Quarterly Publication ISSN 2383 - 3572

Global Journal of Environmental Science and Management

Volume 13, Number 1, Winter 2027

Global Journal of Environmental Science and Management (GJESM)

GJESM

Editor-in-Chief
Professor J. Nouri
GJESM Publisher INC, USA
Email: nourijafar@gmail.com
gjesm.publication@gmail.com

Editor-in-Chief
Professor D. Sivakumar
Kalasalingam Academy of Research and Education, Tamil Nadu, India
Email: sivakumar.gjesm@gmail.com

Managing Editor
Dr. S.M. Tehrani
International Journal of Human Capital in Urban Management
Email: tehranishohre@gmail.com

Technical Editor
Professor M. Samimi
Kermanshah University of Technology
Kermanshah, Iran
Email: m.samimi@kut.ac.ir

Page Designer
A. Rezaye Soltanabadi
Imajaran Danesh, Tehran, Iran
Email: ardavanre@gmail.com

Editorial Contact Information
621 W. Chapman Ave, Orange, CA 92868 USA
Phone: +1(949)405 0540
Email: gjesm.publication@gmail.com

Website: https://www.gjesm.net/
https://www.gjesm.com/
https://www.gjesm.org/

Publication Center
GJESM Publisher INC
gjesm.publication@gmail.com

QUARTERLY PUBLICATION

Editorial Board

Professor V.K. Gupta; *University of Johannesburg, South Africa*

Professor M. Sillanpää; *Lappeenranta University of Technology, Finland*

Professor A. Fauzi Ismail; *Universiti Technologi Malaysia, Malaysia*

Professor A.T. Peterson; *University of Kansas, USA*

Professor A. Cerda; *University of Valencia, Spain*

Professor J.-D. Gu; *University of Hong Kong, P.R. China*

Professor S.I. Allakhverdiev; *Russian Academy of Sciences, Russia*

Professor D. Wen; *University of Leeds, UK*

Professor T. Yigitcanlar; *Queensland University of Technology, Australia*

Professor A. Z. Aris; *Universiti Putra Malaysia, Malaysia*

Professor K. Yetilmezsoy, *Yildiz Technical University, Turkey*

Professor K.E. Noll; *Illinois Institute of Technology, USA*

Professor J. Nouri; *Tehran University of Medical Sciences, Iran*

Professor D. Sivakumar; *Kalasalingam Academy of Research and Education, India*

Professor J. Aravind; *Saveetha Institute of Medical and Technical Sciences, India*

Professor T. Mkilma; *The University of Dodoma, Tanzania*

GJESM is licensed under a "Creative Commons Attribution 4.0 International (CC-BY 4.0)"
Publication authorization is certified by the Ministry of Culture and Islamic Guidance; No. 93/3629; 14 May 2014
Scientific-Research grade is accredited by the Ministry of Science, Research and Technology; No. 3/18/59975; 20 June 2015

Let s work together to publish the knowledge
and science to serve better the environment

Circulation: 500

pISSN: 2383 - 3572 **eISSN: 2383 - 3866**

Aims and Scope

Global Journal of Environmental Science and Management (GJESM) is an international scholarly refereed research journal which aims to promote the theory and practice of environmental science and management. A broad outline of the journal's scope includes; peer reviewed original research articles, case and technical reports, reviews and analyses papers, short communications and notes to the editor, in interdisciplinary information on the practice and status of research in environmental science and management, both natural and man-made. The main aspects of research areas include, but are not exclusive to; environmental chemistry and biology, environments pollution control and monitoring, transport and fate of pollutants in the environment, concentrations and dispersion and trace of wastes in air, water, and soil, point and non-point sources pollution, heavy metals and organic compounds in the environment, atmospheric pollutants and trace gases, solid and hazardous waste management; soil biodegradation and bioremediation of contaminated sites; environmental impact assessment, industrial ecology, ecological and human risk assessment; improved energy management and auditing efficiency and environmental standards and criteria.

Vision and Mission

Global Journal of Environmental Science and Management (GJESM) publishes original. Peer-reviewed and technical environmental articles serve those environmental science and management through the on time quarterly publication with reliable information. GJESM is an integral partner with the scientific and technical communities, delivering superior information products and services that foster communication, build insights and enables individual and collective advancement in environmental research. Providing environmental science and management information to the general public with descriptions of contemporary advances in environmental issues to be used in improving environmental protection and management.

Abstracting and Indexing

Web of Science (ESCI); Scopus; Scimago Journal Rank (SJR); ProQuest (Agricultural and Environmental Science + Natural Science Collection + Ulrichsweb); Chemical Abstract (CAS); CABI Abstract; Global Health Abstract; Agricola; Committee on Publication Ethics (COPE); PubMed-NCBI; DOAJ; Open J-Gate; Google Scholar; Academia.edu; Geomar; WorldCat; Academic Resource Index; Environmental XPRT; Information Matrix for the Analysis of Journals (MIAR); Bibliothek Humburg; ScienceMedia; JournalTOCs; MSRT; ISC; RICeST; SID; Civilica; Magiran.

Serial # 49

Global Journal of Environmental Science and Management
GJESM

Publisher and Editor-in-Chief
Professor J. Nouri

eISSN 2383 3866
pISSN 2383 3572

Quarterly Full Open Access Peer Reviewed Publication

Journal Abbreviation: Global J. Environ. Sci. Manage.

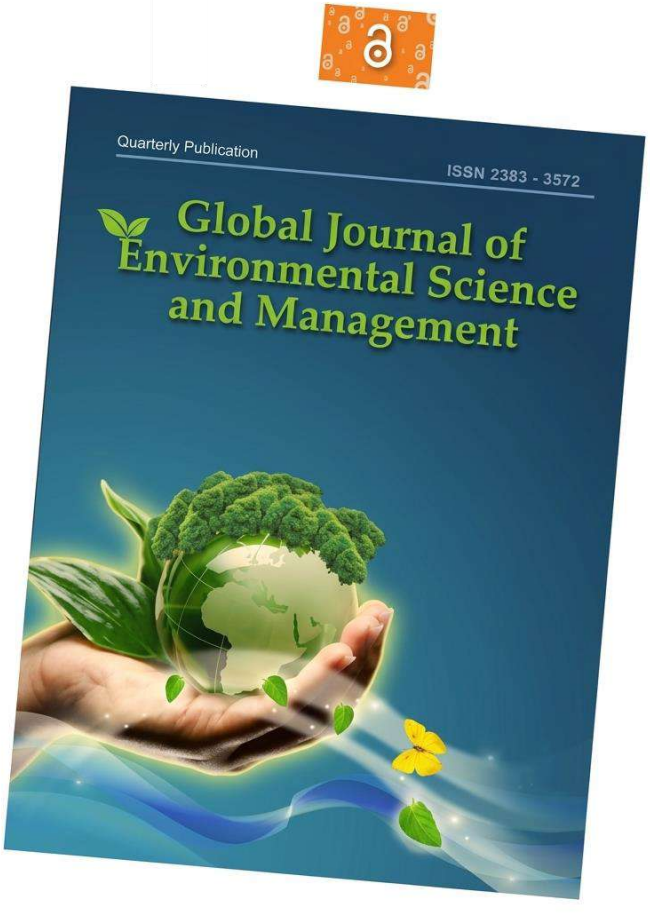

CALL FOR PAPERS

Publication benefits in GJESM Journal

- Online Publication Journal
- Online Submission and Reviewing
- Online Status Inquiry
- Double Blind Review
- Fast-Track Review and Publication
- Immediate Publication on the Net
- Article Podcasts Implementation
- Indexed in **Scopus** Database with **Cite Score = 5.8**
- Scopus Percentile (**WORLD TOP-TEN: 95th in Social Science**)
- **Scopus Q1 Category**
- Indexed in **Web of Science** Database with **IF = 2.3**
- **Web of Science JCR with Q2 Category**

Journal Website:
https://www.gjesm.net
https://www.gjesm.com

Email:
gjesm.publication@gmail.com

Phone:
+1(949)405 4538
+1(949)405 0540

Address:
623 W. Chapman Ave, Orange, CA 92868 USA

Global
Journal of Environmental Science and Management

Volume 13, Issue 1 Winter 2027

1.	Integration of the online river water quality monitoring management framework based on inclusive governance **S. Yudo, D.N. Martono, D. Sutjiningsih, B. Kurniawan (INDONESIA)**	1
2.	Environmental deoxyribonucleic acid metabarcoding reveals fish diversity in subtropical island mangrove rivers **B.G.S. Pananganan, S.G. Salmo III, T. Sado, Y. Isowa, H. Imai, Y. Sato, H. Nagai, M. Bazuin, T. Yamamoto, S. Imura, K. Ishigaki, H. Motomura, M. Miya, T. Kajita (JAPAN/ PHILIPPINES/ INDONESIA)**	27
3.	The effect of agricultural taxes and local agricultural policies onenhancing food security and environmental sustainability **M.S. Setyowati, R.K. Hanum (INDONESIA)**	51
4.	Polymer-specific mechanical recycling of pre-sorted post-consumer municipal plastics for enhanced environmental sustainability **D. Shankar, J. Nouri, Ho Soonmin, B. Hitesh, M. Sankaramuthukumar (INDIA/ USA/ IRAN/MALAYSIA)**	69
5.	Sustainability assessment for multi-activity coastal areas using an integrated hierarchical decision-making framework **Desrizal, B. Widigdo, G. Yulianto, F. Kurniawan, Sulistiono (INDONESIA)**	97
6.	Satellite-based assessment of high Andean wetlands and carbon sequestration under the influence of climate change **Y.M. Mamani-Arpasi, J.A. Mamani Gomez, G. Huanca Chambi, M. Quispe Tisnado, C.E. Yupanqui Bendita, E. Calizaya Chura, E.G. Moreno Terrazas (PERÚ)**	123
7.	Environmental status of silky sharks in Eastern Indian Ocean from length-based catch data **A. Budiarto, I. Yulianto, B. Wiryawan, A.A. Taurusman, M.D. Iskandar, I. Ziegler, S. Gigentika, S. Agustina (INDONESIA/ GERMANY)**	141
8.	The impact of environmental, economic, and social sustainability under intensive agriculture **S. Chandran, T. Ramachandran, D. Sivakumar, A. Ambika (INDIA)**	163
9.	Inflow modeling strategies designed to enhance the ecological sustainability of hydroelectric reservoir operation planning **I. Mulyawati, I.R.S. Salami, M. Marselina, A. Sabar (INDONESIA)**	189
10.	Driving sustainable development goal alignment through green consumption marketing and public mind **S. Petchariya, J. Prasara-A, N. Thiengkamol, V. Sinvayupak, T.K. Thiengkamol (THAILAND)**	213
11.	Ecological diversity in soil properties and bacterial communities in tropical coastal areas with contrasting electrical conductivity **L. Fauziah, Y. Nuraini, Soemarno, N.D. Lestari, Djajadi, N. Aini (INDONESIA)**	231
12.	Multivariate and index-based evaluation of long-term reclaimed wastewater quality and reuse suitability **E.R. Tarawneh (JORDAN)**	251
13.	Environmental modeling of yellowfin tuna fishing grounds integrating oceanographic and biological parameters using generalized additive model **D. Simbolon, E.S.Y. Siregar, R.I. Wahju, I. Yulianto, V.P. Siregar, T.A. Pianto, Rosmasita, M.S. Sangadji, F. Andika, R.A. Mulyadi, M.Y.U. Putra, Rasidi (INDONESIA)**	273

14.	Life cycle assessment and identification of embodied carbon hotspots in a reinforced concrete factory **N. Suriyanon, W. Suriyanon, N. Suriyanon, N. Watkate (THAILAND)**	303
15.	Valorization and physicochemical characterization of municipal solid waste gasification tar derived aliphatic hydrocarbon-rich oils **M. Ridwan, P. Setyono, M.T.S. Budiastuti (INDONESIA)**	327
16.	Analytic hierarchy process-based criterion weighting for water resources management projects **O. Gorbunov, C. Sinsabvarodom, D. Rinchumphu, P. Sangunsri, N. Phichetkunbodee (THAILAND/ TAIWAN)**	347
17.	Temporal water-quality variability and its implications for environmental management of sand lobster aquaculture **I.N.P. Winata, I.M. Radjawane, S. Nurdjaman, I.N. Radiarta, D. Sidik, Deby, S.K. Pratiwi, S. Makmur, A.A. Utama, A. Suman, Husnah (INDONESIA)**	369
18.	Ecological drivers of *Hygrocybe* and *Xylaria* occurrences in a tropical Karst forest **S.H. Larekeng, A.H. Salman, H.A. Amanah, Tine Grebenc, M.B. Akzad, M. Restu, M.D. Usman, R. Prayudyaningsih, Asrianny (INDONESIA/ SLOVENIA)**	391
19.	Consumer awareness, participation, and accessibility in sustainable electronic waste management **D. Fitria, D.R. Nugraheni, H. Herdiansyah, M. Qamruzzaman (INDONESIA/ BANGLADESH)**	413
20.	Integrated system dynamics modeling for sustainable fisheries provisioning services **A.N.K.B.P. Iskandar, D. Iskandar, Sunardi, Zahidah, R. Adji, R. Sunaryanto, S.S. Antarlina, B.N. Marwoto, W. Basuki, N. Ismail (INDONESIA)**	433
21.	Environmental health conditions associated with childhood stunting during the first 1000 days of life **A. Muthia, D. Utari, T.E.B. Soesilo (INDONESIA)**	457
22.	Artificial intelligence-driven approaches for detection, fate, transport, and remediation of microplastic pollution in aquatic systems **M. Kamaraj, H.A. Bhavithra, B. Rajalakshmi, J. Aravind (INDIA)**	479
23.	Environmental risks of pest management practices in smallholder coconut plantations **M.L.A. Hosang, Susilawati, J.C. Alouw, M. Puspitasari, R.E. Senewe, Sujak, Rohimatun, R.T. Hutasoit, Subiyakto, Nurindah, D.A. Sunarto, R.G.U.I. Meththananda, B.A.N. Pinaria (INDONESIA/ SRI LANKA)**	501
24.	A bibliometric and systematic analysis of artificial intelligence and the transition towards smart geotourism **T. Aguirre-Suárez, M. Pérez-Chiquito, H. Cochea-Tomalá, P. Escandón-Panchana (ECUADOR/ SPAIN)**	523
25.	Bridging single-species models to ecosystem-based maximum sustainable yield for environmental sustainability in marine fisheries **S. Triharyuni, A.K. Supriatna, N. Anggriani, R. Puspasari (INDONESIA)**	553

Global J. Environ. Sci. Manage. 13(1): 01-26, Winter 2027, Serial #49

Global Journal of Environmental Science and Management
(GJESM)

Homepage: https://www.gjesm.net/

Podcasts

ORIGINAL RESEARCH ARTICLE

Integration of the online river water quality monitoring management framework based on inclusive governance

S. Yudo[1], D.N. Martono[2,*], D. Sutjiningsih[3], B. Kurniawan[1]

[1]Research Center for Clean Technology and Environment, National Research and Innovation Agency, BJ. Habibie Science and Technology Area, South Tangerang City, 15314, Banten Province, Indonesia

[2]Faculty of Environmental Sciences, University of Indonesia, Central Jakarta, DKI Jakarta, 10430, Indonesia

[3]Faculty of Engineering, University of Indonesia, Depok City, West Java Province, 16424, Indonesia

ARTICLE INFO

Article History:
Received 09 April 2026
Revised 13 June 2026
Accepted 15 July 2026

Keywords:
Data quality
Inclusive governance
Multi-stakeholder collaboration
Online river water quality monitoring
System performance

ABSTRACT

BACKGROUND AND OBJECTIVES: Online river water quality monitoring systems are increasingly used to support pollution control. Nonetheless, the efficacy of these systems remains constrained by key technical and organizational challenges, namely high data variability, sensor instability, restricted interoperability, and decentralized institutional governance. These challenges reduce the trustworthiness of online data for evidence-based pollution control policy and decision-making. The study objectives were to develop an integrated framework to improve data quality, system performance, and coordination in the governance of online river water quality monitoring river water quality monitoring in watersheds across Indonesia.

METHODS: A transdisciplinary methodological approach was applied by combining 1) Integrated data quality management to assess data completeness, accuracy, validity span and stability; 2) Key performance indicators measured by the analytical hierarchy process to evaluate the performance of online river water quality monitoring systems; and 3) Soft systems methodology to build a governance-oriented conceptual model through rich descriptions, root definitions, conceptual models and evaluation of the 3Es (efficacy, efficiency and effectiveness). This study analyzed environmental data collected between 2023 and 2025 from four monitoring stations representing the upstream and downstream reaches of the Ciliwung and Cisadane Rivers. To complement these quantitative findings, semi-structured interviews were conducted with a broad range of stakeholders, including government agencies, vendors, academics, researchers, the media, community-based non-governmental organizations, and local communities residing near the four stations.

FINDINGS: An analysis of data quality demonstrated robust completeness (99–100 percent), highly variable non-zero completeness across all stations, high validity across the range for dissolved oxygen, hydrogen potential, and temperature (greater than 95 percent), and large fluctuations in stability at stations affected by tidal and sediment dynamics. The system performance index was 61.18 percent. Synthesizing soft systems methodology highlighted key operational barriers, such as fragmented roles, low trust towards online data, and lack of community participation. Consequently, this study developed an online river water quality monitoring management framework designed to prioritize digital interoperability, transparency, accountability, and multi-stakeholder governance.

CONCLUSION: The inclusive governance-based online river water quality monitoring framework provides an empirically informed conceptual framework for organizing data-quality, performance, and governance improvements, improved collaboration among government agencies. Subject to contextual adaptation and prospective validation, this framework offers valuable insights for management design in other watersheds, ultimately contributing to the advancement of digital environmental governance in developing nations.

DOI:10. 22034.gjesm.2027.01.01

This is an open access article under the CC BY license (http://creativecommons.org/licenses/by/4.0/)

NUMBER OF REFERENCES	NUMBER OF FIGURES	NUMBER OF TABLES
81	10	6

*Corresponding Author:
Email: dwi.nowo11@ui.ac.id
Phone: +857 1089 2249
ORCID: 0000-0003-2362-9066

Note: Discussion period for this manuscript open until March 01, 2027 on GJESM website at the “Show Article”.

INTRODUCTION

Rivers play a vital role in supporting ecological processes, socio-economic activities, and providing essential services such as domestic water supply, fisheries, agriculture, and recreation (Singh *et al.,* 2020; Debnath *et al.,* 2021). Fluvial systems have experienced progressive environmental degradation, driven primarily by rapid urbanization and industrial expansion (Kumar *et al*., 2017; Chen *et al*., 2022). This phenomenon is seen in many developing countries, including Indonesia. Carvalho *et al*. (2019) and UNEP (2021) emphasized that monitoring river water quality is important for understanding pollutant behavior, identifying pollution sources, and supporting effective environmental management and intervention strategies. In recent years, river water quality monitoring has transitioned from labor-intensive manual sampling protocols toward automated, real-time data acquisition leveraging Internet of Things (IoT)-enabled (Zhang *et al*., 2020; Singh *et al*., 2022). Sustainable development goal 6.3 (SDG 6.3) is to improve water quality by reducing pollution and treating wastewater (Kremere *et al*., 2019). Recently, the advancement of sensor technology has enabled the development of online river water quality monitoring systems that are always on and can sense critical parameters such as dissolved oxygen (DO), chemical oxygen demand (COD), biochemical oxygen demand (BOD), potential of hydrogen (pH), turbidity, temperature, conductivity and nutrient concentrations (Farouk *et al*., 2023; Rajendran *et al*., 2025). To enhance the national environmental monitoring network, the Ministry of Environment (KLH) has established online river water quality monitoring (ORWQM) as a core strategic initiative. The number of ORWQM stations in Indonesia has continued to increase from 2015 to 2024, reaching 347 stations in different watersheds (KLHK, 2024). Institutionally, ORWQM can be a national strategic instrument for KLH and local governments to achieve the SDG 6.3 target on water pollution control. ORWQM assessments should focus on three key areas: data quality, system performance and inclusive governance. Ultimately, the proposed framework provides a conceptual basis to validate ORWQM data integrity, evaluate system performance across multidimensional indicators, and design highly adaptive, transparent, and participatory governance models. The literature on stakeholder engagement in water management suggests that effective participation relies on clarity of purpose, transparency, accountability, capacity, access to information, and ongoing evaluation (Akhmouch and Clavreul, 2016). Soft Systems Methodology (SSM) is used to develop a governance model that clarifies actor roles, institutional fragmentation, levels of trust in online data, and the need for multi-stakeholder coordination. Existing research demonstrates that poor-quality environmental data—specifically when inaccurate, incomplete, unstable, or invalid—compromises the integrity of monitoring programs and obstructs evidence-based policy formulation (Wang and Strong, 1996; Batini and Scannapieco, 2016). In Indonesia, inconsistent sensor data and missing values are frequently reported, limiting the use of online measurements for modeling, pollution law enforcement, early warning system (EWS), and compliance reporting (Wahyono and Yudo, 2022; Yudo *et al.,* 2023; Yudo *et al*., 2026). In tandem with data-related limitations, institutional and governance bottlenecks pose formidable obstacles to the enduring viability of the ORWQM system. Different government agencies, such as KLH, the Watershed Management Agency (BPDAS), the River Basin Organization (BBWS), the Environment Agency (DLH) at the provincial and district levels, and local government, have overlapping mandates in water resource management. Institutional fragmentation, coupled with the absence of both formal coordination mechanisms and an integrated data sharing framework hinder the efficiency and accountability of the monitoring system

(OECD, 2015; World Bank, 2017). Experiences from other countries suggest that the monitoring systems are more likely to have a positive impact on policy if they are supported by open data initiatives, community engagement and multi-stakeholder management (Gupta *et al*., 2020; Dong *et al*., 2023; Domínguez-Rendón *et al*., 2024). In Indonesia, citizen participation in river management remains limited. Furthermore, monitoring data are frequently not effectively disseminated to local communities or river-centric non-governmental organizations (NGOs), thereby hindering collaborative surveillance and timely pollution response efforts (Shao and Bishop, 2021; Basuki *et al*., 2024; Sulistiyowati and Uyun, 2024). Prior research has predominantly concentrated on isolated technical dimensions, such as enhancing sensor accuracy and developing predictive water quality models, or has alternatively focused on formal governance frameworks for pollution control (Ratolojanahary *et al*., 2019; Talagala *et al*., 2019; Zhou, 2020; Cao *et al*., 2022). Several studies highlight the importance of integrated, multi-stakeholder watershed governance (Behmel *et al.,* 2018; Lim *et al.,* 2022). Existing ORWQM assessments generally address sensor performance, data analytics, and institutional governance separately, leaving a gap in explaining how data-quality problems affect system performance and translate into governance actions. To bridge this critical literature gap, this study establishes a comprehensive socio-technical framework that systematically couples TDQM–ODQEM data-quality diagnosis, key performance indicator (KPI) – analytic hierarchy process (AHP) performance prioritization, and SSM-based governance redesign. Its novelty lies in a traceable pathway from identifying whether online data are complete, valid, stable, and usable, to prioritizing performance constraints and converting them into governance activities, clearer institutional roles, and coordination mechanisms. Consequently, the proposed framework consolidates diagnostic, evaluative, and participatory functions into a unified managerial logic, offering strong potential to facilitate evidence-based pollution-control decisions upon prospective implementation and empirical evaluation. This study aims to determine the extent to which the community understands the functions and benefits of the ORWQM stations, as well as their concerns about the condition of the surrounding river water quality. Furthermore, the study evaluates community willingness and capacity to participate in environmental monitoring, while identifying key systemic barriers, such as institutional distrust, constrained digital literacy, and information asymmetry—that may compromise the efficacy of ORWQM governance. This survey aims to measure the extent to which community perceptions are based on subjective data obtained quantitatively through a questionnaire instrument. This study was carried out at the Graduate School of Sustainable Development, Universitas Indonesia, Jakarta, Indonesia, in 2025.

MATERIALS AND METHODS

The study area

This study used four ORWQM stations as samples. The two stations are located on the Ciliwung River (Manggarai and Kelapa Dua) and the two stations are located on the Cisadane River (Empang Dam and Kali Sabi). The four monitoring stations were purposively selected to ensure river-basin representation, ORWQM data availability, and relevance to regional pollution-control efforts. The Ciliwung and Cisadane Rivers were chosen because they are strategic rivers in the Jakarta, Bogor, Depok, Tangerang and Bekasi areas and are part of priority watersheds (Yulianto *et al*., 2021). Differences among Manggarai, Kelapa Dua, Empang Dam, and Kali Sabi are interpreted in terms of station locations, hydrodynamic conditions, sediment influences, urban/industrial pressures, sensor behavior, and institutional maintenance contexts. Alternative explanations, including stable environmental conditions, sensor resolution, communication disruptions, and operational downtime, are considered to avoid over-attribution of patterns to

a single cause. According Wahjono (2016), the technology of ORWQM has been applied to priority watersheds, namely Ciliwung and Cisadane rivers. The four monitoring stations used in this study were Manggarai, Kelapa Dua, Empang Dam, and Kali Sabi, chosen because they represent the spatial variation and pollution levels in the Ciliwung and Cisadane Rivers. Manggarai Station monitors the lower reaches of the Ciliwung River in the densely populated metropolitan area of Jakarta, while Kelapa Dua Station captures the transitional middle to lower reaches, which are significantly influenced by residential development and land-use alterations. In the Cisadane River, Empang Dam Station represents the upper reaches of the system, while Kali Sabi Station represents the lower reaches, which are affected by domestic, urban, and industrial activities. Fig. 1 illustrates the spatial distribution of the four monitoring stations across the Jakarta, Tangerang, Bogor, and Depok areas on Java Island, while Table 1 details their respective physical addresses and geographic coordinates. ORWQM stations are installed along riverbanks in several watersheds in the upper, middle, and lower reaches of rivers (Fig. 2a). This system plays a crucial role in water resource management (Tsatsaros *et al.,* 2021; Rodriguez *et al.,* 2021), environmental protection, and data-driven decision-making. This system can strengthen oversight, policy evaluation, and inter-agency coordination in river water quality management (Saleh and Stanley, 2023). From a technical perspective, each ORWQM station features an identical hardware configuration (Fig. 2b), comprising sensors, data loggers, batteries, solar cells, modems, and pumps (Wahyono *et al.,* 2026). Some of the data logger functions include: setting the time interval for sending data to the data center via global system for mobile communications, sending data to be displayed on a running text, displaying data on a liquid crystal display (LCD) screen, setting periodic sensor cleaning, setting the pump interval for taking water samples from the river, and setting battery charging (Fig. 2c). Data collection was executed utilizing two multiparameter sensors: the first is a physicochemical sensor that measures 11 parameters, namely electrical conductivity, salinity, total dissolved solids (TDS), DO, temperature, pH, turbidity, nitrate, ammonia, oxidation reduction potential (ORP), and depth. The second is an organic sensor that measures 3 parameters: BOD, COD, and total suspended solids (TSS). This system works by periodically measuring 14 water quality parameters, archiving the logged data locally, and transmitting it at scheduled intervals to a centralized data center.

The data sources

This study used three primary data sources. First, ORWQM data (2023–2025) at four ORWQM stations in the Ciliwung–Cisadane region (Manggarai, Kelapa Dua, Empang Dam, and Kali Sabi) covering 11 water quality parameters (COD, BOD, TSS, DO, pH, nitrate, ammonia, temperature, conductivity, TDS, and turbidity). With data transmission configured at hourly intervals, each station typically registers a minimum of 24 records per day. Consequently, assuming continuous sensor operation, a single station is projected to accumulate approximately 8,760 records annually. One data record consists of 17 columns or fields: Station ID, Date, Time, and several water quality parameters. Second, semi-structured interviews were conducted with 27 cross-sectoral stakeholders, including government representatives, academics/researchers, private vendors, NGOs, media, and station operators. Third, the study gathered empirical data on local residents' perceptions within the immediate vicinity of the four monitoring stations through structured questionnaire surveys.

The methods used

This study uses three stages of analysis, namely: 1) Data quality evaluation with a combined approach of total data quality management (TDQM) and online data quality evaluation model (ODQEM) for performance improvement.

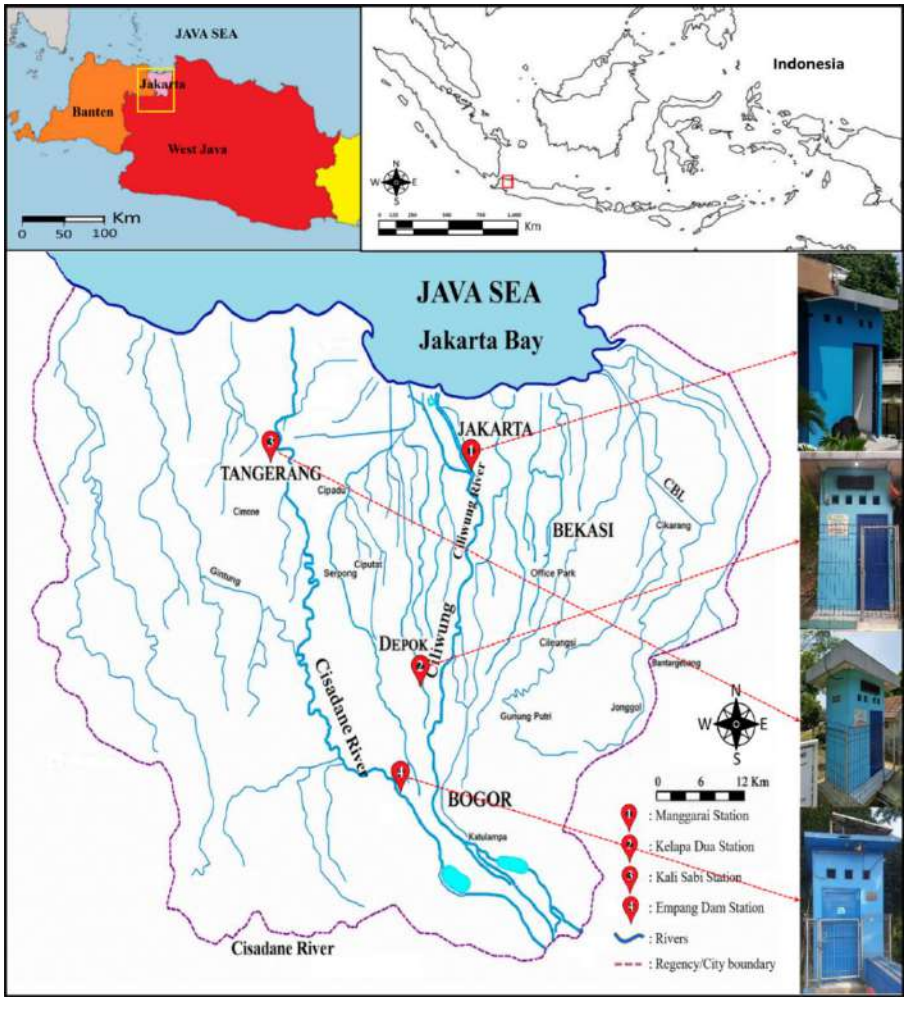

Fig. 1: Geographical location of four stations in the Jakarta, Tangerang, Bogor, and Depok areas on Java Island, Indonesia

Table 1: Location of four ORWQM stations on the Ciliwung River and Cisadane River

No.	Station Name	River	Address	Coordinate	
				Latitude	Longitudes
1	Manggarai	Ciliwung	Tambak Street, RT.07/ RW.04, Pegangsaan, Menteng District, Central Jakarta, DKI Jakarta	-6.20784	106.84851
2	Kelapa Dua	Ciliwung	Arus Alley, RT.07/ RW.01, Srengseng Sawah, Jagakarsa District, South Jakarta, DKI Jakarta.	-6.35264	106.83564
3	Empang Dam	Cisadane	Sedane Street, RT.05/ RW.06, Paledang, Bogor City, West Java Province	-6.60777	106.79288
4	Kali Sabi	Cisadane tributary	Moh. Toha Street, RT.01/ RW.01, Periuk, Periuk District, Tangerang City, Banten, Province	-6.16079	106.62772

TDQM provides a conceptual framework through general data quality dimensions, namely completeness, validity, accuracy, and uniqueness (Wang and Strong, 1996; Wang, 1998). This framework is then adapted with ODQEM technical indicators, namely completeness index (CI), range validity (RV), stability index (SI), accuracy vs lab, and uniqueness (duplicate check); 2) System performance evaluation with a combined method of KPI and AHP. To evaluate the ORWQM system,

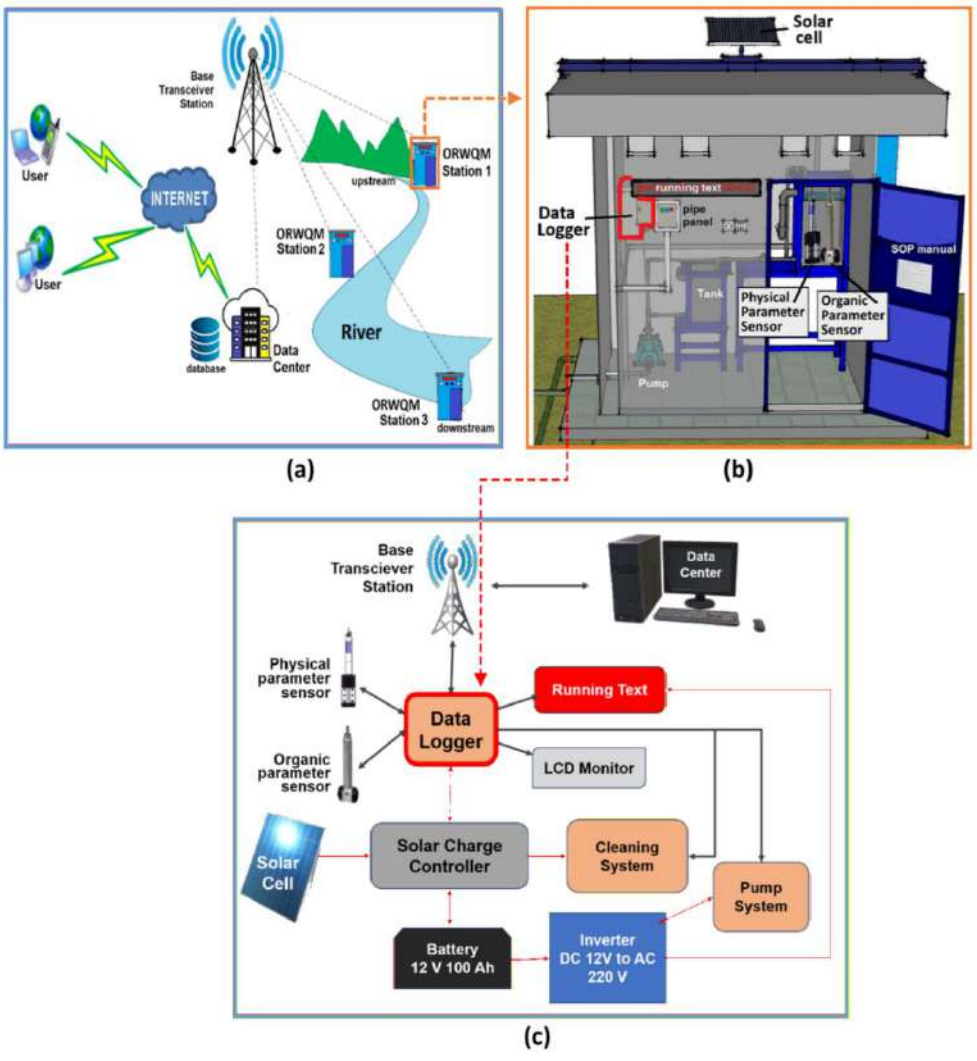

Fig. 2: Diagram of the ORWQM station: (a) Connection system; (b) Station components; and (c) Flow diagram (Modified from Wahyono *et al.,* 2026)

performance assessments are executed by synthesizing the AHP-derived priority weight (Saaty, 1990) with the actual performance scores of each individual KPI (Lo-Iacono-Ferreira *et al.,* 2018; Mamun *et al.,* 2019); 3) Designing a conceptual governance model using the SSM approach. In creating this conceptual model, three SSM components serve as the basis and must be followed: Root definition, Do P, by doing Q, to achieve R (PQR formula), and customers, actors, transformation, worldview, owners, environment (CATWOE). Success indicators are operationalized and evaluated through the '3E' framework, comprising efficacy, efficiency, and effectiveness. This SSM phase analyzes the overall picture, CATWOE analysis, and conceptual modeling to define institutional roles, stakeholder interactions, operational challenges, and governance gaps. Methodologically, this study contributes an integrative mechanism that systematically bridges three established approaches. TDQM-ODQEM generates diagnostic indicators of data usability, then KPI-AHP transforms these indicators and system concerns

derived from stakeholders into weighted priorities, and finally SSM transforms the prioritized issues into root definitions, CATWOE elements, conceptual activities, and governance improvements. This constructs a methodological bridge between quantitative data-quality assessments and qualitative governance redesign, integrating the two by systematically feeding the analytical outputs of each stage as explicit inputs into the next.

Data quality evaluation

The first stage of this research was to analyze data quality at the four stations by evaluating core dimensions adapted from the TDQM (Wang and Strong, 1996; Batini and Scannapieco, 2016). This research used a combined approach between the TDQM and the proposed ODQEM water quality evaluation model. The TDQM provides a conceptual framework through general data quality dimensions: completeness, validity, accuracy, and uniqueness (Wang and Strong, 1996; Wang, 1998). This framework was then adapted to the context of sensor-based ORWQM using the ODQEM technical indicators: CI, RV, SI, accuracy vs lab, and uniqueness (duplicate check). The following formulas are used to calculate each dimension of CI, RV, SI, and accuracy compared to the Lab. The completeness analysis evaluates two core dimensions: structural completeness (the presence of expected time-stamped records) and functional completeness (the proportion of analytically viable, non-zero values). The CI dimension refers to the quantity of available data compared to the total observation time, using Eq. 1 (Egidio *et al.*, 2022; Teh *et al.*, 2020):

$$CI = \frac{N_{\text{valid}}}{N_{\text{expected}}} \times 100\% \quad (1)$$

The more complete the data recorded and stored by the online sensor system, the higher the CI value, approaching 100 percent (%). Low values, on the other hand, indicate missing data, transmission interference, or inactive sensors. RV dimensions account for the percentage of measurements falling within the regulatory ranges, specifically those satisfying water quality standards, using Eq. 2 (Wagner *et al.*, 2006):

$$RV = \frac{N_{\text{in-range}}}{N_{\text{valid}}} \times 100\% \quad (2)$$

As detailed in Table 2, the permissible value ranges are derived from Indonesian regulatory standards: Ministry of Environment and Forestry No. 2 of 2022 and No. 492 of 2016 (KLHK, 2016; PerMen, 2022), as well as the Regulation of the Ministry of Health of the Republic of Indonesia No. 492 of 2010 (Menkes, 2010). High RV with ≥ 90% = the majority of data is realistic, and the sensor is functioning normally. Medium RV (70–90%) = some data points are 'out of range,' possibly due to sensor interference or extreme river conditions. Low RV (< 70%) = the sensor may have a problem (fouling, drift, loss of calibration). RV has been widely used to evaluate the quality of environmental sensor data. Measurement accuracy was evaluated by comparing the online sensor data with laboratory analyses, utilizing the mean absolute error (MAE), using Eq. 3 (Zhang and Thorbun, 2022):

$$MAE = \frac{1}{n}\sum | S_i - L_i | \quad (3)$$

where S_i is the sensor measurement, and L_i is the corresponding laboratory reference value. In the initial analysis, the absolute percentage error was calculated for each sensor-laboratory observation pair and subsequently converted it into a relative accuracy score using Eq. 4 (Hyndman and Koehler, 2006):

$$APE_i = (|S_i - L_i| \,/\, |L_i|) \times 100\%; \text{ and } RAS_i = 100\% - APE_i \quad (4)$$

Percentage-based error measures are commonly used as unit-free measures of relative deviation,

Table 2: Acceptable range for each water quality parameter (PerMen, 2022; Menkes, 2010; KLHK, 2016)

Parameter	Range
BOD	0.1 - 60 milligrams per liter (mg/L)
COD	0.1 - 500 mg/L
Temperature	0° C – 50 degree Clesius (°C)
DO	0 - 15 mg/L; or 0 - 200%
pH	0 - 14 units
Nitrate	0 - 50 mg/L
Nitrite	0 – 10 mg/L
TSS	0 - 500 mg/L
TDS /conductivity/salinity	0 - 100,000 microSiemens per centimeter (µS/cm) or 0 - 100 mS/cm
Turbidity	0 - 1000 nephelometric turbidity unit (NTU)
Ammonia	0 - 100 mg/L as N /0 – 10 mg/L
Depth (pressure)	0 - 10 m or more

although they require caution when reference values are zero or close to zero (Hyndman and Koehler, 2006). The RAS used in this study is an interpretative transformation of APE and is not presented as a conventional statistical agreement metric. In alignment with recent studies on high-frequency river monitoring, evaluating measurement accuracy is essential for validating ORWQM system outputs (Wagner *et al*., 2006; Pellerin *et al.,* 2016). Stability is used as a diagnostic indicator to flag potential flatline behavior. Flatline events are initially identified when identical values persist for three or more consecutive records (QARTOD). This threshold is used as an initial screening rule, not as evidence of sensor failure. Signal flatlining may occur if the sensor experiences sediment-induced fouling, calibration drift, or physical degradation. This indicator has been widely used to evaluate the quality of environmental sensor data, using Eq. 5 (Adu-Manu *et al*., 2017; Zhang *et al.,* 2022):

$$SI = \frac{Number\ of\ flatline\ segments}{Total\ segments} \times 100\% \qquad (5)$$

SI value:

a) A high SI (>90%) indicates stable, reasonable data quality and can be used immediately.
b) A moderate SI (70–90%) indicates quite stable conditions with minor anomalies and needs to be verified by field samples.
c) A low SI (50–70%) indicates unstable data; sensor checks and comparison with manual data are necessary.
d) A very low SI (<50%) indicates very unstable data; sensor maintenance and data imputation are required.

Uniqueness measures the degree to which a dataset is free from duplicate or redundant entries, calculated as the ratio of unique data points to the total number of observations. Uniqueness in ORWQM is determined by the timestamp, which is the time information attached to each time series data point, and each measurement must be unique, by using Eq. 6 (Ehrlinger and Wöß, 2022):

$$Uq = \frac{Number\ of\ unique\ values}{Total\ values} \times 100\% \qquad (6)$$

Uq value of 100% indicates all unique data, and a value <100% indicates redundancy.

System performance evaluation

The next step is to evaluate the performance of the ORWQM system using KPI and AHP instruments. The KPI method is a set of indicators that focus on the performance aspects most critical to the organization's current and future success (Parmenter, 2020). According to Lo-Iacono-Ferreira *et al*. (2018), a KPI serves as an index to quantify critical factors related to established objectives, thereby evaluating organizational performance toward those goals. AHP is a procedure for ranking decision alternatives when decision-makers have multiple

objectives or criteria to consider (Saaty, 1990). The following is the equations for the consistency index (CI) and consistency ratio (CR), according to Saaty (1990):

$$CI = \frac{\lambda_{max} - n}{(n-1)} \quad (7)$$

$$CR = \frac{CI}{RI} \quad (8)$$

The steps involved in evaluating the performance of the ORWQM system (Fig. 3) are: a) Establishing KPIs representing five aspects of the system: technical, institutional, social, economic, and environmental; b) Assign priority weights to each indicator based on the perceptions of experts and stakeholders; c) Collect actual data to measure the actual score of each indicator based on field data and supporting documents; d) Change all measurement results to a 0–1 scale (low–very low) for cross-dimensional comparison. To reconcile the heterogeneous measurement units across indicators—ranging from percentages and ratios to qualitative perceptual scales—raw scores are normalized utilizing both quantitative and qualitative criteria; e) The AHP weight of each indicator is multiplied by its normalized actual score to obtain the indicator's contribution value, using Eq. 9 (Hwang and Yoon, 1981; Triantaphyllou, 2000; Saaty, 2008):

$$I_i = W_i \times S_i \quad (9)$$

Where: I_i = indicator contribution; W_i = AHP weight; S_i = actual score

f) The contribution values of all indicators are then summed to obtain the overall system performance index (PI), using the weighted sum, using Eq. 10 (Hwang and Yoon, 1981; Triantaphyllou, 2000):

$$PI = \sum_{i=1}^{n} (w_i \times S_i) \quad (10)$$

g) The final phase entails interpreting the index results and assessing individual indicator contributions to formulate actionable recommendations for system enhancements. Table 3 the system PI index assessment shows KPI scores based on system performance categories, from low to excellent. This methodology aligns with established guidelines for constructing composite indicators, which mandate explicit and transparent justification for all normalization, weighting, aggregation, and interpretation design choices (OECD, 2008). Given that composite index classification is often sensitive to threshold selection, a sensitivity analysis utilizing alternative category thresholds was performed. The ORWQM performance index remained within a reasonable range under plausible alternatives, indicating that the primary interpretation is robust. However, the numerical scores and the contribution of weighted indicators were emphasized over the categorical labels.

Soft systems methodology

The SSM stages in this study follow the Hardjosoekarto (2012) approach, which is used to understand and address complex, unstructured, multi-stakeholder problem situations. This approach represents an action-oriented investigative framework for addressing adverse conditions, wherein participants systematically analyze the situation to design and implement targeted interventions (Checkland and Poulter, 2020). To navigate unstructured and highly complex situations involving multiple stakeholders with competing priorities, this study utilized the SSM process (Fig. 4) as a diagnostic tool to identify key issues. Semi-structured interviews were conducted with 27 stakeholders representing government agencies, local environmental organizations, academics / researchers, vendors, operators, NGOs, media, and the public. Participants were selected using purposive sampling based on their active involvement in ORWQM planning, operations, data utilization, policy implementation, or

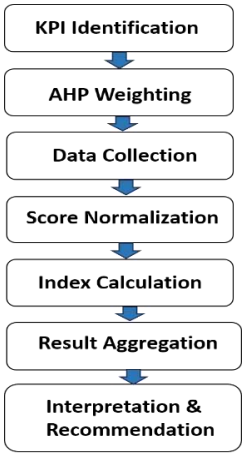

Fig. 3: KPI measurement stages using the AHP method

Table 3: System PI index scoring

Category	KPI value Range	Interpretation
Excellent	≥ 80%	Effective system, high synergy between technical and institutional aspects
Good	65%–79%	System is fairly stable, institutional/social improvements are still needed
Fair	50%–64%	Moderate performance, needs improved coordination and funding support
Low	< 50%	System not yet functioning optimally, fundamental technical and policy issues

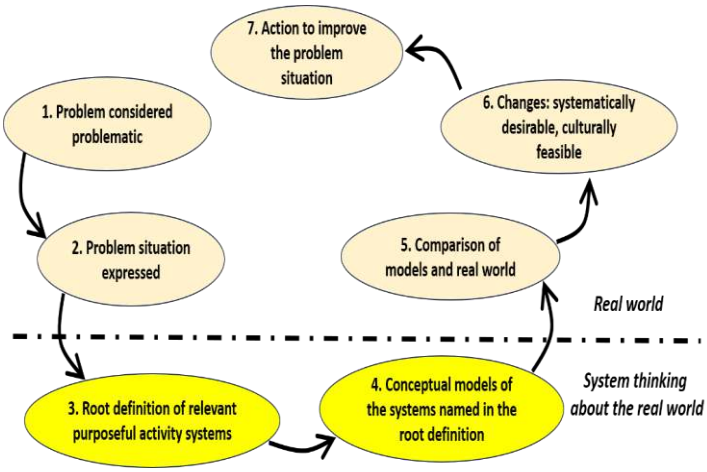

Fig. 4: Steps of SSM (Hardjosoekarto, 2012)

community advocacy. Discussions were guided by a thematic protocol covering operational challenges, data quality, system performance, institutional coordination, public accessibility, and future governance pathways. Specifically, interview transcripts were divided into meaningful statement units, coded, and grouped into recurring themes related to data quality, technical reliability, institutional coordination, financing, public transparency, stakeholder participation, and pollution response. These themes were then used to build a rich picture, formulate the root definition and PQR, identify CATWOE elements, define governance and operational gaps, and develop activities included in the conceptual model. Guided by this foundational understanding, key root definitions designed was developed to model the desired human activity

system. Then, a conceptual model is developed and validated with CATWOE analysis to ensure the clarity of its elements: Customers, Actors, Transformation, Weltanschauung, Owners, and Environmental constraints. The success of the model is assessed based on the 3E principle of efficacy, efficiency, and effectiveness. The next step is the comparison of the conceptual model with the actual conditions to find out gaps, areas for improvement, and potential for intervention. Within the SSM framework, validating social acceptability is essential; this entails assessing whether the system's actors perceive the proposed model as plausible, realistic, and actionable. Through this process, key informants provide insights into the feasibility of model implementation, potential institutional barriers, and the possibility of strengthening inter-institutional coordination mechanisms.

RESULTS AND DISCUSSION

Data quality analysis

Data quality was evaluated across four stations for 2023–2025 using CI, RV and SI accuracy against laboratory measurements, and uniqueness. The findings demonstrate a clear divergence between data availability and actual analytical usability. The United States Geological Survey (USGS) guidance for continuous water quality monitors also states that continuous monitoring data must undergo site selection, field operations, calibration, computation, correction, review, and reporting before it can be used to interpret water quality (Wagner *et al*., 2006). The completeness index (CI) analysis demonstrates near-perfect structural completeness across all four monitoring stations, with values ranging from 99% to 100%. Manggarai had the strongest overall completeness non-zero, with most parameters exceeding 90%, whereas Empang Dam showed substantial gaps for DO (50.5%), pH (59.0%), nitrate (48.0%), and salinity (1.1%) (Fig. 5). These results are also consistent with the study of Behmel *et al*. (2018) who indicated the importance of real-time data reliability to support water quality management. While the Kelapa Dua station exhibited parameter-specific data deficiencies, most notably for TSS and salinity, while Kali Sabi station demonstrated high completeness for nitrate, TDS, salinity, and conductivity, despite suffering from sparse ammonia coverage. Thus, the principal finding is not simply that some stations transmitted more data, but that apparently continuous records could still contain parameter-level failures. These findings underscore the necessity of evaluating completeness in conjunction with validity, stability, and reference measurements rather than conflating mere data availability with data reliability (Wagner *et al*., 2006; Bushnell *et al*., 2020). A comparison across monitoring sites reveals that the Empang Dam station exhibits exceptionally high data completeness (excluding zero-value entries) for key environmental parameters. This means that the Manggarai system can transmit data continuously, and generate data which is easier to use for analysis. This supports the need to interpret completeness together with validity, stability, and reference measurements rather than treating data availability as evidence of reliability (Wagner *et al*., 2006; Bushnell *et al*., 2020: Rozemeijer *et al*., 2025). While these data gaps are likely attributable to sensor malfunctions, operational constraints, maintenance issues, or data-processing errors, the lack of diagnostic records precludes a definitive attribution of their precise causes. Kelapa Dua showed intermediate performance, with relatively good completeness for pH, nitrate, temperature, and turbidity but poorer results for TSS and salinity, indicating parameter-specific rather than system-wide problems. Kali Sabi performed relatively well for nitrate, TDS, salinity, and conductivity but poorly for ammonia. These differences show that key parameters such as DO, pH, turbidity, conductivity/TDS, and temperature respond differently to field conditions and system limitations (Rojas *et al*., 2021).

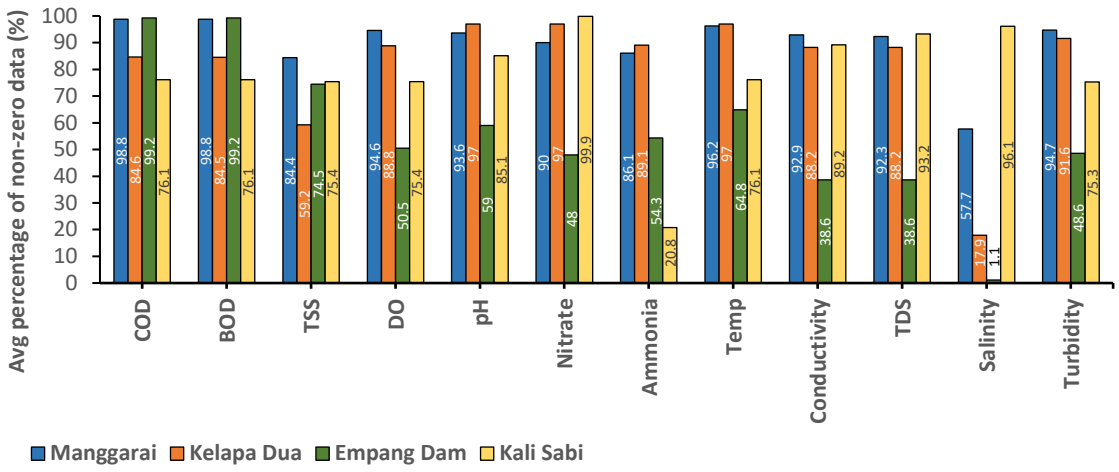

Fig. 5: Percentage of non-zero complete data at the four stations

Range validity

The results of the RV analysis corroborate the idea that data quality of ORWQM cannot be determined only on data completeness. Across nearly all monitored parameters, including TSS, DO, pH, ammonia, temperature, salinity and turbidity, the Manggarai station consistently exhibited elevated RV values. However, the lower RV values for conductivity and TDS suggest that the sensors based on electrodes could be subject to interference. This finding aligns with established continuous monitoring protocols, which emphasize specific conductance as a critical parameter requiring systematic calibration, monitoring, and correction due to its high susceptibility to sensor drift and biofouling (Wagner *et al.*, 2006). The Kelapa Dua Station had a serious problem with nitrate, unlike the Manggarai Station, which had a much smaller RV value than the other measures (Fig. 6). This indicates that the nitrate sensor itself may be problematic, such as interference with the sensor, detection limits or installation problems, despite good performance of the other metrics. These findings align with the high-frequency monitoring study by Rozemeijer *et al.* (2025), which demonstrated that nutrient sensors demand more stringent maintenance and calibration due to their susceptibility to intricate measurement methodologies and fluctuating environmental conditions. At the Empang Dam, the RV values were more consistent than at Kelapa Dua and Kali Sabi. The majority of parameters were inside the valid range, although the total data was not zero, and the stability level was low. Kali Sabi showed the most substantial validity problems for COD, BOD and conductivity measurements. The low validity of COD and BOD is important as they are the major indicators of organic pollution load. The real-time variations in the organic pollution load cannot be reliably captured by the system due to the inherent measurement limitations of COD and BOD proxies. Consequently, readings exceeding these operational thresholds are typically attributable to sensor error, drift, or extreme hydrological conditions. Observations exceeding regulatory water quality thresholds are not automatically considered invalid. If the observations remain within the instrument's physical and specific measurement range, they are still considered valid because they may represent a true pollution event. Regulatory violations are assessed separately as environmental compliance issues, not as data validity filters, requiring further investigation and appropriate management responses when necessary.

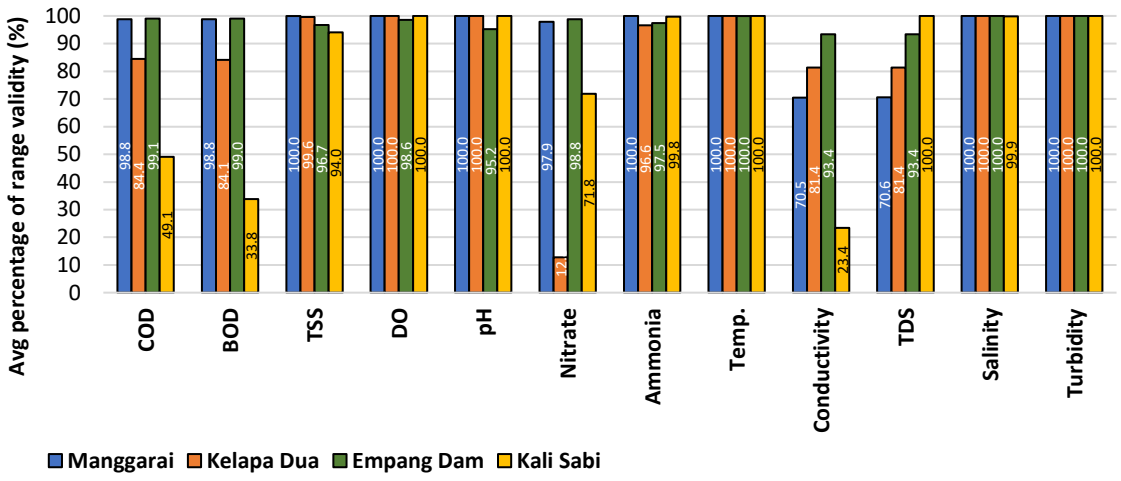

Fig. 6: Percentage of range validity data at the four stations

Stability index (SI)

The SI results reveal marked differences in temporal behavior among stations (Fig. 7) Manggarai was the most stable for COD, BOD, DO, pH, and turbidity, but ammonia, conductivity, TDS, and salinity remained less reliable. Kelapa Dua station exhibited moderate-to-high parameter stability overall, it demonstrated reduced performance regarding TSS and DO. Conversely, the Empang Dam station displayed the most widespread instability, most notably for DO, pH, and nitrate, while the Kali Sabi station was characterized by pronounced fluctuations in pH and temperature. This is in agreement with Shaughnessy *et al*. (2019), who pointed out that data from continuous monitoring of water quality often needs to be fixed to account for sensor drift and fouling before it can be analyzed fully. Rinn *et al*. (2025) confirmed fouling and drift to be especially problematic for nutrient and electrochemical sensors. These results are in line with those of Wagner *et al*. (2006), which showed that the ORWQM system is sensitive to field disturbances, such as sensor contamination, response shifts, calibration errors, and operational disruptions, which can all affect the stability and reliability of the data. Importantly, SI values serve as diagnostic indicators requiring secondary validation, rather than functioning as definitive metrics of operational failure.

Accuracy

Accuracy was assessed by comparing sensor data with manual measurements reported by KLH, although the limited number of paired observations restricts the robustness of the results. At Manggarai Station, pH and temperature demonstrated the highest alignment with reference values, yielding relative accuracy scores of approximately 88–99% alongside minimal absolute errors. These percentages represent relative accuracy, not MAE. Future studies should use more frequent, synchronized sensor and laboratory measurements across different seasons and hydrological conditions. Consistent with USGS guidance, continuous sensor data should also undergo field verification, cleaning, calibration, correction, and quality review before being used for water-quality interpretation (Wagner *et al.*, 2006). A comparison of online sensor data and manual reference measurements at the Kelapa Dua station reveals persistent, moderate-to-high deviations (ranging from 12% to 85%) across key water quality parameters, including COD, BOD, TSS, pH, temperature, and TDS. Such practice is common in ORWQM as data

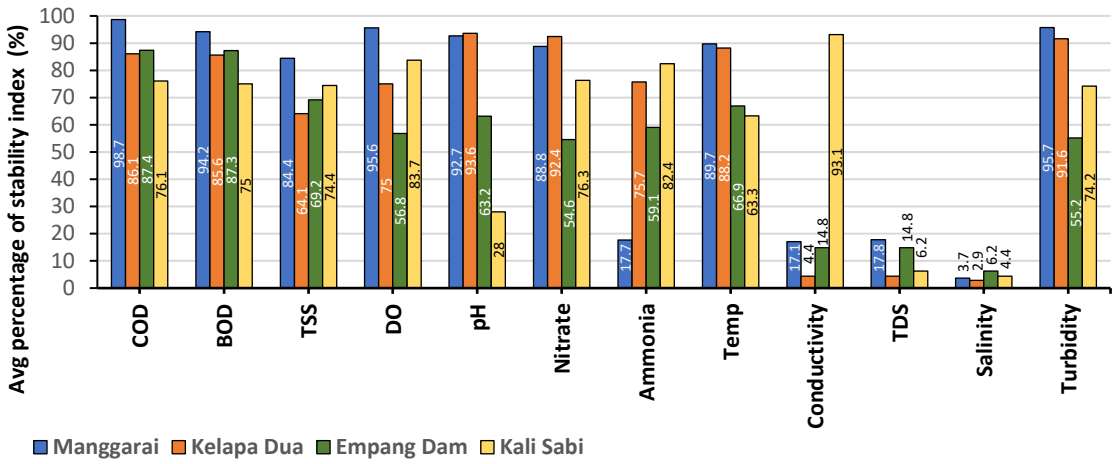

Fig. 7: Percentage of stability Index at the four stations

masking does not work when sensors are tuned off or connection drops out (Teh *et al.*, 2020). The relative accuracy scores at Kali Sabi Station show a wide range in sensor data accuracy over the test period, likely due to sensor instability and technical issues related to the field. Studies on IoT-based water quality monitoring suggest that while real-time systems can improve monitoring efficiency, the accuracy largely relies on the quality of sensors, the design of the system, and the validation of data using reference measurements (Budiarti *et al.*, 2019). The limitations of sparse manual calibration data highlight the need for future studies to employ high-frequency, synchronized sensor and laboratory monitoring across a broader range of seasonal and hydrological regimes. The data-quality metrics identify anomalies but cannot confirm their causes because diagnostic, maintenance, power, communication, and field records were incomplete. Thus, technical failures are treated as plausible explanations alongside environmental variability, sensor resolution, sampling differences, laboratory uncertainty, and data processing. Station-specific discrepancies are likely attributable to interacting environmental, technical, and operational dynamics; consequently, the analysis prioritizes localized, parameter-specific patterns over simple metrics of data availability.

Evaluation of system performance

System performance was assessed through 20 KPIs covering technical, institutional, social, economic, and environmental dimensions (Fig. 8). The indicators were derived from literature and policy review, stakeholder interviews, and empirical findings from the four stations. This structure shifts the assessment from a narrow evaluation of sensor operation to an evaluation of whether the monitoring system can produce credible information, sustain operations, coordinate institutional action, engage users, and contribute to pollution control. Accordingly, technical QA/QC is evaluated as merely one dimension of system performance, rather than being disproportionately cited as the primary driver of operational limitations. A clear process is required for the high frequency water quality detection in terms of data collection, sensor selection, sensor condition maintenance, sensor calibration and data processing

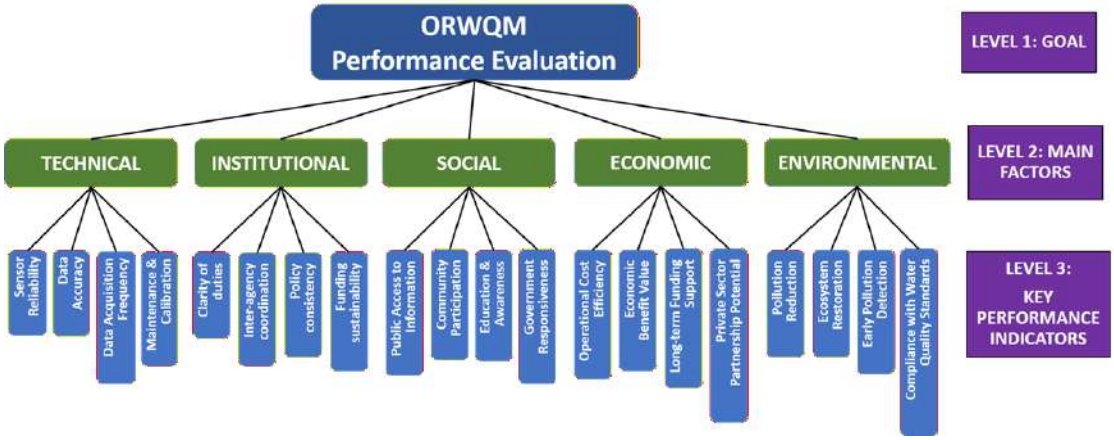

Fig. 8: Hierarchy of ORWQM system performance

(Rozemeijer *et al*., 2025). Calibration, sensor checks, metadata, and quality control are also emphasized to ensure data reliability, as in real-time quality assurance/quality control (QA/QC) systems such as quality assurance/quality control of real-time oceanographic data (QARTOD) (Bushnell *et al*., 2020). Technical indicators include sensor reliability, data accuracy, frequency of data collection, and maintenance and calibration. These four are critical for sensor monitoring reliant systems because water quality instrumentation is highly susceptible to calibration drift, telemetry failures, biofouling, and measurement inaccuracies in the absence of routine maintenance. Reliable real-time data are used worldwide to ensure and control quality, to carry out calibration checks and to validate the data against reference standards or field measurements (Wagner *et al*., 2000). Institutional indicators include unambiguous duties, inter-agency coordination, policy consistency and sustainable funding. These are critical because the success of an ORWQM system depends to a large extent on the relationships between the technical operators, data owners, decision makers and pollution response units. This is consistent with the Organization for Economic Co-operation and Development (OECD) principles on water governance, which designate role clarity, policy coherence, data sharing, financial sustainability, and stakeholder engagement as the structural pillars of effective water resource management (OECD, 2015). Other important social indicators include public access to information, community involvement, education and awareness, and government responsiveness. United Nation-Water (UN-Water) underscores that data transparency and public involvement are vital for water quality improvement, noting that citizen science simultaneously enhances community capacity and strengthens environmental monitoring efforts (UN-Water, 2011; Domínguez-Rendón *et al*., 2024).

Priority weight analysis using the AHP method

The results of the AHP analysis involving 15 sources from various stakeholders showed that environmental variables received the highest weight (0.3174), institutional variables were the second priority (0.208), and technical variables were the third priority (0.2000). The economic dimension (0.1520) underscored the critical importance of cost efficiency and long-term financial sustainability. Similarly, the social dimension (0.1226) yielded a significant contribution, albeit with a marginally lower overall weight. Based on the variable weights above, the maximum eigenvalue is λ_{max} = 5.4199. Based on formula (6) with five factors and the λ_{max} value, a value of 0.01049 was obtained. The random index

(RI) value obtained from the table provided by Saaty (2004) was 1.12 for 7 variables. The consistency ratio (CR) value calculated based on Eq. 8 was 0.00937 or 0.937%, which is much lower than the 10% threshold, indicating acceptable consistency, so the weights given are appropriate for performance assessment. The trend suggests that the experts attach more importance to environmental performance than tool functionality. They say that real-time monitoring should help to detect pollution early, improve the response, and comply with the standards. Water quality data is vital for facilitating early warning systems and rapid response protocols, thereby mitigating both environmental and health risks (UNEP, 2024). The relative significance of environmental parameters in AHP results supports the use of ORWQM as a pollution control tool, rather than a data logging system. The results of the aggregation of the expert pairwise comparison assessments are presented in Table 4.

Priority indicators of each dimension

In terms of technical aspects, data accuracy was the most weighted aspect (42.1%) followed by sensor maintenance and calibration (25.4%), sensor reliability (21.1%) and data collection frequency (11.4%). Findings indicate that experts prioritize the quality and reliability of transmitted data over its sheer volume. This preference aligns with international real-time monitoring standards, which identify calibration, sensor inspection and quality control protocols as essential prerequisites for valid data analysis and decision making (Bushnell *et al*., 2020; Rozemeijer *et al*., 2025). High-frequency data do not inherently reflect high quality or strong performance, particularly when compromised by anomalies, systematic shifts, or a lack of reference validation. Institutionally, policy consistency ranked highest (35.4%), followed by funding sustainability (30.8%), inter-agency coordination (20.3%), and task clarity (13.4%), supporting OECD principles on coherent policies, clear roles, adequate funding, and effective evaluation. Social priorities were education and awareness (35.0%), public participation (26.3%), government responsiveness (24.6%), and information access (14.0%). Despite receiving the lowest weight, public accessibility remains vital for ensuring transparency and facilitating collective action (Domínguez-Rendón *et al*., 2024). Economically, long-term funding (36.1%) was prioritized over economic benefits (30.0%), private partnerships (21.1%), and cost efficiency (12.9%), indicating that sustainable financing should cover capital, operational, and maintenance needs without weakening system functions. Environmentally, compliance with water quality standards ranked highest (29.0%), followed by pollution reduction (28.0%), early detection (22.9%), and ecosystem restoration (20.3%), confirming ORWQM's role in supporting water quality management.

Overall indicator weight priorities

The indicators with the highest global weights were compliance with quality standards (9.2%), pollution reduction (8.9%), data accuracy (8.4%), policy consistency (7.4%), and early pollution detection (7.3%). These priorities establish a logical framework wherein empirical accuracy and coherent policy design collectively facilitate early anomaly detection, regulatory compliance, and subsequent pollution mitigation. The model therefore extends beyond monitoring inputs and processes by linking ORWQM performance to environmental outcomes and response-based action. This supports the use of integrated dashboards, data validation, pollution-response SOPs, and cross-agency reporting mechanisms for timely decision making, effective stakeholder coordination, and continuous improvement. Despite receiving lower weights in the evaluation, public information accessibility and operational cost-efficiency remain indispensable supporting conditions for fostering transparency, accountability, stakeholder acceptance, and long-term system sustainability across diverse institutional, environmental, governance, and community implementation contexts.

Table 4: Geometric mean of pairwise comparisons

Indicators	Technical	Institutional	Social	Economic	Environmental
Technical	1	0.9130	1.7286	1.2080	0.6919
Institutional	1.0953	1	2.4042	1.3638	0.5490
Social	0.5785	0.4159	1	0.7408	0.4693
Economic	0.8278	0.7333	1.3498	1	0.4219
Environmental	1.4453	1.8215	2.1307	2.3700	1

System performance index (PI)

The actual scores of the 20 indicators were assessed on a 0–100 scale, converted to performance scores of 1–4, and multiplied by their respective global AHP weights. The weighted indicator scores were then aggregated to obtain the overall ORWQM system performance index (PI). The resulting PI was 2.447 on a 0–4 scale, equivalent to 61.181%, placing the system in the "adequate" category. This result indicates that the system is operational but still requires improvement to achieve a higher level of effectiveness. The index should be interpreted as a diagnostic measure of the gap between indicator priorities and actual operational performance rather than as a stand-alone value (Nardo *et al*., 2005; OECD, 2008). At the aspect level, the technical aspect achieved the highest performance index (2.847), followed by the institutional (2.797), economic (2.576), environmental (2.527), and social aspects (1.380). Thus, technical and institutional performance was relatively stronger, while the social aspect showed the largest performance gap. However, the environmental and economic aspects contributed the most to the overall PI, with weighted scores of 0.714 and 0.701, respectively, because of their higher aspect weights. These findings confirm that the overall index reflects both the relative importance and actual performance of the technical, institutional, social, economic, and environmental dimensions (Vilanova *et al*., 2015; Sakai, 2024). Tables 5 and 6 present the indicator-level calculations and their aggregation into the overall System PI. Collectively, these dimensions yield an overall System PI of 2.447 on a 0–4 scale, corresponding to an efficiency level of 61.181%.

Studies on the implementation of the OECD water governance indicator framework at the local level have also shown that problems are often located not only in regulations or institutions but also in the implementation of operational instruments (Akhmouch and Clavreul, 2016; OECD, 2018). Within the ORWQM framework, the utility of dashboard data is maximized when coupled with defined operational pathways, including field verification, early warning notifications, systematic incident reporting and rapid responses to localized pollution sources. The lowest score was in the social aspect with an index of 1.380. This value shows that the benefits of the system have not yet been fully reached the community; users of information and actors in environmental monitoring. Citizen science initiatives in water quality monitoring have been shown to build community capacity and raise ecological literacy; however, their ability to drive governance accountability is highly contingent upon robust information accessibility and prompt regulatory action (Tsatsaros *et al*., 2021; Domínguez-Rendón *et al*., 2024) and these results are in line with that literature. The low social index indicates the need to transform the dashboard from a data platform into a tool for risk communication, environmental education, a complaint channel and a collaborative medium between the government, river communities, schools, universities and environmental NGOs. Despite secure long-term economic benefits and funding, cost-efficiency and private-sector synergy require further cultivation. This is consistent with OECD guidelines asserting that sound financing and budgeting are fundamental to the sustainable governance of water policies and the lifecycle

Table 5: AHP weight and performance score of the ORWQM indicators

Aspect	Indicator	Local weight	Global weight	Actual score	Performance score (1–4)	Weighted score
Technical	Sensor reliability	0.209	0.034	82	3	0.102
Technical	Data accuracy	0.419	0.068	78	3	0.204
Technical	Data acquisition frequency	0.11	0.018	95	4	0.071
Technical	Maintenance and calibration	0.263	0.043	65	2	0.085
Institutional	Clarity of duties	0.134	0.017	75	3	0.051
Institutional	Inter-agency coordination	0.203	0.026	65	2	0.052
Institutional	Policy consistency	0.354	0.045	75	3	0.135
Institutional	Funding sustainability	0.308	0.039	80	3	0.117
Social	Public access to information	0.139	0.022	60	2	0.044
Social	Community participation	0.255	0.04	55	1	0.04
Social	Education and awareness	0.365	0.057	50	1	0.057
Social	Government responsiveness	0.241	0.038	65	2	0.075
Economic	Operational cost efficiency	0.194	0.053	70	2	0.106
Economic	Economic benefit value	0.297	0.081	75	3	0.243
Economic	Long-term funding support	0.279	0.076	75	3	0.228
Economic	Private-sector partnership potential	0.229	0.062	65	2	0.125
Environmental	Pollution reduction	0.262	0.074	70	2	0.148
Environmental	Ecosystem restoration	0.211	0.06	65	2	0.12
Environmental	Early pollution detection	0.244	0.069	75	3	0.207
Environmental	Compliance with water-quality standards	0.283	0.08	78	3	0.24

Table 6: Aspect-level performance and overall ORWQM system PI

Aspect	Aspect weight	Weighted aspect score	Aspect performance index (0-4)
Technical	0,162	0,462	2,847
Institutional	0,127	0,355	2,797
Social	0,157	0,216	1,380
Economic	0,272	0,701	2,576
Environmental	0,283	0,714	2,527
System PI (0–4)	1,000		2,447
System PI (%)			61,181

management of infrastructure (OECD, 2018). Strengths are early detection and compliance with quality standards in the environmental sector but ecosystem restoration and pollution reduction need to be more integrated with source control programmes. Studies on real-time monitoring show that ORWQM systems can aid in early warning and rapid action against pollution concerns (Hou *et al*., 2014; Zhang *et al*., 2020; Saleh and Stanley, 2023). In summary, performance evaluation results highlight five overarching priorities for system improvement: (1) improving the quality of QA/QC, calibration and sensor maintenance; (2) aligning policies and division of tasks between agencies; (3) ensuring funding for long-term operations and maintenance; (4) expanding public access, data literacy and community engagement; and (5) integrating ORWQM data with oversight mechanisms, law enforcement and ecosystem restoration.

Conceptual model design of inclusive governance-based ORWQM

The conceptual model design was developed using SSM through field observations, surveys of communities living around the stations and semi-structured interviews with 23 informants representing government, community, academics / researchers, vendors, NGOs/river communities and the media. The SSM findings revealed three main challenges in managing ORWQM. Primarily, data quality requires further refinement; while sensors deliver continuous real-time streams, a subset of the generated data fails to satisfy established validity criteria. Calibration,

validation, technical interpretation, QA and QC are required. Second, the response to the pollution indication is not uniform and the rapid action procedures, field verification and source tracing are not always timely. Third, collaboration remains absent in governance because coordination among KLH, DLH, BBWS, vendors, academics, communities, and the media has not been integrated into a mechanism to ensure system sustainability. This directly contradicts QARTOD guidelines, which stress that rigorous quality control testing, sensor management, and the active involvement of qualified scientific, technical, and data management personnel are essential to ensure sensor data integrity in decision-making processes (Bushnell *et al.,* 2020). Based on the results of the rich picture (Fig. 9) and CATWOE analysis, a root definition was obtained that describes a human activity system involving the KLH, the DLH, BBWS, academics, vendors, the public, river communities, and the media to transform ORWQM sensor data into valid, easily accessible, and actionable water quality information to strengthen river water pollution control in a fast, transparent, collaborative, and sustainable manner. refines the overarching root definition into three constituent sub-root definitions, specifically focusing on strengthening national governance, maximizing technical system and rapid response capabilities, and fostering public participation and empowerment. The overall formulation is reduced to three interrelated conceptual models. The first conceptual model focuses on improving national governance and policy frameworks to address fragmented authority, inadequate inter-agency coordination, and inconsistent data standards and SOPs. Here, the KLH is the national policy maker and data manager. The DLH implements and uses regional data, the BBWS coordinates river and infrastructure management, and the National Development Planning Agency (BAPPENAS) supports funding and integration in development plans. This methodology aligns with the OECD (2015) framework, which conceptualizes water governance as a multi-level system integrating policies, institutions, instruments, financing, and accountability mechanisms. The second conceptual model is on the effectiveness of technical systems, maintenance and rapid response to link the real-time data and pollution control measures. The third conceptual model highlights community empowerment and multi-stakeholder collaboration, which enables data transparency and social support to sustain the system. Surveys near ORWQM stations demonstrate that broad public support coexists with limited community understanding of station functions, with most residents receiving only direct water quality data. A study by Domínguez-Rendón *et al*. (2024) found that community participation in water quality monitoring can empower community organizations or NGOs to improve data collection and reporting, environmental literacy, and bridge the gap between policymakers and citizens affected by pollution. These three models together form an inclusive governance-based ORWQM management framework (Fig. 10). This framework uses data quality analysis as a technical diagnosis, KPI-AHP results as the basis for prioritizing performance improvements, and SSM as the basis for developing practical institutional changes through collaborative stakeholder engagement processes. The workflow systematically advances from data quality validation to a KPI-AHP-based performance evaluation, culminating in conceptual modeling and the subsequent execution of the inclusive governance framework. This approach extends previous studies (Behmel *et al*., 2016; Li *et al*., 2018; Faybishenko *et al*., 2022; Mansouri *et al*., 2023) which primarily focused on the technical aspects of tools and data collection, emphasizing the importance of good data, responsive systems, well-coordinated institutions, and public engagement. This integration is expected to lead to evidence-based ORWQM management, efficient pollution control, river ecosystem protection, and adaptive, accountable, and sustainable governance. The proposed model

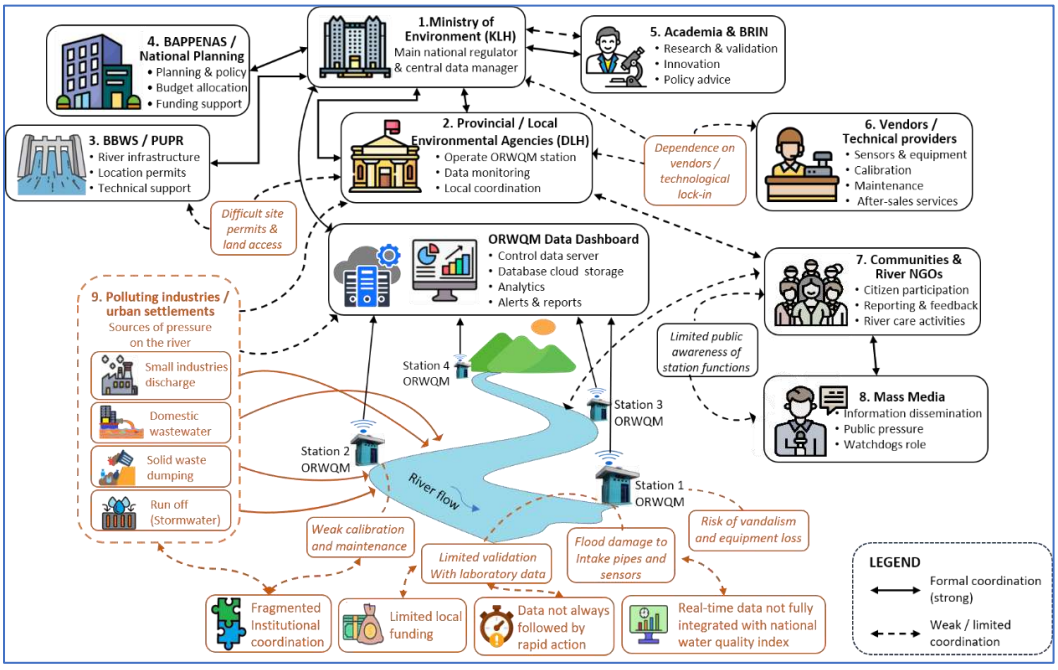

Fig. 9: Rich picture

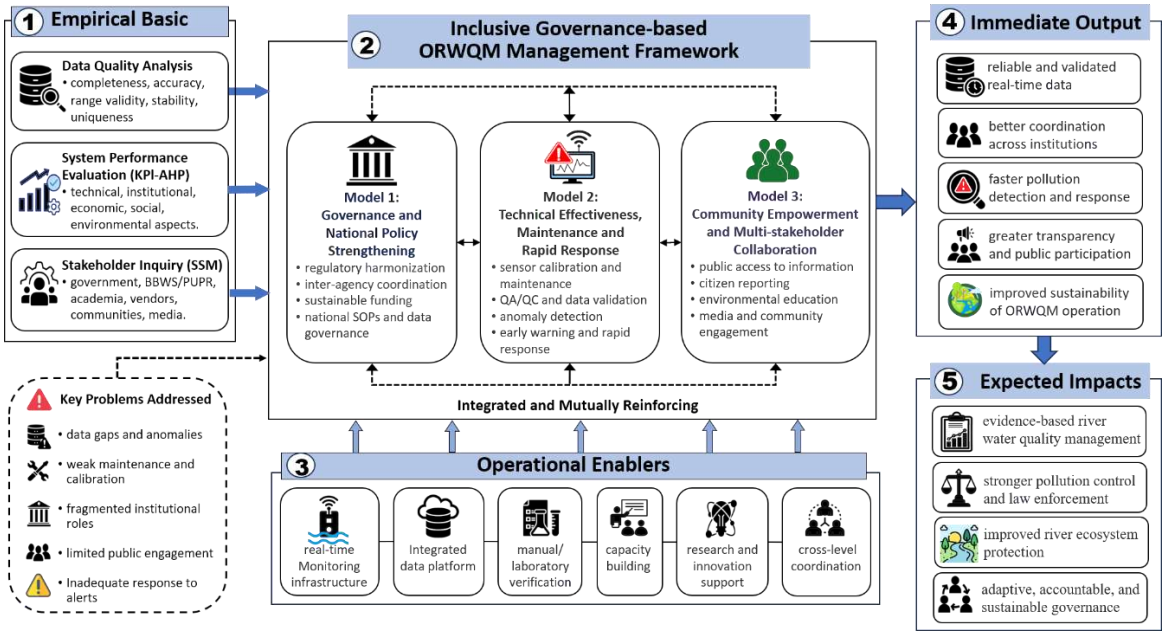

Fig. 10: Integrated ORWQM management framework based on inclusive governance

contends that the policy utility of real-time data is strictly contingent upon satisfying three core criteria: technical validity, institutional responsiveness, and public accessibility. Data without validation and calibration is vulnerable to misinterpretation. In the absence of SOPs for rapid response, the collected data risk becoming merely passive digital archives rather than tools for active

intervention. Systems lose social legitimacy without transparency and public participation. The inclusive governance-based ORWQM framework bridges technical data analytics, KPI-AHP-derived improvement priorities, and the overarching demand for a transparent, adaptive, and sustainable river management paradigm. This proposed ORWQM framework based on inclusive governance serves as a bridge between the results of technical data analysis, improvement priorities through KPI-AHP, and the need for a more transparent, adaptive, and sustainable river management model.

Limitations and future research

This study has several limitations that should be considered when interpreting the findings. First, the four ORWQM stations were purposively selected to represent contrasting upstream–downstream and urban–industrial gradients across the Ciliwung and Cisadane watersheds. Consequently, the findings offer analytical transferability rather than statistical generalizability to the broader network of ORWQM stations in Indonesia. Second, variable data coverage across stations and a modest number of paired validation samples limits the evaluation of long-term sensor reliability. This constraint risks failing to account for parameter-specific bias, sensor calibration drift, or temporal and environmental discrepancies during sample collection. Third, the KPI–AHP results depend on expert judgment and may be influenced by the composition and perspectives of the expert panel, while the composite PI may vary under alternative normalization, weighting, and aggregation procedures. Fourth, stakeholder recruitment was purposive, and the community survey relied on self-reported data, the study is subject to potential selection, recall, and social desirability biases. Fifth, the SSM findings are context-specific because they reflect the institutional arrangements, stakeholder relationships, and governance conditions of the two studied watersheds. Finally, a key limitation of this study is that the proposed framework has yet to undergo prospective evaluation through longitudinal implementation or external validation across alternative watersheds. Future research should therefore expand the number and diversity of stations, increase the frequency of laboratory comparisons, examine alternative index-construction scenarios, include broader stakeholder groups, and evaluate the framework prospectively across different watershed contexts.

CONCLUSION

This multiple case study aims to understand the ORWQM conditions at four stations with different upstream-downstream characteristics, urbanization, and industrial influences in the Ciliwung-Cisadane watershed. Therefore, the performance results at each station cannot be statistically generalized to all ORWQM stations in Indonesia. This study proposes an inclusive governance-based ORWQM management framework that systematically integrates data quality evaluation, system performance assessment, and multi-stakeholder governance. The results reveal that successful ORWQM implementation requires more than technological infrastructure and real-time data; it demands rigorous data quality, operational dependability, robust institutional coordination, long-term financial viability, data transparency, and stakeholder engagement. Thus, ORWQM needs to be understood as a socio-technical system that connects data, institutions, decision-making, and pollution control. Data quality evaluation indicates that data completeness at the four stations is generally high, but some data still require validation due to zero values, negative anomalies, low validity ranges, and uneven stability. These conditions are potentially attributable to environmental influences and technical anomalies, such as biofouling, sensor drift, power instability, or data transmission failures. These findings emphasize that completeness alone is insufficient to describe data quality, as numerically complete data can be pseudo-

complete if they are not valid, stable, or accurate. The system evaluation results indicate that the ORWQM composite PI falls within the 'good' threshold; however, the underlying weighting framework heavily prioritizes institutional aspects, followed by technical and economic considerations. This indicates that performance improvements are not solely achieved through sensor device improvements but also require institutional strengthening, clarity of authority, coordination between actors, improved operating procedures, data interoperability, follow-up mechanisms, and sustainable maintenance funding. The SSM synthesis yielded a conceptual model of ORWQM governance that integrates policies, real-time monitoring systems, early warning, rapid response, and public participation. This model fortifies the cooperative capacity of pentahelix stakeholders encompassing government bodies, academia, private sector vendors, the public or NGOs, and the media to promote transparency, accountability, mutual oversight, and rapid response to potential pollution indications. Converting raw data into validated and accessible information is expected to support more coordinated decision-making, although this benefit was not tested in this study. The main contribution of this study lies in the development of a conceptual framework that synthesizes data quality, system performance, and inclusive governance into a unified ORWQM management model. While this framework possesses the potential to facilitate early detection, rapid incident response, regulatory compliance, inter-institutional coordination, and evidence-based policymaking, its operational effectiveness, feasibility, and implementation outcomes remain unexamined under diverse environmental and institutional conditions through practical field applications. Application to other watersheds requires further adaptation and validation based on local hydrological conditions, monitoring infrastructure, data availability, institutional capacity, regulations, and stakeholder characteristics.

AUTHOR CONTRIBUTIONS

S. Yudo, the corresponding author, conducted the investigation, comprehensive analysis, literature review, and manuscript preparation. D.N. Martono conducted the selection and review of the methodology used. D. Sutjiningsih were involved in the conceptualization and review of the manuscript; B. Kurniawan supervised the writing process. All authors read and approved the final manuscript.

ACKNOWLEDGEMENT

This study was supported by internal funding [No. 3/III.5/HK/2025] from the Research Organization for Life Sciences and Environmental, National Research and Innovation Agency, Indonesia

CONFLICT OF INTEREST

The authors declare that there is no conflict of interest regarding the publication of this manuscript. In addition, the ethical issues, including plagiarism, informed consent, misconduct, data fabrication and/or falsification, double publication and/or submission, and redundancy, have been completely observed by the authors.

OPEN ACCESS

©2026 The author(s). This article is licensed under a Creative Commons Attribution 4.0 International License, which permits use, sharing, adaptation, distribution, and reproduction in any medium or format, as long as you give appropriate credit to the original author(s) and the source, provide a link to the Creative Commons license, and indicate if changes were made. The images or other third-party material in this article are included in the article's Creative Commons license, unless indicated otherwise in a credit line to the material. If material is not included in the article's Creative Commons license and your intended use is not permitted by statutory regulation or exceeds the permitted use, you will

need to obtain permission directly from the copyright holder. To view a copy of this license, visit: http://creativecommons.org/licenses/by/4.0/

PUBLISHER'S NOTE

GJESM Publisher remains neutral with regard to jurisdictional claims in published maps and institutional affiliations.

POSTIVE AI STATEMENT

During the preparation of this work, the author(s) have used Artificial Intelligence (AI), Grammarly, in order to correct grammatical errors, suggest corrections, and reduce typos. After using this tool/service, the authors reviewed and edited the content as needed and take full responsibility for the content of the publication.

ABBREVIATIONS

%	Percent
3E	Efficacy, efficiency, effectiveness
°C	Degree Celcius
AHP	Analytic hierarchy process
BAPPENAS	Badan Perencanaan Pembangunan Nasional (National Development Planning Agency)
BBWS	Balai Besar Wilayah Sungai (River Basin Organization)
BOD	*Biochemical oxygen demand*
BPDAS	Balai Pengelola Daerah Aliran Sungai (Watersheds Management Center)
CATWOE	Customers, actors,
CI	Completeness index
COD	Chemical oxygen demand
CR	Consistency ratio
DAS	Daerah aliran sungai
DLH	Dinas Lingkungan Hidup
DO	*Dissolved oxygen*
EWS	Early warning system
KLH	Kementerian Lingkungan Hidup
KLHK	Kementerian Lingkungan Hidup dan Kehutanan (Ministry of Environment and Forestry)
KPI	Key performance indicator
LCD	Liquid crystal display
MAE	Mean absolute error
mg/L	Milligram per liter
µS/cm	MicroSiemens per centimeter
NGOs	Non-governmental organizations
O&M	Operation and maintenance
NTU	Nephelometric turbidity unit
ODQEM	Online data quality evaluation management
OECD	Organization for economic co-operation and development
ORP	Oxidation reduction potential
ORWQM	Online river water quality monitoring
pH	Potential of hydrogen
PI	Performance index
PQR	P (What) Q (How) R (Why)
QA/QC	Quality assurance/quality control
QARTOD	Quality assurance/quality control of real-time oceanographic data
RV	Range validity
SDGs	Sustainable development goals
SI	Stability index
SOP	Standard operating procedure
SSM	Soft systems methodology
TDQM	Total data quality management
TDS	Total dissolved solids
TSS	Total suspended solids
UN	United nation
UNEP	United Nations Environment Programme
UQ	Uniqueness
USGS	United States Geological Survey
WHO	World Health Organization

REFERENCES

Adu-Manu, K.S.; Katsriku, F.A.; Abdulai, J.D.; Engmann, F., (2020). Smart River Monitoring Using Wireless Sensor Networks. Wireless Commun. Mobile Comput., 1-19 **(19 pages).**

Akhmouch, A.; Clavreul, D., (2016). Stakeholder engagement for inclusive water governance: "practicing what we preach" with the OECD water governance initiative. Water. 8(5): 204: 1–17 **(17 pages).**

Barcelo-Ordinas, J.M.; Doudou, M.; García-Vidal, J.; Badache, N., (2019). Self-calibration methods for uncontrolled environments in sensor networks: a reference survey. Ad Hoc Networks, 88: 142–159 **(18 pages).**

Batini, C.; Scannapieco, M., (2016). Data and information quality: dimensions, principles and techniques. Springer International Publication.

Basuki, T.M.; Indrawati, D.R.; Nugroho, H.Y.S.H.; Pramono, I.B.; Setiawan, O.; Nugroho, N.P.; Nada, F.M.H.; .Nandini, R.; Savitri, E.; Adi, R.N.;

Purwanto; Sartohadi, J., (2024). Water pollution of some major rivers in Indonesia: The status, institution, regulation, and recommendation for its mitigation. Pol. J. Environ. Stud., 33(4): 3515-3530 **(16 pages).**

Behmel, S.; Damour, M.; Ludwig, R.; Rodríguez, M.J., (2018). Participative approach to elicit water quality monitoring needs from stakeholder groups–An application of integrated watershed management. J. Environ. Manage., 218: 540–554 **(15 pages).**

Behmel, S.; Damour, M.; Ludwig, R.; Rodríguez, M.J., (2016). Water quality monitoring strategies: a review and future perspectives. Sci. Total Environ., 571: 1312–1329 **(18 pages)**.

Budiarti, R.P.N.; Tjahjono, A.; Hariadi, M.; Purnomo, M.H., (2019). Development of IoT for automated water quality monitoring system. In 2019 International Conference on Computer Science, Information Technology, and Electrical Engineering, (ICOMITEE). IEEE: 211-216 (**6 pages).**

Buelvas, J.; Múnera, D.; Tobón, V.D.P.; Aguirre, J.; Gaviria, N., (2023). Data quality in IoT-based air quality monitoring systems: a systematic mapping study. Water Air Soil Pollut., 234(4): 1–23 **(23 pages).**

Bushnell, M.; Bailey, K.; Bosch, J.; Burger, E.; Dorton, J.; Easley, R.; Heitsenrether, B.; King, J.; Grissom, K.; Tamburri, M.; Thomas, J.; Waldmann, C., (2020). QARTOD-prospects for real-time quality control manuals, how to create them, and a vision for advanced implementation. IOOS. 1–22 **(22 pages).**

Carvalho, L.; Mackay, E.B.; Cardoso, A.C.; Baattrup-Pedersen, A.; Birk, S.; Blackstock, K.L.; Borics, G.; Borja, A.; Feld, C.K.; Ferreira, M.T.; Globevnik, L.; Grizzetti, B.; Hendry, S.; Hering, D.; Kelly, M.; Langaas, S.; Meissner, K.; Panagopoulos, Y.; Penning, E.; Rouillard, J.; Sabater, S.; Schmedtje, U.; Spears, B.M.; Venohr, M.; van de Bund, W.; Solheim, A.L., (2019). Protecting and restoring Europe's waters: an analysis of the future development needs of the Water Framework Directive. Sci. Total Environ., 658: 1228–1238 **(11 pages)**.

Cao, H.; Zhang, L.; Qi, Y.; Yang, Z.; Li, X.; (2022). Government auditing and environmental governance: Evidence from China's auditing system reform. Environ. Impact Assess. Rev., 93: 106705: 1-10 **(10 pages).**

Checkland, P.; Poulter, J., (2020). Soft systems methodology. In Systems approaches to making change: A practical guide (pp. 201-253). London: Springer London.

Chen, S.S.; Kimirei, I.A.; Yu, C.; Shen, Q.; Gao, Q., (2022). Assessment of urban river water pollution with urbanization in East Africa. Environ. Sci. Pollut. Res., 29(27): 40812–40825 **(14 pages).**

Debnath, A.; Singh, P.K.; Sharma, Y.C., (2021). Metallic contamination of global river sediments and latest developments for their remediation. J. Environ. Manage., 298: 113378: 1–20 **(20 pages)**.

Domínguez-Rendón, E.; Villada-Canela, M.; Muñoz-Pizza, D.M., (2024). Community strengthening through citizen monitoring of water quality: A systematic review. Plos One. 19(7): e0305723: 1–21 **(21 pages).**

Dong, L.; Wang, Z.; Zhou, Y., (2023). Public participation and the effect of environmental governance in China: A systematic review and meta-analysis. Sustainability. 15(5): 4442: 1-16 **(16 pages).**

Egidio, E.; Mancini, S.; De Luca, D.A.; Lasagna, M., (2022). The impact of climate change on groundwater temperature of the Piedmont plain (NW Italy). Water. 14: 1–16 **(16 pages).**

Ehrlinger, L.; Wöß, W., (2022). A survey of data quality measurement and monitoring tools. In frontiers in big data (Vol. 5). Front. Media S.A. 1-30 **(30 pages).**

Farouk, M.I.H.Z.; Jamil, Z.; Latip, M.F.A., (2023). Towards online surface water quality monitoring technology: A review. Environ. Res., 238: 1-11 **(11 pages).**

Faybishenko, B.; Versteeg, R.; Pastorello, G.; Dwivedi, D.; Varadharajan, C.; Agarwal, D., (2022). Challenging problems of quality assurance and quality control (QA/QC) of meteorological time series data. Stochastic Environ. Res. Risk Assess., 1–14 **(14 pages).**

Gupta, A.; Boas, I.; Oosterveer, P., (2020). Transparency in global sustainability governance: to what effect?. J. Environ. Plann. Policy Manage, 22(1): 84-97 **(14 pages).**

Hyndman, R.J.; and Koehler, A.B., (2006). Another look at measures of forecast accuracy. Int. J. Forecas., 22(4): 679-688 **(10 pages).**

Hou, D.; Ge, X.; Huang, P.; Zhang, G.; Loáiciga, H., (2014). A real-time, dynamic early-warning model based on uncertainty analysis and risk assessment for sudden water pollution accidents. Environ. Sci. Pollut. Res., 21(14): 8878-8892 **(15 pages).**

Hardjosoekarto, S., (2012). Soft Systems Methodology (Metodologi Serba Sistem Lunak). Jakarta: Universitas Indonesia Press.

Hwang, C.L.; and Yoon, K., (2012). Multiple attribute decision making: methods and applications a state-of-the-art survey. Springer Science & Business Media.

KLHK, (2024). Laporan kinerja direktorat pengendalian pencemaran air [Performance report of the directorate of water pollution control]. Ministry of Environment and Forestry of the Republic of Indonesia. 1–84 **(84 pages).**

KLHK, (2016). Regulation of the Minister of Environment and Forestry Number P.68/MENLHK/SETJEN/KUM.1/8/2016 concerning Domestic Wastewater Quality Standards

Kremere, E.; Morgan, E.; Obani, P., (2019). SDG6-Clean water and sanitation: balancing the water cycle for sustainable life on earth. Emerald Group Publishing.

Kumar, P.; Masago, Y.; Mishra, B. K.; Jalilov, S.; Rafiei Emam, A.; Kefi, M.; Fukushi, K., (2017). Current assessment and future outlook for water resources considering climate change and a population burst: A case study of Ciliwung River, Jakarta City, Indonesia. Water. 9(6): 410: 1–15 **(15 pages).**

Li, X.T.; Zhai, J.; Zheng, G.F.; Yuan, C.F., (2018). Quality assessment for open government data in China. In Proceedings of the 2018 10th International Conference on Information Management and Engineering. 110–114 **(5 pages).**

Lim, C.H.; Wong, H.L.; Elfithri, R.; Teo, F.Y., (2022). A review of stakeholder engagement in integrated river basin management. Water. 14(19): 1-19 **(19 pages).**

Lo-Iacono-Ferreira, V.G.; Capuz-Rizo, S.F.; Torregrosa-López, J.I., (2018). Key Performance Indicators to optimize the environmental performance of higher education institutions with environmental management system: A case study of Universitat Politecnica de Valencia. J. Cleaner Prod., 178 (2018) 846e865: 846–865 **(20 pages).**

Mansouri, T.; Moghadam, M.R.S.; Monshizadeh, F.; Zareravasan, A., (2023). IoT data quality issues and potential solutions: a literature review. Comput. J., 66(3): 615–625 **(11 pages).**

Mamun, K.A.; Islam, F.R.; Haque, R.; Khan, M.G.M.; Prasad, A.N.; Haqva, H.; Mudliar, R.R.; Mani, F.S., (2019). Smart water quality monitoring system design and KPIs analysis: case sites of Fiji surface water. Sustainability. 11(24): 1–21 **(21 pages).**

Menkes, (2010). Regulation of the Minister of Health of the Republic of Indonesia No. 492 of 2010 concerning drinking water quality requirements.

Nardo, M.; Saisana, M.; Saltelli, A.; Tarantola, S.; Hoffman, A.; and Giovannini, E., (2005). "Handbook on constructing composite indicators: methodology and user guide", OECD Statistics Working Papers, No. 2005/03, OECD Publishing, Paris.

OECD, (2008). Handbook on constructing composite indicators: methodology and user guide. OECD Publishing.

OECD, (2015). OECD principles on water governance. OECD Publishing.

OECD, (2018). Cost-Benefit Analysis and the Environment: Further Developments and Policy Use. OECD Publishing, Paris.

Parmenter, D., (2020). Key performance indicators: developing, implementing, and using winning KPIs. 2nd Edition. John Wiley & Sons, Inc., Hoboken, New Jersey.

PerMen, (2022). Regulation of the Minister of Environment and Forestry Number 2 of 2022 concerning Operational Instructions for the Use of Physical Special Allocation Funds for Assignments in the Environmental and Forestry Sectors for the 2022 Fiscal Year.

Pellerin, B.A.; Stauffer, B.A.; Young, D.A.; Sullivan, D.J.; Bricker, S.B.; Walbridge, M.R.; Clyde, Jr.G.A.; Shaw, D.M., (2016). Emerging tools for continuous nutrient monitoring networks: Sensors advancing science and water resources protection. JAWRA J. Am. Water Resour. Assoc, 52(4): 993-1008 **(16 pages).**

PPRI, (2021). Peraturan Pemerintah Nomor 22 Tahun 2021 tentang Perlindungan, Pengorganisasian, dan Pengelolaan Lingkungan Hidup [Government Regulation Number 22 of 2021 concerning Environmental Protection, Organization, and Management].

Talagala, P.D.; Hyndman, R.J.; Leigh, C.; Mengersen, K.; Smith-Miles K., (2019). A feature-based procedure for detecting technical outliers in water-quality data from in situ sensors. Water Resour. Res., 55: 8547–8568 **(22 pages).**

Ramirez, G.; Fuentes, O.; Tweedie, C.E., (2011). Assessing data quality in a sensor network for environmental monitoring. In 2011 Annual Meeting of the North American Fuzzy Information Processing Society. IEEE: 1–6 **(6 pages).**

Ratolojanahary, R.; Ngouna, R.H.; Medjaher, K.; Junca-Bourié, J.; Dauriac, F.; Sebilo, M., (2019). Model selection to improve multiple imputation for handling high rate missingness in a water quality dataset. Expert Syst. Appl., 131: 299–307. **(9 pages).**

Rajendran, G.B.; Geetha T.; Reddy R.R.; Kandasamy K.K., (2025). Machine learning for river water quality monitoring: assessing seasonal and agricultural influences. Environ. Earth Sci., 84(21): 1–30 **(30 pages).**

Rinn, P.; Boruta, F.; Czermak, P.; Ebrahimi, M., (2025). Fouling control of ion-selective electrodes (ISES) in aquatic and aquacultural environments: a comprehensive review. Sensors, 25(24): 1-37 **(37 pages).**

Rodriguez, R.; Pastorini, M.; Etcheverry, L.; Chreties, C.; Fossati, M.; Castro, A.; Gorgoglione, A., (2021). Water-quality data imputation with a high percentage of missing values: A machine learning approach. Sustainability. 13(11): 1–17 **(17 pages).**

Rojas, J.J.H.; Bonifacio, R.F.A.; Peña, J.M.B.; Leon, D.R.Q.; Peña, C.D.R.; Torres, K.G.P., (2025). Sensors and IoT for water quality monitoring: a systematic review of technologies and field validation. J. Rob. Control. 6(6): 2844–2858 **(15 pages).**

Rozemeijer, J.; Jordan, P.; Hooijboer, A.; Kronvang, B.; Glendell, M.; Hensley, R.; Rinke, K.; Stutter, M.; Bieroza, M.; Turner, R.; Mellander, P.E.; Thorburn, P.; Cassidy, R.; Appels, J.; Ouwerkerk, K.; Rode, M., (2025). Best practice in high-frequency water quality monitoring for improved management and assessment: a novel decision workflow. Environ. Monit. Assess., 197(4): 1–23 **(23 pages).**

Saaty, T.L., (1990). How to make a decision: analytic hierarchy process. European Eur. J. Oper. Res., 48: 9-26 **(17 pages).**

Sakai, H., (2024). Review of research on performance indicators for water utilities. AQUA—Water Infrastruct. Ecosyst. Soc., 73(2): 167-182 **(16 pages).**

Saaty, T.L., (2008). Decision making with the analytic hierarchy process. Int. J. Services Sci., 1(1): 83-98 **(16 pages).**

Saleh, T.; Stanley, M., (2023). Real-time water quality monitoring. Int. Inst. for Sustainable Dev. (IISD): 1-19 **(19 pages).**

Shaughnessy, A.R.; Prener, C.G.; Hasenmueller, E.A., (2019). An R package for correcting continuous water quality monitoring data for drift. Environ. Monit. Assess., 191(7): 1-10 **(10 pages).**

Singh, S.; Rai, S.; Singh, P.; Mishra, V.K., (2022). Real-time water quality monitoring of river ganga (India) using internet of things. Ecol. Inf., 71: 1-15 **(15 pages).**

Singh, V.; Nagpoore, N.K.; Lehri, A., (2020). Monitoring and assessment of pollution load in surface water of River Ganga around Kanpur, India: A study for suitability of this water for different uses. Environ. Technol. Innov., 18: 1–14 **(14 pages).**

Shao, G.P.; and Bishop, I.J., (2025) Citizen science in river monitoring: a systematic literature review of the whys and hows. Front. Environ. Sci. 13: 1-13 **(13 pages).**

Teh, H.Y.; Kempa-Liehr, A.W.; Wang, K.I.K., (2020). Sensor data quality: A systematic review. J. Big Data, 7(1): 1-49 **(49 pages).**

Tsatsaros, J.H.; Bohnet, I.C.; Brodie, J.E.; Valentine, P., (2021). A transdisciplinary approach supports community-led water quality monitoring in river basins adjacent to the Great Barrier Reef, Australia. Mar. Pollut. Bull., 170: 1-11 **(11 pages).**

Triantaphyllou, E., (2000). Multi-criteria decision making methods. In Multi-criteria decision making methods: A comparative study (pp. 5-21). Springer, Boston, MA.

UNEP, (2021). Progress on ambient water quality. Global indicator 6.3.2 updates and acceleration needs. United Nations Environment Programme. 1–64 **(64 pages).**

UNEP, (2024). Progress on ambient water quality: mid-term status of SDG indicator 6.3.2 and acceleration needs, with a special focus on Health. United Nations Environment Programme.

UN-Water, (2011). Water quality: Policy brief. United Nations Water.

Sulistiyowati, E.; Uyun, S., (2024). Participatory water quality monitoring system for the gajahwong river, Yogyakarta City, Indonesia. Engagement: Jurnal Pengabdian Kepada Masyarakat [J. Community Service]. 8(1): 101-116 **(16 pages).**

Vilanova, M.R.N.; Magalhães Filho, P.; Balestieri, J.A.P., (2015). Performance measurement and indicators for water supply management: review and international cases. Renewable Sustainable Energy Rev., 43: 1–12 **(12 pages).**

Wagner, R.J.; Boulger Jr, R.W.; Oblinger, C.J.; Smith, B.A., (2006). Guidelines and standard procedures for continuous water-quality monitors: station operation, record computation, and data reporting (No. 1-D3): 1–51 **(51 pages).**

Wagner, R.J.; Mattraw, H.; Ritz, G.F.; Smith, B.A., (2000). Guidelines and standard procedures for continuous water-quality monitors: site selection, field operation, calibration, record computation, and reporting: USGS Water-Resources Investigations Report 2000-4252, iv: 1-53 **(53 pages).**

Wahjono, H.D., (2016). Penerapan teknologi ORWQM kualitas air untuk DAS prioritas di sungai ciliwung dan sungai cisadane [Implementation of online water quality monitoring technology for priority watersheds in the ciliwung river and cisadane river]. Jurnal Air Indonesia [Indones. Water J.]. 9(1): 63-77 **(15 pages).**

Wahyono, H.D.; and Yudo, S., (2022). Application of AI to filter anomalous data from sensors in an online water quality monitoring system. In international conference on sustainable environment, agriculture and tourism (ICOSEAT 2022), Atlantis Press. 623–631 **(9 pages).**

Wahyono, H.D.; Santoso, A.D.; Goh, G.G.G.; Setiaji, G.; Salim, M.A.; Kustianto, I.; Alhasa, K.M.; Yudo, S.; Sudinda, T., (2026). An integrated real-time water quality monitoring system for sustainable management in tropical reservoirs. Global J. Environ. Sci. Manage. 12(2): 873–896 **(24 pages).**

Wang, R.Y.; Strong, D.M., (1996). Beyond accuracy: What data quality means to data consumers. J. Manag. Inf. Syst., 12(4): 5–34 **(30 pages).**

World Bank, (2017). World Development Report 2017: Governance and the law, World Bank, Washington, DC.

Yudo, S.; Wahyono, H.D.; Alhasa, K.M.; Warto; Zulaikha, S.; Pandiangan, Y.S.H., (2023). Water quality data analysis from the onlimo monitoring system at 16 stations in priority watersheds and lakes. In IOP Conference Series: Earth and Environmental Science. 1201(1),: 012052. IOP Publishing. 1-9 **(9 pages).**

Yudo, S.; Martono, D.N.; Sutjiningsih, D.; Kurniawan, B., (2026). Assessing data quality in real-time river water quality monitoring using multi-parameter indicators: a case study of ciliwung and cisadane, Indonesia. LIMNOTEK Perairan Darat Tropis di Indonesia [J. Limnol. Water Resour.,]. 32(1): 20–34 **(15 pages).**

Yulianto, F.; Nugroho, G.; Aruba Chulafak, G.; Suwarsono, S., (2021). Improvement in the accuracy of the postclassification of land use and land cover using landsat 8 data based on the majority of segment-based filtering approach. Sci. World J., 1: 1-22 **(22 pages).**

Zhang, J.; Sheng, Y.; Chen, W.; Lin, H.; Sun, G.; Guo, P., (2020). Design and analysis of a water quality monitoring data service platform. Comput. Mater. Continua., 66(1): 389-405 (**17 pages**).

Zhang, X.; Ma, L.; Zhu, Y.; Lou, W.; Xie, B.; Sheng, L.; Hu, H.; ·Zheng, K.; Gu, Q., (2022). Temporal stability analysis for the evaluation of spatial and temporal patterns of surface water quality. Water Resour. Manage, 36(4): 1413-1429 **(17 pages).**

Zhou, Y., (2020). Real-time probabilistic forecasting of river water quality under data missing situation: Deep learning plus post-processing techniques. J. Hydrol., 589: 1-17 **(17 pages).**

AUTHOR (S) BIOSKETCHES

Yudo, S., Ph.D. Candidate, Senior Researcher at Research Centre for Environment and Clean Technology, National Research and Innovation Agency, South Tangerang, Banten, Indonesia, 15314.
- Email: *satmoko.yudo@brin.go.id*
- ORCID: 0000-0002-0572-2550
- Web of Science Researcher ID: JBR-9897-2023
- Scopus Author ID: 57441416900
- Homepage: https://brin.go.id/

Martono, D.N., Ph.D., Professor at Graduate School of Sustainable Development, Universitas Indonesia, Jakarta, Indonesia, 10430.
- Email: *dwi.nowo11@ui.ac.id*
- ORCID: 0000-0003-2362-9066
- Web of Science Researcher ID: KGX-5681-2024
- Scopus Author ID: 57212672757
- Homepage: https://sil.ui.ac.id/

Sutjiningsih, D., Dr., Professor at Graduate School of Sustainable Development, Universitas Indonesia, Jakarta, Indonesia, 10430.
- Email: *dwita@eng.ui.ac.id*
- ORCID: 0000-0002-3497-6285
- Web of Science Researcher ID: AAB-1495-2019
- Scopus Author ID: 55836126600
- Homepage: https://sil.ui.ac.id/

Kurniawan, B., Ph.D., Researcher at Research Center for Limnology and Water Resources, National Research and Innovation Agency, Cibinong, Bogor, Indonesia, 16911.
- Email: *budi.kurniawan@brin.go.id*
- ORCID: 0009-0005-5566-8264
- Web of Science Researcher ID: MQA-8256-2025
- Scopus Author ID: 57209043416
- Homepage: https://brin.go.id/

HOW TO CITE THIS ARTICLE:
Yudo, S.; Martono, D.N.; Sutjiningsih, D.; Kurniawan, B., (2026). Integration of the online river water quality monitoring management framework based on inclusive governance. Global J. Environ. Sci. Manage., 13(1): 01-26.

DOI: 10.22034/gjesm.2027.01.01
URL: https://www.gjesm.net/article_735445.html

Global Journal of Environmental Science and Management
(GJESM)

Homepage: https://www.gjesm.net/

Podcasts

ORIGINAL RESEARCH ARTICLE

Environmental deoxyribonucleic acid metabarcoding reveals fish diversity in subtropical island mangrove rivers

B.G.S. Pananganan[1,2], S.G. Salmo III[2,3,4], T. Sado[5,6], Y. Isowa[2], H. Imai[7], Y. Sato[8], H. Nagai[7], M. Basyuni[9], T. Yamamoto[2,10], S. Imura[2], K. Ishigaki[2], H. Motomura[11], M. Miya[5,12], T. Kajita[1,2,*]

[1]*United Graduate School of Agricultural Sciences, Kagoshima University, 1-21-30 Korimoto, Kagoshima 890-0065, Japan*

[2]*Iriomote Station, Tropical Biosphere Research Center, University of the Ryukyus, 870 Uehara, Taketomi-cho, Yaeyama-gun, Okinawa 907-1541, Japan*

[3] *Department of Environmental Science, School of Science and Engineering, Ateneo de Manila University, Loyola Heights, 1108 Quezon City, Philippines*

[4]*Institute of Biology, College of Science, University of the Philippines Diliman, Quezon City, Philippines*

[5]*Department of Ecology and Environmental Sciences, Natural History Museum and Institute, Chiba, Japan*

[6]*National Institute for Environmental Studies, Lake Biwa Branch Office, Otsu, Japan*

[7]*Faculty of Science, University of the Ryukyus, 1 Senbaru, Nishihara, Okinawa 903-0213, Japan*

[8]*Research Laboratory Center, Faculty of Medicine, University of the Ryukyus, 1076 Kiyuna, Ginowan, Okinawa, Japan*

[9]*Center of Excellence for Mangrove, Universitas Sumatera Utara, Medan, Indonesia*

[10]*Hijirigaoka High and Junior High School, Tama University, Tokyo, Japan*

[11]*The Kagoshima University Museum, 1-21-30 Korimoto, Kagoshima 890-0065, Japan*

[12]*Research Organization for Nano and Life Innovation Waseda University 513, Waseda-tsurumaki-cho, Shinjuku-ku, Tokyo, Japan*

ARTICLE INFO

Article History:
Received 25 April 2026
Revised 30 June 2026
Accepted 03 August 2026

Keywords:
Aquatic biodiversity
Community composition
Conservation monitoring
Environmental management
Species richness

DOI:10.22034.gjesm.2027.01.02

ABSTRACT

BACKGROUND AND OBJECTIVES: Reliable biodiversity data are essential for management in World Heritage landscapes. Nevertheless, the ichthyofaunal diversity of short mangrove rivers remains insufficiently characterized because traditional survey methods demand high logistical effort, unrestricted site access, and advanced taxonomic knowledge. The study objectives were to document fish diversity across multiple short, protected island rivers and compressed freshwater-to-mangrove gradients and to provide baseline molecular data from samples collected before the World Heritage inscription.

METHODS: Environmental water samples were collected in 2017 and 2020 along freshwater-to-mangrove gradients in four river systems. Following metabarcoding analyses, operational taxonomic units were classified using reference databases, phylogenetic placement, and expert taxonomic knowledge. Sequencing-depth rarefaction, incidence-based rarefaction and coverage standardization, distance-based redundancy analysis, permutational multivariate analysis of variance, and a Procrustes-based species-richness-controlled null model were used to evaluate sampling completeness and community structure.

FINDINGS: A total of 174 operational taxonomic units representing 47 families and 110 genera were detected, including 20 Red List species. Taxonomic assignment revealed that roughly 74 percent of operational taxonomic units corresponded to formally recognized species. Furthermore, community compositions were largely river-specific, showing restricted overlap among the studied aquatic systems. Diversity was generally higher in lower estuarine reaches associated with mangroves. Community composition was significantly associated with salinity and location, with distance-based redundancy analysis explaining 53.4 percent of adjusted variation. Gobiidae comprised 28 percent of the total operational taxonomic units and showed strong concordance with whole-community patterns, suggesting that the family is a major and ecologically characteristic component of fish assemblages in the short subtropical mangrove rivers.

CONCLUSION: The historical samples documented high and spatially structured fish diversity in short mangrove rivers within a World Heritage landscape. Accordingly, the generated dataset provides an irreplaceable pre-designation molecular baseline to support subsequent monitoring and environmental evaluations. Rarefaction and coverage standardization indicated substantial completeness of the retained operational taxonomic unit dataset while confirming that river-level comparisons require caution. The high richness and freshwater to estuarine distribution of Gobiidae indicate that the family is a major component of these assemblages. Integration of this baseline dataset with contemporary monitoring programs and environmental covariates will facilitate long-term biodiversity evaluations.

This is an open access article under the CC BY license (http://creativecommons.org/licenses/by/4.0/)

NUMBER OF REFERENCES	NUMBER OF FIGURES	NUMBER OF TABLES
52	6	2

*Corresponding Author:
Email: tkaji@cs.u-ryukyu.ac.jp
Phone: +81 980 85 6560
ORCID: 0000-0003-1232-4179

Note: Discussion period for this manuscript open until March 01, 2027 on GJESM website at the "Show Article".

INTRODUCTION

Information on species diversity is fundamental to ecosystem assessment (Stuart-Smith *et al.,* 2013; Sheaves *et al.,* 2014). Diversity metrics, including species inventory, presence of native, endangered, and invasive species, species richness, and spatial distribution patterns, have been used to formulate policies for environmental conservation and management programs (Convention on Biological Diversity, 1992; Davies *et al.,* 2017). Despite its critical importance, establishing comprehensive baseline inventories of species diversity is frequently hindered by logistical limitations, a deficit in specialized taxonomic knowledge, considerable financial costs, and prohibitions against invasive sampling techniques in conserved ecosystems (Chiarucci *et al.,* 2011; Feller *et al.,* 2010). Species diversity data are typically compiled from conventional faunal and floral surveys, which require substantial time and effort to capture or collect specimens in the field (Thomsen and Willerslev, 2015).

Over the past 15 years, the use of environmental deoxyribonucleic acid (eDNA) in biodiversity monitoring has become widely established (Oka *et al.,* 2021; Valentini *et al.,* 2016). eDNA refers to genetic material that organisms release into the surrounding environment through processes such as movement, feeding, reproduction, and mortality. Biodiversity monitoring based on eDNA is recognized as non-invasive, rapid, and cost-effective (Yamamoto *et al.,* 2017). In Japan, fish biodiversity studies using MiFish primers (Miya *et al.,* 2015, 2020) have been widely conducted. In addition, official protocols for utilizing eDNA in freshwater fish environmental assessments have been established by governmental bodies; correspondingly, eDNA surveys have cataloged fish diversity at over 550 coastal sites nationwide (ANEMONE DB, 2026; Minamoto *et al.,* 2021). Beyond coastal ecosystems, eDNA is increasingly being applied across a variety of habitats, contributing to the management and conservation of biodiversity. Although the method is now widely used, multi-river assessments of short, protected island mangrove systems remain uncommon, particularly across compressed freshwater-to-estuarine gradients.

Despite the importance of species diversity information for conservation and management in World Heritage landscapes, fish diversity in short mangrove rivers on Iriomote Island lacks comprehensive documentation. Iriomote Island, located near the westernmost edge of Japan, is a subtropical island characterized by extensive native forests, numerous short rivers, mangrove forests, and surrounding coral reefs. Most of Iriomote Island is protected within Iriomote-Ishigaki National Park, and much of its interior consists of roadless and uninhabited forested catchments. Accordingly, numerous island rivers preserve an uninterrupted ecological gradient extending from headwater streams through freshwater networks and mangrove estuaries directly with coastal zones. Such continuous gradients under minimal direct residential or urban influence constitute a rare, near-natural reference system for examining biodiversity patterns, including the spatial organization of fish assemblages, across connected freshwater, mangrove, and coastal ecosystems. This spatial continuity sets Iriomote Island apart from numerous regional mangrove ecosystems, where pervasive human activities disrupt river catchments from headwaters to estuaries and mask natural gradients of community organization.

In 2021, the island was inscribed as part of a United Nations Educational, Scientific and Cultural Organization (UNESCO) World Natural Heritage property under the criterion of outstanding universal value for biodiversity (UNESCO World Heritage Centre, 2021). Subsequent to this designation, rigorous biodiversity tracking and recreational use management are critical to safeguarding ecological integrity against escalating anthropogenic and tourist-induced pressure. Taketomi Town has introduced

ecotourism-based management measures under the Ecotourism Promotion Act, including the designation of several nature-experience fields such as Specific Natural Tourism Resources and the establishment of daily visitor limits and prior approval requirements for entry. These measures apply to five fields, including river-related areas such as the Hinai and Nishida rivers, and are intended to prevent degradation caused by overuse. However, such regulations may also increase attention to other accessible rivers and mangrove areas within the same World Heritage landscape. At present, quantitative baseline data on aquatic biodiversity remain limited for many of these short river systems, making it difficult to evaluate ecological changes associated with tourism use or to design long-term monitoring programs.

Conventional biodiversity surveys based on visual observation and specimen collection are difficult to sustain across multiple river systems over long periods because of limited accessibility, high sampling effort, and the need for taxonomic expertise (Chiarucci *et al.,* 2011; Lee *et al.,* 2014; Zainal Abidin *et al.,* 2022; Pananganan *et al.*, 2026). This limitation is particularly important in mangrove rivers, which are popular for ecotourism activities such as canoeing but are challenging environments for aquatic faunal surveys due to turbidity, tidal influence, and habitat complexity. Except along the steep southern coastline, mangroves occur in more than 30 river systems throughout Iriomote Island. Most mangrove areas are associated with short rivers less than 10 kilometers (km) in length, whereas only a few larger river systems, such as the Urauchi and Nakara rivers, support extensive mangrove forests. Notwithstanding the record of over 400 fish species in the Urauchi River (Suzuki and Senou, 2005), fish diversity in numerous other short river systems remains largely under documented, primarily owing to the inherent challenges of conducting such investigations (Lee *et al.*, 2014; Nagelkerken *et al.*, 2008; Naputo *et al.*, 2024). The contribution of the present study therefore lies not just in the use of eDNA metabarcoding alone, but also in characterizing multiple short, minimally disturbed forest-to-estuary river systems, examining freshwater-to-estuarine differentiation within rivers, and providing a reproducible historical dataset that may serve as a reference for comparison with more modified mangrove catchments.

The samples analyzed in this study were collected in 2017 and 2020, before Iriomote Island was inscribed as part of a UNESCO World Natural Heritage property in 2021. Accordingly, the collected samples yield an irreplaceable pre-impact molecular baseline—through retrospective analysis—that will enable the evaluation of future variations in fish distribution and community structure. Because the four rivers were not sampled contemporaneously, the study does not estimate an independent year effect; cross-river comparisons are interpreted as descriptive patterns in historical datasets generated with comparable fish metabarcoding workflows. Here, fish assemblages in four short mangrove river systems were characterized using eDNA metabarcoding. The aims of this study were: 1) to document fish diversity detected by eDNA in four short river systems; 2) to compare diversity among rivers and identify distributional patterns; and 3) to assess fish community composition in relation to environmental variation. Collectively, these aims sought to generate foundational molecular metrics from pre-inscription samples, thereby enabling longitudinal biodiversity assessments of these short mangrove river basins via standardized methods.

MATERIALS AND METHODS

The study area

The four study rivers are located on Iriomote Island (24°20′ N, 123°45′ E), part of the Yaeyama Islands in Okinawa Prefecture, Japan (Fig. 1). This subtropical island is characterized by mountainous terrain, extensive native forests, and numerous rivers draining into coral reef–fringed coastal

waters. Sampling sites were established along the Ayanda (A1–A2), Udara (U1–U6), Nakara (N1–N6), and Yutun (Y1–Y7) rivers. The map (Fig. 1), was generated in quantum geographic information system (QGIS) v3.44 using coastline and water-network data obtained from the Geospatial Information Authority of Japan (GSI; https://www.gsi.go.jp/). The sampling design spanned environmental gradients from mangrove-dominated estuaries to freshwater reaches across the Udara, Nakara, and Yutun river basins, with longitudinal distances from the respective river mouths to the terminal upstream sampling sites measuring 1.8, 6.9, and 3.5 km, respectively. In the Ayanda River, sampling was limited to two sites located approximately 500 meters (m) from the river mouth due to inaccessibility. The rivers vary in total length (3–8.75 km), elevation gradient, and extent of mangrove coverage (Fig. 1; Table 1). The four rivers were selected because they are short, relatively undisturbed systems that together include mangrove-estuarine and upstream freshwater habitats. The Udara, Ayanda, and Nakara rivers are accessible only by boat and do not have residential settlements within their catchments. The Yutun River has a road near its lower reach, but its catchment is also uninhabited and remains largely forested. The four study rivers therefore experience little direct influence from residential development, agriculture, or urban runoff, although they differ in river length, mangrove extent, accessibility, and environmental configuration. Owing to the absence of a probabilistic sampling framework, these sites lack statistical representation of the wider fluvial systems on Iriomote Island and cannot be generalized to mangrove river basins elsewhere. All sampling locations are situated within relatively undisturbed habitats designated as category 1 special zones under Japan's National Park Act, making them well suited for evaluating fish diversity patterns along river–estuary gradients within this UNESCO World Heritage site. Primary field collections for the Nakara River were executed in 2017, whereas empirical records for the Ayanda, Udara, and Yutun Rivers were compiled from a previous study (Sato *et al.*, 2022). Because the Nakara dataset was collected in 2017 and the other datasets in 2020, year and river identity are confounded and cannot be separated statistically.

Sampling and collection

Environmental DNA sampling along the freshwater–mangrove gradient was conducted in the Nakara River on 6 September 2017 between 07:30 and 09:52 during a receding tide (high tide: 200 centimeters (cm) at 07:35; low tide: 24 cm at 13:58). At each site, a bucket was randomly thrown ten times into the middle of the river. At each site, two replicate water samples were collected using sterile syringes. For each replicate, up to 1,000 milliliters (mL) of water was filtered through a 0.45 micrometers (μm) Sterivex filter (Merck), following Miya *et al.* (2015). Filtration at Site 5 was limited to 800 mL due to high turbidity. To account for potential exogenous contamination, a field blank of purified water was processed concurrently with all experimental samples utilizing identical procedures. Filtered samples and blanks were stored in a cooler box at 4 degrees Celsius (°C) during transport and subsequently preserved at −20 °C. All equipment was sterilized before use, and collection containers were decontaminated with bleach followed by thorough rinsing with running freshwater before sampling. Environmental parameters, including salinity (in percent (%) and temperature, were measured at each site using a conductivity meter (Mother Tool Co., Ltd.) and a digital thermometer (Tanita Co., Ltd.), respectively. Categorical classification was applied to vegetation types, whereas elevation metrics and distances from the sea were derived from global positioning system (GPS) coordinates. For the Ayanda, Udara, and Yutun rivers, water samples and vertebrate metabarcoding sequence data were obtained from Sato *et al.* (2022), which included MiFish-based analysis of fish eDNA from the same sampling sites. The sampling design

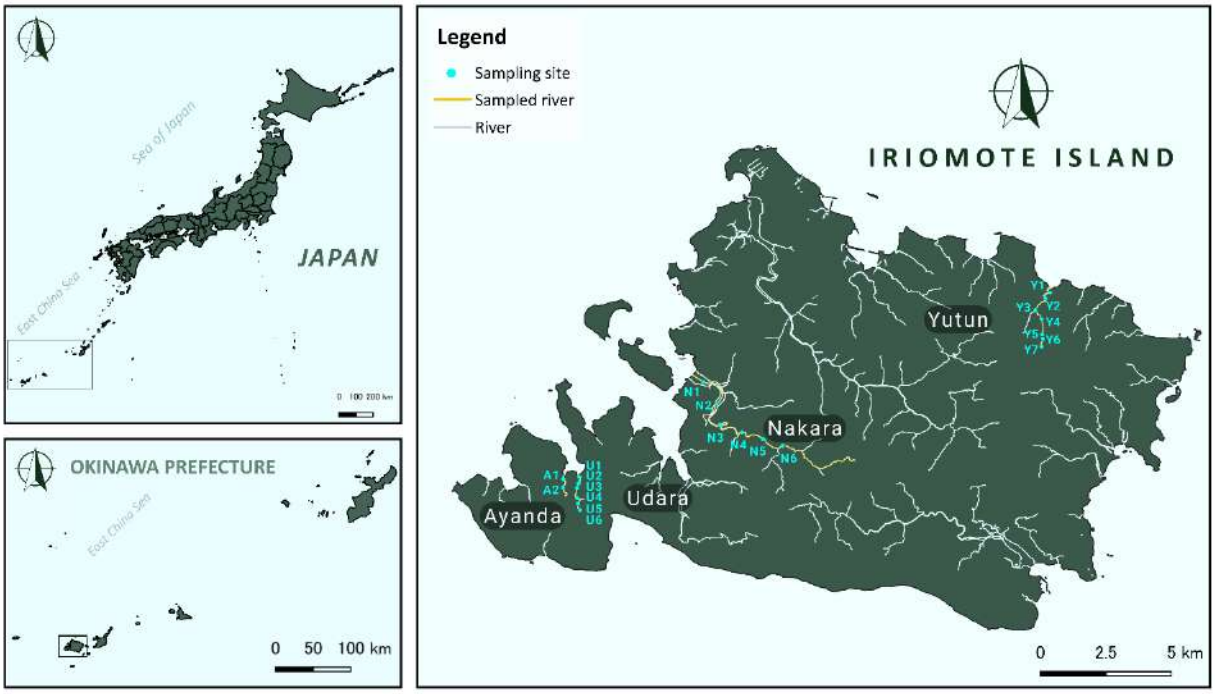

Fig. 1: Geographical location of the study area along with the sampling sites across four rivers on Iriomote Island, Okinawa, Japan

Table 1: Sampling site details across four rivers on Iriomote Island

Site	Lat.	Long.	Elev. (m)	Dist. (km)	Env.	Veg.	Temp. (°C)	Sal. (%)	Vol. (mL)
N1	24.3489	123.7560	0	0.63	ETY	Mf	29.5	3.1	1000
N2	24.3408	123.7610	0	2.06	ETY	Mf	29.7	3.33	1000
N3	24.3328	123.7623	6.2	3.38	ETY	Mf	31	2.65	1000
N4	24.3299	123.7705	9.4	5.08	ETY	Mf	29.3	0.45	1000
N5	24.3274	123.7785	17.4	6.1	FWR	Sf	27.5	0.1	800
N6	24.3249	123.7859	70.6	6.92	FWR	Sf	26.9	0	1000
A1	24.3123	123.7031	10.7	0.28	ETY	Mf	24.5: 33.2	2.74: 3.31	600:800
A2	24.3090	123.7030	11.9	0.39	ETY	Mf	21.5: 32.1	1.22: 2.59	800:800
U1	24.3131	123.7092	20.31	0.22	ETY	Mf	25.3: 33.2	0.93: 3.02	600:800
U2	24.3106	123.7088	6.85	0.49	ETY	Mf	18.9: 30.4	0.74: 2.56	1000:700
U3	24.3089	123.7083	14.31	0.74	ETY	Mf	18.4: 27.5	0.01: 0.07	1000:800
U4	24.3051	123.7083	49.39	1.2	FWR	Sf	18.5: 27.4	0.01: 0.02	950:800
U5	24.3030	123.7086	61.17	1.54	FWR	Sf	19.0: 27.5	0.01: 0.02	1000:1000
U6	24.3006	123.7093	70.54	1.85	FWR	Sf	19.5: 26.8	0.01: 0.01	1000:1000
Y1	24.3828	123.8869	22.24	0.31	ETY	Mf	22.1: 31.9	2.71: 2.83	1000:900
Y2	24.3807	123.8852	5.17	0.73	ETY	Mf	18.8: 28.4	0.26: 0.83	1000:1000
Y3	24.3761	123.8814	61.89	1.45	FWR	Sf	19.2: 26.9	0.01: 0.01	1000:1000
Y4	24.3727	123.8837	105.87	2	FWR	Sf	18.4: 26.1	0.01: 0.01	1000:1000
Y5	24.3669	123.8840	258	2.67	FWR	Sf	18.3: 28.1	0.01: 0.01	1000:1000
Y6	24.3653	123.8842	304.38	2.86	FWR	Sf	18.3: 25.6	0.01: 0.01	1000:1000
Y7	24.3623	123.8838	286.36	3.5	FWR	Sf	18.6: 26.7	0.01: 0.01	1000:1000

Site – Ayanda River (A1–A2), Udara River (U1–U6), Nakara River (N1–N6), and Yutun River (Y1–Y7); Geographic coordinates, Lat. – latitude, Long. – longitude; Elev. (m) – Elevation (meter); Dist. (km) – Distance from the sea (kilometer); Env. – environment, ETY – estuary, FWR – freshwater; Veg. – Vegetation, Sf – subtropical forest, Mf – mangrove forest; Temp. (°C) – water temperature (degree Celsius); Sal. (%) – Salinity (percent); Vol. – water volume. Data for sampling sites in three rivers (Ayanda, Udara, and Yutun) were obtained from Sato *et al.* (2022). For the Ayanda, Udara, and Yutun rivers, paired values separated by a colon represent measurements from January and July 2020, respectively.

and laboratory procedures were comparable to those applied in the Nakara River. The number of sampling sites differed among rivers, with two, six, and seven sites established for the Ayanda, Udara, and Yutun rivers, respectively, and sampling was conducted across two seasons (January and July 2020). Further methodological details are provided in Sato *et al.* (2022). Thus, the design comprised six Nakara sites sampled once with two field replicates per site, whereas Ayanda, Udara, and Yutun contained two, six, and seven sites, respectively, sampled in two seasons. Owing to inter-fluvial disparities in sampling effort, cumulative river-level richness metrics were analyzed qualitatively and descriptively rather than as strictly standardized comparative units.

DNA extraction and purification, paired-end library preparation, and next-generation sequencing (NGS)

Frozen water samples collected from the Nakara River were transported to the Natural History Museum and Institute, Chiba, Japan for eDNA metabarcoding analysis using MiFish primers. DNA extraction and purification were performed following Miya *et al*. (2015) using the DNeasy blood and tissue Kit (Qiagen). Extractions were carried out in a single analytical batch, with a corresponding extraction blank (EB) included to assess and control for potential contamination risks. All DNA extracts were stored at −20 °C until library preparation. Paired-end libraries were prepared using a two-step polymerase chain reaction (PCR) protocol (Miya et *al.*, 2015) with three MiFish primer sets (U, U2, and E). Each first-round PCR had a total volume of 12 microliters (µL) containing KAPA HiFi HotStart ReadyMix (KAPABIOSYSTEMS), template DNA, and nuclease-free water. For each sample, eight technical replicates were performed, along with negative controls. Thermal cycling conditions consisted of an initial denaturation at 95 °C for 3 minutes (min); 35 cycles of 98 °C for 20 s, 65 °C for 15 s, and 72 °C for 15 s; followed by a final extension at 72 °C for 5 min. Amplicons with ~370 base pairs (bp) were verified by agarose gel electrophoresis and purified using the NucleoMag® NGS Clean-up and Size Select Kit (MACHEREY-NAGEL). In the second PCR, dual-index Illumina adapters were attached under the following conditions: 95 °C for 3 min; 10 cycles of 98 °C for 20 s and 72 °C for 15 s; with a final extension at 72 °C for 5 min. Libraries were then pooled, size-selected using 2 % E-Gel SizeSelect II agarose gels (Thermo Fisher Scientific), purified, and quality-checked before sequencing. Sequencing was performed on an Illumina MiSeq (Illumina) platform using the v2 Reagent Kit Mini (2 × 150 bp) (Illumina), with a 5% PhiX control (Illumina) spike-in, following the manufacturer's protocols. For the Ayanda, Udara, and Yutun rivers, metabarcoding analyses were conducted as described in Sato *et al*. (2022). In brief, comparable MiFish-based protocols, including similar primeros sets and sequencing platforms, were applied, enabling consistency across datasets.

Bioinformatics analyses and taxonomic annotations

Initial bioinformatics processing was conducted using quantitative insights into microbial ecology version 2 (QIIME2) (version 2022.2.1; Bolyen *et al.,* 2019) following a standard paired-end workflow. Raw sequencing data from all four rivers were imported into the QIIME2 environment, and adapter sequences were removed using the Cutadapt plugin (Martin, 2011). Sequence quality profiles were examined to guide subsequent filtering steps. Paired-end reads were merged and processed for denoising and chimera removal using the DADA2 plugin (version 2022.2.0; Callahan *et al.,* 2016), resulting in the generation of amplicon sequence variants (ASVs). The ASVs were subsequently clustered at a 99% sequence identity threshold using the VSEARCH plugin (Rognes *et al.,* 2016), and a representative read was selected from each cluster. Sequence reads shorter than 140 bp were excluded from further

analyses. Taxonomic assignment was performed by querying the sequence reads against the NCBI nucleotide database using blastn (Zhang *et al.,* 2000). Sequences assigned to fish taxa and showing at least 75% sequence identity to reference sequences were retained as operational taxonomic units (OTUs) in this study for subsequent analyses, whereas non-fish OTUs and OTUs showing less than 75% sequence identity to reference sequences were removed. No universal minimum read-count or sample-occurrence threshold was applied. To optimize the precision and robustness of taxonomic assignments, annotations were assessed via a multi-criterion framework encompassing sequence identity metrics, phylogenetic topology, and expert taxonomy. Subsequent validation was performed using established distribution databases, expert evaluations, FishBase (Froese and Pauly, 2024), and the Catalog of All Japanese Fish Species Online (version 25; Motomura, 2024). Based on these criteria, OTUs were classified into four confidence categories. Category 1 comprised species-level assignments supported by sequence identity greater than 98.5%, phylogenetic placement, and consistency with known distributions. This classification additionally integrated taxa acknowledged as discrete species in Japan, albeit lacking formally designated or nomenclaturally valid scientific names. Category 2 comprised OTUs matching multiple species within a single genus. Category 3 comprised OTUs clustering with taxa from multiple genera within the same family. Category 4 comprised unannotated OTUs precluded from robust family-level assignment, characteristically resolving as distinct or divergent phylogenetic lineages devoid of proximal reference matches. Detailed taxonomic assignment criteria and the complete taxonomic annotation table, including representative sequences and sample-level occurrence and read-count data, are available in the Open Science Framework (OSF) repository under Project ID wqdb8. All raw sequence data for the Nakara River are available in the National Center for Biotechnology Information (NCBI) BioProject database with accession number PRJNA897101, while sequence data for the Ayanda, Udara, and Yutun rivers are deposited in the DNA Data Bank of Japan (DDBJ) sequence read archive with accession number DRA012231.

Data management and statistical analysis

Negative controls (field blanks, extraction blanks, and PCR negatives) were processed alongside all samples. Only a small number of taxa were detected in these controls (n = 5), each at very low read abundance (3–6 reads), and without consistent patterns across control types. Accordingly, these detections were regarded as negligible, primarily reflecting minor background contamination or sequencing artifacts, including index misassignment. As a conservative measure, read counts for these taxa were subtracted from the corresponding samples on a per-taxon basis before downstream analyses. Adequacy of sequencing depth across individual biological libraries was appraised through read-based rarefaction of the retained operational taxonomic unit (OTU) matrix, wherein expected OTU richness was derived as a function of escalating rarefied sequence reads (Fig. 2a–d). The number of rarefied sequence reads was plotted on a logarithmic scale, and each curve represented one biological library. River-level gamma richness was evaluated from site-by-OTU incidence data using q = 0 rarefaction and extrapolation to twice the observed number of sampling sites, following the iNEXT framework (Fig. 2e). Richness was also standardized to the maximum incidence-based sample coverage (C) shared by all four rivers (C = 0.927) (Fig. 2f). These rarefaction and coverage-standardization analyses were based on the unaggregated sample-by-OTU read-count matrix, with biological libraries and seasonal samples retained separately. The matrix and analysis scripts are available in the OSF repository under Project ID fh4vg. These analyses evaluated the completeness of the retained OTU dataset but did not estimate taxon-specific detection

probabilities. Fish community diversity was assessed using species richness, the Shannon diversity index (H'), following standard ecological approaches. eDNA read counts were normalized using total standardization in the vegan package (decostand, method = "total"), converting counts to relative abundances to account for variation in sequencing depth among samples (Oksanen *et al*., 2025). Variation in community composition among sites was examined using non-metric multidimensional scaling (NMDS) ordination based on Bray–Curtis dissimilarity (Kruskal, 1964; Bray and Curtis, 1957). The influence of environmental variables on community composition was evaluated using distance-based Redundancy Analysis (db-RDA) (Legendre and Anderson, 1999) and a permutational multivariate analysis of variance (PERMANOVA) (Anderson, 2017) using Bray-Curtis distances. Multivariate dispersion was tested using PERMDISP (betadisper) to verify PERMANOVA assumptions. Before analysis, the continuous environmental predictors were standardized (z-score transformation). Multicollinearity among predictors was assessed using variance inflation factors (VIF), while identification of the most parsimonious model was based on adjusted R^2 and permutation tests (999 permutations) using stepwise forward selection (ordiR2step). Owing to collinearity between sampling year and individual river identity, year was omitted from the set of independent predictors to prevent model distortion. To characterize whether the spatial configuration of Gobiidae corresponded with broader community structure, Bray–Curtis dissimilarity matrices were calculated separately for the 49 gobiid OTUs and the 125 non-gobiid OTUs. Each matrix was represented by the first two positive axes of principal coordinates analysis (PCoA), and configurational agreement was quantified using a symmetric Procrustes correlation. To test whether the observed agreement exceeded that expected from gobiid OTU richness alone, an OTU-richness-controlled null model randomly selected 49 OTUs without replacement from the non-gobiid pool, compared each subset with the remaining 76-OTU community, and repeated this procedure 9,999 times. Standardized effect sizes and one-sided empirical p values were calculated directly from the generated null distribution. Rarefaction, coverage-standardization, and Gobiidae null-model analyses were conducted in Python, whereas NMDS, db-RDA, PERMANOVA, and PERMDISP were conducted in R (R Core Team, 2023) using the vegan package (Oksanen *et al.*, 2025). Data visualization, including bar plots, heatmaps, and ordination biplots, was performed using the ggplot2 package (Wickham, 2016). Figures were modified for presentation clarity using the Canva online design platform (https://www.canva.com). Data and analysis scripts are deposited in the OSF repository under Project IDs wqdb8 and fh4vg.

RESULTS AND DISCUSSION

eDNA fish data overview

A total of 1.9 million reads were generated across all sites, yielding 174 OTUs across the four rivers. After subtraction of the low-level detections observed in the negative controls, no control-associated reads remained in the retained dataset. The complete curated sample-by-OTU matrix, including sample-level read counts and season-specific occurrences, is available in the Open Science Framework (OSF) repository under Project ID wqdb8 with DOI: 10.17605/OSF.IO/WQDB8. Asymptotic trajectories observed in the rarefaction curves across the majority of biological libraries imply that incremental sequencing depth would capture negligible additional OTUs following the implemented curation workflow (Fig. 2a-d). River-level incidence-based rarefaction and extrapolation showed increasing gamma richness with additional sites (Fig. 2e). At the maximum incidence-based sample coverage shared by all four rivers (C = 0.927), standardized richness was estimated as 48.3 OTUs for Ayanda, 76.0 for Udara, 123.2 for Nakara, and 46.8 for Yutun (Fig. 2f). The Ayanda estimate required

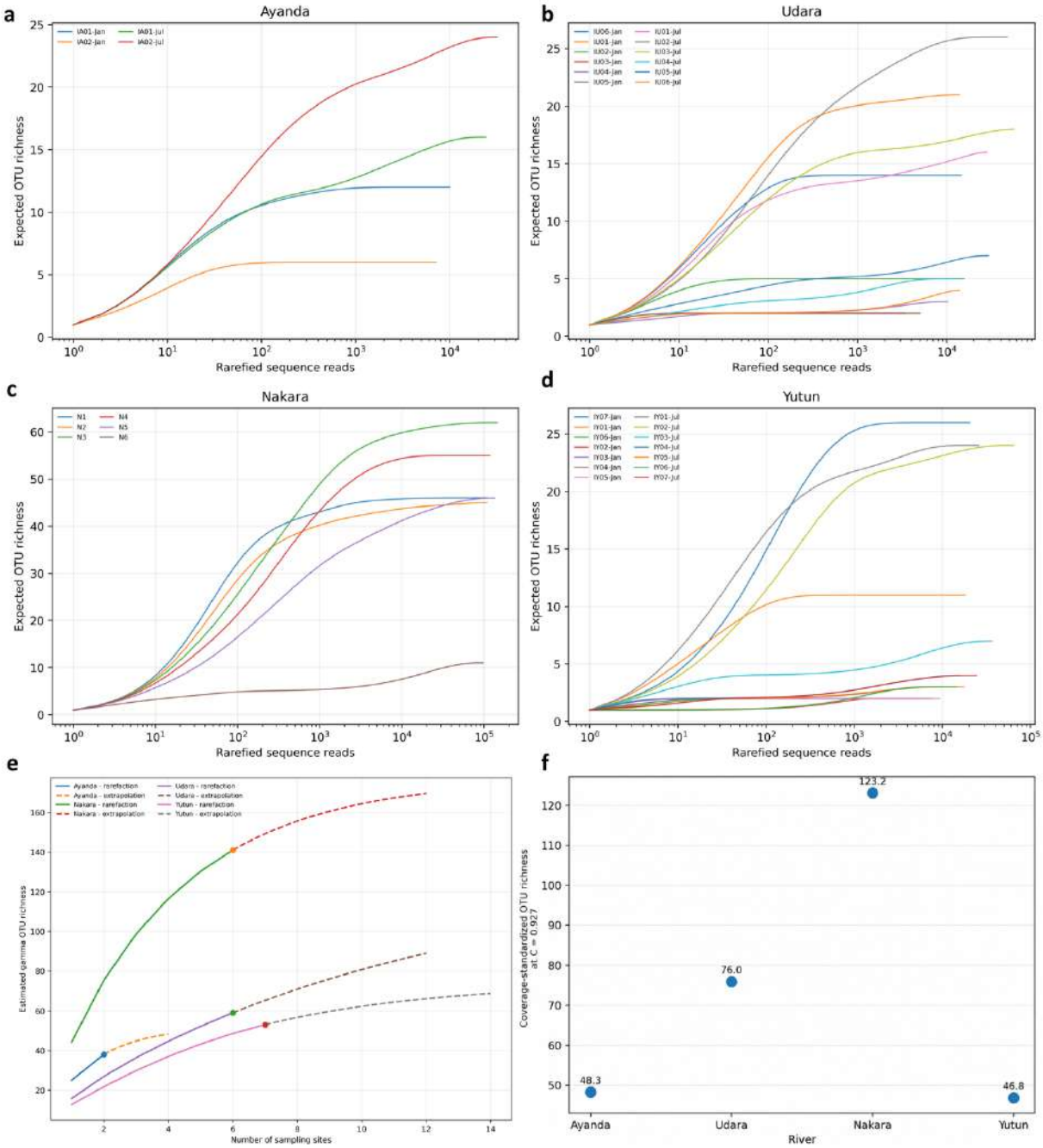

Fig. 2: Sequencing-depth rarefaction of individual biological libraries from the four rivers (a–d), incidence-based rarefaction and extrapolation of river-level OTU richness (e), and coverage-standardized richness at C = 0.927 (f)

extrapolation from only two sites and should be interpreted cautiously. Of the 174 retained OTUs, 136 (78.2%) were assigned to Category 1, 33 (19.0%) to Category 2, 3 (1.7%) to Category 3, and 2 (1.1%) to Category 4. Of the ones assigned to Category 1, 128 OTUs (73.6% of all OTUs) were assigned to formally named species, whereas eight represented distinct but formally unnamed

taxa recognized in Japan. Across the four river systems, Nakara had the highest observed richness (141 OTUs), whereas Ayanda had the lowest observed richness (38 OTUs). Of the total, 145 OTUs (83.3%) showed a 100% match to reference sequences, with Nakara contributing the largest share (118 OTUs) (Table 2). Within this subset, 38 OTUs could not be assigned to species-level identification, either as a consequence of inadequate taxonomic resolution in reference libraries or due to sequence identity overlap among multiple species. Overall, 165 OTUs (94.8%) showed >98.5% similarity to reference sequences, whereas 9 OTUs (5.2%) fell below this threshold. Taxonomic assignment identified 47 families, 110 genera, and 128 species, with Nakara having the highest observed counts across all ranks. A total of 20 species listed as Critically Endangered (CR), Endangered (EN), Vulnerable (VU), or Near Threatened (NT) in the Japanese, Okinawa Prefectural, or International Union for Conservation of Nature (IUCN) Red Lists were detected, with Nakara having the highest observed number (15 species). Within the Gobiidae, 49 OTUs corresponding to 48 species were recorded across the four rivers, representing 28.2% of the total OTUs and constituting the most species-rich family among the 47 identified families.

Comparative diversity across rivers

Observed OTU richness and diversity indices varied along environmental gradients across the four river systems. The highest OTU richness was observed at mid- to lower-elevation sites: N1–N5 (45–64 OTUs) in the Nakara River, U1–U3 (19–36 OTUs) in the Udara River, Y1–Y2 (30–38 OTUs) in the Yutun River, and A1–A2 (23–28 OTUs) in the Ayanda River (Fig. 3a). In contrast, upstream sites showed lower richness, including Y3–Y7 (4–7 OTUs) in the Yutun River, U4–U6 (4–8 OTUs) in the Udara River, and N6 (12 OTUs) in the Nakara River. Shannon diversity across the 21 sampling sites ranged from 0.52 to 3.40 (Fig. 3b). Values were generally higher in estuarine and lower-river sections associated with mangrove vegetation and lowest in upstream headwaters. Within the sampled sites, OTU richness and evenness were generally higher toward downstream reaches, and Nakara sites N1–N3 had the highest observed Shannon values (>3.0). Because the rivers differed in sampling year, number of sites, and sampling occasions, river-level differences are descriptive and cannot be attributed solely to river characteristics. A total of 14 OTUs (8%) were shared among all four rivers, whereas most OTUs (107; 62%) were unique to a single river, with the majority occurring in the Nakara River (82 OTUs), followed by the Udara (13), Yutun (8), and Ayanda (4) rivers. Notably, *Rhinogobius yaima* and *Anguilla marmorata* were primarily associated with upstream habitats. In contrast, estuarine and mangrove-associated species, including *Planiliza macrolepis*, *Planiliza melinopterus*, *Mugil cephalus*, and *Lutjanus argentimaculatus*, were detected mainly in lower-river and brackish environments (Fig. 3c). Conservation-relevant taxa were also detected. In total, 20 Red List species were recorded: 16 species are listed on Japan's Red List (Ministry of the Environment, 2020); 16 species on the Okinawa Red List (Okinawa Prefectural Government, 2017); and 4 species on the IUCN Red List (IUCN, 2025) (Fig. 3d). Among these, *Acanthopagrus pacificus* and *Zenarchopterus dunckeri* were detected in all four rivers, and the Nakara River had the highest observed number of Red List species, while the Yutun River had the lowest observed number.

Fish community composition and environmental correlates

NMDS ordination showed separation among several groups of sites across rivers (stress = 0.058; Fig. 4a). Hierarchical clustering identified two

Table 2: Summary of OTU and taxonomic diversity detected across four river systems on Iriomote Island

OTU dataset	Ayanda	Udara	Nakara	Yutun	Total
No. of OTUs	38	59	141	53	174
OTUs with 100% similarity	35	52	118	48	145
OTUs > 98.5% similarity	36	57	132	51	165
OTUs < 98.5% similarity	2	2	9	2	9
Taxonomic composition					
No. of families	19	24	44	22	47
No. of genera	33	46	93	38	110
No. of species (assigned)	33	44	104	43	128
OTUs not assigned to the species level	12	9	31	9	38
Japan and IUCN Red List (CR, EN, VU, NT)	5	8	15	3	20
Number of Gobiidae species	6	16	36	15	48

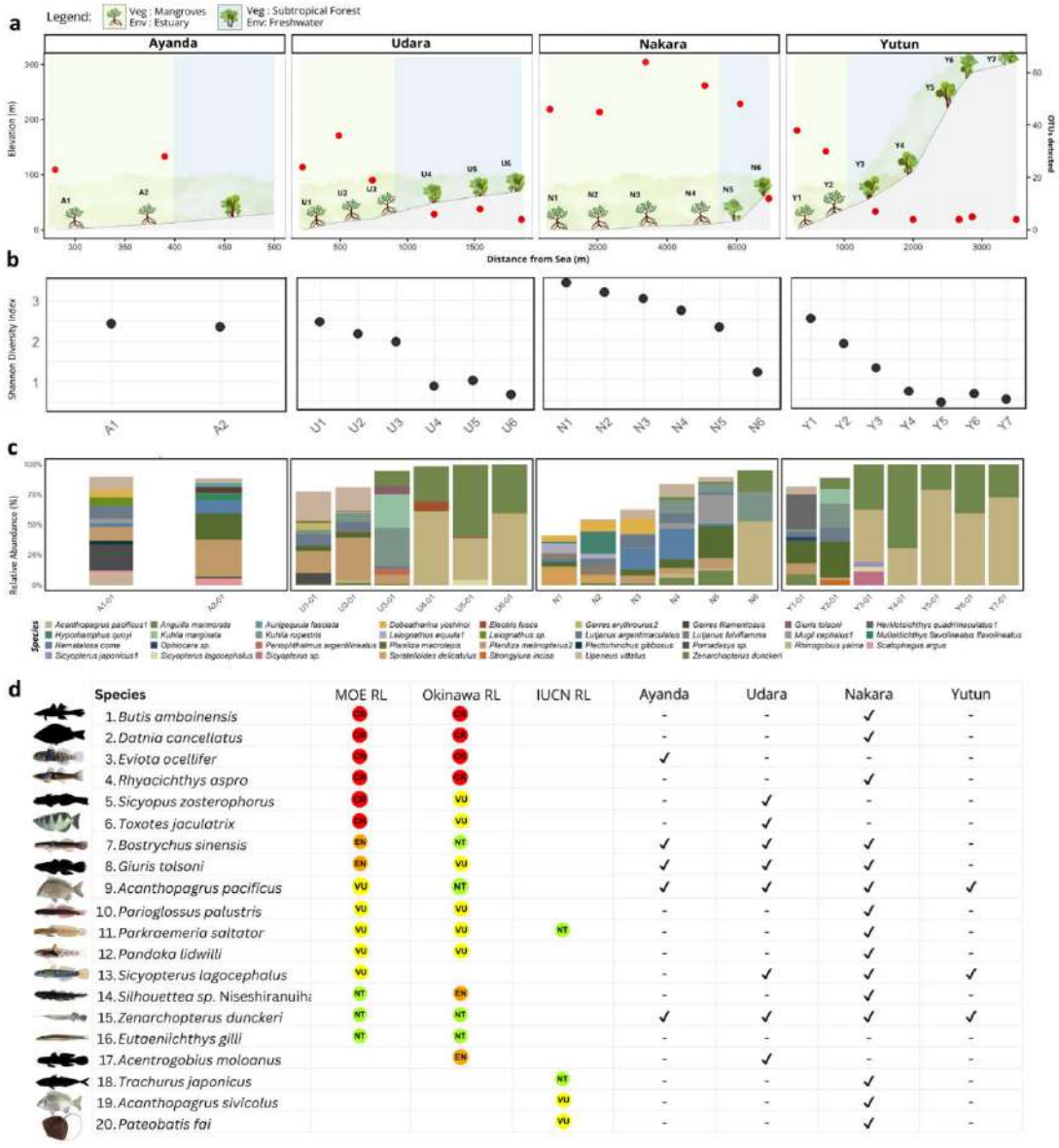

Fig. 3: Site-level fish OTU richness (a), Shannon diversity (b), community composition based on total-standardized relative-read abundance (c), and occurrence of Red List species (d) across the four rivers. Green and blue indicate estuarine and freshwater sites, respectively. Photographs in panel d reproduced with permission from ©KPMNH (T. Suzuki and H. Senou) and ©KAUM (H. Motomura)

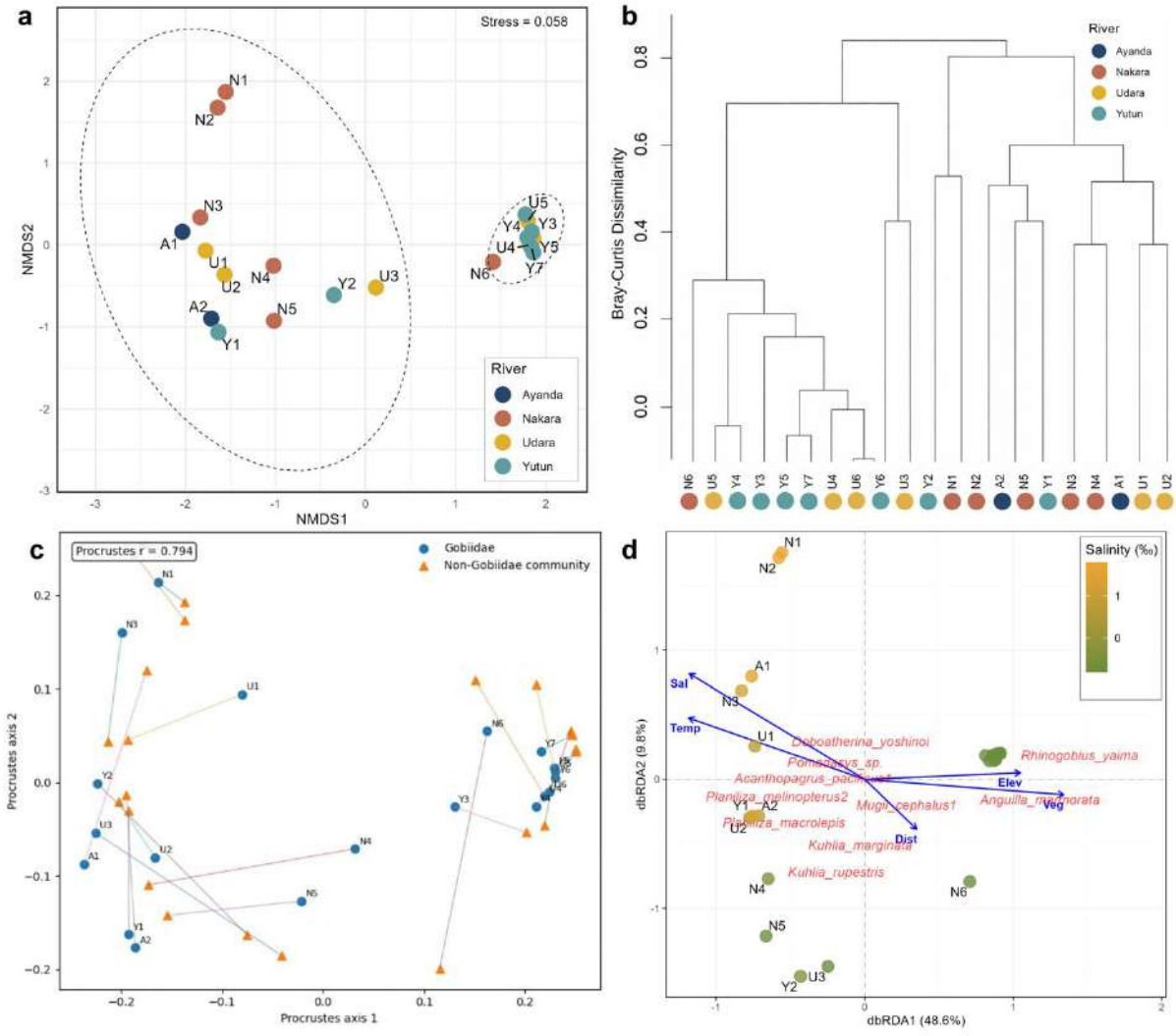

Fig. 4: NMDS ordination (a), hierarchical clustering (b), Procrustes comparison of Gobiidae and non-gobiid community configurations (c), and db-RDA ordination relating fish assemblages to measured environmental variables (d).

major assemblages: Cluster 1 comprised upstream freshwater sites (U4-6, N6, Y3-7), while Cluster 2 included estuarine and lower-reach sites (A1-2, U1-3, N1-2, Y1-2) (Fig. 4b). Isolated ordination analyses of the 49 gobiid OTUs demonstrated substantial concordance between the spatial structuring of Gobiidae and that of the 125 non-gobiid OTUs (Fig. 4c). In the Procrustes plot (Fig. 4c), circles and triangles represent the configurations of Gobiidae and the non-gobiid fish community, respectively. Lines connect the paired positions of each site after optimal rotation and scaling, with attenuated line lengths indicating increased congruence between the alternative spatial configurations. The symmetric Procrustes correlation based on the first two positive PCoA axes was r = 0.794. In the OTU-richness-controlled null model, the mean correlation for 9,999 randomly selected non-gobiid subsets of 49 OTUs was 0.782 (SD = 0.082; 95% null interval = 0.631–0.903). The observed value had a standardized effect size of 0.15 and a one-sided empirical

p value of 0.492 (50.8th percentile), indicating that the congruence was not greater than expected for a random OTU subset of equivalent richness. Furthermore, heatmaps showed clear habitat segregation, wherein freshwater sampling stations demonstrated elevated relative read abundances of amphidromous taxa, contrasted by a prominent representation of brackish and marine-associated species within estuarine reaches (Figs. 5 and 6). Few species were detected across multiple river systems, while occurrence and relative abundance patterns of several were distinct, river- and site-specific. The stepwise-selected db-RDA model retained Location and Salinity as selected measured covariates, explaining 53.4% of the total adjusted variation ($p=0.001$; VIF < 2) (Fig. 4d). Analysis of multivariate dispersion via PERMDISP demonstrated homogeneity among river basins ($F = 0.43$, $p = 0.746$), whereas significant heterogeneity was observed between freshwater and estuarine sampling locations ($F = 46.93$, $p = 0.001$). PERMANOVA detected significant differences associated with Location (pseudo-$F = 3.94$, $p = 0.001$) and River system (pseudo-$F = 2.15$, $p = 0.023$), while Temperature and Elevation showed no significant marginal effects ($p > 0.05$). Factor-level effect sizes indicated that River ($R^2 = 0.120$) and Location ($R^2 = 0.073$) contributed most to community variation.

Observed fish diversity in short mangrove rivers

An eDNA metabarcoding survey detected 174 OTUs across four short mangrove river systems along freshwater-to-mangrove gradients (Table 2). While the Nakara River accounted for 141 OTUs (inclusive of 104 species-level annotations), this elevated metric potentially mirrors intrinsic ecological heterogeneity coupled with augmented spatial coverage, temporal sampling discrepancies, and methodological or reference-database constraints. Comparisons with Japanese river and coastal studies (Ahn *et al.*, 2020; Kume *et al.*, 2021) are therefore descriptive rather than evidence that Nakara is intrinsically more diverse. Within the sampled datasets, estuarine sites associated with mangroves had higher observed richness than upstream freshwater sites (Fig. 3a-c). In Yutun, richness ranged from 4–7 OTUs at upstream sites Y3–Y7 to 30–38 OTUs at downstream sites Y1–Y2, while the two sampled Ayanda sites also contained diverse assemblages. These patterns are consistent with salinity transitions and habitat complexity (Elliott and Whitfield, 2011; Nagelkerken *et al.*, 2008), but they may also be influenced by sampling conditions and eDNA transport (Deiner *et al.*, 2017; Harrison *et al.*, 2019; Oka *et al.*, 2021). Moreover, the pronounced Shannon diversity indices recorded at several mangrove stations align with the concurrent identification of freshwater, estuarine, and marine taxa (Sheaves *et al.*, 2014; Nagelkerken *et al.*, 2008). In Udara, 59 OTUs were detected, with 34% matching species recorded by conventional surveys (Inoue *et al.*, 2016); differences may reflect sampling effort, detectability, DNA persistence, and reference-database completeness (Deiner *et al.*, 2017). The observed low compositional overlap among river basins may be indicative of underlying habitat and watershed heterogeneity; however, methodological artifacts—namely, disparities in sampling effort and temporal intervals—alongside transient biological occurrences and imperfect detectability remain confounding alternative explanations that are unresolvable within the current dataset. Sequencing-depth curves approached asymptotes for most libraries, and coverage standardization retained Nakara as the river with the highest estimated richness at the common coverage of 0.927 (123.2 OTUs; Fig. 2f). Although this outcome demonstrates that disparities in sampling

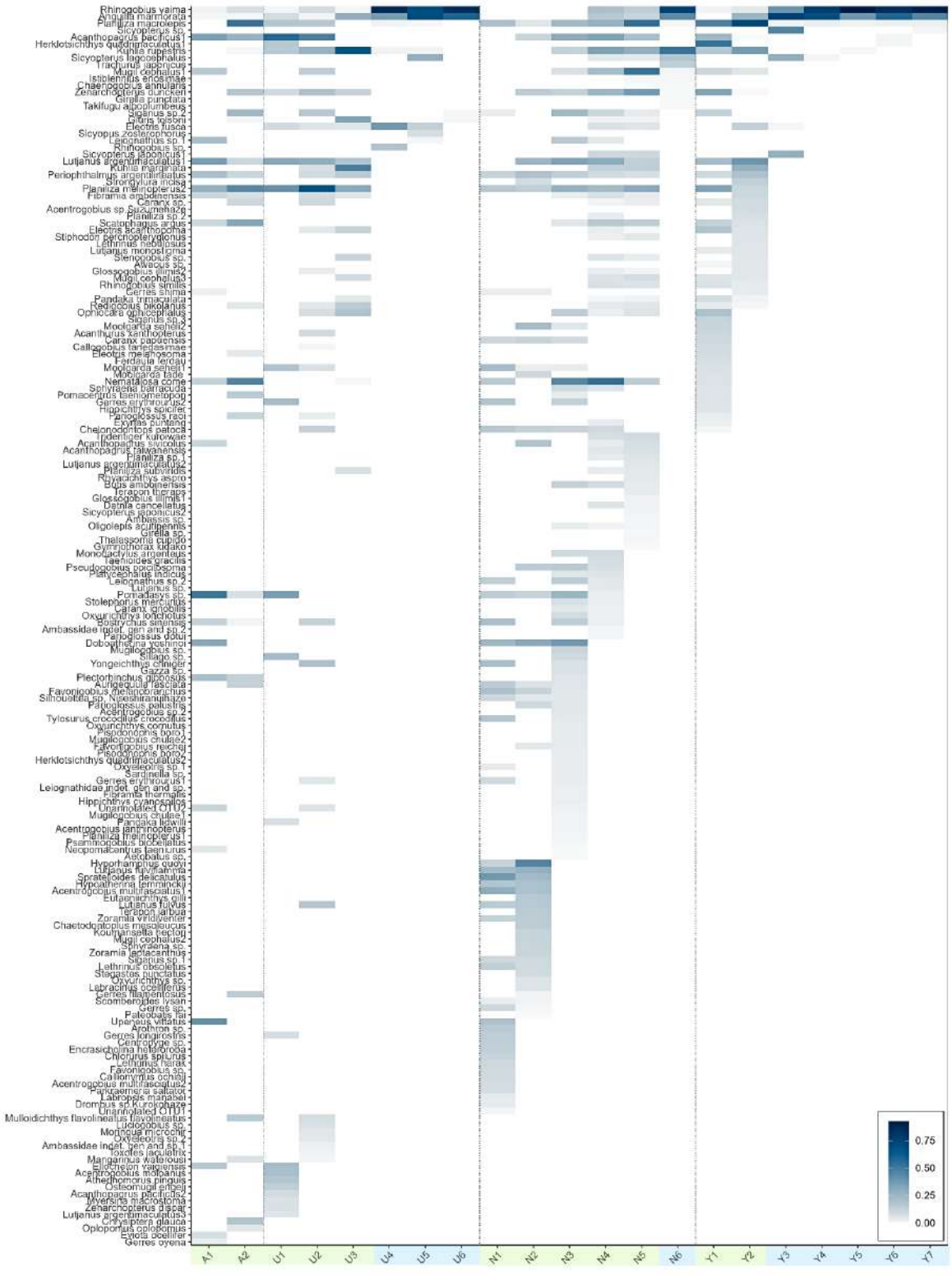

Fig. 5: Heatmap of total-standardized relative read abundances of all fish OTUs across the 21 sampling sites; blue and green denote freshwater and estuarine sites, respectively, and darker cells indicate higher relative values

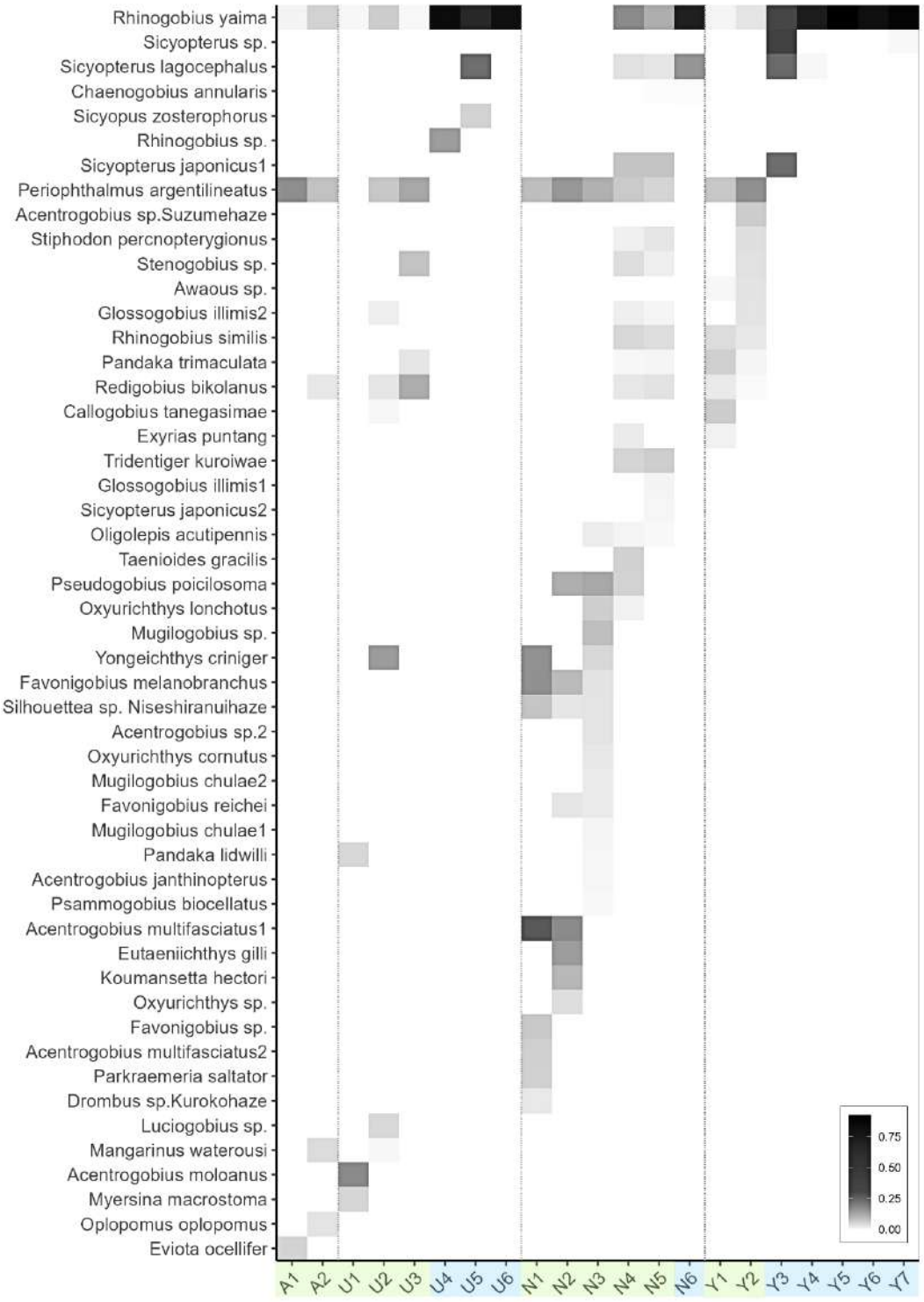

Fig. 6: Heatmap of total-standardized relative read abundances of Gobiidae OTUs across the 21 sampling sites; blue and green denote freshwater and estuarine sites, respectively, and darker cells indicate higher relative values

completeness are insufficient to drive Nakara's pronounced richness, it precludes the exclusion of potential artifacts stemming from temporal variation, habitat area, or underlying methodological and environmental divergences. Several amphidromous Red List species, including *Sicyopterus lagocephalus* and *Rhyacichthys aspro* (Fig. 3d), were detected in upstream reaches, consistent with the importance of river–sea connectivity for their life cycles (McDowall, 2009). Overall, the study provides a historical molecular inventory and illustrates the potential of eDNA for broad, non-invasive ichthyofaunal assessment, while not replacing temporally replicated or conventional surveys (Thomsen and Willerslev, 2015; Pananganan *et al.*, 2026). An important context for interpreting these observations is the low level of direct catchment development in the study rivers. Much of the interior of Iriomote Island is roadless, uninhabited, and protected within a national park, allowing these river systems to retain continuous forest-freshwater-mangrove-coastal connections. In many tropical mangrove regions, upstream settlements, roads, agriculture, and modified runoff can influence aquatic habitats and complicate interpretation of community patterns. Accordingly, the investigated fluvial systems provide valuable historical baseline observations derived from relatively undisturbed catchments, facilitating critical comparative assessments with anthropogenic-modified mangrove systems. Nevertheless, because the rivers differed in sampling years, sampling effort, length, and habitat configuration, the present results should not be treated as a universal benchmark for mangrove rivers.

Measured environmental correlates of community structure and distributional patterns

The ordination and constrained analyses identified associations between fish assemblages and the measured environmental variables. The NMDS ordination indicated separation between freshwater and estuarine locations across river systems, and the low stress value suggests that the ordination provides a reliable representation of underlying community differences (Fig. 4a). Habitat-related structuring was apparent across analyses. Both hierarchical clustering (Fig. 4b) and heatmap patterns (Figs. 5–6) identified two broad assemblages: upstream freshwater sites, where amphidromous taxa were more common, and lower-reach estuarine sites, which showed greater representation of brackish and marine-associated species. In the db-RDA, salinity and spatial location were retained as significant explanatory variables, with the primary ordination axis accounted for 48.6% of the total variation (Fig. 4d). These associations are consistent with turnover along the freshwater-to-mangrove gradient, but they do not establish causation or ecological thresholds. Freshwater sites showed higher relative read representation of low-salinity and amphidromous taxa such as *Anguilla marmorata* and *Rhinogobius yaima*, whereas estuarine sites showed greater representation of euryhaline and marine taxa, including *Planiliza, Kuhlia, Lutjanus,* and *Acanthopagrus* (Fig. 4d). PERMANOVA detected river-associated differences, and multivariate dispersion among rivers was homogeneous (PERMDISP, $p = 0.746$), suggesting that the river-level differences likely reflect shifts in community structure rather than unequal within-river variability. However, river identity is also confounded with sampling year, thereby absorbing unquantified variation attributable to intrinsic geomorphology, mangrove spatial extent, catchment scale, hydrological dynamics, and contextual sampling conditions. Gobiidae was the most OTU-rich family, accounting for 49 of 174 OTUs (28.2%). The gobiid heatmap showed marked taxon-specific partitioning from freshwater reaches to mangrove-estuarine sites

(Fig. 6), and the PCoA configurations of Gobiidae and the remaining fish community showed substantial correspondence (Procrustes r = 0.794) (Fig. 4c). However, the OTU-richness-controlled null model showed that this agreement was not greater than expected for a randomly selected 49-OTU subset (null mean r = 0.782, standardized effect size = 0.15, one-sided empirical p = 0.492). The analysis therefore does not identify Gobiidae as a statistically superior surrogate or validated indicator of the entire community. Rather, its high OTU richness, pervasive distribution across the fluvial–estuarine continuum, and distinctly structured habitat affinities underscore Gobiidae as a major and ecologically characteristic component of fish assemblages in short subtropical mangrove rivers (Itsukushima, 2023). Frequent amphidromous life histories and habitat specialization provide ecological context for this distribution (Patzner *et al.,* 2011; Yamasaki *et al.,* 2015), while cryptic and endemic gobiid lineages emphasize the need for continued taxonomic validation and connectivity studies. Collectively, these findings corroborate significant associations among biological assemblage structure, spatial positioning, and salinity gradients across the datasets, while underscoring the plausible contribution of unquantified environmental and temporal factors.

eDNA method performance, limitations, and management implications

Approximately 74% of OTUs were assigned to named species, a relatively high proportion compared with several eDNA surveys in Southeast Asian mangrove systems (Naputo *et al.,* 2024; Zainal Abidin *et al.,* 2022; Cooper *et al.,* 2026; Nob *et al.,* 2026). Nevertheless, 38 OTUs could not be uniquely resolved because of multiple reference matches or gaps and redundancies in public databases. The comparatively extensive availability of 12S reference sequences for Japanese fishes likely contributed to the achieved resolution, but incomplete reference libraries remain a major limitation (Miya *et al.,* 2015, 2020). The 174 OTUs therefore constitute a standardized historical molecular inventory rather than a complete census of the fish fauna. Evaluation of sequencing depth via rarefaction demonstrated that the majority of libraries achieved satisfactory sampling saturation concerning retained OTUs; furthermore, incidence-based standardization ensured that species richness was evaluated under conditions of comparable estimated completeness. These analyses do not demonstrate complete recovery of the river fish fauna or eliminate temporal and spatial detection limitations. The broader value of this inventory lies partly in documenting fish assemblages in relatively undisturbed forested catchments, thereby providing a reference for evaluating future ecological change within Iriomote Island and for comparison with more modified mangrove river systems elsewhere. Methodological constraints governed spatial and temporal coverage, wherein the Nakara River received a single sampling event in 2017, contrasted by bi-seasonal sampling in 2020 across the Ayanda, Udara, and Yutun catchments, alongside disparities in site densities among river basins. Because sampling year and river identity are confounded, observed cross-river differences cannot be separated from interannual and sampling-effort effects. Dissolved oxygen, pH, turbidity, nutrients, tidal stage, flow velocity, and discharge were not measured consistently and could not be evaluated as covariates. Moreover, analytical constraints are introduced by PCR amplification biases, primer specificity limitations, extracellular DNA transport and degradation dynamics, restricted detectability of rare or transient taxa, inherent risks of false-positive and false-negative classifications, and incomplete taxonomic coverage within reference databases.

The study design did not permit quantitative estimation of detection probabilities (Miya *et al.,* 2020). The use of a single mitochondrial 12S rRNA marker restricts resolution among some closely related taxa, and relative read counts cannot be interpreted directly as biomass or numerical abundance because they are affected by DNA shedding, transport, degradation, and amplification efficiency (Antinero *et al.*, 2025; Deiner *et al.*, 2017; Harrison *et al.*, 2019; Thomsen and Willerslev, 2015; Pananganan *et al.,* 2026). Environmental DNA metabarcoding should therefore complement rather than replace conventional capture, visual, and voucher-based surveys. Notwithstanding the transferability of the sampling framework to alternative mangrove networks, the direct extrapolation of specific richness metrics, taxonomic inventories, and environmental relationships remains unwarranted in the absence of localized reference databases and temporal replication. Future work should include repeated seasonal and interannual sampling, broader spatial coverage, explicit detection models, and integration with hydrological, habitat, and conventional biological observations.

CONCLUSION

Using MiFish environmental DNA metabarcoding, this study detected 174 OTUs representing 47 families and 110 genera across four short river systems, including 20 Red List species and numerous taxa associated with river–sea connectivity. Given that sampling occurred between 2017 and 2020, preceding the island's formal designation as a World Heritage site in 2021, the resulting dataset establishes a historical molecular baseline. Sequencing-depth rarefaction indicated substantial recovery of the retained OTUs in most libraries, and coverage standardization retained Nakara as the river with the highest estimated richness at the common coverage of 0.927. These quantitative outputs describe distinct sampling intervals and therefore preclude synchronous or temporally standardized comparative evaluations across river basins. Within the sampled datasets, observed richness was generally higher in mangrove-estuarine reaches, and community composition was associated with salinity and spatial location. Individual rivers contained partly distinct assemblages; however, unequal sampling effort, different sampling years, and unmeasured environmental variables preclude attributing all among-river differences solely to river characteristics. Gobiidae was the most OTU-rich family and showed marked taxon-specific partitioning across freshwater and mangrove-estuarine habitats. The spatial configuration of the subset exhibited broad concordance with the remainder of the fish assemblage; however, the OTU-richness-controlled null model failed to demonstrate statistically significant congruence exceeding expected stochasticity. These findings identify Gobiidae as a major and ecologically characteristic component of short subtropical river–mangrove assemblages. Environmental DNA metabarcoding provides a non-invasive and repeatable inventory method for protected and difficult-to-access environments, but it cannot directly estimate abundance and should complement conventional surveys. Future surveillance protocols necessitate longitudinal and cross-system replication—encompassing expanded seasonal and inter-annual sampling across additional river basins—while concurrently synthesizing molecular datasets with hydrological, habitat, and anthropogenic visitor-use data. The sampling framework may be transferable to other mangrove systems, although local richness values and taxonomic patterns should not be generalized without regional validation. As a historical dataset from minimally disturbed and largely forested catchments, these observations may also provide

a useful reference for comparative monitoring in more modified tropical and subtropical mangrove rivers. Consequently, while the historical baseline provides critical contextual insights, it does not intrinsically dictate conservation strategies or visitor-use policies within the World Heritage landscape.

AUTHOR CONTRIBUTIONS

B.G.S. Pananganan conceived and designed the study, analyzed and interpreted the data, performed the statistical analysis, drafted the manuscript, and critically revised the manuscript. S.G. Salmo III contributed to manuscript drafting, critical revision of the manuscript, and funding acquisition. T. Sado contributed to data acquisition. Y. Isowa contributed to data analysis and interpretation, statistical analysis, and manuscript drafting. H. Imai contributed to the study conception and design, data acquisition, funding acquisition, and supervision. Y. Sato contributed to conception and design, data acquisition, and funding acquisition. H. Nagai contributed to data acquisition. M. Basyuni contributed to manuscript drafting, critical revision of the manuscript, and funding acquisition. T. Yamamoto contributed to data acquisition. S. Imura contributed to data acquisition and provided administrative, technical, or material support. K. Ishigaki contributed to data acquisition and provided administrative, technical, or material support. H. Motomura contributed to data analysis and interpretation, critical revision of the manuscript, funding acquisition, and supervision. M. Miya contributed to the study conception and design, data acquisition, and funding acquisition. T. Kajita contributed to the conception and design of the study, data acquisition, data analysis and interpretation, manuscript drafting and critical revision, statistical analysis, funding acquisition, and supervision.

ACKNOWLEDGMENTS

The authors thank Katsuya Ito and Rintaro Shimoda for their assistance with field sampling. This study forms part of the first author's Ph.D. dissertation, and the co-authors have provided consent for the submission and publication.

FINANCIAL SUPPORTS

This work was supported by JSPS Core-to-Core Program [JPJSCCB20200007 and JPJSCCB20240006], JSPS KAKENHI Fund [21KK0115, 20H03311, 21H03651, 23K20304, 24K02087], JST [e-ASIA JPMJSC21E5, CREST JPMJCR13A2, COI-NEXT JPMJPF2206 and JPMJPF2102], the Ocean Shot Research Grant Program (OPRI-SPF), TBRC Grant “Project Type” 2019-2020 and the Foreign Researcher Invitation Program of the Tropical Biosphere Research Center, University of the Ryukyus.

CONFLICT OF INTEREST

The authors declare that there is no conflict of interest regarding the publication of this manuscript. In addition, ethical issues, including plagiarism, informed consent, misconduct, data fabrication and/or falsification, double publication and/or submission, and redundancy, were observed by the authors.

OPEN ACCESS

©2027 The author(s). This article is licensed under a Creative Commons Attribution 4.0 International License, which permits use, sharing, adaptation, distribution and reproduction in any medium or format, as long as you give appropriate credit to the original author(s) and the source, provide a link to the Creative Commons license, and indicate if changes were made. The images or other third-party material in this article are included in the article’s Creative Commons license, unless indicated otherwise in a credit line to the material. If material is not included in the

article's Creative Commons license and your intended use is not permitted by statutory regulation or exceeds the permitted use, you will need to obtain permission directly from the copyright holder. To view a copy of this license, visit: http://creativecommons.org/licenses/by/4.0/

PUBLISHER'S NOTE

GJESM Publisher remains neutral regarding jurisdictional claims regarding published maps and institutional affiliations.

POSITIVE AI STATEMENT

During the preparation of this work, the authors used ChatGPT to assist with English language editing, formatting, and manuscript organization. After using this tool, the authors reviewed and edited the content as needed and took full responsibility for the content of the publication.

ABBREVIATIONS

%	Percent
µL	microliters
µm	micrometers
°C	degrees Celsius
ASV	Amplicon sequence variant
bp	base pairs
C	incidence-based sample coverage
cm	Centimeter
CR	Critically Endangered
db-RDA	Distance-based redundancy analysis
DDBJ	DNA Data Bank of Japan
Dist.	Distance
DNA	Deoxyribonucleic acid
DOI	Digital Object Identifier
E	East
eDNA	Environmental deoxyribonucleic acid
EN	Endangered
Env.	environment
ETY	estuary
EB	extraction blank
FWR	freshwater
F	pseudo-F statistic
GPS	global positioning system
GSI	Geospatial Information Authority of Japan
H'	Shannon diversity index
IUCN	International Union for Conservation of Nature
Lat.	latitude
Long.	longitude
KAUM	Kagoshima University Museum
KPMNH	Kanagawa Prefectural Museum of Natural History
km	kilometer
Mf	mangrove forest
NGS	next-generation sequencing
m	meter
mL	milliliters
min	minutes
NCBI	National Center for Biotechnology Information
NMDS	Non-metric multidimensional scaling
NT	Near Threatened
N	North
OSF	Open Science Framework
OTU	Operational taxonomic unit
p	p value
PCoA	Principal coordinates analysis
PCR	Polymerase chain reaction
PERMANOVA	Permutational multivariate analysis of variance
QGIS	Quantum Geographic Information System
QIIME2	Quantitative Insights into Microbial Ecology Version 2
r	correlation coefficient
rRNA	ribosomal ribonucleic acid
Sal.	Salinity
Sf	subtropical forest
Temp.	water temperature

Veg.	Vegetation
VIF	Variance inflation factor
Vol.	water volume
VU	Vulnerable
UNESCO	United Nations Educational, Scientific and Cultural Organization

REFERENCES

Ahn, H.; Kume, M.; Terashima, Y.; Ye, F.; Kameyama, S.; Miya, M.; Yamashita, Y.; Kasai, A., (2020). Evaluation of fish biodiversity in estuaries using environmental DNA metabarcoding. PLoS ONE. 15(10): e0231127 **(15 pages)**.

Anderson, M., (2017). Permutational multivariate analysis of variance (PERMANOVA). Wiley StatsRef: Statistics Reference Online. 1-15 **(15 pages)**.

ANEMONE DB, (2026). A database for biodiversity surveys using eDNA metabarcoding.

Antinero, A.; Balaba, M.; Leopardas, V.; Aspe, N.; Kajita, T., (2025). Is it really there? Addressing inadequate sampling and false detection in environmental DNA metabarcoding. J. Environ. Sci. Manage., 27(2): 61-76 **(17 pages)**.

Bolyen, E.; Rideout, J.R.; Dillon, M.R.; Bokulich, N.A.; Abnet, C.C.; Al-Ghalith, G.A.; Alexander, H.; Alm, E.J.; Arumugam, M.; Asnicar, F.; Bai, Y.; Bisanz, J.E.; Bittinger, K.; Brejnrod, A.; Brislawn, C.J.; Brown, C.T.; Callahan, B.J.; Caraballo-Rodríguez, A.M.; Chase, J.; Cope, E.K.; Da Silva, R.; Diener, C.; Dorrestein, P.C.; Douglas, G.M.; Durall, D.M.; Duvallet, C.; Edwardson, C.F.; Ernst, M.; Estaki, M.; Fouquier, J.; Gauglitz, J.M.; Gibbons, S.M.; Gibson, D.L.; Gonzalez, A.; Gorlick, K.; Guo, J.; Hillmann, B.; Holmes, S.; Holste, H.; Huttenhower, C.; Huttley, G.A.; Janssen, S.; Jarmusch, A.K.; Jiang, L.; Kaehler, B.D.; Kang, K.B.; Keefe, C.R.; Keim, P.; Kelley, S.T.; Knights, D.; Koester, I.; Kosciolek, T.; Kreps, J.; Langille, M.G.I.; Lee, J.; Ley, R.; Liu, Y.X.; Loftfield, E.; Lozupone, C.; Maher, M.; Marotz, C.; Martin, B.D.; McDonald, D.; McIver, L.J.; Melnik, A.V.; Metcalf, J.L.; Morgan, S.C.; Morton, J.T.; Naimey, A.T.; Navas-Molina, J.A.; Nothias, L.F.; Orchanian, S.B.; Pearson, T.; Peoples, S.L.; Petras, D.; Preuss, M.L.; Pruesse, E.; Rasmussen, L.B.; Rivers, A.; Robeson, M.S.; Rosenthal, P.; Segata, N.; Shaffer, M.; Shiffer, A.; Sinha, R.; Song, S.J.; Spear, J.R.; Swafford, A.D.; Thompson, L.R.; Torres, P.J.; Trinh, P.; Tripathi, A.; Turnbaugh, P.J.; Ul-Hasan, S.; Van der Hooft, J.J.J.; Vargas, F.; Vázquez-Baeza, Y.; Vogtmann, E.; Von Hippel, M.; Walters, W.; Wan, Y.; Wang, M.; Warren, J.; Weber, K.C.; Williamson, C.H.D.; Willis, A.D.; Xu, Z.Z.; Zaneveld, J.R.; Zhang, Y.; Zhu, Q.; Knight, R.; Caporaso, J.G., (2019). Reproducible, interactive, scalable and extensible microbiome data science using QIIME 2. Nat. Biotechnol., 37(8): 852-857 **(6 pages)**.

Bray, J.R.; Curtis, J.T., (1957). An ordination of the upland forest communities of southern Wisconsin. Ecol. Monogr., 27(4): 325-349 **(25 pages).**

Callahan, B.J.; McMurdie, P.J.; Rosen, M.J.; Han, A.W.; Johnson, A.J.A.; Holmes, S.P., (2016). DADA2: High-resolution sample inference from Illumina amplicon data. Nat. Methods. 13(7): 581-583 **(3 pages)**.

Chiarucci, A.; Bacaro, G.; Scheiner, S., (2011). Old and new challenges in using species diversity for assessing biodiversity. Philos. Trans. R. Soc. B Biol. Sci., 366(1576): 2426-2437 **(12 pages).**

Convention on Biological Diversity, (1992). Secretariat of the Convention on Biological Diversity Montreal **(36 pages).**

Cooper, E.K.T.; Trillo, J.P.; Tucong, E.J.A.; Evasco Jr., A.C.; Nob, C.J.R.; Pananganan, B.G.S.; Leopardas, V.E.; Honghong Jr., J.E.; Don, P.N.; Hinoguin, A.D.P.; Aspe, N.M.; Gonzales, R.C.; Dolorosa, R.G.; Basyuni, M.; Kajita, T., (2026). Genetic reference gaps limit eDNA metabarcoding and biodiversity monitoring of tropical mangrove ecosystems. Environ. DNA. 8(3): e70280 **(19 pages).**

Davies, T.E.; Maxwell, S.M.; Kaschner, K.; Garilao, C.; Ban, N.C., (2017). Large marine protected areas represent biodiversity now and under climate change. Sci. Rep., 7(1) **(7 pages)**.

Deiner, K.; Bik, H.; Mächler, E.; Seymour, M.; Lacoursière-Roussel, A.; Altermatt, F.; Creer, S.; Bista, I.; Lodge, D.; de Vere, N.; Pfrender, M.; Bernatchez, L., (2017). Environmental metabarcoding: Transforming how we survey animal and plant communities. Mol. Ecol., 26(21): 5872-5895 **(24 pages)**.

Elliott, M.; Whitfield, A.K., (2011). Challenging paradigms in estuarine ecology and management. Estuar. Coast. Shelf Sci., 94(4): 306-314 **(9 pages)**.

Feller, I.C.; Lovelock, C.E.; Berger, U.; McKee, K.L.; Joye, S.B.; Ball, M.C., (2010). Biocomplexity in mangrove ecosystems. Annu. Rev. Mar. Sci., 2(1): 395-417 **(23 pages)**.

Froese, R.; Pauly, D., (2024). FishBase.

Harrison, J.; Sunday, J.; Rogers, S., (2019). Predicting the fate of eDNA in the environment and implications for studying biodiversity. Proc. R. Soc. B Biol. Sci., 286(1915) **(9 pages)**.

Inoue, T.; Nanjo, K.; Mizutani, A.; Kitano, T.; Kawano, H., (2016). Fish community structure in the Udara River, Amitori Bay, Iriomote Island. Jpn. J. Ichthyol., 63: 63-79 **(17 pages)**.

Itsukushima, R., (2023). Broad-scale environmental factors determining fish species composition of river estuaries in the Japanese Archipelago. Estuaries Coasts, 46(7): 1829-1843 **(15 pages)**.

IUCN, (2025). The IUCN Red List of Threatened Species. Version 2025-1.

Kruskal, J.B., (1964). Nonmetric multidimensional scaling: A numerical method. Psychometrika, 29(2): 115-129 **(15 pages)**.

Kume, M.; Lavergne, E.; Ahn, H.; Terashima, Y.; Kadowaki, K.; Ye, F.; Kameyama, S.; Kai, Y.; Henmi, Y.; Yamashita, Y.; Kasai, A., (2021). Factors structuring estuarine and coastal fish communities across Japan using environmental DNA metabarcoding. Ecol. Indic., 121: 107216 **(8 pages)**.

Lee, S.Y.; Primavera, J.; Dahdouh-Guebas, F.; McKee, K.; Bosire, J.; Cannicci, S.; Diele, K.; Fromard, F.; Koedam, N.; Marchand, C.; Mendelssohn, I.; Mukherjee, N.; Record, S., (2014). Ecological role and services of tropical mangrove ecosystems: A reassessment. Glob. Ecol. Biogeogr., 23(7): 726-743 **(18 pages)**.

Legendre, P.; Anderson, M., (1999). Distance-based redundancy analysis: Testing multispecies responses in multifactorial ecological experiments. Ecol. Monogr., 69(1): 1-24 **(24 pages)**.

Martin, M., (2011). Cutadapt removes adapter sequences from high-throughput sequencing reads. EMBnet.journal, 17(1): 10-12 **(3 pages)**.

McDowall, R.M., (2009). Why be amphidromous: Expatrial dispersal and the place of source and sink population dynamics? Rev. Fish Biol. Fish., 20(1): 87-100 **(14 pages)**.

Minamoto, T.; Miya, M.; Sado, T.; Seino, S.; Doi, H.; Kondoh, M.; Nakamura, K.; Takahara, T.; Yamamoto, S.; Yamanaka, H.; Araki, H.; Iwasaki, W.; Kasai, A.; Masuda, R.; Uchii, K., (2021). An illustrated manual for environmental DNA research: Water sampling guidelines and experimental protocols. Environ. DNA, 3(1): 8-13 **(6 pages)**.

Ministry of the Environment, (2020). The Ministry of the Environment Red List. [In Japanese].

Miya, M.; Sato, Y.; Fukunaga, T.; Sado, T.; Poulsen, J.Y.; Sato, K.; Minamoto, T.; Yamamoto, S.; Yamanaka, H.; Araki, H.; Kondoh, M.; Iwasaki, W., (2015). MiFish, a set of universal PCR primers for metabarcoding environmental DNA from fishes: Detection of more than 230 subtropical marine species. R. Soc. Open Sci., 2(7): 150088 **(33 pages)**.

Miya, M.; Gotoh, R.; Sado, T., (2020). MiFish metabarcoding: A high-throughput approach for simultaneous detection of multiple fish species from environmental DNA and other samples. Fish. Sci., 86(6): 939-970 **(32 pages)**.

Motomura, H. 2024. List of Japan's all fish species. Current standard Japanese and scientific names of all fish species recorded from Japanese waters. The Kagoshima University Museum, Kagoshima. Online (Excel) version 25.

Nagelkerken, I.; Blaber, S.J.; Bouillon, S.; Green, P.; Haywood, M.; Kirton, L.G.; Meynecke, J.-O.; Pawlik, J.; Penrose, H.M.; Sasekumar, A.; Somerfield, P.J., (2008). The habitat function of mangroves for terrestrial and marine fauna: A review. Aquat. Bot., 89(2): 155-185 **(31 pages)**.

Naputo, C.; Isowa, Y.; Gerona-Daga, M.E.; Artigas, M.D.; Kajita, T.; Salmo, S., III, (2024). Application of eDNA metabarcoding in the assessment of fish biodiversity in Philippine mangroves: Challenges and opportunities. Reg. Stud. Mar. Sci., 77: 103642 **(10 pages)**.

Nob, C.; Isowa, Y.; Trillo, J.; Pananganan, B.; Cooper, E.; Hinoguin, A.; Evasco, A.; Honghong, J.; Aspe, N.; Dolorosa, R.; Mendoza, T.; Gevaña, D.; Bobiles, R.; Tolentino, J.; Tucong, E.; Noval-Don, P.; Gonzales, R.; Leopardas, V.; Kajita, T., (2026). Mangrove-associated fish biodiversity in selected Philippine bioregions during the northeast (Amihan) monsoon: Insights from eDNA metabarcoding for biomonitoring. Environ. DNA, 8(2): e70273 **(14 pages)**.

Oka, S.; Doi, H.; Miyamoto, K.; Hanahara, N.; Sado, T.; Miya, M., (2021). Environmental DNA metabarcoding for biodiversity monitoring of a highly diverse tropical fish community in a coral reef lagoon: Estimation of species richness and detection of habitat segregation. Environ. DNA, 3(1): 55-69 **(15 pages)**.

Okinawa Prefectural Government, (2017). Threatened wildlife in Okinawa, third edition (Animals): Red data Okinawa **(673 pages)**.

Oksanen, J.; Simpson, G.L.; Blanchet, F.G.; Kindt, R.; Legendre, P.; Minchin, P.R.; O'Hara, R.B.; Solymos, P.; Stevens, M.H.H.; Szoecs, E.; Wagner, H.; Barbour, M.; Bedward, M.; Bolker, B.; Borcard, D.; Carvalho, G.; Chirico, M.; De Caceres, M.; Durand, S.; Evangelista, H.B.A.; FitzJohn, R.; Friendly, M.; Furneaux, B.; Hannigan, G.; Hill, M.O.; Lahti, L.; McGlinn, D.; Ouellette, M.-H.; Ribeiro Cunha, E.; Smith, T.; Stier, A.; Ter Braak, C.J.F.; Weedon, J., (2025). vegan: Community Ecology Package. R package version 2.7-2.

Pananganan, B.G.S.; Juliano, M.G.; Isowa, Y.; Ramirez, M.D.A.; Motomura, H.; Kajita, T., (2026). eDNA reveals extraordinary fish diversity in the Urauchi River, Iriomote Island, Japan, a UNESCO World Heritage Site. PeerJ. 14: e21399 **(22 pages)**.

Patzner, R.; Tassell, J.V.; Kovacic, M., (2011). The biology of gobies. Science Publishers, Enfield, NH, Boca Raton, FL. **(702 pages).**

R Core Team, (2023). R: A language and environment for statistical computing. R Foundation for Statistical Computing, Vienna, Austria.

Rognes, T.; Flouri, T.; Nichols, B.; Quince, C.; Mahé, F., (2016). VSEARCH: A versatile open source tool for metagenomics. PeerJ, 4: e2584 **(22 pages)**.

Sato, Y.; Hermawan, I.; Kakita, T.; Okano, S.; Imai, H.; Nagai, H.; Kimura, R.; Yamashiro, T.; Kajita, T.; Toma, C., (2022). Analysis of human clinical and environmental Leptospira to elucidate the eco-epidemiology of leptospirosis in Yaeyama, subtropical Japan. PLoS Negl. Trop. Dis., 16(3): e0010234 **(24 pages)**.

Sheaves, M.; Baker, R.; Nagelkerken, I.; Connolly, R., (2014). True value of estuarine and coastal nurseries for fish: Incorporating complexity and dynamics. Estuaries Coasts. 38(2): 401-414 **(14 pages)**.

Stuart-Smith, R.; Bates, A.; Lefcheck, J.; Duffy, J.E.; Baker, S.; Thomson, R.; Stuart-Smith, J.; Hill, N.; Kininmonth, S.; Airoldi, L.; Becerro, M.; Campbell, S.; Dawson, T.; Navarrete, S.; Soler, G.; Strain, E.A.; Willis, T.; Edgar, G., (2013). Integrating abundance and functional traits reveals new global hotspots of fish diversity. Nature. 501(7468): 539-542 **(4 pages)**.

Suzuki, T.; Senou, H., (2005). A preliminary checklist of fishes in the Urauchi River and Tudumari Beach, Iriomote Island. In: Urauchi River Basin Research Group, (Ed.), Summary report II on biodiversity and traditional resource use in the estuary of the Urauchi River, Iriomote Island. [In Japanese] **(12 pages).**

Thomsen, P.F.; Willerslev, E., (2015). Environmental DNA: An emerging tool in conservation for monitoring past and present biodiversity. Biol. Conserv., 183: 4-18 **(15 pages)**.

UNESCO World Heritage Centre, (2021). Amami-Ōshima Island, Tokunoshima Island, Northern part of Okinawa Island, and Iriomote Island [World Heritage List, Site No. 1574].

Valentini, A.; Taberlet, P.; Miaud, C.; Civade, R.; Herder, J.; Thomsen, P.F.; Bellemain, E.; Besnard, A.; Coissac, E.; Boyer, F.; Gaboriaud, C.; Jean, P.; Poulet, N.; Roset, N.; Copp, G.H.; Geniez, P.; Pont, D.; Argillier, C.; Baudoin, J.-M.; Peroux, T.; Crivelli, A.J.; Olivier, A.; Acqueberge, M.; Le Brun, M.; Møller, P.R.; Willerslev, E.; Dejean, T., (2016). Next-generation monitoring of aquatic biodiversity using environmental DNA metabarcoding. *Mol. Ecol.* 25(4): 929–942 **(14 pages).**

Wickham, H., (2016). Data Analysis. In: ggplot2. Use R! Springer, Cham. 189-201 **(13 pages)**.

Yamamoto, S.; Masuda, R.; Sato, Y.; Sado, T.; Araki, H.; Kondoh, M.; Minamoto, T.; Miya, M., (2017). Environmental DNA metabarcoding reveals local fish communities in a species-rich coastal sea. Sci. Rep., 7(1): 40368 **(12 pages)**.

Yamasaki, Y.; Nishida, M.; Suzuki, T.; Mukai, T.; Watanabe, K., (2015). Phylogeny, hybridization, and life history evolution of Rhinogobius gobies in Japan, inferred from multiple nuclear gene sequences. Mol. Phylogenet. Evol., 90: 20-33 **(14 pages)**.

Zainal Abidin, D.H.; Mohd Nor, S.A.; Lavoué, S.; Rahim, M.A.; Mohammed Akib, N.A., (2022). Assessing a megadiverse but poorly known community of fishes in a tropical mangrove estuary through environmental DNA (eDNA) metabarcoding. Sci. Rep., 12: 16346 **(16 pages)**.

Zhang, Z.; Schwartz, S.; Wagner, L.; Miller, W., (2000). A greedy algorithm for aligning DNA sequences. J. Comput. Biol., 7: 203–214 **(14 pages)**.

AUTHOR (S) BIOSKETCHES

Pananganan, B.G.S., Ph.D., Researcher, United Graduate School of Agricultural Sciences, Kagoshima University, 1-21-30 Korimoto, Kagoshima, Japan/ Iriomote Station, Tropical Biosphere Research Center, University of the Ryukyus, 870 Uehara, Taketomi-cho, Yaeyama-gun, Okinawa 907-1541, Japan.
- Email: *bernadeth.pananganan@gmail.com*
- ORCID: 0009-0007-5687-4734
- Web of Science ResearcherID: QSO-2830-2026
- Scopus Author ID: 60414469700
- Homepage: https://scholar.google.com/citations?user=MiSoWSIAAAAJ&hl=en

Salmo, S. G. III, Ph.D., Associate Professor, Institute of Biology, University of the Philippines Diliman, National Science Complex, Regidor St, Diliman, Quezon City, Philippines.
- Email: *sgsalmo@up.edu.ph*
- ORCID: 0000-0001-6807-4397
- Web of Science ResearcherID: T-4794-2018
- Scopus Author ID: 36097541900
- Homepage: https://biology.science.upd.edu.ph/profile-severino-g-salmo-iii/

Sado, T., Ph.D., Researcher, National Institute for Environmental Studies (NIES), Lake Biwa Branch Office, Otsu, Japan.
- Email: *zacco_evolans@yahoo.co.jp*
- ORCID: 0000-0003-2137-0759
- Web of Science ResearcherID: FWF-4461-2022
- Scopus Author ID: 8611680800
- Homepage: https://www.nies.go.jp/en/about/organization/biwako.html

Isowa, Y., Ph.D., Assistant Professor, Iriomote Station, Tropical Biosphere Research Center, University of the Ryukyus, 870 Uehara, Taketomi-cho, Yaeyama-gun, Okinawa 907-1541, Japan.
- Email: *yukinobuisowa@gmail.com*
- ORCID: 0009-0009-5733-4355
- Web of Science ResearcherID: CVK-5709-2022
- Scopus Author ID: 55341544900
- Homepage: https://nrid.nii.ac.jp/ja/nrid/1000070782572/

Imai, H., Ph.D., Professor, Faculty of Science, University of the Ryukyus, 1 Senbaru, Nishihara, Okinawa 903-0213, Japan.
- Email: *imai@cs.u-ryukyu.ac.jp*
- ORCID: 0000-0002-3793-1146
- Web of Science ResearcherID: FBS-6434-2022
- Scopus Author ID: 36723639800
- Homepage: https://researchmap.jp/read0119238?lang=en

Sato, Y., Ph.D., Associate Professor, Research Laboratory Center, Faculty of Medicine, University of the Ryukyus, 1076 Kiyuna, Ginowan, Okinawa, Japan.
- Email: *yuksato@cs.u-ryukyu.ac.jp*
- ORCID: 0000-0001-5175-6316
- Web of Science ResearcherID: KUS-0356-2024
- Scopus Author ID: 23393502000
- Homepage: https://researchmap.jp/7000004491?lang=en

Nagai, H., Ph.D., Researcher, Faculty of Science, University of the Ryukyus, 1 Senbaru, Nishihara, Okinawa 903-0213, Japan
- Email: *atyidaenagai@gmail.com*
- ORCID: 0009-0006-9515-3270
- Web of Science ResearcherID: NA
- Scopus Author ID: 57558715200
- Homepage: https://www.researchgate.net/scientific-contributions/Hiroto-Nagai-2218273199

Basyuni, M., Ph.D., Professor, Faculty of Forestry, Universitas Sumatera Utara, 2nd Campus of USU, Kwala Bekala, Deli Serdang Regency, North Sumatra 20355, Indonesia.
- Email: *m.basyuni@usu.ac.id*
- ORCID: 0000-0003-1120-8571
- Web of Science ResearcherID: D-8537-2015
- Scopus Author ID: 15055287200
- Homepage: https://fhut.usu.ac.id/en/lecturer/mohammad-basyuni

Yamamoto, T., Teacher, Hijirigaoka High & Junior High School, Tama University, Tokyo, Japan.
- Email: *t.yamamoto.vm@gmail.com*
- ORCID: 0009-0004-5306-2560
- Web of Science ResearcherID: NA
- Scopus Author ID: NA
- Homepage: https://www.hijirigaoka.ed.jp/

Imura, S., Technical Staff, Iriomote Station, Tropical Biosphere Research Center, University of the Ryukyus, 870 Uehara, Taketomi-cho, Yaeyama-gun, Okinawa 907-1541, Japan
- Email: *s-imura@cs.u-ryukyu.ac.jp*
- ORCID: 0009-0001-0257-0344
- Web of Science ResearcherID: FAC-0443-2022
- Scopus Author ID: 54896092200
- Homepage: https://tbc.skr.u-ryukyu.ac.jp/iriomote/en/staff

Ishigaki, K., Technical Staff, Iriomote Station, Tropical Biosphere Research Center, University of the Ryukyus, 870 Uehara, Taketomi-cho, Yaeyama-gun, Okinawa 907-1541, Japan.
- Email: *keiichi@cs.u-ryukyu.ac.jp*
- ORCID: 0009-0003-4967-1673
- Web of Science ResearcherID: CVR-5998-2022
- Scopus Author ID: 55523658300
- Homepage: https://tbc.skr.u-ryukyu.ac.jp/iriomote/en/staff

Motomura, H., Ph.D., Professor, The Kagoshima University Museum, Kagoshima University, 1-21-30 Korimoto, Kagoshima 890-0065, Japan.
- Email: *motomura@kaum.kagoshima-u.ac.jp*
- ORCID: 0000-0002-7448-2482
- Web of Science ResearcherID: 0-4081-2014
- Scopus Author ID: 7202353066
- Homepage: https://www.museum.kagoshima-u.ac.jp/staff/motomura/motomura.html

Miya, M., Ph.D., Visiting Senior Researcher, Research Organization for Nano & Life Innovation, Waseda University, Tokyo, Japan.
- Email: masaki_miya@me.com
- ORCID: 0000-0002-9791-9886
- Web of Science ResearcherID: FMW-1314-2022
- Scopus Author ID: 7005173446
- Homepage: https://researchmap.jp/mum-usagi

Kajita, T., Ph.D., Professor, Iriomote Station, Tropical Biosphere Research Center, University of the Ryukyus, 870 Uehara, Taketomi-cho, Yaeyama-gun, Okinawa 907-1541, Japan.
- Email: *tkaji@cs.u-ryukyu.ac.jp*
- ORCID: 0000-0003-1232-4179
- Web of Science ResearcherID: NA
- Scopus Author ID: NA
- Homepage: https://researchmap.jp/read0076992?lang=en

HOW TO CITE THIS ARTICLE:
Pananganan B.G.S.; Salmo, S.G.III; Sado, T.; Isowa, Y.; Imai, H.; Sato, Y.; Nagai, H.; Basyuni, M.; Yamamoto, T.; Imura, S.; Ishigaki, K.; Motomura, H.; Miya, M.; Kajita, T., (2027). Environmental deoxyribonucleic acid metabarcoding reveals fish diversity in subtropical island mangrove rivers. Global J. Environ. Sci. Manage., 13(1): 27-50.

DOI: 10.22034/gjesm.2027.01.02
URL: https://www.gjesm.net/article_735558.html

Global Journal of Environmental Science and Management
(GJESM)

Homepage: https://www.gjesm.net/

Podcasts

ORIGINAL RESEARCH ARTICLE

The effect of agricultural taxes and local agricultural policies on enhancing food security and environmental sustainability

M.S. Setyowati[1,*], R.K. Hanum[2]

[1]Faculty of Administrative Science, Universitas Indonesia, Depok, 16424 Indonesia

[2]Institute for the Assessment and Application of Administrative Sciences, Faculty of Administrative Science, Universitas Indonesia, Depok, 16424 Indonesia

ARTICLE INFO

Article History:
Received 15 April 2026
Revised 18 June 2026
Accepted 22 July 2026

Keywords:
Agricultural productivity
Agricultural tax policy
Environmental sustainability
Food security
Sustainable development goals

DOI:10.22034.gjesm.2027.01.03

ABSTRACT

BACKGROUND AND OBJECTIVES: Indonesia is currently working towards sustainability in line with Sustainable Development Goal 2 (Zero Hunger). Anticipated demographic growth to 10.8 billion by the year 2050 is expected to place unprecedented strain on global food security and production systems. The study objectives were to examine the biophysical factors, production inputs, economic conditions, socio-technological factors, agricultural business management, and agricultural tax policies regional agricultural policies and, ultimately, agricultural productivity.

METHODS: This quantitative study employed structured questionnaires administered to a sample of 200 farmers in Surabaya. The instrument used a one-to-five Likert scale covering biophysical factors, economic factors, tax policy, tax morale, and agricultural productivity. Data was analyzed using partial least squares-structural equation modeling version 3. The analytical procedure comprised three distinct phases: first, evaluating the outer model for convergent and discriminant validity; second, conducting reliability assessments; and third, testing the inner model via bootstrapping to determine the coefficient of determination, the effect size, and hypothesis significance. Hypothesis significance was determined using t-statistic values of at least 1.96 and p-values of no more than 0.05.

FINDINGS: Four hypotheses were rejected: economic factor on regional agricultural policy (p-value 0.557), agricultural taxation policy on tax morale (p-value 0.072), tax awareness on agricultural productivity (p-value 0.058), and tax morale on agricultural productivity (p-value 0.208). The findings reveal that regional agricultural policies are substantially driven by three key dimensions: biophysical factors (beta coefficient of 0.251, probability value of 0.000), production inputs (beta coefficient of 0.253, probability value of 0.002), and agricultural business management (beta coefficient of 0.228, probability value of 0.007). Agricultural tax policy significantly affects tax awareness (beta coefficient of -0.229, probability value of 0.000), while tax administration efficiency also significantly affects tax awareness (beta coefficient of -0.345, probability value of 0.000) and tax morale (beta coefficient of -0.634, probability value of 0.000), since clarity on procedures, benefits, and regulations fosters public responsibility and awareness of taxpayer obligations and rights.

CONCLUSION: Elevating agricultural output demands comprehensive frameworks characterized by active farmer participation, supportive regulatory policies, targeted outreach regarding tax frameworks, and enhanced coordination between industry stakeholders and governmental bodies. Regional agricultural policies and tax awareness significantly influence agricultural productivity. These findings offer practical insights for policymakers aiming to strengthen agricultural governance and tax compliance frameworks in support of sustainable rural development.

This is an open access article under the CC BY license (http://creativecommons.org/licenses/by/4.0/)

NUMBER OF REFERENCES	NUMBER OF FIGURES	NUMBER OF TABLES
51	2	8

*Corresponding Author:
Email: milla.s@ui.ac.id
Phone: +6221 7884 9087
ORCID: 0000-0002-7525-5521

Note: Discussion period for this manuscript open until March 01, 2027 on GJESM website at the "Show Article".

INTRODUCTION

Agricultural systems are facing climate change and environmental degradation, which can reduce agricultural production (Van *et al.,* 2026). Agriculture is also an important sector for human survival because it is a basic need and is related to food sources needed for survival (Bangun, 2024). The agricultural sector is fundamentally linked to national food security. Between 2001 and 2021, global agricultural output expanded by 54 percent (%), and production is projected to rise further in tandem with an anticipated population growth of 59% to 102% (Fukase and Martin, 2020). Food security is a top priority for all countries, especially developing countries where the population can grow faster than developed countries (Pawlak and Kołodziejczak, 2020). Therefore, the role of the agricultural sector is very important because it is the main line in achieving food security (Ndwiga *et al.,* 2025). Characterized by extensive scholarly investigation, sustainable agriculture has emerged as a prominent paradigm undergoing widespread implementation and conceptual evolution (Mufida, 2024; Hadi *et al.,* 2025). The agricultural sector can be the foundation of food security; if agricultural products run sustainably, the need for food can be met, and problems such as hunger and malnutrition can be avoided (Gil *et al.*, 2019). Furthermore, the agricultural sector is experiencing rapid expansion, with diverse technological innovations increasingly deployed to sustain community food requirements. Agriculture by relying on soil media alone will not be enough at this time, so new innovations have emerged that aim to realize sustainable agriculture, such as hydroponic techniques, vertical culture, and aeroponics to meet the increasing market demand (Garzón *et al.*, 2023). This goal is in line with the second Sustainable development goals (SDG) (zero hunger) and SDG 12 (responsible consumption and production) programs to end hunger, achieve food security, and realize sustainable agriculture (Bizikova *et al.*, 2020). Effective maintenance of food security promotes public health improvements and ensures the adequate intake of essential dietary nutrients (Pandey and Pandey, 2023). This is in line with the goal of SDG 3 (good health and well-being), which is to maintain health and improve fitness for all ages. Women play an important role in the agricultural sector, which aims to increase food security and nutrients contained in food ingredients as well as to market agricultural products (Abraham and Pingali, 2020). Furthermore, strengthening the agricultural sector indirectly advances SDG 5 (gender equality) by recognizing women as vital contributors alongside men in agricultural management (Arintyas, 2024). In addition, agriculture plays a crucial role in reducing climate change. The amount of vegetation that occurs can be one of the steps to protect the environment and reduce global, SDG 13 (climate action), which aims to keep climate change from changing to extremes, has become a global agenda to prevent other natural disasters (Castro *et al.*, 2019; Schaafsma *et al.*, 2019). According to the 2023 agricultural census conducted by Statistics Indonesia, individual agricultural holdings increased by 7.45%, rising from 29,342,202 units to 31,705,295 units (Statistics Indonesia, 2023). Although there is an increase in land ownership, it does not prevent the import of agricultural products to meet the consumption needs of the community. Even from January to February 2024, rice imports amounted to 880,820 tons worth United States Dollar (USD) 564.51 million. This volume has experienced a significant increase of 93% compared to January to February 2023. This challenge stems from a decline in agricultural output, which has failed to keep pace with the escalating consumption demands of the population. The situation related to agricultural imports also involves challenges that local farmer face. Despite expanded land ownership, local farmers often struggle to advance due to persistent reliance on outdated agricultural practices and technologies. The absence of innovation may result in reduced

productivity and inefficiencies in farming (Syarifudin and Saputra, 2024). Furthermore, the problem on the reduction of local productivity also poses threats to food security. The concurrent pressures of rapid global population growth and climate change on agricultural systems heighten the imperative for sustainable and efficient farming practices (Touch *et al.*, 2024). In the policy-making perspective, the pursuit of specific objectives often conflicts with some priorities (Benni *et al.*, 2024). To illustrate, although environmental conservation frameworks are essential for long-term sustainability, they may inadvertently constrain agricultural yields and concurrently drive up consumer expenditures. Furthermore, to implement the policy, one the most important thing is public acceptance (Sager and Gofen, 2022). A key factor of a high willingness of public to accept the agricultural initiatives lies in the diverse objectives encompassed by agricultural (Nguyen *et al.*, 2021). To achieve a strong level of public support, it is essential to ensure that the policy accepted by taxpayers and consumers (Benni *et al.*, 2024). Government can build trust and legitimacy among the public and simultaneously ensure the public support for the agricultural policies (Nguyen *et al.*, 2021). Agriculture is foundational to macroeconomic stability; wherein optimized land management serves as a critical driver for improving rural and domestic economic well-being. To put context, properly managed agricultural land can generate more returns, simultaneously increasing the livelihoods of farming communities' household income (Robinson, 2024). Achieving these objectives necessitates collaborative efforts between farmers and governmental bodies. Supportive agricultural policies can enhance productivity by facilitating access to essential resources, including quality seeds, markets, subsidies, and tax incentives. Nowadays various countries are widely applying taxation related to the environment. The move aims to improve land management, reduce pollution, improve energy efficiency, protect biodiversity, and reduce the effects of climate change (Fendrich *et al.*, 2022). The Agriculture for Development strategy can be used to overcome problems by using two approaches, the "supply side" and the "demand side" (Bridle *et al.*, 2020; Janvry and Sadoulet, 2020). Data on agricultural processes is used to support the potential increase that will likely arise in the future (Khan *et al.*, 2021). Economic instruments that can be provided to support the development of the agricultural sector can include taxes, subsidies, and emission relief allowances (Deboe, 2020). The financial incentives provided can also be subsidies and tax breaks (Oebel *et al.*, 2025). Fiscal instruments such as subsidies and tax relief are designed to mitigate agricultural operating costs, enabling producers to allocate additional resources toward production enhancement. Likewise, these financial tools may incentivize the farmers to have high quality equipment, techniques, seeds, and many more related to the operational of the farm. Additionally, incentive mechanisms can be utilized to evaluate the efficacy of transitions towards a sustainable food security framework. By that, incentives not only enhance the agricultural productivity but also encourage farmers to adopt with the innovative and environmentally friendly practices. Likewise, the good design of tax incentives may encourage the modern practices of agricultural making the process more effective and the goods produced in high quality (Pineiro *et al.*, 2020). Furthermore, the implementation of tax incentives can facilitate progress toward achieving higher-quality food production systems (Michalke *et al.*, 2023; Milošević *et al.*, 2020; Oebel *et al.*, 2025). Align with that, incentive programs must be regularly developed and evaluated to ensure the effectiveness towards farmers need and agricultural development. Kusuma and Simanungkalit, (2022) have researched how the provision of tax incentives in the form of reducing Income Tax by 25 instalments for corporate taxpayers is on the agenda for national recovery in Indonesia (Kusuma and Simanungkalit, 2022). This study investigates the policy implementation

variables proposed in the G Edwards III framework. Specifically, the research model incorporates communication, bureaucratic structure, resources, disposition, and implementation (Kusuma and Simanungkalit, 2022). Taing and Chang (2020) also researched tax compliance carried out by people in Cambodia. This study uses the theory of planned behavior (TPB) using three components, namely attitudes, subjective norms and perceived behavioral control, which is further developed into variables: tax morality, tax justice, tax complexity, tax information, and tax awareness. Empirical results demonstrate that citizen tax compliance in Cambodia is shaped by multiple determinants, including the efficacy of local authorities, institutional trust, access to tax information, and individual tax awareness (Taing and Chang, 2020). Furthermore, Yin *et al.* (2022) conducted research on how adequate policies and infrastructure can affect the sustainable improvement of agricultural land and aim to increase food security in China. Grounded in the extended theory of planned behavior, this investigation utilizes this theoretical framework to conceptualize and derive its key research variables. Socio-psychological factors, production inputs, improvement of biodiversity systems, attitudes, and environmental factors are studied and adjusted to the research context. The variables of this study use the modification of variables from previous studies (Khan *et al.*, 2021; Viaggi *et al.*, 2021; Oebel *et al.*, 2025; Michalke *et al.*, 2023; Milošević *et al.*, 2020; Kusuma and Simanungkalit, 2022; Taing and Chang, 2020; Yin *et al.*, 2022) to adapt to the context of the research being conducted and to maintain its relevance. Despite a growing body of literature on agricultural policy and tax compliance, empirical research remains scarce regarding how agricultural taxation frameworks and local governance collectively influence farmer behavior and productivity within a unified structural model across developing economies. This study aims to address this gap by integrating the TPB (Taing and Chang, 2020) and the G. Edward III (Kusuma and Simanungkalit, 2022) policy implementation model to examine: 1) how biophysical factors, production inputs, economic conditions, socio-technological factors, and agricultural business management influence regional agricultural policies; 2) how agricultural tax policies and tax administration efficiency shape tax awareness and tax morale among farmers; and 3) how regional agricultural policies, tax. This study was conducted in Surabaya, Indonesia in 2024, providing empirical evidence from an urban-agricultural context within a developing economy.

MATERIALS AND METHODS

A purposive sampling technique was employed to select participating farmers based on the following criteria: 1) aged 18 years or above, 2) currently working as farmers, and 3) owning agricultural land in the Surabaya area. (Fig. 1). The sampling frame was developed through coordination with local agricultural extension officers and farmer group leaders who maintained registers of active farmers in the study area. Prospective participants were recruited by enumerators at their respective agricultural holdings or via regional farmer association assemblies. The survey achieved an 85% response rate, corresponding to 200 completed questionnaires out of 235 individuals solicited. Based on the data collection results, respondents were dominated by people over 40 years old (56%), followed by age 21-30 (34.5%), and age 31-40 (9.5%). Most respondents were male (92.5%), with female respondents at 7.5%. Educational background was dominated by high school graduates (47%), followed by elementary school graduates (21.5%), applied bachelor's degree graduates (19%), and junior high school graduates (12.5%). Marital status: married (69%), unmarried (23.5%), and divorced (7.5%). Monthly expenditure: USD 55.56 - 222.22 (78.5%), more than USD 222.22 (13.5%), and less than USD 55.56 (8%). The selection of Surabaya as the study area is justified by its unique geographical profile. Despite its status as a largely urbanized

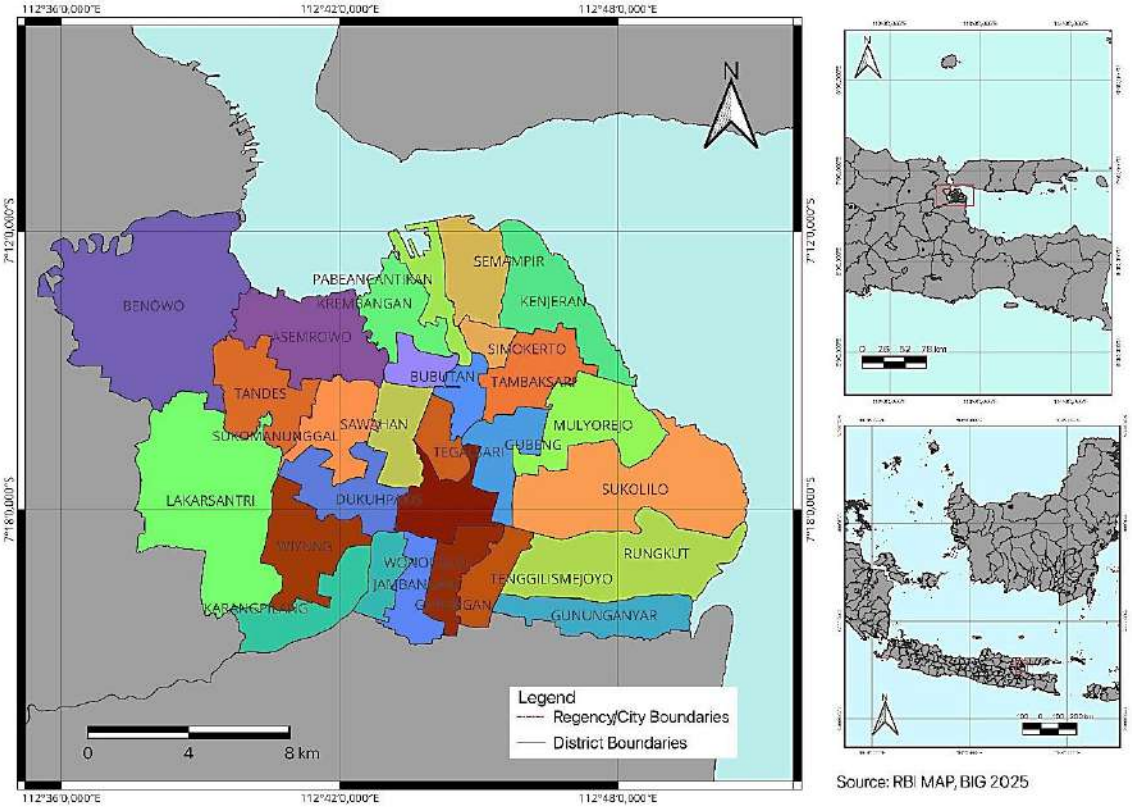

Fig. 1: Geographical location of the study area in the Surabaya, Indonesia

metropolitan territory, it contains peri-urban and suburban agricultural sectors that sustain persistent farming activities. Surabaya presents a unique setting where agriculture coexists with rapid urban development, highlighting challenges such as land conversion, market access, and technology adoption. Agricultural activities mainly include vegetable, fruit, and ornamental plant cultivation on small- to medium-sized farms. Evidence derived from this case study offers valuable implications for regional agricultural governance, elucidating both the obstacles and prospective advantages inherent in peri-urban agricultural systems. The marital status of the dominating respondents was married with 69%, unmarried with 23.5%, and divorced with 7.5%. The monthly expenditure of most respondents was in the range of USD 55.56 to USD 222.22, accounting for 78.5% of respondents, followed by those spending more than USD 222.22 (13.5%), while 8% of respondents spent less than USD 55.56 per month To appropriately contextualize the research and uphold the psychometric reliability and structural validity of the proposed model, necessary methodological modifications were incorporated into the research framework and measurement design to ensure consistency and robustness. The survey instrument is proposed to be able to collect information from respondents covering biophysical factors, production inputs, economy, social technology, agricultural business management, agricultural tax policy, tax administration efficiency, regional agricultural policy, tax awareness, tax morale, and agricultural productivity. This study uses a Likert scale of 1 until (–) 5 as a research indicator with 1 equal to (=) strongly disagree; 2= disagree; 3= neutral; 4= Agree; 5= Strongly agree (Table 1).

Table 1: Measurement items and scale of the study variables

Variable	Item code	Measurement Item	Scale
Agricultural business management (ABM)	ABM1	I implement effective production planning to improve farming efficiency and productivity.	1–5 Likert
	ABM2	I maintain proper financial management by recording farming income and expenditures.	
	ABM3	I use information technology to improve inventory and agricultural logistics management.	
	ABM4	I implement effective marketing strategies to improve product competitiveness.	
	ABM5	I have adequate capability to manage farming risks, including weather and market risks.	
Agricultural productivity (AP)	AP1	Agricultural productivity in my area has increased over time.	1–5 Likert
	AP2	The farming techniques and technologies I use improve crop yields and farming efficiency.	
	AP3	The quality of my agricultural products meets market standards and receives positive responses.	
	AP4	I manage my farmland effectively, including crop management, irrigation, and pest control.	
	AP5	My overall agricultural productivity is higher than the average productivity of surrounding farms.	
Agricultural taxation policy (ATP)	ATP1	The agricultural tax imposed on my harvest is fair and not burdensome.	1–5 Likert
	ATP2	The agricultural tax payment process is simple and easy.	
	ATP3	Information regarding agricultural taxation is easily accessible and understandable.	
	ATP4	The government provides attractive tax incentives for productive farmers.	
	ATP5	Agricultural tax revenues are used to finance programs that benefit farmers.	
Biophysical factors (BPF)	BPF1	The quality of agricultural land in my area is adequate to support crop cultivation.	1–5 Likert
	BPF2	The availability of irrigation water in my area is sufficient for agricultural activities.	
	BPF3	The climate in my area is suitable for cultivating the crops I grow.	
	BPF4	The soil fertility in my area is adequate to support crop growth.	
	BPF5	The elevation of my farmland affects the productivity of my crops.	
	BPF6	The drainage conditions of my farmland adequately support crop growth.	
	BPF7	Pests and plant diseases are often serious problems affecting agricultural production in my area.	
	BPF8	The topography (land contour) of my farmland influences soil erosion and crop productivity.	
Economic factors (EF)	EF1	The selling price of agricultural products in the local market affects my farming profits.	1–5 Likert
	EF2	Access to export markets influences my income and financial stability.	
	EF3	Increases in production costs, such as fertilizers and fuel, reduce my farming profit margins.	
	EF4	Market uncertainty and commodity price fluctuations influence my farming investment and production decisions.	
	EF5	Government policies related to subsidies, taxation, and agricultural regulations significantly affect my farm profitability.	
Production input factors (PIF)	PIF1	The availability of organic and inorganic fertilizers in my area is sufficient to meet my farming needs.	1–5 Likert
	PIF2	Access to and availability of high-quality seeds influence my crop yields.	
	PIF3	The prices of production inputs such as seeds, fertilizers, and pesticides are affordable for farmers in my area.	
	PIF4	Changes in the prices of production inputs frequently influence my farming decisions.	
	PIF5	The quality and availability of fuel for agricultural machinery affect the efficiency and productivity of my farm.	
	PIF6	The quality and availability of agricultural equipment and machinery influence farming efficiency.	
Regional agricultural policy (RAP)	RAP1	The local government provides adequate infrastructure to support agricultural activities.	1–5 Likert
	RAP2	The local government provides easy access to fertilizers, pesticides, and high-quality seeds.	
	RAP3	The local government provides beneficial agricultural extension services.	
	RAP4	The local government assists farmers in marketing their agricultural products.	
	RAP5	Current regional agricultural policies are fair and supportive of farmers.	
Socio-technological factors (STF)	STF1	The use of agricultural technology has improved my farming efficiency and productivity.	1–5 Likert
	STF2	Participation in farmer networks or local farmer groups facilitates knowledge sharing and improves my farming practices.	
	STF3	Environmental awareness and sustainability issues have influenced my farming practices.	
	STF4	Access to and use of social media has helped expand my agricultural business network and product marketing.	
	STF5	Training and education in modern agricultural technology have improved my ability to adopt new innovations.	
Tax awareness (TA)	TA1	I always try to calculate and report my income accurately for tax purposes.	1–5 Likert
	TA2	I understand the importance of the Indonesian tax system.	
	TA3	I recognize the importance of contributing to the country through tax payments.	
	TA4	I always make tax payments on time in accordance with the applicable regulations.	

Tax administration efficiency (TAE)	TAE1	The current agricultural tax administration procedures are simple and easy to understand.	1–5 Likert
	TAE2	The time required to complete agricultural tax administration is fast and efficient.	
	TAE3	Tax officers provide clear information and adequate assistance regarding agricultural taxation.	
	TAE4	The cost of completing agricultural tax administration is reasonable and affordable.	
	TAE5	Information regarding agricultural taxation is transparent and easily accessible.	
Tax morale (TM)	TM1	Paying taxes is my moral responsibility as a citizen.	1–5 Likert
	TM2	I believe that the taxes I pay are used appropriately for rural infrastructure development.	
	TM3	I would feel guilty if I failed to pay my taxes as required.	
	TM4	Paying taxes is my contribution to the development of society and the country.	
	TM5	Paying taxes reflects my compliance with laws and regulations.	
	TM6	I believe that the taxes I pay contribute to improving farmers' welfare.	

The following is the proposed research framework (Fig. 2). This study employs partial least squares-structural equation modeling (PLS-SEM), a well-established method for evaluating relationships between complex constructs (Lohmöller, 1989). PLS-SEM is widely applied across diverse disciplines to examine complex variables (Guenther *et al.*, 2023; Sarstedt *et al.*, 2022), and it is used here to test and analyze the proposed hypotheses. Furthermore, because PLS-SEM accommodates both intricate and straightforward model structures, it serves as a versatile analytical approach adaptable to various research frameworks. The software used in this study is smart partial least squares (SmartPLS) version 3, which includes testing the inner, outer, and bootstrapping models. Surabaya was selected as the study area because it represents one of Indonesia's largest urban-agricultural interfaces, where smallholder and commercial farming coexist alongside urban policy governance — a context well suited to examining the intersection of agricultural policy and tax compliance. Respondents were recruited via purposive sampling, targeting active farmers aged 18 or older who owned agricultural land within Surabaya. Prior to distributing the questionnaires, enumerators visited farming communities to outline the study's objectives and verify the eligibility of potential respondents. All participants provided informed consent; participation was voluntary and responses were collected anonymously to protect confidentiality. Ethical approval was obtained through the research governance framework of Universitas Indonesia. The 200 valid responses are sufficient for the proposed PLS-SEM model complexity (Hair *et al.*, 2017). PLS-SEM was selected over covariance-based SEM due to the model's complexity, the relatively small sample size, and the absence of a normality assumption for the data — conditions under which PLS-SEM demonstrates robust performance (Hair *et al.*, 2019b; Guenther *et al.*, 2023).

Hypothesis development

The hypotheses in this study are based on two theoretical frameworks. The TPB posits that personal conduct is governed by attitudinal, normative, and control constructs. Applied to the taxation domain, this implies that taxpayer attitudes, normative pressures regarding compliance, and perceived administrative ease dictate tax morale and awareness, thereby exerting a direct influence on compliance behavior (Taing and Chang, 2020). G. Edward III's policy implementation model states that the effectiveness of a policy depends on communication, resources, disposition, and bureaucratic structure; in this study, this means that how well agricultural and tax-related policies are communicated, resourced, and administratively structured determines their influence on regional agricultural policy and, ultimately, agricultural productivity, as per Kusuma and Simanungkalit (2022). Based on this framework, the following hypotheses are proposed:

H1: Biophysical factors significantly affect regional agricultural policy.

H2: Production input factors significantly affect regional agricultural policy.

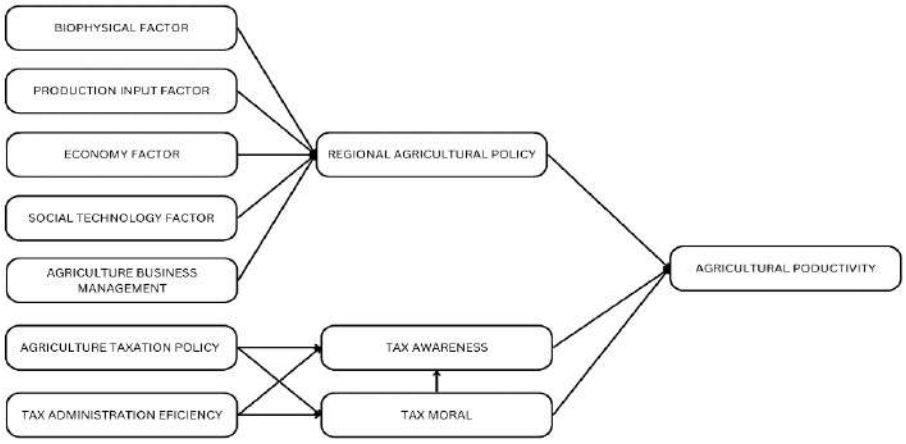

Fig. 2: Research framework

H3: Economic factors significantly affect regional agricultural policy.
H4: Socio-technological factors significantly affect regional agricultural policy.
H5: Agricultural business management significantly affects regional agricultural policy.
H6a: Agricultural taxation policy significantly affects tax awareness.
H6b: Agricultural taxation policy significantly affects tax morale.
H6c: Tax administration efficiency significantly affects tax awareness.
H6d: Tax administration efficiency significantly affects tax morale.
H6e: Tax morale significantly affects tax awareness.
H7a: Regional agricultural policy significantly affects agricultural productivity.
H7b: Tax awareness significantly affects agricultural productivity.
H7c: Tax morale significantly affects agricultural productivity.

RESULTS AND DISCUSSION

A series of tests were carried out in the study, including convergence validity tests, reliability tests, and discrimination validity tests. The convergence validity test consists of outer loadings and average variance extracted (AVE) values. To establish adequate convergent validity, individual indicator loadings ought to surpass the threshold of 0.7, thereby confirming that the latent variable explains a significant proportion of the variance associated with each measure (Hair *et al.*, 2012). Meanwhile, according to Chin (1998), the outer loading value is greater than 0.5 is quite adequate (Chin, 1998). If the outer loading value is below 0.5, it can be considered insignificant or weak, so it should be removed to improve the measurement model (Hair *et al.*, 2019a). In this study, several indicators have a value below 0.5, these indicators are removed to increase the significance value and to make sure there is no overlap indicator that may caused an error. Furthermore, AVE value exceeding 0.5 confirms convergent validity, indicating that a single latent variable accounts for more than half of the variance across its indicators (Bougie and Sekaran, 2019). The test results showed that the AVE value of each variable was eligible because the value showed more than 0.5. Furthermore, internal consistency reliability was evaluated using Cronbach's alpha to establish the lower bound of reliability, alongside composite reliability to assess the true reliability of the construct. The Cronbach alpha and Composite Reliability values must be at least 0.6. The Composite Reliability value so that if it shows a value above 0.7, the test variables' reality can be said to have a high value. In the study, all indicators are acceptable because they

have met the Cronbach Alpha (CA) and composite reliability (CR) standards. The validity and reliability results are fully summarized in Table 2. In addition, discriminant validity was evaluated using the Fornell-Larcker criterion, which requires the square root of the AVE for each construct to exceed its correlations with all other latent variables. The full results of the Fornell-Larcker and Heterotrit-Monotrait ratio (HTMT) test are shown in Tables 3 and 4. HTMT was used to validate the discriminant validity and the result shows that most construct pairs have met the recommended standard. Furthermore, three construct biophysical factor, economic factor, and agricultural business management—exhibited values exceeding 0.90, indicating a high degree of collinearity or association between constructs. This finding can be theoretically justified because these constructs are related to agricultural production systems. Furthermore, Fornell Larcker criterion, cross-loadings, AVE, CR, and CA are supporting the measurement model.

Structural models and hypotheses

The evaluation of the R^2 (variance) and f^2 (effect size) matrices was used to measure the structural model. The R^2 value is divided into three categories, namely 0.75 (firm), 0.50 (moderate), and 0.25 (weak) (Hair *et al.*, 2019a; Hair *et al.*, 2017). R^2 is also used to determine whether the tested model is good. In this study, all variables with R^2 values in the moderate category. Furthermore, the tax awareness construct yielded a value of 0.506, indicating that the independent variables account for 50.6 of the variance in the dependent variable, while the remaining 49.4% is explained by other extraneous factors. Other variables are regional agricultural policy, which has a value of 0.579, which means that independent variables can explain 57.9% of the distribution of dependent variables. In contrast, the remaining 42.1% cannot be explained by independent variables. The R^2 value of the agricultural productivity and tax moral requires further enhancement, as the obtained values fall below the acceptable threshold of 0.50. Meanwhile, the R square adjusted value is used to overcome if there is a problem that often occurs in the R square value, namely an increase in value if independent variables are added to the model. R square adjusted is also used to measure the confidence level in adding the correct independent variable to increase the model's predictive power. In this study, the variables of tax awareness and regional agricultural policy have a sufficient model predictive power because the R square adjusted value is more than 0.5. The comprehensive results detailing the coefficient of determination (R^2) and adjusted R^2 values are presented in Table 5. Meanwhile, the f^2 value with a value higher than 0.35 has a significant effect, higher than 0.15 has a moderate effect, and higher than 0.02 has a negligible effect. In this study, the regional agricultural policy variable greatly influences agricultural productivity because it has a value of 0.367 (greater than (>) 0.35) and tax administration efficiency has a great influence in tax morale because the result shows 0.446 > 0.35. Furthermore, tax administration efficiency and tax morale exert a moderate effect on tax awareness, as indicated by f^2 values exceeding 0.15. Tax awareness and tax morale moderately influence agriculture. Furthermore, biophysical, agricultural business management, social technology, and production input factors have a negligible influence on regional agricultural policy. Meanwhile other variables that has correlation also shows negligible influence because the results show > 0.02 and two correlated variable has no effect since the results are < 0.02. The complete results of the f^2 test are in Table 6. Predictive relevance test (Q^2) is useful to measuring the quality from a structural model and ability to predict data especially endogenous latent variables (Table 7). Q^2 is also used as a complement to R^2 test. According to Hair *et al.* (2012), $Q^2 \leq 0$ is indicated insignificant predictive relevance. $Q^2 > 0.02$ is indicated weak predictive relevance. $Q^2 > 0.15$ is indicated moderate predictive relevance. $Q^2 > 0.35$ is indicated strong

Table 2: Validity and reliability test results

Variables	Indicators	Outer loading	AVE	CA	CR	Status
Agriculture business management (ABM)	ABM3	0.895	0.835	0.804	0.910	Valid
	ABM4	0.932				
Agricultural productivity (AP)	AP1	0.805	0.671	0.760	0.859	Valid
	AP2	0.747				
	AP3	0.899				
Agriculture taxation policy (ATP)	ATP2	0.996	0.693	0.714	0.811	Valid
	ATP4	0.628				
Biophysical factor (BPF)	BPF3	0.791	0.674	0.518	0.805	Valid
	BPF8	0.850				
Economy factor (EF)	EF1	0.671	0.552	0.610	0.784	Valid
	EF4	0.674				
	EF5	0.866				
Production Input Factor (PIF)	PIF5	0.847	0.739	0.647	0.850	Valid
	PIF6	0.872				
Regional agricultural policy (RAP)	RAP3	0.810	0.746	0.669	0.854	Valid
	RAP5	0.914				
Social technology factor (STF)	STF1	0.801	0.591	0.772	0.852	Valid
	STF2	0.800				
	STF3	0.778				
	STF4	0.690				
Tax awareness (TA)	TA1	0.694	0.558	0.607	0.789	Valid
	TA3	0.670				
	TA4	0.862				
Tax administration efficiency (TAE)	TAE1	0.904	0.859	0.840	0.924	Valid
	TAE3	0.949				
Tax moral (TM)	TM1	0.786	0.582	0.860	0.893	Valid
	TM2	0.814				
	TM3	0.729				
	TM4	0.711				
	TM5	0.720				
	TM6	0.809				

Table 3: Fornell-Larcker test

Variables	AP	ATP	ABM	BPF	EF	PIF	RAP	STF	TAE	TA	TM
AP	0.819										
ATP	0.054	0.833									
ABM	0.740	-0.032	0.914								
BPF	0.569	0.108	0.552	0.821							
EF	0.576	0.096	0.486	0.344	0.743						
PIF	0.464	0.069	0.395	0.201	0.176	0.859					
RAP	0.653	-0.185	0.607	0.518	0.372	0.556	0.864				
STF	0.559	0.164	0.547	0.353	0.578	0.578	0.630	0.769			
TAE	-0.440	0.533	-0.530	-0.459	-0.479	-0.126	-0.576	-0.429	0.927		
TA	0.468	-0.490	0.527	0.521	0.308	0.181	0.570	0.238	-0.646	0.747	
TM	0.377	-0.256	0.489	0.422	0.585	0.287	0.446	0.421	-0.591	0.565	0.763

predictive relevance. Based on the results, tax morale (0.178 > 0.15), agricultural productivity (0.273 > 0.15), and tax awareness (0.259 > 0.15) have moderate predictive relevance. Concurrently, regional agricultural policy demonstrates robust predictive relevance within the structural model (0.416 > 0.35). Next step is testing the proposed hypothesis that uses bootstrapping techniques. For the hypothesis to be accepted, the minimum t-test value is 1.96, and the maximum probability value (p-value) 0.05. This threshold was adopted because it represents

Table 4: HTMT test result

Variables	AP	ATP	ABM	BPF	EF	PIF	RAP	STF	TAE	TA	TM
AP	1										
ATP	0.374	1									
ABM	0.958	0.276	1								
BPF	0.943	0.671	0.841	1							
EF	0.912	0.325	0.722	0.701	1						
PIF	0.599	0.405	0.533	0.357	0.516	1					
RAP	0.815	0.514	0.771	0.836	0.589	0.867	1				
STF	0.699	0.528	0.668	0.564	0.790	0.772	0.859	1			
TAE	0.577	0.520	0.607	0.639	0.633	0.155	0.749	0.498	1		
TA	0.660	0.557	0.771	0.895	0.560	0.297	0.864	0.465	0.823	1	
TM	0.447	0.298	0.563	0.589	0.711	0.484	0.559	0.470	0.619	0.704	1

Table 5: R Square results

Endogenous constructs	R^2	R^2 adjusted
Agricultural productivity	0.442	0.434
Regional agricultural policy	0.579	0.568
Tax awareness	0.506	0.498
Tax moral	0.354	0.347

Table 6: F square results

Variable	AP	ABM	ATP	BPF	EF	PIF	RAP	STF	TAE	TA	TM
AP											
ABM							0.064				
ATP										0.075	0.007
BPF							0.103				
EF							0.002				
PIF							0.092				
RAP	0.367										
STF							0.084				
TAE										0.119	0.446
TA	0.013										
TM	0.005									0.120	

Table 7: Q square results

Variables	SSO	SSE	Q^2 (=1-SSE/SSO)
Agricultural productivity	600.000	435.933	0.273
Regional agricultural	400.000	233.438	0.416
Tax awareness	600.000	444.463	0.259
Tax morale	1200.000	986.561	0.178

a widely recommended benchmark in PLS-SEM analyses, and the study utilized two-tailed hypotheses evaluated at a 95% confidence level. If the hypothesis test results do not meet the standards, the results are rejected. In this study, ten hypotheses meet the standards so that the hypothesis decision is accepted. Simultaneously, the other three hypotheses were rejected because the test results showed that they did not meet the set standards. Table 8 describes in detail the results of the bootstrapping tests that have been carried out.

Theoritical implication

Previous theories were adapted to form variables used to study social phenomena in this study. These variables are outlined in the form of a questionnaire distributed to farmers in Surabaya. Furthermore, the findings indicate that biophysical factors exert a significant effect on regional agricultural policy. This relationship is driven by environmental challenges, including climate change, resource scarcity, and deforestation, requiring proactive mitigation to sustain long-term agricultural productivity.

Table 8: Hypothesis results

Hypothesis	Original sample (O) or beta coefficient (β)	Sample mean (M)	Standard deviation (SD)	t-statistics (|O/SD|)	p-value	Decision
H1 biophysical factor → regional agricultural policy	0.251	0.253	0.060	4.210	0.000	Accepted
H2 production input factor → regional agricultural Policy	0.253	0.256	0.058	4.355	0.000	Accepted
H3 economy factor→ regional agricultural policy	-0.039	-0.029	0.067	0.588	0.557	Declined
H4 social technology factor → regional agricultural policy	0.293	0.290	0.076	3.846	0.000	Accepted
H5 agriculture business management → regional agricultural policy	0.228	0.227	0.084	2.717	0.007	Accepted
H6a agriculture taxation policy → tax awareness	-0.229	-0.234	0.065	3.546	0.000	Accepted
H6b agriculture taxation policy → tax moral	0.082	0.082	0.045	1.803	0.072	Declined
H6c tax administration efficiency → tax awareness	-0.345	-0.344	0.074	4.656	0.000	Accepted
H6d tax administration efficiency → tax moral	-0.634	-0.636	0.050	12.650	0.000	Accepted
H6e tax moral → tax awareness	0.303	0.304	0.048	6.248	0.000	Accepted
H7a regional agricultural policy → agricultural productivity	0.560	0.568	0.042	13.380	0.000	Accepted
H7b tax awareness → agricultural productivity	0.112	0.109	0.059	1.901	0.058	Declined
H7c tax moral → agricultural productivity	0.064	0.064	0.051	1.260	0.208	Declined

The existence of agricultural regional policies that serve to protect biodiversity is the opinion by Klitgaard (2020), which states that biophysical factors are related to the environment and energy; if the problems that arise are not appropriately addressed, it will be able to cause macro scale economic problems (Klitgaard, 2020). In addition, the second hypothesis testing the effect of production input factors on regional agricultural policy yielded statistically significant results. This outcome is attributed to the vital role of agricultural inputs—such as seeds, fertilizers, pesticides, and machinery, which serve as essential capital assets driving farming operations. The existence of innovations that support the development of agricultural inputs through research and development (RnD) can significantly improve the quality and quantity (Manogna, 2021). The production input factor is the basis for forming policies that can comprehensively regulate the price of seeds, fertilizers, and access to funding for farmers. Furthermore, the third hypothesis examining the effect of economic factors on regional agricultural policy yielded statistically non-significant results. This outcome suggests that prevailing economic conditions, including local market prices, export market access, and regulatory frameworks—have not generated equitable profitability for the farming community. Consequently, multi-perspective regional policies are necessary to bolster the economic welfare of farmers in Indonesia. The fourth hypothesis, social technology factor to regional agricultural policy, shows significant results. This result is due to the existence of public facilities, agricultural governance systems that have been integrated with technology, and intercommunity relations in agricultural product transactions that can be easily applied, especially in Surabaya, so it requires other aspects to be able to influence regional agricultural policies, previous research conducted by Khan *et al.* (2021) and Viaggi *et al.* (2021) on the use of data for public interest can be applied currently in the region Surabaya. In addition, the fifth hypothesis examining the

relationship between agricultural business management and regional agricultural policy yielded a statistically significant effect. This indicates that sound management practices in the agricultural sector serve as a foundational mechanism for formulating and strengthening regional policies. After all, with business management applied to agriculture, the management of the purchase of production inputs, finance, and distribution as stated in the previous study by Viaggi *et al.* (2021). Furthermore, Agriculture Taxation Policy to Tax Awareness have a significant effect. The existence of a tax policy that has a legal basis can be the basis for the public to know how regulations work so that morals to pay taxes are formed, and awareness to pay taxes grows by research conducted by Taing and Chang (2020). Concurrently, Agriculture Taxation Policy to Tax Moral has no significant effect because individual morale regarding tax shaped through their attitude and perception. Tax administration efficiency to tax awareness and tax administration efficiency to tax moral have a significant effect because a well-organized administrative system can realize the efficiency of administrative services to serve tax payments so that it can foster morale and tax awareness as a study conducted by Lencucha *et al.* (2020). Tax moral exerts a statistically significant effect on tax awareness. This relationship is grounded in the psychological dimensions and intrinsic motivation associated with tax compliance, fostering a heightened sense of obligation toward tax payments, consistent with previous findings by Taing and Chang (2020). Regional agricultural policy to agricultural productivity, is accepted because there are consistent regulations and can regulate the needs of farmers well to bring macro impacts, can increase agricultural productivity because all necessary access can be easily reached as a study conducted by Liu *et al.* (2020). Tax awareness affects agricultural productivity and has insignificant results because productivity in agriculture have no correlation with individual awareness about tax. Despite considering dimensions such as procedural knowledge of tax payment and anticipated benefits, these factors may not exert a statistically significant effect on enhancing agricultural productivity, largely owing to fluctuations in subsidies and fiscal incentives. The last hypothesis, tax moral affects agricultural productivity, is rejected because it does not have a significant effect, although tax morality may trigger awareness to implement tax obligations.

Practical implications

The tax applied to the agricultural sector is an effort made by the government to reduce carbon emissions and realize a sustainable life. Both biophysical factors and production inputs exert a statistically significant effect on agricultural policy. These dimensions serve as a critical foundation for governmental policy refinement, as they address essential environmental, energy, and land needs such as seeds, fertilizers, and pesticides—vital for agricultural production. The sustainability implications of agricultural production are also closely associated with the management and reuse of water resources, particularly where wastewater is considered as an alternative source for agricultural production and is evaluated from both weak- and strong-sustainability perspectives (Rosas Baños and García Salazar, 2026). Economic factors have not been able to significantly affect regional agricultural policies because economic effects such as selling prices in the local market, access to export markets, and government policies on regulations have not increased the profitability that can be felt, so the need for other aspects that can be applied to increase the effects that can be felt. Furthermore, social and technological factors exert a significant effect on regional agricultural policies. This relationship is driven by advanced data applications, the internet of things (IoT), artificial intelligence (AI), and sensors, which enhance societal well-being, optimize environmental outcomes, and substantially boost community-wide economic development. Such technological and policy-oriented approaches are particularly relevant to climate-resilient

agricultural systems, where the management of underutilized climate-resilient crops can contribute to the sustainability and adaptive capacity of farming systems (Ismail *et al.,* 2026). However, this factor can be a record of the government's foundation to make policies that support the improvement of public facilities for agriculture. Furthermore, business management to manage agriculture is also important because the production, harvesting, packaging, and distribution processes will be well integrated. Regional agricultural policies designed to safeguard agricultural business processes can be effectively formulated to ensure the streamlined distribution of agricultural products from producers to consumers. In this context, the integration of environmental, social, and economic indicators into land-use planning provides an important basis for developing agricultural policies that balance productivity with broader sustainability objectives (Freire-Granda *et al.,* 2026). The existence of an excellent agricultural tax policy affects tax awareness and tax morale because a well-regulated policy will clarify how the community should take steps to carry out tax payment obligations. An excellent agricultural tax policy supported by suitable administrative frameworks, foster operational efficiency. This environment cultivates tax awareness by facilitating accessible payment procedures and highlighting tangible benefits for taxpayers. Meanwhile, agriculture tax policy has no significant effect on tax morale because this behavior comes from individual reasons. Regional agricultural policies correlate to increase agricultural productivity because the ease of access that is protected and provided through policies will significantly make it easier for farmers to carry out agricultural processes, from production to distribution to consumers. Furthermore, neither tax awareness nor tax morale exerts a statistically significant effect on agricultural productivity, as this factor is primarily governed by external determinants such as biophysical factors. Through available data, the government can help small-scale farmers to get the necessary subsidies. Finally, tax morality cannot significantly affect agricultural productivity. Because tax morality functions primarily as an attitudinal encouragement rather than an operational mechanism, it fails to generate observable empirical changes in productivity outcomes.

Limitations and further research

This study has several limitations. First, since the data collection was restricted to Surabaya—a predominantly urban metropolitan area—the findings possess limited generalizability to agricultural regions characterized by distinct socioeconomic and institutional profiles. Consequently, subsequent studies should broaden its geographic scope and increase sample size. Second, cross-sectional design prevents causal inference; longitudinal research is recommended. Third, the reliance on self-reported Likert-scale perceptions across all constructs—rather than objective metrics such as yield per hectare or farm income—raises potential concerns regarding measurement validity and common method bias. Consequently, subsequent investigations should incorporate procedural safeguards alongside objective productivity indicators. Fourth, the analysis did not assess mediation, moderation, or subgroup differences, which may limit insight into boundary conditions of the model. Fifth, four hypotheses were rejected — economic factors, agriculture tax policy on tax moral, tax awareness on agriculture productivity, and tax moral on agriculture productivity— suggesting the need for additional variables or refined instruments to capture these relationships more fully.

CONCLUSION

This study integrated the TPB and the G. Edward III policy implementation model to examine determinants of regional agricultural policy and agricultural productivity among farmers in Surabaya, Indonesia. Using PLS-SEM with 200 respondents, 10 of 13 hypotheses were supported. Economic factors do not significantly affect regional agricultural policies (β=-0.039, t-

statistics=0.588, p-value=0.557) because they have not maximized all necessary economic aspects, and the effects felt by the community have not been significant. Consequently, it is recommended that economic considerations—integral components of policy formulation be duly integrated to ensure that the resulting socioeconomic benefits permeate the broader community. Steps taken to improve significant outcomes on economic factors. Agricultural taxation policy factors do not significantly affect on tax morale (β=0.082, t-statistics =1.803, p-value=0.072). The existence of agriculture tax policy is an external factor comparing individual morals to applied tax. The morale (β=0.066, t-statistics=1.260, p-value=0.208) and awareness (β=0.064, t-statistics=1.901, p-value=0.058) hypothesis of taxes also does not significantly affect agricultural productivity because moral perception has yet to take the form of action and can only trigger the desire to implement taxes. Furthermore, relationships demonstrating statistically significant effects require careful management and continuous monitoring to ensure that their socioeconomic benefits remain sustainable for the community. For instance, biophysical factors (β=0.251, t-statistics=4.210, p-value=0.000) warrant careful consideration as they encompass critical environmental, energy, and macroeconomic dimensions. Production inputs (β=0.253, t-statistics=4.355, p-value=0.000) that are capital for the sustainability of agricultural production so that all farmers can access easy access through policies that are milestones. Social technology factor (β=0.293, t-statistics=3.846, p-value=0.000) because developed technology can help many factors such as tax administration more effective and efficient. Agricultural business management is vital for farming communities, as it encompasses both production and distribution channels, thereby exerting a significant effect on the continuous refinement of regional agricultural policies. Agricultural tax policy (β=-0.229, t-statistics=3.546, p-value=0.000 on tax awareness) and the efficiency of tax administration (β=-0.345, t-statistics=4.656, p-value=0.000 on tax awareness; β=-0.634, t-statistics=12.650, p-value=0.000 on tax moral) can have a significant effect on morale and tax awareness because there is clarity about the flow, benefits, and regulations of implementation can be easily understood by the public, forming a sense of responsibility, carrying out their obligations as taxpayers, and knowing what rights will be received if they obey tax regulations. Furthermore, tax morals encourage taxes so that tax awareness emerges and does what taxpayers should do. Finally, neither tax morale nor tax awareness exerts a statistically significant effect on agricultural productivity, given that productivity growth relies heavily on biophysical conditions rather than individual awareness and moral factors. Future research should replicate and extend this model using longitudinal designs, objective productivity measures, and samples drawn from diverse agricultural regions to enhance generalization.

AUTHOR CONTRIBUTIONS

M.S. Setyowati, the corresponding author, has contributed to data curation, investigation, resources, writing review and editing project administration. R.K. Hanum, has contributed to methodology, writing, original draft preparation, writing and review and editing, visualization, and supervision, and funding acquisition. All authors have read and agreed to the published version of the manuscript.

ACKNOWLEDGEMENT

The authors would like to thank to Directorate of Research and Development, Universitas Indonesia and member of the cluster research which facilitates this study to run well. This work was supported by the Hibah Publikasi Terindeks Internasional (PUTI) Q1 2024, Directorate of Research and Development, Universitas Indonesia [Grant numbers NKB-193/UN2.RST/HKP.05.00/2024].

CONFLICT OF INTEREST

The authors declare that there is no conflict of interest regarding the publication of this

manuscript. In addition, ethical issues, including plagiarism, informed consent, misconduct, data fabrication and/or falsification, double publication and/or submission, and redundancy have been completely observed by the authors.

OPEN ACCESS

©2027 The author(s). This article is licensed under a Creative Commons Attribution 4.0 International License, which permits use, sharing, adaptation, distribution and reproduction in any medium or format, as long as you give appropriate credit to the original author(s) and the source, provide a link to the Creative Commons license, and indicate if changes were made. The images or other third-party material in this article are included in the article's Creative Commons license, unless indicated otherwise in a credit line to the material. If material is not included in the article's Creative Commons license and your intended use is not permitted by statutory regulation or exceeds the permitted use, you will need to obtain permission directly from the copyright holder. To view a copy of this license, visit: http://creativecommons.org/licenses/by/4.0/

PUBLISHER'S NOTE

GJESM Publisher remains neutral regarding jurisdictional claims in published maps and institutional affiliations.

POSITIVE AI STATEMENT

During the preparation of this work the author(s) have used Artificial Intelligence (AI) [Quillbot] to [grammar checking]. After using this tool/service, the authors reviewed and edited the content as needed and took full responsibility for the content of the publication.

ABBREVIATIONS

%	Percent
–	Until
=	Equal to
>	Greater than
β	Beta coefficient
|O/SD|	T statistics
ABM	Agriculture business management
AP	Agricultural productivity
ATP	Agriculture taxation policy
AI	Artificial Intelligence
AVE	Average variance extracted
BPF	Biophysical factor
CA	Cronbach alpha
CR	Composite reliability
EF	Economy factor
f^2	Effect size
FAO	Food and Agriculture Organization
IoT	Internet of things
HTMT	Heterotrit-Monotrait ratio
M	Sample mean
O	Original sample
NGOs	Non-governmental organization
p-value	Probability value
PIF	Production Input Factor
PLS-SEM	Partial least squares-structural equation modeling
R^2	Variance
RAP	Regional agricultural policy
RnD	Research and Development
SDGs	Sustainable development goals
SD	Standard Deviation
SmartPLS	Smart partial least squares
STF	Social technology factor
TA	Tax awareness
TM	Tax moral
TPB	Theory Of Planned Behaviour
USD	United States Dollar

REFERENCES

Abraham, M.; Pingali, P., (2020). Transforming smallholder agriculture to achieve the SDGs. In: The Role of Smallholder Farms in Food and Nutrition Security. Springer: 173-209 **(37 pages)**.

Arintyas, A.P.R.D.A., (2024). Women, agriculture, and villages: A community of empowerment study to achieve wellbeing and sustainable development. J. Agrosociol. Sustain. 2(1): 1-16 **(16 pages).**

Bangun, L.P., (2024). Strategic transformations for realizing food security in Indonesia. Crit. Issue Sustain. Future. 1(2): 123-129 (7 pages).

Benni, N.E.; Irek, J.; Finger, R.; Mack, G.; Ammann, J., (2024). Citizens' perceptions of agricultural policy goals - evidence from Switzerland. Food Policy. 125(102643): 1-21 **(21 pages)**.

Bizikova, L.; Jungcurt, S.; McDougal, K.; Tyler, S., (2020). How can agricultural interventions enhance contribution to food security and SDG 2.1? Global Food Secur., 26: 100450 **(8 pages)**.

Bougie, R.; Sekaran, U., (2019). Research Methods for Business: A Skill-Building Approach (8th ed.). John Wiley & Sons Ltd **(432 pages)**.

Bridle, L.; Magruder, J.; McIntosh, C.; Suri, T., (2020). Experimental insights on the constraints to agricultural technology adoption. CEGA White Papers **(38 pages)**.

Castro, P.; Azul, A.M.; Leal Filho, W.; Azeiteiro, U.M., (2019). Climate Change-Resilient Agriculture and Agroforestry Ecosystem Services and Sustainability. Springer.

Chin, W.W., (1998). The partial least squares approach to structural equation modelling. In: Marcoulides, G.A. (Ed.), Modern Methods for Business Research (pp. 295-336). Lawrence Erlbaum Associates Publishers **(42 pages)**.

Deboe, G., (2020). Economic and environmental sustainability performance of environmental policies in agriculture. OECD Food, Agriculture and Fisheries. **(140 pages).**

Fendrich, A.N.; Barretto, A.; Sparovek, G.; Gianetti, G.W.; Luz Ferreira, J.; Souza Filho, C.F.M.; Appy, B.; Guedes, C.M.G.; Leitão, S., (2022). Taxation aiming environmental protection: The case of Brazilian Rural Land Tax. Land Use Policy. 119: 106164 **(12 pages)**.

Freire-Granda, D.; Velastegui-Montoya, A.; Meiguins de Lima, A.; Marcos, A.; Ramirez, A.; Escandón-Panchana, P.C., (2026). Key geographical indicators for environmental, social and economic sustainability of land use. Global J. Environ. Sci. Manage., 12(4): 2133-2156 **(24 pages).**

Fukase, E.; Martin, W., (2020). Economic growth, convergence, and world food demand and supply. World Dev., 132:104954 **(23 pages)**.

Garzón, J.; Montes, L.; Garzón, J.; Lampropoulos, G., (2023). Systematic review of technology in aeroponics: Introducing the technology adoption and integration in sustainable agriculture model. Agronomy. 13(10): 251 7 **(23 pages)**.

Gil, J.D.B.; Reidsma, P.; Giller, K.; Todman, L.; Whitmore, A.; Ittersum, M., (2019). Sustainable development goal 2: Improved targets and indicators for agriculture and food security. Ambio. 48(7): 798-812 **(15 pages)**.

Guenther, P.; Guenther, M.; Ringle, C.M.; Zaefarian, G.; Cartwright, S., (2023). Improving PLS-SEM use for business marketing research. Ind. Mark. Manage., 111: 127-142 **(16 pages)**.

Hadi, S.; Aprisco, H.; Abdillah, M.F., (2025). The exemplary role of farmer institutional administrators as a strengthener for the holistic and integrative reform of the agricultural development paradigm. Holistic: J. Trop. Agric. Sci. 3(1): 21-43 **(23 pages).**

Hair, J.F.; Sarstedt, M.; Pieper, T.M.; Ringle, C.M., (2012). The use of partial least squares structural equation modeling in strategic management research: A review of past practices and recommendations for future applications. Long Range Plan., 45(5-6): 320-340 **(21 pages)**.

Hair, J.F.; Matthews, L.M.; Matthews, R.L.; Sarstedt, M., (2017). PLS-SEM or CB-SEM: Updated guidelines on which method to use. Int. J. Multivariate Data Anal., 1(2): 107-123 **(27 pages)**.

Hair, J.F.; Babin, B.J.; Anderson, R.E.; Black, W.C., (2019a). Multivariate Data Analysis (8th ed.). Cengage Learning. EMEA **(834 pages)**.

Hair, J.F.; Risher, J.J.; Sarstedt, M.; Ringle, C.M., (2019b). When to use and how to report the results of PLS-SEM. Eur. Bus. Rev., 31(1): 2-24 **(23 pages)**.

Ismail, N.; Cepriadi; Rianto, Y.; Catursaptani, R.; Habiburrahman, I.; Basuki, W.; Sihono, S.; Herniwati; Hadiarto, A.; Indriatama, W.M.; Iskandar, D.; Rosadi, A.H.Y.; Daulay, H.; Santoso, A.D., (2026). Environmental management of underutilized climate-resilient crops on sustainability of sorghum farming in emerging agricultural system. Global J. Environ. Sci. Manage., 12(4): 2013-2040 **(28 pages).**

Janvry, A.; Sadoulet, E., (2020). Using agriculture for development: Supply- and demand-side approaches. World Dev., 133:105003 **(14 pages)**.

Khan, N.; Ray, R.L.; Sargani, G.R.; Ihtisham, M.; Khayyam, M.; Ismail, S., (2021). Current progress and future prospects of agriculture technology: Gateway to sustainable agriculture. Sustainability. 13(9): 4883 **(31 pages)**.

Klitgaard, K., (2020). Sustainability as an economic issue: A biophysical economic perspective. Sustainability. 12(1): 364 **(21 pages)**.

Kusuma, A.I.G.K.C.B.; Simanungkalit, Y.T.S., (2022). Implementasi insentif pajak menurut model G Edward III. Jurnal Pajak dan Keuangan Negara (PKN), 3(2): 236-248 **(13 pages)**.

Lencucha, R.; Pal, N.E.; Appau, A.; Thow, A.M.; Drope, J., (2020). Government policy and agricultural production: A scoping review to inform research and policy on healthy agricultural commodities. Global Health. 16:11 **(15 pages)**.

Liu, J.; Wang, M.; Yang, L.; Rahman, S.; Sriboonchitta, S., (2020). Agricultural productivity growth and its determinants in south and southeast Asian countries. Sustainability. 12(12): 4981 **(21 pages)**.

Lohmöller, J.-B., (1989). Latent Variable Path Modeling with Partial Least Squares. Springer.

Manogna, R.L., (2021). Innovation and firm growth in agricultural inputs industry: Empirical evidence from India. J. Agribus. Dev. Emerg. Econ., 11(5): 506-519 **(14 pages)**.

Michalke, A.; Köhler, S.; Messmann, L.; Thorenz, A.; Tuma, A.; Gaugler, T., (2023). True cost accounting of organic and conventional food production. J. Clean. Prod., 408: 137134 **(13 pages)**.

Milošević, G.; Kulić, M.; Durić, Z.; Durić, O., (2020). The taxation of agriculture in the republic of Serbia as a factor of development of organic agriculture. Sustainability. 12(8): 3261 **(17 pages).**

Mufida, R.F., (2024). Enhancing sustainability of agricultural land use in Indonesia: Integrating water, energy, and food resources for achieving long-term development goal. Peatland Agric. Clim. Change J. 1(2): 71-80 **(10 pages).**

Ndwiga, O.W.; Mutambu, D.; Manguriu, D.; Mucheru-Muna, M., (2025). Communication factors influencing smallholder farmers' adoption of climate change adaptation measures in Kenya's Embu County. J. Environ. Sci. Sustain. Dev. 8(2): 523-545 **(23 pages).**

Nguyen, Q.; Spilker, G.; Bernauer, T., (2021). The (still) mysterious case of agricultural protectionism. Int. Interact., 47(3): 391-416 **(26 pages)**.

Oebel, B.; Stein, L.; Michalke, A.; Stoll-Kleemann, S.; Gaugler, T., (2025). Towards true prices in food retailing: The value added tax as an instrument transforming agri-food systems. Sustainable Sci., 20: 1705-1722 **(18 pages)**.

Pandey, P.C.; Pandey, M., (2023). Highlighting the role of agriculture and geospatial technology in food security and sustainable development goals. Sustainable Dev., 31(5): 3282-3295 **(14 pages)**.

Pawlak, K.; Kołodziejczak, M., (2020). The role of agriculture in ensuring food security in developing countries: Considerations in the context of the problem of sustainable food production. Sustainability. 12(13): 5488 **(20 pages)**.

Pineiro, V.; Arias, J.; Durr, J.; Elverdin, P.; Ibáñez, A.M.; Kinengyere, A.; Opazo, C.M.; Owoo, N.; Page, J.R.; Prager, S.D.; Torero, M., (2020). A scoping review on incentives for adoption of sustainable agricultural practices and their outcomes. Nat. Sustainable. 3: 809-820 **(12 pages)**.

Robinson, G.M., (2024). Global sustainable agriculture and land management systems. Geogr. Sustainable. 5(4): 637-646 **(10 pages)**.

Rosas Baños, M.; García Salazar, E.M., (2026). Wastewater uses for agricultural production from weak and strong sustainability perspectives. Global J. Environ. Sci. Manage., 12(2): 667-686 **(20 pages).**

Sager, F.; Gofen, A., (2022). Policy of implementation: Organizational and institutional arrangements in policy implementation. Governance. 35(2): 347-364 **(18 pages)**.

Sarstedt, M.; Radomir, L.; Moisescu, O.I.; Ringle, C.M., (2022). Latent class analysis in PLS-SEM: A review and recommendations for future applications. J. Bus. Res., 138: 398-407 **(10 pages)**.

Schaafsma, M.; Ferrini, S.; Turner, R.K., (2019). Assessing smallholder preferences for incentivised climate-smart agriculture using a discrete choice experiment. Land Use Policy. 88(104153) **(10 pages)**.

Statistics Indonesia, (2023). Complete Enumeration Results of the 2023 Census of Agriculture. Badan Pusat Statistik **(114)**.

Syarifudin, A.; Saputra, R., (2024). Revisiting food security policy: Indonesia's readiness for crisis. J. Public Health Oxford, 46(4): e762-e763 **(2 pages)**.

Taing, H.B.; Chang, Y., (2020). Determinants of tax compliance intention: Focus on the theory of planned behavior. Int. J. Public Adm., 44(1): 62-73 **(12 pages)**.

Touch, V.; Tan, D.K.Y.; Cook, B.R.; Liu, D.L.; Cross, R.; Tran, T.A.; Utomo, A.; Yous, S.; Grunbuhel, C.; Cowie, A., (2024). Smallholder farmers' challenges and opportunities: Implications for agricultural production, environment and food security. J. Environ. Manage., 370:122536 **(19 pages)**.

Van, B.; Vu Thi, H.; Ho Luong, X., (2026). Determinants of home composting behavior in supporting sustainable agriculture among smallholder farmers: A case study in the Thai Nguyen province of Vietnam. J. Environ. Sci. Sustain. Dev. 9(1): 247-262 **(16 pages).**

Viaggi, D.; Raggi, M.; Villanueva, A.J.; Kantelhardt, J., (2021). Provision of public goods by agriculture and forestry: Economics, policy and the way ahead. Land Use Policy. 107: 105273 **(6 pages)**.

Yin, Y.; Zhang, Y.; Li, F.; Jiao, J.; Lebailly, P.; Zhang, Y.; Yin, C., (2022). Driving mechanism for farmers' participation in improving farmland ecosystem: Evidence from China. J. Clean. Prod., 380(1): 134895 **(14 pages)**.

AUTHOR (S) BIOSKETCHES

M.S. Setyowati., Ph.D., Professor. Faculty of Administrative Science, Universitas Indonesia, Depok, Indonesia.
- Email: *milla.s@ui.ac.id*
- ORCID: 0000-0002-7525-5521
- Web of Science ResearcherID: GWM-8574-2022
- Scopus Author ID: 57096051400
- Homepage: https://fia.ui.ac.id/id/dr-milla-sepliana-setyowati-s-sos-m-ak/

R.K. Hanum., B.Sc., Junior researcher. Institute for the Assessment and Application of Administrative Sciences, Faculty of Administrative Science, Universitas Indonesia, Depok, Indonesia.
- Email: *rastiniakh@gmail.com*
- ORCID: 0000-0002-2685-0770
- Web of Science ResearcherID: NA
- Scopus Author ID: NA
- Homepage: https://garuda.kemdiktisaintek.go.id/author/view/7601619

HOW TO CITE THIS ARTICLE:
Setyowati, M.S.; Hanum, R.K., (2027). The effect of agricultural taxes and local agricultural policies on enhancing food security and environmental sustainability. Global J. Environ. Sci. Manage., 13(1): 51-68.

DOI: 10.22034/gjesm.2027.01.03
URL: https://www.gjesm.net/article_735498.html

Global Journal of Environmental Science and Management
(GJESM)

Homepage: https://www.gjesm.net/

Podcasts

ORIGINAL RESEARCH ARTICLE

Polymer-specific mechanical recycling of pre-sorted post-consumer municipal plastics for enhanced environmental sustainability

D. Shankar[1], J. Nouri[2,3,*], Ho Soonmin[4], B. Hitesh[5], M. Sankaramuthukumar[6]

[1]Department of Pharmaceutical Chemistry, KM College of Pharmacy, Madurai 625107, Tamil Nadu, India

[2]1137 Spectrum, Irvine, Orange County 92618 USA

[3]Department of Environmental Health Engineering, Tehran University of Medical Sciences, Tehran, Iran

[4]Faculty of Health and Life Sciences, INTI International University, Putra Nilai 71800, Negeri Sembilan, Malaysia

[5]Department of Management, Mittal School of Business, Lovely Professional University, Phagwara, Punjab, 144411 India

[6]Kalasalingam Business School, Kalasalingam Academy of Research and Education, Krishnankoil, Tamil Nadu, 626126 India

ARTICLE INFO

Article History:
Received 16 June 2026
Revised 19 August 2026
Accepted 20 September 2026

Keywords:
Carbon footprint reduction
Energy efficiency
Environmental sustainability
Material recovery
Mechanical recycling
Resource optimization
Waste minimization

DOI:10. 22034.gjesm.2027.01.04

ABSTRACT

BACKGROUND AND OBJECTIVES: Mechanical recycling of municipal plastic waste can reduce landfill burden, energy demand, and environmental impacts while recovering reusable polymers. The study objectives were to assess the performance of polyethylene terephthalate, high-density polyethylene, and low-density polyethylene using polymer-specific pre-processing methods, shredding, thermal consolidation, and compression moulding. The assessment focused on waste minimization, material recovery, energy requirements, estimated carbon dioxide emission reductions, sustainability, and mechanical and thermal performance.

METHODS: A total of 37 kilograms of pre-sorted post-consumer polyethylene terephthalate, high-density polyethylene, and low-density polyethylene was separately processed using polymer-specific treatment and compression moulding. Environmental performance was evaluated within a cradle-to-gate framework using secondary emission factors, and the Sustainability Index was derived from predefined parameters. Recycled materials were evaluated for mechanical and thermal properties. Exploratory one-way analysis of variance assessed polymer differences, with probability values adjusted using the Benjamini–Hochberg false discovery rate procedure.

FINDINGS: Waste reduction and material recovery rates exceeded 95 percent for all polymers, with low-density polyethylene achieving the highest recovery of 99 percent. Low-density polyethylene also showed the lowest energy consumption of 0.95 kilowatt-hours per kilogram and the observed sustainability index of 82.6 ± 2.1, although polymer-specific differences in the Sustainability Index were not statistically significant**.** Polyethylene terephthalate showed the highest tensile strength (55.2 megapascals), compressive strength (83.4 megapascals), density (1.36 grams per cubic centimetre), and carbon dioxide emission reduction (2.10 kilograms of carbon dioxide per kilogram). High-density polyethylene showed intermediate performance. Analysis of variance indicated polymer-specific differences, with F-statistic values of 1.72–412.3 and probability values of <0.001–0.27. After Benjamini–Hochberg adjustment, most physical and mechanical properties, energy consumption, and carbon dioxide emission reduction showed significant differences, whereas landfill diversion and the Sustainability Index did not differ significantly.

CONCLUSION: Polymer-specific mechanical recycling of pre-sorted post-consumer polyethylene terephthalate, high-density polyethylene, and low-density polyethylene achieved high material recovery while maintaining mechanical and thermal properties. The polymers showed differences in material recovery, energy consumption, carbon dioxide emission reduction, and evaluated material properties. Further evaluation using heterogeneous municipal plastic waste and larger-scale processing is required.

This is an open access article under the CC BY license (http://creativecommons.org/licenses/by/4.0/)

NUMBER OF REFERENCES	NUMBER OF FIGURES	NUMBER OF TABLES
49	9	10

*Corresponding Author:
Email: nourijafar@gmail.com
Phone: +1(949)405 0540
ORCID: 0000-0002-9982-3546

INTRODUCTION

Environmental sustainability targets the effective use of resources, reduction of waste, and minimization of emissions to mitigate environmental degradation and climate change (Alrazen *et al.,* 2025). Rapid industrial growth and urbanization have significantly increased material consumption, resulting in escalating waste generation and depletion of natural resources (Gabisa *et al.,* 2023). Among municipal solid waste components, plastics present a major challenge due to their high production volume, durability, and persistence in the environment, which contributes to pollution, greenhouse gas emissions, and microplastic formation (Law and Narayan, 2022; Mogollón-Arismendy *et al.,* 2026). Effective recycling can reduce these impacts while supporting material recovery and circular use of resources. Municipal solid waste contains several commonly used plastic polymers, including polyethylene terephthalate (PET), high-density polyethylene (HDPE), and low-density polyethylene (LDPE), which are widely utilized in packaging and consumer products (Van Eygen *et al.,* 2018). Improper disposal of these polymers through landfilling or uncontrolled dumping leads to long-term environmental hazards, including soil and water contamination, microplastic proliferation, and greenhouse gas emissions (Lahtela *et al.,* 2019; Nurhasanah *et al.,* 2026). The increasing leakage of plastics into terrestrial and aquatic ecosystems further emphasizes the need for better waste management practices that consider both environmental performance and economic feasibility (Go *et al.,* 2024; Gao *et al.,* 2025). Recycling is recognized as a key intervention for sustainable development because it can reduce dependence on virgin materials, conserve energy, and lower carbon emissions compared with conventional production pathways (Santos *et al.,* 2024). Among recycling technologies, mechanical recycling remains widely used for thermoplastics because of its established processing methods, comparatively low energy requirements, and economic feasibility (Sultan *et al.,* 2025). When appropriately optimized, mechanical recycling enables the production of secondary materials with properties suitable for various applications, extending product life cycles and strengthening circular material flows (Antonopoulos *et al.,* 2021). However, the efficiency and sustainability of mechanical recycling are highly dependent on polymer type, processing conditions, and feedstock quality, necessitating polymer-specific evaluation (Pishehvarz and Azamat, 2024). PET, for instance, has been extensively studied due to its high recyclability, while HDPE and LDPE, despite their widespread use and presence in municipal plastic waste, have received comparatively less attention (Tonini *et al.,* 2021). Flexible polymers such as LDPE often present additional challenges related to sorting, property degradation, and process control, highlighting the need for systematic and polymer-specific recycling approaches (Zhao and You, 2022). While recycling is widely acknowledged for its environmental and economic benefits, current research often focuses on individual polymers or isolated indicators, limiting the integration of recovery efficiency, energy demand, material performance, and environmental outcomes within a common assessment framework (Liang *et al.,* 2023). Existing studies typically evaluate energy savings, carbon footprint reduction, or mechanical performance separately, with limited experimental validation of their combined evaluation under comparable recycling conditions (Papo and Corona, 2022). Consequently, experimental studies that examine multiple performance indicators together are needed to compare recycling outcomes across different polymers and identify differences in recovery efficiency, energy demand, material performance, and environmental effects (Mitrano and Wohlleben, 2020). Developing such integrated approaches can provide a clearer basis for assessing polymer-specific recycling performance

and its relevance to municipal plastic waste management (Xu *et al.,* 2020; Nurhasanah *et al.,* 2025). Given the increasing global emphasis on circular economy strategies and climate change mitigation, evaluating polymer-specific mechanical recycling is important for understanding how different polymers perform under comparable processing conditions (Moliner *et al.,* 2024). Understanding how different polymers respond to recycling processes can inform decisions regarding segregation, processing parameters, and end-use applications, provided that such differences are established through direct experimental comparison (Chen *et al.,* 2021). By linking polymer characteristics, recycling efficiency, and sustainability outcomes, such research provides a basis for comparing selected polymer streams and assessing their potential contribution to municipal plastic recycling strategies (Faraca and Astrup, 2019; Selvakumar *et al.,* 2023). The present study provides an experimentally validated, polymer-specific comparison of PET, HDPE, and LDPE under comparable conditions, integrating recovery efficiency, energy consumption, material properties, estimated carbon dioxide emission reduction, landfill diversion, and a sustainability index using experimental data and one-way analysis of variance (ANOVA) with Benjamini–Hochberg false discovery rate (FDR) adjustment. The study focuses on selected pre-sorted post-consumer polymer streams identified in collected municipal plastic waste, excluding multilayer, ambiguously identified, severely degraded, and visibly contaminated plastics, and therefore does not represent the complete municipal plastic waste stream**.** The aims of this study are i) to assess the effectiveness of mechanical recycling in terms of waste reduction, material recovery, and process reproducibility; ii) to evaluate the mechanical, physical, and environmental performance of recycled polymers, including tensile and compressive strength, density, water absorption, carbon dioxide (CO_2) emission reduction, and landfill diversion, and integrate these measures into a sustainability index (SI); iii) to evaluate differences in the physical, mechanical, and environmental properties of recycled PET, HDPE, and LDPE using exploratory one-way ANOVA with Benjamini–Hochberg FDR adjustment; and iv) to develop a polymer-specific framework for recycling strategy assessment and practical recommendations for improving environmental sustainability and supporting further evaluation of broader recycling systems. The study was conducted at K.M. College of Pharmacy, Madurai, Tamil Nadu, India, in 2026.

MATERIALS AND METHODS

Plastic waste is a major environmental concern due to its accumulation in ecosystems and contribution to greenhouse gas emissions. Mechanical recycling provides an effective approach by converting post-consumer plastics into reusable materials with lower energy demand and carbon footprint than virgin plastics (Ragaert *et al.,* 2017). This study experimentally evaluated the sustainability of recycling PET, HDPE, and LDPE through a controlled mechanical recycling process, assessing material recovery, energy consumption, mechanical and physical properties, and CO_2 emission reduction against virgin-plastic controls (Silva *et al.,* 2025).

Study area

The study was conducted around the Perungudi Solid Waste Dumping Yard, Chennai, Tamil Nadu, India, a major municipal landfill serving the southern zones of the city. The site is located between 12.96–12.97° N latitude and 80.24–80.25° E longitude, adjacent to the Pallikaranai marshland and surrounded by residential, commercial, and institutional areas including Velachery, Taramani, and Thoraipakkam. Waste samples were collected within a 10 kilometers (km) radius of the Perungudi solid waste dumping yard to ensure representativeness. The region has a tropical savanna climate, with an average annual temperature of 28 degrees Celsius (°C) and annual rainfall of 1000 millimeter (mm), primarily during

the northeast monsoon (October–December 2025). The collected samples were transported to K.M. College of Pharmacy, Madurai, Tamil Nadu, India, where sorting, processing, and experimental evaluations were conducted. Samples were stored under controlled laboratory conditions before processing.

Materials used

The materials employed, processing equipment, and experimental and quality control procedures adopted in this study were used to support reliable and reproducible recycling results.

i. *Plastic waste materials:* Post-consumer PET, HDPE, and LDPE plastics were selected based on their prevalence in municipal waste and recyclability. Polymer identity was confirmed using resin identification codes, while multilayer and composite plastics were excluded. Single-layer bottles, containers, and carry bags collected within one sampling period were used to ensure material homogeneity (Jeswani *et al.,* 2021).
ii. *Processing materials and equipment:* Plastics were washed with water and mild detergent, air-dried, shredded into 10–15 mm flakes, and subjected to controlled melting and compression moulding without additives (Shan *et al.,* 2023).
iii. *Experimental design and replication:* The collected 740 kilograms (kg) of collected municipal solid waste comprised organic/wet waste (63.5 percent (%); 469.90 kg), paper/cardboard (9.5%; 70.30 kg), plastics (5.0%; 37.00 kg), textiles (3.0%; 22.20 kg), glass (2.5%; 18.50 kg), metals (1.5%; 11.10 kg), rubber/leather (1.5%; 11.10 kg), and inert/other fractions (13.5%; 99.90 kg), based on the mean composition of three representative samples (total = 100%). The plastic fraction (37 kg) was manually segregated and sorted into PET, HDPE, and LDPE, with 100 g of each polymer used as the standardized sample for each independent recycling run (Jeswani *et al.,* 2021).
iv. *Safety, randomization, and calibration:* Standard laboratory safety procedures were followed. The prepared polymer samples served as the sampling frame, and three independent samples were randomly selected from each prepared batch using a simple random-number procedure prior to recycling and subsequent testing. Randomization was applied during sample selection to ensure that no specific sample position or processing order was preferentially selected. All equipment was calibrated before use. Measurement uncertainties were ±0.5 megapascals (MPa) for mechanical strength and ±0.01 grams per cubic centimetre (g/cm^3) for density (Silva *et al.,* 2025).

Methodology overview

The methodology comprised the collection, segregation, washing, shredding, melting, moulding, testing, and environmental assessment of post-consumer plastics. The cradle-to-gate assessment included electricity, detergent use, material losses, and recycled-material production, while excluding collection, transport, wastewater treatment, and upstream infrastructure due to the controlled laboratory scope. No allocation or avoided-burden credits were applied. Physical and mechanical testing was followed by environmental assessment, and the workflow is shown in Fig. 1.

Collection of plastic waste

Plastic waste was collected from residential, commercial, and institutional areas within a single municipal boundary during one continuous collection period. The sampling represented available municipal plastic streams during this period and was not intended to assess seasonal or temporal variation. Manual collection was used to remove non-plastic contaminants without

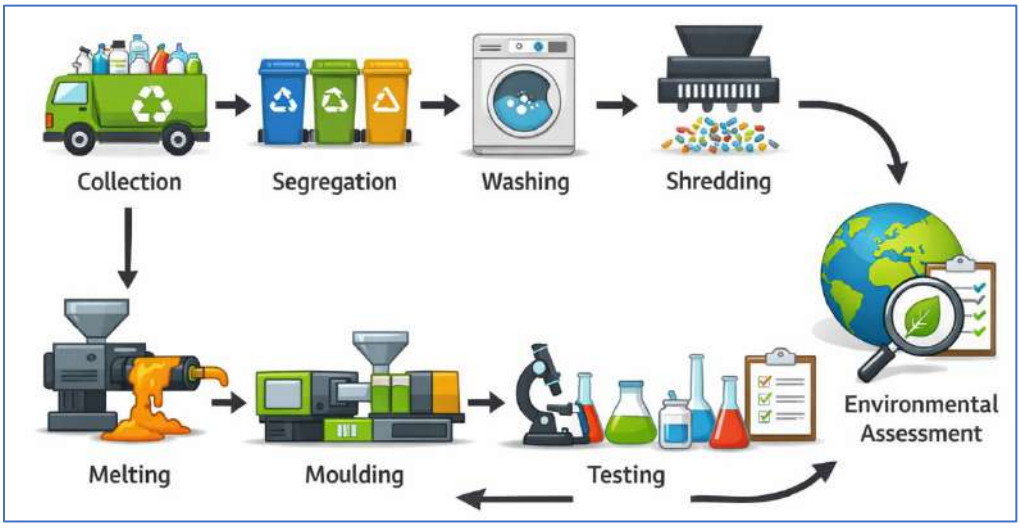

Fig. 1: The overall workflow methodology

washing. Plastics were segregated into PET, HDPE, and LDPE for quantitative analysis and recycling-efficiency evaluation (Ragaert *et al.,* 2017; Silva *et al.,* 2025).

Segregation of plastic waste

Collected plastics were segregated to avoid polymer incompatibility and ensure uniform subsequent processing. Manual sorting separated PET, HDPE, and LDPE using resin identification codes, visual appearance, rigidity, and tactile characteristics. Plastics that were uncertain in identification, multilayered, severely degraded, or visibly contaminated were excluded. Coloured plastics were retained within the same polymer category and matched with corresponding virgin controls (Jeswani *et al.,* 2021).

Pre-Treatment of plastic waste

Segregated plastics were washed with 0.5% non-ionic detergent at a 10:1 water-to-plastic ratio for 15 min at 30 ± 2 °C, rinsed twice, and air-dried for 24 h at 28 ± 2 °C and 55–65% relative humidity. Mass variation below 0.1% between successive measurements indicated adequate drying; however, residual moisture content prior to PET melting was not directly quantified. The plastics were then shredded into 10–15 mm flakes and stored in sealed containers to prevent moisture uptake and recontamination (Jeswani *et al.,* 2021; Silva *et al.,* 2025).

Recycling process

Shredded flakes were recycled using a laboratory hydraulic hot-press (20-ton capacity) with a 150 × 150 mm stainless-steel mould at 3 MPa. Heating was performed at 10 °C/min to 265 °C for PET, 185 °C for HDPE, and 165 °C for LDPE (±5 °C), with an 8 min residence time after reaching the set temperature. The material was compressed and cooled at 5 °C/min to 45 °C for demoulding. Specimens were prepared at 3 mm thickness. Three independent recycling batches were produced for each polymer, with test specimens prepared from each batch (Ragaert *et al.,* 2017; Shan *et al.,* 2023).

Cradle-to-gate energy and greenhouse-gas assessment

The environmental evaluation was conducted as a cradle-to-gate energy and greenhouse-gas assessment, not a full LCA. It included electricity for washing, shredding, melting, and moulding, detergent use, and material losses. Collection, transport, wastewater treatment, and upstream infrastructure were outside the system boundary,

and no allocation or avoided-burden credits were applied. Energy demand was expressed per kg of recycled polymer, and greenhouse-gas emissions as kg CO_2-eq/kg of recycled material using specified electricity and material emission factors. Thus, the assessment provides process-level energy and greenhouse-gas estimates rather than a complete life-cycle profile.

Assessment methodology

Plastic recycling effectiveness was evaluated using physical, mechanical, and environmental indicators. Waste reduction and material recovery rates (MRRs) were used to quantify waste conversion and material recovery. Energy use during shredding, heating, and moulding was measured using calibrated digital energy meters. Density, water absorption, tensile strength, compressive strength, elongation at break, and hardness were determined according to American Society for Testing and Materials (ASTM) methods (ASTM D792, D570, D638, and D695). Environmental performance was assessed through CO_2 emission reduction, landfill diversion, and resource conservation. The study was limited to the properties and tests listed in Table 1, with the corresponding measurement techniques, test conditions, specimen requirements, applied load or crosshead speed, where relevant, measurement frequency, and calculation methods considered in the reported analyses. Standardized measurements followed the corresponding ASTM methods, including ASTM D695 for compressive strength, while mass flow index (MFI), differential scanning calorimetry (DSC) based melting temperature and crystallinity, and thermogravimetric analysis (TGA) for thermal stability were determined using the procedures specified in Table 1. Study-specific environmental and sustainability indicators were calculated using the equations provided in Table 1.

Statistical analysis

All data are expressed as mean ± standard deviation (SD). Differences in the physical, mechanical, and environmental properties among recycled PET, HDPE, and LDPE were evaluated using exploratory one-way ANOVA at a probability vlaue (p) < 0.05. P-values were adjusted using the Benjamini–Hochberg FDR procedure. Because replicate-level data were unavailable and complete assumption checks could not be performed, ANOVA results were interpreted as exploratory, not definitive population-level effects (Durairaj, 2024). Statistical analyses were performed using Microsoft Excel 2021 and OriginPro 2022.

RESULTS AND DISCUSSION

Plastic waste collection, pre-treatment, and recycling

The collected plastic waste was systematically characterized, segregated, pre-treated, and processed for recycling. These sequential steps ensured consistent material quality and enabled reliable evaluation of recycling performance.

Composition of collected plastic waste

The composition of plastic waste collected from different municipal sources was analyzed to determine sector-wise contributions and polymer distribution. Fig. 2 presents the PET, HDPE, and LDPE quantities from residential, commercial, and institutional sources. Municipal solid waste samples were collected during March 2026 in a single sampling period. The 37 kg plastic fraction comprised PET 15 kg (40.54%), HDPE 12 kg (32.43%), and LDPE 10 kg (27.03%). These percentages reflect the study's specific feedstock polymer composition rather than general municipal waste. Standardized 100 g polymer samples were prepared from three independent batches (Jeswani *et al.,* 2021), serving as true replicates to ensure statistical independence. Additionally, waste from residential, commercial, and institutional sources was analyzed for sector-wise contributions and polymer distribution. Fig. 2 presents the quantities and percentage contributions of PET, HDPE, and LDPE from these urban municipal waste generation categories.

Table 1: Physical, mechanical, and environmental / sustainability properties of polymers

Property name	Symbol	Unit	Equation/ Description	Standard references
Physical property				
Density	ρ	g/cm³	$\rho = W_a / (W_a - W_w) \times \rho_w$, Archimedes' method (ASTM D792)	ASTM D792-20
Water absorption	WA	%	$WA (\%) = (W_f - W_i) / W_i \times 100$, ASTM D570	ASTM D570-98
Moisture content	MC	%	$MC (\%) = (W_i - W_o) / W_i \times 100$	ASTM D6980-04
Melt flow index	MFI	g/10 min	Measured via melt flow tester (ASTM D1238); mass extruded per 10 min under load	ASTM D1238-13
Melting temperature	T_m	°C	Determined from DSC as peak of melting endotherm	ASTM D3418-21
Vicat softening temperature	T_{vst}	°C	Measured using Vicat apparatus (ASTM D1525); temperature at 1 mm penetration	ASTM D1525-09
Crystallinity	X_c	%	$X_c (\%) = (\Delta H_m / \Delta H_m^\circ) \times 100$, DSC method	ASTM D3418-21
Thermal stability (onset)	T_{onset}	°C	Determined from TGA; temperature at onset of significant weight loss	ASTM E1131-20
Mechanical property				
Tensile strength	σ_t	MPa	$\sigma_t = F_{max} / A_o$, ASTM D638	ASTM D638-22
Compressive strength	σ_c	MPa	$\sigma_c = F_c / A_c$, ASTM D695	ASTM D695-10
Elongation at break	ε_b	%	$\varepsilon_b (\%) = (L_f - L_o) / L_o \times 100$	ASTM D638-22
Young's modulus	E	Gigapascals (GPa)	$E = \sigma / \varepsilon$, slope of stress–strain curve in elastic region	ASTM D638-22
Impact strength	IS	Kilojoules per square metre (kJ/m²)	IS = Energy absorbed / cross-sectional area, Charpy/Izod test	ASTM D256-97
Shore D hardness	H^D	Shore D	Measured using Shore D durometer (ASTM D2240)	ASTM D2240-15(2021)
Environmental / sustainability				
Waste reduction efficiency	WRE	%	$WRE (\%) = [(W_i - W_f) / W_i] \times 100$	Study-specific calculated indicator; no direct ASTM standard
Material recovery rate	MRR	%	$MRR (\%) = (M_r / M_i) \times 100$	
Landfill diversion	LFD	%	$LFD (\%) = (M_r / M_w) \times 100$	
Recycling rate	RR	%	$RR (\%) = (M_r / M_w) \times 100$	
Energy consumption	E_{total}	Kilowatt-hours per kilogram (kWh/kg)	$E_{total} = E_s + E_h + E_m$	
CO_2 emission reduction	CO_2	Kilograms of carbon dioxide per kilogram (kg CO_2/kg)	$CO_2 = (EF_v - EF_r) \times Q$	
SI	SI	–	$SI = [(w_1 \times N_{WRE}) + (w_2 \times N_{MSF})] / (w_3 \times NE_{total}) \times 100$	

Note: W_a = weight of the specimen in air; W_w = weight of the specimen in water; ρ_w = density of water; W_i = initial dry weight of the specimen; W_f = final weight after water immersion; W_o = oven-dried weight; ΔH_m = measured melting enthalpy from Differential Scanning Calorimetry; ΔH_m° = enthalpy of a fully crystalline polymer; F_{max} = maximum tensile force applied; A_o = original cross-sectional area; F_c = compressive force; A_c = cross-sectional area under compression; L_o = original gauge length; L_f = gauge length at break; σ = applied stress; ε = strain; W_i = initial waste mass; W_f = final waste mass after processing; M_r = recovered material mass; M_i = initial input material mass; M_D = mass diverted from landfill; M_w = total waste polymer mass; E_s = energy consumed during shredding; E_h = energy consumed during heating; E_m = energy consumed during moulding; EF_v = emission factor of virgin polymer; EF_r = emission factor of recycled polymer; Q = quantity of polymer processed; N_{WRE} = normalized waste reduction efficiency; N_{MSF} = normalized mechanical strength factor; NE_{total} = normalized total energy consumption; w_1, w_2 and w_3 = weighting coefficients assigned to WRE, MSF and E_{total}, respectively.

The residential, commercial, and institutional sources contributed 40.54%, 32.43%, and 27.03%, respectively, to the 37 kg plastic feedstock. Such polymer-specific establishes a basis for subsequent recycling processes, as Lahtela *et al.* (2019) highlighted source-dependent variation in plastic composition and the importance of polymer identification. In comparison, Faraca and Astrup (2019) reported substantial impurity levels in plastics from recycling centres, emphasizing the influence of feedstock quality. Accordingly, the present composition establishes the experimental feedstock baseline rather than a general estimate of municipal plastic-waste composition.

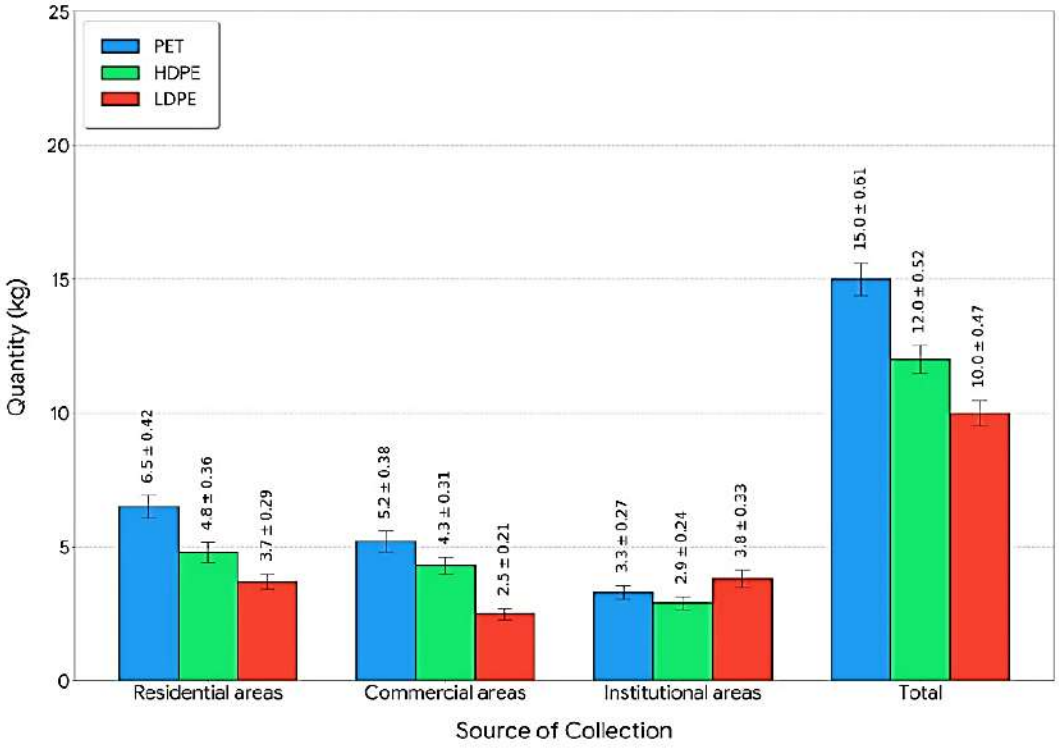

Fig. 2: Sector-wise distribution of PET, HDPE, and LDPE collected from municipal sources

Segregation of plastic waste

Segregation effectiveness was evaluated from the final polymer-specific distribution. Fig. 3 shows PET as the largest fraction (40.54%), followed by HDPE (32.43%) and LDPE (27.03%). Low SDs indicate good reproducibility of manual segregation. Effective polymer separation is important because feedstock composition and contamination affect recovery efficiency. Antonopoulos *et al.* (2021) reported PET sorting rates of 45–97% and HDPE sorting rates of 13–95% across European material recovery facilities, with recycling rates of 63–90% for PET and 70–88% for HDPE. Output purity ranged from 80–98% for selected recycled polymer streams. Lahtela *et al.* (2019) reported considerable variation in sorting efficiency across material recovery facilities, highlighting the importance of effective polymer identification and separation. Therefore, the present segregation results demonstrate a consistent feedstock composition appropriate for polymer-specific recycling.

Pre-treatment of plastic waste

Fig. 4 presents the material loss of PET, HDPE, and LDPE during pre-treatment. PET showed the lowest loss (1.33%), followed by HDPE (1.67%), while LDPE showed the highest loss (2.00%); the overall experimentally determined pre-treatment loss was 1.57%, corresponding to approximately 0.58 kg of the 37.00 kg initial feedstock. Approximately 36.42 kg remained post-pretreatment, indicating minimal mass loss. While Alrazen *et al.* (2025) highlighted key mechanical recycling stages (collection, sorting, grinding, washing, drying, granulation) where contamination and degradation can affect material quality, current findings indicate effective contaminant removal and exceptionally high material retention throughout the process.

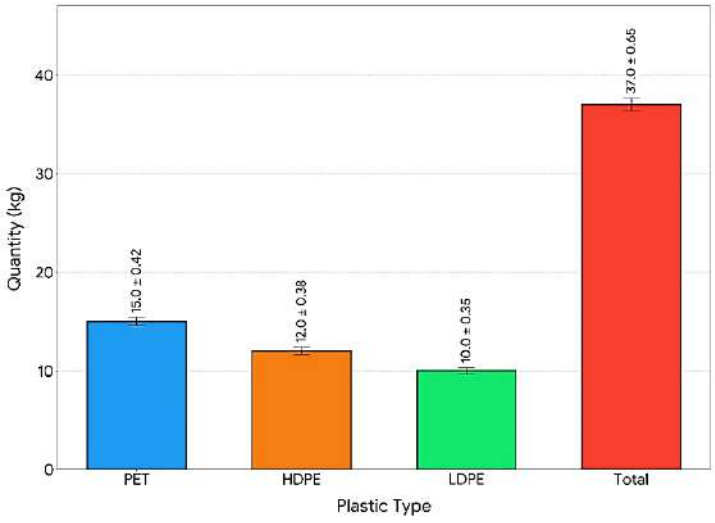

Fig. 3: Quantity and percentage of PET, HDPE, and LDPE plastics

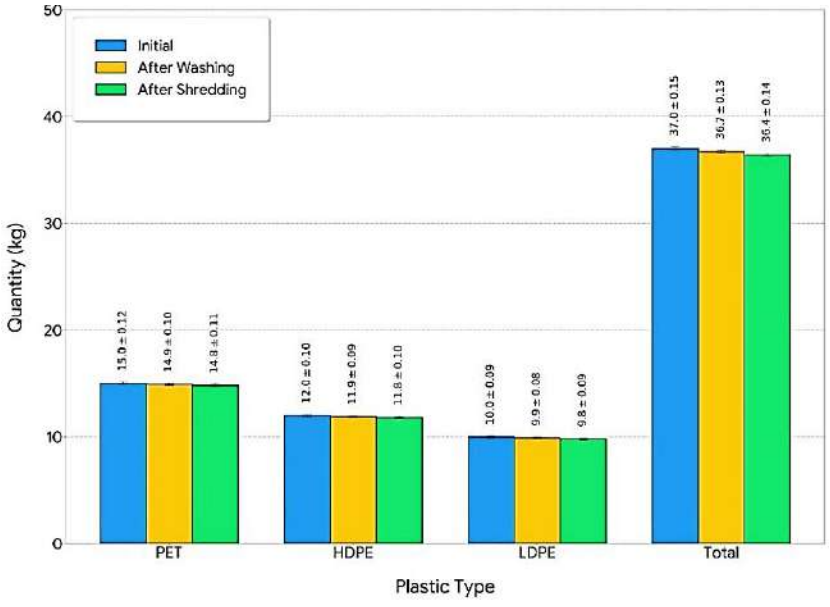

Fig. 4: Material loss of PET, HDPE, and LDPE during pre-treatment

Recycling process

Fig. 5 presents the recycling process parameters for PET, HDPE, and LDPE, evaluated based on specimen uniformity, surface characteristics, and reproducibility. PET was processed at 250 °C for 15 min with 20 min cooling, whereas HDPE and LDPE were processed at 145 °C and 120 °C, respectively. PET processing at 250 °C is consistent with its reported melting behaviour of approximately 250–260 °C. Industrially, Antonopoulos *et al.* (2021) reported PET and HDPE recycling rates of 63–90% and 70–88%, respectively, while Szostak *et al.* (2020) reported 60.6 ± 20.4 wt% plastic available for processing in a full-scale packaging-waste plant (max 10% moisture, 5% impurities). Controlled preparation promoted reproducible and uniform specimens, although degradation and scale-up feasibility warrant further investigation.

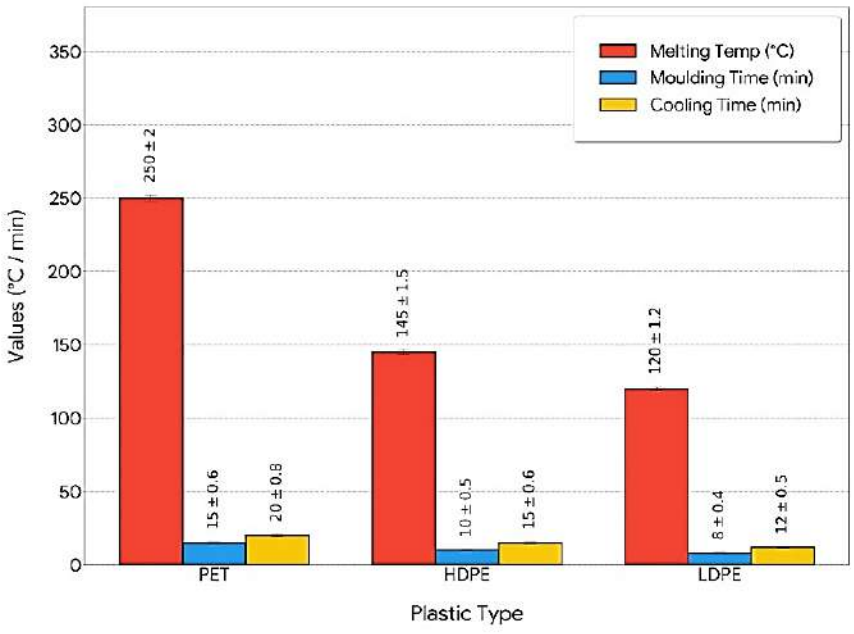

Fig. 5: Recycling process parameters for PET, HDPE, and LDPE

Process efficiency and environmental performance

The efficiency and environmental performance of recycling PET, HDPE, and LDPE were evaluated using waste reduction, material recovery, energy consumption, CO_2 emission reduction, mechanical strength, and the SI. These indicators collectively evaluate the technical performance and environmental sustainability of polymer-specific mechanical recycling. Mechanical recycling remains the most widely adopted recycling route, although contamination, polymer degradation, and incompatibility among mixed plastics can influence recycled-product quality (Alrazen *et al.,* 2025).

Waste reduction and material recovery

Waste reduction efficiency (WRE) and MRR, which measure converted proportion and reusable material, are key mechanical recycling indicators. Fig. 6 shows high performance across polymers: LDPE achieved the highest values (WRE: 99.0 ± 0.5%; MRR: 98.7 ± 0.5%) due to favorable melt behavior and lower processing temperatures, followed by HDPE (WRE: 96.0 ± 1.0%; MRR: 95.5 ± 1.0%) and PET (WRE: 95.8 ± 0.8%; MRR: 95.2 ± 0.5%), indicating minor losses during cutting, heating, and moulding. Small differences between WRE and MRR suggest limited downstream material losses. While these values show high controlled laboratory recovery, industrial rates vary due to feedstock heterogeneity, contamination, and overall high sorting efficiency (Antonopoulos *et al.,* 2021), representing process-specific rather than universal rates.

Mass balance of polymer-specific mechanical recycling

A mass-balance assessment was performed to quantify the distribution of plastic material from the initial feedstock through pre-treatment and final recovery (Table 2). The initial feedstock was 37.00 kg, comprising 15.00 kg PET, 12.00 kg HDPE, and 10.00 kg LDPE. Pre-treatment loss was 1.57% (0.58 kg), leaving 36.42 kg. Synthesized losses were 0.24 kg PET, 0.19 kg HDPE, and 0.16 kg LDPE. MRR-based recovered masses were 35.61 kg (14.28 kg PET, 11.46 kg HDPE, 9.87 kg LDPE), with unrecovered masses of 0.72 kg PET, 0.54 kg HDPE, and 0.13 kg LDPE. Mass-weighted overall WRE and

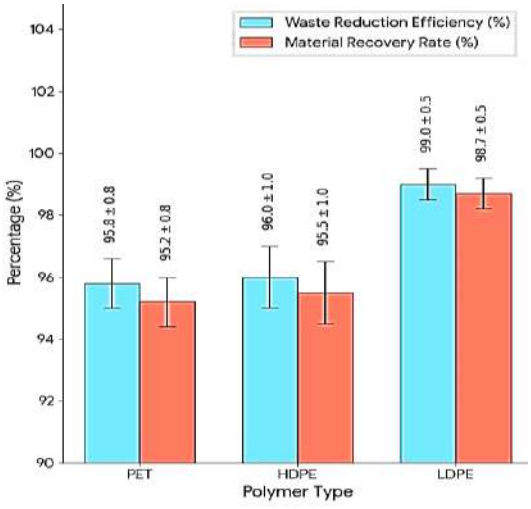

Fig. 6: WRE and MRR of PET, HDPE, and LDPE

Table 2: Mass balance of polymer-specific mechanical recycling of municipal plastics

Mass-balance component	PET (kg)	HDPE (kg)	LDPE (kg)	Total (kg)
Initial plastic feedstock	15.00	12.00	10.00	37.00
Pre-treatment loss	0.24	0.19	0.16	0.58 (1.57%)
Material remaining after pre-treatment	14.76	11.81	9.84	36.42
Final recovered recycled product*	14.28	11.46	9.87	35.61
Unrecovered mass based on MRR*	0.72	0.54	0.13	1.39
WRE (%)	95.8 ± 0.8	96.0 ± 1.0	99.0 ± 0.5	96.73
MRR (%)	95.2 ± 0.5	95.5 ± 1.0	98.7 ± 0.5	96.24

Note: *Final recovered recycled-product and unrecovered masses are derived from the reported MRR values and should not be interpreted as direct measurements at individual processing stages. Polymer-specific pre-treatment losses are proportionally synthesized from the experimentally determined overall pre-treatment loss of 1.57% and the initial polymer feedstock masses.

MRR were 96.73% and 96.24%, respectively, demonstrating high material retention under controlled processing conditions. Pre-treatment losses were calculated from the overall loss and initial proportions, while recovered and unrecovered masses were independently calculated from MRR values as separate mass-balance stages. Measured masses were experimental; percentages and mass-balance values were calculated, and emission factors were literature-derived estimates.

Energy consumption

Energy consumption was assessed for shredding, heating/melting, and moulding to determine polymer-specific energy requirements. Table 3 shows that PET exhibited the highest total energy consumption (10.50 ± 0.20 kWh/kg), followed by HDPE (10.30 ± 0.19 kWh/kg) and LDPE (9.20 ± 0.18 kWh/kg). The higher PET requirement is attributed to its higher processing temperature, whereas LDPE required less energy because of its lower processing temperature. Heating and melting dominated energy consumption, making thermal processing as the main area for optimization. While Alrazen *et al.* (2025) highlighted energy demand and process conditions as key mechanical recycling considerations, direct comparisons remain limited because reported values vary significantly across studies with equipment, throughput, processing duration, polymer composition, and system boundaries.

CO_2 emission reduction and landfill diversion

Environmental performance was evaluated using landfill diversion and CO_2 emission reduction as separate environmental indicators (Table 4).

Table 3: Energy consumption during recycling for PET, HDPE, and LDPE

Polymer	Energy shredding (kWh/100 g)	Energy heating/melting (kWh/100 g)	Energy moulding (kWh/100 g)	Total energy (kWh/kg)
PET	0.20 ± 0.01	0.65 ± 0.02	0.20 ± 0.01	10.50 ± 0.20
HDPE	0.22 ± 0.01	0.60 ± 0.02	0.21 ± 0.01	10.30 ± 0.19
LDPE	0.18 ± 0.01	0.55 ± 0.02	0.19 ± 0.01	9.20 ± 0.18

Note: Total energy was calculated as the sum of shredding, heating/melting, and moulding energy and normalized to 1 kg. For example, PET: (0.20 + 0.65 + 0.20) kWh/100 g = 10.50 kWh/kg.

Table 4: CO_2 Emission reduction and landfill diversion performance of recycled PET, HDPE, and LDPE

Polymer	Landfill diversion (%)	EF_v (kg CO_2-eq/kg)	EF_r (kg CO_2-eq/kg)	Q (kg)	CO_2-eq reduction (kg CO_2-eq/kg)	CO_2 emission reduction (kg CO_2/kg)	Mechanical strength factor
PET	85 ± 2	3.00	0.90	1.00	2.10	2.10 ± 0.08	1.15 ± 0.03
HDPE	80 ± 3	2.50	0.65	1.00	1.85	1.85 ± 0.06	1.10 ± 0.02
LDPE	75 ± 2	2.20	0.70	1.00	1.50	1.50 ± 0.05	1.05 ± 0.03

Landfill diversion measures original waste kept from landfills, whereas material recovery measures processed input recovered as usable material. PET had the highest landfill diversion (85 ± 2%) and CO_2 emission reduction (2.10 ± 0.08 kg CO_2/kg), followed by HDPE (80 ± 3%; 1.85 ± 0.06 kg CO_2/kg) and LDPE (75 ± 2%; 1.50 ± 0.05 kg CO_2/kg). Landfill diversion was interpreted separately from Fig. 6 MRRs using initial input, recovered material, and processing losses. Thus, diversion (75–85%) includes non-recyclable fractions and original waste losses, whereas MRR (95–99%) indicates the recyclable material retained following processing. Environmental benefits differed among polymers because of material characteristics, processing requirements, and avoided virgin-material production. Gabisa *et al.* (2023) demonstrated that recycling can reduce life-cycle greenhouse-gas emissions and resource depletion, while also identifying potential microplastic-emission trade-offs. Papo and Corona (2022) also reported environmental benefits from recycled HDPE compared with virgin HDPE, despite economic and social trade-offs. Accordingly, these CO_2 values reflect process-specific avoided emissions within the defined system boundaries. Therefore, they should not be interpreted as direct statistical comparisons between recycled and virgin polymers. Future research should incorporate broader lifecycle perspectives to validate environmental trade-offs.

Physical properties

Fig. 7 demonstrates clear polymer-specific differences in the physical, thermal, structural, and rheological behaviour of recycled PET, HDPE, and LDPE. Recycled PET exhibited the highest density (1.36 ± 0.02 g/cm³) and melting temperature (250 ± 3 °C), whereas HDPE showed the highest crystallinity (72 ± 3%) and LDPE the highest melt flow index (12.6 ± 0.5 g/10 min). PET also showed comparatively higher water absorption (0.28 ± 0.03%), while HDPE exhibited the lowest moisture uptake (0.12 ± 0.02%). These differences may be attributed to polymer structure, chain configuration, crystallinity, and recycling history. Basalp *et al.* (2020) similarly reported that polymer type and recycling conditions significantly influence physical and processing characteristics, confirming the distinct properties of PET, HDPE, and LDPE.

Mechanical properties

Fig. 8 presents the mechanical behaviour of recycled PET, HDPE, and LDPE. PET exhibited the highest tensile strength (55.2 ± 1.8 MPa) and Young's modulus (2.45 ± 0.08 GPa), indicating higher stiffness and tensile strength. In contrast, LDPE showed the highest elongation at break (560 ± 20%) due to greater flexibility, whereas HDPE provided intermediate strength and ductility. Basalp *et al.* (2020) similarly reported marked mechanical differences among recycled polymers,

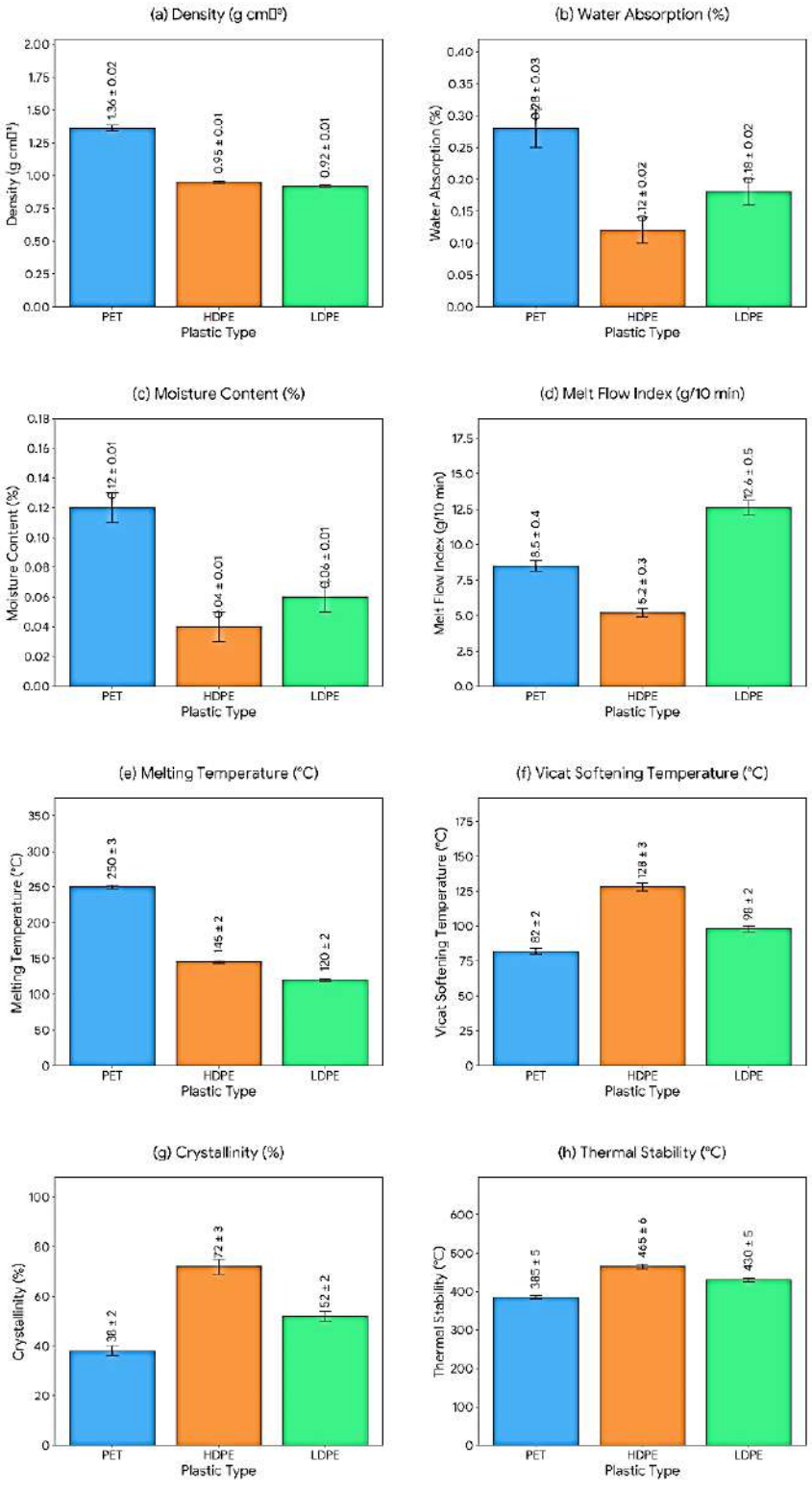

Fig. 7: Physical properties of recycled PET, HDPE, and LDPE

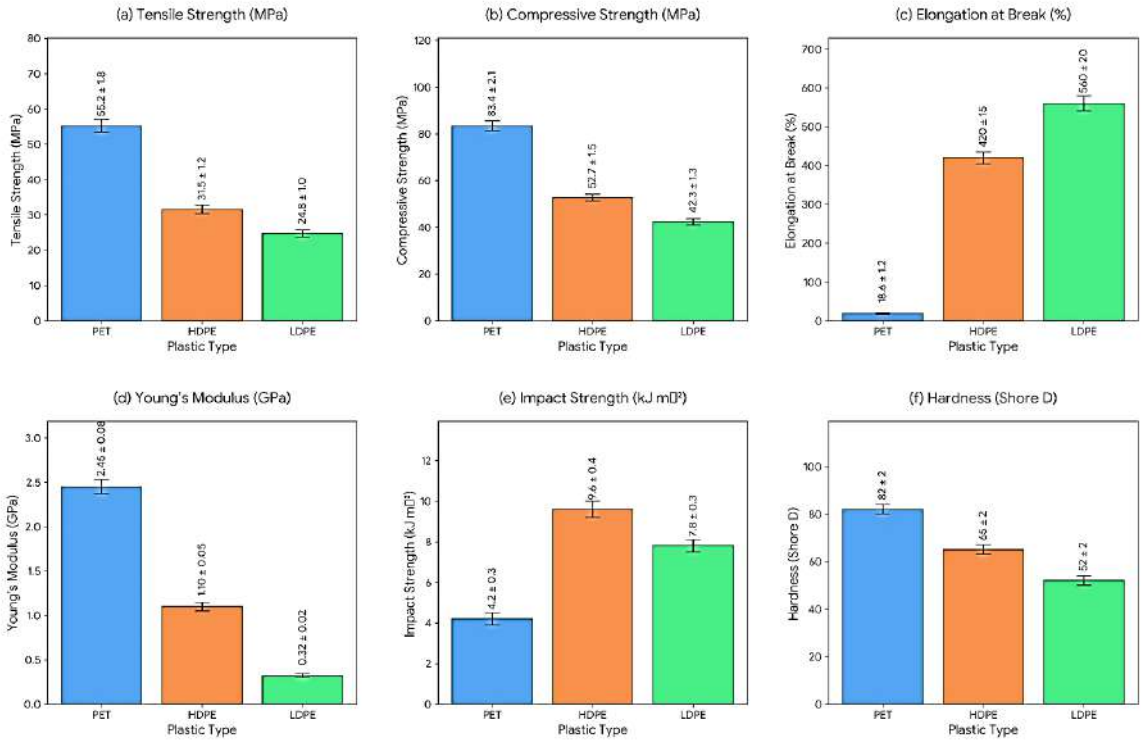

Fig. 8: Mechanical properties of recycled PET, HDPE, and LDPE

attributing them to polymer type, composition, and processing history. Thus, these findings demonstrate a clear strength-ductility trade-off and support polymer-specific selection for rigid, dimensionally stable, and flexible applications.

Environmental impact assessment (EIA)

The environmental performance of recycled PET, HDPE and LDPE was assessed using landfill diversion, energy consumption, CO_2-equivalent (CO_2-eq) emission reduction and the integrated sustainability index (SI) under the cradle-to-gate boundary (Fig. 9). PET showed 85 ± 2% landfill diversion, followed by HDPE (80 ± 3%) and LDPE (75 ± 2%). These differences may be associated with variations in polymer structure, feedstock characteristics and separation efficiency (Antonopoulos *et al.,* 2021). The energy requirements were 0.22, 0.49 and 0.91 kWh/kg for PET, HDPE and LDPE, respectively, based on the LCI presented in Table 5. PET achieved a CO_2-eq emission reduction of 2.10 ± 0.08 kg CO_2-eq/kg, followed by HDPE (1.85 ± 0.06 kg CO_2-eq/kg) and LDPE (1.50 ± 0.05 kg CO_2-eq/kg). These differences indicate variations in estimated environmental impacts associated with polymer-specific recycling processes within the defined system boundary (Papo and Corona, 2022). The dimensionless SI combined normalized waste reduction, mechanical strength, and energy consumption with equal weighting, yielding 78.1 ± 2.5 for PET, 80.0 ± 2.8 for HDPE, and 82.6 ± 2.1 for LDPE. These scores represent the study conditions and normalization framework, not absolute quantities. Sensitivity analysis verified robustness across alternative weightings, and the SI serves as a decision-support metric rather than an LCA substitute. PET showed greater landfill diversion and CO_2-eq reduction, whereas LDPE required less energy and exhibited a higher SI, highlighting

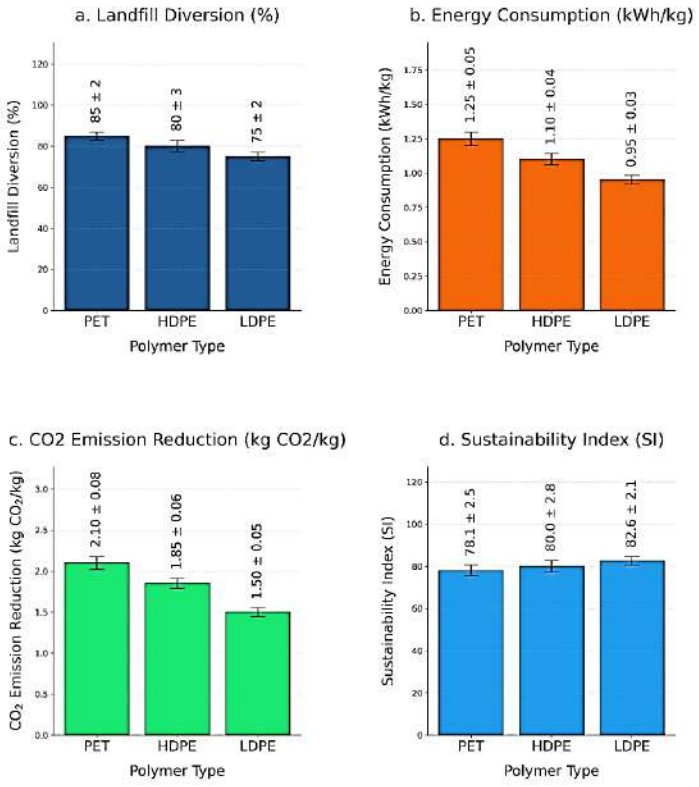

Fig. 9: Environmental performance and SI of recycled plastics

polymer-specific environmental performance is critically and directly influenced by the underlying feedstock, processing configuration, and recycling conditions employed during production (Gabisa *et al.,* 2023; Alrazen *et al.,* 2025).

LCA

The LCA evaluated mechanically recycled PET, HDPE, and LDPE using 1 kg of recycled plastic as the functional unit and a cradle-to-gate boundary encompassing collection, transportation, segregation, washing, pre-treatment, shredding, drying, recycling, and product formation. Use and end-of-life stages were not included because the system boundary terminated at the production gate. The assessment followed ISO 14040 and ISO 14044 for goal and scope, inventory, impact assessment, and interpretation. Published results were used only as contextual benchmarks due to differences in functional units, feedstock quality, recycling routes, and system boundaries (Gabisa *et al.,* 2023).

Life cycle inventory (LCI) analysis

LCI data were established for a functional unit of 1 kg recycled plastic within the defined cradle-to-gate system boundary (Table 5). PET and HDPE each required 1.04 kg of plastic input to produce 1.00 kg of recycled output, whereas LDPE required 1.01 kg, corresponding to material losses of 0.04, 0.04 and 0.01 kg, respectively. LDPE exhibited the lowest material loss and higher material recovery under the evaluated processing conditions. Electricity consumption was 0.22, 0.49 and 0.91 kWh/kg for PET, HDPE and LDPE, respectively, while washing-water consumption was 2.24, 1.56 and 2.00 L/kg. Chemical/detergent inputs were 0.002, 0.003 and 0.024 kg/kg, respectively, and wastewater generation was 2.13, 1.48 and 1.90 L/kg for PET, HDPE and LDPE, respectively.

Table 5: LCI data for recycled plastics (per kg)

Parameter	PET	HDPE	LDPE
Plastic input (kg/kg recycled plastic)	1.04	1.04	1.01
Recycled output (kg/kg recycled plastic)	1.00	1.00	1.00
Material loss (kg/kg recycled plastic)	0.04	0.04	0.01
Electricity consumption (kWh/kg)	0.22	0.49	0.91
Washing-water consumption (L/kg)	2.24	1.56	2.00
Chemical/detergent input (kg/kg)	0.002	0.003	0.024
Wastewater generation (L/kg)	2.13	1.48	1.90
Transport requirement (km)	60	60	50
Material-loss treatment	Process loss	Process loss	Process loss
Functional unit for recycle plastic	1 kg	1 kg	1 kg
System boundary	Cradle-to-gate	Cradle-to-gate	Cradle-to-gate

Transport requirements were 60 km for PET and HDPE and 50 km for LDPE. These inventory differences indicate variations in polymer characteristics, feedstock requirements and processing conditions. Feedstock quality and contamination can further influence material recovery and recycling efficiency in heterogeneous plastic streams. Faraca and Astrup (2019) identified feedstock quality and contamination as key constraints in mechanical recycling, while Alrazen *et al.* (2025) highlighted processing configuration and feedstock quality as important determinants of recycling performance.

Life cycle impact assessment (LCIA)

Environmental and sustainability indicators are presented in Table 6. PET recorded the highest landfill diversion (85 ± 2%) and CO_2-eq emission reduction (2.10 ± 0.08 kg CO_2-eq/kg), followed by HDPE (80 ± 3%; 1.85 ± 0.06 kg CO_2-eq/kg) and LDPE (75 ± 2%; 1.50 ± 0.05 kg CO_2-eq/kg). Energy savings relative to virgin plastic increased from 62% for PET to 65% for HDPE and 68% for LDPE. The mechanical strength factor decreased from 1.15 ± 0.03 for PET to 1.10 ± 0.02 for HDPE and 1.05 ± 0.03 for LDPE, whereas SI increased from 78.1 ± 2.5 to 80.0 ± 2.8 and 82.6 ± 2.1, respectively. SI was calculated using the complete study-specific formulation, with the mechanical strength factor defined as the ratio of recycled to corresponding virgin-polymer compressive strength. These environmental benefits are consistent with Papo and Corona (2022) and Gabisa *et al.* (2023). Differences among polymers reflect material recovery, feedstock characteristics, energy requirements, and processing conditions. Faraca and Astrup (2019) highlighted the effects of feedstock quality and contamination, while Alrazen *et al.* (2025) emphasized processing configuration and feedstock characteristics. Direct numerical comparison remains limited by variations in functional units, system boundaries, feedstock composition, recycling efficiency, transport assumptions, and processing conditions.

Insights and implications of LCA findings

The life cycle assessment linked polymer characteristics to energy demand and sustainability, with heating and melting identified as the main hotspots (58 to 62%). PET required the highest heating energy (0.65 ± 0.02 kWh/100 g), while shredding contributed 17 to 20% and moulding 18 to 21%, identifying thermal processing as the main energy-reduction opportunity, consistent with Alrazen *et al.* (2025). A ±10% change in heating energy altered the Sustainability Index (SI) by ±6% for PET, ±5% for HDPE, and ±4% for LDPE, whereas material-loss changes caused less than ±2% variation, confirming energy demand as the dominant driver. These SI sensitivity were obtained by recalculating the complete SI equation after independently varying heating energy by ±10%, while keeping other components unchanged, representing net SI changes rather than direct inverse proportionality.

Table 6: LCIA Indicators

Impact category	PET	HDPE	LDPE
Landfill diversion (%)	85 ± 2	80 ± 3	75 ± 2
CO_2 emission reduction (kg CO_2/kg)	2.10 ± 0.08	1.85 ± 0.06	1.50 ± 0.05
Energy savings vs virgin (%)	62	65	68
Mechanical strength factor	1.15 ± 0.03	1.10 ± 0.02	1.05 ± 0.03
SI	78.1 ± 2.5	80.0 ± 2.8	82.6 ± 2.1

The environmental assessment applied polymer-specific emission factors for virgin plastics (2.75 kg CO_2-eq/kg for PET, 1.82 for HDPE, 1.95 for LDPE) and recycled counterparts (0.65 for PET, 0.64 for HDPE, 0.45 for LDPE) on a cradle-to-gate basis using India-relevant conditions for 2025, with electricity emissions at 0.70 kg CO_2-eq/kWh and greenhouse gases expressed on a 100-year global warming basis. Compared to virgin plastics, recycled PET, HDPE, and LDPE achieved energy savings of 62%, 65%, and 68%, respectively, with CO_2 reductions of 2.10, 1.85, and 1.50 kg CO_2/kg. PET provided the highest CO_2 reduction, while LDPE achieved the highest energy saving and SI. Gabisa *et al.* (2023) similarly reported greenhouse gas benefits. Low standard deviations for energy consumption (±0.03 to 0.05 kWh/kg) and material loss (0.01 to 0.04 kg) indicate good repeatability, though LCA outcomes remain sensitive to the electricity mix, transport, allocation, and feedstock quality (Faraca and Astrup, 2019). The findings support polymer-specific approaches targeting thermal energy reduction, material recovery, feedstock quality, and virgin-material substitution rather than a generalized recycling approach.

Polymer-specific mechanical recycling pathway for municipal plastics

The polymer-specific recycling pathway achieved effective material recovery, with low pre-treatment losses (1.33–2.00%) and satisfactory recycled-material performance, highlighting the importance of controlled segregation and feedstock quality. These findings support the observations of Faraca and Astrup, 2019, who identified contamination and sorting quality as critical constraints in municipal plastic recycling, while Alrazen *et al.* (2025) highlighted the influence of polymer properties and process configurations. Heating and melting accounted for 58 to 62% of energy demand, with PET requiring the highest heating energy (0.65 ± 0.02 kWh/100 g). LDPE achieved the highest SI (82.6 ± 2.1), whereas PET showed the greatest carbon reduction (2.10 kg CO_2/kg), indicating that energy efficiency and carbon mitigation vary by polymer type. The results indicate that polymer-specific optimization of thermal processing and material recovery is superior to a generalized municipal strategy.

Statistical analysis of recycled plastics

Exploratory one-way ANOVA with Benjamini–Hochberg FDR adjustment identified significant polymer-specific differences across most physical, mechanical, energy, and carbon-reduction properties. However, landfill diversion and the Sustainability Index did not show statistically significant differences.These findings are consistent with the polymer-specific performance characteristics reported by (Alrazen *et al.,* 2025), while providing quantitative evidence under controlled mechanical recycling conditions.

One-way ANOVA and Tukey post-hoc analysis of polymer properties

The physical, mechanical, and environmental properties of recycled PET, HDPE, and LDPE were evaluated to assess material performance and sustainability. The study provides an integrated, polymer-specific assessment linking process efficiency, physical and mechanical properties, environmental indicators, ANOVA, and the sustainability index. Original one-way ANOVA results are retained in Table 7 as exploratory

Table 7: One-way ANOVA and Benjamini–Hochberg FDR-adjusted comparison of polymer properties

Property category	Evaluated parameter	F-statistic (F)	p-value (p)	FDR-adjusted p	Significance level
Physical	Density (g/cm³)	152.3	<0.001	0.0023	***
	Water absorption (%)	9.42	0.016	0.0192	*
	Moisture content (%)	12.58	0.010	0.0138	*
	Melt flow index (g/10 min)	18.35	0.005	0.0082	**
	Melting temperature (°C)	246.7	<0.001	0.0023	***
	Vicat softening temperature (°C)	27.8	0.002	0.0040	**
	Crystallinity (%)	96.4	<0.001	0.0023	***
	Thermal stability (Onset °C)	14.2	0.008	0.0120	**
Mechanical	Tensile strength (MPa)	178.6	<0.001	0.0023	***
	Compressive strength (MPa)	148.1	<0.001	0.0023	***
	Elongation at break (%)	412.3	<0.001	0.0023	***
	Young's modulus (GPa)	203.5	<0.001	0.0023	***
	Impact strength (kJ/m²)	21.7	0.004	0.0072	**
	Shore D hardness	165.4	<0.001	0.0023	***
Environmental / Sustainability	Landfill diversion (%)	2.18	0.22	0.2329	ns
	Energy consumption (kWh/kg)	6.03	0.033	0.0371	*
	CO_2 emission reduction (kg CO_2/kg)	10.52	0.014	0.0180	*
	SI	1.72	0.27	0.2700	ns

Note: ***Highly significant (p < 0.001); **Significant (p < 0.01); *Moderately significant (p < 0.05); ns: Not significant.

statistical descriptors, with multiple-testing adjustment using the Benjamini–Hochberg FDR procedure. Complete replicate-level observations, sample sizes, residual diagnostics, normality tests, and homogeneity-of-variance assessments were not available for all parameters; consequently, the ANOVA results are interpreted as exploratory rather than definitive evidence of population-level effects.

i. *Physical properties:* The evaluated physical properties included density, water absorption, moisture content, melt flow index, melting temperature, Vicat softening temperature, crystallinity, and thermal stability. The F-statistic ranged from 9.42 to 246.7, with p-values from <0.001 to 0.016. After FDR adjustment, values remained below 0.05 for all eight parameters (0.0023–0.0192), indicating consistent polymer-level differences across the evaluated properties. PET had a density of 1.36 g/cm³, compared with 0.95 g/cm³ for HDPE and 0.92 g/cm³ for LDPE. PET also showed higher thermal resistance, while HDPE and LDPE showed greater flexibility. These differences are consistent with reported influences of polymer type, crystallinity, degradation history, and processing conditions, although the experimental design does not demonstrate causal relationships among these factors Alrazen *et al.* (2025).

ii. *Mechanical properties:* All mechanical parameters showed exploratory differences, with F-statistics of 21.7–412.3 and p-values of ≤0.004; FDR-adjusted p-values remained below 0.01. PET showed higher tensile strength (55.2 MPa) and compressive strength (83.4 MPa) than HDPE (31.5 and 52.7 MPa) and LDPE (24.8 and 42.3 MPa), respectively. PET had lower elongation at break (18.6%) than HDPE (420%) and LDPE (560%), indicating greater stiffness and lower ductility. However, molecular weight, intrinsic viscosity, oxidation indices, molecular-weight distribution, branching, and other direct degradation indicators were not evaluated; consequently, specific molecular or structural mechanisms cannot be established. These results describe polymer differences under the study conditions without establishing causal structure–property relationships. Published studies similarly report that recycled-polymer performance is influenced by polymer type, recycling history, molecular changes, crystallinity, contamination, and processing conditions (Das and Ali, 2025).

iii. *Environmental and sustainability properties:* The exploratory analysis indicated differences in energy consumption and CO_2 emission reduction, whereas landfill diversion and SI showed no clear differences after multiple-testing adjustment. The reported F-statistic were 2.18, 6.03, 10.52, and 1.72 for landfill diversion, energy consumption, CO_2 emission reduction, and SI, respectively. The corresponding FDR-adjusted p-values were 0.2329, 0.0371, 0.0180, and 0.2700. The CO_2 emission reduction values were 2.10 kg CO_2/kg for PET, 1.85 kg CO_2/kg for HDPE, and 1.50 kg CO_2/kg for LDPE, while energy consumption showed a smaller polymer-level difference. These sustainability characteristics should be interpreted in relation to collection, sorting, contamination, feedstock quality, recycling efficiency, and process configuration rather than attributed solely to polymer type, as these factors can collectively influence recycling performance and environmental outcomes (Faraca and Astrup, 2019).

PET exhibited higher density, tensile strength, and compressive strength, but lower elongation at break, whereas HDPE and LDPE showed greater ductility and flexibility. Sustainability indicators showed less polymer-level differentiation than physical and mechanical properties. The reported statistics are retained for transparency but treated as exploratory because the available information does not permit complete verification of inferential ANOVA assumptions prior to drawing definitive statistical conclusions.

Sustainability assessment

This section evaluates the environmental sustainability of polymer-specific mechanical recycling for PET, HDPE, and LDPE by integrating landfill diversion, energy consumption, carbon reduction, and material performance indicators. The findings provide an experimental basis for supporting circular economy practices and climate mitigation, with comparisons made against previous global and regional studies.

Contribution of recycling to environmental sustainability

Mechanical recycling significantly reduced landfill burden while generating reusable secondary materials. Landfill diversion efficiencies reached 85 ± 2% for PET, 80 ± 3% for HDPE, and 75 ± 2% for LDPE, exceeding typical previous studies ranges for post-consumer recycling (50–85%, Edjabou *et al.,* 2021). WRE and material recovery exceeded 95% for all polymers, with LDPE achieving 99 ± 0.5%, compared to typical industrial recovery rates of 60–90% (Tonini *et al.,* 2021). These high recovery values reflect the selected feedstock, as severely degraded, contaminated, ambiguous, and multilayer plastics were excluded and therefore should not be interpreted as representative of unsorted municipal plastic recycling. Pre-treatment losses remained minimal (total loss: 1.57%), which is lower than the 2–10% commonly reported (Van Eygen *et al.,* 2018). Additionally, microplastic mitigation is relevant: well-managed recycling reduces microplastic release by 56.8 million particles per year, whereas uncontrolled processes can increase particle release up to 2.4×10^9 particles per year (Gabisa *et al.,* 2023), emphasizing the importance of optimized pre-treatment and handling.

Reduction in carbon footprint

Substantial CO_2 emission reductions were achieved, strongly dependent on polymer-specific embodied carbon and recovery efficiency. PET exhibited the highest reduction (2.10 ± 0.08 kg CO_2 per kg), followed by HDPE (1.85 ± 0.06 kg CO_2 per kg) and LDPE (1.50 ± 0.05 kg CO_2 per kg), within the previous studies range for mechanical recycling (0.37–0.65 kg CO_2 per kg, Vollmer *et al.,* 2020) and consistent with global GHG mitigation scenarios of 67 Megatonnes of carbon dioxide equivalent (Mt CO_2-eq) (Gabisa *et al.,* 2023). Despite lower landfill diversion, LDPE achieved the highest SI (82.6 ± 2.1) due to its lower energy requirement, confirming that environmental performance depends on recovery efficiency, carbon intensity, and energy consumption. Mechanical recycling can provide greater greenhouse-gas benefits than alternative

treatment pathways under optimized conditions, while the European Union (EU) recycling rate of only 19.6% (Amadei *et al.,* 2025b) highlights the continuing gap in plastic recycling performance.

Energy savings through recycling

Total energy consumption varied by polymer and processing requirements. PET required 1.25 ± 0.05 kWh per kg, HDPE 1.10 ± 0.04 kWh per kg, and LDPE 0.95 ± 0.03 kWh per kg, which is consistent with previous studies ranges for mechanical recycling (0.9–1.5 kWh per kg, Szostak *et al.,* 2020). Heating and melting accounted for approximately 58–62% of total energy consumption. Lower LDPE processing temperature reduced energy requirements while maintaining mechanical performance. Effective process control during shredding, heating, and moulding helped minimize energy losses, reinforcing the environmental advantage of mechanical recycling relative to chemical recycling, which can consume similar or higher energy under pyrolysis/gasification scenarios (0.37–0.65 kg CO_2 per kg, Vollmer *et al.,* 2020). These results demonstrate that polymer-specific optimization of energy use is crucial for maximizing sustainability.

Long-term sustainability implications

Sustainability outcomes were assessed using landfill diversion, mechanical performance, energy efficiency, and carbon mitigation. Exploratory one-way ANOVA with Benjamini–Hochberg FDR adjustment identified polymer-specific differences in most physical and mechanical properties, energy consumption, and CO_2 emission reduction, but not for landfill diversion or the sustainability index. These differences are observational and do not establish causal or long-term sustainability effects. The findings provide a controlled experimental baseline within the defined system boundary. CO_2-eq reductions were 2.10, 1.85, and 1.50 kg CO_2-eq/kg for PET, HDPE, and LDPE, respectively, relative to corresponding virgin polymers. These are not directly comparable with absolute recycling impacts of 0.37–0.65 kg CO_2-eq/kg from previous LCA studies. Facility-scale recovery comparisons were interpreted cautiously because feedstock, contamination, sorting losses, process scale, and system boundaries differ. The high recovery reflects controlled laboratory process efficiency rather than municipal-scale recycling performance. Similarly, the material-recovery yield is process-level, whereas the EU recycling rate of 19.6% represents broader post-consumer waste management outcomes. These values were therefore considered contextual benchmarks. Recycling outcomes vary with feedstock composition, process configuration, energy sources, and system boundaries (Nordahl and Scown, 2024; Tonini *et al.,* 2021). Table 8 provides broader evidence from previous studies on climate impacts, recycling rates, resource use, and potential environmental risks associated with plastic recycling.

Sustainability context

Mechanical recycling is widely recognized as the most environmentally favorable plastic waste management pathway when polymer purity and process efficiency are adequately controlled. Previous LCA and material flow analysis studies have shown that sustainability outcomes are highly polymer-dependent, reflecting trade-offs among energy demand, greenhouse gas mitigation, material recovery, and mechanical performance (Tonini *et al.,* 2021; Van Eygen *et al.,* 2018). Literature values in Table 9 are used as contextual references, not universal performance thresholds. The comparison assesses whether experimental indicators fall within or exceed reported ranges without implying comparative performance. Differences among studies may reflect feedstock quality, process configuration, functional units, and system boundaries. Similarly, SI values depend on the selected indicators and weighting formulation and should not be interpreted as universally valid inherent sustainability rankings across polymers without comprehensive sensitivity and uncertainty analyses.

Table 8: Previous studies benchmarks for sustainability metrics of plastic recycling

Aspect	Recycling pathway / Context	Reported value (Range)	Key Interpretation	Source
Global GHG reduction	Substitution of virgin plastics with recycled polymers	67 Mt CO_2-eq (global scenario)	Large climate benefit from replacing virgin polymers	Gabisa *et al.* (2023)
Mechanical recycling GWP	Mechanical recycling of plastics (LCA studies)	0.37–0.65 kg CO_2 per kg	Lower climate impact compared with incineration and virgin production	Vollmer *et al.* (2020)
Chemical recycling GWP	Pyrolysis / gasification routes	0.37–0.65 kg CO_2 per kg	Can be competitive with mechanical recycling under optimized conditions	Vollmer *et al.* (2020)
Emission reduction vs incineration	Chemical recycling (pyrolysis)	Up to 70% GHG reduction	Strong advantage over energy-recovery incineration	Krell *et al.* (2025)
EU recycling rate	Post-consumer plastic waste (EU-27)	19.6%	Indicates limited circularity despite policy efforts	Amadei *et al.* (2025a)
Recycled plastic use in EU	Secondary plastics used in new products	5.5 Mt/y	Highlights gap between waste generation and recycled content demand	Amadei *et al.* (2025b)
Microplastic reduction	Use of recycled materials (system-level)	56.8 million particles per year	Recycling reduces leakage when well managed	Gabisa *et al.* (2023)
Microplastic increase (risk)	Mechanical recycling without mitigation	2.4×10^9 particles per year	Emphasizes need for improving process controls	Gabisa *et al.* (2023)

Table 9: Sustainability performance of mechanical recycling previous studies and present study

Indicator	Previous studies benchmark	Present study	Interpretation	Source
MRR (%)	60–90	PET 95.2; HDPE 95.5; LDPE 98.7	Recovery exceeds typical industrial values	Tonini *et al.* (2021)
Pre-treatment loss (%)	2–10	Total loss 1.57	Highly efficient washing and shredding	Van Eygen *et al.* (2018)
Energy consumption (kWh/kg)	0.9–1.5	PET 1.25; HDPE 1.10; LDPE 0.95	Consistent with optimized systems	Szostak *et al.* (2020)
CO_2 reduction (kg CO_2/kg)	1.1–3.0	PET 2.10; HDPE 1.85; LDPE 1.50	Within global mitigation ranges	Gabisa *et al.* (2023)
Landfill diversion (%)	50–85	PET 85; HDPE 80; LDPE 75	PET reaches upper benchmark	Edjabou *et al.* (2021)
Tensile strength trend	PET > HDPE > LDPE	55.2 > 31.5 > 24.8 MPa	Confirms polymer hierarchy	Das and Ali (2025)
SI	Energy–quality trade-off	PET 78.1; HDPE 80.0; LDPE 82.6	LDPE favored by low energy demand	Nordahl and Scown (2024)

Contextual comparison of material recovery and process efficiency

The comparison of material recovery and process efficiency is primarily relevant to feedstock condition and process control rather than numerical performance ranking. Previous studies report substantial variation in sorting efficiency, contamination, and recovery across heterogeneous plastic streams (Faraca and Astrup, 2019; Antonopoulos *et al.* 2021). The controlled, pre-segregated feedstock used in this study therefore represents a defined experimental condition distinct from heterogeneous municipal or industrial streams. The processing sequence and polymer-specific thermal conditions are considered in Table 10 to distinguish methodological effects from material-specific observations. Table 10 demonstrates that methodological and system-level differences affect recycling-result interpretation. The 1.57% overall processing loss was lower than impurity levels reported in previous studies, reflecting the manually segregated, controlled feedstock (Faraca and Astrup, 2019), while broad sorting and recycling ranges show that industrial recovery depends on feedstock and facility conditions (Antonopoulos *et al.,* 2021). Thus, the present polymer proportions indicate feedstock composition, not solely recovery efficiency within the analyzed industrial recovery streams.

Table 10: Comparison of previous studies with the present polymer-specific recycling results

Parameter	Previous study result	Present study result	Critical comparison	Source
Waste source & composition	PP and PE were consistently represented in CDW plastic; 86.11 kg manually separated and 57.74 kg mechanically sorted.	37 kg collected: PET 40.54%, HDPE 32.43%, LDPE 27.03%.	Confirms source-dependent polymer composition.	Lahtela *et al.* (2019)
Feedstock quality and loss	Impurities up to 28%; recycling potential 52% hard plastics, 59% films and 79% PVC.	PET 1.33%, HDPE 1.67%, LDPE 2.00% loss; overall 1.57%.	Lower loss reflects controlled, pre-segregated feedstock.	Faraca and Astrup (2019)
Sorting and recycling	PET sorting 45–97%, recycling 63–90%; HDPE sorting 13–95%, recycling 70–88%; purity 80–98%.	PET 40.54%, HDPE 32.43%, LDPE 27.03%.	Present values are composition data, not recovery rates.	Antonopoulos *et al.* (2021)
Recycling pathway	Collection → sorting → grinding → washing → drying → granulation.	Segregation → washing → drying → shredding → polymer-specific thermal processing.	Follows established mechanical recycling with polymer-specific processing.	Alrazen *et al.* (2025)
Processing conditions	No directly comparable polymer-specific conditions reported.	PET 250 °C/15 min; HDPE 145 °C/10 min; LDPE 120 °C/8 min.	Provides differentiated polymer-specific process control.	Alrazen *et al.* (2025)
Mechanical performance	Recycled MixPO WPC 5.8 MPa and recycled LLDPE WPC 5.5 MPa tensile strength.	PET 55.2, HDPE 31.5, LDPE 24.8 MPa.	Higher values are not directly comparable due to different material formulations.	Basalp *et al.* (2020)
Application potential	Recycled PP rebar showed 12.2 ± 0.6 kN maximum load.	Tensile strengths: PET 55.2, HDPE 31.5, LDPE 24.8 MPa.	Indicates reuse potential, but geometry and testing metrics differ.	Das and Ali (2025)
Energy consumption	Recycled-HDPE bottle system: 0.08 kWh/FU for 58.20 g HDPE.	PET 1.25, HDPE 1.10, LDPE 0.95 kWh/kg.	Different functional units and boundaries prevent direct comparison.	Papo and Corona (2022)
CO_2 reduction	Global recycling scenario indicated −67 Mt CO_2-eq and about 50 Mt resource savings.	PET 2.10, HDPE 1.85, LDPE 1.50 kg CO_2/kg.	Both indicate benefits, but scales and boundaries differ.	Gabisa *et al.* (2023)
Landfill diversion	No directly comparable polymer-specific value reported.	PET 85 ± 2%, HDPE 80 ± 3%, LDPE 75 ± 2%.	Provides polymer-specific landfill-diversion evidence.	Present study
LCA energy hotspot	No directly comparable hotspot percentage reported.	Heating/melting 52.6–56.0%; washing/shredding 28–30%; moulding/cooling 16–18%.	Heating and melting are the principal energy hotspots.	Present study
Energy savings	Recycled-material systems generally reduce impacts relative to virgin materials.	PET 62%, HDPE 65%, LDPE 68% savings.	Demonstrates polymer-specific energy savings within the defined boundary.	Present study
Statistical significance	No directly comparable three-polymer dataset.	Most physical/mechanical properties significant; energy and CO_2 significant; landfill diversion and SI non-significant.	Shows stronger polymer effects on material properties than sustainability indicators.	Present study
SI	No directly comparable integrated SI reported.	PET 78.1 ± 2.5, HDPE 80.0 ± 2.8, LDPE 82.6 ± 2.1.	Shows that sustainability is not determined solely by mechanical strength.	Present study
Overall performance	Previous studies emphasize feedstock heterogeneity, sorting limitations, contamination and environmental benefits.	Polymer-specific processing produced differentiated material, energy, environmental and sustainability outcomes.	Supports differentiated recycling strategies for municipal plastics.	Present study

PET showed the highest tensile strength (55.2 MPa), whereas HDPE and LDPE showed greater flexibility; comparisons indicate reuse potential, although differences in formulation, geometry, and testing metrics limit direct comparison (Basalp *et al.,* 2020; Das and Ali, 2025). Environmental comparisons are similarly affected by functional units, system boundaries, process assumptions, and impact categories. The present system required 0.95–1.25 kWh/kg and achieved 1.50–2.10 kg CO_2/kg reduction, while previous studies reported broader life-cycle outcomes under different conditions (Papo and Corona, 2022; Gabisa *et al.,* 2023). Heating and melting contributed 52.6–56.0% of total energy demand, making thermal processing the principal hotspot. Physical and mechanical properties showed greater differentiation than selected sustainability indicators. PET had the highest mechanical performance, while LDPE had the lowest energy demand (0.95 kWh/kg) and highest SI (82.6 ± 2.1). The SI a study-specific composite indicator rather than an inherent polymer property. Overall, the results indicate a trade-off between performance and sustainability and support polymer-specific segregation and processing under controlled conditions.

Circular economy perspective

In the context of circular economy implementation, polymer-specific mechanical recycling supported material utilization, resource efficiency, and reduced environmental burden. MRRs (95.2–98.7%) exceeded industrial benchmarks (60–90%), while pre-treatment loss (1.57%) was below reported ranges (2–10%), indicating effective material retention through segregation and pre-treatment (Van Eygen *et al.,* 2018; Tonini *et al.,* 2021). Energy consumption (0.95–1.25 kWh/kg) was within optimized ranges (0.9–1.5 kWh/kg), with lower LDPE demand demonstrating the importance of polymer-specific processing (Szostak *et al.,* 2020). CO_2 reductions (1.50–2.10 kg CO_2/kg) were within reported ranges (1.1–3.0 kg CO_2/kg), while landfill diversion (75–85%) aligned with benchmarks (50–85%) (Edjabou *et al.,* 2021; Gabisa *et al.,* 2023). The SI trend (LDPE > HDPE > PET) highlighted the role of energy efficiency, with LDPE showing higher sustainability despite lower landfill diversion (Nordahl and Scown, 2024). High recovery, low material losses, optimized energy use, and substantial carbon dioxide reduction support polymer-specific recycling for material recovery, reduced virgin-material dependence, and climate mitigation.

Implications for environmental sustainability

Mechanical recycling under controlled feedstock conditions reduced landfill burden, material losses, energy consumption, and carbon dioxide emissions while maintaining mechanically robust recycled materials. PET achieved the greatest CO_2 reduction, whereas LDPE showed the highest SI due to its lower energy demand. These findings indicate that sustainable polymer-specific recycling requires a balance among material recovery, mechanical performance, and energy efficiency rather than maximizing diversion alone. However, the experimental feedstock excluded multilayer, composite, severely degraded, and visibly contaminated plastics; therefore, the findings may not fully capture the variability present in heterogeneous municipal plastic waste.

Limitations of the study

Recovery values exceeding 95% were obtained under controlled laboratory conditions using well-sorted, relatively homogeneous PET, HDPE, and LDPE feedstocks. Multilayer, composite, severely degraded, and visibly contaminated plastics were excluded. Polymer identification was based on resin codes and physical characteristics with pre-segregation cross-checking, while independent FTIR confirmation was not performed. Therefore, recovery and environmental performance may not reflect heterogeneous municipal waste or industrial conditions. The study also lacked pilot- or industrial-scale validation and detailed techno-economic assessment. Thus, the polymer-specific recycling framework provides a basis for potential broader application rather than direct evidence of

large-scale implementation. Further research should include heterogeneous feedstocks, scale-up trials, techno-economic assessment, and LCA. As sampling occurred during a single collection period in March 2026, seasonal variation could not be assessed, and the reported PET, HDPE, and LDPE proportions are specific to the study feedstock rather than representative of year-round or regional composition. Uncertainty in energy-meter measurements, material-property testing, and CO_2-eq emission factors may also propagate into the overall energy, environmental, and sustainability indicators. Therefore, these vital resulting metrics should be interpreted strictly within the defined experimental conditions and system boundary.

Novelty and research gap

This study addresses an important research gap by integrating process efficiency, energy demand, physical and mechanical performance, CO_2 reduction, recovery, and overall sustainability into a polymer-specific assessment of PET, HDPE, and LDPE under controlled mechanical recycling conditions.

i. *Research gap:* Unlike previous studies that often examine individual material, process, or environmental indicators, the present study combines physical and mechanical performance with experimentally measured energy and environmental outcomes under common controlled recycling conditions.
ii. *Novel knowledge:* The experiment provides directly measured polymer-specific relationships among stage-specific energy demand, material properties, recovery, CO_2 reduction, and sustainability indicators that cannot be inferred from established intrinsic differences among PET, HDPE, and LDPE alone.
iii. *Statistical contribution:* Exploratory one-way ANOVA with Benjamini–Hochberg FDR adjustment provides a systematic assessment of polymer-specific differences across measured performance, energy, and sustainability indicators.
iv. *SI contribution:* The integrated framework provides a quantitative basis for assessing polymer-specific recycling performance through the study-specific SI, while its formulation, normalization, weighting, units, and mathematical consistency are explicitly clarified and the SI is not presented as the sole basis of novelty.
v. *Practical significance:* The findings provide a controlled laboratory baseline for evaluating polymer-specific recycling performance and energy-environment trade-offs, supporting further investigation of resource-efficient recycling strategies without implying direct municipal-scale optimization or large-scale implementation.

The principal novelty lies in the experimentally resolved polymer-specific dataset and integrated comparative framework developed under common controlled recycling conditions, providing a quantitative baseline for future pilot- and industrial-scale validation.

Recommendations and future perspectives

Processing conditions should be polymer-specific, particularly temperature, moulding time, and cooling. Energy-saving strategies such as preheating and optimized mechanical processing should focus on energy-intensive polymers such as PET. Future work should evaluate hybrid recycling streams and validate these findings through industrial-scale trials. These strategies can improve material quality, energy efficiency, and environmental performance while supporting circular plastic management.

CONCLUSION

Mechanical recycling of municipal plastic waste enhances environmental sustainability while producing reusable materials with preserved mechanical integrity and supporting circular economy objectives through material utilization (material recovery: 95.2–98.7%) and low process losses (1.57%). PET, HDPE, and LDPE were processed through polymer-specific pre-treatment, shredding, thermal consolidation, and

compression moulding, allowing systematic evaluation of WRE, material recovery, energy consumption, CO_2 emission reduction, mechanical performance, and SI. High process efficiency was observed, with waste reduction and material recovery exceeding 95% across all polymers, with LDPE achieving the highest recovery of 99%. PET exhibited the highest tensile strength (55.2 MPa), compressive strength (83.4 MPa), density (1.36 g/cm^3), and CO_2 emission reduction (2.10 kg CO_2/kg), while LDPE showed the lowest energy consumption (0.95 kWh/kg) and the highest observed SI (82.6 ± 2.1). HDPE displayed intermediate values across several evaluated parameters. Exploratory one-way ANOVA showed polymer-specific differences, with F-statistics of 1.72–412.3 and p-values of <0.001–0.27. After Benjamini–Hochberg FDR adjustment, most physical and mechanical properties, energy consumption, and CO_2 emission reduction were significant, whereas landfill diversion and SI were not. These differences represent observed polymer-specific variation under the experimental conditions and do not establish causal structure–property relationships. Density, crystallinity, mechanical performance, energy consumption, and carbon mitigation were therefore treated as observed recycling-performance indicators. The study's novelty lies in integrating mechanical, physical, and environmental indicators within a unified sustainability framework. The evaluated ranges were 0.95–1.25 kWh/kg energy consumption, 1.50–2.10 kg CO_2/kg CO_2 emission reduction, and 75–85% landfill diversion. The laboratory-scale design and well-sorted feedstocks limit extrapolation to mixed municipal waste and industrial conditions. Thus, the findings do not establish climate-change mitigation, industrial-scale performance, long-term sustainability, or broader circular-economy outcomes. PET showed higher tensile and compressive strength, HDPE intermediate mechanical characteristics, and LDPE greater flexibility and the highest observed SI. These findings support polymer-specific pre-treatment and processing. Future studies should evaluate mixed polymer streams, additional polymer types, low-energy processing, industrial-scale validation, and comprehensive life cycle assessment to examine broader environmental and economic implications.

AUTHOR CONTRIBUTIONS

D. Shankar conceived and designed the study, developed the methodology, conducted the investigation and experimental work, collected and analysed the data, and prepared the original manuscript draft. J. Nouri supervised the study, coordinated the project, and critically revised the manuscript. Ho Soonmin supervised the study, critically evaluated the work, interpreted the data, validated the scientific findings, and conducted the final review of the manuscript. B. Hitesh contributed to the literature review, analytical interpretation, and manuscript revision. M. Sankaramuthukumar contributed to methodological development, environmental sustainability analysis, supervision, and project coordination. All authors contributed to the interpretation of the findings, critically reviewed the manuscript, approved the final version, and agreed to all aspects of the work.

ACKNOWLEDGEMENT

The authors gratefully acknowledge the institutional support provided by K M College of Pharmacy; Tehran University of Medical Sciences; INTI International University; Lovely Professional University; and Kalasalingam Academy of Research and Education. The authors also acknowledge the academic and technical support received during the study and manuscript preparation.

CONFLICT OF INTEREST

The authors declare that they have no competing interests. Furthermore, the authors confirm that all ethical guidelines, including the prevention of plagiarism, misconduct, data falsification and fabrication, and redundant or duplicate submissions, were fully observed and maintained.

OPEN ACCESS

©2027 The author(s). This article is licensed under a Creative Commons Attribution 4.0 International License, which permits use, sharing, adaptation, distribution and reproduction in any medium or format, as long as you give appropriate credit to the original author(s) and the source, provide a link to the Creative Commons license, and indicate if changes were made. The images or other third-party material in this article are included in the article's Creative Commons license, unless indicated otherwise in a credit line to the material. If material is not included in the article's Creative Commons license and your intended use is not permitted by statutory regulation or exceeds the permitted use, you will need to obtain permission directly from the copyright holder. To view a copy of this license, visit: http://creativecommons.org/licenses/by/4.0/

PUBLISHER'S NOTE

GJESM Publisher remains neutral with regard to jurisdictional claims in published maps and institutional affiliations.

POSITIVE AI STATEMENT

During the preparation of this work, the authors used QuillBot and Grammarly for English grammar and language improvement. After using these tools, the authors reviewed and edited the content as needed and take full responsibility for the content of the publication.

ABBREVIATIONS

εb	Elongation at break
p	Probability value
ρ	Density
σc	Compressive strength
σ_t	Tensile strength
T_m	Melting temperature
T_{onset}	Thermal stability onset temperature
T_{vst}	Vicat softening temperature
%	Percent
°C	Degree Celsius
ANOVA	Analysis of variance
ASTM	American Society for Testing and Materials
CO_2	Carbon dioxide
CO_2-eq	CO_2-equivalant
DSC	Differential scanning calorimetry
E	Young's modulus
EIA	Environmental impact assessment
EU	European Union
FDR	False discovery rate
GPa	Gigapascals
GHG	Greenhouse gas
g	Gram
g/cm^3	Grams per cubic centimetre
H^D	Shore D hardness
h	Hours
HDPE	High-density polyethylene
IS	Impact strength
kg	Kilograms
kg CO_2/kg	Kilograms of carbon dioxide per kilogram
kg CO_2-eq/kg	Kilogram carbon dioxicde-equivalant per kg
kJ/m^2	Kilojoules per square metre
km	Kilometre
kWh/kg	Kilowatt-hours per kilogram
LCA	Life cycle assessment
LCI	Life cycle inventory
LCIA	Life cycle impact assessment
LFD	Landfill diversion
LDPE	Low-density polyethylene
MFI	Melt flow index
MC	Moisture content
min	Minutes
mm	Millimetre
MPa	Megapascals
MRR	Material recovery rate
Mt CO_2-eq	Megatonnes of carbon dioxide equivalent
Mt/y	Megatonnes per year
PET	Polyethylene terephthalate
SD	Standard deviation
SI	Sustainability index
TGA	Thermogravimetric analysis
WA	Water absorption
Xc	Crystallinity

REFERENCES

Alrazen, H.A.; Aminossadati, S.M.; Mahmood, H.A.; Hussein, A.K.; Ahmad, K.A.; Dol, S.S.; Jabbar, S.; Algayyim, S.J.M.; Konarova, M.; Fattah, I.M.R., (2025). A review of the pathways, limitations, and perspectives of plastic waste recycling. Mater. Renewable Sustainable Energy. 14(3): 50 **(37 pages).**

Amadei, A.M.; Rigamonti, L.; Tosches, D.; Sala, S., (2025a). Combining MFA and LCA models to unveil the EU plastic value chain impacts. Resour. Conserv. Recycl., 219: 108279 **(15 pages).**

Amadei, A.M.; Venturelli, S.; Manfredi, S., (2025b). Plastics materials flows in the EU-27 and their environmental impacts. Joint Research Centre, European Commission, JRC142860, Publications Office of the European Union, Luxembourg. **(106 pages).**

Antonopoulos, I.; Faraca, G.; Tonini, D., (2021). Recycling of post-consumer plastic packaging waste in the EU: Recovery rates, material flows, and barriers. Waste Manage., 126: 694–705 **(12 pages).**

ASTM International, (2020). ASTM D792-20, Standard test methods for density and specific gravity (relative density) of plastics by displacement. ASTM International, West Conshohocken, PA **(4 pages).**

ASTM International, (2015). ASTM D2240-15, Standard test method for rubber property—durometer hardness. ASTM International, West Conshohocken. PA **(18 pages).**

ASTM International, (2021). ASTM D3418-21, Standard test method for transition temperatures and enthalpies of fusion and crystallization of polymers by differential scanning calorimetry. ASTM International, West Conshohocken, PA **(8 pages).**

ASTM International, (1998). ASTM D570-98, Standard test method for water absorption of plastics. ASTM International, West Conshohocken. PA **(3 pages).**

ASTM International, (2009). ASTM D1525-09, Standard test method for vicat softening temperature of plastics. ASTM International, West Conshohocken, PA **(10 pages).**

ASTM International, (2004). ASTM D6980-04, Standard test method for determination of moisture in plastics by loss in weight. ASTM International, West Conshohocken, PA **(5 pages).**

ASTM International, (2020). ASTM E1131-20, Standard test method for compositional analysis by thermogravimetry. ASTM International, West Conshohocken, PA **(10 pages).**

ASTM International, (2013). ASTM D1238-13, Standard test method for melt flow rates of thermoplastics by extrusion plastometer. ASTM International, West Conshohocken, PA **(16 pages).**

ASTM International, (1997). ASTM D256-97, Standard test methods for determining the izod pendulum impact resistance of plastics. ASTM International, West Conshohocken, PA **(21 pages).**

ASTM International, (2010). ASTM D695-10, Standard test method for compressive properties of rigid plastics. ASTM International, West Conshohocken, PA **(7 pages).**

ASTM International, (2022). ASTM D638-22, Standard test method for tensile properties of plastics. ASTM International, West Conshohocken, PA, USA **(2 pages).**

Basalp, D.; Tihminlioglu, F.; Sofuoglu, S.C.; Inal, F.; Sofuoglu, A., (2020). Utilization of municipal plastic and wood waste in industrial manufacturing of wood plastic composites. Waste Biomass Valorization. 11(10): 5419–5430 **(12 pages).**

Chen, H.L.; Nath, T.K.; Chong, S.; Foo, V.; Gibbins, C.; Lechner, A.M., (2021). The plastic waste problem in Malaysia: management, recycling and disposal of local and global plastic waste. SN Appl. Sci., 3(4): 437 **(15 pages).**

Das, A.J.; Ali, M., (2025). Sustainable development and assessment of low-strength/high-toughness recycled plastic rebars for structural elements under light loads. Sustainability. 17(11): 4997 **(21 pages).**

Durairaj, S., (2024). Sorption capacity of *Eichhornia crassipes* (Mart.) Solms for zinc removal from electroplating industry wastewater. Environ. Sci. Pollut. Res., 31(21): 30849–30866 **(18 pages).**

Edjabou, M.E.; Takou, V.; Boldrin, A.; Petersen, C.; Astrup, T.F., (2021). The influence of recycling schemes on the composition and generation of municipal solid waste. J. Cleaner Prod., 295: 126439 **(48 pages).**

Faraca, G.; Astrup, T., (2019). Plastic waste from recycling centres: Characterisation and evaluation of plastic recyclability. Waste Manage., 95: 388–398 **(11 pages).**

Gabisa, E.W.; Ratanatamskul, C.; Gheewala, S.H., (2023). Recycling of plastics as a strategy to reduce life cycle GHG emission, microplastics and resource depletion. Sustainability, 15(15): 11529 **(13 pages).**

Gao, Y.; Liu, X.; Chen, W.; Cabrera Serrenho, A.; Cimpan, C.; Liu, G., (2025). High-Resolution Mapping of the Nordic Plastic Cycle Suggests Capacity Expansion for Both Mechanical and Chemical Recycling. ACS Sustainable Resour. Manage., 2(11): 2024–2034 **(11 pages).**

Go, M.; Ybañez, A.; Illano, A.; Cababat, F.; De La Calzada, L., (2024). Microplastics in beach sediments, seawater, and common fish in tourist destinations. Global J. Environ. Sci. Manage., 10(4): 1993–2008 **(16 pages).**

Jeswani, H.K.; Krüger, C.; Russ, M.; Horlacher, M.; Antony, F.; Hann, S.; Azapagic, A., (2021). Life cycle environmental impacts of chemical recycling via pyrolysis of mixed plastic waste in comparison with mechanical recycling and energy recovery. Sci. Total Environ., 769: 144483 **(15 pages).**

Krell, K.; Keller, F.; Gräbner, M., (2025). Life cycle greenhouse gas emission assessment of pyrolysis-based chemical recycling of post-consumer waste: focus on feedstock composition, oil processing and balancing consistency. Waste Manage., 206: 115090 **(11 pages).**

Lahtela, V.; Hyvärinen, M.; Kärki, T., (2019). Composition of plastic fractions in waste streams: Toward more efficient recycling and utilization. Polym., 11(1): 69 **(7 pages).**

Law, K.L.; Narayan, R., (2022). Reducing environmental plastic pollution by designing polymer materials for managed end-of-life. Nat. Rev. Mater., 7(2): 104–116 **(13 pages).**

Liang, H.; Dong, H.; Zhang, C.; Geng, Y.; Liu, X.; Liu, G.; Zhong, C., (2023). Combining LCA-MFA models to identify China's plastic value chain environmental impact mitigation pathways. iScience, 26(9): 1–21 **(21 pages).**

Mitrano, D.M.; Wohlleben, W., (2020). Microplastic regulation should be more precise to incentivize both innovation and environmental safety. Nat. Commun., 11(1): 5324 **(12 pages).**

Mogollón-Arismendy, M.; Hernández-Martínez, A.; Pinedo-Hernández, J.; Fuentes-Gandara, F.A., (2026). Microplastic pollution and risk assessment in urban beaches of the Caribbean region. Global J. Environ. Sci. Manage., 12(4): 1639–1662 **(24 pages).**

Moliner, C.; Pasquale, G.; Arato, E., (2024). Municipal plastic waste recycling through pyrogasification. Energies, 17(5): 1206 **(14 pages).**

Nordahl, S.L.; Scown, C.D., (2024). Recommendations for life-cycle assessment of recyclable plastics in a circular economy. Chem. Sci., 15(25): 9397–9407 **(11 pages).**

Nurhasanah, Hasrianti; Hakim, L.; Riani, E.; Cordova, M.R., (2025). Fate and dynamics of microplastics in the municipal waste composting process. Global J. Environ. Sci. Manage., 11(4): 1671–1686 **(16 pages).**

Nurhasanah, Hasrianti; Hakim, L.; Riani, E.; Cordova, M.R., (2026). Dynamics of microplastics along landfill leachate pathways and treatment processes. Global J. Environ. Sci. Manage., 12(3): 1083–1102 **(20 pages).**

Papo, M.; Corona, B., (2022). Life cycle sustainability assessment of non-beverage bottles made of recycled High Density Polyethylene. J. Clean. Prod., 378: 134442 **(12 pages).**

Pishehvarz, G.; Azamat, J., (2024). Perspectives of Material Flow Analysis in Plastic Waste Management. Plastic Waste Management: Methods and Applications, 279–309 **(30 pages).**

Ragaert, K.; Delva, L.; Van Geem, K., (2017). Mechanical and chemical recycling of solid plastic waste. Waste Manag., 69: 24–58 **(35 pages).**

Santos, G.; Esmizadeh, E.; Riahinezhad, M., (2024). Recycling construction, renovation, and demolition plastic waste: review of the status quo, challenges and opportunities. J. Polym. Environ., 32(2): 479–509 **(31 pages).**

Selvakumar, S.; Boomiraj, K.; Durairaj, S.; Kumar, V., (2023). Performance evaluation of a lab-scale subsurface flow-constructed wetland system for textile industry wastewater treatment. Environ. Sci. Pollut. Res., 30(46): 102708–102724 **(17 pages).**

Shan, C.; Pandyaswargo, A.H.; Onoda, H., (2023). Environmental impact of plastic recycling in terms of energy consumption: A comparison of Japan's mechanical and chemical recycling technologies. Energies. 16(5): 2199 **(15 pages).**

Silva, R.J.O.; Graf, K.; Leite Ribeiro Okimoto, M.L., (2025). Plastic waste recycling: An overview of the mechanical, chemical, and thermal technologies. J. Eng. Appl. Sci., 72: 251 **(29 pages).**

Sultan, M.; Ali, N.; Naseem, M.; Islam, M.; Kareem, A.; Yang, Y.; Khan, F.; Gul, S.; Khan, A.; Ali, F.; Al Balushi, R.A., (2025). Management of bioplastic waste: a critical analysis of biodegradation and recycling approaches. J. Polym. Res., 32(10): 362 **(35 pages).**

Szostak, E.; Duda, P.; Duda, A.; Górska, N.; Fenicki, A.; Molski, P., (2020). Characteristics of plastic waste processing in the modern recycling plant operating in Poland. Energies. 14(1): 35 **(17 pages).**

Tonini, D.; Garcia-Gutierrez, P.; Nessi, S., (2021). Environmental effects of plastic waste recycling. European Commission **(51 pages).**

Van Eygen, E.; Laner, D.; Fellner, J., (2018). Integrating high-resolution material flow data into the environmental assessment of waste management system scenarios: The case of plastic packaging in Austria. Environ. Sci. Technol., 52(19): 10934–10945 **(12 pages).**

Vollmer, I.; Jenks, M.J.F.; Roelands, M.C.P.; White, R.J.; van Harmelen, T.; de Wild, P.; van der Laan, G.P.; Meirer, F.; Keurentjes, J.T.F.; Weckhuysen, B.M., (2020). Beyond mechanical recycling: giving new life to plastic waste. Angew. Chem. Int. Ed., 59(36): 15402–15423 **(22 pages).**

Xu, Q.; Xiang, J.; Ko, J.H., (2020). Municipal plastic recycling at two areas in China and heavy metal leachability of plastic in municipal solid waste. Environ. Pollut., 260: 114074 **(9 pages).**

Zhao, X.; You, F., (2022). Life cycle assessment of microplastics reveals their greater environmental hazards than mismanaged polymer waste losses. Environ. Sci. Technol., 56(16): 11780–11797 **(18 pages).**

AUTHOR (S) BIOSKETCHES

Shankar, D., M.Pharm., Associate Professor, Department of Pharmaceutical Chemistry, K M College of Pharmacy, Madurai 625107, Tamil Nadu, India.
- Email: *shankar131979@gmail.com*
- ORCID: 0009-0008-5889-7005
- Web of Science ResearcherID: OKS-5617-2025
- Scopus Author ID: 57220417594
- Homepage: https://kmcp.ac.in/rt-faculty/mr-d-shankar/

Nouri, J., Ph.D., Professor, [1]Department of Environmental Health Engineering, Tehran University of Medical Sciences, Tehran, Iran; [2]1137 Spectrum, Irvine, Orange County 92618 USA.
- Email: *nourijafar@gmail.com*
- ORCID: 0000-0002-9982-3546
- Web of Science ResearcherID: B-2614-2008
- Scopus Author ID: 22951700700
- Homepage: http://old.tums.ac.ir/faculties/jnouri

Soonmin Ho, Ph.D., Professor, Faculty of Health and Life Sciences, INTI International University, Putra Nilai,71800, Negeri Sembilan, Malaysia.
- Email: *soonmin.ho@newinti.edu.my*
- ORCID: 0000-0002-3697-5091
- Web of Science ResearcherID: NA
- Scopus Author ID: 35790219600
- Homepage: https://newinti.edu.my/?s=Ho+Soon+Min

Hitesh, B., Ph.D. Candidate, Department of Management, Mittal School of Business, Lovely Professional University, Phagwara 144411, Punjab, India.
- Email: *hmgmt72@gmail.com*
- ORCID: 0009-0003-1029-8090
- Web of Science ResearcherID: QSO-4171-2026
- Scopus Author ID: 60732972400
- Homepage: https://www.lpu.in/faculty/staff-profile.php?EmpCode=21576

Sankaramuthukumar, M., Ph.D., Assistant Professor, Kalasalingam Business School, Kalasalingam Academy of Research and Education, Krishnankoil 626126, Tamil Nadu, India.
- Email: *sksmkumar149@gmail.com*
- ORCID: 0009-0006-3246-3693
- Web of Science ResearcherID: *QWC-8339-2026*
- Scopus Author ID: NA
- Homepage:https://scholar.google.com/citations?view_op=list_works&hl=en&hl=en&user=ThDzOoUAAAAJ

HOW TO CITE THIS ARTICLE:
Shankar, D.; Nouri, J.; Soonmin Ho; Hitesh, B.; Sankaramuthukumar, M., (2027). Polymer-specific mechanical recycling of pre-sorted post-consumer municipal plastics for enhanced environmental sustainability. Global J. Environ. Sci., Manage., 13(1): 69-96.

DOI: 10.22034/gjesm.2027.01.04
URL: https://www.gjesm.net/article_735764.html

Global Journal of Environmental Science and Management
(GJESM)

Homepage: https://www.gjesm.net/

Podcasts

CASE STUDY

Sustainability assessment for multi-activity coastal areas using an integrated hierarchical decision-making framework

Desrizal[1,2], B. Widigdo[3], G. Yulianto[3], F. Kurniawan[3,4], Sulistiono[3,*]

[1]Study Program of Coastal and Marine Resources Management, Department of Aquatic Resources Management, Faculty of Fisheries and Marine Sciences, IPB University, Bogor, West Java, 16680 Indonesia

[2]Department of Aquatic Resources Management, Faculty of Sciences, Nahdlatul Ulama University of West Sumatra, Padang, 25136 Indonesia

[3]Department of Aquatic Resources Management, Faculty of Fisheries and Marine Sciences, IPB University, Bogor, 16680, West Java, Indonesia

[4]Center for Coastal and Marine Resources Studies, International Research Institute for Maritime, Ocean and Fisheries, IPB University, Bogor, West Java, 16127 Indonesia

ARTICLE INFO

Article History:
Received 24 May 2026
Revised 06 July 2026
Accepted 12 August 2026

Keywords:
Analytic hierarchy process
Analytic network process
Composite sustainability index
Cross-activity dependence
Multi-criteria decision analysis

DOI:10. 22034.gjesm.2027.01.05

ABSTRACT

BACKGROUND AND OBJECTIVES: Sustainability assessments of multi-activity coastal areas generally evaluate each utilization activity independently, leaving interdependencies unaccommodated and risking biased contribution estimates under conventional hierarchical weighting. This constraint carries profound implications for settings where anthropogenic activities vie for finite ecological space, most notably within tropical coastal socio-ecological systems in developing countries. The study objectives were to develop an activity-based sustainability assessment framework integrating hierarchical and network-based multi-criteria weighting to estimate the relative contribution of three activities: small-scale capture fisheries, vannamei shrimp ponds, and coastal tourism, in the coastal area of Pariaman City, Indonesia.

METHODS: Assessments covered 36 indicators across four sustainability dimensions: ecological, social, economic, and governance, with a 17-node interdependence network built from 14 indicators showing cross-activity dependencies through shared resources and identified causal pathways. Hierarchical weights for individual activities were derived independently by fifteen experts across three sectoral panels. Additionally, network-based weighting to account for inter-activity interactions was performed by a subset of five cross-sectoral experts. All pairwise comparison matrices satisfied the predetermined consistency threshold. The resilience of the regional index to weighting uncertainty was tested through sensitivity analysis.

FINDINGS: Network-based weights ranked vannamei shrimp ponds above small-scale capture fisheries and coastal tourism, but far less dominantly than under hierarchical weighting, which treated ponds as an extreme outlier by ignoring their negative influence on shared water quality and spatial resources. With a near-uniform contribution value of 0.554 across all three activities, the regional index underscores that intervention prioritization requires integrating interdependent cross-activity contributions rather than relying exclusively on standalone activity assessments. The moderately sustainable category held consistently across sensitivity scenarios, although activity contribution order proved more sensitive to weighting uncertainty.

CONCLUSION: Accounting for interdependence corrects the hierarchical approach's over-estimation of vannamei shrimp ponds and reveals a greater contribution from small-scale capture fisheries and coastal tourism than independent estimates suggest. The sustainability contribution of a given activity cannot be reliably determined in isolation from cross-sectoral interdependencies, highlighting the primary utility of this framework as a decision-support mechanism for coastal management.

This is an open access article under the CC BY license (http://creativecommons.org/licenses/by/4.0/)

NUMBER OF REFERENCES	NUMBER OF FIGURES	NUMBER OF TABLES
88	7	8

*Corresponding Author:
Email: ecep_s@apps.ipb.ac.id
Phone: +6281 3170 11347
ORCID: 0000-0002-8151-9546

INTRODUCTION

Coastal areas support over 2.4 billion livelihoods but face intensifying environmental pressures (Newton *et al*., 2020). In tropical developing countries, fisheries, aquaculture, and tourism share spatial zones and ecological foundations (Berkes, 2017; FAO, 2022; Stacey *et al*., 2021). Assessments focused on individual activities fail to capture the cross-sectoral trade-offs generated by these spatial overlaps (Folke *et al*., 2016; Hossain *et al*., 2020). Activity expansion in shared ecological space creates direct cross-sector effects. Shrimp aquaculture has caused over 1 million hectares of mangrove loss in Indonesia since the 1970s (Arifanti *et al*., 2021; Richards and Friess, 2016; Widigdo *et al*., 2024). These mangroves serve as nursery grounds for small-scale fisheries, which support ~90% of Indonesian fishing households (Rahmat and Neilson, 2023; Sari *et al*., 2021; Stacey *et al*., 2021; Yuliana *et al*., 2026a; Yuliana *et al*., 2026b). Aquaculture effluent compromises aquatic environmental quality, impairing fisheries and tourism, whereas tourism expansion simultaneously engenders spatial competition for marine resource utilization (Ketaren *et al*., 2026; Silalahi *et al*., 2024). In Pariaman, West Sumatra, vannamei shrimp farming expanded rapidly, yet only 19% of 58 ponds held full legal status (Desrizal *et al*., 2025). Meanwhile, small-scale fisheries declined, and coastal tourism grew across provincial marine destinations (Zamzami *et al*., 2023). These interconnections complicate management. Policies that benefit one sector may harm others sharing the same space. Consequently, Pariaman serves as an empirically representative case for integrated sustainability assessment. Multi-criteria evaluations in tropical coastal regions predominantly employ the analytic hierarchy process (AHP), a methodology prized for its transparent hierarchical framework (Cabrera and Lee, 2022). However, AHP assumes criterion independence. Evidence shows this systematically underestimates governance's role in coastal sustainability (Cabrera and Lee, 2022). Research modelling interdependence through analytic network process (ANP) demonstrates that priority rankings can shift significantly compared to independent approaches (Tuyen, 2024). Empirical Empirical findings further demonstrate that trade-offs are predominantly driven by spatial overlap among activity zones rather than intrinsic individual characteristics (Kurniawan *et al*., 2023), thereby exposing a fundamental limitation of conventional hierarchical methodologies. The independence assumption impedes representation of feedback relationships. This leaves inter-activity linkages unaddressed (Daimi and Rebai, 2023; Jorge-García and Estruch-Guitart, 2022). AHP remains appropriate for assessments with simple hierarchical structures, such as coastal-use suitability (Pourebrahim *et al*., 2010; Tian *et al*., 2013). However, when elements have reciprocal relationships that a one-way structure cannot represent, ANP is more suitable (Navarro *et al*., 2022). This study evaluates an environmental context wherein small-scale capture fisheries, intensive *vannamei* shrimp ponds, and coastal tourism sectors concurrently vie for shared ecological resources and space. Four sustainability dimensions (ecological, social, economic, and governance) mutually influence each activity. This interdependence necessitates AHP-ANP integration, not because ANP is inherently superior, but because the problem's characteristics demand it. AHP offers hierarchical clarity for weighting dimensions and indicators within each activity. ANP models dependency networks across activities (Sánchez-Garrido *et al*., 2022; Ziemba, 2019). Despite their utility, comprehensive methodologies coupling the AHP-ANP for concurrent multi-activity assessments in individual coastal areas are notably limited, especially within tropical coastal regions in developing countries (Chuang *et al*., 2018; Daimi and Rebai, 2023). Conventional assessments predominantly quantify sustainability contributions on a per-activity basis, presupposing an absence of cross-sectoral interdependencies (Kadoić *et al*., 2017; Saaty, 2008). This presumption is structurally unsound in multi-activity coastal regions. For example, shrimp

farming degrades water quality that supports fisheries productivity and tourism appeal. Unregulated pond expansion generates spatial conflicts. Governance failures propagate across activities through shared regulatory frameworks (Boyd *et al*., 2020; Ofori *et al*., 2023). These dynamics bias priorities toward sectorally dominant activities. They obscure reciprocal influences and undermine management effectiveness. The extent to which cross-sectoral interdependence shapes sustainability priorities remains empirically unverified. This knowledge gap necessitates a holistic assessment framework capable of concurrently evaluating the contributions of coastal activities. This study extends existing AHP-ANP methodologies through three primary contributions. First, by employing utilization activities instead of administrative sectors as the unit of analysis, the framework facilitates the estimation of both intrinsic sustainability (AHP) and systemic influence (ANP) for identical analytical entities. Second, the ANP network uses only indicators representing shared resources or theoretically identified causal pathways. This improves interpretability. Third, the composite index is decomposed to the indicator level. This identifies hub nodes driving divergence between AHP and ANP estimates. Collectively, these integrated features set the current framework apart from prior implementations in the literature. This study aims to develop and implement an activity-based sustainability assessment framework for the coastal area of Pariaman, West Sumatra, Indonesia. It covers three concurrent activities: small-scale capture fisheries, vannamei shrimp farming, and coastal tourism. The framework integrates AHP-ANP to model interdependencies between activities explicitly. Fieldwork was conducted in 2024.

MATERIALS AND METHODS

Study area

The study was conducted in the coastal area of Pariaman, West Sumatra, Indonesia (approximately 0°24′00″ – 0°52′32″ S and 99°57′44″ – 100°25′14″ E), encompassing the coastal administrative areas of Padang Pariaman Regency and Pariaman City, as shown in Fig. 1. Field investigations were conducted across nine coastal sub-districts, a setting characterized by intensive spatial interactions among three core sectors: small-scale capture fisheries, vannamei shrimp aquaculture, and coastal tourism. Small-scale capture fisheries are characterized by a fleet dominated by vessels of ≤5 gross tonnage (GT) (1,346 units, comprising 1,338 outboard-motor vessels and 8 motorboats without engines), while 18 vessels of 10–30 GT were excluded from the small-scale fisheries scope. Vannamei shrimp aquaculture covers approximately 72.3 ha of active ponds, and coastal tourism receives more than 2.3 million visitors annually (BPS Pariaman City, 2025; BPS Padang Pariaman Regency, 2025). The region also experiences mangrove conversion pressures and documented spatial-use conflicts (Firdaus *et al*., 2021), providing a representative setting for examining sustainability in a multi-use tropical coastal system. The selection of these three sectors reflects the restricted nature of industrial development in the region, coupled with the socio-economic dependence of coastal populations on small-scale capture fisheries, vannamei shrimp aquaculture, and tourism-related enterprises. In contrast, agriculture-based livelihoods, particularly paddy farming, are concentrated farther inland and are therefore outside the coastal utilization area examined in this study (Firdaus *et al*., 2021; Stanford *et al*., 2014).

Research framework

This study uses a quantitative multi-criteria decision analysis (MCDA) design with seven sequential stages: 1) identification of initial indicators through a literature search of coastal sustainability assessments; 2) selection and validation of indicators with experts and field stakeholders until 36 final indicators are obtained; 3) field measurement of indicators and preparation of a Saaty-scale paired-comparison questionnaire; 4) expert panel completion of the

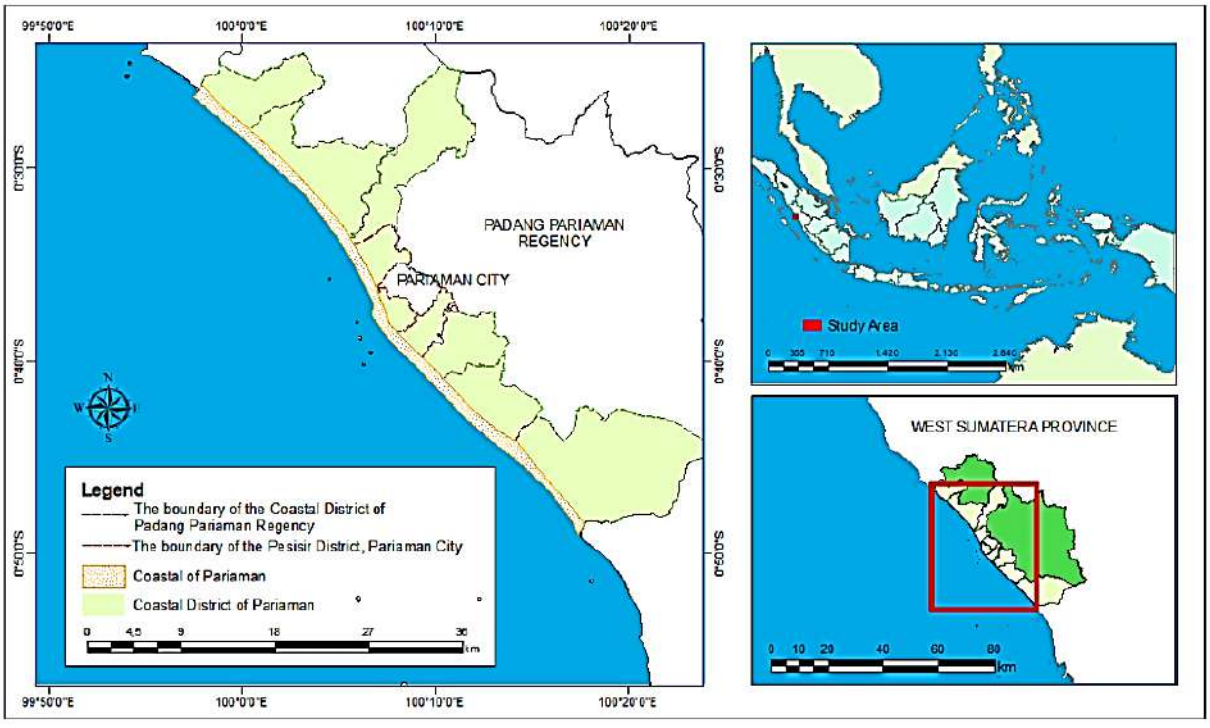

Fig. 1: Geographical location of the study área in the Pariaman coast, Indonesia

paired-comparison matrix; 5) calculation of dimension and indicator weights via the AHP; 6) construction of inter-activity interdependence networks and weight estimation via the ANP; and 7) evaluation of result robustness through sensitivity analysis, described sequentially in the following sub-sections. Utilization activities, rather than sectors or actors, serve as the primary unit of analysis in this study. These activities are evaluated across four dimensions: ecology (E), social (S), economic (K), and governance (G), using a total of 36 indicators. The proposed AHP-ANP integration is executed biennially—first, by applying AHP to determine the relative importance weights of dimensions and indicators per activity, and second, by employing ANP to estimate inter-activity contribution weights based on systemic dependencies within the network (Huang and Chen, 2024a; Kheybari *et al*., 2020; Saaty, 1996, 2004) as presented in Fig. 2.

Identification and validation of sustainability indicators

A review of coastal sustainability assessments was conducted to identify candidate indicators encompassing ecological, social, economic, and governance dimensions relevant to small-scale capture fisheries, vannamei shrimp ponds, and coastal tourism. A total of 36 indicators (4 dimensions × 3 indicators × 3 activities) were established to represent each sustainability dimension in a balanced manner per activity while keeping the expert-elicitation burden reasonable. The preliminary indicator set underwent a validation process involving regional experts and local stakeholders, including artisanal fishers, tourism representatives, pond management personnel, and community authorities, thereby verifying its contextual relevance to Pariaman's utilization context. The primary evidence offered for the indicator set's ability to represent sustainability comprehensively is this deliberate

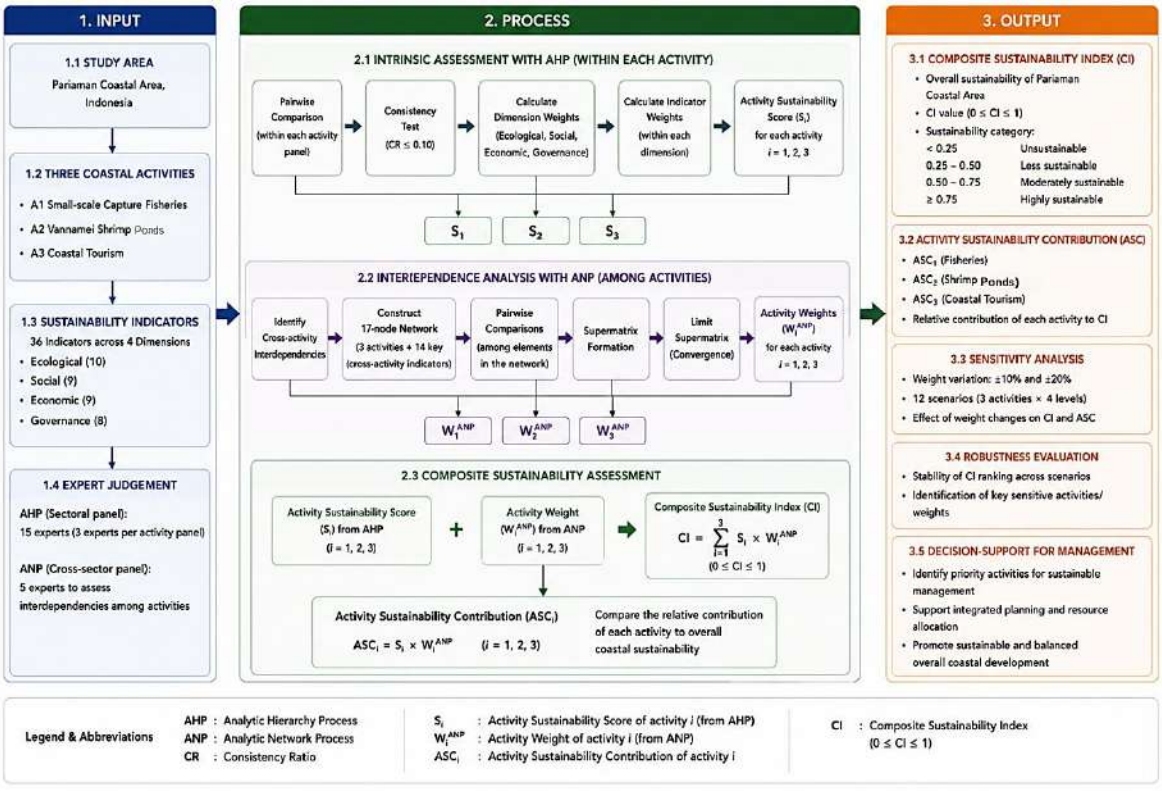

Fig. 2: Research framework for activity-based sustainability assessment (Integrating AHP and ANP to evaluate the sustainability contribution of coastal activities)

structural balance, three indicators allocated to each of the four dimensions (ecological, social, economic, and governance) within each activity, combined with expert and stakeholder validation of each candidate indicator's relevance; this constitutes a systematic, expert-informed basis for coverage rather than an independent statistical test of representativeness, and is acknowledged as such. The validated indicators were operationalized through field measurements and min–max normalization to a 0–1 scale, followed by AHP paired-comparison weighting to determine their relative importance.

Data collection

Secondary data were collected from agency documents and databases (West Sumatra Provincial Marine and Fisheries Agency, Padang Pariaman Regency Fisheries Office, BPS Pariaman City and Padang Pariaman Regency, Tourism and Culture Offices of Pariaman City and Padang Pariaman Regency) to identify and verify the 36 sustainability indicators and regional characteristics (fleet size, pond area, tourist numbers). Primary data were collected through two channels: (a) direct field measurements of the 36 indicators (September 2024-January 2025) across the Pariaman coastal zone, used to calculate indicator values (*Xi*) normalised to 0–1 via the Min-Max method; and (b) an expert-completed Saaty-scale paired-comparison questionnaire (Saaty, 2008), used for weighting indicators, dimensions, and activities and for modelling relationships between elements, secondary data and field measurements identify and verify regional conditions, while expert assessments weight and model inter-element relationships. In-situ data collection involved 65

sampling locations designated for artisanal fisheries, 50 for vannamei shrimp ponds, and 25 for coastal tourism operations. These points were allocated among the eight coastal sub-districts in proportion to the spatial extent of each activity. Water quality indicators, which exhibit the greatest temporal variability, were measured through three repeated observations during the study period to capture both short-term and seasonal variation. Because the remaining indicators demonstrated greater temporal stability, data collection for these variables was conducted once during the five-month monitoring period. All primary field observations were complete. Occasional incompleteness occurred in secondary data, where agency sources reported differing values for the same regional statistic. In these instances, the most credible and current source, typically the most recent official agency publication, was selected as the reference value. A purposive two-layer expert selection design was implemented. Fifteen experts were assigned to three sectoral panels (five per activity: small-scale capture fisheries, vannamei shrimp ponds, and coastal tourism), with each panel conducting paired comparisons exclusively within its sector. Furthermore, inter-activity comparisons and ANP network interdependencies were evaluated by a subgroup of five specialists possessing cross-sectoral expertise in coastal-marine spatial planning and tourism management. The selection criteria included: 1) a minimum of a Bachelor's degree, with most holding Bachelor's or Doctoral qualifications; 2) at least ten years of relevant professional experience (actual range: 10–20 years); 3) active engagement as academics, researchers, structural officials, or field practitioners; and 4) demonstrated contextual understanding of Pariaman City and Padang Pariaman Regency. The five-expert panel size follows the general AHP-ANP convention that assessment validity depends more on expert-domain competence than respondent count (Darko *et al*., 2019; Saaty, 2014; Srđević and Srđević, 2024); the diversity of backgrounds among academics, government officials, and field practitioners ensures sectoral panels handle within-activity relationships and cross-sectoral panels handle the inter-activity relationships requiring an integrative perspective. Their disciplinary backgrounds and experience are summarized in Table 1. The panel members—possessing between 10 and 24 years of expertise across academic, governmental, and practical sectors, were strategically assigned: sectoral panels managed intra-activity dynamics, while cross-sectoral specialists governed inter-activity interactions. Code legend: AC = Academic Expert; GS = Government Structural Expert; FP = Field Practitioner; ANP = expert panel selected specifically for the ANP (cross-sectoral) analysis.

Despite its smaller size relative to the 15-member sectoral panels, the five-member ANP cross-sectoral panel was purposely constituted to integrate all four dimensions of sustainability collectively, avoiding narrow representation of any isolated dimension (Table 1). ANP1's background in coastal resource management anchors the ecological and governance dimensions. ANP3's mandate in regional development planning, which within the Indonesian regency planning agency structure typically integrates economic and social welfare programming with spatial governance, anchors the economic, social, and governance dimensions. ANP4's role in marine and fisheries spatial planning anchors the ecological and governance dimensions. ANP5's experience in field-level integrated coastal management grounds the social dimension in community-level practice. ANP2's expertise in multi-criteria decision-support methodology is intentionally cross-dimensional, requiring the weighting procedure to synthesize all dimensions rather than privileging any individual aspect. This reflects cross-sectoral coastal governance roles, where administrative responsibilities may shift over time across institutions, jurisdictions, policy frameworks, and evolving environmental management priorities.

Table 1: Characteristics of the expert panels (AHP sectoral panels, n = 15; ANP cross-sectoral panel, n = 5). No expert held a direct financial or operational interest in the three utilization activities assessed

Code	Panel	Affiliation category	Area of expertise	Academic discipline	Experience (y)
AC1	AHP	Academic	Small-scale capture fisheries	Fisheries Resource Utilization	18
AC2	AHP	Academic	Aquaculture	Aquaculture	16
AC3	AHP	Academic	Coastal tourism	Tourism	14
AC4	AHP	Academic	Coastal zone management	Coastal Resources	20
AC5	AHP	Academic	Resource economics	Marine Economics	17
GS1	AHP	Government official	Development planning	Regional Planning	19
GS2	AHP	Government official	Coastal and marine spatial planning	Marine and Fisheries Affairs	18
GS3	AHP	Government official	Tourism	Public Administration	13
GS4	AHP	Government official	Environment	Environmental Engineering	15
GS5	AHP	Government official	Spatial planning	Regional Planning	21
FP1	AHP	Field practitioner	Capture fisherman	Small-Scale Capture Fisheries	24
FP2	AHP	Field practitioner	Shrimp farmer	Aquaculture	10
FP3	AHP	Field practitioner	Tourism operator	Tourism	15
FP4	AHP	Field practitioner	Fisheries extension officer	Fisheries Extension	20
FP5	AHP	Field practitioner	NGO / coastal community	Coastal Management	14
ANP1	ANP (cross-sectoral)	Academic	Coastal zone management (Ecological, Governance dimensions)	Coastal Resources	20
ANP2	ANP (cross-sectoral)	Academic	Decision support systems (cross-dimensional / methodological integration)	Industrial Management	18
ANP3	ANP (cross-sectoral)	Government official	Regional development planning (Economic, Social, Governance dimensions)	Regional Planning	19
ANP4	ANP (cross-sectoral)	Government official	Marine and fisheries affairs (Ecological, Governance dimensions)	Coastal and Marine Spatial Planning	18
ANP5	ANP (cross-sectoral)	Field practitioner	Integrated coastal management (Social, Ecological dimensions)	Coastal Management	24

Therefore, panel members were selected for broad and balanced coverage of relevant sustainability dimensions rather than narrowly defined or position-specific roles.

Development of the integrated AHP–ANP assessment framework

The proposed framework integrates AHP and ANP to accommodate two analytical needs: AHP derives priority weights from the hierarchical structure of sustainability indicators. In contrast, ANP models interdependence relationships between activities and indicators that a hierarchical structure cannot represent, combining indicator priorities with interdependence influence, as presented in Fig. 3.

AHP

The AHP model was organised as a four-level hierarchy: assessment goal, coastal activities, sustainability dimensions, and indicators (Fig. 4). This structure enabled the independent determination of each coastal activity's intrinsic sustainability score. Each activity, including small-scale capture fisheries, vannamei shrimp ponds, and coastal tourism, was evaluated using the same four dimensions: ecological, social, economic, and governance across 36 indicators. Pairwise comparisons were conducted only within each activity's hierarchy, consistent with the conventional AHP assumption of independence between activities. The AHP generates the dimension weight per activity (Wi_dimension) and

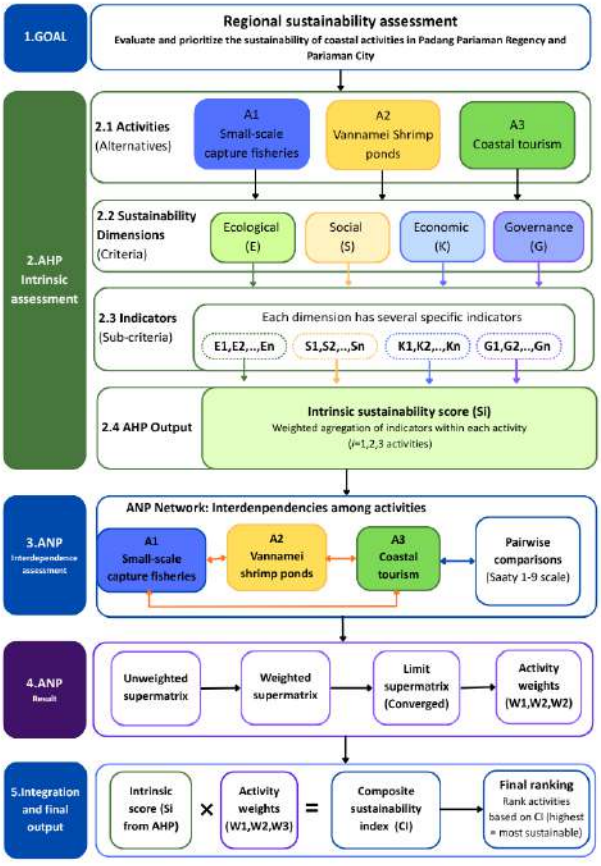

Fig. 3: Analytical structure of the integrated AHP–ANP assessment framework, illustrating how AHP-derived intrinsic sustainability scores (Si) and ANP-derived interdependence-based activity weights (Wi_ANP) are combined to obtain the regional composite index (CI) (A1 = Small-scale capture fisheries; A2 = Vannamei shrimp ponds; A3 = Coastal tourism)

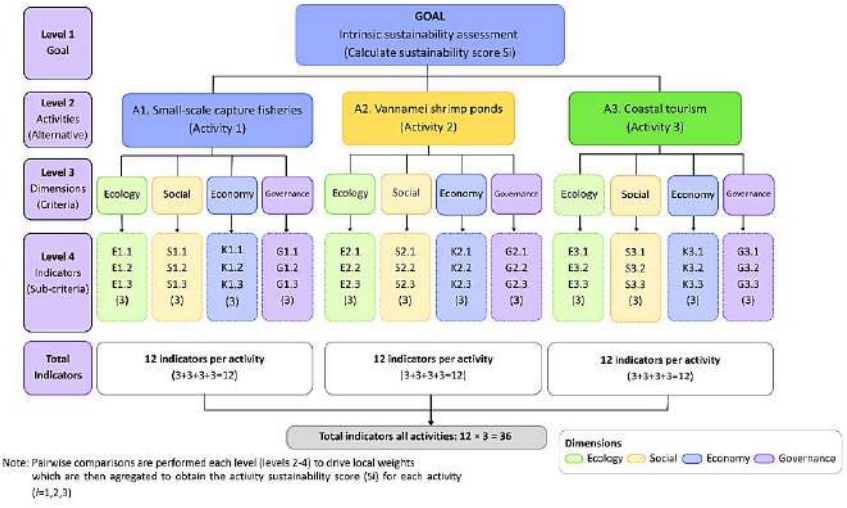

Fig. 4: AHP hierarchical structure for intrinsic sustainability assessment, showing the four-level pairwise-comparison structure (goal, activity, dimension, indicator) used to derive each activity's intrinsic sustainability score (Si) independently of the others (A1 = Small-scale capture fisheries; A2 = Vannamei shrimp ponds; A3 = Coastal tourism)

the indicator weight per dimension per activity (Wi_indicator) based on pairwise comparison assessments using the Saaty scale (1–9) (Saaty and Vargas, 2012). Fifteen experts, organised into three sectoral panels of five members each, conducted assessments exclusively within their respective sectors. The geometric mean of each panel's assessments was used to construct the aggregate matrix input, and consistency was verified using the Consistency Ratio (CR < 0.10). Rather than utilizing a dedicated consensus workshop, expert disagreements were reconciled by aggregating individual pairwise-comparison matrices via geometric means and applying a per-matrix CR screen, consistent with the standard AHP/ANP aggregation-of-individual-judgements (AIJ) framework. The sustainability score per activity (Si) is calculated using Eq. 1 (Saaty, 2008):

$$S_i = \sum(W_j \times \sum(W_k \times X_{ijk})) \quad (1)$$

Where: *Wj* is the weight of dimension *j*, *Wk* is the weight of indicator *k* in dimension j, and *Xijk* is the normalised value of indicator *k* of dimension *j* for activity *i*.

Development of the ANP network

Not all indicators enter the ANP network, since not all have a significant influence relationship on activities outside their own sector; most are sector-specific and already adequately represented through AHP weights within their respective activities; meaning only those forming inter-activity pathways of influence are modelled as ANP nodes. Nodes were selected based on two jointly applied criteria: 1) shared resources or conditions influenced by multiple activities, such as water quality affected by ponds but impacting fisheries and tourism; and 2) a theoretically identified causal pathway from one activity to another, supported by domain knowledge and coastal literature (for example, the water-quality pathway from pond effluent to fisheries and tourism performance cited above is documented in the shrimp-aquaculture wastewater management literature, e.g., by (Iber and Kasan, 2021). This methodological strategy is consistent with standard ANP protocols that emphasize theory- and expert-driven network architecture construction over automated filtering procedures (Saaty, 1996, 2004). Indicators present in more than one activity were not automatically designated as nodes. For example, Labour Absorption appears in both fisheries and ponds but satisfies neither criterion, as each absorbs labour with different skill sets and does not compete for the same resources. The 36 indicators underwent individual screening against two distinct benchmarks: shared environmental resources or conditions influenced by concurrent activities, and theoretically grounded inter-activity causal pathway. The research team, in consultation with the cross-sectoral expert panel, conducted qualitative screening based on expert knowledge and established ANP network-construction practices rather than numerical scoring. A notable limitation stems from its qualitative foundation. Without continuous scoring mechanisms, indicators near criterion thresholds are inherently more vulnerable to analyst or reviewer discretion. Excluding a borderline indicator could shift individual node weights; however, the overall network topology, defined by which activities are linked through shared resources, is expected to remain robust given the criteria's clear conceptual foundation. Application of these criteria to the 36 final indicators resulted in the network structure presented in Table 2.

ANP

The ANP comprised nine dependency blocks representing inter-cluster influences within the utilization network: 1) Ecology to activities; 2) Social to activities; 3) Economic to activities; 4) Governance to activities; 5) Activities to ecology; 6) Activities to social; 7) Activities to economic; 8) Activities to governance; and 9) Inner dependence of activities to activities. A paired-comparison matrix was constructed for each individual block based on evaluations provided by five subject-

Table 2: ANP network structure results from the implementation of screening criteria

Stages	Total
Final indicator (from AHP)	36
Indicator meets screening criteria (unique node)	14
Activity nodes added	+3
Total ANP network nodes	17

matter experts, generating 111 comparison pairs collected through a structured questionnaire. Consistency was evaluated for all 29 matrices; 26 matrices achieved a consistency ratio (CR) below 0.10, while the three 2×2 matrices were inherently consistent. The structure of the ANP network is illustrated in Fig. 5. The unweighted supermatrix (W) was constructed by populating each column with the priority vector derived from its respective comparison matrix. Subsequently, each column was normalised to sum to 1.0, resulting in the Weighted Supermatrix. The Supermatrix limit W^{∞} was determined through repeated powering (W^2, W^4, W^8, W^{16}) until convergence was achieved (Saaty, 1996, 2004; Saaty and Vargas, 2006). The final ANP weight (Wi_ANP) is the mean of the activity row at limit W^{16}, normalised so Σ*Wi*_ANP = 1.0, with all computations performed in Microsoft Excel using a specially developed supermatrix method.

Data analysis

Composite sustainability assessment

The AHP generates an intrinsic sustainability score (*Si*) for each activity based on its specific dimension and indicator weights. Although the standard AHP framework presumes strict independence among activities, this condition is not met in the Pariaman coastal zone, characterized by significant operational interactions via shared resources and spatial overlap. Consequently, the AHP-derived Si scores are not utilized as final outputs; rather, the composite area index incorporates ANP activity weights (Wi_ANP) to appropriately adjust each activity's relative contribution by capturing structural interdependencies through supermatrix convergence. As a result, the composite sustainability index (*CI*) reflects regional sustainability as an interconnected system rather than as a sum of independent achievements. In accordance with the standard weighted aggregation approach for composite indicators, the intrinsic sustainability score of each activity (*Si*) is combined with its relative activity weight (*Wi*) to calculate *CI*, ensuring that each activity's contribution is proportional to both its performance and its relative importance (Nardo *et al*., 2005):

$$CI = \sum(S_i \times W_i) \quad (2)$$

Where: *Si* is the sustainability score of activity *i* (from AHP) and Wi is the weight of activity *i* (both Wi_AHP and normalised Wi_ANP).

To compare the relative impacts of the three activities on overall regional sustainability—regardless of their intrinsic sustainability scores—each activity's contribution to the regional *CI* is quantified as the product of *Si* × *Wi*. Regional CI and activity contribution were calculated in two versions, using *Wi*_AHP and *Wi*_ANP, to compare the methodological implications of both weighting approaches. A decomposition follows directly from the weighted aggregation formulation, where *Si* × *Wi* represents activity *i*'s individual contribution to the composite index (CI). Sustainability levels are classified according to the four-tier system established by Rapfis (Kavanagh and Pitcher, 2004): unsustainable (<0.25), less sustainable (0.25-0.50), moderately sustainable (0.50-0.75), and highly sustainable (≥0.75). The same classification framework is utilized for both *Si* and *CI*. Because both frameworks share a conceptual 0–1 sustainability scale, the threshold

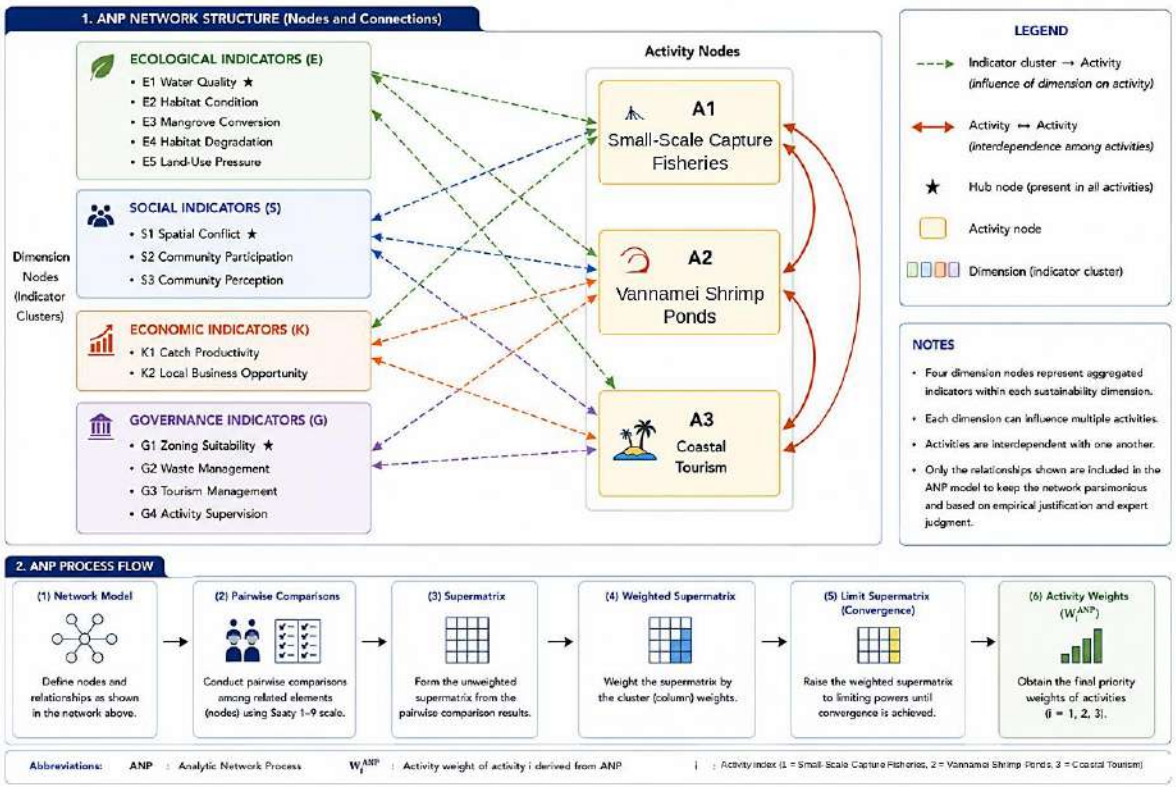

Fig. 5: ANP network structure for cross-activity interdependencies (Conceptual structure used to derive activity weights, W_i^{ANP}). A1 = Small-scale capture fisheries; A2 = Vannamei shrimp ponds; A3 = Coastal tourism

originally formulated for Rapfish multidimensional scaling (MDS) ordination is extended to the AHP-ANP composite index, with cross-method adaptation explicitly acknowledged as a study limitation. The transparency and simplicity principles for composite-index construction outlined by Nardo *et al*. (2005) underlie the choice of a discrete categorisation scheme in general, though the handbook does not explicitly prescribe specific thresholds.

Sensitivity analysis

To test the robustness of results against uncertainty in the estimated ANP weights, a one-at-a-time (OAT) sensitivity analysis varied each activity's weight (*Wi*_ANP) by ±10% and ±20% of baseline values, following variation magnitudes conventional in systematic reviews of MCDA sensitivity analyses (Więckowski and Sałabun, 2023). For target activity *i* that is varied by *d*, the new weight is calculated using Eq. 3 (Więckowski and Sałabun, 2023):

$$w_i' = w_i \times (1 + d) \quad (3)$$

The remaining weight $(1 - w_i')$ is then distributed to the other two activities (*j,k*) in proportion to their baseline weight ratio, using Eqs. 4 and 5 (Więckowski and Sałabun, 2023):

$$w_j' = w_j \times \frac{1-w_i'}{w_j+w_k} \quad (4)$$

$$w_k' = w_k \times \frac{1-w_i'}{w_j+w_k} \quad (5)$$

The redistribution follows a proportional normalization scheme commonly used in weighted sensitivity analysis, keeping total weight equal to one while preserving the relative

proportions among the remaining activities, using Eq. 6 (Więckowski and Sałabun, 2023):

$$wi' + wj' + wk' = wi' + (1 - wi') = 1 \qquad (6)$$

By construction, the total weight equals one in every scenario. A total of 12 scenarios (three activities × four variation levels) were recalculated to obtain the regional *CI* and activity priority ranking under each scenario. Rather than utilizing Monte Carlo or other probabilistic sensitivity procedures, an OAT design was implemented. This choice reflects the methodological constraints of relying on a five-expert panel for ANP weight estimation, which lacks the statistical power necessary to generate reliable probability distributions and avoids engendering a false sense of analytical precision. OAT sensitivity analysis instead produces directly interpretable, deterministic bounds on weight uncertainty appropriate to a small, purposively selected expert panel. Consequently, sensitivity analysis was restricted to uncertainty in the ANP activity weights (Wi-ANP). Potential variations from indicator measurements, environmental dynamics, socioeconomic constraints, and network topology were excluded from the simulation and acknowledged as limitations.

RESULTS AND DISCUSSION

Final Indicators and ANP nodes

The screening process, based on shared resources and causality pathways of interactivity, identified 14 of the 36 indicators as valid ANP nodes (Table 3). Three nodes (E1, S1, G1) serve as hubs, fulfilling both the screening criteria and connecting multiple activities. The 14 nodes are unevenly distributed across four dimensions: ecology (5), governance (4), social (3), and economic (2). This distribution suggests that inter-activity influence in Pariaman's coastal area is primarily governed by ecological mechanisms and the management of shared resources such as waters, land, and mangroves, as well as spatial management instruments. The pronounced sector-specificity of socioeconomic mechanisms corroborates standard ANP methodology, which dictates that influence pathways and structural interdependencies must be delineated before defining network architecture, avoiding the assumption of equivalent node weights (Kadoić *et al*., 2017). These nodes provide the foundation for the ANP network analysed in the following subsection.

AHP-derived dimension weights and intrinsic sustainability assessment

The AHP assessment produced two complementary outputs: (i) local weights reflecting experts' relative importance judgments for each sustainability dimension and indicator, and (ii) intrinsic sustainability scores reflecting each activity's observed field indicator performance. The sustainability profiles of the three activities spanning ecological, social, economic, and governance dimensions are delineated in Fig. 6, with comprehensive AHP-derived weights, indicator weights, and activity sustainability scores (*Si*) summarized in Tables 4a–4c. AHP yielded consistent matrices across all panels (CR = 0.001--0.092; mean 0.026; all < 0.10). Coastal tourism scored highest (*Si* = 0.695), followed by fisheries (0.529) and shrimp ponds (0.486). Ponds performed weakest in governance (Table 4a-c) (Saaty, 2008). All three activities fell within the moderate sustainability range (0.486–0.695). The tourism-fisheries gap (0.166) exceeded the fisheries-ponds gap (0.043), indicating ponds and fisheries perform similarly while tourism stands apart. AHP weights (*Wd*, *Wi*) reflect expert judgments of importance, whereas scores (*Xi, Si*) reflect field performance. Their product (*Wd* × *Wi* × *Xi*) identifies intervention priorities: high importance with low performance signals urgency, while high importance with high performance indicates strength. The ecological dimension dominated all activities, demonstrating maximal factor weights and optimal performance.

Table 3: Indicator nodes in the ANP network and cross-activity dependency justification

Code	Indicator	Sustainability dimension	Cross-activity dependency justification
E1	Water quality ★	Ecology	Shared resource: ponds pollute the waters → reduce fisheries productivity and tourist attractions. Critical hub nodes.
E2	Habitat conditions	Ecology	Tourism damages habitats → impacts fisheries. Two-way causality.
E3	Mangrove conversion	Ecology	Ponds convert mangroves → destroy nursery grounds and ecotourism bases.
E4	Habitat destruction	Ecology	Tourism and fisheries compete using the same habitat.
E5	Land use pressures	Ecology	Space competition: ponds, tourism, fishing settlements.
S1	Space conflict★	Social	Present in all three activities. Social hub nodes: formalising the pressures of space competition.
S2	Community participation	Social	Community-based tourism influences relevant participation for fisheries and ponds.
S3	Public perception	Social	The perception of coastal conditions is influenced by all three activities at once.
K1	Catch productivity	Economy	It is directly influenced by ecological quality (pond effect). Economic-ecological bridge.
K2	Local business opportunities	Economy	Tourism creates opportunities that can be taken advantage of by fishermen and farmers.
G1	Zoning suitability★	Governance	Present in all three activities. Governance hub nodes: the primary instrument for regulating inter-activity interactions.
G2	Waste management	Governance	Pond waste directly affects the quality of water → fisheries and tourism.
G3	Tourism area management	Governance	Tourism management affects the common ecological conditions.
G4	Activity supervision	Governance	Fisheries supervision affects the intensity of catches, which has an impact on tourist habitats.

★ = Hub node — comes as a cross-activity co-indicator

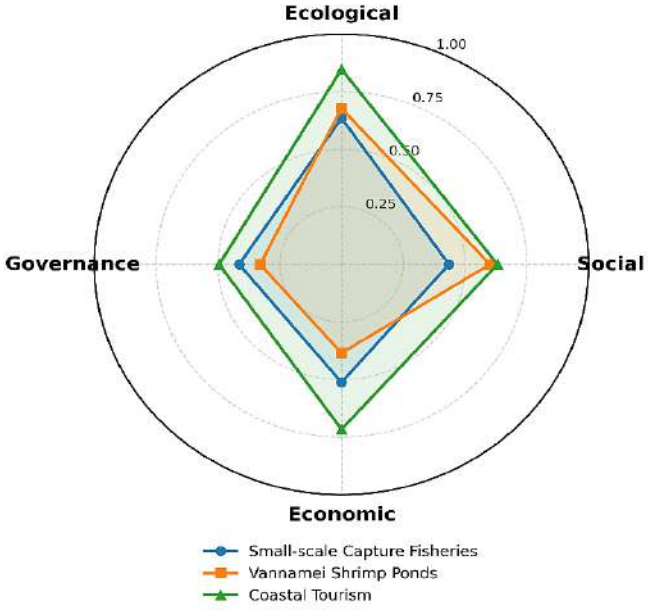

Fig. 6: Intrinsic sustainability profiles of the three coastal activities across the ecological, social, economic, and governance dimensions based on the AHP assessment

Tourism's top score (*Si* = 0.695) was driven by ecology (*Wd* = 0.473; performance = 0.829). Conversely, ponds' lowest score (0.486) stemmed not from ecology (score = 0.660) but from governance: high weight (*Wd* = 0.333) yet poor performance (0.313). This high-importance / low-performance combination makes governance, not ecology, the pond's main intervention priority.

Table 4a: Tiered weights, indicator weights, and sustainability scores (*Si*) for small-scale capture fisheries

Dimensions	Wd	Indicator	*Wi*	*Wd × Wi*	*Xi*	Contribution
		Pressure capture	0.161	0.0783	0.430	0.0337
Ecology	0.487	Quality of coastal waters	0.517	0.2519	0.850	0.2140
		Coastal habitat conditions	0.323	0.1572	0.339	0.0533
		Labor absorption	0.506	0.0685	0.401	0.0275
Social	0.135	Community dependency	0.393	0.0532	0.463	0.0246
		Utilization conflicts	0.101	0.0137	0.329	0.0045
		Fishermen's income	0.401	0.0835	0.377	0.0315
Economy	0.208	Capture productivity	0.408	0.0849	0.546	0.0464
		Stability of the fishery business	0.191	0.0398	0.637	0.0254
		Regulatory compliance	0.467	0.0790	0.386	0.0305
Governance	0.169	Activity monitoring	0.222	0.0375	0.345	0.0129
		Zoning suitability	0.311	0.0526	0.462	0.0243
Total	1.000			1.000		*Si* = 0.529

Table 4b: Tiered weights, indicator weights, and sustainability scores (*Si*) for vannamei shrimp ponds

Dimensions	Wd	Indicator	Wi	Wd × Wi	Xi	Contribution
		Mangrove conversion	0.172	0.0657	0.380	0.0250
Ecology	0.381	Pond water quality	0.632	0.2408	0.795	0.1914
		Land use pressures	0.196	0.0747	0.470	0.0351
		Labor absorption	0.418	0.0467	0.590	0.0275
Social	0.112	Land use conflicts	0.147	0.0164	0.662	0.0109
		Impact on society	0.435	0.0486	0.580	0.0282
		Pond productivity	0.292	0.0508	0.392	0.0199
Economy	0.174	Profit of the business	0.425	0.0740	0.362	0.0268
		Production stability	0.283	0.0494	0.352	0.0174
		Licensing compliance	0.248	0.0827	0.450	0.0372
Governance	0.333	Waste management	0.647	0.2156	0.235	0.0507
		Zoning suitability	0.104	0.0348	0.470	0.0163
Total	1.000			1.000		*Si* = 0.486

Table 4c: Tiered weights, indicator weights, and sustainability scores (*Si*) for coastal tourism

Dimensions	Wd	Indicator	*Wi*	*Wd × Wi*	*Xi*	Contribution
		Destruction of coastal habitats	0.176	0.0833	0.680	0.0566
Ecology	0.473	Tourism waste and waste	0.572	0.2708	0.800	0.2166
		Quality of coastal waters	0.252	0.1190	1.000	0.1190
		Community participation	0.533	0.0675	0.627	0.0423
Social	0.127	Public perception	0.373	0.0472	0.628	0.0297
		Space utilization conflicts	0.094	0.0119	0.450	0.0054
		Tourism revenue	0.257	0.0404	0.650	0.0262
Economy	0.157	Number of tourist visits	0.583	0.0916	0.634	0.0581
		Local business opportunities	0.160	0.0251	1.000	0.0251
		Management of tourist areas	0.146	0.0355	0.450	0.0160
Governance	0.243	Tourism facilities and regulations	0.624	0.1517	0.508	0.0771
		Zoning suitability	0.230	0.0559	0.404	0.0226
Total	1.000			1.000		Si = 0.695

Wd = dimension weights in the activity; *Wi* = the weight of the indicator in dimensions; *Wd × Wi* = global weight indicator; *Xi* = Min-Max normalised indicator value (range 0–1); Contribution = *Wd × Wi × Xi; Si* = activity composite sustainability score = Σ contribution.

A similar pattern occurs in tourism: governance is high-weighted (*Wd*=0.243, ranked 2nd) but its performance is far below ecology (0.476 vs 0.829), although still better than ponds in absolute terms. In contrast, capture fisheries demonstrate an intermediary profile characterized by a relatively equitable pressure gradient across governance (0.401) and social (0.418) indicators. At the indicator level, the importance-performance pattern remains consistent: the highest-weighted indicators within the ecology dimension are also the strongest performers. Specifically, coastal

water quality in fisheries (*Wi*=0.517, *Xi*=0.850) and pond water quality in ponds (*Wi*=0.632, *Xi*=0.795) represent both the most important and best-performing indicators in their respective dimensions. In contrast, waste management in ponds, which is the highest-weighted governance indicator (*Wi*=0.647) coupled with the lowest performance score (*Xi*=0.235), thereby highlighting it as the critical leverage point demanding immediate intervention in the comprehensive evaluation. First, AHP results indicate governance-not ecology- as the primary weakness for shrimp ponds (*Si* governance = 0.313), consistent with documented pond-waste threats to shared water quality (hub node E1) (Boyd *et al*., 2022; de Lacerda *et al*., 2021; Iber and Kasan, 2021; McSherry *et al*., 2023). Second, ecological stress in aquaculture is significant, as intensive aquaculture imposes a high ecological burden in tropical coastal areas (Akram *et al*., 2023; Ariadi *et al*., 2025; Boyd *et al*., 2022; Goldberg *et al*., 2020; Ottinger *et al*., 2022; Rizky *et al*., 2025). While this phenomenon is pertinent at the regional scale, within the context of Pariaman, ecological stress is predominantly channeled through governance deficits rather than direct ecological degradation of the ponds. Third, tourism-related environmental risk is a concern, as community-based tourism is generally susceptible to environmental degradation if not managed effectively (Boustead and Bhatta, 2021; Kakkar and Upadhyay, 2025; Reddy, 2018).

ANP weights

The ANP network is built from 17 nodes (14 indicators selected in Section 3.1 plus 3 activity nodes), organised in nine dependency blocks. Before interpreting the ANP weights, consistency of all paired-comparison matrices forming this network was first verified. All 29 ANP matrices were valid, with excellent consistency: 26 met CR < 0.10 (range 0.000–0.060, mean ≈ 0.014), while 3 matrices in the Economy→Activity block are 2×2, consistent by definition (Table 5). Absence of entries in the Economic→Pond block stems from the lack of direct relevance between the network's economic indicators and the model-specific shrimp pond, rather than implying a broader generalization concerning the economic profile of shrimp aquaculture beyond this framework. The final ANP weight, obtained from the supermatrix limit, is compared with the AHP weight in Table 6. Ponds showed the largest weight correction (Δ = −0.200; 0.588 to 0.388), while fisheries and tourism increased moderately (Δ = +0.103 and +0.097). The ranking (ponds > fisheries > tourism) remained stable, but relative magnitudes shifted---a pattern consistent with prior AHP-ANP comparisons (Jorge-García and Estruch-Guitart, 2022; Lin *et al*., 2024). By failing to account for negative mutual interactions, AHP disproportionately overestimates sectorally dominant activities (Kadoić *et al*., 2017; Saaty, 2006). In contrast, ANP corrects this bias, producing a balanced and proportional weight distribution. The implications for decision-making are substantial: AHP supports stringent restrictions on pond operations (weight 0.588), whereas ANP advocates for more balanced, integrated management, as reflected in the more proportional weights (0.388:0.360:0.252). This correction reflects the network structure, not a mathematical artefact. Three hub nodes link activities: water quality (E1), spatial conflicts (S1), and zoning suitability (G1). Ponds exert the greatest pressure on these hubs (via E1 and G1), explaining their largest weight reduction. Fisheries and tourism, as net recipients of hub-node impacts, gained relative weight. These hub nodes further validate the structural constraints of AHP, demonstrating that a purely hierarchical design fails to account for the interconnected network properties characteristic of shared indicators (Chen and Ren, 2017; Gonzalez-Urango *et al*., 2023; Huang and Chen, 2024b; Lin *et al*., 2024; Saaty, 1996; Ziemba, 2019). Rather than relying solely on the application of ANP, the principal contribution of this study resides in demonstrating how the inclusion of activity interdependencies shifts the evaluated sustainability profile of each

Table 5: Summary of the consistency ratio (CR) values of all ANP matrices

Dependency blocks	n Spouse	Matrix	CR Min	CR Max	Status
Ecology → Activity (E→A)	10 per activity	3	0.007	0.044	✓ Consistent
Social → Activities (S→A)	3 per activity	3	0.006	0.058	✓ Consistent
Economy → Activity (K→A)	1 per activity	2 *	0.000	0.000	✓ Consistent
Governance → Activities (T→A)	6 per activity	3	0.008	0.027	✓ Consistent
Ecology → Activities (A→E)	3 per E node	5	0.005	0.046	✓ Consistent
Social → Activities (A→S)	3 per node S	3	0.001	0.042	✓ Consistent
Economic → Activities (A→K)	3 per node K	2	0.001	0.028	✓ Consistent
Governance → Activities (A→T)	3 per node T	4	0.001	0.060	✓ Consistent
Inner dependence (A→A)	3	3	0.018	0.051	✓ Consistent

*Economic Block → Shrimp ponds = 0 (no relevant ANP economic node for shrimp ponds)

Table 6: Activity weight comparison: AHP vs normalised ANP

Activities	*Wi*_AHP	Rank AHP	*Wi*_ANP ternorm	Rank ANP	Δ (ANP−AHP)	n
Vannamei shrimp pond	0.588	1	0.388	1	−0.200*	5
Small-scale capture fisheries	0.257	2	0.360	2	+0.103*	5
Coastal tourism	0.155	3	0.252	3	+0.097*	5
Total	1.000	-	1.000	-	-	-

|Δ| ≥ 0.05 = methodologically substantial difference; n = number of experts; *CI and activity contribution*

Table 7: Composite index of regional sustainability: AHP vs ANP comparison

Activities	*Si*	*Wi*_AHP	*Si*×*Wi*_AHP	*Wi*_ANP Norm	*Si*×*Wi*_ANP	Δ
Small-scale capture fisheries	0.529	0.257	0.136	0.360	0.190	+0.054
Vannamei shrimp pond	0.486	0.588	0.286	0.388	0.189	−0.097
Coastal tourism	0.695	0.155	0.107	0.252	0.175	+0.068
CI Area	-	-	0.529	-	0.554	+0.025

sector. In contrast, the conventional AHP assumes strict independence across activities and thus obscures these coupled effects. While including interdependencies does not affect the priority order, it changes the relative magnitude of each activity's contribution, thereby providing a more proportionate foundation for decision-making than an independent hierarchical approach. Although AHP assesses each activity's intrinsic sustainability profile independently, the observed patterns indicate that several priority issues extend beyond individual activities due to shared environmental resources. These cross-activity relationships are explicitly addressed in the subsequent ANP analysis. The AHP-ANP result produced three levels of information with distinct meanings: *Si* shows each activity; Wi_ANP shows an activity's relative influence within the interacting system; and activity contribution (*Si* × *Wi*_ANP) shows each activity's effective contribution to regional sustainability as an interaction between its performance and its systemic importance, rather than mere mathematical multiplication. Integrating the activity *Si* with the interdependence-based activity weight (*Wi*_ANP) yielded a regional *CI* of 0.554, compared with 0.529 using AHP weights (Table 7). The activity with the highest *Si* (tourism, 0.695) received greater weight in ANP (0.252) than in AHP (0.155), so its positive contribution is better represented in *CI*; conversely, ponds received a lower ANP weight, reducing their negative contribution. Both *CI* values are classified as moderately sustainable (0.50–0.75) according to Kavanagh and Pitcher (2004). The regional status remains unchanged between the AHP and ANP approaches. The difference between *CI*_ANP and *CI*_AHP (+0.025) is numerically small; however, its significance arises from a structural shift in activity weights due to interdependence (*Wi*_AHP to *Wi*_ANP), rather than from measurement uncertainty or random variation. This makes the

difference methodologically significant despite its limited magnitude. The activity contribution (*Si* × *Wi*_ANP) exhibits a distinct pattern compared to *Si* and *Wi*_ANP individually. Fisheries (0.190), Ponds (0.189), and Tourism (0.175) contribute almost equally to the regional *CI*, despite notable differences in their *Si* and *Wi*_ANP values. This equivalence arises from the interaction between an activity's performance (*Si*) and its systemic importance (*Wi*_ANP). To illustrate, tourism achieves strong performance metrics despite limited systemic influence, whereas ponds display diminished performance alongside substantial systemic importance, resulting in virtually equivalent net contributions when combined. From a policy perspective, the aggregated contribution is particularly informative because it precisely captures the relative functional role of each activity within the regional sustainability framework. The primary management implication arises from the near-equal contribution pattern, which results from the interdependency structure captured by the ANP rather than the *CI* value alone. Because Ponds, Fisheries, and Tourism are interdependent through hub nodes, *CI*_AHP, which does not account for this interdependence, would suggest unilateral restrictions on Ponds. Under *Wi*_AHP, the contribution of Ponds (0.286) appears erroneously dominant. *CI*_ANP, which includes interdependency, instead recommends a synergistic co-management approach across all three activities. This recommendation stems from the capacity of ANP to capture inter-activity feedback and dependencies, distinguishing it from approaches driven strictly by higher quantitative *CI* outcomes. Indicator level reveals that three ecological indicators dominate: fisheries water quality (13.9%), pond water quality (13.4%), and tourism waste management (9.9%). Together, these account for 37% of *CI* despite comprising only 3 of 36 indicators. All three are also the best-performing field indicators (*Xi* = 0.850, 0.795, 0.800). Thus, the moderate sustainability classification rests primarily on favorable environmental conditions, not on social, economic, or governance strengths (Kesaulya *et al*., 2024; Oktorie *et al*., 2025; Romadhon *et al*., 2025; Zhang *et al*., 2024). This perspective is consistent with previous research indicating that a moderate overall sustainability score may mask substantial performance deficits across non-ecological dimensions (Joesidawati and Suwarsih, 2022; Munir and Misbah, 2025). Benchmarking these findings against existing coastal sustainability literature reveals notable instances of both methodological convergence and divergence. Convergence is evident in the repeated observation that environmental quality, particularly water quality, is a decisive attribute in coastal assessments, including waterfront sustainability in Pariaman, partial Indonesian Marine Health Index (IKLI) applications in Ambon and Baguala Bays, coastal tourism risk assessments on small islands, and coastal water quality studies in tourism-intensive marine áreas (Al-Qadami *et al*., 2025; Kesaulya *et al*., 2024; Kurniawan *et al*., 2023; Oktorie *et al*., 2025; Romadhon *et al*., 2025). However, divergence is also notable: while the present study identifies ecology as the principal source of strength, many earlier Rapfish/MDS-based studies in fisheries and coastal systems have found ecology, institutions, ethics, or socio-economic conditions to be the main sources of fragility, with overall systems often rated as less sustainable or only marginally sustainable (Jimenez *et al*., 2021; Parsaulian *et al*., 2024; Wulandari *et al*., 2026). This contrast suggests that Pariaman's multi-activity coastal system is not unusual in achieving only a moderate sustainability classification. Notwithstanding this trend, the profile remains distinctive as its performance is underpinned primarily by advantageous ecological states rather than progress in governance, institutional frameworks, market resilience, or social capacity, which are routinely emphasized as critical leverage domains in prior research (Engen *et al*., 2024; Jimenez *et al*., 2021; Munir and Misbah, 2025; Parsaulian *et al*., 2024; Wulandari *et al*., 2026). Methodologically, this comparison should be viewed as contextual

rather than confirmatory. By employing integrated AHP-ANP weighting, the present framework runs the risk of disproportionately amplifying the impact of a small subset of highly weighted, high-performing indicators. In contrast, many benchmark studies utilise Rapfish/MDS, IKLI/Ocean Health Index (OHI), coastal water quality indices, or Earth-observation-based indicators, each differing in attribute structure, scale, and weighting logic (Jimenez *et al*., 2021; Joesidawati and Suwarsih, 2022; Kurniawan *et al*., 2023; Valenti *et al*., 2018; Widyawati *et al*., 2024; Zhang *et al*., 2024). Therefore, the comparison with West Pasaman is informative but not strictly equivalent: its same-province score of 49.67 situates the present CI of 0.554 (55.4/100) within a comparable regional range, yet the West Pasaman result was primarily driven by dependence on fishing, environmental knowledge, harvest handling, and customary rules, reflecting a different sustainability structure from the ecology-led configuration observed here (Parsaulian *et al*., 2024). Furthermore, emerging scholarship underscores that coastal sustainability trajectories rely heavily on intersectoral dynamics among fisheries, aquaculture, and tourism. Such interactions mediate the redistribution of benefits and vulnerabilities throughout socio-ecological networks, driven explicitly by tourism pressure, aquaculture intensification, and climate change (Alsaleh and Wang, 2025; Kyvelou and Ierapetritis, 2020; Weatherdon *et al*., 2016). Fig. 7 confirms two things: the most striking shift among the three activities is in Pond weight when switching from AHP to ANP (panel a), and both weighting approaches still yield the same regional CI status of moderately sustainable despite different absolute values (panel b). The uniformity of this outcome confirms that the core findings of the study remain invariant to variations in the weighting approach employed. At the same time, differences at the activity level remain relevant for targeted intervention planning. Although both AHP and ANP classify the area as moderately sustainable, ANP's practical advantage lies in three interrelated points: the regional sustainability status is unchanged, the distribution of activity contributions changes substantially, and management intervention priorities differ between the two approaches. Although different methodologies may align on a region's overall status, they frequently exhibit divergent priorities. It is these variations in priority, rather than differences in status, that directly inform and drive practical decision-making. Beyond the methodological comparison, the CI 0.554 value itself carries substantive significance for the region. Sitting in the lower half of the moderately sustainable category (0.50-0.75) suggests considerable room for improvement before reaching highly sustainable status (0.75). Furthermore, the comparable contribution values observed across the three activities (0.190, 0.189, 0.175) demonstrate that improving regional sustainability gains cannot be achieved through sector-specific optimization alone. A simultaneous, cross-sectoral intervention strategy is essential, aligning directly with the network interdependencies captured by ANP. ANP's ability to systematically capture dependencies and feedback between criteria makes it a more capable instrument than AHP for reflecting real-world system complexity, more effectively bridging the gap between models and decision-making (Moslem *et al*., 2023; Sari *et al*., 2024). It loosens AHP's assumption of independence between criteria (Chen and Huang, 2023) and can be used to prioritize indicators and investigate relationships between criteria (Eriş *et al*., 2022). Sustainability assessments that consider spatial competition among economic activities, such as fisheries, aquaculture, and tourism, present a management challenge that is increasingly recognized in the applied MCDA literature (Zekić *et al*., 2025). The current study overcomes this limitation by proposing a composite index that accounts for performance metrics and systemic significance inherent to each activity.

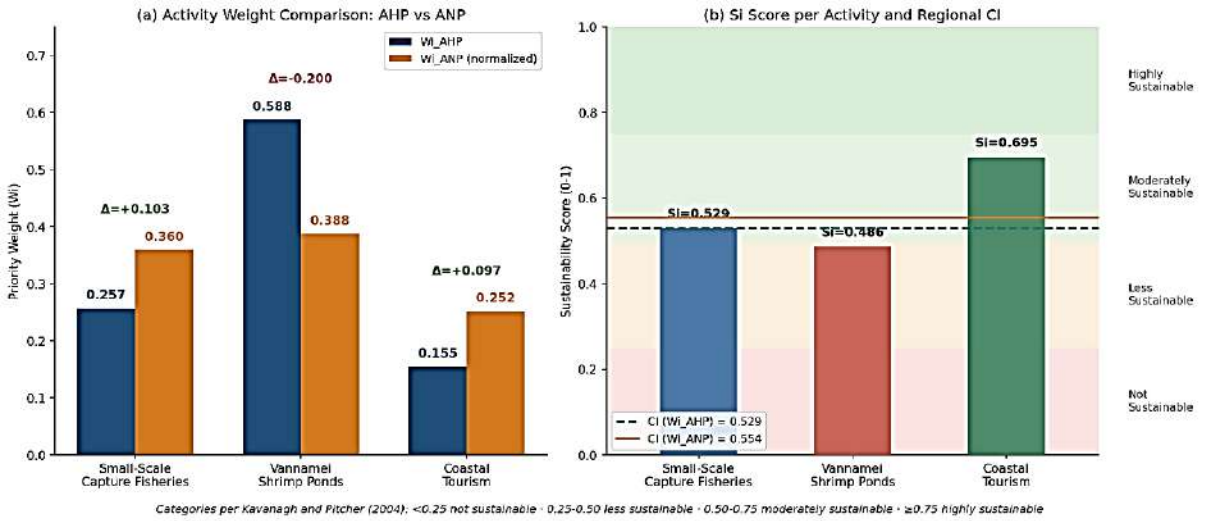

Fig. 7: Comparison of the weight of normalised *Wi*_AHP vs *Wi*_ANP activities (a) and the Pariaman coastal regional Sustainability composite Index (*CI*) (b). Both approaches produce the status: moderately sustainable (Kavanagh and Pitcher, 2004)

Table 8: Results of analysis of the sensitivity of the ANP weight to the regional *CI* and the order of priority of activities (variation ±10% and ±20%)

Varied Activities	Variasi	*Wi*_A1	*Wi*_A2	*Wi*_A3	*CI*	Weight sequence (*Wi*)	Order of contributions (*Si*×*Wi*)
Small-Scale Capture Fisheries	-20%	0.288	0.432	0.281	0.557	A2>A1>A3	A2>A3>A1*
Small-Scale Capture Fisheries	-10%	0.324	0.410	0.267	0.556	A2>A1>A3	A2>A3>A1*
Small-Scale Capture Fisheries	+10%	0.396	0.366	0.238	0.553	A1>A2>A3*	A1>A2>A3
Small-Scale Capture Fisheries	+20%	0.431	0.344	0.224	0.551	A1>A2>A3*	A1>A2>A3
Vannamei Shrimp Ponds	-20%	0.405	0.310	0.284	0.563	A1>A2>A3*	A1>A3>A2*
Vannamei Shrimp Ponds	-10%	0.382	0.349	0.268	0.558	A1>A2>A3*	A1>A3>A2*
Vannamei Shrimp Ponds	+10%	0.337	0.427	0.236	0.550	A2>A1>A3	A2>A1>A3*
Vannamei Shrimp Ponds	+20%	0.314	0.466	0.220	0.546	A2>A1>A3	A2>A1>A3*
Coastal Tourism	-20%	0.384	0.414	0.202	0.545	A2>A1>A3	A1>A2>A3
Coastal Tourism	-10%	0.372	0.401	0.227	0.549	A2>A1>A3	A1>A2>A3
Coastal Tourism	+10%	0.347	0.375	0.278	0.559	A2>A1>A3	A3>A1>A2*
Coastal Tourism	+20%	0.335	0.362	0.303	0.564	A2>A1>A3	A3>A1>A2*

A1 = Small-scale capture fisheries; A2 = Vannamei shrimp ponds; A3 = Coastal tourism. The sign (*) indicates the sequence changed from baseline (A2 > A1 > A3 for weight; A1 > A2 > A3 for Si×Wi's contribution). All 12 scenarios remained in the category of moderately sustainable (0.50–0.75).

Robustness results

Regional *CI* across all 12 tested scenarios ranged from 0.545 to 0.564 (baseline = 0.554), with a maximum deviation of only ±0.010 from baseline, remaining under 2% (approximately 1.8%) and consistently within the moderately sustainable class (Table 8). For individuals interested in the main conclusions, attention should be directed to the *CI* and Contribution Order (*Si*×*Wi*) columns, as they are vital for understanding the resilience of the outcomes. Additional fields are provided for detailed verification. The sustainability status classification (moderately sustainable, 0.50–0.75) did not change in any scenario, indicating the study's main conclusion that Pariaman's coastal area has a sufficiently sustainable status is robust against ANP weighting uncertainty of up to ±20%. However, the order of activity contribution to *CI* (*Si*×*Wi*_ANP) is much more sensitive than *CI* itself. At baseline, the margin between small-scale capture fisheries' contribution (0.190) and vannamei shrimp ponds' (0.189) is only 0.001,

much smaller than the margin in gross weight (*Wi*_ANP: 0.388 vs 0.360; margin 0.028). Consequently, rank reversals manifested across 8 out of 12 evaluated scenarios, including all instances where the vannamei shrimp pond weight was adjusted, including all instances where the vannamei shrimp pond weight. Such a small margin suggests that the two activities make comparable contributions to regional sustainability, precluding any inference of model error. Consequently, management strategies should avoid rigid prioritization between fisheries and shrimp ponds. This pattern aligns with the established finding in the composite index literature that robustness at the aggregate level and sensitivity at the level of constituent components are independent properties, each requiring separate evaluation (Choi, 2019; Wang *et al*., 2026). Far from indicating a structural flaw, the observed rank reversal underscores the model's sensitivity in differentiating between varying levels of spatial uncertainty. The composite index remains stable because it aggregates all three activities' contributions, making regional sustainability status independent of the specific order between activities; at the activity level, the contribution order is sensitive because it is empirically close to a tie, not because of methodological weakness. A genuinely robust framework should reveal these differences in sensitivity across levels, rather than uniformly reporting all results as 'stable' or 'unstable' regardless of level. While weighting uncertainty does not undermine the stability of regional sustainability status for long-term planning, the prioritization sequence between fisheries and aquaculture ponds requires flexibility. Given their near-equivalent contributions to the composite index, decisions must integrate qualitative and contextual drivers exogenous to the analytical framework. Sensitivity analysis shows the framework has two important characteristics: stable enough to produce a consistent region-level sustainability assessment, yet sensitive enough to detect small changes in relative contribution between activities, a combination that makes the framework suitable as a decision-support tool, able to distinguish genuinely stable findings from those still dependent on weight uncertainty.

Limitations

Internal validation relies on consistency ratios and the *CI*_ANP (0.554) versus *CI*_AHP (0.529) comparison. This demonstrates interpretable ranking shifts from incorporating interdependence. However, independent datasets, historical trends, or external benchmarks are unavailable, limiting external validation. Future empirical validation of the framework's regional composite index estimates against longitudinal monitoring datasets or independent sustainability metrics will be essential to corroborate model outputs and substantiate confidence beyond internal structural consistency. The AHP-ANP weights and *CI* values are specific to Pariaman's biophysical, socio-economic, and institutional context. To establish broader applicability, cross-site validation across analogous tropical coastal settings is required. Expanding the framework beyond three activities would increase ANP complexity combinatorially, raising the expert-elicitation burden and inconsistency risk. The framework is also inherently cross-sectional; it does not capture climate change, seasonal variability, or long-term land-use change that could alter activity interdependencies. Accounting for these shifting dynamics calls for systematic, iterative re-evaluation or the coupling of the framework with dynamic simulation models. The ANP network structure and weights reflect expert judgement rather than empirical interaction data. This introduces potential anchoring and framing biases that consistency ratios cannot detect. The 36-indicator set is also non-unique; alternative indicators could yield different weights and *CI* values. Because min-max normalization relies heavily on sample extrema, it exhibits limited robustness when encountering out-of-range data during prospective application. Consequently,

precise numerical reproduction requires the same expert panel, indicator set, and sample—an inherent constraint of expert-elicitation-based MCDA.

Policy implications

Priority setting extends beyond a simple numerical ranking. Given the marginal differences in activity contributions (Fisheries 0.190, Ponds 0.189, Tourism 0.175), governance frameworks should avoid depending solely on quantitative *Si* or *Wi*_ANP outputs, balancing them instead against underlying socioeconomic importance, ecological vulnerabilities, and stakeholder preferences. Targeted hub-node interventions outperform blanket restrictions. The correction of Ponds' weight (0.588 to 0.388) traces to three shared nodes: water quality, spatial conflicts, and zoning suitability. Interventions on pond effluent standards, spatial-use resolution, and zoning compliance would simultaneously benefit fisheries and tourism. A core strength of the framework lies in its ability to separate intrinsic sustainability dynamics from broader, indirect regional externalities. Ponds' low intrinsic score (*Si* = 0.486) reflects weak governance, yet the network reveals their wastewater degrades shared water quality and spatial nodes—a dynamic invisible to activity-level assessment. Policymakers should thus evaluate *Si* and *Wi*_ANP jointly. Decision-makers can apply the framework in four steps. First, use activity contributions (*Si* × *Wi*_ANP) to identify systemic weight. Second, trace hub nodes affected by each activity to locate cross-sectoral intervention points. Third, prioritize shared nodes for the greatest management return. Ultimately, the observed parity in activity contributions underscores the requirement for an integrated, multi-sectoral intervention framework; discrete, single-activity measures are insufficient to drive substantial shifts in the regional *CI*. The framework is a static, cross-sectional tool, not a forecasting model. Its supermatrix structure can support ex-ante scenario comparison using hypothetical indicator values, such as projected pond expansion. Nonetheless, achieving precise predictive capability requires integrating dynamic simulation models. The conclusion that hierarchical assessments tend to overestimate locally dominant, negatively interdependent sectors is broadly generalizable to other multi-activity resource conflicts. However, the specific numerical weights remain context-specific. Subsequent methodological extensions could integrate the framework with GIS for spatial deployment, employ, Bayesian networks for probabilistic modeling of hub-node interactions, or incorporate System Dynamics to simulate temporal feedback loops. Such integration pathways outline future development trajectories rather than existing framework capabilities.

CONCLUSION

This study developed and implemented an activity-based sustainability assessment framework integrating AHP and ANP for multi-activity coastal areas in Pariaman, West Sumatra. AHP calculated activity-level sustainability scores across four dimensions and 36 indicators. Coastal tourism scored highest (0.695), small-scale capture fisheries ranked middle (0.529), and vannamei shrimp ponds scored lowest (0.486). By structuring the system into five clusters comprising 14 indicator nodes and three activity nodes, the ANP network explicitly captured complex inter-activity dependencies. Regional *CI* calculated under both weighting schemes showed significant methodological implications. ANP corrected the overestimation of shrimp ponds from Wi_AHP = 0.588 to Wi_ANP = 0.388 (Δ = -0.200). Small-scale capture fisheries (+0.103) and coastal tourism (+0.097) strengthened after interdependence was incorporated. This finding demonstrates that reliance on AHP's foundational independence assumption generates contribution estimates unreflective of the complex interactions characteristic of multi-functional coastal environments. The ANP-weighted CI (0.554)

provides a more valid planning basis than the AHP-based *CI* (0.529). Both fall within the moderately sustainable category. Three hub nodes (coastal water quality, space utilization conflicts, and zoning suitability) provide empirical evidence of inter-activity dependency mechanisms directly relevant to integrated coastal zone management. Effective management of Pariaman's coastal area demands targeted interventions at three pivotal junctures—improving water quality, resolving spatial incompatibilities, and augmenting cross-sectoral governance. These leverage points affect the sustainability of more than one activity simultaneously. The main contribution of this research lies in the activity-based assessment framework itself, which is not merely the application of AHP-ANP to a new case, but an approach that explicitly models interdependencies between activities. It distinguishes between region-level stability and activity-level sensitivity. By offering a transferable decision-support architecture, the proposed framework facilitates systematic coastal sustainability assessments in comparable multi-activity areas. It is especially relevant for tropical regions with similar coastal utilization patterns. The theoretical contribution demonstrates that hierarchical assessment systematically overestimates locally dominant activities that are negatively interdependent with others. An interdependence-aware network layer corrects this overestimation traceably by identifying hub nodes. The practical contribution translates this correction into targeted, hub-node-based management guidance. This replaces the blanket single-activity restrictions implied by purely hierarchical assessments. The underlying two-layer logic is not limited to coastal systems. By synthesizing an intrinsic hierarchical evaluation with a network-based layer that accounts for competitive interactions over shared resources, the approach establishes a robust logic transferable to broader natural resource management contexts. Examples include river-basin water allocation among agricultural, industrial, and municipal users, or multi-use forest landscapes where logging, agriculture, and conservation zones interact through shared hydrological and habitat connectivity. Subsequent studies might expand the utility of the framework by incorporating evolving environmental conditions, broader ecosystem service portfolios, increased stakeholder participation in indicator curation, and advanced analytical approaches including System Dynamics, Bayesian networks, or spatially explicit modelling. These enhancements would strengthen both the predictive capability and the applicability of the framework to a wider range of coastal and non-coastal resource management settings.

AUTHOR CONTRIBUTIONS

Desrizal, contributed to the conceptualization, methodology, software, validation and writing the original draft. B. Widigdo, assisted with the methodology, validation, formal analysis and resources. G. Yulianto, contributed to writing, reviewing and visualization. F. Kurniawan, assisted with writing, reviewing and editing. Sulistiono, the corresponding author, supervised the project, writing, reviewing and editing.

ACKNOWLEDGEMENT

The authors thank all experts who participated in the assessment, and the relevant agencies (Marine and Fisheries Service West Sumatra Province; Fisheries, Environment, Tourism, and Spatial Planning Services of Padang Pariaman and Pariaman City) for field data support. The authors also sincerely acknowledge the Indonesian Education Scholarship (BPI), the Centre for Higher Education Funding and Assessment (PPAPT), Ministry of Education, Science and Technology (Kemdiksaintek), and the Indonesian Endowment Fund for Education (LPDP) for their financial support [0005/J5.2.3./BPI.06/9/2022], which made this research possible.

CONFLICT OF INTEREST

The authors declare that there is no conflict of interest regarding the publication of this manuscript. In addition, the ethical issues, including plagiarism, informed consent, misconduct, data fabrication and/or falsification, double publication and/or submission, and redundancy, have been completely observed by the authors.

OPEN ACCESS

©2027 The author(s). This article is licensed under a Creative Commons Attribution 4.0 International License, which permits use, sharing, adaptation, distribution and reproduction in any medium or format, as long as you give appropriate credit to the original author(s) and the source, provide a link to the Creative Commons license, and indicate if changes were made. The images or other third-party material in this article are included in the article's Creative Commons license, unless indicated otherwise in a credit line to the material. If material is not included in the article's Creative Commons license and your intended use is not permitted by statutory regulation or exceeds the permitted use, you will need to obtain permission directly from the copyright holder. To view a copy of this license, visit: http://creativecommons.org/licenses/by/4.0/

PUBLISHER'S NOTE

GJESM Publisher remains neutral with regard to jurisdictional claims in published maps and institutional affiliations.

POSITIVE AI STATEMENT

During the preparation of this work, the author(s) have used Artificial Intelligence (AI) tools, Claude (Anthropic), ChatGPT (OpenAI) and Grammarly, to assist in data compilation and verification, as well as refinement of the manuscript language. After using this tool/service, the authors reviewed and edited the content as needed and take full responsibility for the content of the publication.

ABBREVIATIONS

%	Percent
A1, A2, A3	Activity code (Table 7): A1 = Small-scale capture fisheries, A2 = Vannamei shrimp ponds, A3 = Coastal tourism
AHP	Analytic hierarchy process
ANP	Analytic network process
BPS	Central bureau of statistics (Badan Pusat Statistik), Indonesia
CI	Composite sustainability index
CR	Consistency ratio
E, S, K, G	Sustainability dimension code: Ecology, Social, Economy, Governance
FAO	Food and agriculture organization
GIS	Geographic information system
GT	Gross tonnage
IKLI	Indonesian marine health index (Indeks Kesehatan Laut Indonesia)
MCDA	Multi-criteria decision analysis
MDS	Multidimensional scaling
NGO	Non-governmental organization
OAT	One-at-a-time
OECD	Organisation for economic co-operation and development
OHI	Ocean Health Index
Si	Sustainability score per activity
Wi	Weight/priority vector
WQI	Water quality index

REFERENCES

Akram, H.; Hussain, S.; Mazumdar, P.; Chua, K. O.; Butt, T. E.; Harikrishna, J. A., (2023). Mangrove health: A review of functions, threats, and challenges associated with mangrove management practices. Forests. 14(9): 1-38 **(38 pages).**

Al-Qadami, E.H.H.; Razi, M.A.M.; Shah, S.M.H.; Mokhtar, A.; Mahamud, M.; Jamal, M.H.; Ismail, Z.A., (2025). Marine water and sediment quality assessment of mainland Kedah and Langkawi Island shorelines: A case study. IOP Conference Series: Earth Environ. Sci., 1453(1): 1-12 **(12 pages).**

Alsaleh, M.; Wang, X., (2025). Aquaculture growth and coastal tourism development in the context of sustainable blue economy. Sustainable Dev., 33(2): 2030-2046 **(17 pages).**

Ariadi, H.; Musa, M.; Mahmudi, M.; Hertika, A. M. S., (2025). The waste load and carrying capacity on intensive shrimp farming: A mini review. Ecol. Eng. Environ. Technol., 26(4): 323–333 **(11 pages).**

Arifanti, V.B.; Novita, N.; Subarno; Tosiani, A., (2021). Mangrove deforestation and CO_2 emissions in Indonesia. IOP Conference Series: Earth Environ. Sci., 874(1): 1-10 **(10 pages).**

Berkes, F., (2017). Environmental governance for the anthropocene? Social-ecological systems, resilience, and collaborative learning. Sustainability. 9(7): 1232 **(1 page).**

BPS Padang Pariaman Regency, (2025). Padang Pariaman Regency in figures 2025. BPS-Statistics Padang Pariaman Regency, 26: 1–749 **(749 pages).**

BPS Pariaman City, (2025). Pariaman City in figures 2025. BPS-Statistics Pariaman Municipality, 22: 1–564 **(564 pages).**

Boustead, R.; Bhatta, S., (2021). Assessment of the social impacts of community based tourism. Z. Tourismuswiss. 13(2): 268-302 **(35 pages).**

Boyd, C.E.; D'Abramo, L.R.; Glencross, B.D.; Huyben, D.C.; Juarez, L.M.; Lockwood, G.S.; McNevin, A.A.; Tacon, A.G.J.; Teletchea, F.; Tomasso, J.R.; Tucker, C.S.; Valenti, W.C., (2020). Achieving sustainable aquaculture: Historical and current perspectives and future needs and challenges. J. World Aquacult. Soc., 51(3): 578-633 **(56 pages).**

Boyd, C.E.; Davis, R.P.; McNevin, A.A., (2022). Perspectives on the mangrove conundrum, land use, and benefits of yield intensification in farmed shrimp production: A review. J. World Aquacult. Soc., 53(1): 8-46 **(39 pages).**

Cabrera, J.S.; Lee, H.S., (2022). Coastal zone environment integrity assessment for sustainable management: Part 1. Development of adaptive expert-driven coastal zone health index framework. J. Mar. Sci. Eng., 10(9): 1-19 **(19 pages).**

Chen, C.Y.; Huang, J.J., (2023). Integrating dynamic Bayesian networks and analytic hierarchy process for time-dependent multi-criteria decision-making. Mathematics. 11(10): 1-12 **(12 pages).**

Chen, L.; Ren, J., (2017). Multi-attribute sustainability evaluation of alternative aviation fuels based on fuzzy ANP and fuzzy grey relational analysis. J. Air Transp. Manage., 68: 176–186 **(11 pages).**

Chuang, Y.H.; Yu, R.F.; Chen, W.Y.; Chen, H.W.; Su, Y.T., (2018). Sustainable planning for a coastal wetland system with an integrated ANP and DPSIR model for conflict resolution. Wetlands Ecol. Manage., 26(6): 1-12 **(12 pages).**

Daimi, S.; Rebai, S., (2023). Sustainability performance assessment of Tunisian public transport companies: AHP and ANP approaches. Socio-Econ. Plann. Sci., 89: 101680 **(1 page).**

Darko, A.; Chan, A. P. C.; Ameyaw, E. E.; Owusu, E. K.; Pärn, E.; Edwards, D. J., (2019). Review of application of analytic hierarchy process (AHP) in construction. Int. J. Constr. Manage., 19(5): 436–452 **(17 pages).**

de Lacerda, L. D.; Ward, R. D.; Godoy, M. D. P.; Meireles, A. J. de A.; Borges, R.; Ferreira, A. C., (2021). 20-years cumulative impact from shrimp farming on mangroves of northeast brazil. **Front. For. Glob. Change.,** 653096 (4): 1-17 **(17 pages).**

Desrizal, D.; Widigdo, B.; Yulianto, G.; Kurniawan, F.; Sulistiono, S., (2025). Legal status of aquaculture ponds and coastal compliance in Padang Pariaman. IOP Conference Series.: Earth Environ. Sci., 1543(1): 1-13 **(13 pages).**

Engen, S.; Hausner, V.H.; Mikkelsen, E.; Gundersen, H.; Christie, H.; Falk-Andersson, J.; Halpern, B.S.; Fauchald, P., (2024). Co-creating coastal sustainability goals and indicators. Sustainable Sci., 19(4): 1327-1343 **(17 pages).**

Eriş, M.B.; Sezer, E.D.G.; Ocak.; Z., (2023). Prioritization of the factors affecting the performance of clinical laboratories using the AHP and ANP techniques. Netw. Model. Anal. Health Inform. Bioinforma. 12 (1): 5 **(1 page).**

FAO, (2022). The state of world fisheries and aquaculture 2022. FAO, Rome, Italy. 1-266 **(266 pages).**

Firdaus, M.; Sulistiono; Widigdo, B., (2021). Brackishwater pond development: present status and problems in the Padang Pariaman Regency of West Sumatra, Indonesia. E3S Web Conference. 05009 (322):1-12 **(12 pages).**

Folke, C.; Biggs, R.; Norström, A.V.; Reyers, B.; Rockström, J., (2016). Social-ecological resilience and biosphere-based sustainability science. Ecol. Soc., 21(3): 41 **(1 page).**

Goldberg, L.; Lagomasino, D.; Thomas, N.; Fatoyinbo, T., (2020). Global declines in human-driven mangrove loss. Global Change Biol., 26(10): 5844-5855 **(12 pages).**

Gonzalez-Urango, H.; Mu, E.; Ujwary-Gil, A.; Florek-Paszkowska, A., (2023). Analytic network process in economics, finance and management: Contingency factors, current trends and further research. Expert Syst. Appl., 121415 (237): 1-13 **(13 pages).**

Hossain, M.S.; Gain, A.K.; Rogers, K.G., (2020). Sustainable coastal social-ecological systems: How do we define "coastal"?. Int. J. Sustainable Dev. World Ecol., 27(7): 577-582 **(6 pages).**

Huang, J. J.; Chen, C. Y., (2024a). Resource allocation of cooperative alternatives using the analytic hierarchy process and analytic network process with shapley values. Algorithms. 17(4): 1-15 **(15 pages).**

Huang, J. J.; Chen, C. Y., (2024b). Using markov random field and analytic hierarchy process to account for Interdependent criteria. Algorithms, 17(1): 1-13 **(13 pages).**

Iber, B. T.; Kasan, N. A., (2021). Recent advances in Shrimp aquaculture wastewater management. Heliyon. 7(11): 1-9 **(9 pages).**

Il Choi, H., (2019). Assessment of aggregation frameworks for composite indicators in measuring flood vulnerability to climate change. Sci. Rep., 19371(9): **(1 page).**

Jimenez, É.A.; Gonzalez, J.G.; Amaral, M.T.; Lucena Frédou, F., (2021). Sustainability indicators for the integrated assessment of coastal small-scale fisheries in the Brazilian Amazon. Ecol. Econ., 181: 1-14 **(14 pages).**

Joesidawati, M.I.; Suwarsih, S., (2022). Measurement of Indonesian Marine Health Index to assess the health of the coastal ecosystem of Tuban, East Java. IOP Conference Series: Earth Environ. Sci., 1036(1): 1-13 **(13 pages).**

Jorge-García, D.; Estruch-Guitart, V., (2022). Comparative analysis between AHP and ANP in prioritization of ecosystem services - A case study in a rice field area raised in the Guadalquivir marshes (Spain). Ecol. Inform., 70 (101739): 1-11 **(11 pages).**

Kadoić, N.; Ređep, N.B.; Divjak, B., (2017). Decision making with the analytic network process. Int. J. Anal. Hierarchy Process:1-7 (**7 pages).**

Kakkar, S.; Upadhyay, P., (2025). Structural challenges and sustainability deficits in rural tourism: A conceptual review of long-term economic and environmental impacts on local communities. Adv. Int. J. Res., 6(6): 1-5 **(5 pages).**

Kavanagh, P.; Pitcher, T.J., (2004). Implementing Microsoft Excel software for Rapfish: A technique for the rapid appraisal of fisheries status. Fish. Cent. Res. Rep., 12(2): 1-80 **(80 pages).**

Kesaulya, I.; Haumahu, S.; Nikijuluw, V.P.H.; Djakiman, C., (2024). A partial analysis of ocean health index based on clean waters and biodiversity goals in Ambon and Baguala bays, Maluku. Depik, 13(1): 64-71 **(8 pages).**

Ketaren, D. G. K.; Radjawane, I. M.; Latief, H.; Sidik, F.; Trenggono, S. W.; Diantara, S. D.; Setyawidati, N. A. R.; Akbar, M. I.; Raja, J. A. L.; Farkhan, M. A.; Kasim, K.; Maharani, S., (2026). Impacts of mangrove land use change on carbon stocks in coastal ecosystems. Global J. Environ. Sci. Manag.. 12(3): 1041-1060 **(20 pages).**

Kheybari, S.; Rezaie, F.M.; Farazmand, H., (2020). Analytic network process: An overview of applications. Appl. Math. Comput., 124780 (367): **(1 pages).**

Kyvelou, S.S.I.; Ierapetritis, D.G., (2020). Fisheries sustainability through soft multi-use maritime spatial planning and local development co-management: Potentials and challenges in Greece. Sustainability. 12(5): 1-26 **(26 pages).**

Kurniawan, F.; Adrianto, L.; Bengen, D.G.; Prasetyo, L.B., (2023). Hypothetical effects assessment of tourism on coastal water quality in the Marine Tourism Park of the Gili Matra Islands, Indonesia. Environ. Dev. Sustainable. 25(8): 7959-7985 **(27 pages).**

Lin, G.; Zhang, Q.; Zhang, Y.; Shen, C.; Xu, H.; Wang, S., (2024). Performance assessment of public transport networks: An AHP-ANP approach. Heliyon. 10(22): 1-11 **(11 pages).**

McSherry, M.; Davis, R.P.; Andradi-Brown, D.A.; Ahmadia, G.N.; Van Kempen, M.; Wingard Brian, S., (2023). Integrated mangrove aquaculture: The sustainable choice for mangroves and aquaculture?. Front. For. Global Change., 1094306(6): 01-08 **(8 pages).**

Moslem, S.; Solieman, H.; Oubahman, L.; Duleba, S.; Senapati, T.; Pilla, F., (2023). Assessing public transport supply quality: A comparative analysis of analytical network process and analytical hierarchy process. J. Soft Comput. Decis. Anal., 1(1): 124-138 **(15 pages).**

Munir, M.; Misbah, A., (2025). Sustainability analysis of skipjack tuna catch based on multidimensional scaling (MDS) in the coastal area of Pasuruan Regency. AGROMIX, 16(1): 155-167 **(13 pages).**

Nardo, M.; Saisana, M.; Saltelli, A.; Tarantola, S.; Hoffmann, A.; Giovannini, E., (2005). Handbook on constructing composite indicators: Methodology and user guide. OECD Statistics Working Papers, OECD Publishing, Paris, France: 1-109 **(109 pages).**

Navarro, I.J.; Martí, J.V.; Yepes, V., (2022). Analytic network process-based sustainability life cycle assessment of concrete bridges in coastal regions. Sustainability. 14(17): 1-16 **(16 pages).**

Newton, A.; Icely, J.; Cristina, S.; Perillo, G.M.E.; Turner, R.E.; Ashan, D.; Cragg, S.; Luo, Y.; Tu, C.; Li, Y.; Zhang, H.; Ramesh, R.; Forbes, D.L.; Solidoro, C.; Béjaoui, B.; Gao, S.; Pastres, R.; Kelsey, H.; Taillie, D.; Kuenzer, C., (2020). Anthropogenic, direct pressures on coastal wetlands. Front. Ecol. Evol., 8: 144 **(29 pages).**

Ofori, S.A.; Kodikara, S.K.A.; Jayatissa, L.P.; Madarasinghe, S.K.; Nijamdeen, T.W.G.F.M.; Dahdouh-Guebas, F., (2023). What is the ecological footprint of aquaculture after 5 decades of competition between mangrove conservation and shrimp farm development?. Aquat. Conserv. Mar. Freshw. Ecosyst., 33(1): 15-28 **(14 pages).**

Oktorie, O.; Dewata, I.; Barlian, E.; Hermon, D.; Putra, A., (2025). Assessing the sustainability of lagoon-based environmental waterfront in the coastal zone of Pariaman City, Indonesia. Geogr. Technol., 20(2): 134-149 **(16 pages).**

Ottinger, M.; Bachofer, F.; Huth, J.; Kuenzer, C., (2022). Mapping aquaculture ponds for the coastal zone of Asia with Sentinel-1 and Sentinel-2 time series. Remote Sens., 14(153): 1-25 **(25 pages).**

Parsaulian, B.; *et al*., (2024). Re-thinking Indonesian fisheries policy: empowerment of a hidden asset for sustainable fisheries in West Pasaman District, West Sumatra, Indonesia. Int. J. Environ. Impacts. 7(1): 1-16 **(16 pages).**

Pourebrahim, S.; Hadipour, M.; Mokhtar, M.B.; Hj Mohamed, M.I., (2010). Analytic network process for criteria selection in sustainable coastal land use planning. Ocean Coast. Manage., 53(9): 544-551 **(8 pages).**

Rahmat, Y.N.; Neilson, J., (2023). The ebb and flow of capital in Indonesian coastal production systems. Singapore J. Trop. Geogr., 44(2): 300-321 **(22 pages).**

Reddy, G.P.O., (2018). Spatial data management, analysis, and modeling in gis: principles and applications. Springer international publishing, Cham, Switzerland: 127-142 **(16 pages).**

Richards, D.R.; Friess, D.A., (2016). Rates and drivers of mangrove deforestation in Southeast Asia, 2000-2012. Proc. Natl. Acad. Sci. U.S.A., 113(2): 344-349 **(6 pages).**

Rizky, P. N.; Halim, A. M.; Nisa, A. C.; Prama, E. A.; Ulfauza, Oktahimawan, M. K., (2025). Spatial variability of water and sediment quality in pond outlet: Implications for coastal ecosystems in mangrove areas, Pasuruan, East Java. HAYATI J. Biosci., 32(5): 1313–1323 **(11 pages).**

Romadhon, A.; Rini, D.A.S.; Hilyana, S., (2025). Ecological risk assessment for sustainable tourism on Saobi Island, Indonesia. Asian J. Ethnobiol., 8(2): 291-300 **(10 pages).**

Saaty, T. L., (2004). Fundamentals of the analytic network process — Dependence and feedback in decision-making with a single network. J. Syst. Sci. Syst. Eng., 13(2): 129–157 **(29 pages).**

Saaty, T.L., (2006). An analytic network process model for financial-crisis forecasting. Int. J. Forecast., 22(1): 1-15 **(15 pages).**

Saaty, T.L., (2008). Decision making with the analytic hierarchy process. Int. J. Services Sci., 1(1): 83-98 **(17 pages).**

Saaty, T.L., (2014). Analytic hierarchy process. In: Balakrishnan, N.; Colton, T.; Everitt, B.; Piegorsch, W.; Ruggeri, F.; Teugels, J.L. (Eds.), Wiley StatsRef: Statistics Reference Online. John Wiley & Sons, Hoboken, NJ, USA **(15 pages).**

Saaty, T.L., (1996). Decision Making with dependence and feedback: The Analytic Network Process. RWS Publications, Pittsburgh, PA, USA: 1-2 **(2 pages).**

Saaty, T.L.; Vargas, L.G., (2006). Decision Making with the Analytic Network Process: Economic, Political, Social and Technological Applications with Benefits, Opportunities, Costs and Risks. Springer, New York, NY, USA: 1-283 **(283 pages).**

Saaty, T.L.; Vargas, L.G., (2012). Models, Methods, Concepts and Applications of the Analytic Hierarchy Process, Second Edition. Springer, New York, NY, USA: 1-342 **(342 pages).**

Sánchez-Garrido, A.J.; Navarro, I.J.; García, J.; Yepes, V., (2022). An adaptive ANP and ELECTRE IS-based MCDM model using quantitative variables. Mathematics. 10(12): 1-24 **(24 pages).**

Sari, I.; Ichsan, M.; White, A.; Raup, S.A.; Wisudo, S.H., (2021). Monitoring small-scale fisheries catches in Indonesia through a fishing logbook system: Challenges and strategies. Mar. Policy. 134: 104770: 1-7 **(7 pages).**

Sari, R.; Kurniastuti, I.; Sulistiyani, E., (2024). Comparative analysis of prioritization model between AHP and ANP for project portfolio management SI/IT Surabaya City Government. Appl. Technol. Comput. Sci. J., 6(2): 88-95 **(8 pages).**

Silalahi, H. T.; Basyuni, M.; Aritonang, E. Y.; Slamet, B.; Hartini, K. S.; Wee, A. K. S., (2024). Management of mangrove landscape and ecosystem for ecotourism. Global J. Environ. Sci. Manage., 10(4): 1977–1992 **(16 pages).**

Srđević, B.; Srđević, Z., (2024). Multi-model assessing and visualizing consistency and compatibility of experts in group decision-making. Mathematics. 12(11): 1-21 **(21 pages).**

Stacey, N.; Gibson, E.; Loneragan, N.R.; Warren, C.; Wiryawan, B.; Adhuri, D.S.; Steenbergen, D.J.; Fitriana, R., (2021). Developing sustainable small-scale fisheries livelihoods in Indonesia: Trends, enabling and constraining factors, and future opportunities. Mar. Policy. 132: 1-12 **(12 pages).**

Stanford, R.J.; Wiryawan, B.; Bengen, D.G.; Febriamansyah, R.; Haluan, J., (2014). Improving livelihoods in fishing communities of West Sumatra: More than just boats and machines. Mar. Policy. 45: 16-25 **(10 pages).**

Tian, W.; Bai, J.; Sun, H.; Zhao, Y., (2013). Application of the analytic hierarchy process to a sustainability assessment of coastal beach exploitation: A case study of the wind power projects on the coastal beaches of Yancheng, China. J. Environ. Manage., 115: 251-256 **(6 pages).**

Tuyen, V.V., (2024). Prioritization of coastal environmental risks under climate change in Quang Ngai, Vietnam: An integrated analytic network process—Risk score approach. Acadlore Trans. Geoscience. 3(4): 237-251 **(15 pages).**

Valenti, W.C.; Kimpara, J.M.; Preto, B. de L.; Moraes-Valenti, P., (2018). Indicators of sustainability to assess aquaculture systems. Ecol. Indic., 88: 402-413 **(11 pages).**

Wang, P.; O'Brien, F.; Son, J.Y.; Heo, S.; Bell, M.L.; Dubrow, R.; Chen, K., (2026). An updated modeling framework and sensitivity analysis of methodology for the climate health vulnerability index. Nat. Commun., 17: 1417 **(1 page).**

Weatherdon, L.V.; Magnan, A.K.; Rogers, A.D.; Sumaila, U.R.; Cheung, W.W.L., (2016). Observed and projected impacts of climate change on marine fisheries, aquaculture, coastal tourism, and human health: An update. Front. Mar. Sci., 3: 48 **(21 pages).**

Widigdo, B.; Ilman, M.; Santoso, N.; Sulistiono; Kusmana, C.; Krisanti, M., (2024). Performance of integrated mangrove-aquaculture (IMA) in District of Sidoarjo, East Java Indonesia. Bio-Web Conference. 92: 01022: 1-9 **(9 pages).**

Widyawati, K.; Kusmana, C.; Pertiwi, S.; Sulistyantara, B., (2024). Rapid assessment of the sustainability status of tourism area management through MDS-Rapfish R in Situ Rawa Kalong, Depok City, West Java, Indonesia. Int. J. Sustain. Dev. Plan., 19(6): 2059-2068 **(10 pages).**

Więckowski, J.; Sałabun, W., (2023). Sensitivity analysis approaches in multi-criteria decision analysis: A systematic review. Appl. Soft Comput., 148: 110915: 1-19 **(19 pages).**

Wulandari, U.; Purwanti, P.; Setyohadi, D.; Abidin, Z., (2026). Multidimensional rapfish analysis of Danish seine fisheries in Brondong, Indonesia: Ecological, economic, social, technological, and ethical perspectives. Fish. Aquat. Sci., 29(3): 152-165 **(14 pages).**

Yuliana, E.; Nurilmala, M., Rahadiati, A.; Farida, I.; Kurniawati, H.; Agustina, S.; Difah, D. A.; Pertiwi, P. R.; Wicaksana, B. E.; Ramilo, R. V.; Djatmiko, W. A., (2026a). Provisioning ecosystem services through the sustainable management of fish resources extracted by small-scale fishers. Global J. Environ. Sci. Manage., 12(3): 1311-1332 **(21 pages).**

Yuliana, E.; Winata, A.; Setijorini, L. E.; Yani, D. E.; Fathani, M. H.; Djatmiko, W. A., (2026b). Biodiversity-oriented criteria for measuring the effectiveness of mangrove ecosystem rehabilitation success. Global J. Environ. Sci. Manage., 12(4): 1-20 **(20 pages).**

Zamzami, L.; Azwar, Darman Moenir, H., (2023). Enhancing social resilience and addressing economic uncertainty in small-scale fishing households along the west coast of West Sumatra. Bio-Web of Conference. 74: 1-10 **(10 pages).**

Zekić, A.; Gundić, A.; Grbić, L.; Vukić, M., (2025). The application of multi-criteria analysis to coastal zone management decision-making. Sustainability. 17(13): 6194: 1-17 **(17 pages).**

Zhang, L.; Zuo, J.; Chen, B.; Liao, J.; Yan, M.; Bai, L.; Sutrisno, D.; Hashim, M.; Mamun, M.M.A. Al., (2024). Improved indicators for the integrated assessment of coastal sustainable development based on Earth observation data. Int. J. Digit. Earth. 17(1): 1-21 **(21 pages).**

Ziemba, P., (2019). Inter-criteria dependencies-based decision support in the sustainable wind energy management. Energies. 12(4): 749: 1-29 **(29 pages).**

AUTHOR (S) BIOSKETCHES

Desrizal, Ph.D. Candidate, Study Program of Coastal and Marine Resources Management, Department of Aquatic Resources Management, Faculty of Fisheries and Marine Sciences, IPB University, Bogor, 16680, West Java, Indonesia. Department of Aquatic Resources Management, Faculty of Sciences, Nahdlatul Ulama University of West Sumatera, Padang, 25136, Indonesia.
- Email: *chaniagodesrizal@apps.ipb.ac.id*
- ORCID: 0000-0002-7888-3574
- Web of Science ResearcherID: NA
- Scopus Author ID: 60177383400
- Homepage:https://ipb.ac.id

Widigdo, B., Ph.D., Professor, Department of Aquatic Resources Management, Faculty of Fisheries and Marine Sciences, IPB University, Bogor, 16680, West Java, Indonesia.
- Email: *widigdo@apps.ipb.ac.id*
- ORCID: 0000-0002-8926-3573
- Web of Science ResearcherID: NA
- Scopus Author ID: 57193567053
- Homepage: https://ipb.ac.id

Yulianto, G., Ph.D., Lecturer, Department of Aquatic Resources Management, Faculty of Fisheries and Marine Sciences, IPB University, Bogor, 16680, West Java, Indonesia.
- Email: *gyo@apps.ipb.ac.id*
- ORCID: 0000-0003-4946-3877
- Web of Science ResearcherID: NA
- Scopus Author ID: 57221489619
- Homepage: https://ipb.ac.id

Kurniawan, F., Ph.D., Lecturer, Department of Aquatic Resources Management, Faculty of Fisheries and Marine Sciences, IPB University, Bogor, 16680, West Java, Indonesia.
- Email: *ferykurniawan@apps.ipb.ac.id*
- ORCID: 0000-0003-4342-2169
- Web of Science ResearcherID: NA
- Scopus Author ID: 57188824120
- Homepage: https://ipb.ac.id

Sulistiono, Ph.D., Professor, Department of Aquatic Resources Management, Faculty of Fisheries and Marine Sciences, IPB University, Bogor, 16680, West Java, Indonesia.
- Email: *ecep_s@apps.ipb.ac.id*
- ORCID: 0000-0002-8151-9546
- Web of Science ResearcherID: AAD-4846-2022
- Scopus Author ID: 57360844200
- Homepage: https://ipb.ac.id

HOW TO CITE THIS ARTICLE:
Desrizal; Widigdo, B.; Yulianto, G.; Kurniawan, F.; Sulistiono, (2027). Sustainability assessment for multi-activity coastal areas using an integrated hierarchical decision-making framework. Global J. Environ. Sci. Manage., 13(1): 97-122.

DOI: 10.22034/gjesm.2027.01.05
URL: https://www.gjesm.net/article_735588.html

Global Journal of Environmental Science and Management
(GJESM)

Homepage: https://www.gjesm.net/

Podcasts

ORIGINAL RESEARCH ARTICLE

Satellite-based assessment of high Andean wetlands and carbon sequestration under the influence of climate change

Y. Mamani-Arpasi[1], J.A. Mamani Gomez[2,3], G. Huanca Chambi[1], M. Quispe Tisnado[1], C.E. Yupanqui Bendita[1], E. Calizaya Chura[1], E.G. Moreno Terrazas[4,*]

[1]*Universidad Nacional de Juliaca, San Román, 21101 Perú*

[2]*Institute for Research in Water Science and Technology, National University of Altiplano, Puno, 21001 Perú*

[3]*Faculty of Civil Engineering, Architecture and Urbanism, State University of Campinas, Campinas, 13083-970 Brazil*

[4]*Facultad de Ciencias Biológicas. Universidad Nacional del Altiplano, Puno, 21001 Perú*

ARTICLE INFO

Article History:
Received 12 May 2026
Revised 20 July 2026
Accepted 27 August 2026

Keywords:
Humidity
Rain
Temperature
Watershed
Wind

DOI:10. 22034.gjesm.2027.01.06

ABSTRACT

BACKGROUND AND OBJECTIVES: High-Andean wetlands play an important role in providing ecosystem services, particularly carbon sequestration. Yet, anthropogenic climate change threatens to restrict their spatial footprint and curtail their overall efficacy as atmospheric carbon sinks. Therefore, the study objectives were to estimate carbon uptake in High-Andean wetlands using satellite imagery and to evaluate its relationship with climatic variables in the Huancané Basin, Peru.

METHODS: Google Earth Engine and RStudio integrated development environment (v4.3.1) were used with JavaScript and R programming languages. Wetland extents were delineated across seasonal wet and dry phases via Linear Spectral Unmixing applied to Landsat 5–8 imagery. Subsequent to the conversion of digital numbers to surface reflectance, the wetland index was implemented to estimate carbon uptake using oderate resolution imaging spectroradiometer gross primary productivity and net primary productivity datasets. Climate data were obtained from the National Aeronautics and Space Administration power platform, and the relationships between wetland extent, carbon dioxide sequestration, and climatic variables were analyzed.

FINDINGS: Wetland coverage declined across both seasons over the study duration, experiencing contractions of 109.43 square kilometers during the wet season and 85.60 square kilometers during the dry season between 2010 and 2022. Carbon uptake also showed a decreasing trend during both seasons. Values ranged from 9.985 to 28.234 kilograms of carbon per square meter during the wet season and from 7.091 to 19.103 kilograms of carbon per square meter during the dry season. Significant relationships were found between wetland extent, carbon uptake, and climatic variables ($p<0.05$). Arid climatic trends, characterized by diminished precipitation, elevated temperature ranges, lower relative humidity, and increased wind speeds, corresponded closely with contractions in wetland extent and reduced carbon uptake.

CONCLUSION: The results indicate that recent climatic changes have contributed to the degradation of high-Andean wetlands and to a reduction in their carbon uptake capacity in the Huancané Basin. These results provide vital baselines for tracking wetland trajectories, informing climate change mitigation and conservation frameworks to guide future ecosystem management and sustainable planning in fragile mountain regions worldwide.

This is an open access article under the CC BY license (http://creativecommons.org/licenses/by/4.0/)

NUMBER OF REFERENCES	NUMBER OF FIGURES	NUMBER OF TABLES
46	7	4

*Corresponding Author:
Email: emoreno@unap.edu.pe
Phone: +51 951 677 041
ORCID: 0000-0001-6356-8806

INTRODUCTION

High-Andean wetlands play a key role in the provision of ecosystem services (Huaraca *et al.,* 2025), and are often regarded as oases because they sustain life in these arid environments (de la Fuente *et al.,* 2021). These ecosystems also contribute to the regional carbon balance, mainly through their capacity to accumulate organic matter (Malerba *et al.,* 2023; Ghosh *et al.,* 2025; Zhang *et al.,* 2025a), which is generally associated with plant communities dominated by cushion plants and grasses (Chimner, 2020). Within these systems, water availability and low thermal regimes sustain biological activity and carbon fixation across soils and vegetation, thereby modulating atmospheric carbon dioxide (CO_2) fluxes. (Suárez Duque *et al.,* 2016; Wicaksono *et al.,* 2016). Their functioning is therefore influenced by variations in water availability, temperature, and anthropogenic pressures such as grazing and fire (Garcia and Otto, 2015; Chimner, 2020; Huaraca *et al.,* 2025). Carbon storage and carbon dynamics in wetlands vary according to ecosystem type, vegetation cover and hydrological conditions (Cui *et al.,* 2021; Vorobyev *et al.,* 2024). This coupling has been extensively characterized across forest ecosystems (He *et al.,* 2022) as well as within marine-terrestrial transitional zones, with particular emphasis on blue carbon dynamics in coastal wetlands (Padhy *et al.,* 2020; Hamzeh and Azizi, 2023; Malerba *et al.,* 2023; Antony *et al.,* 2025; Chen *et al.,* 2025). In this context, carbon stock refers to the amount of carbon stored in a defined ecosystem pool, whereas carbon flux describes the transfer of carbon between the ecosystem and the atmosphere over time. Whereas Carbon sequestration denotes the net accumulation of carbon in an ecosystem, productivity signifies the rate of vegetation-mediated carbon; consequently, this study, centers on carbon uptake derived from MODIS productivity metrics, as opposed total ecosystem carbon stocks or net carbon sequestration. In addition, seasonal hydrological cycles influence carbon storage processes (Cui *et al.,* 2021). In floodplain environments, carbon emissions may exceed the amount of carbon stored (Das *et al.,* 2024; Vorobyev *et al.,* 2024), as previously accumulated carbon can be released through degradation processes (Senger *et al.,* 2021). These structural modifications complicate the derivation of reliable estimates regarding actual wetland carbon storage (Ghosh *et al.,* 2025). Therefore, this factor should be considered when assessing carbon storage in these ecosystems. Hitherto, research on carbon storage in High-Andean wetlands has relied primarily on vegetation biomass estimates and radiocarbon dating (Hribljan *et al.,* 2015; Llanos *et al.,* 2026). Although informative, these approaches have limitations, including high costs, restricted temporal coverage and complex procedures for long-term assessments. Consequently, there is a pressing need for accessible methodologies that enable scalable, large-scale monitoring. Remote sensing has become a widely used tool for evaluating changes in wetland extent, surface moisture and vegetation cover through the integration of optical and radar imagery, as well as for monitoring phenological dynamics using Landsat-Sentinel harmonisation and structural analyzes (He *et al.,* 2022; Malerba *et al.,* 2023; Fan *et al.,* 2023; Choi *et al.,* 2024; Ingalls *et al.,* 2024; Antony *et al.,* 2025; Shinkarenko and Bartalev, 2025). In this study, high-Andean wetlands are defined as water-saturated ecosystems characterized by hydrological regimes that drive vegetation dynamics and associated ecological processes. Furthermore, hotspot identification and CO_2 emission assessments have been conducted using UAV sensors, neural networks and spectral indices to estimate aboveground biomass and quantify the contribution of submerged vegetation (Belloli *et al.,* 2022; Liu *et al.,* 2023; Chen *et al.,* 2025; Li *et al.,* 2025;). Land-use change monitoring systems and greenhouse gas emission assessments also support regional inventories and climate targets

(Wannasiri and Chaksan, 2023; Zhang *et al.,* 2025a). Together, these methodologies provide efficient, scalable frameworks for assessing net carbon assimilation and functional dynamics of High-Andean wetlands, overcoming the principal constraints of conventional approaches. In this context, the High-Andean wetlands of the Huancané Basin represent strategic ecosystems because of their carbon storage capacity and marked seasonality. The novelty of this study lies in the integrated assessment of High-Andean wetland extent and carbon uptake across wet and dry seasons using multi-temporal Landsat and MODIS data, together with their associations with climatic variability in the Huancané Basin. This approach provides a basin-scale assessment of temporal variations in wetland extent and carbon uptake within a High-Andean ecosystem where such empirical data remains limited. The primary objectives of this study are to evaluate spatial variations in wetland extent, quantify net carbon assimilation by wetland vegetation, analyze the relationships among wetland coverage, net carbon uptake, climate-induced environmental variables. This study was carried out in the Huancané Basin, Peru, in 2010-2022.

MATERIALS AND METHODS

Study area

The Huancané watershed, located in the Puno Region, Peru, covers an area of 3,633.52 square kilometers (km²) and ranges in elevation from 3,806 meters above sea level (m a.s.l.) to 5,059 m a.s.l., at Surupana Hill. The geology is diverse and includes Cretaceous formations such as Huancané, Chupa, Muni and Moho, as well as the Cotacucho, Muñani and Vilquechico groups. Agricultural land occupies 414.04 km² with 11.40 percent (%) of the watershed in the lower areas and is characterised by low agricultural suitability, although it is used for grazing and permanent crops. The climate is cold and very humid, with annual precipitation ranging from 650 to 700 millimeters (mm) and mean temperatures between 4.5 and 5.2 degrees Celsius (°C). The dominant vegetation comprises High-Andean grasslands, whereas the hyperhumid subtropical subalpine páramo constitutes the primary ecological zone, covering more than half of the watershed. The region shows marked seasonality, with a wet season from November to March and a dry season from April to October (Fig. 1). The distribution of High-Andean wetlands is concentrated primarily within the upper sections of the Huancané Basin, restricted to localities exhibiting supportive hydrological conditions and seasonal water retention. Their spatial distribution is heterogeneous across the basin, reflecting differences in elevation, topography and local hydrological conditions.

Assessment of wetland extent

Wetland extent during the wet and dry seasons (2010–2022) was estimated using Landsat 5 Thematic Mapper (TM) and Landsat 8 Operational Land Imager (OLI) imagery with a spatial resolution of 30 meters (m). Landsat 5 TM and Landsat 8 OLI imagery were obtained from Google Earth Engine and converted from digital numbers to top-of-atmosphere (TOA) reflectance prior to spectral-index calculation. Mosaic and clip workflows were implemented within Google Earth Engine (GEE) to derive composite imagery covering the Huancané Basin. Only images with cloud cover below 10% were used. The corresponding Landsat sensor was used for each year of the study period. The geospatial tools, data sources, and analytical purposes used in the study are summarized in Table 1. Wetland extent was derived from Landsat-based spectral indices, whereas carbon uptake was estimated independently from MODIS productivity products, ensuring that wetland classification and area estimates were not employed as input variables for estimating carbon uptake calculations. The imagery was processed in RStudio integrated development environment (RStudio) using the normalized difference vegetation index (NDVI), normalized difference water index (NDWI) and NDII spectral indices to

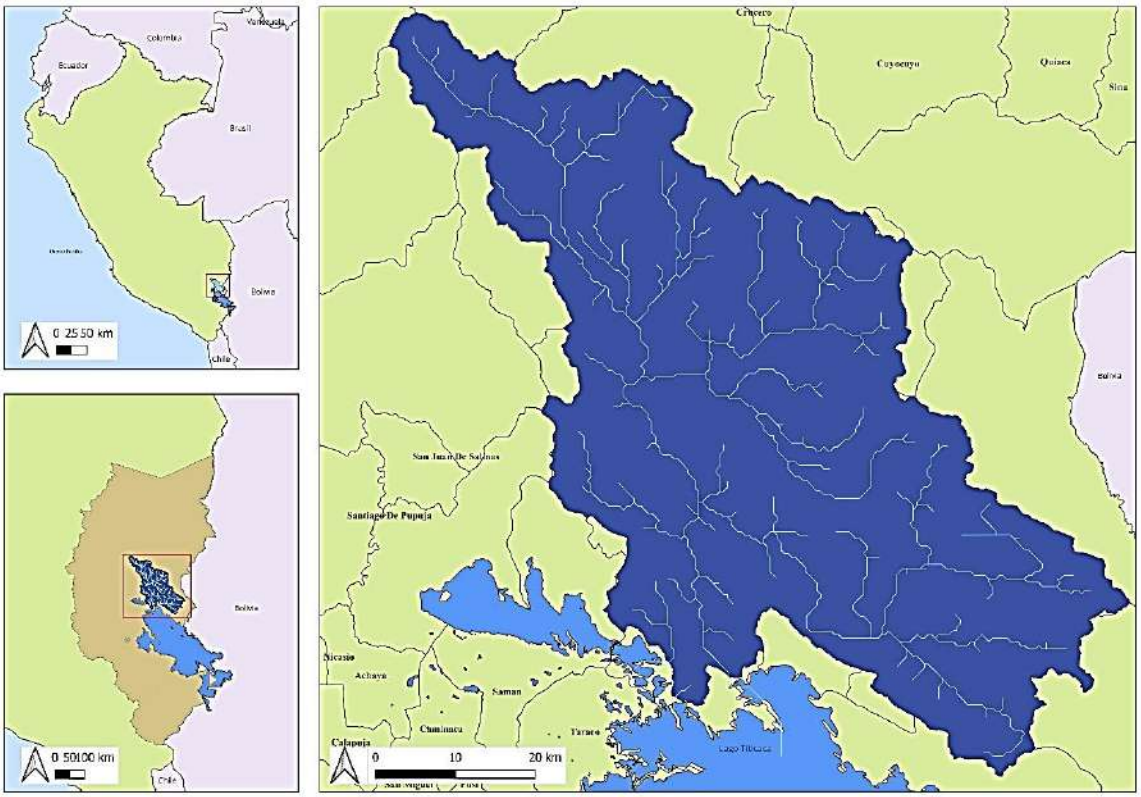

Fig. 1: Geographic location of the study area in the Huancané Basin, Puno Region in Peru

Table 1: Data sources and geospatial tools

Tool	Purpose	Data used
Google Earth Engine (JavaScript)	Satellite image processing, area calculation, GPP/NPP estimation	Landsat 5 and 8, MODIS (GPP, NPP)
RStudio v4.3.1	Spectral index calculation and statistical analysis (NDVI, NDWI, NDII, WI)	Satellite imagery and climatic time series
NASA power	Historical meteorological data	Temperature, precipitation, humidity and wind

characterize vegetation, vegetation water content and soil moisture, respectively (Table 2). The linear spectral unmixing (LSU) method was employed to generate the wetland index (WI) and classify wetland pixels, with the WI computed by integrating spectral data from the NDWI and NDII in accordance with the R-based analytical framework. The resulting WI was used to identify and delineate wetland areas during the wet and dry seasons. The resulting wetland extent was calculated for each year and season from the delineated wetland areas. The absence of independent quantitative accuracy evaluations and reference sample datasets precluded formal validation of the wetland classification across the study period. The uncertainty associated with the remote-sensing estimates was considered in relation to the characteristics of the datasets and processing steps used in the analysis. Potential errors in classifying wetlands could arise due to difficulties in spectrally resolving pixels alongside the spatial complexity found within the 30 m Landsat imagery. For carbon uptake, uncertainty is associated with the spatial and temporal characteristics of the MODIS productivity products and their conversion to carbon units.

Table 2: Spectral indices used for wetland assessment

Index	Application
$\text{NDVI} = \frac{\rho\text{NIR} - \rho\text{RED}}{\rho\text{NIR} + \rho\text{RED}}$	Vegetation
$\text{NDWI} = \frac{\rho\text{GREEN} - \rho\text{NIR}}{\rho\text{GREEN} + \rho\text{NIR}}$	Vegetation water content
$\text{NDII} = \frac{\rho\text{NIR} - \rho\text{SWIR}}{\rho\text{NIR} + \rho\text{SWIR}}$	Soil moisture

Furthermore, disparities in spatial resolution between Landsat and MODIS data may influence the alignment between wetland extent and carbon uptake estimates. These sources of uncertainty were considered when interpreting temporal patterns and relationships between wetland extent, carbon uptake and climatic variables. The wetland classification reflects aggregate spatial coverage and does not differentiate between distinct wetland typologies or internal ecological conditions within the mapped domain.

Estimation of Carbon Uptake

JavaScript was used within the GEE platform to evaluate the net primary productivity (NPP) of wetland vegetation as an indicator of carbon uptake. MODIS products from NASA's Earth Observing System (EOS) were used for this analysis. The MOD17A2HGF 8-Day Global 500 m product, which provides gross primary productivity (GPP), and the MOD17A3HGF Annual Global 500 m product, which provides annual NPP, were used. The Landsat-derived wetland polygons were imported into GEE and used as spatial masks to clip the MODIS productivity layers, restricting the carbon uptake estimates to the mapped wetland areas. Because of the difference in spatial resolution between Landsat (30 m) and MODIS (500 m), MODIS pixels along wetland boundaries may contain mixed land-cover information, which was considered as a methodological limitation. An algorithm workflow was implemented within GEE to approximate NPP at an 8-day temporal resolution by allocating annual NPP proportionally based on the relative contribution of each 8-day interval to total annual GPP using Eq. 1 (Ouattara *et al.*, 2025):

$$NPP_{8d} = \left(\frac{GPP_{8d}}{GPP_{anual}}\right) xNPP_{annual} \quad (1)$$

This technique operated on the assumption that the temporal progression of annual NPP followed the relative share contributed by each 8-day period to annual GPP. The resulting 8-day NPP estimates were then aggregated according to the corresponding wet and dry seasons. The resulting NPP values were quantified in kilograms of carbon per square meter (kg C/m²) and utilized to assess variations in carbon uptake between the wet and dry seasons. The spectral indices were calculated from the Landsat reflectance bands, and the Bofedal Index (BI) was subsequently derived from the combination of NDWI and NDII using the normalized-difference formulation. Specifically, NDWI was calculated from Landsat 5 bands 4 and 2, while NDII was calculated from bands 5 and 4. The derived indices were subsequently integrated to calculate the BI, which served to delineate wetland extents across both the wet and dry seasons. The complete methodological workflow, including Landsat processing, wetland delineation, MODIS productivity estimation, and seasonal carbon-uptake assessment, is presented in Fig. 2.

Analysis of environmental variables and climate change

Meteorological data were obtained from the NASA POWER database for the Huancané Basin. Climate data were extracted for a representative location within the basin (15.0743° S, 69.6493° W; 4,258 m a.s.l.), selected through remote sensing analysis in an open area free from topographic and structural obstructions. Monthly and annual records spanning 2010–2022 were compiled, including accumulated precipitation (mm), maximum and minimum temperature (°C), relative humidity (%), and wind speed (m/s) to assess climatic variability over the study period.

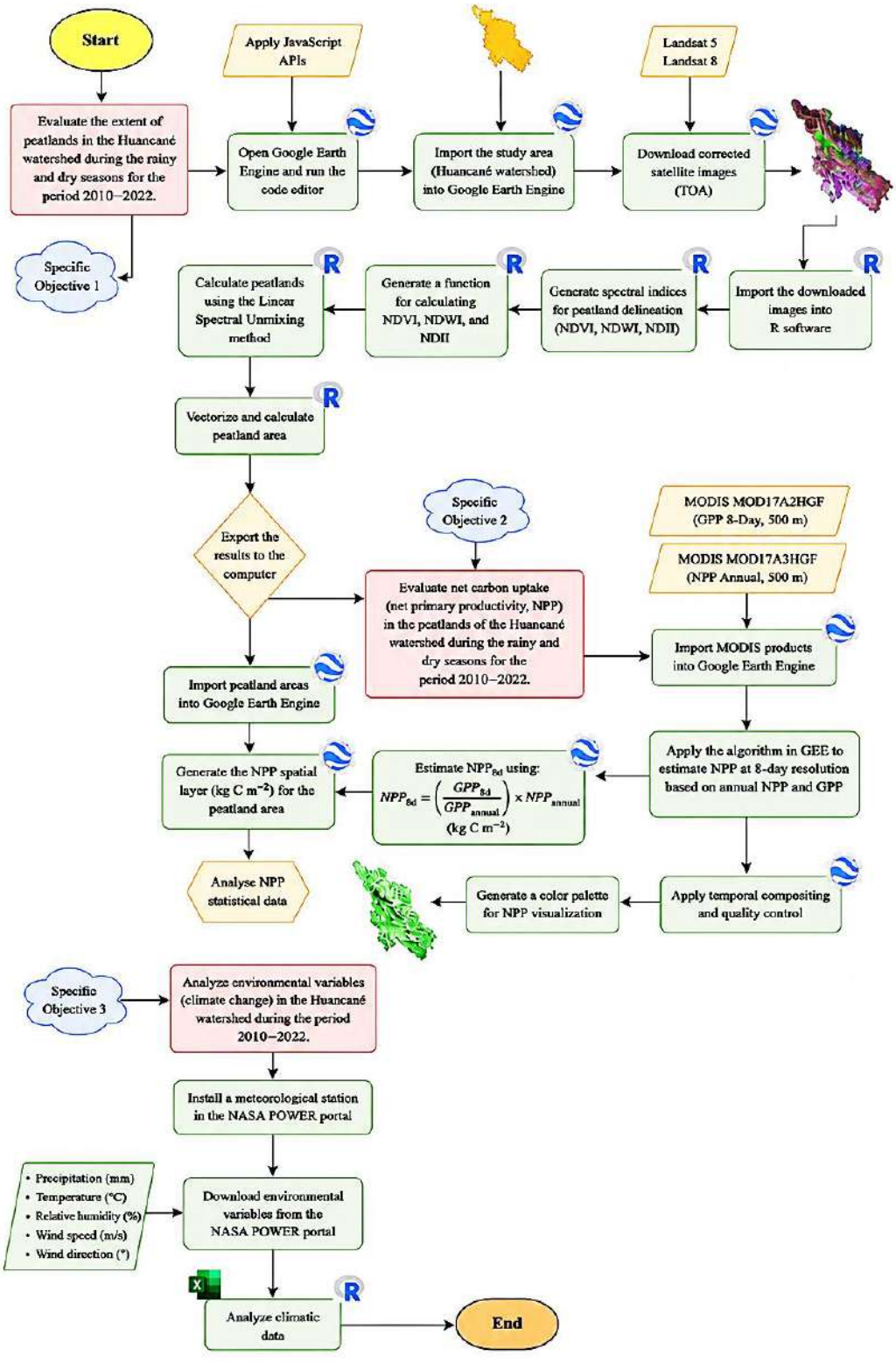

Fig. 2: Methodological workflow

Statistical analysis

Inferential statistics were used to evaluate the associations between Carbon uptake, wetland extent and climatic variables. Data normality was assessed using the Shapiro–Wilk test ($\alpha = 0.05$). Pearson correlation analysis was then applied to evaluate the linear associations between Carbon uptake, wetland extent and climatic variables. Owing to the limited number of temporal observations spanning 2010 to 2022, the magnitude of the correlation coefficients was evaluated with appropriate circumspection.

RESULTS AND DISCUSSION

Assessment of wetland area in the Huancané Basin during the wet and dry seasons

The analysis of wetland area in the Huancané Basin during the wet season between 2010 and 2022 showed a decreasing trend. The maximum wetland extents were documented at the commencement of the study period, whereas the minimum values were registered during the concluding years. Wetland area ranged from 28.63 km² to 181.72 km², with a mean value of 129.42 km², showing a progressive reduction in wetland cover under wet conditions (Fig. 3A). A similar decrease was observed during the dry season, with lower values towards the end of the study period (Fig. 3B). Wetland area ranged from 21.77 km² to 116.26 km², with a mean value of 85.35 km², reflecting a marked contraction under dry conditions. Although a comparable overall trajectory was observed across both seasons (Fig. 3C), the magnitude of the reduction was more pronounced during the wet season. Interannual fluctuations were observed, with increases in 2013, 2017 and 2020, which were subsequently succeeded by a sustained downward trajectory through the final years of the investigation, culminating in minimum values in 2022. The results show a marked decrease in wetland area between 2010 and 2022 during both seasons, with a greater reduction in the most recent years. This contraction aligns with findings from other regions indicating that High-Andean wetlands exhibit pronounced vulnerability to climatic variability and anthropogenic pressures (Fan *et al.,* 2023; Shinkarenko and Bartalev, 2025). The observed decline was associated with changes in precipitation and temperature (Cui *et al.,* 2021; Zhang *et al.*, 2025b). However, anthropogenic factors such as agricultural expansion and grazing may also influence wetland extent, although these factors were not quantitatively assessed in the present study. The evidence suggests that variations in climate across the 2010–2022 study timeframe corresponded with alterations in wetland expanse and carbon uptake dynamics in the Huancané Basin. In recent years, glaciers have decreased and, in some areas of the Peruvian Andes, have disappeared completely (Chimner, 2020). Glacier changes may influence water availability in Andean wetland systems, although their specific contribution to water availability in the Huancané Basin was not quantified in this study (Fan *et al.,* 2023). Climate change also influences precipitation and evaporation (Cui *et al.,* 2021). Because rising temperatures can significantly alter evapotranspiration rates, thermal parameters are routinely integrated into climate-change projections and future environmental scenarios (Cui *et al.,* 2021; Ngoc Tu *et al.,* 2025). The temporal fluctuations observed in 2013, 2017 and 2020 (Fig. 3C) suggest a gradual contraction pattern with periods of temporary stability, which is characteristic of High-Andean wetlands exposed to prolonged water stress (Ngoc Tu *et al.,* 2025). These fluctuations may also be related to glacier recharge and soil infiltration processes, which later supply water to wetlands (Chimner, 2020; Das *et al.,* 2024). As demonstrated by Fan *et al.* (2023) and Shinkarenko and Bartalev (2025), High-Andean wetlands can undergo episodic expansions in spatial extent, whereas persistent constraints on water availability ultimately dictate the overarching contraction trajectory and shape long-term ecosystem carbon dynamics.

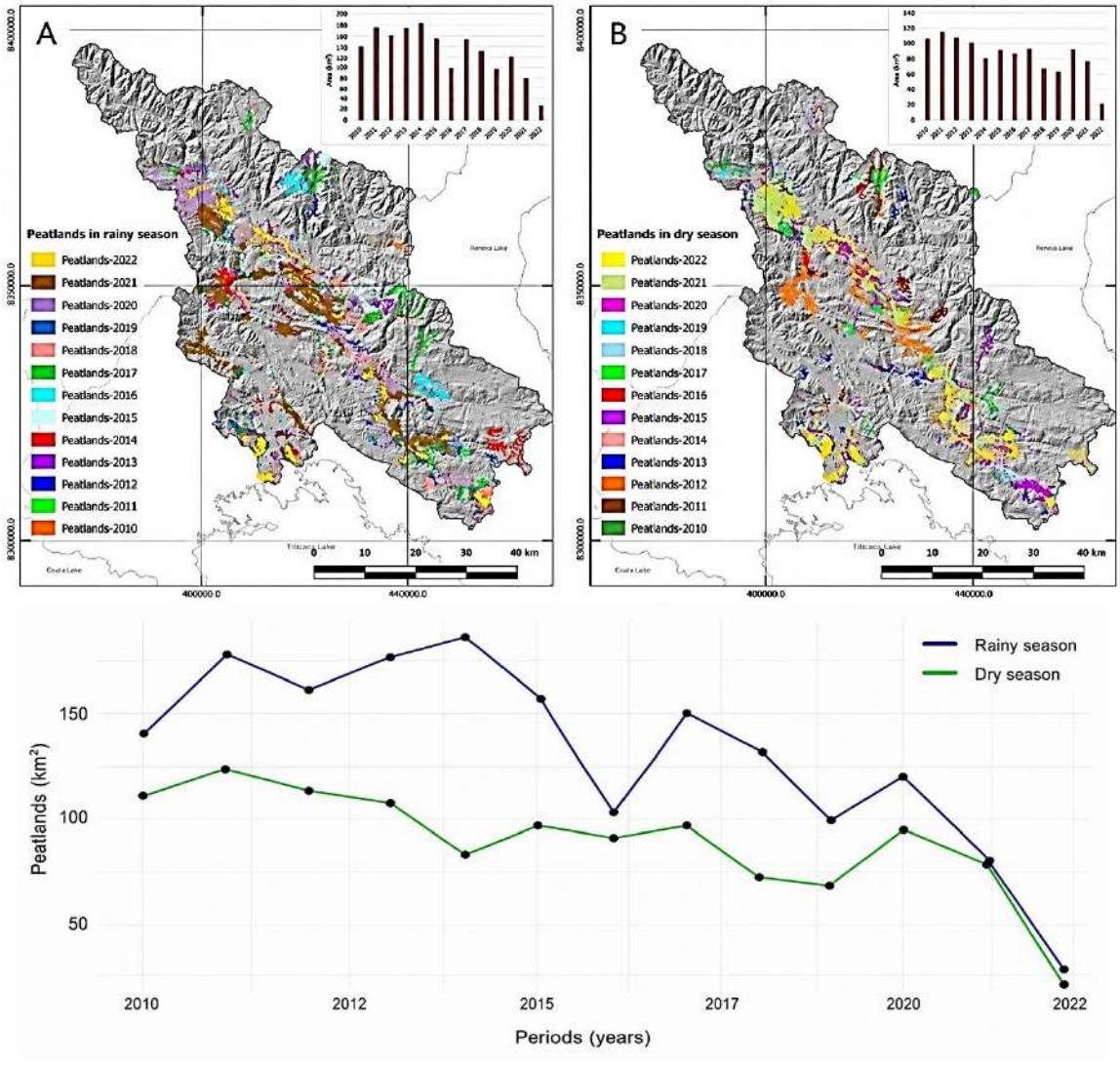

Fig. 3: Wetland area during the wet season (A) and dry season (B). Temporal variation in wetland area during the wet and dry seasons (C)

From an ecological perspective, the continued reduction in wetland area may affect aquatic vegetation, water retention, associated biogeochemical processes and biodiversity (Belloli *et al.,* 2022; Das *et al.,* 2024; Ghosh *et al.,* 2025). Fig. 4A shows the relationship between wetland area during the wet season and time. The linear regression equation shows a negative trend, with a coefficient of determination of R^2 = 0.615, indicating that 61.5% of the variation in wetland area is explained by time (Fig. 4A). Fig. 4B illustrates the relationship between dry-season wetland area and time, with the corresponding regression equation further confirming a negative trajectory. The coefficient of determination (R^2 = 0.624) indicates that 62.4% of the variation in wetland area is explained by time (Fig. 4B). These findings corroborate the aforementioned trends, wherein an inverse association was identified between precipitation and wetland extent. As water availability decreases, associated vegetation is reduced or lost, limiting the capacity of these ecosystems to sequester CO_2 and maintain long-term carbon storage.

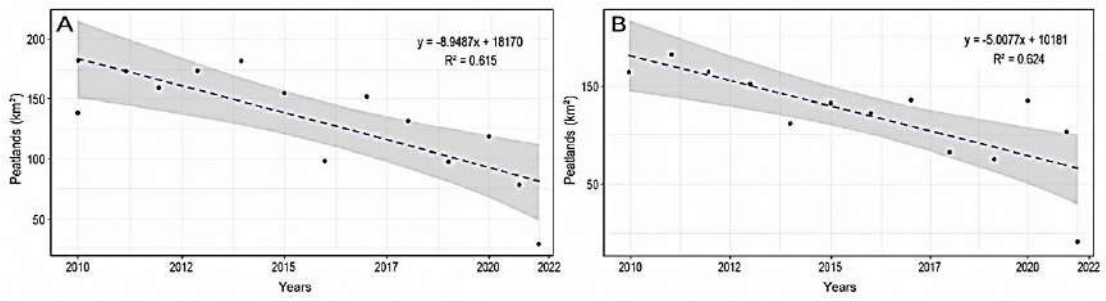

Fig. 4: Linear regression of wetland area during the wet season (A) and dry season (B) over time

Similar patterns have been reported in High-Andean wetlands of Ecuador and Peru, where reductions in water and vegetation cover are considered early indicators of ecosystem degradation (Chimner, 2020; Huaraca *et al.,* 2025). The negative trajectories documented across both seasons signify a broader reduction in wetland extent throughout the study period, notwithstanding interannual variability, with analogous spatial and temporal dynamics documented elsewhere in the Andes. For example, studies in wetlands of northern Chile based on long-term Landsat image series have shown that wetland area fluctuations are strongly influenced by interannual climatic variability associated with events such as the El Niño-Southern Oscillation (ENSO), as well as by the balance between groundwater recharge and potential evaporation. These processes drive decades-long cycles of wetland expansion and contraction over several decades (de la Fuente *et al.,* 2021), implying that the reductions documented in this study align with broader transformation patterns observed in High-Andean wetlands under varying climatic and hydrological conditions (Withaningsih *et al.*, 2026).

Assessment of net carbon uptake in the wetlands of the Huancané Basin

The results show that net carbon uptake fluctuated between 2010 and 2022, with an overall decreasing trend. The highest values were recorded at the beginning of the wet period and the lowest values towards the end of the study period, ranging from 9.985 to 28.234 kg C/m², with a mean value of 20.22 kg C/m², indicating high spatial and temporal variability (Fig. 5A). During the dry season, values ranged from 7.091 to 19.103 kg C/m² (mean = 13.658 kg C/m²; standard deviation = 3.300), showing moderate variability and an approximately normal distribution (Fig. 5B). The reduction in net carbon uptake was evident during both seasons and was more pronounced during the dry season (Fig. 5C). Carbon uptake in wetlands ranged from 7.091 to 28.234 kg C/m², showing high spatial and temporal variability. This heterogeneity reflects the contrasting structure and functioning of mountain wetlands. Previous remote-sensing studies have shown that similar environmental gradients generate distinct spatial patterns of carbon uptake (Junttila *et al.,* 2021; Belloli *et al.,* 2022). The combination of optical and radar sensors reinforces the inference that the detected variability stems from underlying ecological processes rather than methodological artefacts (Fan *et al.,* 2023; Shinkarenko and Bartalev, 2025). During periods of water deficit, photosynthesis capacity becomes constrained as plants close their stomata to minimize transpirational loss. Consequently, carbon assimilation decreases due to diminished photosynthetic rates (Llanos *et al.,* 2026), a pattern that aligns with wetland observations where climatic seasonality dictates interannual fluctuations in net CO_2 fluxes (Wang *et al.,* 2024; Zhang *et al.,* 2025b). Studies covering longer time periods have also reported significant changes in wetland extent, biomass and carbon

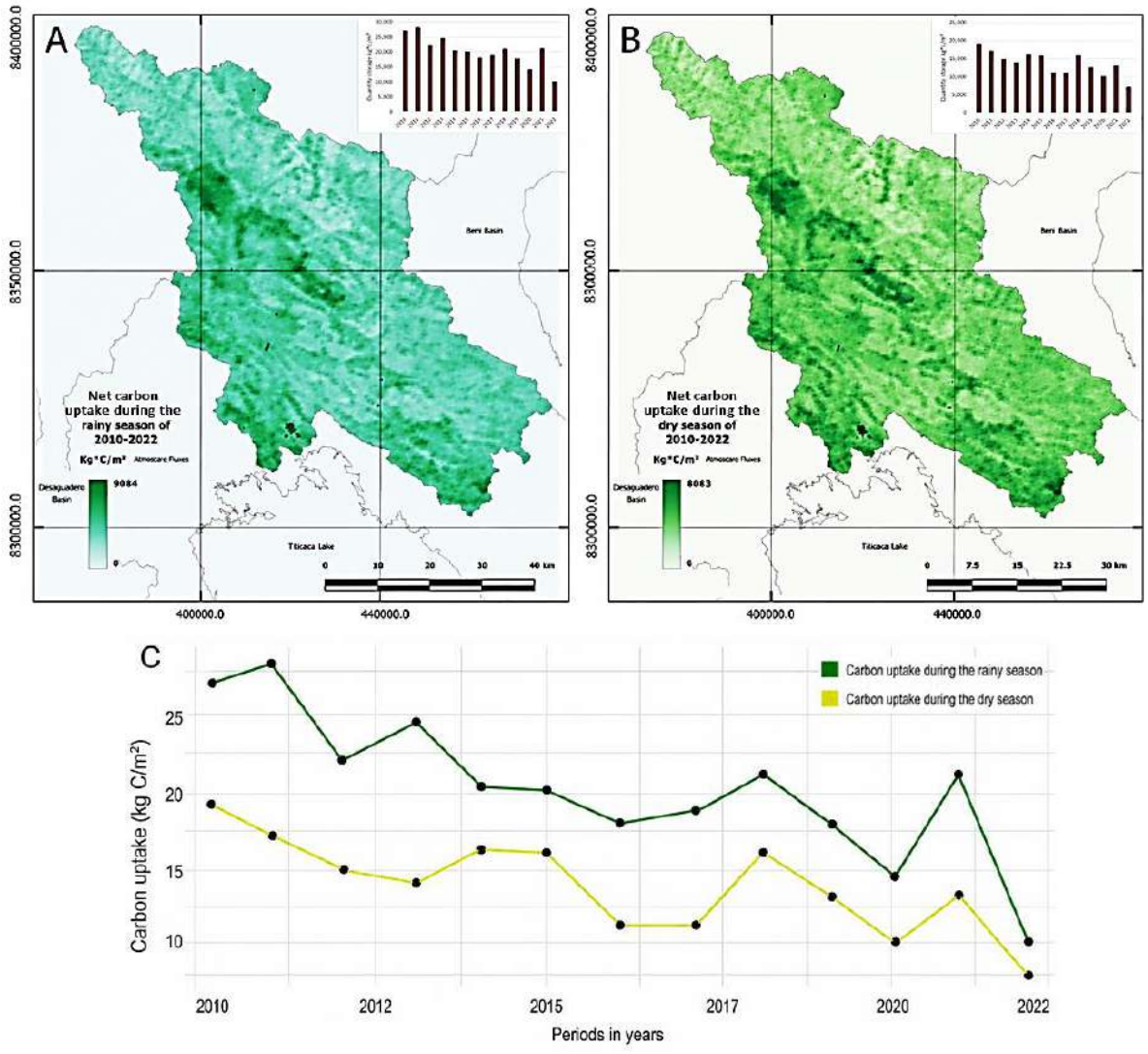

Fig. 5: Carbon uptake in wetlands during the wet season (A) and dry season (B) between 2010 and 2022, Temporal variation in net carbon uptake during the wet and dry seasons (C)

accumulation associated with hydroclimatic variability (de la Fuente *et al.,* 2021). These findings suggest that the decline in Carbon uptake observed in the Huancané Basin is consistent with responses reported for wetlands under changing environmental conditions and that these ecosystems do not respond linearly to changing climatic conditions. Methodologically, remote sensing provides a robust framework for connecting spectral indices and biomass metrics to ecosystem carbon dynamics (Senger *et al.,* 2021; Malerba *et al.,* 2023; Ngoc Tu *et al.,* 2025). This interpretation aligns with prior studies demonstrating that wetlands exhibit extreme vulnerability to hydrological disruptions, wherein minor fluctuations in water availability can induce substantial shifts in carbon storage (Christiani *et al.,* 2024). Studies from other regions have reported carbon values that provide a broader context for the estimates obtained in this study (7.091–28.234 kg C/m²), although differences in ecosystem type and carbon pools should be

considered. In Colombia, values between 0.7 and 1.5 kg C/m² were reported (Peña *et al.,* 2009). In Huascarán National Park, average values of 3 kg C/m² were reported for wet meadows and 109.2 kg C/m² for peatlands (Chimner *et al.,* 2023). In Bolivia, values of 104 kg C/m² in Manasaya and 57.2 kg C/m² in other wetland areas were reported (Hribljan *et al.,* 2015). In Ecuador, values of 136.2 kg C/m² in Antisana and 164.7 kg C/m² in Cajas were reported (Suárez Duque *et al.,* 2016). The discrepancies noted among values reported for the Huascarán, Bolivian, and Ecuadorian peatlands are largely attributable to the accounting of subsurface peat deposits alongside aboveground vegetation. Conversely, studies conducted in Colombia concentrated on biomass and necromass rather than aggregate wetland carbon storage. These comparative insights underscore the critical role of biomass, necromass and peat deposits as primary carbon reservoirs in wetland ecosystems. The regression analysis showed a significant inverse relationship between time and Carbon uptake (kg C/m²). Detailed regression statistics are provided in Table 3. During the wet season, temporal progression accounted for 68.4% of the total variance ($R^2 = 0.684$), denoting a persistent reduction in wetland carbon sequestration efficiency (Fig. 6A). A similar negative trend was observed during the dry season (Fig. 6B), where the model explained 60.3% of the variation in carbon uptake ($R^2 = 0.603$). Additionally, a direct correlation analysis showed a positive association between wetland extent and carbon uptake during both the wet season ($r = 0.699$, $p = 0.0079$) and dry season ($r = 0.621$, $p = 0.0236$ (Table 4). This association indicates that years with greater wetland extent tended to coincide with higher carbon uptake. These correlations, however, do not infer causation, given that carbon uptake can be confounded or mediated by local vegetation attributes, soil properties and hydrological conditions. The negative relationship between time and carbon uptake suggests a progressive decline in the ecological functioning of the wetlands. Constrained water availability can suppress plant productivity and photosynthetic carbon fixation, ultimately reducing carbon sequestration over time. Comparable trends have been documented in High-Andean wetlands, where hydrological shifts govern vegetation cover, biomass accumulation, and overall carbon cycling (Wicaksono *et al.,* 2016; Hoyt *et al.,* 2020; Malerba *et al.,* 2023). The decline observed in the Huancané Basin is therefore likely to be associated with a gradual reduction in water availability, which may be affecting both vegetation productivity and the capacity of wetlands to carbon uptake. Although the regression analysis demonstrates a linear trend, the underlying mechanisms governing carbon uptake are inherently more complex, likely driven by multifaceted interactions among climatic factors, vegetation dynamics, and soil properties (Zhang, *et al.,* 2025b). Given the relatively short time series, linear regression was used to characterise the overall temporal trend rather than imply a strictly linear ecological response. This interpretation is consistent with previous studies showing that wetland responses can vary among periods and locations. For example, a multitemporal study of wetlands in the upper Santa River Basin demonstrated that observed ecological shifts were significantly associated with fluctuations in soil moisture and vegetation cover. Their results showed that wetland responses may differ among periods and sectors, even when the overall trend remains unchanged, reflecting the influence of spatial heterogeneity and temporal environmental variability on wetland ecological dynamics.Similarly, palaeoecological records from Andean peatlands revealed marked changes in carbon accumulation rates during particular decades (Garcia and Otto, 2015) suggesting that these ecosystems do not respond uniformly over time. Consequently, the linear trend observed in this study may represent the general behaviour of the system, while smaller-scale variations remain undetected by the model due to temporal resolution and inherent environmental variability.

Table 3: Temporal linear regression statistics for wetland extent and carbon uptake during 2010–2022

Response variable	Season	n	Slope	SE	95% CI for slope	R^2	p-value
Wetland extent (km²)	Wet	13	−8.949	2.135	−13.647 to −4.251	0.615	0.0015
Wetland extent (km²)	Dry	13	−5.008	1.172	−7.587 to −2.428	0.624	0.0013
Carbon uptake (kg C/m²)	Wet	13	−1.046	0.214	−1.518 to −0.575	0.684	0.0005
Carbon uptake (kg C/m²)	Dry	13	−0.658	0.161	−1.013 to −0.304	0.603	0.0018

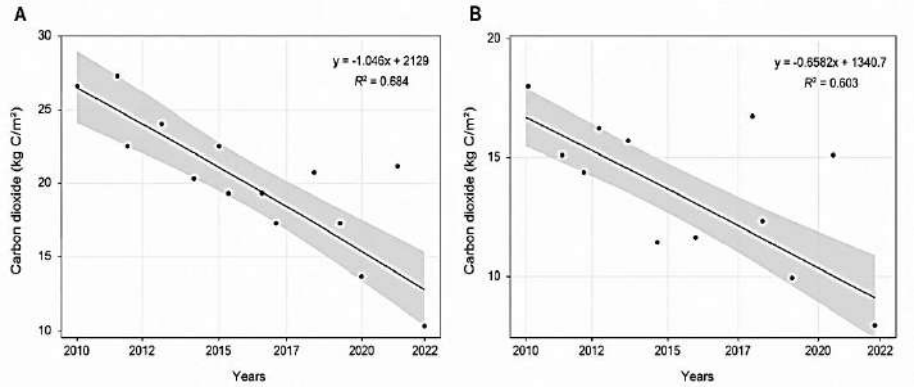

Fig. 6: 1 Linear regression of carbon uptake against time during the wet season (A) and dry season (B)

Table 4: Statistical analyzes of wetland extent, carbon uptake and environmental variables during 2010–2022

Variable / relationship	Season	n	Pearson's *r*	95% CI	p-value
Cumulative precipitation (mm)	Wet	13	0.91	0.72–0.97	2×10^{-5}
Cumulative precipitation (mm)	Dry	13	0.89	0.67–0.97	5.4×10^{-5}
Maximum temperature (°C)	Wet	13	−0.79	−0.93–−0.42	0.0009
Maximum temperature (°C)	Dry	13	−0.78	−0.93–−0.40	0.0016
Relative humidity (%)	Wet	13	0.80	0.45–0.94	0.0011
Relative humidity (%)	Dry	13	0.75	0.34–0.92	0.003
Wind speed (m/s)	Wet	13	−0.78	−0.93–−0.40	0.0015
Wind direction (°)	Dry	13	−0.86	−0.96–−0.59	4×10^{-5}
Wetland extent (km²)	Wet	13	0.699	0.240–0.902	0.0079
Wetland extent (km²)	Dry	13	0.621	0.106–0.873	0.0236

The seasonal analysis suggests that carbon dynamics extend beyond cyclical intra-annual variations to encompass broader interannual trends. Supported by correlation metrics showing positive associations between precipitation and carbon uptake in both wet (r = 0.91) and dry season (r = 0.88) season, these results indicate that increased moisture availability acts as a primary catalyst for elevated carbon sequestration (Figs. 7A and B). This pattern is consistent with observations from mountain wetlands, where the dry season acts as a critical period that amplifies cumulative respiratory losses (de la Fuente *et al.,* 2021). From an ecological perspective, the carbon balance becomes particularly vulnerable during dry conditions. From a methodological perspective, remote-sensing-based regression assumes a stable relationship between spectral response, biomass and carbon storage. Previous studies indicate that this relationship is suitable for detecting interannual trends, although uncertainty remains because of spatial heterogeneity and phenological variability (Shinkarenko and Bartalev, 2025). Therefore, the R^2 values primarily indicate temporal consistency of the observed pattern rather than absolute ecological precision under field conditions, where spatial heterogeneity, measurement uncertainty, and seasonal variability may influence relationships and interpretations.

Environmental variable analysis of climate change in the Huancané Basin

During the study period, annual precipitation decreased from 1289.8 mm in 2012 to 626.5 mm in 2022, with a mean value of 989.31 ± 180.98 mm, indicating a sustained reduction in water inputs and moderate interannual variability. Temperature showed a progressive increase, rising from 7.89 °C in 2011 to 14.89 °C in 2022. Mean maximum temperature was 11.42 ± 2.03 °C, whereas mean minimum temperature was −0.01 ± 0.57 °C. Relative humidity decreased from 83.98% in 2011 to 72.78% in 2022, with a mean value of 78.63 ± 3.24%, reflecting a shift towards drier conditions. Wind speed remained relatively stable (2.07 ± 0.05 m/s) (Fig. 7). Correlation analysis revealed robust positive associations between carbon uptake and annual precipitation during both the wet (r = 0.91) and dry (r = 0.89) seasons. Similarly, relative humidity exhibited positive correlations with carbon uptake during the wet (r = 0.80) and dry (r = 0.75) season. Conversely, temperature demonstrated a strong negative correlation with carbon uptake during in both seasons (r = −0.83), indicating that elevated temperatures constrain carbon assimilation (Table 4). Relative humidity and precipitation emerge as critical environmental determinants controlling vegetation development and, consequently, carbon fixation pathways. Studies in wetlands of northern Chile have shown that prolonged dry periods are associated with higher carbon losses, suggesting that reduced precipitation may increase CO_2 release through respiration and organic matter decomposition under less anoxic conditions (de la Fuente *et al.,* 2021; Syamdidi *et al.,* 2026). Alterations in precipitation regimes can additionally modulate the decomposition rates (Llanos *et al.,* 2026). In Huascarán National Park, wetland types with greater water saturation, such as peatlands, were found to store substantially larger amounts of carbon than less saturated wet meadows (Chimner *et al.,* 2023). Similarly, studies of Andean peatlands have shown that deep carbon deposits develop under long-term saturated conditions (Hribljan *et al.,* 2015; Benavides *et al.,* 2023). Together, these findings highlight the importance of hydrological regimes in modulating carbon storage dynamics across High-Andean wetlands. Temperature and wind speed showed negative associations with carbon uptake during the study period. For instance, a prior study reported a decline in carbon accumulation over a 65-year period preceding 1980, driven by regional warming that accelerated organic matter degradation in response to broader climatic shifts and glacier retreat. These processes altered the hydrological flows required for wetlands to maintain their function as carbon sinks (Llanos *et al.,* 2026). Elevated temperatures can accelerate organic matter decomposition rates and ecosystem respiration, thereby enhancing carbon release to the atmosphere (Junttila *et al.,* 2021; Masocha and Mhangara, 2025). These results support the importance of temperature and precipitation as key variables in studies of carbon storage and carbon uptake in wetland ecosystems (Chen *et al.,* 2025; Ngoc Tu *et al.,* 2025), consistent with evidence that land-use changes can alter ecosystem carbon stocks (Ketaren *et al.,* 2026).

Hydrological trends and implications

From a climatic perspective, regional evidence supports the pattern identified in this study. Studies of hydroclimatic fluctuations within the tropical Andes indicate a projected rise in both the occurrence and magnitude of droughts in southern Peru (Vuille *et al.,* 2018; IPCC, 2021). At a global scale, Johnson *et al.* (1999) reported that wetlands associated with the Herbert River in Australia declined by 70% between 1943 and 1996. Additionally, assessments by the IPCC underscore the pronounced susceptibility of diverse wetland ecosystems to climate change driven by their strict dependence on sustained water availability and hydrological equilibrium (Garcia and Otto, 2015). Reduced water availability restricts vegetation productivity and limits carbon assimilation, while structural

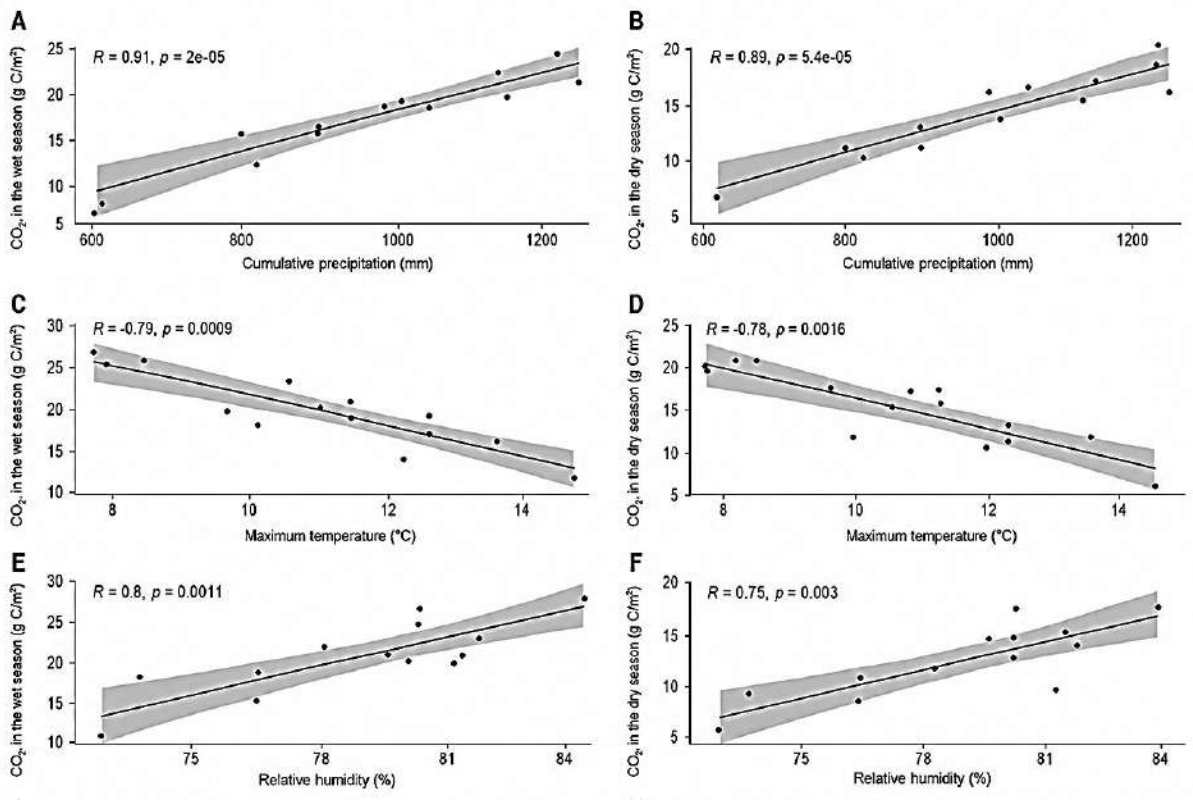

Fig. 7: Correlation between carbon uptake and environmental variables during the wet season (left column) and dry season (right column). Precipitation (A, B), temperature (C, D), relative humidity (E, F)

changes in plant communities further modify ecosystem carbon storage. Such trends align with impairment stimulates the oxidation of organic matter, driving the release of CO_2 and auxiliary greenhouse gases (Hribljan *et al.,* 2015). When wetlands experience prolonged loss of saturation, their capacity to function as carbon sinks may decline, increasing net carbon emissions. These changes have important implications for climate-change mitigation. Overall, scientific evidence indicates that wetlands are highly vulnerable to climate change because of their dependence on hydrological balance and sensitivity to drought and warming (López-Moreno *et al.,* 2017).

CONCLUSION

Wetland extent decreased in the Huancané Basin between 2010 and 2022 in both seasons. The decrease was 109.43 km² in the wet season and 85.60 km² in the dry season. Carbon uptake also showed a decreasing trend during this period. Values ranged from 9.985 to 28.234 kg C/m² in the wet season and from 7.091 to 19.103 kg C/m² in the dry season. The temporal regression modeling demonstrated that variations in time explained 68.4% of carbon uptake dynamics within the wet season and 60.3% during the dry season. Accordingly, parallel reductions in wetland extent and carbon uptake were recorded throughout the study duration. The substantial decrease in wetland extent during the wet season demonstrates that hydrological contractions were not confined to the dry period, manifesting instead across the full seasonal cycle. Wetland extent was positively correlated with carbon uptake in both seasons. The correlation was r = 0.699 in the wet season and r = 0.621 in the dry season. Interannual comparisons indicate that years featuring more extensive wetland coverage generally demonstrated enhanced carbon

sequestration capacity. However, this relationship does not indicate that reduced wetland area directly caused decreased carbon uptake. Carbon uptake is also influenced by vegetation characteristics, soil properties, and hydrological conditions; therefore, changes in wetland extent should be evaluated alongside these factors. During the study period, precipitation and relative humidity decreased, while temperature increased. Carbon uptake was positively correlated with precipitation and relative humidity and negatively correlated with temperature in both seasons, indicating that water availability and temperature were associated with temporal variation in carbon uptake in these High-Andean wetlands. The persistence of these inter-seasonal relationships suggests a consistent climatic influence on carbon assimilation across the annual cycle. However, as the study relied on observational satellite and climatic data, these relationships should be interpreted as associations rather than causal effects. The relative contributions of climate variability, natural variability, and anthropogenic pressures cannot be separated under the current study design. The use of Landsat imagery, MODIS productivity products, Google Earth Engine and NASA POWER data allowed changes in wetland extent and carbon uptake to be evaluated over the 2010–2022 period. The combination of these datasets was useful for examining wetland dynamics together with climatic conditions across the Huancané Basin. Landsat provided the spatial information required to evaluate changes in wetland extent, while MODIS productivity products allowed carbon uptake to be examined over the same period. However, the difference in spatial resolution between Landsat and MODIS and the lack of independent field validation should be considered when interpreting the estimates. Such constraints assume particular relevance when correlating wetland extent with carbon uptake, given that the respective datasets resolve the ecosystem across differing spatial scales. The decrease in wetland extent and carbon uptake observed in the Huancané Basin shows the need to keep monitoring these ecosystems. In particular, changes in precipitation, temperature and water availability should be followed over time. Furthermore, ground-truth data on vegetation biomass, soil moisture, and edaphic carbon stocks would strengthen cross-validation of satellite estimates and improve understanding of ecosystem carbon uptake. Additional information on elevation, land use, and human activities could further explain basin-scale differences. Extending the time series would help determine whether the observed 2010–2022 decline is continuing. Future monitoring combining ground-based observations with satellite telemetry could provide higher-resolution assessments of wetland dynamics and carbon sequestration and clarify whether the Huancané Basin trends reflect ongoing change or longer-term variability in High-Andean wetland ecosystems.

AUTHOR CONTRIBUTIONS

Y.M. Mamani-Arpasi conceived the study, developed the methodology, conducted the investigation, curated the data, performed the formal analysis, prepared the visualizations, and prepared the original manuscript draft and revised the manuscript. J.A. Mamani Gomez contributed to the methodology, performed validation, and reviewed and edited the manuscript. G. Huanca Chambi performed validation, provided resources, and reviewed and edited the manuscript. M. Quispe Tisnado curated the data, performed validation, and reviewed and edited the manuscript. C.E. Yupanqui Bendita provided resources, performed validation, and reviewed and edited the manuscript. E. Calizaya Chura performed validation and reviewed and edited the manuscript. E.G. Moreno Terrazas supervised the study, contributed to the methodology, performed validation, administered the project, and reviewed and edited the manuscript.

ACKNOWLEDGEMENT

Authors would like to thank the Universidad Nacional de Juliaca, San Román as well as Institute for Research in Water Science and Technology,

National University of Altiplano, Perú. This study received no external funding.

CONFLICT OF INTEREST

The authors declare that there is no conflict of interest regarding the publication of this manuscript. In addition, ethical issues, including plagiarism, informed consent, misconduct, data fabrication and/or falsification, double publication and/or submission, and redundancy, were observed by the authors.

OPEN ACCESS

©2027 The author(s). This article is licensed under a Creative Commons Attribution 4.0 International License, which permits use, sharing, adaptation, distribution and reproduction in any medium or format, as long as you give appropriate credit to the original author(s) and the source, provide a link to the Creative Commons license, and indicate if changes were made. The images or other third-party material in this article are included in the article's Creative Commons license, unless indicated otherwise in a credit line to the material. If material is not included in the article's Creative Commons license and your intended use is not permitted by statutory regulation or exceeds the permitted use, you will need to obtain permission directly from the copyright holder. To view a copy of this license, visit: http://creativecommons.org/licenses/by/4.0/

PUBLISHER'S NOTE

GJESM Publisher remains neutral with regard to jurisdictional claims in published maps and institutional affiliations.

NEGATIVE AI STATEMENT

The authors declared that no AI tools or services were used or not highly applied during the preparation of this work.

ABBREVIATIONS

%	Percent
°C	Degrees Celsius
CO_2	Carbon dioxide
ENSO	El Niño–Southern Oscillation
EOS	Earth observing system
GEE	Google Earth Engine
GPP	Gross primary productivity
IPCC	Intergovernmental Panel on Climate Change
kg	Kilogram
kg C/m²	Kilograms of carbon per square meter
km	Kilometer
km²	Square kilometer
LSU	Linear spectral unmixing
m	Meter
m a. s. l.	Meter above sea level
M/s	Meters per second
mm	Millimeter
MODIS	Moderate resolution imaging spectroradiometer
NASA	National Aeronautics and Space Administration
NDII	Normalized difference infrared index
NDVI	Normalized difference vegetation index
NDWI	Normalized difference water index
NPP	Net primary productivity
OLI	Operational land imager
POWER	Prediction of Worldwide Energy Resources
R^2	Coefficient of determination
RStudio	RStudio integrated development environment
%	Percent
TM	Thematic mapper
TOA	Top of atmosphere
WI	Wetland index

REFERENCES

Antony, S.; Perumal, K.; Devi, S.S.; Shajahan, S.; Kumar, A.B., (2025). Exploring blue carbon research in India: current landscape and future avenues. Mar. Pollut. Bull., 219: 118269 **(18 pages).**

Belloli, T.F.; Guasselli, L.A.; Kuplich, T.M.; Ruiz, L.F.C.; Arruda, D.C.; Etchelar, C.B.; Simioni, J.D., (2022). Estimation of aboveground biomass and carbon in palustrine wetland using bands and multispectral indices derived from optical satellite imageries PlanetScope and Sentinel-2A. J. Appl. Remote Sens., 16(3): 034516 **(21 pages).**

Benavides, J.C.; Vitt, D.H.; Cooper, D.J., (2023). The High-Elevation Peatlands of the Northern Andes, Colombia. Plants. 12(4): 955 **(17 pages).**

Chen, J.; Lu, Y.; Liu, F.; Gao, G.; Xie, M., (2025). Remote sensing evidence of blue carbon stock increase and attribution of its drivers in coastal China. Remote Sens., 17(15): 2559 **(22 pages).**

Chimner, R., (2020). Andes, bofedales, and the communities of Huascarán National Park, Peru. Wetl. Sci. Pract., 37(4): 246-254 **(9 pages).**

Chimner, R.A.; Resh, S.C.; Hribljan, J.A.; Battaglia, M.; Bourgeau-Chavez, L.; Bowser, G.; Lilleskov, E.A., (2023). Mountain wetland soil carbon stocks of Huascarán National Park, Peru. Front. Plant Sci., 14: 1-8 **(8 pages).**

Choi, I.H.; Lee, E.R.; Jung, H.S., (2024). Performance comparison of water body detection from Sentinel-1 SAR and Sentinel-2 optical imagery using Attention U-Net model. Korean J. Remote Sens., 40(5): 507-523 **(17 pages)**.

Christiani, P.; Rana, P.; Räsänen, A.; Pitkänen, T.P.; Tolvanen, A., (2024). Detecting spatial patterns of peatland greenhouse gas sinks and sources with geospatial environmental and remote sensing data. Environ. Manage., 74(3): 461-478 **(18 pages)**.

Cui, Q.; Ammar, M.E.; Iravani, M.; Kariyeva, J.; Faramarzi, M., (2021). Regional wetland water storage changes: The influence of future climate on geographically isolated wetlands. Ecol. Indic., 120: 106941 **(17 pages)**.

Das, T.; Pal, S.; Debanshi, S., (2024). Effect of water presence consistency on balance between CH4 emission and CO2 sequestration in floodplain wetland. Acta Geophys., 73(2): 1847-1864 **(18 pages)**.

de la Fuente, A.; Meruane, C.; Suárez, F., (2021). Long-term spatiotemporal variability in high Andean wetlands in northern Chile. Sci. Total Environ. 756, 143830 **(13 pages)**.

Fan, C.; Yang, J.; Zhao, G.; Dai, J.; Zhu, M.; Dong, J.; Liu, R.; Zhang, G., (2023). Mapping phenology of complicated wetland landscapes through harmonizing Landsat and Sentinel-2 imagery. Remote Sens., 15(9): 2413 **(19 pages)**.

Garcia, E.; Otto, M., (2015). Ecohydrological characterization of High-Andean wetlands based on multi-temporal remote sensing images in the case of Upper Santa River, Ancash, Peru. Ecol. Apl., 14(1-2): 115 **(11 pages).**

Ghosh, R.; Haldar, M.; Debanshi, S.; Pal, S., (2025). Role of ox-bow lakes towards carbon sink and resilience of warming effect. Spat. Inf. Res., 33(4): 6369-6392 **(13 pages).**

Hamzeh, M.A.; Azizi, N., (2023). Estimating blue carbon storage in the mangrove forest of Gaz-Harra wetland, Strait of Hormoz. Reg. Stud. Mar. Sci., 66: 103142 **(09 pages).**

He, L.; Byrne, B.; Yin, Y.; Liu, J.; Frankenberg, C., (2022). Remote-sensing derived trends in gross primary production explain increases in the CO2 seasonal cycle amplitude. Glob. Biogeochem. Cycles, 36(9) **(16 pages).**

Hoyt, A.M.; Chaussard, E.; Seppalainen, S.S.; Harvey, C.F., (2020). Widespread subsidence and carbon emissions across Southeast Asian peatlands. Nat. Geosci., 13(6): 435-440 **(06 pages).**

Hribljan, J.A.; Cooper, D.J.; Sueltenfuss, J.; Wolf, E.C.; Heckman, K.A.; Lilleskov, E.A.; Chimner, R.A., (2015). Carbon storage and long-term rate of accumulation in high-altitude Andean peatlands of Bolivia. Mires Peat, 15: 1-14 **(14 pages).**

Huaraca, L.; Bourrel, L.; Zapata-Ríos, X.; Páez-Bimos, S.; Lahuatte, B.; Galeas, R.; Fuentes, P.; Frappart, F., (2025). Multitemporal monitoring of Ecuadorian Andean high wetlands using radar and multispectral remote sensing. Water, 17(11): 1637 **(30 pages).**

Ingalls, T.C.; Li, J.; Sawall, Y.; Martin, R.E.; Thompson, D.R.; Asner, G.P., (2024). Imaging spectroscopy investigations in wet carbon ecosystems: A review of the literature from 1995 to 2022 and future directions. Remote Sens. Environ., 305: 114051 **(23 pages).**

IPCC, (2021). Ecosystems and conservation: Wetlands. Intergovernmental Panel on Climate Change.

Johnson, A.K.L.; Ebert, S.P.; Murray, A.E., (1999). Distribution of coastal freshwater wetlands and riparian forests in the Herbert River catchment and implications for management of catchments adjacent the Great Barrier Reef Marine Park. Environ. Conserv., 26(3): 229-235 **(07 pages).**

Junttila, S.; Kelly, J.; Kljun, N.; Aurela, M.; Klemedtsson, L.; Lohila, A.; Nilsson, M.B.; Rinne, J.; Tuittila, E.S.; Vestin, P.; Weslien, P.; Eklundh, L., (2021). Upscaling northern peatland CO2 fluxes using satellite remote sensing data. Remote Sens., 13(4): 1-23 **(23 pages).**

Ketaren, D.G.K.; Radjawane, I.M.; Latief, H.; Sidik, F.; Trenggono, S.W.; Diantara, S.D.; Setyawidati, N.A.R.; Akbar, M.I.; Raja, J.A.L.; Farkhan, M.A.; Kasim, K.; Maharani, S. (2026). Impacts of mangrove land-use change on carbon stocks in coastal ecosystems. Global J. Environ. Sci. Manage., 12(3): 1041-1060 **(20 pages).**

Li, Y.; Henrion, M.; Moore, A.; Lambot, S.; Opfergelt, S.; Vanacker, V.; Jonard, F.; Van Oost, K., (2025). Hot spots, hot moments, and spatiotemporal drivers of soil CO2 flux in temperate peatlands using UAV remote sensing. Biogeosciences, 22(21): 6369-6392 **(24 pages).**

Liu, B.; Sevick, T.; Jung, H.; Kiskaddon, E.; Carruthers, T., (2023). Quantifying the potential contribution of submerged aquatic vegetation to coastal carbon capture in a delta system from field and Landsat 8/9 Operational Land Imager (OLI) data with deep convolutional neural network. Remote Sens., 15(15): 3765 **(24 pages).**

Llanos, R.; Moreira-Turcq, P.; Turcq, B.; Cordeiro, R.; Espinoza-Villar, R.; Huaman-Navarro, Y.; Condom, T.; Willems, B., (2026). Drastic change in Andean peatland carbon accumulation in the 1980s. Glob. Earth Surf. Process. Change, 5: 100014 **(11 pages).**

López-Moreno, J.I.; Valero-Garcés, B.; Mark, B.; Condom, T.; Revuelto, J.; Azorín-Molina, C.; Bazo, J.; Frugone, M.; Vicente-Serrano, S.M.; Alejo-Cochachin, J., (2017). Hydrological and depositional processes associated with recent glacier recession in Yanamarey catchment, Cordillera Blanca (Peru). Sci. Total Environ., 579: 272-282 **(12 pages).**

Malerba, M.E.; Duarte de Paula Costa, M.; Friess, D.A.; Schuster, L.; Young, M.A.; Lagomasino, D.; Serrano, O.; Hickey, S.M.; York, P.H.; Rasheed, M.; Lefcheck, J.S.; Radford, B.; Atwood, T.B.; Ierodiaconou, D.; Macreadie, P., (2023). Remote sensing for cost-effective blue carbon accounting. Earth-Sci. Rev., 238: 104337 **(16 pages).**

Masocha, B.L.; Mhangara, P., (2025). Satellite-driven assessment of methane trends, seasonal variability, and emission hotspots in Botswana's Central and Ngamiland Regions. Environ. Monit. Assess., 197(10): 1-18 **(18 pages).**

Ngoc Tu, N.; Lü, H.; He, W.; Xu, P.; Zhao, M.; Liu, S.; Zhu, Y.; Lei, X., (2025). Automated machine learning integrating multi-source satellite observations to predict gross and net CO2 fluxes of coastal wetlands in China. Environ. Res. Lett., 20: 084011 **(17 pages).**

Ouattara, B., Thiel, M., Forkuor, G., Mouillot, F., Laris, P., Tondoh, E. J., & Sponholz, B. (2025). Fire Impacts, vegetation Recovery, and environmental drivers in West African savannas (2014–2023): A High-Resolution remote sensing assessment. International Journal of Applied Earth Observation and Geoinformation, 143, 1–22 **(22 pages)**.

Padhy, S.R., Bhattacharyya, P., Dash, P.K., Reddy, C.S., Chakraborty, A. and Pathak, H., (2020), Seasonal fluctuation in three mode of greenhouse gases emission in relation to soil labile carbon pools in degraded mangrove, Sundarban, India. Sci. Total Environ., 705:135909 **(12 pages)**.

Peña, E.J.; Sandoval, H.; Zuñiga, O.; Torres, M., (2009). Estimates of carbon reservoirs in high-altitude wetlands in the Colombian Andes. J. Agric. Rural Dev. Trop. Subtrop., 110(2): 115-126 **(12 pages)**.

Senger, D.F.; Saavedra Hortua, D.A.; Engel, S.; Schnurawa, M.; Moosdorf, N.; Gillis, L.G., (2021). Impacts of wetland dieback on carbon dynamics: A comparison between intact and degraded mangroves. Sci. Total Environ., 753: 141817 **(13 pages)**.

Shinkarenko, S.S.; Bartalev, S.A., (2025). Application of remote sensing data in large-scale monitoring of wetlands. Cosmic Res., 62(1): S100-S114 **(15 pages)**.

Suárez Duque, D.; Acurio, C.; Chimbolema, S.; Aguirre, X., (2016). Análisis del carbono secuestrado en humedales altoandinos de dos áreas protegidas del Ecuador. Ecol. Apl., 15(2): 171-177 **(07 pages)**.

Syamdidi; Putri, M.R.; Bernawis, L.I; Wahyudin, R.A.; Trenggono, S.W.; Diantara, S.D.; Yuwono, T.; Sakti, W.I.; Arthatiani, F.Y.; Simamora, D.C.; Sabina, A.; Wahid, L.O.M.A.; Radiarta, I.N., Kasim, K., (2026). Temporal and seasonal influences concerning the carbon footprint of pelagic fisheries. Global J. Environ. Sci. Manage., 12(3): 1169-1190 **(22 pages).**

Vorobyev, S.N.; Kolesnichenko, L.G.; Kolesnichenko, Y.; Prokushkin, A.S.; Lugovaya-Dolmatova, A.V.; Karlsson, J.; Pokrovsky, O.S., (2024). Floodplain carbon dioxide emissions strongly exceed those of the main river stem: A case study of the Ob River, western Siberia. J. Hydrol., 638: 131468 **(12 pages)**.

Vuille, M.; Carey, M.; Huggel, C.; Buytaert, W.; Rabatel, A.; Jacobsen, D.; Soruco, A.; et Villacis, M.; Yarleque, C.; Elison Timm, O.; Condom, T.; Salzmann, N.; Sicart, J.E., (2018). Rapid decline of snow and ice in the tropical Andes: Impacts, uncertainties and challenges ahead. Earth-Sci. Rev., 176: 195-213 **(19 pages)**.

Wang, J.; Yu, G.; Han, L.; Yao, Y.; Sun, M.; Yan, Z., (2024). Ecosystem carbon exchange across China's coastal wetlands: Spatial patterns, mechanisms, and magnitudes. Agric. For. Meteorol., 345: 109859 **(11 pages)**.

Wannasiri, W.; Chaksan, A., (2023). Land use change monitoring systems for spatial GHG emissions and removals assessment in Chiang-Mai, Thailand. Chem. Eng. Trans., 106: 655-660. **(06 pages)**.

Wicaksono, P.; Danoedoro, P.; Hartono; Nehren, U., (2016). Mangrove biomass carbon stock mapping of the Karimunjawa Islands using multispectral remote sensing. Int. J. Remote Sens., 37(1): 26-52 **(27 pages)**.

Withaningsih, S.; Nurmilah, S.; Utama, G.L., (2026). The role of carbon sequestration and biodiversity in agroforestry for climate change mitigation. Global J. Environ. Sci. Manage., 12(1): 431-452 **(22 pages).**

Zhang, Q.; Wei, S.; Chu, X.; Zhang, X.; Gong, Z.; Wang, X.; Song, W.; Xie, B.; Han, G., (2025a). Climate and vegetation jointly determine the interannual variation of net ecosystem CO2 fluxes over 12 years in a restored coastal wetland. Agric. For. Meteorol., 373: 110760 **(10 pages)**.

Zhang, Y.; Lin, W.; Ye, Y.; Li, Y., (2025b). Accounting for land use carbon emissions considering differences in wetland types to support the achievement of SDG 13.2.2. Land Degrad. Dev., 36(4): 1106-1120 **(15 pages)**.

AUTHOR (S) BIOSKETCHES

Mamani-Arpasi, Y., M.Sc., Researcher, Universidad Nacional de Juliaca, San Román 21101, Peru.
- Email: *ymmamania.doc@unaj.edu.pe*
- ORCID: 0000-0002-5643-4516
- Web of Science ResearcherID: QUU-4958-2026
- Scopus Author ID: NA
- Homepage: https://dina.concytec.gob.pe/appDirectorioCTI/VerDatosInvestigador.do?id_investigador=67262

Mamani Gomez, J.A., Ph.D., Professor, Institute for Research in Water Science and Technology, National University of the Altiplano, Puno 21001, Peru; Faculty of Civil Engineering, Architecture and Urbanism, State University of Campinas, Campinas 13083-970, Brazil.
- Email: *jmamani@unap.edu.pe*
- ORCID: 0000-0001-7694-7549
- Web of Science ResearcherID: HSD-9922-2023
- Scopus Author ID: 57193374056
- Homepage: https://ctivitae.concytec.gob.pe/appDirectorioCTI/VerDatosInvestigador.do?id_investigador=0034104

Huanca Chambi, G., M.Sc., Researcher, Universidad Nacional de Juliaca, San Román 21101, Peru.
- Email: *g.huancac@unaj.edu.pe*
- ORCID: 0000-0003-0107-8056
- Web of Science ResearcherID: NA
- Scopus Author ID: NA
- Homepage:https://ctivitae.concytec.gob.pe/appDirectorioCTI/VerDatosInvestigador.do?id_investigador=174664

Quispe Tisnado, M., M.Sc., Researcher, Universidad Nacional de Juliaca, San Román 21101, Peru.
- Email: *miltonqtisnado@gmail.com*
- ORCID: 0009-0001-7744-5935
- Web of Science ResearcherID: NA
- Scopus Author ID: NA
- Homepage: https://ctivitae.concytec.gob.pe/appDirectorioCTI/VerDatosInvestigador.do?id_investigador=222452

Yupanqui Bendita, C.E., M.Sc., Researcher, Universidad Nacional de Juliaca, San Román 21101, Peru.
- Email: *ucesareyb@gmail.com*
- ORCID: 0000-0002-7750-7016
- Web of Science ResearcherID: NA
- Scopus Author ID: 59975381800
- Homepage: https://ctivitae.concytec.gob.pe/appDirectorioCTI/VerDatosInvestigador.do?id_investigador=96030

Calizaya Chura, E., M.Sc., Researcher, Universidad Nacional de Juliaca, San Román 21101, Peru.
- Email: *edgarclzy@gmail.com*
- ORCID: 0009-0007-4060-2670
- Web of Science ResearcherID: NA
- Scopus Author ID: 59976620700
- Homepage:https://ctivitae.concytec.gob.pe/appDirectorioCTI/VerDatosInvestigador.do?id_investigador=472633

Moreno Terrazas, E.G., Ph.D., Professor, Faculty of Biological Sciences, National University of the Altiplano, Puno 21001, Peru.
- Email: *emoreno@unap.edu.pe*
- ORCID: 0000-0001-6356-8806
- Web of Science ResearcherID: HPE-0519-2023
- Scopus Author ID: 57221246484
- Homepage: https://ctivitae.concytec.gob.pe/appDirectorioCTI/VerDatosInvestigador.do?id_investigador=40556

HOW TO CITE THIS ARTICLE:
Mamani-Arpasi, Y.; Mamani Gomez, J.A.; Huanca Chambi, G.; Quispe Tisnado, M.; Yupanqui Bendita, C.E.; Calizaya Chura, E.; Moreno Terrazas, E.G., (2027). Satellite-based assessment of high Andean wetlands and carbon sequestration under the influence of climate change. Global J. Environ. Sci. Manage., 13(1): 123-140.

DOI: 10.22034/gjesm.2027.01.06
URL: https://www.gjesm.net/article_735656.html

Global J. Environ. Sci. Manage. 13(1): 141-162, Winter 2027, Serial #49

Global Journal of Environmental Science and Management
(GJESM)

Homepage: https://www.gjesm.net/

Podcasts

CASE STUDY

Environmental status of silky sharks in Eastern Indian Ocean from length-based catch data

A. Budiarto[1,2], I. Yulianto[1,3,4], B. Wiryawan[1,3], A.A. Taurusman[1,*], D. Iskandar[1], I. Ziegler[5], S. Gigentika[4,6], S. Agustina[4,7]

[1]*Department of Fisheries Resources Utilization, Faculty of Fisheries and Marine Sciences, IPB University, Dramaga, Bogor, West Jawa, Indonesia*

[2]*Ministry Marine Affairs and Fisheries, Indonesia*

[3]*Rekam Nusantara Foundation, Bogor, West Java, Indonesia*

[4]*Scientific Forum for Sustainable Fisheries in West Nusa Tenggara, Indonesia*

[5]*Deutsche Stiftung Meeresschutz (German Foundation for Marine Conservation), Badstr, München, 481379 Germany*

[6]*Marine Science, Faculty of Agriculture, Mataram University, Mataram, West Nusa Tenggara, Indonesia*

[7]*Indonesia Ocean Program, Yayasan Konservasi Alam Nusantara, Indonesia*

ARTICLE INFO

Article History:
Received 13 May 2026
Revised 20 July 2026
Accepted 24 August 2026

Keywords:
Catch-per-unit-effort
Length-based indicators
Length-based indicators
Silky shark
Shark fisheries management

DOI:10. 22034.gjesm.2026.04.07

ABSTRACT

BACKGROUND AND OBJECTIVES: Silky sharks (*Carcharhinus falciformis*) are among the most exploited pelagic species in the Eastern Indian Ocean, yet their population dynamics remain poorly documented. The study objectives were to evaluate the status of silky shark populations landed by artisanal fisheries at Tanjung Luar Port, West Nusa Tenggara, by combining length-based indicators with standardized catch-per-unit-effort modelling to detect early warning signs of overexploitation.

METHODS: Data were collected between 2017 and 2023, covering 33,129 individuals captured by bottom longline, surface longline, and gillnet gears. Biological parameters included length-frequency distribution and sex ratio, while operational indicators comprised trip frequency, vessel numbers, and fishing days per trip. Standardization of catch-per-unit-effort was achieved via a dual-component delta framework. The architecture integrated a binomial generalized linear mixed model evaluating encounter probability with a negative-binomial generalized additive model analyzing positive catch rates, while explicitly controlling for provincial fishing grounds, effort duration in fishing days, gear typology, vessel-level random effects, and all potential two-way interactive effects.

FINDINGS: Catch-per-unit-effort displayed consistent biannual peaks in May and November, reflecting seasonal variation in availability or catchability, but overall abundance declined steadily. Length-frequency distributions demonstrated truncated population structures heavily skewed toward juveniles fractions, with the majority of individuals falling below published length-at-maturity thresholds. A persistent female bias was evident, with females comprising more than half of annual catches and reaching ~71 percent in 2023. Effort dynamics showed declining efficiency; Catch-per-unit-effort decreased as trip frequency increased, while total catch was maintained only through increased fishing trips. Furthermore, the manifestation of fleet growth alongside shortened operational windows exemplifies tactical adaptations capable of temporarily concealing structural biological degradation.

CONCLUSION: The convergence of biological and operational signals highlights a fishery increasingly sustained by juvenile recruitment rather than adult spawning biomass, raising precautionary concerns about reduced spawning potential. Precautionary measures are urgently required to safeguard spawning potential and ensure long-term sustainability. Recommended policy measures entail the enforcement of seasonal closures during critical aggregation phases, restrictions on juvenile removal, technical gear adjustments to curtail retention, and the application of effort constraints calibrated against vessel- and trip-level operational parameters.

This is an open access article under the CC BY license (http://creativecommons.org/licenses/by/4.0/)

NUMBER OF REFERENCES	NUMBER OF FIGURES	NUMBER OF TABLES
35	6	4

*Corresponding Author:
Email: azbas@apps.ipb.ac.id
Phone: +62813 1871 8700
ORCID: 0000-0002-8707-3223

Note: Discussion period for this manuscript open until March 01, 2027 on GJESM website at the “Show Article”.

INTRODUCTION

Shark fisheries in Indonesia have operated since the 1970s, initially as bycatch in tuna fisheries but later developing into targeted fisheries, particularly among small-scale fishers at major landing sites. This transition has been propelled by escalating domestic and international demand for shark-derived commodities, encompassing meat, fins, and cartilage (Dulvy *et al.,* 2021). At the global scale, reported elasmobranch catches reached approximately 731,000 tons in 1994, with Asia contributing around 60 percent (%) of total landings. Indonesia, together with India, Japan, and Pakistan, accounted for nearly 75% of global shark and ray catches. Notwithstanding a downward trend in average annual landings to 631,393 tonnes over the 2019–2022 interval (FAO 2024), Indonesia persistently commands the position of the world's primary shark producer, having reigned as the principal shark-catching nation across the entire 2007–2022 span (FAO 2024). This sustained exploitation has resulted in global population declines, of pelagic sharks and rays, estimated at more than 71% over the past five decades, largely driven by high fishing pressure and bycatch mortality (Pacoureau *et al.,* 2021). The vulnerability of chondrichthyan species is underscored by Dulvy *et al*., (2021), who noted that over one-third are currently threatened with extinction. Complementary findings from the International Union for Conservation of Nature (IUCN) global reassessment demonstrate that 32.6% of sharks and ray species are threatened, with this proportion escalating to 37.5% when accounting for Data Deficient taxa, largely due to intense overfishing and incidental bycatch mortality. Tropical and subtropical coastal waters, particularly in the Indo-Pacific region, were identified as areas with disproportionately high extinction risk, especially for large-bodied shark species inhabiting shallow waters, and the study further emphasized that current fisheries management measures remain insufficient to reverse ongoing global declines in shark populations. Silky sharks (*Carcharhinus falciformis*) are ecologically important apex predators in the Eastern Indian Ocean, contributing to pelagic food-web stability by regulating prey populations and linking tuna-associated ecosystems (Murray *et al.,* 2023). The life-history traits of slow growth, delayed maturation, and low fecundity impart acute vulnerability to anthropogenic harvesting, threatening to rapidly deplete reproductive stock structure and undermine long-term population resilience. These trends have prompted increasing international concern and the call for strengthening conservation and management measures for exploited shark species. Such management-oriented approaches increasingly require systematic assessment frameworks and evidence-based analytical strategies to support environmental decision-making (Mohamed and Rezk, 2025). The silky shark (*Carcharhinus falciformis*) is among the species of greatest conservation concern and has been listed under Appendix II of the Convention on International Trade in Endangered Species of Wild Fauna and Flora (CITES) in 2016, allowing international trade only when sustainability, legality, and traceability requirements are met (Dharmadi and Fahm, 2015). Indonesia, issued a non-detriment finding (NDF) for silky sharks in 2019 to support science-based management. The global population trajectory of the silky shark exhibits an estimated decline of 47–54% across three generations, encapsulating regional variations in demographic change. Consequently, the severity of this contraction, when evaluated in conjunction with prevailing data uncertainties, underpins its formal categorization as Vulnerable globally (Rigby *et al.,* 2021). Current evidence from the Indian Ocean shows truncated size structures dominated by juveniles, limited representation of mature individuals, and seasonal recruitment pulses that are insufficient to offset adult depletion (Hall *et al*., 2012; Clavareau *et al*., 2020). These exploitation patterns highlight the risk of

reproductive depletion under sustained fishing pressure. Silky sharks are widely distributed in tropical and subtropical waters and are captured both in targeted shark fisheries and as bycatch in tuna longline and gillnet fisheries (White *et al.,* 2006; Grant *et al.,* 2018). In addition, industrial purse-seine sets deploying fish aggregating devices (FADs) disproportionately capture juvenile silky sharks as primary bycatch, with respective incidence levels markedly elevated in the Indian Ocean (99.7%) compared to the Atlantic (97.9%). Across both oceans, elasmobranch catches were substantially higher in sets associated with FADs (>40%) compared to free-school tuna sets (<17%), although species-specific differences were evident. Elasmobranch catches were dominated by juvenile individuals (30.7–100%), exhibited relatively high at-haulback mortality rates (24.3–63.9%), and showed unbalanced sex ratios, with females comprising 13.3–66.7% of catches. Analyses of Indian Ocean purse-seine sets reveal that silky shark bycatch over FADs was overwhelmingly juvenile-dominated (99.7%), with a marginal female demographic bias and a recorded haulback mortality rate of 60.5%. The identified spatial and seasonal patterns provide important information for improving monitoring and management strategies of elasmobranch bycatch (Clavareau *et al.,* 2020). In Indonesian archipelagic waters, silky sharks are broadly distributed across the Indian Ocean, South China Sea, Makassar Strait, and Banda Sea, with juveniles cohorts frequently captured in coastal fisheries. Available evidence suggests that silky sharks have declined by approximately 70% from historical levels in the Western Central Pacific (WCPFC) due to non sustainable fishing pressure being the only Regional Fisheries Management Organization (RFMO) that has succeeded in performing a stock assessment for silky sharks. According to FAO (2017) data, global catches expanded throughout the 1990s and early 2000s before experiencing a sharp downturn post-2000, ultimately contracting to less than 20% of their initial levels by 2014. IOTC reports an average retained catch of 2,062 t of silky sharks per year (y) for the period of 2020 – 2024, with more than 60% of catches taken by Indonesia, Sri Lanka, and Taiwan in their line, longline, and coastal purse seine fisheries. Pakistan's and Iran's gillnet fisheries also account for about 30% of the retained catches (IOTC, 2025) although silky sharks are often not reported at species level in gillnet fisheries as such reporting is not mandatory for this gear in Indian Ocean Tuna Commission (IOTC) Resolution 15/01. Furthermore, silky sharks are also the most common shark bycatch in industrial DFAD purse seine fisheries and there subject to high at vessel and post release mortality rates (Hutchinson *et al.,* 2015; Onandia *et al.*, 2021). Throughout the 2005–2015 period, Indonesian shark production fluctuated between 2,500 to 6,700 tons annually, with approximately 20% of landings comprising members of the family Carcharhinidae. Major fishing centres include Tanjung Luar, adjacent to the Indian Ocean and operating primarily in fisheries management area (FMA) 573 (Yulianto *et al.,* 2018). Silky sharks dominate landings in these fisheries, accounting for more than 30–40% of total shark catches in several years (y). Fishers in Tanjung Luar primarily target sharks in Southern Sumbawa, Sumba Islands, eastern Flores, and Timor Island, as part of the FMA 573 (Yulianto *et al.,* 2018). The IOTC (2025) reported that the stock status of silky shark (*Carcharhinus falciformis*) in the Indian Ocean remains "Unknown" due to substantial uncertainties in catch data, catch-per-unit-effort (CPUE) trends, and the lack of reliable stock assessment indicators (Hinton and Maunder, 2003). Nevertheless, the species is identified as one of the most vulnerable sharks in Indian Ocean fisheries owing to low biological productivity and high susceptibility to longline and purse seine gears, ranking second and fifth in vulnerability, respectively, within the IOTC ecological risk assessment. Furthermore, available evidence indicates that silky shark abundance has experienced sustained declines over recent decades despite limited quantitative metrics. In

data-limited fisheries such as Indonesia, length-based catch indicators are particularly useful because they provide direct information on population structure, maturity composition, and recruitment signals without requiring full stock assessments. Recognized broadly as diagnostic early-warning proxies for overexploitation, these metrics provide the basis for this investigation; by synthesizing length-based indicators with CPUE modeling, this study bridges regional data gaps across Indonesian waters to evaluate preliminary vulnerabilities. Specifically, we evaluate artisanal landings at Tanjung Luar Port to provide the first combined length-based and standardized CPUE assessment of silky shark environmental status in the Eastern Indian Ocean. This fills a critical gap in understanding how artisanal fisheries contribute to exploitation patterns and population decline. Ultimately, these empirical outcomes are intended to advance an updated scientific framework capable of supporting evidence-based, sustainable governance structures for the local silky shark fishery (Yulianto *et al.,* 2018). The aims of this study are to evaluate the status of silky shark populations landed by artisanal fisheries, by combining length-based indicators with standardized catch-per-unit-effort modelling to detect early warning signs of overexploitation. This study has been contacted in the Tanjung Luar Fishing Port, West Nusa Tenggara Province, during 2017 and 2023.

MATERIALS AND METHODS

Data collection

The study evaluated a major shark landing site in West Nusa Tenggara, Indonesia (Fig. 1). Data were collected from 83 fishing vessels operating between 2017 and 2023. These vessels employed three types of fishing gear: bottom longline (BL), surface longline (SL), and gillnet (GN). The trip and catch composition data were collected to ensure standardized records detailed in Table 1. The fleet operating in Tanjung Luar was dominated by wooden vessels, with approximately 75% having a gross tonnage (GT) of 5 or less, while only 25% ranged between 6 and 28 GT. Engine power is modest (15–60 HP), which constrains operational range and confirms that these vessels are artisanal to semi-industrial in scale. With an average length of 15 to 20 meters (m) and operations restricted exclusively to the Indonesian EEZ, these vessels are exempt from mandatory inclusion in the IOTC register of active vessels (RAV) and its corresponding regulatory mandates. Fishing grounds reported by the fleet span across West Nusa Tenggara (NTB) and East Nusa Tenggara (NTT), with occasional records from other provinces. Larger vessels (46–60 HP) are capable of reaching fishing grounds further afield, including Sumba Island, Savu Sea, Flores Sea, Java Sea, and Makassar Strait, whereas smaller vessels (<46 HP) remain closer to Lombok and Sumbawa, typically operating in Awang Bay, Alas Strait, and Panjang Island (Yulianto *et al.*, 2018). The silky shark (*Carcharhinus falciformis*) as shown in Fig. 2 is a member of the family Carcharhinidae within the order Carcharhiniformes, class Chondrichthyes. It is widely distributed in tropical and subtropical waters, occurring from the surface to depths of around 500 m, but records extend to 4000 m in some regions. In the Indian Ocean, individuals are born at 65–81 centimeters (cm) total length (TL) and reach maturity at approximately 216 cm in females TL and 208 cm TL in males (Rigby *et al.,* 2021), with an estimated lifespan of about 20 y (Hall *et al.,* 2012). Sexual maturity is attained around 13 y in males and around 15 y in females. The species is viviparous, exhibiting a gestation period of 9–12 months and fecundity ranging from 2 to 18 pups per litter at intervals of 2 to 3 y, with reproductive output increasing as a function of female body size. Silky sharks are highly migratory and often associated with tuna schools, a behavioral trait that increases their exposure to fishing pressure. Their slow growth, late maturity, and low reproductive output make them particularly vulnerable to sustained and intensive overexploitation.

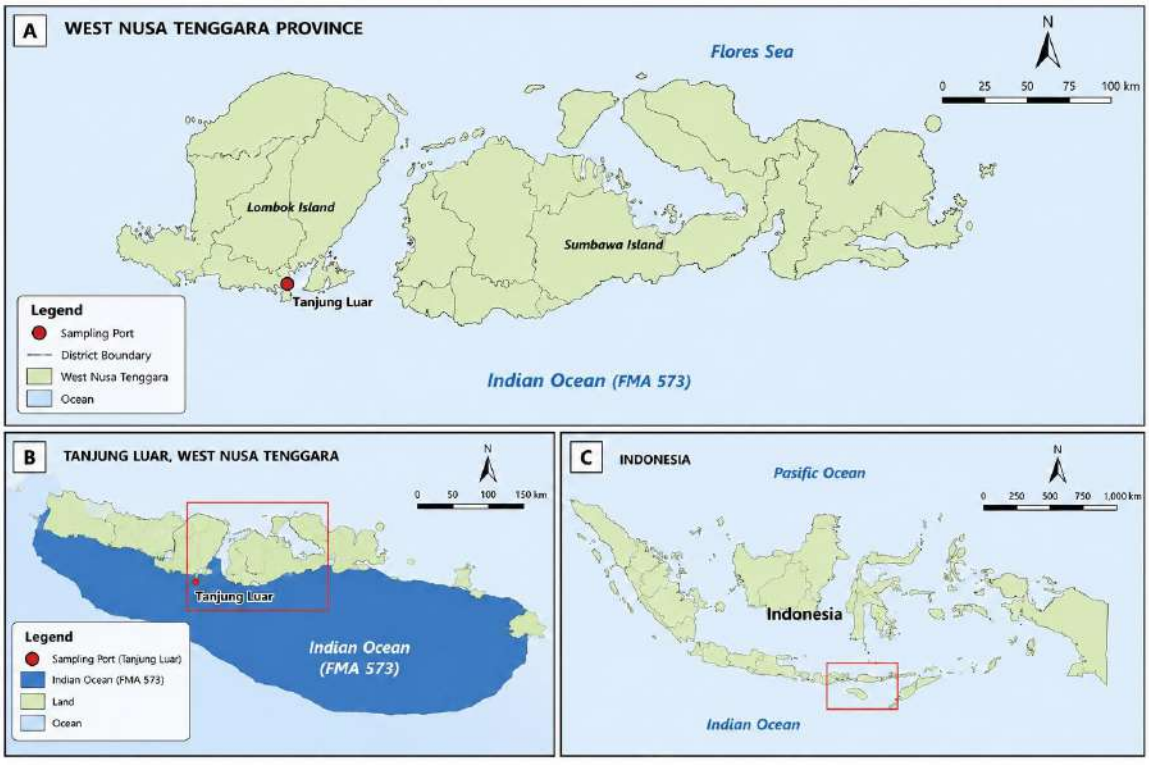

Fig. 1: Geographical location of the study area in Tanjung Luar, West Nusa Tenggara, Indonesia



Fig. 2: Silky shark measurement at Tanjung Luar Port

A cumulative total of 33,129 silky sharks were measured across 2017–2023 from the catch landings of 83 commercial vessels deploying bottom longline, surface longline, and gillnet gears. Dedicated enumerators were present at Tanjung Luar Port throughout the year to continuously record the data using the parameter data shown in Table 1.

Table 1: Parameters data for the fishing trip in Tanjung Luar fishing port

Category	Variable	Description
Trip information	Trip ID and date	Unique identifier and date of fishing trip
	Vessel name	Name of the fishing boat; engine power, and tonnage
	Fishing gear type and code	Fishing Gear: Bottom longline (BL), Surface longline (SL), Gillnet (GN)
	Trip duration (days)	Number of days spent fishing
	Fishing ground	Area of operation at provincial level (West Nusa Tenggara, East Nusa Tenggara, and Others)
Catch composition	Family and species	Taxonomic identification
	Morphometric measurements	Body size metrics recorded per individual
	— Total Length	Measured in cm
	— Fork Length	Measured in cm
	Sex (F/M)	Biological sex is determined at landing

Data analysis

Three main analyses were conducted to evaluate the biology and fishing effort of silky sharks (*Carcharhinus falciformis*), including length frequency distribution (LFD), sex ratio, and standardized CPUE. LFD data were analysed to explore the size distribution of the silky sharks across ys, sexes, and fishing gear. Distributions were constructed using 1 cm TL intervals and stratified by sex and gear type. Annual and seasonal variation was visualized using ridgeline density plots to elucidate recruitment pulses, the truncation of larger size classes, and gear-specific selectivity. This analytical approach facilitated the evaluation of juvenile-to-adult ratios, recruitment dynamics, and gear selectivity, patterns, thereby yielding critical insights into stock status and overall population health (Dharmadi and Fahm, 2015). Sex composition was used to detect potential bias in catches. The proportion of females and males was calculated annually and by gear type. Statistical differences in the sex ratio were tested using chi-square tests, with significance set at $p < 0.05$. To further evaluate variation across ys, size classes, seasons, and gears, a generalized linear model (GLM, binomial logit) was fitted with sex as the response variable and predictors including y, month, gear, fishing ground, and total length. This analytical approach enabled the identification of seasonal segregation, gear specific selectivity, and size-related variations in sex composition. Female proportions with 95% confidence intervals were reported annually, and effect sizes were emphasised over p-values given the large sample sizes. Deviations from a 1:1 sex ratio were interpreted in relation to reproductive dynamics and possible selective fishing pressure. Because direct stock assessment data are frequently unavailable, CPUE serves as a standard proxy for relative abundance (Maunder *et al.*, 2006; Campbell, 2004). In this study, CPUE was applied to standardize catch rates and determine the primary variables influencing shark abundance. By standardizing CPUE, temporal and spatial variation in fishing effort can be accounted for, allowing more reliable inference about population trends and fishing pressure. CPUE was calculated as the number of sharks caught per trip, adjusted for the duration of each trip. Standardized catch per unit effort (CPUE) was estimated using a two-stage delta-model framework to accommodate the zero catches typically observed in shark fisheries (Lo *et al.*, 1992). The delta approach decomposes the catch process into an encounter-probability component and a positive-catch component, thereby enabling the independent modeling of factors governing occurrence and relative abundance. For the encounter component, a generalized linear mixed model (GLMM) with a binomial error distribution and logit link was fitted using y, month, fishing gear (gear), provincial level fishing ground (FG), and all plausible two-way interactions among these variables. Vessel identity (boat name) was included as a random intercept to account for differences in fishing power among vessels.

Fishing effort (trip day) was incorporated as a logarithmic offset term to standardize catches to a common unit of effort. For the positive-catch component, a generalized additive model (GAM) featuring a negative-binomial error distribution and a log-link function was fitted using identical explanatory variables and interaction terms. This model yielded the lowest Akaike's Information Criterion (AIC) value of 13,193 alongside acceptable levels of overdispersion, while simultaneously generating biologically interpretable CPUE estimates. Vessel-specific effects were incorporated using a random-effect smooth terms (boat name, bs = "re"). The model fpr GAM with negative binomial, using Eq. 1 (Wood, 2017):

Catch ~ Year + Month + Gear + Fishing ground + offset[log(Trip Days)] (1)

To determine the optimal models for both the encounter-probability and a positive-catch components, a global model incorporating year (Y), month, fishing gear (gear), provincial level FG, and all plausible two-way interactions among these variables were fitted and evaluated to explain the variance in CPUE. Model selection was conducted using the MuMIn package. Candidate models were generated using the pdredge function, which systematically constructs and evaluates all permissible subsets of the global model. Models were ranked according to AIC, providing a balance between model fit and complexity. The effort offset and vessel effects were retained throughout the model selection process, as they functioned as foundational standardization parameters rather than candidate explanatory variables. Parallel processing was implemented using doParallel to improve computational efficiency, using Eqs. 2 to 7 (Hoyle *et al.*, 2024):

$$CPUE_t = P_t \, x \, C_t \quad (2)$$

Where:

$P_t = P_r \, (Y_t > 0)$

$C_t = E(Y_t \mid Y_t > 0$

$Y_i \sim Binomial \, (1, p_i)$

$$logit(pi) = \beta_0 + \beta_{year} + \beta_{month} + \beta_{Gear} + \beta_{fg} + \beta(gear \, x \, fg) + boat \, name \, (i) + offset \, (\log(effort)) \quad (3)$$

$$Boat \, name \, (i) \sim N \, (0, \sigma^2 boat \, name)$$
$$Y_i \mid Y_i > 0 \sim NB(\mu_i, \theta) \quad (4)$$

$$\log(\mu_i) = \beta_0 + \beta_{year} + \beta_{month} + \beta_{Gear} + \beta_{fg} + \beta(gear \, x \, fg) + s(boat \, name \,) + offset \, (\log(effort) \quad (5)$$

$$AIC = -2 \log(L) + 2K \quad (6)$$

$$Var(CPUE) = C^2 Var(P) + P^2 Var(C) \quad (7)$$

$$SE \, (CPUE) = \sqrt{Var(CPUE)}$$

$$95\% \, CI = CPUE \, \pm 1.96 \, x \, SE$$

The final encounter model selected by AIC retained y, month, gear, fishing ground, and the gear × fishing ground interaction, together with the vessel random effect and effort offset. The final positive-catch GAM retained y, month, gear, fishing round, gear × fishing, the vessel random-effect smooth term, and the effort offset. Annual and monthly standardized indices were subsequently estimated using marginal means obtained from the emmeans package (Lenth, 2023). The delta method was applied to compute the variance and confidence intervals of the delta-CPUE index (Walter and Ortiz, 2012).

RESULTS AND DISCUSSION

Fishing catches and trips

The silky sharks, landed at Tanjung Luar Fishing Port between 2017 and 2023, were dominated by surface longline vessels (Tables 2 and 3). 149 fishing trips were recorded in 2017 and 388 fishing trips in 2023. In contrast, bottom longline vessels

Table 2: Number of trips with silky sharks landed in Tanjung Luar port, West Nusa Tenggara from 2017 to 2023

Fishing gear	2017	2018	2019	2020	2021	2022	2023
Bottom longline	43	48	18	16	35	41	60
Gillnet	-	-	-	-	-	-	1
Surface longline	149	217	265	174	199	247	388

Table 3. Number of individuals landed in Tanjung Luar port, West Nusa Tenggara from 2017 to 2023

Fishing gear	2017	2018	2019	2020	2021	2022	2023
Bottom longline	123	89	22	33	64	85	161
Gillnet	-	-	-	-	-	-	5
Surface longline	2,905	4,899	5,935	3,811	4,505	5,253	5,239

made fewer trips, ranging from 16 in 2020 to 60 in 2023, and only one trip of gillnet was recorded in 2023. The number of individuals landed reflected this pattern of fishing effort. Surface longlines consistently accounted for the majority of silky shark catches, with annual landings ranging from 2,905 individuals in 2017 to a peak of 5,935 in 2019, and remaining above 3,800 individuals thereafter. Throughout the monitoring period, annual yields of silky sharks captured by bottom longlines did not exceed 170 individuals, with gillnet operations similarly recording a negligible catch of 5 individuals in 2023. A total of 33.129 individuals were measured, with morphometric data recorded for total length (TL) and sex. Surface longline was the predominant fishing gear for silky shark exploitation in Tanjung Luar, accounting for the highest number of trips and landed individuals across all years. Although cumulative landings experienced significant growth from 2017 to 2022, the sharp escalation in fishing trips observed in 2023 was not mirrored by proportional increase in catch volumes, thereby precipitating a marked decline in catch per trip. This sharp increase in trips coincided with a growth in the number of active vessels operating from Tanjung Luar, reflecting an expansion of the fleets. Median trip duration remained relatively stable, but overall fishing days and cumulative effort rose, indicating that catch levels were sustained through intensified activity rather than stable population productivity. The observed pattern may stem from diminished stock availability or catchability induced by heightened fishing pressure, thereby pointing toward potential early warnings of overexploitation. These indications of declining catch efficiency are further contextualized by sex-ratio evaluations, providing critical insights into demographic stability and population vulnerabilities under prolonged fishing mortality.

Sex ratio

Of the 33,129 samples collected between 2017 and 2023, the sex of 32,077 individuals was successfully determined females consistently comprised more than 50% of the catch. (Fig. 3a). Male proportions ranged from 29.1% in 2023 to 47.8% in 2019, with the strongest female dominance observed in 2022 and 2023. Based on chi-square test, the sex ratio was significantly skewed toward females ($p < 0.001$) in six of seven years (Table 4). The year 2019 was the most balanced, with males comprising 47.8% of the catch and a p-value of 0.009, indicating a weaker but still statistically significant deviation. To evaluate sex-specific patterns, a generalized linear model utilizing a binomial logit link was constructed; sex served as the dependent variable, while gear configuration, management zone, year, month, and total length functioned as independent predictors. The model confirmed that female probability increased significantly over time ($p < 0.001$) and declined with increasing size ($p < 0.001$). Importantly, several monthly contrasts were significant ($p < 0.05$), indicating seasonal variation in sex ratios, consistent with potential migration or segregation. Gear and zoning effects were weaker and not statistically

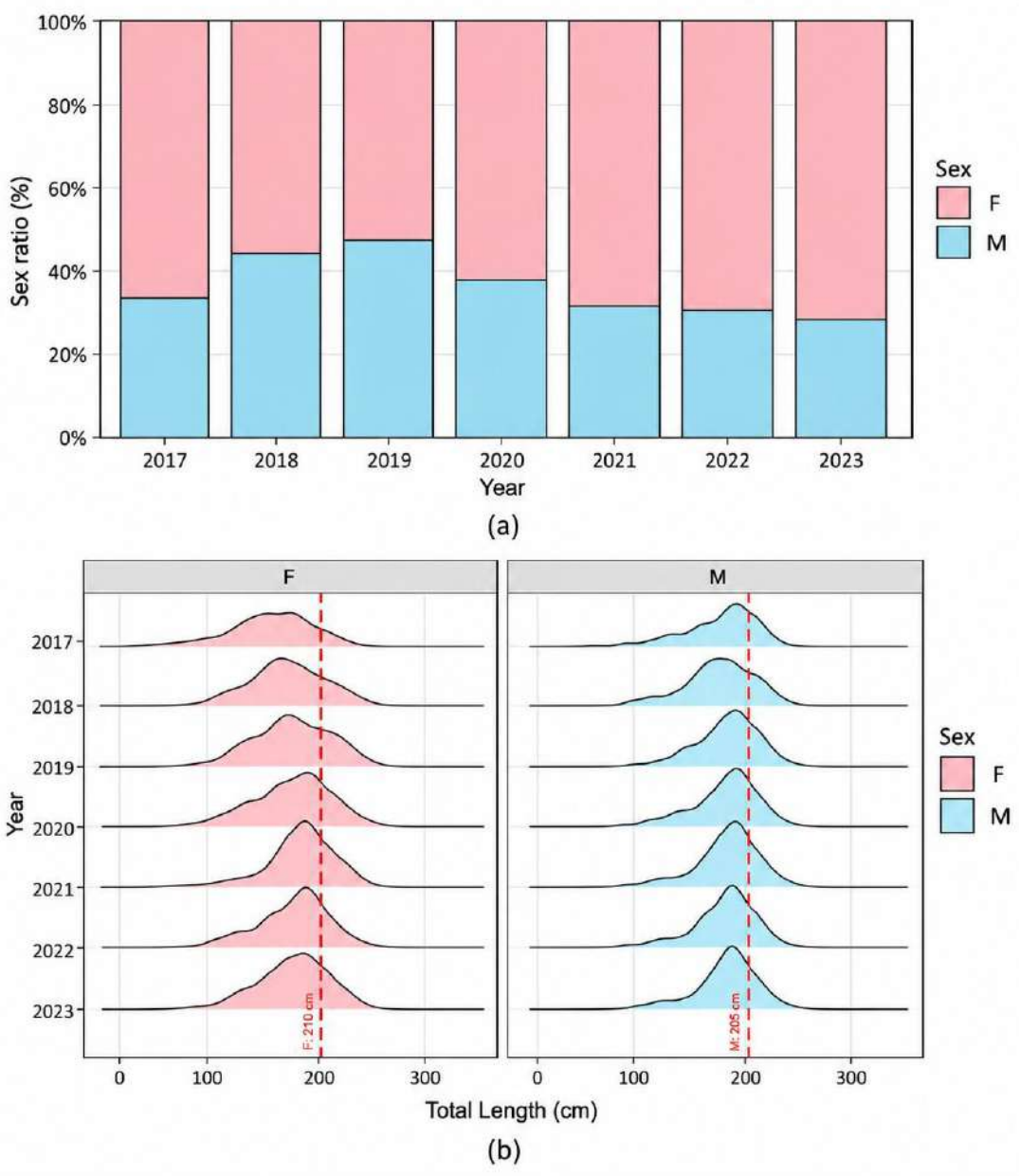

Fig. 3. Annual sex ratio (%) (a) and length-frequency distribution by sex (b) of silky sharks (Carcharhinus falciformis) landed at Tanjung Luar fishing port, Eastern Indian Ocean, 2017–2023

Table 4: Annual sex ratio of silky sharks landed at Tanjung Luar fishing port (2017–2023)

Year	Female	Male	Total	prop_M	p_value
2017	2041	987	3028	0.326	2.61e- 83
2018	2764	2189	4953	0.442	3.21e- 16
2019	3056	2802	5858	0.478	9.46e- 4
2020	2441	1403	3844	0.365	1.48e- 63
2021	3090	1465	4555	0.322	9.57E-131
2022	3671	1667	5338	0.312	1.56E-169
2023	3853	1578	5431	0.291	1.41E-215

significant. Across years, modal total lengths were concentrated at approximately 150–200 cm TL. Females consistently had broader distributions and larger median lengths than males (Fig. 3b). However, the upper tail of the distribution became progressively thinner, particularly between 2019 and 2023, and the interquartile ranges narrowed slightly in 2019 and 2023. A post-2018 decline was likewise observed in the median length of females, in contrast to male median lengths, which varied without exhibiting any clear directional trend. This pattern is consistent with disproportionate removal of larger females, however, sexual segregation, habitat use, and gear selectivity may also contribute to the observed female bias. Female proportions ranged from 52% to 71% annually. A salient feature of the landings is a persistent female bias (> 50% females annually and ~71% in 2023) alongside larger median TLs in females (this study). Sex-biased catches can arise from sexual segregation, gear selectivity, and seasonal movement. Furthermore, sex-specific spatial segregation, such as the utilization of distinct migration routes or depth zones by adult females, may result in heightened seasonal susceptibility to longline fisheries interactions. Evidence of sexual segregation is well documented in other shark species, such as *Squalus acanthias* and grey reef sharks (*Carcharhinus amblyrhynchos*) (Heupel and Simpfendorfer, 2014). Although less studied in silky sharks, emerging research indicates spatial structuring and potential sex-specific segregation in the Indo-Pacific and Eastern Pacific (Li *et al.*, 2023; Talwar *et al.*, 2025). These findings indicate that female silky sharks experience spatially and temporally variable vulnerability to specific fisheries. Furthermore, the convergence of sex-ratio biases with size-class truncation leads to the selective removal of larger, late-maturing females—a demographic shift that substantially depresses population fecundity and aggregate spawning biomass (Joung *et al.*, 2008; Grant *et al.*, 2018). Reports from the Indian Ocean similarly note the high vulnerability of silky sharks to longline and purse seine, consistent with the ecological risk assessment that ranked the species among the least productive and most susceptible to these gears. The IOTC Scientific Committee further highlighted that silky sharks are long-lived, late maturing, and have low reproductive output, making them particularly prone to overfishing, with current stock status in the Indian Ocean considered uncertain (IOTC, 2025; Simeon *et al.*, 2018; Curnick *et al.*, 2020). From a monitoring perspective, sex ratio and sex-specific size distributions are sensitive key indicators of reproductive stress in elasmobranch fisheries. A consistently female-skewed catch, which shows a reduction in the number of large females as detailed in this document, supports the need for sex-specific strategies and targeted conservation measures. These include protecting mature females through size/slot limits, minimizing retention via gear modifications and live-release protocols, and restricting catch effort to prevent overfishing in seasonal hotspots frequently visited by adult females during critical reproductive periods and aggregation seasons (Joung *et al.*, 2008; Curnick *et al.*, 2020).

Stock status and health from length-based indicators

From the recorded data, the modal peaks were found being between 150–200 cm TL, with females generally exhibiting broader distributions and higher frequencies than males (Fig 3b). Median lengths ranged from 191.0 cm to 198.2 cm for females and 183.4 cm to 189.6 cm for males, indicating that females were consistently larger across all ys. The temporal trend in length by sex showed stable median lengths across the study period, with females consistently larger than males. This sex-specific divergence is evident in Fig. 4, where male size distributions remain variable but stable, while female medians compress downward over time (Fig. 4b). Slight contractions in the interquartile ranges during 2019 and 2023 indicated a decrease in dispersion among landed body sizes (Fig. 4a).

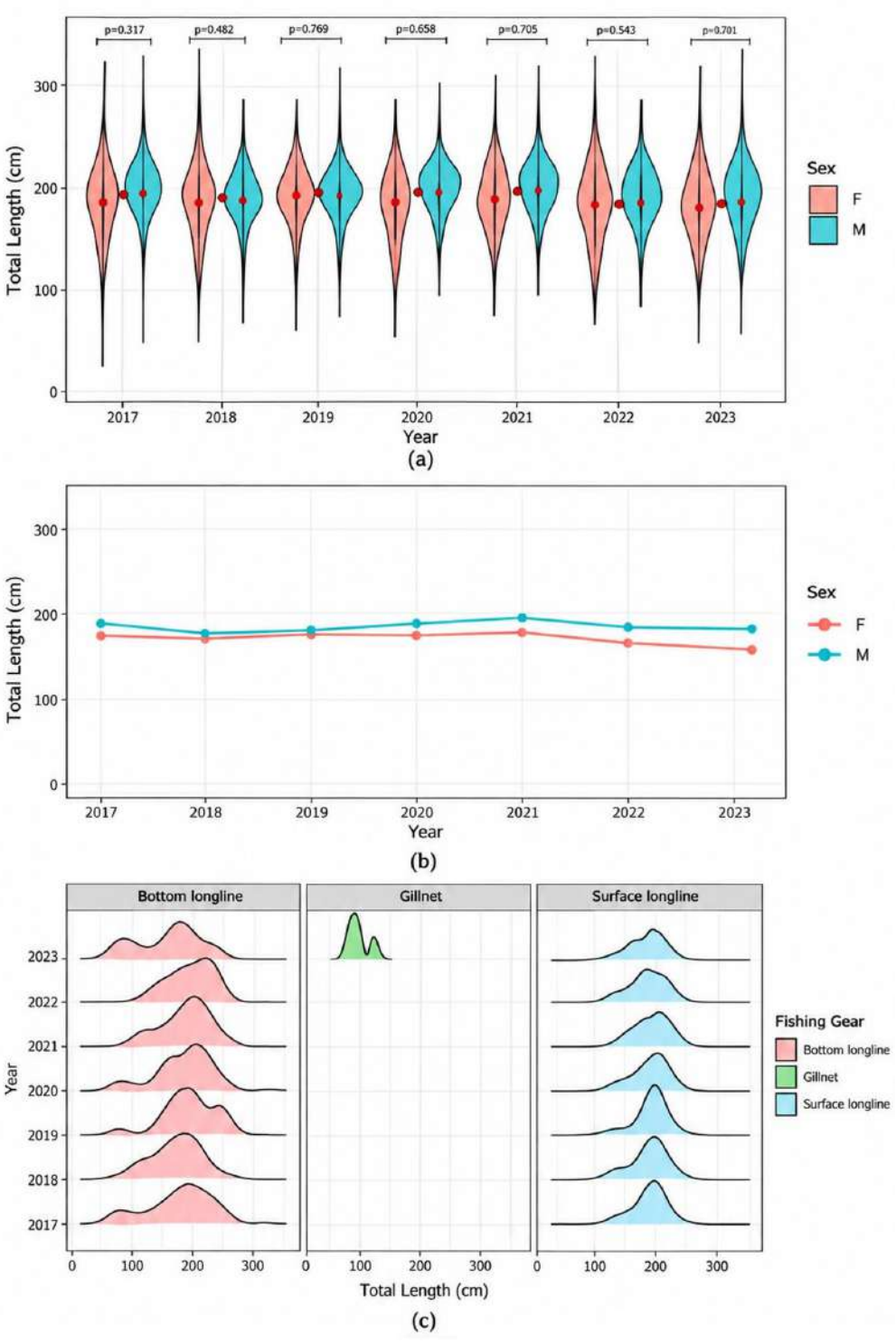

Fig. 4: The LFD of silky shark total length (cm) by y and sex (F = female, M = male) (a and b) and by fishing gear (c) landed at Tanjung Luar fishing port, 2017–2023

The length distribution by gear (Fig 4c) showed revealed clear differences in selectivity. Surface longlines consistently captured the widest range of sizes, including individuals above the published length-at-maturity thresholds (F ≈ 216 cm TL; M ≈ 208 cm TL). In contrast, bottom longline catches were heavily skewed toward smaller sharks, with most individuals below maturity size. Gillnets (GN), were introduced only in 2023, and therefore contribute only limited data, but captured mid-sized individuals (~180 cm TL). Apparent shifts in selectivity between years are driven primarily by changes in fleet gear composition, such as the introduction of gillnets, rather than alterations in longline configuration. Length–frequency patterns from 2017–2023 point to a landed catch increasingly composed of sub-mature individuals. Modal sizes were concentrated at 150–200 cm TL, female medians exceeded male medians throughout, and the upper tail of the distribution became progressively thinner between 2019 and 2023 (Fig 4a), indicative of size truncation under sustained overexploitation. As illustrated in Fig. 4b, male median values fluctuate without a discernible directional trend, while female medians have exhibited a downward trajectory since 2018. Formal statistical testing confirmed significant interannual variation in female median lengths (Kruskal–Wallis $\chi^2 = 668.78$, df = 6, $p < 0.001$), with pairwise Wilcoxon tests indicating that female median TL in 2023 was significantly lower than in earlier years (adjusted $p < 0.001$). This pattern suggests that the decline in female size is driven not by narrowing of the median per se, but by reduced frequency of large females in landings. When benchmarked against published length-at-maturity (Lm) thresholds for silky sharks in the Indian Ocean, females ≈ 216 cm TL and males ≈ 208 cm TL (Rigby *et al.,* 2021) the majority of landed individuals at Tanjung Luar are caught below published length-at-maturity thresholds (immature). That pattern raises precautionary concerns regarding diminished spawning potential, given that the fishery lands predominantly sub-mature individuals that have not yet contributed to the reproductive output of the stock (Joung *et al.*, 2008; IOTC, 2025). Notwithstanding the absence of statistical significance for gear effects in the models, documented evidence reveals that the use of wire leaders and shark lines elevates shark retention efficiency compared to nylon monofilament leaders; thus, prohibiting such gear could mitigate longline-related mortality in silky sharks populations by >30% (D'Alberto *et al.*, 2024). The life-history backdrop reinforces the risk of over-exploitation: silky sharks grow slowly and mature late (e.g., sexes-combined k ≈ 0.084/y; $L\infty$ ≈ 332 cm TL), implying limited capacity to rebound once spawning stock diminishes (Joung *et al.*, 2008; Grant *et al.*, 2018). At the ocean-basin scale, the ~71% decline in oceanic shark and ray abundance since 1970 underscores that exploitation rates typical of contemporary pelagic fleets readily outpace the replacement potential of slow-growing elasmobranchs (Pacoureau *et al.*, 2021). Collectively, the dominance of sub-Lm fish, the loss of large size classes, and the female–male size separation in this study indicate a fishery in which spawning cohorts are being eroded, and recruitment is increasingly relied upon to sustain catches. While length-based monitoring offers a robust early-warning framework under data-limited scenarios, sustained compression of maximum size distributions, especially within female cohorts, reflects elevated fishing mortality and stock overexploitation, necessitating urgent precautionary oversight (Joung *et al.*, 2008; Pacoureau *et al.*, 2021). The compression of size structure is consistent with precautionary warning signals about reduced contribution of large mature individuals. These length-based patterns are complemented by the standardized CPUE trends.

Stock status and health from standardized CPUE

Based on the selected model (GAM-NB within a two-stage delta approach), the standardized CPUE for silky sharks showed a clear peak in 2018 (10.81 ± 1.32), before declining steadily to

5.18 ± 0.88 in 2023. Annual values demonstrate a gradual downward trajectory: 8.32 ± 1.14 in 2017, 7.83 ± 1.33 in 2019, 7.62 ± 1.37 in 2020, 9.97 ± 1.18 in 2021, and 9.00 ± 0.99 in 2022 (Fig. 5a). A linear regression revealed a significant negative temporal trend (slope = –0.64 CPUE/y, 95% CI: –0.95 to –0.49, p = 0.020), explaining ~56% of the variance. This confirms that CPUE experienced a significant temporal decline, despite the absence of statistically significant differences among annual medians when evaluated independently. The monthly CPUE (Fig. 5b.) across seven years of data collection showed that the highest values consistently occurred in May and November, indicating a biannual seasonal pattern in silky shark availability or catchability within the Eastern Indian Ocean. Based on simulation from the model, a significant positive correlation was detected between catch volumes and trip frequency, whereas standardized CPUE correlated inversely with the total number of fishing trips (Figs. 6a and 6b). Based on the data collected throughout the survey period, the number of fishing trips per boat remained the same, however there was a significant increase in the number of boats (Fig. 6c). To strengthen the analysis, we examined trip-level data (Fig. 5d–e), which provide hundreds of observations per y. Pronounced interannual fluctuations in fishing trip duration were observed (Fig. 6d) , with median values varying across years alongside several outlying data points denoting exceptionally extended trips. The dual-axis plot of annual CPUE and number of trips (Fig. 6e) illustrates the contrasting trajectories of declining catch efficiency and increasing fishing effort, reinforcing the conclusion that effort compensation is insufficient to maintain catch rates. This pattern suggests that changes in fishing effort are not only driven by fleet size but also by the duration of individual trips, which may further influence catchability and standardized CPUE trends. Standardized CPUE revealed a pronounced 2018 peak (~10.8 ind/day) followed by a steady decline to 2023 (~5.2 ind/day). The index shows a sustained downward trajectory since its 2018 peak. This implies that the heightened values recorded in 2018 do not necessarily denote an increase in absolute stock abundance; instead, they are more plausibly attributed to operational modifications, including fleet motorization—that artificially inflated catchability (Maunder *et al.*, 2006; Hoyle *et al.*, 2024). Uncertainty estimates from the delta method provide plausible confidence bounds around the standardized index, though broader structural model uncertainty (spatial redistribution, catchability changes) should be considered when interpreting trends. The IOTC assessment itself emphasizes that nominal CPUE may not reliably reflect abundance, underscoring the need for precautionary interpretation of standardized indices. It is important to emphasize that the patterns identified herein constitute localized signals specific to FMA 573 and should not be extrapolated to resolve the broader regional stock-status ambiguities emphasized by IOTC. Rather, they provide complementary evidence of declining catch rates that must be considered within the wider context of ongoing uncertainty at the Indian Ocean scale. The persistence of seasonal peaks in May and November across seven ys indicates a seasonal signal in availability/catchability, which is consistent with prior work in Indonesia's FMA 573 documenting a seasonal structure in silky shark abundance indices during 2015–2016, and is also supported by tagging and fishery evidence from the central Indian Ocean showing high residence in the upper 100 m, diel use of seamounts, and dominance of juveniles in longline and purse-seine catches (Simeon *et al.*, 2018; Curnick *et al.*, 2020). Temporal and spatial overlap with seasonal aggregations and migratory corridors generates predictable windows of elevated catchability, rendering stocks acutely susceptible to overexploitation absent appropriate limitations on fishing mortality (Simeon *et al.*, 2018; Curnick *et al.*, 2020). Methodologically, the choice of a flexible additive framework accords with CPUE

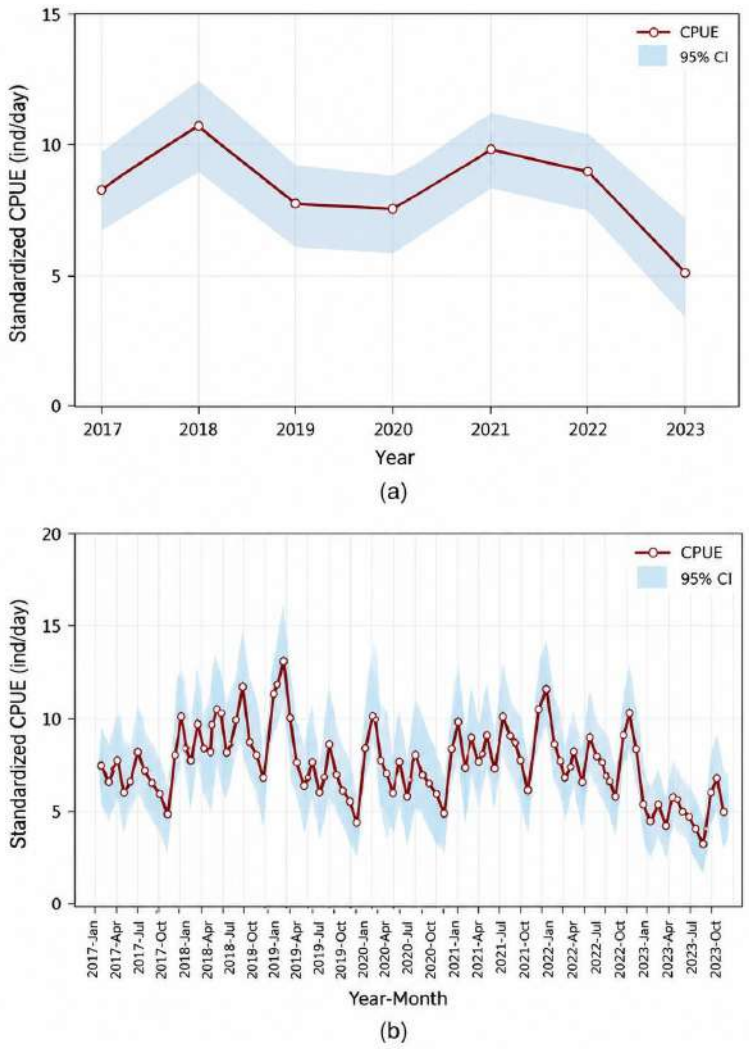

Fig. 5: Annual (a) and monthly (b) trend of standardized CPUE (ind/day/GT) for silky sharks (*Carcharhinus falciformis*) landed at Tanjung Luar fishing port, Eastern Indian Ocean, 2017-2023

good practice. Contemporary guidance emphasizes distinguishing density and catchability covariates, incorporating spatial/temporal effects, and conducting uncertainty estimation beyond point predictions; adherence to these principles generally yields indices less prone to bias than raw CPUE (Maunder *et al.*, 2006; Hoyle *et al.*, 2024). Notwithstanding rigorous standardization, CPUE indices must be cross-verified against independent biological indicators, including size-frequency distributions, maturity stages, and sex ratios—under conditions of shifting fleet dynamics, given that behavioral redistributions of effort can decouple catch rates from absolute population abundance (Maunder *et al.*, 2006; Hoyle *et al.*, 2024). In the present case, the post-2018 decline in standardized CPUE, together with size truncation and sex skew, strongly suggests declining stock availability and abundance rather than improved catchability. This interpretation aligns with broader Indo-Pacific assessments that highlight the vulnerability of silky sharks to sustained exploitation and the need effective precautionary management measures to support long-term population stability and resilience (IOTC, 2025; Pacoureau *et al.*, 2021).

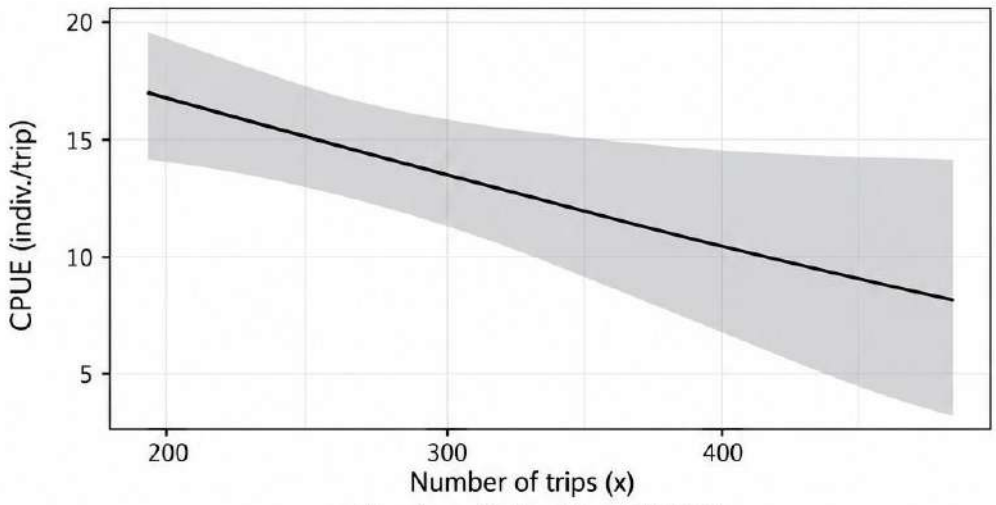

a. Number of trips (x) vs CPUE (y)

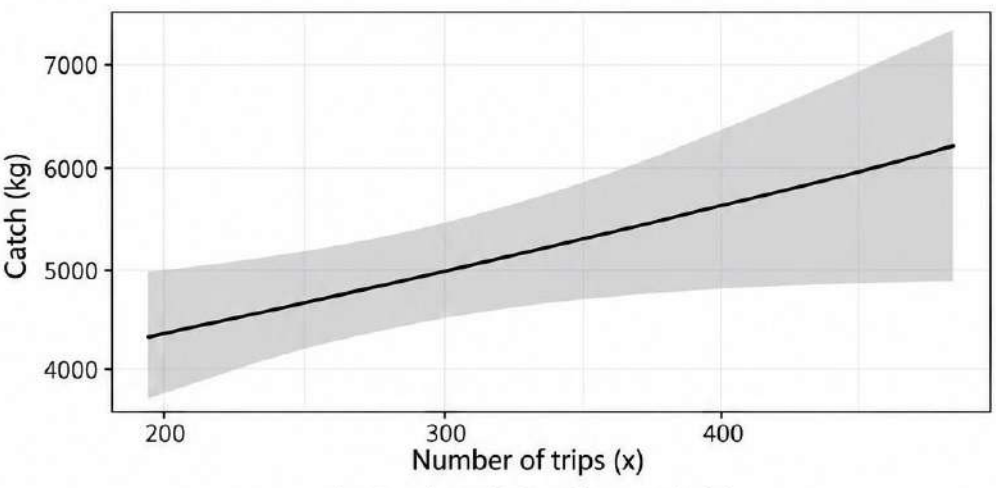

b. Number of trips (x) vs catch (y)

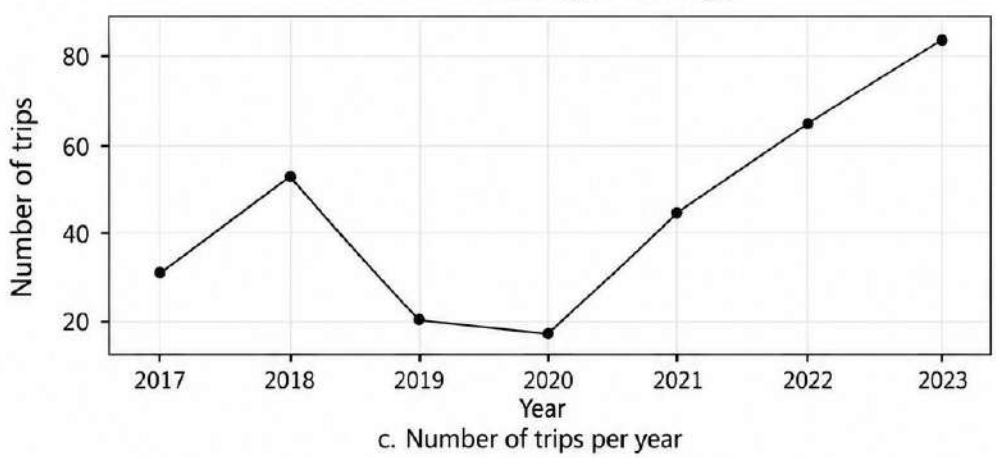

c. Number of trips per year

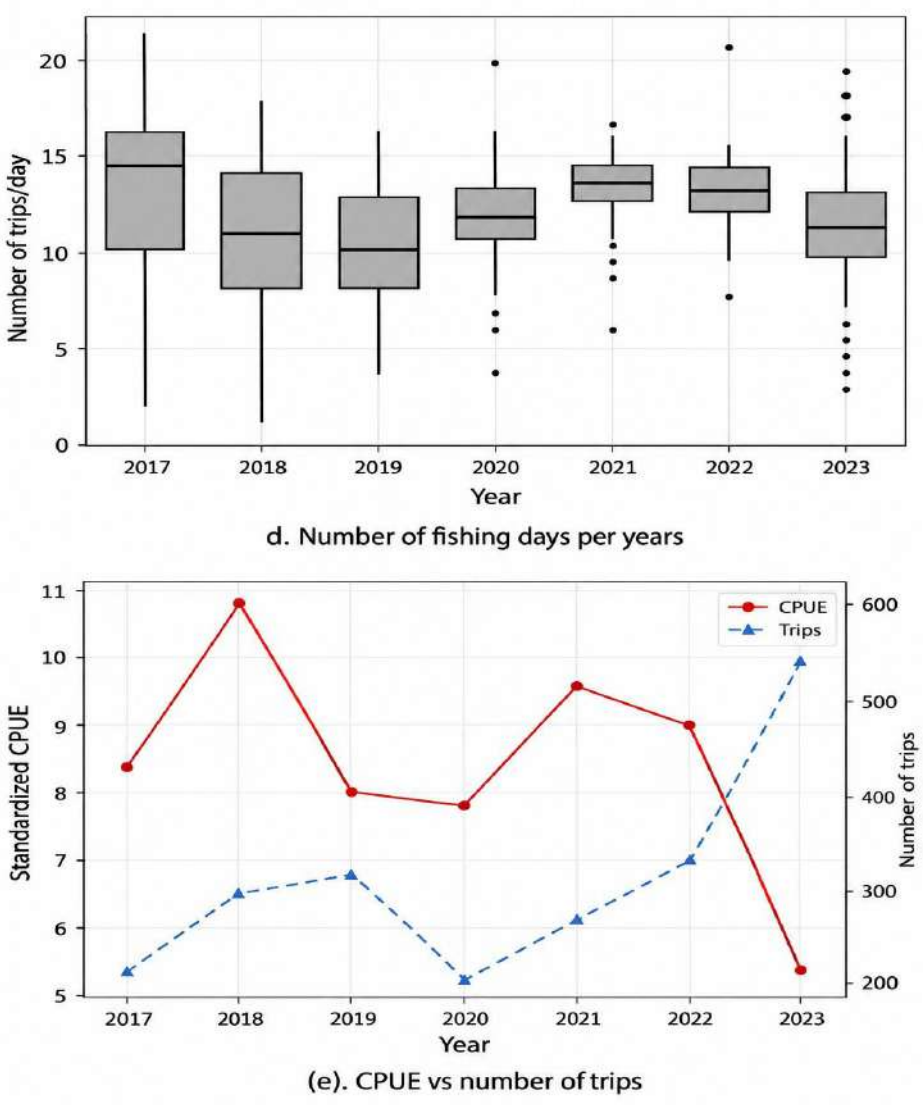

Fig. 6: Key indicators of silky shark fishery dynamics at Tanjung Luar, in the Eastern Indian Ocean

Fleet growth, effort redistribution, and effort creep

Operational signals from this study show that trip frequency increased while standardized CPUE declined, and total catch was maintained primarily by more trips and more boats rather than by stable per-trip efficiency (Figs. 4a and 5b). Such patterns are consistent with an effort-compensation behaviors frequently observed in fisheries experiencing stock depletion; as catch efficiency diminishes, fleets systematically scale up effort to sustain constant aggregate landings, notwithstanding the requirement for trip-level verification (Harley *et al.*, 2001; Maunder *et al.*, 2006). Simultaneously, growth in vessel numbers and shifts in trip characteristics can lead to spatial expansion or concentration of effort, increasing overlap with nursery grounds and migratory corridors. The literature terms the underlying process effort creep, technological and behavioral changes that raise effective fishing power relative to nominal effort, thereby biasing CPUE and potentially masking biological decline unless standardization explicitly accounts for spatial/temporal redistribution and targeting

(Campbell, 2004; Hoyle *et al.,* 2024). In Indonesia, the 2014 policy package, including the moratorium on ex-foreign vessels and the ban on at-sea transshipment, reduced industrial effort and re-shaped fleet behavior, with mixed short-term production effects but evidence of local fleet adjustments (more domestic vessels and trips) that can elevate exposure of oceanic/coastal shark habitats (Arthatiani and Apriliani, 2016; Zulbainarni *et al.*, 2022). Within this policy context, the trend of increasing landings through additional trips, coupled with diminishing returns per trip is both economically and biologically unsustainable. This observation is consistent with theoretical frameworks and case studies that indicate CPUE may appear stable or decline gradually even as fish abundance decreases, especially in fisheries characterized by aggregation (Harley *et al.*, 2001; Maunder *et al.*, 2006).

Management implications

The synthesis of biological, abundance, and operational indicators points to a fishery showing multiple precautionary warning signals. Length-based indicators suggest increasing representation of sub-mature individuals alongside a potential reduction in the contribution of large, older fish to commercial landings. Concurrently, standardized CPUE has exhibited a downward trajectory since 2018, despite concurrent increases in annual fishing trips and vessel counts, reflecting an effort-compensation pattern consistent with declining abundance (Maunder *et al.*, 2006; Campbell, 2004). The progressive loss of large females in length-frequency distributions is consistent with the declining CPUE index, together indicating reduced availability of mature individuals and erosion of reproductive potential under sustained fishing pressure. Seasonal CPUE peaks occurring in May and November point to distinct intervals of elevated catch rates, likely driven by increased catchability or stock availability—though any corresponding seasonal management measures implemented during these months should be rigorously validated against independent biological evidence prior to implementation (Simeon *et al.*, 2018; Curnick *et al.*, 2020). These converging signals require immediate, precautionary action. Building on these converging signals and the need for immediate precautionary action, a structured package of management measures must be implemented. First, seasonal closures or effort limitations during May and November are proposed as a precautionary hypothesis, given that these months consistently exhibit elevated CPUE metrics. Although catch rates in isolation do not definitively confirm the presence of spawning aggregations or concentration of mature females, these seasonal signals warrant rigorous investigation and could justify preliminary management trials. Second, the protection of mature females remains an important precautionary consideration, given their critical role in population recovery. Notwithstanding these considerations, the high prevalence of sub-mature specimens in the catch necessitates that size-selective regulations, including minimum landing sizes, maximum limits, or slot configurations, be critically appraised in light of empirical population structure. As a precautionary hypothesis, live-release protocols could be applied for individuals below the published maturity threshold (Lm50 ≈ 216 cm TL for females (Rigby *et al.,* 2021), with complementary gear modifications, particularly in surface longline fisheries to reduce capture rates and minimize haul-back and post-release mortality of large sharks (Joung *et al.*, 2008). Third, effective fishing effort must be strictly controlled and monitored to prevent further decline in stock abundance. Such measures necessitate comprehensive regulatory frameworks that extend beyond restrictions on vessel capacity and trip frequency to incorporate fine-scale variations in fishing power—including hook spacing, set density, and soak duration—thereby avoiding the pitfalls of relying exclusively on nominal effort metrics. Concurrently, spatio-

temporal standardization of CPUE must be maintained, with routine sensitivity analyses to ensure that abundance indices remain robust under changing fleet behavior and fishing strategies (Campbell, 2004; Hoyle *et al.*, 2024). Furthermore, monitoring frameworks must remain streamlined and practical. By institutionalizing sex-ratio and length recording, stratified by gear type and fishing area as core performance indicators, managers can better detect rebuilding of the upper-tail female size clusters essential for sustaining spawning potential. These signals can then be leveraged as near-real-time feedback to dynamically adapt seasonal fishing closures and size regulations (Grant *et al.*,2018; Maunder *et al.*, 2006). Given the post-2014 restructuring of Indonesian industrial fisheries (moratorium on ex-foreign vessels; transshipment ban) and stronger enforcement, local measures at Tanjung Luar should align with national and regional frameworks to avoid displacement and leakage (Arthatiani and Apriliani, 2016; Zulbainarni *et al.*, 2022). Since silky sharks exhibit high mobility and extensive migratory behavior, collaborative frameworks with the IOTC addressing bycatch mitigation, comprehensive data exchange for retained and discarded fractions, and synchronized regional surveillance are paramount to precluding the spatial displacement of fishing mortality that could erode localized conservation achievements (IOTC, 2025). In addition to local and national measures, international cooperation is indispensable. In the IOTC Area of Competence small juveniles of 120 cm and less (Clavareau *et al.*, 2020) are frequently taken as bycatch in industrial purse seine tuna fisheries setting on drifting FADs and subject to high on-board and post release mortality (Hutchinson *et al.*, 2015; Onandia *et al.*, 2021). Thereby, estimates from external studies suggest that purse seiners increase fishing-related mortality of juvenile silky sharks by approximately 100,000 animals per y (Ziegler, 2022; Ziegler, 2025), this estimate derives from sources external to the present study, while sub-adults and adults are removed by industrial and artisanal longliners and gillnetters. Finally, participatory implementation will determine durability. Co-designing the seasonal pilots programs with fishers, maintaining transparency in reporting, and supplying interim transition aid during closures collectively foster regulatory compliance and alleviate immediate socio-economic burdens, thereby reinforcing the conversion of ecological restoration into stable medium-term yields and economic returns (Simeon *et al.*, 2018; Zulbainarni *et al.*, 2022). In summary, this focused set of seasonal, sex-specific, and effort-based measures in the Eastern Indian Ocean silky shark fishery supported by pragmatic monitoring and regional coordination constitutes a clear and implementable pathway to halt decline and start rebuilding spawning biomass of silky sharks in the Eastern Indian Ocean.

CONCLUSION

This study demonstrates that the silky shark fishery in at the FMA 573 in the Eastern Indian Ocean is showing the sign of increasing vulnerability under sustained fishing pressure. Length-based metrics demonstrate that catches are heavily skewed toward immature specimens; coupled with the progressive scarcity of large females, this underscores a population truncation wherein older, larger cohorts contribute minimally to total landings. At the same time, standardized CPUE exhibited a persistent decline after 2018 despite increasing fishing effort, indicating that catch levels are being maintained through greater fishing activity rather than stable population productivity. The synthesis of these biological and fishery-dependent metrics underscores a growing dependency on annual recruitment pulses, signaling that the stock's long-term resilience to contemporary exploitation pressure is severely compromised. The findings highlight the importance of integrating biological indicators with standardized abundance indices to evaluate stock condition in data-limited shark fisheries. Particular priority should be given to monitoring

length-based indicators, including median total length, size-frequency distribution, proportion of individuals below length-at-maturity thresholds, representation of large mature size classes, and sex-specific length distributions. Such indicators furnish pragmatic early-warning signals regarding alterations in demographic structure, reproductive output, and exploitation dynamics across data-limited shark fisheries. Seasonal management measures, improvements in gear selectivity, and more comprehensive effort controls may provide opportunities to reduce mortality on vulnerable life stages and support stock recovery. It is essential to note that although the underlying data derive exclusively from landings at Tanjung Luar within FMA 573, the nomadic nature of silky sharks means that the associated fishing grounds encompass a much wider geographic distribution across various provincial waters within Indonesia's EEZ. The patterns identified herein represent localized signals from FMA 573 that may reflect broader exploitation pressures across the Eastern Indian Ocean basin. Given silky sharks' extensive migrations and transboundary exploitation, these fishery-dependent signals are specific to Tanjung Luar, highlighting localized vulnerabilities while acknowledging unresolved large-scale regional stock-status uncertainty and data gaps requiring monitoring, coordinated assessments, and improved regional fisheries information systems. Conservation outcomes will therefore depend not only on precautionary local implementation but also on alignment between national management actions and wider regional initiatives. Long-term sustainability will require a management approach that balances ecological objectives with the needs of fishing communities. Strengthening collaboration among fishers, managers, researchers, and regional institutions can improve compliance, support adaptive management, and enhance the effectiveness of conservation measures. Synthesizing these lines of evidence specifically, the contraction of standardized catch rates coupled with demographic shifts combined with changes in size and sex distributions, furnishes critical precautionary signals. These trends underscore an imperative for intensified surveillance, rigorous quantitative stock modeling, and adaptive regulatory frameworks designed to secure the long-term ecological persistence of the silky shark fishery across the Eastern Indian Ocean.

AUTHOR CONTRIBUTIONS

A. Budiarto conceived, design, and overseeing sample collection, and prepared the initial manuscript draft. B. Wiryawan reviewed the manuscript and provided critical feedback. I. Yulianto prepared the analysis data, interpreted the results, and assisted in manuscript preparation. A.A. Taurusman contributed to manuscript review and provided comments on the interpretation of results. M.D. Iskandar reviewed the manuscript and provided input on data interpretation. I. Ziegler contributed to the manuscript review and provided feedback on the discussion. S. Gigentika reviewed the manuscript and provided constructive comments. S. Agustina performed the statistical analysis, provided figure and table, and prepared the manuscript draft.

ACKNOWLEDGEMENT

The authors would like to thank the Wildlife Conservation Society Indonesia Program and Scientific Forum for Sustainable Fisheries in West Nusa Tenggara for providing support and data. This research was funded by Sustainable Fisheries and Communities Trust through Rekam Nusantara Foundation with Reference Number [267/SPK/YRJAN/VII/2024].

CONFLICT OF INTEREST

The authors declare that there is no conflict of interests regarding the publication of this manuscript. In addition, the ethical issues, including plagiarism, informed consent, misconduct, data fabrication and/or falsification, double publication and/or submission, and redundancy have been completely observed by the authors.

OPEN ACCESS

©2027 The author(s). This article is licensed under a Creative Commons Attribution 4.0 International License, which permits use, sharing, adaptation, distribution and reproduction in any medium or format, as long as you give appropriate credit to the original author(s) and the source, provide a link to the Creative Commons license, and indicate if changes were made. The images or other third-party material in this article are included in the article's Creative Commons license, unless indicated otherwise in a credit line to the material. If material is not included in the article's Creative Commons license and your intended use is not permitted by statutory regulation or exceeds the permitted use, you will need to obtain permission directly from the copyright holder. To view a copy of this license, visit: http://creativecommons.org/licenses/by/4.0/

PUBLISHER'S NOTE

GJESM Publisher remains neutral with regard to jurisdictional claims in published maps and institutional affiliations.

POSITIVE AI STATEMENT

During the preparation of this work the author(s) have used Artificial Intelligence (AI) Copilot and ChatGPT in order to rephrase and improve the paragraph as well as revise the R script. After using this tool/service, the authors reviewed and edited the content as needed and take full responsibility for the content of the publication.

ABBREVIATIONS

%	Percent
ABARES	Australian Bureau of Agricultural and Resource Economics and Sciences
ACIAR	Australian Centre for International Agricultural Research
AIC	Akaike Information Criterion
BL	Bottom longline
CC BY	Creative Commons Attribution
CITES	Convention on International Trade in Endangered Species of Wild Fauna and Flora
cm	Centimeter
CPUE	Catch-per-unit-effort
dFAD	Drifting fish aggregating device
DOI	Digital object identifier
EEZ	Exclusive economic zone
F	Female
FAD	Fish aggregating device
FAO	Food and Agriculture Organization of the United Nations
FG	fishing ground
Fig.	Figure
FL	Fork length
FMA	Fisheries management area
GAM	Generalized additive model
GAM-NB	Generalized additive model with negative binomial distribution
GJESM	Global Journal of Environmental Science and Management
GLM	Generalized linear model
GN	Gillnet
GT	Gross tonnage
HP	Horsepower
IOTC	Indian Ocean Tuna Commission
IUCN	International Union for Conservation of Nature
LFD	Length-frequency distribution
Lm	Length at maturity
m	Meter
M	Male
MMAF	Ministry of Marine Affairs and Fisheries
NA	Not available
NB	Negative binomial
NDF	Non-detriment finding
NTB	West Nusa Tenggara
NTT	East Nusa Tenggara
RAV	Record of Active Vessels
RFMO	Regional Fisheries Management Organization
SL	Surface longline
TL	Total length
WCPFC	Western and Central Pacific Fisheries Commission
WPEB	Working Party on Ecosystems and Bycatch
y	Years

REFERENCES

Arthatiani, F.Y.; Apriliani, T., (2016). Dampak kebijakan moratorium kapal eks asing terhadap kondisi perikanan tuna: studi kasus di DKI jakarta. Jurnal Kebijakan Sosial Ekonomi Kelautan dan Perikanan. 5: 71 **(8 pages).**

Campbell, R.A., (2004). CPUE standardisation and the construction of indices of stock abundance in a spatially varying fishery using general linear models. Fish. Res., 70(2–3) (**18 pages**).

CITES, (2016). CoP17 Proposal 42: Inclusion of *Carcharhinus falciformis* in Appendix II. Convention on International Trade in Endangered Species of Wild Fauna and Flora, Geneva. pp. 1–15 **(15 pages).**

Clavareau, L.; Sabarros, P.; Escalle, L.; Bach, P.; Abascal, F.; Lopez, J.; Murua, H.; Alayoón, P.J.; Ramos, M.; Ruiz, J.; Mérigot, B., (2020). Elasmobranch bycatch distributions and mortality: Insights from the European tropical tuna purse-seine fishery. Global Ecol. Conserv., 24: e01211. (**12 pages**).

Curnick, D.J.; Carlisle, A.B.; Gollock, M.; Schallert, R.J.; Hussey, N.E.; Chapple, T.K.; Tickler, D.M.; Block, B.A.; Jacoby, D.M.P., (2020). Behavior and ecology of silky sharks around the Chagos Archipelago and evidence of Indian Ocean-wide movement. Front. Mar. Sci., 7: 596619 (**18 pages**).

D'Alberto, B.; Patterson, H.; Bromhead, D., (2024). The influence of wire leaders and shark lines on shark bycatch in pelagic longline fisheries: A review and implications for the IOTC (ABARES Research Report 24.04). Canberra: Australian Bureau Agriculture Resources Economics and Sciences. (**32 pages**).

Dharmadi, F.; Fahmi. (2015). Pelagic shark fisheries of Indonesia's Eastern Indian Ocean Fisheries Management Region. Afr. J. Mar. Sci., 37(2): 249-258 **(9 pages).**

Dulvy, N.; Pacoureau, N.; Rigby, C.; Pollom, R.; Jabado, R.; Ebert, D.; Finucci, B.; Pollock, C.; Cheok, J.; Derrick, D.; Herman, K.; Sherman, C.; VanderWright, W.; Lawson, J.; Walls, R.; Carlson, J.; Charvet, P.; Bineesh, K.; Fernando, D.; Ralph, G.; Matsushiba, J.; Hilton-Taylor, C.; Fordham, S.; Simpfendorfer, C., (2021). Overfishing drives over one-third of all sharks and rays toward a global extinction crisis. Curr. Biol., 31(21): 4773-4787 (**27 pages**).

FAO, (2024). The State of World Fisheries and Aquaculture 2024: Blue Transformation in action. Food and Agriculture Organization of the United Nations, Rome, **(264 pages).**

Grant, M.; Smart, J.; White, W.; Baje, L.; Simpfendorfer, C., (2018). Life history characteristics of the silky shark Carcharhinus falciformis from the central west Pacific. Mar. Freshwater Res., 69(5): 562–573 (**12 pages**).

Hall, N.G., Bartron, C., White, W.T. Dharmadi, Potter, I.C., (2012). Biology of the silky Fish biol., 80(5): 1320-1341 **(22 pages).**

Harley, S.J.; Myers, R.A.; Dunn, A., (2001). Is catch-per-unit-effort proportional to abundance?. Canad. J. Fish. Aquat. Sci., 58(9): 1760-1772 (**13 pages**).

Heupel, M.R.; Simpfendorfer, C.A., (2014). Importance of environmental and biological drivers in the presence and space use of a reef-associated shark. Mar. Ecol. Progress Series. 496: 47–57 (**11 pages**).

Hinton, M.G.; Maunder, M.N., (2003). Methods for standardizing CPUE and how to select among them (SCRS/2003/034). Inter-American Tropical Tuna Commission. (**11 pages**).

Hoyle, S.D.; Campbell, R.A.; Ducharme-Barth, N.D.; Grüss, A.; Moore, B.R.; Thorson, J.T.; Tremblay-Boyer, L.; Winker, H.; Zhou, S.; Maunder, M.N., (2024). Catch per unit effort modelling for stock assessment: A summary of good practices. Fish. Res., 265: 106860 (**22 pages**).

Hutchinson, M.; Itano, D.; Muir, J.; Leroy, B.; Holland, K., (2015). Post-release survival of juvenile silky sharks captured in tropical tuna purse seine fishery. Mar. Ecol. Progress Series. 521: 143-154 (**12 pages**).

IOTC, (2025). Report of the 28th Session of the IOTC Scientific Committee. China, 1-5 December 2025. IOTC-2025-SC28-R[E]: 269 pp. (Appendix 27: Executive Summary Silky Shark. 194. (**269 pages**).

Joung, S.J.; Chen, C.T.; Lee, H.H.; Liu, K.M., (2008). Age, growth, and reproduction of silky sharks (Carcharhinus falciformis) in northeastern Taiwan waters. Fish. Res., 90(1-3): 78-85 **(8 pages).**

Lenth, R.V., (2023). emmeans: Estimated marginal means, aka least-squares means (Version 1.8.8) [R package]. CRAN. (**1 page**).

Li, C.Y.J.; Tsai, W.P.; Ranatunga, R.R.M.K.P.; Samidon, M.; Liu, S.Y.V. (2023). Genetic stock structure of the silky shark (Carcharhinus falciformis) in the Indo-Pacific Ocean. PLOS ONE. 18(10): e0292743 (**17 pages**).

Lo, N.C.H.; Jacobson, L.D.; Squire, J.L., (1992). Indices of relative abundance from fish spotter data based on delta-lognormal models. Canad. J. Fish. Aquat. Sci., 49(12), (**11 pages**).

Maunder, M.N.; Sibert, J.R.; Fonteneau, A.; Hampton, J.; Kleiber, P.; Harley, S.J., (2006). Interpreting catch per unit effort data to assess the status of individual stocks and communities. ICES J. Mar. Sci., 63(8): 1373-1385 (**13 pages**).

Mohamed, A.F.; Rezk, H., (2025). Neuro-fuzzy inference system and white shark optimization of coagulationflocculation of aquaculture wastewater treatment. Global J. Environ. Sci. Manage., 11(3): 857-874 **(18 pages).**

Murray, S.; Meeuwig, J.J.; Thompson, C.D.H.; Mouillot, D., (2023). Identifying the drivers of silky shark distribution and an evaluation of protection measures. Environ. Biol. Fish., 106: 1693-1713 (**21 pages**).

Pacoureau, N.; Rigby, C.L.; Kyne, P.M.; Sherley, R.B.; Winker, H.; Carlson, J.K.; Fordham, S.V.; Barreto, R.; Fernando, D.; Francis, M.P.; Jabado, R.W.; Herman, K.B.; Liu, K.M.; Marshall, A.D.; Pollom, R.A.; Romanov, E.V.; Simpfendorfer, C.A.; Yin, J.S.; Kindsvater, H.K.; Dulvy, N.K., (2021). Half a century of global decline in oceanic sharks and rays. Nature, 589(7843): 567–571 (**5 pages**).

Rigby, C.L.; Sherman, C.S.; Chin, A.; Simpfendorfer, C., (2021). Carcharhinus falciformis (amended version of 2017 assessment). The IUCN Red List of Threatened Species 2021: e.T39370A205782570. (**27 pages**).

Simeon, B.M.; Muttaqin, E.; Mardhiah, U.; Ichsan, M.; Dharmadi.; Prasetyo, A.P.; Fahmi.; Yulianto, I., (2018). Increasing abundance of silky sharks in the Eastern Indian Ocean: Good news or a reason to be cautious?. Fishes, 3(3): 29 (**12 pages**).

Talwar, B.S.; Semmens, B.X.; Aires-da-Silva, A.; Griffiths, S.; Humberstone, J.; Hutchinson, M.; Lopez, J.; Minte-Vera, C.; Ovando, D.; Román-Verdesoto, M.; Siu, S.; Bellquist, L.F., (2025). Informing the spatial management of silky shark (*Carcharhinus falciformis*) in the Eastern Pacific Ocean. Rev. Fish Biol.Fish., 35(4): 1031-1062 (**32 pages).**

Walter, J.F.; Ortiz, M., (2012). Derivation of the delta-lognormal variance estimator and recommendation for approximating variances for two-stage CPUE standardization models. Collective Volume of Scientific Papers ICCAT, 68 (1), (**5 pages**).

White, W.T.; Last, P.R.; Stevens, J.D.; Yearsley, G.K.; Fahmi.; Dharmadi., (2006). Economically important sharks and rays of Indonesia. ACIAR Monograph No. 124. Canberra: Australian Centre for International Agricultural Research (**338 pages**).

Wood, S.N., (2017). Generalized additive models: An introduction with R (2nd ed.). CRC Press. (**50 pages**).

Yulianto, I.; Booth, H.; Ningtias, P.; Kartawijaya, T.; Santos, J.; Sarmintohadi; Kleinertz, S.; Campbell, S.J.; Palm, H.W.; Hammer, C. (2018). Practical measures for sustainable shark fisheries: Lessons learned from an Indonesian targeted shark fishery. PLoS One, 13(11): e0206437 **(18 pages).**

Ziegler, I., (2022). Carcharhinus falciformis - A massive bycatch in the industrial purse seine industry but systematically underreported and deprived of any protection in the Indian Ocean. IOTC Working Party on Ecosystems, IOTC-2025-WPEB21(AS)-25 **(28 pages)**.

Ziegler I., (2025). Resolution 2025-08, an opportunity to step up science driven conservation and management measures for sharks in tuna and multi-species fisheries at IOTC. IOTC Working Party on Ecosystems and Bycatch, IOTC-2025-WPEB21(AS)-25 **(27 pages).**

Zulbainarni, N.; Sukarsih, Y.; Jahroh, S.; Abdullah, A., (2022). Economic valuation of moratorium and transhipment policy to tuna fisheries business, study case in Bitung, North Sulawesi. J. Manage. Agribisnis. 19(1): 79–92 **(14 pages).**

AUTHOR (S) BIOSKETCHES

Budiarto, A., Ph.D. Candidate, Department of Fisheries Utilization, Faculty of Fisheries and Marine Sciences, IPB University, Dramaga, Bogor, Jawa Barat, Indonesia.
- Email: *arisbudiarto@gmail.com*
- ORCID: 0000-0003-3741-5552
- Web of Science ResearcherID: NA
- Scopus Author ID: NA
- Homepage: https://kkp.go.id/

Yulianto, I., Ph.D., Researcher, Department of Fisheries Utilization, Faculty of Fisheries and Marine Sciences, IPB University, Dramaga, Bogor, Jawa Barat, Indonesia.
- Email: *irfan@rekam.or.id*
- ORCID: 0000-0003-4116-9171
- Web of Science ResearcherID: NA
- Scopus Author ID: 55557876500
- Homepage: www.rekam.org

Wiryawan, B., Ph.D, Professor, Department of Fisheries Utilization, Faculty of Fisheries and Marine Sciences, IPB University, Dramaga, Bogor, Jawa Barat, Indonesia.
- Email: *budywi@apps.ipb.ac.id*
- ORCID: 0000-0003-1958-5769
- Web of Science ResearcherID: QUU-5976-2026
- Scopus Author ID: 55845748300
- Homepage: www.ipb.ac.id

Taurusman, A.A., Ph.D, Associate Professor, Department of Fisheries Utilization, Faculty of Fisheries and Marine Sciences, IPB University, Dramaga, Bogor, Jawa Barat, Indonesia.
- Email: *azbas@apps.ipb.ac.id*
- ORCID: 0000-0002-8707-3223
- Web of Science ResearcherID: GNH-4493-2022
- Scopus Author ID: 56724229500
- Homepage: www.ipb.ac.id

Iskandar, M.D, Ph.D, Associate Professor, Department of Fisheries Utilization, Faculty of Fisheries and Marine Sciences, IPB University, Dramaga, Bogor, Jawa Barat, Indonesia.
- Email: *dahri@apps.ipb.ac.id*
- ORCID: 0009-0009-8930-6631
- Web of Science ResearcherID: NA
- Scopus Author ID: 57383494100
- Homepage: www.ipb.ac.id

Ziegler, I. Ph.D., Associate Professor German Foundation for Marine Conservation, Badstr. 4 81379 München, Germany.
- Email: *iris.ziegler@stiftung-meeresschutz.org*
- ORCID: 0009-0000-4535-111X
- Web of Science ResearcherID: NA
- Scopus Author ID: NA
- Homepage: https://www.stiftung-meeresschutz.org/leitbild/iris-ziegler-hai-und-fischereiexpertin/

Gigentika, S. Ph.D., Assistant Professor, Marine Science, Faculty of Agriculture, Mataram University; Scientific Forum for Sustainable Fisheries in West Nusa Tenggara, Indonesia.
- Email: *gigentika@unram.ac.id*
- ORCID: 0000-0002-9252-915X
- Web of Science ResearcherID: AAG-2639-2021
- Scopus Author ID: 57191169068
- Homepage: https://unram.ac.id/en/

Agustina, S., Master, Indonesia Ocean Program, Yayasan Konservasi Alam Nusantara, Indonesia.
- Email: *siska.agustina@ykan.or.id*
- ORCID: 0000-0003-0000-8072
- Web of Science ResearcherID: NFS-9587-2025
- Scopus Author ID: 57210140242
- Homepage: https://www.ykan.or.id/id/

HOW TO CITE THIS ARTICLE:
Budiarto, A.; Yulianto, I.; Wiryawan, B.; Taurusman, A.A. Iskandar, M.D.; Ziegler, I.; Gigentika, S.; Agustina, S., (2027). Environmental status of silky sharks in Eastern Indian Ocean from lengh-based catch data. Global J. Environ. Sci. Manage., 13(1): 141-162.

DOI: 10.22034/gjesm.2026.03.07
URL: https://www.gjesm.net/article_735644.html

Global Journal of Environmental Science and Management
(GJESM)

Homepage: https://www.gjesm.net/

Podcasts

ORIGINAL RESEARCH ARTICLE

The impact of environmental, economic, and social sustainability under intensive agriculture

S. Chandran[1], T. Ramachandran[2], D. Sivakumar[3,*], A. Ambika[4]

[1]School of Management Distance Education, SRM Institute of Science and Technology, Kattankulathur, Chennai 603203, Tamil Nadu, India

[2]Department of Management, College of Management, SRM Institute of Science and Technology, Kattankulathur, Chennai 603203, Tamil Nadu, India

[3]Department of Agricultural Engineering, Kalasalingam Academy of Research and Education, Krishnankoil, Virudhunagar 626126, Tamil Nadu, India

[4]Department of Electronics and Communication Engineering, B. S. Abdur Rahman Institute of Science and Technology, Vandalur, Chennai 600048, Tamil Nadu, India

ARTICLE INFO

Article History:
Received 10 April 2026
Revised 15 May 2026
Accepted 22 July 2026

Keywords:
Agro-chemicals
Economic impact
Environmental impact
Intensive cultivation
Societal impact
Sustainable development

ABSTRACT

BACKGROUND AND OBJECTIVES: Intensive agriculture has substantially increased agricultural productivity but is increasingly associated with environmental degradation, resource depletion, and socio-economic challenges. The study objectives were to evaluate the sustainability impacts of intensive agricultural practices across environmental, economic, and social dimensions in Namakkal district, Tamil Nadu, India, with particular emphasis on resource utilization, ecological stress, and the factors influencing sustainable agricultural development.

METHODS: Primary data were collected during 2025 from 663 eligible farmers selected through multistage stratified random sampling across eight taluks of Namakkal District using a structured questionnaire. Farms were classified as traditional or intensive based on cultivation practices. Relationships among the study variables were examined using correlation analysis, analysis of variance, regression analysis, and non-parametric statistical tests.

FINDINGS: The findings revealed a strong positive relationship between landholding size and family size (correlation coefficient = 0.7214), indicating close structural and demographic linkages within farming systems. Intensive agriculture was significantly associated with land expansion (correlation coefficient = 0.658), environmental pollution (correlation coefficient = 0.519), and declining health conditions among farming communities (correlation coefficient = 0.412). Approximately 63 percent of respondents reported land degradation, while 65 –78 percent reported salinity and nutrient depletion, reflecting perceived ecological stress. The regression model explained 7.1 percent of the variation in agricultural production (coefficient of determination = 0.071), indicating modest explanatory power. Questionnaire reliability was satisfactory (Cronbach's alpha = 0.824), supporting the internal consistency of the survey instrument.

CONCLUSION: Intensive agriculture is associated with higher short-term agricultural productivity but is also associated with environmental degradation, increases health risks, and places greater pressure on natural resources. These findings may inform strategies to improve the environmental, economic, and social dimensions of agricultural sustainability through sustainable soil management, balanced agrochemical application, efficient irrigation, and policy support. While the study is limited to a single district and cross-sectional data, it provides empirical evidence to inform future longitudinal and multi-regional investigations.

DOI:10. 22034.gjesm.2027.01.08

This is an open access article under the CC BY license (http://creativecommons.org/licenses/by/4.0/)

NUMBER OF REFERENCES	NUMBER OF FIGURES	NUMBER OF TABLES
37	7	10

*Corresponding Author:
Email: d.sivakumar@klu.ac.in
Phone: +91-9790973774
ORCID: 0000-0001-5228-0145

Note: Discussion period for this manuscript open until March 01, 2027 on GJESM website at the “Show Article”.

INTRODUCTION

Agriculture plays a crucial role in driving the economic growth and overall prosperity of a nation, particularly in India where nearly two-thirds of the population depends on it for livelihood despite ongoing structural changes in the economy. The agricultural sector is a major contributor to gross domestic product (GDP) and employment while ensuring food security and supplying raw materials to agro-processing, textile, and other agro-based industries. Its role extends beyond production, as it sustains rural livelihoods, promotes regional development, and contributes to environmental, social, and economic sustainability (Bathaei and Štreimikienė, 2023). The concept of sustainable development itself has long been subject to critical scrutiny regarding its definition, scope, and operational boundaries (Lélé, 1991), and bibliometric evidence confirms a growing body of global research adopting the environmental, economic, and social sustainability (triple bottom line) framework to evaluate sustainability outcomes. Increasing population pressure has intensified food demand, challenging agriculture to increase productivity while minimizing environmental degradation. However, conventional farming has caused ecological stress through excessive chemical inputs, groundwater depletion, and soil degradation. Declining agricultural growth directly affects GDP, employment, and poverty, destabilizing the national economy (Kaur, 2014). Indian agriculture faces major challenges despite growth opportunities. Financial constraints, market uncertainty, and economic reforms have increased farmer vulnerability and distress, including suicides (Mariappan and Zhou, 2019). Environmental concerns linked to chemical-intensive farming practices have been widely documented, particularly the degradation caused by excessive fertilizer use and the need for region-specific sustainable alternatives (Rosas Baños and García Salazar, 2026). Sustainability research emphasizes balancing natural resource use with productivity growth through increased cropped area, cropping intensity, and efficiency (Mózner *et al.,* 2012). Broader reviews of agricultural sustainability concepts and assessment methods further reinforce the multidimensional and evolving nature of these frameworks (Lampridi *et al.,* 2019). Further studies highlight India's broader sustainability challenges, including fragmented landholdings, climate change, technological gaps, and policy inefficiencies (Kareemulla *et al.,* 2017; Das *et al.,* 2020). At the micro level, studies in the district show crop diversification driven by profitability and market conditions, with shifts from tapioca to sorghum and maize. Extension services improve productivity and land use, while sustainability assessments emphasize integrated farm planning and resource optimization (Ramasubramaniyan *et al.,* 2016). Policy research also highlights sustainable input distribution, particularly biofertilizers, for long-term agricultural viability. Most previous research has examined environmental, economic, and policy aspects independently, with limited integration across these dimensions. Limited research integrates socio-economic factors, production intensity, and environmental degradation using large-scale primary data at the district level (Mózner *et al.,* 2012). Few studies also examine how government support interacts with farming intensity or assess environmental, economic, and social sustainability within a unified framework. Accordingly, this study adopts the triple bottom line framework, evaluating environmental (soil quality, pollution, and resource use), economic (cultivated area, production, income, and input use), and social (household characteristics, family labour, health, and institutional support) dimensions using primary data from 663 farmers. A key contribution of this research is the combined assessment of socio-economic, environmental, and production-related aspects of intensive agriculture using a single analytical approach. Using multiple established statistical methods, the study examines relationships between agricultural

intensity and sustainability outcomes, providing empirical evidence to support balanced agricultural planning and policy development (Rockström *et al.,* 2017; Ologunde and Nunes, 2026). Unlike previous studies that addressed these dimensions separately, this research integrates them within a district-level assessment. The environmental concerns associated with intensive agriculture, including soil degradation and excessive fertilizer use, are well documented (Lampridi *et al.,* 2019; Das *et al.,* 2020). This integrated approach addresses the limited availability of comprehensive empirical evidence from intensively cultivated regions such as Namakkal District. Integrated strategies combining policy support, efficient resource management, and eco-friendly farming are essential for long-term agricultural sustainability. Accordingly, this study evaluates the environmental, economic, and social dimensions of agricultural sustainability using the triple bottom line framework. The aims of the study are as follows: i) to analyze the socio-economic characteristics of farmers and evaluate the role of government support and policy interventions in promoting sustainable agricultural practices; ii) to examine the relationship between intensive agricultural practices and agricultural productivity, with particular emphasis on fertilizer, pesticide, and irrigation use; and iii) to assess farmers' reported environmental conditions associated with intensive farming and identify potential strategies for improving agricultural sustainability. This study was carried out at SRM Institute of Science and Technology, Chennai, Tamil Nadu, India, during 2025.

MATERIALS AND METHODS

Study area and research design

The study was conducted in selected talukas of an intensive agricultural region with high input use and diversified cropping systems, making it suitable for assessing agricultural sustainability (Bathaei and Štreimikienė, 2023). A descriptive and analytical research design was adopted to evaluate the environmental, social, and economic dimensions of sustainability (Kaur, 2014). Primary data on farming practices, resource use, input management, and institutional support were analyzed to examine the relationship between agricultural intensification and sustainability outcomes.

Sampling design

A multistage stratified random sampling technique was used to select respondents from Namakkal District, Tamil Nadu (11°00′–11°36′ N, 77°28′–78°30′ E). The district has a semi-arid tropical climate, receiving approximately 850–900 mm of annual rainfall and an average annual temperature of 28–30 °C. Intensive cultivation of tapioca, maize, sorghum, groundnut, and other field crops, supported by canal, tank, and groundwater irrigation, provides a suitable setting for assessing intensive agricultural systems. A pilot survey involving 40 farmers (approximately 6% of the final sample) was conducted to validate the questionnaire. The final sample of 663 farmers was determined using the Slovin method. Sampling involved three stages: selection of eight taluks (Namakkal, Rasipuram, Tiruchengode, Paramathivelur, Kolli Hills, Sendamangalam, Kumarapalayam, and Mohanur), identification of farmers from 454 villages, and proportionate random selection of respondents. Only farmers actively engaged in cultivation and farm management were included, ensuring representative coverage across farm categories and geographical areas of the district (Etikan and Bala, 2017).

Data collection procedure

Primary data were collected through a structured questionnaire administered to farmers in the selected villages. A total of 700 farmers were approached during the survey, of whom 20 farmers declined participation and 17 responses were excluded due to incomplete information.

Finally, 663 valid responses were considered for analysis, resulting in a response rate of 94.7%. The sampling approach ensured adequate representation of both traditional and intensive cultivation systems, classified based on farming practices such as fertilizer and pesticide use, irrigation intensity, cropping frequency, and cultivation characteristics, thereby capturing variability in agricultural practices and sustainability outcomes across the study area (Goswami *et al.,* 2017; Kareemulla *et al.,* 2017). The questionnaire was administered through field surveys among farmers practicing diverse cropping and irrigation systems. Responses covered farming practices, input use, environmental perceptions, production activities, and government support. The survey was designed to ensure clear, complete, and locally relevant information for assessing the environmental, economic, and social dimensions of agricultural sustainability.

Data type and variables

Both general and specific categories of data were collected to ensure a holistic understanding of agricultural systems. General data included demographic characteristics of farmers, such as age, education, gender, family structure, farming system classification, cropping intensity, and environmental perceptions related to agriculture. These variables were used to assess the socio-economic and structural characteristics of farming households, including crop output, input costs, total production value, and net farm income. They also provided information on economic performance, productivity, and input–output relationships under intensive and traditional farming systems (Mariappan and Zhou, 2019; Bobitan *et al.,* 2023).

Data processing and presentation

After data collection, all responses were systematically coded, categorized, and organized for analysis. The data were structured into tables to facilitate classification and comparison across different variables of agricultural sustainability. In addition, bar charts were used to visually represent key agricultural indicators, enabling clear interpretation of trends in farming practices, Bar charts were used to visually present key agricultural indicators, enabling clear interpretation of trends in farming practices, input usage, and sustainability-related outcomes (Rani *et al.,* 2021). This structured presentation ensured effective summarization of complex datasets and supported further statistical analysis and interpretation of relationships among environmental, social, and economic variables.

Development of research instrument

A structured questionnaire was developed based on the research objectives and sustainability framework to collect primary data on agricultural practices. It covered crop cultivation, crop rotation, pest management, organic farming, soil and water management, fertilizer and pesticide use, biodiversity conservation, energy use, socio-economic characteristics, awareness, government support, farming constraints, and future farming intentions. It provided comprehensive coverage of the environmental, economic, and social dimensions of agricultural sustainability (Mariappan and Zhou, 2019).

Questionnaire development and validation

A structured questionnaire was developed based on the study objectives and the agricultural sustainability framework. The questionnaire collected primary data on socio-economic characteristics, farming practices, environmental impacts, institutional support, and production factors. It was developed based on relevant literature and adapted to the agricultural conditions of Namakkal District. Subject experts reviewed the instrument to ensure content validity and clarity. A pilot survey was conducted to assess and improve the wording and sequence of the questions. The final questionnaire covered the key dimensions of agricultural sustainability. Construct validity was established by aligning the

variables with the sustainability framework, and internal consistency was confirmed using Cronbach's alpha (α) before statistical analysis (Parihar *et al.,* 2015; Mariappan and Zhou, 2019; Scheper *et al.,* 2023).

Questionnaire structure

The structured questionnaire was developed to collect primary data on socio-economic, farm-level, environmental, institutional, and production-related aspects of agriculture in the study area, ensuring comprehensive coverage of sustainable farming dimensions.

Personal information

Variables such as gender, qualification, age, number of family members involved in cultivation, and status of employment level in the family were collected to understand the socio-economic characteristics of farmers (Mariappan and Zhou, 2019).

Environmental impact

Environmental variables included characteristics of air, water, and soil affected by cultivation, loss of health standards due to intensive cultivation, loss of productivity of cattle and biodiversity, harmful chemical impacts on land quality, human health, cattle and biodiversity, and substitutes for chemical fertilizers and pesticides (Parihar *et al.,* 2015).

Government and institutional support

Variables included fiscal incentives from government budg*et a*llocations and institutional support mechanisms to manage environmental impacts of intensive cultivation (Ramasubramaniyan *et al.,* 2016).

Production and innovation

The indicators included increased land productivity from intensive cultivation, willingness to pay compensation for pollution, adoption of bio-fertilizers and bio-pesticides, ability to maintain production using eco-friendly inputs, soil nutrient depletion, soil quality deterioration, and the younger generation's interest in technology-driven and innovative farming practices (Scheper *et al.,* 2023). Table 1 presents the questionnaire components structured based on the study framework, covering the key dimensions of personal information, farm characteristics, environmental impacts, government and institutional support, and production and innovation aspects of agricultural practices.

Measurement scale, coding procedure, and reliability assessment

Environmental impact, government and institutional support, production and innovation, and farmers' sustainability perceptions were assessed using a five-point Likert scale ranging from 1 (strongly disagree) to 5 (strongly agree), where higher scores indicated stronger agreement. A pilot study involving 40 farmers from marginal, small, medium, and large farm categories was conducted to assess the clarity and suitability of the questionnaire. Responses were numerically coded before statistical analysis. Categorical variables (gender, education level, farming category, cultivation system, and irrigation pattern) were coded according to their response categories, whereas continuous variables (age, cultivated area, production, income, and input usage) were recorded in their original values. Likert-scale responses were coded from 1 to 5, and composite construct scores were calculated by averaging the corresponding item responses to ensure consistency across measures and facilitate subsequent statistical analysis and interpretation. The internal consistency and reliability of the measurement scale were assessed using the α coefficient. The overall reliability value (α = 0.824) indicated satisfactory internal consistency among the questionnaire items. Reliability was evaluated before statistical analysis to ensure the consistency and suitability of the measurement instrument for capturing the intended constructs and supporting subsequent empirical analysis of the study.

Table 1: Questionnaire components based on study framework

Section	Variables included (from study instrument)
Personal Information	Gender, qualification, age, number of family members involved in cultivation, status of employment level in the family.
Farm Characteristics	Total area of cultivation, type of land pattern, crop pattern (major and minor crops), irrigation pattern, traditional vs. intensive cultivation, annual income
Environmental Impact	Air, water, soil characteristics affected by cultivation, health impacts, livestock productivity loss, biodiversity loss, harmful chemical effects, substitutes for fertilizers and pesticides.
Government and Institutional Support	Fiscal incentives from government budget, institutional support for environmental management in intensive cultivation.
Production and Innovation	Increase in production, willingness to pay compensation for pollution, production using bio-fertilizers, willingness to switch to bio-inputs, soil nutrient depletion, youth technological adoption.

Sustainability challenges framework

The sustainability of the agricultural sector is shaped by interrelated environmental, social, and economic constraints that collectively influence farming systems and long-term productivity outcomes (Mariappan and Zhou, 2019; Scheper *et al.,* 2023). In this context, a structured framework of challenges has been developed to better understand the multidimensional pressures affecting agriculture in the study region, as presented in Table 2. Table 2 shows that environmental degradation in agriculture is mainly associated with soil erosion, resource depletion, and chemical pollution, reducing ecosystem health and agricultural productivity. Social challenges such as unemployment, migration, and labour shortages increase the vulnerability of farming communities. Economic challenges, including indebtedness, limited market access, and low livelihood security, reduce agricultural resilience. These findings highlight the need for integrated strategies that improve environmental, social, and economic sustainability.

Environmental assessment indicators

Environmental indicators were evaluated using farmers' perceptions and field observations collected through a structured questionnaire rather than laboratory or instrumental measurements. The survey captured farmers' perceptions of soil quality, land degradation, salinity, water quality, contamination, climatic variation, and the environmental effects of intensive farming. Particular emphasis was given to fertilizer use and its perceived effects on soil and water resources. These perception-based indicators were used to evaluate the environmental impacts of intensive agricultural practices within the study area (Ju *et al.,* 2007). The environmental indicators were derived from farmers' responses to the structured questionnaire. They reflect farmers' observations and perceptions rather than direct measurements of soil, water, or climatic conditions.

Analytical framework

The analytical framework was based on a cause–effect approach to examine how intensive agricultural practices, government support, farmers' awareness, and market price fluctuations influence agricultural sustainability. The study adopted the triple bottom line framework, incorporating environmental, economic, and social dimensions. Environmental sustainability comprised fertilizer application, soil and land quality, pollution, climatic conditions, and land-use patterns, reflecting farmers' perceptions of environmental pressures and resource conditions within the agricultural production system. Economic sustainability considered government support, cultivation area, production, fertilizer and pesticide use, irrigation practices, and marketable surplus. Social sustainability included farmers' socio-economic characteristics, family labour participation, and perceived health impacts of intensive cultivation. These dimensions were integrated to provide a comprehensive sustainability assessment (Lampridi *et al.,* 2019).

Table 2: Challenges for the sustainability of the agricultural sector in the current context

Environmental perspective	Social perspective	Economic perspective
Eutrophication, erosion, landslides, flooding, clogging of irrigation channels, crop failure, and deforestation.	Unemployment due to rainfall variability, water scarcity, and labour shortage.	Burden of loans and accumulation of bad debts.
Depletion of resources; pollution and greenhouse gas emissions from chemical fertilizers affecting water, soil, and air.	Marketable surplus issues and lack of stable markets.	Inability to meet basic livelihood requirements and lifestyle maintenance.
Insufficient irrigation and electricity resources.	Migration of farmers to urban areas.	Difficulty in supplying food for increasing population demand.

Ethical considerations

This study involved a questionnaire-based survey of farmers and did not include any clinical interventions or collection of sensitive personal information. Prior to data collection, all participants were informed about the objectives and purpose of the study, and informed consent was obtained before participation. Participation was voluntary, and respondents were assured of the confidentiality and anonymity of their responses. The collected data were used solely for research purposes in accordance with institutional and ethical guidelines.

Statistical analysis

The collected data were analyzed using multiple statistical techniques to evaluate agricultural sustainability. Analysis of variance (ANOVA) was used to examine relationships in intensive cultivation practices and test the research hypotheses. The assumptions of normality, homogeneity of variance, independence, linearity, and multicollinearity were assessed before analysis. The Mann–Whitney U test (Z-test) compared traditional and intensive farming systems, while the Kruskal–Wallis H test (H-test) assessed the relationship between agricultural production and environmental pollution. The % analysis examined the distribution of respondents across categories. Row-wise analysis, together with mean, standard deviation (SD), and Pearson correlation (r), was used to identify variable relationships. Regression analysis determined factors affecting agricultural production, and the Chi-square (χ^2) test evaluated the impact of government support on farming outcomes (James *et al.,* 2013). Collectively, these statistical tools enabled a comprehensive and multi-dimensional assessment of agricultural sustainability.

RESULTS AND DISCUSSION

Socio-economic and farm profile characteristics

The socio-economic and farm characteristics of respondents provide a foundation for understanding agricultural decision-making and sustainability in the study area. Household structure, demographic profile, education, and farm size influence farming practices, resource use, productivity, and adaptation strategies. Fig. 1 presents the % analysis of the distribution of respondents' responses across key socio-economic and farm profile variables. Gender composition (Fig. 1a) shows male dominance at 93% (617 individuals) and female participation at 7% (46 individuals). This distribution reflects unequal access to agricultural resources, land ownership, and decision-making roles, indicating structural gender disparity within farming systems. Female participation remains limited, suggesting constrained participation in formal agricultural activities and farm management processes (Goswami *et al.,* 2017). Age distribution (Fig. 1b) indicates concentration in older cohorts, with 40–50 years at 38% and above 50 years at 29.9%. The 21–30 years group accounts for 12.7%, while the 15–20 years category shows no representation. This pattern reflects an ageing farming population and limited youth involvement

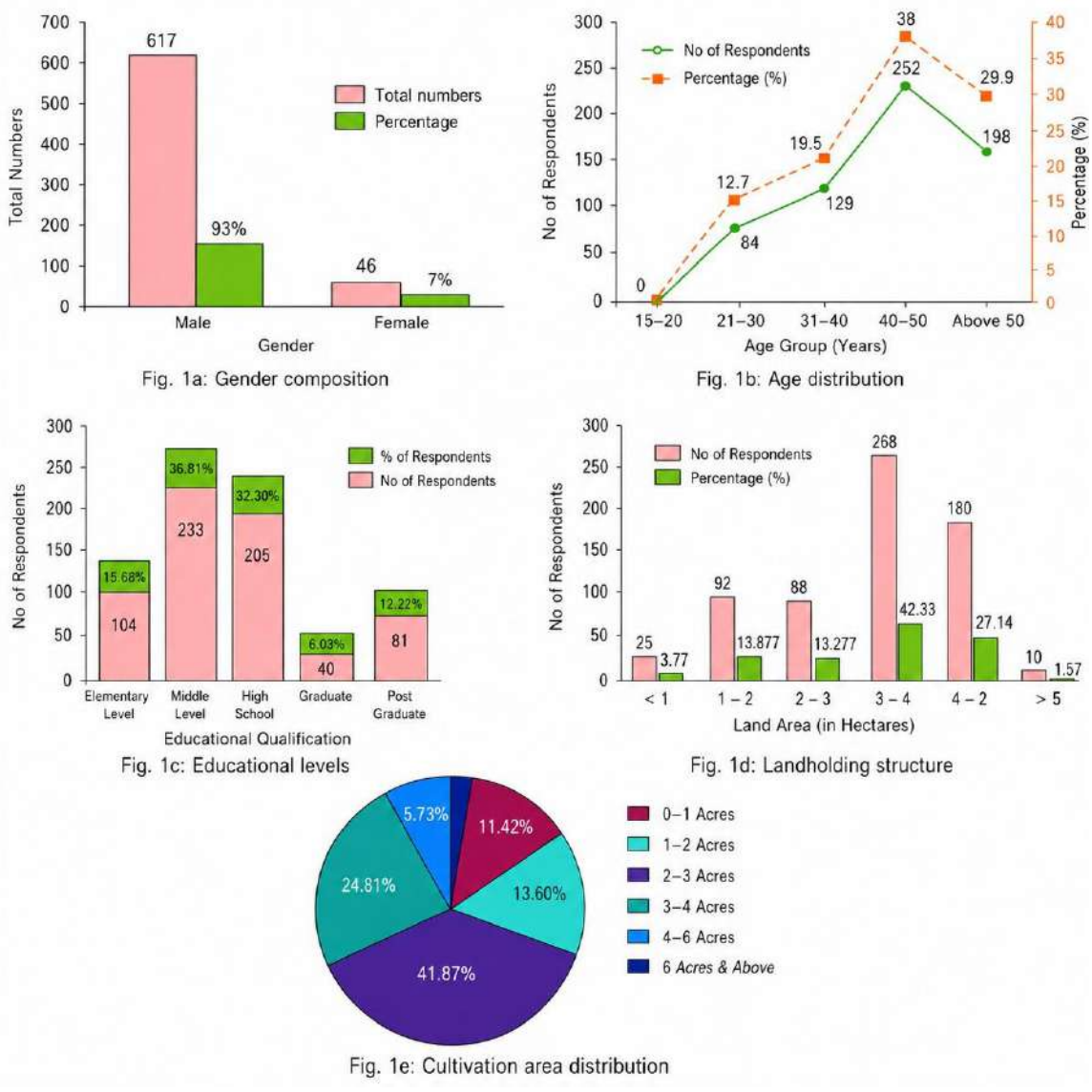

Fig. 1: The distribution % of respondents' responses

indicate potential challenges for labour continuity and innovation adoption in agriculture (Kareemulla *et al.,* 2017). Educational levels (Fig. 1c) are dominated by middle education at 35.11% and high school at 32.39%. Postgraduate qualification accounts for 12.22%, while graduates represent 6%. The distribution was dominated by respondents with basic education, while higher educational attainment remained limited, reflecting a mixed knowledge system combining experiential and formal agricultural understanding. Landholding structure (Fig. 1d) shows 3–4 hectares (ha) at 42.33% and 4–5 ha at 27.14%. Small holdings below 1 ha constitute 3.77%, while holdings above 5 ha account for 1.57%. The pattern indicates dominance of medium-scale farming units with relatively uniform operational capacity and similar resource requirements across respondents, reflecting strong dependence on landholding and livelihood

assets. Cultivation area distribution (Fig. 1e) shows dominance of 3–4 ha and above 4 ha categories. The 0–1 ha category accounted for the smallest proportion, whereas the 1–2 ha and 2–3 ha categories represented intermediate shares. The pattern indicates prevalence of medium to large-scale cultivation systems, suggesting higher operational capacity and dependence on household labour within semi-uniform farming structures. Fig. 1 shows that most respondents were male, middle-aged, and had moderate educational levels. Most farms ranged from 1–4 ha, with strong dependence on household labour. Limited participation of youth and women reflects the characteristics of smallholder farming systems and may influence sustainability outcomes across the study area.

Relationship between family size, income and area of cultivation

A cross-sectional analysis was conducted to examine the association between household demographic structure, income levels, and landholding patterns among the farming community.

Family size and area of cultivation:

Table 3 presents the distribution of family size across different categories of land area under cultivation in ha among the study respondents, highlighting the relationship between household composition and landholding structure within the agricultural system. Table 3 shows that 31% of landholdings were marginal farms below 3 ha, while 69% were small and medium farms of 3 ha and above. The average landholding size was approximately 3.3 ha, indicating the predominance of medium-scale farming. Family size showed a positive correlation with landholding size (r = 0.7214), suggesting that larger households generally managed larger farms. This relationship is likely associated with greater family labour availability but does not necessarily imply higher farm productivity or more efficient agricultural resource utilization.

Agricultural dependency

Table 4 presents the distribution of annual income across different categories of area under cultivation among the study respondents, illustrating the relationship between farm size and income levels within the agricultural system. From Table 4, it may be observed that the income pattern shows that 36% of farmers earn above United States Dollars (USD) 1,170 annually, while a substantial proportion remains within lower income categories, reflecting financial instability linked with inefficient cost management (Bobitan *et al.,* 2023). Higher income levels were generally associated with larger landholdings, whereas lower incomes were more common among small and marginal farmers. The income distribution indicates economic differences across farm categories, reflecting unequal resource availability. These findings highlight the need to strengthen market access and income opportunities for smaller farms.

Environmental sustainability and related factors

Environmental sustainability was assessed using indicators related to fertilizer application, soil quality, land quality, climatic conditions, pollution, and land-use patterns. The assessment was based on farmers' responses collected through a structured questionnaire instead of direct field or laboratory measurements. Therefore, the results represent farmers' perceptions of environmental changes associated with intensive agricultural practices. In the study area, respondents identified fertilizer application, land quality, and land-use patterns as the main factors affecting soil health, climatic conditions, and ecological stability. The following sections present the environmental assessment derived from responses from 663 farmers. These findings should be interpreted as perception-based observations rather than directly measured environmental parameters, providing context for locally perceived environmental pressures, degradation, and sustainability challenges in agricultural systems.

Table 3: Family size by landholding category in ha

Land area (ha)	Up to 2	3	≥ 4	Total
< 1	17	8	2	27
1 – 2	55	12	25	92
2 – 3	16	50	22	88
3 – 4	32	150	86	268
≥ 4	14	49	125	188
Total	134	269	260	663

Table 4: Distribution of annual income across different categories of area under cultivation

Annual income (USD)	Up to 2 ha	2 – 4 ha	Above 4 ha	Total
Up to 292	48	48	24	120
292–585	8	83	9	100
585–877	48	63	17	128
877–1,170	7	52	20	79
Above 1,170	6	110	120	236
Total	117	356	190	663

Note: Annual income categories were converted from Indian Rupees (₹) to United States Dollars (USD) using the average 2025 exchange rate (US$1 = ₹85.50) to facilitate international comparison.

Effect of fertilizer application on soil quality

Fig. 2 presents farmers' reported perceptions of soil salinity associated with different fertilizer types. Respondents most frequently associated ammonium sulphate with increased soil salinity (116 responses), followed by potassium fertilizer (98 responses). Urea was associated with 66 cases of nutrient deficiency and 62 cases of salinization, while phosphate fertilizer shows 30 salinization and 15 nutrient deficiency cases. Nitrogenous fertilizer records 15 salinization cases, and natural fertilizer shows 58 salinization and 12 deficiency cases. These results align with 24% soil organic carbon (SOC) reduction and 40% microbial biomass decline (Bonanomi *et al.,* 2011) and 25–75% carbon depletion (Lal, 2013), consistent with recent evidence that Intensive agricultural practices increasingly accelerate soil degradation (Al-Sammarraie and Kaplan, 2025) and that such degradation constitutes a pressing global environmental concern (Bünemann *et al.,* 2018). Present findings indicate 65–78% nutrient depletion and 63% land degradation, reflecting substantial soil deterioration. Farmers' perceptions indicated that prolonged intensive fertilizer application was associated with increased soil salinity, nutrient imbalance, and reduced soil quality.

Effect of fertilizer application on land quality and environmental conditions

Farmers' perceptions of land quality reflected the cumulative effects of agricultural inputs on soil, water, and surrounding environmental conditions. Fig. 3 shows contamination as the dominant impact with 519 out of 663 responses, followed by bad smell (62), turbidity (37), loss of biochemical oxygen demand (BOD) (26), and colour change (19), consistent with environmental pollution under high agrochemical usage (Mengel, 1993; Jwaideh and Dalin, 2025). Fertilizer-wise analysis showed that diammonium phosphate (DAP) recorded the highest contamination (147), followed by urea (130) and potassium fertilizer (118). Ammonium sulphate caused 36 contamination cases with turbidity and BOD impacts, while phosphate fertilizer caused 21 contamination and 19 bad-smell cases; nitrogenous fertilizer had minimal effects. These findings align with the ecological impacts observed under intensive farming systems (Mózner *et al.,* 2012). The study found a significant positive correlation between intensive farming and environmental pollution (r = 0.519), indicating that increased chemical fertilizer use is associated with soil salinization, land degradation, and environmental degradation.

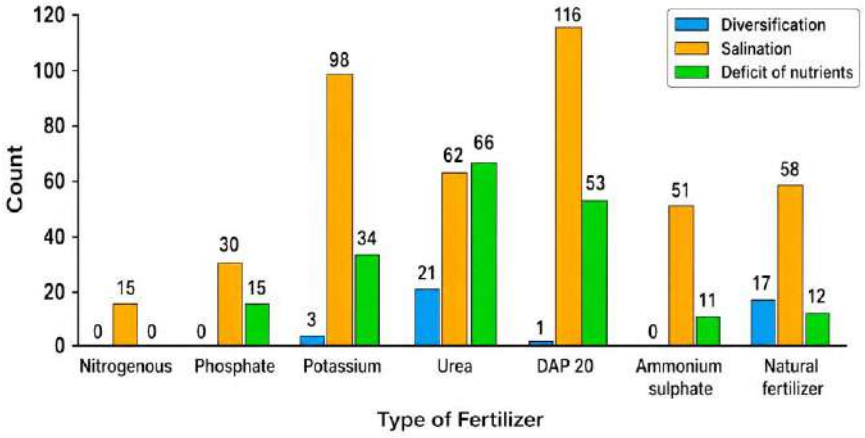

Fig. 2: Distribution of soil quality impacts of fertilizer application

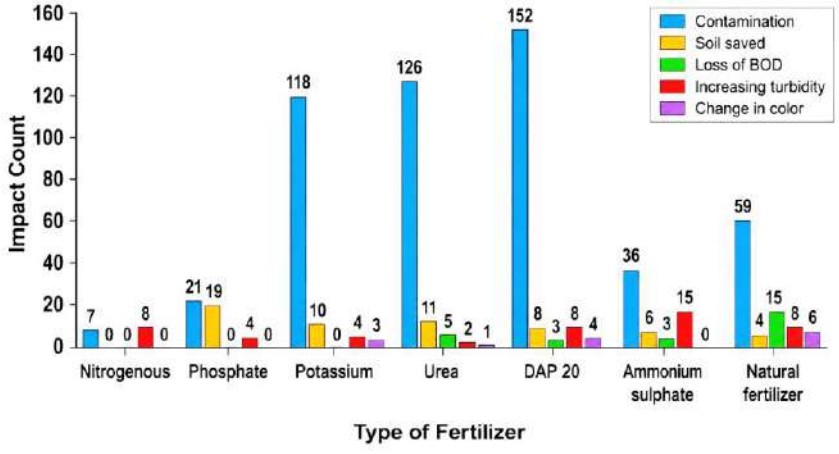

Fig. 3: Distribution of environmental and land quality impacts of fertilizer application

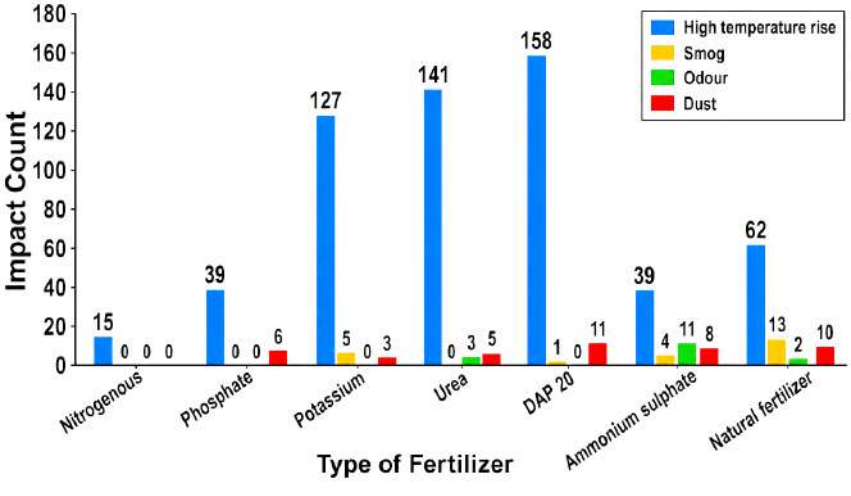

Fig. 4: Distribution of climatic impacts of fertilizer application

Effect of fertilizer application on climatic conditions

Climatic conditions in agricultural regions are increasingly associated with chemical input use, particularly fertilizers that affect temperature, air quality, and particulate emissions. Fig. 4 shows high temperature rise as the dominant effect with 581 out of 663 responses, followed by dust formation (43), smog occurrence (23), and odour impacts (16), consistent with climate impacts linked to soil carbon depletion of 25–75% (Lal, 2013; Imelda and Hidayat, 2024). Fertilizer-wise distribution showed that DAP recorded the highest number of temperatures rise cases (158), followed by urea (141) and potassium fertilizer (127). Ammonium sulphate showed combined effects on temperature, smog, odour, and dust, whereas natural fertilizer showed relatively moderate impacts. These findings are consistent with reports that abiotic stresses, such as salinity, reduce crop productivity (Parihar *et al.,* 2015). Farmers also perceived increased temperature and moisture stress under intensive farming. However, these results are based on farmers' perceptions and statistical analysis, not direct climatic measurements. Therefore, the present study does not establish a causal relationship between fertilizer use and temperature change.

Land pattern and area of cultivation

Land use patterns provide insight into environmental conditions, agricultural intensity, and resource distribution across the study region. Fig. 5 shows terrestrial barren land as the predominant land-use category with 356 out of 663 responses, followed by wet land (203), grassland (46), fallow land (37), and other land (21). Area-wise distribution indicates the highest concentration within the 2–4 ha category (356), followed by above 4 ha (190) and up to 2 ha (117), indicating predominance of medium-scale farming systems. This pattern reflects semi-arid conditions and land-use pressure, consistent with enhanced land-use utilization under intensive systems (Adhikari *et al.,* 2017) and irrigation-induced instability and land-use changes (Bosco and Simeoni, 2018; Ologunde and Nunes, 2026), while also indicating that expansion of cultivated area under intensive practices contributes to increased resource exploitation and ecological imbalance. The present findings revealed a strong positive correlation between intensive farming and cultivated land expansion (r = 0.658), consistent with increased land-use pressure and environmental stress associated with intensive agricultural systems (Adhikari *et al.,* 2017).

Farmers' perceptions of environmental impacts of intensive cultivation

Farmers' perceptions indicated that intensive agriculture was associated with environmental concerns. About 78% of respondents linked land contamination to chemical fertilizer use, while 65% associated soil degradation with salinization caused by intensive fertilizer application. In addition, 13% reported that natural fertilizers alone were insufficient for achieving satisfactory crop production. These findings suggest that excessive fertilizer use is perceived to adversely influence soil conditions in intensive farming systems (Ju *et al.,* 2007). Soil quality deterioration associated with continuous input-intensive agricultural practices has also been widely documented, highlighting its adverse effects on soil health and ecosystem functions (Bonanomi *et al.,* 2011; Bünemann *et al.,* 2018). The present findings indicate that intensive agriculture is associated with natural resource degradation through excessive input use. However, the current results are based on farmers' perceptions rather than direct soil or water measurements. They reflect perceived environmental stress and highlight the need for integrated nutrient management and sustainable intensification (Kaur, 2014; Rockström *et al.,* 2017).

Statistical analysis for integrated triple bottom line sustainability

A combination of statistical techniques was used to evaluate the environmental, economic, and

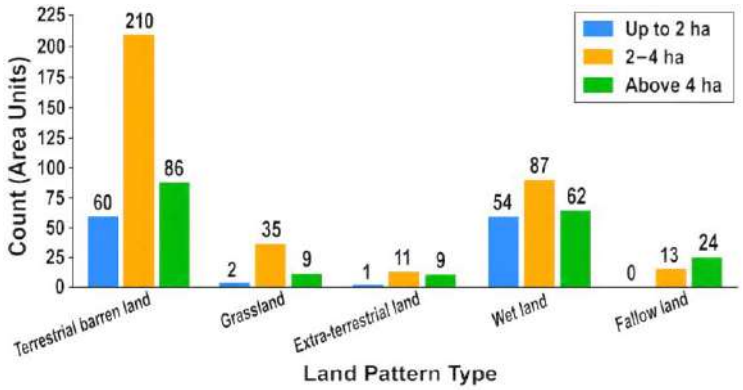

Fig. 5: Distribution of land patterns across different categories of area under cultivation

Table 5: Combined ANOVA results on agricultural sustainability variables

Source of variation	Sum of squares (SS)	Degrees of freedom (df)	Mean square (MS)	F-value	p-value	Effect size (η^2)
Government support and intensive cultivation						
Between Groups	35380.916	18	1965.606	8.998	< 0.001***	0.021
Within Groups	140680.65	644	218.448			
Total	176061.56	662				
Area of cultivation to intensive cultivation						
Between Groups	16144.933	6	2690.822	11.038	< 0.001***	0.092
Within Groups	159916.63	656	243.775			
Total	176061.56	662				
Health impact of intensive cultivation						
Between Groups	159.11	170	0.936	16.981	< 0.001***	0.854
Within Groups	27.119	492	0.0551			
Total	186.229	662				
Pollution due to intensive cultivation						
Between Groups	1661.255	170	9.772	15.619	< 0.001***	0.844
Within Groups	307.915	492	0.626			
Total	1969.17	662				

Note: Total degrees of freedom were calculated as $N - 1$ (N = 663); *p < 0.05; **p < 0.01; ***p < 0.001.

social dimensions of sustainability under intensive cultivation. The triple bottom line framework was adopted to examine relationships among agricultural practices, production, government support, environmental conditions, and social outcomes. ANOVA compared sustainability indicators across groups (Table 5). Pearson correlation (r) was used to assess relationships among continuous variables, and multiple regression was performed to evaluate the effects of fertilizer type, pesticide type, and irrigation pattern on agricultural production. The Z-test was applied to compare marketable surplus between traditional and intensive cultivation systems, while the χ^2 test and H-test examined associations among categorical variables and pollution-related responses, respectively.

ANOVA analysis

ANOVA was used to examine differences in key agricultural sustainability variables across intensive cultivation groups. Intensive cultivation categories were treated as grouping variables, while government support, area of cultivation, perceived health impacts, and perceived pollution were considered dependent variables. The analysis was based on 663 respondents with df = 662 (N − 1). It was used to determine whether differences among the variables were statistically significant within the study area. Table 5 shows

the combined ANOVA results, indicating significant differences among agricultural sustainability variables related to intensive cultivation.

Government support and intensive cultivation

It may be observed from Table 5 that the ANOVA results indicate a statistically significant relationship between government support measures and intensive cultivation, with an F-value of 8.998 and significance level of $p < 0.001$. The corresponding $\eta^2 = 0.201$ indicates a large practical effect, suggesting that government support explains approximately 20.1% of the variation in intensive cultivation practices. These findings are consistent with the role of policy interventions and institutional frameworks in influencing sustainability outcomes (Das *et al.,* 2020). The higher mean square (MS) between groups compared to the within-group mean square suggests that variations in government policies, subsidies, and institutional assistance significantly influence the adoption and intensity of cultivation practices, aligning with stakeholder-based governance approaches (Gillund *et al.,* 2016). This confirms that government support acts as a key determinant in shaping agricultural intensification patterns, with the present findings indicating a positive association between government support and the adoption of sustainable practices across respondent groups.

Area of cultivation and intensive cultivation

It may be observed from Table 5 that the analysis shows a significant impact of cultivated land area on intensive cultivation, with an F-value of 11.038 and $p < 0.001$. The corresponding effect size ($\eta^2 = 0.092$) indicates a moderate practical effect, suggesting that cultivated land area explains approximately 9.2% of the variation in intensive cultivation practices. These findings are consistent with the expansion of cultivated area under agricultural intensification (Adhikari *et al.,* 2017). The results indicate that farm size significantly influences agricultural intensification. Larger landholdings generally require greater inputs, labour, and management. The significant variation among groups suggests that cultivated area is an important factor influencing agricultural management practices and the level of intensification.

Social sustainability perceived health impacts of intensive cultivation

Social sustainability was examined through farmers' socio-economic characteristics, family labour participation, perceived health impacts, and institutional support. These indicators provide an understanding of how intensive agriculture influences farmers' livelihoods, well-being, and social conditions. It may be observed from Table 5 that the ANOVA results reveal a highly significant association between intensive cultivation categories and perceived health impacts, with an F-value of 16.981 and $p < 0.001$. The corresponding effect size ($\eta^2 = 0.854$) indicates a large practical effect, demonstrating that intensive cultivation explains approximately 85.4% of the variation in perceived health impacts. This finding is consistent with evidence linking pesticide exposure to chronic diseases, including cancer and neurological disorders (Horrigan *et al.,* 2002; Rani *et al.,* 2021). Perceived pollution responses were significantly associated with intensive cultivation categories ($F = 15.619$, $p < 0.001$). These results reflect farmers' perceptions rather than direct health or environmental measurements. Respondents consistently perceived that intensive cultivation, particularly the use of chemical inputs, was associated with adverse health and environmental effects. A moderate positive correlation ($r = 0.412$) was observed between intensive agricultural practices and perceived health impacts (Rani *et al.,* 2021).

Pollution due to intensive cultivation

It may be observed from Table 5 that the findings show a significant relationship between intensive cultivation and pollution levels, with an F-value of 15.619 and $p < 0.001$. The corresponding effect

size (η^2 = 0.844) indicates a large practical effect, suggesting that intensive cultivation accounts for approximately 84.4% of the variation in pollution levels. These findings are consistent with evidence of environmental contamination characterized by nutrient losses of up to −53 kilograms per hectare per year (kg/ha/y) and phosphorus surplus of up to 18.1 kg/ha/y (Muhammed *et al.,* 2018). The significant difference between the between-group and within-group variation indicates that perceived pollution varied with cultivation intensity. Farmers associated intensive agricultural practices with increased air, water, and soil pollution. A significant positive correlation (r = 0.519) further supports this relationship (Mengel, 1993). To further examine this relationship, the impact of government and institutional support on intensive cultivation is presented in the following section. Government and institutional financial support showed a significant positive association with intensive cultivation practices.

Economic sustainability and government support

Economic sustainability was evaluated using indicators related to government and institutional support, area of cultivation, agricultural production, fertilizer and pesticide use, irrigation practices, and productivity. These variables reflect the economic performance of intensive agriculture and the influence of agricultural inputs and policy support on agricultural output and resource use. Government and institutional support play an important role in influencing cultivation practices and the adoption of intensive farming methods, consistent with national policies promoting sustainable and climate-resilient agriculture (Keshyagol *et al.,* 2026). An analysis was carried out to examine the association of government and institutional support with key variables such as intensive cultivation, cattle and biodiversity, productivity, and environmental quality. Table 6 presents the impact of government and institutional support on intensive cultivation and related variables and Fig. 6 presents corresponding leverage plots illustrating these relationships. The results presented in Table 6 and Fig. 6 illustrate the relationship between government and institutional support and selected variables associated with intensive cultivation. Government and institutional support showed a significant positive association with intensive cultivation (Standardized regression coefficient (β) = 0.118888, p < 0.0001), indicating that policy support is significantly related to the adoption of intensive cultivation practices. However, the association with cattle and biodiversity was non-significant (p = 0.957), as were the associations with increase in productivity (p = 0.4085) and damage in environmental quality (p = 0.2489). The leverage plots in Fig. 6 show a strong relationship between government and institutional support and intensive cultivation, whereas the relationships with biodiversity, productivity, and environmental quality were weak. Accordingly, the null hypothesis was rejected for intensive cultivation and retained for cattle and biodiversity, increase in productivity, and environmental quality. The ANOVA results showed that government support, area of cultivation, health impact, and pollution were significantly associated with intensive cultivation (p < 0.001). However, government and institutional support had no significant direct effect on productivity or environmental degradation under the present study conditions.

Correlation analysis

Correlation analysis was performed to examine the relationship between land-use pattern and selected agricultural input variables. It helps identify the direction and strength of association between fertilizer use, pesticide use, and irrigation pattern with land-use dynamics. Table 7 shows the correlation between land pattern and the selected independent variables. The results indicate the strength and direction of the relationships. These findings represent statistical associations only and should not be interpreted as evidence of causal relationships.

Table 6: Government and institutional support and its impact on intensive cultivation

Term	Estimate	Standard error (SE)	t-value	p-value
Intercept (Government and institutional support)	1.943634	0.185725	10.47	< 0.0001***
Impact on the intensive cultivation	0.118888	0.021204	5.61	< 0.0001***
Cattle and biodiversity	0.020169	0.370876	0.054	0.957
Increase in productivity	-0.061935	0.074888	-0.83	0.4085
Damage in environment quality	-0.044279	0.038372	-1.15	0.2489

Note: *p < 0.05; **p < 0.01; ***p < 0.001.

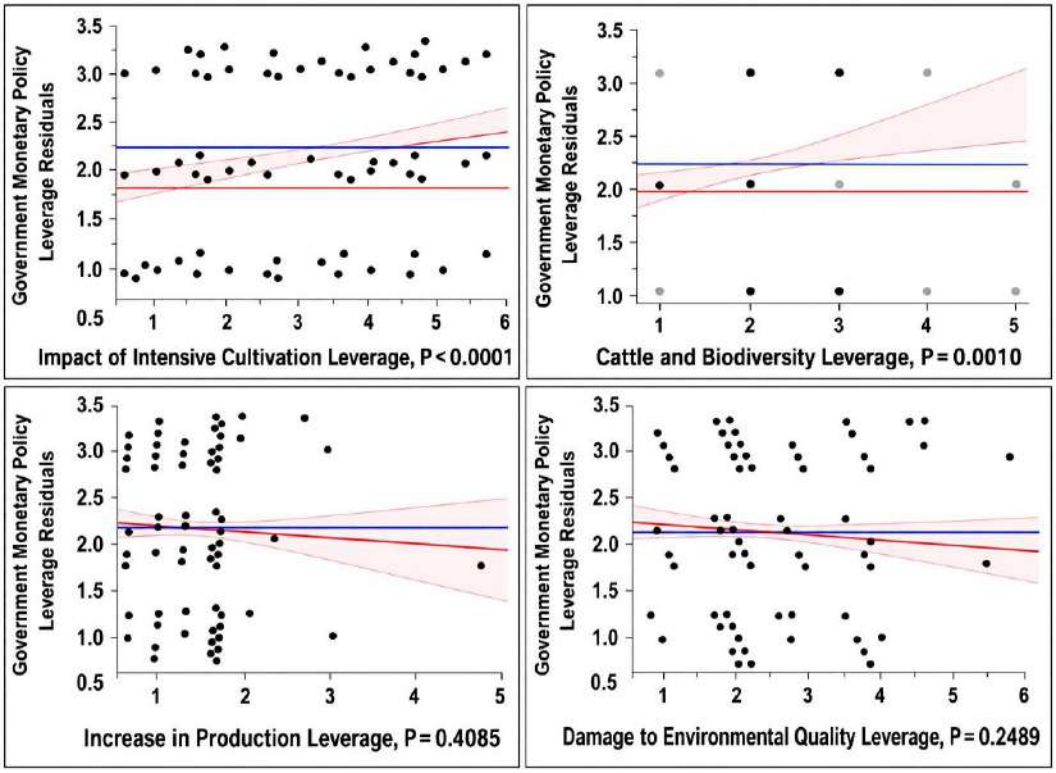

Fig. 6: Leverage plots

Land pattern and fertilizer use

It may be found from Table 7 that the correlation analysis shows a significant negative relationship between land-use pattern and fertilizer use (r = −0.105**). This finding indicates a limited inverse association between fertilizer use and land-use patterns. Although statistically significant, the very weak correlation suggests that fertilizer use should not be regarded as a primary determinant of land-use patterns. The negative direction suggests that intensification through fertilizer use may contribute to changes in traditional land management systems (Ju *et al.,* 2007).

Land pattern and pesticide use

It may be found from Table 7 that the relationship between land-use pattern and pesticide use is weak and not statistically significant (r = 0.045). This indicates that pesticide application does not have a meaningful impact on changes in land-use patterns within the study area. The weak and non-significant correlation suggests that the study did not detect a meaningful linear relationship between these variables, but does not establish their complete independence or absence of other potential relationships (Rani *et al.,* 2021).

Table 7: Correlation between dependent variable and independent variables

Variables	Mean	SD	N	r
Land pattern (last five years)	2.27	1.491	663	-
Fertilizer use	4.43	1.520	663	− 0.105**
Pesticide use	3.35	1.675	663	0.045
Irrigation pattern	2.80	1.927	663	− 0.158***

Note: *p < 0.05; **p < 0.01; ***p < 0.001 (2-tailed). N = sample size; r = Pearson correlation coefficient.

Land pattern and irrigation pattern

It may be found from Table 7 that land-use pattern shows significant negative correlations with fertilizer use (r = − 0.105**) and irrigation pattern (r = − 0.158***), indicating that changes in agricultural input and irrigation management are associated with variations in land-use configuration and cultivation patterns. In contrast, pesticide use showed a weak and non-significant relationship (r = 0.045), indicating little association with land-use dynamics. Fertilizer use and irrigation practices were more closely related to agricultural intensification and land management decisions. These findings are consistent with earlier studies on farming practices and irrigation-driven land-use change (Alhassan *et al.,* 2016; Keshyagol *et al.,* 2026). The observed relationships are further supported by the correlations with cultivated land expansion (r = 0.658), pollution (r = 0.519), and health impacts (r = 0.412), indicating interrelated sustainability outcomes under intensive agriculture.

Regression analysis

Multiple regression analysis was employed to assess the combined effect of key agricultural inputs on the increase in agricultural production**.** It was used to determine the extent to which fertilizer use, pesticide use, and irrigation pattern predict variations in agricultural productivity. Table 8 presents the multiple regression analysis for increase in agricultural production, showing the effect of key agricultural inputs on production. Table 8 presents the multiple linear regression analysis examining the effects of fertilizer use, pesticide use, and irrigation pattern on agricultural production. The regression model was statistically significant (F = 16.807, p < 0.001*). The R^2 value of 0.071 indicates that the model explained 7.1% of the variation in agricultural production, indicating modest explanatory power. This suggests that other factors, such as climatic conditions, soil properties, crop type, farm management, market conditions, and socio-economic characteristics, also influence production. Therefore, the results should be interpreted as statistical associations rather than causal relationships. The general form of the multiple linear regression model is given in Eq. 1 (James *et al.,* 2013):

$$Y = a + b_1X_1 + b_2X_2 + b_3X_3 + e \quad (1)$$

Where: Y represents agricultural production, a is the intercept (constant), b_1, b_2, and b_3 are the regression coefficients, X_1 denotes fertilizer use, X_2 denotes pesticide use, X_3 denotes irrigation pattern, and e represents the random error term. Based on the estimated coefficients obtained in the present study, the fitted multiple linear regression, using Eq. 2 (Present study):

$$Y = 1.206 + 0.40X_1 + 0.38X_2 - 0.34X_3 \quad (2)$$

The intercept (1.206) was statistically significant (SE = 0.069, t = 17.398, p < 0.001*), indicating the baseline agricultural production. Fertilizer use showed a significant positive association with agricultural production (B = 0.40, β = 0.126, p = 0.002). Pesticide use also showed a significant positive relationship (B = 0.38, β = 0.132, p = 0.001), consistent with previous findings (Affandi *et al.,* 2026). In contrast, irrigation pattern showed a significant negative association with agricultural

Table 8: Multiple regression analysis for increase in production

Model component	Variable	Unstandardized regression coefficient (B)	SE	β	t-value	p-value
Model summary	Coefficient of determination (R^2)	0.071	—	—	—	< 0.001***
	F change	16.807	—	—	—	< 0.001***
	Numerator degrees of freedom (df1)	4	—	—	—	—
	Denominator degrees of freedom (df2)	659	—	—	—	—
Constant		1.206	0.069	—	17.398	< 0.001***
Independent variable	Type of fertilizer (X_1)	0.40	0.128	0.126	3.123	0.002**
	Type of pesticide (X_2)	0.38	0.117	0.132	3.255	0.001**
	Type of irrigation (X_3)	− 0.34	0.088	− 0.145	-3.852	< 0.001***

Note: *p < 0.05; **p < 0.01; ***p < 0.001.

production (B = −0.34, β = −0.145, p < 0.001*), indicating lower production at higher coded levels of the variable (Goswami *et al.,* 2017). Overall, fertilizer use, pesticide use, and irrigation pattern were significantly associated with agricultural production. These results represent statistical associations based on the coding of the predictor variables and should not be interpreted as causal effects (James *et al.,* 2013).

Non-parametric analysis of surplus, production, and environmental factors

Non-parametric tests were used because the analyzed variables did not satisfy the normality assumption required for parametric tests. These distribution-independent methods were applied to examine differences and associations among key variables. They were used to assess variations in marketable surplus, production, government support, and environmental factors under different cultivation practices. Table 9 presents the non-parametric test statistics, including the Z-test, χ^2 test, and H-test, for the selected variables. Table 9 shows that the Z-test identified significant differences in marketable and marketed surplus between traditional and intensive cultivation systems. The χ^2 test showed significant associations between increased production and willingness to pay (p < 0.001) and between government support and intensive cultivation (p < 0.001). The H-test indicated a significant difference in perceived pollution with increased production (p < 0.001), suggesting greater environmental stress under higher production. These findings are consistent with previous studies reporting improved profitability under alternative farming systems and sustainable agricultural management practices (Mariappan and Zhou, 2019).

Reliability assessment of the measurement instrument

The reliability of the questionnaire was evaluated using the corrected item–total correlation (CITC) and α if Item Deleted. The questionnaire included 10 constructs, each comprising five items, giving a total of 50 items. Fig. 7 presents the item-wise reliability results. The CITC values ranged from 0.651 to 0.781, exceeding the recommended threshold of 0.30, indicating satisfactory internal consistency. The highest CITC was observed for AS4 (0.781), followed by AS2 (0.772) and AS5 (0.763), while the lowest value was recorded for GS1 (0.651). The α if Item Deleted values ranged from 0.801 to 0.894, indicating that removing any item did not improve the overall reliability. Therefore, all questionnaire items were retained for further analysis, confirming their contribution to measuring agricultural sustainability across the study's key dimensions and ensuring adequate measurement consistency.

Table 9: Non-parametric test statistics (Z-test, χ^2 test, and H-test)

Test	Variables	Statistic	df	p-value
Z-test	Marketable surplus (Traditional vs. Intensive cultivation)	Z = −3.243	—	0.001**
Z-test	Marketed surplus (Traditional vs. Intensive cultivation)	Z = −5.104	—	< 0.001***
χ^2 test	Increase in production vs. Willingness to pay	χ^2 = 32.593	1	< 0.001***
χ^2 test	Government support vs. Impact on intensive cultivation	χ^2 = 657.679	17	< 0.001***
H-test	Pollution (air, water, and soil) vs. Increase in production	H = 50.737	1	< 0.001***

Note: *p < 0.05; **p < 0.01; ***p < 0.001.

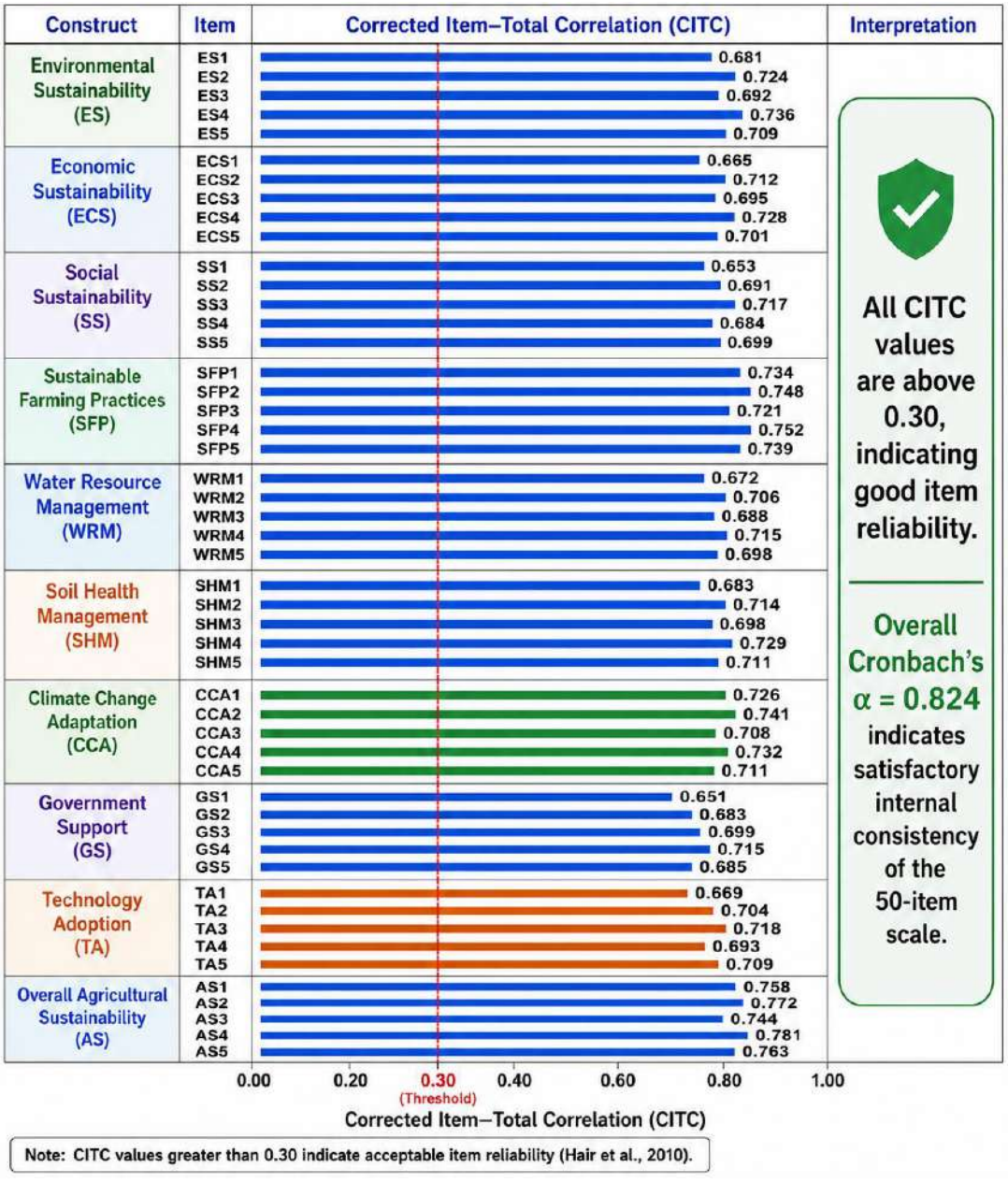

Fig. 7: Item-wise reliability assessment of the agricultural sustainability questionnaire

Validity assessment of measurement instrument

The quality of the measurement instrument was evaluated through internal consistency reliability, content validity, and construct validity to ensure the reliability, validity, and appropriateness of the questionnaire for statistical analysis.

Internal consistency reliability

The internal consistency of the measurement instrument was evaluated using the α coefficient. The overall questionnaire achieved an α value of 0.824, exceeding the recommended threshold of 0.70 and indicating satisfactory reliability. The α if Item Deleted values ranged from 0.801 to 0.894, indicating that removing any item would not substantially improve reliability. Therefore, all 50 questionnaire items were retained for subsequent statistical analyses.

Content validity

Content validity was established through an extensive review of previous agricultural sustainability studies and the study objectives. The questionnaire covered environmental, economic, social, institutional, technological, and resource management dimensions. A pilot study involving 40 farmers from marginal, small, medium, and large farm categories was conducted to assess the clarity, relevance, and applicability of the questionnaire. Feedback from the pilot survey was incorporated into the final questionnaire before the main data collection.

Construct validity

Construct validity was supported through the satisfactory performance of the corrected CITC values. The CITC values (0.651–0.781) indicate that all items were appropriately associated with their underlying constructs and adequately represented the intended dimensions of agricultural sustainability. The absence of low item-total correlation values demonstrates satisfactory coherence among the measurement items, confirming that the questionnaire reliably captured the multidimensional characteristics of agricultural sustainability.

Comparative evaluation of previous and present study results

A structured comparison of the impacts of intensive agriculture was performed using quantitatively measurable indicators derived from earlier studies and present field observations. Table 10 presents these indicators with corresponding values, enabling a systematic evaluation of the consistency and variation across studies. From Table 10, it could be noted that the earlier studies have reported significant environmental and socio-economic challenges associated with intensive agriculture, including a 24% reduction in SOC, 40% decline in microbial biomass, and 25–75% depletion of soil organic carbon, indicating deterioration of soil biological functions and carbon dynamics (Bonanomi *et al.,* 2011; Lal, 2013). In comparison, the present study reported 63% perceived land degradation and 65–78% perceived nutrient depletion, along with a 13% reduction in perceived organic fertilizer effectiveness, indicating concerns about declining soil quality and function. Although earlier studies used direct soil measurements, the present study reflects farmer perceptions; both highlight soil vulnerability under intensive cultivation. Previous investigations quantified nutrient imbalance through a nitrogen surplus of 4328 kg/ha/y, phosphorus surplus of 1337 kg/ha/y, and nitrogen losses of −53 kg/ha/y, demonstrating inefficient nutrient cycling in intensive farming systems (Ju *et al.,* 2007; Muhammed *et al.,* 2018). Similarly, the present study identified excessive fertilizer application and perceived soil fertility decline, suggesting that increased nutrient inputs may not always result in improved nutrient-use efficiency. Previous research has also documented environmental pollution associated with agrochemical-intensive agriculture (Mengel, 1993), while the present study observed a significant association between intensive

Table 10: Contextual evaluation of sustainability indicators under intensive agricultural systems

Sustainability indicator	Evidence from previous studies	Evidence from present study	Interpretation
Soil quality and carbon dynamics	SOC reduction (24%), microbial biomass decline (40%), and soil carbon depletion (25–75%) reported under intensive agriculture (Bonanomi *et al.,* 2011; Lal, 2013)	Farmers reported land degradation (63%), nutrient depletion (65–78%), and reduced organic fertilizer efficiency (13%)	Both studies indicate declining soil quality; however, previous studies used measured soil parameters, whereas the present study reflects farmer-level observations
Nutrient management	Nitrogen surplus (4328 kg/ha/y), phosphorus surplus (1337 kg/ha/y), and nitrogen losses (−53 kg/ha/y) reported under intensive agriculture (Ju *et al.,* 2007; Muhammed *et al.,* 2018)	Excess fertilizer application and declining soil fertility were reported by farmers	Indicates possible inefficiencies in nutrient management under intensive cultivation
Environmental pollution	Intensive agrochemical use associated with increased pollution risks (Mengel, 1993)	Significant association between intensive agriculture and pollution perception (r = 0.519)	Suggests farmer-perceived environmental stress associated with intensive practices
Land-use pressure	Intensive systems improve land-use efficiency but increase resource pressure (Adhikari *et al.,* 2017)	Significant association between intensive farming and land-use intensification (r = 0.658)	Indicates increasing cultivation pressure within the study region
Health concerns	Agricultural chemical exposure linked with potential health risks (Rani *et al.,* 2021)	Significant association between intensive cultivation and reported health impacts (r = 0.412)	Highlights farmer concerns regarding chemical exposure and health outcomes
Socio-economic dependence	Agricultural livelihoods associated with land ownership and household labour (Goswami *et al.,* 2017)	Landholding size showed a strong association with family size (r = 0.7214)	Indicates continued dependence on family labour in intensive farming systems

agricultural practices and environmental pollution (r = 0.519), along with farmer-reported concerns related to salinity, dust accumulation, and climatic stress indicators. Earlier studies reported that intensive agriculture improves land-use efficiency but increases pressure on agricultural resources (Adhikari *et al.,* 2017), which is comparable with the present finding of a significant relationship between intensive farming practices and land-use intensification (r = 0.658). Previous evidence has highlighted potential health risks associated with prolonged agricultural chemical exposure (Rani *et al.,* 2021), and the present study similarly identified a significant association between intensive agricultural practices and reported health impacts (r = 0.412). Furthermore, previous studies emphasized the dependence of farming livelihoods on household labour and land ownership (Goswami *et al.,* 2017), while the present study observed a strong relationship between landholding size and family size (r = 0.7214), indicating continued dependence on family labour in intensive farming systems. The present findings are generally consistent with earlier studies on soil degradation, nutrient imbalance, environmental stress, health impacts, and socio-economic dependence. However, these relationships indicate statistical associations rather than causal effects, as the study used cross-sectional survey data. Reported land degradation (63%) and nutrient depletion (65–78%) may reflect local soil conditions, climate, cropping intensity, irrigation, and management practices. Differences from previous studies may arise from farmers' perceptions rather than direct environmental measurements. Significant associations between intensive cultivation and pollution (r = 0.519), land-use intensification (r = 0.658), health impacts (r = 0.412), and landholding size and family size (r = 0.7214) are consistent with previous findings. These relationships should therefore be interpreted within the local agricultural context rather than as evidence of causality.

Recommendations

Sustainable agricultural development requires targeted policy and management interventions. Since government support, area of cultivation, health impact, and pollution were significantly associated with intensive cultivation ($p < 0.001$), strengthening financial assistance, crop insurance, and timely access to institutional credit should be prioritized. The regression analysis showed positive associations of fertilizer and pesticide use with agricultural production, while irrigation pattern showed a negative association, indicating the need to improve irrigation management practices. Awareness programmes on the efficient and safe use of agricultural inputs should also be strengthened to reduce environmental and health risks. Future research should further examine conservation agriculture and climate-smart technologies to support sustainable agricultural development (Caldara *et al.,* 2026). Overall, the findings support enhanced institutional support, efficient resource management, and evidence-based policy interventions to promote long-term agricultural sustainability (Ţopa *et al.,* 2025).

Contribution of the study

This study contributes to the understanding of agricultural sustainability by integrating environmental, economic, and social dimensions within a unified analytical framework. Government support, area of cultivation, health impact, and pollution were significantly associated with intensive cultivation ($F = 9.542$, 13.266, 17.115, and 15.739; $p < 0.001$). Regression analysis showed positive associations of fertilizer and pesticide use with agricultural production, whereas irrigation pattern showed a negative association. Non-parametric tests also indicated significant associations among marketable surplus, production, and environmental factors ($p < 0.001$). This integrated assessment provides comprehensive evidence to support sustainable agricultural management and evidence-based policy decisions for resilient and environmentally responsible farming systems.

Limitations of the study

The study was limited to a single district, which may restrict the generalizability of the findings. The analysis was based on primary survey data and may be subject to respondent bias. Although multiple statistical methods were applied, some models showed moderate explanatory power, suggesting that additional factors may influence the observed outcomes. Multiple statistical tests were conducted without formal adjustment for multiple comparisons, which may have increased the likelihood of Type I error. The hierarchical data structure was not explicitly considered, which may have affected SE precision. Finally, the significant relationships represent statistical associations rather than causal effects due to the cross-sectional design. Future longitudinal and experimental studies should examine causal mechanisms.

Scope for future research

Future research should include multiple districts and states to improve the generalizability of the findings. Longitudinal studies are needed to examine the long-term environmental and socio-economic impacts of intensive cultivation and to better assess causal relationships. F Future studies should incorporate direct soil, water, and environmental measurements alongside environmental, institutional, and socio-economic variables to improve model explanatory performance. They should also assess agricultural subsidies, organic farming, and sustainable resource management across diverse agroecological conditions.

CONCLUSION

The study demonstrates that intensive cultivation is associated with variations in the environmental, economic, and social dimensions of agricultural sustainability, highlighting the interactions among production practices, resource utilization, and farmer-level socio-economic conditions. The statistical analyses indicate that

agricultural intensification is related to both structural characteristics and institutional factors, with implications for sustainability outcomes. ANOVA results showed significant differences among intensive cultivation-related variables, including government support, cultivated area, pollution perception, and reported health impacts, indicating that intensification is associated with multiple sustainability concerns. Government financial support showed a significant positive association with intensive cultivation practices; however, its relationship with productivity-related and environmental indicators was limited, suggesting the need for improved alignment between policy support and sustainability objectives. Correlation analysis indicated significant relationships between land-use patterns and selected agricultural input variables, including fertilizer use and irrigation practices, whereas pesticide use showed no significant association. Regression analysis showed that fertilizer and pesticide use were positively associated with agricultural production, while irrigation practices showed a negative association, emphasizing the importance of efficient input and water management strategies. However, the regression model explained a relatively small proportion of the variation in agricultural production (R^2 = 0.071), indicating that additional environmental, managerial, and socio-economic factors not included in the model are also likely to influence production outcomes. Additional statistical analyses indicated significant relationships among production practices, institutional support, and sustainability-related indicators, suggesting that agricultural sustainability requires consideration of both productivity and resource management dimensions. The findings provide empirical insights for policymakers, agricultural planners, and extension agencies to develop strategies promoting efficient fertilizer management, improved irrigation practices, responsible input use, and sustainable cultivation approaches. However, the study is limited by its cross-sectional survey design, geographical focus on Namakkal District, reliance on farmers' self-reported responses, and the modest explanatory power of the regression model, which may restrict the generalizability of the findings beyond the sampled farming population. Although significant relationships were identified between intensive cultivation indicators and sustainability outcomes, these associations do not establish causal relationships. Future studies should incorporate longitudinal observations, multi-location assessments, and direct field measurements of soil, water, and environmental parameters to further evaluate long-term sustainability outcomes. Although the present study did not directly evaluate advanced digital technologies, future research may also examine the potential of remote sensing and geographic information system to improve sustainability assessment and support evidence-based agricultural planning. Sustainable agricultural development requires balancing production objectives with efficient resource utilization, improved management practices, institutional support, and farmer capacity development to enhance the resilience and sustainability of farming systems.

AUTHOR CONTRIBUTIONS

S. Chandran contributed to the conceptualization of the study, methodology development, data collection, formal analysis, investigation, environmental sustainability assessment, interpretation of the findings, visualization, and preparation of the original manuscript draft. T. Ramachandran contributed to study supervision, research design, methodology refinement, validation, manuscript review, and editing. D. Sivakumar contributed to conceptual guidance, critical review, technical editing, and final approval of the manuscript. A. Ambika contributed to data validation, visualization, manuscript review, language editing, and final approval of the manuscript. All authors read and approved the final manuscript and agree to be accountable for all aspects of the work.

ACKNOWLEDGEMENT

The authors sincerely acknowledge the SRM Institute of Science and Technology, Kattankulathur, Chennai, Kalasalingam Academy of Research and Education, Krishnankoil, and B. S. Abdur Rahman Institute of Science and Technology, Vandalur, Chennai, for providing the academic support and research facilities required for this study. The authors thank all farmers and respondents for their voluntary participation and valuable contributions to this research.

CONFLICT OF INTEREST

The authors declare no conflict of interest regarding this manuscript. Ethical standards, including informed consent, originality, research integrity, and avoidance of fabrication, falsification, duplicate publication, and redundant submission, were strictly observed.

OPEN ACCESS

©2026 The author(s). This article is licensed under a Creative Commons Attribution 4.0 International License, which permits use, sharing, adaptation, distribution and reproduction in any medium or format, as long as you give appropriate credit to the original author(s) and the source, provide a link to the Creative Commons license, and indicate if changes were made. The images or other third-party material in this article are included in the article's Creative Commons license, unless indicated otherwise in a credit line to the material. If material is not included in the article's Creative Commons license and your intended use is not permitted by statutory regulation or exceeds the permitted use, you will need to obtain permission directly from the copyright holder. To view a copy of this license, visit: http://creativecommons.org/licenses/by/4.0/

PUBLISHER'S NOTE

GJESM Publisher remains neutral with regard to jurisdictional claims in published maps and institutional affiliations.

POSITIVE AI STATEMENT

During the preparation of this manuscript, the authors used QuillBot to improve the clarity and readability of the text. Following the use of this tool, the authors critically reviewed and revised the manuscript as necessary and accept full responsibility for the accuracy, integrity, and content of the final publication.

ABBREVIATIONS

%	Percent
ANOVA	Analysis of Variance
B	Unstandardized regression coefficient
BOD	Biochemical oxygen demand
CITC	Corrected item–total correlation
DAP	Diammonium phosphate
df	Degrees of freedom
df_1	Numerator degrees of freedom
df_2	Denominator degrees of freedom
F-value	F-statistic
GDP	Gross domestic product
ha	Hectare(s)
H-test	Kruskal–Wallis H statistic
Kg/ha/y	Kilograms per hectare per year
MS	Mean square
N	Sample size
p-value	Probability (significance) value
r	Pearson correlation coefficient
R^2	Coefficient of determination
SD	Standard deviation
SE	Standard error
SOC	Soil organic carbon
SS	Sum of squares
t-value	t-statistic
US$	United States Dollars
Z-test	Mann–Whitney U statistic
α	Cronbach's alpha coefficient
η^2	Effect size
χ^2	Chi-square statistic
β	Standardized regression coefficient

REFERENCES

Adhikari, P.; Araya, H.; Aruna, G.; Balamatti, A.; Banerjee, S.; Baskaran, B.; Barah, B.C.; Behera, D.; Berhe, T.; Boruah, P.; Dhar, S.; Edwards, S.; Fulford, M.; Gujja, B.; Ibrahim, H.; Kabir, H.; Kassam, A.; Khadka, B.; Koma, Y.S.; Natarajan, S.; Perez, R.; Sen, D.; Sharif, A.; Singh, G.; Styger, E.; Thakur, A.K.; Tiwari, A.; Uphoff, N.; Verma, A., (2017). System of crop intensification for more productive, resource-conserving, climate-resilient, and sustainable agriculture: Experience with diverse crops in varying agroecologies. Int. J. Agric. Sustainability. 16(1): 1–28 **(28 pages)**.

Affandi; Sutanto, K.D.; Wiratno, R.; Murtiningsih, A.; Meilin, O.; Endarto, M.; Istianto; Handoko, A.; Sebayang, D.; Hutapea, R.C.; Wicaksono, N.; Wardani, S.W.; Manwan, S.; Wuryantini, S.; Agustini, D.W.; Utami. (2026). Integrated pest control and environmental risk management for sustainable chili pepper production. Global J. Environ. Sci. Manage. 12(2): 989–1010 **(22 pages).**

Al-Sammarraie, M.A.J.; Kaplan, S., (2025). Precision agriculture strategies to reduce the impacts of soil degradation: A comprehensive review. CABI Rev. 20: 0037 **(20 pages).**

Alhassan, A.; Salifu, H.; Adebanji, A.O., (2016). Discriminant analysis of farmers' adoption of improved maize varieties in Wa Municipality, Upper West Region of Ghana. SpringerPlus. 5(1): 1514 **(12 pages).**

Bathaei, A.; Štreimikienė, D., (2023). A systematic review of agricultural sustainability indicators. Agriculture. 13(2): 241 **(19 pages).**

Bobitan, N.; Dumitrescu, D.; Burca, V. (2023). Agriculture's efficiency in the context of sustainable agriculture—A benchmarking analysis of financial performance with data envelopment analysis and Malmquist index. Sustainability. 15(16): 12169 **(28 pages).**

Bonanomi, G.; D'Ascoli, R.; Antignani, V.; Capodilupo, M.; Cozzolino, L.; Marzaioli, R.; Puopolo, G.; Rutigliano, F.A.; Scelza, R.; Scotti, R.; Rao, M.A.; Zoina, A., (2011). Assessing soil quality under intensive cultivation and tree orchards in Southern Italy. Appl. Soil Ecol. 47(3): 184–194 **(11 pages).**

Bosco, G.; Simeoni, L., (2018). Environmental impact of intensive farming in sloping areas. MATEC Web Conf. 174: 01001 **(11 pages).**

Bünemann, E.K.; Bongiorno, G.; Bai, Z.; Creamer, R.E.; De Deyn, G.; De Goede, R.; Fleskens, L.; Geissen, V.; Kuyper, T.W.; Mäder, P.; Pulleman, M.; Sukkel, W.; Van Groenigen, J.W.; Brussaard, L.., (2018). Soil quality – A critical review. Soil Biol. Biochem. 120: 105–125 **(21 pages).**

Caldara, M.; Di Gregorio, L.; Sarvi, M.; Graziano, S.; Bindo, A.; Salo, T.; Nolfi, L.; Costanzo, M.; Lamanna, G.; Scanferla, V.; Varese, G.C.; Bernini, R.; Palojarvi, A.; Marmiroli, N.; Bevivino, A., (2026). Impacts on soil health of soil improvers derived from agri-food processing residues: A systematic review with a focus on European field studies. J. Soil Sci. Plant Nutr. 26: 2858–2883 **(26 pages).**

Das, J.; Jha, S.; Goyal, M.K.; Surampalli, R.Y., (2020). Challenges of sustainability in agricultural management. Sustainability: Fundam. Appl. 339–356 **(18 pages).**

Etikan, I.; Bala, K. (2017). Sampling and sampling methods. Biom. Biostat. Int. J., 5(6): 215–217 **(3 pages).**

Gillund, F.T.; Myhr, A.I.; Utskarpen, A.; Hilbeck, A., (2016). Stakeholder views on sustainability assessment of genetically modified potato. Int. J. Agric. Sustainability 14(3): 357–376 **(20 pages).**

Goswami, R.; Saha, S.; Dasgupta, P., (2017). Sustainability assessment of smallholder farms in developing countries. Agroecol. Sustainable Food Syst. 41(5): 546–569 **(24 pages).**

Horrigan, L.; Lawrence, R.S.; Walker, P., (2002). How sustainable agriculture can address the environmental and human health harms of industrial agriculture. Environ. Health Perspect. 110(5): 445–456 **(12 pages).**

Imelda; Hidayat, R., (2024). Climate change impacts, adaptation and mitigation in the agricultural sector. Global J. Environ. Sci. Manage., 10(3): 1457-1476 **(20 pages).**

James, G.; Witten, D.; Hastie, T.; Tibshirani, R., (2013). An Introduction to Statistical Learning. Springer, New York **(426 pages).**

Ju, X.T.; Kou, C.L.; Christie, P.; Dou, Z.X.; Zhang, F.S., (2007). Changes in the soil environment from excessive application of fertilizers and manures to two contrasting intensive cropping systems on the North China Plain. Environ. Pollut. 145(2): 497–506 **(10 pages).**

Jwaideh, M.A.A.; Dalin, C., (2025). The multi-dimensional environmental impact of global crop commodities. Nat. Sustainability 8(4): 396–410 **(15 pages).**

Kareemulla, K.; Venkattakumar, R.; Samuel, M.P., (2017). An analysis on agricultural sustainability in India. Curr. Sci. 112(2): 258–266 **(9 pages).**

Kaur, N., (2014). Impact of intensive agriculture on natural resource base of Punjab. Agric. Rev. 35(4): 279–286 **(8 pages).**

Keshyagol, K.; Vanarotti, M.; Madiwal, S.; Kulkarni, P.; Bongale, A.M., (2026). Sustainable farming systems integrating soil health, water use efficiency and crop productivity for climate resilience. Discover Sustainability. 7: 481 **(51 pages).**

Lal, R., (2013). Intensive agriculture and the soil carbon pool. J. Crop Improv., 27(6): 735-751 **(17 pages).**

Lampridi, M.G.; Sørensen, C.G.; Bochtis, D., (2019). Agricultural sustainability: a review of concepts and methods. Sustainability, 11(18): 5120 **(27 pages).**

Lélé, S.M., (1991). Sustainable development: a critical review. World Dev., 19(6): 607-621 **(15 pages).**

Mariappan, K.; Zhou, D., (2019). Farmers' suicide and organic farming opportunity in India. Sustainability, 11(8): 2400 **(17 pages).**

Mengel, K., (1993). Impact of intensive agriculture on resources and environment. In: Optimization of Plant Nutrition, Springer, Dordrecht, 613-617 **(5 pages).**

Mózner, Z.; Tabi, A.; Csutora, M., (2012). Modifying the yield factor based on more efficient use of fertilizer – the environmental impacts of intensive and extensive agricultural practices. Ecol. Indic., 16: 58-66 **(9 pages).**

Muhammed, S.E.; Coleman, K.; Wu, L.; Bell, V.A.; Davies, J.A.; Quinton, J.N.; Carnell, E.J.; Tomlinson, S.J.; Dore, A.J.; Dragosits, U.; Naden, P.S.; Glendining, M.J.; Tipping, E.; Whitmore, A.P., (2018). Impact of two centuries of intensive agriculture on soil carbon, nitrogen and phosphorus cycling in the UK. Sci. Total Environ., 634: 1486-1504 **(19 pages).**

Ologunde, O.H.; Nunes, M.R., (2026). Redefining soil health and food security through tropical conservation agriculture. Commun. Sustainability, 1: 82 **(11 pages).**

Parihar, C.M.; Singh, S.; Singh, R.; Singh, V.P.; Prasad, S.M., (2015). Effect of salinity stress on plants and its tolerance strategies: a review. Environ. Sci. Pollut. Res., 22(6): 4056-4075 **(20 pages).**

Ramasubramaniyan, R.; Vasanthakumar, J.; Hansra, B.S., (2016). Knowledge and adoption of conservation agriculture technologies by the farming community in different agro-climatic zones of Tamil Nadu state in India. J. Agric. Sci. 8(11): 154–169 **(16 pages).**

Rani, L.; Thapa, K.; Kanojia, N.; Sharma, N.; Singh, S.; Grewal, A.S.; Srivastav, A.L.; Kaushal, J., (2021). An extensive review on the consequences of chemical pesticides on human health and environment. J. Cleaner Prod., 283: 124657 **(129 pages).**

Rockström, J.; Williams, J.; Daily, G.; Noble, A.; Matthews, N.; Gordon, L.; Wetterstrand, H.; DeClerck, F.; Shah, M.; Steduto, P.; De Fraiture, C. (2017). Sustainable intensification of agriculture for human prosperity and global sustainability. Ambio, 46(1): 4–17 **(14 pages).**

Rosas Baños, M.; García Salazar, E.M. (2026). Wastewater uses for agricultural production from weak and strong sustainability perspectives. Global J. Environ. Sci. Manage. 12(2): 667–686 **(20 pages).**

Scheper, J.; Badenhausser, I.; Kantelhardt, J.; Kirchweger, S.; Bartomeus, I.; Bretagnolle, V.; Clough, Y.; Gross, N.; Raemakers, I.; Vilà, M.; Trello, C.J.; Kleijn, D., (2023). Biodiversity and pollination benefits trade off against profit in an intensive farming system. Proc. Natl. Acad. Sci. U.S.A., 120(28): e2212124120 **(24 pages).**

Țopa, D.-C.; Căpșună, S.; Calistru, A.-E.; Ailincăi, C., (2025). Sustainable practices for enhancing soil health and crop quality in modern agriculture: a review. Agric., 15(9): 998 **(38 pages).**

AUTHOR (S) BIOSKETCHES

Chandran, S., Ph.D. Candidate, School of Management Distance Education, SRM Institute of Science and Technology, Kattankulathur, Chennai 603203, Tamil Nadu, India.
- Email: *chandras4@srmist.edu.in*
- ORCID: 0009-0001-2637-3310
- Web of Science ResearcherID: NA
- Scopus Author ID: NA
- Homepage: https://srmistdistanceeducation.in/facultyandstaff/

Ramachandran, T., Ph.D., Professor, Department of Management, College of Management, SRM Institute of Science and Technology, Kattankulathur, Chennai 603203, Tamil Nadu, India.
- Email: *ramachat@srmist.edu.in*
- ORCID: 0000-0002-5633-0303
- Web of Science ResearcherID: QSO-2480-2026
- Scopus Author ID: 56627799420
- Homepage: https://www.srmist.edu.in/faculty/dr-t-ramachandran/

Sivakumar, D., Ph.D., Professor, Department of Agricultural Engineering, Kalasalingam Academy of Research and Education, Krishnankoil, Virudhunagar 626126, Tamil Nadu, India.
- Email: *d.sivakumar@klu.ac.in*
- ORCID: 0000-0001-5228-0145
- Web of Science ResearcherID: Y-6145-2019
- Scopus Author ID: 55611586900
- Homepage: https://www.kalasalingam.ac.in/course/b-sc-hons-agriculture/

Ambika, A., Ph.D., Assistant Professor (Selection Grade), Department of Electronics and Communication Engineering, B. S. Abdur Rahman Institute of Science and Technology, Vandalur, Chennai 600048, Tamil Nadu, India.
- Email: *ambika@crescent.education*
- ORCID: 0000-0003-1628-2543
- Web of Science ResearcherID: ACH-8800-2022
- Scopus Author ID: 57210460307
- Homepage: https://www.researchgate.net/profile/Ambika-A-2

HOW TO CITE THIS ARTICLE:
Chandran, S.; Ramachandran, T.; Sivakumar, D., Ambika, A., (2027). The impact of environmental, economic, and social sustainability under intensive agriculture. Global J. Environ. Sci., Manage., 13(1): 163-188.

DOI: 10.22034/gjesm.2027.01.08
URL: https://www.gjesm.net/article_735501.html

Global J. Environ. Sci. Manage. 13(1): 189-212, Winter 2027, Serial #49

Global Journal of Environmental Science and Management
(GJESM)

Homepage: https://www.gjesm.net/

Podcasts

CASE STUDY

Inflow modeling strategies designed to enhance the ecological sustainability of hydroelectric reservoir operation planning

I. Mulyawati[1], I.R.S. Salami[2,], M. Marselina[2], A. Sabar[2,3]*

[1]*Environmental Engineering Graduate Program, Faculty of Civil and Environmental Engineering, Institut Teknologi Bandung, Bandung 40132 Indonesia*

[2]*Department of Environmental Engineering, Faculty of Civil and Environmental Engineering, Institut Teknologi Bandung, Bandung 40132 Indonesia*

[3]*Department of Environmental Engineering, Faculty of Infrastructure and Regional Technology, Institut Teknologi Sumatera, South Lampung 35365 Indonesia*

ARTICLE INFO

Article History:
Received 03 May 2026
Revised 17 July 2026
Accepted 18 August 2026

Keywords:
Environmental flows
Inflow forecasting
Karian Reservoir
Markov Chain
Monsoonal tropics
Multiple linear regression

ABSTRACT

BACKGROUND AND OBJECTIVES: The rapid global expansion of water infrastructure alters major rivers, causes severe biodiversity declines, and destabilizes aquatic ecosystems. Amid intensifying eco-hydrological pressures, accurate prediction of reservoir inflow remains imperative to safeguard downstream aquatic ecosystems, yet data-sparse tropical environments chronically impair the generalizability of deep learning architectures due to pronounced overfitting. The study objectives were to evaluate three statistical inflow modeling frameworks, representative of design-era hydrological understanding, against the observed 1998–2023 flow regime to identify the most reliable forecasting approach for supporting environmental-flow-informed reservoir operation planning under monsoonal variability.

METHODS: Using a multi-decadal hydro-meteorological dataset from 1998 to 2023 (n = 312 monthly time steps) at Karian Reservoir in Banten Province, Indonesia, three primary modeling approaches were tested: Autoregressive Integrated Moving Average, Markov Chain, and Multiple Linear Regression. To rigorously assess model diagnostics and predictive performance across historical drought and wet regimes, the Pearson correlation coefficient, Kling-Gupta efficiency, and operational trajectory metrics were integrated.

FINDINGS: Deterministic multiple linear regression achieved the highest overall predictive accuracy with a Pearson correlation coefficient of 0.74, a Kling-Gupta efficiency of 0.64, and a superior operational trajectory guideline correlation of 0.85. The observed enhancement in model efficacy stems from the methodical integration of lagged streamflow predictors that effectively characterize catchment-scale moisture persistence. Conversely, the Autoregressive Integrated Moving Average model exhibited the weakest diagnostic capability (Pearson correlation coefficient = 0.62; Kling-Gupta efficiency = 0.60) due to systematic overestimation of dry-season baseflows, risking artificial inflation of safe water availability. Meanwhile, the stochastic Markov yielded a commensurate aggregate Kling-Gupta efficiency score of 0.66 and exhibited a superior proficiency in replicating long-term probability distributions.

CONCLUSION: While Multiple Linear Regression shows the strongest performance for monthly operational scheduling, the Markov Chain model offers a complementary probabilistic framework for screening extended seasonal drought risk. Independent out-of-sample validation against a held-out 2019–2023 period revealed substantial performance degradation for both models (Multiple Linear Regression Nash-Sutcliffe efficiency declining from 0.61 to 0.02; Markov Chain Nash-sutcliffe efficiency declining from 0.28 to -1.01), directly evidencing non-stationary rainfall-inflow relationships. Ultimately, these results establish that the evaluated models serve as an initial decision-support tool for raw water allocation planning, though their sustained operational reliability necessitates systematic recalibration.

DOI:10. 22034.gjesm.2027.01.09

This is an open access article under the CC BY license (http://creativecommons.org/licenses/by/4.0/)

NUMBER OF REFERENCES	NUMBER OF FIGURES	NUMBER OF TABLES
63	9	3

*Corresponding Author:
Email: indahrss@itb.ac.id
Phone: +628170292093
ORCID: 0000-0003-4108-1110

Note: Discussion period for this manuscript open until March 01, 2027 on GJESM website at the “Show Article”.

INTRODUCTION

A reservoir is an engineered ecological system whose operation governs downstream hydrological regimes, aquatic habitat continuity, and riparian ecosystem health (Chan *et al*., 2025). Global water-infrastructure expansion has altered more than two-thirds of the world's large rivers, precipitating biodiversity declines and destabilizing deltaic environments (Grill *et al*., 2019). Integrating hydrological forecasting with reservoir operation reinforces overall system performance and protects downstream aquatic ecosystems by substituting inflexible release rules with dynamic, environmentally responsive strategies (Zarei *et al*., 2021). Accurate inflow forecasting directly underpins outflow discharge calculations, storage stability, and environmental flow delivery, especially as anthropogenic climate change alters basin-scale hydrological regimes (Jayanti *et al*., 2025; Null *et al*., 2024; Anand and Oinam, 2019). Despite advances in deep learning for streamflow prediction, robust statistical models—namely multiple linear regression (MLR), Markov chain, and autoregressive integrated moving average (ARIMA)—remain widely preferred in data-scarce tropical regions where complex black-box models often overfit limited records and lack physical interpretability (Hasan *et al*., 2025; Dimitriadou and Nikolakopoulos, 2022; Gupta and Kumar, 2022). A salient manifestation of this challenge is observed in the Karian Reservoir—a multipurpose engineering project in Banten Province, Indonesia—that mirrors the intricate eco-hydrological trade-offs inherent to large-scale tropical reservoirs (Wahyono *et al*., 2026). Karian must simultaneously fulfill five Phase 1 operational objectives: urban raw water supply, Ciujung River irrigation, municipal releases, run-of-river hydropower, flood control, and a minimum environmental flow of 3.06 m^3/s (Mulyawati *et al*., 2024; BBWS C3, 2025). At 24% of mean annual flow, this environmental release meets the Tennant (1976) "satisfactory" threshold during the wet season but falls below "fair" in the dry season. Legally, Indonesian regulations mandate incorporating river-maintenance flow into every dam's operating pattern, tied to the Q95% dependable discharge (Government of Indonesia, 2011; Ilmi, 2022). Critically, Karian's target releases were derived from a Q355 low-flow index computed from 1970–2004 hydrological records (KOICA, 2006). This epoch precedes both significant upstream land-use transformations (18.3% since 2000) (Arianti *et al*., 2015) and documented ENSO-driven rainfall shifts (Aldrian and Dwi Susanto, 2003). The obsolescence of traditional design-era assumptions under evolving hydrological regimes has received global attention via climate modeling; nonetheless, empirical testing against multi-decadal observational records is notably deficient (Yang *et al*., 2017; Yang *et al*., 2021; Mazvimavi *et al*., 2024). Furthermore, prior evaluations of Indonesian multipurpose reservoirs like Citarum (Arwin and Bourqueil, 1992) and Saguling (Marselina *et al*., 2017) evaluated operating policies under baseline hydrology without testing whether historical forecasting models remain valid decades later. A unique circumstance at Karian is that while inaugurated in 2024 for flood control and irrigation, its full raw water supply function targeting Jabodetabek will only be complete by 2027. Thus, no direct operational record exists. To address this, the 1998–2023 inflow series in this study was retrospectively reconstructed via hydraulic routing from continuous long-term gauging stations. Additionally, unlike existing literature emphasizing economic priorities, the present investigation examines the four primary competing demands—hydropower, raw water supply, irrigation, and environmental flow—with equal weighting. Existing literature comparing ARIMA, Markov Chain, and MLR typically evaluates forecast accuracy alone (Mulyawati *et al*., 2025; Magar and Jothiprakash, 2011; Margini *et al*., 2022) or omits explicit environmental-flow thresholds in multi-objective operational

simulations (Jayanti *et al*., 2025). This study bridges the identified knowledge gap by undertaking a systematic benchmark evaluation of the three data-sparse statistical models using the multi-decadal (1998–2023) reconstructed hydrological sequence of the Karian Reservoir. Model performance was evaluated using the Pearson correlation coefficient (r), Nash-sutcliffe efficiency (NSE), and Kling-Gupta Efficiency (KGE). Propagating these predictive outputs through a reservoir operational model allows for an assessment of whether design-era environmental thresholds remain hydrologically defensible amid current monsoonal regimes, cross-validated using Tennant's (1976) methodology. This study aims to identify the most reliable inflow forecasting method for supporting environmental-flow-informed, multi-sectoral reservoir operation planning under a shifted monsoonal hydrological regime. This study has been conducted in the Karian Reservoir watershed in Banten Province, Indonesia, in 2023.

MATERIALS AND METHODS

Study area

This study was conducted at the Karian Reservoir, located in Sajira District, Lebak Regency, Banten Province, Indonesia (Fig. 1). The reservoir has an effective storage capacity of 207 million cubic meter (Mm^3) and drains water from a watershed area of approximately 288 square kilometers (km^2), most of which is fed by the Ciberang River. Based on continuous monthly hydrological records from 1998 to 2023 (n = 312 monthly time steps), the mean annual flow (MAF) was determined to be 12.81 m^3/s (Table 1) (Atieh *et al*., 2017). Key temporal hydrological metrics, such as flow duration curve (FDC) quantiles, extreme discharge months, and inter-annual variability observed in January, are consolidated in Table 1 to maintain narrative conciseness. This pattern of strong monsoonal seasonality and inter-annual variability is consistent with the influence of climate variability driven by the ENSO (Aldrian and Dwi Susanto, 2003). The reliable water discharge of 9.51 m^3/s is fully allocated to various downstream sectors, leaving no operational margin. Consequently, the design water discharge for drought conditions of 4.0 m^3/s obtained from historical feasibility studies (KOICA, 2006; BBWS C3, 2025) sets the benchmark for ecological planning. This threshold assumes heightened significance during arid periods, when discrepancies between managed discharge volumes and required environmental flows yield the most pronounced ecological impairment (Sedghi-Asl and Poursalehan, 2025).

Data collection and preprocessing

Secondary multi-decadal hydrological records (1997–2023) were retrieved from the Korea International Cooperation Agency (KOICA) and Balai Besar Wilayah Sungai Cidanau-Ciujung-Cidurian (BBWS C3). The compiled dataset encompasses daily and monthly reservoir surface elevations, inflow discharges, and spatial rainfall from six monitoring stations: P1 (Banjar Irigasi), P2 (Ciminyak Cilaki), P3 (Sampang Peundeuy), P4 (Sajira), P5 (Cimarga), and P6 (Pasir Ona). Gaps in precipitation records were reconstructed via the continuous imputation technique formulated by Arwin and Bourqueil (1992). Candidate donor stations were identified via Thiessen polygon proximity, and multi-variable regression combinations (2 to 4 variables) yielding the highest coefficient of determination (R^2) were selected to construct a gap-free time series (Qiu *et al*., 2024). Although raw records span 1997–2023 (n = 324 monthly steps), the year 1997 was used exclusively to calculate lag-1 predictors (P1 at t-1, P4 at t-1, and Qin at t-1), required for MLR, ARIMA, and Markov Chain models. This yielded a robust, highly effective calibration and continuous long-term forecasting period of 1998–2023 (n = 312). To verify the long-term data consistency and homogeneity of the datasets, the double mass curve approach (Sriwongsitanon *et al*., 2023) was implemented, and spatial mean areal rainfall was determined through Thiessen polygon interpolation.

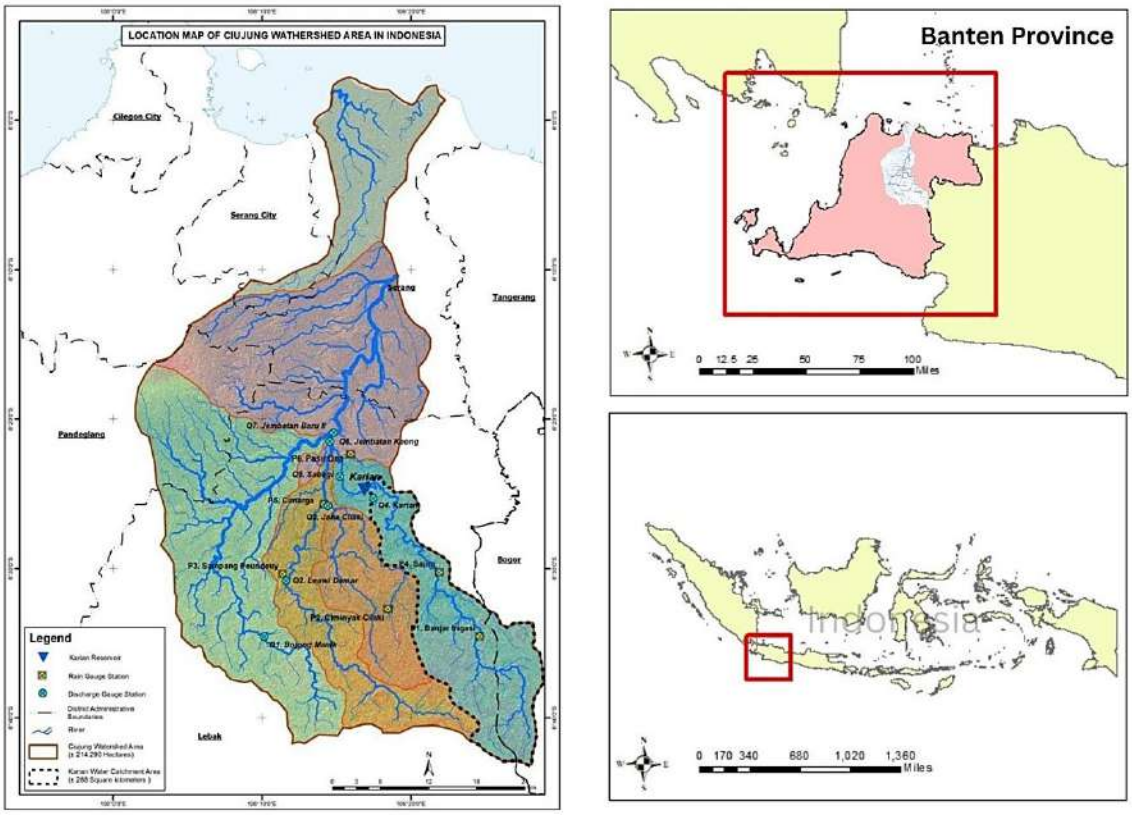

Fig. 1: Geographical location of the study area in the Karian Reservoir watershed in Banten Province, Indonesia, showing the downstream Ciujung River system and the spatial distribution of the hydro-meteorological monitoring network (six rainfall stations, P1-P6) across the 288 km2 Ciberang sub-watershed draining into the 207 million m³ Karian Reservoir

Table 1: Summary of monthly and inter-annual hydrological statistics for Karian Reservoir (1998-2023, n=312)

Statistic	Value
Mean annual flow	12.81 m^3/s
Q80 (flow duration curve quantile)	9.51 m^3/s
Q90 (flow duration curve quantile)	7.67 m^3/s
Highest monthly mean discharge	February: 23.04 m^3/s
Lowest monthly mean discharge	September: 7.53 m^3/s
Most extreme inter-annual range (single month)	January: 1.18-45.61 m^3/s

Due to the absence of a direct gauging station at the reservoir inlet and the ongoing operational ramp-up (with raw water completion targeted for 2027), a synthetic inflow baseline (Q_{in}) was reconstructed from downstream reference stations Q_5 (Sabagi) and Q_7 (Jembatan Baru II) via contemporaneous MLR (Mulyawati *et al.*, 2024). Unlike the lag-1 predictive models, this baseline reconstruction is executed without any underlying lag architecture. For the 1997–2004 period, this reconstructed series showed strong agreement with KOICA's original area-ratio-scaled estimates (Pearson r = 0.916, R^2 = 0.840; Evans, 1996), confirming methodological consistency with design-era baselines. Building upon prior investigations within the catchment (Mulyawati *et al.*, 2025), this comprehensive study directly extends previous work through three key methodological advancements:

1. Standardizing rainfall imputation across all six stations via multiple linear regression.

2. Expanding model performance evaluation to include RMSE, MAE, NSE, MAPE, moving-block bootstrap confidence intervals, and paired-sample significance tests.
3. Propagating forecasts into a full reservoir operation simulation to evaluate environmental-flow target adequacy.

To preserve the integrity of the observational record, extreme hydrological anomalies (such as January inflow rates varying between 1.18 to 45.61 m^3/s) were retained unconditionally, omitting any data capping or exclusion. Preserving this full inter-annual variability was essential to reliably parameterize Weibull-based hydrologic year—categorized as dry, normal, and wet, thereby enabling a realistic representation of operational drought and flood risks in the monsoonal modeling framework simulation.

Flow estimation models

Three robust statistical inflow modeling approaches were evaluated within a unified comparative framework using the quality-controlled dataset (1998–2023, n = 312).

MLR

The MLR model established an explicit linear relationship between contemporary reservoir inflow and antecedent hydro-meteorological predictors (Bargam *et al*., 2024). To accommodate seasonal non-stationarity in the rainfall-inflow relationship, and consistent with the month-specific structure adopted for the Markov Chain transition probabilities and inherent to the seasonal ARIMA specifications the MLR model was parameterized monthly. This generated twelve coefficient sets with uniform predictor architectures but varying numerical values. A pooled-coefficient benchmark demonstrated markedly inferior efficacy (r = 0.40, NSE = 0.16, compared to r = 0.74, NSE = 0.54 in Table 2), validating the month-stratified strategy. Implications regarding the reduced per-month sample size (n = 26-27 years per month) are evaluated in the Discussion. The predictor selection itself was based on upstream spatial positioning and physical hydrological connectivity. These formulations retained three lagged predictors—$P1_{t-1}$ (Banjar Irigasi rainfall), $P4_{t-1}$ (Sajira rainfall), and Qin_{t-1} (lagged inflow), using Eq. 1 (Bargam *et al*., 2024):

$$Q_{in,t} = \beta_0 + \beta_1 P1_{t-1} + \beta_2 P4_{t-1} + \beta_3 Q_{in,t-1} + \epsilon_t \quad (1)$$

Where: β_0 is the intercept, β_1 to β_3 are the partial regression coefficients, and ϵ_t represents the residual error term at time step t.

Markov chain model

Framed as a discrete, stochastic lag-1 process, the Markov chain model parameterized monthly inflows into three discrete states of dry, normal, and wet, using historical monthly distribution quantiles. Following the methodology of Aksoy (2003) as extended in contemporary infrastructure management, month-specific transition probabilities were computed to capture seasonal shifts in transition behavior (Rezaeianzadeh *et al*., 2016; Jayanti *et al*., 2025). The transition probability P_{ij} from state i to state j was mathematically derived using Eq. 2 (Aksoy, 2003):

$$P_{ij} = \frac{n_{ij}}{\sum_{j=1}^{m} n_{ij}} \quad (2)$$

Where: n_{ij} represents the observed historical transitions from state i to state j, and m denotes the total number of defined states (m = 3).

ARIMA model

The ARIMA model exploited the internal autocorrelation structure of the time series. The general model is formulated as $\phi(B)(1-B)^d Q_{in,t} = \Theta(B)\epsilon_t$, where $\phi(B)$ is the autoregressive operator of order p, Θ(B) is the moving average operator of order q, B is the backshift operator ($BX_t = X_{t-1}$), and d is the order of non-seasonal differencing required to achieve stationarity. The optimal

seasonal ARIMA $(p,d,q)(P,D,Q)_s$ structure was rigorously identified via autocorrelation function (ACF) and partial autocorrelation function (PACF) evaluation, minimizing the Akaike information criterion (AIC) (Box *et al*., 2015).

Weibull classification, operation trajectories, and reservoir simulation

The classification of annual inflow volumes into dry, normal, and wet hydrological years was performed using the Weibull plotting position method, thereby facilitating the derivation of return periods and dependability thresholds. Operation guideline trajectories were subsequently derived from a deterministic Rippl Method mass-balance reservoir simulation, using Eq. 3 (Rippl, 1883; Alrayess *et al*., 2017):

$$S_{t-1} = S_t + Q_{in,t} - Q_{out,t} - E_t \quad (3)$$

Where: S_t is the active reservoir storage at month t, constrained strictly between the dead storage level and the 207 million m^3 maximum capacity; $Q_{in,t}$ is the modeled or observed monthly inflow; $Q_{out,t}$ is the total managed outflow release; and E_t represents net evaporative and seepage losses, with long-term active capacity also contingent on catchment sediment yield into the impoundment (Aness *et al*., 2026).

The upper storage boundary (Q_{max} stock) used in the simulation was conservatively set at 200 million m^3, marginally below the reservoir's nominal effective capacity of 207 million m^3, as a simplifying assumption for the statistical simulation exercise. The allocation scheme designated the Tangerang raw water supply as an inflexible, high-priority diversion (6.45 m^3/s) for the duration of every computational time step. Environmental flow performance within $Q_{out,t}$ was dynamically evaluated against the seasonal eco-hydrological thresholds established by the Tennant (1976) method to quantify the ecological reliability of each modeling approach (McMahon and Adeloye, 2005; Shekohideh *et al*., 2026). In fulfillment of the required operational-algorithm specifications for the reservoir simulation, the conversion of operational guidelines into actual implementation followed a two-stage recursive monthly mass-balance procedure. In the first stage, the target (guideline) release T(t) required to keep the reservoir exactly on its Weibull-derived guideline storage trajectory was back-calculated for each month using Eq. 4 (Arwin and Bourqueil, 1992; Loucks and van Beek, 2017; Marselina *et al*., 2016):

$$T(t) = S(t) - Sguideline(t+1) + Qanticipated(t) - E(t) \quad (4)$$

Where: S(t) is the storage carried over from the previous month, Sguideline(t+1) is the target storage prescribed by the applicable reliability-class guideline trajectory for month t+1, Qanticipated(t) is the inflow anticipated for month t from the model under evaluation (ARIMA, Markov Chain, or MLR), and E(t) is net evaporative and seepage loss.

During the second stage, the release T(t) derived from Eq. 4 was held constant while the anticipated inflow was replaced by the actual historical or synthetic inflow Qactual(t), was substituted for the expected inflow to compute the corresponding actual storage through Eq. 5 (Arwin and Bourqueil, 1992; Loucks and van Beek, 2017; Marselina *et al*., 2016):

$$Sactual(t+1) = S(t) + Qactual(t) - T(t) - E(t) \quad (5)$$

The resulting Sactual(t+1) then replaces S(t) as the initial condition for the following month's calculation (Eq. 5 recomputed for month t+1), and the two-stage procedure (Eqs. 4 and 5) is applied recursively across the full 1998-2023 simulation horizon, separately for each of the three inflow models. The proposed recursive coupling serves as the propagation of forecast errors within the reservoir system. Specifically, the release policy is dictated by the guideline trajectory coupled with

the projected inflow, whereas the physical storage dynamics are governed by the realized inflow. Thus, trajectory discrepancies observed in Figs. 7 to 9 serve as a direct measure of the monthly forecast error inherent in the inflow-prediction model. Instead of utilizing a formal multi-objective optimization algorithm (such as dynamic or linear programming), the reservoir simulation framework presented in the Results and Discussion relies on this procedure to define operational constraints and decision rules. This approach was deliberately chosen to evaluate the performance of legacy operating assumptions under historical inflow regimes rather than to derive an optimized release policy—an objective reserved for subsequent research.

Model performance evaluation

Model diagnostic accuracy was systematically validated utilizing r and the modified KGE framework (Gupta *et al*., 2009; Mitze *et al*., 2025). The KGE metric decomposes model performance across three mathematical dimensions: linear correlation (r), bias ratio (β), and variability ratio (γ). A KGE = 1 indicates a perfect match between simulated (s) and observed (o) values, while KGE ≥ 0.75 signifies a highly satisfactory predictive capability, using Eq. 6 (Gupta *et al*., 2009; Mitze *et al*., 2025):

$$r = \frac{[n \cdot \Sigma QoQs - \Sigma Qo \cdot \Sigma Qs]}{\sqrt{[n \cdot \Sigma Qo^2 - (\Sigma Qo)^2][n \cdot \Sigma Qs^2 - (\Sigma Qs)^2]}}$$

$$KGE = 1 - \sqrt{[(r-1)^2 + (\beta-1)^2 + (\gamma-1)^2]} \quad (6)$$

Where: $\beta = \mu_s/\mu_0$ (the ratio of simulated and observed means) and $\gamma = CV_s/CV_o = (\sigma_s/\mu_s)/(\sigma_o/\mu_o)$ (the ratio of simulated and observed coefficients of variation).

The bias ratio (β) component of KGE has direct practical significance for environmental-flow reliability independent of the aggregate KGE score: a model with β > 1 systematically overestimates available discharge, creating the false operational safety margin discussed for ARIMA below, whereas β < 1 would systemacally understate available water and could trigger unnecessarily conservative curtailment; either bias directly affects whether the mandated 3.06 m^3/s environmental release is reliably met, regardless of the model's overall KGE value. In order to enhance the r and KGE metrics and to respond to the reviewers' concerns about the thoroughness of the statistical analysis, four supplementary error metrics were calculated for each model: the root mean square error (RMSE), the mean absolute error (MAE), the NSE, and the mean absolute percentage error (MAPE), in accordance with the methodologies outlined by Moriasi *et al*. (2007) and Lewis (1982). RMSE and MAE quantify the average magnitude of prediction error in the original discharge units (m^3/s), NSE expresses model skill relative to the observed mean as a naive predictor (NSE > 0.5 considered satisfactory), and MAPE expresses the average relative error as a percentage. The RMSE-observations standard deviation ratio (RSR = RMSE/SD of observed values) was additionally computed to classify overall model performance (RSR <= 0.7 considered satisfactory; Moriasi *et al.,* (2007). In addition to point-accuracy metrics, the statistical significance of deviations between the simulated inflow series and the historical (Q_4synthetic) inflow series was rigorously evaluated for each model. Because a Shapiro-Wilk normality test rejected the assumption of normally distributed residuals for all three models ($p < 0.001$), both a parametric paired t-test and a non-parametric Wilcoxon signed-rank test were applied, testing the null hypothesis that no systematic difference exists between simulated and historical inflow values at alpha = 0.05, with the non-parametric result treated as the primary evidence given the non-normal residual distribution. Uncertainty in the reported performance metrics was further quantified using a moving block bootstrap procedure (Künsch, 1989), rather than conventional independent-and-identically-distributed (IID) resampling, because

monthly inflow records exhibit pronounced seasonal autocorrelation that i.i.d. resampling would disrupt, artificially narrowing the estimated uncertainty. For each model, 2,000 bootstrap replicates of the 312-month record were generated by resampling contiguous 12-month blocks with replacement (preserving the annual wet-dry seasonal cycle within each block), and r, KGE, RMSE, MAE, NSE, and MAPE were recalculated for every replicate. The 2.5th and 97.5th percentiles of each resulting bootstrap distribution were taken as the 95% confidence interval (CI) for that metric. Statistical robustness for pairwise model comparisons was established solely in the absence of 95% Cis. Conversely, overlapping intervals suggest that apparent variations in point estimates cannot be separated from sampling uncertainty across the 26-year monthly time series.

RESULTS AND DISCUSSION

This study regularly evaluates the predictive performance of the three dynamic inflow modeling approaches and dissects their operational implications for the Karian reservoir system. The empirical findings are structured to present a comparative statistical validation of the ARIMA, Markov chain, and MLR models, followed by a non-parametric analysis of reliable discharges and reservoir storage trajectories. Finally, this chapter examines the downstream propagation of forecasting variances within long-term multi-objective optimization frameworks, culminating in strategic perspectives for environmentally sustainable water resource governance amidst monsoonal climate shifts.

ARIMA model performance

Performance evaluation of the ARIMA model demonstrated intrinsic structural deficiencies in representing highly dynamic tropical streamflow regimes. The predictive capability of the ARIMA model, alongside the comparative statistical performance metrics of all evaluated frameworks, is summarized in Table 2. As indicated by the statistical criteria, the ARIMA model achieved a correlation coefficient (r) of 0.62 and a KGE of 0.60, exhibiting the weakest overall predictive performance among the three paradigms. To assess the temporal fidelity of the model across sequential time steps, Fig. 2 illustrates a multi-decadal comparison between the reconstructed historical streamflow and the corresponding ARIMA forecasts. As visible in Fig. 2, the ARIMA model systematically compresses predicted peak discharges during the November-March wet season and persistently overestimates baseflows during the June-October dry season. This behavior arises from ARIMA's reliance on stationary linear combinations of past errors and lagged observations, a mechanism that attenuates the non-linear hydrologic extremes induced by monsoonal shifts. In tropical catchments like the Ciberang basin, dry-season baseflows are sustained predominantly by groundwater recession rather than immediate atmospheric forcing, a physical process whose dynamics cannot be effectively decoupled by the stationary stochastic framework of the ARIMA model from rapid monsoonal transitions occurring in April and October. This systematic dry-season overestimation creates a false sense of water availability: when integrated into the Rippl mass-balance simulation, the inflated inflow estimates falsely raise calculated reservoir storage and mask imminent deficits, shifting the release schedule toward aggressive early allocations for urban raw water and hydropower and leaving no buffer for the downstream Ciujung River. The resulting artificial drawdown pushes discharges below critical eco-flow thresholds during the April-September period (Simeone *et al.*, 2024), when the mandated 3.06 m^3/s environmental release is already below the Tennant (1976) "fair" threshold of 3.84 m^3/s (30% of MAF), creating conditions under which riparian ecosystems, macroinvertebrate habitats, and benthic communities would plausibly face elevated stress based on established eco-hydrological relationships; the present study did not directly

Table 2: Comparative statistical performance of ARIMA, MLR, and Markov chain inflow models for Karian reservoir

Metric	ARIMA	Markov Chain (3-class)	MLR
R (guideline vs actual trajectory)	0.76	0.80	0.85
Calibration (1998–2023) Correlation (r)	0.62	0.67	0.74
Calibration (1998–2023) KGE	0.60	0.66	0.64
RMSE (m^3/s)	4.97	4.69	4.08
MAE (m^3/s)	3.45	3.21	2.63
NSE	0.32	0.40	0.54
MAPE (%)	33.2	29.8	26.1

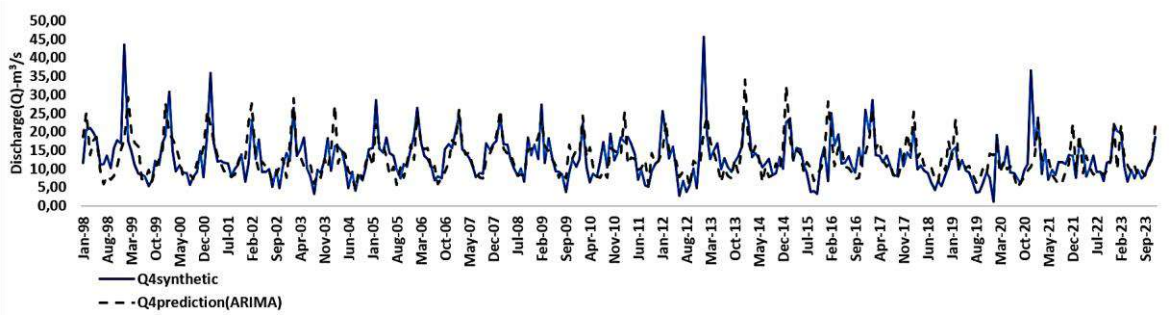

Fig. 2: Comparison of historical (Q4synthetic) and ARIMA-predicted monthly inflow discharge (1998-2023); the model systematically compresses wet-season peaks and overestimates dry-season baseflows, yielding the weakest fit among the three models (r = 0.62, KGE = 0.60, RMSE = 4.97 m^3/s)

measure these biological responses, so this inference remains a hypothesis for future ecological monitoring rather than an established outcome. Despite these forecasting limitations, the ARIMA framework preserves core utility for capturing seasonal autocorrelation structures and multi-year macro-scale trends pertinent to overarching infrastructural planning. Consistent with its weakest r and KGE, the ARIMA model also recorded the least favorable error metrics among the three frameworks (Table 2): RMSE = 4.97 m^3/s, MAE = 3.45 m^3/s, NSE = 0.32 (below the 0.5 satisfactory threshold of Moriasi *et al*. (2007), and MAPE = 33.2%. Despite this comparatively weaker point-to-point accuracy, a paired t-test (p = 0.937) and a Wilcoxon signed-rank test (p = 0.470) both failed to reject the null hypothesis of no systematic difference between ARIMA-simulated and historical inflow values, indicating that ARIMA's shortcomings manifest as reduced precision and event-scale responsiveness rather than a directional (systematic) bias.

Markov chain model performance

By shifting from a deterministic time-series architecture to a probabilistic formulation, the Markov Chain model facilitated a deeper comprehension of underlying state-transition dynamics. The stochastic model reached an event-scale correlation (r) of 0.67 and an aggregate KGE of 0.66 (Table 2). To observe how the probabilistic discretization translates into a continuous hydrograph trajectory, the chronological performance of the Markov Chain framework is displayed in Fig. 3. A particularly striking finding is the KGE statistical parity between the Markov Chain and the more responsive MLR model. Although constrained by lower event-scale correlation, the Markov Chain achieves comparable aggregate fidelity in replicating the long-term historical probability distribution of reservoir inflow, independently of localized, real-time hydrometeorological predictors. This capability stems from the model's underlying mathematical formulation.

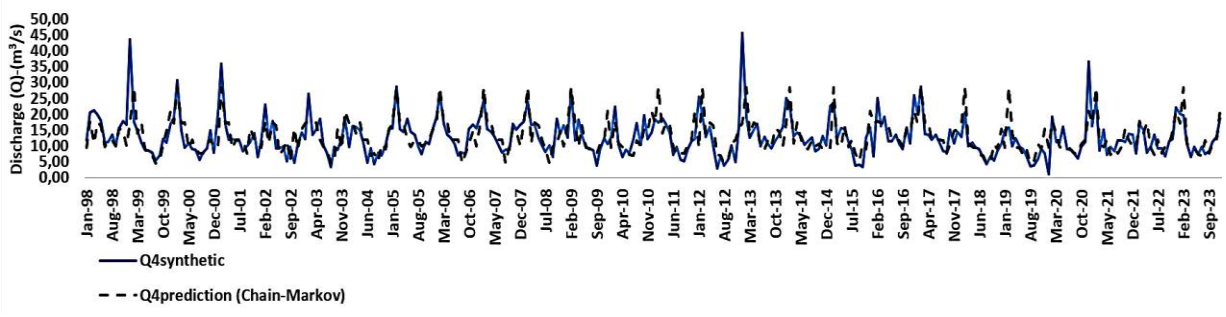

Fig. 3: Comparison of historical (Q4synthetic) and Markov Chain-predicted monthly inflow discharge (1998-2023); despite a lower event-scale correlation than MLR, the model closely reproduces the long-term probability distribution of historical inflow (r = 0.67, KGE = 0.66)

By discretizing the inflow hydrograph into three distinct probabilistic states and estimating the lag-1 Markovian transition matrix (Pij), water resource managers can quantify the probability of the system persisting in a 'dry' state across consecutive months. This framework effectively captures the temporal clustering of drought characteristic of the monsoonal tropics, where extended dry spells are driven by macroclimatic oscillations such as ENSO and the Indian Ocean Dipole (IOD) rather than isolated single-month fluctuations. Such prolonged dry spells are highly consequential, reducing available downstream discharge to the critical R10 threshold of just 1.22 m^3/s. The quantification of these transition probabilities provides a foundation for proactive "hedging rules". By executing gradual supply reductions at the onset of the dry season, systems can circumvent the need for sudden, reactive multi-sectoral allocation cuts near dead storage thresholds (Jehanzaib *et al.*, 2020; Yaseen *et al.*, 2018), ensuring the preservation of the 3.06 m^3/s environmental baseline during vulnerable low-flow window. In terms of point-accuracy error metrics (Table 2), the Markov Chain model achieved RMSE = 4.69 m^3/s, MAE = 3.21 m^3/s, NSE = 0.40, and MAPE = 29.8%, positioning it between ARIMA and MLR: an improvement over ARIMA across all four metrics, yet still below the 0.5 NSE threshold considered satisfactory by Moriasi *et al.* (2007). As with the other two models, a paired t-test (p = 0.518) and a Wilcoxon signed-rank test (p = 0.137) both failed to reject the null hypothesis of no systematic difference between Markov Chain-simulated and historical inflow values, confirming that the model's comparatively lower point-to-point precision does not reflect a systematic bias. Notwithstanding this positive cumulative performance, the Markov chain methodology entails specific methodological limitations necessitating careful consideration. First, the model's transition probabilities are entirely dependent on the historical record used to estimate them (1998-2018 in the calibration-only formulation reported above), and, as demonstrated by the independent validation results, these probabilities do not automatically adapt if the underlying climatic regime shifts. Second, the formulation relies on the premise of stationary, time-invariant state-transition probabilities, which could fail under the non-stationary environmental forcing—including intensified ENSO/IOD cycles and land-use modifications—underlying the broader scope of this retrospective analysis. Consequently, conducting formal tests of stationarity (such as transition-homogeneity or Markov-order diagnostics) is identified as a key direction for future work. Third, the model's three-state (dry/normal/wet) discretization operates at a coarser resolution than the continuous forecasts produced by ARIMA and MLR, trading event-scale precision for robustness in capturing long-term probabilistic drought patterns across dynamic, highly variable hydrological environments under changing climate conditions.

MLR model performance

Evaluation of the alternative approaches revealed that the MLR model attained the highest cumulative predictive accuracy and temporal sensitivity at the event scale. It achieved a correlation coefficient (r) of 0.74 and a KGE of 0.64 (Table 2). The temporal alignment and high precision of this deterministic baseline model across the historical 1998–2023 timeline are illustrated in Fig. 4. The correlation coefficient of r = 0.74, the highest among the three evaluated models, corroborates that a well-formulated multivariate linear structure captures the dominant rainfall-discharge teleconnections governing inflow variability at Karian, translating into accurate tracking of individual monthly high- and low-flow fluctuations with direct operational relevance for release scheduling and adaptive spillway management. This predictive robustness is anchored in the model's predictor combination, P1t-1 (Banjar Irigasi), P4t-1 (Sajira), and the lagged inflow Qin,t-1, of which the lagged inflow term is the dominant driver while the two rainfall stations contribute secondary, spatially-distributed information on upstream hydrological connectivity to the reservoir inlet (see robustness check below). Specifically, the lagged inflow term in particular functions as a mathematical proxy for the physical transit time between precipitation and downstream channel response, capturing the catchment's "memory". In steep tropical regimes, soil moisture dynamics operate as a natural low-pass filter that dampens high-frequency variability, ultimately dictating the translation of prior precipitation and baseflow recession into sustained runoff (Hasan *et al*., 2025; Wang *et al*., 2023). The high operational trajectory correlation (R = 0.85) achieved during the reservoir trajectory simulation confirms that MLR's linear formulation effectively approximates this physical lag-time behavior. In contrast to data-intensive machine learning algorithms that demand heavy computational overhead and rigorous long-term sensor calibration, this calibrated MLR structure offers water authorities a transparent, verifiable, and lightweight alternative for operational forecasting. The framework effectively links raw statistical inputs to monthly management schedules, allowing reservoir operations and sectoral water distribution to be governed by mechanistic catchment moisture trends instead of generalized statistical norms. The additional error metrics computed for MLR corroborate its superior performance (Table 2): RMSE = 4.08 m^3/s and MAE = 2.63 m^3/s were the lowest among the three models, NSE = 0.54 was the only value exceeding the 0.5 satisfactory threshold of Moriasi *et al.* (2007), and MAPE = 26.1% was likewise the lowest. A paired t-test (p = 0.923) and a Wilcoxon signed-rank test (p = 0.757) both failed to reject the null hypothesis of no systematic difference between MLR-simulated and historical inflow values, indicating that MLR combines the best point-accuracy performance among the three models with an absence of systematic bias over the 1998-2023 calibration period. To ascertain whether the observed point-estimate divergences among the three models remain resilient against sampling variability, 95% confidence intervals were generated using a moving block bootstrap approach (B = 2,000; utilizing 12-month blocks). MLR's advantage in MAE was robust specifically against ARIMA, and its NSE advantage over ARIMA was likewise robust, as the respective 95% CIs did not overlap (MLR MAE: 2.33-2.98 m^3/s vs ARIMA: 3.05-3.90 m^3/s; MLR NSE: 0.46-0.64 vs ARIMA: 0.20-0.44); MLR's MAE advantage over Markov Chain (2.94-3.55 m^3/s) was not statistically robust, as the two 95% CIs overlapped narrowly. However, the 95% CIs for r, KGE, RMSE, and MAPE overlapped substantially across all three models, meaning that the apparent ranking on these metrics falls within the bounds of sampling uncertainty given the 26-year monthly record and should not be over-interpreted as a robust, generalizable difference. Consequently, the MLR model is best interpreted as yielding the most competitive point estimates across all evaluated metrics—demonstrating a statistically robust advantage over ARIMA specifically in terms of

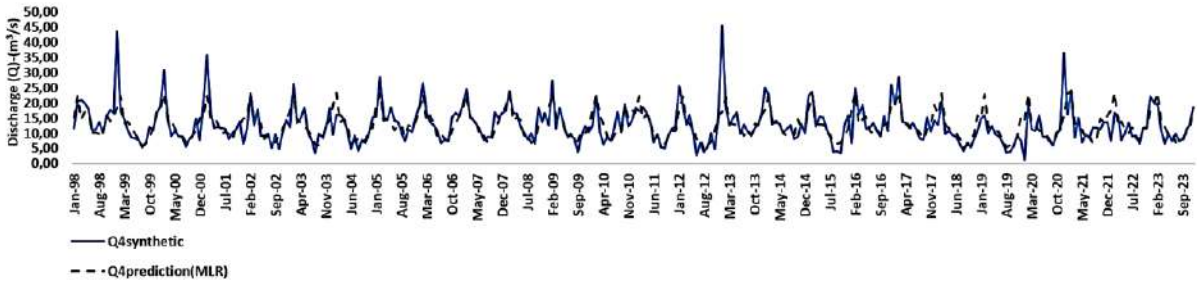

Fig. 4: Comparison of historical (Q4synthetic) and MLR-predicted monthly inflow discharge (1998-2023), showing the closest event-scale tracking among the three models (r = 0.74, KGE = 0.64, RMSE = 4.08 m^3/s), driven primarily by the lagged-inflow predictor

mean absolute error and NSE—rather than exhibiting uniform superiority across every performance dimension. As detailed in Materials and Methods, the twelve month-specific MLR models (Eq. 1) that together generate the calibration series evaluated in Table 2 each rely on a comparatively small per-month sample (n = 26-27 years). Examining the coefficients of these twelve models individually shows that the lagged inflow term (Qin,t-1) is by far the most consistently significant predictor ($p < 0.05$ in 7 of 12 months, concentrated in the May-November transition and dry-season months), whereas P4,t-1 (Sajira) is significant in only one month and P1,t-1 (Banjar Irigasi) is not statistically significant in any month; variance inflation factors remained below 2 throughout, indicating that this pattern reflects genuine predictor importance rather than multicollinearity, and confirming that MLR's predictive skill is driven primarily by the catchment-memory mechanism encoded in Qin,t-1, with the upstream rainfall stations contributing secondary, spatially-distributed information. Leave-one-out cross-validation of these twelve month-specific models shows negative out-of-sample R2 in 6 of 12 months (mean overfitting gap = 0.30), indicating that, taken individually, several of the month-specific models are statistically fragile at this sample size. This trade-off is evaluated against the considerably enhanced overall goodness-of-fit afforded by monthly stratification relative to a pooled-coefficient configuration (r = 0.40, NSE = 0.16; as stated in Materials and Methods section), a convention conceptually analogous to the seasonal parameterization already incorporated into the comparative ARIMA and Markov Chain formulations. Reported MLR performance in Table 2 should therefore be interpreted as the aggregate behavior of twelve seasonally-specific models rather than of a single model generalizing across a large, homogeneous 312-month sample, and the per-month overfitting risk identified here is noted as a limitation in the Study limitations section. Beyond the sample-size and seasonal stratification issues previously addressed, a further structural drawback inherent to the MLR architecture is its rigid linear formulation. Rainfall-runoff mechanisms within steep tropical basins are characterized by distinct threshold-dependent non-linearities. These include storm flow activation governed by antecedent soil moisture saturation limits, as well as non-linear infiltration and groundwater recession behaviors that exceed the representational capacity of conventional linear modeling architecture. This is a plausible contributing explanation for MLR's own moderate (not outstanding) r and KGE values (Table 2) and for the sharp performance degradation observed under independent out-of-sample validation (see above), since nonlinear catchment behavior that differs between the calibration and validation periods cannot be captured by a fixed linear coefficient set. Future work extending this comparison to nonlinear or hybrid statistical models (e.g., ARIMA-LSTM, as noted in the

Outlook) would help isolate how much of the observed performance gap is attributable to linearity itself versus non-stationarity. To explicitly evaluate the independence between the calibration and validation samples, all three modeling frameworks—ARIMA, MLR, and the Markov chain—were further subjected to a strict chronological train-test split. For both the MLR and Markov Chain, state classification thresholds, transition probabilities, and the twelve month-specific regression coefficients (Eq. 1) were derived exclusively from the 1998-2018 dataset. These calibration-derived parameters were subsequently applied without modification or re-fitting to the independent 2019-2023 evaluation period. For ARIMA, the model order was independently re-identified via automated seasonal ARIMA selection on a training subset (n=263) rather than applied from the full-record specification reported in Table 2, yielding ARIMA(1,0,0)(1,1,0)[12] with drift, distinct from the full-record SARIMA(2,0,1)(2,1,2)[12] model; this training/testing split (n=263/61) operates on the undifferenced 1997-2023 series required for ARIMA's seasonal differencing and consequently begins approximately one month earlier than the calendar-aligned 1998-2018/2019-2023 split used for MLR and Markov Chain, though the two splits are closely comparable in both timing and proportion (81%/19% versus 81%/19%). Aggregate performance across all three models and both periods is summarized in Table 3. Although predictive performance declines across the independent validation dataset for all three modeling frameworks, the extent of degradation varies substantially among them. For MLR, NSE falls from 0.61 (calibration) to 0.02 (validation), a value indistinguishable from a naive mean predictor, and MAPE more than doubles from 21.9% to 50.2%. In contrast, the Markov Chain model exhibits an even more pronounced degradation: its state-classification thresholds, transition probabilities, and state-conditional mean discharges, all parameterized exclusively on the 1998-2018 data, achieve NSE = 0.28 in calibration but fall to NSE = -1.01 in validation. This indicates that the calibration-derived model performs worse than utilizing the simple historical mean for the 2019–2023 evaluation period, accompanied by an increase in MAPE from 30.8% to 81.6%. ARIMA, by contrast, shows comparatively modest degradation: NSE falls only from 0.37 (training) to 0.29 (testing), and its correlation coefficient decreases only slightly, from 0.66 to 0.60, despite ARIMA having the lowest calibration-period accuracy of the three models in Table 2. This divergent behavioral pattern provides key insights: the purely autoregressive, seasonally differenced structure of the ARIMA model does not depend on exogenous rainfall or lagged-inflow predictors whose relationship to Qin may itself be shifting, which plausibly makes it less sensitive to the specific form of non-stationarity affecting the exogenous-predictor-dependent MLR and state-transition-dependent Markov Chain models, even though this parsimonious structure simultaneously limits its overall absolute predictive accuracy. This degradation was not an artifact of the particular split year chosen for MLR: repeating the same procedure at six additional split points boundaries spanning 2012-2021 consistently yielded near-zero or negative validation NSE (range: -0.22 to 0.07), irrespective of where the calibration-validation threshold was established. Rather than weakening the central hypothesis, this phenomenon—most pronounced in the Markov chain simulations and observable even within ARIMA's minor degradation—reinforces the fundamental premise of this investigation. Specifically, models calibrated against past hydrological regimes cannot be presumed transferable to future periods in the presence of a non-stationary precipitation-discharge dynamic, regardless of whether the underlying architecture is regression-based, stochastic, or autoregressive. This underscores the necessity for continuous retrospective appraisal of design-era assumptions in lieu of their indefinite operational reuse. The calibration-only

Table 3: MLR, Markov Chain and ARIMA performance under chronological calibration (1998-2018) versus independent out-of-sample validation (2019-2023)

Metric	MLR calibration (1998-2018, n=252)	MLR validation (2019-2023, n=60)	Markov Chain calibration (1998-2018, n=252)	Markov Chain validation (2019-2023, n=60)	ARIMA training (n=263)	ARIMA Testing (n=61)
r (Pearson correlation)	0.78	0.56	0.66	0.32	0.66	0.60
RMSE (m^3/s)	3.85	5.48	5.19	7.86	4.92	4.64
MAE (m^3/s)	2.48	3.65	3.45	5.35	3.41	3.34
NSE	0.61	0.02	0.28	-1.01	0.37	0.29
MAPE (%)	21.9	50.2	30.8	81.6	29.6	47.3

performance reported in Table 2 (MLR: r = 0.74, NSE = 0.54; Markov Chain: r = 0.67, KGE = 0.66; ARIMA: r = 0.62, KGE = 0.60; all computed by fitting and evaluating on the full 1998-2023 record) should accordingly be interpreted as an upper-bound estimate of in-sample fit quality rather than a guarantee of forecasting skill on unseen future periods.

Hydrological year classification and operation guideline trajectories

To bridge the inflow forecast with practical field enforcement, a non-parametric frequency analysis was performed. In lieu of alternative return-period estimators (such as the Gumbel, Log-Pearson III, and California/Hazen formulations), the Weibull plotting-position method was adopted. This approach is favored due to its unbiased nature and prominent status in Indonesian hydrological practice for dependability and return-period assessment. Crucially, unlike parametric distribution-fitting approaches (e.g., Log-Pearson III), it dispenses with a-priori assumptions regarding the parent probability distribution of monthly inflow, thereby mitigating uncertainties stemming from the catchment's limited 26-year instrumental record. Weibull probability analysis applied to the multi-decade dataset yielded reliable discharge thresholds of 9.51 m^3/s (P80% or R5 dry, representing dry year conditions), 15.65 m^3/s (P50% or R2 normal, representing normal year conditions), and 21.66 m^3/s (P20% or R5 Wet, representing wet year conditions). The full seasonal variation of these reliable flows across the various reliability classes is structurally illustrated in Fig. 5. The R5 discharge limit was adopted as the primary basis for Phase 1 water allocation, allocating 6.45 m^3/s for the Tangerang raw water covered tunnel and a nominal 3.06 m^3/s for the downstream flow of the Ciujung River. Crucially, the R5-estimated discharge surpasses the baseline operational threshold of 2.20 m^3/s previously stipulated by the regional water authority (BBWS C3 2025) with an incremental addition of 0.86 m^3/s, thereby yielding a 39.09% upward adjustment. This adjustment closes approximately 47.78% of the operational gap towards the ideal design drought discharge reference of 4.0 m^3/s required for full ecosystem preservation (KOICA, 2006), with a remaining gap of 0.94 m^3/s remaining unmet. However, under severe R_{10} hydrological constraints, the residual streamflow entering the Ciujung River sharply declines to 1.22 m^3/s. Such streamflow volumes fall critically short of the thresholds required to operate the 1.8 megawatt (MW) run-of-river hydropower turbines and maintain downstream aquatic ecosystem integrity, underscoring the severe ecological susceptibility of the catchment. To systematically manage these risks, long-term operation guideline trajectories were derived using the Rippl Method mass-balance reservoir simulation. The resulting monthly volume trajectories for each hydrological year class are detailed in Fig. 6. As depicted in Fig. 6, reservoir storage behavior exhibits highly seasonal and monsoon-dependent characteristics. Active storage begins at a relatively low level in January, with wet-year volumes starting at approximately 39.55 million m^3, normal-year volumes at 20.14 million m^3, and dry-year volumes at 6.46 million m^3.

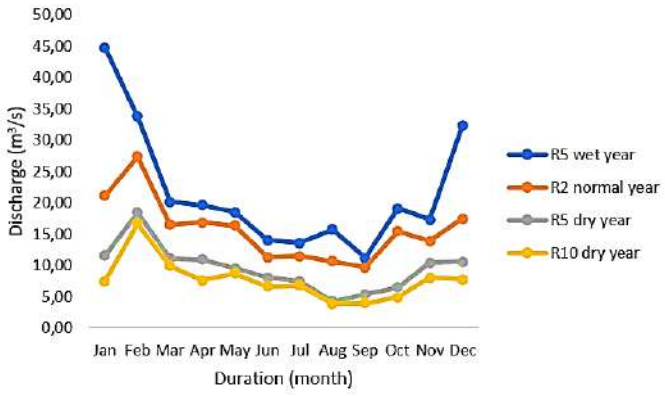

Fig. 5: Monthly distribution of Karian Reservoir dependable discharges across four Weibull reliability classes (R_5 wet year to R_{10} dry year), showing the sharp dry-season contraction from the R5 Dry threshold of 9.51 m^3/s to a residual R10 discharge of just 1.22 m^3/s

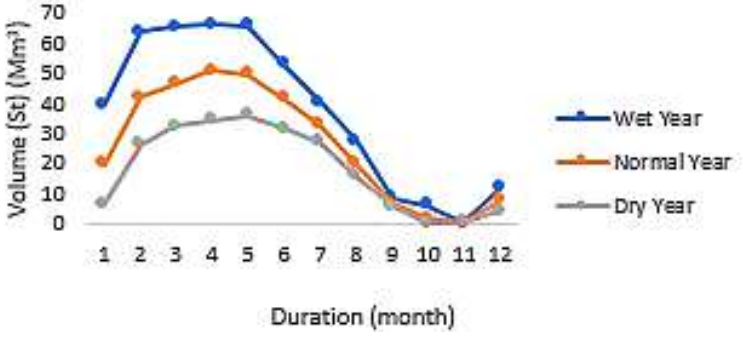

Fig. 6: Three-class operation guideline trajectory curves for Karian Reservoir (dry, normal, and wet year classifications) derived from the Rippl mass-balance simulation, showing active storage accumulating to a wet-year peak of 66.42 million m3 in April before contracting to near-zero levels during the September-November low-flow period

Active storage volumes exhibit a progressive accumulation phase throughout the monsoon, reaching absolute peak capacity in April for both wet-year (66.42 million m^3) and normal-year (50.86 million m^3) conditions, while peaking slightly later in May (36.07 million m^3) in dry-year conditions. In contrast, water storage volumes exhibit a severe depletion phase beginning in June, driven by the steep decline in basin inflows characteristic of the dominant dry monsoon pattern. This downward trend culminates in near-zero active storage volumes during the critical September–November period, with storage reaching absolute zero in October (dry conditions) and November (wet and normal conditions). This interval of extreme low storage manifests as an annual bottleneck of ecological vulnerability, marked by the potential collapse of required downstream environmental flows within the critical Ciujung River reach. In accordance with established hydrodynamic and ecological principles observed in similar systems, such near-zero storage states would theoretically intensify vulnerability to localized saltwater encroachment in the estuary and associated habitat impacts, notwithstanding the omission of direct salinity and biodiversity measurements in the current study (Bauer *et al*., 2025).

Reservoir operation simulation

To evaluate how inflow forecasting errors propagate into long-term infrastructure behavior, the three generated inflow time series were integrated as direct forcing vectors into reservoir operation simulations. Model trajectories generated under the ARIMA, Markov chain, and

MLR frameworks are presented in comparative alignment across Figs. 7, 8, and 9. The ARIMA-forced simulation (Fig. 7) achieved a guideline-to-actual trajectory correlation (R) of 0.76. During the 1998–2005 wet seasons, actual simulated storage trajectories frequently exceeded target guideline envelopes due to the underestimation of high-flow periods by the ARIMA model. This indicates a high risk of uncontrolled spillway losses and unutilized hydro-potential. The probabilistic Markov chain simulation (Fig. 8) achieved an improved R of 0.8, displaying more consistent trajectory tracking and tighter adherence to the target boundary conditions across both average and wet sequences. The MLR-forced simulation (Fig. 9) achieved superior predictive capability with a correlation coefficient of R = 0.85, establishing a stable discharge regime while effectively mitigating large excursions from target guidelines. This outcome provides empirical evidence favoring the operational use of MLR-based inflow scenarios for long-term planning, with the caveat noted above that this advantage is statistically robust for MAE and NSE but not yet distinguishable from sampling uncertainty for r, KGE, RMSE, and MAPE. Crucially, while keeping all internal operational boundary constraints fixed, all three models mathematically confirm that the Karian Reservoir possesses adequate structural capacity to satisfy Phase 1 mandatory multi-sectoral release obligations under standard climatological conditions. However, the MLR framework minimizes risk by preventing abrupt over-releases.

Eco-hydrological trade-offs and multi-sectoral allocation dynamics

Integrating these forecasting structures into the multi-objective water balance equation illuminates the severe operational trade-offs inherent to the Karian Reservoir system under hydrological constraints. Severe inflow reductions reaching extreme dry-year thresholds (R10) diminish the residual operational margin to negligible levels, thereby intensifying the trade-off between human water infrastructure requirements and downstream aquatic ecological survival (Poff *et al*., 2010; Arthington *et al*., 2024). This convergence between infrastructure operation and river ecosystem service provision underscores the value of coupling landscape-scale ecological assessments with reservoir release planning (Dede *et al*., 2023). Total reservoir discharge is routed through two distinct, physically segregated conduits. A closed tunnel supplies the fixed-priority, legally non-negotiable urban raw water withdrawal for Tangerang, whose design allocation evolved from an original 9.1 m^3/s to 12.4 m^3/s before settling at the current Phase 1 value of 6.45 m^3/s. An open channel, feasibility-study design capacity 5.5 m^3/s, first routes water through the 1.8 MW run-of-river hydroelectric power plant turbines before releasing the same water to the Ciujung/Ciberang system to jointly serve raw water supply, irrigation, and river-maintenance (environmental) flow; the feasibility study did not subdivide this 5.5 m^3/s into separate, individually protected sub-allocations for each use; it estimated a combined river-maintenance requirement of approximately 4.0 m^3/s but did not wall this off as a reserved quantity within the 5.5 m^3/s design total. Crucially, the prevailing rule structure fails to treat environmental flow as an adaptive constraint capable of dynamically adjusting releases during low-storage events. Throughout this study, the frequently referenced 3.06 m^3/s environmental flow figure is more accurately defined as the total open-channel residual under R5 dry-year dependable-flow conditions. Specifically, this figure represents the 9.51 m3/s total inflow minus the 6.45 m^3/s tunnel withdrawal, which is shared among raw water supply, irrigation, and river maintenance. As raw water and irrigation draws draw from this shared pool, actual water availability for ecological integrity is heavily constrained. Consequently, the ecological-risk assessments evaluated against Tennant thresholds serve as conservative, upper-bound estimates of e-flow stress rather than exact measurements of dedicated environmental allocations (BBWS C3, 2025) allocates the Karian-side intake serving the Serang area as 1.5 m^3/s raw

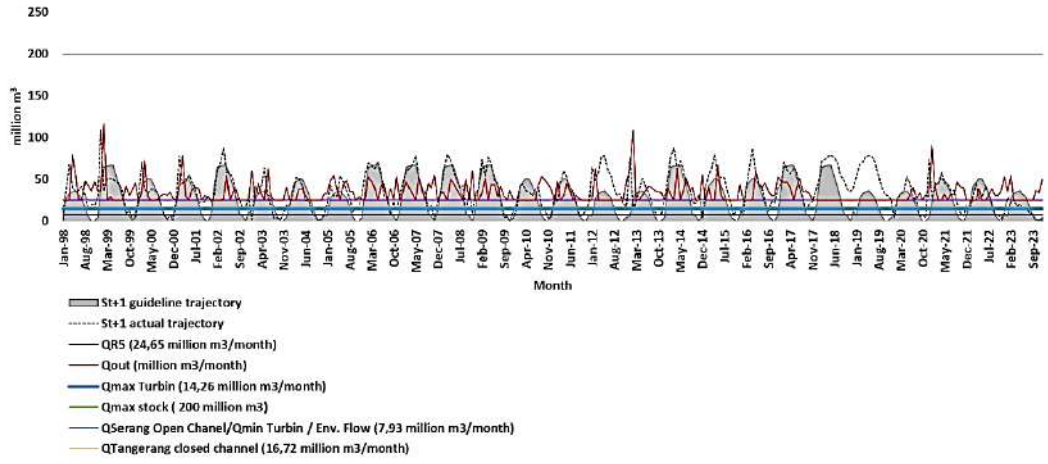

Fig. 7: ARIMA-based reservoir operation simulation showing St+1 guideline and actual trajectories with operational parameters (1998–2023); actual storage frequently overshoots the guideline envelope during 1998-2005 wet seasons (R = 0.76), indicating a risk of uncontrolled spillway losses

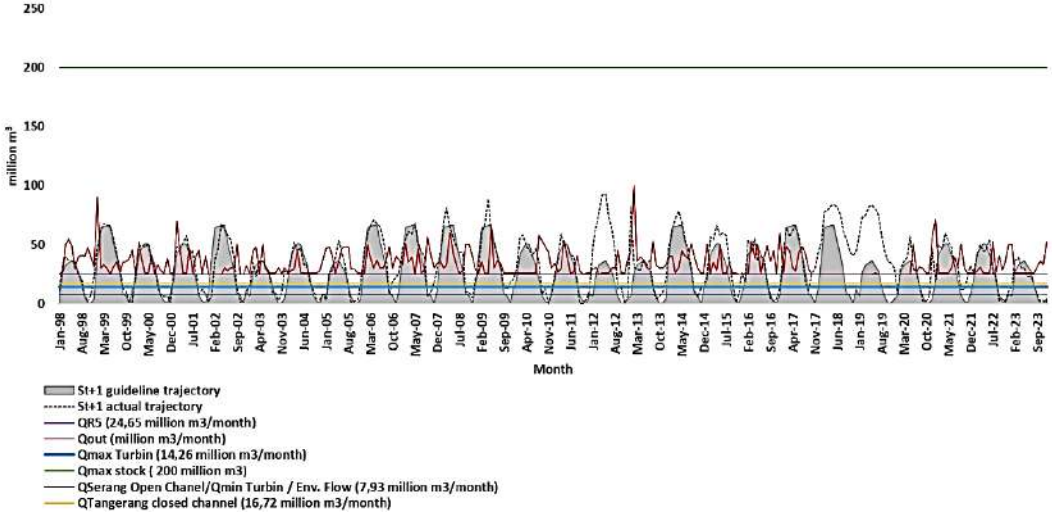

Fig. 8: Markov chain-based reservoir operation simulation showing St+1 guideline and actual trajectories with operational parameters (1998–2023), displaying more consistent trajectory tracking than ARIMA (R = 0.80) across both average and wet sequences

water supply plus 0.7 m^3/s irrigation (2.2 m^3/s total), without an explicit environmental-flow or hydropower line item comparable to the original feasibility study's provisions; whether this reflects an actual removal of environmental-flow consideration from current operational planning, or simply its omission from this particular planning summary while it is retained in other unpublished technical documents, could not be determined from the materials available to this study and is noted here as an area requiring clarification with the implementing agency rather than as an established finding. The performance of operational simulations reveals significant vulnerabilities when utilizing uncoupled or systematically biased models like ARIMA. Specifically, under R10 conditions, these predictive inaccuracies force the designated 3.06 m^3/s environmental flow down to a deficient minimum of 1.22 m^3/s. This extreme truncation would be expected to severely diminish the river's ecological assimilative capacity; based on

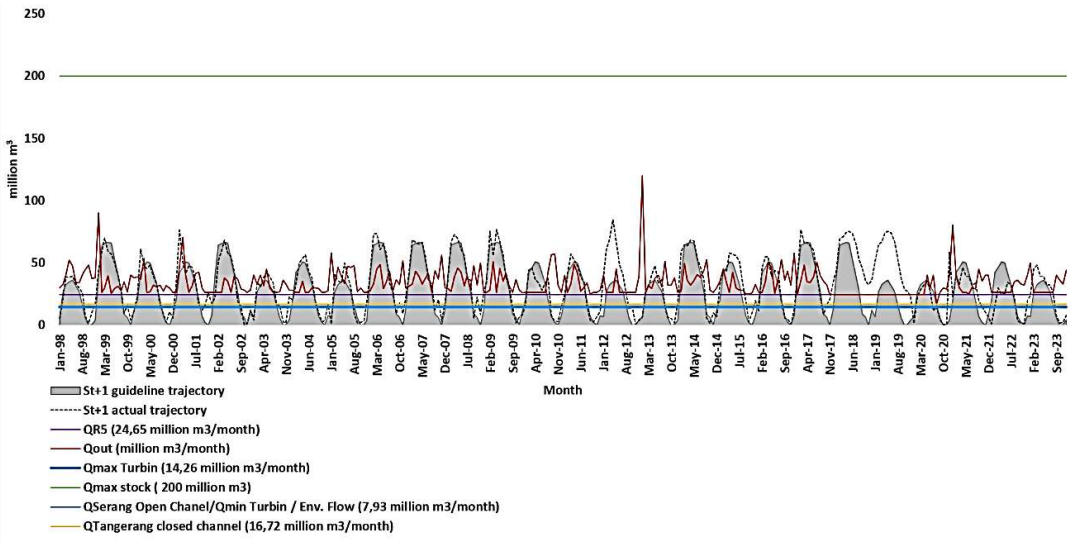

Fig. 9: MLR-based reservoir operation simulation showing St+1 guideline and actual trajectories with operational parameters (1998–2023); the closest adherence to the guideline envelope among the three models (R = 0.85) yields the most stable, risk-minimizing discharge pattern

mechanisms documented in comparable low-flow systems, such conditions could plausibly contribute to dissolved oxygen depletion and saltwater estuarine intrusion upstream, although these water-quality and salinity responses were not directly measured in the present study (Wu *et al.*, 2023). As previously noted, the R5-derived allocation narrows the historical design gap by approximately 39.09% relative to the minimum threshold recommended by the regional authority. Despite this improvement, a deficit of 0.94 m^3/s remains against the complete ecosystem-preservation objective (KOICA, 2006). Conversely, by deploying the complementary MLR-Markov Chain decision-support architecture proposed in this study, reservoir operators can balance these trade-offs dynamically (Li and Zhu, 2025). This methodological framework must comprehensively address multiple socio-environmental dimensions. Crucially, it needs to balance social legitimacy and water-quality trade-offs among the local communities dependent on the shared reservoir (Al-Afeshat *et al.*, 2025). The MLR provides the short-term precision needed to maximize run-of-river hydropower generation during transient wet intervals (Yajure-Ramírez, 2026), while the Markov chain framework provides the long-term probabilistic warning required to trigger ecological water rationing, preventing the complete collapse of downstream riparian eco-services during macroclimatic anomalies (Huang *et al.*, 2026).

Outlook for advancing sustainable reservoir management

This comparative study highlights that while the deterministic MLR model excels as an operational tool for creating guideline trajectories (R = 0.85, r = 0.74, KGE = 0.64), the Markov Chain model acts as a vital probabilistic instrument to safeguard against severe drought risks. Incorporating this complementary MLR-Markov Chain approach offers a low-cost, practically implementable decision-support approach that accounts for hydrological environmental-flow thresholds, rather than a validated ecologically sensitive system, since ecological outcomes were not directly evaluated in this study (see Study limitations). This framework can guide water authorities in simultaneously balancing all five competing Phase 1 strategic mandates at the Karian Reservoir. A primary limitation of this study is its reliance on the reconstructed Q_{in} synthetic inflow record. Nevertheless, this framework exhibits inherent limitations under conditions of hydrological non-stationarity. Such regime

shifts—stemming from anthropogenic climate change, intensive land-use alterations, and amplified ENSO/IOD teleconnections across the Indonesian archipelago—pose ongoing challenges to long-term projections (Irwandi *et al*., 2021). To advance sustainable reservoir management in tropical monsoonal zones, future research should prioritize three key domains:

- Development of hybrid ARIMA-LSTM (long short-term memory) networks and gradient boosting machines to better map non-stationary, non-linear peak discharge variations (Kratzert *et al*., 2019).
- Integration of downscaled CMIP6 climate change projections and dynamic land-use conversion scenarios directly into the water balance equation.
- To build regional resilience against extreme climate anomalies, this comparative eco-hydrological evaluation framework warrants systematic replication. Specifically, its application should be extended to other strategic, multipurpose tropical reservoirs throughout Southeast Asia.

The empirical evidence established through this multi-model framework demonstrates that transitioning from traditional linear approaches to a complementary MLR-Markov chain paradigm provides a robust, data-driven foundation for tropical reservoir management worldwide. Crucially, the MLR and Markov Chain components were formulated, calibrated, and validated as independent frameworks within this study, omitting any joint calibration or optimized structural coupling. The framing of these models as 'complementary' is therefore strictly conceptual. It denotes their separate operational roles in short-term guideline generation versus long-term drought-risk screening, rather than an interconnected modeling architecture. By accurately capturing seasonal inflow variations and quantifying drought state-transition probabilities, this two-model approach offers a transferable framework that may inform operation planning at other tropical monsoonal reservoirs facing similar trade-offs between hydropower generation and downstream environmental flow protection, pending validation across additional basins and climate scenarios.

Study limitations and future directions

Several methodological limitations of this study warrant consideration. First, eco-flow compliance was evaluated strictly using hydrological proxy thresholds (specifically the Tennant method) rather than direct *in situ* biological sampling. Qualitative inferences regarding ecological risk—such as dissolved oxygen depletion or benthic habitat stress, are fundamentally anchored to minimum volumetric discharge thresholds established for aquatic habitat preservation. They do not stem from direct empirical observations of biological responses. Future research should integrate multi-seasonal biological monitoring with hydrodynamic modeling to empirically validate ecological outcomes under simulated release strategies. Second, because the Karian Reservoir lacks an operational inlet gauging station, the reconstructed inflow (Qin) baseline cannot be independently validated through on-site measurements. While internal consistency with legacy estimates (KOICA area-ratio) was verified, both approaches rely on the same downstream reference station (Q7), representing an inherent monitoring constraint to be prioritized in future instrumentation efforts. Third, the predictive performance obtained here ($r = 0.62–0.75$, KGE = 0.60–0.66) is more conservative than metrics reported in longer-record tropical reservoir studies. For instance, comparative applications of Markov Chain, NRECA, ARIMA, and continuous models at Jatigede Reservoir, Indonesia achieved substantially higher accuracy (Jayanti *et al*., 2023), while MLR, ARIMA, and SARIMA models at Koyna Reservoir, India (Magar and Jothiprakash, 2011) and across East Java reservoirs (Margini *et al*., 2022) also demonstrated strong predictive performance. These regional discrepancies do not stem from any methodological shortcoming. Instead, they reflect Karian's shorter 26-year record, the retention of extreme events, and dynamic monsoonal

variability. Moreover, fitting month-specific MLR models on 26–27 years of data introduces sampling uncertainty, leading to variable out-of-sample generalization despite outperforming a single pooled formulation. Subsequent studies should evaluate alternative modeling strategies, including harmonic regression and partial pooling. Incorporating these frameworks will help capture finer seasonal dynamics while optimizing sample efficiency. Finally, because all models were calibrated for a single monsoonal catchment (Karian/Ciberang), extending this framework to catchments with distinct hydroclimatic regimes (such as snowmelt influence or bimodal rainfall) will require structural adjustments and independent re-validation.

CONCLUSION

This study evaluated three low-data statistical inflow forecasting frameworks—MLR, Markov Chain, and ARIMA—against the Karian Reservoir's historical hydrological record (1998–2023) to examine whether design-era operational assumptions remain hydrologically defensible under present-day flow regimes. The historical calibration period (1998–2018) revealed considerable variation in functional performance characteristics across the evaluated methodologies. MLR achieved the highest calibration accuracy ($r = 0.74$, KGE = 0.64, $R = 0.85$) by effectively leveraging lagged inflow variables to capture catchment storage memory and temporal persistence. While delivering a comparable overall efficiency (KGE = 0.66), the Markov Chain framework excelled in capturing complex hydrological patterns. Specifically, it exhibited enhanced capability in reproducing long-term probability distributions and structural low-flow characteristics. Conversely, ARIMA produced the weakest baseline performance ($r = 0.62$, KGE = 0.60), largely driven by a systematic overestimation of dry-season baseflow. This constraint reveals a fundamental structural limitation of the ARIMA model. Specifically, it lacks the technical capacity to accommodate extreme seasonal fluctuations without introducing substantial signal distortion in monsoonal hydrological systems. Critically, independent out-of-sample validation (2019–2023) revealed a severe performance degradation across all frameworks. The NSE for MLR plummeted from 0.61 to 0.02, while the Markov Chain framework dropped drastically from 0.28 to -1.01. The marked degradation in predictive capability confirms the presence of hydrological non-stationarity across the catchment. This degradation demonstrates that traditional models parameterized on past hydroclimatic regimes require continuous adaptive recalibration to maintain long-term reliability. Consequently, these empirical findings directly address the primary objective of this study: no single low-data statistical model evaluated here is dependably robust for static operational deployment over long horizons. Furthermore, the original design-era environmental-flow target of 3.06 m^3/s must be re-categorized as provisional. Adhering to inflexible historical release rules compromises downstream aquatic ecosystems and water-supply security. As runoff patterns deviate increasingly from stationary historical baselines, these systems face compounded operational vulnerabilities. The broader scientific and practical implications of these findings highlight the urgent need to transition from deterministic, static reservoir operating policies toward dynamic, risk-based operational strategies in data-scarce tropical basins. Relying solely on historical statistical relationships creates a false sense of operational security, particularly during prolonged dry spells or extreme convective rainfall events. By illustrating the performance decay of conventional statistical models under non-stationary hydroclimatic regimes, this work highlights a critical operational requirement. Specifically, it emphasizes the imperative to incorporate real-time feedback mechanisms into modern reservoir management frameworks. Adaptive management protocols must replace legacy operational rules to reconcile competing demands between municipal water supply, flood control, and downstream ecological integrity.

These findings should, however, be interpreted with due consideration of specific methodological constraints. First, the analysis relied on a single reconstructed catchment inflow dataset, which may carry unresolved observational uncertainties or spatial aggregation biases from streamflow routing approximations. Second, rather than utilizing direct in-situ biological sampling of fish or macroinvertebrate communities, ecological adequacy was assessed via hydrological proxy indicators. Specifically, this study adopted the Tennant methodology to establish environmental flow requirements. Third, because calibration was restricted to a single reservoir catchment, specific numerical parameters and degradation rates observed here may not transfer to other climatic zones or topographically diverse catchments without independent local revalidation.

AUTHOR CONTRIBUTIONS

I. Mulyawati, prepared in data curation, formal analysis, investigation, visualization and preparing the manuscript draft. I.R.S. Salami, the first promotor and corresponding author, supervised the first author, contributed to conceptualization, and reviewed the manuscript. M. Marselina, the second promotor, also supervised the first author and contributed to conceptualization and manuscript review. A. Sabar, the third promotor, supervised the first author, contributed to conceptualization, and reviewed the manuscript.

ACKNOWLEDGEMENT

I. Mulyawati was supported by the Center for Higher Education Funding and Assessment (PPAPT), Ministry of Higher Education, Science, and Technology of the Republic of Indonesia, and the Indonesia Endowment Fund for Education (LPDP), Ministry of Finance of the Republic of Indonesia, through the Beasiswa Pendidikan Indonesia (BPI) for doctoral studies [Grant number: 202101121537]. The authors gratefully acknowledge BBWS C3, Banten Province, Indonesia, for providing hydrological monitoring network data and the location map of Karian Reservoir during a series of field visits conducted between 2021 and 2025.

CONFLICT OF INTEREST

The authors declare that there is no conflict of interests regarding the publication of this manuscript. In addition, the ethical issues, including plagiarism, informed consent, misconduct, data fabrication and/or falsification, double publication and/or submission, and redundancy have been completely observed by the authors.

OPEN ACCESS

©2027 The author(s). This article is licensed under a Creative Commons Attribution 4.0 International License, which permits use, sharing, adaptation, distribution and reproduction in any medium or format, as long as you give appropriate credit to the original author(s) and the source, provide a link to the Creative Commons license, and indicate if changes were made. The images or other third-party material in this article are included in the article's Creative Commons license, unless indicated otherwise in a credit line to the material. If material is not included in the article's Creative Commons license and your intended use is not permitted by statutory regulation or exceeds the permitted use, you will need to obtain permission directly from the copyright holder. To view a copy of this license, visit: http://creativecommons.org/licenses/by/4.0/

PUBLISHER'S NOTE

GJESM Publisher remains neutral with regard to jurisdictional claims in published maps and institutional affiliations.

POSITIVE AI STATEMENT

During the preparation of this work the author(s) have used Artificial Intelligence (AI) [Quillbot] in order to improve English language clarity, grammar accuracy, and academic phrasing of the manuscript. After using this tool/service, the authors reviewed and edited the content as needed and take full responsibility for the content of the publication.

ABBREVIATIONS

%	Percent
ACF	Autocorrelation function
AIC	Akaike information criterion
ARIMA	Autoregressive integrated moving average
BBWS C3	Balai Besar Wilayah Sungai Cidanau-Ciujung-Cidurian
BPI	Beasiswa Pendidikan Indonesia
CMIP6	Coupled Model Intercomparison Project Phase 6
DPI	Dots per inch
ENSO	El Niño-Southern Oscillation
FDC	Flow duration curve
IID	Independent-and-identically-distributed
IOD	Indian Ocean Dipole
KGE	Kling-Gupta efficiency
KOICA	Korea International Cooperation Agency
LPDP	Lembaga Pengelola Dana Pendidikan (Indonesia Endowment Fund for Education)
LSTM	Long short-term memory
MAF	Mean annual flow
m^3/s	Cubic meter per second
MLR	Multiple linear regression
MW	Megawatt
n	Sample size / number of time steps
NSE	Nash-sutcliffe efficiency
PPAPT	Pusat Pembiayaan dan Asesmen Pendidikan Tinggi (Center for Higher Education Funding and Assessment)
r	Pearson correlation coefficient
R	Operational trajectory correlation coefficient

REFERENCES

Aksoy, H., (2003). Markov chain-based modeling techniques for stochastic generation of daily intermittent streamflows. Adv. Water Resour., 26(6): 663–671 (**9 pages**).

Al-Afeshat, A.; Zoubi, M.M.; Abu-Afifeh, Q.Y.; Al-Jawaldeh, H.; Qutishat, T.A.; Masoud, A.M.N.; Rahbeh, M., (2025). Interrelation of dams sustainability with the local communities and water quality. Global J. Environ. Sci. Manage., 11(1): 157–176 (**20 pages**).

Aldrian, E.; Dwi Susanto, R., (2003). Identification of three dominant rainfall regions within Indonesia and their relationship to sea surface temperature. Int. J. Climatol., 23(12): 1435–1452 (**18 pages**).

Arianti, D.; Murtilaksono, K.; Barus, B., (2015). Evaluation of land use for design flood discharge prediction in Ciberang watershed, Banten Province. TATALOKA, 17(2): 76–86 **(11 pages).**

Arwin; Bourqueil, M., (1992). Modelisation des ressources en eau et leur exploitation énergétique sur l'exemple du bassin supérieur de Citarum en Indonesie. Doctoral Thesis. Toulouse, INPT (**250 pages**).

Alrayess, H.; Zeybekoglu, U.; Ulke, A., (2017). Different design techniques in determining reservoir capacity. Eur. Water, 60: 107–115 (**9 pages**).

Anand, V.; Oinam, B., (2019). Future climate change impact on hydrological regime of river basin using SWAT model. Global J. Environ. Sci. Manage., 5(4): 471–484 (**14 pages**).

Aness, W.Th.; Hadadin, N.A.; Zoubi, M.M.; Abu-Afifeh, Q.Y.; Al-Afeshat, A.F.; Al-Jawaldeh, H.F.; Qutishat, T.A.; AlHalaigah, M.R.; Alnizami, N.H.; Aljarrah, A.; Alta'any, Y.A.; Alzubaidi, A.J., (2026). Runoff and sediment dynamics modeling for erosion risk reduction and sustainable watershed management. Global J. Environ. Sci. Manage., 12(2): 813–836 (**24 pages**).

Arthington, A.H.; Tickner, D.; McClain, M.E.; Acreman, M.C.; Anderson, E.P.; Babu, S.; Dickens, C.W.S.; Horne, A.C.; Kaushal, N.; Monk, W.A.; O'Brien, G.C.; Olden, J.D.; Opperman, J.J.; Owusu, A.G.; Poff, N.L.; Richter, B.D.; Salinas-Rodríguez, S.A.; Shamboko Mbale, B.; Tharme, R.E.; Yarnell, S.M., (2024). Accelerating environmental flow implementation to bend the curve of global freshwater biodiversity loss. Environ. Rev., 32(3): 387–413 (**27 pages**).

Atieh, M.; Taylor, G.; Sattar, A.M.A.; Gharabaghi, B., (2017). Prediction of flow duration curves for ungauged basins. J. Hydrol., 545: 383–394 (**12 pages**).

Balai Besar Wilayah Sungai Cidanau-Ciujung-Cidurian (BBWSC3), (2025). Spatial data of Karian Reservoir watershed. Unpublished technical dataset, Ministry of Public Works and Housing, Banten, Indonesia.

Bargam, B.; Boudhar, A.; Kinnard, C.; Bouamri, H.; Nifa, K.; Chehbouni, A., (2024). Evaluation of the support vector regression (SVR) and the random forest (RF) models accuracy for streamflow prediction under a data-scarce basin in Morocco. Discov. Appl. Sci., 6: 306 (**18 pages**).

Bauer, J.; Dörr, F.; Vu, H.T.D.; Schenk, A.; Tran, H.V.; Pham, V.C.; Börsig, N.; van der Linden, R.; Nguyen, N.H.; Eiche, E.; Norra, S., (2025). Seawater intrusion in river delta systems. Inter-annual dynamics and drivers of salinity variations in the southern Mekong Delta, Vietnam. J. Hydrol., 661: 133745 (**13 pages**).

Box, G.E.P.; Jenkins, G.M.; Reinsel, G.C.; Ljung, G.M., (2015). Time series analysis: Forecasting and control. 5th Edn. John Wiley and Sons, New Jersey, USA. (**712 pages**).

Chan, J.C.F.; Lam, B.Y.K.; Dudgeon, D.; Liew, J.H., (2025). Global consequences of dam-induced river fragmentation on diadromous migrants: A systematic review and meta-analysis. Biol. Rev., 100(5): 2020–2037 (**18 pages**).

Dede, M.; Sunardi, S.; Lam, K.C.; Withaningsih, S., (2023). Relationship between landscape and river ecosystem services. Global J. Environ. Sci. Manage., 9(3): 637–652 (**16 pages**).

Dimitriadou, S.; Nikolakopoulos, K.G., (2022). Multiple linear regression models with limited data for the prediction of reference evapotranspiration of the Peloponnese, Greece. Hydrology, 9(7): 124 (**18 pages**).

Evans, J.D., (1996). Straightforward Statistics for the Behavioral Sciences. Brooks/Cole Publishing Company, Pacific Grove, CA, USA (**600 pages**).

Government of Indonesia, (2011). Government Regulation No. 38/2011 concerning Rivers (Peraturan Pemerintah No. 38 Tahun 2011 tentang Sungai). State Secretariat of the Republic of Indonesia, Jakarta.

Grill, G.; Lehner, B.; Thieme, M.; Geenen, B.; Tickner, D.; Antonelli, F.; Babu, S.; Borrelli, P.; Cheng, L.; Crochetiere, H.; Ehalt Macedo, H.; Filgueiras, R.; Goichot, M.; Higgins, J.; Hogan, Z.; Lip, B.; McClain, M.E.; Meng, J.; Mulligan, M.; Nilsson, C.; Olden, J.D.; Opperman, J.J.; Petry, P.; Reidy Liermann, C.; Sáenz, L.; Salinas-Rodríguez, S.; Schelle, P.; Schmitt, R.J.P.; Snider, J.; Tan, F.; Tockner, K.; Valdujo, P.H.; van Soesbergen, A.; Zarfl, C., (2019). Mapping the world's free-flowing rivers. Nature, 569(7755): 215–221 (**7 pages**).

Gupta, A.; Kumar, A., (2022). Two-step daily reservoir inflow prediction using ARIMA-machine learning and ensemble models. J. Hydro-Environ. Res., 45: 39–52 (**14 pages**).

Gupta, H.V.; Kling, H.; Yilmaz, K.K.; Martinez, G.F., (2009). Decomposition of the mean squared error and NSE performance criteria: Implications for improving hydrological modelling. J. Hydrol., 377(1–2): 80–91 (**12 pages**).

Hasan, K.; Islam, M.S.; Mitu, K.N.; Salam, M.I.; Aghashahi, N., (2025). Evaluating the performance of CHIRPS and CPC precipitation data for streamflow

forecasting using multiple linear regression and Long Short-Term Memory Neural Network model. MethodsX, 15: 103443 (**15 pages**).

Huang, B.; Peng, T.; Fan, T.; Singh, V.P.; Dong, X.; Lin, Q.; Chang, W.; Liu, J.; Huang, Y.; Guo, J.; Li, Y.; Yu, D., (2026). Assessment of dynamic drought risk and transition characteristics by combining an indicator-based approach and Markov chain model. Nat. Hazards, 122(4): 141 (**29 pages**).

Ilmi, M.K., (2022). Determination of environmental flow in Dodokan watershed based on Tennant and flow duration curve (FDC) method. Media Ilm. Tek. Sip, 10(2): 115-123 **(9 pages)**.

Irwandi, H.; Rosid, M.S.; Mart, T., (2021). The effects of ENSO, climate change and human activities on the water level of Lake Toba, Indonesia: A critical literature review. Geosci. Lett., 8(21): 1-13 (**13 pages**).

Jayanti, M.; Sabar, A.; Ariesyady, H.D.; Marselina, M.; Qadafi, M., (2023). A comparison of three water discharge forecasting models for monsoon climate region: A case study in Cimanuk-Jatigede watershed, Indonesia. Water Cycle, 4: 17-25 **(9 pages).**

Jayanti, M.; Marganingrum, D.; Plamonia, N.; Santoso, H.; Marselina, M.; Ariesyady, H.D.; Sabar, A., (2025). The operation optimization of multipurpose reservoir between ARIMA, continuous, and Markov Chain models on Jatigede reservoir, Indonesia. Water Cycle, 6: 399–411 (**13 pages**).

Jehanzaib, M.; Shah, S.A.; Yoo, J.; Kim, T.-W., (2020). Investigating the impacts of climate change and human activities on hydrological drought using non-stationary approaches. J. Hydrol., 588: 125052 (**16 pages**).

KOICA, (2006). Hydrology study: Main report - Feasibility study for Karian multipurpose dam project. Korea International Cooperation Agency and Directorate General of Water Resources, Ministry of Public Works, Seoul and Jakarta. (**185 pages**).

Kratzert, F.; Klotz, D.; Herrnegger, M.; Sampson, A.K.; Hochreiter, S.; Nearing, G.S., (2019). Toward improved predictions in ungauged basins: Exploiting the power of machine learning. Water Resour. Res., 55(12): 11344–11354 (**11 pages**).

Künsch, H.R., (1989). The jackknife and the bootstrap for general stationary observations. *Ann. Statist.*, 17(3): 1217-1241 (**25 pages**).

Li, C.; Zhu, T., (2025). Integrating Eco-Index and Hydropower Optimization for Cascade Reservoir Operations in the Lancang–Mekong River Basin. Water. 17(20): 2966 (**19 pages**).

Loucks, D.P.; van Beek, E., (2017). Water resource systems planning and management: an introduction to methods, models, and applications. Springer, Cham (624 pages)**.**

Lewis, C.D., (1982). Industrial and business forecasting methods. Butterworths, London, United Kingdom (**143 pages**).

Magar, R.B.; Jothiprakash, V., (2011). Intermittent reservoir daily-inflow prediction using lumped and distributed data multi-linear regression models. J. Earth Syst. Sci., 120(6): 1067-1084 (**18 pages**).

Margini, N.F.; Anwar, N.; Wardoyo, W.; Prastyo, D.D.; Yusop, Z., (2022). Monthly inflow forecasting of three multi-purpose reservoirs. Int. J. Adv. Sci. Eng. Inf. Technol., 12(6): 2190-2195 (**6 pages**).

Marselina, M.; Sabar, A.; Salami, I.R.S.; Marganingrum, D., (2016). Management optimization of Saguling reservoir with Bellman dynamic programming and "Du Couloir" iterative method. Forum Geografi, 30(1): 14-23 (**10 pages**).

Marselina, M.; Sabar, A.; Salami, I.R.S.; Marganingrum, D., (2017). Model prakiraan debit air dalam rangka optimalisasi pengelolaan Waduk Saguling-Kaskade Citarum. J. Tek. Sip., 24(1): 99-108 (**10 pages**).

Mazvimavi, D.; Kapangaziwir, E.; Gumbo, A.D., (2024). Assessing the effects of non-stationarity on reservoir yield estimations: A case study of the Southern Okavango Integrated Water Development system in Botswana. River Res. Appl., 40(1): 3–13 **(11 pages).**

McMahon, T.A.; Adeloye, A., (2005). Water resources yield. Water Resources Publications, Colorado, USA. (**234 pages**).

Mitze, F.; Jacobs, S.R.; Breuer, L.; Campos Zeballos, J.; Weeser, B., (2025). Evaluating hydrological model performance using varying amounts of participatory monitoring water level data. PLOS Water, 4(9): e0000405 **(21 pages)**.

Moriasi, D.N.; Arnold, J.G.; Van Liew, M.W.; Bingner, R.L.; Harmel, R.D.; Veith, T.L., (2007). Model evaluation guidelines for systematic quantification of accuracy in watershed simulations. *Trans. ASABE*, 50(3): 885-900 (**16 pages**).

Mulyawati, I.; Siti Salami, I.R.; Marselina, M.; Sabar, A., (2024). The development of inflow discharge for the karian multipurpose reservoir in the pursuit of reservoir management optimization. E3S Web Conference, 485: 04009 (**13 pages**).

Mulyawati, I.; Salami, I.R.S.; Marselina, M.; Sabar, A., (2025). A comparison of Markov Chain, Sarima and multiple linear regression for forecasting discharge. Int. J. Innov. Res. Sci. Stud., 8(3): 4176-4188 **(13 pages).**

Null, S.E.; Zeff, H.; Mount, J.; Gray, B.; Sturrock, A.M.; Sencan, G.; Dybala, K.; Thompson, B., (2024). Storing and managing water for the environment is more efficient than mimicking natural flows. Nat. Commun., 15(1): 5462 (**13 pages**).

Poff, N.L.; Richter, B.D.; Arthington, A.H.; Bunn, S.E.; Naiman, R.J.; Kendy, E.; Acreman, M.; Apse, C.; Bledsoe, B.P.; Freeman, M.C.; Henriksen, J.; Jacobson, R.B.; Kennen, J.G.; Merritt, D.M.; O'Keeffe, J.H.; Olden, J.D.; Rogers, K.; Tharme, R.E.; Warner, A., (2010). The ecological limits of hydrologic alteration (ELOHA): A new framework for developing regional environmental flow standards. Freshwater Biol., 55(1): 147–170 (**24 pages**).

Qiu, H.; Chen, H.; Xu, B.; Liu, G.; Huang, S.; Nie, H.; Xie, H., (2024). Multiple types of missing precipitation data filling based on ensemble artificial intelligence models. Water, 16(22): 3192 (**18 pages**).

Rezaeianzadeh, M.; Stein, A.; Cox, J.P., (2016). Drought forecasting using Markov chain model and artificial neural networks. Water Resour. Manag., 30(7): 2245–2259 (**15 pages**).

Rippl, W., (1883). The capacity of storage-reservoirs for water-supply. Proc. Inst. Civ. Eng., 71: 270–278 (**9 pages**).

Simeone, C.E.; Hammond, J.C.; Archfield, S.A.; Broman, D.P.; Condon, L.E.; Eldardiry, H.; Olson, C.G.; Steyaert, J.C., (2024). Declining reservoir reliability and increasing reservoir vulnerability: Long-term observations reveal longer and more severe periods of low reservoir storage for major United States reservoirs. Geophys. Res. Lett., 51(16): e2024GL109476 **(12 pages)**.

Sedghi-Asl, M.; Poursalehan, S.-J., (2025). Hydro-environmental flow classification of rivers (case study: Beshar River, Iran). Ecol. Indic., 178: 114049 (**13 pages**).

Shekohideh, H.; Vafakhah, M.; Sadeghi, S.H.R.; Moosavi, V., (2026). Evaluating the reliability, resilience, and vulnerability of water resources: the impact of minimum, maximum, environmental flows, and water quality. Appl. Water Sci., 16(8): 1-22 **(22 pages)**.

Sriwongsitanon, N.; Kaprom, C.; Tantisuvanichkul, K.; Prasertthonggorn, N.; Suiadee, W.; Bastiaanssen, W.G.M.; Williams, J.A., (2023). The Combined Power of Double Mass Curves and Bias Correction for the Maximisation of the Accuracy of an Ensemble Satellite-Based Precipitation Estimate Product. Hydrology, 10(7): 154 (**21 pages**).

Tennant, D.L., (1976). Instream flow regimens for fish, wildlife, recreation and related environmental resources. Fisheries, 1(4): 6–10 (**5 pages**).

Wahyono, H.D.; Santoso, A.D.; Goh, G.G.G.; Setiaji, G.; Salim, M.A.; Kustianto, I.; Alhasa, K.M.; Yudo, S.; Sudinda, T.W., (2026). An integrated real-time water quality monitoring system for sustainable management in tropical reservoirs. Global J. Environ. Sci. Manage., 12(2): 873–896 (**24 pages**).

Wang, M.; Wyatt, B.M.; Ochsner, T.E., (2023). Accurate statistical seasonal streamflow forecasts developed by incorporating remote sensing soil moisture and terrestrial water storage anomaly information. J. Hydrol., 626: 130154 **(39 pages)**.

Wu, H.; Tu, X.; Chen, X.; Singh, V.P.; Alfonso, L.; Lin, K.; Liu, Z.; Lai, R., (2023). A framework for water supply regulation in coastal areas by avoiding saltwater withdrawal considering upstream streamflow distribution. Sci. Total Environ., 905: 167181 (**17 pages**).

Yang, T.; Asanjan, A.A.; Welles, E.; Gao, X.; Sorooshian, S.; Liu, X., (2017). Developing reservoir monthly inflow forecasts using artificial intelligence and climate phenomenon information. Water Resour. Res., 53(4): 2786–2812 (**27 pages**).

Yang, Y.; Roderick, M.L.; Yang, D.; Wang, Z.; Ruan, F.; McVicar, T.R.; Zhang, S.; Beck, H.E., (2021). Streamflow stationarity in a changing world. Environ. Res. Lett., 16: 064096 (**9 pages**).

Yajure-Ramírez, C.A., (2026). Hydropower generation forecasting in regulated systems using two-stage feature selection. Acad. Green Energy, 3(1): 1-8 **(8 pages)**.

Yaseen, Z.M.; Karami, H.; Ehteram, M.; Mohd, N.S.; Mousavi, S.F.; Hin, L.S.; Kisi, O.; Farzin, S.; Kim, S.; El-Shafie, A., (2018). Optimization of reservoir operation using new hybrid algorithm. KSCE J. Civil Eng., 22(11): 4668–4680 (**13 pages**).

Zarei, M.; Bozorg-Haddad, O.; Baghban, S.; Delpasand, M.; Goharian, E.; Loáiciga, H.A., (2021). Machine-learning algorithms for forecast-informed reservoir operation (FIRO) to reduce flood damages. Sci. Rep., 11(1): 24295 (**21 pages**).

AUTHOR (S) BIOSKETCHES

I. Mulyawati., Ph.D. Candidate, Environmental Engineering Graduate Program, Faculty of Civil and Environmental Engineering, Institut Teknologi Bandung, Jl. Ganesha 10, Bandung 40132, Indonesia
- Email: *ira_mulyawati@usahid.ac.id*
- ORCID: 0000-0003-1589-0715
- Web of Science ResearcherID: QTU-9749-2026
- Scopus Author ID: 58893875300
- Homepage: https://usahid.ac.id/jabatan/wakil-ketua-program-studi-teknik-lingkungan/

I.R.S. Salami., Ph.D., Professor, Department of Environmental Engineering, Faculty of Civil and Environmental Engineering, Institut Teknologi Bandung, Jl. Ganesha 10, Bandung 40132, Indonesia
- Email: *indahrss@itb.ac.id*
- ORCID: 0000-0003-4108-1110
- Web of Science ResearcherID: DAAD-8781-2020
- Scopus Author ID: 25628844800
- Homepage: https://itb.ac.id/staf/profil/indah-rachmatiah-siti-salami

M. Marselina., Ph. D., Associate Professor, Department of Environmental Engineering, Faculty of Civil and Environmental Engineering, Institut Teknologi Bandung, Jl. Ganesha 10, Bandung 40132, Indonesia
- Email: *mariana.marselina@yahoo.com*
- ORCID: 0000-0002-6441-8639
- Web of Science ResearcherID: MAH-0537-2025
- Scopus Author ID: 56114581600
- Homepage: https://itb.ac.id/staf/profil/mariana-marselina-s

A. Sabar., Ph.D., Professor, Department of Environmental Engineering, Faculty of Civil and Environmental Engineering, Institut Teknologi Bandung, Jl. Ganesha 10, Bandung 40132, Indonesia.
Department of Environmental Engineering, Faculty of Infrastructure and Regional Technology, Institut Teknologi Sumatera, Jl. Terusan Ryacudu, Desa Way Hui, Kecamatan Jati Agung, Kabupaten Lampung Selatan, Provinsi Lampung, Kode Pos 35365, Indonesia.
- Email: *arwinsabar@yahoo.com*
- ORCID: 0009-0003-6460-863X
- Web of Science ResearcherID: KHX-9222-2024
- Scopus Author ID: 57194021491
- Homepage: https://ftsl.itb.ac.id/kelompok-keahlian/teknologi-pengelolaan-lingkungan/ar/

HOW TO CITE THIS ARTICLE:
Mulyawati, I.; Salami, I.R.S.; Marselina, M.; Sabar, A., (2027). Inflow modeling strategies designed to enhance the ecological sustainability of hydroelectric reservoir operation planning. Global J. Environ. Sci. Manage., 13(1): 189-212.

DOI: 10.22034/gjesm.2027.01.09
URL: https://www.gjesm.net/article_735608.html

Global Journal of Environmental Science and Management
(GJESM)

Homepage: https://www.gjesm.net/

Podcasts

ORIGINAL RESEARCH ARTICLE

Driving sustainable development goal alignment through green consumption marketing and public mind

S. Petchariya[1], J. Prasara-A[1,*], N. Thiengkamol[1], V. Sinvayupak[2], T. K. Thiengkamol[2]

[1]Graduate Program in Sustainable Environmental Management, Faculty of Environment and Resource Studies, Mahasarakham University, Khamriang Sub-District, Kantarawichai District, Mahasarakham 44150 Thailand

[2]Rajamangala University of Technology Phra Nakhon, Samsen Rd. Vachira Phayaban, Dusit, Bangkok 10300 Thailand

ARTICLE INFO

Article History:
Received 01 May 2026
Revised 03 July 2026
Accepted 04 August 2026

Keywords:
Green consumption behavior
Green marketing
Linear structural equation model
Public mind
Sustainable development goals

DOI:10. 22034.gjesm.2027.01.10

ABSTRACT

BACKGROUND AND OBJECTIVES: Sustainable development demands synchronized efforts across socioeconomic and environmental domains, specifically targeting poverty alleviation, food security, and environmental stewardship. Although sustainable consumption patterns and ecological marketing act as established catalysts for environmental transitions, the specific socio-civic pathways translating micro-level pro-environmental behaviors into macro-level policy alignment remain underexplored. To bridge this gap, the study objectives were to evaluate the direct and indirect pathways through which green consumption behavior and green marketing drive local alignment with the sustainable development goals through the mediating role of the public mind among residents in Nonthaburi Province, Thailand.

METHODS: A quantitative survey design was executed to gather data from 400 residents across administrative districts in Nonthaburi Province using proportionate stratified random sampling. The researchers collected primary data through structured questionnaires employing a 5-point Likert scale. Analytical procedures encompassed descriptive statistics, confirmatory factor analysis, and structural equation modeling to validate construct relationships and assess overall structural model fit.

FINDINGS: The results of structural equation modeling indicate that both green consumption behavior and green marketing significantly influence the realization of local sustainable development goals, operating through both direct pathways and indirect pathways mediated by public consciousness. The public mind demonstrated the strongest direct influence on sustainable development goals realization ($\beta = 0.69$, $p < 0.01$), followed by direct impacts from green consumption behavior ($\beta = 0.35$, $p < 0.01$) and green marketing ($\beta = 0.28$, $p < 0.01$). Additionally, green consumption behavior was the primary driver of public mind activation ($\beta = 0.37$, $p < 0.01$), surpassing green marketing ($\beta = 0.27$, $p < 0.01$). The validated structural model accounted for substantial variance in sustainable development goals alignment ($R2 = 0.97$) and the public mind ($R2 = 0.77$).

CONCLUSION: Green consumption behavior and green marketing are critical precursors to cultivating a collective public mind, which bridges individual eco-conscious actions with macro-level alignment of Sustainable Development Goals. Municipal authorities ought to embed the mobilization of public ecological awareness into environmental governance policies. Furthermore, this structural framework offers a scalable model adaptable to other rapidly urbanizing provinces in Southeast Asia.

This is an open access article under the CC BY license (http://creativecommons.org/licenses/by/4.0/)

NUMBER OF REFERENCES	NUMBER OF FIGURES	NUMBER OF TABLES
42	3	10

*Corresponding Author:
Email: jittima.p@msu.ac.th
Phone: +66 4375 4435
ORCID: 0000-0003-3490-6567

Note: Discussion period for this manuscript open until March 01, 2027 on GJESM website at the “Show Article”.

INTRODUCTION

Global challenges—such as widening economic inequality, social disparity, and environmental degradation—continue to threaten global human well-being and ecosystem stability. In response, international policy agendas increasingly emphasize actionable strategies targeting environmental health, food security, and socioeconomic resilience. The United Nations formalized these global priorities through the 17 sustainable development goals (SDGs) for the 2015–2030 planning horizon (United Nations, 2023). Operationalizing macro-level national sustainability targets demands context-specific implementation at both the municipal and provincial tiers of governance. Nonthaburi Province, Thailand, offers an ideal empirical setting for this investigation due to its dense population, rapid urbanization, and economic integration with metropolitan Bangkok. Nonthaburi serves as a microcosm of Thailand's broader urban sustainability challenges—specifically regarding SDG 1 (No Poverty), SDG 2 (Zero Hunger), SDG 3 (Good Health and Well-Being), and SDG 6 (Clean Water and Sanitation). Attaining these target outcomes at the local level necessitates coordinated adaptations across consumer acquisition patterns and corporate operational strategies (Agarwal *et al.,* 2025). Within this transition, green marketing (GM) and Green Consumption Behavior (GCB) serve as essential operational and psychological catalysts (Zheng *et al.,* 2025). However, environmental management literature reveals a persistent "behavior–operations divide": consumer studies rely heavily on self-reported survey models evaluating private purchase intentions (Islam and Khan, 2024), whereas technical management studies focus predominantly on physical resource metrics such as carbon intensity and waste streams (Rajić *et al.,* 2022). In examining the cognitive mechanisms driving sustainable transitions, value-belief-norm (VBN) theory provides a structured framework mapping the progression from core human values to concrete ecological action (Stern, 2000). VBN theory posits that core biospheric, altruistic, and egoistic value orientations systematically shape an individual's ecological worldview, traditionally measured via the New ecological paradigm (NEP) scale (Stern, 2000). This worldview activates an awareness of consequences (AC) regarding environmental threats, followed by Ascribed responsibility (AR), wherein individuals recognize personal efficacy in mitigating ecological damage (Joo *et al.,*2022). The joint engagement of AC and AR attribution stimulates personal moral norms, functioning as internal moral imperatives that transcend immediate self-regarding motivations to promote ecological behavior (White *et al.,*2019). VBN theory effectively explains both private sustainable choices and public civic engagement (Çam *et al.,*2025), addressing critical analytical gaps in rational-choice frameworks by capturing moral and altruistic motives (Soulami *et al.,* 2026; Kamolteeravit *et al.,*2026). Operating in tandem with VBN frameworks is prosocial orientation—a psychological disposition that mirrors a sustained commitment to individual and societal welfare. Comprising intergenerational concern (generativity), empathic awareness, and altruistic value balancing, prosocial mindedness translates underlying values into active civic engagement and ethical decision-making (Çam *et al.,*2025). While scholarly discourse on sustainable consumption frequently centers on micro-level household decision-making, a notable gap remains regarding how individual ecological practices integrate into broader policy frameworks and municipal administrative processes. To bridge this critical research gap, this study conceptualizes and operationalizes the public mind (PM) as an intervening, macro-level socio-civic construct. To establish PM as a

genuinely novel theoretical construct—distinct from the relabeling of pre-existing concepts—requires clear conceptual parameters that separate it from internal psychological constructs and private domestic actions. Whereas personal moral norms operate internally through self-sanction, personal conscience, and individual moral duty (Stern, 2000), PM focuses *outwardly* on institutional governance, public policies, and systemic societal structures. Similarly, while pro-environmental attitudes and general environmental concern reflect localized, private actions—such as purchasing eco-friendly products or saving electricity (Soulami *et al.,* 2026)—PM operates directly within the public sphere by driving active stewardship through participation in municipal sustainability initiatives, support for environmental regulations, and demands for corporate accountability. Furthermore, PM extends past traditional boundaries of civic participation. While standard civic duty emphasizes general engagement in democratic processes, PM uniquely synthesizes ecological awareness with civic responsibility, conceptualizing environmental sustainability as a critical collective resource (Stern, 2000). By serving as an outward-facing socio-civic bridge, PM helps mitigate the persistent "intention–behavior gap" associated with price premiums, eco-label skepticism, and corporate greenwashing (Bonera *et al.,* 2020; White *et al.*, 2019). It reorients consumer decision-making from short-term individual trade-offs toward long-term systemic accountability and collective stewardship. Rather than providing a mere regional replication of existing models, the principal theoretical contribution of this study lies in its structural re-specification of pro-environmental decision-making within a multi-level structural equation modeling (SEM) framework. Through the integration of VBN frameworks and prosocial mindedness, the current research reveals how internalized moral mechanisms transcend individual self-interest to catalyze organizational stewardship and macro-level SDG alignment. This study aims to demonstrate how internal moral activation and social empathy transcend private utility to activate institutional stewardship, civic accountability, and collective decarbonization demand. Consequently, this structural framework offers a novel, scalable lens for understanding how consumer psychology translates into macro-level environmental governance across modern service ecosystems. This study was carried out in Nonthaburi Province in Thailand in 2025.

MATERIALS AND METHODS

To empirically evaluate this conceptual model using SEM, five theoretically derived hypotheses have been formulated:

H_1: GCB directly and positively predicts the activation of the PM among residents.

H_2: GM directly and positively predicts the activation of the PM among residents.

H_3: GCB directly and positively influences local SDG alignment.

H_4: GM directly and positively influences local SDG alignment.

H_5: The PM directly influences SDG alignment and significantly mediates the relationships between exogenous drivers (GCB and GM) and SDG fulfillment.

Target population and sampling strategy

The study target population comprised 1,322,280 registered residents in Nonthaburi Province, located in central Thailand (Fig. 1), during the 2025 period. Sampling was conducted across administrative districts in 2025 using a proportionate stratified random sampling technique. Based on Taro Yamane's formula (Yamane, 1973), $n = N / (1 + Ne^2)$, at a 95 percent (%) confidence level and a margin of error e = 0.05.

The calculated sample size was 399.88, which rounded up to 400. The sampling was conducted across Nonthaburi's 6 administrative districts proportional to population size. Out of 430 distributed questionnaires, 400 complete responses were retrieved (93.02% response rate).

Measurement instrument and scale development

The research instrument was a structured questionnaire using a 5-point Likert scale (ranging from 1 = Strongly Disagree to 5 = Strongly Agree). The specified content validity index (Index of item-objective congruence (IOC) = 1.00) was evaluated by 5 experts. An initial pool of 21 items was evaluated by 5 experts. Four items with IOC scores below 0.80 were eliminated or revised during pre-testing, resulting in unanimous expert agreement (IOC = 1.00) for the final 17 retained items. This comfortably exceeds the standard 0.5 threshold (Rovinelli and Hambleton, 1977). Reliability metric values (α = 0.943 for GCB, 0.935 for GM, 0.956 for PM, and 0.934 for SDGs; overall α = 0.967) surpass the widely accepted 0.8 minimum (Cronbach, 1951; Hair *et al.*, 2019). To ensure measurement reliability and construct validity, the questionnaire items were adapted from previously validated instruments in the existing literature rather than developed ad hoc. The questionnaire measured four main constructs; GCB: items X1–X4, GM: items X5–X8, PM: items Y1–Y5, and SDGs: items Y6–Y9. To adapt the scales for local respondents in Nonthaburi Province while maintaining semantic equivalence, a standard translation and back-translation procedure was conducted. To ensure cross-cultural equivalence, the questionnaire was first translated into Thai by two bilingual specialists in environmental management, followed by a blind back-translation into English conducted by an independent native English translator. Any minor discrepancies were resolved through discussion to ensure conceptual clarity and consistency across all constructs. All items were evaluated using a 5-point Likert scale.

Data analysis

The demographic explanation employs descriptive analysis in terms of frequency and percentage. The confirmatory factor analysis and Linear Structural Relations (LISREL) analysis (Joreskog and Sorbom, 1996) were employed for model verification. Similar structural equation modeling techniques have proven effective in fostering civic engagement in ecological restoration initiatives and empowering social capital across environmental management contexts (Listiana and Ariyanto, 2024a, 2024b).

Common method variance (CMV)

To evaluate potential common method bias resulting from single-source, self-reported survey data, Harman's single-factor test was performed. The unrotated single-factor solution accounted for 34.82% of the total variance, remaining well below the standard 50% critical threshold (Podsakoff *et al.*, 2003). This confirms that CMV is not a confounding issue of substantial concern within the data analyzed.

Descriptive statistics

To summarize the dataset, baseline descriptive statistics, including the mean ($\bar{x}$), Standard deviation (S.D.), skewness, and kurtosis, were computed. The assumption of normality was tested by examining the ratios of skewness and kurtosis to their respective standard errors, with all values meeting the acceptable criteria ranging between -1.96 and 1.96. To further validate this normal distribution, the Shapiro-Wilk and Kolmogorov-Smirnov tests were conducted. Both tests yielded non-significant results ($p > 0.05$) across all items, confirming the data met the criteria for normality (Shapiro and Wilk 1965;

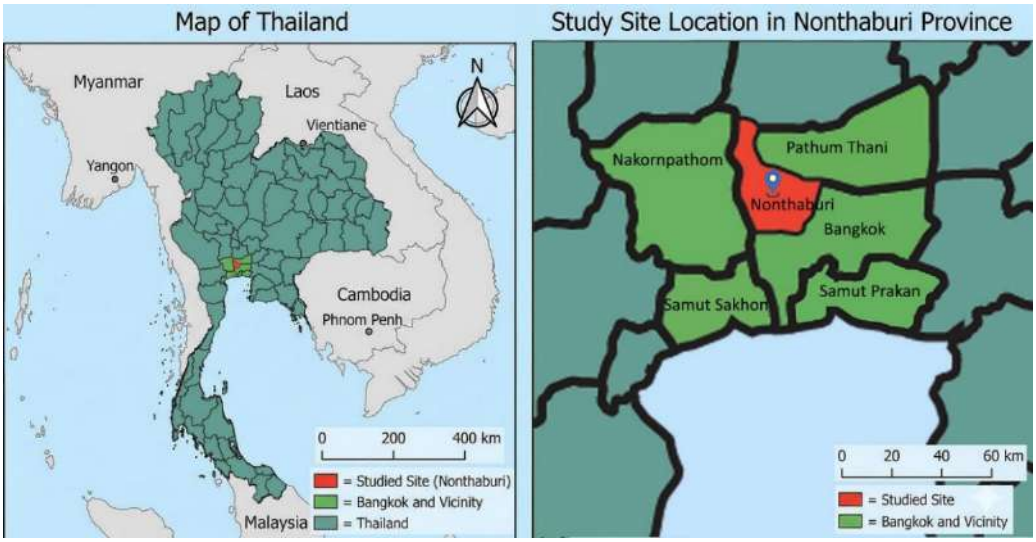

Fig. 1: Geographical location of the study area in Nonthaburi province, Thailand

Razali and Wah, 2011). However, for n = 400, formal normality tests like Kolmogorov-Smirnov and Shapiro-Wilk tests can be overly sensitive to minor deviations. Thus, data normality was primarily verified using skewness (< 2.0) and kurtosis (< 7.0) thresholds as recommended for SEM.

Inferential statistics

Confirmatory factor analysis alongside LISREL estimation procedures was utilized to validate the proposed model. Confirmation of the proposed model of sustainable development based on green consumption, GM, and the PM was performed by confirming statistical values X^2 ratio (less than 5), and critical number (more than 200). Moreover, GFI > 0.90, AGFI > 0.90, and RMSEA less than 0.05 are acceptable values (Joreskog and Sorbom, 1996).

RESULTS AND DISCUSSION

Demographic characteristics of the people in Nonthaburi Province

The demographic analysis of the sample (n = 400) in Nonthaburi Province revealed an average age of 33.56 years, with women comprising the majority (n = 222, 55.50%). It was found that the sample group was mostly Buddhists, with 360 people or 90.00%. As for domicile, it was found that the sample group was mostly from Nonthaburi province, with 400 people or 100.00%. The family characteristics of the 230-person indicated that single-family households constituted the largest proportion, accounting for 57.50%. The current residence characteristics of the 220-person sample group were owning their own homes the most, accounting for 55.00%. The monthly income of the sample group was an average of 17,970.48 baht per month. The marital status of the 180-person sample group was mostly single, or 45.00%. The highest level of education of the 174-person sample group was having completed an associate's degree/vocational certificate, the most, or 43.50%. The occupation was mostly company employees, 140 people, or 35.00%.

Symbols used to present data analysis results of model verification

To ensure a common understanding in interpreting the meaning of the data, the

following symbols and abbreviations are defined for data analysis and presentation: Symbols used to represent statistical values.

Mean ($\bar{x}$)
Standard deviation (S.D.)
Goodness of fit index (GFI)
Adjusted goodness of fit index (AGFI)
Root mean square error of approximation (RMSEA)
Chi-square (X^2)
Degree of freedom (Df)
Level of statistical significance (P-value)
Direct effects (DE)
Indirect effects (IE)
Total effects (TE)

Symbols and abbreviations used to represent latent variables

Causal variables

1) Exogenous Variables:

GCB: X1 (Green meal consumption), X2 (Green energy utility behavior), X3 (Green traveling behavior), X4 (Green local product consumption behavior).

Green Marketing (GM): X5 (Green Products), X6 (Green design), X7 (Green label), X8 (Green packaging).

2) Endogenous and Outcome Variables:

Public Mind (PM): Y5 (Self Public Mind), Y6 (Event Impression), Y7 (Self Awareness), Y8 (Role Model), Y9 (Environmental Impression).

SDGs: Y1 (No Poverty/ SDG 1), Y2 (Zero Hunger/ SDG 2), Y3 (Good Health/ SDG 3), Y4 (Clean Water and Sanitation/ SDG 6).

Symbols and abbreviations used to represent observed variables

X1 represents GMC
X2 represents GEB
X3 represents GT
X4 represents GLPC
X5 represents GP
X6 represents GD
X7 represents GL
X8 represents GPk

End-Result Variables

Y1 represents NP
Y2 represents ZH
Y3 represents GH
Y4 represents CWS
Y5 represents SM
Y6 represents EI
Y7 represents SA
Y8 represents EM
Y9 represents EnI

Preliminary analysis and descriptive evaluation

Initial assessment of the measurement model entailed analyzing the descriptive statistics of the observed variables across the four primary constructs among the sampled residents of Nonthaburi Province (n = 400). Overall, mean scores ($\bar{x}$) across all items indicated high to very high levels of respondent agreement. Specifically, GCB was measured using four items (X1–X4), with X1 recording the highest mean score ($\bar{x}$ = 4.50), followed by X3 ($\bar{x}$ = 4.47), X2 ($\bar{x}$ = 4.43), and X4 ($\bar{x}$ = 4.32). Similarly, the GM construct comprised four items (X5–X8), led by X7 ($\bar{x}$ = 4.56), X5 ($\bar{x}$ = 4.47), X6 ($\bar{x}$ = 4.45), and X8 ($\bar{x}$ = 4.39). For PM, operationalized via five observed variables (Y5–Y9), Y7 yielded the highest mean rating ($\bar{x}$ = 4.62), followed by Y8 ($\bar{x}$ = 4.56), Y5 ($\bar{x}$ = 4.53), Y6 ($\bar{x}$ = 4.46), and Y9 ($\bar{x}$ = 4.43). Finally, SDG alignment was confirmed through four items (Y1–Y4), where Y3 achieved the highest rating ($\bar{x}$ = 4.55), followed by Y1 ($\bar{x}$ = 4.51), Y2 ($\bar{x}$ = 4.47), and Y4 ($\bar{x}$ = 4.45). Prior to structural modeling, univariate normality was examined across all manifest variables to ascertain data appropriateness (Table 1). The skewness values for all indicators were negative, reflecting the high average scores and left-skewed distributions. Kurtosis estimates exhibited a balanced spread of minor positive and negative values. Crucially, all absolute skewness values

Table 1: Latent variable, observed variable, $\bar{x}$, S.D., skewness, kurtosis, and evaluation level

Main variable	Observed variable	$\overline{X}$	S.D.	Skewness	Kurtosis	Evaluation level
1. GCB	X1	4.50	0.46	-0.83	0.55	Highest
	X2	4.43	0.38	-0.32	0.66	High
	X3	4.47	0.41	-0.49	0.15	High
	X4	4.32	0.44	-0.47	0.51	High
2. GM	X5	4.47	0.40	-0.53	0.50	High
	X6	4.45	0.42	-0.82	0.44	High
	X7	4.56	0.42	-0.55	0.21	Highest
	X8	4.39	0.41	-0.29	0.27	High
3. PM	Y1	4.53	0.46	-0.71	0.20	Highest
	Y2	4.46	0.47	-0.56	0.03	High
	Y3	4.62	0.39	-0.92	0.77	Highest
	Y4	4.56	0.42	-0.82	0.70	Highest
	Y5	4.43	0.45	-0.58	0.26	High
4. SDGs	Y6	4.51	0.44	-0.27	-0.73	Highest
	Y7	4.47	0.46	-0.31	-0.68	High
	Y8	4.55	0.43	-0.32	-0.84	Highest
	Y9	4.45	0.47	-0.58	0.67	High

remained strictly below 2.00, and absolute kurtosis values were well under 7.00, comfortably satisfying standard recommended benchmarks for normal distribution (Kline, 2023). The findings demonstrate that the dataset adheres to univariate normality requirements, validating the implementation of maximum likelihood estimation for the ensuing structural equation modeling analyses. As shown in Table 1, the item mean scores across constructs were relatively high, reflecting strong overall environmental awareness among the surveyed sample. In assessing the distributional characteristics of the dataset, tests for univariate normality were conducted. All skewness values ranged between -0.27 and -0.83, remaining strictly within the recommended threshold of skewness < 2.00 (and kurtosis < 7.00) for structural equation modeling (Kline, 2023). The findings demonstrate that even with negative skewness, the dataset conforms to the univariate normality guidelines necessary for maximum likelihood parameter estimation.

1) Results of the analysis of the correlation coefficient between observable variables

In this study, the sample group consisted of 400 people in Nonthaburi province. The average values of the observed variables in each component are at high coefficients between all the variables, as shown in Table 2.

2)Confirmatory factor analysis (CFA) of latent variables

The CFA for both exogenous and endogenous latent constructs was conducted in two systematic stages. Prior to evaluating the structural configuration of the exogenous constructs—GCB and GM— comprehensive evaluations of sampling adequacy and data appropriateness were conducted. For the GCB construct, Bartlett's Test of Sphericity yielded a highly significant result (X^2 = 1,356.923, p < 0.01). In addition, the Kaiser-Meyer-Olkin (KMO) measure of sampling adequacy reached 0.823, comfortably exceeding the recommended 0.60 threshold (Kaiser, 1974). The resulting metrics indicate robust intercorrelations among the manifest indicators, verifying that the dataset is well-suited for structural factor evaluation. Prior to evaluating the structural model, individual measurement models were assessed for each construct to establish construct validity and unidimensionality. As consolidated in Fig. 2 (a–d), all four confirmatory components—GCB, GM, PM, and

Table 2: Coefficients among all the variables

Correlations																	
	X1	X2	X3	X4	X5	X6	X7	X8	Y1	Y2	Y3	Y4	Y5	Y6	Y7	Y8	Y9
X1	1																
X2	0.518**1																
X3	0.451**0.409**1																
X4	0.397**0.442**0.379**1																
X5	0.403**0.446**0.445**0.441**1																
X6	0.468**0.387**0.284**0.267**0.287**1																
X7	0.330**0.310**0.401**0.293**0.359**0.536**1																
X8	0.366**0.412**0.393**0.409**0.433**0.360**0.421**1																
Y1	0.521**0.382**0.244**0.326**0.361**0.450**0.392**0.367**1																
Y2	0.252**0.305**0.145**0.344**0.204**0.281**0.272**0.264**0.343**1																
Y3	0.395**0.384**0.254**0.223**0.293**0.488**0.364**0.265**0.501**0.450**1																
Y4	0.230**0.266**0.300**0.212**0.252**0.221**0.405**0.279**0.418**0.371**0.405**1																
Y5	0.216**0.250**0.199**0.305**0.278**0.194**0.355**0.345**0.357**0.402**0.287**0.359**1																
Y6	0.199**0.234**0.274**0.356**0.340**0.228**0.363**0.371**0.296**0.299**0.217**0.331**0.480**1																
Y7	0.207**0.318**0.146**0.321**0.226**0.295**0.267**0.207**0.330**0.398**0.397**0.361**0.411**0.294**1																
Y8	0.245**0.298**0.157**0.194**0.260**0.383**0.371**0.195**0.391**0.269**0.376**0.271**0.324**0.245**0.461**1																
Y9	0.300**0.279**0.231**0.312**0.374**0.244**0.227**0.383**0.405**0.395**0.238**0.255**0.385**0.389**0.323**0.369**1																

** Correlation is significant at the 0.01 level (2-tailed). * Correlation is significant at the 0.05 level (2-tailed).

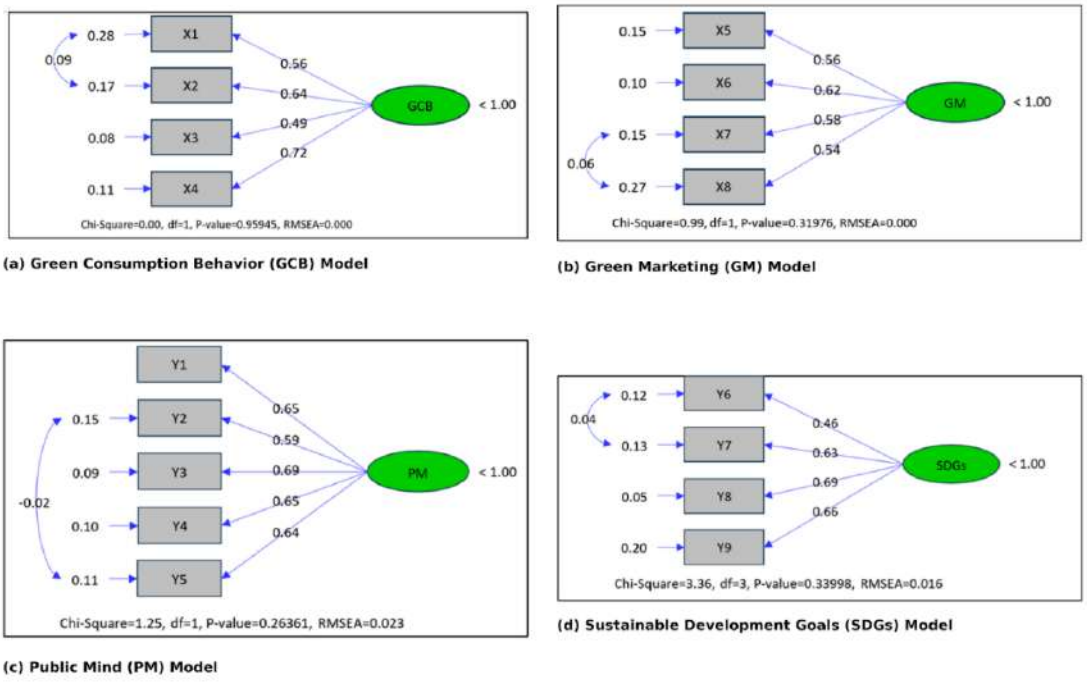

Fig. 2: CFA measurement models for study components: (a) GCB; (b) GM; (c) PM; (d) SDGs

Table 3: Confirmatory components of GCB

Components of GCB	Weight	SE	t-test	R^2
X1	0.56	0.032	17.63**	0.52
X2	0.64	0.029	21.97**	0.70
X3	0.49	0.021	22.26**	0.74
X4	0.72	0.029	24.80**	0.82
X^2 = 0.00 df = 4 P = 0.9594				
GFI = 1.00 AGFI = 0.99 RMSEA = 0.000 RMR =0.0018				

** Statistical significance at the 0.01 level

Table 4: Confirmatory components of GM

Components of GM	Weight	SE	t	R^2
X5	0.56	0.027	21.13**	0.68
X6	0.62	0.026	23.51**	0.79
X7	0.58	0.017	21.34**	0.69
X8	0.54	0.031	17.39**	0.52
X^2 = 0.99 df = 1 P = 0.31976				
GFI =1.00 AGFI =1.00 RMSEA = 0.000 RMR =0.0022				

** Statistical significance at the 0.01 level

SDGs—demonstrated acceptable empirical data fit, meeting standard statistical thresholds $p > 0.05$ and RMSEA < 0.05). As illustrated in Fig. 2(a) and Table 3, the CFA results for the GCB construct, based on four observable variables, indicate an acceptable model fit index with the empirical data. Additionally, the standardized factor loadings for the manifest indicators were positively spanning from 0.49 to 0.72—and accounted for 52.00% to 82.00% of the variance within the GCB model. For the GM construct, Bartlett's Test of Sphericity produced a highly significant value of 1,223.872 (p < 0.01), and the KMO Measure of Sampling Adequacy was 0.856. Fig. 2 illustrates adequate inter-variable correlations, confirming their appropriateness for subsequent factor analysis, with comprehensive results presented in Fig. 2(b) and Table 4. Based on Fig. 2(b) and Table 4, the CFA for the GM construct, which comprises four observable variables, demonstrates a strong fit with the empirical data. Additionally, the observed variables yielded positive factor loadings ranging from 0.54 to 0.62, accounting for 52.00% to 79.00% of the variance within the GM model. In analyzing the endogenous variables related to Nonthaburi residents' PM and their contribution to the SDGs, preliminary diagnostic evaluations were performed to ascertain data appropriateness. For the PM components, Bartlett's Test of Sphericity was statistically significant at the 0.01 level, and the KMO Measure of Sampling Adequacy yielded an acceptable index of 0.88. The resulting indices demonstrate robust intercorrelation among the variables, substantiating the appropriateness of the PM construct is highly appropriate for further structural analysis, with comprehensive findings presented in Fig. 2(c) and Table 5. As detailed in Fig. 2(c) and Table 5, the CFA for the PM construct, based on five observable variables, demonstrates an acceptable model fit with empirical data. Furthermore, the manifest indicators yielded positive standardized factor loadings—spanning from 0.59 to 0.69, which accounted for 69.00% to 86.00% of the total variance within the PM model. Moving to the SDGs construct, data suitability tests confirmed that the items are highly appropriate for factor extraction. Bartlett's Test of Sphericity was statistically significant (p < 0.01), and the KMO Measure of Sampling Adequacy yielded an outstanding index of 0.98. These metrics demonstrate a strong intercorrelation among the variables, as detailed comprehensively in Fig. 2(d) and Table 6. As illustrated in Fig. 2(d) and Table 6, the CFA results for the SDGs construct, which comprises four observable variables, reveal an acceptable fit with the empirical data. Additionally, the manifest indicators yielded positive standardized factor loading spanning from 0.37 to 0.63—which accounted for 64.00% to 91.00% of the variance within the measurement model. To evaluate the structural relationships and influence of GCB, GM, and the PM on the fulfilment of the SDGs within Nonthaburi Province, a correlation analysis was conducted. The resulting correlation coefficients, illustrating the interdependencies among these variable components, are summarized in Table 7.

Table 5: Confirmatory components of PM of Nonthaburi people

Components confirming the PM of the Nonthaburi people	Weight	SE	t	R^2
Y1	0.65	0.026	24.72**	0.79
Y2	0.59	0.027	22.01**	0.69
Y3	0.69	0.027	25.90**	0.84
Y4	0.65	0.028	25.39**	0.86
Y5	0.64	0.025	24.50**	0.79
X^2 = 1.25 df = 1 P = 0.26361				
GFI = 1.00 AGFI = 1.00 RMSEA = 0.023 RMR = .0000				

** Statistical significance at the 0.01 level

Table 6: Confirmatory components of SDGs of Nonthaburi people

Component SDGs of the Nonthaburi province people	Weight	SE	t-test	R^2
Y6	0.46	0.022	20.84**	0.64
Y7	0.63	0.026	23.81**	0.75
Y8	0.69	0.025	27.84**	0.91
Y9	0.66	0.026	25.25**	0.81
X^2 = 3.36 df = 3 P = 0.33998				
GFI = 1.00 AGFI = 1.00 RMSEA = 0.016 RMR = 0.00021				

** Statistical significance at the 0.01 level

Table 7: Correlation coefficient matrix among components of GCB, GM, and the PM of Nonthaburi people in alignment with the SDGs

Variables	GCB	GM	PM	SDGs
GCB	1.00			
GM	0.85**	1.00		
PM	0.87**	0.88**	1.00	
SDGs	0.89**	0.90**	0.93**	1.00

From Table 7, the relationship between the variables in general was positively at statistically significant at the 0.01 level, with a correlation coefficient for each pair ranging from 0.79 to 0.93. An examination of the association between the PM of Nonthaburi residents and their contribution to the SDGs revealed a peak correlation of 93.00%. Subsequences were GM and SDGs of Nonthaburi people with a correlation coefficient of 90.00, and GCB and SDGs of Nonthaburi people with a correlation coefficient of 89.00. The PM of Nonthaburi people and GM have a relationship of 88.00%, and the PM of Nonthaburi people and GCB have a relationship of 87.00%, and GCB and GM have a relationship of 85.00%, respectively. A linear structural relationship analysis was performed to assess the intricate interactions governing sustainability in Thailand, specifically investigating how the exogenous constructs of GCB and GM, alongside the mediating variable of PM, affect SDG alignment among residents of Nonthaburi Province. The detailed results illustrating these linear relationships and structural pathways are presented in Fig. 3 and Table 8. As illustrated in Fig. 3 and detailed in Table 8, the structural equation model successfully confirms the empirical data, establishing statistically significant linear relationships among GCB, GM, PM, and localized SDG attainment among the residents of Nonthaburi Province. In particular, PM serves as an essential mediating pathway, demonstrating a substantial and statistically significant direct influence on SDG attainment (β = 0.69). Concurrently, GCB demonstrates a significant direct effect on PM (β = 0.37) and SDG alignment (β = 0.35), alongside an indirect effect of 0.26 on SDGs mediated through PM (total effect = 0.61). Similarly, GM exhibits statistically significant direct effects on both PM (β = 0.27) and SDGs (β = 0.28), while contributing an

Table 8: Results of the influence of the causal variables of GCB and GM, and the intervention variable of PM in achieving SDGs of the Nonthaburi people

Causal variables	Results of variables					
	PM			SGDs		
	TE	IE	DE	TE	IE	DE
GC	0.37** (0.06)	-	0.37** (0.06)	0.61** (0.11)	0.26** (0.03)	0.35** (0.05)
GM	0.27** (0.07)	-	0.27** (0.07)	0.47** (0.10)	0.19** (0.02)	0.28** (0.08)
PM	-	-	-	0.69** (0.08)	-	0.69** (0.08)
X^2 = 238.20; df = 136		P = 0.00000		X^2/ df = 1.75		
GFI=0.94; AGFI = 0.92; CN=298.78		RMSEA = 0.049		RMR = 0.0093		

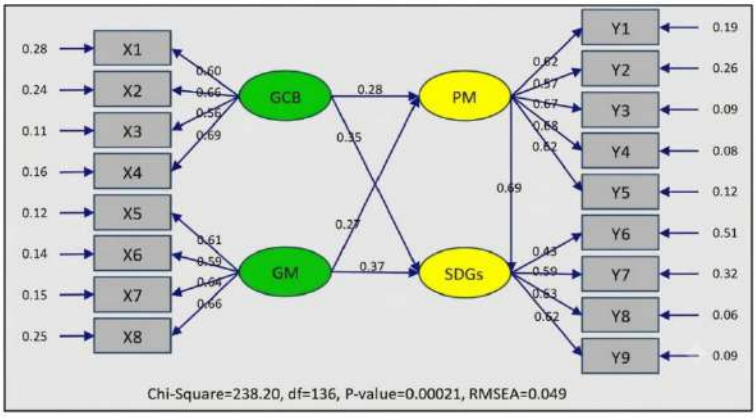

Fig. 3: Structural equation model for the SDG alignment of the people of Nonthaburi Province

indirect effect of 0.19 on SDG attainment via PM (total effect = 0.47). Collectively, these structural path coefficients reveal that although green mindsets and purchasing behavior independently foster regional SDG attainment, their overall impact on localized sustainability is considerably magnified through the mediating influence of the PM.

Hypothesis testing results

Based on the structural model parameters presented in Table 8, all five proposed hypotheses (H_1–H_5) received full empirical support:

H_1 is supported: GCB exerted a statistically significant direct positive effect on PM activation (β = 0.37, p < 0.01).

H_2 is supported: GM directly and positively predicted PM activation (β = 0.27, p < 0.01).

H_3 is supported: GCB demonstrated a significant direct positive effect on local SDG fulfillment (β = 0.35, p < 0.01).

H_4 is supported: GM significantly and directly influenced local SDG alignment (β = 0.28, p < 0.01).

H_5 is supported: PM exerted the strongest direct positive effect on SDG alignment (β = 0.69, p < 0.01) while significantly mediating the indirect structural pathways from GCB (IE = 0.26, p < 0.01) and GM (IE = 0.19, p < 0.01) to SDG realization.

3) *Composite reliability (CR) and average variance extracted (AVE)*

Based on the standardized factor loadings (λ), CR and AVE for all four constructs were calculated as shown in Table 9. All constructs exceed the 0.70 threshold for CR and the 0.50 threshold for AVE, establishing robust convergent validity. Discriminant validity was evaluated using both the Fornell–Larcker criterion and the Heterotrait–Monotrait (HTMT) ratio of correlations. As

Table 9: Measurement model assessment and discriminant validity

Part A: Convergent Validity and Construct Reliability				
Construct	Standardized Loadings (λ)	CR (> 0.70)	AVE (> 0.50)	Result
GCB	0.721, 0.837, 0.860, 0.906	0.901	0.695	Validated
GM	0.825, 0.889, 0.831, 0.748	0.894	0.68	Validated
PM	0.889, 0.831, 0.917, 0.927, 0.889	0.951	0.794	Validated
SDGs	0.800, 0.866, 0.954, 0.900	0.933	0.778	Validated
Part B: Discriminant Validity (Fornell-Larcker and HTMT Ratios)				
Construct	(1) GCB	(2) GM	(3) PM	(4) SDGs
(1) GCB	**0.834**	0.518	0.605	0.458
(2) GM	0.432	**0.825**	0.572	0.482
(3) PM	0.512	0.488	**0.891**	0.718
(4) SDGs	0.389	0.415	0.624	0.882

Note: Bold diagonal values represent the square root of AVE (√AVE). Values in the lower triangle are inter-construct correlations (Fornell–Larcker criterion). Italicized values in the upper triangle represent HTMT ratios (all < 0.85).

presented in Table 9, the square root of the AVE (√AVE) for each construct was greater than its correlations with all other constructs, satisfying the Fornell–Larcker criterion (Fornell and Larcker, 1981). Furthermore, all HTMT ratios stayed under the conservative benchmark of 0.85 (Henseler *et al*., 2015), thereby substantiating clear construct differentiation and robust discriminant validity throughout the model.

4) *Structural model fit and hypothesis testing*

To evaluate the overall predictive capacity and structural integrity of the proposed model, goodness-of-fit indices were evaluated for the full structural specification (df = 136). As shown in Table 10, the structural model met standard recommended goodness-of-fit thresholds (X^2 = 238.20, df = 136, X^2/df = 1.75, p < 0.001). The comparative and absolute fit indices comfortably m*et a*l standard recommended thresholds (Hu and Bentler, 1999; Hair *et al*., 2019): GFI = 0.94, AGFI = 0.92, RMSEA = 0.049, RMR = 0.0093, and Hoelter's Critical N (CN) = 298.78 (well above the 200 benchmark). These parameters confirm that the full structural model is robust, properly identified, and free from overfitting concerns. The standardized structural equations governing the empirical model, derived from LISREL parameter estimates, using Eqs. 1 and 2 (Joreskog and Sorbom, 1996; Kline, 2023):

$$SDGs = 0.69 \times PM + 0.35 \times GCB + 0.28 \times GM \quad (1)$$
$$[R^2 = 0.97]$$

$$PM = 0.37 \times GCB + 0.27 \times GM \quad (2)$$
$$[R^2 = 0.77]$$

As specified in Eq. 1, the PM exerts the strongest direct influence on SDG realization (β = 0.69, p < 0.01), followed by Green Consumption Behavior (β = 0.35, p < 0.01) and GM (β = 0.28, p < 0.01). Together with indirect effects mediated through PM (0.26 for GCB and 0.19 for GM), the total effects on SDG alignment reach 0.61 for GCB and 0.47 for GM. The structural model accounts for 97.0% of the variance in SDG fulfillment (R^2 = 0.97). This high R^2 stems from strong bivariate linear correlations among respondents' eco-conscious attitudes (r = 0.85 to 0.93). These findings demonstrate a strong linear association among self-reported civic attitudes; consequently, subsequent investigations should integrate objective behavioral metrics to corroborate actual long-term SDG impacts. Furthermore, Eq. 2 demonstrates that GCB is the primary determinant of PM activation (β = 0.37, p < 0.01)

Table 10: Goodness-of-fit indices for the full structural model

Fit index	Reported value	Recommended threshold	Source/ benchmark	Fit Status
Chi-square (X^2)	238.20	—	—	—
Degrees of freedom (df)	136	—	—	—
Normed Chi-square (X^2/df)	1.75	< 3.00	Hair *et al.* (2019)	Excellent
Goodness-of-fit index (GFI)	0.94	> 0.90	Hu and Bentler (1999)	Acceptable
Adjusted GFI (AGFI)	0.92	> 0.80	Chau (1997)	Excellent
Root Mean Sq. Error of Approx. (RMSEA)	0.049	< 0.06 (or < 0.08)	Hu and Bentler (1999)	Excellent
Root Mean Square Residual (RMR)	0.0093	< 0.05	Kline (2023)	Excellent
Critical N (CN)	298.78	> 200	Hoelter (1983)	Satisfactory

followed by GM (β = 0.27, p < 0.01), jointly explaining 77.0% of the variance in PM (R^2 = 0.77). The empirical findings of this study provide critical insights into the structural relationships between GCB, GM, PM, and SDG fulfillment among residents in Nonthaburi Province, Thailand. By integrating consumer behavioral constructs with socio-civic responsibility, the structural equation model demonstrates exceptional explanatory power, accounting for 97% of the variance in SDG fulfillment (R^2 = 0.97) and 77% of the variance in PM (R^2 = 0.77). These empirical outcomes significantly expand existing theoretical frameworks regarding the operationalization of municipal sustainability transitions across rapidly urbanizing settings in Southeast Asian contexts, while reinforcing the growing evidence that consumer behavioral mechanisms play a central role in advancing green consumption and sustainability-oriented civic engagement in the digital era (Soulami *et al.,* 2026).

The centrality of the PM in driving SDG realization

The identification of PM as the most potent direct determinant of local SDG realization illuminates civic consciousness as the core operational catalyst for regional sustainability. This aligns closely with the core tenets of VBN theory (Stern, 2000; Stern and Dietz, 1994), which posits that pro-environmental personal norms and altruistic values are essential drivers of public-sphere environmental action. Similar empirical studies, such as Liu *et al.* (2018) and Soemantri *et al.* (2025), have demonstrated that when individuals develop a heightened sense of shared responsibility and ecological citizenship, public-sphere sustainability initiatives experience significantly higher adoption rates. Unlike conventional consumer frameworks that treat social responsibility as a peripheral factor, the present findings show that PM is a key mechanism linking individual behavioral intentions to municipal SDG advancement.

GCB as a catalyst for socio-civic mindedness

The structural analysis revealed that GCB directly impacts SDG realization while serving as the leading antecedent to PM activation. This dual role substantiates the psychological spillover hypothesis highlighted by Hong *et al.* (2024) and Paço *et al.* (2019), wherein individual eco-conscious actions (such as waste sorting, energy conservation, and purchasing eco-labeled goods) gradually reinforce a collective civic identity. As citizens routinely engage in sustainable procurement practices, their intrinsic commitment to environmental stewardship deepens, consequently reinforcing their aggregate PM. These findings complement the work of Lu and Tam (2024) and Ogiemwonyi *et al.* (2023), confirming that private-sphere consumer choices actively nurture public-sphere civic duties.

Reconciling the dual pathways of GM

GM was found to have statistically significant direct effects on both SDG alignment and PM development. Previous literature has presented mixed conclusions regarding the efficacy of GM;

while studies by Dangelico and Vocalelli (2017) and Agarwal *et al.* (2025) emphasized its positive role in shaping sustainable values, others such as Paço *et al.* (2019) and Ozola (2025) noted that green advertising often exerts a weak direct influence on actual behavior when perceived merely as commercial promotion. This study resolves these conflicting views by showing that GM is most effective when focused on public education and civic value alignment rather than product promotion. Transparent marketing communication that emphasizes civic responsibility shapes consumer behavior and strengthens collective public consciousness.

Practical and policy implications

Despite the positive structural influence of green marketing and consumption behaviors, promoting these strategies involves potential unintended consequences and socio-economic trade-offs that demand careful governance. First, excessive or unverified environmental marketing can trigger consumer doubt and greenwashing concerns, which undermine public trust and reduce community engagement (Thiyas *et al.,* 2025). Second, economic trade-offs, specifically the premium pricing associated with certified green products, present substantial financial barriers for lower-income households. These price premiums threaten to widen the intention-behavior gap, wherein favorable ecological attitudes fail to manifest as enduring daily sustainable routines, consequently marginalizing broader civic engagement in municipal SDG frameworks (Khang, 2026). From a municipal management perspective, the findings offer a clear framework for local administrative organizations in Nonthaburi Province and similar urbanizing regions. Because PM serves as the principal mediator, policy interventions should not rely solely on transactional green incentives or promotional marketing. Instead, municipal authorities ought to integrate PM activation directly into civic educational initiatives, community-driven waste reduction networks, and participatory environmental governance frameworks. Enhancing public recognition of individual civic actions can reduce the intention-behavior gap, strengthen long-term community alignment with SDGs, and improve municipal environmental governance.

Critical interpretation and international comparisons

Rather than merely reflecting statistical pathways, the empirical findings reveal that while GCB and GM act as essential behavioral catalysts, PM functions as the critical mechanism transforming individual action into broader SDG alignment. This underscores that marketing mechanisms and personal eco-friendly choices remain insufficient in the absence of a foundational commitment to civic duty and social responsibility. This observed pattern is consistent with recent international empirical literature spanning diverse socio-economic contexts. In Asia, empirical research by Yue *et al.* (2020) in China demonstrated that individual environmental responsibility directly predicts GCB, mediated by personal environmental concern and civic awareness. Within European contexts characterized by mature environmental regulation and advanced green infrastructure, Geiger *et al.* (2018) emphasized that structural SDG alignment depends upon internalized socio-environmental values rather than superficial market mechanisms. Furthermore, evidence from Latin America by Severo *et al.* (2018) in Brazil confirms that sustainable consumption behavior depends fundamentally on social responsibility and environmental consciousness, demonstrating that marketing practices only yield long-term SDG alignment when rooted in public mindset and reinforced through civic engagement.

CONCLUSION

This study investigated the structural relationships linking GCB, GM, and the PM to SDG alignment among residents in Nonthaburi Province, Thailand. Demonstrating robust structural validity, the model explains 97% of the total variance in SDG alignment (R^2 = 0.97) and 77% of the variance in PM activation (R^2 = 0.77). Importantly, the empirical results corroborate that PM acts as an essential bridge connecting individual eco-friendly choices to city-level sustainability goals, with daily green consumption habits having a greater structural impact on civic engagement than passive exposure to commercial advertising. Practically, these results offer a strategic roadmap for local administrative organizations in Nonthaburi Province and comparable urbanizing regions across Southeast Asia. To maximize SDG progress, municipal authorities should move beyond standard promotional campaigns and prioritize civic infrastructure that fosters collective environmental stewardship. Policy measures should focus on community-led waste reduction networks, support for green energy, and targeted financial incentives for local eco-certified businesses to reduce barriers to long-term environmental participation. Several limitations highlight avenues for future research. First, the cross-sectional design restricted to Nonthaburi Province limits immediate generalizability; future studies should employ longitudinal panel designs across diverse administrative regions. Second, to address potential self-reporting biases, subsequent investigations ought to incorporate objective behavioral metrics alongside physical carbon footprint accounting frameworks and environmental performance indicators. Finally, future empirical efforts should utilize multi-group SEM to examine socio-demographic moderation (e.g., income, age, and policy enforcement) to further refine localized sustainability strategies.

AUTHOR CONTRIBUTIONS

S. Petchariya collected the data, analyzed the data, interpreted the results, and wrote a draft of the manuscript. J. Prasara-A, the corresponding author, supervised the first author, conceived the research idea, designed the experiment, interpreted the results, wrote and revised the manuscript, and finalized the manuscript. N. Thiengkamol supervised the first author, conceived the research idea, designed the experiment, interpreted the results, and revised the manuscript. V. Sinvayupak prepared all the maps and figures and checked the references. T.K. Thiengkamol analyzed the data and interpreted the results.

ACKNOWLEDGEMENT

This study was financially supported by Mahasarakham University with the financial support number: [6909025]. The authors sincerely thank all participants for their cooperation and valuable contributions to the research.

CONFLICT OF INTEREST

The authors declare that there is no conflict of interest regarding the publication of this manuscript. In addition, ethical issues, including plagiarism, informed consent, misconduct, data fabrication and/or falsification, double publication and/or submission, and redundancy have been completely observed by the authors.

OPEN ACCESS

©2027 The author(s). This article is licensed under a Creative Commons Attribution 4.0 International License, which permits use, sharing, adaptation, distribution and reproduction in any medium or format, as long as you give appropriate credit to the original author(s) and the source, provide a link to the Creative Commons license, and indicate if changes were made. The images or other third-party material in this article are

included in the article's Creative Commons license, unless indicated otherwise in a credit line to the material. If material is not included in the article's Creative Commons license and your intended use is not permitted by statutory regulation or exceeds the permitted use, you will need to obtain permission directly from the copyright holder. To view a copy of this license, visit: http://creativecommons.org/licenses/by/4.0/

PUBLISHER'S NOTE

GJESM Publisher remains neutral regarding jurisdictional claims in published maps and institutional affiliations.

POSITIVE AI STATEMENT

During the preparation of this work, the authors have used Artificial Intelligence (AI) [Grammarly] to improve the readability and style of writing. After using this tool/service, the authors reviewed and edited the content as needed and took full responsibility for the content of the publication.

ABBREVIATIONS

%	Percent
α	Cronbach's Alpha Coefficient
β	Standardized Regression Coefficient
%	Percent
λ	Standardized factor loadings
$\bar{x}$	Mean
χ2	Chi-square
AC	Awareness of consequences
AGFI	Adjusted goodness of fit index
AVE	Average variance extracted
AR	Ascribed responsibility
CFA	Confirmatory factor analysis
CMV	Common method variance
CN	Hoelter's Critical N
CR	Composite reliability
CWS	Clean water and sanitation
DE	Direct effects
df	Degree of freedom
EI	Event impression
EnI	Environmental impression
GCB	Green consumption behavior
GD	Green design / Green distribution
GEB	Green energy utility behavior
GFI	Goodness of fit index
GH	Good health and well-being
GL	Green label
GLPC	Green local product consumption
GM	Green marketing
GMC	Green meal consumption
GP	Green products
GPB	Green purchasing
GPk	Green packaging
GT	Green traveling
HTMT	Heterotrait–Monotrait
IE	Indirect effects
IOC	Index of item-objective congruence
KMO	Kaiser-Meyer-Olkin
LISREL	Linear structural relations
NEP	New Ecological Paradigm
NP	No poverty
PM	Public mind
p-value	Level of statistical significance
RMR	Root mean square residual
RMSEA	Root mean square error of approximation
RM	Role model
SA	Self-awareness
S.D.	Standard deviation
SDGs	Sustainable Development Goals
SEM	Structural equation modeling
SM	Self-public mind
TE	Total effects
TPB	Theory of Planned Behavior
UN	United Nations
VBN	Value-Belief-Norm
ZH	Zero hunger

REFERENCES

Agarwal, S.; Kweh, Q.L.; Goh, K.; Wider, W., (2025). Redefining marketing strategies through sustainability: Influencing consumer behavior in the circular economy: A systematic review and future research roadmap. Clean. Respons. Consump., 16: 100298 **(14 pages)**.

Bonera, M.; Corvi, E.; Codini, A.P.; Ma, F., (2020). Sustainable consumer behavior. MDPI Books, 1–208 **(208 pages)**.

Çam, E.; Yilmaz, O.; Kaya, M., (2025). The resale–repurchase cycle: How consumer perceptions of gain and loss shape sustainable consumption. Soc. Responsib. J., 21(9): 1874–1889 **(16 pages)**.

Chau, P.Y.K., (1997). Reexamining a model for evaluating information center success using a structural equation modeling approach. Decis. Sci., 28(2): 309–334 **(26 pages)**.

Cronbach, L.J., (1951). Coefficient alpha and the internal structure of tests. Psychometrika, 16(3): 297–334 **(38 pages)**.

Dangelico, R.M.; Vocalelli, D., (2017). "Green Marketing": An analysis of definitions, strategy steps, and tools through a systematic review of the literature. J. Clean. Prod., 165: 1263–1279 **(17 pages)**.

Fornell, C.; Larcker, D.F., (1981). Evaluating structural equation models with unobservable variables and measurement error. J. Mark. Res., 18(1): 39–50 **(12 pages)**.

Geiger, S.M.; Fischer, D.; Schrader, U., (2018). Measuring what matters in sustainable consumption: An integrative framework for the selection of relevant behaviors. Sustainable Dev., 26(1): 18–33 **(16 pages)**.

Hair, J.F.; Babin, B.J.; Anderson, R.E.; Black, W.C., (2019). Multivariate data analysis. 8th Ed., Cengage Learning, EMEA, Cheriton House, North Way, Andover, Hampshire, SP10 5BE, United Kingdom **(834 pages)**.

Henseler, J.; Ringle, C.M.; Sarstedt, M., (2015). A new criterion for assessing discriminant validity in variance-based structural equation modeling. J. Acad. Mark. Sci., 43(1): 115–135 **(21 pages)**.

Hoelter, J.W., (1983). The analysis of covariance structures: Goodness-of-fit indices. Sociol. Methods Res., 11(3): 325–344 **(20 pages)**.

Hong, Y.; Al Mamun, A.; Masukujjaman, M.; Yang, Q., (2024). Significance of the environmental value-belief-norm model and its relationship to green consumption among Chinese youth. Asia Pac. Manage. Rev., 29(1): 127-140 **(14 pages)**.

Hu, L.T.; Bentler, P.M., (1999). Cutoff criteria for fit indexes in covariance structure analysis: Conventional criteria versus new alternatives. Struct. Equ. Model. Multidiscipl. J., 6(1): 1–55 **(55 pages)**.

Islam, Q.; Khan, S.M.F.A., (2024). Assessing consumer behavior in sustainable product markets: A structural equation modeling approach with partial least squares analysis. Sustainability. 16(8): 3400 **(21 pages)**.

Joo, Y.; Kim, N.; Park, S., (2022). How do humans value urban nature? Developing the perceived biophilic design scale (PBDs) for preference and emotion. Urban For. Urban Green., 78: 127730 **(13 pages)**.

Jöreskog, K.G.; Sörbom, D., (1996). LISREL 8: User's reference guide. Scientific Software International, Chicago, United States **(378 pages)**.

Kaiser, H.F., (1974). An index of factorial simplicity. Psychometrika. 39(1): 31–36 **(6 pages)**.

Kamolteeravit, N.; Prasara-A, J.; Thiengkamol, N.; Thiengkamol, T.K., (2026). Carbon footprint and environmental management behaviors among students achieving sustainability in higher education. Global J. Environ. Sci. Manage., 12(2): 857–872 **(16 pages)**.

Khang, T.N., (2026). The moderating role of renewable energy in the relationship between economic growth and carbon intensity. Global J. Environ. Sci. Manage., 12(2): 771-792 **(22 pages).**

Kline, R.B., (2023). Principles and practice of structural equation modeling. 5th Ed., Guilford Publications, New York, United States **(494 pages)**.

Listiana, I.; Ariyanto, D., (2024a). Enhancing coastal community participation in mangrove rehabilitation through structural equation modeling. Global J. Environ. Sci. Manage., 10(2): 873–890 **(18 pages)**.

Listiana, I.; Ariyanto, D., (2024b). Structural equation modeling for social capital empowerment in supporting mangrove rehabilitation. Global J. Environ. Sci. Manage., 10(4): 2031–**2044 (14 pages)**.

Liu, X.; Zou, Y.; Wu, J., (2018). Factors influencing public-sphere pro-environmental behavior among Mongolian college students: A test of value–belief–norm theory. Sustainability, 10(5): 1384 **(15 pages)**.

Lu, P.N.; Tam, P., (2024). Managerial recommendations for enhancing green consumption behavior and sustainable consumption. Emerg. Sci. J., 8(6): 2245-2266 **(22 pages)**.

Ogiemwonyi, O.; Alam, M.N.; Alshareef, R.; Alsolamy, M.; Azizan, N.; Mat, N., (2023). Environmental factors affecting green purchase behaviors of the consumers: Mediating role of environmental attitude. Clean. Environ. Syst., 10: 100130 **(10 pages)**.

Ozola, I., (2025). Green marketing impact on behavioural change for sustainable consumption in green economy. In Proceedings of the 25th International Multidisciplinary Scientific GeoConference Proceedings SGEM2025, Ecology, Environmental Economics, Education, and Legislation, 25 (5.1): 779-786 **(8 pages)**.

Paço, A.; Shiel, C.; Alves, H., (2019). A new model for testing green consumer behaviour. J. Clean. Prod., 207: 998–1006 **(9 pages)**.

Podsakoff, P.M.; MacKenzie, S.B.; Lee, J.Y.; Podsakoff, N.P., (2003). Common method biases in behavioral research: A critical review of the literature and recommended remedies. J. Appl. Psychol., 88(5): 879–903 **(25 pages).**

Rajić, S.; Đorđević, V.; Tomašević, I.; Djekic, I., (2022). The role of food systems in achieving the sustainable development goals: Environmental perspective. Bus. Strategy Environ., 31(3): 988-1001 **(14 pages)**.

Razali, N.M.; Wah, Y.B., (2011). Power comparisons of Shapiro–Wilk, Kolmogorov–Smirnov, Lilliefors and Anderson–Darling tests. J. Stat. Model. Anal., 2(1): 21–33 **(13 pages)**.

Rovinelli, R.J.; Hambleton, R.K., (1977). On the use of content specialists in the assessment of criterion-referenced test item validity. Dutch J. Educ. Res., 2(2): 49–60 **(12 pages)**.

Severo, E.A.; de Guimarães, J.C.F.; Dorion, E.C.H., (2018). Cleaner production, social responsibility and eco-innovation: Generations' perception for a sustainable future. J. Clean. Prod., 186: 91–103 **(13 pages)**.

Shapiro, S.S.; Wilk, M.B., (1965). An analysis of variance test for normality (complete samples). Biometrika, 52(3/4): 591–611 **(21 pages)**.

Soemantri, T.S.; Anzhari, K.; Kosasih, O.; Murwani, I.A., (2025). Value-belief-norm theory and pro-environmental behavior: A study on blue collar workers in Jakarta. JRSSEM., 5(2), 3323–3330 **(8 pages)**.

Soulami, M , Benchekroun, S , Galiulina, A and Sayarh, I., (2026). A bibliometric and systematic analysis of consumer behavior toward green consumption in the digital age. Global J. Environ. Sci. Manage., 12(3): 1567-1590 **(24 pages)**.

Stern, P., (2000). Toward a coherent theory of environmentally significant behavior. J. Soc. Issues, 56(3): 407–424 **(18 pages)**.

Stern, P.C.; Dietz, T., (1994). The value basis of environmental concern. J. Soc. Issues. 50(3): 65–84 **(20 pages)**.

Thiyas, U.N.; Riyanto, A.; Widjaya, F.E.; WidjaJa, E. Diastuti, R.; Suryani; Erlambang, Y.; Abbas, N.; Trihadi, S.E.Y.; Sulistiono, W., (2025). Environmental and institutional sustainability of a regional public rice enterprise employing multidimensional scaling. Global J. Environ. Sci. Manage., 11(4): 1687-1710 **(24 pages).**

White, K.; Habib, R.; Hardisty, D.J., (2019). How to SHIFT consumer behaviors to be more sustainable: A framework for social science review and research agenda. J. Mark., 83(3): 22–49 **(28 pages)**.

Yamane, T., (1973). Statistics: An introductory analysis. 3rd Ed., Harper and Row, New York, United States **(1,130 pages)**.

Yue, B.; Sheng, G.; She, S.; Xu, J., (2020). Impact of consumer environmental responsibility on green consumption behavior in China: The role of environmental concern and price sensitivity. Sustainability. 12(5): 2074 **(16 pages)**.

Zheng, S.; Han, J.; Gandolfi, F.; Alturise, F.; Alkhalaf, S., (2025). Fostering eco-conscious tourists: How sustainable marketing drives green consumption behaviors. Acta Psychol., 255: 104900 **(13 pages)**.

AUTHOR (S) BIOSKETCHES

Petchariya, S., Ph.D. Candidate, Graduate Program in Sustainable Environmental Management, Faculty of Environment and Resource Studies, Mahasarakham University, Khamriang Sub-District, Kantarawichai District, Mahasarakham 44150, Thailand.
- Email: *reamosk119@gmail.com*
- ORCID: 0009-0006-9705-1112
- Web of Science ResearcherID: NA
- Scopus Author ID: NA
- Homepage: http://env.msu.ac.th/

Prasara-A, J., Ph.D., Associate Professor, Graduate Program in Sustainable Environmental Management, Faculty of Environment and Resource Studies, Mahasarakham University, Khamriang Sub-District, Kantarawichai District, Mahasarakham 44150, Thailand.
- Email: *jittima.p@msu.ac.th*
- ORCID: 0000-0003-3490-6567
- Web of Science ResearcherID: ABD-9585-2021
- Scopus Author ID: 37119357400
- Homepage: http://env.msu.ac.th/

Thiengkamol, N., D.Ed., Visiting Lecturer, Graduate Program in Sustainable Environmental Management, Faculty of Environment and Resource Studies, Mahasarakham University, Khamriang Sub-District, Kantarawichai District, Mahasarakham 44150, Thailand.
- Email: *mahidol@gmail.com*
- ORCID: 0000-0002-9731-7033
- Web of Science ResearcherID: AGL-1712-2022
- Scopus Author ID: 54406317000
- Homepage: https://www.researchgate.net/profile/Nongnapas-Thiengkamol

Sinvayupak, V., Ph.D., Lecturer, International College, Rajamangala University of Technology Phra Nakhon, Samsen Rd. Vachira Phayaban, Dusit, Bangkok 10300, Thailand.
- Email: *sinvayupak@gmail.com*
- ORCID: 0009-0002-4586-7006
- Web of Science ResearcherID: NA
- Scopus Author ID: 55210873400
- Homepage: https://www.rm.co.th/namecard/ohm/

Thiengkamol, T.K., Ph.D. Lecturer, International College, Rajamangala University of Technology Phra Nakhon, Samsen Rd. Vachira Phayaban, Dusit, Bangkok 10300, Thailand.
- Email: *tanarat.th@gmail.com*
- ORCID: 0009-0007-9843-6994
- Web of Science ResearcherID: OSH-9670-2025
- Scopus Author 55210842100
- Homepage: https://www.researchgate.net/profile/Tanarat-Thiengkamol-2

HOW TO CITE THIS ARTICLE:
Petchariya, S.; Prasara-A, J.; Thiengkamol, N.; Sinvayupak, V.; Thiengkamol, T.K., (2027). Driving sustainable development goal alignment through green consumption marketing and public mind. Global J. Environ. Sci. Manage., 13(1): 213-230.

DOI: 10.22034/gjesm.2027.01.10
URL: https://www.gjesm.net/article_735559.html

Global Journal of Environmental Science and Management
(GJESM)

Homepage: https://www.gjesm.net/

Podcasts

ORIGINAL RESEARCH ARTICLE

Ecological diversity in soil properties and bacterial communities in tropical coastal areas with contrasting electrical conductivity

L. Fauziah[1,2], Y. Nuraini[3], Soemarno[3], N.D. Lestari[3], Djajadi[2], N. Aini[4,*]

[1]Postgraduate Program, Faculty of Agriculture, Brawijaya University, Jl., Malang, 65145 Indonesia

[2]Research Center for Estate Crops, Research Organization for Agriculture and Food, the National Research and Innovation Agency of the Republic of Indonesia, Jl., Cibinong, Bogor, 16911 Indonesia

[3]Department of Soil Science, Faculty of Agriculture, Brawijaya University, Jl., Malang, 65145 Indonesia

[4]Department of Agronomy, Faculty of Agriculture, Brawijaya University, Jl., Malang, 65145 Indonesia

ARTICLE INFO

Article History:
Received 12 May 2026
Revised 17 July 2026
Accepted 19 August 2026

Keywords:
Coastal soil
Electrical conductivity
Saline soil
Soil bacterial community
Soil physicochemical properties
Tropical agricultural soil

DOI:10. 22034.gjesm.2027.01.11

ABSTRACT

BACKGROUND AND OBJECTIVES: Coastal soil salinization is an environmental constraint that alters soil physicochemical conditions and may restructure microbial communities, while field patterns may also reflect land use and co-varying soil properties. The study objectives were to characterize soil physicochemical conditions together with bacterial diversity, composition, community dissimilarity, and predicted ecological functions at three tropical coastal sites in Palang, Tuban, East Java, with contrasting electrical conductivity.

METHODS: Electrical conductivity at sampling sites PA8, PA9, and PA10 was 13.68, 3.74, and 0.50 decisiemens per meter, respectively. A single composite soil sample was collected and analyzed from each site and subjected to near full-length bacterial small-subunit ribosomal ribonucleic acid gene amplicon sequencing. Following quality filtering and denoising, amplicon sequence variants were resolved, and taxonomic assignments were performed against a curated ribosomal reference database. Observed richness, Shannon and Gini-Simpson indices, Bray-Curtis and Weighted UniFrac principal coordinate analyses, taxonomic relative abundance, and taxonomy-based predicted functions were summarized descriptively. Site-to-site variations in exchangeable sodium, organic carbon, cation exchange capacity, phosphorus availability, soil texture, and culturable bacterial abundance were also compared among sites**.** Due to the confounding of site identity, electrical conductivity, land use, and other edaphic properties, replicated inference of salinity effects was not feasible.

FINDINGS: PA8 had 2,052 observed sequence variants and a Shannon index of 9.61; PA9 had 5,205 variants and a Shannon index of 11.39; and PA10 had 3,145 variants and a Shannon index of 11.03. Taxonomic profiles differed among sites. PA8 was characterized by Bacillota, Bacillales, and Incertae_Sedis_14; PA9 by Bacillota/Pseudomonadota, Bacillales, and Neobacillus; and PA10 by Chloroflexota, Anaerolineales, and UTCFX1. Weighted UniFrac distances were 0.3266 for PA9–PA10, 0.4850 for PA8–PA9, and 0.5226 for PA8–PA10. Predicted chemoheterotrophy accounted for 20.46 percent, 16.97 percent, and 23.88 percent of post-filter reads at sites PA8, PA9, and PA10, respectively. PA8 also had the highest exchangeable sodium, whereas PA10 had the highest organic carbon, cation exchange capacity, Olsen-available phosphorus, and culturable bacterial abundance**.**

CONCLUSION: While intra-site analyses revealed marked heterogeneity in physicochemical parameters and bacterial community structures, the observational framework of this study limits direct causal attribution to salinity gradients and restricts the extrapolation of findings to wider salinity categories. The findings provide a site-specific environmental baseline and hypotheses for future replicated studies.

This is an open access article under the CC BY license (http://creativecommons.org/licenses/by/4.0/)

NUMBER OF REFERENCES	NUMBER OF FIGURES	NUMBER OF TABLES
51	5	5

*Corresponding Author:
Email: nra-fp@ub.ac.id
Phone: +62813 3411 0303
ORCID: 0000-0002-5600-0443

Note: Discussion period for this manuscript open until March 01, 2027 on GJESM website at the “Show Article”.

INTRODUCTION

Coastal soil salinization is a major environmental constraint in tropical agricultural landscapes because excessive soluble salts can reduce soil water availability, disturb ionic and nutrient balance, and impose osmotic and ionic stress on plants and soil microorganisms (Dong *et al.*, 2022; Hailu and Mehari, 2021; Tarolli *et al.*, 2024). In coastal environments, these hydrological stresses are frequently exacerbated by seawater intrusion, saline water influxes, impeded drainage, and evaporative enrichment. For soil bacteria, increased osmotic stress and ionic imbalance can constrain growth and resource use, modify competitive interactions, and favor taxa able to maintain cellular homeostasis under saline conditions. Consequently, bacterial richness, evenness, taxonomic composition, and phylogenetically structured community dissimilarity can exhibit substantial spatial variation across salt-affected soils. Furthermore, these spatial distributions can be modulated by confounding covariates, including organic carbon concentrations, soil potential of hydrogen (pH), moisture dynamics, sodium chemistry, and anthropogenic land use (Dong *et al.*, 2022; Li *et al.*, 2023; Rath *et al.*, 2019). Such interactions between agroecological conditions, soil chemical properties, and microbial diversity have also been documented in tropical agricultural systems, highlighting the importance of evaluating microbial patterns alongside site-specific environmental characteristics (Tarigan *et al.*, 2026). Electrical conductivity (EC) is therefore used here as the descriptor of soluble-salt conditions, whereas sodicity-related measurements are treated separately. 16S ribosomal ribonucleic acid (16S rRNA) gene amplicon sequencing enables culture-independent characterization of bacterial communities and is widely used to compare community composition across environmental samples (Dreier *et al.*, 2022). Empirical evaluations of agricultural and coastal saline soils consistently demonstrate distinct shifts in bacterial richness, structural diversity, and taxonomic configurations under varying salinity regimes. The magnitude and direction of these patterns are strongly context dependent and may covary with pH, organic carbon, moisture, sodium-related chemistry, and other site properties (Dong *et al.*, 2022; Hindersah *et al.*, 2023; Li *et al.*, 2023; Mucsi *et al.*, 2024; Rath *et al.*, 2019). Mechanistically, elevated soluble salts can impose osmotic constraints and alter nutrient and cation availability, whereas pH, organic carbon, and moisture modify substrate supply and habitat conditions. Consequently, such interconnected edaphic drivers modulate microbial assembly by governing taxon persistence and relative abundance profiles, which directly shape both within-sample richness and between-sample structural divergence. Thus, current evidence supports salinity as an important ecological filter but does not imply a universal or strictly monotonic bacterial response across soils. The contribution of salinity cannot be separated from co-varying soil properties without independent biological replication or a design that decouples those factors. Such constraints are particularly salient within tropical coastal agroecosystems, where salinity regimes evolve amidst complexly varied agricultural practices and edaphic management frameworks. The broader importance of integrating biodiversity considerations with coastal landscape management has likewise been emphasized in studies of mangrove-based coastal resilience and ecosystem rehabilitation (Utomo *et al.*, 2026; Yuliana *et al.*, 2026). Taxonomy-based tools such as functional annotation of prokaryotic taxa (FAPROTAX) can additionally generate hypotheses about potential ecological functions, but these predictions do not measure functional genes, transcripts, enzymes, or process rates (Louca *et al.*, 2016; Sansupa *et al.*, 2021). Accordingly, the knowledge gap addressed here is not whether salinity affects soil bacteria in general. Instead, it concerns the limited site-specific baseline information for tropical coastal agricultural soils of East Java. To address this gap, this study integrates nearly full-length 16S rRNA profiling with empirical soil chemistry, amplicon sequence variant (ASV) diversity, taxonomic composition, pairwise community dissimilarity, and conservatively

interpreted functional potential. The present study therefore provides a descriptive survey of three geographically distinct coastal sites in Palang, Tuban, with contrasting measured EC. PA8, PA9, and PA10 were each represented by one composite sequencing sample. Consequently, site identity, land use, EC, and other soil properties were confounded, and the study was not designed to estimate replicated salinity-treatment effects or isolate salinity from other site characteristics. Specifically, the objectives of this study are to document soil environmental parameters and to describe observed ASV richness and diversity, bacterial taxonomic relative abundance, pairwise community dissimilarity, and inferred ecological functions across three coastal gradients characterized by divergent EC levels. Site-specific environmental and bacterial patterns were identified to guide future replicated studies. The present study was conducted in coastal agricultural soils of Palang, Tuban, East Java, Indonesia in 2025.

MATERIALS AND METHODS

Research approach and design

This study was an exploratory, field-based observational survey of three geographically distinct sites within Palang Subdistrict that were purposively selected to span contrasting measured EC conditions. In order to mitigate potential temporal confounding, sampling across all three locations was conducted within the same synchronized field campaign in November 2025. The sampling sites, coded PA8, PA9, and PA10, were individual sites rather than biological replicates of salinity or EC treatments, and one composite sequencing sample was analyzed from each site. Site selection did not ensure that bacterial differences represented EC alone. Consequently, potential confounding persisted among site-specific factors, including land-use patterns, sodium chemistry, organic carbon dynamics, cationic profiles, management regimens, and both quantified and unquantified environmental parameters. Accordingly, alpha-diversity metrics, taxonomic profiles, ordination patterns, and predicted functions were interpreted descriptively, and no inferential test was used to claim a salinity-treatment effect.

Study area

This study was conducted at three coastal sites in Palang Subdistrict, Tuban Regency, East Java, Indonesia (Fig. 1). PA8 was located in Leran Wetan, Palang, Tuban, at 6°54′26.4″ south (S) 112°10′12.6″ east (E). PA9 was located in Karang Lor, Cepokrejo, Palang, Tuban, at 6°54′47.2″ south and 112°09′51.6″ east. PA10 was located in Wangun Bara, Wangun, Palang, Tuban, at 6°56′09.1″ south and 112°09′52.8″ east. Field records identified the land-use categories as a salt-producing pond at PA8, paddy/fallow land at PA9, and paddy land at PA10. These land-use disparities represent potential site-level confounding variables rather than experimentally controlled experimental parameters. Site selection was based on contrasting measured EC rather than replicated salinity treatments. EC was determined using a 1:5 soil-to-water suspension and interpreted using the criteria of Eviati *et al.* (2023), in which <1; 1–2; 2–3; 3–4; and >4 dS/m correspond to very low, low, moderate, high, and very high EC classes, respectively. On this basis, PA8 (13.68 dS/m), PA9 (3.74 dS/m), and PA10 (0.50 dS/m) corresponded to very high, high, and very low EC classes. To avoid implying true experimental replication, the study locations are designated throughout the comparative interpretation as the highest-EC site (PA8), intermediate-EC site (PA9), and lowest-EC site (PA10). These descriptors are site specific and do not constitute formal saline, sodic, or saline-sodic soil classification.

Soil sample collection

At each site, soil was collected from five sampling points without a fixed geometric sampling pattern, with approximately 10 meters (m) spacing between successive points. Surface litter and vegetation were removed before sampling. Approximately 500 grams (g) of soil was retrieved from the entire 0–20 centimeters (cm) depth layer at each designated point using a clean shovel,

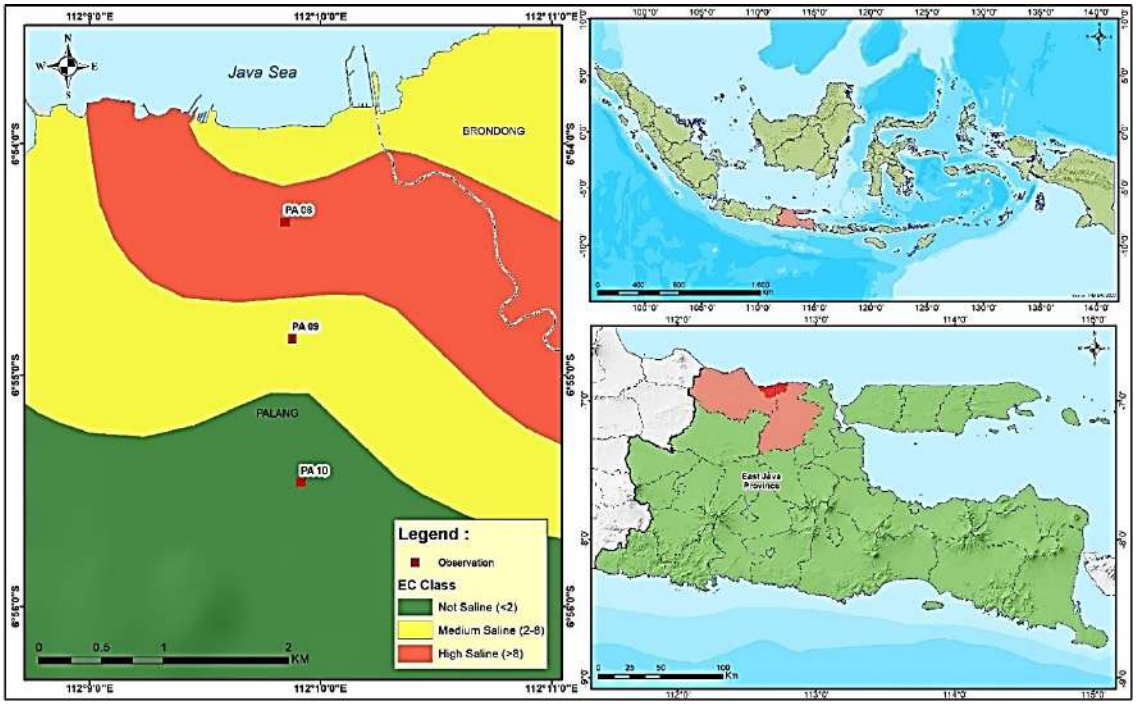

Fig. 1: Geographical location of the study area and sampling locations in Palang Subdistrict, Tuban Regency, East Java, Indonesia. (PA8, PA9, and PA10 represent the highest-, intermediate-, and lowest-EC sites in the present three-site comparison, respectively. The background EC strata shown in the original field map (<2, 2–8, and >8 dS/m) were used only for preliminary reconnaissance and are not treated as replicated salinity classes in the revised analysis)

which was decontaminated with water between successive sampling sites to prevent cross-contamination. The five subsamples were manually mixed and homogenized on a clean tray or clean plastic surface, yielding approximately 2.5 kilograms (kg) of bulk soil per site. A 100 g aliquot of each homogenized composite sample was placed in a clean resealable plastic ziplock bag for molecular analysis. The molecular aliquots were frozen for approximately 24 hours (h) in the freezer compartment of a two-door refrigerator before shipment. To maintain cold chain integrity during transit, specimens were transported in insulated, aluminum-foil-lined containers equipped with ice packs via priority overnight delivery, departing midday and arriving at the analytical facility on the subsequent afternoon. Due to the absence of continuous temperature logging during shipment, precise transit temperatures are not formally documented. Thus, each site contributed one composite biological sequencing sample; compositing improved within-site spatial coverage but did not create independent biological replication. Separate homogenized material from the same site composite was used for physicochemical analysis and was air-dried, gently crushed, and sieved through a 2 millimeters (mm) sieve before analysis (Carter and Gregorich, 2008; Sparks *et al.*, 1996).

Soil physicochemical analysis

Soil physicochemical characterization included EC, pH, organic carbon (C), exchangeable sodium (Na), potassium (K), calcium (Ca), and magnesium (Mg), cation exchange capacity (CEC), gravimetric moisture content, available and potential phosphorus (P), and particle-size distribution. EC was determined using a 1:5 soil-to-water suspension. A 10 g portion of air-dried soil passed through a 2 mm sieve was mixed with 50 milliliters (mL) of distilled water, mechanically shaken for 1 h, and measured with a conductivity meter. The procedure followed the approach reported previously (Eviati *et al.*, 2023). The soil chemical

properties and pH values detailed in Table 1 were derived from official analytical reports issued by the East Java soil laboratory reports. Soil pH was measured electrometrically at a 1:5 soil-to-water (H_2O) ratio. Soil organic carbon content was quantified using the Walkley and Black (1934) wet oxidation procedure coupled with spectrophotometric determination. Exchangeable K, Ca, Mg, and Na were extracted by percolation with 1 molar per liter (mol/L) ammonium acetate (NH_4OAc) at pH 7 and measured by atomic absorption spectrometry. CEC was determined by NH_4OAc percolation followed by 10 percent (%) sodium chloride (NaCl) displacement and titrimetry. Moisture content was determined gravimetrically by oven drying, available P by the Olsen method, potential P by 25% hydrochloric acid extraction, and texture by the hydrometer method. In accordance with laboratory advisories noting that cumulative extractable base cations may surpass measured CEC thresholds, individual cation and CEC values were retained as descriptive measurements but were not utilized to derive base saturation or exchangeable sodium percentage (ESP), prompting the exclusion of ESP from the refined analytical framework. Culturable bacterial abundance was determined by the total plate count (TPC) method on Nutrient Agar. Soil samples were stored frozen for approximately 2–3 days before analysis. A 1 g aliquot was taken while still partially frozen and mixed with 9 mL sterile 0.85% NaCl solution to obtain a 10−1 suspension. After vortex homogenization, tenfold serial dilutions were prepared to 10−6, with each tube vortexed before transfer. Aliquots of 1 mL from the 10−3, 10−4, and 10−5 dilutions were plated in duplicate by the pour-plate method with molten Nutrient Agar allowed to cool until warm. Plates were incubated at room temperature for 24 h. Bacterial enumeration was performed on replicate plates containing between 30 and 300 colonies per plate. The corresponding mean counts were adjusted using the reciprocal dilution factor to quantify culturable bacterial density in colony-forming units (CFU)/g soil (Pepper and Gerba, 2015).

Bacterial gene sequencing and taxonomic analysis

Deoxyribonucleic acid (DNA) extraction was performed by PT Aurora on the composite soil aliquots using the VAMNE Magnetic Stool/Soil DNA Extraction Kit (DMA5101, Vazyme Biotech Co., Ltd.) following the manufacturer's soil-DNA protocol. The manufacturer specifies 200 mg soil input for sample pretreatment with Lysis Buffer/ribonuclease A (RNase A), followed by mechanical disruption, inhibitor removal with the manufacturer-designated inhibitor-removal buffer, magnetic-bead binding and washing, and low-salt elution. The exact soil mass processed for each of the three extracts was not recorded in the documentation available to the authors and is therefore not stated as a sample-specific value. Furthermore, the available laboratory records lacked documentation regarding distinct absorbance-ratio acceptance thresholds at 260/280 nm and 260/230 nm, as well as the corresponding extraction-blank results. Downstream amplicon qualification, however, was documented by the sequencing provider using 0.8% agarose-gel examination and Qubit 2.0 fluorometry before pooling. Nearly full-length 16S rRNA genes were amplified with barcoded 27F (AGRGTTYGATYMTGGCTCAG) and 1492R (RGYTACCTTGTTACGACTT) primers. Polymerase chain reaction (PCR) was performed in 25 µL reactions containing 2× KAPA HiFi HotStart ReadyMix, 2.5 micromolar per litter (µmol/L) forward and reverse primers, and approximately 10 ng DNA template. Thermal cycling comprised 95 degrees Celsius (°C) for 3 minutes (min); 25 cycles of 95 °C for 30 s, 57 °C for 30 s, and 72 °C for 1 min; followed by 72 °C for 1 min. Qualified PCR products were combined in equal proportions and purified using AMPure PB beads. A 600 ng pooled amplicon was utilized to prepare a single-molecule real-time (SMRT) library employing the SMRTbell Prep Kit 3.0. Sequencing was conducted on a PacBio Sequel IIe using an SMRT 8M Cell with chemistry version 2, and secondary processing was carried out using the SMRT analysis pipeline v11.0.0. The resulting reads had median lengths of approximately 1,449–1,549 base pairs (bp). Full-

length PacBio sequencing and subsequent 16S analysis were conducted by Genomics (Taiwan) under project ID NT260119024. Primer sequences were removed before amplicon sequence variant (ASV) inference using Cutadapt v4.6 (Martin, 2011) with minimum length 1, overlap 3, error rate 0.1, reverse-complement search, and discard-untrimmed. Bioinformatic processing used nf-core/ampliseq v2.14.0 (Straub *et al.*, 2020). Read quality was evaluated with FastQC sequence quality-control software v0.12.1 (Andrews, 2010) and summarized with MultiQC quality-control reporting software v1.27 (Ewels *et al.*, 2016). Sequence-variant inference used divisive amplicon denoising algorithm 2 (DADA2) v1.30.0 (Callahan *et al.*, 2016), and downstream analysis used the quantitative insights into microbial ecology 2 (QIIME 2) framework v2024.10.1 (Bolyen *et al.*, 2019). In DADA2 filterAndTrim, minLen and maxLen were 1,000 and 1,600 bp, respectively. Reads passing filtering were denoised using the DADA2 error model, dereplicated, and screened for chimeras to generate ASVs. Given that the dataset comprised PacBio long-read amplicons rather than than paired-end short reads, read merging was omitted. Taxonomy assignment was performed in QIIME 2 using a primer-specific Naive Bayes classifier (Bokulich *et al.*, 2018), which was trained on the SILVA ribosomal ribonucleic acid gene database (SILVA) version 138.2 reference set clustered at 99% similarity (Quast *et al.*, 2012; Robeson *et al.*, 2021). The 99% value refers to the reference-sequence set used for classifier construction and is not a taxonomic assignment threshold or evidence of 99% species identity. ASVs with taxonomic strings containing mitochondria or chloroplast were removed before downstream analyses. ASVs, rather than traditional species-level taxonomic assignments, served as the primary units for all diversity analyses. Furthermore, parameters not explicitly documented in the sequencing report were neither reconstructed nor inferred from software defaults.

Diversity and community structure analysis

Alpha diversity was summarized at the ASV level using observed ASV richness, the Shannon index (Shannon, 1948), and the Gini-Simpson index (Simpson, 1949). The number of observed ASVs measures detected richness, the Shannon diversity index integrates both richness and relative abundance distribution, and the Gini-Simpson index summarizes evenness while allocating greater weight to dominant populations. Sequencing-depth adequacy was assessed from rarefaction curves generated from the post-taxonomic-filter ASV table. For beta diversity, Bray-Curtis dissimilarity was selected to describe abundance-based compositional differences without phylogenetic information, whereas Weighted UniFrac incorporated both relative abundance and phylogenetic branch lengths. Pairwise distance relationships were visualized using principal coordinate analysis (PCoA) (Gower, 1966). Given that individual sites were represented by single composite samples, downstream alpha- and beta-diversity measures were interpreted strictly in a descriptive capacity without the application of inferential statistical tests. For Weighted UniFrac, the QIIME 2 provenance of the verified weighted_unifrac distance artifact was inspected directly. Representative ASV sequences were aligned with multiple alignment using fast fourier transform (MAFFT) in q2-alignment v2024.10.0 using 20 threads with parttree disabled. The alignment was masked using a maximum gap frequency of 1.0 and minimum conservation of 0.4, after which a phylogenetic tree was constructed with FastTree in q2-phylogeny v2024.10.0 using 20 threads and midpoint-rooted. Weighted UniFrac distance matrices were generated using the rooted tree within the QIIME 2 beta-phylogenetic framework. Hierarchical clustering was excluded, as a dataset of three observations is insufficient for reliable group-level inference and adds no independent analytical value beyond the pairwise distance matrix. The Bray-Curtis metric was originally described by Bray and Curtis (1957).

Predicted ecological function analysis

Predicted ecological functions were generated with FAPROTAX 2025 from the processed 16S rRNA taxonomic table (Louca *et al.*, 2016). By mapping prokaryotic taxa to curated putative ecological functions, FAPROTAX provides heuristic functional predictions grounded in taxonomy rather than direct measurements. For quantitative comparison among the three samples, the abundance assigned to each functional category was divided by the post-taxonomic-filter read total for that sample (42,745 reads for PA8, 81,678 for PA9, and 34,447 for PA10) and expressed as a percentage. Because individual taxa may be mapped to multiple functional groups within FAPROTAX, these categories are not mutually exclusive, precluding cumulative relative abundances of exactly 100%. Coverage was calculated as the proportion of post-filter reads belonging to taxa assigned to at least one FAPROTAX group. Selected profiles are summarized in Table 5. Consequently, these functional predictions should not be construed as direct measurements of functional-gene abundance, transcriptional activity, enzymatic rates, cellular abundance, or in situ metabolic processes.

Analytical reliability and reproducibility

Reliability and reproducibility were addressed at multiple stages of the workflow. Amplicon products were evaluated by 0.8% agarose-gel examination and Qubit 2.0 fluorometry before pooling. Read quality was evaluated using FastQC (v0.12.1) and aggregated via MultiQC (v1.27). Absolute read counts were preserved throughout primer trimming, DADA2 filtering, denoising, chimera removal, and taxonomic filtering. ASVs were generated using the DADA2 error model rather than similarity-based operational taxonomic unit clustering, and taxonomy was assigned with a primer-specific Naive Bayes classifier trained from SILVA 138.2. Rarefaction output was used to assess sequencing-depth behavior, and the Weighted UniFrac tree-construction workflow and distance artifact were verified directly from QIIME 2 provenance. FAPROTAX execution parameters, including the software workflow version, sample-specific normalization denominator, and annotation coverage metrics, were fully documented. For auditability, the raw reads are archived in the National Center for Biotechnology Information (NCBI) Sequence Read Archive (SRA). Parameters not documented in the laboratory or bioinformatic records were left unassigned rather than inferred from software defaults. While this practice safeguards workflow traceability, it does not compensate for the inherent lack of biological replication within EC conditions.

RESULTS AND DISCUSSION

Soil physicochemical characteristics across the three sites

The three sites showed distinct physicochemical profiles rather than a uniform gradient across all measured soil properties (Table 1). PA8 had the highest EC (13.68 dS/m) and exchangeable Na (30.71 cmol(+)/kg), together with the lowest CEC (12.83 cmol(+)/kg). PA10 had the lowest EC (0.50 dS/m) but the highest organic C (1.45%), CEC (28.41 cmol(+)/kg), Olsen-available P (42 mg/kg), potential P (1,110 mg/kg), and TPC (8.5×10^4 CFU/g). PA9 represented the intermediate-EC site (3.74 dS/m) and showed comparatively low organic C and P availability. Under the 1:5 soil–water EC criteria of Eviati *et al.* (2023), PA8, PA9, and PA10 corresponded to very high, high, and very low EC classes, respectively. All soils were classified as clay, but clay content varied substantially among sites. ESP and base saturation were not calculated from the reported exchangeable-cation and CEC values. Overall, the sites differed in salinity, Na status, carbon and nutrient availability, cation-retention capacity, and soil physical properties.Such co-variation is ecologically important because soluble salts and Na enrichment can impose osmotic and ionic constraints, whereas organic C, pH, nutrient availability, and soil physicochemical properties can modify microbial resource availability and habitat conditions (Basak *et al.*, 2022; Dong *et al.*, 2022; Xie *et al.*, 2017). Furthermore, Agricultural

Table 1: Physicochemical characteristics and total plate counts of soil samples from Three coastal sites in Palang, Tuban, East Java

Parameter	Unit	PA8	PA9	PA10
Electrical conductivity	dS/m	13.68	3.74	0.50
pH (H_2O)	–	8.50	8.04	8.80
Organic C	%	1.01	0.62	1.45
Exchangeable Na	cmol(+)/kg	30.71	4.15	4.84
Exchangeable K	cmol(+)/kg	2.67	0.49	0.23
Exchangeable Ca	cmol(+)/kg	41.62	44.25	49.73
Exchangeable Mg	cmol(+)/kg	28.45	7.20	6.08
Cation exchange capacity	cmol(+)/kg	12.83	22.02	28.41
Gravimetric moisture content	%	7.86	6.61	7.74
Olsen-available P	Mg/kg	18	8	42
Potential P	Mg/kg	640	550	1,110
Clay fraction	%	42	75	78
Textural class	–	Clay	Clay	Clay
Total plate count	$\times 10^4$ CFU/g	0.7	2.4	8.5

Note: PA8, PA9, and PA10 represent the highest-, intermediate-, and lowest-EC sites, respectively, in this three-site comparison. Exchangeable cations and CEC are presented as reported by the analytical laboratory. Because the summed exchangeable base cations exceeded the measured CEC in some samples, these values were not used to derive ESP or base saturation. TPC represents culturable bacterial abundance under the applied culture conditions. Gravimetric moisture content represents laboratory-determined soil moisture rather than in-situ field moisture.

management practices can additionally drive variations in soil bacterial communities through mediated effects on edaphic conditions (Lee *et al.*, 2020). Therefore, subsequent bacterial community differences among PA8, PA9, and PA10 should be interpreted as site-specific responses to contrasting physicochemical environments rather than as effects of EC alone. TPC served solely as a measure of culturable bacterial density under the applied culture conditions, precluding its use as an estimate of total bacterial abundance (Janssen *et al.*, 2002).

Sequencing quality, sequence variant processing, and taxonomic assignment

Sequencing and read-processing metrics are summarized in Table 2. Cutadapt retained 99.3–99.6% of reads after primer trimming. DADA2 input counts were 58,005 for PA8, 109,492 for PA9, and 63,589 for PA10, yielding 42,816, 81,885, and 34,586 non-chimeric reads, respectively, after filtering, denoising, and chimera removal. PA10 consequently showed a lower overall DADA2 retention rate (54.4%) than PA8 (73.8%) and PA9 (74.8%). Although FastQC and MultiQC indicated elevated sequence-duplication levels (79.0–86.2%), these metrics were retained solely as quality-control indicators, given that sequence recurrence alone does not confirm technical PCR duplicates. Rarefaction curves were therefore used as an additional assessment of sequencing depth rather than as evidence that differences in read retention were fully eliminated. The high sequence retention observed following primer trimming indicates that primer removal incurred minimal sequence loss. In contrast, the substantial reduction during DADA2 processing reflects the cumulative impact of quality filtering, error correction, ASV inference, and chimera removal. These steps are integral to DADA2-based processing of full-length PacBio 16S rRNA amplicons and are intended to distinguish biological sequence variants from sequencing and PCR-derived errors (Callahan *et al.*, 2019). The reduced retention of PA10 necessitates cautious interpretation of comparative richness values, given that alpha-diversity metrics can be influenced by unequal effective sequencing depth and filtering stringency. Rarefaction provides a useful means of evaluating the influence of uneven sequencing effort, but it does not by itself demonstrate that richness estimates are free from depth-related effects (Schloss, 2024). Likewise, FastQC duplication metrics quantify repeated sequences and may indicate enrichment bias, including PCR over-amplification, but they are not sufficient on their own to identify the origin of duplicated reads. Consequently, differences in

Table 2: Sequencing quality and sequence variant processing summary

Parameter	PA8	PA9	PA10
Sequencing mode	PacBio Sequel IIe	PacBio Sequel IIe	PacBio Sequel IIe
Cutadapt total processed	58,427	109,973	63,981
Cutadapt passing filters	58,005	109,492	63,589
DADA2 input	58,005	109,492	63,589
DADA2 filtered	56,332	106,240	61,624
DADA2 denoised	43,485	82,776	34,820
DADA2 non-chimeric	42,816	81,885	34,586
Reads after taxonomic filtering	42,745	81,678	34,447
DADA2 non-chimeric retention (%)	73.8	74.8	54.4
FastQC sequence duplication (%)	84.2	86.2	79.0
Median read length (bp)	1,549	1,499	1,449
Mean Phred quality score	~40	~40	~40

sequencing depth and retention served strictly as methodological context for the descriptive analyses rather than as evidence of biological divergence among PA8, PA9, and PA10.

Alpha diversity of bacterial communities

Alpha-diversity profiles differed descriptively among the three sites (Table 3). PA9 showed the highest observed ASV richness (5,205) and Shannon diversity (11.39), followed by PA10 with 3,145 ASVs and a Shannon index of 11.03, whereas PA8 had the lowest values (2,052 ASVs; Shannon = 9.61). Gini-Simpson indices were consistently high, ranging from 0.9951 at PA8 to 0.9993 at PA10, indicating low dominance across the three communities. The Chao1 index was omitted from final evaluations since processed values matched observed ASV richness and lacked verifiable singleton or doubleton counts. Rarefaction curves were instead implemented to gauge sequencing-depth behavior. The lower richness and Shannon diversity at PA8 coincided with the highest EC and exchangeable Na, which is consistent with reports that elevated salinity can impose environmental filtering and reduce microbial diversity in salt-affected soils (Canfora *et al.*, 2014; Zhang *et al.*, 2019). However, bacterial diversity does not respond uniformly to salinity. Zhao *et al.* (2018) showed that pH can be as important as salinity in structuring bacterial communities, while Dong *et al.* (2022) reported strong compositional shifts without a corresponding reduction in bacterial richness. The higher richness at PA9 therefore should not be interpreted as evidence that intermediate EC maximized bacterial diversity. PA9 also had the greatest post-taxonomic-filter sequencing depth (81,678 reads), although PA10 contained fewer reads than PA8 yet retained greater observed richness, indicating that sequencing depth alone does not explain the observed ranking. Because uneven sequencing effort poses an ongoing technical challenge for alpha-diversity contrasts, rarefaction was employed as an additional safeguard to evaluate depth-dependent biases (Schloss, 2024). Because each site was represented by only one composite sequencing sample and soil properties and land use covaried with site identity, the alpha-diversity pattern is best interpreted as a site-specific outcome rather than a direct EC effect.

Table 3: Observed richness and alpha diversity indices of soil bacterial communities

Site	Observed ASVs	Shannon index	Gini-Simpson index
PA8	2,052	9.61	0.9951
PA9	5,205	11.39	0.9990
PA10	3,145	11.03	0.9993

Note: PA8 = highest-EC site; PA9 = intermediate-EC site; PA10 = lowest-EC site in the present three-site comparison.

Bacterial taxonomic composition across the three sites

Significant compositional divergence in bacterial communities was observed among the three sites (Fig. 2). PA8 showed the greatest relative representation of Bacillota (24.54%) and Bacillales (21.38%), with *Incertae_Sedis_14* (13.43%) and *Thalassobacillus* (11.46%) as the most represented genera. PA9 showed near-equal proportions of Bacillota (20.12%) and

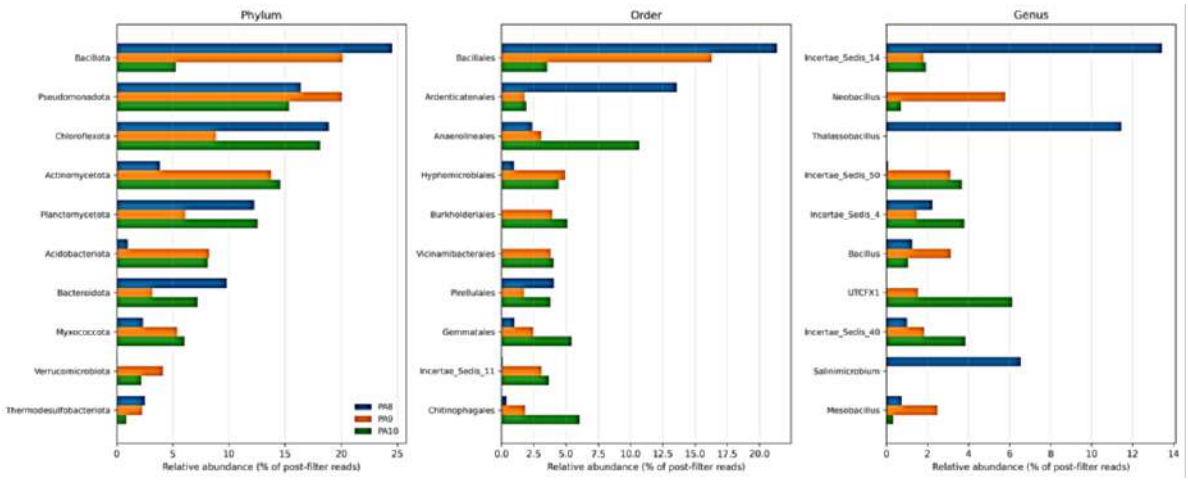

Fig. 2: Relative-abundance profiles of the ten bacterial taxa with the highest summed abundance across PA8, PA9, and PA10 at (a) phylum, (b) order, and (c) genus levels. Values represent percentages of all post-taxonomic-filter reads within each sample; taxa outside the displayed top ten are not shown. Each site is represented by one composite sequencing sample, and taxonomic differences are interpreted descriptively.

Pseudomonadota (20.07%), with Bacillales (16.30%) and *Neobacillus* (5.79%), whereas PA10 was characterized by Chloroflexota (18.14%), Anaerolineales (10.69%), and UTCFX1 (6.12%). These percentages were calculated relative to the total post-filtering read count per sample, thereby reflecting relative sequence proportions rather than absolute bacterial population size (Props *et al.*, 2017). The greater representation of Bacillota/Bacillales and *Thalassobacillus* at PA8 is ecologically compatible with previous evidence that saline conditions can restructure bacterial communities and favor lineages possessing greater salt tolerance (Dong *et al.*, 2022; Rath *et al.*, 2019). Consequently, observed profile differences cannot be isolated to EC owing to confounding variations in salinity, edaphic properties, and land management across PA8, PA9, and PA10. The detected taxa are therefore interpreted as site-associated community configurations rather than salinity-selected populations. Species-level annotations were excluded from the main ecological interpretation. Nearly full-length 16S rRNA sequencing provides substantially greater taxonomic resolution than partial-gene sequencing and, when combined with high-accuracy PacBio sequencing and appropriate denoising, can discriminate closely related sequence variants (Callahan *et al.*, 2019; Johnson *et al.*, 2019). Notwithstanding its advantages, full-length 16S profiling remains limited in achieving absolute species-level discrimination because sequence overlap occurs among distinct taxa, and multiple, divergent 16S gene variants can coexist within a single genome. Ecological interpretation was therefore restricted to phylum-, order-, and genus-level patterns.

Dominant bacterial taxa across the three sites

Table 4 highlights distinct taxonomic configurations among the three sites. PA8 was characterized by Bacillota (24.54%), Bacillales (21.38%), and *Incertae_Sedis_14* (13.43%); PA9 by near co-representation of Bacillota and Pseudomonadota (20.12% and 20.07%), Bacillales (16.30%), and *Neobacillus* (5.79%); whereas PA10 was characterized by Chloroflexota (18.14%), Anaerolineales (10.69%), and UTCFX1 (6.12%). The observed variations reveal localized reorganization of bacterial relative abundance across sites rather than a linear or continuous taxonomic transition in response to the EC gradient. Salinity can act as an environmental filter and alter bacterial community composition, but its effects commonly covary with pH, organic matter, and other edaphic conditions, making causal attribution difficult in field gradients (Dong *et al.*, 2022; Rath *et al.*, 2019). Furthermore, the

Table 4: Dominant bacterial taxa at phylum, order, and genus levels across the three sites

Taxonomic level	PA8 / highest EC	Relative abundance (%)	PA9 / intermediate EC	Relative abundance (%)	PA10 / lowest EC	Relative abundance (%)
Phylum	Bacillota	24.54	Bacillota / Pseudomonadota	20.12 / 20.07	Chloroflexota	18.14
Order	Bacillales	21.38	Bacillales	16.30	Anaerolineales	10.69
Genus	Incertae_Sedis_14	13.43	Neobacillus	5.79	UTCFX1	6.12

elevated relative abundance of *Thalassobacillus* at PA8 aligns with the known halophilic traits of this genus, which is frequently documented in saline soils and other hypersaline ecosystems (Tuesta-Popolizio *et al.*, 2021). Nevertheless, the present data do not demonstrate physiological salt tolerance or salinity-driven selection of the detected taxa because EC varied together with land use, organic C, exchangeable cations, CEC, and other site properties. PA9 and PA10 should therefore likewise be interpreted as distinct site-associated taxonomic assemblages rather than communities specifically selected by intermediate or low EC.

Heatmap patterns of dominant bacterial taxa

The genus-level heatmap revealed distinct site-associated abundance patterns (Fig. 3). PA8 was distinguished by the high relative representation of *Incertae_Sedis_14* (13.43%), *Thalassobacillus* (11.46%), *Salinimicrobium* (6.56%), and *Microbulbifer* (4.67%), whereas PA9 showed greater representation of *Neobacillus*, *Bacillus*, and *Mesobacillus*. PA10 displayed a contrasting profile dominated by UTCFX1 and several unresolved *Incertae_Sedis* groups. The prevalence of *Thalassobacillus* at PA8 is ecologically expected given the classification of this genus as a moderate-to-extreme environmental halophiles (Tuesta-Popolizio *et al.*, 2021). Collectively, prior studies on saline environments demonstrate that progressive salinization alters bacterial community composition through selective osmotic and ionic pressures, though both the scale and taxonomic composition of these responses are tightly governed by local environmental factors (Nan *et al.*, 2022; Rath *et al.*, 2019; Zhang *et al.*, 2024). The phylum-level heatmap reinforced this site differentiation (Fig. 4). PA8 was characterized by greater representation of Bacillota, whereas PA9 showed near co-representation of Bacillota and Pseudomonadota, and PA10 showed greater representation of Chloroflexota together with Actinomycetota and Planctomycetota. Chloroflexota comprises phylogenetically and metabolically diverse lineages occurring across terrestrial and aquatic environments; its higher representation at PA10 therefore cannot be assigned to a specific ecological function from 16S data alone (Wiegand *et al.*, 2023). The distinct clustering patterns are best understood as site-specific taxonomic assemblages rather than isolated responses to salinity, because EC shared strong collinearity with land-use practices, organic carbon, exchangeable cations, CEC, and broader environmental gradients. This caution is particularly important in field salinity studies, where salinity effects can be difficult to separate from co-varying edaphic factors (Dong *et al.*, 2022; Rath *et al.*, 2019).

Beta diversity and bacterial community structure

PCoA provided a descriptive visualization of differences among the three composite bacterial communities identified (Fig. 5). Non-phylogenetic compositional dissimilarity evaluated via Bray–Curtis ordination placed PA8, PA9, and PA10 at distinct coordinates, axes PCoA1 and PCoA2 accounted for 53.42% and 46.58% of the explained variation, respectively. Weighted UniFrac, which additionally incorporates phylogenetic branch lengths and relative abundance, showed the strongest separation of PA8, with distances of 0.4850 to PA9 and 0.5226 to PA10, compared with 0.3266 between PA9 and PA10. This concordance between abundance-based and phylogenetic outcomes reveals that the three sites variations involved shifts both in taxonomic relative abundance and in the structural distribution of

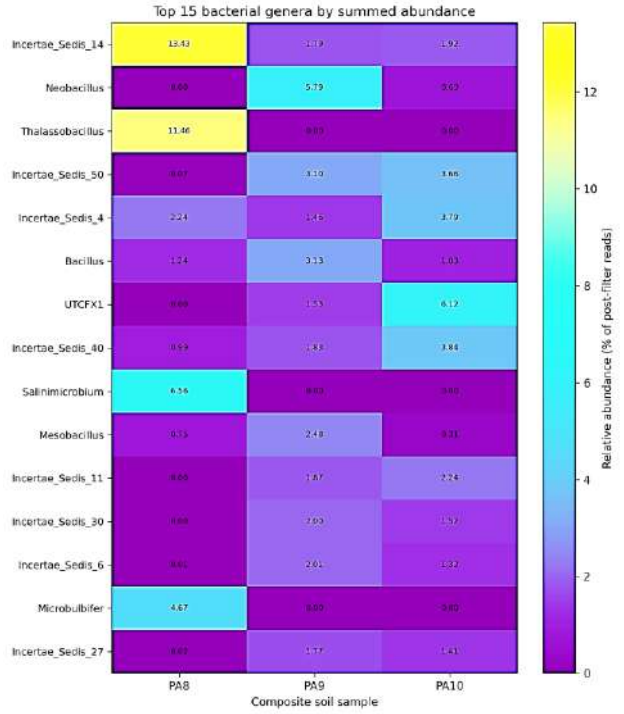

Fig. 3: Heatmap of the 15 bacterial genera with the highest summed abundance across PA8, PA9, and PA10. Cell values represent within-sample relative abundance based on all post-taxonomic-filter reads; no z-score standardization or clustering was applied

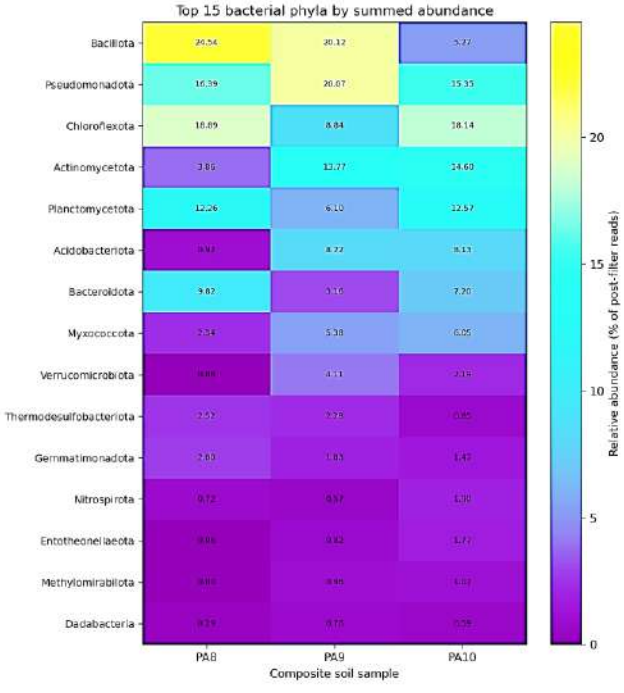

Fig. 4: Heatmap of the 15 bacterial phyla with the highest summed abundance across PA8, PA9, and PA10. Cell values represent within-sample relative abundance based on all post-taxonomic-filter reads; no z-score standardization or clustering was applied

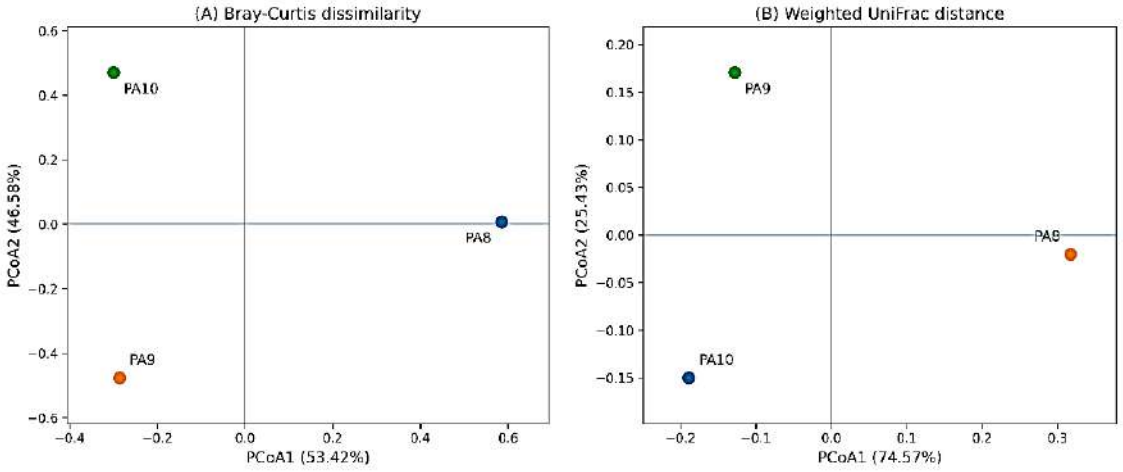

Fig. 5: Principal coordinate analysis (PCoA) of the three composite soil bacterial communities based on (A) Bray-Curtis dissimilarity and (B) Weighted UniFrac distance. Bray-Curtis PCoA1 and PCoA2 represent 53.42% and 46.58% of the displayed variation, whereas Weighted UniFrac PCoA1 and PCoA2 represent 74.57% and 25.43%, respectively. Each point represents one composite sequencing sample from PA8, PA9, or PA10. The ordinations are descriptive and do not represent replicated salinity treatments or inferential group comparisons

phylogenetically distinct lineages (Lozupone *et al.*, 2007; Lozupone and Knight, 2005). The greater phylogenetic dissimilarity of PA8 is consistent with its distinct taxonomic profile, including greater relative representation of Bacillota/Bacillales and several site-associated genera. Salinity serves as a key selective force influencing bacterial assemblage composition; however, the ubiquitous co-variance of field salinity gradients with auxiliary edaphic parameters limits the direct attribution of community shifts to salinity alone (Dong *et al.*, 2022; Rath *et al.*, 2019). In the present study, PA8 also differed in land use, exchangeable Na, CEC, and other measured and unmeasured environmental characteristics; its separation in ordination space is therefore interpreted as site-specific community differentiation rather than evidence of a salinity-driven treatment effect. Owing to the lack of replication (one composite sample per site), estimating within-condition variability was not feasible, thereby constraining the analytical design to descriptive comparisons in the absence of justifiable inferential testing (Anderson, 2001).

Predicted ecological functions of bacterial communities

FAPROTAX indicated distinct site-specific functional potentials related to carbon, nitrogen, and sulfur transformations (Table 5). Functional prediction indicated that Chemoheterotrophy constituted the primary metabolic pathway across the study sites (reaching 23.88% at PA10, 20.46% at PA8, and 16.97% at PA9), whereas proportional representation for aerobic chemoheterotrophy was maximized at PA9 and PA10. PA8 showed a particularly distinctive predicted profile, with substantially higher nitrate reduction (11.46%) and greater representation of aromatic-compound degradation, cellulolysis, xylanolysis, and chitinolysis relative to the alternative sites. Sulfate respiration was also more represented at PA8 and PA9 than at PA10. These contrasts are consistent with the different taxonomic compositions observed among the sites because FAPROTAX assigns ecological functions from taxonomic identities based on documented functions of cultured representatives rather than from direct measurements of functional genes or metabolic activity (Louca *et al.*, 2016; Sansupa *et al.*, 2021). The functional predictions should therefore be interpreted cautiously. Only 34.36%, 19.97%, and 26.07% of reads from PA8, PA9, and PA10, respectively, were assigned to at least one FAPROTAX category, indicating that substantial portions of the communities were outside the available functional annotations. Because predicted functional profiles derive directly from

Table 5: Selected FAPROTAX-predicted functional profiles expressed as percentage of post-taxonomic-filter reads

Predicted ecological function	PA8 (%)	PA9 (%)	PA10 (%)
Chemoheterotrophy	20.46	16.97	23.88
Aerobic chemoheterotrophy	3.98	8.41	7.86
Nitrate reduction	11.46	1.37	3.47
Aromatic compound degradation	5.22	1.70	0.62
Cellulolysis	4.68	0.29	0.19
Xylanolysis	4.67	0.03	0.00
Chitinolysis	4.67	0.01	0.00
Sulfate respiration	2.52	2.28	0.85
Fermentation	0.87	0.68	0.99
Methylotrophy	0.00	0.49	0.06
Methanotrophy	0.00	0.49	0.06
Ureolysis	0.00	0.31	0.39
Coverage: reads assigned to ≥1 FAPROTAX group	34.36	19.97	26.07

taxonomic assignments, they cannot substitute for direct measurements of gene abundance, metabolic expression, enzymatic kinetics, or in-situ biogeochemical turnover rates. This methodological constraint is supported by previous findings demonstrating that FAPROTAX generates valuable ecological hypotheses for soil bacterial communities yet may omit functions or taxa, and that predicted carbon-, nitrogen-, and sulfur-cycling assemblages do not invariably align with empirically quantified functional genes (Sansupa *et al.*, 2021; Yang *et al.*, 2022). Accordingly, the higher predicted nitrate reduction and organic-substrate degradation at PA8, and the contrasting carbon- and sulfur-related profiles at PA9 and PA10, are interpreted as site-associated functional hypotheses rather than evidence that EC or salinity altered biogeochemical process rates.

Ecological synthesis of site-specific patterns

Across the three sites, bacterial richness, Shannon diversity, taxonomic composition, phylogenetic dissimilarity, and predicted functional profiles did not form a simple monotonic sequence with EC. PA8, the highest-EC and highest-Na concentrations, exhibited the lowest observed ASV richness and Shannon diversity alongside a distinct taxonomic and Weighted UniFrac profile. In contrast, site PA9, with intermediate EC, displayed the highest observed richness and diversity, whereas site PA10, with the lowest EC, showed intermediate richness paired with a divergent phylum-, order-, and genus-level configuration. This non-monotonic pattern is ecologically plausible because salinity can exert strong environmental filtering on soil microbial communities, while its effects on richness, community composition, and assembly may vary among soil environments and interact with other edaphic factors (Dong *et al.*, 2022; Zhang *et al.*, 2019). In addition, broader edaphic analyses show that soil microbial assemblages are governed by multivariate interactions involving salinity, pH, and organic carbon, with the relative importance of individual drivers contingent upon depth and local environmental conditions (Xie *et al.*, 2017). Several mechanisms could therefore plausibly contribute to the contrasts observed among PA8, PA9, and PA10, including osmotic and ionic filtering, differences in carbon and nutrient availability, pH and cation balance, soil physicochemical conditions, and land-use or management history (Dong *et al.*, 2024; Lee *et al.*, 2020; Zhang *et al.*, 2019). In parallel, recent metagenomic findings highlight that microbial adaptation to salinity is mediated by clade-specific physiological constraints and metabolic interactions involving carbon assimilation, underscoring the ecological complexity and context-dependency of these community-level shifts (Dong *et al.*, 2024). However, these environmental properties varied simultaneously with site identity in the present study, and each EC condition was represented by only one composite sequencing sample. Consequently, the relative contribution of EC, Na-related chemistry, carbon

availability, pH, land use, or other unmeasured environmental factors cannot be separated or ranked from the present dataset. Consequently, these findings are interpreted as hypothesis-generating evidence of site-specific bacterial ecological organization under contrasting environmental conditions rather than as definitive proof of a direct salinity-driven functional response.

Study limitations

Attribution to salinity is limited by the observational design. PA8, PA9, and PA10 are three geographically distinct sites, and EC covaried with organic C, exchangeable Na, CEC, land use, texture, and other measured or unmeasured properties. For example, PA8 had EC of 13.68 dS/m, organic C of 1.01%, exchangeable Na of 30.71 cmol(+)/kg, and CEC of 12.83 cmol(+)/kg. PA9 had corresponding values of 3.74 dS/m, 0.62%, 4.15 cmol(+)/kg, and 22.02 cmol(+)/kg. PA10 had values of 0.50 dS/m, 1.45%, 4.84 cmol(+)/kg, and 28.41 cmol(+)/kg. The limited sample size of three site-level observations precludes the statistical partitioning or adjustment required to isolate an independent effect of salinity from co-varying environmental factors. The observed bacterial differences are therefore interpreted as site-specific associations rather than salinity effects. The composite-sampling design improves spatial coverage within each sampled site but does not provide biological replication. Each sequencing sample pooled soil from five field points within a site. The physical pooling and homogenization of component points precluded independent sequencing, thereby preventing the quantification or retention of fine-scale spatial heterogeneity within the final dataset. Ecological significance is therefore restricted to a descriptive snapshot of the pooled bacterial community at each site at the time of sampling. The observed contrasts are useful for identifying candidate taxa, diversity patterns, and community-distance profiles for future testing, but they do not establish a population-level response for an EC condition. Furthermore, the lack of independent biological replication prevents formal statistical evaluation of salinity-driven community responses. Within-condition variance, standard errors, confidence intervals, and a treatment-level error term cannot be estimated from one composite sequencing observation per EC condition. Accordingly, group-level inferential tests, analysis of variance, and regression of microbial metrics against EC were not used to infer a salinity effect. PCoA, alpha-diversity values, relative-abundance profiles, and FAPROTAX outputs are presented descriptively only. The findings cannot be generalized to high-, intermediate-, or low-EC soil classes beyond the sampled sites. Further methodological constraints stem from the incomplete documentation of historical management practices, including irrigation regimes, fertilization protocols, drainage infrastructure, and prior land-use history. Laboratory gravimetric moisture was measured and is reported in Table 1; however, in-situ field soil moisture and soil temperature were not recorded. Moreover, 16S rRNA amplicon sequencing provides compositional relative-abundance data rather than absolute population sizes. TPC represents only culturable bacteria under the applied culture conditions, species-level assignments remain uncertain for many taxa, and FAPROTAX outputs are predictions rather than direct functional measurements. Collectively, these methodological constraints constrain causal and regional extrapolation, positioning the present findings as a site-specific, hypothesis-generating baseline.

CONCLUSION

Distinct variations in bacterial communities across high-, moderate- and low-salinity conditions were found in the saline agricultural soils located at time of sampling. High-salinity soil yielded peak values for EC and sodium saturation coupled with depressed organic carbon, minimal richness and Shannon diversity, a singular

taxonomic configuration, and distinct spatial ordination patterns. These distinctive ecoevolutionary patterns suggests that salinity and sodium accumulation acted as potent ecological filters limiting community breadth, while favoring the establishment of high-salt-tolerating bacterial taxa. Bacterial diversity, however, did not exhibit a linear decline relative to salinity gradient. Moderate soil salinity corresponded with peak richness and Shannon diversity, coinciding with elevated organic carbon content and cation exchange capacity. This pattern aligns with eco-evolutionary theory, suggesting that organic carbon availability partially buffers estuarine bacteria against salt stress, whereas high-salinity soils may experience a shift in which key metabolic generalists are supplanted by specialized, stress-tolerant taxa. The distinction between the samples from low-salinity soil and the other groups due to their bacterial profile was less in proximity with, also based on tick richness estimated by pneumonic acid as well as culturable bacteria abundance, suggesting a differential response of the indicators of bacterium exposure to conditions in which they thrive during analysis. Taxonomic composition underwent marked structural shifts along the salinity gradient. Bacillota and Bacillales were the primary phyla in the high-salinity soil, accompanied by salt-associated genera (*Thalassobacillus, Salinimicrobium* and *Microbulbifer*). Conversely, low-salinity soil exhibited a higher relative abundance of Chloroflexota, Anaerolineales and several uncultured indigenous bacterial lineages. These changes illustrate that salinity affected bacterial diversity, as well as the identity and relative dominance of taxa at multiple taxonomic levels. Collectively, ordination frameworks demonstrated that spatial variation in bacterial assemblages reflected multivariate edaphic interactions rather than a direct, singular response to soil salinity gradients. The high-salinity condition was most closely related to EC, exchangeable sodium percentage and exchangeable sodium and had negative loadings relative to most bacterial diversity attributes in the ordination space. The bacterial assemblages documented under moderate and low salinity exhibited stronger associations with organic carbon resources, alleviated salt constraints, and ionic homeostasis. These relationships underpin a multivariate understanding of how bacterial communities respond to saline soil environments. Functional prediction revealed potential role of indigenous bacterial communities in chemoheterotrophic carbon utilization, sulfur transformation, nitrogen cycling, fermentation and complex organic compounds degradation. These functional assignments reflect estimated ecological potential rather than direct measurements of empirical gene expression, enzymatic activity, or biogeochemical process rates. According to this assessment, the response of bacteria to salinity is thus linear on a bacterial richness scale and driven by salt concentration, sodium enrichment, organic carbon content and the soil cation balance. Moreover, indigenous bacterial communities not only serve as bioindicators of saline-soil conditions, but also represent potential microbial resources for bio-remediation and soil recovery under elevated salinity. However, functional gene analysis and direct measurements of microbial activity are required to confirm these predicted ecological roles.

AUTHOR CONTRIBUTIONS

L. Fauziah designed and formulated this study, conducted field sampling, analyzed the data, interpreted the results, and prepared the draft manuscript. N. Aini supervised this study, provided methodological guidance, participated in data interpretation, and critically reviewed the manuscript. Y. Nuraini contributed by supervising this study, providing methodological guidance, participating in data interpretation, and critically reviewing the manuscript. Soemarno contributed

to data interpretation and critically reviewed the manuscript. N.D. Lestari contributed to data interpretation and critically reviewed the manuscript. Djajadi also contributed to data interpretation and critically reviewed the manuscript. All authors have read and approved the final version of this manuscript.

ACKNOWLEDGEMENT

The authors gratefully acknowledge financial support from the Professor Grant Program of Universitas Brawijaya for the 2025 fiscal year. The support was provided under contract number [08254.6/UN.10.F0401/B/KS/2025]. The authors also acknowledge the National Research and Innovation Agency of the Republic of Indonesia for institutional support during this research. Appreciation is extended to the laboratory staff and field assistants for their technical assistance with soil sampling, microbial isolation, and molecular analysis.

CONFLICT OF INTEREST

The authors declare that there is no conflict of interest regarding the publication of this manuscript. In addition, all relevant ethical requirements were observed by the authors. These include plagiarism, informed consent, misconduct, data fabrication and/or falsification, double publication and/or submission, and redundancy.

OPEN ACCESS

©2027 The author(s). This article is licensed under a Creative Commons Attribution 4.0 International License, which permits use, sharing, adaptation, distribution and reproduction in any medium or format, as long as you give appropriate credit to the original author(s) and the source, provide a link to the Creative Commons license, and indicate if changes were made. The images or other third-party material in this article are included in the article's Creative Commons license, unless indicated otherwise in a credit line to the material. If material is not included in the article's Creative Commons license and your intended use is not permitted by statutory regulation or exceeds the permitted use, you will need to obtain permission directly from the copyright holder. To view a copy of this license, visit: http://creativecommons.org/licenses/by/4.0/

PUBLISHER'S NOTE

GJESM Publisher remains neutral with regard to jurisdictional claims in published maps and institutional affiliations.

POSITIVE AI STATEMENT

During manuscript preparation, ChatGPT, an AI tool developed by OpenAI, was used for English-language editing and editorial assistance. This included grammatical correction, sentence restructuring, improved clarity and organization, and refinement of author-prepared scientific text. The tool was also used to improve the presentation of interpretations developed by the authors from the original data and analyses. ChatGPT was not used to generate, modify, fabricate, or replace experimental data, laboratory results, statistical outputs, or bioinformatic results. It was also not used to independently determine the study methodology or scientific conclusions. All AI-assisted suggestions were critically reviewed, verified against the original data and relevant literature, and revised by the authors. The authors retain full responsibility for the accuracy, integrity, and final content of this publication.

ABBREVIATIONS

%	Percent
°C	Degrees Celsius
16S rRNA	16S ribosomal ribonucleic acid
µmol/L	Micromolar per liter
AI	Artificial intelligence
ASV	Amplicon sequence variant
bp	Base pair
C	Carbon
Ca	Calcium

CEC	Cation exchange capacity
CFU	Colony-forming unit
cm	Centimeter
cmol(+)/kg	Centimoles of positive charge per kilogram of soil
DADA2	Divisive Amplicon Denoising Algorithm 2
DNA	Deoxyribonucleic acid
dS/m	Decisiemens per meter
E	East
EC	Electrical conductivity
ESP	Exchangeable sodium percentage
FAPROTAX	Functional Annotation of Prokaryotic Taxa
FastQC	FastQC sequence quality-control software
g	Gram
H_2O	Water
h	Hour
K	Potassium
kg	Kilogram
MAFFT	Multiple alignment using fast fourier transform
m	Meter
min	Minute
Mg	Magnesium
mL	Milliliter
mm	Millimeter
mol/L	Molar per liter
MultiQC	MultiQC quality-control reporting software
Na	Sodium
NaCl	Sodium chloride
NCBI	National Center for Biotechnology Information
nm	Nanometer
NH_4OAc	Ammonium acetate
P	Phosphorus
PA8	Highest-EC sampling site
PA9	Intermediate-EC sampling site
PA10	Lowest-EC sampling site
PCoA	Principal coordinate analysis
PCR	Polymerase chain reaction
pH	Potential of hydrogen
QIIME 2	Quantitative Insights Into Microbial Ecology 2
RNase A	Ribonuclease A
SILVA	SILVA ribosomal ribonucleic acid gene database
SMRT	Single-molecule real-time
S	South
SRA	Sequence Read Archive
TPC	Total plate count

REFERENCES

Anderson, M.J., (2001). A new method for non-parametric multivariate analysis of variance. Austral Ecol., 26(1): 32-46 **(15 pages)**.

Andrews, S., (2010). FastQC: a quality control tool for high throughput sequence data. Babraham Bioinformatics, Cambridge, UK.

Basak, N.; Rai, A.K.; Barman, A.; Mandal, S.; Sundha, P.; Bedwal, S.; Kumar, S.; Yadav, R.K.; Sharma, P.C., (2022). Salt affected soils: global perspectives. In: Salt affected soils: reclamation and management. Springer, Cham, Switzerland, 107-129 (**23 pages**).

Bokulich, N.A.; Kaehler, B.D.; Rideout, J.R.; Dillon, M.; Bolyen, E.; Knight, R.; Huttley, G.A.; Caporaso, J.G., (2018). Optimizing taxonomic classification of marker-gene amplicon sequences with QIIME 2's q2-feature-classifier plugin. Microbiome, 6(1): 90 (**17 pages**).

Bolyen, E.; Rideout, J.R.; Dillon, M.R.; Bokulich, N.A.; Abnet, C.C.; Al-Ghalith, G.A.; Alexander, H.; Alm, E.J.; Arumugam, M.; Asnicar, F.; Bai, Y.; Bisanz, J.E.; Bittinger, K.; Brejnrod, A.; Brislawn, C.J.; Brown, C.T.; Callahan, B.J.; Caraballo-Rodríguez, A.M.; Chase, J.; Cope, E.K.; Da Silva, R.; Diener, C.; Dorrestein, P.C.; Douglas, G.M.; Durall, D.M.; Duvallet, C.; Edwardson, C.F.; Ernst, M.; Estaki, M.; Fouquier, J.; Gauglitz, J.M.; Gibbons, S.M.; Gibson, D.L.; Gonzalez, A.; Gorlick, K.; Guo, J.; Hillmann, B.; Holmes, S.; Holste, H.; Huttenhower, C.; Huttley, G.A.; Janssen, S.; Jarmusch, A.K.; Jiang, L.; Kaehler, B.D.; Kang, K.B.; Keefe, C.R.; Keim, P.; Kelley, S.T.; Knights, D.; Koester, I.; Kosciolek, T.; Kreps, J.; Langille, M.G.I.; Lee, J.; Ley, R.; Liu, Y.X.; Loftfield, E.; Lozupone, C.; Maher, M.; Marotz, C.; Martin, B.D.; McDonald, D.; McIver, L.J.; Melnik, A.V.; Metcalf, J.L.; Morgan, S.C.; Morton, J.T.; Naimey, A.T.; Navas-Molina, J.A.; Nothias, L.F.; Orchanian, S.B.; Pearson, T.; Peoples, S.L.; Petras, D.; Preuss, M.L.; Pruesse, E.; Rasmussen, L.B.; Rivers, A.; Robeson, M.S.; Rosenthal, P.; Segata, N.; Shaffer, M.; Shiffer, A.; Sinha, R.; Song, S.J.; Spear, J.R.; Swafford, A.D.; Thompson, L.R.; Torres, P.J.; Trinh, P.; Tripathi, A.; Turnbaugh, P.J.; Ul-Hasan, S.; van der Hooft, J.J.J.; Vargas, F.; Vázquez-Baeza, Y.; Vogtmann, E.; von Hippel, M.; Walters, W.; Wan, Y.; Wang, M.; Warren, J.; Weber, K.C.; Williamson, C.H.D.; Willis, A.D.; Xu, Z.Z.; Zaneveld, J.R.; Zhang, Y.; Zhu, Q.; Knight, R.; Caporaso, J.G., (2019). Reproducible, interactive, scalable and extensible microbiome data science using QIIME 2. Nat. Biotechnol., 37(8): 852-857 **(6 pages)**.

Bray, J.R.; Curtis, J.T., (1957). An ordination of the upland forest communities of southern Wisconsin. Ecol. Monogr., 27(4): 325-349 (**25 pages**).

Callahan, B.J.; McMurdie, P.J.; Rosen, M.J.; Han, A.W.; Johnson, A.J.A.; Holmes, S.P., (2016). DADA2: high-resolution sample inference from Illumina amplicon data. Nat. Methods, 13(7): 581-583 (**3 pages**).

Callahan, B.J.; Wong, J.; Heiner, C.; Oh, S.; Theriot, C.M.; Gulati, A.S.; McGill, S.K.; Dougherty, M.K., (2019). High-throughput amplicon sequencing of the full-length 16S rRNA gene with single-nucleotide resolution. Nucleic Acids Res., 47(18): e103 (**12 pages**).

Canfora, L.; Bacci, G.; Pinzari, F.; Lo Papa, G.; Dazzi, C.; Benedetti, A., (2014). Salinity and bacterial diversity: to what extent does the concentration of salt affect the bacterial community in a saline soil? PLoS ONE, 9(9): e106662 (**15 pages**).

Carter, M.R.; Gregorich, E.G., (2008). Soil sampling and methods of analysis. 2nd ed. CRC Press, Boca Raton, USA (**1224 pages**).

Dong, Y.; Chen, R.; Graham, E.B.; Yu, B.; Bao, Y.; Li, X.; You, X.; Feng, Y., (2024). Eco-evolutionary strategies for relieving carbon limitation under salt stress differ across microbial clades. Nat. Commun., 15(1): 6013 (**12 pages**).

Dong, Y.; Zhang, J.; Chen, R.; Zhong, L.; Lin, X.; Feng, Y., (2022). Microbial community composition and activity in saline soils of coastal agro-ecosystems. Microorganisms, 10(4): 835 (**16 pages**).

Dreier, M.; Meola, M.; Berthoud, H.; Shani, N.; Wechsler, D.; Junier, P., (2022). High-throughput qPCR and 16S rRNA gene amplicon sequencing as complementary methods for the investigation of the cheese microbiota. BMC Microbiol., 22(1): 48 (**18 pages**).

Eviati; Sulaeman; Herawaty, L.; Anggria, L.; Usman; Tantika, H.E.; Prihatini, R.; Wuningrum, P., (2023). Petunjuk teknis edisi 3: Analisis kimia tanah, tanaman, air, dan pupuk. Kementerian Pertanian Republik Indonesia, Bogor, Indonesia (**271 pages**).

Ewels, P.; Magnusson, M.; Lundin, S.; Käller, M., (2016). MultiQC: summarize analysis results for multiple tools and samples in a single report. Bioinformatics, 32(19): 3047-3048 (**2 pages**).

Gower, J.C., (1966). Some distance properties of latent root and vector methods used in multivariate analysis. Biometrika, 53(3-4): 325-338 (**14 pages**).

Hailu, B.; Mehari, H., (2021). Impacts of soil salinity/sodicity on soil-water relations and plant growth in dry land areas: a review. J. Nat. Sci. Res., 12(3): 1-10 (**10 pages**).

Hindersah, R.; Pratiwi, E.; Fatma, Y.S.; Simarmata, T., (2023). Diversity and structure of bacterial communities in saline and non-saline rice fields in Cilacap Regency, Indonesia. Open Agric., 8(1): 20220225 (**11 pages**).

Janssen, P.H.; Yates, P.S.; Grinton, B.E.; Taylor, P.M.; Sait, M., (2002). Improved culturability of soil bacteria and isolation in pure culture of novel members of the divisions Acidobacteria, Actinobacteria, Proteobacteria, and Verrucomicrobia. Appl. Environ. Microbiol., 68(5): 2391-2396 (**6 pages**).

Johnson, J.S.; Spakowicz, D.J.; Hong, B.Y.; Petersen, L.M.; Demkowicz, P.; Chen, L.; Leopold, S.R.; Hanson, B.M.; Agresta, H.O.; Gerstein, M.; Sodergren, E.; Weinstock, G.M., (2019). Evaluation of 16S rRNA gene sequencing for species and strain-level microbiome analysis. Nat. Commun., 10(1): 5029 (**11 pages**).

Lee, S.A.; Kim, J.M.; Kim, Y.; Joa, J.H.; Kang, S.S.; Ahn, J.H.; Kim, M.; Song, J.; Weon, H.Y., (2020). Different types of agricultural land use drive distinct soil bacterial communities. Sci. Rep., 10(1): 17418 (**12 pages**).

Li, D.; Qiu, H.; Tian, G.; Zhao, Y.; Zhou, X.; He, S., (2023). Soil salinity is the main factor influencing the soil bacterial community assembly process under long-term drip irrigation in Xinjiang, China. Front. Microbiol., 14: 1291962 (**10 pages**).

Louca, S.; Parfrey, L.W.; Doebeli, M., (2016). Decoupling function and taxonomy in the global ocean microbiome. Science, 353(6305): 1272-1277 (**6 pages**).

Lozupone, C.; Knight, R., (2005). UniFrac: a new phylogenetic method for comparing microbial communities. Appl. Environ. Microbiol., 71(12): 8228-8235 (**8 pages**).

Lozupone, C.A.; Hamady, M.; Kelley, S.T.; Knight, R., (2007). Quantitative and qualitative beta diversity measures lead to different insights into factors that structure microbial communities. Appl. Environ. Microbiol., 73(5): 1576-1585 (**10 pages**).

Martin, M., (2011). Cutadapt removes adapter sequences from high-throughput sequencing reads. EMBnet.journal, 17(1): 10-12 **(3 pages)**.

Mucsi, M.; Borsodi, A.K.; Megyes, M.; Szili-Kovács, T., (2024). Response of the metabolic activity and taxonomic composition of bacterial communities to mosaically varying soil salinity and alkalinity. Sci. Rep., 14(1): 7460 (**15 pages**).

Nan, L.; Guo, Q.; Cao, S.; Zhan, Z., (2022). Diversity of bacterium communities in saline-alkali soil in arid regions of Northwest China. BMC Microbiol., 22(1): 11 (**12 pages**).

Pepper, I.L.; Gerba, C.P., (2015). Cultural methods. In: Pepper, I.L.; Gerba, C.P.; Gentry, T.J. (Eds.), Environmental microbiology. 3rd ed. Academic Press, San Diego, USA, 195-212 (**18 pages**).

Props, R.; Kerckhof, F.M.; Rubbens, P.; De Vrieze, J.; Hernandez Sanabria, E.; Waegeman, W.; Monsieurs, P.; Hammes, F.; Boon, N., (2017). Absolute quantification of microbial taxon abundances. ISME J., 11(2): 584-587 (**4 pages**).

Quast, C.; Pruesse, E.; Yilmaz, P.; Gerken, J.; Schweer, T.; Yarza, P.; Peplies, J.; Glöckner, F.O., (2012). The SILVA ribosomal RNA gene database project: improved data processing and web-based tools. Nucleic Acids Res., 41(D1): D590-D596 (**7 pages**).

Rath, K.M.; Fierer, N.; Murphy, D.V.; Rousk, J., (2019). Linking bacterial community composition to soil salinity along environmental gradients. ISME J., 13(3): 836-846 (**11 pages**).

Robeson II, M.S.; O'Rourke, D.R.; Kaehler, B.D.; Ziemski, M.; Dillon, M.R.; Foster, J.T.; Bokulich, N.A., (2021). RESCRIPt: reproducible sequence taxonomy reference database management. PLoS Comput. Biol., 17(11): e1009581 (**37 pages**).

Sansupa, C.; Wahdan, S.F.M.; Hossen, S.; Disayathanoowat, T.; Wubet, T.; Purahong, W., (2021). Can we use Functional Annotation of Prokaryotic Taxa (FAPROTAX) to assign the ecological functions of soil bacteria? Appl. Sci., 11(2): 688 (**17 pages**).

Schloss, P.D., (2024). Rarefaction is currently the best approach to control for uneven sequencing effort in amplicon sequence analyses. mSphere, 9(2): e00354-23 (**18 pages**).

Shannon, C.E., (1948). A mathematical theory of communication. Bell Syst. Tech. J., 27(3): 379-423 (**45 pages**).

Simpson, E.H., (1949). Measurement of diversity. Nature, 163(4148): 688 (**1 page**).

Sparks, D.L.; Page, A.L.; Helmke, P.A.; Loeppert, R.H.; Soltanpour, P.N.; Tabatabai, M.A.; Johnston, C.T.; Sumner, M.E., (1996). Methods of soil analysis. Part 3. Chemical methods. Soil Science Society of America, Madison, USA (**1390 pages**).

Straub, D.; Blackwell, N.; Langarica-Fuentes, A.; Peltzer, A.; Nahnsen, S.; Kleindienst, S., (2020). Interpretations of environmental microbial community studies are biased by the selected 16S rRNA (gene) amplicon sequencing pipeline. Front. Microbiol., 11: 550420 (**18 pages**).

Tarigan, R.; Lisnawita; Tantawi, A.R.; Hermanto, C., (2026). The impact of agroecological conditions on culturable bacterial and fungal diversity and soil chemical properties in chili pepper. Global J. Environ. Sci. Manage., 12(4): 2111-2132 **(22 pages).**

Tarolli, P.; Luo, J.; Park, E.; Barcaccia, G.; Masin, R., (2024). Soil salinization in agriculture: mitigation and adaptation strategies combining nature-based solutions and bioengineering. iScience, 27(2): 108830 (**8 pages**).

Tuesta-Popolizio, D.A.; Velázquez-Fernández, J.B.; Rodriguez-Campos, J.; Contreras-Ramos, S.M., (2021). Thalassobacillus, a genus of extreme to moderate environmental halophiles with biotechnological potential. World J. Microbiol. Biotechnol., 37(9): 147 (**13 pages**).

Utomo, B.; Dimyati, M.; Dewanti, R.; Trihatmoko, E.; Utami, P., (2026). Sustaining mangrove-based silvofishery to support coastal landscape resilience and explore ecotourism potential. Global J. Environ. Sci. Manage., 12(4): 1965-1988 **(24 pages).**

Walkley, A.; Black, I.A., (1934). An examination of the Degtjareff method for determining soil organic matter and a proposed modification of the chromic acid titration method. Soil Sci., 37(1): 29-38 (**10 pages**).

Wiegand, S.; Sobol, M.; Schnepp-Pesch, L.K.; Yan, G.; Iqbal, S.; Vollmers, J.; Müller, J.A.; Kaster, A.K., (2023). Taxonomic re-classification and expansion of the phylum Chloroflexota based on over 5000 genomes and metagenome-assembled genomes. Microorganisms, 11(10): 2612 (**19 pages**).

Xie, K.; Deng, Y.; Zhang, S.; Zhang, W.; Liu, J.; Xie, Y.; Zhang, X.; Huang, H., (2017). Prokaryotic community distribution along an ecological gradient of salinity in surface and subsurface saline soils. Sci. Rep., 7(1): 13332 (**10 pages**).

Yang, Z.; Peng, C.; Cao, H.; Song, J.; Gong, B.; Li, L.; Wang, L.; He, Y.; Liang, M.; Lin, J.; Lu, L., (2022). Microbial functional assemblages predicted by the FAPROTAX analysis are impacted by physicochemical properties, but C, N and S cycling genes are not in mangrove soil in the Beibu Gulf, China. Ecol. Indic., 139: 108887 (**15 pages**).

Yuliana, E.; Winata, A.; Setijorini, L.E.; Yani, D.E.; Fathani, M.H.; Djatmiko, W.A., (2026). Biodiversity-oriented criteria for measuring the effectiveness of mangrove ecosystem rehabilitation success. Global J. Environ. Sci. Manage., 12(4): 1619-1638 **(20 pages).**

Zhang, G.; Bai, J.; Zhai, Y.; Jia, J.; Zhao, Q.; Wang, W.; Hu, X., (2024). Microbial diversity and functions in saline soils: a review from a biogeochemical perspective. J. Adv. Res., 59: 129-140 (**12 pages**).

Zhang, K.; Shi, Y.; Cui, X.; Yue, P.; Li, K.; Liu, X.; Tripathi, B.M.; Chu, H., (2019). Salinity is a key determinant for soil microbial communities in a desert ecosystem. mSystems, 4(1): e00225-18 (**9 pages**).

Zhao, S.; Liu, J.J.; Banerjee, S.; Zhou, N.; Zhao, Z.Y.; Zhang, K.; Tian, C.Y., (2018). Soil pH is equally important as salinity in shaping bacterial communities in saline soils under halophytic vegetation. Sci. Rep., 8(1): 4550 (**11 pages**).

AUTHOR (S) BIOSKETCHES

Fauziah, L., Ph.D. Candidate, Postgraduate Program, Faculty of Agriculture, Brawijaya University, Jl. Veteran No. 10–11, Malang 65145, Indonesia; Researcher, Research Center for Estate Crops, Research Organization for Agriculture and Food, National Research and Innovation Agency of the Republic of Indonesia, Jl. Raya Jakarta–Bogor Km 46, Cibinong, Bogor 16911, Indonesia.
- Email: *lili025@brin.go.id*
- ORCID: 0000-0002-7515-574X
- Web of Science ResearcherID: QWC-1004-2026
- Scopus Author ID: 58157153600
- Homepage: https://simpeg.brin.go.id/admin/kepegawaian/pegawai/profilen

Nuraini, Y., Professor, Department of Soil Science, Faculty of Agriculture, Brawijaya University, Jl. Veteran No. 10–11, Malang 65145, Indonesia.
- Email: *ynuraini@ub.ac.id*
- ORCID: 0009-0002-3056-1135
- Web of Science ResearcherID: JLL-1344-2023
- Scopus Author ID: 56271859000
- Homepage: https://fbipk.ub.ac.id/profil-dosen/

Soemarno, Professor, Department of Soil Science, Faculty of Agriculture, Brawijaya University, Jl. Veteran No. 10–11, Malang 65145, Indonesia.
- Email: *smno@ub.ac.id*
- ORCID: 0000-0002-7058-6495
- Web of Science ResearcherID: JLL-7442-2023
- Scopus Author ID: 55876886500
- Homepage: https://fbipk.ub.ac.id/profil-dosen/

Lestari, N.D., Lecturer and Researcher, Department of Soil Science, Faculty of Agriculture, Brawijaya University, Jl. Veteran No. 10–11, Malang 65145, Indonesia.
- Email: *nd.lestari@ub.ac.id*
- ORCID: 0000-0002-0496-2819
- Web of Science ResearcherID: NA
- Scopus Author ID: 57205465015
- Homepage: https://fbipk.ub.ac.id/profil-dosen/

Djajadi, Professor and Researcher, Research Center for Estate Crops, Research Organization for Agriculture and Food, National Research and Innovation Agency of the Republic of Indonesia, Jl. Raya Jakarta–Bogor Km 46, Cibinong, Bogor 16911, Indonesia.
- Email: *djaj001@brin.go.id*
- ORCID: 0000-0003-0931-4519
- Web of Science ResearcherID: QWC-1160-2026
- Scopus Author ID: 55204846200
- Homepage: https://simpeg.brin.go.id/admin/kepegawaian/pegawai/profilen

Aini, N., Professor, Department of Agronomy, Faculty of Agriculture, Brawijaya University, Jl. Veteran No. 10–11, Malang 65145, Indonesia.
- Email: *nra-fp@ub.ac.id*
- ORCID: 0000-0002-5600-0443
- Web of Science ResearcherID: GPK-1954-2022
- Scopus Author ID: 57219657937
- Homepage: https://fbipk.ub.ac.id/profil-dosen/

HOW TO CITE THIS ARTICLE:
Fauziah, L.; Nuraini, Y.; Soemarno; Lestari, N.D.; Djajadi; Aini, N., (2027). Ecological diversity in soil properties and bacterial communities in tropical coastal areas with contrasting electrical conductivity. Global J. Environ. Sci. Manage., 13(1): 231-250.

DOI: 10.22034/gjesm.2027.01.11
URL: https://www.gjesm.net/article_735607.html

Global J. Environ. Sci. Manage. 13(1): 251-272, Winter 2027, Serial #49

Global Journal of Environmental Science and Management
(GJESM)

Homepage: https://www.gjesm.net/

Podcasts

ORIGINAL RESEARCH ARTICLE

Multivariate and index-based evaluation of long-term reclaimed wastewater quality and reuse suitability

E.R. Tarawneh

Civil and Environmental Engineering Department, Mutah University, Karak, Jordan

ARTICLE INFO

Article History:
Received 09 June 2026
Revised 12 August 2026
Accepted 15 September 2026

Keywords:
Index-based evaluation
Multivariate methods Positive matrix factorization
Reclaimed wastewater Source apportionment

DOI:10.22034.gjesm.2027.01.12

ABSTRACT

BACKGROUND AND OBJECTIVES: Reclaimed wastewater is important in water-scarce regions, but safe reuse requires sustained effluent quality. The study objectives were to evaluate the quality and reuse potential of effluent discharged from the Karak domestic wastewater treatment plant in Jordan over the 2016–2025 period. The investigation employed a comprehensive framework integrating regulatory standards, water quality indices, temporal trend evaluations, multivariate statistical techniques, and positive matrix factorization.

METHODS: Seventeen physicochemical and microbiological parameters were assessed against Jordanian Standard 893:2021. Water quality index and water pollution index were applied as supplementary screening tools, and parameter-contribution and sensitivity analyses evaluated the magnitude of influence exerted by specific variables and the underlying weighting framework. Linear trends were estimated from 30 campaigns using ordinary least-squares regression, reporting slope, coefficient of determination, and p-value; *Escherichia coli* was evaluated on the log10 scale. Principal component analysis, hierarchical cluster analysis, and Environmental Protection Agency Positive Matrix Factorization 5.0 characterized covariance, similarity, and stable effluent-quality profiles.

FINDINGS: Average parameter-level compliance ranged from 50 to 65 percent across reuse and discharge categories, with limitations from residual organic matter, suspended solids, nutrients, bicarbonate, phenol, fats, oils and grease, and *Escherichia coli*. Across all categories, water quality index values surpassed 100. Subsequent sensitivity evaluations revealed that *Escherichia coli* drove approximately 99.99 percent of the weighted index for Class D irrigation and groundwater recharge, whereas phenol dominated Classes B and C. Equal weighting reduced mean Class C water quality index below 100, confirming weighting sensitivity without changing the regulatory compliance conclusion. Water pollution index decomposition also showed dominant *Escherichia coli* influence. Significant decreasing linear trends occurred for biochemical oxygen demand, chemical oxygen demand, total dissolved solids, total suspended solids, total nitrogen, phosphate-phosphorus, chloride, and sodium adsorption ratio, whereas dissolved oxygen, phenol, and nitrate-nitrogen increased. Principal component analysis explained 89.54 percent of variance through four components, and positive matrix factorization resolved four stable profiles contributing 54.0, 20.3, 16.7, and 9.1 percent.

CONCLUSION: Index magnitudes were strongly affected by restrictive standards and dominant parameters, while temporal trends indicated directional change without establishing causal treatment mechanisms. Direct Jordanian Standard 893:2021 compliance should remain the primary basis for reuse decisions. Confirming underlying causal mechanisms or targeted treatment interventions necessitates higher-frequency monitoring protocols that encompass influent, hydraulic, operational, and source-specific metrics.

This is an open access article under the CC BY license (http://creativecommons.org/licenses/by/4.0/)

NUMBER OF REFERENCES	NUMBER OF FIGURES	NUMBER OF TABLES
50	3	9

*Corresponding Author:
Email: erat@mutah.edu.jo
Phone: +962 79 009 8490
ORCID: 0000-0003-4580-753X

Note: Discussion period for this manuscript open until March 01, 2027 on GJESM website at the “Show Article”.

INTRODUCTION

Jordan faces severe structural water scarcity driven by limited renewable resources, irregular rainfall, demographic pressure, refugee influxes, climate change, and long-term stress on groundwater and surface-water systems. Renewable freshwater availability has fallen to approximately 61 cubic meters (m^3) per capita per year, while rainfall was about 39.5 percent (%) below the long-term average, according to the Ministry of Water and Irrigation (MWI, 2024, 2025b). During 2025, national water allocations relied on groundwater, surface water, and treated wastewater for approximately 58%, 26%, and 16% of demand, respectively. Total utilization reached approximately 1189 million cubic meters (MCM), exceeding the estimated aggregate availability of 1088.25 (MWI, 2025a, 2025b). This persistent deficit increases the strategic importance of reclaimed domestic wastewater. National policy promotes treated wastewater reuse to reduce freshwater demand and support irrigation and industry (Ammary, 2007; Rosas Baños and García Salazar, 2026). Jordan operated 29 wastewater treatment plants in 2025, with about 233 MCM per year design capacity and 214.4 MCM of treated wastewater production (MWI, 2025b). During 2021, approximately 167 of 186 MCM generated was reclaimed and redirected predominantly toward agricultural irrigation in the Jordan Valley subsequent to freshwater blending (MWI, 2023). Effluent reuse serves to substitute freshwater resources, facilitate aquifer recovery, and boost overall resource productivity (Fardous and Al-Hadidi, 2007); furthermore, under controlled quality parameters, wastewater-derived nutrients can substantially lower conventional fertilizer demands (Kalavrouziotis *et al.,* 2023; Ofori *et al.,* 2021). Safe reuse nevertheless depends on sustained effluent quality. Residual organic matter, suspended solids, nutrients, salts, pathogens, and trace contaminants may constrain reuse and threaten soils, crops, surface water, groundwater, and public health (Al-Hazmi *et al.,* 2023; Ukoha-Onuoha and Horsfall, 2026). In Jordan, salinity, chloride, soil properties, sodium adsorption ratio, and crop sensitivity are recognized irrigation constraints (Al-hasanat *et al.,* 2025), and variable treatment performance can undermine compliance with physicochemical and microbiological standards (Ait-Mouheb *et al.,* 2018; Breulmann *et al.,* 2019; Moghaddam *et al.,* 2017). Furthermore, additional pollutant inputs can originate from domestic effluents, unauthorized industrial discharges, stormwater intrusion, septic systems, agricultural return flows, and urban runoff (De Gisi *et al.,* 2017), directly compromising receiving-water quality and the safety of reclaimed water reuse (Dharmadhikari *et al.,* 2023). Integrated monitoring is therefore required to diagnose deterioration and guide wastewater treatment plant (WWTP) management (Nayak and Panda, 2026). Due to the temporal variability inherent in water-quality monitoring metrics, evaluating discrete regulatory parameters in isolation presents significant challenges for environmental synthesis and decision-making (Gupta and Gupta, 2021; Moeinzadeh *et al.,* 2024). Water-quality indices condense multidimensional datasets into standardized scores that streamline classification, comparative evaluation, longitudinal trend analysis, and risk communication (Rana and Ganguly, 2020). Consequently, such frameworks have become central to the assessment of drinking water supplies, irrigation systems, surface waters, groundwater reserves, and wastewater effluents (Abbasi and Abbasi, 2012; Yan *et al.,* 2022; Manna and Biswas, 2023; Patel *et al.,* 2023; Anyango *et al.,* 2024). Wastewater-specific applications include modified wastewater reuse index (WRI) for Jordan (Alfarra *et al.,* 2011), the wastewater polishing index (Verlicchi *et al.,* 2011), and wastewater quality index (WWQI)-based evaluations for agricultural reuse or disposal in Iran, Algeria, Egypt, and Jordan (Jamshidzadeh and Tavangari Barzi , 2020;

Bessedik *et al.,* 2021; Ayoub and El-Morsy, 2021; Alihosseini *et al.,* 2020; Abualhaija, 2023). Index-based assessment can also be strengthened by multivariate and source-apportionment methods, which help identify the processes underlying poor index scores (Chidiac *et al.,* 2023; Kachroud *et al.,* 2019). While extant literature largely emphasizes broad WWQI classification or single-plant assessments, the integration of water quality index (WQI) and water pollution index (WPI) with multivariate statistics and receptor-based source apportionment remains notably scarce. No published study was identified that applies this integrated framework to Karak domestic wastewater treatment plant (DWWTP). The resulting evidence gap is important because reuse decisions in this water-scarce setting require simultaneous evaluation of effluent quality, temporal variability, pollution status, and controlling processes. Combining index-based assessment with multivariate and source-apportionment techniques provides a stronger basis for reuse evaluation, treatment-performance diagnosis, and environmental decision-making. Prior applications of wastewater indices highlight the effectiveness of integrated frameworks in assessing treated effluent quality, determining reuse viability, and monitoring compliance with discharge mandates (Alfarra *et al.,* 2011; Verlicchi *et al.,* 2011; Bessedik *et al.,* 2021; Ayoub and El-Morsy, 2021; Alihosseini *et al.,* 2020). This study aims to evaluate the suitability of effluent from the Karak DWWTP for reliable and sustainable water reuse using an integrated methodological framework. Specifically, the study framework integrates the WQI and WPI for effluent classification;; principal component analysis (PCA) to isolate key variables and latent pollution structures; hierarchical cluster analysis (HCA) to group quality profiles; and positive matrix factorization (PMF) for source apportionment and identification of underlying controlling factors. This study was conducted at the Karak DWWTP, located in Wadi Al-Karak, Karak, Jordan, over a ten-year monitoring during 2016 to 2025.

MATERIALS AND METHODS

The study area

Karak DWWTP is in Wadi Al-Karak, Karak, southern Jordan, about 120 kilometers (km) south of Amman, and serves Karak city and surrounding districts with a total population of about 40,232 according to the Department of Statistics (DOS, 2026). Originally commissioned in 1988 as a trickling-filter system, the facility was retrofitted in 2018 with a mechanical activated-sludge process while maintaining a baseline design capacity of 800 cubic meters per day (m^3/d) (MWI, 2023). Actual flows subsequently reached about 1,000–1,200 m^3/d, with annual treated discharge estimated at 419,750 cubic meters per year (m^3/y) (approximately 1,150 m^3/d), indicating hydraulic loading above design capacity (MWI, 2023). Final effluent is discharged to Wadi Al-Karak and supports planned and informal reuse. A 9-km pipeline conveys part of the effluent to the Al-Rasees agricultural project for forest-tree irrigation, while local farmers irrigate lemon, olive, fodder maize, alfalfa, and barley. Approximately 496.48 dunums equivalent to approximately 49.65 hectare (ha) are irrigated under 13 formal agreements reported by MWI (2023). The residual effluent is directed toward the Wadi Al-Karak Dam, which possesses a nominal design storage capacity of approximately 2MCM, subsequently supporting regional irrigation networks and groundwater recharge initiatives (MWI, 2025a). The plant therefore forms an important component of the local non-conventional water-resource system.

Wastewater sampling and chemical analysis

Treated domestic wastewater effluent from the Karak DWWTP was monitored over a ten-year period from 2016 to 2025. Samples were collected from the final-effluent discharge point at four-month intervals, translating to three distinct sampling campaigns annually yielding a cumulative total of 30 campaign-level observations. During each campaign, three independent grab samples were obtained from

the WWTP outlet; with the final value for each parameter established as the arithmetic mean of triplicate measurements. The overall precision of the triplicate measurements, expressed as relative standard deviation (RSD), was generally ≤5% for most parameters. Sampling, preservation, transportation and laboratory analysis followed standard methods (Baird *et al.,* 2017). Samples were transported under cooled conditions and stored at 4 degrees Celsius (°C) until analysis. Seventeen physicochemical and microbiological parameters were monitored, including potential of hydrogen (pH), dissolved oxygen (DO), five-day biochemical oxygen demand (BOD_5), chemical oxygen demand (COD), total dissolved solids (TDS), total suspended solids (TSS), fats, oils and grease (FOG), methylene blue active substances (MBAS), nitrate-nitrogen (NO_3-N), total nitrogen (T-N), phosphate-phosphorus (PO_4-P), chloride (Cl), bicarbonate (HCO_3), sodium adsorption ratio (SAR), *Escherichia coli* (*E. coli*), and intestinal pathogenic nematode eggs (IPN). The dataset was supplied by Jordan's Ministry of Environment under the National Water Quality Monitoring Project. A summary of the monitored parameters, analytical units, and corresponding analytical methods is presented in Table 1. Due to a temporal resolution constrained to three campaigns annually, the monitoring record is suited for evaluating long-term trends rather than resolving seasonal, short-term hydraulic fluctuations or episodic operational events. The treatment system changed from trickling filters to mechanically operated activated sludge in 2018. Due to limited pre-conversion observations and a lack of matched operational records, temporal patterns observed between 2016–2025 are presented descriptively rather than explicitly linked to the facility modification.

Calculation of the water quality index

The WQI was used as a supplementary screening indicator to summarize multi-parameter effluent quality relative to the applicable Jordanian Standard (JS) 893:2021 reuse/discharge category. Within each category, calculations incorporated exclusively those parameters for which JS 893: 2021 mandates an applicable numerical limit or range, while parameters lacking defined limits were excluded from both the category aggregate and its denominator. The Jordanian permissible limits (JS 893:2021) for reclaimed domestic wastewater according to reuse category are presented in Table 2. The WQI was calculated using Eq. 1 (Brown *et al.,* 1972). Because the applied WQI methodology was not specifically developed as a reclaimed-wastewater risk-assessment framework, the resulting index values are interpreted as comparative screening indicators and not as a replacement for direct regulatory compliance assessment.

$$QI = \sum_{i=1}^{n} \frac{Wi \times Qi}{\sum_{i=1}^{n} Wi} \quad (1)$$

Where: Wi denotes the unit weight of the ith parameter, Qi denotes the water quality rating of the ith parameter, and (n) denotes the number of the involved parameters in the calculation. The water quality rating (Qi) was calculated, using Eq. 2 (Brown *et al.,* 1972):

$$Qi = 100 \times \left[\frac{(Vi - Vid)}{(Si - Vid)}\right] \quad (2)$$

Where: Vi is the measured value of the ith parameter, Vid is the reference or ideal value used in the WQI calculation, and Si is the applicable JS 893:2021 limit for the intended use. In the calculations that generated the reported WQI series, Vid was 0 for non-pH parameters and 7.5 for pH. Because this methodological convention lacks wastewater-specific calibration, posing interpretive challenges for parameters such as dissolved oxygen; therefore, WQI magnitude is evaluated conservatively, absolute index values are decoupled from health-risk implications, and direct parameter-by-parameter compliance remains the primary reuse criterion for water reuse. Wi is inversely proportional to Si, using Eq. 3 (Brown *et al.,* 1972):

Table 1: Monitored parameters, analytical units, and corresponding analytical methods

Parameter	Unit	Reference method (Ayres *et al.,* 1996; HACH, 2006; Baird *et al.,* 2017)	Method
pH	Standard units (SU)	SM 4500-H^+ B, 2017	Electrometric method
DO	Milligram per liter (mg/L)	HACH Method 10360 (HACH, 2006)	Luminescence measurement of dissolved oxygen (LDO) in water and wastewater
BOD_5	mg/L	SM 5210-B, 2017	5-day biochemical oxygen demand test
COD	mg/L	SM 5220-B, 2017	Open reflux method
TDS	mg/L	SM 2540-C, 2017	Total dissolved solids dried at 180 °C
TSS	mg/L	SM 2540-D, 2017	Total suspended solids dried at 103–105°C
FOG	mg/L	SM 5520-B, 2017	Liquid-Liquid, Partition- Gravimetric Method
Phenol	mg/L	SM 5530-C, 2017	Chloroform extraction method
MBAS	mg/L	SM 5540-C, 2017	Anionic surfactants as MBAS
NO_3 – N	mg/L	SM 4110-B, 2017	Ion chromatography with chemical suppression of eluent conductivity
T-N	mg/L	Calculation	-
PO4-P	mg/L	SM 4500-P, C, 2017	Vanadomolybdophosphoric acid colorimetric method
Cl	mg/L	SM 4500-Cl, D, 2017	Potentiometric method
HCO3	mg/L	SM 2320-B, 2017	Titration method
SAR	Unitless	Calculation	-
E. coli	Most probable number (MPN) 100/mL	SM 9221-F, 2017	*Escherichia coli* procedure using fluorogenic substrate
IPN	Eggs/L	Modified Bailenger Method, World Health Organization (WHO) report 1996	Modified Bailenger Method

$$Wi = \frac{K}{Si} \quad (3)$$

Where: K is the constant of proportionality and is computed, using Eq. 4 (Brown *et al.,* 1972):

$$\mathrm{K} = \frac{1}{\sum \frac{1}{\mathrm{Si}}} \quad (4)$$

Water quality is classified into five categories based on WQI values: Excellent water quality (WQI value 0- 25), Good water quality (WQI value 26-50), Poor water quality (WQI value 51-75), Very poor water quality (WQI value 76-100), Unsuitable for the intended use (WQI value >100), where the lower the WQI value, the better the water quality, and the higher the WQI value, the poorer the water (Brown *et al.,* 1972; Tyagi *et al.,* 2013; Kachroud *et al.,* 2019).

Calculation of the water pollution index

Additionally, the WPI served as a supplementary screening tool, standardizing observed concentrations against applicable regulatory thresholds and aggregating the resulting pollution loads free of subjective weights (Hossain and Patra, 2020; Syeed *et al.,* 2023). As for WQI, each reuse/discharge category used only parameters with an applicable JS 893:2021 limit; non-applicable parameters were omitted from that category-specific calculation and denominator, as documented in Table 2. The WPI was calculated using Eq. 5 (Hossain and Patra, 2020). Regulatory compliance with individual critical parameters, particularly microbiological limits, served as the primary decision criterion, as composite index scores can obscure the disparate environmental and public health consequences of different exceedances across healthcare facilities and geographic regions under varying regulatory conditions.

$$\mathrm{WPI} = \frac{1}{\mathrm{n}} \sum_{\mathrm{i}=1}^{\mathrm{n}} \mathrm{PLi} \quad (5)$$

Where: Pli is the pollution load of the ith parameter; (n) represents the number of all parameters. The calculation of the pollution load (PLi) was performed using Eq. 6 (Hossain and Patra, 2020):

Table 2: Jordanian permissible limits (JS 893:2021) for reclaimed domestic wastewater according to reuse category

Parameter	Unit	artificial recharge of groundwater aquifers	discharge into streams, wadies and water bodies	Irrigation reuse-Class A	Irrigation reuse-Class B	Irrigation reuse-Class C	Irrigation reuse-Class D
pH	SU	6-9	6-9	6-9	6-9	6-9	1 or…6-9
DO	mg/L	>2	>1	>2	-	-	>2
BOD_5	mg/L	15	60	30	100	200	15
COD	mg/L	50	150	100	200	300	50
TDS	mg/L	1500	1500	1500	1500	1500	1500
TSS	mg/L	50	60	50	100	100	15
FOG	mg/L	8	8	8	8	8	2
Phenol	mg/L	0.02	0.02	0.02	0.02	0.02	0.02
MBAS	mg/L	25	25	100	100	100	15
NO_3-N	mg/L	7	20	16	16	16	16
T-N	mg/L	20	70	70	70	70	70
PO_4-P	mg/L	5	5	10	10	10	10
Cl	mg/L	350	500	500	500	500	500
HCO_3	mg/L	400	400	400	400	400	400
SAR	Unitless	6	6	9	9	9	9
E. coli	MPN 100/mL	1.1	1000	100	1000	-	1.1
IPN	Eggs/L	≤1	≤1	≤1	≤1	≤1	≤1

Note: "-'' indicates that no permissible limit was specified
pH is checked within range; DO is checked as a minimum; other numeric parameters are checked as maximum limits
Class A: parks, playgrounds, and sides of roads inside the cities
Class B: fruit trees, sides of roads outside the cities, and green areas
Class C: field crops, industrial crops, and forest trees
Class D: cut flowers

$$PLi = 1 + \left(\frac{Ci - Si}{Si}\right) \quad (6)$$

Where: Ci is the laboratory-analyzed concentration of the ith parameter, Si denotes each Jordanian parameter's standard or maximum acceptable limit. The calculation of PLi for the pH parameter is based on the pH value, using Eqs. 7 and 8 (Hossain and Patra, 2020):

$$\mathrm{PLi} = \frac{\mathrm{Ci\text{-}7}}{\mathrm{Sia\text{-}7}} \text{ , If the pH < 7} \quad (7)$$

$$\mathrm{PLi} = \frac{\mathrm{Ci\text{-}7}}{\mathrm{Sib\text{-}7}} \text{ , If the pH > 7} \quad (8)$$

Where: Si_a denotes the lowest permissible pH value for the intended use, Si_b denotes the highest allowable pH value for the intended use.

The classifications of water quality based on WPI results are divided into four categories: excellent water quality (WPI value < 0.5), good water quality (WPI value 0.5-0.75), moderately polluted water (WPI value 0.75-1), and highly polluted water (WPI value >1) (Hossain and Patra, 2020). Parameter-contribution and sensitivity analyses were executed utilizing the identical annual category-specific standards and parameter configurations applied for the reported indices. For WQI, parameter leverage was quantified as the fixed weighted-term contribution, 100(WiQi)/Σ(WjQj), aggregated over the 2016–2025 annual calculations. A leave-one-parameter-out calculation was used for selected dominant terms, with K renormalized after omission, and an equal-weight WQI (arithmetic mean of Qi across applicable parameters) was calculated to test dependence on the inverse-standard weighting scheme. For WPI, individual parameter contributions were determined as 100PLi/ΣPLj, and WPI was subsequently re-evaluated excluding *E. coli* instances where applicable standard applied. These sensitivity calculations quantify mathematical leverage within the indices and are not interpreted as causal pollutant-source apportionment. Ordinary least-squares regression was applied to evaluate linear temporal trends spanning 2016–2025, utilizing the 30

campaign-level observations across each of the 16 quantitative parameters retained within the multivariate dataset. Time was represented as decimal year according to the actual routine sampling months (January = year, May = year + 4/12, and September = year + 8/12), so the regression slope represents the average change per year. For each parameter, the slope, coefficient of determination (R^2), and two-sided p-value for the slope were reported. *E. coli* was analyzed on the base-10 logarithmic (log_{10}) scale because of its several-order-of-magnitude range; all other parameters were analyzed on their measured scales. The regressions quantify monotonic temporal association across the entire record rather than serving as indicators of seasonal dynamics, intervention outcomes, or causal treatment-process responses. Because 16 parallel regressions were evaluated, nominal p-values are presented transparently and interpreted strictly as exploratory evidence.

Multivariate statistical analysis

Principal component analysis

PCA was applied to the 30 campaign-level observations and 16 variables retained after exclusion of IPN (pH, DO, BOD_5(f), COD, TDS, TSS, FOG, phenol, MBAS, NO_3–N, T-N, PO_4–P, Cl^-, HCO_3^-, SAR and *E. coli*). Variables were standardized and PCA was performed on the correlation matrix. The Kaiser-Meyer-Olkin (KMO) value was 0.82 and Bartlett's test was significant ($\chi^2 = 1052.18$, degrees of freedom (df) = 120, $p < 0.001$), indicating that the observed correlation structure was suitable for dimension reduction; these tests do not, however, remove the limitation of the low observation-to-variable ratio (30:16). Consequently, PCA is applied as an exploratory pattern recognition technique rather than as a definitive or broadly generalizable latent-process model. Components with eigenvalues >1 were retained and varimax rotation was used to aid interpretation. Seasonal, causal, and pre- or post-upgrade inferences were intentionally excluded from the PCA interpretation, as data were restricted to three annual campaigns and lacked paired process or operational available. Analyses were conducted using International Business Machines (IBM) Statistical Package for the Social Sciences (SPSS) Statistics version 26.

Hierarchical cluster analysis

HCA was used as a complementary description of similarity among the same 16 standardized effluent-quality variables. Agglomerative hierarchical clustering was performed using squared Euclidean distance and Ward's minimum-variance linkage, with the resulting dendrogram evaluated for coherent variable groupings. Because HCA and PCA were derived from the same 30 × 16 dataset, HCA is not construed as an independent validation of PCA nor as conclusive evidence of causal pollutant sources. Its added value is descriptive, illustrating which variables merge at shorter linkage distances and indicating whether covariance groupings align broadly consistent with the PCA structure. Note that IPN was excluded due to its non-detection across all analyzed samples.

Positive matrix factorization

PMF was applied as an exploratory receptor-model analysis to resolve non-negative statistical factor profiles in the final-effluent dataset. U.S. Environmental Protection Agency (EPA) PMF 5.0 decomposes the observed concentration matrix into factor-contribution and factor-profile matrices while weighting observations by uncertainty (Paatero and Tapper, 1994; Norris *et al.,* 2014). The input matrix incorporated the identical 16 final-effluent variables utilized in the multivariate analyses; with IPN excluded due to its non-detection across the samples. Importantly, the analysis did not include influent concentrations, source fingerprints, process-unit samples, hydraulic/operational records, rainfall, sludge characteristics or disinfection data. Consequently, the extracted factors are interpreted strictly as statistical profiles or potential process-associated patterns rather than

verified external pollutant sources or established treatment mechanisms. The measured matrix X was decomposed into G and F under non-negativity constraints using Eq. 9 (Norris *et al.,* 2014).

$$\chi_{ij} = \sum_{k=1}^{P} g_{ik} f_{kj} + e_{ij} \quad (9)$$

Where: x_{ij} is the measured concentration of variable j in sample i, g_{ik} is the contribution of factor k, f_{kj} is the factor profile, e_{ij} is the residual, and p is the number of resolved factors. The optimal solution was obtained by minimizing the uncertainty-weighted objective function, using Eq. 10 (Norris *et al.,* 2014):

$$Q = \sum_{i=1}^{n} \sum_{j=1}^{m} \left(\frac{e_{ij}}{u_{ij}}\right)^2 \quad (10)$$

Where: u_{ij} represents the observation-specific uncertainty. Uncertainties were calculated following the EPA PMF 5.0 equation-based approach: values at or below the method detection limit (MDL) were assigned u_{ij} =5/6×MDLj, whereas values above the MDL were assigned, using Eq. 11 (Norris *et al.,* 2014):

$$u_{ij} = \sqrt{\left(EF_j x_{ij}\right)^2 + \left(0.5 MDL_j\right)^2} \quad (11)$$

Where: EFj is the species-specific error fraction. The PMF input contained 30 observations for each of the 16 modeled variables and no missing values. Species-specific MDLs and error fractions were used in the uncertainty calculation. Based on the signal-to-noise assessment, 13 variables were classified as strong, while FOG, NO_3-N and *E. coli* were classified as weak and down-weighted by tripling their uncertainties. These preprocessing choices defined the uncertainty structure used to weigh the PMF input matrix. The relative contribution of each factor to each variable was calculated using Eq. 12, while the corresponding factor contribution was determined using Eq. 13.

$$C_{kj} = \sum_{i=1}^{n} g_{ik} f_{kj} \quad (12)$$

$$RC_{kj} = \frac{C_{kj}}{\sum_{k=1}^{p} C_{kj}} \times 100 \quad (13)$$

Where: RC_{kj} is the relative contribution of factor k to variable j. Candidate PMF solutions were evaluated through a comprehensive suite of diagnostics, including convergence criteria, Q statistics, scaled residuals, observed-predicted agreement, species-specific Q/Qexpected ratios, interpretability, bootstrap mapping, displacement (DISP) and bootstrap-displacement (BS-DISP) analyses. Three-, four- and five-factor solutions were examined; the four-factor solution was selected because it provided the best balance between numerical fit, factor separation and interpretability. For the selected solution, all 100 base runs converged; Q(true), Q(robust) and Q(expected) were 244.495, 228.335 and 218, respectively, giving Q(robust)/Q(expected)=1.047. A total of 98.54% of scaled residuals were within +/-3, all species-specific Q/Qexpected values were below 2, and bootstrap mapping to the corresponding base factors ranged from 93% to 98%. DISP and BS-DISP showed no factor swaps, supporting limited rotational ambiguity. While these diagnostics confirm the internal numerical stability of the selected solution, they do not independently validate the environmental or causal identity of the factors. Accordingly, the extracted factors represent descriptive statistical groupings or prospective process patterns, requiring supplementary operational or source verification to establish causal links. Although the diagnostics collectively validate the mathematical stability of the four-factor model, environmental interpretation is inherently constrained by the limits of the available final-effluent evidence. Therefore, the relative contributions of each variable across all PMF factors sum to 100%. The average contribution of each PMF factor to the overall source/process apportionment was calculated, using Eq. 14 (Paatero and Tapper, 1994; Brown *et al.,* 2015):

$$AFC_k = \frac{\sum_{j=1}^{m} C_{kj}}{\sum_{k=1}^{p}\sum_{j=1}^{m} C_{kj}} \times 100 \quad (14)$$

Where: AFC_k is the average contribution of factor k. Accordingly, factor-profile bar charts were used to visualize the relative contributions of the studied variables to the resolved PMF factors, while the factor-contribution pie chart summarized the average contribution of each factor to the total apportioned effluent-quality matrix. The PMF results were interpreted as source and process apportionment, relying on the proportional share of each variable assigned to every respective factor profile alongside the average factor contributions.

Descriptive statistics

Descriptive statistics were performed for each measured effluent parameter to summarize the central tendency, variability, and distribution of the WWTP dataset. The statistical descriptors included the mean, standard deviation (SD), median (Q2), minimum, maximum, coefficient of variation (CV), first quartile (Q1), and third quartile (Q3). These analyses were performed utilizing SPSS Statistics (version 26) to establish a preliminary characterization of the effluent quality dataset and to lay the groundwork for subsequent multivariate analysis.

Quality assurance and quality control

All analyses were performed at the Royal Scientific Society laboratories under International Organization for Standardization/International Electrotechnical Commission (ISO/IEC) 17025 accreditation. Quality assurance (QA) and quality control (QC) procedures followed ISO/IEC 17025:2017 and accredited methods to ensure data traceability, precision, and accuracy. Each analytical batch incorporated calibration verification, procedural blanks, control standards, and duplicate analyses where applicable, whereas analytical accuracy and matrix effects were evaluated using certified reference materials and/or matrix-spike recoveries. Analytical results were validated against method-specific criteria, including calibration linearity, blank response, spike recovery, and relative percentage difference, with corrective action and reanalysis executed upon non-compliance to ensure that exclusively quality-assured data were integrated into the final report.

RESULTS AND DISCUSSION

Effluent characterization and compliance assessment

The ten-year final-effluent record (Table 3) shows partial compliance with JS 893:2021. pH was within the permissible range across categories, while DO, TDS, MBAS, SAR and IPN eggs showed full or near-full compliance where standards were applicable. Chloride concentrations satisfied regulatory thresholds established for irrigation and surface-discharge; however, they exceeded acceptable constraints for artificial groundwater recharge applications. The most frequent limitations involved BOD_5, COD and TSS, together with T-N, PO_4-P, HCO_3^-, phenol and *E. coli*. While these patterns align with inadequate regulation of residual organics, suspended solids, nutrients, alkalinity and microbiological parameters, the final-effluent dataset alone is insufficient to determine whether individual exceedances stem from influent fluctuations, hydraulic variations, operational dynamics, disinfection efficiencies, or extraneous factors. *E. coli* exceedances are therefore described as evidence of insufficient final microbial quality relative to the standard rather than proof of a specific disinfection failure. Instances of HCO_3^- non-compliance manifested despite complete compliance with TDS/SAR standards, demonstrating that alkalinity-related irrigation limitations can emerge independently of overall salinity/sodicity conditions. The 50–65% average parameter-level compliance is an unweighted descriptive summary and does not account for differences in the environmental or public-health significance of individual exceedances. Uncompromising adherence to each

Table 3: Descriptive statistics and compliance summary of the final effluent quality for Karak DWWTP over the ten years (2016 -2025) monitoring period

Parameter	Mean ±SD	Median	Min-Max	Q1	Q3	CV (%)	Compliance percentage against each Jordanian reclaimed wastewater reuse standard category JS 893:2021					
							Irrigation reuse-Class A	Irrigation reuse- Class B	Irrigation reuse-Class C	Irrigation reuse-Class D	Discharge into streams, wadies and water bodies	Artificial groundwater recharge
pH	7.68 ± 0.15	7.69	7.30-7.93	7.60	7.80	2	100%	100%	100%	100%	100%	100%
DO	5.78 ± 1.11	5.71	3.85-8.00	4.94	6.54	19	100%	N/A	N/A	100%	100%	100%
BOD5	104.45 ± 85.55	70.25	11.70-286.00	37.39	140.00	82	10%	57%	83%	3%	43%	3%
COD	399.96 ± 267.75	501.00	60.80-840.00	132.93	573.25	67	20%	40%	43%	0%	33%	0%
TDS	1105.50 ± 135.77	1120.00	880.00-1280.00	970.00	1231.25	12	100%	100%	100%	100%	100%	100%
TSS	213.59 ± 138.10	277.50	24.00-430.00	60.25	317.50	65	17%	37%	37%	0%	23%	17%
FOG	8.72 ± 1.31	8.00	8.00-12.90	8.00	8.85	15	57%	57%	57%	0%	57%	57%
Phenol	0.03 ± 0.01	0.02	0.02-0.04	0.02	0.03	29	17%	17%	17%	17%	17%	17%
MBAS	1.24 ± 0.62	1.52	0.15-1.80	0.74	1.69	50	100%	100%	100%	100%	100%	100%
NO3-N	4.34 ± 7.71	1.00	0.23-29.90	0.88	3.48	178	93%	93%	93%	93%	93%	80%
T-N	95.60 ± 33.03	100.12	31.40-199.24	83.03	112.56	35	20%	20%	20%	20%	20%	0%
PO4-P	16.47 ± 8.07	19.35	0.73-24.20	13.65	22.80	49	20%	20%	20%	20%	20%	20%
Cl	322.50 ± 42.23	327.00	261.00-378.00	283.00	362.25	13	100%	100%	100%	100%	100%	50%
HCO3	701.53 ± 124.31	725.00	449.00-850.00	708.75	768.00	18	0%	0%	0%	0%	0%	0%
SAR	4.92 ± 0.51	5.00	3.94-5.55	4.64	5.35	10	100%	100%	100%	100%	100%	100%
E. coli	7.37E+05 ± 5.61E+05	5.77E+05	3.30E+02-1.8E+06	2.97E+05	1.02E+06	140	0%	3%	N/A	0%	3%	0%
IPN	-	-	-	-	-	-	100%	100%	100%	100%	100%	100%
Average of parameter-level compliance percentages							56%	59%	65%	50%	59%	50%
Main restriction (parameter(s) that limit each intended use according to Jordanian standards)							HCO_3^-, *E. coli*, BOD_5, COD, TSS, Phenol, T-N, PO_4-P	HCO_3^-, *E. coli*, Phenol, T-N, PO_4-P, TSS, COD	HCO_3^-, Phenol, T-N, PO_4-P, TSS, COD	COD, TSS, FOG, HCO_3^-, *E. coli*, BOD_5, Phenol, T-N, PO_4-P	HCO_3^-, *E.coli*, Phenol, T-N, PO_4-P, TSS, COD, BOD_5	COD, T-N, HCO_3^-, *E. coli*, BOD_5, TSS, Phenol, PO_4-P, Cl^-

Note: Class A: parks, playgrounds, and sides of roads inside the cities. Class B: fruit trees, sides of roads outside the cities, and green areas. Class C: field crops, industrial crops, and forest trees. Class D: cut flowers. The arithmetic mean was calculated for all tests except for Escherichia coli, for which the geometric mean was calculated. n = 30 sampling campaigns (3 campaigns per year over 2016–2025). Mean ± SD was calculated from campaign-level mean values over the 2016–2025 monitoring period. -: Not detected (0 eggs/L). Parameters not mentioned in the Jordanian reclaimed wastewater reuse standard category JS 893 were not included in compliance calculations; Compliance percentage= (number samples meeting the applicable Jordanian reuse/discharge standard ÷ total numeric samples) × 100. N/A: Not applicable because no standard available.

applicable JS 893:2021 limit continues to serve as the foundational criterion for operational management decisions.

WQI based reclaimed wastewater assessment

All annual WQI values exceeded 100 (Table 4), but the parameter-contribution analysis showed that the index was strongly concentrated in a small number of weighted terms (Table 5). Across 2016–2025, phenol accounted for 52.02% of the Class A weighted WQI term and 98.42% and 99.31% of Classes B and C, respectively, whereas *E. coli* accounted for 99.985% of Class D and 99.986% of artificial-recharge WQI. For Class A, *E. coli* accounted for an additional 46.27%. Consequently, the pronounced magnitudes observed in Class D and artificial recharge assessments stem primarily from the interplay between elevated *E. coli* concentrations and the highly rigorous 1.1 MPN/100 mL criterion, rather than from uniformly extreme deterioration in all measured variables. Excluding *E. coli* and renormalizing the WQI reduced the 2016–2025 mean from 878,860.47 to 132.04 for Class D and from 881,753.08 to 128.58 for artificial recharge; both remained above 100. Class A similarly decreased from 236.07 to 126.87. Conversely, excluding phenol decreased the mean WQI to 65.74 for Class B and 28.66 for Class C, illustrating that the numerical classification of both categories is particularly vulnerable to the stringent phenol threshold and the inverse-standard weighting configuration. The annual WQI pattern was lower in 2021–2022 and higher again in 2024–2025 (Table 4). This finding is documented exclusively as a descriptive temporal pattern only. A weighting-scheme sensitivity test using equal parameter weights changed the 2016–2025 mean Class C WQI from 125.00 to 89.74, whereas the other five reuse/discharge categories remained above 100. Thus, the absolute WQI magnitude and, for Class C, even the screening class are sensitive to weighting assumptions. This sensitivity does not alter the overarching management conclusion, given that direct parameter-specific compliance with JS 893:2021 remains the primary criterion and Class C continues to exhibit recurring regulatory exceedances. The dataset cannot definitively attribute interannual variation to hydraulic loading, influent composition, process control, disinfection efficacy, or the 2018 plant conversion because operational data are unavailable and sampling was limited to three annual campaigns.

WPI based reclaimed wastewater assessment

WPI similarly indicated limited reuse suitability, but its message differed from WQI for Class C irrigation. Class C had the lowest WPI values and averaged 0.91, whereas WQI remained >100 and individual parameters still failed applicable standards (Table 6). Accordingly, WPI is not interpreted as evidence that Class C reuse is compliant or generally feasible. Class C is described only as the least impaired category in the WPI screening, while direct JS 893:2021 compliance, especially microbiological and other critical limits, remains the controlling decision criterion. The WPI parameter decomposition established that *E. coli* serves as the primary mathematical contributor across all categories governed by microbiological standard (Table 7). *E. coli* accounted for 99.57% of mean Class A WPI, 97.45% of Class B, 95.74% of discharge, 99.991% of Class D and 99.993% of artificial-recharge WPI. Class C, for which no *E. coli* limit is specified in the applied category, showed a distributed WPI structure led by TSS (15.61%), HCO3 (12.82%), PO4-P (12.04%), T-N (9.98%), COD (9.75%) and phenol (9.36%). Excluding *E. coli* and recalculating WPI reduced the mean values to 1.52 for Class A, 0.99 for Class B, 1.58 for discharge, 2.82 for Class D and 2.36 for artificial recharge. Consequently, *E. coli* drives the exceptionally high WPI in stricter categories, while substantial physicochemical pollution persists, particularly in Class D and artificial recharge applications. Thus, the Class C mean WPI of 0. 91 should be interpreted as a screening metric rather than definitive regulatory compliance.

Table 4: annual values of WQI for the effluent of Karak DWWTP during 2016–2025

Year	Irrigation reuse-Class A	Irrigation reuse-Class B	Irrigation reuse-Class C	Irrigation reuse-Class D	Discharge into streams and wadies or water bodies	Artificial recharge of groundwater aquifers
2016	302	110	108	1543915	118	1548998
2017	291	105	103	1497596	114	1502526
2018	287	106	104	1451283	116	1456061
2019	284	109	108	1404972	119	1409598
2020	288	109	108	1435848	120	1440576
2021	135	103	103	247115	112	247926
2022	129	114	114	103552	126	103890
2023	178	116	115	494134	124	495759
2024	234	195	195	308956	203	309971
2025	232	194	193	301235	202	302225
Average 2016-2025	236	126	125	878860	135	881753

Notes: Class A: parks, playgrounds, and sides of roads inside the cities. Class B: fruit trees, sides of roads outside the cities, and green areas. Class C: field crops, industrial crops, and forest trees. Class D: cut flowers. Lower WQI values reveal better effluent quality and compliance with the relevant standards, while higher values reveal poorer water quality.

Table 5: Parameter-contribution and targeted sensitivity analysis of mean WQI (2016–2025)

Category	Mean WQI	Dominant weighted-term contribution	Targeted sensitivity
Class A	236.07	Phenol 52.02%; *E. coli* 46.27%; DO 1.17%	Without *E. coli*: 126.87 (>100)
Class B	126.11	Phenol 98.42%; *E. coli* 0.88%; PO4-P 0.25%	Without phenol: 65.74
Class C	125.00	Phenol 99.31%; PO4-P 0.26%; FOG 0.21%	Without phenol: 28.66
Class D	878,860.47	*E. coli* 99.985%; phenol 0.014%	Without *E. coli*: 132.04 (>100)
Discharge	135.41	Phenol 89.59%; DO 8.09%; PO4-P 0.92%	Equal-weight sensitivity assessed in text
Artificial recharge	881,753.08	*E. coli* 99.986%; phenol 0.014%	Without *E. coli*: 128.58 (>100)

Note: Contributions are mathematical shares of the weighted WQI terms, not environmental-risk shares. Leave-one-parameter-out values were recalculated with K renormalized after omission.

Table 6: Annual values WPI for the effluent of Karak DWWTP during 2016–2025, evaluated against Jordanian standards (JS 893:2021) for reclaimed domestic wastewater according to reuse purposes (JSMO, 2021)

Year	Irrigation reuse- Class A	Irrigation reuse- Class B	Irrigation reuse-Class C	Irrigation reuse- Class D	Discharge into streams and wadies or water bodies	Artificial recharge of groundwater aquifers
2016	590	64	1.16	53480	61	53479
2017	572	62	1.12	51875	59	51875
2018	555	60	1.10	50271	57	50270
2019	537	58	1.08	48667	55	48666
2020	549	59	1.06	49736	56	49735
2021	95	11	0.74	8558	11	8558
2022	40	5	0.57	3584	5	3584
2023	189	21	0.52	17113	20	17113
2024	119	13	0.89	10697	13	10697
2025	116	13	0.89	10430	13	10430
Average 2016-2025	336	37	0.91	30441	35	30441

Notes: Class A: parks, playgrounds, and sides of roads inside the cities. Class B: fruit trees, sides of roads outside the cities, and green areas. Class C: field crops, industrial crops, and forest trees. Class D: cut flowers. Lower WPI values reveal compliance with the relevant standards; whereas higher values reveal greater pollution

Table 7: Parameter contributions and *E. coli*-exclusion sensitivity of mean WPI (2016–2025)

Category	Mean WPI	Dominant WPI contribution	WPI without *E. coli*
Class A	336.25	*E. coli* 99.57%; TSS 0.08%; COD 0.07%	1.52
Class B	36.50	*E. coli* 97.45%; TSS 0.37%; COD 0.34%	0.99
Class C	0.912	TSS 15.61%; HCO3 12.82%; PO4-P 12.04%; T-N 9.98%	N/A (no *E. coli* standard)
Class D	30,441.16	*E. coli* 99.991%; TSS 0.003%; COD 0.002%	2.82
Discharge	34.97	*E. coli* 95.74%; DO 0.97%; TSS 0.60%	1.58
Artificial recharge	30,440.73	*E. coli* 99.993%; COD 0.002%; BOD5 0.001%	2.36

Note: WPI contribution (%) = 100PLi/ΣPLj, aggregated across the annual calculations. *E. coli*-exclusion WPI was recalculated with the number of included parameters reduced accordingly.

Linear temporal trend analysis (2016–2025)

Regression across the 30 campaign observations identified several systematic long-term changes in final-effluent quality (Table 8). Significant decreasing slopes (nominal $p < 0.05$) were observed for BOD_5 (−10.844 mg/L/y), COD (−60.290 mg/L/y), TDS (−39.861 mg/L/y), TSS (−33.637 mg/L/y), T-N (−5.089 mg/L/y), PO_4-P (−1.726 mg/L/y), Cl (−11.675 mg/L/y), and SAR (−0.117 units/y). DO increased significantly (+0.170 mg/L/year), while phenol (+0.00187 mg/L/y) and NO_3-N (+1.483 mg/L/y) also showed significant upward trends. The strongest linear temporal fits were observed for TDS ($R^2 = 0.742$), Cl ($R^2 = 0.658$), phenol ($R^2 = 0.545$), TSS ($R^2 = 0.511$), and SAR ($R^2 = 0.456$). Trends in pH, FOG, MBAS and HCO_3 were not statistically significant, and the log10 *E. coli* slope was negative but marginal (−0.0923 log10 MPN/100 mL/y; $R^2 = 0.130$; $p = 0.0508$). These outcomes illustrate interannual directionality within the monitored timeline; however, they neither resolve seasonal cycles nor confirm that the 2018 treatment conversion or unmeasured operational variables drove the observed temporal shifts.

PCA-based identification of water quality drivers

The four retained varimax-rotated PCA components explained 89.54% of the variance (Table 9). Given the 30:16 observation-to-variable ratio, the PCA is interpreted as exploratory covariance structure. principal component 1 (PC1; 46.25%) was characterized mainly by BOD_5(f), COD, TSS, TDS, PO_4-P, Cl and SAR, describing a broad residual organic/solids/salinity covariance domain. These co-loadings indicate that the variables exhibited synchronous variations within the monitored final effluent; however, they cannot independently isolate a common source or substantiate a specific treatment mechanism. Comparable variable groupings have been reported in wastewater multivariate studies (Pantsar-Kallio *et al.,* 1999; Singh *et al.,* 2005; Kumari and Tripathi, 2014). Bold number: loading value ≥ 0.60, indicating heavy loading. PC2 (15.79%) was characterized by pH, FOG and T-N; PC3 (15.25%) by phenol, MBAS, NO_3-N and HCO_3; and PC4 (12.25%) mainly by DO and *E. coli* (Table 8). These components are described as statistical associations: a pH–FOG–T-N pattern, a phenol–MBAS–NO_3-N–HCO_3 pattern, and a DO–*E. coli* pattern. Although biological or operational mechanisms, including nitrogen transformation, aeration, sedimentation, disinfection, and detergent-derived inputs, serve as plausible hypotheses, they cannot be definitively confirmed through final-effluent covariance análisis alone. The absence of influent, process-unit, operational and source-profile data prevents causal attribution. Accordingly, these components are interpreted as statistical associations and patterns rather than definitive process drivers or source signatures and should therefore be considered hypotheses requiring independent operational and source-specific verification through targeted investigations.

Table 8: Linear temporal trends in final-effluent quality parameters across 30 monitoring campaigns, 2016–2025

Parameter	Slope	R^2	p-value	Direction
pH	+0.00906 SU/y	0.031	0.3521	No significant trend
DO	+0.170 mg/L/y	0.204	0.0122	Increase
BOD_5	−10.844 mg/L/y	0.138	0.0430	Decrease
COD	−60.290 mg/L/y	0.437	7.06×10^{-5}	Decrease
TDS	−39.861 mg/L/y	0.742	9.80×10^{-10}	Decrease
TSS	−33.637 mg/L/y	0.511	9.11×10^{-6}	Decrease
FOG	−0.156 mg/L/y	0.123	0.0576	No significant trend
Phenol	+0.00187 mg/L/y	0.545	3.20×10^{-6}	Increase
MBAS	−0.0635 mg/L/y	0.091	0.1053	No significant trend
NO_3-N	+1.483 mg/L/y	0.319	0.00115	Increase
T-N	−5.089 mg/L/y	0.204	0.0121	Decrease
PO_4-P	−1.726 mg/L/y	0.394	0.000205	Decrease
Cl	−11.675 mg/L/y	0.658	5.41×10^{-8}	Decrease
HCO_3	−1.022 mg/L/y	0.001	0.8993	No significant trend
SAR	−0.117 units/y	0.456	4.21×10^{-5}	Decrease
E. coli (log_{10})	−0.0923 log_{10}/y	0.130	0.0508	Marginal decrease

Note: Slopes are from ordinary least-squares regression against decimal year using all 30 campaign observations. *E. coli* was analyzed on the log_{10} scale; all other parameters were analyzed on their measured scales. p-values are two-sided and presented as exploratory nominal values.

Table 9: Factor analysis scores following varimax rotation for final-effluent quality parameters at Karak DWWTP, 2016–2025

Parameter	PC1	PC2	PC3	PC4
pH	-0.29	**0.75**	-0.09	0.47
DO	-0.30	0.04	0.17	**0.89**
BOD5	**0.71**	0.35	0.20	0.38
COD	**0.85**	0.40	-0.03	0.40
TDS	**0.92**	0.25	-0.27	-0.25
TSS	**0.80**	0.39	-0.05	0.18
FOG	0.41	**0.75**	-0.14	0.19
Phenol	-0.27	-0.29	**0.88**	0.29
MBAS	0.49	-0.04	**0.84**	-0.19
NO3-N	-0.41	0.23	**0.65**	0.35
T-N	0.42	**0.87**	0.08	-0.04
PO4-P	**0.90**	0.19	0.28	-0.29
Cl	**0.95**	0.04	0.18	-0.08
HCO3	0.49	0.17	**0.79**	-0.38
SAR	**0.93**	0.05	-0.09	-0.09
E. coli	0.39	0.39	-0.24	**0.67**
Eigen value	8.35	4.41	3.59	2.75
Total variance (%)	**46.25**	**15.79**	**15.25**	**12.25**
Cumulative variance (%)	46.25	62.04	77.29	89.54
Possible source/driver	Residual organic–solids–salinity–phosphorus effluent matrix	Nitrogen–FOG–pH operational factor	Phenolic– surfactant/nitrification–alkalinity factor	Oxygenation–microbial effluent-quality factor

Hierarchical clustering of wastewater quality patterns

HCA grouped the final-effluent variables into four clusters (Fig. 1). Cluster 1 comprised BOD_5, COD, TSS, TDS, Cl, SAR and PO_4-P, showing a residual organic/solids/salinity covariance grouping. This broadly resembles PC1 but is not independent validation because both analyses use the same 30 × 16 standardized datasets. HCA provides valuable linkage information by identifying variables that agglomerate at shorter distances, thereby serving as a complementary descriptive perspective on the underlying correlation structure. Cluster 2 comprised pH, FOG and T-N (Fig. 1). This grouping is reported as an association among these variables in the final effluent. While associations with nitrogen transformation, grease dynamics, pH/alkalinity balance, or aeration remain mechanistically sound, they cannot be validated in the absence of paired process and influent data; consequently, Cluster 2 is construed strictly as a co-variation pattern rather than proof of a distinct treatment mechanism. Cluster 3 grouped phenol, MBAS, NO_3-N and HCO_3 (Fig. 1). The cluster may be consistent with a mixed trace-organic/nutrient/alkalinity pattern, but neither a detergent source nor a specific nitrification mechanism is established by the clustering. The grouping is used only to describe co-variation in the monitored final effluent. Cluster 4 comprised DO and *E. coli* (Fig. 1). Their proximity indicates co-variation within the dataset, not a demonstrated causal link between oxygenation and microbial removal or disinfection. Because no disinfection, hydraulic or process-operating data were available, the cluster is described as a DO–microbiological quality association requiring independent confirmation. Overall, HCA showed four covariance groupings broadly consistent with the PCA structure. While this consistency substantiates a coherent descriptive pattern within the dataset, it does not provide independent validation, identify specific pollution sources, or confirm underlying treatment mechanisms.

PMF based source apportionment

The four-factor PMF solution comprised one dominant and three lower-average statistical profiles (Fig. 2); Factor 1, 54.0%; Factor 2, 20.3%; Factor 3, 16.7%; and Factor 4, 9.1%. These percentages characterize the mean apportioned matrix derived from the PMF model and should not be construed as the proportional contributions of verified external pollutant sources. Environmental interpretation is based on the variables with the largest relative contributions within each profile, and the labels are descriptive hypotheses that require independent influent, source or operational data for validation. Lower-average factors may still be important when they dominate regulatory-critical variables such as FOG, *E. coli*, phenol or MBAS. Factor 1 (54.0%) was characterized by Cl (86.0%), TDS (80.5%), HCO_3 (80.1%), SAR (79.1%), COD (78.0%), TSS (68.5%) and BOD_5 (61.7%) (Fig. 3). This profile is therefore described as a mineralized–organic residual pattern, reflecting co-apportionment of salinity/alkalinity indicators with residual organic/solids variables. It is not treated as a single confirmed pollutant source. Although the profile aligns with persistent final-effluent matrix neither source origin nor underlying treatment mechanism can be definitively resolved from effluent monitoring data in isolation. Factor 2 (20.3%) was characterized by PO_4-P (77.0%), NO_3-N (75.5%), T-N (70.1%) and pH (67.0%) (Fig. 3). It is therefore described as a nutrient–pH statistical pattern. Although nitrogen transformation and alkalinity dynamics serve as plausible process interpretations, the profile fails to confirm a specific nitrification, denitrification or polishing mechanism due to the absence of corresponding process measurements.

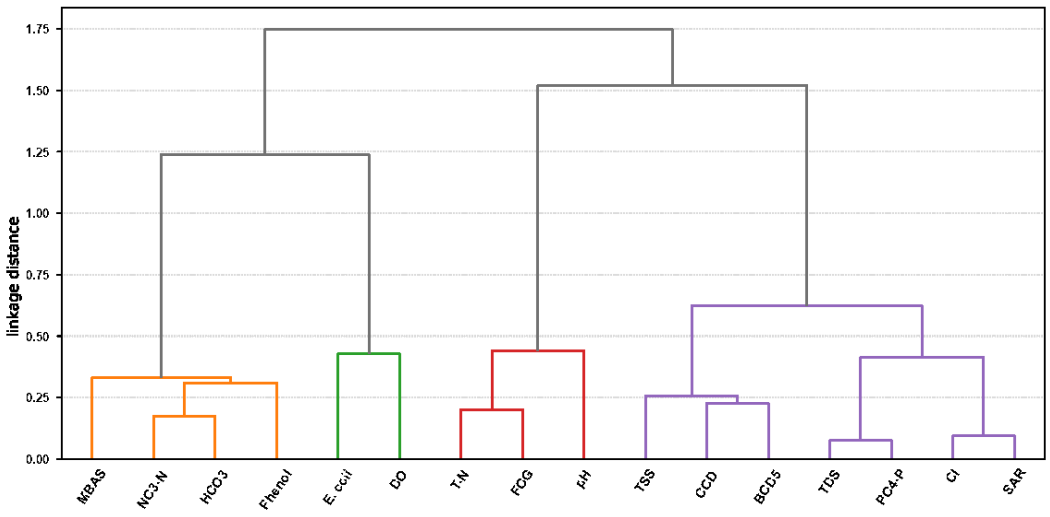

Fig. 1: Hierarchical cluster analysis dendrogram of final effluent-quality parameters from Karak DWWTP during 2016–2025

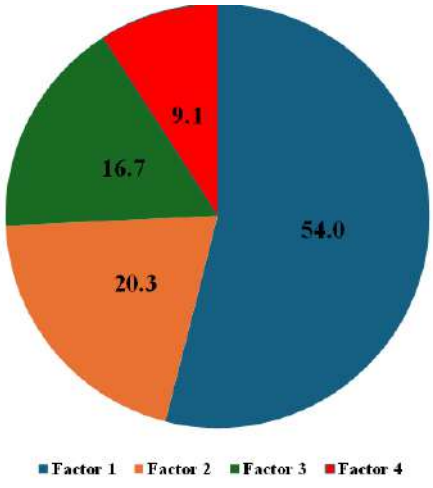

Fig. 2: Average contributions of PMF factors

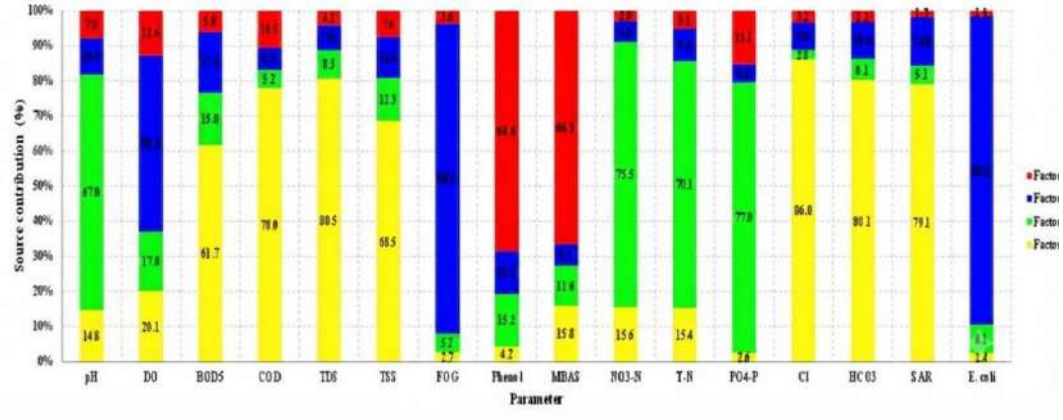

Fig. 3: Relative contributions of studied variables to PMF factors

Factor 3 (16.7%) was characterized most strongly by FOG (88.5%) and *E. coli* (88.0%), with a substantial DO contribution (50.3%) (Fig. 3). This is described as a FOG–microbiological–DO association. Owing to a constrained sampling frequency of three annual campaigns and the absence of flow or operational records, this profile cannot be construed as evidence of episodic, short-term operational or hydraulic events, nor does it substantiate a specific carryover mechanism. Although this factor holds environmental significance by dominating two compliance-sensitive indicators, the co-apportionment results do not confirm that FOG induced microbial carryover, nor do they establish that shifts in aeration/disinfection generated the observed pattern. Factor 4 (9.1%) was characterized by phenol (68.4%) and MBAS (66.5%) (Fig. 3). It is therefore described as a phenol–MBAS trace-organic/surfactant statistical pattern. MBAS is an anionic-surfactant indicator, but phenol is not source-specific; consequently, the factor cannot be assigned confidently to domestic detergents, cleaning agents or a particular external source from the present data. Achieving definitive source attribution necessitates targeted influent and source characterization efforts. Collectively, the PMF profiles delineate dominant, matrix-wide co-apportionment patterns from lower-average profiles that exert a disproportionate influence on specific sensitive variables. This is useful for prioritizing follow-up monitoring, but it does not convert statistical factors into confirmed sources. Accordingly, numerical PMF stability is considered separately from statistical factor structure and from environmental/process hypotheses, which require independent validation.

Implications for wastewater reuse and environmental management strategies

Management implications are based first on direct JS 893:2021 exceedances and only secondarily on the statistical patterns. The most defensible priorities are improved control of residual organics/solids, nutrients, FOG, phenol/MBAS and *E. coli*, together with management of bicarbonate and chloride where relevant to the intended reuse. Priority should therefore be given to sustained compliance with individual critical parameters rather than reliance on composite indices or statistical factor scores alone. Routine monitoring should also be strengthened to identify persistent exceedances and support timely corrective management. Because comprehensive operational data regarding aeration configuration, sludge age, secondary clarification, disinfection, FOG removal, nutrient-removal setups, influent compositions, and energy/economic requirements were unavailable, the findings cannot justify recommending specific unit-process upgrades, such as tertiary filtration, anoxic/anaerobic zones, ultraviolet (UV) irradiation, ozonation, or advanced desalination. Such options necessitate rigorous, site-specific engineering assessments prior to selection or deployment. Furthermore, the reintroduction of restricted irrigation should only be entertained once sustained, category-specific compliance is verified through higher-frequency monitoring, with a particular emphasis on microbiological and other critical parameters.

Study limitations

This study has several limitations that directly constrain interpretation. The dataset contains 30 campaign-level observations for 16 variables, with only three campaigns per year; therefore, PCA, HCA and PMF are exploratory and cannot resolve seasonal or short-term operational events. Although the 2018 conversion from trickling filters to activated sludge falls within the monitoring period, limited pre-upgrade observations and a lack of paired operational data preclude definitive causal attribution between the pre- and post-conversion phases. Only final effluent was

analyzed; no influent, process-unit, hydraulic, rainfall, sludge, disinfection or source-profile data were available, so multivariate components and PMF factors represent statistical associations or potential process-associated patterns rather than confirmed sources or mechanisms. Furthermore, the monitoring protocol encompassed a restricted suite of contaminants, omitting pharmaceuticals, emerging pollutants, heavy metals, comprehensive pathogen indicators or antibiotic resistance markers. WQI and WPI are screening tools whose results depend on parameter selection, reference standards and aggregation; they do not replace direct compliance with critical regulatory limits. These constraints are now explicitly integrated into the formulation of management implications, emphasizing that subsequent investigations should couple high-frequency surveillance with comprehensive influent characterization and detailed process-operational records. The linear trend analysis evaluates monotonic change over the complete 2016–2025 record; it does not resolve seasonal cycles and cannot isolate the effect of the 2018 treatment conversion from other unmeasured temporal changes.

CONCLUSION

This study provides an integrated assessment of long-term final-effluent quality and reuse suitability at Karak DWWTP during 2016–2025. Direct comparison against JS 893:2021 standards revealed that the effluent remained limited in its suitability for multiple intended applications, constrained predominantly by residual organic matter, suspended solids, nutrients, bicarbonate, phenol, FOG, and *E. coli*. The observed exceedances indicate that reuse suitability varied substantially among intended applications and that compliance with individual critical parameters remains more informative than a single aggregated measure of water quality. WQI and WPI were useful as supplementary screening tools, but the additional parameter-contribution and sensitivity analyses demonstrated that their magnitudes can be strongly controlled by a small number of variables and by category-specific standards. *E. coli* overwhelmingly dominated the most restrictive Class D irrigation and groundwater-recharge indices, whereas phenol exerted the greatest WQI influence in Classes B and C. This contrast demonstrates that high composite-index values may arise from different controlling parameters depending on the intended reuse category, thereby requiring parameter-specific examination before management decisions are made. Furthermore, an equal-weight sensitivity analysis further demonstrated that index classification are sensitive to variations in weighting architectures, emphasizing the necessity of interpreting composite indices in conjunction with direct, parameter-specific compliance rather than as independent indicators of treatment efficacy or health risk. Accordingly, composite indices are best regarded as screening and prioritization tools that complement, rather than replace, regulatory assessment of critical microbiological, chemical, and physicochemical parameters. The 2016–2025 linear trend analysis provided an additional temporal perspective. Significant declines in BOD5, COD, TDS, TSS, T-N, PO4-P, chloride, and SAR indicate improvement in several organic, solids, nutrient, and salinity-related indicators, while significant increases in DO, phenol, and NO3-N show that improvement was not uniform across all parameters. These trends outline directional shifts within the monitored effluent; however, they cannot be construed as indicators of specific treatment mechanisms due to the absence of corresponding influent, hydraulic, operational, and process-unit records. PCA, HCA, and PMF similarly identified coherent covariance, similarity, and factor-profile structures, but these

statistical patterns do not independently establish causal sources or treatment pathways. Overall, direct JS 893:2021 compliance remains the primary basis for reuse decisions. Given the parameters of the monitored conditions, practices such as unrestricted irrigation, environmentally sensitive surface-water discharge, and artificial groundwater recharge are scientifically unwarranted. Such applications should be considered only after sustained category-specific compliance, higher-frequency monitoring, and verification of critical parameters. Future assessments should combine higher-frequency monitoring with influent, operational, hydraulic, process-unit, and source-specific measurements so that temporal changes, treatment performance, source attribution, and required process interventions can be evaluated with greater confidence and stronger engineering and management relevance for sustainable wastewater reuse and environmental protection.

AUTHOR CONTRIBUTIONS

E.R. Tarawneh was solely responsible for the conceptualization and design of the study, data collection, data analysis and interpretation, and preparation and revision of the manuscript and final approval of the submitted version.

ACKNOWLEDGEMENT

The author gratefully acknowledges the Ministry of Environment, Amman, Jordan, for providing the data used in this study.

CONFLICT OF INTEREST

The author declares that there is no conflict of interest regarding the publication of this manuscript. In addition, ethical issues, including plagiarism, informed consent, misconduct, data fabrication and/or falsification, double publication and/or submission, and redundancy have been completely observed by the authors.

OPEN ACCESS

©2027 The author(s). This article is licensed under a Creative Commons Attribution 4.0 International License, which permits use, sharing, adaptation, distribution and reproduction in any medium or format, as long as you give appropriate credit to the original author(s) and the source, provide a link to the Creative Commons license, and indicate if changes were made. The images or other third-party material in this article are included in the article's Creative Commons license, unless indicated otherwise in a credit line to the material. If material is not included in the article's Creative Commons license and your intended use is not permitted by statutory regulation or exceeds the permitted use, you will need to obtain permission directly from the copyright holder. To view a copy of this license, visit: http://creativecommons.org/licenses/by/4.0/

PUBLISHER'S NOTE

GJESM Publisher remains neutral regarding jurisdictional claims in published maps and institutional affiliations.

POSITIVE AI STATEMENT

During the preparation of this work the author(s) have used AI (ChatGPT – OpenAI) to enhance the readability, grammar, and structure of the manuscript. After using this tool/service, the author reviewed and edited the content as needed and takes full responsibility for the content of the publication.

ABBREVIATIONS

%	Percent
°C	Degrees Celsius
log_{10}	Base-10 logarithm
HCO_3	Bicarbonate
BOD_5	Biochemical oxygen demand
BS-DISP	Bootstrap–displacement
COD	Chemical oxygen demand

Cl	Chloride
R^2	Coefficient of determination
CV	Coefficient of variation
m^3	Cubic meters
m^3/d	Cubic meters per day
m^3/y	Cubic meters per year
DISP	Displacement
DO	Dissolved oxygen
DWWTP	Domestic wastewater treatment plant
E. coli	Escherichia coli
G	Factor contribution
F	Factor profile
FOG	Fats, oils, and grease
Q1	First quartile
ha	Hectare
HCA	Hierarchical cluster analysis
IBM	International Business Machines
IPN	Intestinal pathogenic nematode eggs
KMO	Kaiser-Meyer-Olkin
km	Kilometers
LDO	Luminescence measurement of dissolved oxygen
Q2	Median
MDL	Method detection limit
MBAS	Methylene blue active substance
mg/L	Milligram per liter
MCM	Million cubic meters
MPN	Most probable number
NO_3–*N*	Nitrate-nitrogen
PO_4–*P*	Phosphate -phosphorus
PLi	Pollution load
PMF	Positive matrix factorization
PCA	Principal component analysis
QA	Quality assurance
QC	Quality control
RSD	Relative standard deviation
SAR	Sodium adsorption ratio
SPSS	Statistical package for the social sciences
TSS	Suspended solids
Q3	Third quartile
TDS	Total dissolved solids
T-N	Total nitrogen
EPA	U.S. Environmental Protection Agency
WWQI	Wastewater quality index
WRI	Wastewater reuse index
WWTP	Wastewater treatment plant
WPI	Water pollution index
WQI	Water quality index
AI	Artificial intelligence
df	Degrees of freedom
DOS	Department of Statistics
ISO/IEC	International Organization for Standardization/International Electrotechnical Commission
JS	Jordanian Standard
JSMO	Jordan Standards and Metrology Organization
MWI	Ministry of Water and Irrigation
N/A	Not applicable
PC	Principal component
pH	Potential of hydrogen
SD	Standard deviation
SU	Standard units
UV	Ultraviolet
WHO	World Health Organization

REFERENCES

Abbasi, T.; Abbasi, S.A., (2012). Water quality indices Elsevier.

Abualhaija, M., (2023). Applying the quality and pollution indices for evaluating the wastewater effluent quality of Kufranja wastewater treatment plant, Jordan. Water Conserv. Manage., 7(1): 06–11 **(6 pages)**.

Ait-Mouheb, N.; Bahri, A.; Thayer, B. Ben; Benyahia, B.; Bourrié, G.; Cherki, B.; Condom, N.; Declercq, R.; Gunes, A.; Héran, M.; Kitir, N.; Molle, B.; Patureau, D.; Pollice, A.; Rapaport, A.; Renault, P.; Riahi, K.; Romagny, B.; Sari, T.; Sinfort, C.; Steyer, J.-P.; Talozi, S.; Topcuoglu, B.; Turan, M.; Wéry, N.; Yıldırım, E.; Harmand, J., (2018). The reuse of reclaimed water for irrigation around the Mediterranean Rim: a step towards a more virtuous cycle? Reg. Environ. Change., 18(3): 693–705 **(13 pages)**.

Al-hasanat, A.; Chemack, F.; Sabbahi, S.; Nouiri, I.; Karanis, P.; Ayed, L. Ben, (2025). Exploring treated wastewater reuse as an alternative option to cope with water scarcity: comparative review in Tunisia and Jordan. Water Pract. Technol., 20(12): 2881–2898 **(18 pages)**.

Al-Hazmi, H.E.; Mohammadi, A.; Hejna, A.; Majtacz, J.; Esmaeili, A.; Habibzadeh, S.; Saeb, M.R.; Badawi, M.; Lima, E.C.; Mąkinia, J., (2023). Wastewater reuse in agriculture: Prospects and challenges. Environ. Res., 236: 116711 **(26 pages)**.

Alfarra, A.; Kemp-Benedict, E.; Hötzl, H.; Sader, N.; Sonneveld, B., (2011). A framework for wastewater reuse in Jordan: utilizing a modified wastewater reuse index. Water Resour. Manage., 25(4): 1153–1167 **(15 pages)**.

Alihosseini, S.H.; Torabian, A.; Semiromi, F.B., (2020). Evaluation of treated municipal wastewater effluent for agricultural irrigation purposes using the fuzzy effluent quality index (FEQI). Water Supply. 20(1): 148–156 **(9 pages)**.

Ammary, B.Y., (2007). Wastewater reuse in Jordan: present status and future plans. Desalination, 211(1–3): 164–176 **(13 pages)**.

Anyango, G.W.; Bhowmick, G.D.; Bhattacharya, N.S.; Sahoo Bhattacharya, N., (2024). A critical review of irrigation water quality index and water quality management practices in micro-irrigation for efficient policy making. Desalin. Water Treat., 318: 100304 **(17 pages)**.

Ayoub, M.; El-Morsy, A., (2021). Applying the wastewater quality index for assessing the effluent quality of recently upgraded meet Abo El-koum wastewater treatment plant. J. Ecol. Eng., 22(2): 128–133 **(6 pages)**.

Ayres, R.M.; Mara, D.D.; Organization, W.H., (1996). Analysis of wastewater for use in agriculture: a laboratory manual of parasitological and bacteriological techniques World Health Organization.

Baird, R.; Rice, E.; Eaton, A., (2017). Standard methods for the examination of water and wastewaters, Water Environment Federation, Chair Eugene W. Rice, American Public Health Association Andrew D. Eaton, American Water Works Association.

Bessedik, M.; Abdelbaki, C.; Badr, N.; Tiar, S.M.; Megnounif, A., (2021). Application of water quality indices for assessment of influent and effluent wastewater from wastewater treatment plant of Oran City, Algeria. Desalin. Water Treat., 236: 306–317 **(12 pages)**.

Breulmann, M.; Müller, R.A.; Al-Subeh, A.; Subah, A.; Afferden, M. van, (2019). Reuse of treated wastewater and biosolids in Jordan: Nationwide evaluation. Helmholtz Centre for Environmental Research – UFZ, with support from the Ministry of Water and Irrigation.

Brown, R.M.; Mccleiland, N.J.; Deiniger, R.A.; O'Connor, M.F., (1972). Water quality index–crossing the physical barrier (Jenkis, SH ed) Proceeding.

Brown, S.G.; Eberly, S.; Paatero, P.; Norris, G.A., (2015). Methods for estimating uncertainty in PMF solutions: Examples with ambient air and water quality data and guidance on reporting PMF results. Sci. Total Environ., 518–519: 626–635 **(10 pages)**.

Chidiac, S.; Najjar, P. El; Ouaini, N.; Rayess, Y. El; Azzi, D. El, (2023). A comprehensive review of water quality indices (WQIs): history, models, attempts and perspectives. Rev. Environ. Sci. Bio. Technol., 22(2): 349–395 **(47 pages)**.

Dharmadhikari, S.; Jain, A.; Pawar, N.; Chaudhari, P.K., (2023). Direct reuse of wastewater: problem, challenge, and future direction, in: Antimicrobial resistance in wastewater and human health. Elsevier.

DOS, (2026). Population estimates at the end of 2025. Amman: Department of Statistics.

Fardous, A.-N.; Al-Hadidi, L., (2007). Waste water management and reuse in Jordan: Water resources in the Middle East: Israel-Palestinian water issues—from conflict to cooperation. springer.

Gisi, S. De; Casella, P.; Cellamare, C.M.; Ferraris, M.; Petta, L.; Notarnicola, M., (2017). Wastewater reuse. Encycl. Sustain. Technol., 4(2008): 53–68 **(16 pages)**.

Gupta, S.S.K.; Gupta, S.S.K., (2021). A critical review on water quality index tool: Genesis, evolution and future directions. Ecol. Inform., 63: 101299 **(13 pages)**.

HACH, (2006). Hach Method 10360: Luminescence Measurement of Dissolved Oxygen (LDO®) in Water and Wastewater.

Hossain, M.; Patra, P.K., (2020). Water pollution index–A new integrated approach to rank water quality. Ecol. Indic., 117: 106668 **(9 pages)**.

Jamshidzadeh, Z.; Tavangari Barzi, M., (2020). Wastewater quality index (WWQI) as an assessment tool of treated wastewater quality for agriculture: a case of North Wastewater Treatment Plant effluent of Isfahan. Environ. Sci. Pollut. Res., 27(7): 7366–7378 **(13 pages)**.

JSMO, (2021). Jordan standards and metrology organization (JSMO): standard specification "water—reclaimed domestic wastewater". JS 893:2021, 4th ed.

Kachroud, M.; Trolard, F.; Kefi, M.; Jebari, S.; Bourrié, G., (2019). Water quality indices: challenges and application limits in literature. Water, 11(2): 361 **(26 pages)**.

Kalavrouziotis, I.K.; Kyritsis, S.S.; Koukoulakis, P.H., (2023). Benefits from reclaimed wastewater and biosolid reuse in agriculture and in the environment, in: Water Management and Circular Economy. Elsevier, 273–302 **(30 pages).**

Kumari, M.; Tripathi, B.D., (2014). Source apportionment of wastewater pollutants using multivariate analyses. Bull. Environ. Contam. Toxicol., 93(1): 19–24 **(6 pages)**.

Manna, A.; Biswas, D., (2023). Assessment of drinking water quality using water quality index: a review. Water Conserv. Sci. Eng., 8(1): 6 **(18 pages)**.

Moeinzadeh, H.; Yong, K.-T.; Withana, A., (2024). A critical analysis of parameter choices in water quality assessment. Water Res., 258: 121777 **(10 pages)**.

Moghaddam, V.K.; Changani, F.; Mohammadi, A.; Hadei, M.; Ashabi, R.; Majd, L.E.; Mahvi, A.H., (2017). Sustainable development of water resources based on wastewater reuse and upgrading of treatment plants: a review in the Middle East. Desalin. Water Treat., 65: 463–473 **(11 pages)**.

MWI, (2023). Wastewater in Jordan. Amman: Ministry of Water and Irrigation.

MWI, (2024). National water strategy 2023–2040. Amman: Ministry of Water and Irrigation.

MWI, (2025a). Jordan water sector: facts and figures 2025. Amman: Ministry of Water and Irrigation.

MWI, (2025b). Water budget 2025. Amman: Ministry of Water and Irrigation. Directorate of Policies and Strategic Planning.

Nayak, B.; Panda, P.K., (2026). A comprehensive review of water quality analysis. Int. J. Image Graph., 26(04): 2650033 **(15 pages)**.

Norris, G.; Duvall, R.; Brown, S.; Bai, S., (2014). EPA positive matrix factorization (PMF) 5.0 fundamentals and user guide, US Environmental Protection Agency, Washington, DC.

Ofori, S.; Puškáčová, A.; Růžičková, I.; Wanner, J., (2021). Treated wastewater reuse for irrigation: Pros and cons. Sci. Total Environ., 760: 144026 **(15 pages)**.

Paatero, P.; Tapper, U., (1994). Positive matrix factorization: A non-negative factor model with optimal utilization of error estimates of data values. Environmetrics. 5(2): 111–126 **(16 pages)**.

Pantsar-Kallio, M.; Mujunen, S.-P.; Hatzimihalis, G.; Koutoufides, P.; Minkkinen, P.; Wilkie, P.J.; Connor, M.A., (1999). Multivariate data analysis of key pollutants in sewage samples: a case study. Anal. Chim. Acta, 393(1–3): 181–191 **(11 pages)**.

Patel, P.S.; Pandya, D.M.; Shah, M., (2023). A systematic and comparative study of Water Quality Index (WQI) for groundwater quality analysis and assessment. Environ. Sci. Pollut. Res., 30(19): 54303–54323 **(21 pages)**.

Rana, R.; Ganguly, R., (2020). Water quality indices: challenges and applications—an overview. Arab. J. Geosci., 13(22): 1190 **(11 pages)**.

Rosas Baños, M.; García Salazar, E.M., (2026). Wastewater uses for agricultural production from weak and strong sustainability perspectives. Global J. Environ. Sci. Manage., 12(2): 667-686 **(20 pages).**

Singh, K.P.; Malik, A.; Mohan, D.; Sinha, S.; Singh, V.K., (2005). Chemometric data analysis of pollutants in wastewater: A case study. Anal. Chim. Acta, 532(1): 15–25 **(11 pages)**.

Syeed, M.M.M.; Hossain, M.S.; Karim, M.R.; Uddin, M.F.; Hasan, M.; Khan, R.H., (2023). Surface water quality profiling using the water quality index, pollution index and statistical methods: A critical review. Environ. Sustain. Indic., 18: 100247 **(23 pages)**.

Tyagi, S.; Sharma, B.; Singh, P.; Dobhal, R., (2013). Water quality assessment in terms of water quality index. Am. J. water Resour., 1(3): 34–38 **(5 pages)**.

Ukoha-Onuoha, E.; Horsfall, I.T., (2026). The evolution of wastewater reuse for irrigation: Lessons learned and future directions. Next Sustainable. 7: 100253 **(13 pages)**.

Verlicchi, P.; Masotti, L.; Galletti, A., (2011). Wastewater polishing index: a tool for a rapid quality assessment of reclaimed wastewater. Environ. Monit. Assess., 173(1–4): 267–277 **(11 pages)**.

Yan, T.; Shen, S.-L.; Zhou, A., (2022). Indices and models of surface water quality assessment: Review and perspectives. Environ. Pollut., 308: 119611 **(19 pages)**.

AUTHOR (S) BIOSKETCHES

E.R. Tarawneh, Ph.D., Assistant Professor, Civil and Environmental Engineering Department, Mutah University, Al-karak, Jordan.

- Email: *erat@mutah.edu.jo*
- ORCID: 0000-0003-4580-753X
- Web of Science Researcher ID: GLN-6252-2022
- Scopus Author ID: 57191833368
- Homepage: https://academic.mutah.edu.jo/erat/sitepages/Home.aspx

HOW TO CITE THIS ARTICLE:
Tarawneh, E.R., (2027). Multivariate and index-based evaluation of long-term reclaimed wastewater quality and reuse suitability. Global J. Environ. Sci. Manage., 13(1): 251-272.

DOI: 10.22034.gjesm.2027.01.12
URL: https://www.gjesm.net/article_735752.html

Global Journal of Environmental Science and Management
(GJESM)

Homepage: https://www.gjesm.net/

Podcasts

ORIGINAL RESEARCH ARTICLE

Environmental modeling of yellowfin tuna fishing grounds integrating oceanographic and biological parameters using generalized additive model

D. Simbolon[1], E.S.Y. Siregar[1,*], R.I. Wahju[1], I. Yulianto[1,2], V.P. Siregar[3], T.A. Pianto[4], Rosmasita[5], M.S. Sangadji[6], F. Andika[5], R.A. Mulyadi[5], M.Y.U. Putra[5], Rasidi[5]

[1]*Department of Fisheries Resources Utilization, Faculty of Fisheries and Marine Science, IPB University, Jl Raya Dramaga, Bogor, Jawa Barat, 16680 Indonesia*

[2]*Fisheries Resource Center of Indonesia, Rekam Nusantara Foundation, Jl Sempur, Bogor, West Java, 16129 Indonesia*

[3]*Department of Marine Science and Technology, Faculty of Fisheries and Marine Science, IPB University, Jl Raya Dramaga, Bogor, Jawa Barat, 16680 Indonesia*

[4]*Research Center for Limnology and Water Resources, National Research and Innovation Agency, Jl Jl Raya Jakarta, Cibinong, West Java, 16911 Indonesia*

[5]*Doctoral Program of Marine Fisheries Technology, Faculty of Fisheries and Marine Science, IPB University, Jl Raya Dramaga, Bogor, Jawa Barat, 16680 Indonesia*

[6]*Marine Technology Study Program, Faculty of Fisheries and Marine Science, IPB University, Jl Raya Dramaga, Bogor, Jawa Barat, 16680 Indonesia*

ARTICLE INFO

Article History:
Received 29 May 2026
Revised 05 August 2026
Accepted 11 September 2026

Keywords:
Environmental modeling
Fisheries management
Generalized additive model
Yellowfin tuna
Fishing grounds
Oceanographic variability

DOI:10. 22034.gjesm.2027.01.13

ABSTRACT

BACKGROUND AND OBJECTIVES: Marine environmental variability influences the distribution, productivity, and habitat suitability of yellowfin tuna (Thunnus albacares). However, fishing-ground assessment based primarily on environmental conditions or production may overlook the biological suitability of harvested fish. The study objectives were to develop an integrated generalized additive model framework for assessing yellowfin tuna fishing grounds. The framework combined oceanographic conditions and fishing operational factors with production potential and fish size through two complementary Generalized additive models.

METHODS: The study was conducted in the waters of West Sumatra, eastern Indian Ocean, Indonesia. Fisheries and oceanographic data covered 2019–2024, while biological observations covered 2019, 2020, and 2024. Oceanographic predictors included sea surface temperature, chlorophyll-a concentration, sea surface salinity, and sea surface height. Fisheries predictors included fishing year, month, gear, spatial location, and vessel capacity. A total of 8,771 yellowfin tuna fork-length measurements were analyzed. A fork length of 99 centimeters was used as the maturity-based threshold. Two complementary generalized additive models were developed. The Fishing Ground–Environment, Technology, and Production model used catch as the production response. The Fishing Ground–Environment, Technology, and Size model used fork length as the biological response.

FINDINGS: Sea surface temperature ranged from 29.37–30.45 degrees Celsius. Chlorophyll-a concentration ranged from 0.21–0.43 milligrams per cubic meter. Sea surface salinity ranged from 33.29–33.87 practical salinity units. Sea surface height ranged from 0.46–0.59 meters. Overall, 94 percent of fish were harvest-suitable. The production model had an Akaike information criterion of 155,482.9 and cumulative deviance explained of 11.5 percent. The size model had an Akaike information criterion of 77,913.73 and cumulative deviance explained of 28.74 percent. Medium to high fishing-ground potential occurred more frequently around the Mentawai Islands. Temporal integration identified highly potential and potential fishing-period statuses based on relative production potential and the landing-based biological size indicator.

CONCLUSION: The integrated generalized additive model framework links environmental conditions, fishing operations, production, and biological size. This approach provides a more selective basis for adaptive and sustainable management of yellowfin tuna fisheries.

This is an open access article under the CC BY license (http://creativecommons.org/licenses/by/4.0/)

NUMBER OF REFERENCES	NUMBER OF FIGURES	NUMBER OF TABLES
45	12	9

*Corresponding Author:
Email: emmasuriyantisiregar@gmail.com
Phone: +6823 8486 6054
ORCID: 0000-0003-2477-0950

INTRODUCTION

Marine environmental variability influences ecosystem structure, productivity, habitat suitability, and the distribution of pelagic species in tropical systems such as the eastern Indian Ocean (Ducklow *et al.,* 2022; Cartwright *et al.,* 2021). Yellowfin tuna (*Thunnus albacares*) is a highly migratory pelagic predator that responds to environmental variation, making it an important species for examining ecological responses to oceanographic variability (Siregar *et al.,* 2018; Fu *et al.,* 2025; Siregar *et al.,* 2025b). Understanding the relationship between environmental conditions and yellowfin tuna distribution is consequently important for environmental assessment and sustainable management of marine resources. Oceanographic variables, including sea surface temperature (SST), chlorophyll-a concentration (Chl-a), sea surface salinity (SSS), and sea surface height (SSH), represent important physical and biogeochemical characteristics of the marine environment. Their spatial and temporal variability reflects processes such as ocean circulation, water-mass dynamics, productivity gradients, and nutrient enrichment, which influence the distribution, abundance, and habitat utilization of pelagic fish (Siregar *et al.,* 2025a). SST represents thermal conditions, Chl-a provides an indicator of surface productivity, SSS reflects water-mass characteristics and salinity gradients, and SSH represents surface-ocean dynamics and spatial variability. These environmental variables have been used to examine yellowfin tuna distribution and potential fishing grounds, including GAM-based analysis in West Sumatra and remote-sensing-based assessment in the eastern Indian Ocean off Sumatra (Feng *et al.,* 2025; Siregar *et al.,* 2025a). Favorable combinations of these environmental conditions may therefore be associated with variation in yellowfin tuna occurrence and fishing activity. Consequently, SST, Chl-a, SSS, and SSH were selected as complementary oceanographic predictors for evaluating the associations between environmental variability, yellowfin tuna production, and fish size in the study area. However, environmental suitability alone does not necessarily indicate that fish occurring in these areas are biologically appropriate for harvesting or that the areas have high production potential. Biological characteristics provide an important complementary dimension for evaluating the suitability of marine resources. Fish size structure reflects population composition, ontogenetic development, habitat utilization, and ecological responses to environmental variability. Individuals of different sizes may exhibit different habitat preferences, swimming capabilities, feeding strategies, and responses to environmental conditions (Ostman *et al.,* 2023). Therefore, fish size can provide biological information that cannot be obtained from environmental variables, fish occurrence, or catch indicators alone. This consideration is particularly important for fisheries management because fish size is closely related to biological maturity and harvest suitability (Cacciamani *et al.,* 2025; Siregar *et al.,* 2026). Areas with favorable environmental conditions may contain fish that are not yet biologically suitable for harvesting and should therefore not automatically be classified as sustainable fishing grounds. The consideration of biological size is particularly relevant because harvesting immature fish can reduce the reproductive potential of fish populations and increase the risk of growth overfishing. Fish that have not reached an appropriate size for harvest may contribute substantially to future population recruitment and therefore require greater consideration in fisheries management (Mendoza *et al.,* 2024). Thus, the identification of fishing grounds based solely on oceanographic suitability may overestimate their suitability from a biological perspective. Integrating fish size with environmental information can provide a more comprehensive assessment of fishing-ground suitability and support management strategies that consider both resource availability and

biological sustainability. In addition to environmental and biological conditions, fishing technology and operational characteristics influence fishing distribution and production. Fishing gear, vessel capacity, effort, and temporal patterns affect fishing efficiency and vessels' ability to exploit areas under different environmental conditions. Consequently, fishing-ground assessment should consider environmental and biological suitability alongside fishing operations. However, these dimensions are commonly evaluated separately, limiting integrated assessment of fishing-ground suitability. Generalized additive models (GAMs) provide a flexible statistical framework for examining complex and nonlinear relationships between environmental predictors and biological or fisheries responses. Since the introduction of GAMs by Hastie and Tibshirani (1990), these models have been widely applied in ecological and fisheries research because they can accommodate nonlinear responses without requiring a predetermined functional form. GAMs have been used to investigate species–environment relationships, habitat suitability, abundance, and spatiotemporal patterns of pelagic fishes, including yellowfin tuna, bigeye tuna, skipjack tuna, and other commercially important species (Siregar *et al.,* 2018; Azeez *et al.,* 2021; Koropitan *et al.,* 2021; Wang *et al.,* 2022; Lin *et al.,* 2025). The flexibility of GAMs provides an appropriate basis for evaluating multiple environmental, biological, and fishing operational factors within complementary frameworks. Despite increasing GAM application in marine environmental modeling, most fishing-ground studies focus primarily on environmental indicators, fish occurrence, abundance, catch, or catch-per-unit-effort (CPUE). Recent studies have similarly emphasized environmental determinants and integrated resource assessment (Takrina *et al.,* 2023; Shahat *et al.,* 2026). Although these approaches effectively identify areas with favorable environmental conditions or higher fishing productivity, they provide limited information on whether fish are biologically appropriate for harvesting. Similarly, biological size structure is rarely incorporated as an explicit response variable, while fishing technology is often considered separately from environmental and biological conditions. Consequently, existing approaches may identify favorable or highly productive fishing areas without simultaneously evaluating biological suitability and operational characteristics. The novelty of this study lies in developing an integrated environmental modeling framework for yellowfin tuna fishing-ground assessment that combines oceanographic conditions, biological size, and fishing operational characteristics through two complementary GAMs. The first model, fishing ground–environment, technology, and production (FG-ETP), evaluates yellowfin tuna production in relation to environmental and fishing operational factors. The second model, fishing ground–environment, technology, and size (FG-ETS), evaluates yellowfin tuna size in relation to environmental and fishing operational factors using landing-based biological observations. The outputs of these models are integrated temporally to combine production potential with biological size suitability. Unlike conventional fishing-ground approaches emphasizing environmental suitability, catch, or productivity, the proposed framework incorporates production potential and biological size for a more comprehensive assessment of fishing-ground suitability. This integrated approach is consistent with recent resource-management frameworks incorporating environmental and human-use factors (Díaz-Ponce *et al.,* 2026). The integrated framework provides an exploratory approach for assessing yellowfin tuna fishing-ground potential by identifying statistical associations among environmental conditions, fishing operations, production, and biological size, but it does not by itself demonstrate management effectiveness or sustainable fisheries outcomes. This study aims to: 1) evaluate the relationships between oceanographic parameters, fishing technology,

and yellowfin tuna production using the FG-ETP model; 2) evaluate the relationships between oceanographic parameters, fishing technology, and yellowfin tuna fish size using the FG-ETS model; and 3) integrate the outputs of FG-ETP and FG-ETS temporally to characterize yellowfin tuna fishing periods according to production potential and biological size suitability. The study was conducted in the waters of West Sumatra, eastern Indian Ocean, Indonesia, using oceanographic and fisheries data covering 2019–2024, with biological fish-size observations available for 2019, 2020, and 2024.

MATERIALS AND METHODS

Study area and data sources

The study was conducted in the waters of West Sumatra, eastern Indian Ocean, Indonesia, between 11° north (N), –4° south (S) and 95°E–101° east (E) (Fig. 1), including the western Sumatran coastal waters and waters surrounding the Mentawai Islands. The study period was January–December 2024, while the datasets covered January 2019–December 2024. The study integrated environmental, fisheries, and biological datasets. Oceanographic data comprised SST, Chl-a, SSS, and SSH obtained from the Copernicus Marine Environment Monitoring Service (CMEMS) at 0.25° × 0.25° spatial and monthly temporal resolutions. Fisheries data were obtained from the PPS Bungus fishing logbook and included catch (C), fishing location, year, month, fishing gear, vessel capacity expressed as gross tonnage (GT), and fishing effort (E). Biological data comprised fork length (FL) and weight measurements of yellowfin tuna collected in 2019, 2020, and 2024, totaling 8,771 individuals. The 2019–2020 records were obtained from the PPS Bungus database, whereas 2024 measurements were collected during fish landings. Differences in sampling procedures among years may have contributed to variation in FL; therefore, year-related patterns were interpreted as differences in sampled landings rather than definitive changes in population size structure.

Environmental, biological, and fisheries data

The study used oceanographic, biological, and fisheries data from the waters of West Sumatra, eastern Indian Ocean, Indonesia. The four oceanographic variables SST, Chl-a, SSS, and SSH were obtained from CMEMS and processed using Ferret 7.6. Environmental datasets were checked for consistency in parameter definitions, units, and spatial and temporal coverage, then clipped to 1°N–4°S and 95°E–101°E. Monthly environmental fields were matched with fisheries observations by fishing year, month, and geographic location, with each observation assigned the corresponding 0.25° × 0.25° environmental grid cell. Biological observations were recorded at landing ports without equivalent fishing coordinates; therefore, they were not spatially matched with environmental fields or fishing locations but were aggregated monthly and integrated through the FG-ETS model. The fisheries dataset included yellowfin tuna catch (kg), fishing effort based on tuna handline operations, fishing gear, vessel capacity, fishing year and month, and geographic coordinates. CPUE was calculated using Eq. 1 (Chang *et al.*, 2011):

$$CPUE_i = \frac{Catch_i}{Effort_i} \quad (1)$$

Where: $CPUE_i$ is the catch per unit effort at observation *i*, C_i is yellowfin tuna catch, and E_i is fishing effort. CPUE was used as an indicator of relative fishing productivity, while the production GAM used catch in kilograms as the response variable. Standardized CPUE obtained through the FPI procedure was used to support the interpretation of relative fishing productivity and was not used as the response variable in the production GAM. Because different fishing gears have different catching capabilities, CPUE was

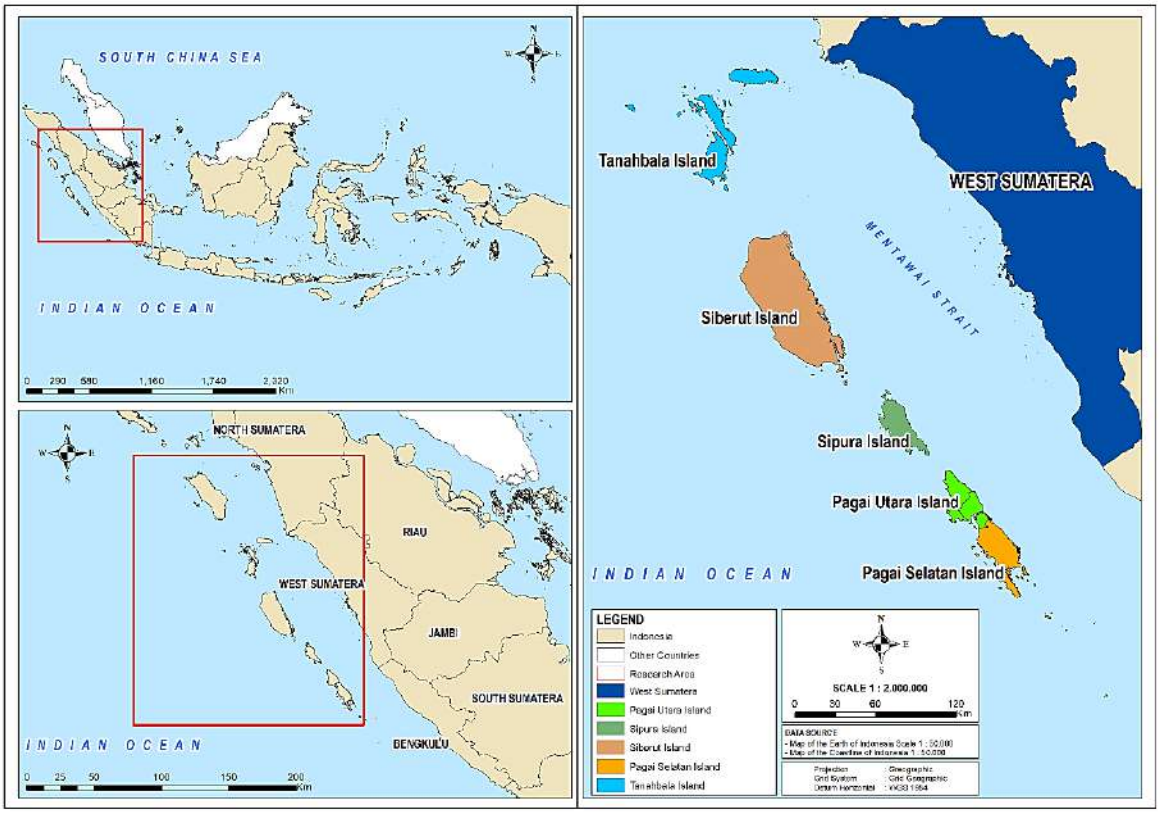

Fig. 1: Geographical location of the study area in the eastern Indian Ocean off West Sumatra, Indonesia

standardized using the Fishing Power Index (FPI), with tuna handline selected as the reference fishing gear. The FPI was estimated to account for differences in relative fishing power among gear types. The FPI was estimated to account for differences in relative fishing power among gear types. The FPI was determined using Eq. 2 (Sparre and Venema, 1998):

$$FPI = \frac{CPUE_r}{CPUE_s} \quad (2)$$

Where: CPUEr is the catch per unit effort of the fishing gear being standardized and CPUEs is the catch per unit effort of the reference fishing gear (tuna handline). The standardized CPUE was used to support the interpretation of relative fishing productivity, whereas fishing gear was retained as a categorical predictor in the GAM to account for gear-specific effects on the production response. Thus, FPI standardization and the gear effect in the GAM served different analytical purposes and were not applied as two successive corrections to the same response variable. CPUE calculation and FPI standardization were performed computationally in R. For the production GAM, fishing effort was incorporated as a log-transformed offset [log(EFFORT)] to account for differences in fishing intensity among observations. Biological observations consisted of 8,771 yellowfin tuna FL measurements collected in 2019, 2020, and 2024. Fork-length observations were available only for these three sampling years, whereas fisheries and environmental data covered the period from 2019 to 2024. The maximum observed FL was determined using Eq. 3 (Hasan *et al.*, 2021; Ostman *et al.*, 2023):

$$L_{max} = \max(FL) \quad (3)$$

Where: Lmax is the maximum observed FL and FL is the fork length of an individual fish. The asymptotic length (L_∞) was estimated using the empirical relationship in Eq. 4 (Laban *et al.,* 2024; Vicente and Palla, 2024; Nurdin *et al.,* 2025):

$$L_\infty = \frac{L_{max}}{0.99} \quad (4)$$

The length at first maturity (Lm) was subsequently estimated using Eq. 5 (Chen *et al.,* 2021; Morbey and Pauly, 2022):

$$\log_{10}(Lm) = -0.0782 + 0.8979 \log_{10}(L_\infty) \quad (5)$$

These empirical relationships provide a length-based approximation of L∞ and Lm,0.95 when direct biological maturity observations are unavailable. Because L∞ was derived from the maximum observed fork length of the landing sample, the resulting Lm,0.95 was interpreted as an empirical estimate for the sampled population rather than as a direct population-specific maturity estimate. The empirical relationships used for estimating Lmax and Lm were derived from previously reported length-based relationships and assume that the observed maximum length provides a reasonable basis for estimating the asymptotic length (Chen *et al.,* 2021; Hasan *et al.,* 2021; Morbey and Pauly, 2022). The calculation conducted in the present study yielded an estimated Lm,0.95 of 98.63 centimeters (cm) FL. The calculation conducted in the present study yielded an estimated Lm,0.95 of 98.63 cm FL. This value was operationally rounded to 99 cm FL and used as a biological maturity-based threshold for size classification in the present study. The resulting size categories are presented in Table 1. The 99 cm FL threshold was derived from the biological analysis conducted in the present study rather than adopted directly from previous studies. The classification was subsequently used as the biological criterion in the FG-ETS analysis and in the temporal integration of FG-ETP and FG-ETS (Siregar *et al.,* 2026).

Table 1: Biological size classification of yellowfin tuna based on the 99 cm FL threshold

Size category	Classification criterion
Below maturity-based threshold	FL < 99 cm
At or above maturity-based threshold	FL ≥ 99 cm

Environmental modeling using GAMs

Statistical modeling in this study was conducted using GAMs to quantify potentially nonlinear relationships between yellowfin tuna responses and environmental and fishing operational factors. GAMs were selected because of their ability to represent complex nonlinear relationships under spatially and temporally heterogeneous environmental conditions. The modeling procedure included data preparation and integration, specification of response and explanatory variables, model formulation, multicollinearity assessment, model selection, and model evaluation. The fisheries, biological, and environmental datasets were harmonized before analysis. The modeling framework incorporated yellowfin tuna responses, oceanographic variables, and fishing operational factors, with fork length representing the biological size response and catch representing the production response. Thus, the final FG-ETP model used catch as the response variable, with fishing effort incorporated as a log-transformed offset [log(EFFORT)]. CPUE and FPI-standardized CPUE were not used as response variables in the GAM. Catch was selected as the production response because it represents the realized fishing production, while the effort offset accounts for differences in fishing intensity among observations. This specification allows the model to estimate relative production potential while accounting for variation in fishing effort. The use of fisheries-dependent observations may introduce sampling bias because fishing activity can be concentrated in areas perceived as productive. This potential bias was not completely eliminated in the present study; therefore, the FG-ETP results were interpreted as relative production potential associated with observed

fishing activity rather than as unbiased estimates of environmental habitat suitability. The general form of the GAM was expressed using Eq. 6 (Hastie *et al.,* 1986; Wood, 2006; Simpson, 2024):

$$g(\mu_i) = \beta_0 + \sum_{k=1}^{p} s_k(X_{ik}) \quad (6)$$

Where: g(μi) is the link function relating the expected value of the response variable to the predictors, β0 is the model intercept, sk(X_{ik}) is the smoothing function for the k-th covariate, X_{ik} is the value of the k-th covariate for observation i, and p is the number of covariates included in the model. The additive formulation allows each covariate to contribute partially to the response without assuming a predetermined linear relationship (Hastie *et al.,* 1986; Wood, 2006; Simpson, 2024). Smoothing functions were applied to continuous variables to represent potentially non-linear relationships between predictors and responses, whereas categorical variables were included as factors without smoothing. The smooth functions allowed the models to identify nonlinear relationships and potential threshold-like changes in the responses across the observed ranges of the oceanographic variables. The relationships were evaluated from the estimated smooth terms, effective degrees of freedom (edf), test statistics, p-values, and partial-effect plots. Interaction terms were not systematically tested in the present study; therefore, the models were interpreted primarily as additive relationships among the selected predictors. The predictors included SST, Chl-a, SSS, SSH, fishing year, fishing month, fishing gear, fishing location, and vessel capacity, depending on the response variable being modeled. Multicollinearity among explanatory variables was assessed using the variance inflation factor (VIF), with VIF values below 5 considered indicative of no substantial multicollinearity. The fisheries and environmental datasets were checked for consistency in variable definitions, units, spatial and temporal coverage, and data completeness before fitting the GAMs. Environmental values were examined against their observed ranges, and biological measurements were checked for consistency with the recorded measurement units and observed length range. Candidate models were compared using Akaike's information criterion (AIC), cumulative deviance explained (CDE), where available, statistical significance, and ecological relevance (Mammel *et al.,* 2022; Gang *et al.,* 2023; Owiredu *et al.,* 2024). The best-supported model was selected based on the lowest AIC, higher explanatory performance, and adequate statistical and ecological support. Spatial and temporal autocorrelation were not explicitly tested or modeled in the present analysis; therefore, potential dependence among observations may remain and could affect parameter uncertainty and model performance. The modeling was implemented in R using the Mixed GAM Computation Vehicle (mgcv) package. The significance of smooth terms was evaluated using estimated degrees of freedom, reference degrees of freedom (Ref.df), test statistics, and p-values. Model diagnostics included assessment of residual patterns and model assumptions to evaluate model adequacy and reliability. Model adequacy was evaluated primarily using AIC, CDE, statistical significance of model terms, and examination of model residual patterns. The selected models were further interpreted based on the edf, Ref.df, test statistics, and p-values of the smooth terms. Given that the objective of the GAM analysis was to identify non-linear relationships between the response variables and environmental and fishing operational factors, the evaluation focused on model fit, explanatory performance, and residual patterns rather than on incorporating additional correlation structures.

Integration of FG-ETS and FG-ETP models

The outputs of FG-ETP and FG-ETS models were integrated to link yellowfin tuna production potential with fish-size suitability over the same periods. The FG-ETP model was used to characterize fishing-ground potential based on predicted yellowfin tuna production, whereas the FG-ETS model was used to characterize the

biological dimension based on monthly estimated marginal means (EMMs) of FL. Monthly EMMs of FL were estimated separately for each reference fishing gear, with other covariates and model terms accounted for according to the fitted FG-ETS model specification. The EMMs were not averaged across fishing gears, but were calculated separately to compare the predicted monthly FL patterns among the reference fishing gears. The EMM estimates were presented with 95% confidence intervals to indicate the uncertainty around the estimated monthly FL for each reference fishing gear. The integration was conducted temporally because the biological size data did not have spatial coverage equivalent to the fishing logbook data. Therefore, fish-size information was integrated according to the corresponding month rather than being spatially overlaid with the production predictions. A scoring approach was used to combine fishing-production potential and biological size suitability into a composite indicator. The normalized INDEX FG values ranged from 0 to 1 and were classified into three equal-interval categories: Low (0–0.33), Medium (0.34–0.66), and High (0.67–1.00), with scores of 1, 2, and 3, respectively. These thresholds were based on equal-interval classification of the normalized INDEX FG rather than on quantiles, natural breaks, standard deviations, or biological criteria. The FG-ETS biological output was classified according to the monthly EMMs of FL relative to the maturity-based threshold of 99 cm FL. Months with EMMs of FL < 99 cm were classified as below the maturity-based threshold and assigned a score of 1, whereas months with EMMs of FL ≥ 99 cm were classified as at or above the maturity-based threshold and assigned a score of 3. The binary scoring scheme was used to distinguish months below and at or above the maturity-based threshold, consistent with the objective of identifying periods in which the observed mean fish size was at or above the estimated maturity-based threshold. The score was applied to the monthly EMM rather than to individual fish, so the classification represents the average biological size condition of the monthly landings. The scoring criteria used for the two model outputs are presented in Table 2 (Criteria and scores for integration of FG-ETP and FG-ETS). The scores from the two models were then summed to obtain the total integrated score using Eq. 7 (Siregar *et al.,* 2026):

$$S_{total} = S_{FG-ETP} + S_{FG-ETS} \quad (7)$$

Where: Stotal is the total integrated score, SFG-ETP is the production-potential score, and SFG-ETS is the biological-size suitability score. The resulting total scores were used to classify fishing-ground status into three categories: Less Potential (2–3), Potential (4), and Highly Potential (5–6). The quantitative distinction among the categories was based on the predefined scoring scheme rather than on additional statistical significance testing. FG-ETP scores of 1, 2, and 3 represented Low, Medium, and High relative production potential, respectively, while FG-ETS scores of 1 and 3 represented fish sizes below and at or above the 99 cm maturity-based threshold, respectively. The total score therefore ranged from 2 to 6, with Potential corresponding to a total score of 4 and Highly Potential corresponding to scores of 5–6. Ecologically, Highly Potential represented periods combining relatively higher production potential with a biological size condition at or above the maturity-based threshold, whereas Potential represented a lower production-potential category while the biological size condition remained at or above the threshold. The classification of fishing-ground status based on the integrated score is presented in Table 3 (Classification of fishing-ground status based on the integrated score) (Syah *et al.,* 2020; Siregar *et al.,* 2026). A Less Potential fishing ground indicates that production potential and fish-size suitability do not simultaneously support fishing activity. A Potential fishing ground indicates a moderately favorable combination of production and biological suitability, whereas a highly potential

Table 2: Criteria and scores for integration of FG-ETP and FG-ETS

Indicator	Category	Score
FG-ETP	Low	1
	Medium	2
	High	3
FG-ETS	FL < 99 cm	1
	FL ≥ 99 cm	3

Table 3: Classification of fishing-ground status based on the integrated score

Total score	Fishing-ground status
2–3	Less Potential
4	Potential
5–6	Highly Potential

fishing ground represents high production potential supported by fish sizes that have reached the maturity-based threshold. The temporal integration was conducted for each month and subsequently interpreted according to the four monsoonal seasons. The resulting monthly status was used to strengthen the interpretation of fishing-ground potential by incorporating biological information into production-based fishing-ground assessment. Thus, the integrated approach identifies fishing periods not only according to production potential but also according to the biological suitability of the yellowfin tuna caught.

RESULTS AND DISCUSSION

Environmental and biological variability

The waters of West Sumatra exhibited pronounced spatial and temporal variability in oceanographic conditions during 2019–2024, with distinct characteristics among the coastal waters of West Sumatra, the Mentawai Islands, and the offshore waters of the Indian Ocean. Such variability is important for yellowfin tuna because oceanographic conditions influence habitat suitability, productivity, and the distribution of pelagic fish (Safruddin *et al.,* 2022). SST ranged from 29.37 to 30.45 degrees Celsius (°C), with relatively cooler conditions during the Northwest Monsoon. Temperatures increased during the First Transition Season and subsequently declined toward the Second Transition Season. The highest SST occurred in May, indicating that the First Transition Season represented the main warming phase of the study area (Fig. 2). Chl-a ranged from 0.21 to 0.43 milligrams per cubic meter (mg/m³), with concentrations increasing toward September–November (Fig. 3). SSS ranged from 33.29 to 33.87 practical salinity units (psu), with the highest values occurring during July–August (Fig. 4). SSH ranged from 0.46 to 0.59 meters (m) and reached its highest values during the First Transition Season before declining toward the Second Transition Season (Fig. 5). Spatially, the environmental parameters also showed clear differences among the coastal waters, the Mentawai Islands, and offshore waters (Figs. 2–5). Relatively higher SSH values during the First Transition Season extended across the coastal waters and much of the Mentawai Islands. Lower values became more widespread toward the offshore Indian Ocean during the Second Transition Season (Fig. 5). These spatial gradients reflect differences in water-mass characteristics and surface-ocean dynamics across the study region. The combined variation of SST, Chl-a, SSS, and SSH indicates that the study area comprises heterogeneous environmental conditions that vary systematically among seasons and regions. Such variability provides an ecological basis for the spatial and temporal responses of yellowfin tuna and supports the use of nonlinear environmental modeling (Wiryawan *et al.,* 2020; Wu *et al.,* 2022). Biological observations comprised 8,771 yellowfin tuna measured during 2019, 2020, and 2024. The FL frequency distributions for the three years are presented in Fig. 6, while the comparison of length-frequency distributions among years is shown in Fig. 7. The overall mean FL was 127.58 ± 19.64 cm, with annual mean FL values of 123.95 cm in 2019, 134.07 cm in 2020, and 131.23 cm in 2024. The size distributions were generally unimodal and dominated by medium- to large-sized individuals, with relatively few small fish. However, the dominant size class shifted among years, from 110–120 cm in 2019 to 140–150 cm in 2020 and 130–140 cm in 2024.

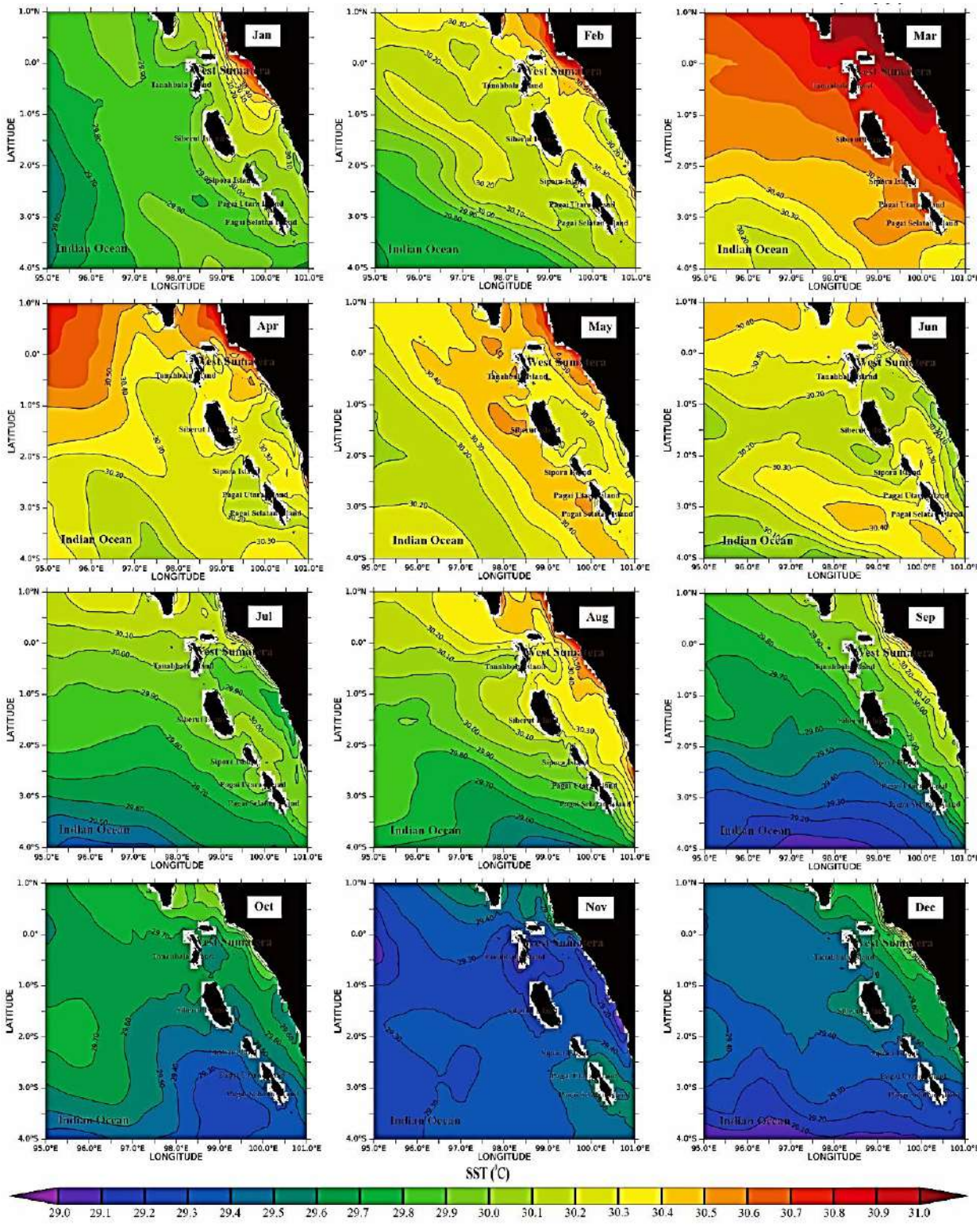

Fig. 2: Spatial distribution of SST based on monthly-averaged values aggregated over the period 2019, 2020, and 2024 in the waters of West Sumatra

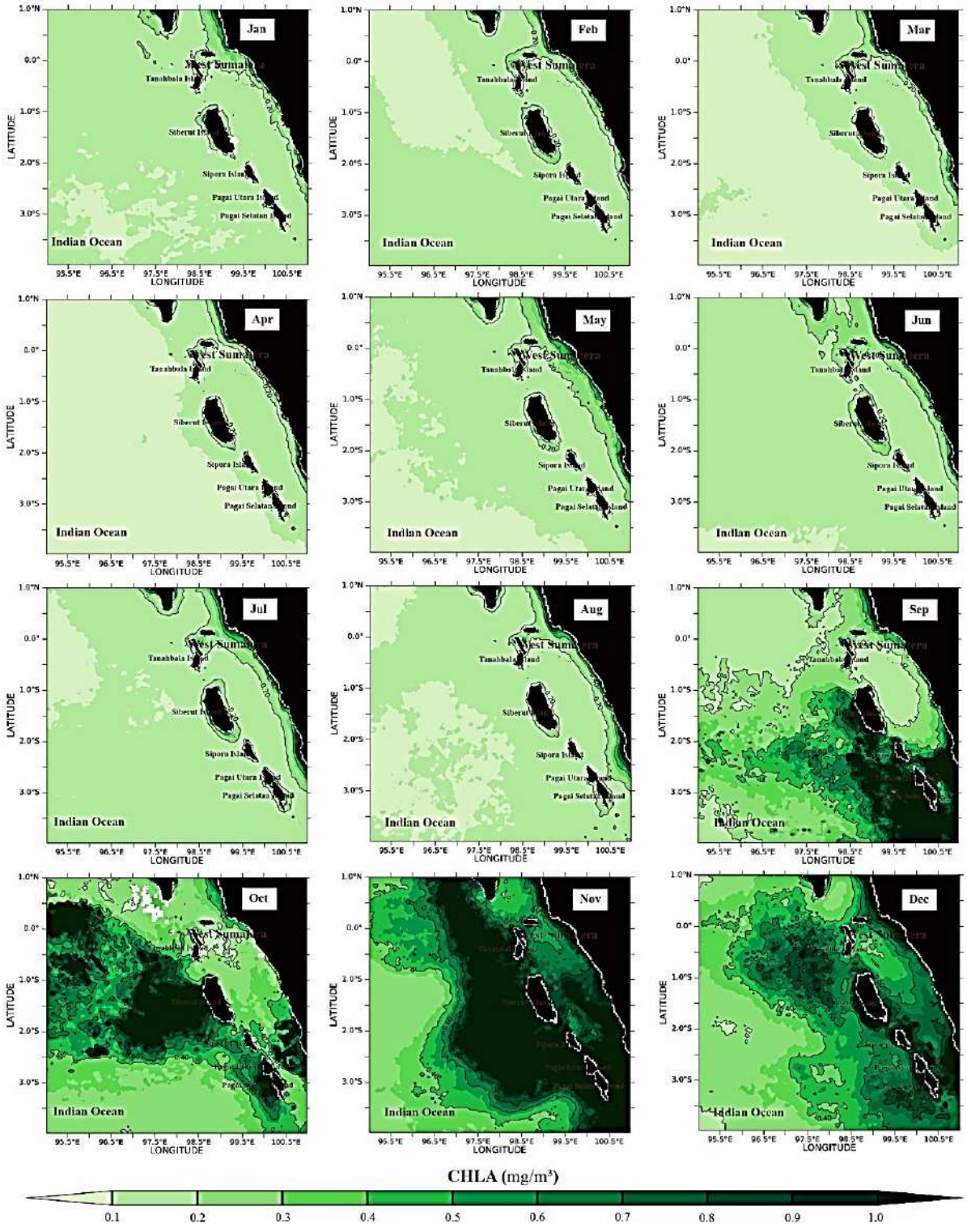

Fig. 3: Spatial distribution of multi-year monthly-averaged chlorophyll-a (2019, 2020, and 2024) in the waters of West Sumatra

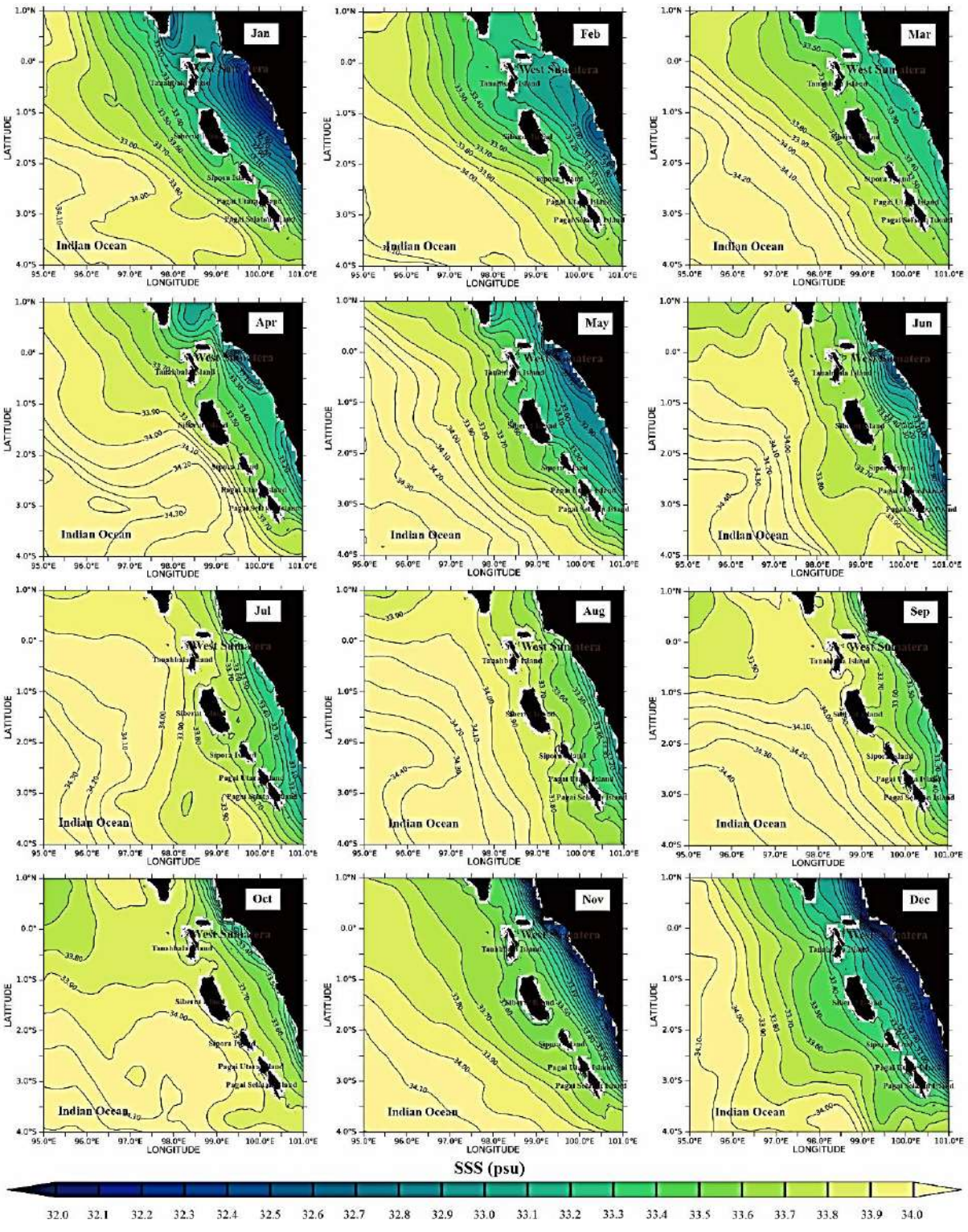

Fig. 4: Spatial distribution map of multi-year monthly-averaged sea surface salinity (2019, 2020, and 2024) in the waters of West Sumatra

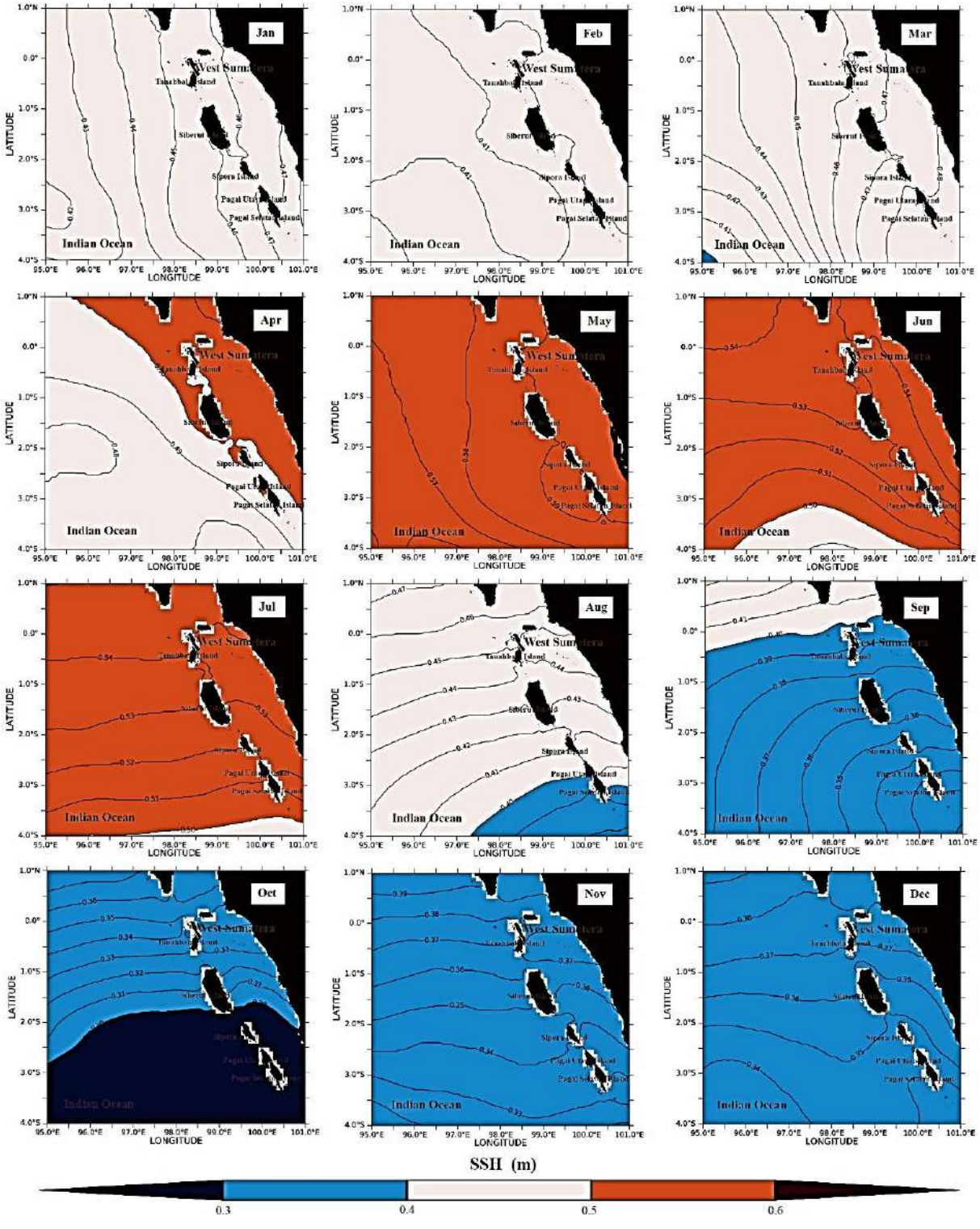

Fig. 5: Spatial distribution map of multi-year monthly-averaged sea surface height (2019, 2020, and 2024) in the waters of West Sumatra

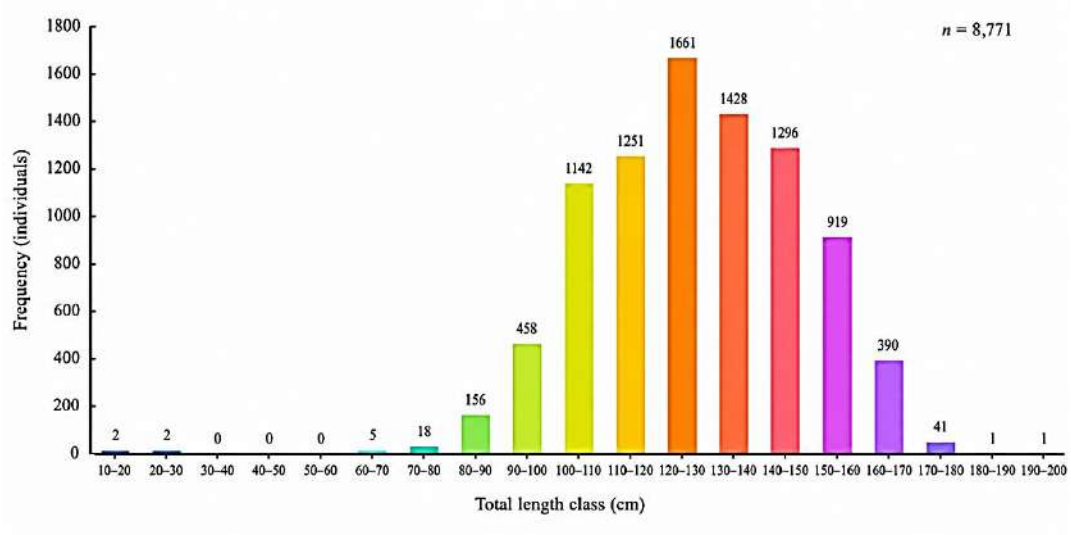

Fig. 6: FL frequency distribution of yellowfin tuna in 2019, 2020, and 2024

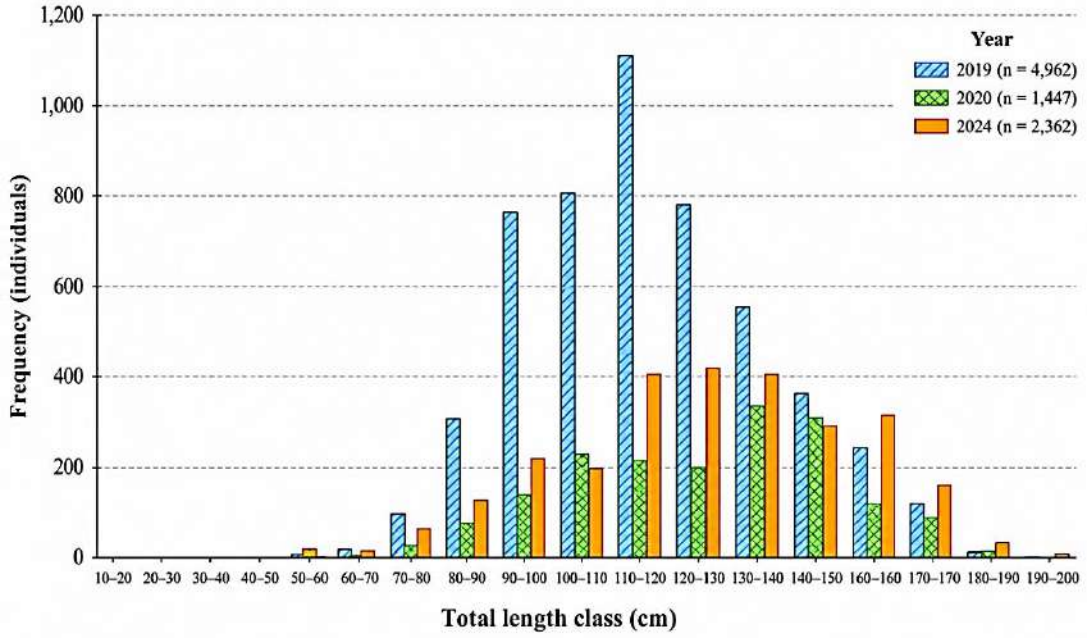

Fig. 7: Comparison of yellowfin tuna FL frequency distributions among years

This pattern indicates temporal variation in catch size structure while maintaining an overall dominance of medium- to large-sized fish. The biological parameters and estimated maturity-based threshold are summarized in Table 4. The estimated Lm,0.95 was 98.63 cm FL and was operationally rounded to 99 cm FL. Based on this maturity-based threshold, 8,207 individuals, representing 94 percent (%), were at or above the threshold, whereas 564 individuals (6%) were below the threshold (Fig. 8). The high proportion

Table 4: Biological parameters and estimated length at first maturity (Lm) of yellowfin tuna

Parameter	Value
Number of individuals (N)	8,771
Lmax (cm)	193
L∞ (cm)	203.16
Lm (cm)	98.63 (rounded to 99)

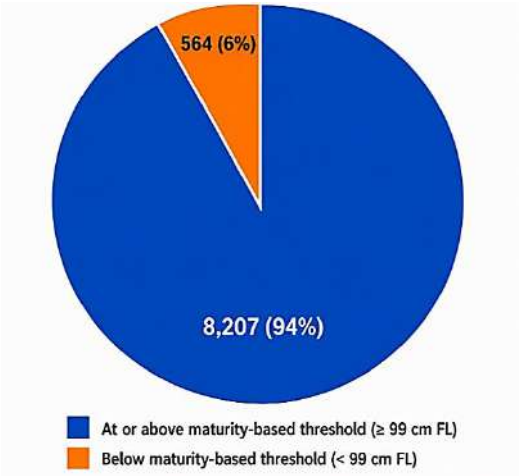

Fig. 8: Size composition of yellowfin tuna above and below the maturity-based threshold based on pooled data from 2019, 2020, and 2024

of fish at or above the maturity-based threshold indicates that sampled landings were predominantly composed of individuals meeting the selected criterion. However, this reflects only landing size composition and does not indicate stock sustainability, spawning biomass, fishing mortality, or recruitment status. Fish length provides an important indicator of size structure and growth stage (Hutubessy *et al.,* 2021; Ostman *et al.,* 2023). The 99 cm threshold, derived from estimated length at first maturity, was used to distinguish fish at or above the maturity-based threshold from those below it. Mean FL varied among gears, ranging from approximately 127 cm for tuna handline to 132 cm for troll line, 129 cm for purse seine, and 130 cm for tuna longline. The proportion of harvest-suitable fish ranged from 93.2% to 97.1%, suggesting that fishing technology contributed to variation in catch size composition, consistent with the role of gear selectivity in pelagic fish populations (Pechon *et al.,* 2022; Orbesen *et al.,* 2025). Overall, oceanographic variability represents the environmental dimension of fishing potential, while fish size provides a biological criterion for harvest suitability. These results provide the basis for subsequent GAM analysis of production and biological responses to environmental and fishing operational factors.

Environmental modeling using GAMs

The GAM analysis demonstrated that yellowfin tuna production and fish size were associated with a combination of environmental, temporal, spatial, and fishing operational factors rather than with a single predictor. The models incorporated SST, Chl-a, SSS, and SSH, together with fishing year, fishing month, fishing gear, GT, and spatial information. This combination is relevant because yellowfin tuna is a highly mobile pelagic species whose distribution and catch may vary with changing environmental conditions and fishing operations (Siregar *et al.,* 2018; Wu *et al.,* 2022; Vaihola *et al.,* 2023). Two response dimensions were evaluated to provide complementary information for fishing-ground assessment. Yellowfin tuna catch represented the production dimension, whereas FL represented the biological size dimension. These response variables describe different aspects of fishing-ground suitability because high production potential does not necessarily indicate that the fish present are biologically suitable for harvest, while favorable fish-size conditions alone do not indicate high fishing productivity. The VIF assessment for the FG-ETP model is presented in Table 5. The VIF values for the continuous covariates ranged from 1.12 to 3.03, with the lowest value observed for X4 (1.12) and the highest for X7 (3.03). All numerical

Table 5: Variance inflation factor (VIF) for the FG-ETP model

Code	Model Variable	VIF	Interpretation
X1	Fishing technology	1.26	No multicollinearity
X2	Fishing technology	2.64	Low multicollinearity
X3	Fishing technology	–	Categorical variable
X4	Fishing technology	1.12	No multicollinearity
X5	Fishing technology	1.30	No multicollinearity
X6	Environmental parameter	1.71	No multicollinearity
X7	Environmental parameter	3.03	Low multicollinearity
X8	Environmental parameter	2.58	Low multicollinearity
X9	Environmental parameter	1.78	No multicollinearity
X10	Fishing technology	1.20	No multicollinearity

Note: Y1 represents the response variable in the FG-ETP model. X3 is a categorical variable and therefore is not presented with a numerical VIF value like continuous covariates.

VIF values were below the threshold of 5, indicating no substantial multicollinearity among the continuous predictors used in the FG-ETP model. X3 was retained as a categorical predictor and therefore was not assigned a numerical VIF value. The relatively low VIF values indicate that the predictors provided relatively distinct information for explaining variation in yellowfin tuna production and support their joint inclusion in the GAM. Low multicollinearity is important because strong linear relationships among predictors can reduce estimation stability and complicate the interpretation of individual covariate contributions (Siregar, 2026). The candidate GAMs developed for yellowfin tuna production and fish size are presented in Table 6 and Table 7, respectively. The comparison of candidate models showed that retaining the environmental and fishing operational predictors generally improved model performance. For both response variables, removal of predictor terms resulted in higher AIC values and lower CDE values within the respective candidate-model comparisons. The selected models therefore retained the predictor combinations that provided the strongest statistical and ecological support for explaining yellowfin tuna production and fish size. Among the four candidate models, Model 1 was selected as the best-supported production model, with the lowest AIC (155,482.9) and highest CDE (11.5%). Sequential removal of predictors increased AIC and reduced CDE, indicating that the complete predictor structure provided the strongest performance. The selected model incorporated temporal, spatial, environmental, and fishing operational predictors and identified significant effects of the spatial smooth s(X4, X5), SSH, GT, SSS, SST, and Chl-a on yellowfin tuna production. The spatial smooth indicated spatial heterogeneity in production, while the environmental variables and GT reflected associations with oceanographic conditions and fishing operational capability. The partial-effect plots showed predominantly nonlinear relationships between the predictors and yellowfin tuna production (Fig. 9). Fishing year, month, and gear showed distinct responses, while the spatial smooth reinforced the spatial variation identified by the model. Chl-a, SST, SSH, and SSS also exhibited nonlinear responses across their observed ranges, with Chl-a varying rather than increasing continuously with production. SST also showed a curved response, indicating that yellowfin tuna production was associated with a range of thermal conditions rather than a simple linear increase. SSH and SSS similarly showed changes in the magnitude and direction of their partial effects across the observed ranges. These patterns support previous findings that yellowfin tuna responses are associated with interacting environmental gradients rather than a single environmental optimum (Siregar *et al.,* 2018; Wu *et al.,* 2022; Vaihola *et al.,* 2023). The partial effect of GT was also nonlinear, indicating that production did not increase proportionally across the entire range of GT. Production increased over

Table 6: Candidate GAMs for yellowfin tuna production

Model	Candidat model	Family	Link	AIC	CDE (%)
1	Y1 ~ X1 + X2 + X3 + s(X4, X5) + s(X6) + s(X7) + s(X8) + s(X9) + s(X10)	Negative Binomial (θ = 0.875)	log	155,482.9	11.5
2	Y1 ~ X1 + X2 + X3 + s(X4, X5) + s(X6) + s(X7) + s(X8) + s(X10)	Negative Binomial (θ = 0.871)	log	155,533.4	11.1
3	Y1 ~ X1 + X2 + X3 + s(X4, X5) + s(X6) + s(X7) + s(X10)	Negative Binomial (θ = 0.859)	log	155,714.4	9.98
4	Y1 ~ X1 + X2 + X3 + s(X4, X5) + s(X6) + s(X10)	Negative Binomial (θ = 0.857)	log	155,746.7	9.67

Note: Y1 = yellowfin tuna catch; X1 = fishing year; X2 = fishing month; X3 = fishing gear; X4 = longitude; X5 = latitude; X6 = Chl-a; X7 = SST; X8 = SSH; X9 = SSS; X10 = vessel capacity (GT); s(·) = smooth function; CDE.

Table 7: Candidate GAMs for yellowfin tuna fish size

No.	Pilihan model	Family	Link	AIC	CDE (%)
1	Y2 ~ X1 + X2 + X3 + X4 + s(X5) + s(X6) + s(X7) + s(X8) + s(X9)	Poisson	log	77,913.73	28.74
2	Y2 ~ X1 + X2 + X3 + X4 + s(X5) + s(X6) + s(X7) + s(X8)	Poisson	log	78,022.46	28.29
3	Y2 ~ X1 + X2 + X3 + X4 + s(X5) + s(X7) + s(X8)	Poisson	log	78,260.55	27.35
4	Y2 ~ X1 + X2 + X3 + X4 + s(X5) + s(X7)	Poisson	log	78,631.90	25.91
5	Y2 ~ X1 + X2 + X3 + X4 + s(X5)	Poisson	log	79,127.56	24.01

Y2 = yellowfin tuna FL; X1 = fishing year; X2 = fishing month; X3 = fishing gear; X4 = fish-size category; X5 = GT; X6 = SSH; X7 = Chl-a; X8 = SST; X9 = SSS; s(·) = smooth function; CDE = cumulative deviance explained.

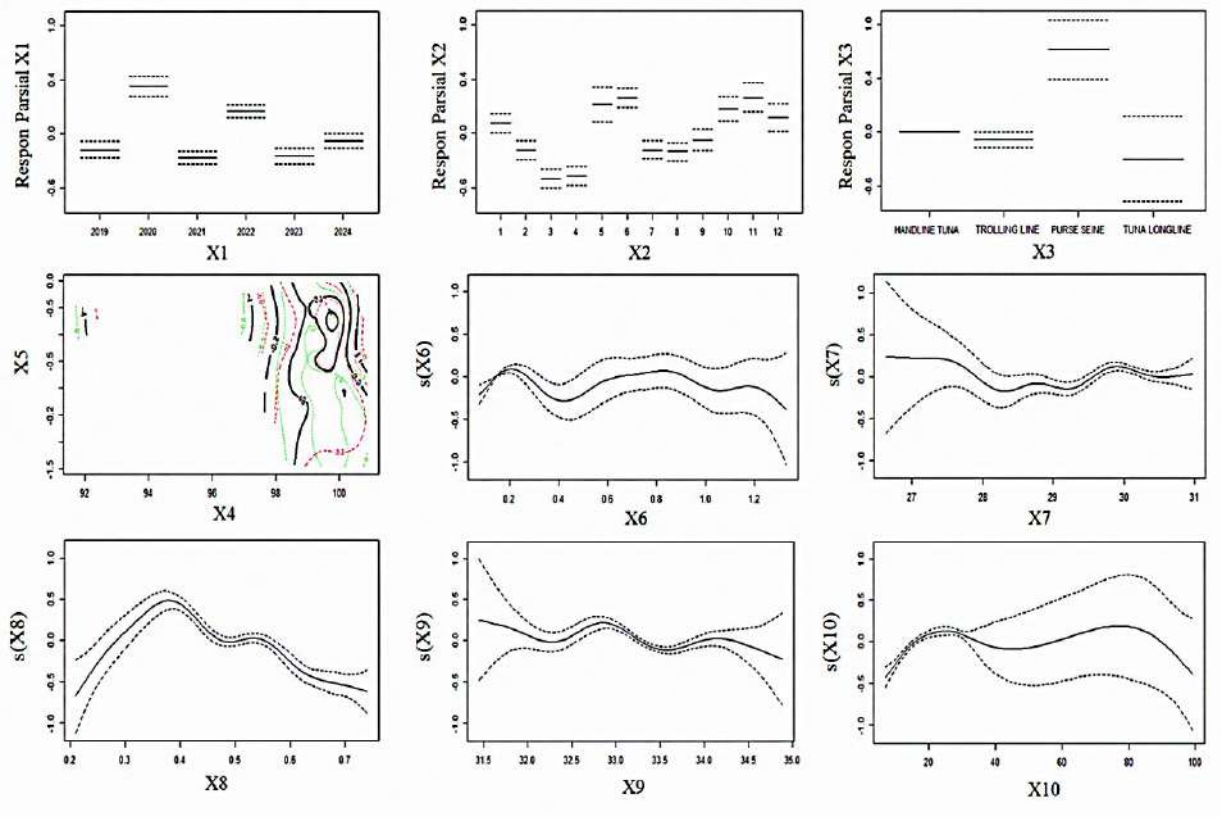

Fig. 9: Partial effects of environmental and fishing operational factors on yellowfin tuna production (Y_1) in the FG-ETP model. X1 = fishing year; X2 = fishing month; X3 = fishing gear; X4 = longitude; X5 = latitude; X6 = Chl-a; X7 = SST; X8 = SSH; X9 = sea surface salinity (SSS); and X10 = vessel capacity (GT)

part of the observed GT range before declining at higher values. This pattern indicates that realized production varied nonlinearly across the observed GT range. The association with GT should be interpreted as an operational relationship rather than a causal effect, because GT may be related to other fishing characteristics, including fishing gear, vessel type, fishing location, and fishing effort. The contribution of spatial and environmental terms indicates that realized production was associated with variation in environmental conditions and fishing operations. This is consistent with the ecological interpretation that yellowfin tuna distribution is related to oceanographic variability, while realized catch additionally depends on how fishing activities are conducted within these environmental conditions. Similar interactions among environmental and operational factors have been reported for pelagic tuna fisheries (Hua *et al.,* 2025). Despite the influence of these predictors, the selected production model explained 11.5% of cumulative deviance. The relatively low CDE indicates that a substantial proportion of production variability remained unexplained. Yellowfin tuna catch may also be affected by prey availability, fish aggregation behavior, fishing decisions, changes in fishing intensity, and other environmental or operational variables not included in the model. Similar complexity has been reported in pelagic fisheries, where environmental variability alone does not fully explain variations in catch and fishing performance (Wang *et al.,* 2023). Therefore, predicted production should be interpreted as relative production potential rather than as a deterministic prediction of catch. A limitation of the present study is that prediction uncertainty and the stability of the spatial classification were not quantified using confidence or prediction intervals. Consequently, the stability of areas classified as high potential under uncertainty could not be directly assessed. Future studies should incorporate spatial prediction uncertainty and sensitivity analysis to evaluate the robustness of fishing-ground classifications and identify areas that remain consistently classified as high potential when prediction uncertainty is considered. The VIF assessment for the FG-ETS model is presented in Table 8. The VIF values for the continuous covariates ranged from 1.28 to 5.21, with the lowest value observed for X5 (1.28) and the highest for X8 (5.21). Most VIF values were below the threshold of 5, indicating no substantial multicollinearity among most continuous predictors. X3 and X4 were retained as categorical predictors and therefore were not assigned numerical VIF values. The relatively low VIF values indicate that most predictors provided relatively distinct information for explaining variation in yellowfin tuna FL. However, the VIF value of X8 (5.21) indicated moderate multicollinearity, which should be considered when interpreting its contribution to the FG-ETS model. Model 1 was selected as the best-supported biological model, with the lowest AIC (77,913.73) and highest CDE (28.74%). Sequential removal of predictors increased AIC and reduced CDE, indicating that the complete predictor structure provided the strongest model performance. The selected size model identified SSS, SSH, GT, Chl-a, and SST as important predictors of yellowfin tuna FL, indicating associations with water-mass characteristics, surface-ocean dynamics, productivity, and thermal conditions (Wu *et al.,* 2022; Srioktoviana *et al.,* 2024). The partial-effect plots further demonstrated nonlinear relationships between fish size and the model predictors (Fig. 10). Fishing year showed differences in predicted FL among the observation years, while fishing month produced substantial variation across the annual cycle. These temporal effects indicate that the size structure of yellowfin tuna catches was not constant throughout the year or among observation years. Such variation may reflect changes in habitat use, movement, population composition, or the seasonal availability of different size groups. Fishing gear produced a pronounced difference in predicted FL**.** Handline, troll line, and purse seine showed relatively similar predicted fish sizes, whereas

Table 8: Variance inflation factor (VIF) for the FG-ETS model

Code	Model Variable	VIF	Interpretation
X1	Fishing technology	2.05	Low multicollinearity
X2	Fishing technology	4.82	Low multicollinearity
X3	Fishing technology	–	Categorical variable
X4	Fish biological factor	–	Categorical variable
X5	Fishing technology	1.28	No multicollinearity
X6	Environmental parameter	4.32	Low multicollinearity
X7	Environmental parameter	1.77	No multicollinearity
X8	Environmental parameter	5.21	Moderate multicollinearity
X9	Environmental parameter	2.03	Low multicollinearity

Note: Y2 is the response variable in FG-ETS; X3 and X4 are categorical variables and therefore have no numerical VIF values.

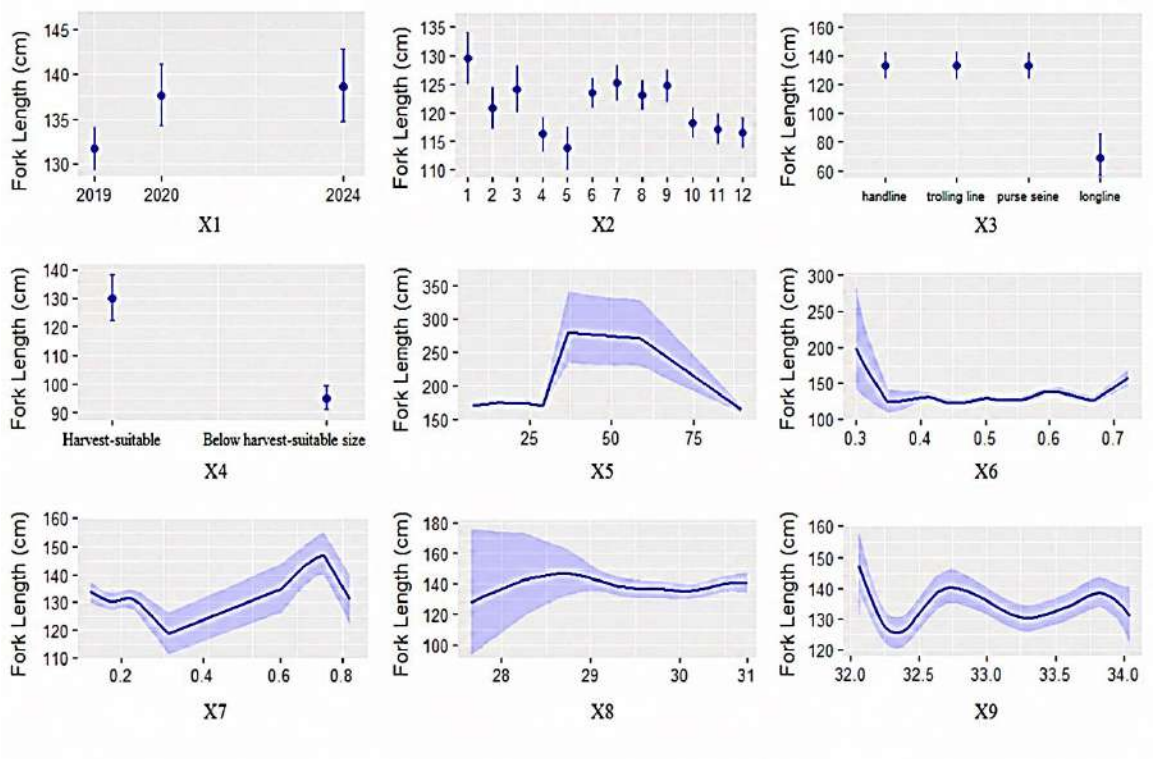

Fig. 10: Partial effects of biological, environmental, and fishing operational factors on yellowfin tuna fork length (Y_2) in the FG-ETS model. X1 = fishing year; X2 = fishing month; X3 = fishing gear; X4 = fish-size category; X5 = GT; X6 = SSH; X7 = Chl-a; X8 = SST; and X9 = SSS

tuna longline displayed a markedly lower response. The parametric results also showed different gear effects, including a positive coefficient for troll line and a negative coefficient for tuna longline relative to the reference gear. These findings indicate that fishing technology contributed to the size composition of the catch. Differences among gears may reflect variation in gear selectivity, fishing depth, fishing location, and operational strategy, consistent with previous evidence that gear characteristics influence the size structure of pelagic catches (Pechon *et al.,* 2022; Orbesen *et al.,* 2025). The fish-size category clearly distinguished predicted FL, with the harvest-suitable category showing substantially larger values than the below-harvest-suitable category. This distinction supports the subsequent fishing-ground integration based on the 99 cm FL maturity-based threshold. GT showed a nonlinear association with predicted FL, with fish size

increasing across part of the observed range before declining at higher vessel capacities. This relationship may reflect differences in fishing area, operational strategy, or gear characteristics associated with GT rather than a direct biological effect of vessel size. The environmental smooth terms also showed nonlinear responses. SSH initially declined before stabilizing, while Chl-a, SST, and SSS exhibited curved relationships with predicted FL across their observed ranges. These patterns indicate that fish size was associated with varying environmental conditions, consistent with the influence of thermal conditions, productivity, water-mass characteristics, and surface-ocean dynamics on habitat use and prey distribution. Ontogenetic differences may further influence the responses of different size groups (Srioktoviana *et al.,* 2024). The selected size model explained 28.74% of cumulative deviance within its candidate-model comparison. The remaining variation indicates that FL is also influenced by biological processes not explicitly included in the model, such as growth, population structure, movement, recruitment, and feeding ecology. The model should therefore be interpreted as describing relationships between environmental and operational factors and fish size rather than as a complete deterministic explanation of individual FL. Taken together, the two GAM analyses showed that yellowfin tuna production and fish size were associated with overlapping environmental, temporal, spatial, and fishing operational factors. The production model was designated FG-ETP, representing production potential, while the fish-size model was designated FG-ETS, representing biological suitability. Both responses showed nonlinear relationships with several predictors, supporting the use of GAMs. The complementary outputs of FG-ETP and FG-ETS provided the basis for subsequent spatial-temporal assessment and integration of production potential with biological size suitability. The spatial and temporal distribution of fishing-ground potential based on FG-ETP predictions is presented in Fig. 11. Because these predictions were not independently validated against withheld observations or an external dataset, they should be interpreted as model-based relative production potential rather than independently validated fishing-ground occurrence. Spatial or temporal cross-validation was not conducted and should be incorporated in future research to assess predictive performance and classification robustness. Spatially, moderate to high potential areas were predominantly concentrated around the Mentawai Islands and adjacent coastal waters, whereas offshore western areas generally showed lower potential. Temporally, fishing-ground potential varied among months. During the West Monsoon, relatively high potential areas occurred in December, followed by a reduction in January and February. During the First Transition Season, higher potential was particularly evident in March, while the distribution became more spatially variable in April and May. During the East Monsoon, moderate to high potential areas were more evident from June to August, particularly around the Mentawai Islands and adjacent waters. During the Second Transition Season, relatively high potential areas were again observed in September, followed by a gradual reduction in October and November. These spatial and temporal patterns indicate that yellowfin tuna fishing-ground potential was not uniformly distributed but varied according to the seasonal environmental and fishing conditions represented in the FG-ETP model. The concentration of predicted potential fishing grounds around the Mentawai Islands suggests that this region may provide relatively favorable conditions for yellowfin tuna production. The temporal shifts in predicted fishing-ground distribution indicate that fishing-area suitability varies throughout the annual cycle. However, the predicted values represent model-based relative production potential rather than deterministic fish abundance or definitive fishing-ground classifications, as FG-ETP explained only 11.5% of cumulative deviance and was not independently validated against withheld or external observations. Spatial or

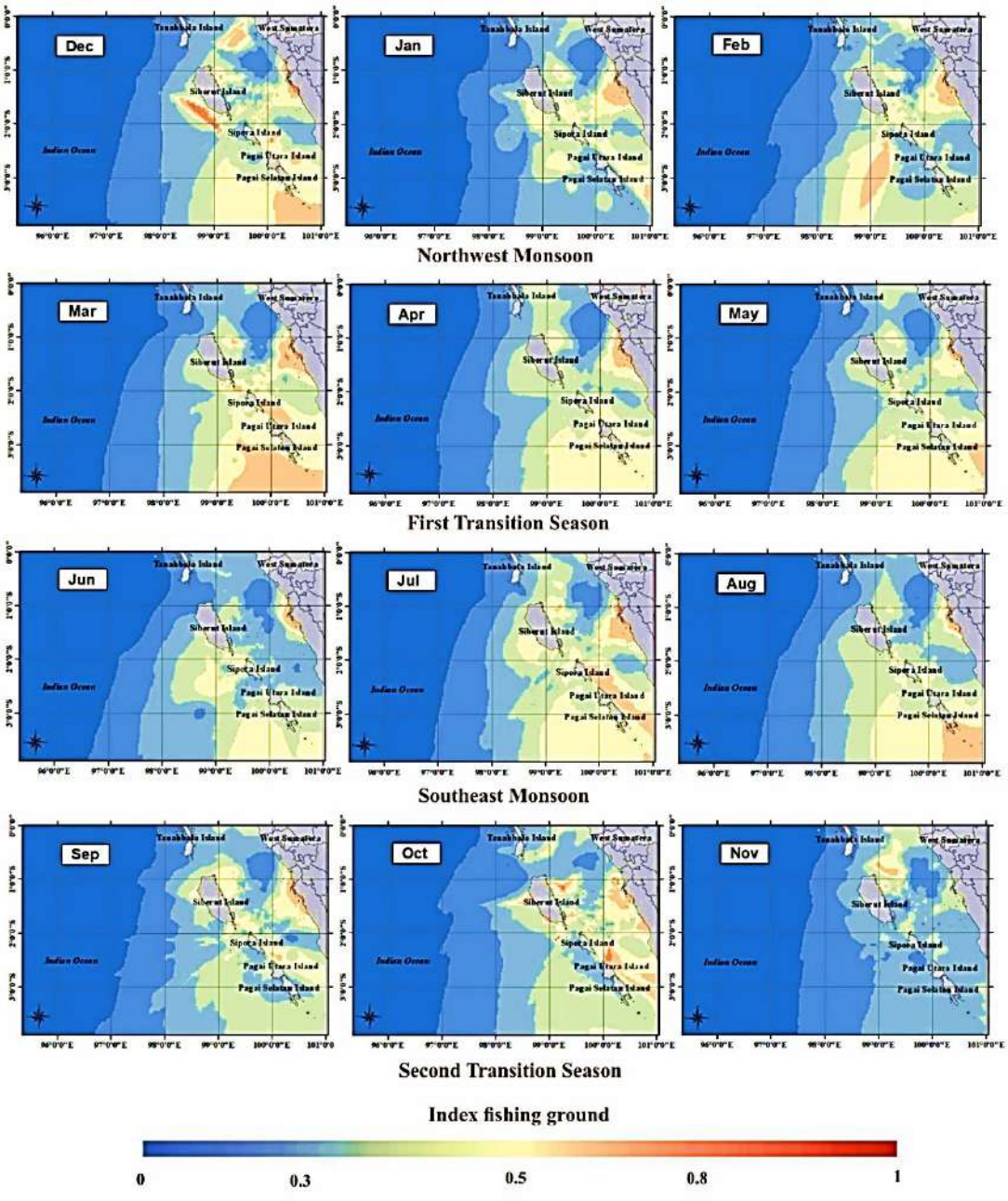

Fig. 11: Spatial and temporal distribution of yellowfin tuna fishing-ground potential based on predictions from the FG-ETP model in the waters of West Sumatra

temporal cross-validation was not conducted, and prediction uncertainty was not quantified; therefore, the generalizability and stability of the spatial classifications remain uncertain, particularly in unsampled areas. The estimated marginal means (EMMs) of yellowfin tuna fork length (FL) from FG-ETS varied among months and reference fishing gears (hand line tuna, pancing tonda, purse seine, and tuna longline), with confidence intervals indicating uncertainty in the estimates (Fig. 12). The temporal pattern was generally similar across gears: FL was relatively

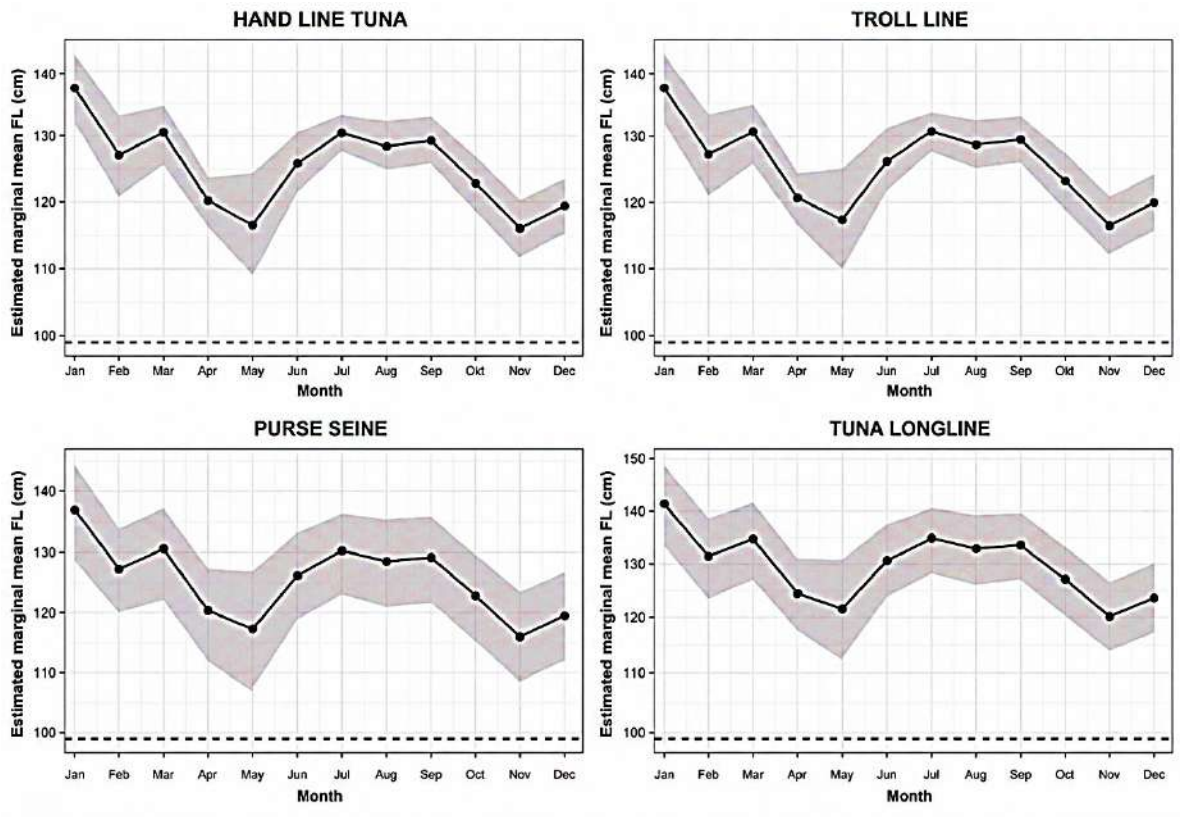

Fig. 12: Monthly estimated marginal means of fork length (FL) of yellowfin tuna based on the FG-ETS model for four reference fishing gears. The shaded areas represent confidence intervals, and the dashed line indicates the 99 cm FL maturity-based threshold

high in January, decreased in February, increased in March, declined during April–May, increased from June to September, and declined again during October–November before a slight increase in December. During the West Monsoon, January showed the highest estimated FL (approximately 136–141 cm), followed by lower values in February (127–132 cm); December remained slightly higher than the November minimum but below January.

Temporal integration of fishing-ground production potential and biological size suitability

The temporal integration of FG-ETP and FG-ETS combined yellowfin tuna production potential with the biological size condition on a monthly basis. The biological observations were obtained at the landing port and were not associated with fishing coordinates equivalent to those recorded in the fisheries logbook. Therefore, the integration was performed temporally rather than through direct spatial overlay. The study did not quantitatively evaluate spatial agreement or mismatch between FG-ETP production potential and the FG-ETS biological size condition. Instead, the integration compared the two dimensions at the monthly temporal scale, with FG-ETP representing relative spatial production potential and FG-ETS representing the biological size condition of landed yellowfin tuna. Consequently, the integrated categories represent temporal correspondence between production potential and biological size condition rather than direct spatial overlap. The integrated results showed that fishing-ground status varied among months, whereas the biological size component remained consistently high throughout the study period overall (Table 9).

Table 9: Temporal integration of FG-ETP and FG-ETS for yellowfin tuna fishing-ground status

Season	Month	FG-ETP category	Score	FG-ETS category	Score	Total score	Fishing-ground status
Northwest monsoon	December	High	3	High	3	6	Highly potential
	January	Medium	2	High	3	5	Highly potential
	February	Medium	2	High	3	5	Highly potential
First transition season	March	High	3	High	3	6	Highly potential
	April	Low	1	High	3	4	Potential
	May	Low	1	High	3	4	Potential
Southeast monsoon	June	Medium	2	High	3	5	Highly potential
	July	Medium	2	High	3	5	Highly potential
	August	Medium	2	High	3	5	Highly potential
Second transition season	September	Medium	2	High	3	5	Highly potential
	October	Low	1	High	3	4	Potential
	November	Low	1	High	3	4	Potential

Note: FG-ETS categories were determined from monthly EMMs of fork length (FL) relative to the 99 cm maturity-based threshold. All months were classified as high because the EMMs FL for the four reference fishing gears remained above 99 cm.

During the Northwest Monsoon, December was classified as Highly Potential, while January and February remained Highly Potential despite lower production-potential categories. During the First Transition Season, March was Highly Potential, whereas April–May were Potential. During the East Monsoon, June–August was consistently Highly Potential. In the Second Transition Season, September was Highly Potential, while October–November were Potential. As shown in Table 9, Highly Potential status occurred during December–March and June–September, when higher production potential coincided with fish sizes at or above the maturity-based threshold. April–May and October–November was classified as Potential because production potential was lower, while biological size remained above the threshold. Thus, temporal variation in integrated status was primarily associated with FG-ETP, whereas FG-ETS remained in the higher category throughout the evaluated months. The consistently high FG-ETS classification indicates that monthly EMMs of FL remained above the 99 cm maturity-based threshold. Although mean FL differed among sampling years, classification was based on monthly EMMs relative to the threshold rather than pooled individual observations. Therefore, the consistently high classification reflects the monthly mean size condition of the available observations and does not imply identical size distributions among years. Consequently, differences in integrated fishing-ground status were primarily associated with changes in FG-ETP production potential. This indicates that production potential varied seasonally even when the biological size condition remained favorable. The absence of the Less Potential category resulted from the consistently high biological suitability score, with 94% of sampled yellowfin tuna at or above the 99 cm maturity-based threshold. Thus, monthly changes between Highly Potential and Potential were primarily determined by FG-ETP production potential. The 94% proportion reflects the sampled landings and should not be interpreted as evidence of population-wide size structure or sustainable exploitation. The composite categories represent relative fishing-ground potential based on the predefined scoring framework and were not independently validated against fishing success or fisheries-management indicators. Highly Potential periods represented higher production potential coinciding with fish reaching the maturity-based threshold, whereas Potential periods had lower production potential despite suitable fish size. This integration adds a biological dimension to conventional fishing-ground assessment based on environmental suitability, catch, or fishing productivity and strengthens the interpretation of fishing potential

from a sustainability perspective (Hutubessy *et al.,* 2021; Ostman *et al.,* 2023). The combined assessment of production potential and fish size provides a more comprehensive basis for identifying fishing periods that are both productive and biologically appropriate.

Environmental and fisheries management implications

The results demonstrate that yellowfin tuna fishing grounds in the waters of West Sumatra are dynamic in both space and time and cannot be represented by a single permanent fishing zone. The relatively higher production potential observed around the Mentawai Islands and during specific periods, particularly December and March, indicates that environmental variability should be incorporated into adaptive fishing-ground management. Changes in SST, Chl-a, SSS, and SSH may alter environmental conditions and consequently influence the spatial and temporal patterns of modeled fishing production potential (Siregar *et al.,* 2018; Wu *et al.,* 2022; Hua *et al.,* 2025). The identified oceanographic conditions provide context for spatial and temporal variation in fishing-ground potential. Areas and periods with relatively higher FG-ETP production potential can be prioritized for fisheries monitoring and seasonal fishing planning, while the consistently high FG-ETS component provides a biological reference based on the 99 cm FL maturity-based threshold. Temporal integration therefore links environmental conditions, production potential, and fish-size composition, supporting management attention to relatively productive periods while maintaining size monitoring. However, these implications represent potential management applications rather than demonstrated effects because spatial predictions were not independently validated and biological observations were not spatially matched with fishing locations. The higher potential around the Mentawai Islands and during selected periods may reflect the combined statistical association of production with SST, Chl-a, SSS, and SSH, representing thermal conditions, productivity, water-mass characteristics, and surface-ocean dynamics. However, these relationships represent statistical associations rather than demonstrated causal mechanisms, and the low CDE of FG-ETP indicates that other factors contribute to the observed patterns. The integration of FG-ETP and FG-ETS indicates that fishing-ground assessment should consider both production potential and biological suitability. All evaluated months had fish sizes above the 99 cm FL maturity-based threshold, while differences in fishing-ground status were primarily associated with temporal changes in production potential. This approach distinguishes periods of relatively high production supported by biologically suitable fish from periods with lower production potential (Hutubessy *et al.,* 2021; Ostman *et al.,* 2023). From a fisheries management perspective, areas with higher FG-ETP potential can be prioritized for monitoring, while Highly Potential periods can support seasonal fishing planning. The 99 cm FL threshold provides a biological reference for monitoring landed yellowfin tuna. Areas with lower production potential should not automatically be considered unfavorable habitats because the model represents relative potential rather than deterministic catch. The relatively low CDE (11.5%) highlights the importance of prediction uncertainty; therefore, predicted fishing-ground patterns should be considered decision-support information rather than definitive representations of fish abundance or catch. The exclusion of additional environmental and habitat descriptors, including dissolved oxygen, ocean currents, mixed-layer depth, primary productivity, bathymetry, and prey-related variables, may have limited the representation of processes associated with yellowfin tuna distribution. These variables provide information not fully represented by SST, Chl-a, SSS, and SSH. Consequently, the identified patterns represent relative model-based associations within the selected predictor set rather than a complete representation of habitat

suitability. Future studies could incorporate additional physical, biological, and habitat descriptors with appropriate model comparison and validation. The scientific novelty of this study lies in integrating production potential and biological size with environmental and fishing operational information within a unified fishing-ground assessment framework. FG-ETP represents the spatial dimension of relative production potential, while FG-ETS represents the monthly biological-size dimension based on the maturity-based threshold; their integration evaluates whether higher production potential coincides with biologically suitable fish. This framework extends conventional assessments based primarily on environmental conditions or fishing production by combining four complementary dimensions: environmental conditions, fishing operations, production potential, and biological size. However, it remains an exploratory decision-support approach because biological observations were obtained from landings without spatial matching to fishing locations, and FG-ETP had relatively low explanatory performance. Future studies should incorporate longer time series, repeated biological sampling, climate-related indicators, and fishing-pressure measures using time-varying or spatiotemporal GAMs to strengthen fisheries assessment.

CONCLUSION

The study demonstrates that yellowfin tuna fishing-ground suitability in the waters of West Sumatra is associated with environmental variability, fishing operations, production potential, and biological size. Environmental conditions ranged from 29.37–30.45 °C for SST, 0.21–0.43 mg/m³ for Chl-a, 33.29–33.87 PSU for SSS, and 0.46–0.59 m for SSH. Among 8,771 measured fish, mean FL was 127.58 cm, with 8,207 individuals (94%) at or above the 99 cm FL maturity-based threshold, demonstrating the complementary value of biological size in fishing-ground assessment. The selected FG-ETP model identified spatial variation, SSH, GT, SSS, SST, and Chl-a as influential predictors of production, while FG-ETS identified SSS, SSH, GT, Chl-a, and SST as important predictors of FL, with temporal and fishing-gear effects also contributing. The nonlinear responses indicate that production and fish size were not proportionally related to individual predictors. FG-ETP and FG-ETS therefore provided complementary information for fishing-ground assessment. Their CDE values were 11.5% and 28.74%, respectively, indicating meaningful relationships but substantial unexplained variation. Consequently, the outputs should be interpreted as relative model-based patterns rather than deterministic estimates of fish abundance or catch, particularly in areas with limited observations where prediction uncertainty was not independently quantified. Relatively higher fishing-ground potential occurred more frequently around the Mentawai Islands and adjacent waters, while lower potential generally occurred offshore toward the west. Potential also varied seasonally, with relatively higher production potential particularly evident in December and March. These findings can support seasonal fishing planning and effort allocation, while the 99 cm FL maturity-based threshold provides a biological reference for monitoring landed fish size and supporting selective fishing practices. Temporal integration of FG-ETP and FG-ETS produced two fishing-ground statuses: Highly Potential and Potential. The absence of the Less Potential category resulted from the consistently high biological suitability component. Highly Potential periods combined relatively higher production potential with fish sizes above the 99 cm FL threshold, whereas Potential periods had lower production potential despite suitable fish size. This integration demonstrates the value of combining production potential with biological size in fishing-ground assessment. The findings support an adaptive and selective approach to fisheries management in the waters of West Sumatra. Fishing-ground management should

consider changing spatial and seasonal conditions rather than fixed fishing zones, while lower predicted potential should not automatically be interpreted as unfavorable habitat because of the relatively low CDE of FG-ETP. Other factors, including prey availability, fish aggregation, population structure, movement, recruitment, and fishing decisions, may contribute to unexplained variation. Overall, the proposed framework extends conventional fishing-ground assessment by integrating environmental conditions, fishing operations, production potential, and biological size through complementary GAMs, providing a basis for identifying fishing periods according to relative production potential and biological harvest suitability while recognizing uncertainty in model-based predictions.

AUTHOR CONTRIBUTIONS

E.S.Y. Siregar, the corresponding author, conceptualized the study, conducted data processing and analysis, developed the GAMs, prepared the maps and figures, interpreted the results, and prepared the manuscript. D. Simbolon supervised the research, contributed to the study design and methodology, and critically reviewed the manuscript. R.I. Wahju contributed to the fisheries methodology, data interpretation, and manuscript review. I. Yulianto contributed to fisheries data analysis, interpretation of the results, and manuscript review. V.P. Siregar contributed to spatial analysis and interpretation of fishing-ground distribution. T.A. Pianto contributed to data analysis and interpretation. Rosmasita contributed to data processing and manuscript review. M.S. Sangadji contributed to fisheries data analysis and interpretation. F. Andika contributed to data processing and analysis. R.A. Mulyadi contributed to data processing and interpretation. M.Y.U. Putra contributed to data processing and manuscript review. Rasidi contributed to data processing and manuscript review. All authors reviewed and approved the final version of the manuscript.

ACKNOWLEDGEMENT

This study was financially supported by the Indonesia Endowment Fund for Education (LPDP) and the Indonesian Education Scholarship (BPI) under the following funding decision numbers: [SKPB3734/LPDP/LPDP.3/2024;
01014/BPPT/BPI.06/9/2023;
00433/BPPT/BPI.06/9/2023;
02418/BPPT/BPI.06/9/2023;
00663/BPPT/BPI.06/9/2023;
and 02342/BPPT/BPI.06/9/2023]. The authors gratefully acknowledge the financial support provided through these scholarship programs. The authors also sincerely thank the Center for Higher Education Funding and Assessment (PPAPT) and the Ministry of Education, Science, and Technology (Kemdiktisaintek), Indonesia, for their administrative support and assistance throughout the scholarship and research process. The authors further express their sincere appreciation to the supervisors for their invaluable guidance, constructive suggestions, and continuous support throughout the research and preparation of this manuscript.

CONFLICT OF INTEREST

The authors declare that there is no conflict of interest regarding the publication of this manuscript. The authors also declare that no ethical issues, including plagiarism, informed consent, misconduct, data fabrication and/or falsification, duplicate publication and/or submission, or redundancy, are involved in this study.

OPEN ACCESS

©2027 The author(s). This article is licensed under a Creative Commons Attribution 4.0 International License, which permits use, sharing, adaptation, distribution and reproduction in any medium or format, as long as you give appropriate credit to the original author(s) and the source, provide a link to the Creative Commons license, and indicate if changes were made. The images or

other third-party material in this article are included in the article's Creative Commons license, unless indicated otherwise in a credit line to the material. If material is not included in the article's Creative Commons license and your intended use is not permitted by statutory regulation or exceeds the permitted use, you will need to obtain permission directly from the copyright holder. To view a copy of this license, visit: http://creativecommons.org/licenses/by/4.0/

PUBLISHER'S NOTE

GJESM Publisher remains neutral regarding jurisdictional claims with regard to published maps and institutional affiliations.

POSITIVE AI STATEMENT

During the preparation of this work, the author(s) have used Artificial Intelligence [ChatGPT] in order to language editing and proofreading. After using this tool/service, the authors reviewed and edited the content as needed and take full responsibility for the content of the publication.

ABBREVIATIONS

%	Percent
°C	Degree Celsius
AI	Artificial intelligence
AIC	Akaike's information criterion
BPI	Indonesian Education Scholarship
C	Catch
CDE	Cumulative deviance explained
Chl-a	Chlorophyll-a concentration
cm	Centimeter
CMEMS	Copernicus Marine Environment Monitoring Service
CPUE	Catch per unit effort
E	Fishing effort
edf	Estimated degrees of freedom
EMMs	Estimated marginal means
FG-ETP	Fishing Ground–Environment, Technology, and Production
FG-ETS	Fishing Ground–Environment, Technology, and Size
FL	Fork length
FPI	Fishing power index
GAM	Generalized additive model
GT	Gross tonnage
kg	Kilogram
km	Kilometer
L∞	Asymptotic length
Lm	Length at first maturity
Lm,0.95	Length at which 95% of individuals reach maturity
Lmax	Maximum observed length
LPDP	Indonesia Endowment Fund for Education
m	Meter
mg/m³	Milligrams per cubic meter
mgcv	Mixed GAM Computation Vehicle
n	Number of observations
PSU	Practical salinity unit
R²	Coefficient of determination
Ref.df	Reference degrees of freedom
SD	Standard deviation
SSH	Sea surface height
SSS	Sea surface salinity
SST	Sea surface temperature
VIF	Variance inflation factor

REFERENCES

Azeez, P.A.; Raman, M.; Rohit, P.; Shenoy, L.; Kumar, A.; Mohammed, K.; Damodaran, D., (2021). Predicting potential fishing grounds of ribbonfish (Trichiurus lepturus) in the north-eastern Arabian Sea, using remote sensing data. Int. J. Remote Sens., 42(1): 322–342 **(21 pages).**

Cacciamani, R.; Caserta, V.; Guizzardi, S.; Santojanni, A.; Colella, S.; Domenichetti, F.; Donato, F.; Angelini, S., (2025). How fishing pressures and environmental changes can impact the mean size of fish resources: A case study of small pelagics in the Adriatic Sea. Front. Mar. Sci., 170(12): 1–19 **(19 pages).**

Cartwright, P.J.; Fearns, P.R.C.S.; Branson, P.; Cuttler, M.V.W.; O'Leary, M.; Browne, N.K.; Lowe, R.J., (2021). Identifying metocean drivers of turbidity using 18 years of MODIS satellite data: Implications for marine ecosystems under climate change. Remote Sens., 13(3): 1–27 **(27 pages).**

Chang, S.; Hoyle, S.; Liu, H., (2011). Catch rate standardization for yellowfin tuna (Thunnus albacares) in Taiwan's distant-water longline fishery in the western and central Pacific Ocean, with consideration of target change. Fish. Res., 107(1–3): 210–220 **(11 pages).**

Chen, Z.C.; Jennifer, B.; Weiwei, X.; Cui, L.; Elaine, C.; Pauly, D., (2021). The ratio of length at first maturity to maximum length across marine and freshwater fishes. J. Fish Biol., 101(2): 400–407 **(8 pages).**

Díaz-Ponce, M.; Villón-Perero, S.; Escandón-Panchana, J.; Pico-Saltos, R.; Escandón-Panchana, P., (2026). Socio environmental and territorial factors affecting urban management of artisanal fishing port. Global J. Environ. Sci. Manage., 12(2): 897-920 **(24 pages).**

Ducklow, H.; Cimino, M.; Dunton, K.H.; Fraser, W.R.; Hopcroft, R.R.; Ji, R.; Miller, A.J.; Ohman, M.D.; Sosik, H.M., (2022). Marine pelagic ecosystem responses to climate variability and change. BioScience., 72(9): 827–850 **(24 pages).**

Feng, S.; Yang, X.; Li, M.; Hua, Z.; Tian, S.; Zhu, J., (2025). Spatial prediction and environmental response of skipjack tuna resources from the perspective of geographic similarity: A case study of purse seine fisheries in the western and central Pacific. J. Mar. Sci. Eng., 13(8): 1–23 **(23 pages).**

Fu, Z.; Bai, J.; Ma, Z., (2025). Physiological adaptations and stress responses of juvenile yellowfin tuna (*Thunnus albacares*) in aquaculture: An integrative review. Aquat. Life Ecosyst., 1(1): 1–14 **(14 pages).**

Gang, L.; Zhengwei, L.; Yangming, C.; Lijin, Z.; Xinjun, C., (2023). CPUE estimation and standardization based on VMS: A case study for squid-jigging fishery in the equatorial eastern Pacific Ocean. Fishes., 8(2): 1–13 **(13 pages).**

Hasan, M.R.; Hossain, M.; Yeamin, Z.M.; Sumaya, T.; Ashekur, M.R.; Uttam, K.S.; Jun, O., (2021). Evaluating the size at sexual maturity for 20 fish species (Actinopterygii) in wetland (Gajner Beel) ecosystem, north-western Bangladesh through multi-model approach: A key for sound management. Acta Ichthyol. Piscat., 51(1): 29–36 **(8 pages).**

Hastie, T.J.; Tibshirani, R., (1986). Generalized additive models. Stat. Sci., 1(3): 297–310 **(14 pages).**

Hastie, T.J.; Tibshirani, R., (1990). Generalized additive models. Stanford University, Department of Statistics and Division of Biostatistics.

Hua, Z.; Yang, X.; Li, M.; Feng, S.; Zhu, J., (2025). Spatial heterogeneity-based explainable machine learning methods modeling the relationship between yellowfin tuna fishery resources and the environment in the Pacific Ocean. Fishes., 10(8): 1–24 **(24 pages).**

Hutubessy, B.; Haruna; Hipaploly, L., (2021). Status of yellowfin tuna (*Thunnus albacares*) handline fisheries based on length of maturity. IOP Conference Series: Earth Environ. Sci., 800(1): 1–8 **(8 pages).**

Koropitan, A.F.; Kholilullah, I.; Yusfiandayani, R., (2021). Modeling mackerel tuna (*Euthynnus affinis*) habitat in southern coast of Java: Influence of seasonal upwelling and negative IOD. Hayati J. Biosci., 28(4): 271–285 **(15 pages).**

Laban, M.; Ashiraf, K.; Monic, N.; Vianny, N.; William, O.; Jos, S.; Maarten, V.S., (2024). Estimates of life-history and growth parameters of exploited fish species in lakes Edward and George: Implications on exploitation status, population dynamics, management, and conservation of native species. J. Fish Biol., 106(2): 201–215 **(15 pages).**

Lin, W.; Niu, M.; Lu, F.; Zuo, T.; Wang, J.; Li, Y.; Cheng, Z.; Sun, J., (2025). Spatiotemporal distribution of ichthyoplankton and their relationship with environmental factors in the waters around the Yellow River estuary, China. Front. Mar. Sci., 12(2): 1–12 **(12 pages).**

Mammel, M.; Naimullah, M.; Vayghan, A.H.; Hsu, J.; Lee, M.; Wu, J.; Wang, Y.; Lan, K., (2022). Variability in the spatiotemporal distribution patterns of greater amberjack in response to environmental factors in the Taiwan Strait using remote sensing data. Remote Sens., 14(12): 1–20 **(20 pages).**

Mendoza, Z.R.; Nishizaki, O.S.; Pardo, M.A.; Herzka, S.Z.; Wells, R.J.D.; Rooker, J.R.; Falterman, B.J.; León, M.J.D., (2024). Mesoscale activity drives the habitat suitability of yellowfin tuna in the Gulf of Mexico. Sci. Rep., 14: 1–13 **(13 pages).**

Morbey, Y.E.; Pauly, D., (2022). Juvenile-to-adult transition invariances in fishes: Perspectives on proximate and ultimate causation. J. Fish Biol., 101(4): 874–884 **(11 pages).**

Nurdin, E.; Muhammad, T.; Pratiwi, L.; Asep, M.; Duranta, D.K.; Tirtadanu; Tegoeh, N.P.; Anthony, S.P., (2025). Stock status of skipjack tuna (*Katsuwonus pelamis* Linnaeus, 1758) using length-based assessment in Cenderawasih Bay, Indonesia. Sains Malays., 54(5): 1209–1220 **(12 pages).**

Orbesen, E.S.; Foster, D.G.; Blankinship, D.R.; Cushner, S.; Bergmann, C.; Serafy, J.E., (2025). Assessment of "weak hook" effects on fish catches and sizes in a pelagic longline fishery. Mar. Coast. Fish., 17(9): 1–13 **(13 pages).**

Ostman, O.; Hommik, K.; Bolund, E.; Heikinheimo, O.; Olin, M.; Lejk, A.M.; Olsson, J., (2023). Size-based indicators for assessments of ecological status of coastal fish communities. ICES J. Mar. Sci., 80(1): 2478–2489 **(12 pages).**

Owiredu, S.A.; Onyango, S.O.; Song, E.; Kim, K.; Kim, B.; Lee, K., (2024). Enhancing chub mackerel catch per unit effort (CPUE) standardization through high-resolution analysis of Korean large purse seine catch and effort using AIS data. Sustainability. 16(3): 1–19 **(19 pages).**

Pechon, R.R.; Emelyn, A.D.; Al-Azeez, T.P.; Kimber, M.A.; Maria, A.F., (2022). Relative abundance and size composition of tuna caught by major fishing gears landed in the General Santos Fish Port Complex, Philippines. Philipp. J. Fish., 29(1): 67–77 **(11 pages).**

Safruddin; Hidayat, R.; Farhum, S.T.A.; Zainuddin, M., (2022). The use of statistical models in identifying skipjack tuna habitat characteristics during the southeast monsoon in the Bone Gulf, Indonesia. Biodiversitas., 23(4): 2231–2237 **(7 pages).**

Shahat, M.A.A.; Sayed, D.S.; Qorqor, M.M.; Abdel Hamed, H.N., (2026). An integrated framework for sustainable natural resources management in freshwater lakes. Global J. Environ. Sci. Manage., 12(4): 2061-2086 **(26 pages).**

Simpson, G.L., (2024). Gratia: An R package for exploring generalized additive models. J. Open Source Softw., 9(104): 1–10 **(10 pages).**

Siregar, E.S.Y.; Siregar, V.P.; Agus, S.B., (2018). Analisis daerah penangkapan ikan tuna sirip kuning *Thunnus albacares* di perairan Sumatera Barat berdasarkan model GAM. J. Ilmu Teknol. Kelaut. Trop., 10(2): 501–516 **(16 pages).**

Siregar, E.S.Y.; Simbolon, D.; Wahju, R.I.; Yulianto, I.; Siregar, V.P., (2025a). Prediction of potential fishing ground for *Thunnus albacares* (Bonnaterre, 1788) using maximum entropy models in the waters of West Sumatra. AACL Bioflux., 18(3): 1532–1546 **(15 pages).**

Siregar, E.S.Y.; Simbolon, D.; Wahju, R.I.; Yulianto, I.; Siregar, V.P., (2025b). Yellowfin tuna (*Thunnus albacares*) fisheries sustainability: A weight-length analysis in the West Sumatra waters. J. Teknol. Perikan. Kelaut., 16(3): 282–293 **(12 pages).**

Siregar, E.S.Y.; Simbolon, D.; Wahju, R.I.; Yulianto, I.; Siregar, V.P., (2026). Ontogenetic size composition and life-stage structure of yellowfin tuna (*Thunnus albacares*) in West Sumatra waters, Indonesia. Adv. Biol. Earth Sci., 11(2): 644–662 **(19 pages).**

Siregar, E.S.Y., (2026). Pemodelan daerah penangkapan ikan madidihang berbasis parameter oseanografi dan biologi dengan menggunakan generalized additive model. Ph.D. Dissertation, IPB University, Bogor, Indonesia.

Sparre, P.; Venema, S.C., (1998). Introduction to tropical fish stock assessment. Part 1: Manual. FAO Fisheries Technical Paper No. 306. FAO, Rome, Italy.

Srioktoviana, S.K.; Mukti, Z.; Rachmat, H.; Alfira, Y.; Muzzneena, A.M.; Farhum, S.; Safruddin, (2024). Exploring the relationship between salinity front and the distribution and abundance of yellowfin tuna (*Thunnus albacares*) in the western Banda Sea, Center of Indonesia Coral Triangle. IOP Conference Series: Earth Environ. Sci., 1410(1): 1–10 **(10 pages).**

Syah, A.F.; Yanti Siregar, E.S.; Siregar, V.P.; Agus, S.B., (2020). Application of remotely sensed data and maximum entropy model in detecting potential fishing zones of yellowfin tuna (*Thunnus albacares*) in the eastern Indian Ocean off Sumatera. Conf. Ser. J. Phys., 1569(4): 1–10 **(10 pages).**

Takrina, N.D.; Chuan O.M.; Afifudin, M.I.; Tristan, L.; Arif, I.; Adiwibowo, A., (2023). Modeling the tropical fish community related to the land uses and environmental determinants. Global J. Environ. Sci. Manage., 9(3): 515-530 **(16 page).**

Vaihola, S.; Yemane, D.; Kininmonth, S., (2023). Spatiotemporal patterns in the distribution of albacore, bigeye, skipjack, and yellowfin tuna species within the exclusive economic zones of Tonga for the years 2002 to 2018. Diversity., 15(8): 1–21 **(21 pages).**

Vicente, J.A.; Palla, H.P., (2024). Length-weight relationship and population dynamics of fringescale sardinella, *Sardinella fimbriata* (Clupeiformes, Clupeidae), from Malampaya Sound, Palawan, Philippines. Zoodiversity., 58(5): 391–402 **(12 pages).**

Wang, J.; Cheng, Y.; Lu, H.; Chen, X.; Lin, L., (2022). Water temperature at different depths affects the distribution of neon flying squid (*Ommastrephes bartramii*) in the northwest Pacific Ocean. Front. Mar. Sci., 8: 1–10 **(10 pages).**

Wang, Zhang, F.; Geng, Z.; Zhang, Y.; Zhu, J.; Dai, X., (2023). Effects of climate variability on two commercial tuna species abundance in the Indian Ocean. Fishes., 8(2): 1–12 **(12 pages).**

Wiryawan, B.; Loneragan, N.; Mardhiah, U.; Kleinertz, S.; Wahyuningrum, P.I.; Pingkan, J.; Wildan; Timur, P.S.; Duggan, D.; Yulianto, I., (2020). Catch per unit effort dynamic of yellowfin tuna related to sea surface temperature and chlorophyll in southern Indonesia. Fishes., 5(3): 1–16 **(16 pages).**

Wood, S.N., (2006). Generalized additive models: An introduction with R. Chapman and Hall/CRC.

Wu, Y.L.; Lan, K.W.; Evans, K.; Chang, Y.J.; Chan, J.W., (2022). Effects of decadal climate variability on spatiotemporal distribution of Indo-Pacific yellowfin tuna population. Sci. Rep., 12: 1–13 **(13 pages).**

AUTHOR (S) BIOSKETCHES

Simbolon, D., Ph.D., Professor, Department of Fisheries Resources Utilization, Faculty of Fisheries and Marine Science, IPB University, Jl Raya Dramaga, Bogor, Jawa Barat, 16680 Indonesia.
- Email: *domu@apps.ipb.ac.id*
- ORCID: 0000-0001-7075-6792
- Web of Science ResearcherID: CAG-0277-2022
- Scopus Author ID: 57195333551
- Homepage: https://www.researchgate.net/profile/Domu-Simbolon

Siregar, E.S.Y., Ph.D., Assistant Professor, Department of Fisheries Resources Utilization, Faculty of Fisheries and Marine Science, IPB University, Jl Raya Dramaga, Bogor, Jawa Barat, 16680 Indonesia.
- Email: *emmasuriyantisiregar@gmail.com*
- ORCID: 0000-0003-2477-0950
- Web of Science ResearcherID: OGO-4386-2025
- Scopus Author ID: 57214822277
- Homepage: https://www.researchgate.net/profile/Emma-Yanti-Siregar/research

Wahju, R.I., Ph.D., Professor, Department of Fisheries Resources Utilization, Faculty of Fisheries and Marine Science, IPB University, Jl Raya Dramaga, Bogor, Jawa Barat, 16680 Indonesia.
- Email: *ronnywa@apps.ipb.ac.id*
- ORCID: 0009-0001-5419-3675
- Web of Science ResearcherID: GPP-2506-2022
- Scopus Author ID: 7801620906
- Homepage: https://www.researchgate.net/profile/Ronny-Wahju

Yulianto, I., Ph.D., Associate Professor, Department of Fisheries Resources Utilization, Faculty of Fisheries and Marine Science, IPB University, Jl Raya Dramaga, Bogor, Jawa Barat, 16680 Indonesia and Fisheries Resource Center of Indonesia, Rekam Nusantara Foundation, Jl Sempur, Bogor, West Java, 16129 Indonesia.
- Email: irfan-yu@apps.ipb.ac.id
- ORCID: 0000-0003-4116-9171
- Web of Science ResearcherID: QXJ-4049-2026
- Scopus Author ID: 55557876500
- Homepage: https://www.researchgate.net/profile/Irfan-Yulianto

Siregar, V.P., Ph.D., Professor, Department of Marine Science and Technology, Faculty of Fisheries and Marine Science, IPB University, Jl Raya Dramaga, Bogor, Jawa Barat, 16680 Indonesia.
- Email: *vincentius@apps.ipb.ac.id*
- ORCID: 0009-0003-2801-7939
- Web of Science ResearcherID: GPP-5332-2022
- Scopus Author ID: 56102074300
- Homepage: https://www.researchgate.net/profile/Vincentius-Siregar

Pianto, T.A., Ph.D. Candidate, Researcher, Research Center for Limnology and Water Resources, National Research and Innovation Agency, Jl Jl Raya Jakarta, Cibinong, West Java, 16911 Indonesia.
- Email: *tegu023@brin.go.id*
- ORCID: 0009-0008-7160-5329
- Web of Science ResearcherID: QXI-9555-2026
- Scopus Author ID: 56118598400
- Homepage: https://www.researchgate.net/profile/Teguh-Pianto

Sangadji, M.S., Ph.D. Candidate, Doctoral Student, Marine Technology Study Program, Faculty of Fisheries and Marine Science, IPB University, Jl Raya Dramaga, Bogor, Jawa Barat, 16680 Indonesia.
- Email: *sidiksangadji@gmail.com*
- ORCID: 0009-0001-1981-398X
- Web of Science ResearcherID: NA
- Scopus Author ID: NA
- Homepage: https://www.researchgate.net/profile/Muhamad-Sangadji?ev=hdr_xprf

Rosmasita., Ph.D. Candidate, Doctoral Student, Marine Technology Study Program, Faculty of Fisheries and Marine Science, IPB University, Jl Raya Dramaga, Bogor, Jawa Barat, 16680 Indonesia.
- Email: *rosmasita1994@gmail.com*
- ORCID: 0000-0001-7511-1248
- Web of Science ResearcherID: QWF-2875-2026
- Scopus Author ID: 57209251196
- Homepage: https://www.researchgate.net/profile/Rosmasita-Rosmasita

Andika, F., Ph.D. Candidate, Doctoral Student, Marine Technology Study Program, Faculty of Fisheries and Marine Science, IPB University, Jl Raya Dramaga, Bogor, Jawa Barat, 16680 Indonesia.
- Email: *fauziandikabunga@gmail.com*
- ORCID: 0009-0000-0700-0036
- Web of Science ResearcherID: KOD-4344-2024
- Scopus Author ID: 56820149700
- Homepage: https://www.researchgate.net/profile/Fauzi-Andika?ev=hdr_xprf

Mulyadi, R.A., Ph.D. Candidate, Doctoral Student, Marine Technology Study Program, Faculty of Fisheries and Marine Science, IPB University, Jl Raya Dramaga, Bogor, Jawa Barat, 16680 Indonesia.
- Email: *ramaagus1992@gmail.com*
- ORCID: 0009-0005-6639-3753
- Web of Science ResearcherID: NA
- Scopus Author ID: 60430004500
- Homepage: https://www.researchgate.net/profile/Rama-Agus-Mulyadi?ev=hdr_xprf

Putra, M.Y.U., Ph.D. Candidate, Doctoral Student, Marine Technology Study Program, Faculty of Fisheries and Marine Science, IPB University, Jl Raya Dramaga, Bogor, Jawa Barat, 16680 Indonesia.
- Email: *umsiniputra@yahoo.com*
- ORCID: 0000-0002-4596-0561
- Web of Science ResearcherID: NA
- Scopus Author ID: NA
- Homepage: https://www.researchgate.net/profile/Muh-Olii?ev=hdr_xprf

Rasidi., Ph.D. Candidate, Doctoral Student, Marine Technology Study Program, Faculty of Fisheries and Marine Science, IPB University, Jl Raya Dramaga, Bogor, Jawa Barat, 16680 Indonesia.
- Email: *rasidiburhan1980@gmail.com*
- ORCID: 0009-0003-3605-7527
- Web of Science ResearcherID: NA
- Scopus Author ID: 57216532463
- Homepage: https://www.researchgate.net/lab/Rasidi-Burhan-Lab

HOW TO CITE THIS ARTICLE:
Simbolon, D.; Siregar, E.S.Y.; Wahju, R.I.; Yulianto, I.; Siregar, V.P.; Pianto, T.A.; Rosmasita; Sangadji, M.S.; Andika, F.; Mulyadi, R.A.; Putra, M.Y.U.; Rasidi., (2027). Environmental modeling of yellowfin tuna fishing grounds integrating oceanographic and biological parameters using a generalized additive model. Global J. Environ. Sci. Manage., 13(1): 273-302.

DOI: 10.22034/gjesm.2027.01.13
URL: https://www.gjesm.net/article_735743.html

Global Journal of Environmental Science and Management
(GJESM)

Homepage: https://www.gjesm.net/

Podcasts

ORIGINAL RESEARCH ARTICLE

Life cycle assessment and identification of embodied carbon hotspots in a reinforced concrete factory

N. Suriyanon[1], W. Suriyanon[2,*], N. Suriyanon[2], N. Watkate[1]

[1]Department of Civil Engineering, Faculty of Engineering, Chiang Mai University, Chiang Mai, Thailand

[2]Department of Civil and Environmental Engineering, Rajamangala University of Technology Lanna, Chiang Mai, Thailand

ARTICLE INFO

Article History:
Received 21 May 2026
Revised 23 August 2026
Accepted 25 September 2026

Keywords:
Embodied carbon
Greenhouse gas
Industrial buildings
Life cycle assessment
Pre-use embodied carbon
Reinforced concrete

DOI:10.22034.gjesm.2027.01.14

ABSTRACT

BACKGROUND AND OBJECTIVES: Reducing embodied carbon is a key strategy for delivering low-carbon buildings because emissions from construction materials and activities represent a substantial share of total building life-cycle emissions. While extensive scholarly research has addressed embodied carbon within the residential and commercial sectors, comprehensive hotspot analyses concerning industrial facilities remain scarce, particularly within the geographical context of Thailand. The study objectives were to quantify the embodied carbon of a reinforced concrete factory building and identified carbon hotspots at the life-cycle module, building-component, and material levels to support evidence-based mitigation during the building pre-use stage.

METHODS: A reinforced concrete factory building in Thailand with a gross floor area of 90.00 square meters was selected as the case study. Embodied carbon was assessed using life cycle assessment in accordance with International Organization for Standardization 14040 and 14044 and British Standard European Norm 15978. The system boundary, established from a cradle-to-practical-completion perspective, encompassed the production and transport of construction materials, on-site energy consumption during construction, and construction waste management. Carbon hotspots were analyzed at the life-cycle module, building-component, and resource type levels.

FINDINGS: The total embodied carbon was 29,353.47 kilograms of carbon dioxide equivalent, corresponding to 326.15 kilograms of carbon dioxide equivalent per square meter. Construction material production was the dominant emission source, contributing 78.10 percent of total embodied carbon. On-site construction energy use accounted for 12.09 percent of the impact, followed by construction waste management at 5.25 percent, and the transportation of construction materials at 4.56 percent. The reinforced concrete structural system generated the highest embodied carbon at 10,533.29 kilograms of carbon dioxide equivalent, followed by the wall system at 7,527.36 kilograms of carbon dioxide equivalent. Concrete, structural steel, and corrugated steel roofing with associated components accounted for 23.13 percent, 18.31 percent, and 16.73 percent of the total impact, respectively. Collectively, these three resource categories accounted for 58.17 percent of total embodied carbon.

CONCLUSION: Construction material production represents the principal opportunity for reducing embodied carbon in reinforced concrete factory buildings. Improvements in construction energy efficiency and construction waste management can provide additional emission reductions. The proposed hotspot-based assessment framework establishes a comprehensive embodied carbon inventory for reinforced concrete industrial facilities in Thailand, thereby providing actionable guidance for low-carbon design architectural, material optimization, and construction management.

This is an open access article under the CC BY license (http://creativecommons.org/licenses/by/4.0/)

NUMBER OF REFERENCES	NUMBER OF FIGURES	NUMBER OF TABLES
39	5	5

*Corresponding Author:
Email: wanidaenv@rmutl.ac.th
Phone: +81 950 7534
ORCID: 0009-0009-1393-8085

Note: Discussion period for this manuscript open until March 01, 2027 on GJESM website at the "Show Article".

INTRODUCTION

The building sector is a major source of greenhouse gas (GHG) emissions, primarily from construction material production, transportation, and on-site construction activities. As countries pursue carbon neutrality and sustainable development, life cycle assessment (LCA) and carbon accounting have become important tools for systematically identifying major emission sources and supporting evidence-based decision-making for low-carbon buildings and sustainable infrastructure (Pomponi and Moncaster, 2016; Röck *et al.*, 2020; de Cadenet *et al.*, 2025). LCA serves as a systematic methodology for systematically evaluating the environmental burdens of products and systems across sequential life-cycle phases. By quantifying impacts at each stage, LCA facilitates the identification of emission-intensive processes and highlights critical targets for mitigation (Rashif *et al.*, 2025). Accordingly, LCA and carbon footprint assessment are increasingly used to support sustainability decision-making, including comparing alternatives, evaluating GHG mitigation measures, and identifying environmental hotspots to inform evidence-based decisions (Rashif *et al.*, 2025; de Cadenet *et al.*, 2025; Firmansyah *et al.*, 2025). In building LCA, GHG emissions are frequently evaluated through the framework of whole life carbon (WLC), which encompasses both embodied and operational carbon components. Embodied carbon arises from material production, transportation, construction, maintenance, replacement, demolition, and end-of-life processes, whereas operational carbon results from energy consumption during building use (Cabeza *et al.*, 2014; Lützkendorf and Balouktsi, 2022). As energy-efficient building strategies become more widespread, the relative share of operational carbon has decreased, whereas embodied carbon has emerged as an increasingly significant component of total life-cycle emissions, particularly within high-performance structures (Pomponi and Moncaster, 2016; Röck *et al.*, 2020; Lützkendorf and Balouktsi, 2022). Early design decisions, including building form, structural systems, and material selection, can substantially influence embodied carbon (Gauch *et al.*, 2023). Consequently, reliable embodied carbon datasets are essential for identifying carbon hotspots and prioritizing mitigation strategies, including the adoption of low-carbon materials, enhanced structural efficiency, and optimized construction practices (Myint and Shafique, 2024; Amarasinghe *et al.*, 2025). However, studies specifically assessing the embodied carbon of built assets in Thailand remain limited. Although recent research has quantified the embodied carbon of roads and drainage systems in Thai housing developments (Suriyanon *et al.*, 2026), studies focusing on buildings—particularly reinforced concrete factory buildings, remain scarce. Consequently, the Thai construction industry lacks empirical evidence and benchmark values to support comparison, target setting, and the selection of appropriate GHG mitigation measures during the building pre-use stage. In recent years, scholarly investigation into embodied building carbon (EBC) has expanded significantly, encompassing comparative evaluations of alternative design and construction strategies, component-level hotspot identification, and the advancement of specialized assessment methodologies and decision-support tools. Studies of residential, commercial, and high-rise buildings have consistently shown that structural systems and major construction materials frequently dominate embodied carbon emissions. For example, Monahan and Powell (2011) compared embodied carbon across alternative affordable housing construction systems in the United Kingdom, while Jayawardana *et al.* (2021) identified masonry wall systems as a major hotspot in multi-storey residential buildings in Sri Lanka. Similar assessments have been conducted for commercial buildings and green office buildings (Samson and Pope, 2012; Sandaruwan *et al.*, 2024), as well as

residential construction projects in North America (Zuluaga and Saxe, 2025). Investigations into high-rise and large-scale structures have further analyzed how structural systems, building configurations, and construction methodologies influence embodied carbon emissions. Wan Omar (2018) evaluated the embodied carbon intensity of several building types in Malaysia, while Teng and Pan (2019) assessed a prefabricated public residential building in Hong Kong at material and whole-building levels. More recent studies have evaluated modular high-rise reinforced concrete structures, public housing complexes, and high-rise residential buildings, generating critical hotspot data and benchmark values to facilitate low-carbon design and decision-making (Sachchithananthan *et al.*, 2024; Agustiningtyas *et al.*, 2024; Zhang and Wang, 2016). In Thailand, Liwthaisong *et al.* (2025) assessed a six-storey reinforced concrete outpatient building and found that concrete and reinforcing steel were the major sources of embodied carbon. Furthermore, methodological advancements in embodied carbon assessment have been achieved through the application of process-based, input–output, and hybrid LCA frameworks (Li *et al.*, 2014; Zhang and Wang, 2016). In addition, the integration of building information modeling (BIM) with LCA enables more rapid quantity take-off, carbon estimation, and visualisation during the design stage (Huang *et al.*, 2023; Kanangkaew *et al.*, 2026). Recent reviews further highlight the potential of machine learning and multi-criteria decision-making frameworks to improve the efficiency, contextual relevance, and practical application of embodied carbon assessments (Shi *et al.*, 2025). At the macro-systemic level, researchers have underscored the critical need for reliable benchmarks, localized environmental product declarations, harmonized assessment standards, and robust institutional and policy frameworks to ensure effective implementation (Drewniok *et al.*, 2023; Greer *et al.*, 2023; Amarasinghe *et al.*, 2025; Santos *et al.*, 2025). Despite these advances, research on industrial buildings remains limited relative to that on residential and commercial buildings. Rodrigues *et al.* (2018) assessed an industrial building and found that construction materials were the primary contributors to embodied carbon. Nevertheless, findings from international studies cannot be directly extrapolated to Thailand because embodied carbon is heavily governed by context-specific determinants, such as material emission factors, national energy grid characteristics, and regional construction practices. Therefore, assessing reinforced concrete factory buildings in Thailand and identifying carbon hotspots at the building-component, material, and life-cycle-stage levels are essential for establishing locally relevant evidence and prioritising effective mitigation measures. In the present study, the dataset was augmented with supplementary entries and subsequently subjected to comprehensive review and revision to enhance data fidelity. It builds on earlier work by Watkate and Suriyanom (2024), which reported a preliminary assessment of the building's embodied carbon (EBC). The scope of the study was also expanded to provide a more in-depth analysis of carbon hotspots across building components, resource types, and life-cycle stages. The findings are intended to inform engineering decisions pertaining to architectural design, material specification, procurement strategies, on-site energy utilization, and waste management practices. The study also provides data and a methodological foundation for future benchmark development and embodied carbon assessments of buildings in Thailand. Conducted in 2024, this study evaluates the embodied carbon of a reinforced-concrete industrial facility in Thailand through a LCA framework focusing specifically on the pre-use stage.

MATERIALS AND METHODS

Case study and study scope

A reinforced concrete factory building located in Chiang Mai Province, Thailand, with a gross floor area of 90.00 square meters (m^2), was selected as

the case study. This particular project was adopted for evaluation as its architectural configuration and material framework closely mirror the baseline characteristics of small-sized manufacturing buildings throughout Thailand. The building is a single-storey industrial facility. The assessment scope covered GHG emissions associated with structural works, architectural works, and construction support works, while mechanical, electrical, and plumbing (MEP) systems were excluded. The scope was established based on two primary considerations. First, the assessment focused on building elements characterized by high material consumption, as these components predominantly drive embodied carbon and constitute likely carbon hotspots. Second, MEP systems were excluded to minimize analytical uncertainty stemming from project-specific service installations, which vary substantially according to facility functions, operational parameters, and system configurations. This variability limits meaningful cross-project comparisons and reduces the value of the results for benchmarking. In addition, MEP systems comprise a wide range of materials and equipment with diverse manufacturing routes and raw material compositions, meaning that emission estimation often relies on numerous assumptions when selecting appropriate emission factors (EFs). Consequently, the exclusion of MEP systems enhances the reliability and consistency of the embodied carbon findings, thereby reinforcing their utility as a benchmark reference case for industrial facilities within the Thai construction sector. Nevertheless, excluding MEP systems may result in an underestimation of the total pre-use embodied carbon; therefore, the reported results should be interpreted as representing only the structural, architectural, and construction-support works included within the defined system boundary. The structural system of the subject building comprised reinforced concrete spread footings, columns, and floor slabs, whereas the roof framework was constructed using structural steel members. Architectural works comprised two external wall systems—painted, cement-rendered concrete block walls and corrugated steel sheet cladding on steel framing—as well as expanded polystyrene (EPS) sandwich-panel internal partitions, corrugated steel sheet roof covering, and a smooth plaster ceiling finish. Regarding construction support activities, the life cycle inventory (LCI) accounted for general electricity consumption, administrative air-conditioning use, wastewater treatment via an on-site facility system, and solid waste management. Additionally, auxiliary resources, including temporary office container units and operational consumable materials such as A4 paper, were integrated into the life-cycle inventory. These activities were defined according to the available project records to represent greenhouse gas emissions generated during the pre-use stage of the building life cycle. The primary data used for developing the LCI and assessing embodied carbon and carbon hotspots during the pre-use stage were obtained from the construction drawings, technical specifications, and the bill of quantities (BOQ). These project documents furnished the quantitative parameters necessary to conduct material take-off and subsequent embodied carbon computations.

Research framework

The research framework adopted in this study was formulated in accordance with LCA principles for embodied carbon evaluation. The assessment commenced with the definition of the study objectives and system boundary, followed by data collection for the preparation of the LCI. Appropriate EFs were subsequently selected and integrated with the inventory data to quantify the embodied carbon associated with the case-study building. Subsequently, the computed results were then systematically analyzed to isolate primary carbon hotspots across both the life-cycle stages and structural building component, as illustrated in the overarching research framework presented in Fig. 1.

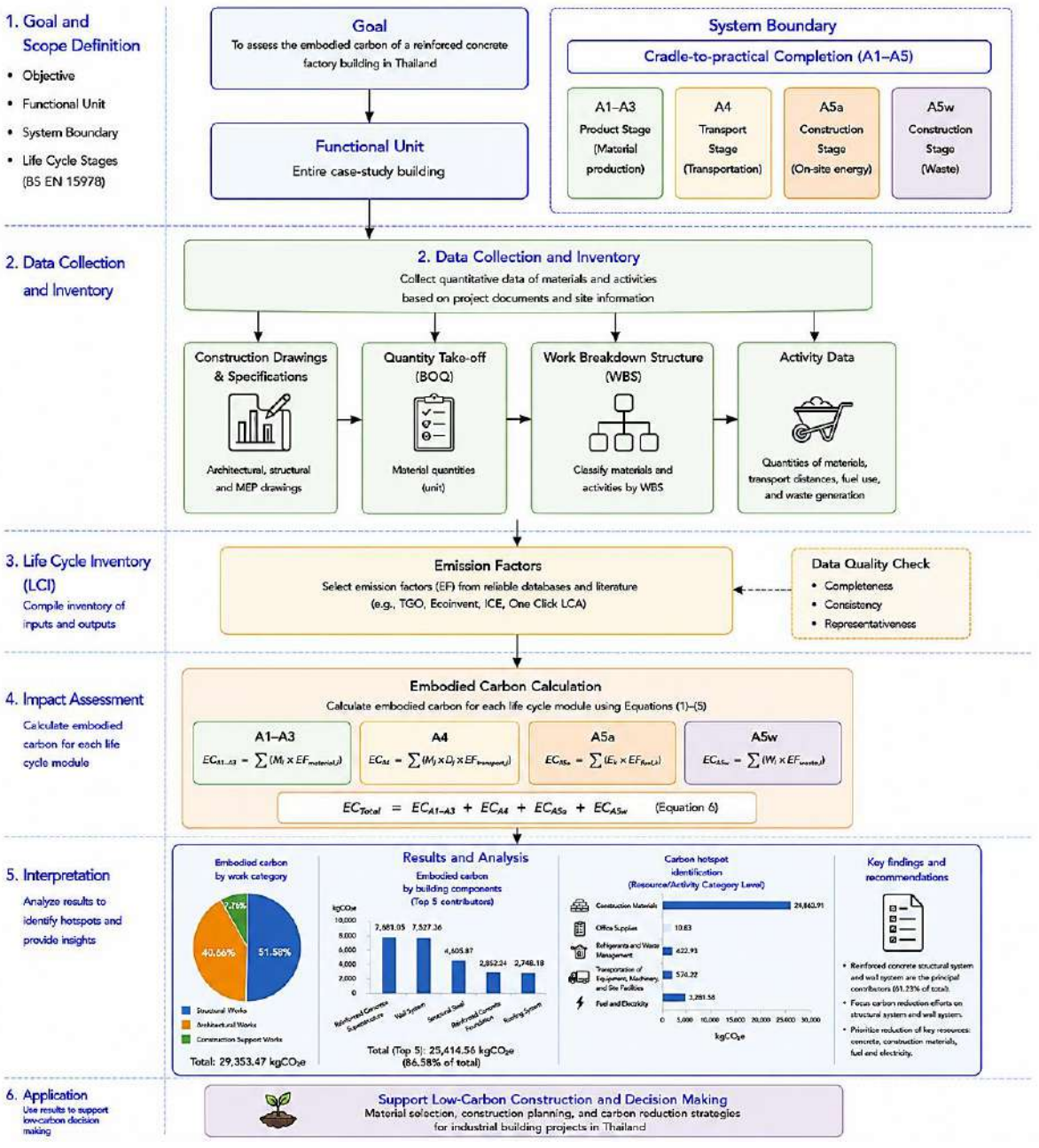

Fig. 1: Research framework adopted in this study

System boundary

The embodied carbon assessment was conducted following the principles of LCA in accordance with International Organization for Standardization (ISO) 14040:2006 (ISO, 2006a) and ISO 14044:2006 (ISO, 2006b), thereby ensuring that the assessment process was systematic, transparent, and reproducible. The system boundary at the building level was established based on BS EN 15978:2011 (BSI, 2011), with the assessment focusing exclusively on the pre-use stage of the building life

cycle. The system boundary was established under a cradle-to-practical completion approach, incorporating modules A1–A3 (material production), A4 (transportation), A5a (on-site energy use and construction activities), and A5w (waste management). In accordance with BS EN 15978, transportation of construction machinery and temporary site facilities was allocated to A4, while on-site fuel and electricity use, refrigerant emissions, and temporary site utility activities were allocated to A5a. Construction waste transportation and treatment were allocated to A5w. The use stage (modules B1–B7) and end-of-life stage (modules C1–C4) were omitted because the primary objective of this study was to identify embodied carbon hotspots and carbon mitigation opportunities addressable during the building design and construction phases. For the embodied carbon calculation, quantitative data obtained from the construction drawings and the BOQ were compiled into the LCI and linked with the corresponding EFs for construction materials, transportation, energy and fuel use, and construction waste management. This comprehensive inventory formed the methodological foundation for calculating greenhouse gas emissions across the established assessment boundary. The entire case-study building, with a gross floor area of 90.00 m^2, was defined as the reference unit for the assessment. To facilitate comparison with existing building LCAs, the outcomes were further normalized per square meter of gross floor area, expressed in kilogram carbon dioxide equivalent ($kgCO_2e/m^2$), establishing a standardized reference metric independent of structural scale. The system boundary implemented in this study is illustrated in Fig. 2.

Data collection

The data used in this study comprised both primary and secondary data sources. The primary data were quantified directly from the case-study project and included; 1) construction material quantities, 2) fuel and energy consumption of construction equipment during on-site activities, and 3) transportation distances for construction materials and equipment to the project site. The secondary data consisted of greenhouse gas EFs for construction materials, transportation, fuels, electricity consumption, and construction waste management. A work breakdown structure (WBS) was utilized to categorize the facility into discrete construction components, thereby systematically integrating material quantities, transportation activities, on-site processes, and construction waste management into the embodied carbon assessment. This structured methodology allowed the evaluation outcomes to be examined across both life-cycle modules and structural components, thereby supporting the efficient identification of primary carbon hotspots. Priority was given to EFs developed by domestic organizations and relevant stakeholders, such as manufacturer-published databases and the Thailand Greenhouse Gas Management Organization (TGO). Where local EFs were unavailable or insufficient, reliable data obtained from published studies and internationally recognized databases were adopted. This data selection strategy was formulated to enhance both the accuracy and representativeness of the evaluation while preserving full alignment with core LCA principles. Furthermore, this methodological strategy aligns with the recommendations of De Wolf *et al.* (2017), who stressed the necessity of utilizing granular activity data alongside well-defined system boundaries and transparent data sources to improve the reliability and comparability of embodied carbon evaluations.

Data quality, allocation, cut-off criteria, and assumptions

Project-specific data were used where available, while secondary EFs prioritized Thailand-specific and temporally relevant sources. To prevent double counting, resources and activities were allocated to their corresponding building components and life-cycle modules in accordance

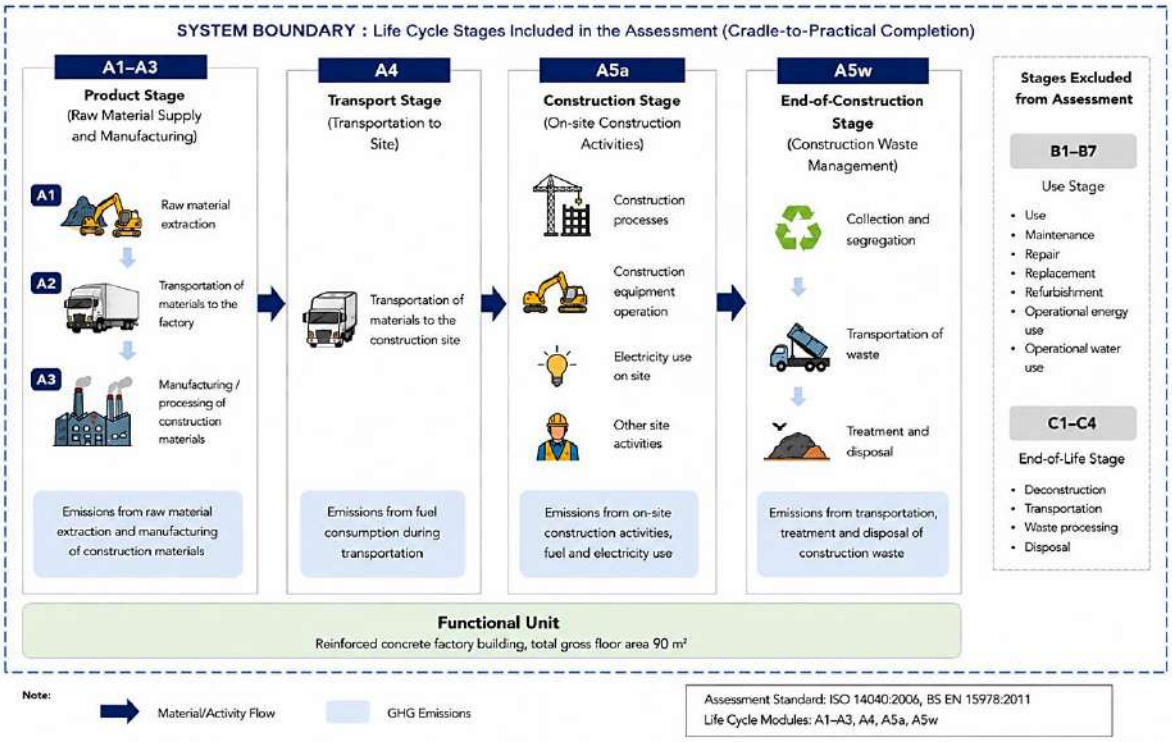

Fig. 2: System boundary of the embodied carbon assessment based on the cradle-to-practical completion approach

with the WBS and established system boundary, ensuring that no intentional cut-off criteria were applied to major activities within the assessment scope. Data quality was considered in terms of geographical, temporal, and technological representativeness and completeness. Secondary data and necessary assumptions were recognized as sources of uncertainty and considered in the sensitivity and uncertainty analysis. Emissions associated with air-conditioning refrigerant and on-site wastewater treatment were estimated from available project activity data combined with the corresponding secondary EFs. Where complete project-specific information was unavailable, necessary assumptions were applied; consequently, these figures should be interpreted as approximate contributions to construction-support emissions. A one-at-a-time sensitivity analysis was performed for the principal hotspot resources by varying the emission factors for concrete, structural steel, corrugated steel, diesel, and electricity by ±20% from the baseline values. Sensitivity analyses of relative contributions and hotspot classifications were conducted to verify outcome stability. Contributors were subsequently ordered by their proportional embodied carbon output to isolate critical hotspots. Principal carbon hotspots were defined as the highest-ranked contributors that collectively accounted for more than 50% of the total pre-use embodied carbon.

Embodied carbon calculation

The embodied carbon of the case-study building was quantified by multiplying the activity data associated with each process by the corresponding greenhouse gas emission factor (EF). This methodology facilitated the quantification of greenhouse gas emissions associated with individual activities across the

established system boundary. The embodied carbon calculation was performed using Eq. 1 (Gibbons *et al*., 2025):

$$EC_{Total} = \Sigma(Q_i \times EF_i) \quad (1)$$

Where: EC_{Total} is the total embodied carbon emissions in $kgCO_2e$, Q_i is the activity data for activity i (e.g., material quantity, transportation distance, fuel consumption, or electricity consumption), and EF_i is the greenhouse gas emission factor corresponding to activity i ($kgCO_2e$ per unit of activity). Upon disaggregating the assessment across the life-cycle modules encompassed by the system boundary, embodied carbon emissions were quantified independently for each individual stage.

1) Construction material production (A1–A3)

Embodied carbon emissions associated with the production of construction materials in modules A1–A3 were calculated by multiplying the quantity of each construction material by its corresponding greenhouse gas emission factor, using Eq. 2 (Gibbons *et al*., 2025):

$$ECA_{1-3} = \Sigma(M_i \times EF_{material,i}) \quad (2)$$

Where: ECA_{1-3} is the embodied carbon emissions from construction material production ($kgCO_2e$), M_i is the quantity of construction material item i (unit), and $EF_{material,i}$ is the greenhouse gas emission factor for construction material item i in kilogram carbon dioxide equivalent per unit ($kgCO_2e$/unit).

2) Transportation of construction materials (A4)

Embodied carbon emissions associated with the transportation of construction materials in module A4 were calculated from the material quantity, transportation distance, and corresponding transportation emission factor, using Eq. 3 (Gibbons *et al*., 2025):

$$ECA_4 = \Sigma(M_i \times D_i \times EF_{transport,i}) \quad (3)$$

Where: ECA_4 is the embodied carbon emissions from the transportation of construction materials ($kgCO_2e$), M_i is the quantity of construction material item i (unit), D_i is the transportation distance for construction material item i in kilometer (km), and $EF_{transport,i}$ is the greenhouse gas emission factor for the transportation of construction material item *i* ($kgCO_2e$/unit-km). Transportation emissions were quantified by multiplying material-specific transportation distances by their corresponding emission factors. Vehicle types and transport modes were assigned based on available project logistics records, whereas transport activity levels were quantified using the transported mass and delivery distance.

3) Fuel and energy use during construction (A5a)

Embodied carbon emissions associated with fuel and energy consumption during construction in module A5a were calculated by multiplying the quantity of each fuel or energy source consumed by its corresponding greenhouse gas emission factor, as expressed in Eq. 4 (Gibbonsn *et al*., 2025):

$$ECA_{5a} = \Sigma(F_i \times EF_{fuel,i}) \quad (4)$$

Where: ECA_{5a} is the embodied carbon emissions from fuel and energy consumption during construction ($kgCO_2e$), F_i is the quantity of fuel or energy source i consumed during construction (unit), and $EF_{fuel,i}$ is the greenhouse gas emission factor for fuel or energy source i ($kgCO_2e$/unit).

4) Construction waste management (A5w)

Embodied carbon emissions associated with construction waste management in module A5w were calculated by multiplying the quantity of each construction waste stream by its corresponding waste-management emission factor, using Eq. 5 (Gibbons *et al*., 2025):

$$ECA_{5w} = \Sigma(W_i \times EF_{waste,i}) \quad (5)$$

Where: ECA_{5w} is the embodied carbon emissions from construction waste management ($kgCO_2e$), W_i is the quantity of construction waste stream *i* (unit), and $EF_{waste,i}$ is the greenhouse gas emission factor for the management of construction waste stream i ($kgCO_2e$/unit). Emissions associated with construction waste were quantified based on the generated waste volume and its corresponding waste-management emission factors. Waste-treatment pathways were determined in accordance with available project documentation, supplemented by reasoned assumptions where granular records were absent. The total embodied carbon of the building was calculated as the sum of greenhouse gas emissions from all life-cycle modules included within the system boundary, namely construction material production (A1–A3), transportation of construction materials (A4), fuel and energy use during construction (A5a), and construction waste management (A5w), using Eq. 6 (Gibbons *et al*., 2025):

$$EC_{Total} = ECA_{1\text{-}3} + ECA_4 + ECA_{5a} + ECA_{5w} \quad (6)$$

Where: EC_{Total} is the total embodied carbon emissions of the building ($kgCO_2e$), $ECA_{1\text{-}3}$ is the embodied carbon emissions from construction material production ($kgCO_2e$), ECA_4 is the embodied carbon emissions from the transportation of construction materials ($kgCO_2e$), ECA_{5a} is the embodied carbon emissions from fuel and energy consumption during construction ($kgCO_2e$), and ECA_{5w} is the embodied carbon emissions from construction waste management ($kgCO_2e$). Eqs. 1 through 6 were utilized to quantify embodied carbon across the project, building-component, and life-cycle-module levels. Subsequently, the computed outcomes were utilized to evaluate the distribution of embodied carbon emissions, isolate primary carbon hotspots, and inform the formulation of targeted greenhouse gas mitigation strategies for reinforced-concrete factory industrial facilities. The resource-level, building-component, and life-cycle-module results were cross-checked to ensure consistency, and all classification totals reconciled with the overall pre-use embodied carbon of 29,353.47 $kgCO_2e$. The refrigerant-related emission reported under module A5a originated from temporary construction-site office air conditioning and were consequently classified as construction-site office and was therefore treated as a construction-support activity rather than components of the permanent building MEP systems.

RESULTS AND DISCUSSION

Embodied carbon by building component

The embodied carbon assessment of the reinforced concrete manufacturing facility was conducted for the pre-use stage, encompassing material production, transport logistics, on-site energy consumption, and waste management. The results indicated that the building generated a total embodied carbon of 29,353.47 $kgCO_2e$ (Fig. 3), corresponding to an embodied carbon intensity of 326.15 kilogram carbon dioxide equivalent per square meter ($kgCO_2e/m^2$) based on the total gross floor area. As shown in Fig. 3, structural works contributed the largest share of embodied carbon, accounting for 15,139.16 $kgCO_2e$, followed by architectural works with 11,939.44 $kgCO_2e$, and construction support works with 2,274.87 $kgCO_2e$. The corresponding embodied carbon ratio for structural works: architectural works: construction support works was 1 : 0.79 : 0.15. The findings reveal that the embodied carbon of the analyzed building was largely driven by structural and architectural categories, whereas construction-support operations accounted for only a minor fraction of overall emissions. This distribution suggests that overall embodied carbon reduction strategies should primarily target structural and architectural components, where the greatest mitigation potential can be achieved, before extending improvement measures to construction support activities. To isolate the primary drivers of embodied carbon, a granular evaluation was conducted at the building-component level. These findings are detailed in Table 1 and Fig. 4.

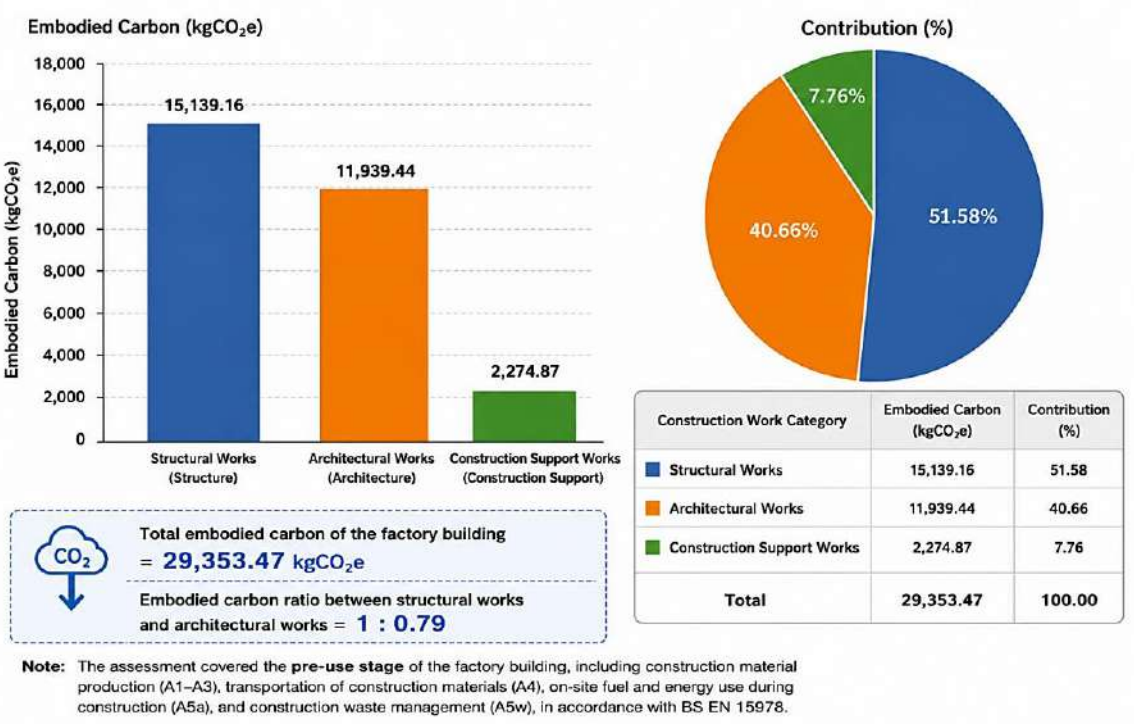

Construction Work Category	Embodied Carbon ($kgCO_2e$)	Contribution (%)
Structural Works	15,139.16	51.58
Architectural Works	11,939.44	40.66
Construction Support Works	2,274.87	7.76
Total	29,353.47	100.00

Fig. 3: Total embodied carbon emissions of the case-study factory building classified by construction work category

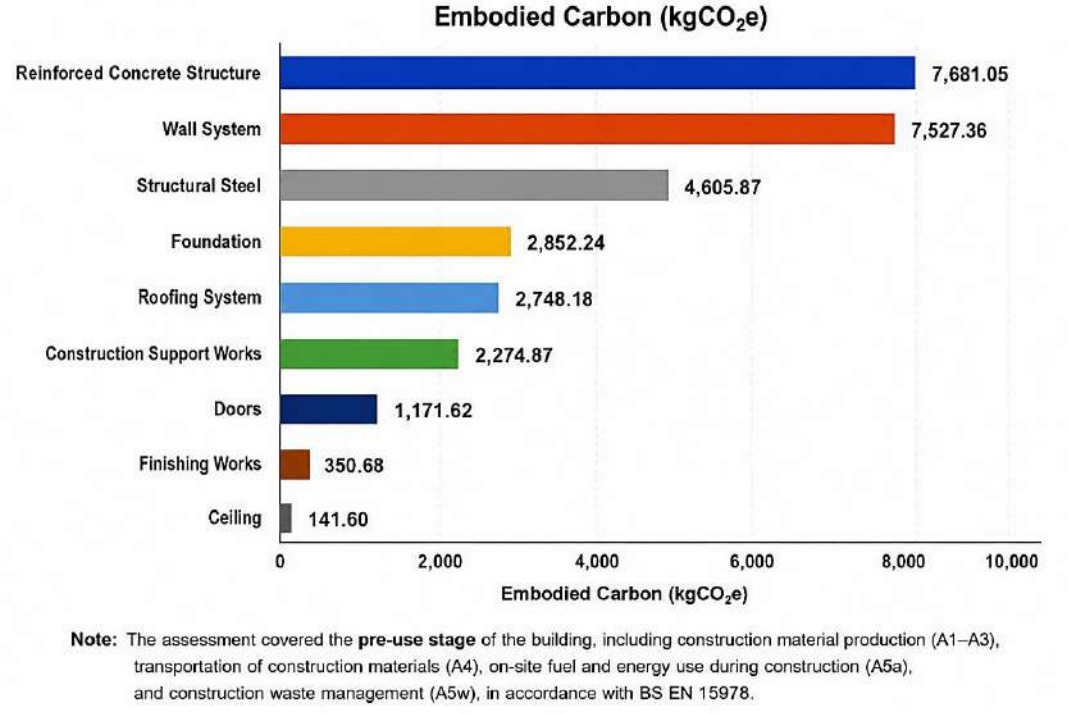

Fig. 4: Embodied carbon emissions and their distribution by building component

Table 1. Embodied carbon emissions and contribution classified by building component

Building component	Embodied carbon ($kgCO_2e$)	Contribution in percent (%)
Structural works		
– Reinforced Concrete Foundation	2,852.24	9.72
– Reinforced Concrete Superstructure	7,681.05	26.17
– Structural Steel	4,605.87	15.69
Architectural works		
– Roofing System	2,748.18	9.36
– Wall System	7,527.36	25.64
– Doors	1,171.62	3.99
– Finishing Works	350.68	1.19
– Ceiling	141.60	0.48
Construction support works		
– Construction Support Works	2,274.87	7.75
Total	29,353.47	100.00

As presented in Table 1 and Fig. 4, within the structural works category, the reinforced concrete structural system (including both the foundation and superstructure) generated a total embodied carbon of 10,533.29 $kgCO_2e$, which was substantially higher than that of the structural steel system, accounting for 4,605.87 $kgCO_2e$. The embodied carbon ratio between the reinforced concrete structural system and the structural steel system stood at 1 : 0.44, demonstrating that reinforced concrete served as the primary contributor to embodied carbon within the structural works category. Within the architectural works category, the wall system generated 7,527.36 $kgCO_2e$, whereas the remaining architectural components, including the roof, doors, finishes, and ceiling system, contributed a combined embodied carbon of 4,412.08 $kgCO_2e$. The corresponding embodied carbon ratio between the wall system and the remaining architectural components stood at 1 : 0.59, indicating that embodied carbon within the architectural works category was heavily concentrated in the wall assembly. When these results were considered collectively, the reinforced concrete structural system (foundation and superstructure) together with the wall system accounted for a combined embodied carbon of 18,060.65 $kgCO_2e$, representing 61.53% of the total embodied carbon of the building. This finding demonstrates that these two building elements served as the primary sources of embodied carbon throughout the pre-use phase. Consequently, prioritizing carbon reduction measures for the reinforced concrete structural system and the wall assembly is expected to yield the highest mitigation potential for reducing the overall embodied carbon of reinforced concrete industrial facilities before addressing secondary building components.

Embodied carbon by resource type

In addition to the analysis at the building-component level, embodied carbon emissions were further classified according to resource type to provide an alternative perspective on the sources of greenhouse gas emissions within the project. This analysis was designed to isolate the specific materials and resources driving overall embodied carbon, accounting for the fact that individual building components generally incorporate diverse materials with varying greenhouse gas emission intensities. Classifying embodied carbon at the resource level provides a more detailed basis for identifying material-specific carbon hotspots and supports the development of targeted carbon reduction strategies through improved material selection

and construction management practices. Furthermore, these insights offer valuable guidance for decision-making during the building design and procurement phases, enabling embodied carbon reduction opportunities to be integrated early in the project lifecycle. The classification results are presented in Table 2. As presented in Table 2, concrete was the largest contributor to embodied carbon, accounting for 6,790.47 $kgCO_2e$ (23.13%), followed by structural steel with 5,374.10 $kgCO_2e$ (18.31%), and corrugated steel sheets and associated materials with 4,911.09 $kgCO_2e$ (16.73%). Cumulatively, these three material classifications accounted for 58.17% of the project's aggregate embodied carbon. This disproportionate contribution—whereby a mere triad of resource categories generated over half of the cumulative emissions—demonstrates that greenhouse gas outputs were heavily skewed toward a select subset of inputs rather than uniformly distributed across the construction material resources. Accordingly, these three resource categories can be clearly identified as resource-level carbon hotspots, representing the highest-priority targets for further analysis and the development of embodied carbon reduction strategies. The concentration of embodied carbon in these materials can be attributed to the combined effects of their relatively large quantities and emission-intensive production processes. While concrete was predominantly utilized across the foundation and superstructure, structural and corrugated steel were extensively integrated within the primary framing, roofing assemblies, and wall enclosures. Consequently, both material quantity and emission intensity contributed to their dominant shares of pre-use embodied carbon. When considered together with the results of the building-component analysis (Table 1), a consistent pattern emerged. Concrete (6,790.47 $kgCO_2e$; 23.13%) together with reinforcing steel (1,529.78 $kgCO_2e$; 5.21%) constituted the principal materials used in the reinforced concrete structural system, which generated a combined embodied carbon of 10,533.29 $kgCO_2e$. constituted the primary resource linked to high-emission elements, predominantly driving the structural steel framework (4,605.87 $kgCO_2e$) while making substantial contributions to the wall assembly, which recorded a cumulative embodied carbon of 7,527.36 $kgCO_2e$. Correspondingly, corrugated steel sheeting and ancillary materials (4,911.09 $kgCO_2e$; 16.73%) served as the principal inputs for the roofing subsystem (2,748.18 $kgCO_2e$; 9.36%), alongside maintaining a notable material presence within the wall system. In addition, EPS panels (1,652.76 $kgCO_2e$; 5.63%) were identified as another major resource directly associated with the wall system. These findings are consistent with the observation that the wall system was the largest contributor to embodied carbon within the architectural works category. Among the energy-related resources, diesel fuel generated 1,645.06 $kgCO_2e$ (5.60%), while electricity consumption contributed 1,625.74 $kgCO_2e$ (5.54%). Both resources individually accounted for more than 5% of the total embodied carbon, indicating that energy use during the pre-use stage represented another significant source of greenhouse gas emissions. Combined, diesel fuel and electricity accounted for 3,270.80 $kgCO_2e$, representing to 11.14% of the total embodied carbon, thereby identifying these inputs as significant energy-related carbon hotspots within the project lifecycle. In contrast, gasoline contributed only 10.78 $kgCO_2e$ (0.04%), representing a negligible contribution compared with diesel fuel and electricity. Conversely, several resources, including crushed stone, sand, office paper, gasoline, partition wall accessories, steel formwork, and office containers, each contributed less than 1% of the total embodied carbon. Although these resources inputs were operationally essential for project execution, their cumulative contribution to overall embodied carbon remained comparatively negligible relative to the primary resource categories. Consequently, carbon reduction measures focusing exclusively

Table 2: Embodied carbon emissions and contribution classified by resource type

Resource	Embodied Carbon ($kgCO_2e$)	Contribution (%)
Construction materials		
Crushed stone	39.28	0.13
Sand	145.15	0.49
Eucalyptus Timber	871.63	2.97
Reinforcing Steel	1,529.78	5.21
Concrete	6,790.47	23.13
Cement	817.25	2.78
Structural Steel	5,374.10	18.31
Welding Electrode	217.05	0.74
Tap Water	378.87	1.29
Concrete Blocks	444.43	1.51
Corrugated steel sheets and associated materials	4,911.09	16.73
EPS Panels	1,652.76	5.63
Partition Wall Accessories	49.27	0.17
Clear Glass	183.39	0.62
Extruded Aluminum	339.40	1.16
Rolling Steel Door	648.10	2.21
Ceiling panels and associated materials	141.53	0.48
Paint	330.36	1.13
Office supplies		
A4 Paper	10.83	0.04
Refrigerants and Waste Management		
Refrigerant (R-143a)	238.26	0.81
Methane from the On-site Septic Tank	211.68	0.72
Solid waste disposal	172.99	0.59
Transportation of equipment, machinery, and site facilities		
Steel Formwork	39.52	0.13
Construction Machinery	411.22	1.40
Construction Tools	64.40	0.22
Office Container	59.08	0.20
Fuel and electricity		
Diesel Fuel	1,645.06	5.60
Gasoline	10.78	0.04
Electricity	1,625.74	5.54
Total	29,353.47	100.00

on these low-contributing resources are unlikely to achieve substantial reductions in the overall embodied carbon of the project when compared with strategies targeting the identified carbon hotspots. Overall, categorized by both resource type and building component exhibited a consistent pattern, demonstrating that the embodied carbon footprint of the case-study building was predominantly governed by a select subset of key material inputs concentrated within the highest-emission building components. These resources included the principal materials used in the reinforced concrete structural system, the structural steel system, and the roofing and wall systems within the architectural works category. In addition, diesel fuel and electricity emerged as prominent energy-related emission sources warranting explicit integration into life-cycle carbon reduction frameworks. These findings collectively indicate that mitigation strategies should prioritize high-emission inputs—specifically concrete, structural steel, corrugated steel assemblies, alongside operational diesel and electricity consumption. Improving material selection while enhancing fuel and energy efficiency during construction is expected to achieve the greatest reduction in the overall embodied carbon of reinforced concrete factory building projects. Sensitivity analysis showed that varying the emission factors of the five principal hotspot resources by ±20% affected the total embodied carbon but did not substantially change

the overall hotspot pattern. Concrete remained the dominant contributor, while structural steel and corrugated steel remained among the three major material hotspots. Similarly, diesel fuel and electricity continued to function as notable energy-related contributors. These findings demonstrate that the primary carbon hotspots identified in this investigation exhibited overall robustness against plausible fluctuations in associated emission factors.

Embodied carbon by life-cycle module

Following the building-component and resource-type evaluations, which isolated the primary embodied carbon contributors at both the assembly and material building-component and resource levels, this section examines embodied carbon through a complementary lens by categorizing greenhouse gas emissions according to life-cycle modules. The analysis considers the four modules included within the assessment boundary, namely construction material production (A1–A3), transportation of construction materials (A4), fuel and energy use during construction (A5a), and construction waste management (A5w). Classification by life-cycle module provides additional insight into the distribution of embodied carbon by identifying system-level carbon hotspots, thereby indicating where greenhouse gas emissions predominantly occur rather than which materials are responsible for the emissions. This perspective facilitates the development of mitigation strategies better synchronized with the operational dynamics of distinct life-cycle stages. For instance, when the preponderance of embodied carbon stems from the material production stage, primary emphasis must be directed toward low-carbon material substitution, environmentally preferable suppliers selection, and material specification optimization. Conversely, where emissions are primarily associated with transportation, construction energy use, or construction waste management, greater attention should be directed toward logistics optimization, improved energy efficiency, and waste minimization during construction. Consequently, the life-cycle module analysis corroborates the insights established in preceding sections, thereby furnishing a more robust foundation for prioritizing embodied carbon abatement strategies. The life-cycle module breakdown of the embodied carbon assessment (Fig. 5) showed that construction material production (A1–A3) contributed 22,926.93 $kgCO_2e$, accounting for 78.10% of the total embodied carbon. This was followed by fuel and energy use during construction (A5a) with 3,547.33 $kgCO_2e$ (12.09%), construction waste management (A5w) with 1,540.83 $kgCO_2e$ (5.25%), and transportation of construction materials (A4) with 1,338.38 $kgCO_2e$ (4.56%). These results indicate that the embodied carbon of the case-study factory building was predominantly concentrated in the construction material production stage (A1–A3). In comparison, fuel and energy use during construction (A5a) and construction waste management (A5w) played secondary roles, together accounting for 17.34% of the total embodied carbon. Among all evaluated life-cycle modules, material transportation (Module A4) accounted for the lowest share of cumulative embodied carbon within the scope of this study. Overall, the life-cycle module analysis demonstrates that the majority of embodied carbon originated from the construction material production stage (A1–A3), with additional contributions from fuel and energy use during construction, construction waste management, and transportation of construction materials. These findings furnish a critical empirical baseline for the holistic interpretation of outcomes, bridging them with the component-level and material-specific evaluations detailed in the subsequent section.

Integrated analysis of embodied carbon by building component, resource/activity type, and life-cycle module

Although the analyses of building components, resource/activity types, and life-cycle modules

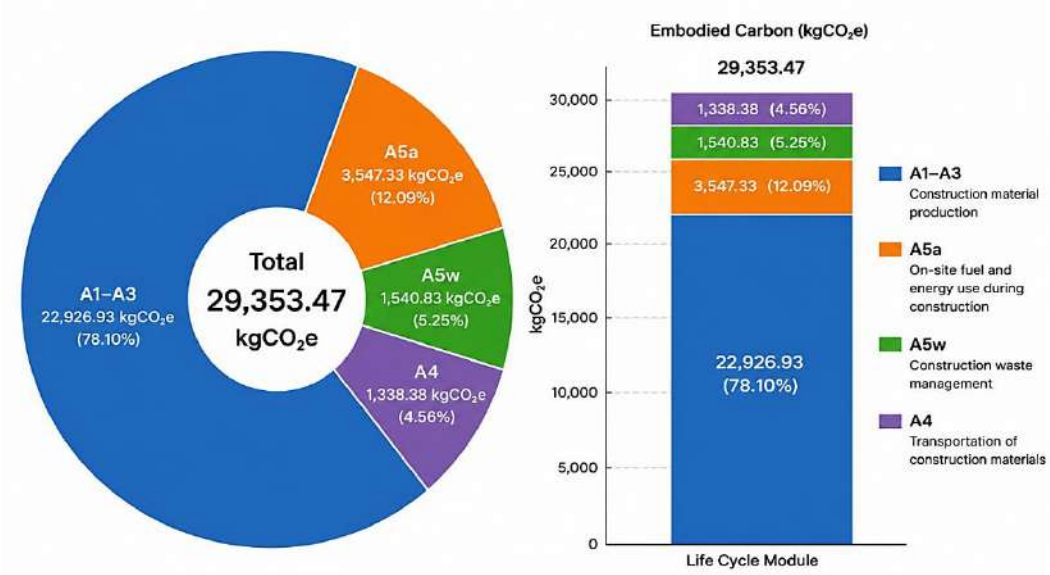

Fig. 5: Embodied carbon emissions and percentage contribution classified by the life-cycle module of the factory building

successfully identified the major sources of embodied carbon from different perspectives, consideration of each dimension independently does not fully reveal the practical relationships among them. Specifically, it fails to identify which resources or construction activities drive the embodied carbon of individual building components, nor does it specify the life-cycle modules where these emissions predominantly occur. To address this limitation, this section presents an integrated analysis of embodied carbon based on the combined framework of building component–resource/activity–life-cycle module (A1–A3, A4, A5a, and A5w). This integrated classification identifies the primary emission-contributing resources and activities associated with individual building components, alongside the specific life-cycle modules where greenhouse gas emissions are concentrated. These results are presented in Tables 3 to 5. The integrated analysis presented in Table 3 shows that the structural works generated a total embodied carbon of 15,139.16 $kgCO_2e$. The majority of emissions originated from the construction material production stage (A1–A3), which accounted for 11,842.17 $kgCO_2e$ (78.22%). The principal material contributors were concrete, with a total embodied carbon of 6,790.47 $kgCO_2e$ (44.85%), including 6,457.69 $kgCO_2e$ from A1–A3; structural steel, contributing 3,868.70 $kgCO_2e$ (25.55%), of which 3,657.82 $kgCO_2e$ originated from A1–A3; and reinforcing steel, contributing 1,514.38 $kgCO_2e$ (10.00%), including 1,348.75 $kgCO_2e$ from A1–A3. For the transportation stage (A4), total emissions amounted to 894.37 $kgCO_2e$ (5.91%), with transportation of construction machinery representing the largest individual contributor (346.36 $kgCO_2e$). During the construction stage (A5a), total embodied carbon was 1,230.69 $kgCO_2e$ (8.13%), with diesel fuel consumption accounting for the majority of emissions (1,208.34 $kgCO_2e$). In the construction waste management stage (A5w), total emissions reached 1,171.93 $kgCO_2e$ (7.74%), of which eucalyptus timber contributed the largest share (788.83 $kgCO_2e$). The integrated analysis presented in Table 4 indicates that the architectural works generated a total embodied carbon of 11,939.44 $kgCO_2e$, with emissions overwhelmingly concentrated in the construction material production stage (A1–A3), which accounted for 11,079.01 $kgCO_2e$ (92.79%).

Table 3: Embodied carbon emissions and contribution of structural works classified by resource/activity type and life-cycle module

Resource/activity	A1–A3	A4	A5a	A5w	Total	Contribution (%)
Construction materials						
– Sand	54.08	51.15	–	–	105.23	0.70
– Steel Formwork	–	39.52	–	–	39.52	0.26
– Eucalyptus Timber	67.98	14.82	–	788.83	871.63	5.76
– Reinforcing Steel	1,348.75	110.81	–	54.82	1,514.38	10.00
– Concrete	6,457.69	112.02	–	220.76	6,790.47	44.85
– Cement	3.97	1.37	–	11.31	16.65	0.11
– Structural Steel	3,657.82	114.67	–	96.21	3,868.70	25.55
– Welding Electrode	133.53	4.89	–	–	138.42	0.91
Transportation of machinery, tools and temporary site facilities						
– Construction Machinery	–	346.36	–	–	346.36	2.29
– Construction Tools	–	64.40	–	–	64.40	0.43
Fuel and electricity						
– Diesel Fuel	117.57	30.17	1,208.34	–	1,356.08	8.96
– Gasoline	0.78	4.19	5.81	–	10.78	0.07
– Electricity	–	–	16.54	–	16.54	0.11
Total	11,842.17	894.37	1,230.69	1,171.93	15,139.16	100.00

Table 4: Embodied carbon emissions and contribution of architectural works classified by resource/activity type and life-cycle module

Resource/activity	A1–A3	A4	A5a	A5w	Total	Contribution (%)
Construction materials						
– Concrete Blocks	386.34	56.36	–	1.73	444.43	3.72
– Reinforcing Steel	13.51	1.05	–	0.84	15.40	0.13
– Crushed Stone	7.30	30.64	–	1.34	39.28	0.33
– Sand	17.96	16.99	–	4.97	39.92	0.33
Tap Water	378.87	–	–	–	378.87	3.17
Cement	770.67	29.89	–	0.04	800.60	6.71
Corrugated steel sheets and associated materials	4,768.48	15.35	–	127.26	4,911.09	41.13
Structural Steel	1,404.98	48.10	–	52.32	1,505.40	12.61
Welding Electrode	76.50	2.13	–	–	78.63	0.66
EPS Panels	1,604.50	46.83	–	1.43	1,652.76	13.84
Partition Wall Accessories	49.21	0.00	–	0.06	49.27	0.41
Clear Glass	174.75	8.64	–	–	183.39	1.54
Extruded Aluminum	333.85	5.55	–	–	339.40	2.84
Rolling Steel Door	630.18	17.92	–	–	648.10	5.43
Ceiling panels and associated materials	120.92	16.71	–	3.90	141.53	1.19
Paint	315.94	14.42	–	–	330.36	2.77
Transportation of machinery, tools and temporary site facilities						
Construction machinery	–	64.86	–	–	64.86	0.54
Fuel and electricity						
Diesel Fuel	25.05	6.43	257.50	–	288.98	2.42
Electricity	–	–	27.17	–	27.17	0.23
Total	11,079.01	381.87	284.67	193.89	11,939.44	100.00

The largest material contributor was corrugated steel sheets and associated materials, with a total embodied carbon of 4,911.09 $kgCO_2e$ (41.13%), comprising 4,768.48 $kgCO_2e$ from A1–A3 and 127.26 $kgCO_2e$ from A5w. This was followed by EPS panels, contributing 1,652.76 $kgCO_2e$ (13.84%), including 1,604.50 $kgCO_2e$ from A1–A3 and 46.83 $kgCO_2e$ from A4, and structural steel, contributing 1,505.40 $kgCO_2e$ (12.61%), of which 1,404.98 $kgCO_2e$ originated from A1–A3 and 48.10 $kgCO_2e$ from A4. During the construction stage (A5a), total embodied carbon amounted to 284.67 $kgCO_2e$, with diesel fuel consumption representing the largest individual contributor (257.50 $kgCO_2e$). Within the transportation stage (A4), transportation of construction machinery was identified as another notable emission source, contributing 64.86 $kgCO_2e$. The integrated analysis

Table 5. Embodied carbon emissions and contribution of construction support works classified by resource/activity type and life-cycle module

Resource/activity	A1–A3	A4	A5a	A5w	Total	Contribution (%)
Office supplies						
A4 Paper	5.75	3.06	–	2.02	10.83	0.48
Refrigerants and waste management						
Air-Conditioning Refrigerant (R-143a)	–	–	238.26	–	238.26	10.47
Methane from the On-site Septic Tank	–	–	211.68	–	211.68	9.31
Transportation of machinery, tools and temporary site facilities						
Office Container	–	59.08	–	–	59.08	2.60
Construction waste management						
Construction Waste	–	–	–	172.99	172.99	7.60
Fuel and electricity						
Electricity	–	–	1,582.03	–	1,582.03	69.54
Total	5.75	62.14	2,031.97	175.01	2,274.87	100.00

presented in Table 5 shows that the construction support works generated a total embodied carbon of 2,274.87 $kgCO_2e$, exhibiting a markedly different emission pattern from the other two work categories. Emissions were overwhelmingly concentrated in the construction stage (A5a), contributing 2,031.97 $kgCO_2e$ (89.32%) of the total embodied carbon. Electricity consumption emerged as the dominant emission hotspot, occurring entirely within module A5a and accounting for 1,582.03 $kgCO_2e$ (69.54%). Additional major contributors included air-conditioning refrigerant (238.26 $kgCO_2e$) and methane emissions from the onsite septic tank (211.68 $kgCO_2e$). Within the construction waste management stage (A5w), the principal hotspot was construction waste, contributing 172.99 $kgCO_2e$, whereas in the transportation stage (A4), the largest contributor was the transportation of office containers, accounting for 59.08 $kgCO_2e$. These results indicate that the embodied carbon associated with construction support works stems primarily from energy consumption and temporary site utility systems. Overall, the integrated building component–resource/activity–life-cycle module classification demonstrates that embodied carbon hotspots are highly specific to individual work categories and their respective emission mechanisms. For the structural works, embodied carbon was predominantly driven by structural materials during the production stage (A1–A3), alongside stage-specific hotspots linked to diesel fuel consumption in stage A5a and eucalyptus timber in stage A5w. The architectural works were dominated by materials used in the building envelope and roofing systems, with emissions concentrated almost entirely in A1–A3. In contrast, the construction support works were principally driven by energy consumption and temporary site utility systems during A5a. These findings provide a comprehensive foundation for interpreting embodied carbon emissions from an engineering perspective and establish a robust basis for comparison with previous studies in the subsequent Discussion section.

Engineering implications and practical applications

The findings of this study demonstrate that the embodied carbon of the reinforced concrete factory building was predominantly associated with the construction material production stage (A1–A3) and was concentrated in a limited number of high-emission building components. Notably, the reinforced concrete structural system, wall system, and structural steel system collectively accounted for 67.50% of the building's total embodied carbon. From an engineering perspective, these findings advocate for a hotspot-based approach to embodied carbon mitigation, prioritizing reduction efforts on highy-emission

building components before addressing elements with lower relative contributions. Such an approach is expected to achieve greater reductions in the overall embodied carbon of the project than strategies that distribute mitigation efforts uniformly across all building components. This finding aligns with the broader application of LCA in environmental management, where identifying key environmental hotspots serves as an established foundation for prioritizing mitigation strategies and supporting evidence-based decision-making across diverse infrastructure and facility systems (Buadit *et al.,* 2026). The results further indicate that the design stage represents the most influential decision point for reducing embodied carbon because it determines the selection of construction materials, material quantities, and structural systems, all of which directly influence greenhouse gas emissions during the construction material production stage (A1–A3). Consequently, decisions made during the early design phase have a substantial influence on the embodied carbon performance of the building throughout the pre-use stage and provide the greatest opportunity for implementing effective carbon reduction measures. Consequently, design-phase mitigation strategies should be tailored to address the specific emission mechanisms driving the highest-emitting building components. For the reinforced concrete structural system, highly effective mitigation measures include adopting low-carbon concrete, the incorporating supplementary cementitious materials (SCMs), utilizing reinforcing steel with high recycled content, and implementing material-efficient structural designs (Cabeza *et al.,* 2014). For the structural steel system, priority should be given to selecting steel products with higher recycled content and optimizing structural detailing and member configurations to minimize material consumption (Akbarnezhad and Xiao, 2017). For wall system, mitigation efforts should prioritize selecting low-carbon construction materials while simultaneously minimizing material losses and enhancing installation efficiency (Pomponi and Moncaster, 2016). These mitigation measures are presented as potential strategies based on the identified hotspots rather than as quantitatively evaluated alternatives. Their actual carbon-reduction potential depends on project-specific material availability, emission factors, structural requirements, and design constraints; therefore, quantitative scenario assessment is recommended for future research. These strategies are particularly relevant because wall systems typically encompass extensive surface areas, rendering them more vulnerable to material waste generated during cutting, fitting, and installation processes. Although the construction material production stage (A1–A3) represented the dominant source of embodied carbon in the present study, the results also highlight the management significance of the remaining life-cycle modules, particularly A4 (transportation of construction materials) and A5 (construction activities). Emissions associated with stage A4 are highly dependent on transportation distances and project-specific logistics, increasing substantially when construction materials are procured from geographically distant suppliers (Zuluaga and Saxe, 2025). Likewise, emissions generated during stage A5a (fuel and energy consumption during construction) and stage A5w (construction waste management) reflect the efficacy of onsite management practices, indicating that reductions can be achieved through improved energy conservation, optimized equipment utilization, and enhanced waste diversion strategies (Myint and Shafique, 2024). Accordingly, mitigation measures targeting the A4–A5 modules should be regarded as complementary strategies that enhance overall carbon reduction performance, even though their contributions remain lower than those of A1–A3. From an engineering perspective, embodied carbon assessment should be embedded into the building design process as a core decision-making criterion to optimize both material carbon intensity and required material

quantities. This objective can be achieved by incorporating the principles of material efficiency (Drewniok *et al.,* 2023) and structural optimization (Abushama *et al.,* 2025), together with the systematic use of Environmental Product Declarations (EPDs) to support transparent and evidence-based comparisons of alternative construction materials (Santos *et al.,* 2025). Ultimately, low-carbon factory building design must be anchored in the localization of primary embodied carbon hotspots, guiding the deployment of targeted mitigation measures aligned with their respective emission drivers. These measures should be complemented by improvements in logistics planning and onsite construction management during the A4–A5 life-cycle modules to maximize embodied carbon reduction at the project level.

Comparison with previous studies

Comparisons with previous studies should be interpreted cautiously because of differences in system boundaries, building size, reference units, and included materials. Compared to the industrial factory building evaluated by Rodrigues *et al.* (2018), the case-study building in this research exhibited lower embodied carbon values across both total emissions and emissions per unit floor area. This difference is likely attributable to variations in building characteristics and functional requirements. The factory building evaluated by Rodrigues *et al.* (2018) was larger and structurally more complex, featuring greater building height, multiple stories, and basement levels. Furthermore, as a heavy industrial facility, it required substantially thicker reinforced concrete floor slabs to support heavy machinery and large inventory loads. Climatic variations may also have influenced the performance requirements of the building envelope, thereby elevating the embodied carbon associated with specific architectural components relative to the present case study. Overall, the findings of the present study reinforce a consistent trend reported in the embodied carbon literature, namely that the construction material production stage (A1–A3) constitutes the dominant source of embodied carbon in buildings. This observation aligns with the findings of Cabeza *et al*. (2014), Röck *et al*. (2020), and Myint and Shafique (2024), who demonstrated that the production of primary construction materials, notably cement and steel, is highly energy-intensive, serving as the primary driver of greenhouse gas emissions during the pre-use stage of buildings. These findings also corroborate the recommendations of Santos *et al*. (2025), who underscored that embodied carbon reduction must commence during the design phase, as material selection and specification decisions critically dictate emissions associated with stages A1–A3. Overall, the findings of this study support the growing body of evidence demonstrating that A1–A3 is the primary contributor to embodied carbon in buildings. Concurrently, these findings underscore that the relative importance of other life-cycle stages, specifically modules A5a and A5w, depends heavily on project-specific variables, including building type, functional requirements, and construction practices. These findings further reinforce the importance of adopting a LCA-based approach to identify project-specific carbon hotspots and prioritize mitigation strategies according to their relative contribution to overall greenhouse gas emissions, as recommended in recent environmental management studies. Consequently, the interpreting embodied carbon results and designing mitigation strategies must account for individual project characteristics alongside prior empirical evidence, ensuring that carbon reduction measures remain both technically sound and practically effective for factory construction within the Thai construction context. Furthermore, transparent quantification of embodied carbon can provide reliable evidence to support sustainability reporting, improve environmental transparency, and facilitate evidence-based decision-making for low-carbon construction practices across diverse project contexts and scales.

Limitations and future research

Although this study provides a systematic assessment of the embodied carbon for a reinforced concrete factory building and identifies primary carbon hotspots across both life-cycle and building-component levels, several limitations should be considered when acknowledged the findings. First, the assessment was limited to the pre-use stage, comprising construction material production (A1–A3), transportation of construction materials (A4), fuel and energy use during construction (A5a), and construction waste management (A5w), in accordance with BS EN 15978. The use stage (B1–B7) and end-of-life stage (C1–C4) were excluded, the findings primarily reflect pre-use embodied carbon and do not capture the full life-cycle environmental impacts of the building. Second, the embodied carbon calculations were based on EFs obtained from published databases and reference sources. These figures may deviate from the specific carbon intensities linked to products provided by individual manufacturers. As a result, the accuracy of the assessment depends on the extent to which the selected EFs represent the materials used in the project. The use of product-specific Environmental Product Declarations (EPDs) would improve both the accuracy and transparency of future embodied carbon assessments. Third, because this study relies on a single factory building case study, caution is warranted when generalizing these findings to alternative building typologies or construction projects characterized by differing architectural configurations, structural configurations, material specifications, and operational conditions. Nevertheless, the assessment framework and analytical approach developed in this study can readily be applied to other projects by adapting the activity data and EFs to reflect project-specific conditions. Future research should address these limitations by extending the assessment to Whole Life Carbon, incorporating both the use stage (B1–B7) and the end-of-life stage (C1–C4) to provide a more comprehensive understanding of the environmental impacts throughout the building life cycle. In addition, future studies should improve data quality by utilizing product-specific EPDs and considering variations in manufacturing processes, material sources, and construction practices under real project conditions. Generalizing these insights would benefit from incorporating broader case studies that capture varying facility typologies, structural frameworks, and material profiles, thereby allowing a more rigorous appraisal of the determinants governing embodied carbon. Furthermore, future research should focus on developing assessment tools and decision-support frameworks that facilitate the integration of embodied carbon assessment into the building design process. This could be achieved through the integration of Building Information Modeling (BIM) with EPD databases, enabling real-time embodied carbon assessment during the design stage. Such advancements would also facilitate structural optimization and the evaluation of low-carbon material alternatives by concurrently balancing embodied carbon, construction cost, and structural performance, thereby delivering practical and evidence-based solutions for project-level mitigation.

CONCLUSION

This study assessed the embodied carbon of a reinforced concrete factory building in Thailand using the LCA methodology. The assessment was limited to the pre-use stage, encompassing construction material production (A1–A3), transportation of construction materials (A4), fuel and energy use during construction (A5a), and construction waste management (A5w). The results showed that the building generated a total embodied carbon of 29,353.47 $kgCO_2e$, equivalent to 326.15 $kgCO_2e/m^2$ based on a gross floor area of 90.00 m^2. Classification by building component revealed that embodied carbon was predominantly concentrated in elements requiring high volumes of construction materials. The reinforced concrete structural system generated the highest embodied carbon

(10,533.29 $kgCO_2e$), followed by the wall system (7,527.36 $kgCO_2e$). Consequently, these two building components emerged as the primary carbon hotspots within the case-study facility. This trend aligns with the resource-based analysis, which demonstrated that embodied carbon is predominantly driven by a select group of major construction materials. Concrete contributed 6,790.47 $kgCO_2e$ (23.13%), followed by structural steel with 5,374.10 $kgCO_2e$ (18.31%), and corrugated steel sheets and associated materials with 4,911.09 $kgCO_2e$ (16.73%). Collectively, these three resource categories accounted for 58.17% of the total embodied carbon. Concrete was primarily associated with the reinforced concrete structural system, whereas structural steel and corrugated steel sheets predominated in the steel framework and the building envelope, particularly within the wall and roofing assemblies. Furthermore, construction-phase energy resources made substantial contributions, with diesel fuel accounting for 1,645.06 $kgCO_2e$ (5.60%) and electricity consumption contributing 1,625.74 $kgCO_2e$ (5.54%), underscoring potential pathways for emission mitigation via enhanced energy governance and optimized onsite practices. Classification by life-cycle module further demonstrated that the dominant source of embodied carbon was construction material production (A1–A3), contributing 22,926.93 $kgCO_2e$ (78.10%), followed by fuel and energy use during construction (A5a) with 3,547.33 $kgCO_2e$ (12.09%), construction waste management (A5w) with 1,540.83 $kgCO_2e$ (5.25%), and transportation of construction materials (A4) with 1,338.38 $kgCO_2e$ (4.56%). These findings suggest that carbon reduction frameworks must prioritize manufacturing-phase emissions from construction materials, alongside optimizing onsite energy performance and curbing construction waste. When the results were examined collectively across the dimensions of building component–resource–life-cycle module, distinct emission mechanisms were identified for each work category. The structural works were primarily driven by structural materials during A1–A3, with additional stage-specific emissions arising from diesel fuel consumption during A5a and eucalyptus timber during A5w. Conversely, the architectural works were governed by materials employed in the building envelope and roofing assemblies, with emissions overwhelmingly concentrated in stages A1–A3. Conversely, the construction support works were characterized by emissions associated predominantly with energy consumption and temporary site utility systems during stage A5a. This integrated analysis enabled the systematic identification of both the critical construction materials and onsite construction activities responsible for embodied carbon emissions within each work category, thereby providing a robust basis for developing mitigation strategies tailored to their respective emission mechanisms. Consequently, these insights hold meaningful implications for both future research directions and professional execution. Designers, structural engineers, and architects can utilize the identified carbon hotspots to optimize design solutions and incorporate low-carbon materials at the early design stage. Project owners and procurement teams can use the hotspot rankings to establish material specifications and prioritize mitigation measures with the greatest carbon reduction potential. Project managers and construction contractors can utilize these outcomes to refine operational energy strategies and minimize waste generation during site implementation. Furthermore, government agencies and professional organizations may use the results as supporting evidence for developing embodied carbon management guidelines and benchmark values for factory buildings within the Thai construction sector, promoting consistent assessment practices and informed decisions.

AUTHOR CONTRIBUTIONS

N. Suriyanon contributed to the overall project conceptualization of the study, research methodology, data collection, interpretation of the results, and review of the manuscript.

W. Suriyanon, the corresponding author, contributed to research supervision, interpretation of the results, and review and revision of the manuscript. Nakorn Suriyanon contributed to the life cycle assessment, embodied carbon and hotspot analyses, interpretation and discussion of the results, preparation of figures and tables, and manuscript preparation. N. Watkate contributed to data collection, verification of construction-related data, interpretation of the results, and review of the manuscript.

ACKNOWLEDGEMENT

The authors gratefully acknowledge the support and cooperation of the project owner and construction personnel involved in the case-study factory building in Chiang Mai Province, Thailand, for providing the construction drawings, technical specifications, Bill of Quantities (BOQ), and other relevant project information used in this study. The authors also acknowledge Chiang Mai University and Rajamangala University of Technology Lanna for their academic support and facilities that contributed to the completion of this study.

CONFLICT OF INTEREST

The authors declare that there is no conflict of interests regarding the publication of this manuscript. In addition, the ethical issues, including plagiarism, informed consent, misconduct, data fabrication and/or falsification, double publication and/or submission, and redundancy have been completely observed by the authors.

OPEN ACCESS

©2027 The author(s). This article is licensed under a Creative Commons Attribution 4.0 International License, which permits use, sharing, adaptation, distribution and reproduction in any medium or format, as long as you give appropriate credit to the original author(s) and the source, provide a link to the Creative Commons license, and indicate if changes were made. The images or other third-party material in this article are included in the article's Creative Commons license, unless indicated otherwise in a credit line to the material. If material is not included in the article's Creative Commons license and your intended use is not permitted by statutory regulation or exceeds the permitted use, you will need to obtain permission directly from the copyright holder. To view a copy of this license, visit: http://creativecommons.org/licenses/by/4.0/

PUBLISHER'S NOTE

GJESM Publisher remains neutral with regard to jurisdictional claims in published maps and institutional affiliations.

POSITIVE AI STATEMENT

During the preparation of this work, the authors used ChatGPT (OpenAI) to assist with English language editing, grammatical correction, and improving the clarity and readability of the manuscript. After using this tool/service, the authors reviewed and edited the content as needed and take full responsibility for the content of the publication.

ABBREVIATIONS

%	Percent
A1–A3	Construction material production
A4	Transportation of construction materials
A5a	Fuel and energy use during construction
A5w	Construction waste management
BIM	Building Information Modeling
BOQ	Bill of Quantities
BS EN	British Standard European Norm
CO_2	Carbon dioxide
CO_2e	Carbon dioxide equivalent

EF	Emission factor
EPD	Environmental Product Declaration
EPS	Expanded polystyrene
GHG	Greenhouse gas
ISO	International Organization for Standardization
$kgCO_2e$	Kilogram carbon dioxide equivalent
km	Kilometer
LCA	Life Cycle Assessment
LCI	Life Cycle Inventory
MEP	Mechanical, Electrical, and Plumbing
m^2	Square meter
SCMs	Supplementary Cementitious Materials
TGO	Thailand Greenhouse Gas Management Organization (Public Organization)
WBS	Work Breakdown Structure
WLC	Whole Life Carbon

REFERENCES

Abushama, K.; Hawkins, W.; Pelecanos, L.; Ibell, T., (2025). Optimisation of embodied carbon and construction cost of concrete, steel and timber piles. Dev. Built Environ., 22: 100656 **(13 pages).**

Agustiningtyas, R.S.; Takaguchi, H.; Prasetya, A.B.; Kubota, T., (2024). Embodied energy and carbon assessment of existing affordable apartments in Indonesia. J. Asian Archit. Build. Eng., 23(6): 2057-2070 **(14 pages).**

Akbarnezhad, A.; Xiao, J., (2017). Estimation and minimization of embodied carbon of buildings: A review. Buildings. 7(1): 5 **(17 pages).**

Amarasinghe, I.; Liu, T.; Stewart, R.A.; Mostafa, S., (2025). Paving the way for lowering embodied carbon emissions in the building and construction sector. Clean Technol. Environ. Policy. 27(4): 1825-1843 **(19 pages).**

BSI, (2011). BS EN 15978:2011 Sustainability of construction works—assessment of environmental performance of buildings—calculation method. British Standards Institution, London, UK.

Buadit, T.; Janmaimool, P.; Bhatta, J.; Ounsaneha, W.; Rattanapan, C., (2026). Minimizing the environmental impact of hospitals by focusing on carbon footprint reduction. Global J. Environ. Sci. Manage., 12(4): 2157-2178 **(22 pages).**

Cabeza, L.F.; Rincón, L.; Vilariño, V.; Pérez, G.; Castell, A., (2014). Life cycle assessment (LCA) and life cycle energy analysis (LCEA) of buildings and the building sector: A review. Renew. Sustainable Energy Rev., 29: 394-416 **(23 pages).**

de Cadenet, V.; Komkum, W.; Raksa, P.; Boondaeng, P.; Parinyakulset, P., (2025). Carbon footprint associated with a small-scale emissions reduction initiative for sustainable event management. Global J. Environ. Sci. Manage., 11(3): 941-962 **(22 pages).**

De Wolf, C.; Pomponi, F.; Moncaster, A., (2017). Measuring embodied carbon dioxide equivalent of buildings: A review and critique of current industry practice. Energy Build., 140: 68-80 **(13 pages).**

Drewniok, M.P.; Cruz Azevedo, J.M.; Dunant, C.F.; Allwood, J.M.; Cullen, J.M.; Ibell, T.; Hawkins, W., (2023). Mapping material use and embodied carbon in UK construction. Resour. Conserv. Recycl., 197: 107056 **(15 pages).**

Firmansyah, I.; Santoso, A.D.; Nuha, N.; Sahwan, F.L.; Suryanto, F.; Wahyono, S., (2025). Environmental impact of car wash services by performing life cycle perspective. Global J. Environ. Sci. Manage., 11(1): 261-276 **(16 pages).**

Gauch, H.L.; Dunant, C.F.; Hawkins, W.; Cabrera Serrenho, A., (2023). What really matters in multi-storey building design? A simultaneous sensitivity study of embodied carbon, construction cost, and operational energy. Appl. Energy, 333: 120585 **(14 pages).**

Gibbons, O.P.; Orr, J.J.; Arnold, W., (2025). How to calculate embodied carbon. Third edition. The Institution of Structural Engineers, London, UK.

Greer, F.; Raftery, P.; Brager, G.; Horvath, A., (2023). A perspective on tools for assessing the building sector's greenhouse gas emissions and beyond. Environ. Res.: Infrastruct. Sustainability. 3(4): 043001 **(18 pages).**

Huang, M.Q.; Chen, X.L.; Ninić, J.; Bai, Y.; Zhang, Q.B., (2023). A framework for integrating embodied carbon assessment and construction feasibility in prefabricated stations. Tunn. Undergr. Space Technol., 132: 104920 **(19 pages).**

ISO, (2006a). ISO 14040:2006 Environmental management—Life cycle assessment—Principles and framework. International Organization for Standardization, Geneva, Switzerland.

ISO, (2006b). ISO 14044:2006 Environmental management—Life cycle assessment—Requirements and guidelines. International Organization for Standardization, Geneva, Switzerland.

Jayawardana, A.S.; Perera, N.G.R.; Perera, L.A.S.R., (2021). "Cradle to Gate" assessment of material related embodied carbon: A design stage stratagem for mid-rise housing in Sri Lanka. Energy Build., 230: 110542 **(12 pages).**

Kanangkaew, S.; Suriyanon, N.; Rinchumphu, D.; Jokkaw, N.; Kaewmoracharoen, M.; Pang, D.; Charnwasununth, P., (2026). BIM-based embodied carbon assessment during the pre-construction phases. IOP Conf. Ser.: Earth Environ. Sci., 1629(1): 012053 **(9 pages).**

Li, X.; Yang, F.; Zhu, Y.; Gao, Y., (2014). An assessment framework for analyzing the embodied carbon impacts of residential buildings in China. Energy Build., 85: 400-409 **(10 pages).**

Liwthaisong, S.; Chaithongrat, T.; Aksorn, P., (2025). Reinforced concrete and embodied carbon in construction: Challenges and pathways to reduction in Thailand. Eng. Appl. Sci. Res., 52(2): 125-134 **(10 pages).**

Lützkendorf, T.; Balouktsi, M., (2022). Embodied carbon emissions in buildings: Explanations, interpretations, recommendations. Build. Cities, 3(1): 964-973 **(10 pages).**

Monahan, J.; Powell, J.C., (2011). An embodied carbon and energy analysis of modern methods of construction in housing: A case study using a lifecycle assessment framework. Energy Build., 43(1): 179-188 **(10 pages).**

Myint, N.N.; Shafique, M., (2024). Embodied carbon emissions of buildings: Taking a step towards net zero buildings. Case Stud. Constr. Mater., 20: e03024 **(20 pages).**

Pomponi, F.; Moncaster, A., (2016). Embodied carbon mitigation and reduction in the built environment: What does the evidence say? J. Environ. Manage., 181: 687-700 **(14 pages).**

Rashif, M.N.; Hartini, S.; Sari, D.P.; Ramadan, B.S.; Matsumoto, T.; Balasbaneh, A.T., (2025). Life cycle assessment of biomass waste briquettes as renewable energy. Global J. Environ. Sci. Manage., 11(1): 207-224 **(18 pages).**

Rodrigues, V.; Martins, A.A.; Nunes, M.I.; Quintas, A.; Mata, T.M.; Caetano, N.S., (2018). LCA of constructing an industrial building: Focus on embodied carbon and energy. Energy Procedia. 153: 420-425 **(6 pages).**

Röck, M.; Saade, M.R.M.; Balouktsi, M.; Rasmussen, F.N.; Birgisdottir, H.; Frischknecht, R.; Habert, G.; Lützkendorf, T.; Passer, A., (2020). Embodied GHG emissions of buildings—The hidden challenge for effective climate change mitigation. Appl. Energy. 258: 114107 **(19 pages).**

Sachchithananthan, M.; Ramachandra, T.; Geekiyanage, D., (2024). A simplified guide towards incentivising embodied carbon assessment: A case of high-rise residential building. In: Proc. 12th World Constr. Symp., Sri Lanka. 54-65 **(12 pages).**

Sandaruwan, I.P.T.; Manoharan, K.; Kulatunga, U., (2024). Cradle-to-gate embodied carbon assessment of green office building using life cycle analysis: A case study from Sri Lanka. J. Build. Eng., 88: 109155 **(13 pages).**

Samson, M.; Pope, R.J., (2012). A comparative embodied carbon assessment of commercial buildings. Struct. Eng., 90(10): 38-49 **(12 pages).**

Santos, A.K.; Ferreira, V.M.; Dias, A.C., (2025). Promoting decarbonisation in the construction of new buildings: A strategy to calculate the embodied carbon footprint. J. Build. Eng., 103: 112037 **(15 pages).**

Shi, Y.; Cao, X.; Yang, X., (2025). Assessment and reduction of embodied carbon emissions in buildings: A systematic literature review of recent advances. Energy Build., 345: 116058 **(23 pages).**

Suriyanon, N.; Suriyanon, N.; Suriyanon, W.; Doungsoma, T.; Jenvorapoj, K., (2026). Embodied carbon assessment of asphalt concrete roads and integrated drainage systems in Thai housing estates: A case study. Environ. Res. Commun., 8(4): 045022 **(20 pages).**

Teng, Y.; Pan, W., (2019). Systematic embodied carbon assessment and reduction of prefabricated high-rise public residential buildings in Hong Kong. J. Clean. Prod., 238: 117791 **(13 pages).**

Wan Omar, W.M.S., (2018). A hybrid life cycle assessment of embodied energy and carbon emissions from conventional and industrialised building systems in Malaysia. Energy Build., 167: 253-268 **(16 pages).**

Watkate, N.; Suriyanon, N., (2024). Embodied carbon estimation of a factory building. Proceedings of the 29th National Convention on Civil Engineering (NCCE29), Chiang Mai, Thailand, 29–31 May 2024, CEM26-1–CEM26-11 **(11 pages)** (in Thai).

Zhang, X.; Wang, F., (2016). Assessment of embodied carbon emissions for building construction in China: Comparative case studies using alternative methods. Energy Build., 130: 330-340 **(11 pages).**

Zuluaga, S.; Saxe, S., (2025). Leveraging building permit data for large-scale embodied carbon assessment of residential building construction. Environ. Res.: Infrastruct. Sustainability. 5(3): 035015 **(18 pages).**

AUTHOR (S) BIOSKETCHES

Suriyanon, N., Ph.D., Associate Professor, Department of Civil Engineering, Chiang Mai University, Thailand.
- Email: *natee.suriyanon@cmu.ac.th*
- ORCID: 0009-0003-0669-4138
- Web of Science ResearcherID: RBQ-2458-2026
- Scopus Author ID: 54788469300
- Homepage: https://urbanintelligence.eng.cmu.ac.th/experts/urban-management-experts/natee-suriyanon/

Suriyanon, W., Ph.D., Assistant Professor, Department of Civil and Environmental Engineering, Rajamangala University of Technology Lanna, Chiang Mai, Thailand.
- Email: *wanidaenv@rmutl.ac.th*
- ORCID: 0009-0009-1393-8085
- Web of Science ResearcherID: RBQ-8834-2026
- Scopus Author ID: 57330002800
- Homepage: https://lms.rmutl.ac.th/teachers/detail/26177613085019590/ca64d6ac9eb70538c68d70ebcaa3bed90d1c60bcd1cba72fda1e6d52b7414f12

Suriyanon, N., Ph.D., Assistant Professor, Department of Civil and Environmental Engineering, Rajamangala University of Technology Lanna, Chiang Mai, Thailand.
- Email: *jamecu555@rmutl.ac.th*
- ORCID: 0000-0002-6921-4184
- Web of Science ResearcherID: PKQ-5211-2026
- Scopus Author ID: 36983254200
- Homepage: https://lms.rmutl.ac.th/teachers/detail/24620320304433639/70b457950fc3161ee2f399a23558b27815a2993d3fab1bc134c4c7073d83fd86

Watkate, N., M.Eng., Graduate student, Department of Civil Engineering, Chiang Mai University, Thailand.
- Email: *passion.ranger@gmail.com*
- ORCID: 0009-0001-3210-300X
- Web of Science ResearcherID: NA
- Scopus Author ID: NA
- Homepage: https://www.researchgate.net/profile/Nikom-Watkate

HOW TO CITE THIS ARTICLE:
Suriyanon, N.; Suriyanon, W.; Suriyanon, N.; Watkate, N., (2027). Life cycle assessment and identification of embodied carbon hotspots in a reinforced concrete factory. Global J. Environ. Sci. Manage., 13(1): 303-326.

DOI: 10.22034.gjesm.2027.01.14
URL: https://www.gjesm.net/article_736221.html

Global J. Environ. Sci. Manage. 13(1): 327-346, Winter 2027, Serial #49

Global Journal of Environmental Science and Management
(GJESM)

Homepage: https://www.gjesm.net/

Podcasts

ORIGINAL RESEARCH ARTICLE

Valorization and physicochemical characterization of municipal solid waste gasification tar derived aliphatic hydrocarbon-rich oils

M. Ridwan, P. Setyono*, M.T.S. Budiastuti

Department of Environmental Science, Graduate School, Universitas Sebelas Maret, Jalan Ir. Sutami 36A Kentingan, Jebres, Surakarta, Central Java, Indonesia

ARTICLE INFO

Article History:
Received 14 June 2026
Revised 18 August 2026
Accepted 21 September 2026

Keywords:
Aliphatic hydrocarbons oil
Municipal solid waste
Gasification
Physicochemical characterization
Sequential re-pyrolysis
Tar valorization

DOI:10. 22034.gjesm.2027.01.15

ABSTRACT

BACKGROUND AND OBJECTIVES: Municipal solid waste gasification generates tar as a persistent by-product, posing operational and environmental challenges due to its viscosity, instability, and high content of various hydrocarbons. Previous studies demonstrated that the principal constituents of tar were predominantly aliphatic hydrocarbon compounds. The study objectives were to investigate the valorization potential and evaluate the physicochemical properties of the oil fraction derived from tar waste through pyrolysis process from gasification plant of Surakarta landfill, Indonesia.

METHODS: Conversion of tar into aliphatic hydrocarbon-rich oils using a sequential re-pyrolysis method at temperatures ranging from 350–700 degrees Celsius. The physical properties of the pyrolysis products, specifically temperature, viscosity, and density, were determined, while their chemical compositions were evaluated using gas chromatography and infrared spectroscopy. The results of the physicochemical tests were then analyzed and evaluated with those of commercial oil products.

FINDINGS: Pyrolysis produced three liquid fractions based on the sequential re- pyrolysis: tar pyrolysis 1, 2, and 3. Liquid yields of approximately 65–70 weight percent at 500–550 degrees Celsius. Mass spectrometry analysis revealed aliphatic hydrocarbons (alkane–alkene) contents of 86.65, 45.58, and 46.76 percent in tar pyrolysis oil-1, 2, and 3 samples. The identified aliphatic hydrocarbons ranged from 8–21, 12–43, and 9–20 carbon atoms in the respective fractions. The infrared spectra consistently displayed characteristic aliphatic carbon-hydrogen stretching vibrations, thereby confirming that the resulting products are rich in aliphatic hydrocarbons. The produced oils exhibited densities of 801.3–875.4 kilograms per cubic meter and viscosities of 2.304–2.956 centistokes at 40 degrees Celsius, indicating potential for liquid-fuel and hydrocarbon-material applications, although the relatively low flash point of 40–62 degrees celsius requires further upgrading for improved product stability.

CONCLUSION: Sequential re-pyrolysis demonstrated the potential to convert tar into aliphatic hydrocarbon-rich oils, with tar pyrolysis oil-3 showing the highest aliphatic hydrocarbon content (86.65 percent) and a C8–C21 carbon-chain range. The findings demonstrate that tar pyrolysis oil-3 exhibits the highest aliphatic content among the evaluated products, suggesting its viability as an intermediate hydrocarbon feedstock for subsequent upgrading. Further fractionation, upgrading, and scale-up studies are required to determine its suitability for specific fuel or hydrocarbon-material applications.

This is an open access article under the CC BY license (http://creativecommons.org/licenses/by/4.0/)

NUMBER OF REFERENCES	NUMBER OF FIGURES	NUMBER OF TABLES
58	6	10

*Corresponding Author:
Email: prabangsetyono@gmail.com
Phone: +62813 2842 3455
ORCID: 0000-0001-6440-6083

Note: Discussion period for this manuscript open until March 01, 2027 on GJESM website at the “Show Article”.

INTRODUCTION

An escalating municipal solid waste (MSW) crisis is currently being experienced in Indonesia. Approximately 43.458 million tons (Mt) of municipal solid waste were generated in 2023, with an average annual increase of 2–3 percent (%) attributed to urbanization, population growth, and changing consumption patterns (KLH, 2023). Urban centers such as Jakarta, Surabaya, and Bandung contribute significantly to this problem, generating over 1,500–2,500 tons per day (t/d) of waste each city (Himawanto, 2021). Waste sorting at the source and landfill management have been continuously pursued, yet more than 50% of waste still ends up in landfills. Landfill overburdening exerts significant adverse environmental impacts; furthermore, excessive reliance on landfilling creates spatial constraints and leads to the depletion of valuable energy resources embedded within municipal waste streams (Khan *et al*., 2022). Waste management challenges are increasingly being addressed through waste-to-energy (WtE) technology, while greater energy independence is simultaneously being promoted. One such technology, gasification, is increasingly gaining attention as an integrated solution for managing large amounts of waste while recovering energy (Wang *et al.,* 2023a). The national strategic framework incorporates the development of WtE facilities via eco-friendly technologies, aiming to expedite landfill waste management across 12 major urban centers through thermal applications pursuant to Presidential Regulation No. 35 of 2018. The thermal conversion of waste into electrical energy using gasification technology has been implemented in the city of Surakarta, with a processing capacity of 545 t/d and an electrical output of 8 MegaWatts (MW) (Sonjaya, 2021; Wasita, 2023). MSW gasification has emerged as a promising thermochemical technology for converting heterogeneous municipal waste into valuable energy. The primary product of gasification is synthetic gas (syngas), consisting of carbon monoxide (CO), hydrogen (H_2), and methane (CH_4), which is then converted into electricity. This methodological approach corresponds with the expanding global prioritization of sustainable WtE systems, which serve to curtail landfill diversion volumes while efficiently converting waste streams into secondary energy sources (Im-Orb *et al.*, 2016; Niu *et al.*, 2013). However, one of the most persistent and technical issues in MSW gasification is the formation of tar, a complex mixture of heavy hydrocarbons. Previous studies concerning tar generation from waste gasification indicate that the condensate consists primarily of polycyclic aromatic hydrocarbons, including benzene, naphthalene, and toluene (Blanco *et al.*, 2012; Etutu *et al.*, 2016; Pio *et al.*, 2021; Tursunov *et al.*, 2020), as well as aliphatic hydrocarbons including alkanes and alkenes (Chancelice *et al*., 2020; Ni *et al.*, 2013). Tar typically exhibits physical properties characterized as a viscous liquid–solid material, dark brown to black in color, and possessing a distinctive odor (Huang *et al*., 2015). Tar production not only reduces gasification efficiency but also causes operational issues such as pipeline blockages, equipment fouling, reduces the quality of syngas, and catalyst deactivation, ultimately increasing system downtime and maintenance costs (Chan *et al.*, 2020; Pio *et al.*, 2021; Rios *et al.*, 2018). Tar generation occurs during the pyrolysis and partial oxidation phases of the gasification, wherein MSW constituents, including food waste, paper, plastic, and biomass, undergoes thermochemical degradation under sub-stoichiometric oxygen environments (Qin *et al.*, 2010). At lower temperatures below 1000 degrees Celsius (°C), these volatile intermediate compounds fail to completely convert into light gases, leading to the polymerization and condensation of heavier hydrocarbons. This phenomenon is predominantly observed in fixed-bed reactors, which are characterized by lower operating temperatures and nonuniform thermal distribution relative to fluidized-bed or fixed-bed

alternatives (Čespiva *et al.*, 2020; Pio *et al.*, 2021). Other influencing factors include feedstock composition, residence time, heating rate, and the presence or absence of a catalyst. The incorporation of cracking catalysts, including dolomite, olivine, or nickel-based formulations, substantially diminishes tar formation by accelerating secondary gas-phase reactions (Anis and Zainal, 2011). Tar has a fairly high calorific value, ranging from 30 to 40 megajoule per kilogram (MJ/kg). Tar has the potential to be used as a valuable alternative energy source through thermal cracking and compound purification. Tar contains fuel compounds such as paraffin and olefin hydrocarbons (Ni *et al*., 2013; Satyro *et al*., 2023). In a previous study, total paraffin–olefin (alkane–alkene) compounds of 64.80 weight (wt) % in the solid tar extract and 65.98 wt% in the liquid tar extract were reported for tar produced from waste gasification at the Putri Cempo Surakarta Landfill (Ridwan *et al*., 2026). These compounds exhibit strong potential as alternative aliphatic hydrocarbon-based oils for value-added applications, provided that their processing methodologies align with circular economy principles in WtE management (Satyro *et al*., 2023). Thermal cracking is an effective method for breaking complex hydrocarbon bonds (Anis and Zainal, 2011). Based on the abundance of this potential, tar is converted into aliphatic-rich hydrocarbons oil fraction contained alkane-alkene (paraffin-olefin) compound. Liquid aliphatic hydrocarbon condensate is successfully recovered by regulating the system temperature to match the boiling point range of alkane-alkene fractions, utilizing high-temperature thermal cracking as the primary method for converting tar into aliphatic hydrocarbon oil (Niu *et al*., 2024). Temperature variation analysis is employed to determine the optimal paraffin yield percentage (Drissi *et al*., 2019). The resulting oil fraction is then subjected to specification testing and compared with commercial oil products or materials. This study focuses on the conversion of tar and the analysis of liquid fraction products. In parallel, significant quantities of tar are continuously generated as a by-product of MSW gasification at the Putri Cempo Landfill in Surakarta, Indonesia, with a tar yield of approximately 0.7 wt% (Sonjaya, 2021). To address this gap, this study investigates the conversion of real MSW-derived tar into oil light aliphatic hydrocarbon fractions through a sequential pyrolysis process. In contrast to prior investigations dependent on model compounds, this study examines actual tar recovered from an operational landfill gasification facility, thereby offering practical insights under realistic operational conditions. The novelty of this study lies in three key aspects: i) the use of real landfill-derived tar as feedstock, enabling potential of tar upgrading under practical operating conditions; ii) the application of sequential pyrolysis to selectively enhance light aliphatic hydrocarbon fractions; and iii) potential application regarding evaluate the physicochemical analysis of light aliphatic hydrocarbon fractions. Integrating tar valorization technology with MSW gasification systems can potentially mitigate environmental impacts while advancing responsible waste management practices. The findings of this study can serve as a basis for future evidence-based policy-making regarding the responsible implementation of waste-to-energy processes at the Surakarta Landfill gasification plant in Indonesia. This study strives to realize of sustainable development goals (SDGs), particularly SDGs 7 (affordable and clean energy), SDGs 9 (industry, innovation and infrastructure), and SDGs 12 (responsible consumption and production). This study aims to investigate the valorization of tar derived from MSW gasification at the Putri Cempo landfill into light aliphatic-rich hydrocarbon oil fractions through sequential re-pyrolysis process, as well as to evaluate its physicochemical properties. This study was carried out at the MSW gasification plant at Putri Cempo Landfill, Surakarta and environmental engineering laboratory of Univeristas Sebelas Maret, Surakarta, Indonesia during the period of 2025–2026.

MATERIALS AND METHODS

Material preparation

The material used for conversion into light aliphatic hydrocarbon-*rich* oil fractions was tar, which was generated as a by-product of the MSW gasification process at Putri Cempo Landfill, Surakarta, Indonesia. The landfill was designated as the case study site, wherein the generated tar was maintained within a covered storage facility featuring a dedicated collection basin. Approximately 128,000 liters (L) of tar based on storage capacity, had accumulated at the source location and was expected to increase with the continuation of large-scale MSW gasification operations. Tar samples were collected from the by-product storage tank via grab sampling method (Fig. 1). The tar was continuously generated during steady-state operations utilizing a gasification feedstock characterized by consistent properties. Prior to thermal conversion, the collected raw tar was homogenized by mechanical stirring at 300 revolutions per minute (rpm) for 10–15 minutes (min) to obtain a more uniform viscosity and composition (Abatzoglou *et al.,* 2000). The homogenized tar was subsequently used as the feedstock for the sequential pyrolysis process.

Conversion of tar through sequential re-pyrolysis

Prior to thermal conversion, the moisture content of the tar was reduced directly under oxygen-limited conditions in a sealed fixed-bed reactor. Approximately 1000 grams (g) of raw tar was loaded into a crucible and positioned inside the reactor. Subsequently, the reactor was hermetically sealed to prevent the ingress of atmospheric oxygen (Dabai *et al*., 2014). The loaded tar was initially heated to 100–150 °C and maintained at this temperature for 30–60 min. to facilitate the evaporation and removal of residual moisture. After drying, the tar was heated at 10 degrees Celsius per minute (°C/min) to target temperatures ranging from 350 to 700 °C (Abatzoglou *et al*., 2000). Pyrolysis was performed under oxygen-limited conditions in a sealed fixed-bed reactor in the absence of an external carrier or purge gas, with each target temperature maintained for 30 min. Sequential re-pyrolysis was implemented to continuously enhance volatilization and thermal cracking, thereby generating lighter hydrocarbon fractions and condensable liquid products (Fig. 2). The temperature range was selected to evaluate progressive thermal cracking, with 350–450 °C facilitating the volatilization of lighter constituents and temperatures exceeding 600 °C promoting secondary cracking and C–C bond scission (Zhou *et al*., 2019; Drissi *et al*., 2019). The vapors generated during pyrolysis were directed through a continuously flowing cooling-water condensation system, where the condensable products were cooled and recovered as liquid fractions. The sequential re-pyrolysis approach was implemented to assess the thermal conversion of tar into lighter hydrocarbon fractions and to identify the temperature range responsible for the generation of aliphatic-rich liquid products (Wang *et al.,* 2025). The pyrolysis experiments were conducted in duplicate at each temperature re-pyrolysis to improve the reliability and reproducibility of the obtained product yields light hydrocarbon. Furthermore, the re-pyrolysis operation facilitated the generation of distinct heavy and light fractions, which subsequently underwent comparative physicochemical and compositional evaluations (Gholami *et al*., 2021).

Physicochemical analysis of oil fraction

The physical properties analyzed included density, kinematic viscosity, flash point, and pour point (ASTM International, 2021). The chemical compositions were characterized using gas chromatography–mass spectrometry (GC–MS) and Fourier-transform infrared spectroscopy (FT-IR), respectively (Table 1). The chemical composition of the liquid products was characterized using a Shimadzu GCMS-QP2010 SE system with a column temperature range of 50–270 °C, a heating rate of 10 °C/min, and helium as



Fig. 1: Tar (by-product) MSW gasification in Putri Cempo landfill, Surakarta

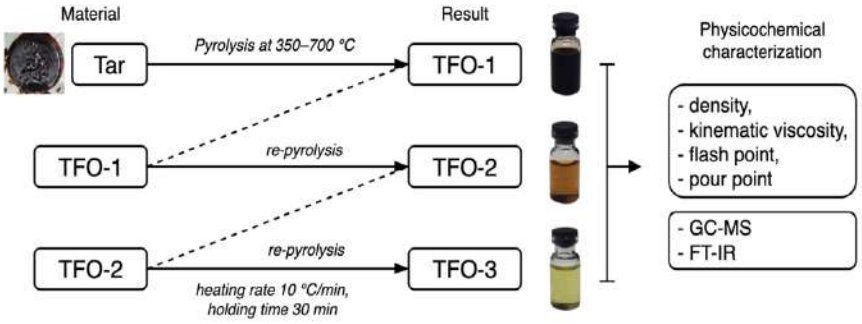

Fig. 2: Schematic diagram of the sequential re-pyrolysis process for tar-derived products and subsequent physicochemical characterization (Note: Tar Pyrolysis Oil-1 (TFO-1), TFO-2, and TFO-3)

Table 1: Physicochemical characterization parameters and analytical methods

Parameter	Unit	Method	Analytical principle
Physical testing			
Density	Kilogram per cubic meter (kg/m^3)	ASTM D4052-22	Oscillating U-tube
Kinematic viscosity	Centistokes (cSt)	ASTM D445-23	Capillary flow-time
Flash point	°C	ASTM D93-20	Pensky–Martens closed cup
Pour point	°C	ASTM D5853-17a	Controlled cooling and flowability
Chemical testing			
Chemical (Organic volatil) compound	Peak area (%)	GC-MS/MS	GC separation and MS/MS detection
Chemical bonds	Wavenumber /cm	FT-IR/IR	Infrared molecular vibration

the carrier gas at 1.7 milliliter per minute (mL/min). Compounds were identified by comparison with mass spectral library matching, and their relative peak areas were utilized to evaluate hydrocarbon fraction distributions. Functional groups were characterized using a Thermo Scientific Nicolet iS10 FT-IR spectrometer with KBr sample preparation. The resulting spectra were evaluated according to characteristic absorption bands to identify major chemical bonds and functional groups (Wang *et al*., 2023b).

RESULTS AND DISCUSSION

This study investigated the potential valorization of MSW gasification tar from the Putri Cempo Landfill, Surakarta, Indonesia, through sequential re-pyrolysis to obtain aliphatic hydrocarbon-rich oil fractions. The physicochemical and chemical properties of the resulting liquid products were assessed to determine the effects of pyrolysis temperature and successive re-pyrolysis stages. Furthermore, these findings offer valuable insights into the prospective recovery of distinct heavy and

lighter aliphatic hydrocarbon fractions from gasification-derived tar as a secondary resource.

Existing characteristics of tar from gasification plant, Surakarta landfill

The main product in the gasification of MSW pellet feedstock at Putri Cempo Landfill with a fixed bed downdraft gasifier produces syngas with a composition of CO (24.78%), CO_2 (18.65%), H_2 (15.6%), and CH_4 (4.06%) at an air fuel ratio (AFR) of 0.3 at 600–750 ^oC (Sonjaya, 2021). Downdraft fixed-bed gasifiers typically generate significantly lower tar yields than updraft and fluidized-bed configurations. The tar examined in this study was derived from steady-state gasification operations, with the RDF maintaining consistent characteristics prior to entering the gasifier (Sonjaya, 2021). Gravimetric tar yields as low as 0.7 wt% have been reported in pilot-scale and parametric studies under optimal superficial velocity conditions and specific reactor configurations (Bhavanam and Sastry, 2011). Tar management at the Surakarta landfill is currently handled through large storage ponds. Moreover, tar frequently deposits within system ducts, pipelines, and associated equipment, as its susceptibility to low-temperature cooling and solidification leads to severe operational blockages (Rakesh and Dasappa, 2018). A tar yield of 0.7 wt% is applied to the gasification of 545 t/d or 545,000 kilograms per day (kg/d) of waste at the Surakarta Landfill, representing a low-to-medium value commonly reported for fixed-bed downdraft reactors processing municipal solid waste under stable operating conditions (Bhavanam and Sastry, 2011). Based on this fraction, the estimated daily tar production reaches 3,815 kg/d, indicating that even at relatively low yields, tar accumulation from municipa-scale operations generates substantial condensate volumes, thereby supporting the technical feasibility of evaluating its potential as an upgrading feedstock for paraffinic (Bhavanam and Sastry, 2011). Based on the analysis of tar compounds in Surakarta landfill using gas chromatography–mass spectrometry (GC-MS), the majority of the content is dominated by aliphatic hydrocarbons in the form of alkanes and alkenes (Table 2). Alkanes and alkenes and their derivatives have been identified as hydrocarbons with carbon atom (C) lengths ≥ C_{13-33} (Ridwan *et al.,* 2026). Previous studies have established that aliphatic hydrocarbon, including paraffins and olefins, are prevalent within tar, originating from the thermal degradation of lignocellulose and complex hydrocarbon compounds during pyrolysis or carbonization (Huang *et al.*, 2015). Other detected compounds were predominantly derivatives of aliphatic hydrocarbons, including alcohols, carboxylic acids, and ethers. In contrast, the proportion of aromatic compounds identified was very low (Table 2). This finding provides an initial basis for further thermal conversion through sequential re-pyrolysis, enabling the selective transformation of heavier hydrocarbon components into lighter aliphatic-rich hydrocarbons oil fractions.

Field observations at Putri Cempo fall within this range. To provide a conservative but realistic assessment, the operational tar formation is approximately at 0.7 wt% (Sonjaya, 2021). Based on the waste gasification process that produces and its associated tar yield, the daily tar production of the gasification plant at the Surakarta landfill is calculated as shown in Eq. 1 (Wang *et al*., 2023a):

$$M_{tar} = M_{msw} \times Y_{tar} \quad (1)$$

Where: M_{tar} tar formation (kg/d); M_{msw} MSW/feed stock (kg/d); Y_{tar} tar yield (kg/kg).

$$M_{tar} = 545{,}000 \text{ kg/d} \times 0.007$$
$$M_{tar} = 3{,}815 \text{ kg/d}$$

Conversion of tar into oil fraction

Sequential re-pyrolysis successfully converted a portion of these heavy molecules into lighter condensable oils. During subsequent thermal treatment, these heavy constituents undergo a

Table 2: Distribution of compounds in tar from MSW Gasification, Surakarta landfill (Ridwan *et al*., 2026)

Compound group	Tar extract		
	Ethyl acetate (%)	Hexane (%)	Heptane (%)
Paraffin (alkane)	22.96	46.37	55.42
Olefin (alkene)	00.00	18.43	10.56
Subtotal aliphatic hydrocarbon	22.96	64.80	65.98
Alcohol	19.29	25.90	31.30
Carboxilic acid	42.08	6.39	-
Aromatic	8.92	2.93	-
Eter	-	-	2.72
Keton	6.76	-	-
Total	100.00	100.00	100.00

progression of volatilization, thermal cracking, dealkylation, and secondary reactions, resulting in continuous shifts in the molecular-weight distribution of the final products (Abatzoglou *et al.,* 2000). Previous studies indicates that elevating thermal severity facilitates the transformation of heavier tar compounds into lighter condensable hydrocarbons, whereas excessive severity can simultaneously accelerate secondary polymerization and char formation (Evans and Milne, 1998). In the present study, sequential re-pyrolysis was therefore applied to promote controlled conversion of the heavy tar matrix into lighter condensable oil fractions while allowing the temperature-dependent evolution of the products to be evaluated. Prior to primary pyrolysis, the raw tar underwent gradual thermal conditioning to minimize the impact of residual moisture. The initial heating step was conducted below approximately 100–120 °C to facilitate the evaporation of physically entrained water while minimizing the occurrence of significant thermal decomposition. This conditioning step was particularly critical because the presence of moisture within the highly viscous tar matrix can significantly affect heat transfer, vapor generation, and the stability of the liquid-phase during subsequent heating. After moisture removal, the temperature was progressively increased to approximately 150–250 °C to facilitate the release of readily volatile constituents before the main cracking reactions occurred at higher temperatures. This stage as a preliminary devolatilization step that stabilizes the feedstock and promotes more consistent thermal conversion (Abatzoglou *et al.,* 2000). Sequential re-pyrolysis was resulting in three liquid fractions representing TPO-1, 2, and 3 (Fig. 3). This re-pyrolysis configuration was engineered to progressively elevate the thermal severity imposed on the tar, thereby promoting the conversion of high-molecular-weight hydrocarbons into lighter condensable fractions. At the lower temperature range, approximately 350–450 °C, the process primarily promoted the volatilization of relatively light and thermally labile constituents, while a considerable proportion of the heavier hydrocarbon matrix remained unconverted. Increasing the pyrolysis temperature enhanced thermal cracking and promoted the cleavage of C–C bonds within the heavier hydrocarbon structures, thereby increasing the formation of lower-molecular-weight vapors that could subsequently be recovered as condensable liquids. In the intermediate temperature range of approximately 500–550 °C, enhanced formation of condensable liquid products is achieved, indicating an optimal balance between heavy tar conversion and the preservation of hydrocarbons within their condensation threshold. At higher temperatures, particularly above 600 °C, more severe secondary cracking may occur, causing a greater fraction of the hydrocarbons to undergo further decomposition into non-condensable gases and other secondary products. Comparable temperature-dependent behavior has been documented during the thermal conversion of

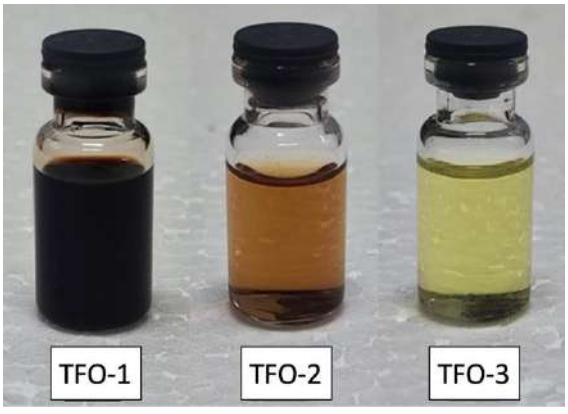

Fig. 3: Tar Pyrolysis Oil (TFO) from the tar sequential re-pyrolysis process (Note: Tar Pyrolysis Oil-1 (TFO-1), TFO-2, and TFO-3)

complex tar and heavy hydrocarbon matrices, wherein elevated temperatures drive both primary cracking and ensuing secondary reactions (Aboelela *et al*., 2023). A favorable temperature range for condensable liquid recovery was observed at 500–550 °C, where liquid production remained relatively high before greater gas-phase conversion occurred at higher temperatures. This trend is consistent with thermal cracking behavior documented for hydrocarbon systems; wherein intermediate temperatures can favor liquid formation while restricting excessive conversion into gaseous products. The implementation of a staged heating strategy enabled precise control over tar thermal conversion across successive temperature ranges, thereby mitigating the excessive polymerization and coke formation typically induced by high-temperature treatment. The resulting products were characterized by relatively high aliphatic hydrocarbon fractions, although further process optimization and upgrading would be required to confirm their potential applications (Aboelela *et al*., 2023; Rios *et al*., 2018). Identical pyrolysis temperature and heating rate were maintained across each successive re-pyrolysis stage. Sequential re-pyrolysis increased the degree of thermal conversion, promoting the transformation of heavier hydrocarbon compounds into lighter fractions. This observation aligns with the enhanced generation of lighter and more volatile hydrocarbon compounds during successive thermal conversion (Heydariaraghi *et al.,* 2016). Consequently, the combined effects of pyrolysis temperature and the number of re-pyrolysis stages establish a robust foundation for assessing the conversion of MSW-derived tar into lighter, aliphatic hydrocarbon-rich liquid fractions (Fig. 3).

Liquid recovery and volumetric characteristics

Experimental findings indicate that the liquid phase constituted the primary product fraction. Accounting for approximately 65–70 wt% of the initial feed based on their density characterization in oil fraction (Table 3). These results indicate that a substantial portion of heavy tar can be converted into recoverable liquid products (Rios *et al*., 2018). Based on the results of the density test on the oil fraction samples, the range obtained was 801.3–875.4 kg/m^3 (Table 7). Based on an assumed liquid recovery of 70 wt%, approximately 0.70 kg of liquid product can be obtained from 1 kg of tar. The corresponding liquid volume was estimated from the measured density using Eqs. 2 and 3 (ASTM International, 2021):

$$m_{liquid} = m_{tar} \times Y_{liquid} = 1\,kg \times 70\,wt\% = 0.70\,kg \quad (2)$$

$$V_{liquid} = \frac{m_{liquid}}{\rho_{liquid}} = \frac{0.70}{875.4} \times 1000 = 0.799\,L \approx 0.80\,L \quad (3)$$

Table 3: Reported tar conversion to oil yields and related research

Feedstock and process	Reactor type	Temperature (°C)	Liquid yield (wt%)	Source
Mixed MSW condensate upgrading	Spiral condenser	450–600	1.2 L from 2 kg (≈60)	Sadewo, 2023
Coal–MSW tar cracking	Fixed-bed catalytic	500–650	55–68	Liu *et al.*, 2017
Stepwise tar pyrolysis	Fixed-bed staged	350–700	65–70	Wang *et al.*, 2025
This study	Fixed-bed staged	350–700	65–70	Ridwan *et al.*, 2027

1 kg tar → 0.70 kg recovered liquid → 0.800 L TFO Where: V_{liquid} is the liquid volume (L), m_{liquid} is the recovered liquid mass (kg), ρ_{liquid} is the liquid density (kg/m³). For the TFO fraction with a density of 875.4 kilograms per meters (kg/m³), the estimated 0.70 kg of recovered liquid corresponds to approximately 0.800 L. Thus, on a standardized basis, 1 kg of tar is estimated to produce approximately 0.800 L of liquid under the assumed 70 wt% recovery. The density of the recovered TFO fractions provides an additional indication of their physical characteristics following sequential re-pyrolysis. Variations in density among the TFO fractions likely originate from distinct molecular composition and hydrocarbon distribution induced by progressive thermal cracking.

The similarity of yields between this study and the stepwise approach reported by Wang *et al.*, (2025) confirms that staged heating effectively prevents premature polymerization, minimizes soot formation, and shifts the product distribution toward lighter hydrocarbons.

1 kg tar → 0.70 kg recovered liquid → 0.800 L TFO (Eqs. 2 and 3), potential daily production, using Eq. 4 (Wang *et al*., 2023a):

$$V_{oil} = M_{tar} \times V_{liquid} \quad (4)$$

Where: V_{oil} daily liquid production (L/d); V_{liquid} liquid recovery yield tar (L/kg)

$V_{oil} = 3{,}815\ \text{kg/d} \times 0.8$

$V_{oil} = 3{,}052\ \text{L/d}$

Physical properties analysis of oil fraction from tar

Oil fraction exhibits a wide range of viscosities, from light to heavy, depending on its specific application. The reference materials used for comparison include paraffin chemical abstracts service (CAS), with the molecular formula $C_nH_2n_2$ (n = 16–24), as well as paraffinic oil 60 and paraffinic oil 95 (Table 4). In addition, the product was also compared with domestic biofuel standards established by Indonesia's Director General of Oil and Gas (Table 5). Paraffin CAS paraffin, commonly as mineral paraffin, is used for analytical purposes due to its high level of purity. Highly purified paraffin, achieving purities of up to 99%, is typically employed in cosmetic, pharmaceutical, and chemical applications, with standard liquid paraffin also demonstrating exceptional stability under ambient conditions (Carlen and Mastrangelo, 2002; Ma *et al.*, 2020). The paraffinic oils 60 and 95 produced by Pertamina are standard products derived from solvent-dewaxed light paraffinic petroleum distillates (CAS No. 64742-56-9). Based on the physicochemical characterization presented in Table 6, the density of the thermally cracked tar fractions ranged from 801.3 to 875.4 kg/m³, while several other properties remained below or outside the applicable reference specifications (Table 7). The comparatively low flash point indicates the presence of volatile hydrocarbons generated via thermal cracking, implying that additional stabilization is essential for applications governed by stringent safety requirements (Sarikoc, 2020). Subsequent upgrading via considered through fractional distillation, hydrotreatment, catalytic treatment, or fuel blending may be implemented to tailor the physical and chemical properties of the recovered liquid (Razavian and Fatemi, 2020; Ula and Kurniadi, 2017). Fractional distillation effectively minimizes light volatile components, whereas

Table 4: Physical properties of paraffin CAS, paraffinic oil 60, and paraffinic oil 95 (Chemwhat, 2025; Pertamina, 2017)

Parameter	Paraffin CAS	Paraffinic Oil 60	Paraffinic Oil 95
Melting point	-24 °C	0 °C	0 °C
Boiling point	300 °C	352 °C	315 °C
Flash point	> 300 °C	> 216 °C	> 211 °C
Density	850 kg/m³ at 20 °C	867.1 kg/m³ at 15 °C	877.6 kg/m³ at 15 °C
Viscosity	–	48.76 cSt at 23 °C	124.1 cSt at 23 °C
Color	White	Liquid, yellow	Liquid, yellow

Table 5: Standard specifications for domestic diesel fuel

Parameter	Unit	Pertamina Dex (B35)*	Dexlite (B35)*	Biodiesel (B40)*
Density	kg/m³	815 – 860	815 – 880	815 – 880
Kinematic Viscosity	cSt	2.0 – 4.5	2.0 – 5.0	2.0 – 5.0
Flash Point	°C, minimum	55	52	52
Pour Point	°C, maximum	18	18	18

*Director general of oil and gas decree No. 447.K/MG.06/DJM/2023 and No. 384.K/MG.06/DJM/2024 concerning standards and quality (specifications) for diesel fuel domestically.

Table 6: Physical properties of oil fraction samples based on re-pyrolysis

Parameter	Method	Unit	Sequental re-pyrolysis		
			PFO-1	PFO-2	PFO-3
Color	-	-	heavy-Dark brown	Medium-brown	light-yellow
Density (15°C)	ASTM D4052-22	kg/m³	875.4	802.1	801.3
Viscosity (40°C)	ASTM D445-23	cSt	2.956	2.404	2.304
Flash Point	ASTM D93-20	°C, minimum	62.0	40.0	45.0
Pour Point	ASTM D5853-17	°C, maximum	-3	+21	+3

Table 7: Comparison of hydrocarbon oil fraction from tar with hydrocarbon oil product

Parameter	Unit	Range of Oil fraction	Commercial Paraffin	Diesel (Domestic)	Result and potential
Density (15°C)	kg/m³	801.3–875.4	780–880	820–850	Close to diesel and paraffin, potential for liquid fuel alternative
Viscosity (40°C)	cSt	2.304–2.956	1.5–3.0	2.0–4.5	Within the operational range, potential for combustion systems
Flash Point	°C	40.0 – 62.3	>60	>52	Too low → safety risk Requires upgrading (distillation/catalytic treatment)
Pour Point	°C	(-3) – (+21)	−10 to 10	−15 to 10	depending on the application

hydrotreatment and catalytic treatment enhance overall hydrocarbon stability. For wax-based applications, blending with microcrystalline wax may improve flexibility and oxidation resistance. Collectively, the physicochemical characterization demonstrates that thermally cracked tar fractions hold promise as intermediate hydrocarbon precursors, although subsequent upgrading remains essential prior to utilization in systems with stringent fuel-quality standards. Fractional distillation, catalytic upgrading, hydrotreatment, and blending can be considered according to the identified property limitations and intended end use (Wang *et al.,* 2022). Additional experimental validation is necessary to establish the most effective upgrading route.

Chemical properties analysis of oil fraction using GC-MS and FT-IR

The GC–MS results provide the relative distribution of compounds based on chromatographic peak areas. The combined results served to assess shifts in hydrocarbon distribution and composition throughout sequential re-pyrolysis (Tables 8 and 9). The three fractions were predominantly composed of

Table 8: Compounds detected by gas chromatography

Peak	TFO-1	Area	TFO-2	Area	TFO-3	Area
	Name	(%)	Name	(%)	Name	(%)
1	2-Isopropyl-1-hexene	0.91	Benzene, 1,3,5-trimethyl- (CAS)	0.96	Benzene, ethyl- (CAS)	0.64
2	Phenol (CAS)	1.82	Phenol, 2-methyl-	1.78	Benzene, 1,2-dimethyl-	1.60
3	1-Decanol (CAS)	2.10	2-propyl-trimethylcyclohexane	2.73	1,8-Nonadiene	0.60
4	Decane (CAS)	1.54	2-Undecene, 4,5-dimethyl-,	1.70	1-Nonene (CAS)	3.82
5	Octane, 3,3-dimethyl-	0.85	4-Dodecene, (Z)-	1.61	Octane (CAS)	4.16
6	1-Octanesulfonyl chloride	4.77	Dodecane (CAS)	1.91	Octane, 2-chloro- (CAS)	1.11
7	Cyclopropane, Octyl-	1.64	tetra propylene	0.90	1-Decene (CAS)	6.63
8	Tetradecane (CAS)	1.34	5,9-dimethyldeca-5,8-diene	2.29	Decane,2,3,5,8, tetramethyl	4.83
9	2-Undecanethiol, 2-methyl-	0.92	Benzene, 1-butyl-	1.29	trans-4-Decene	0.67
10	Benzenemethanol, 4-methyl-	2.32	Benzene, pentyl- (CAS)	1.01	1-Undecene (CAS)	0.84
11	Cyclopropane, Octyl-	4.81	2-Hydroxy-2-phenyl-acetamide	0.98	10-Undecen-1-ol (CAS)	1.22
12	Nony lthiol, isomer mix	8.17	(4E)-4-Dodecene #	2.68	3-Dodecene, (E)-	6.55
13	trans-7-tetradecene	0.91	Naphthalene (CAS)	7.57	Dodecane, 2,6,10-trimethyl	4.16
14	Decane, 2,3,5,8-tetramethyl-	2.29	Tetradecane (CAS)	2.68	1,11-Dodecadiene	0.89
15	2-(2'-Nitro-2'-propenyl)-1-cyclohexanone	1.53	4,5-Dimethyltetrahydro-1,3-oxazine-2-thione	1.11	Cyclopropane, nonyl-	5.92
16	Cyclooctane, 1,4-Dimethyl	1.86	Decane, 2,3,5,8-Tetramethyl-	1.62	Naphthalene	1.39
17	Nonane, 5-(2-Methylpropyl)-	4.12	5-Tetrade Cene, (E)-	3.28	Dodecane, 2,6,10-trimethyl-	4.06
18	1-Heptadecene (CAS)	9.23	Tridecane (CAS)	4.60	4-Dodecene, (Z)-	0.72
19	1-Tridecanol (CAS)	3.16	Isotridecanol-	11.27	1,11-Dodecadiene	0.87
20	3-OCTADECENE, (E)-	7.57	1-UNDECENE, 7-METHYL-	3.79	3-Tetradecene, (Z)-	4.64
21	1,4-Methanonaphthalene,	0.91	1-Heptanol, 2,4-diethyl-	9.62	Tetradecane (CAS)	4.04
22	Umbellulol	0.93	1-Tridecanol (CAS)	2.40	5-Dodecene, (E)-	0.64
23	1-Tridecanol (CAS)	2.33	1-Tridecanol (CAS)	1.94	5-Hydroxy-2-metylpyrimidin	0.68
24	1-Tridecanol (CAS)	1.49	Bicyclo-heptan-3-one, trimethyl	1.48	8-Dodecenol	0.80
25	Bicyclo-heptan-3-one, trimethyl	1.51	1,12-Tridecadiene (CAS)	1.14	3-Tetradecene, (Z)-	4.40
26	5,5-Diethyl-Thiohexan-4-One	1.03	1-Pentadecene (CAS)	5.76	Tetradecane (CAS)	3.69
27	1-Pentadecene (CAS)	6.58	Tetradecane (CAS)	3.49	9-Octadecene, (E)-	3.45
28	Tetradecane (CAS)	3.25	Naphthalene, 1,4-dimethyl-	1.07	Tetradecane (CAS)	3.92
29	Naphthalene, 1,3-dimethyl-	0.94	Benzene, octyl-	1.20	9-Octadecene, (E)-	2.68
30	Naphthalene, 1,5-dimethyl-	0.93	7-HEXADECENE, (Z)-	3.49	Nonadecane	3.76
31	Decane, 2-methyl- (CAS)	1.43	PENTADECANE	3.99	9-Octadecene, (E)-	1.83
32	1-Tridecanol (CAS)	2.85	Naphthalene, 2-ethyl- (CAS)	1.13	Hexadecane	3.63
33	Tetradecane (CAS)	3.89	Isotridecanol-	2.15	9-Octadecene, (E)-	1.13
34	Pyridine-2,4-diol, trimethyl	0.93	1-Tridecanol (CAS)	0.82	Hexadecane	3.06
35	Isodecyl methacrylate	2.24	Isotridecanol-	0.81	9-Eicosene, (E)-	0.67
36	Isotridecanol-	0.97	5-OCTADECENE, (E)-	1.07	Nonadecane (CAS)	2.61
37	7-Hexadecene, (Z)-	1.43	Tetracosane, 3,5,24-trimethyl-	1.87	Nonadecane (CAS)	2.15
38	1-Decanol, 2-hexyl-	2.18	Isotridecanol-	0.80	Heneicosane	1.55
39	Hexadecane (CAS)	1.42				
40	Isotridecanol-	0.89				
Total		**100**	Total	**100**	Total	**100**

Table 9: Hydrocarbon distribution and physical appearance of oil fractions

Fraction	re-pyrolysis stage	Carbon-chain range	Aliphatic hydrocarbon relative peak area (%)	Physical appearance
TFO-1	1 stage	C_9–C_{20}	46.76	Darker/Heavy
TFO-2	2 stages	C_{12}–C_{43}	45.58	Intermediate
TFO-3	3 stages	C_8–C_{21}	86.65	Clearer/Light

aliphatic hydrocarbons, with combined relative peak areas of 46.76% for TFO-1, 45.58% for TFO-2, and 86.65% for TFO-3 (Fig. 4). The aliphatic hydrocarbon class fraction remained relatively similar between TFO-1 and TFO-2 but increased substantially in TFO-3. This elevation indicates that successive re-pyrolysis modifies the hydrocarbon distribution and accelerates the formation of aliphatic hydrocarbon compounds in the final stage. A progressive alteration in physical

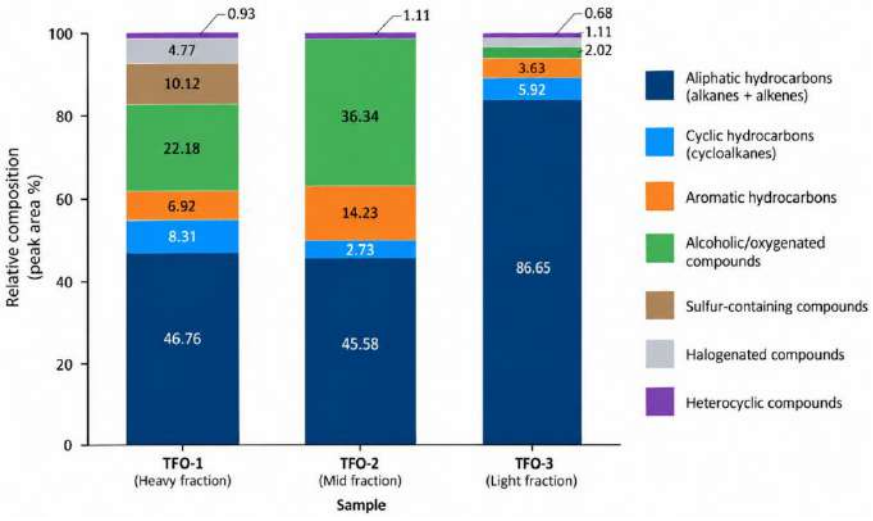

Fig. 4: Relative composition of compound classes identified in TFO-1, TFO-2, and TFO-3 based on GC–MS analysis
(Note: Values are expressed as relative peak area (%). Alkanes and alkenes were combined into a single hydrocarbon class, whereas cycloalkanes were classified separately)

appearance was likewise evident, with the TFO fractions exhibiting increased clarity following sequential re-pyrolysis. Although thermal re-pyrolysis promotes the cleavage of larger hydrocarbon structures into smaller molecules, the extent of this transformation is governed by temperature, residence time, and feedstock composition (Heydariaraghi *et al.,* 2016). However, the visual change alone cannot confirm molecular-weight reduction and is therefore considered a supporting observation. GC–MS results provide evidence of the compound changes, particularly the substantial increase in aliphatic hydrocarbon fraction observed in TFO-3. The broader distribution observed in TFO-2 indicates that intermediate re-pyrolysis did not produce a continuous shift toward shorter-chain hydrocarbons. However, the subsequent increase in the aliphatic hydrocarbon fraction and the narrower carbon-chain range in TFO-3 indicate a substantial change in hydrocarbon distribution during the third stage. Thermal cracking accelerates the breakdown of macromolecular hydrocarbon frameworks and secondary reactions, effectively modifying the distribution of condensable hydrocarbons. Nevertheless, the observed change in color should be regarded as a supporting physical indicator rather than definitive evidence of molecular-weight reduction (Andalia *et al.,* 2025). The GC–MS results, particularly the carbon-chain distribution and aliphatic hydrocarbon composition, provide the primary evidence for evaluating changes in hydrocarbon characteristics. The GC–MS results showed clear changes in the chemical-group distribution during sequential re-pyrolysis (Fig. 4). The aliphatic hydrocarbon fraction increased from 46.76% (TFO-1) and 45.58% (TFO-2) to 86.65% in TFO-3, while the oxygenated fraction decreased to 2.02% in TFO-3. Aromatic compounds accounted for 6.92%, 14.23%, and 3.63% in TFO-1, TFO-2, and TFO-3, respectively. These variations indicate that successive thermal treatment modifies the distribution of condensable compounds, exhibiting the most pronounced aliphatic hydrocarbon enrichment in TFO-3. Thermal cracking drives the decomposition and restructuring of heavier hydrocarbon frameworks via primary and secondary pathways, albeit with the ultimate product composition remaining contingent upon feedstock characteristics and operating conditions (Andalia *et al.,* 2025). The

progressively clearer appearance of the TFO fractions after re-pyrolysis provides a complementary visual indication of changes in the liquid composition, but cannot independently confirm molecular-weight reduction. The presence of sulfur-containing compounds in TFO-1 (10.12% relative peak area) and halogenated compounds in TFO-3 (1.11% relative peak area) should also be considered in evaluating potential applications. These values reflect GC–MS relative peak areas rather than absolute sulfur or halogen concentrations; therefore, direct comparison with fuel specifications necessitates dedicated sulfur and chlorine quantification. Sulfur- and chlorine-containing compounds may contribute to SO_x emissions, corrosion, and other operational concerns during thermal utilization and should therefore be controlled during fuel upgrading (Kusenberg *et al*., 2022; Thi *et al.,* 2021). Among the three fractions, TFO-3 exhibited the highest relative abundance of aliphatic hydrocarbons (86.65%) and the lowest oxygenated fraction (2.02%), indicating its potential as an aliphatic-rich hydrocarbon intermediate for further upgrading. Rather than serving as a direct finished fuel, TFO-3 holds potential for subsequent conversion into marketable fuels or as a substitute material for wax-based products. Fractional distillation, hydrotreatment, catalytic processing, or blending may be considered to improve physicochemical properties and reduce unwanted volatile components or those containing heteroatoms before use in specific end applications (Razavian and Fatemi, 2020; Ula and Kurniadi, 2017). For wax-based applications, advanced formulations incorporating additives such as microcrystalline wax may also be evaluated to optimize product performance. Further evaluation of flash point, viscosity, distillation range, heating value, total sulfur, total chlorine, and other relevant fuel properties is required. Fractional distillation and hydrotreatment have been documented as viable strategies for enhancing the physicochemical characteristics of MSW-derived pyrolysis oils, encompassing flash point, viscosity, and sulfur-related properties (Sarikoc, 2020). The FT-IR spectra in Fig. 5 showed that aliphatic hydrocarbon structures were consistently identified in all TFO fractions (Table 10). Characteristic C–H stretching bands were observed at approximately 2955, 2923, and 2853 /cm, together with CH_2/CH_3 deformation bands near 1456 and 1377 /cm. The band near 721–722 /cm was also consistently detected, supporting the presence of aliphatic hydrocarbon chains (Qiao *et al.,* 2018). These stretching bands indicate that C–H-containing aliphatic structures constitute a major component of TFO fractions, aligning with the high relative abundance of aliphatic hydrocarbons identified by GC–MS. Bands associated with C=C and =C–H vibrations were also identified in all samples. The absorption near 1641–1648/cm can be attributed to C=C stretching, while bands in the approximately 888–992/cm region are associated with =C–H vibrations. he detection of both saturated and unsaturated hydrocarbon-related bands is consistent with the aliphatic hydrocarbon distribution obtained from GC–MS. Overall, FT-IR analysis provided supporting evidence for the chemical changes identified by GC–MS. The prominent aliphatic C–H stretching bands across all TFO fractions indicate a predominance of aliphatic components, whereas the subdued oxygenation signals in TFO-3 align with its lower proportion of oxygen-containing compounds. Nevertheless, FT-IR was used only for structural identification and not for quantitative determination of compound composition or molecular-weight distribution (Mishra *et al.*, 2024; Pannucharoenwong *et al.,* 2026).

Tar based Light hydrocarbon oil fraction potential

These findings demonstrate that successive thermal treatments alter the chemical composition of tar-derived liquids, yielding an intermediate fraction enriched in aliphatic components. TFO-3 exhibited a substantially higher relative abundance of aliphatic hydrocarbons (86.65%) and a lower proportion of

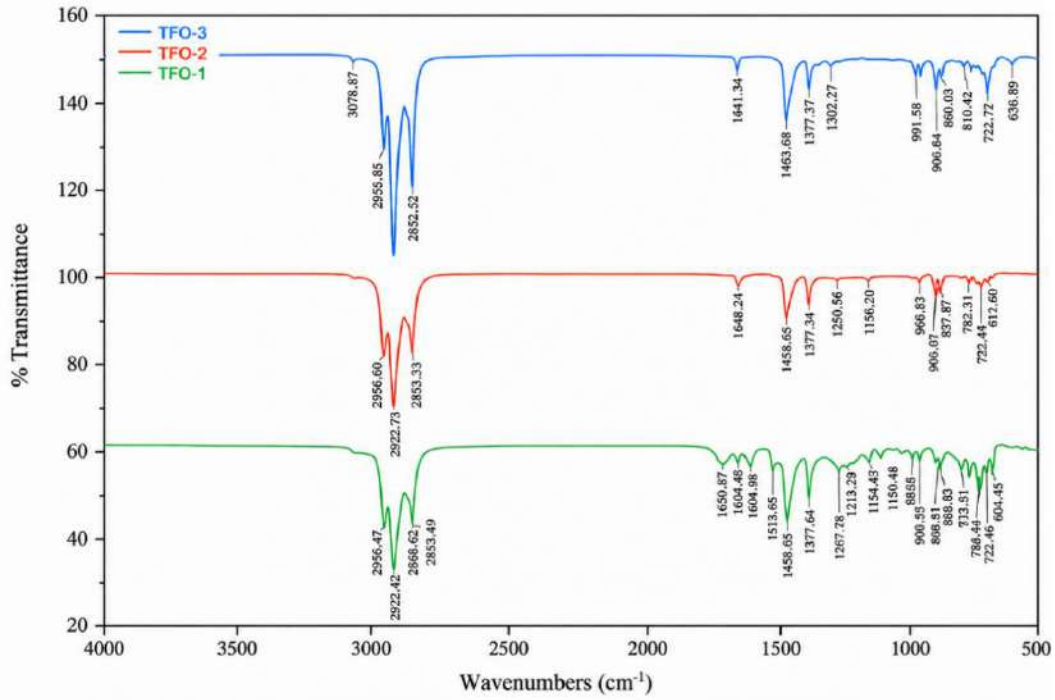

Fig. 5: Infrared spectra of TFO-1, TFO-2, and TFO-3

Table 10: Interpretation of functional groups and compound classifications based infrared spectrum

Compound classification	Functional group	TFO-1 (/cm)	TFO-2 (/cm)	TFO-3 (/cm)	Interpretation	Source
Alkane-Alkene/ Aliphatic hydrocarbons	–CH_3 and –CH_2–	2955.47; 2922.56; 2853.49; 1456.66; 1377.04; 721.46	2955.60; 2922.73; 2853.53; 1458.65; 1377.34; 721.90	2955.85; 2922.73; 2852.52; 1463.68; 1377.37; 721.27	Dominant and consistently identified in all samples	Qiao *et al.*, 2018
	C=C and =C–H	1643.62; 963.55; 908.81; 886–887	1648.24; 966.33; 908.81; 887.67	1641.34; 991.55; 965.10; 908.84; 888.08	Indicated in all samples	Qiao *et al.*, 2018
Aromatic/ cyclic hydrocarbons	Ar–H and aromatic C=C	812.23; 750.54; 668.46	782.31; 733.54	810.42; 781.36; 721.27; 633.98	Indicated, but less prominent than aliphatic structures	Yousef *et al.* 2021
Oxygenated compounds	O–H, C=O, and C–O	1267.88; 1154.27; 1109.99	1269.58; 1155.20	No strong bands in principal region	Weakly indicated in TFO-1 and TFO-2; not prominent in PFO-3	Yousef *et al.* 2021

oxygenated compounds (2.02%) than TFO-1 and TFO-2. Findings from the sequential re-pyrolysis demonstrate that MSW gasification tar serves as a promising feedstock for the recovery of hydrocarbon-rich liquid fractions. Based on estimate a liquid recovery of 70 wt% and an oil density of 875.4 kg/m³, the potential volume of recovered oil fraction was estimated at approximately 3,052 L/d (Eq. 4), equivalent to approximately 1,113,980 L/y or 1,114 m³/y (Fig. 6). This value represents a scenario-based estimate of liquid hydrocarbon recovery and may vary

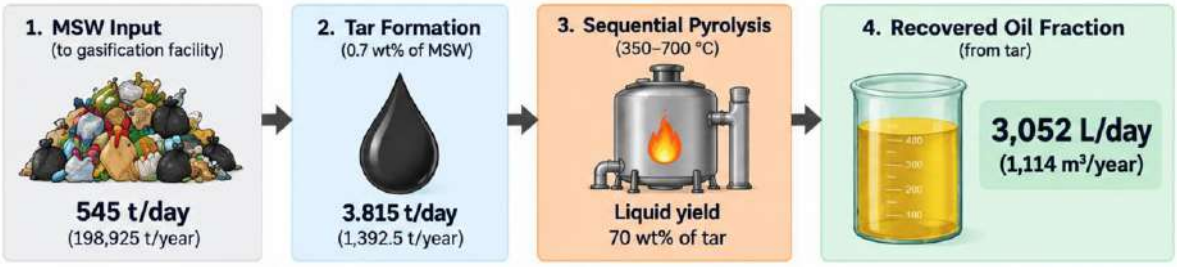

Fig. 6: Potential hydrocarbon oil recovery from tar at the Surakarta landfill

depending on tar composition, pyrolysis conditions, condensation efficiency, and product properties. The recovered liquid is more appropriately evaluated as an intermediate hydrocarbon feedstock rather than applied directly as a fuel. The relatively high aliphatic hydrocarbon content observed in TFO-3 provides a basis for considering applications in fuel-blending components, hydrocarbon feedstocks, or wax material-related formulations after appropriate upgrading. MSW-derived pyrolysis oils typically necessitate post-treatment owing to the unfavorable flash point, viscosities, densities, sulfur contents, and other fuel properties inherent in the crude products. Fractional distillation and hydrotreatment have been reported as practical approaches for improving several of these properties (Faisal *et al.,* 2023). Fractional distillation is recommended as an initial upgrading step to separate light, middle, and heavy boiling fractions. Subsequent evaluations might explore the lighter fraction for fuel-blending applications, whereas heavier fractions can be routed toward further cracking or material utilization. Distillation has been reported to reduce density and viscosity and to improve the characteristics of selected pyrolysis-oil fractions (Wang *et al.,* 2025). Hydrotreatment can subsequently be considered when reduction of unsaturation, sulfur-containing compounds, or other unstable components is required. However, hydrogen consumption, catalyst deactivation, pressure requirements, and process energy demand should be evaluated before scale-up (Osman *et al.*, 2024). Overall, the results support the potential recovery of an aliphatic hydrocarbon-rich intermediate from MSW gasification tar, with TFO-3 showing the most pronounced aliphatic hydrocarbon character.

Environmental implications

The sequential re-pyrolysis of tar provides a potential route for recovering liquid hydrocarbon fractions from a waste stream that would otherwise require further treatment or disposal. From an environmental standpoint, converting tar into an oil fraction minimizes the volume of residual tar requiring direct disposal while simultaneously recovering hydrocarbons as a secondary resource. Pyrolysis has been reported as a waste-valorization pathway capable of recovering energy and material from MSW, although its environmental performance depends strongly on feedstock characteristics and process control (Aswathy and Ramesh, 2026). Furthermore, the contaminants present in MSW–derived tar raise significant environmental concerns. Depending on feedstock composition, pyrolysis systems can generate or concentrate compounds containing sulfur, chlorine, nitrogen, and other contaminants, while emissions such as HCl and SO_2 may require appropriate control. Consequently, the recovered oil should not be regarded as a directly usable fuel without further characterization and, where necessary, upgrading (Javed *et al.*, 2025; Osman *et al.*, 2024). For the obtained TFO fractions, fractional distillation serves as a viable subsequent treatment to separate compounds based on boiling range, while hydrotreatment can be employed to

eliminate sulfur, unsaturated compounds, or other undesirable components. Such upgrading has been reported to improve properties including viscosity, flash point, and sulfur content of MSW-derived pyrolysis oils (Detsios *et al.,* 2024). Overall, the primary environmental benefit of the proposed pathway stems from effective tar reduction and hydrocarbon recovery, rather than from the direct displacement of conventional fuels. The estimated 3,052 L/d oil fraction demonstrates the potential scale of resource recovery. Further assessment through energy balance, emission characterization, contaminant analysis, and life-cycle assessment (LCA) are required to quantify the net environmental benefit. This approach would provide a more robust basis for determining whether sequential re-pyrolysis offers an environmentally preferable pathway for tar management. The recovery of aliphatic hydrocarbon-rich oil fractions from gasification tar supports the relevance of SDG 7, SDG 9, and SDG 12 by demonstrating potential for secondary resource recovery, and waste valorization. Nevertheless, the recovered oil functions primarily as an intermediate product, necessitating further upgrading and characterization prior to its utilization in specific fuel or material applications. Future implementation would also require appropriate product quality standards, emission controls, market mechanisms, and economic incentives to support the utilization of waste-derived hydrocarbon products.

Limitation of this study

This study was conducted at laboratory scale, and therefore, the performance of sequential re-pyrolysis under plant-scale conditions remains to be validated. The estimated oil potential of 3,052 L/d is derived from a scenario-based calculation using assumed tar yield and liquid recovery rates, rather than direct empirical measurements from the gasification facility. Further characterization, including higher heating value, distillation range, sulfur, chlorine, nitrogen, metals, and product stability, is required to determine the suitability of the recovered oil for specific applications. Furthermore, this study did not encompass detailed energy balance, techno-economic evaluations, and LCA. Additionally, fluctuations in MSW composition and gasification operating conditions may influence tar properties and product yield. Therefore, further fractionation and/or catalytic upgrading, together with pilot-scale validation, is recommended to strengthen the assessment of the practical and environmental potential of the recovered hydrocarbon fractions.

CONCLUSION

This study demonstrated the potential valorization of municipal solid waste (MSW) gasification tar from the Putri Cempo Landfill, Surakarta, through sequential re-pyrolysis to obtain aliphatic hydrocarbon-rich liquid fractions. The original tar contained substantial aliphatic hydrocarbons, with combined alkane–alkene contents of 64.80 wt% and 65.98 wt% in the hexane and n-heptane extracts, respectively, indicating potential for further thermal conversion. Sequential re-pyrolysis at 350–700 °C produced condensable liquid fractions, with 500–550 °C identified as a favorable temperature range for liquid recovery under the investigated conditions. The chemical composition underwent significant alteration throughout the sequential re-pyrolysis process. The aliphatic hydrocarbon content was 46.76% in TFO-1, 45.58% in TFO-2, and increased to 86.65% in TFO-3. The alkane content also increased from 20.13% and 20.16% in TFO-1 and TFO-2 to 45.62% in TFO-3. The identified carbon-chain distributions ranged from C9–C20 in TFO-1, C12–C43 in TFO-2, and C8–C21 in TFO-3. The broader carbon range observed in TFO-2 reflects a more extended hydrocarbon distribution, whereas TFO-3 exhibits a comparatively restricted range combined with a maximum alkane–alkene content, collectively confirming its enrichment in aliphatic hydrocarbon. The presence of aliphatic structures was further supported by FT-IR analysis, which

consistently showed characteristic aliphatic C–H stretching bands at approximately 2955–2956, 2922–2923, and 2852–2854 /cm, corresponding to asymmetric and symmetric C–H stretching vibrations of CH_3 and CH_2 groups. Additional absorption bands observed approximately 1456–1464 and 1377 /cm were assigned to CH_2/CH_3 deformation vibrations, whereas signals near721–722 /cm denoted the presence of extended aliphatic hydrocarbon chains. These FT-IR features support the GC–MS results and confirm the predominance of aliphatic hydrocarbon structures in the recovered fractions. The physicochemical characterization showed densities of 801.3–875.4 kg/ m^3 and kinematic viscosities of 2.304–2.956 cSt. The flash points ranging from 40 to 62 °C indicate the presence of relatively volatile components, highlighting the necessity for further treatment in applications requiring stricter alternative fuel or hydrocarbon-material specifications. Fractional distillation, blending, and catalytic or hydrotreatment processes could therefore be considered for subsequent product upgrading. Based on an assumed tar generation rate of 0.7 wt% from 545 t/d of MSW, approximately 3.815 t/d of tar could be generated. Using the liquid recovery basis applied in this study, the potential oil fraction was estimated at approximately 3,052 L/d, equivalent to approximately 1,114 m^3/y. This value reflects a scenario-based potential rather than empirical plant-scale production, depending heavily on tar generation, liquid recovery rates, condensation efficiencies, and product density. sequential re-pyrolysis provides a potential route for recovering aliphatic hydrocarbon-rich liquid products from MSW gasification tar, supporting waste valorization and secondary resource recovery. Further investigations should prioritize pilot-scale validation, product fractionation and upgrading, comprehensive contaminant profiling, energy integration, alongside techno-economic and life-cycle assessments. These developments could strengthen the relevance of the proposed pathway to SDG 7, SDG 9, and SDG 12 through waste-derived resource recovery, technological development, and more efficient utilization of secondary resources.

AUTHOR CONTRIBUTIONS

M. Ridwan conceived and designed, prepared materials, data collection, analytical measurements, drafted manuscript, interpreted results, and edited. P. Setyono conceived and designed, analysis and discussion, reviewed draft, validated and supervised, grant funding, and as corresponding author. M.T.S. Budiastuti performed analysis and discussion, reviewed draft, project administration, and supervision.

ACKNOWLEDGEMENT

The authors would like to express their sincere gratitude to the Research and Community Service Center (LPPM) of Universitas Sebelas Maret and the Ministry of Research, Technology, and Higher Education of the Republic of Indonesia (Menristekdikti) for providing financial support for this research through the Pendidikan Magister menuju Doktor Sarjana Unggul (PMDSU) Program for the 2025 fiscal year, under Contract Number [1186.1/UN27.22/PT.01.03/2025].

CONFLICT OF INTEREST

The authors declare that there is no conflict of interest related to the research and funding. All authors have full independence in conducting research and preparing manuscripts without any pressure or influence from third parties.

OPEN ACCESS

©2027 The author(s). This article is licensed under a Creative Commons Attribution 4.0 International License, which permits use, sharing, adaptation, distribution and reproduction in any medium or format, as long as you give appropriate credit to the original author(s) and the source, provide a link to the Creative Commons license, and indicate if changes were made. The images or other third-party material in this article are included in the article's Creative Commons

license, unless indicated otherwise in a credit line to the material. If material is not included in the article's Creative Commons license and your intended use is not permitted by statutory regulation or exceeds the permitted use, you will need to obtain permission directly from the copyright holder. To view a copy of this license, visit: http://creativecommons.org/licenses/by/4.0/

PUBLISHER'S NOTE

GJESM Publisher remains neutral with regard to jurisdictional claims in published maps and institutional affiliations.

POSITIVE AI STATEMENT

During the preparation of this work, the author(s) have used Artificial Intelligence (AI) [ChatGPT] in order to [to improve the clarity of the language and restructure selected paragraphs]. After using this tool/service, the authors reviewed and edited the content as needed and take full responsibility for the content of the publication.

ABBREVIATIONS

%	Percent
°C	Degree celsius
°C/min	Degree Celsius per minute
/cm	Per centimeter
≥	Greater than or equal to
–CH₃	Methyl
–CH₂–	Methylene
ρ_{liquid}	Liquid density (kg/m³)
wt %	Weight percentage
AFR	Air fuel ratio
ASTM	American Society for Testing and Materials
C	Carbon atom
C–C	Carbon-carbon single bond
C=C	Carbon-carbon double bond
C–H	Carbon-hydrogen single bond
CH_4	Methane
CO	Carbon monoxide
CO_2	Carbon dioxide
cSt	Centistokes
ECHA	European Chemicals Agency
ER	Equivalence ratio
FT-IR	Fourier-transform infrared spectroscopy
g	Grams
GC-MS	Gas chromatography–mass spectrometry
GWP	Global warming potential
HFO	Heavy fuel oil
H_2	Hydrogen
KBr	Kalium Bromida
kg	kilogram
kg/d	Kilogram per day
kg/kg	Kilogram per kilogram
kg/L	Kilogram per liter
kg/m³	Kilogram per cubic meter
KLH	Ministry of Environment (Kementrian Lingkungan Hidup)
L	Liters
LCA	Life cycle analysis
L/d	Liter per day
L/kg	Liter per kilogram
min	Minutes
MJ/kg	Megajoule per kilogram
mL/min	Milliliter per minute
MSW	Municipal solid waste
Mt	Million ton
m_{liquid}	Recovered liquid mass (kg)
M_{msw}	Municipal solid waste feed rate (kg/d)
M_{tar}	Tar formation rate (kg/d)
rpm	Revolutions per minute
SDGs	Sustainable development goals
TEA	Techno-economic analysis
TFO-1	Tar Pyrolysis Oil 1-Sample
TFO-2	Tar Pyrolysis Oil 2-Sample
TFO-3	Tar Pyrolysis Oil 3-Sample
t/d	Ton per day
t/y	Ton per year
VOC	Volatile Organic Compounds
V_{liquid}	Recovered liquid volume (L)
V_{oil}	Daily liquid oil production (L/d)
WtE	Waste to Energy
Y_{liquid}	Tar yield (kg/kg)
Y_{tar}	Liquid recovery yield (wt%)

REFERENCES

Aboelela, D.; Saleh, H.; Attia, A.M.; Elhenawy, Y.; Majozi, T.; Bassyouni, M., (2023). Recent advances in biomass pyrolysis processes for bioenergy production: optimization of operating conditions. Sustainability. 15(14) **(30 pages)**.

Abatzoglou, N.; Barker, N.; Hasler, P.; Knoef, H., (2000). The development of a draft protocol for the sampling and analysis of particulate and organic contaminants in the gas from small biomass gasifiers. Biomass Bioenergy. 18(1): 5–17 **(13 pages)**.

Andalia, W.; Pratiwi, I.; Afrah, B.D.; Akbar, I.; Ammarullah, M.I., (2025). Optimized pyrolysis of household plastic waste in Indonesia for oil production: Hydrocarbon profiling, fuel alternative, and potential biomedical application. Results in Chemistry, 15, 102247 **(12 pages).**

Anis, S.; Zainal, Z.A., (2011). Tar reduction in biomass producer gas via mechanical, catalytic and thermal methods: A review. Renew. Sustain. Energy Rev., 15(5): 2355–2377 **(23 pages)**.

ASTM International, (2021). ASTM D5947-18: Standard test methods for physical dimensions of solid plastics. ASTM International, West Conshohocken, PA, USA.

Aswathy, K.P.; Ramesh, S.T., (2026). Pyrolysis of municipal solid waste: A comprehensive review of process, challenges and future prospects. In J. Anal. Appl. Pyrolysis.,198(107927) **(22 pages)**.

Bhavanam, A.; Sastry, R.C., (2011). Biomass gasification processes in downdraft fixed bed reactors: A review. Int. J. Chem. Eng. Appl., 2(6): 425–433 **(9 pages)**.

Blanco, P.H.; Wu, C.; Onwudili, J.A.; Williams, P.T., (2012). Characterization of tar from the pyrolysis/gasification of refuse derived fuel: Influence of process parameters and catalysis. Energy Fuels. 26(4): 2107–2115 **(9 pages)**.

Carlen, E.T.; Mastrangelo, C.H., (2002). Electrothermally activated paraffin microactuators. J. Microelectromechanical Syst., 11(3), 165–174 **(10 pages)**.

Češpiva, J.; Wnukowski, M.; Niedzwiecki, L.; Skřínský, J.; Vereš, J.; Ochodek, T.; Pawlak-Kruczek, H.; Borovec, K., (2020). Characterization of tars from a novel, pilot scale, biomass gasifier working under low equivalence ratio regime. Renew. Energy, 159: 775–785. **(11 pages).**

Chan, W.P.; Yusoff, S.A.M.B.; Veksha, A.; Giannis, A.; Lim, T.T.; Lisak, G., (2020). Analytical assessment of tar generated during gasification of municipal solid waste: Distribution of GC–MS detectable tar compounds, undetectable tar residues and inorganic impurities. Fuel. 268: 1–10 **(10 pages).**

Chancelice, N.C.; Philémon, Z.B.; Arnaud, M.A.G.; Benoït, N.M., (2020). Aliphatic hydrocarbons extraction from oily sludge using kerosene. Eur. J. Eng. Res. Sci., 5(10): 1137–1141 **(5 pages).**

ChemWhat, (2025). Paraffin CAS 8012-95-1. United Kingdom.

Dabai, F.; Paterson, N.; Millan, M.; Fennell, P.; Kandiyoti, R., (2013). Tar formation and destruction in a fixed bed reactor simulating downdraft gasification: Effect of reaction conditions on tar cracking products. Energy Fuels, 27(3): 1970–1982 **(13 pages).**

Detsios, N.; Maragoudaki, L.; Rebecchi, S.; Quataert, K.; De Winter, K.; Stathopoulos, V.; Orfanoudakis, N.G.; Grammelis, P.; Atsonios, K., (2024). Techno-economic evaluation of jet fuel production via an alternative gasification-driven biomass-to-liquid pathway and benchmarking with the state-of-the-art fischer–tropsch and alcohol-to-jet concepts. Energies, 17(7) **(13 pages).**

Drissi, S.; Ling, T.C.; Mo, K.H., (2019). Thermal efficiency and durability performances of paraffinic phase change materials with enhanced thermal conductivity – A review. Thermochim. Acta, 673: 198–210 **(13 pages)**.

Etutu, T.G.; Laohalidanond, K.; Kerdsuwan, S., (2016). Gasification of municipal solid waste in a downdraft gasifier: Analysis of tar formation. Songklanakarin J. Sci. Technol., 38(2): 221–228 **(8 pages).**

Evans, R.J.; Milne, T.A., (1998). Chemistry of tar formation and maturation in the thermochemical conversion of biomass. Dev. Thermochem. Biomass Convers., 803–816 **(14 pages)**.

Faisal, F.; Rasul, M.G.; Jahirul, M.I., (2023). Upgrading MSW pyrolysis oil through distillation and hydrotreatment for automobile engine applications: A short review. Energy Rep. 9: 555–560. **(6 pages).**

Gholami, Z.; Gholami, F.; Tišler, Z.; Vakili, M., (2021). A review on the production of light olefins using steam cracking of hydrocarbons. Energies. 14(23): 1–24 **(24 pages)**.

Heydariaraghi, M.; Ghorbanian, S.; Hallajisani, A.; Salehpour, A., (2016). Fuel properties of the oils produced from the pyrolysis of commonly-used polymers: Effect of fractionating column. J. Anal. Appl. Pyrolysis. 121: 307–317. **(11 pages).**

Himawanto, D.A., (2021). RDF characteristics of sorted municipal solid waste produced by a helical pyrolyzer. J. Sci. Technol., 10(2): 188–199 **(12 pages)**.

Huang, Q.; Tang, Y.; Lu, S.; Wu, X.; Chi, Y.; Yan, J., (2015). Characterization of tar derived from principle components of municipal solid waste. Energy Fuels. 29(11): 7266–7274 **(9 pages)**.

Im-Orb, K.; Simasatitkul, L.; Arpornwichanop, A., (2016). Analysis of synthesis gas production with a flexible H_2/CO ratio from rice straw gasification. Fuel. 164: 361–373 **(13 pages)**.

KLH, (2023). Waste generation. National Waste Management Information System (SIPSN). Indonesian Minister of the Environment.

Javed, M.H.; Ahmad, A., Rehan, M.; Musharavati, F.; Nizami, A.S.; Khan, M.I.; (2025). Advancing sustainable energy: Environmental and economic assessment of plastic waste gasification for syngas and electricity generation using life cycle modeling. Sustainability. 17(3) **(23 pages).**

Khan, A.H.; López-Maldonado, E.A.; Alam, S.S.; Khan, N.A.; López, J.R.L.; Herrera, P.F.M.; Abutaleb, A.; Ahmed, S.; Singh, L., (2022). Municipal solid waste generation and the current state of waste-to-energy potential: State of art review. Energy Convers. Manage. 267(6) **(15 pages).**

Kusenberg, M.; Zayoud, A.; Roosen, M.; Thi, H.D.; Abbas-Abadi, M.S.; Eschenbacher, A.; Kresovic, U.; De Meester, S.; Van Geem, K.M., (2022). A comprehensive experimental investigation of plastic waste pyrolysis oil quality and its dependence on the plastic waste composition. Fuel Process. Technol., 227: 107090 **(14 pages).**

Liu, S.; Mei, D.; Wang, L.; Tu, X., (2017). Steam reforming of toluene as biomass tar model compound in a gliding arc discharge reactor. Chem. Eng. J., 307: 793–802 **(10 pages)**.

Ma, H.; Xiao, X.; Zhang, X.; Liu, K., (2020). Recent advances for phase-transition materials for actuators. J. Appl. Phys., 128(10) **(21 pages)**.

Mishra, R.K.; Gariya, B.; Savvasere, P.; Dhir, D.; Kumar, P.; Mohanty, K., (2024). Thermocatalytic pyrolysis of waste areca nut into renewable fuel and value-added chemicals. ACS Omega. 9(24): 25779–25792 **(14 pages)**.

Ni, H.; Hsu, C.S.; Ma, C.; Shi, Q.; Xu, C., (2013). Separation and characterization of olefin/paraffin in coal tar and petroleum coker oil. Energy Fuels. 27(9): 5069–5075 **(7 pages)**.

Niu, M.; Huang, Y.; Jin, B.; and Wang, X., (2013). Simulation of syngas production from municipal solid waste gasification in a bubbling fluidized bed using aspen plus. Ind. Eng. Chem. Res., 52(42): 14768–14775 **(8 pages)**.

Niu, Y.; Chi, Z.; Li, M.; Du, J.; Han, F., (2024). Advancements in biomass gasification and catalytic tar-cracking technologies. Mater. Rep. Energy. 4(4): 100295 **(19 pages)**.

Osman, A.I.; Fang, B.; Zhang, Y.; Liu, Y.; Yu, J.; Farghali, M.; Rashwan, A.K.; Chen, Z.; Chen, L.; Ihara, I.; Rooney, D.W.; Yap, P.S., (2024). Life cycle assessment and techno-economic analysis of sustainable bioenergy production: a review. In Environ. Chem. Lett. 22(3): 1115–1154 **(40 pages).**

Pannucharoenwong, N.; Echaroj, S.; Duanguppama, K.; Tanantong, T.; Chaiphet, K.; Turakarn, C.; Ratanadecho, P., (2026). Production of biogasoline from plastic waste through pyrolysis using a temperature-controlled condenser technique. ACS Omega, 11(29): 43735–43747 **(13 pages).**

Pertamina, (2017). Produk Paraffinic Oil 60 dan 95. PT. Pertamina Persero. Indonesia.

Pio, D.T.; Ruivo, L.C.M.; Tarelho, L.A.C.; Frade, J.R.; Kantarelis, E.; Engvall, K., (2021). Tar formation during eucalyptus gasification in a bubbling fluidized bed reactor: Effect of feedstock and reactor bed composition. Energy Convers. Manage., 229(113749). **(19 pages).**

Qiao, Y.; Xu, F.; Xu, S.; Yang, D.; Wang, B.; Ming, X.; Hao, J.; Tian, Y., (2018). Pyrolysis characteristics and kinetics of typical municipal solid waste components and their mixture: Analytical TG-FTIR study. Energy Fuels. 32(10): 10801–10812 **(12 pages).**

Qin, Y.H.; Feng, J.; Li, W.Y., (2010). Formation of tar and its characterization during air-steam gasification of sawdust in a fluidized bed reactor. Fuel. 89(7): 1344–1347 **(4 pages)**.

Rakesh, N.; Dasappa, S., (2018). A critical assessment of tar generated during biomass gasification - Formation, evaluation, issues and mitigation strategies. Renew. Sustain. Energy Rev., 91: 1045–1064 **(20 pages)**.

Razavian, M.; Fatemi, S., (2020). Intensified transformation of low-value residual fuel oil to light fuels with TPABr: EG as deep eutectic solvent with dual functionality at moderate temperatures. Energy Fuels. 34(5): 5497–5510 **(14 pages)**.

Ridwan, M.; Setyono, P.; Budiastuti, M.T.S., (2026). Paraffin-olefin content analysis and potential solutions of tar from municipal solid waste gasification process in Indonesia. Nat. Environ. Pollut. Technol., 7(2): 1–25 **(25 pages)**.

Rios, M.L.V.; González, A.M.; Lora, E.E.S.; Olmo, O.A.A., (2018). Reduction of tar generated during biomass gasification: A review: Biomass Bioenergy. 108, 345–370 **(26 pages)**.

Sadewo, A.B., (2023). Design of a condenser and the effect of the geometry of the condenser's spiral pipe diameter on the amount of gasification oil. J. Mech. Eng., 11(1): 147–154 **(8 pages)**.

Sarikoc, S., (2020). Fuels of the diesel-gasoline engines and their properties. In Diesel Gasol. Engines. IntechOpen. **(13 pages)**.

Satyro, W.C.; Contador, J.C.; Monken, S.F.P.; de Lima, A.F.; Junior, G.G.S.; Gomes, J.A.; Neves, J.V.S.; do Nascimento, J.R.; de Araújo, J.L.; Correa, E.S.; Silva, L.S., (2023). Industry 4.0 implementation projects: The cleaner production strategy—a literature review. Sustainability. 15(3), 1–18. **(18 pages).**

Sonjaya, A.N., (2021). Simulation analysis of municipal solid waste gasification using a fixed-bed downdraft gasifier (Case study: Putri Cempo landfill, Surakarta), Thesis. Universitas Indonesia. **(144 pages).**

Thi, H.D.; Djokic, M.R.; Van Geem, K.M., (2021). Detailed group-type characterization of plastic-waste pyrolysis oils: By comprehensive two-dimensional gas chromatography including linear, branched, and di-olefins. Separations. 8(7): 103. **(18 pages)**.

Tursunov, O.; Suleimenova, B.; Kuspangaliyeva, B.; Inglezakis, V.J.; Anthony, E.J.; Sarbassov, Y., (2020). Characterization of tar generated from the mixture of municipal solid waste and coal pyrolysis at 800 °C. Energy Rep., 6: 147–152. **(6 pages)**.

Ula, S.; Kurniadi, W., (2017). A feasibility study on the industrial-scale production of biodiesel from used cooking oil. J. Mech. Eng., 2(2):1–7 **(7 pages)**.

Wang, S.; Jiao, T.; Zhang, Y.; Hao, M.; Bai, G.; Wang, X.; Liang, P., (2022). Recovery of paraffin from the filter cake used for paraffin decoloration in the Fischer-Tropsch synthetic process. Fuel. 324(PB): 124579. **(8 pages)**.

Wang, B.; Gupta, R.; Bei, L.; Wan, Q.; and Sun, L., (2023a). A review on gasification of municipal solid waste (MSW): Syngas production, tar formation, mineral transformation and industrial challenges. Int. J. Hydrog. Energy. 48(69): 26676–26706 **(31 pages)**.

Wang, X.; He, X.; Wang, X., (2023b). FTIR analysis of the functional group composition of coal tar residue extracts and extractive residues. Appl. Sci., 13(8) **(14 pages)**.

Wang, Q.; Li, T.; Tian, Q.; Wang, N.; Wang, M.; Shen, Y.; Yan, L.; Kong, J.; Chang, L.; Bao, W., (2025). Catalytic upgrading of tar by regulating reactions of coal pyrolysis volatiles over acid-base bifunctional carbon-based composites. Fuel, 387, 134328. **(13 pages).**

Wasita, A., (2023). Realizing alternative energy from mountains of waste in Solo. ANTARA News.

Yousef, S.; Eimontas, J.; Striūgas, N.; Abdelnaby, M.A., (2021). Pyrolysis kinetic behaviour and TG-FTIR-GC–MS analysis of Coronavirus Face Masks. Journal of Analytical and Applied Pyrolysis. 156: 105118 **(10 pages).**

Zhou, Q.; Liu, Q.; Shi, L.; Yan, Y.; Wu, J.; Xiang, C.; Wang, T.; Liu, Z., (2019). Effect of volatiles' reaction on composition of tars derived from pyrolysis of a lignite and a bituminous coal. Fuel. 242: 140–148 **(9 pages)**.

AUTHOR (S) BIOSKETCHES

Ridwan, M., Doctor Candidate, Department of Environmental Science, Graduate School, Universitas Sebelas Maret, Jalan Ir. Sutami 36A Kentingan, Jebres, Surakarta, Central Java, Indonesia.
- Email: *ridwannn@student.uns.ac.id*
- ORCID: 0009-0001-4923-9069
- Web of Science ResearcherID: QUU-6553-2026
- Scopus Author ID: 60685021900
- Homepage: https://pasca.uns.ac.id/s3-ilmu-lingkungan/

Setyono, P., Doctor, Professor, Department of Environmental Science, Graduate School, Universitas Sebelas Maret, Jalan Ir. Sutami 36A Kentingan, Jebres, Surakarta, Central Java, Indonesia.
- Email: *prabangsetyono@gmail.com*
- ORCID: 0000-0001-6440-6083
- Web of Science ResearcherID: AAD-9682-2021
- Scopus Author ID: 56179823100
- Homepage: https://iris1103.uns.ac.id/profil-0024057202.asm

Budiastuti, M.T.S., Doctor, Professor, Department of Environmental Science, Graduate School, Universitas Sebelas Maret, Jalan Ir. Sutami 36A Kentingan, Jebres, Surakarta, Central Java, Indonesia.
- Email: *mariatheresia@staff.uns.ac.id*
- ORCID: 0000-0002-4144-4041
- Web of Science ResearcherID: AAD-8365-2022
- Scopus Author ID: 57194587611
- Homepage: https://iris1103.uns.ac.id/profil-0005125905.asm

HOW TO CITE THIS ARTICLE:
Ridwan, M.; Setyono, P.; Budiastuti, M.T.S., (2027). Valorization and physicochemical characterization of municipal solid waste gasification tar derived aliphatic hydrocarbon-rich oils. Global J. Environ. Sci. Manage., 13(1): 327-346.

DOI: 10.22034/gjesm.2027.01.15
URL: https://www.gjesm.net/article_735772.html

Global J. Environ. Sci. Manage. 13(1): 347-368, Winter 2027, Serial #49

Global Journal of Environmental Science and Management
(GJESM)

Homepage: https://www.gjesm.net/

Podcasts

ORIGINAL RESEARCH ARTICLE

Analytic hierarchy process-based criterion weighting for water resources management projects

O. Gorbunov[1], C. Sinsabvarodom[1], D. Rinchumphu[1,*], P. Sangunsri[2], N. Phichetkunbodee[3]

[1]*Department of Civil Engineering, Chiang Mai University, Thailand*

[2]*Lamphun Irrigation Project, Office of Regional Irrigation 1, Ministry of Agriculture and Cooperatives, Thailand*

[3]*Department of Civil Engineering, National Taiwan University, Taiwan*

ARTICLE INFO

Article History:
Received 20 June 2026
Revised 24 August 2026
Accepted 28 September 2026

Keywords:
Criteria weighting
Decision support
Engineering feasibility
Expert judgment
Irrigation development
Sustainable infrastructure appraisal

DOI:10. 22034.gjesm.2027.01.16

ABSTRACT

BACKGROUND AND OBJECTIVES: Prioritizing water resources projects requires decision-makers to balance hydrological performance, engineering feasibility, environmental and social sustainability, and economic value under limited budgets and implementation resources. Conventional evaluation frameworks are frequently bound to specific project typologies or geographical contexts, thereby constraining their direct applicability across heterogeneous project portfolios. The study objectives were to develop an analytic hierarchy process-based multi-criteria decision-making framework for deriving criterion weights for water resources management project assessment, using Chiang Mai Province, Thailand, as the empirical context.

METHODS: The framework was developed by synthesizing water resources management principles, practical project-assessment considerations, and relevant multi-criteria decision-making literature. The evaluation model comprised four principal dimensions and 18 operational sub-criteria. The Analytical hierarchy process framework was employed to analyze expert judgments elicited from six senior water resources and irrigation specialists, each possessing a minimum of 20 years of professional experience. Individual judgments were subsequently evaluated for consistency and aggregated using the geometric mean. Local weights were calculated using the eigenvector method and combined with the corresponding main-dimension weights to obtain global priorities.

FINDINGS: Engineering and Implementation Feasibility received the highest main-dimension weight (32.58 percent), followed by Economic performance (25.84 percent), Environmental and Social Sustainability (21.87 percent), and Water Resource and Hydrological Performance (19.71 percent). At the global level, cost effectiveness ranked first (13.99 percent), followed by Structural Scale (11.58 percent), Foundation Suitability (10.60 percent), and Storage and Hydrological Adequacy (8.93 percent). These four sub-criteria accounted for 45.10 percent of the total weight. Accounting for 81.88 percent of the total weight and encompassing elements across all four dimensions, the top 11 sub-criteria demonstrate that comprehensive assessment necessitates an integrated approach spanning technical, economic, hydrological, environmental, and social dimensions.

CONCLUSION: By establishing a transparent architecture for criterion organization and context-specific priority derivation, the framework facilitates water resources project evaluation. Integrated with empirical performance data and explicit scoring protocols, it underpins the formulation of robust project screening, portfolio comparative analysis, and budgetary prioritization procedures. The reported weights represent the judgments of the study panel and should be recalibrated for other locations, project types, and stakeholder groups. Subsequent applications of this framework should formulate a structured operational scoring rubric while comprehensively evaluating parameter sensitivity, model robustness, and project-ranking stability.

This is an open access article under the CC BY license (http://creativecommons.org/licenses/by/4.0/)

NUMBER OF REFERENCES	NUMBER OF FIGURES	NUMBER OF TABLES
31	4	9

*Corresponding Author:
Email: damrongsak.r@cmu.ac.th
Phone: +669 5995 9519
ORCID: 0000-0002-6037-4974

Note: Discussion period for this manuscript open until March 01, 2027 on GJESM website at the "Show Article".

INTRODUCTION

Water-resource management is a major challenge for sustainable development because water systems must accommodate increasing demands from population growth, economic activity, agriculture, and urban expansion, while water availability and distribution vary substantially across space and time (Gebre *et al.*, 2021). These vulnerabilities are further exacerbated by climate variability and long-term anthropogenic climate change, which disrupt precipitation regimes, regional water yields, and extreme event frequencies, thereby compounding uncertainty regarding future hydrological resource availability and demand projections (Wu *et al.*, 2025). In many regions, water scarcity therefore reflects not only physical limitations in supply but also rising demand, inefficient resource use, and increasing pressure on ecosystems (Konstadinos *et al.*, 2025; Meskine *et al.*, 2025). Under these conditions, water-resource management must move beyond responding to sector-specific demands toward systematic planning and allocation that balance water security, economic development, user needs, and long-term ecosystem sustainability (Gebre *et al.*, 2021; Wu *et al.*, 2025). The prioritization of water-resource development initiatives constitutes an inherently multidimensional decision-making paradigm. Project suitability depends not only on hydrological potential but also on engineering feasibility, environmental and social implications, and economic viability (Jafari *et al.*, 2026; Sandoval *et al.*, 2025). These criteria encompass both quantitative and qualitative attributes, frequently entailing trade-offs among competing objectives. For instance, enhancing water-delivery efficiency may necessitate substantial capital investment, whereas an alternative that is technically viable may encounter ecological or social-acceptance constraints (Jafari *et al.*, 2026; Sandoval *et al.*, 2025). The problem becomes more consequential when projects must compete for limited budgets, time, and implementation resources, making simultaneous development of all potentially beneficial projects impractical (Chaitongrat *et al.*, 2026; Mochani *et al.*, 2025). Consequently, the primary challenge lies not merely in identifying a singular optimal initiative, but in formulating a transparent evaluative architecture wherein multiple criteria and their relative priorities can be systematically appraised to guide project prioritization (Macchiaroli *et al.*, 2023; Sandoval *et al.*, 2025). Given the need to evaluate multiple criteria and trade-offs simultaneously, multi-criteria decision-making (MCDM) has been widely applied to support water-resource decisions because it can accommodate quantitative and qualitative criteria with different units and levels of importance (Gebre *et al.*, 2021). Among MCDM approaches, the analytic hierarchy process (AHP) is especially advantageous for decomposing complex decision problems into structured hierarchies of objectives, criteria, and sub-criteria, while systematically translating pairwise comparisons into relative priorities (Abastante *et al.*, 2019). This approach enables expert knowledge and professional experience to be expressed as a transparent weighting structure whose internal consistency can be assessed before the priorities are used for project comparison (Sandoval *et al.*, 2025). Consequently, the AHP has consequently been extensively adopted within water-resources and flood-management studies to bridge technical evaluation with structured decision frameworks (Alfian *et al.*, 2026; Kaewwichian *et al.*, 2025). Beyond water-resource management, AHP has also been extended to prioritize environmental risks in concrete construction initiatives across developing economies, effectively synthesizing expert evaluations and stakeholder perspectives through pairwise comparisons (Solaimanian, 2025). Northern Thailand, and Chiang Mai in particular, provides a useful empirical setting for examining this type of multidimensional prioritization problem. The province combines diverse topography, changing land use, and strong

interactions between water systems, economic activities, agriculture, and communities (Chayakul *et al.*, 2026; Gu *et al.*, 2025). Water-resource development must therefore address multiple objectives, including agricultural water supply, flood-related concerns, community needs, and environmental and land-use constraints (Gu *et al.*, 2025; Wu *et al.*, 2025). Studies of irrigation projects in Thailand likewise indicate that technical, environmental, financial, and implementation factors are closely interrelated in project decision-making (Chaitongrat *et al.*, 2026). Accordingly, Chiang Mai serves in this investigation as an empirical setting for developing and testing a multidimensional prioritization framework, rather than acting as its exclusive geographical boundary. The challenge is thus not merely the number of criteria involved, but how those criteria are organized into a structure that can be applied consistently across projects. Recent MCDM and AHP studies in water resources have addressed problems ranging from alternative water-resource assessment and sustainable water management (Konstadinos *et al.*, 2025; Pham *et al.*, 2026) to irrigation-project prioritization and urban water-management measures (Demir *et al.*, 2025; Sandoval *et al.*, 2025). Irrigation-modernization studies further demonstrate the need to consider technical, economic, social, and environmental factors jointly (Jafari *et al.*, 2026). Nevertheless, evaluation criteria employed in prior studies are frequently customized for specific project typologies, spatial settings, or decision objective, thereby constraining their utility as generalized frameworks for heterogeneous water-resource initiatives. Indicator-development research also emphasizes that criteria should be both conceptually comprehensive and operationally applicable (Asadi and Alibaygi, 2026; Li, 2023). Consequently, this underscores a methodological imperative for an integrated operational architecture capable of organizing diverse project dimensions and assigning relative priorities while retaining adaptability to local decision environments. The contribution of the present framework lies not in introducing a new AHP technique, but in consolidating heterogeneous project-assessment considerations into a common hierarchical structure that integrates hydrological, engineering and implementation, environmental and social, and economic dimensions. By bridging four primary dimensions with 18 operational sub-criteria and segregating dimension-level, local, and global priorities, the framework establishes a coherent architecture for synthesizing expert evaluations across multifaceted water-resource project assessment. To address this need, this study develops a framework for prioritizing water-resource projects using four main dimensions and 18 operational sub-criteria covering water resource and hydrological performance, engineering and implementation feasibility, environmental and social sustainability, and economic performance. Expert-based AHP is then applied to derive the relative priorities of the criteria and construct a transparent priority structure. Rather than selecting or ranking individual project alternatives, this study establishes a methodical foundation for deriving the relative weighting of assessment criteria, which, when integrated with project-level performance data and explicit scoring protocols, can systematically guide future project comparison and prioritization across diverse infrastructure development contexts. The proposed framework is intended as an adaptable structure for project prioritization across different decision contexts. Accordingly, this study aims to develop an analytic hierarchy process-based multi-criteria decision-making framework for deriving criterion weights for water resources management project assessment, using Chiang Mai Province, Thailand, as the empirical context. The study was conducted in Chiang Mai Province, Thailand, in 2025 and 2026, using an existing expert-based water-resource project assessment dataset. Chiang Mai Province, Thailand, is used as the empirical setting to illustrate realistic water-resource development conditions.

MATERIALS AND METHODS

Study context and data source

Chiang Mai Province, Thailand, was used as the empirical context for developing and examining the water-resource project prioritization framework. The province contains diverse physical and land-use conditions, including mountainous terrain, agricultural areas, and expanding urban settlements that interact with water systems at multiple spatial scales. These intrinsic characteristics render water-resource planning highly susceptible to hydrological variability, conflicting sectoral demands, and complex land-water feedback loops (Chayakul *et al.*, 2026; Gu *et al.*, 2025). Chiang Mai therefore provides a suitable real-world setting in which project development must simultaneously consider water-resource performance, engineering feasibility, environmental and social implications, and economic performance. In this study, the province functions as an empirical testbed for evaluating the architecture and relative priorities of the proposed framework rather than serving as an isolated case study of a single project. Fig. 1 represent the proposed project area in Chiang Mai province, Thailand. A previous study of water-resource project assessment in Chiang Mai (Sangunsri, 2022) was used primarily to provide contextual background and to illustrate the practical need for a more integrated criterion-weighting framework. Selected project attributes and evaluative criteria from prior studies were integrated with the broader literature to inform the development of the framework. The present study, however, adopts a revised analytical structure consisting of four main dimensions and 18 operational sub-criteria, developed to address the current research objective rather than to reproduce the analytical structure of the previous study. Although Chiang Mai was used as the empirical setting, the conceptual scope of the framework is not restricted to this location. Its four dimensions represent recurring components of multidimensional water-resource project prioritization, whereas the resulting relative weights remain context-sensitive and may vary across regions and management systems (Asadi and Alibaygi, 2026; Pham *et al.*, 2026). Consequently, the research design was structured into three distinct phases: 1) the establishment of the criteria framework, 2) the evaluation of expert judgments via the analytic hierarchy process (AHP), and 3) the subsequent synthesis of local and global criterion weights. The overall analytical workflow and its relationship with the subsequent methodological and results sections are illustrated in Fig. 2.

Criteria structuring and framework development

The criteria framework was developed by synthesizing water resources management principles, technical criteria, and approaches from relevant MCDM studies. The aim was to organize diverse assessment criteria into a clear structure suitable for practical application (Konstadinos *et al.*, 2025; Sandoval *et al.*, 2025). This procedure prioritized both conceptual relevance and operational utility, ensuring that every criterion captured a substantive dimension of the decision process while remaining tethered to empirical project-level data or assessments (Asadi and Alibaygi, 2026; Jafari *et al.*, 2026). The resulting framework comprises four main dimensions and 18 operational sub-criteria. The dimensions are Water Resource and Hydrological Performance, Engineering and Implementation Feasibility, Environmental and Social Sustainability, and Economic Performance. Table 1 outlines the mapping between the criteria established in this study and the corresponding relevant literature. During framework development, conceptually related criteria were also reviewed to minimize potential overlap and double counting. Distinct operational boundaries were enforced between criteria addressing distinct facets of project evaluation. For example, water availability (A1) represents the availability of the water resource that can support project demand, whereas storage

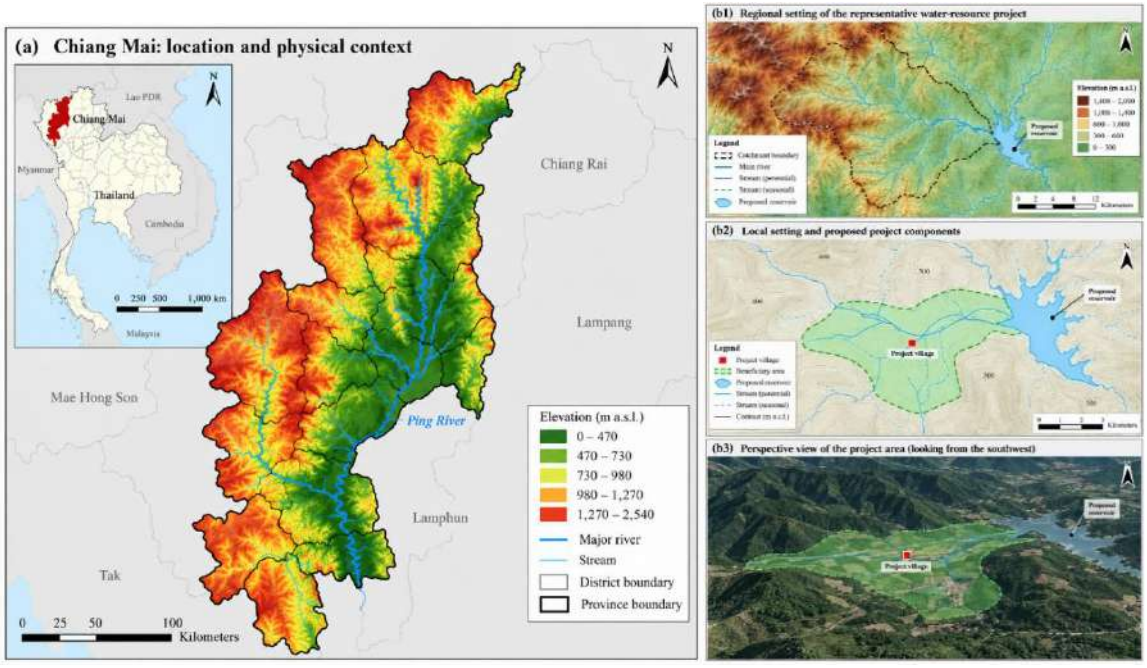

Fig. 1: Geographical location and spatial context and example of a water-resource development setting in Chiang Mai, Thailand (a) location, terrain, elevation, and major drainage characteristics of Chiang Mai Province; (b1) regional setting of an example water-resource project; (b2) local setting and proposed project components, including the reservoir and beneficiary area; and (b3) perspective view of the project area

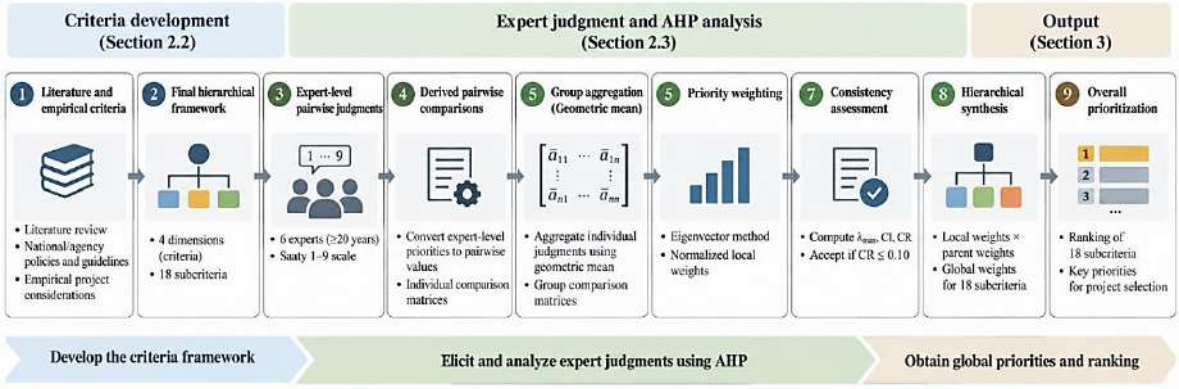

Fig. 2: Analytical workflow for developing the AHP-based criterion-weighting framework for water-resource project assessment

and hydrological adequacy (A2) concerns the adequacy of storage and hydrological conditions for regulating and supplying that resource. Ecological impact (C1) addresses potential consequences of project deployment on local biological conditions, while watershed and conservation constraints (C2) delineate site-specific limitations linked to hydrological and conservation settings. Similarly, cost effectiveness (D2) considers the relationship between project cost and the benefits or service delivered, whereas economic return (D3) represents the economic benefits or returns generated by the project. These distinctions were maintained to reduce conceptual redundancy within the hierarchical structure.

Table 1: Literature synthesis of criteria for water-resource project prioritization

Dimension/ subcriterion	(Pham *et al.*, 2026)	(Shams *et al.*, 2025)	(Mochani *et al.*, 2025)	(Sandoval *et al.*, 2025)	(Chayakul *et al.*, 2026)	(Chaitongrat *et al.*, 2026)	(Lamichhane *et al.*, 2025)	(Macchiaroli *et al.*, 2023)	(Jafari *et al.*, 2026)	(Asadi and Alibaygi, 2026)
A. Water resource and hydrological performance										
A1 Water availability	✓	✓	✓	✓			✓		✓	
A2 Storage and hydrological adequacy	✓	✓	✓	✓			✓		✓	
A3 Irrigation water need				✓			✓		✓	
A4 Irrigation service potential				✓			✓		✓	
B. Engineering and implementation feasibility										
B1 Structural scale		✓	✓	✓					✓	
B2 Earthwork requirement			✓						✓	
B3 Foundation suitability		✓	✓						✓	
B4 site accessibility		✓	✓			✓			✓	
B5 Implementation duration						✓			✓	
C. Environmental and social sustainability										
C1 ecological impact	✓	✓	✓	✓	✓				✓	✓
C2 watershed and conservation constraints		✓	✓	✓	✓				✓	✓
C3 environmental assessment Requirement			✓	✓	✓				✓	✓
C4 beneficiary Coverage				✓			✓		✓	✓
C5 social acceptability and land impact	✓		✓	✓	✓				✓	✓
D. Economic performance										
D1 project cost	✓		✓	✓		✓		✓	✓	
D2 cost effectiveness	✓		✓	✓			✓	✓	✓	
D3 economic return	✓		✓	✓				✓	✓	
D4 long-term economic value	✓		✓	✓				✓	✓	

To facilitate uniform interpretation of the hierarchical structure, the operational definitions of the four primary dimensions and their 18 sub-criteria were explicitly detailed, drawing upon evaluation considerations synthesized during framework development. Table 2 summarizes these operational definitions together with indicative measures or units, where applicable. The illustrative metrics presented in Table 2 delineate how individual criteria can be construed within an operational assessment context; they do not establish a rigid project-scoring or data normalization protocol. The definitions also maintain distinct assessment boundaries among conceptually related sub-criteria, thereby reducing potential overlap within the hierarchy. This operationalized structure formed the basis for the subsequent expert-based AHP weighting procedure.

Expert judgment and AHP analysis

Determining the relative importance of criteria for water resources project prioritization requires both technical knowledge and practical experience in project planning and implementation. Consequently, this study utilized an expert-based

Table 2: Operational definitions of the criteria and sub-criteria used in the AHP framework

Code	Criterion / Subcriterion	Operational definition and indicative measurement
A	Water resource and hydrological performance	Assesses project suitability in terms of water-resource and hydrological conditions relevant to project development and service provision, including water availability, storage adequacy, irrigation need, and irrigation service potential.
A1	Water availability	Availability and adequacy of natural water resources to support project development and operation, represented by long-term mean annual rainfall (mm/y) and mean annual runoff volume (m^3/y or Mm^3/y).
A2	Storage and hydrological adequacy	Adequacy of project storage relative to local hydrological conditions, represented by storage capacity (m^3 or Mm^3), storage-to-annual-runoff ratio (%), and maximum flood discharge (m^3/s).
A3	Irrigation water need	Need for project investment arising from water shortages or unmet irrigation demand, represented by water-deficit conditions, severity or frequency of shortages, and proportion of unmet water demand.
A4	Irrigation service potential	Capacity of the project to serve existing irrigation areas and support future expansion, represented by irrigated area (rai or ha), potential expansion area, and percentage expansion (%).
B	Engineering and implementation feasibility	Assesses the feasibility of project design, construction, and implementation under site conditions, considering structural scale, earthwork requirements, foundation conditions, site accessibility, and implementation duration.
B1	Structural scale	Physical size and complexity of the principal hydraulic structure, represented by structure height (m) and structure length (m).
B2	Earthwork Requirement	Amount of earthwork required for construction, including excavation, filling, and site preparation, represented primarily by earthfill volume (m^3).
B3	Foundation suitability	Suitability of geological and foundation conditions for structural stability and construction, represented by foundation geology or foundation-suitability class based on geological and geotechnical assessment.
B4	Site accessibility	Ease of access from the existing transport network to the construction site, represented by distance from the main road to the project site (km).
B5	Implementation duration	Time required for project preparation, construction, commissioning, and handover, represented by the implementation period (months or years).
C	Environmental and social sustainability	Assesses project suitability in terms of ecological impacts, conservation constraints, environmental assessment requirements, beneficiary coverage, social acceptance, and land-related impacts.
C1	Ecological impact	Direct effects of project development on natural resources and ecosystems, represented by inundated forest area (ha) and information on wildlife or habitat impacts/severity.
C2	Watershed and conservation constraints	Spatial and regulatory constraints associated with watershed protection and conservation areas, represented by watershed class, conservation-area designation, affected area (ha), and degree of restriction.
C3	Environmental assessment requirement	Level of environmental assessment and review required according to project characteristics, scale, location, and anticipated impacts, represented by the required environmental-assessment level or study category.
C4	Beneficiary coverage	Social reach of project benefits, represented by the number of beneficiary households or persons, and where appropriate the proportion of the target population or households (%).
C5	Social acceptability and land impact	Community acceptance and land-related effects associated with project development, represented by public participation or beneficiary acceptance together with land-acquisition area.
D	Economic performance	Assesses project suitability in terms of investment requirements, resource-use efficiency, economic return, and long-term economic value.
D1	Project cost	Absolute financial resources required for project development and construction, represented by construction or total project cost (USD or million USD).
D2	Cost effectiveness	Investment efficiency in terms of physical outputs or services delivered per unit of cost, represented by construction cost per unit water volume (USD/m^3) and construction cost per unit irrigated area (USD/ha).
D3	Economic return	Economic benefits generated relative to project costs over the investment period, represented primarily by the Benefit–Cost Ratio (BCR).
D4	Long-term economic value	Net economic value generated over the analysis period after accounting for the timing of benefits and costs, represented by Net Present Value (NPV; USD or million USD) under a specified discount rate and analysis period.

decision analysis framework, employing purposive, criterion-based sampling to select experts rather relying on random sampling designed to reflect the general population. Selection emphasized relevant professional roles, domain expertise, and experience directly related to the decision problem. This approach is consistent with multi-criteria decision analysis (MCDA) studies that select experts based on specialized qualifications and experience (Min *et al.*, 2025). Similar approaches are used in water-related decision support, where participants are selected for their technical expertise, institutional roles, and knowledge of the system under study (Alfian *et al.*, 2026), and in water governance indicator development, where purposive sampling identifies experts with knowledge relevant to the assessment (Asadi and Alibaygi, 2026). Consequently, the panel was assembled to furnish informed insights rooted in specialized expertise, rather than to achieve statistical representativeness (Caraveo Gomez Llanos *et al.*, 2024). The panel comprised six senior water resources and irrigation professionals, each with at least 20 years of experience in planning, developing, and implementing water resources projects. Their experience included project appraisal, assessment of technical constraints, and operational decision-making, enabling them to provide judgments grounded in professional practice. This selection methodology aligns with the principles of expert-based AHP, which prioritizes specialized knowledge and contextual experience directly pertinent to the decision problem (Caraveo Gomez Llanos *et al.*, 2024). Unlike population surveys, expert-based AHP does not determine panel size using conventional statistical sample-size requirements, as its purpose is to synthesize informed judgments rather than estimate population parameters. Furthermore, panel adequacy is governed by variations in criterion priorities, expert heterogeneity, judgment variability, and ranking stability, rather than being determined by panel size alone (Zeki *et al.*, 2026). The six-member panel should therefore be considered in relation to its qualifications and expertise, and should not be interpreted as a universally appropriate size for all AHP applications (Caraveo Gomez Llanos *et al.*, 2024; Zeki *et al.*, 2026). While Table 3 outlines the professional profiles of the experts, the evaluations rendered by this panel were systematically processed via the AHP across five sequential phases. The expert panel was purposively selected to provide informed professional judgments rather than statistical representation of a broader population. The six participants were senior professionals with at least 20 years of experience in water-resource planning, engineering, or project-related decision-making. Consequently, the derived weighting parameters constitute an expert-driven priority architecture bounded by the professional and institutional milieu of the panel. They should not be interpreted as population-level preferences or as universally applicable weights across all stakeholder groups and decision contexts.

Step 1: Individual pairwise judgments

Expert judgments were collected through AHP pairwise comparisons using Saaty's 1–9 scale, ranging from 1 for equal importance to 9 for extreme importance of one criterion over another (Abastante *et al.*, 2019). The survey instrument administered pairwise comparisons of criteria, requiring experts to designate the more critical parameter and quantify the relative magnitude of difference, as depicted in Fig. 3. Judgments were retained at the individual-expert level to preserve differences in opinion before group aggregation (Alfian *et al.*, 2026; Caraveo Gomez Llanos *et al.*, 2024). The pairwise comparison values were organized into a reciprocal comparison matrix following AHP principles. If a_{ij} represents the importance of criterion i relative to criterion j, the reverse comparison is defined as $a_{ji} = 1/a_{ij}$, while the diagonal entries are $a_{ii} = 1$ (Abastante *et al.*, 2019). This matrix provides the basis for calculating priority weights and assessing consistency in the subsequent steps.

Table 3: Professional profile of the expert panel

Expert	Professional role/category*	Relevant experience	Water-resource responsibility
E1	Senior water-resources development executive	>30 years	Water-resource project planning and construction; contract administration for weirs, reservoirs, conveyance systems, and irrigation structures
E2	Senior engineering director	>30 years	Water-resource project planning; design of weirs, reservoirs, conveyance systems, and irrigation structures
E3	Senior water-management director	>30 years	Water-resource project planning; water management; operation and maintenance of weirs, reservoirs, conveyance systems, and irrigation structures
E4	Senior irrigation-project director	>20 years	Construction and maintenance of water-resource projects; contract administration for weirs, reservoirs, conveyance systems, and irrigation structures
E5	Senior irrigation engineering professional	>20 years	Engineering and implementation of water-resource and irrigation projects
E6	Senior irrigation/water-resources professional	>20 years	Planning, engineering, implementation, and management of water-resource projects

Note: *Expert identities are anonymized as E1–E6. All experts had at least 20 years of relevant professional experience in water-resource and irrigation development.

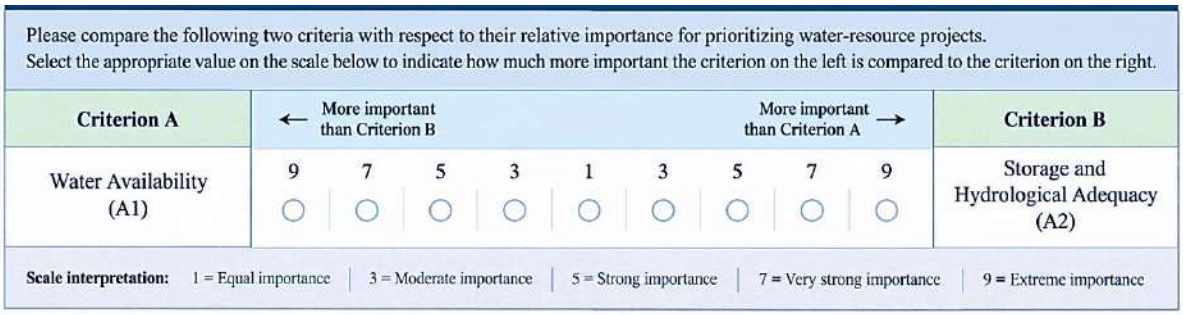

Fig. 3: Example of the pairwise-comparison questionnaire used for expert judgment

Step 2: Construction of individual pairwise comparison matrices

For analysis under the final hierarchy, pairwise comparisons were organized separately for each expert and for each comparison level of the framework. The expert evaluations were structured into reciprocal comparison matrices in accordance with AHP guidelines, thereby preserving individual judgment variances prior to final aggregation. Each pairwise entry quantified the relative significance of one criterion against another (Abastante *et al.*, 2019; Al-Jabal and Al-Khafaji, 2025). Once all individual matrices were constructed, they were combined through group aggregation in the next step.

Step 3: Aggregation of expert judgments

To synthesize individual insights into a unified group comparison matrix, the geometric mean was applied to aggregate the experts' pairwise comparison matrices—a standard procedure in group AHP applications. For each pair of criteria, the group comparison value was calculated, using Eq. 1 (Alfian *et al.*, 2026; Caraveo Gomez Llanos *et al.*, 2024):

$$\bar{a}_{ij} = \left(\prod_{k=1}^{m} a_{ij}^{(k)} \right)^{1/m} \quad (1)$$

Where: $\bar{a}_{ij}$ is the group comparison value between criteria i and j, $a_{ij}^{(k)}$ is the judgment provided by expert k, and m is the number of experts, which was six in this study. The geometric mean was calculated for every pair of criteria at each level of the hierarchy to construct a reciprocal group comparison matrix. This approach preserves the ratio-scale properties of pairwise judgments and is suitable for synthesizing

judgments from multiple experts (Asadi and Alibaygi, 2026).

Step 4. Priority weighting and consistency assessment

Once the group comparison matrix was constructed, criterion weights were derived from the eigenvector corresponding to the maximum eigenvalue, following AHP principles. The weights were normalized to sum to 1 within each comparison set. The consistency of pairwise judgments was then assessed using the maximum eigenvalue ($\lambda_{\max}$), consistency index (CI), and consistency ratio (CR), using Eqs. 2 and 3 (Abastante *et al.*, 2019):

$$CI = \frac{\lambda_{\max} - n}{n-1} \quad (2)$$

and

$$CR = \frac{CI}{RI} \quad (3)$$

Where: n is the number of criteria in the comparison matrix and RI is the random index corresponding to the matrix size. A consistency ratio of $\mathrm{CR} \leq 0.10$ was used to indicate an acceptable level of judgment inconsistency for AHP analysis (Alfian *et al.*, 2026; Caraveo Gomez Llanos *et al.*, 2024). Prior to the final synthesis of priority weights, the consistency of the group matrices was evaluated across every hierarchical tier.

Step 5: Hierarchical synthesis and global prioritization

The local priority weights within each dimension were synthesized to obtain the global priorities of all 1 8 sub-criteria. The global weight of each subcriterion was computed by scaling its local weight against the weight of its corresponding parent dimension, expressed in Eq. 4 (Caraveo Gomez Llanos *et al.*, 2024; Jafari *et al.*, 2026):

$$GW_i = LW_i \times PW_j \quad (4)$$

where GW_i is the global weight of subcriterion i, LW_i is its local weight within its dimension, and PW_j is the priority weight of its parent dimension j. This hierarchical synthesis allows sub-criteria from different dimensions to be compared on a common scale, with the resulting global weights used to rank all 18 sub-criteria (Caraveo Gomez Llanos *et al.*, 2024; Jafari *et al.*, 2026).

RESULTS AND DISCUSSION

Priority structure and consistency

Individual-expert results are reported in Tables 4 to 8 for the main dimensions and their respective sub-criteria, together with the corresponding geometric-mean aggregated results. reveal divergences in expert preference structures that remain obscured when relying solely on aggregated values. Furthermore, all individual comparison matrices met the established consistency threshold (CR < 0.10). It should be emphasized that CR represents the internal consistency of each comparison structure and should not be interpreted as a measure of inter-expert agreement. The individual results also reveal differences in the relative emphasis assigned by the six experts. For example, engineering and implementation feasibility (B) received the highest weight from E1, E3, and E4, whereas environmental and social sustainability (C) was weighted highest by E2 and E6, and economic performance (D) by E5. These variations highlight that satisfying individual consistency thresholds does not ensure uniform priority configurations among experts. Consequently, employing geometric-mean aggregation of the six individual assessments, the synthesized group weights were propagated across the hierarchy to derive the local and global criterion priorities detailed in Table 9. At the main-dimension level, engineering and implementation feasibility (B) received the highest weight at 32.58%, followed

Table 4: Individual expert priorities, consistency, and aggregated results for the main dimensions

Expert	A: Water resource and hydrological performance	B: Engineering and implementation feasibility	C: Environmental and social sustainability	D: Economic performance	λmax	CI	CR
E1	0.251	0.552	0.108	0.090	4.022	0.007	0.008
E2	0.109	0.104	0.433	0.354	4.025	0.008	0.009
E3	0.196	0.480	0.108	0.216	4.021	0.007	0.008
E4	0.185	0.370	0.100	0.345	4.010	0.004	0.004
E5	0.246	0.246	0.210	0.298	4.061	0.020	0.023
E6	0.108	0.216	0.480	0.196	4.021	0.007	0.008
Aggregated	0.197	0.326	0.219	0.258	4.003	0.001	0.001

Table 5: Individual expert priorities, consistency, and aggregated results for the water resource and hydrological performance (A)

Expert	A1: Water availability	A2: Storage and hydrological adequacy	A3: Irrigation water need	A4: Irrigation service potential	λmax	CI	CR
E1	0.308	0.541	0.106	0.044	4.052	0.017	0.019
E2	0.171	0.467	0.171	0.191	4.020	0.007	0.008
E3	0.218	0.461	0.103	0.218	4.006	0.002	0.002
E4	0.345	0.370	0.100	0.185	4.010	0.003	0.004
E5	0.461	0.218	0.218	0.103	4.006	0.002	0.002
E6	0.158	0.615	0.101	0.126	4.041	0.014	0.015
Aggregated	0.275	0.453	0.135	0.137	4.006	0.002	0.002

Table 6: Individual expert priorities, consistency, and aggregated results for the Engineering and Implementation Feasibility (B)

Expert	B1: Structural scale	B2: Earthwork requirement	B3: Foundation suitability	B4: Site accessibility	B5: Implementation duration	λmax	CI	CR
E1	0.289	0.289	0.289	0.102	0.030	5.010	0.002	0.002
E2	0.345	0.082	0.329	0.079	0.165	5.006	0.001	0.001
E3	0.377	0.097	0.377	0.097	0.051	5.003	0.001	0.001
E4	0.341	0.082	0.327	0.072	0.178	5.018	0.005	0.004
E5	0.284	0.241	0.262	0.111	0.103	5.033	0.008	0.007
E6	0.416	0.190	0.291	0.068	0.036	5.060	0.015	0.013
Aggregated	0.355	0.151	0.325	0.091	0.078	5.003	0.001	0.001

Table 7: Individual expert priorities, consistency, and aggregated results for the Environmental and Social Sustainability (C)

Expert	C1: Ecological impact	C2: Watershed and conservation constraints	C3: Environmental assessment requirement	C4: Beneficiary coverage	C5: Social acceptability and land impact	λmax	CI	CR
E1	0.079	0.081	0.081	0.158	0.600	5.003	0.001	0.001
E2	0.120	0.363	0.347	0.077	0.093	5.038	0.009	0.008
E3	0.054	0.214	0.238	0.064	0.4290	5.019	0.005	0.004
E4	0.124	0.347	0.271	0.035	0.223	5.043	0.011	0.010
E5	0.108	0.203	0.203	0.101	0.384	5.010	0.002	0.002
E6	0.095	0.393	0.340	0.086	0.086	5.018	0.004	0.004
Aggregated	0.107	0.272	0.258	0.091	0.272	5.004	0.001	0.001

Table 8: Individual expert priorities, consistency, and aggregated results for the Economic Performance (D)

Expert	D1: Project cost	D2: Cost effectiveness	D3: Economic return	D4: Long-term economic value	λmax	CI	CR
E1	0.082	0.235	0.449	0.235	4.004	0.001	0.001
E2	0.049	0.469	0.241	0.241	4.001	0.001	0.001
E3	0.206	0.662	0.064	0.068	4.031	0.010	0.012
E4	0.177	0.689	0.067	0.067	4.033	0.011	0.012
E5	0.095	0.467	0.277	0.160	4.031	0.010	0.011
E6	0.078	0.559	0.228	0.135	4.031	0.010	0.011
Aggregated	0.113	0.542	0.196	0.149	4.003	0.001	0.001

Table 9: Priority weights of criteria and sub-criteria for water-resource project prioritization

Main dimension [A]	Main weight	Subcriterion [B]	Local weight	Global weight [A × B]	Overall rank
A. Water resource and hydrological performance	0.197	A1 Water availability	0.275	0.054	8
		A2 Storage and hydrological adequacy	0.453	0.089	4
		A3 Irrigation water need	0.135	0.027	15
		A4 Irrigation service potential	0.137	0.027	14
B. Engineering and implementation feasibility	0.326	B1 Structural scale	0.355	0.116	2
		B2 Earthwork requirement	0.151	0.049	10
		B3 Foundation suitability	0.325	0.106	3
		B4 Site accessibility	0.091	0.030	12
		B5 Implementation duration	0.078	0.025	16
C. Environmental and social sustainability	0.219	C1 Ecological impact	0.107	0.023	17
		C2 Watershed and conservation constraints	0.272	0.060	5
		C3 Environmental assessment requirement	0.258	0.056	7
		C4 Beneficiary coverage	0.091	0.020	18
		C5 Social acceptability and land impact	0.272	0.059	6
D. Economic performance	0.258	D1 Project cost	0.113	0.029	13
		D2 Cost effectiveness	0.542	0.140	1
		D3 Economic return	0.196	0.051	9
		D4 Long-term economic value	0.149	0.038	11

by economic performance (D) at 25.84%, environmental and social sustainability (C) at 21.87%, and water resource and hydrological performance (A) at 19.71%. Consequently, the resulting priority hierarchy was established as B>D>C>A, demonstrating that the panel assigned primary importance to engineering and implementation feasibility, followed by closely economic considerations. Consistency assessment of the 4 × 4 group comparison matrix yielded $\lambda_{\max} = 4.0025$, $\mathrm{CI} = 0.0008$, and $\mathrm{CR} = 0.0009$. The resulting CR remained well beneath the 0.10 threshold, confirming satisfactory internal consistency across the primary-dimension comparisons for AHP evaluation. Within dimension A: Water Resource and Hydrological Performance, Storage and Hydrological Adequacy (A2) received the highest local weight at 45.32%, followed by water availability (A1) at 27.49%, Irrigation Service Potential (A4) at 13.65%, and Irrigation Water Need (A3) at 13.54%. Within Dimension B: Engineering and Implementation Feasibility, Structural Scale (B1) ranked first at 35.54%, followed by Foundation Suitability (B3) at 32.53%, Earthwork Requirement (B2) at 15.04%, Site Accessibility (B4) at 9.12%, and Implementation Duration (B5) at 7.77%. A2 and A1 therefore held the highest local priorities within dimension A, while B1 and B3 received substantially greater weights than the remaining sub-criteria within dimension B. within dimension C: Environmental and social sustainability, watershed and conservation constraints (C2) received the highest local weight at 27.24%, closely followed by Social Acceptability and Land Impact (C5) at 27.22%, Environmental assessment requirement (C3) at 25.76%, Ecological Impact (C1) at 10.73%, and beneficiary coverage (C4) at 9.06%. Within dimension D: economic performance, cost effectiveness (D2) received the highest local weight by a clear margin at 54.15%, followed by Economic Return (D3) at 19.61%, Long-Term Economic Value (D4) at 14.90%, and project cost (D1) at 11.34%. These findings demonstrate that conservation constraints and social acceptability were accorded comparable priority within Dimension C, while experts assigned greater significance to cost effectiveness than on overall project expenditure within Dimension D. The global priorities, calculated by multiplying each subcriterion's local weight by its parent-dimension weight, showed that cost effectiveness (D2) ranked first at 13.99%, followed by structural scale (B1) at 11.58%, foundation

suitability (B3) at 10.60%, and Storage and Hydrological Adequacy (A2) at 8.93%. Subsequent priorities comprised watershed and conservation constraints (C2) at 5.96%, social acceptability and Land Impact (C5) at 5.95%, and environmental assessment requirement (C3) at 5.63%. In contrast to local weights, global weights account for both a sub-criterion's relative significance within its parent dimension and the overarching importance of that dimension within the complete hierarchy, thereby establishing a unified basis for comparing and ranking all 18 sub-criteria across the framework (Caraveo Gomez Llanos *et al.*, 2024). Table 9 presents the calculated weights and rankings. The consistency assessment showed that both individual and group pairwise comparison matrices had CR values below the AHP acceptance threshold of 0.10 (Abastante *et al.*, 2019). The individual comparison matrices underlying this analysis had been checked for consistency within the present framework. The main-dimension group matrix had a $CR \approx 0.0009$, while those for Dimensions A and B were approximately $CR \approx 0.0022$ and 0.0007, respectively, indicating high internal coherence. Nevertheless, these exceptionally low CR values should be construed as indicators of the internal mathematical coherence of the derived pairwise relationships rather than as a measure of consensus among experts, given that the CR evaluates alignment solely within an individual comparison matrix rather than inter-expert agreement.

Interpretation and comparison

The analysis revealed differences in the relative importance of the four main dimensions, ranked in descending order as engineering and implementation feasibility (B), economic performance (D), environmental and social sustainability (C), and water resource and hydrological performance (A). Although water resource and hydrological performance (A) received the lowest relative weight among the four primary dimensions (19.71%), this outcome should not be construed as implying that hydrological performance lacks significance in water-resource projects. AHP weights represent relative priorities among the criteria considered within the decision structure rather than the absolute necessity of each dimension. The result indicates that, within the judgments of the present expert panel, engineering and implementation, economic, and environmental and social considerations received greater relative emphasis when the four dimensions were compared simultaneously. Moreover, storage and hydrological adequacy (A2) emerged as the fourth-highest global priority across all 18 sub-criteria at 8.93%, demonstrating that a specific hydrological factor retained substantial significance within the overarching priority architecture. To interpret this priority structure, the following discussion proceeds from the highest- to the lowest-weighted dimension, considering both main-dimension weights and local priorities within each dimension. This methodological strategy clarifies the rationale behind the emphasis assigned by experts to specific dimensions while isolating the underlying sub-criteria that govern those priorities, prior to evaluating the global priorities across all sub-criteria. The highest main-dimension weight assigned to engineering and implementation feasibility (B) indicates that water resources project priorities depend on both water demand and expected returns, as well as the ability to implement projects under engineering constraints and actual site conditions. Within this dimension, structural scale (B1) and foundation suitability (B3) attained the highest priority weights, underscoring their critical bearing on constructability, construction complexity, and implementation risk. This pattern aligns with existing literature on irrigation project prioritization and water infrastructure evaluation, which integrates technical feasibility and operational constraints alongside project benefits (Jafari *et al.*, 2026; Sandoval *et al.*, 2025). Technical and operational risks also play an

important role in prioritizing irrigation projects in Thailand (Chaitongrat *et al.*, 2026). Consequently, these findings reinforce the perspective that initiatives exhibiting substantial water resources or economic viability may not merit high priority when complex structural demands or challenging site conditions hinder execution (Al-Jabal and Al-Khafaji, 2025). The second-highest main-dimension weight assigned to Economic Performance (D) indicates that economic value remains an important consideration in water resources project prioritization, particularly when public budgets and investment resources are limited. Within this dimension, cost effectiveness attained the highest priority weight by a distinct margin at 54.15%, while project cost (D1) registered the lowest. This outcome indicates that experts placed greater emphasis on benefits or outputs relative to expenditure than on aggregate capital investment alone. This pattern is consistent with water infrastructure prioritization studies that use investment efficiency, cost–benefit relationships, and economic returns to support project selection under budget constraints (Macchiaroli *et al.*, 2023; Mochani *et al.*, 2025). Correspondingly, research on irrigation project prioritization underscores the evaluation of capital conversion efficiency—gauging how effectively investments translate into system-wide benefits, rather than relying solely on minimum-cost metrics cost alone (Jafari *et al.*, 2026; Sandoval *et al.*, 2025). These findings highlight cost effectiveness as a key link between budget constraints and the value of the outcomes a project can deliver. The weight assigned to Environmental and Social Sustainability (C), ranked third among the main dimensions, highlights the need to consider sustainability alongside engineering and economic feasibility in water resources project prioritization. Within this dimension, watershed and conservation constraints (C2) alongside Social Acceptability and Land Impact (C5) attained high and nearly equal weights, reflecting the critical significance of both environmental preservation and local stakeholder implications. This pattern is consistent with studies on sustainable water management and environmental decision support that integrate ecological constraints, community participation, and social acceptability into decision-making (Alfian *et al.*, 2026; Shahat *et al.*, 2026). Furthermore, research on water governance and environmental assessment also indicates that technically viable initiatives may encounter execution barriers when conservation impacts, land-use dynamics, and stakeholder concerns are insufficiently addressed (Asadi and Alibaygi, 2026; Chayakul *et al.*, 2026; Jafari *et al.*, 2026). These findings suggest that environmental and social considerations are integral to the project prioritization framework, rather than supplementary issues addressed only at a later stage. Although water resource and hydrological performance (A) recorded the lowest relative weight among the primary dimensions, this outcome should not be construed as implying that hydrological performance lacks significance in water resources development. AHP weights represent relative priorities derived from comparisons across multiple dimensions within a common hierarchy. Within dimension A, storage and hydrological adequacy (A2) received the highest local weight at 45.32% and ranked fourth globally among all sub-criteria, highlighting the continued importance of adequate storage and compatibility with hydrological conditions to project viability. Studies on alternative water resources, sustainable water management, and dam site selection similarly recognize water availability, storage capacity, and hydrological suitability as core fundamental considerations in project evaluation (Konstadinos *et al.*, 2025; Pham *et al.*, 2026; Shams *et al.*, 2025). These findings therefore reflect trade-offs between hydrological adequacy and engineering, economic, environmental, and social constraints, rather than a diminished role for hydrological factors in decision-making (Sandoval *et al.*, 2025). Contrasting these results with alternative AHP and MCDM studies in water resources management

demonstrates that criterion weights fluctuate depending on the decision-making environment, stakeholder composition, and specific characteristics of the problem under study. Cross-country assessments of alternative water resources have found substantial differences in relative priorities across locations, even when similar assessment frameworks are used (Pham *et al.*, 2026). Studies on sustainable water management and irrigation project prioritization likewise report variations in weights associated with resource constraints, project objectives, and expert perspectives (Konstadinos *et al.*, 2025; Sandoval *et al.*, 2025). Similarly, research on flood management, environmental assessment, and water governance indicators shows that stakeholder preferences and institutional context influence the priority structures derived through MCDM (Alfian *et al.*, 2026; Asadi and Alibaygi, 2026; Jafari *et al.*, 2026). Consequently, the weights derived from this study must be construed as a context-sensitive priority configuration, rather than universal values applicable across all geographic settings. Their interpretation requires accounting for localized conditions and the composition of the expert panel, precluding any treatment of the weights in isolation from the specific decision-making environment (Zeki *et al.*, 2026).

Global priority concentration and two-tier priority interpretation

Two complementary views were used to interpret the concentration of global criterion weights. First, the ranked weights showed a visible break after the fourth-ranked subcriterion. The four highest-weighted sub-criteria—cost effectiveness, structural scale (B1), foundation suitability (B3), and storage and hydrological adequacy (A2)—accounted for 45.10% of the total global weight. This categorization is treated as a descriptive high-priority cluster derived from the observed weight distribution rather than as a statistically defined threshold. Second, a cumulative 80% priority threshold was implemented to determine how many ranked sub-criteria comprised the majority of the aggregate weight. The cumulative threshold surpassed 80% at the eleventh-ranked subcriterion, with the leading 11 elements accounting for 81.88% of the total weight. Serving strictly as a descriptive prioritization aid, this benchmark should not be equated with the classical 80/20 rule. Although global ranking establishes the relative order of sub-criteria within a common framework, ranks alone do not fully capture the concentration of priority weights. To examine this distribution, the global weights of all 18 sub-criteria were ordered from highest to lowest, and both individual and cumulative weights were assessed. This methodological strategy isolates the criteria exerting the most pronounced influence on the decision, alongside the broader subset responsible for a substantial portion of the aggregate weight. Cumulative thresholds have previously been used with AHP to identify key factors and support prioritization and screening (Tochaiwat *et al.*, 2023). Concepts related to natural breaks, clustering, and data-driven classification also suggest that grouping can be informed by patterns and changes in the data, alongside predefined thresholds (Lv *et al.*, 2025; Xu *et al.*, 2018). The distribution of global weights showed that cost effectiveness ranked first at 13.99%, followed by structural scale (B1) at 11.58%, foundation suitability (B3) at 10.60%, and Storage and hydrological adequacy (A2) at 8.93%. Collectively, these four criteria represent a cumulative weight of 45.10%. Individual weights declined noticeably after the fourth rank: watershed and conservation constraints (C2) occupy the fifth position with a weight of 5.96%, whereas the remaining subsequent criteria predominantly cluster within the 2% to 6% range. This visible break in the ranked distribution provided the basis for identifying D2, B1, B3, and A2 as the dominant priority cluster. Rather than establishing a theoretical threshold at 45.10%, this interpretation relies on the observed shifts in individual criterion contributions to cumulative

weight. Consequently, this approach isolates the specific cluster of factors exerting the most substantial influence on the overarching priority structure. Focusing on highly weighted criteria is also consistent with other applications of AHP-based prioritization, which use top-ranked items to guide the allocation of attention and resources (Chang *et al.*, 2025). However, the dominant cluster alone may not capture the full breadth of the decision structure. Adopting an 80% cumulative threshold as an analytical screening benchmark in accordance with Pareto-based prioritization principles (Tochaiwat *et al.*, 2023), showed that cumulative weight exceeded 80% at the eleventh rank. The top 11 sub-criteria: D2, B1, B3, A2, C2, C5, C3, A1, D3, B2, and D4, accounted for 81.88% of the total weight. This comprehensive priority set subsumes four primary dimensions: engineering and implementation feasibility, economic performance, environmental and social sustainability, and water resource and hydrological performance. Consequently, while the dominant cluster primarily concentrates on economic factors, engineering feasibility, and hydrological adequacy, capturing approximately 80% of the aggregate priority weight, achieving this threshold concurrently necessitates the incorporation of environmental and social considerations. As shown in Fig. 4, the broader priority set includes key elements from all four main dimensions rather than being concentrated in a single dimension. Although the highest global weights emphasize cost effectiveness and engineering feasibility, extending the assessment to cover a substantial share of cumulative priority highlights the continued importance of hydrological adequacy and environmental and social considerations. These findings underscore the multidimensional complexity of project prioritization, demonstrating that relying exclusively on economic or engineering criteria fails to adequately capture the comprehensive scope of determinants driving the overarching decision-making process. The distribution of global weights supports a two-tier priority interpretation for decision-making. Tier 1 comprises the sub-criteria that exert the greatest influence on the overall priority structure and can serve as an initial focus for rapid screening or preliminary project review. Tier 2 expands the evaluative scope by incorporating a more exhaustive array of critical parameters tailored for comparative assessment and portfolio-level prioritization. Using both tiers help balance efficiency in the decision-making process with adequate coverage of the key factors in the MCDM framework, without implying that lower-ranked criteria are irrelevant to project assessment.

Decision implications, applicability and methodological considerations

The findings facilitate water resources project prioritization by systematically structuring multidimensional decision parameters within a unified analytical framework. This structure enables the relative importance of engineering feasibility, economic performance, environmental and social sustainability, and hydrological performance to be considered systematically. When integrated with project-level performance data and a suitable operational scoring protocol, the resulting criterion-weighting architecture can effectively facilitate subsequent project screening, portfolio comparison, budgetary prioritization, and resource allocation. The framework serves as a decision-support structure that complements existing project appraisal and planning processes rather than replacing the technical, environmental, or economic appraisal of individual projects. At the project level, the AHP priority weights can provide a common weighting structure for comparing multiple projects using the same criteria. Each project would receive project-specific performance scores based on quantitative and qualitative data related to the 18 sub-criteria. Scoring scales for quantitative metrics, including project cost, cost per unit of benefit, storage capacity, irrigated area, and beneficiary coverage, can be systematically

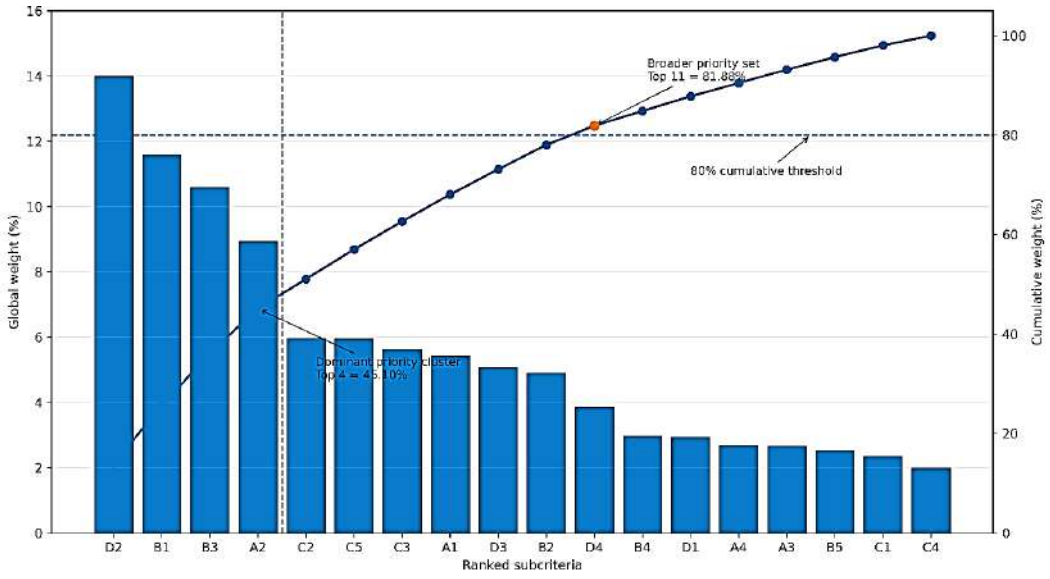

Fig. 4: Ranked global weights of the 18 sub-criteria (bars) and their cumulative weights (line)

derived from empirical measurements. Qualitative criteria, such as foundation suitability, environmental constraints, and social acceptability, can be converted into scores using transparent assessment standards. The integration of these performance scores with the global weights yields composite produce weighted project scores, thereby establishing a robust basis for comparative evaluation and portfolio-level prioritization. The AHP-derived weight of a criterion represents its relative importance in the decision structure and should not be interpreted as the performance score of a project on that criterion. Consequently, the present study does not pursue project-level ranking or empirical validation across a set of alternatives options. Such validation necessitates both project-specific performance data and a systematic operational scoring procedure capable of integrating these metrics with the established criterion weights. Applying the framework to actual project portfolios therefore represents a subsequent stage of evaluation rather than part of the present criterion-weighting analysis. The next step in applying the framework is therefore to develop an operational scoring rubric that links each subcriterion to measurable indicators, scoring scales, and decision thresholds appropriate to the intended context. Regarding practical applicability, the framework, comprising four primary dimensions and 18 sub-criteria, offers a highly transferable decision structure for alternative water resources project prioritization contexts, as it comprehensively encompasses hydrological performance, technical feasibility, socio-environmental sustainability, and economic viability. However, the priority weights obtained in this study should be treated as context-dependent parameters reflecting the characteristics of the study area and the expert judgments used in the analysis. Furthermore, the derived weights must be interpreted within the context of the expert panel composition. While the participants provided seasoned professional insights relevant to water-resource project evaluation, the resulting weights distribution does not necessarily capture the preferences of broader stakeholder cohorts, such as local communities, project beneficiaries, or decision makers operating under different institutional frameworks. Accordingly, applications to other locations or project types should retain or adapt the hierarchical structure as

appropriate while recalibrating criterion weights, scoring scales, and decision thresholds to reflect the relevant stakeholder composition, local priorities, project characteristics, and planning objectives. From a methodological perspective, the AHP weights were elicited from the expert judgments of six specialists possessing extensive, practical experience in water resources and irrigation project planning. In expert-based AHP, panel suitability depends primarily on domain expertise and relevance to the decision problem, rather than statistical representativeness as required in general population surveys (Caraveo Gomez Llanos *et al.*, 2024; Zeki *et al.*, 2026). Consequently, the reported priority weights should be understood as a derived, expert-informed hierarchy that systematically aggregates subjective judgments within the specific criteria framework and operational decision context established in this study. Future research should operationalize the framework for direct application to project portfolios by developing a scoring rubric that links each subcriterion to measurable indicators and by testing the sensitivity and robustness of the results under different weighting assumptions. Comparisons with alternative MCDM methods and applications to portfolios containing larger numbers of projects would also help assess the framework's stability and practical applicability across a wider range of decision settings. The present study employs the AHP as the weighting methodology. This approach is selected because its multi-tiered architecture seamlessly mirrors the structural organization of the four dimensions and 18 sub-criteria, thereby facilitating the derivation of robust criterion weights via structured pairwise comparisons. Other multi-criteria decision-making approaches, such as the Best–Worst Method, Technique for Order Preference by Similarity to Ideal Solution, or Preference Ranking Organization Method for Enrichment Evaluation, involve different elicitation or decision-aggregation procedures and could provide complementary perspectives. A formal cross-method comparison was beyond the analytical scope of the present study; however, future applications could examine whether alternative weighting or ranking methods produce comparable priority structures. Several methodological considerations should be recognized when interpreting the results. First, the criterion weights were elicited from a limited, purposively selected panel of senior experts; consequently, they encapsulate the specific professional and institutional perspectives inherent to this cohort rather than broad population-level or universally generalizable preferences. Second, although individual expert results reveal variation in priority structures, the reliance on expert judgment remains inherently context-dependent, and the consistency ratio evaluates internal judgment consistency rather than agreement among experts. Third, the derived weights were not empirically validated through application to actual project alternatives utilizing project-level performance data. Finally, the study omitted formal methodological stress-testing, such as perturbation-based sensitivity analysis, leave-one-expert-out evaluation, alternative aggregation testing, and ranking-stability verification. These considerations should therefore be taken into account when interpreting and transferring the derived priority structure to other project, stakeholder, or decision contexts.

CONCLUSION

This study developed an analytic hierarchy process-based framework for structuring assessment criteria and determining their relative importance in water resources project prioritization. The framework integrates four main dimensions and 18 sub-criteria covering hydrological performance, engineering and implementation feasibility, environmental and social sustainability, and economic performance. Analysis of judgments from six experienced professionals in the Chiang Mai context produced a common weighting structure for these diverse considerations. Consequently, this study establishes a foundational architecture for

subsequent project evaluations, with its empirical findings determining criterion-specific priorities rather than individual project rankings. Engineering and implementation feasibility received the highest aggregate dimension weight (32.58%), followed sequentially by economic performance (25.84%), environmental and social sustainability (21.87%), and water resource and hydrological performance (19.71%). These priorities indicate that the panel placed particular emphasis on whether projects could be implemented under actual engineering and site constraints. At the subcriterion level, cost effectiveness had the highest global weight (13.99%), followed by structural scale (11.58%), foundation suitability (10.60%), and storage and hydrological adequacy (8.93%). Collectively, these findings indicate that investment efficiency, construction requirements, and the relationship between storage and water supply constitute pivotal considerations within the evaluated decision-making framework. The cumulative-weight analysis provided a complementary interpretation of the priority structure. The four highest-ranked sub-criteria accounted for 45.10% of total weight, identifying a concentrated group of influential factors. Extending the evaluation scope to encompass the top 11 sub-criteria accounts for 81.88% of the cumulative weight while successfully integrating all four primary dimensions. This expanded configuration demonstrates that socio-environmental factors remain fundamentally integral when capturing a substantial proportion of the aggregate priority weight. The two-tier interpretation can guide the initial focus and subsequent breadth of assessment. However, it does not justify excluding lower-ranked criteria or overriding mandatory environmental and regulatory requirements. The principal contribution is the organization of heterogeneous project considerations into an explicit hierarchy with context-specific priorities. Potential applications include project screening, portfolio comparison, and budget prioritization. These applications necessitate project-level performance data, transparent scoring mechanisms, and the appropriate normalization of indicators wherein higher values denote either positive benefits or operational constraints. The framework should therefore complement established technical, environmental, and economic appraisal procedures. Several limitations define the interpretation and transferability of the findings. The assigned weights capture the subjective evaluations of a limited expert panel within the specific decision framework investigated in this study. Their applicability to other stakeholder groups, locations, and project types remains to be assessed. Low consistency ratios indicate internal mathematical coherence of the comparison matrices; they do not establish agreement among experts or predictive validity. Subsequent investigations should focus on formulating an operational scoring rubric, evaluating model sensitivity to expert panel composition and weighting assumptions, and benchmarking outcomes against alternative decision-making methodologies. Applications to diverse project portfolios are also needed to assess ranking stability and practical usefulness. These steps would strengthen the evidence for using the framework in operational water resources planning.

AUTHOR CONTRIBUTIONS

O. Gorbunov was responsible for data curation, formal analysis, and implementation of the AHP analysis. C. Sinsabvarodom conducted validation of the initial results and contributed to critical review of the manuscript. D. Rinchumphu provided project supervision, strategic guidance, and critical revision of the manuscript. P. Sangunsri contributed to the local data recuitement and interpretation of the results. N. Phichetkunbodee contributed to methodological review, interpretation of the analytical results, and critical review of the manuscript. All authors reviewed and approved the final manuscript.

ACKNOWLEDGEMENT

This study was supported by the Presidential Scholarship Ph.D., Program, Chiang Mai University [660651034]. The authors are also thankful for the support from City Research and Development Center, Faculty of Engineering, Chiang Mai University.

CONFLICT OF INTEREST

The authors declare that there is no conflict of interests regarding the publication of this manuscript. In addition, the ethical issues, including plagiarism, informed consent, misconduct, data fabrication and/or falsification, double publication and/or submission, and redundancy have been completely observed by the authors.

OPEN ACCESS

©2027 The author(s). This article is licensed under a Creative Commons Attribution 4.0 International License, which permits use, sharing, adaptation, distribution and reproduction in any medium or format, as long as you give appropriate credit to the original author(s) and the source, provide a link to the Creative Commons license, and indicate if changes were made. The images or other third-party material in this article are included in the article's Creative Commons license, unless indicated otherwise in a credit line to the material. If material is not included in the article's Creative Commons license and your intended use is not permitted by statutory regulation or exceeds the permitted use, you will need to obtain permission directly from the copyright holder. To view a copy of this license, visit: http://creativecommons.org/licenses/by/4.0/

PUBLISHER'S NOTE

GJESM Publisher remains neutral with regard to jurisdictional claims in published maps and institutional affiliations.

POSITIVE AI STATEMENT

During the preparation of this work the author(s) have used Artificial Intelligence (AI) ChatGPT Plus in order to correct English sentences. After using this tool/service, the authors reviewed and edited the content as needed and took full responsibility for the content of the publication.

ABBREVIATIONS

%	Percent
λ_{max}	Maximum eigenvalue of the comparison matrix
A	Water resource and hydrological performance
A1	Water availability
A2	Storage and hydrological adequacy
A3	Irrigation water need
A4	Irrigation service potential
AHP	Analytic hierarchy process
a_{ij}	Pairwise comparison value for criterion i relative to criterion j
$a_{ij}^{(k)}$	Pairwise comparison value provided by expert k
$\bar{a}_{ij}$	Geometric mean of the experts' pairwise comparison values
B	Engineering and implementation feasibility
B1	Structural scale
B2	Earthwork requirement
B3	Foundation suitability
B4	Site accessibility
B5	Implementation duration
BCR	Benefit–cost ratio
C	Environmental and social sustainability
C1	Ecological impact
C2	Watershed and conservation constraints
C3	Environmental assessment requirement
C4	Beneficiary coverage
C5	Social acceptability and land impact
CI	Consistency index
CR	Consistency ratio
D	Economic performance
D1	Project cost

D2	Cost effectiveness
D3	Economic return
D4	Long-term economic value
E1–E6	Expert identifiers 1–6
GW_i	Global weight of subcriterion i
ha	Hectare
i	Subcriterion or criterion index, as applicable
j	Criterion or parent-dimension index, as applicable
k	Expert index
km	Kilometer
LW_i	Local weight of subcriterion i
m	Meter when used as a unit; number of experts in the aggregation equation
MCDA	Multi-criteria decision analysis
MCDM	Multi-criteria decision-making
Mm^3	Million cubic meter
Mm^3/y	Million cubic meter per year
million USD	Million United States dollars
mm	Millimeter
mm/year	Millimeter per year
m^3	Cubic meter
m^3/s	Cubic meter per second
$m^3/year$	Cubic meter per year
n	Number of criteria in a comparison matrix
NPV	Net present value
PW_j	Priority weight of parent dimension j
RI	Random index
USD	United States Dollar
USD/ha	United States dollars per hectare of irrigated area
USD/m^3	United States dollars per cubic meter of water volume

REFERENCES

Abastante, F.; Corrente, S.; Greco, S.; Ishizaka, A.; Lami, I.M., (2019). A new parsimonious AHP methodology: Assigning priorities to many objects by comparing pairwise few reference objects. Expert Syst. Appl., 127: 109-120 **(12 Pages)**.

Al-Jabal, Z.M.; Al-Khafaji, M.S., (2025). SWOT and AHP-based analysis of the reality of irrigation projects' water conveyance systems in Iraq. Civil Environ. Eng., 21(1): 643-670 **(28 Pages)**.

Alfian, D.; Meilianda, E.; Achmad, A.; Syukri, M., (2026). Integrating hydrodynamic modeling and multi-criteria decision support for flood risk management in coastal systems. Global J. Environ. Sci. Manage., 12(3): 1287-1310 **(24 Pages)**.

Asadi, S.; Alibaygi, A., (2026). Revolutionizing local water governance indicators: A combined Fuzzy Delphi and AHP methodological framework. Environ. Sustainability Indic., 31: 101306 **(13 Pages)**.

Caraveo Gomez Llanos, A.F.; Vijaya, A.; Wicaksono, H., (2024). Rating ESG key performance indicators in the airline industry. Environ. Dev. Sustainability. 26(11): 27629-27653 **(25 Pages)**.

Chaitongrat, T.; Kusonkhum, W.; Yuwanasiri, C.; Wiriyaphanit, E.; Lumlerdvoravith, I.; Pang, D., (2026). Clustering and machine learning-based risk prioritization for irrigation construction projects in Thailand. Irrig. Drain., 1-16 **(16 Pages)**.

Chang, J.; Kim, H.; Lalonde, R.; Doraisamy, E.; Vargo, J., (2025). Fuzzy Analytical Hierarchy Process-based Risk Priority Number Approach in Failure Modes and Effects Analysis for Magnetic Resonance Imaging-guided High-dose-rate Brachytherapy for Gynecologic Cancer. Adv. Radiat. Oncol., 10(4): 101731 **(10 Pages)**.

Chayakul, J.; Veldwisch, G.J.; Bruins, B.; Boelens, R., (2026). Scales and sustainability: The politics of riverine landscape governance in Chiang Mai, Thailand. Water. 18(9): 1049 **(28 Pages)**.

Demir, S.; Dilman Gokkaya, M.; Ersoz, N.D., (2025). Prioritization blue-green infrastructure strategies: Developing a hybrid quantitative approach model for sustainable urban water management. Water Resour. Manage., 39(8): 3901-3919 **(19 Pages)**.

Gebre, S.L.; Cattrysse, D.; Van Orshoven, J., (2021). Multi-criteria decision-making methods to address water allocation problems: A systematic review. Water, 13(2): 125 **(28 Pages)**.

Gu, Z.; Phakdimek, S.; Nagami, K.; Komori, D., (2025). Relationship between urbanization-induced land use changes and flood risk: Case study in Chiang Mai, Thailand. Water. 17(3): 327 **(20 Pages)**.

Jafari, M.; Soltani, J.; Shahdany Hashemy, S.M.; Monem, M.J.; Vasheghani Farahani, E.; Tork, H., (2026). Environmental analysis within a multi-criteria evaluation of agricultural water distribution system modernization strategies. Environ. Model. Assess., 31(2): 361-382 **(22 Pages)**.

Kaewwichian, P.; Prapaporn, W.; Nachaisit, P.; Charmongkolpradit, S.; Prasanchum, H.; Chaipanha, W.; Auttha, W.; Duangsa, B., (2025). The adaptive hybrid MCDA for land use prioritization: Case study dry port size analysis. Eng. Access, 12(1): 86-98 **(13 Pages)**.

Konstadinos, M.; Pantazis, G.; Dimitra, L.C.; Christos, M.; Stefanos, N.A.; Giovanna, S.; Mantent, K.J.; Joseph, A.-D., Adombilla, R., (2025). Assessing sustainable water management in a resource-scarce environment (Ghana, West Africa) via the Analytic Hierarchy Process. Agric. Water Manage., 313: 109497 **(8 Pages)**.

Lamichhane, S.; Bista, S.; Khatri, D.; Devkota, N.; Karki, N.; Dawadi, S.; Pradhan, A.M.S., (2025). Application of a multi-criteria decision-making technique to prioritize the irrigation projects in southern Nepal. H_2Open J., 8(3): 100-114 **(15 Pages)**.

Li, J. (2023). Land suitability analysis of urban agriculture for different investment scenarios: Evidence from Fuzhou of China. Heliyon, 9(10): e20817 **(15 Pages)**.

Lv, X.; Lin, H.; Chen, Z., (2025). Prevention and control strategies for rainwater and flood disasters in traditional villages: A concentrated contiguous zone approach. Buildings. 15: 1335 **(17 Pages)**.

Macchiaroli, M.; Dolores, L.; De Mare, G., (2023). Multicriteria decision making and water infrastructure: An application of the Analytic Hierarchy Process for a sustainable ranking of investments. Appl. Sci., 13(14): 8284 **(23 Pages)**.

Meskine, A.; Cherif, E.A.; Zerouali, B.; Ouadja, A.; Santos, C.A.G.; Bailek, N.; Bouznad, I.E.; Baba, A., (2025). Decision-support approaches for sustainable water resource management in northwest Algeria [journal article]. J. Ecol. Eng., 26(7): 24-43 **(20 Pages)**.

Min, V.; Panuwatwanich, K.; Matsumoto, K., (2025). Evaluating key attributes for enhancing contractors' performance in construction waste management: A Multi-Criteria Decision Analysis using the Best Worst Method. Int. J. Constr. Manage., 25(16): 1968-1981 **(14 Pages)**.

Mochani, M.M.; Moridi, A.; Tehrani, M.D.; Khalili, R.; Haghighi, A.T., (2025). Site selection and investment prioritization for small hydropower plants using spatial multi-criteria decision-making models. Water Resour. Manage., 39(13): 6985-7004 **(20 Pages)**.

Pham, N.L.; Su, Y.; Lee, H.-J.; Huh, S.-Y., (2026). Prioritising development criteria for alternative water resources: A comparative AHP analysis of South Korea and Vietnam. Sustainable Water Resour. Manage., 12(2): 21 **(12 Pages)**.

Sandoval, A.; Requelme, N.; Cachipuendo, C., (2025). Multi-criteria decision making (MCDM) methodology for the prioritization of technical irrigation projects. Water Policy. 27(8): 804-822 **(19 Pages)**.

Sangunsri, P. (2022). Application of analytic hierarchy process to select water resource development projects: A case study of Rai Dong village. Faculty of Engineering, Chiang Mai University. Chiang Mai, Thailand. **(122 Pages)**.

Shahat, M.A.A.; Sayed, D.S.; Qorqor, M.M.; Abdel Hamed, H.N., (2026). An integrated framework for sustainable natural resources management in freshwater lakes. Global J. Environ. Sci. Manage., 12(4): 2061-2086 **(26 Pages)**.

Shams, E.M.M.; Sawires, R.; Tawfik, S.N.E.; Youssef, H.R.; Kishida, T., (2025). Optimal sites for rainwater harvesting and proposed dams: A geospatial and analytic hierarchy process-based feasibility study in Western Saudi Arabia. J. Hydrol. Reg. Stud., 62: 102782 **(21 Pages)**.

Solaimanian, S. (2025). Environmental risk assessment of concrete construction projects in developing countries based on Analytical Hierarchy Process method. Green Technol. Sustain., 3(3): 100178 **(10 Pages)**.

Tochaiwat, K.; Rinchumphu, D.; Thumvisuttivarakorn, V., (2023). Measuring influences of residence decision to buy factors by Modified Analytical Hierarchy Process. ABAC J., 43(2): 161-175 **(15 Pages)**.

Wu, W.; Eamen, L.; Dandy, G.; Maier, H.R.; Razavi, S.; Kwakkel, J.; Huang, J.; Kuczera, G., (2025). Beyond the traditional paradigm of water resources management: scenario thinking to address deep uncertainty. J. Hydrol., 661: 133547 **(9 Pages)**.

Xu, H.; Ma, C.; Lian, J.; Xu, K.; Chaima, E., (2018). Urban flooding risk assessment based on an integrated k-means cluster algorithm and improved entropy weight method in the region of Haikou, China. J. Hydrol., 563: 975-986 **(12 Pages)**.

Zeki, M.; Zeki, Ö.; Güner, P.; Kang, H.; Ozkaynak, M., (2026). Scenario-based sample-size requirements for stable hierarchical AHP rankings: A computational simulation and empirically anchored framework. Oper. Res. Perspect., 17: 100408 **(20 Pages)**.

AUTHOR (S) BIOSKETCHES

Gorbunov, O., Ph.D. Candidate, Department of Civil Engineering, Chiang Mai University, Thailand.
- Email: *oleg_gorbunov@cmu.ac.th*
- ORCID: 0009-0006-3899-5228
- Web of Science ResearcherID: NA
- Scopus Author ID: 60102518500
- Homepage: https://urbanintelligence.eng.cmu.ac.th/graduate-students/oleg-gorbunov/

Sinsabvarodom, C., Ph.D., Assistant Professor, Department of Civil Engineering, Chiang Mai University, Thailand.
- Email: *chana.sinsabvarodom@cmu.ac.th*
- ORCID: 0000-0002-1860-4860
- Web of Science ResearcherID: NA
- Scopus Author ID: 56461314900
- Homepage: https://urbanintelligence.eng.cmu.ac.th/experts/urban-resilience-experts/chana-sinsabvarodom/

Rinchumphu, D., Ph.D., Associate Professor, Department of Civil Engineering, Chiang Mai University, Thailand.
- Email: *damrongsak.r@cmu.ac.th*
- ORCID: 0000-0002-6037-4974
- Web of Science ResearcherID: IUN-3065-2023
- Scopus Author ID: 57219602276
- Homepage: https://urbanintelligence.eng.cmu.ac.th/experts/urban-management-experts/damrongsak-rinchumphu/

Sangunsri, P., Civil Engineer, Lamphun Irrigation Project, Office of Regional Irrigation 1, Ministry of Agriculture and Cooperatives, Thailand
- Email: *piyapon_san@rid.go.th*
- ORCID: 0009-0002-1700-2523
- Web of Science ResearcherID: NA
- Scopus Author ID: NA
- Homepage: https://www.lamphunrid.com/main.php

Phichetkunbodee, N., Ph.D. Candidate, Department of Civil Engineering, National Taiwan University, Taiwan.
- Email: *d11521023@ntu.edu.tw*
- ORCID: 0000-0003-4569-669X
- Web of Science ResearcherID: NA
- Scopus Author ID: 57222813126
- Homepage: https://www.ce.ntu.edu.tw/en/home/

HOW TO CITE THIS ARTICLE:
Gorbunov, O.; Sinsabvarodom, C.; Rinchumphu, D.; Sangunsri, P.; Phichetkunbodee, N., (2027). Analytic hierarchy process-based criterion weighting for water resources management projects. Global J. Environ. Sci. Manage., 13(1): 347-368.

DOI: 10.22034/gjesm.2027.01.16
URL: https://www.gjesm.net/article_736229.html

Global Journal of Environmental Science and Management
(GJESM)

Homepage: https://www.gjesm.net/

Podcasts

ORIGINAL RESEARCH ARTICLE

Temporal water-quality variability and its implications for environmental management of sand lobster aquaculture

I.N.P. Winata[1,2], I.M. Radjawane[1,*], S. Nurdjaman[1], I.N. Radiarta[3], D. Sidik[2], Deby[2], S.K. Pratiwi[2], S. Makmur[4], A.A. Utama[4], A. Suman[4], Husnah[4]

[1]Faculty of Earth Sciences and Technology, Bandung Institute of Technology, Bandung, Indonesia

[2]Directorate of Venture Capital Management, Ministry of Marine Affairs and Fisheries, Jakarta Pusat, Indonesia

[3]Agency for Marine and Fisheries Extension and Human Resources Development, Jakarta, Indonesia

[4]Research Center for Biota System, Research Organization for Life Science and Environment, National Research and Innovation Agency, West Java, Indonesia

ARTICLE INFO

Article History:
Received 15 May 2026
Revised 19 August 2026
Accepted 21 September 2026

Keywords:
Adaptive aquaculture management
Biomanagement
Environmental monitoring architecture
Oceanographic variability
Panulirus Homarus
Sustainable aquaculture

DOI:10. 22034.gjesm.2027.01.17

ABSTRACT

BACKGROUND AND OBJECTIVES: Sustainable management of sand lobster aquaculture is often limited by monitoring approaches that summarize environmental conditions using long-term averages, obscuring short-term extremes and spatial variation. The study objectives were to characterize spatial and temporal variations in water quality within a floating net cage aquaculture system, identify their underlying physical drivers, evaluate whether longitudinal growth is governed more by culture duration, initial size, and stocking density than by environmental exposure alone, and translate these empirical relationships into a transferable environmental monitoring framework.
METHODS: The study collected longitudinal growth and environmental data from floating net cage culture in Indonesia. Monitoring covered temperature, salinity, oxygen concentration, potential of hydrogen, and nutrient concentrations across three water depths and multiple sampling times. Non-parametric statistical tests were employed to evaluate depth-dependent variations in dissolved oxygen, while correlation and regression analysis assessed the relationships between wind speed, water temperature, and dissolved oxygen levels. Multivariate statistical ordination summarized dominant environmental gradients, and mixed-effects statistical models, compared through an information-theoretic model selection approach, captured longitudinal growth.
FINDINGS: Dissolved oxygen concentration differed significantly among depths (test statistic 29.27, probability below 0.001), declining by close to a fifth from the surface to three and ten meters. Monthly wind speed closely tracked the concurrent decline in temperature closely (correlation coefficient -0.988, probability below 0.002) but exhibited no statistically significant association with dissolved oxygen, consistent with a wind-driven transition observed during this production cycle. Culture duration, initial size class, and stocking density together explained total length best, with an additive model carrying more than seventy percent of the statistical weight among six candidate models. Growth rate exhibited its strongest association with low-oxygen exposure, followed by temperature and potential of hydrogen condition, an interpretation that warrants caution given the limited independent exposure intervals available.
CONCLUSION: Successful sand lobster aquaculture requires an adaptive environmental monitoring architecture that accounts for depth-related oxygen stratification and wind-driven seasonal variability, alongside coordinated management of culture duration, initial seed size, and stocking density. The analytical framework of integrated site assessment and management for lobster can be adapted to other marine aquaculture systems through the inclusion of species-specific biological indicators and management variables.

This is an open access article under the CC BY license (http://creativecommons.org/licenses/by/4.0/)

NUMBER OF REFERENCES	NUMBER OF FIGURES	NUMBER OF TABLES
54	7	2

*Corresponding Author:
Email: ivonne.mradjawane@gmail.com
Phone: +6281 2214 7833
ORCID: 0000-0002-8116-3180

INTRODUCTION

Marine aquaculture has become one of the fastest-growing food-production sectors worldwide, playing an increasingly important role in food security, coastal livelihoods, and blue-economy development as capture fisheries face pressure from overexploitation and environmental degradation (Norman *et al*., 2019; Mair *et al*., 2023). Among high-value marine commodities, the scalloped or sand spiny lobster, *Panulirus homarus*, has drawn substantial interest owing to its exceptional market value and promising potential for aquaculture expansion (Zhou *et al*., 2026; Minjoyo *et al*., 2024). Because physiological performance, molting, and survival are heavily governed by environmental parameters such as temperature, salinity, dissolved oxygen (DO), and potential of hydrogen (pH) (Vidya and Joseph, 2012; Minjoyo *et al*., 2024); site suitability for lobster aquaculture must be evaluated as a dynamic production challenge rather than a static environmental classification. Conventional aquaculture site-selection approaches commonly assess physicochemical, spatial, and infrastructural variables against species-specific suitability criteria using Geographic Information System (GIS), remote sensing, and multi-criteria decision analysis (Porporato *et al*., 2020; Jayanthi *et al*., 2022). However, these approaches primarily establish environmental or spatial suitability without guaranteeing that a site will achieve favorable biological performance under a specific combination of stocking, feeding, and culture duration, as growth and survival can vary substantially even where ambient environmental conditions are broadly favorable (Kulmiye and Mavuti, 2005; Adiyana *et al*., 2020; Minjoyo *et al*., 2024). An additional drawback of conventional suitability assessments is their reliance on long-term environmental averages, which can mask critical short-term fluctuations and extreme events of ecological significance. Recent integrated water-quality monitoring research has similarly emphasized that conventional manual and stationary monitoring can provide inadequate spatial and temporal resolution, whereas stratified and multi-location monitoring can better resolve depth-dependent and short-term water-quality variation (Wahyono *et al.,* 2026). High-frequency observations from aquaculture sites have shown that DO can vary markedly among seasons and even among cages within the same site (Jeong *et al*., 2024; Breitburg *et al*., 2015), and marine organisms may experience environmental extremes that differ substantially from long-term means (Kroeker *et al*., 2023). This pattern is not limited to temperate systems: a seasonal water-quality assessment of a floating-net-cage site in Pegametan Bay, Bali found DO ranging from 2.6–9.1 milligrams per liter (mg/L) in the dry season versus 3.4–7.7 mg/L in the wet season (Ariadji *et al*., 2024), a spread a single seasonal average would not reveal. Consequently, in longitudinal studies, environmental conditions ought to be characterized as temporally aligned exposure variables rather than relied upon as isolated single-point or averaged measurements. Discrete-time monitoring at fixed depths and sampling occasions, rather than continuous logging, is a common and accepted practice in aquaculture water-quality monitoring (Jeong *et al*., 2024), and depth-resolved profiling of the water column is similarly an established approach for characterizing the vertical DOD structure relevant to cage aquaculture (Oldham *et al.,* 2018). Aside from temporal averaging, environmental parameters often exhibit systematic fluctuations driven by seasonal-scale physical processes. Tidal currents and rainfall-driven discharge are also recognized as important physical drivers of stratification and oxygen dynamics in tropical coastal systems (Lee *et al.,* 2020), though not directly measured here, consistent with prior studies evaluating a single physical driver as a tractable indicator of broader forcing (Soeyanto *et al.,* 2026). In semi-enclosed tropical coastal waters, seasonal wind forcing is a primary control

on circulation, stratification, and oxygen dynamics; a recent study of Jakarta Bay, Indonesia demonstrated a significant wind–transport correlation ($r > 0.5$, $p < 0.01$) supporting an early-warning framework for hypoxia at bay scale (Soeyanto *et al*., 2026). Vertical DO heterogeneity within cage culture systems is well established for pelagic finfish, with larger and deeper enclosures consistently exhibiting lower oxygen saturation than shallower counterparts (Oldham *et al*., 2018). For *P. homarus* specifically, depth-related effects have already been reported in Indonesia: a comparison of sub-mersible cages at 6 m and 8 m in Kepulauan Seribu found no depth effect on immune indicators (Wahjuningrum *et al*., 2022), while a grow-out trial in Pangandaran reported markedly better feed conversion at 5 m than at shallower depths, attributed to greater thermal and oxygen stability (Sarkar *et al*., 2026). However, the intra-water column oxygen-exposure gradient and its direct relationship with with growth performance rather than immune or feed-conversion endpoints, have not yet been quantified for this species. Accordingly, this study establishes the lobster integrated site assessment and management (LISAM) architecture, as a protocol for aligning depth-resolved, physically indexed environmental monitoring with species-specific biological responses to support adaptive management at operating aquaculture facilities. Conceptually, this architecture is built on the premise that environmentally favorable sites do not automatically ensure optimal production, and that sustainable aquaculture planning must synthesize environmental traits, biological performance, operational constraints, and managerial decisions (Jayanthi *et al*., 2022; Mair *et al*., 2023; Zhou *et al*., 2026; Shahat *et al.,* 2026). While demonstrated at a single site in Batam, Indonesia, the analytical architecture underlying LISAM is not specific to this location or species: it is the sequence of depth-resolved environmental characterization, physical-driver identification, and growth-linked biomanagement modelling those transfers, not the specific numerical thresholds reported here. Applying LISAM elsewhere means substituting these with the target system's own values and biomanagement variables. Accordingly, this study aims to characterize the temporal and depth-dependent environmental variability associated with sand lobster aquaculture; isolate its underlying physical drivers, including wind-driven seasonal transitions; evaluate whether longitudinal growth is better predicted by culture duration alone or by multifactorial models incorporating initial size class and stocking density; assess if temporally synchronized environmental exposure metrics improve biological performance predictions after accounting for biomanagement effects and translate these supported relationships into a transferable environmental-monitoring framework for the adaptive management of *P. homarus* aquaculture under tropical coastal conditions. The aim of the study is to apply LISAM architecture, aligning depth-resolved oceanographic monitoring with biomanagement and longitudinal biological performance in sand lobster (*Panulirus homarus*) aquaculture. This study was carried out in Batam Islands, Indonesia. Environmental and biological data were collected in 2025 and 2026.

MATERIALS AND METHODS

Study site and culture system

The study was conducted in the coastal waters of Setokok Island, Batam City, Riau Islands Province, Indonesia, within the Singapore Strait, one of Indonesia's principal centers for sand lobster (*Panulirus homarus*) floating-net-cage (FNC) culture. Data was obtained from representative FNC aquaculture locations, namely marine aquaculture development (BPBL) Batam (Fig. 1), which differ in hydrodynamic characteristics, water exchange, coastal exposure, and site-specific physical conditions while maintaining comparable culture systems. This spatial variability among otherwise comparable sites provides a natural framework for evaluating the

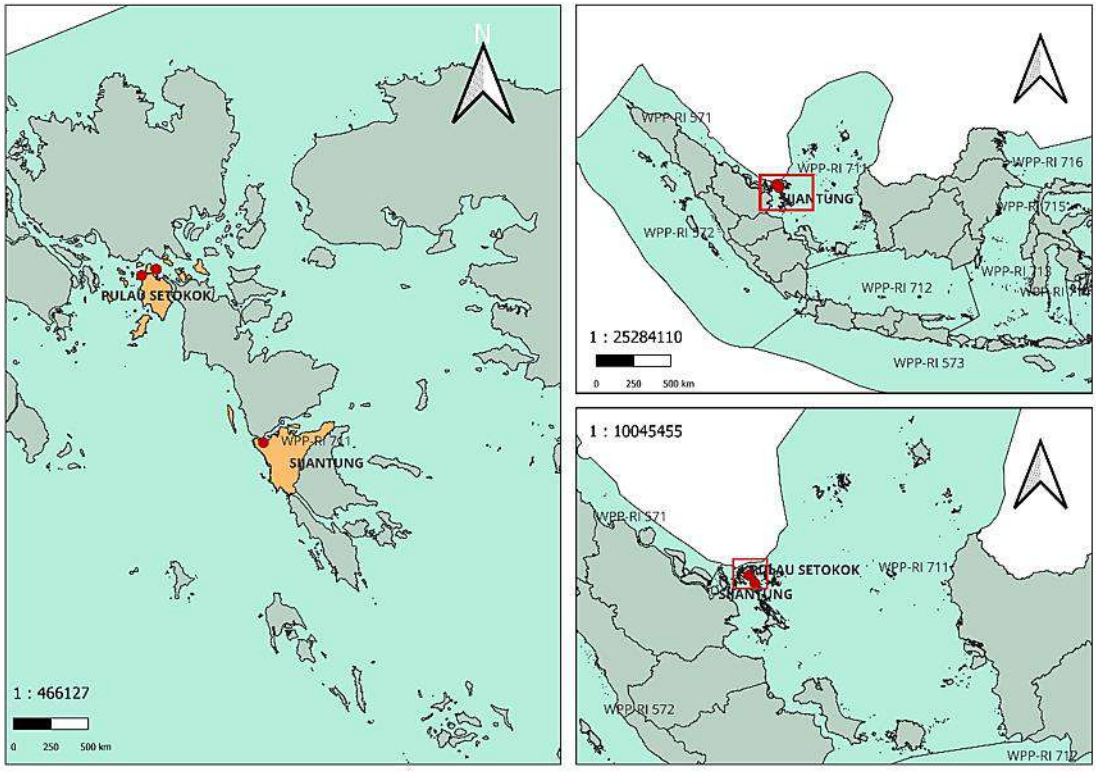

Fig. 1: Geographical location of the study area in Batam Island, Indonesia

complex interplay among environmental conditions, farm management practices, and biological performance (Radhakrishnan *et al*. 2019; FAO, 2024). Field observations were carried out over a single five-month production cycle using a longitudinal monitoring design, wherein oceanographic parameters were measured concurrently with biological sampling at each site to capture both spatial (among-site) and temporal (within-cycle) environmental variability.

Environmental monitoring

Environmental observations collected representative stationary points were retained for quality control but excluded from biological exposure calculations. Culture-site measurements of temperature, DO, pH, and salinity were summarized for each biological growth interval rather than matched to a single sampling date. Exposure metrics encompassed the mean, standard deviation, minimum, and maximum for each variable, alongside stress-oriented indices such as the percentage of observations falling below a defined DO threshold, using Eqs. 1 and 2 (Jeong *et al*., 2024):

$$DO_{<5} = 100(n_{DO<5}/n_{DO}) \quad (1)$$

$$DO_{<4} = 100(n_{DO<4}/n_{DO}) \quad (2)$$

For each growth interval, this proportion aggregated all discrete depth-and-time observations gathered across the interval's monitoring campaigns, encompassing three depths × five diel sampling occasions per campaign, rather than relying on single-point measurement or a simple mean. Nevertheless, exposure itself was characterized by discrete sampling events rather than continuously logged or duration-weighted data. Environmental monitoring events were given equal weight when deriving interval summaries.

Biological growth data

Longitudinal growth and environmental data from sand lobster (*Panulirus homarus*) cultured in FNC were analyzed using a cage-based repeated-measures framework. Due to the logistical constraints of tracking individual lobsters across multiple sampling intervals, statistical analyses treated the rearing cage as the primary experimental unit. The study was conducted at a single site (BPBL Batam) using six floating net cages, representing all combinations of three initial size classes (small, medium, large) and two stocking densities (50 and 75 individuals per cage), with one cage assigned to each combination. Rather than employing a randomized design, treatment allocations were fixed, and replicate cages per treatment combination were omitted. Instead, individual cages underwent repeated sampling across five successive monthly intervals throughout the five-month culture period, thereby providing the robust longitudinal growth datasets examined herein. For each cage and sampling period, mean body weight and total length (TL) were calculated, following cage-based growth assessments commonly used in *P. homarus* culture studies, using Eq. 3 (Prayanti *et al*., 2026):

$$AG = Y_{t_2} - Y_{t_1} \quad (3)$$

Biological performance between two sampling times (t_1, t_2) was quantified as absolute growth (AG). The relative growth (RG) is applied using Eq. 4 (Sun and Wang, 2024):

$$RG = 100\left(Y_{t_2} - Y_{t_1}\right)/Y_{t_1} \quad (4)$$

The specific growth rate (SGR) for body weight is applied using Eq. 5 (Sun and Wang, 2024):

$$SGR = 100\left[\ln\left(W_{t_2}\right) - \ln\left(W_{t_1}\right)\right]/(t_2 - t_1) \quad (5)$$

It is expressed as percent (%) per day. Length growth rate (LGR) was calculated, using Eq. 6 (Kristiana *et al*., 2020):

$$LGR = \left(L_{t_2} - L_{t_1}\right)/(t_2 - t_1) \quad (6)$$

Total length was selected as the primary response metric for the biomanagement models owing to its near-linear trajectory throughout the culture phase. Conversely, SGR was applied in the environmental models to normalize growth performance across monitoring intervals of varying lengths (20–29 days). The continuous predictors were standardized where required, using Eq. 7 (Ignatz *et al*., 2021):

$$z = (x - \bar{x})/s_x \quad (7)$$

Depth-stratified DO analysis

Water quality was monitored at a single representative station within each site across three depths, with sampling conducted five times per diel cycle over five monthly campaigns (September–January), generating a total of 75 distinct depth-resolved observations (3 depths × 5 diel occasions × 5 campaigns). Classifying DO relative to a biological threshold, rather than mean concentration alone, is informative given that DO in tropical floating-net-cage systems is known to vary substantially, with a comparable Indonesian FNC site reporting a range of 2.6–9.1 mg/L across seasons (Ariadji *et al.,* 2024) and in other tropical crustacean aquaculture systems (>37% in shrimp ponds (Tho *et al.,* 2011). Values below this threshold may indicate that the conditions at the site are potentially unsuitable for *Panulirus homorus* culture. To assess water-column stratification of DO, measurements taken at the three sampled depths with 0, 3, and 10 meters (m) were evaluated using the Kruskal–Wallis's test whenever the assumptions of normality or homogeneity of variance were violated. Where the global test indicated a significant difference among depths, pairwise post-hoc comparisons (Tukey's HSD or Dunn's test, respectively) were performed to identify which depth strata differed from one another. This analysis evaluated the influence of cage depth on

DO, to establish whether depth- dependent oxygen stratification constituted a consistent pattern rather than a negligible phenomenon.

Physical correlates of environmental variability

To investigate the physical drivers of observed temporal variability in water quality, monthly wind speeds were analyzed against monthly mean temperature and DO using Pearson correlation, or Spearman's rank correlation for non-normal data, and simple linear regression, reporting regression coefficients, coefficients of determination (R^2), and 95% confidence intervals. This analysis aimed to determine whether seasonal wind forcing could account for the collinearity between culture duration and environmental predictors noted in the Results.

Multivariate environmental characterization

Principal Component Analysis (PCA) was employed to characterize covariance structures among the standardized environmental parameters. Prior to component extraction, sampling adequacy and variable intercorrelation were assessed using the Kaiser–Meyer–Olkin (KMO) measure and Bartlett's Test of Sphericity. Components exhibiting eigenvalues greater than one were retained in accordance with the Kaiser criterion, and Varimax rotation was applied to ease interpretation of the resulting gradients, using Eq. 8 (Jolliffe and Cadima, 2016):

$$PC_k = a_{1k}Z_1 + a_{2k}Z_2 + \cdots + a_{pk}Z_p \quad (8)$$

Where: a_{jk}denotes the loading of standardized variable; $Z_j$on component k.

Biomanagement growth models (LMM)

Longitudinal biological responses were analyzed using Linear Mixed-Effects Models (LMMs). The general model, using Eq. 9 (Augie *et al.*, 2025):

$$Y_{it} = X_{it}\beta + u_i + \varepsilon_{it} \quad (9)$$

Where: $Y_{it}$is the response for cage $i$at time t, βrepresents fixed effects, $u_i \sim N(0, \sigma^2_{cage})$is the cage-specific random intercept, and $\varepsilon_{it}$is the residual error. Temporal dependence within cages was represented using a continuous first-order autoregressive structure, using Eq. 10 (Hamel *et al.*, 2012):

$$\mathrm{Cor}(\varepsilon_{it}, \varepsilon_{is}) = \phi^{|t-s|} \quad (10)$$

A cage-specific random intercept, combined with this within-cage, was considered appropriate, repeated monthly measurements within each of six cages, with no individual-lobster tracking and no additional site to model. This architecture permits cages to vary systematically in their baseline growth while accounting for temporal autocorrelation, wherein measurements separated by shorter intervals within the same cage exhibit stronger correlation than those spaced further apart. Six biologically defined candidate models were subsequently evaluated using Eqs. 11 to 16 (Zuur *et al.*, 2009):

$$M_0: Y \sim 1; \quad (11)$$

$$M_T: Y \sim Time; \quad (12)$$

$$M_{TS}: Y \sim Time \times Size; \quad (13)$$

$$M_A: Y \sim Time + Size + Density; \quad (14)$$

$$M_{TD}: Y \sim Time \times Density + Size; \quad (15)$$

$$M_I: Y \sim Time \times Size + Time \times Density + Size \times Density \quad (16)$$

Environmental–growth association models

Environmental effects on interval-specific SGR were examined as extensions of the biomanagement baseline, using Eq. 17 (Sun and Wang, 2024):

$$SGR \sim Time + Size + Density \quad (17)$$

To prevent over-parameterization given the restricted number of independent environmental exposure periods, standardized temperature, mean DO, low-DO exposure, pH, or salinity were incorporated into models individually. Interactions between environmental variables and biomanagement factors (e.g., density × DO) were not tested, despite evidence from other crustacean species that such interactions may influence biological responses (Kumar *et al.,* 2024). Due to the limited availability of only four independent environmental exposure intervals, the inclusion of additional interaction terms was deemed unfeasible.

Model selection

Candidate models were fitted using maximum likelihood (ML) and ranked using the Akaike information criterion corrected for small sample size small sample (AICc) (Hurvich and Tsai, 1993; Zhu *et al.,* 2009):

$$AIC_c = AIC + \frac{2K(K+1)}{n-K-1} \quad (18)$$

Where: K is the number of estimated parameters and; n is the number of observations. Relative support was quantified, using Eq. 19 (Hodson *et al*., 2024):

$$\Delta_i = AIC_{c,i} - AIC_{c,\min} \quad (19)$$

and Akaike weight, using Eq. 20 (Hodson *et al*., 2024):

$$w_i = \exp(-0.5\Delta_i) / \sum_r \exp(-0.5\Delta_r) \quad (20)$$

Parameter estimation and inference relied exclusively on the single best-supported model rather than incorporating model-averaged estimates across candidate models. The best-supported model was subsequently refitted using restricted maximum likelihood (REML) for final parameter estimation, confidence intervals, variance components, and residual diagnostics. Because multiple enclosures shared identical environmental conditions within each growth interval, the environmental models were interpreted as exploratory.

RESULTS AND DISCUSSION

Temporal variability of water quality

Environmental conditions were characterized using quality-controlled in situ observations collected across the culture period. Across all depths and cage, water temperature averaged 26.235 ± 0.884 °C with range of 27.53–30.20 degree Celcius (°C), salinity averaged 32.447 ± 0.110 Parts per thousand (ppt) (range 32.29–32.62 ppt), DO averaged 5.502 ± 0.350 mg/L (range 5.00–5.95 mg/L), and pH averaged 8.238 ± 0.190 (range 7.97–8.61) (Table 1). Temperature and salinity are established physicochemical drivers of physiological and production performance in spiny lobster aquaculture (Balkhair *et al*., 2012), whereas DO limits aerobic metabolism acts as a primary determinant of stress and growth in cultured crustaceans (Zheng *et al*., 2021; Brennan *et al*., 2016). Nitrate (1.643 ± 0.444 mg/L), phosphate (0.0093 ± 0.0110 mg/L), and chlorophyll-a (2.447 ± 1.052 µg/L) provide additional characterization of the nutrient and productivity regime. Wind direction and wind speed (3.685 ± 2.386 m/s) further describe the physical setting and atmospheric forcing of the study area. Temperature, dissolved oxygen, phosphate, chlorophyll-a, and wind direction departed significantly from normality (all $p < 0.05$) (Table 1), motivating the use of a non-parametric approach for depth comparison. These baseline patterns also provide important context for distinguishing natural environmental variability from depth-related changes in subsequent analyses. Within the LISAM framework, this baseline characterization anchors the initial analytical layer by defining the temporal envelope of water-quality conditions and establishing a foundation for subsequent depth-resolved, wind-driven, multivariate, and ecological analyses.

Table 1: Descriptive statistics of environmental variables

Variable	Unit	Mean	Standard deviation (SD)	Min	Max	Shapiro–Wilk p
pH	–	8.238	0.190	7.97	8.61	0.240
Temperature	°C	29.235	0.884	27.53	30.20	0.020*
Salinity	ppt	32.447	0.110	32.29	32.62	0.378
DO	mg/L	5.502	0.350	5.00	5.95	0.044*
Nitrate	mg/L	1.643	0.444	0.91	2.34	0.496
Phosphate	mg/L	0.0093	0.0110	0.00	0.03	0.004*
Chlorophyll-a	µg L^{-1}	2.447	1.052	1.13	4.02	0.035*
Wind direction	°	-8.92	127.07	-178.54	177.59	0.041*
Wind speed	m/s	3.685	2.238	0.95	7.45	0.527

* $p < .05$, departs from normality

Depth-stratified oxygen distribution

Because DO is not necessarily homogeneous throughout the water column occupied by a floating cage, DO was compared across three sampled depths (0, 3, and 10 m; n = 75 depth-resolved observations). Mean DO was 6.032 ± 0.586 mg/L at the surface, 4.947 ± 0.550 mg/L at 3 m, and 4.940 ± 0.754 mg/L at 10 m. Because Shapiro–Wilk tests indicated non-normal distributions within each depth stratum, the Kruskal–Wallis test was applied as the primary comparison: the global difference among depths was highly significant ($H = 28.61$, $p < 0.001$). Levene's test confirmed homogeneity of variance across depths ($p = 0.410$). Tukey's HSD post-hoc test revealed that surface DO values differed significantly from those at both 3 m and 10 m (both $p < 0.001$), whereas 3 m and 10 m depths showed no significant difference ($p = 0.999$) (Fig. 2). This pattern demonstrates that lobsters maintained at depths of 3 m or greater encounter DO levels near the lower limit of the 5–7 mg/L range deemed acceptable for floating-net-cage *Panulirus homarus* culture (Syahrir et al., 2024), whereas surface-deployed enclosures remain safely above this critical threshold. These findings quantitatively extend depth-related effects previously reported for *P. homarus* in Indonesia (Wahjuningrum *et al*., 2022; Sarkar *et al*., 2026) and depth-related DO stratification in cage aquaculture more broadly (Oldham *et al*., 2018). Within LISAM framework, this vertical configuration establishes a spatially resolved component of the initial analytical layer, thereby complementing the temporal assessment.

Wind as a correlate of the seasonal transition in environmental variability

Monthly wind speed was strongly and significantly associated with the concurrent decline in water temperature (Pearson $r = -0.988$, $p = 0.002$; temperature = 30.69 - 0.392 × wind speed, $R^2 = 0.975$, 95% CI for the slope [-0.506, -0.277]), but was not significantly associated with DO ($r = -0.810$, $p = 0.096$; $R^2 = 0.656$, 95% CI for the slope [-0.241, 0.034]) (Fig. 3). The strong wind–temperature relationship aligns with wind acting as a physical driver of the seasonal transition in environmental variability, thereby offering a mechanistic explanation for the correlation between culture duration and environmental predictors. This pattern aligns with findings by Soeyanto *et al*. (2026), who demonstrated that seasonal wind forcing governs circulation, stratification, and oxygen dynamics in adjacent Jakarta Bay, thereby suggesting a similar wind–transport relationship to underpin a bay-scale early-warning framework for hypoxia. The present analysis extends this concept to the scale of an individual aquaculture operation and links it to measured biological growth responses rather than to hydrodynamic indicators alone. The lack of a statistically significant wind–DO relationship implies that, unlike temperature, oxygen variability at this site is governed by additional mechanisms, such as biological oxygen demand or

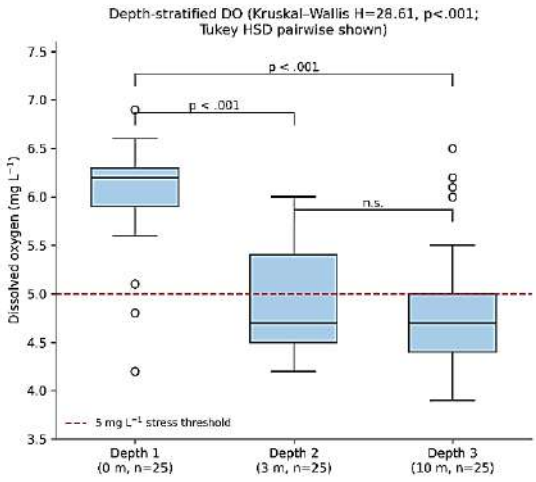

Fig. 2: DO by cage depth (0, 3, 10 m; n = 75). Kruskal–Wallis H = 28.61, p < .001; brackets show Tukey HSD pairwise comparisons

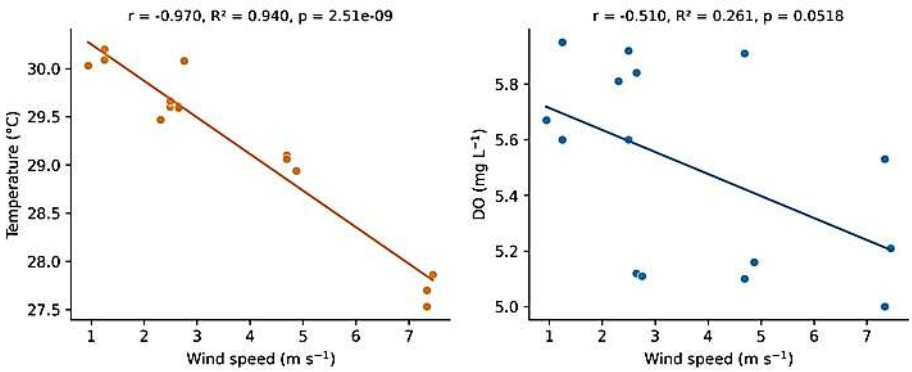

Fig. 3: Monthly wind speed vs. temperature and DO

localized mixing, that wind speed alone does not capture. Within LISAM, wind speed constitutes a low-cost, forecastable physical indicator that can be layered onto the environmental-characterization stage to anticipate the seasonal transition before its biological consequences materialize.

Site characteristics as descriptive context

Site suitability was further characterized using spatial and physical attributes compared across three floating-net-cage (FNC) locations (BPBL Batam, Sijantung, and Taman Laut), to support understanding of how these spatial attributes are interrelated and can be reduced to a small number of interpretable components. This comparative framework complements the single-site environmental and biological monitoring conducted at BPBL Batam, the site selected for cage-based culture in this study, by providing key data on accessibility, proximity to land and marine protected areas (MPA), exposure, bathymetry, and substrate attributes frequently integrated into GIS-based suitability assessments for floating-net-cage lobster aquaculture (Syahrir *et al*., 2024). Accessibility distance ranged from 69.06 to 1,724.51 m (mean 625.06 ± 824.61 m), distance to land ranged from 0 to 140.94 m (mean 53.50 ± 65.09 m), and distance to the nearest MPA ranged from 648.98 to 3,473.03 m (mean 2,162.92 ±

1,232.37 m), indicating considerable variation in spatial accessibility and positioning within the surrounding coastal landscape. Several variables warrant cautious interpretation: the "inside MPA" metric was uniformly zero, denoting that no monitoring sites fall within a protected zone; substrate type was coded categorically on a 1–4 scale, meaning its numerical mean (3.11 ± 0.93) does not represent a physical quantity; and bathymetry exhibited a narrow numerical range (0.9680–0.9878), reflecting a normalized index rather than direct water depth (Mabula *et al*., 2023). To characterize the joint structure among these attributes, PCA was applied. Several methodological limitations must be noted: given the comparison of only three locations, the underlying correlation matrix is necessarily rank-deficient (maximum rank = 2) and several variable pairs exhibit perfect or near-perfect collinearity (e.g., distance to MPA and bathymetry, r = -0.966). The component solution was derived by eigendecomposition of the Pearson correlation matrix. Because only three locations were compared, the matrix rank is mathematically bounded at two, consistent with the reported two-component solution, and is presented here as a low-dimensional descriptive summary of covariation among the three sites rather than a generalizable multivariate structure. Consequently, the resulting components should be interpreted as a descriptive summary of how these attributes covary across the three study locations, rather than as statistically robust or generalizable environmental gradients. Together, two components accounted for 81.46% of the total variance (PC1 = 46.23%, PC2 = 35.23% after Varimax rotation). PC1 was dominated by accessibility distance (0.933), exposure (0.926), and distance to land (0.918); while PC2 was dominated by distance to MPA (-0.973) and bathymetry (0.950); substrate did not load strongly (< 0.50) on either rotated component (Fig. 4). Aligned with the monitoring-architecture principles of LISAM, these site attributes and their multivariate structure serve as a descriptive locational context rather than as fixed-effect predictors within the biological growth models. Formally integrating site-characteristic gradients with growth performance represents a logical next step once future sampling resolves the collinearity.

Multivariate structure of environmental gradients

PCA revealed that the first two components accounted for 84.0% of the total environmental variance. Specifically, the first principal component (PC1) explained 47.8% and was primarily driven by temperature and pH; because DO contributed in the same direction as temperature, PC1 represents a temperature–oxygen versus pH gradient. The second principal component (PC2) explained 36.2% of the variance and was predominantly driven by salinity, which opposed by DO and pH, thereby representing a salinity versus oxygen–pH gradient. The third principal component (PC3) and fourth principal component (PC4) explained only 14.4% and 1.58%, respectively. PCA is frequently employed to condense covariance structures among correlated environmental metrics and to isolate the primary multivariate gradients characterizing complex ecological datasets (Li *et al*., 2017). Condensing multiple correlated environmental metrics into a concise set of interpretable gradients forms the core of LISAM's initial analytical layer. This approach supplies standardized environmental descriptors that can be linked to biological performance without introducing the multicollinearity inherent in incorporating all raw physicochemical variables simultaneously (Zuur *et al*., 2009).

Biomanagement effects on total length growth

Information-theoretic model selection established that the Additive model — incorporating culture time, initial size class, and stocking density entered as additive fixed effects, provided the best-supported explanation for total length variation (AICc = 60.3, Akaike weight = 0.715; Table 2 and Fig. 5. The Time_Density model

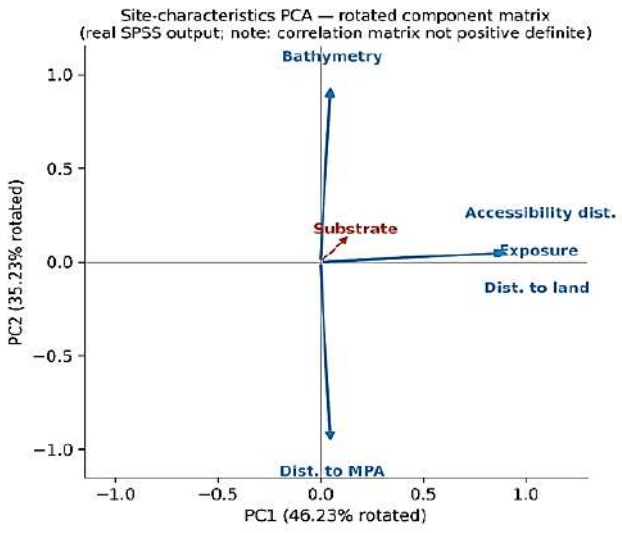

Fig. 4: Site-characteristics PCA

Table 2: AICc-based selection of candidate models for total length growth

Rank	Model	n	K	AICc	ΔAICc	Akaike weight (w_i)	Relative support	Decision
1	Additive	30	8	60.3	0.00	0.715	Strongest	Best-supported model
2	Time density	30	9	62.4	2.10	0.251	Secondary support	Plausible alternative
3	Time size	30	9	66.5	6.17	0.0327	Weak	Considerably less supported
4	Integrated biomanagement	30	13	71.9	11.6	0.00218	Very weak	Little support
5	Time	30	5	105.0	44.8	1.31×10^{-10}	Negligible	Not supported
6	Null	30	4	398.0	337.6–338	3.48×10^{-74}	Negligible	Not supported

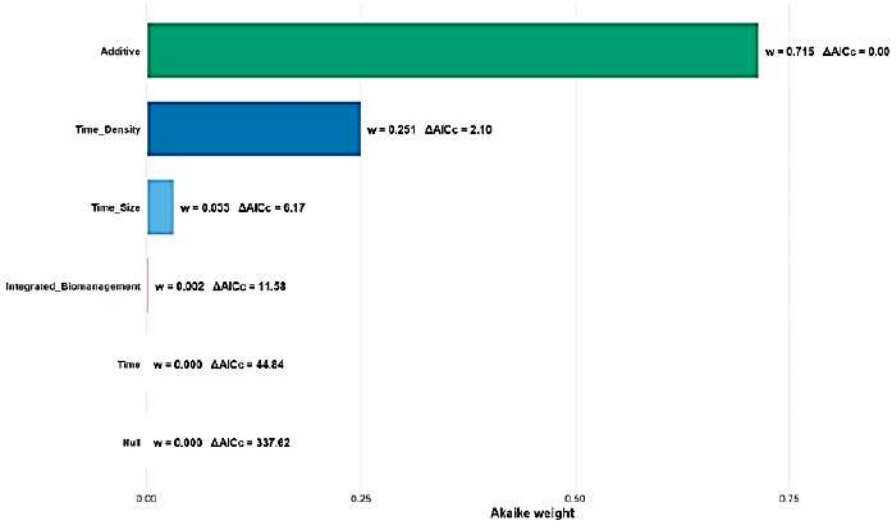

Fig. 5: AICc-based model selection for total length growth of sand lobster (*Panulirus homarus*) seed under different biomanagement hypotheses

received secondary support (AICc = 62.4, weight = 0.251); combined, these two models accounted for approximately 96.6% of cumulative Akaike weight, while the Time_Size interaction, Integrated_Biomanagement, Time-only, and Null models exhibited progressively weaker support. The REML-fitted Additive model confirmed a strong positive effect of culture time (β = 1.260, standard error (SE) = 0.026, p < 0.001); medium-size lobsters were on average 1.280 cm longer than the small-size class (p < 0.001), and large-size lobsters 1.731 cm longer (p < 0.001), after accounting for time and density. Higher stocking density (75 vs. 50 individuals per cage) was associated with a modest, non-significant reduction in length (-0.181 cm, SE = 0.097), consistent with lower-density treatments generally producing better growth in juvenile *P. homarus* (Minjoyo *et al.*, 2024) rather than definitive evidence of a density effect (Fig. 6). The very large ΔAICc values for the Time-only and Null models indicate strong relative support for the Additive structure within this candidate set. Nevertheless, these metrics should be viewed as comparative evidence among the six evaluated models rather than conclusive proof that time, size, and density dictate growth independently of unmeasured variables. Furthermore, the limited support for the more complex Integrated_Biomanagement model indicates that incorporating interaction terms failed to improve model fit sufficiently to penalize the added complexity.

Environmental associations with weight growth

Given that interval-specific environmental exposure was derived from just four independent monitoring intervals across a single ~5-month production cycle, this environmental-growth analysis is treated as exploratory rather than confirmatory; consequently, the reported coefficients and model rankings represent dataset-specific associations rather than generalizable inferential evidence. Building on the biomanagement baseline, environmental variables were evaluated as additional predictors of interval-specific SGR. Among these, the model extending the baseline with low-DO exposure (Bio_DOstress) received the strongest support, followed by temperature and pH; together these three models accounted for approximately 99.5% of cumulative Akaike weight. SGR showed a negative association with culture time (β = -0.767, SE = 0.129), a predictor similarly limited by the four available exposure intervals; relative to the small size class, medium and large lobsters showed lower SGR (β = -0.681, p = 0.017; β = -0.721, p = 0.013), while stocking density showed little association (β = 0.040, p = 0.850). Low-DO exposure showed a positive conditional association with SGR (β = 0.497, SE = 0.129, p < .001). Nevertheless, this estimate derives from only four independent environmental exposure intervals (culture months two through five) in which multiple enclosures shared identical monthly conditions; consequently, the reported p-value should not be construed as indicative of robust statistical certainty. Examined at the interval level, mean SGR declined from 2.87 to 2.50 %/day between the second and third months while mean DO remained unchanged (5.60 mg/L), then rose to 2.75 %/day in the fourth month as mean DO fell to 5.10 mg/L, before both declined together in the fifth month (DO = 5.00 mg/L, SGR = 1.44 %/day). Rather than signaling a genuine dose-dependent trend, this non-monotonic pattern arises from the sparse and uneven parameter combinations available across the four intervals, and it must not be misconstrued as proof that reduced DO enhances lobster growth. To probe this association further, a partial-residual analysis were performed (Fig. 7) to evaluate the relationship between DO and SGR after adjusting for the fitted effects of culture time, size class, and stocking density. The unadjusted bivariate relationship between DO and SGR was positive (r = 0.54, p = 0.007), aligning with the expected biological mechanism whereby higher oxygen availability enhances growth performance.

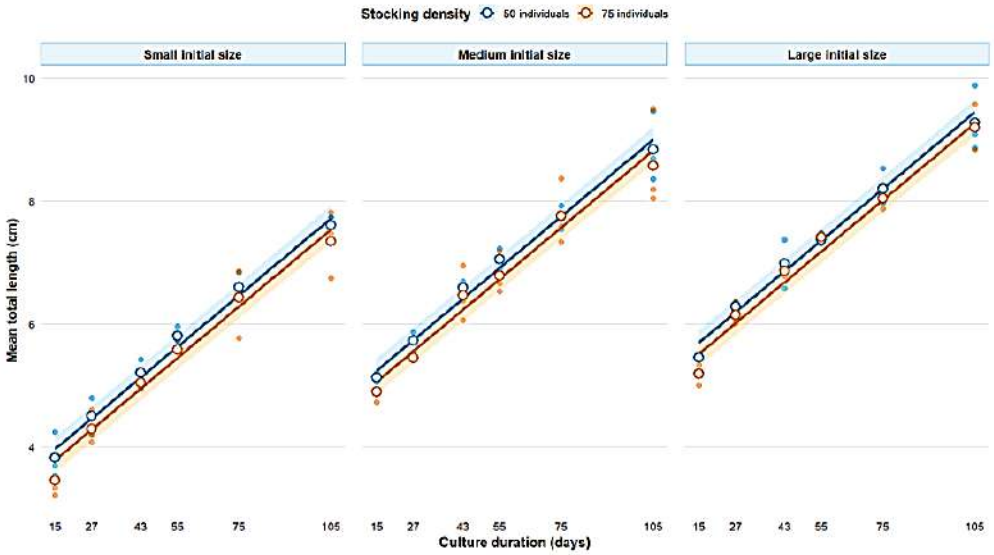

Fig. 6: Observed and model-predicted total length trajectories of sand lobster (*Panulirus homarus*) seed according to initial size class and stocking density

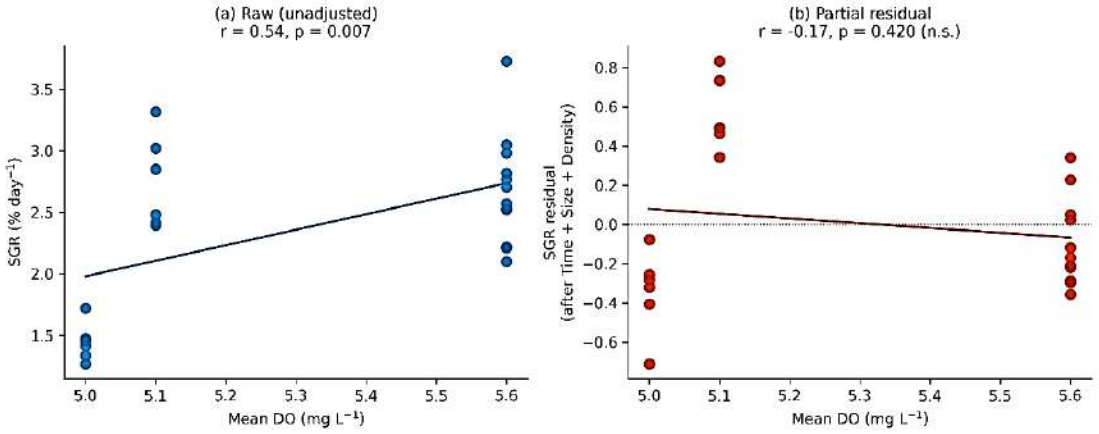

Fig. 7: DO–SGR relationship across 24 cage-interval observations. (a) Raw correlation (r = 0.54, p = 0.007). (b) Partial residual after removing culture time, size class, and stocking density (r = −0.17, p = 0.420, n.s.), indicating the raw association is confounded with the temporal growth trend

This relationship was no longer significant once the shared temporal trend was removed (partial residual r = −0.17, p = 0.420). Furthermore, incorporating DO alongside culture time in the same model also substantially inflated the estimated magnitude of the time effect and triggered a severe rise in multicollinearity (with the condition number surging from 15.8 to 390). This demonstrates that the apparent DO–SGR relationship noted earlier is unstable, arising more parsimoniously from collinearity between DO and culture time than from a genuine, independent influence of oxygen availability on growth. Consequently, this association is not construed as proof that reduced oxygen levels enhance or benefits lobster growth; rather, it is presented strictly as a descriptive trend that merits further examination across additional independent exposure intervals. This association was also interpreted cautiously because culture time was

strongly correlated with temperature (r = -0.947) and pH (r = 0.949), while low-DO exposure was itself correlated with time (r = 0.592) and pH (r = 0.783). This collinearity between culture time and environmental predictors is consistent with, and onsistent with, and physically plausible given, the wind-related seasonal transition, rather than representing an unexplained statistical artefact. Collectively, the biomanagement and environmental evaluations demonstrate that successful sand lobster culture cannot be attributed to management practices or oceanographic conditions in isolation. Culture duration, initial seed size, and stocking density structure the biological growth trajectory, while temporal variability in DO, temperature, and pH provides additional environmental information relevant to culture performance. This represents the third analytical layer of LISAM: identifying which environmental gradients best explain biological performance alongside key biomanagement drivers.

Implications for adaptive environmental management

The biomanagement and environmental-association models identify what matters for sand lobster growth: culture duration, initial size, stocking density, and, more cautiously, DO exposure. The large depth effect on DO (Kruskal–Wallis H = 29.27, $p < 0.001$) means depth is a relevant dimension for environmental monitoring in this system, one that operators should track explicitly rather than assume uniform across the water column. Although depth trends suggest that enclosures positioned closer to the surface would experience higher DO , this study did not evaluate whether surface placement translate to enhanced growth, survival, feed conversion, or welfare. Furthermore, it did it assess how depth influences temperature, hydrodynamics, biofouling, or food availability, variables that covary with depth and could potentially offset any oxygen-related advantage. Repositioning cages toward the surface should therefore be treated as a hypothesis warranting direct experimental testing rather than an operational recommendation. In the interim, monitoring protocols should encompass multiple depth strata; relying on a single surface or mid-column reading risks misrepresenting the actual environmental conditions experienced by lobsters housed deeper within the same enclosure. This matches water-quality guidance for pond and cage aquaculture (Asmah *et al*., 2021), documented crustacean sensitivity to hypoxia (Zheng *et al*., 2021), and known environmental effects on fished lobsters and crabs (Green *et al*., 2014). Within this monitoring framework, routine seasonal variability can be differentiated from potentially critical conditions by comparing new observations against established temporal baseline and predefined biological or environmental trigger levels; can initiate intensified monitoring or proactive management intervention. Wind speed is inexpensive and publicly forecastable through national weather advisories, and the strong wind–temperature relationship (r=-0.988, p=0.0017) turns it into a low-cost indicator for the temperature-related seasonal transition. Operators who monitor these shifts gain valuable lead time to modify feeding, stocking, or harvest schedules before the resulting biological consequences materialize. Consequently, precision-aquaculture research relies on such proxies to anticipate production risks rather than documenting them post-hoc (Kapetsky *et al*., 2013; Falconer *et al*., 2016). However, wind speed showed no significant association with DO (r = -0.810, p = 0.096) in this dataset, so it should not be treated as an early-warning indicator for oxygen risk specifically; oxygen conditions still require direct measurement. Together, the depth and wind results give the biomanagement findings a monitoring logic they lacked before: operators now have grounds for deciding where in the water column, and when in the season, to concentrate monitoring effort. Culture duration, initial seed size, and stocking density govern total length variations, whereas DO, temperature, and pH

provide additional explanatory power regarding weight gain. Integrated statistical assessment of aquaculture water-quality variables can similarly help distinguish relationships among environmental conditions and aquaculture-related responses, supporting the use of multivariable rather than single-parameter assessments (Takarina *et al.,* 2025). Together these results argue against treating site selection and farm management as separate decisions. A physically monitored site will not automatically produce good growth if biomanagement is mismatched to it, and good biomanagement in turn needs a site's environmental variability actively monitored and anticipated, not assumed constant (Giri *et al*., 2023; Radhakrishnan *et al*., 2019). Aquaculture systems behave as coupled social-ecological systems: production outcomes depend on continuous interaction between environmental variability and management decisions, not on either factor alone (Ostrom, 2009; Folke *et al*., 2010). This integrated perspective is consistent with contemporary marine and fisheries strategies that link aquaculture development with environmental sustainability and broader blue-economy objectives (Trenggono *et al.,* 2025). These recommendations rely fundamentally on maintaining the monitoring framework from which they were derived. In this context, adaptive management entails continuously updating operational practices in response to incoming monitoring data, requiring the architecture to be sustained over time rather than deployed merely as a one-time characterization exercise (Costa-Pierce, 2010; Costello *et al*., 2020). To position this contribution more precisely, GIS-based multi-criteria frameworks commonly used for lobster and finfish cage-aquaculture site assessment (Jayanthi *et al*., 2022; Porporato *et al*., 2020; Syahrir *et al*., 2024) are designed to compare candidate locations before operation begins, drawing on static or snapshot environmental and spatial layers to produce a composite suitability score; they do not incorporate depth-resolved temporal monitoring or link their outputs to measured biological performance. In contrast, the LISAM framework is implemented post-site selection. It conceptualizes environmental fluctuations as longitudinal, depth-profiled attributes within an individual operating facility, subsequently connecting them to somatic growth outcomes through the mixed-effects model outlined above. The two approaches are therefore complementary rather than competing: GIS-based multi-criteria assessment remains appropriate for initial site screening, while LISAM addresses the subsequent, and comparatively underdeveloped, problem of managing an operating site once selected. LISAM's novelty sits less in any single statistical technique and more in what it couples together, and at what scale. Separate bodies of research within coastal oceanography and aquaculture provide distinct theoretical and empirical support for depth-related oxygen stratification and wind-driven physical forcing. Linking both physical drivers, at the scale of a single floating-net-cage operation, to measured growth outcomes for a high-value benthic crustacean such as *P. homarus* has not been done before (Zhou *et al*., 2026; Giri *et al*., 2023). Conventional site-selection frameworks (Radiarta *et al*., 2008; Falconer *et al*., 2016; Jayanthi *et al*., 2022; Porporato *et al*., 2020; Syahrir *et al*., 2024) evaluate environmental or spatial suitability largely apart from biomanagement and biological response. LISAM treats environmental characterization, physical-driver identification, biomanagement, and growth modelling as layers of one analytical architecture, producing operational monitoring and management recommendations instead of a static suitability score. The biomanagement models explain why that design matters biologically, without functioning as the central claim. The primary practical outcome is a standardized protocol establishing systematic criteria for selecting monitoring variables, frequencies, and spatial scales. This framework directly responds to contemporary calls for holistic aquaculture

decision-support tools capable of integrating ecological, operational, and adaptive-management facets into a unified workflow (Mair *et al*., 2023; Sampantamit *et al*., 2020). Several parts of this analysis remain preliminary. With only four independent environmental exposure intervals, the environmental-growth analysis (Eq. 17) is formally underpowered for detecting effects independent of culture time; this is demonstrated empirically, not just assumed, by the loss of the DO–SGR signal under partial-residual analysis. Because the cage-based growth assessment utilized a single, non-randomized enclosure per size class–density treatment, cross-combination comparisons warrant cautious interpretation. The depth-stratified DO comparison reflects measurements from a single representative stationary point rather than all six cages, and may not capture cage-to-cage environmental heterogeneity across the site. The original DO–SGR association rests on four independent exposure intervals within a single 5-month production cycle, limiting the ability to separate environmental from temporal effects. This study did not incorporate feeding regime, feed quantity, feed type, feeding frequency, survival/mortality, moulting, disease or health status, shelter availability, handling practices, or other cage-specific management variables, all of which can independently influence growth in *P. homarus* and related palinurid species (Adiyana *et al.,* 2020; Prayanti *et al.,* 2026). Consequently, the documented associations should be viewed as reflecting only the specific set of biomanagement and environmental parameters quantified, rather than an exhaustive account of all growth determinants. The site-characteristics PCA is limited by a non-positive-definite correlation matrix given the current sample size. The wind-speed early-warning idea remains a statistical association, not yet a tested field protocol. Derived likewise from an isolated five-month production cycle, the seasonal and predictive assertions regarding this wind–temperature interaction warrant interpretation as preliminary observations rather than validated, operational early-warning capabilities. More monitoring cycles, full three-site coverage, and an operational trial of the wind indicator would move LISAM toward a fully validated version. LISAM's analytical architecture carries no location-specific parameter. It specifies a type of monitoring (depth-resolved, physically indexed, and growth-linked) not a fixed set of thresholds. Operators can transfer it to other marine aquaculture species and systems (Radhakrishnan *et al*., 2019; Zhou *et al*., 2026) by substituting the relevant environmental variables, depth structure, and biological indicators. This matches calls for aquaculture decision-support frameworks that generalize across species and settings instead of being rebuilt for each case (Kapetsky *et al*., 2013).

CONCLUSION

Successful sand lobster (*Panulirus homarus*) aquaculture in floating net cages requires treating environmental monitoring and biomanagement as one integrated problem across the production cycle. This study characterizes spatial and temporal variations in water quality at an operational aquaculture site and identifies their physical correlates. Furthermore, it quantifies the extent to which growth performance is independently explained by culture duration, initial seed size, and stocking density versus the additional contribution of environmental factors. DO averaged about 6.0 mg/L at the surface and dropped to about 4.9 mg/L at 3 m and 10 m. A Kruskal–Wallis test confirmed this difference ($H = 29.27$, $p < 0.001$), and pairwise comparison showed the surface differed from both deeper strata ($p < 0.001$) while the two deeper strata matched each other. Cages held at 3 m or deeper sit close to the 5 mg/L threshold associated with physiological stress in cultured crustaceans. Monthly wind speed and temperature exhibited a strong inverse seasonal co-variation ($r = -0.988$, $p = 0.002$), whereas wind speed demonstrated no statistically significant association with DO

(r = -0.810, p = 0.096) in this single-site dataset. This coastal system's season transition is a measurable, forecastable driver of the water-quality conditions lobsters experience. Among the evaluated parameters, culture duration, initial seed size, and stocking density collectively provided superior model performance in accounting for total length development. Among six candidate models, an additive model combining these three variables carried the strongest statistical support (Akaike weight = 0.715), well ahead of the next-best model (weight = 0.251). These three variables set the pace of structural growth under the conditions monitored here. SGR followed a different pattern. Low-oxygen exposure carried the strongest environmental signal (β = 0.497, p < 0.001), followed by temperature and pH conditions, even after accounting for time (β = -0.767, p < 0.001), size, and density. Because this relationship is derived from four distinct environmental exposure periods, additional monitoring cycles are required to validate its robustness. Oxygen availability is the physicochemical variable most worth monitoring closely at this class of site. DO concentrations approached the 5 mg/L threshold associated with physiological stress more closely under less favorable cage placement and seasonal timing. Whether relocating aquaculture enclosures closer to the surface—where dissolved oxygen levels remain consistently elevated—translates into enhanced growth, survival, or welfare remains unproven and warrants targeted experimental validation, given that depth simultaneously co-varies with temperature, hydrodynamics, biofouling, and trophic resource availability. Monitor water quality across depth strata, not at a single fixed point. Treat locally forecastable wind conditions as an early indicator of the seasonal transition that precedes oxygen stress, ahead of any signal from DO itself. By integrating species-specific biological indicators and management variables, the analytical framework of LISAM can be readily adapted to other marine aquaculture systems.

AUTHOR CONTRIBUTIONS

I.N.P. Winata conceptualized the study framework and prepared the initial draft of the manuscript. I.M. Radjawane supervised the overall research and provided critical revisions to the manuscript. S. Nurdjaman contributed to research supervision and the literature review, while I.N. Radiarta supported the study through supervision and provided critical comments to strengthen the manuscript. D. Sidik participated in field sampling and data collection, and Deby contributed essential supporting data for the study. S.K. Pratiwi assisted with laboratory analyses. A.A. Utama contributed to data analysis, S. Makmur participated in the interpretation of the results, and Husnah provided critical comments on the manuscript. A. Suman contributed to the development of the conceptual framework and supported the literature review. All authors reviewed and approved the final version of the manuscript prior to publication.

ACKNOWLEDGEMENT

The authors gratefully acknowledge the Research Organization for Earth Sciences and Maritime, Indonesia, for providing academic support and facilitating this doctoral research. We sincerely thank the Marine Aquaculture Development Center (BPBL) Batam, Ministry of Marine Affairs and Fisheries, Indonesia, for granting access to the experimental facilities, field observations, and technical assistance during data collection. Appreciation is also extended to all field technicians and staff who contributed to environmental monitoring, biological sampling, and laboratory analyses throughout the study. The constructive comments and guidance provided by the supervisory committee are gratefully acknowledged and have substantially improved the quality of this research.

CONFLICT OF INTEREST

The authors declare that there is no conflict of interest regarding the publication of this manuscript. In addition, ethical issues, including plagiarism, informed consent, misconduct, data fabrication and/or falsification, double publication and/or submission, and redundancy, were observed by the authors.

OPEN ACCESS

©2027 The author(s). This article is licensed under a Creative Commons Attribution 4.0 International License, which permits use, sharing, adaptation, distribution and reproduction in any medium or format, as long as you give appropriate credit to the original author(s) and the source, provide a link to the Creative Commons license, and indicate if changes were made. The images or other third-party material in this article are included in the article's Creative Commons license, unless indicated otherwise in a credit line to the material. If material is not included in the article's Creative Commons license and your intended use is not permitted by statutory regulation or exceeds the permitted use, you will need to obtain permission directly from the copyright holder. To view a copy of this license, visit: http://creativecommons.org/licenses/by/4.0/

PUBLISHER'S NOTE

GJESM Publisher remains neutral regarding jurisdictional claims in published maps and institutional affiliations.

NEGATIVE AI STATEMENT

The author(s) declared that no AI tools or services were used or highly applied during the preparation of this work.

ABBREVIATIONS

%	Percent
Δ_i	AICc difference for candidate model i
ΔAICc	Difference between the AICc of a candidate model and the minimum AICc
β	Fixed-effect regression coefficient
β	Vector of fixed-effect coefficients
ε_{it}	Residual error for cage $i$at time t
σ^2_{cage}	Between-cage random-intercept variance
ϕ	Temporal autocorrelation parameter
°C	Degree Celsius
%/day	Percent per day
µg/L	Microgram per liter
Additive	Model including additive effects of culture time, initial size class, and stocking density
AG	Absolute Growth
AICc	Akaike information criterion corrected for small sample size
a_{jk}	PCA loading of standardized variable $j$on principal component k
ANOVA	Analysis of variance
Bio_DOmean	Biomanagement model extended with mean dissolved oxygen
Bio_DOstress	Biomanagement model extended with low-DO exposure
Bio_pH	Biomanagement model extended with pH
Bio_Salinity	Biomanagement model extended with salinity
Bio_Temperature	Biomanagement model extended with temperature
BioManagement	Baseline model containing culture time, initial size class, and stocking density
BPBL	Marine Aquaculture Development Center (*Balai Perikanan Budidaya Laut*)
cm	Centimeter
DO	Dissolved Oxygen
FNC	Floating Net Cage
GIS	Geographic Information System

Integrated_Biomanagement	Model incorporating culture time, size, density, and their specified pairwise interactions
K	Number of estimated parameters used in AICc calculation
KMO	Kaiser–Meyer–Olkin
LGR	Length Growth Rate
LISAM	Lobster Integrated Site Assessment and Management
LMM	Linear Mixed-Effects Model
m	Meter
m/s	Meter per second
mg/L	Milligrams per liter
ML	Maximum Likelihood
MPA	Marine Protected Area
n	Number of observations
Null	Model containing an intercept only
PC1	First Principal Component
PC2	Second Principal Component
PC3	Third Principal Component
PC4	Fourth Principal Component
PCA	Principal Component Analysis
pH	Measure of acidity–alkalinity based on hydrogen-ion activity
ppt	Parts per thousand
r	Correlation coefficient
REML	Restricted Maximum Likelihood
RG	Relative Growth
SD	Standard Deviation
SE	Standard Error
SGR	Specific Growth Rate
Time	Model including culture time as the explanatory variable
Time_density	Model including culture time, stocking density, their interaction, and initial size class
Time_size	Model including culture time, initial size class, and their interaction
u_i	Cage-specific random intercept
w_i	Akaike weight of candidate model i
X_{it}	Fixed-effect design/predictor vector for cage $i$at time t
Y_{it}	Biological response for cage $i$at observation time t
Z_j	Standardized environmental variable $j$in PCA

REFERENCES

Adiyana, K.; Zulkarnain, R.; Thesiana, L., (2020). Physiological response and growth performance of spiny lobster (Panulirus homarus) juvenile rearing in recirculating aquaculture system with various shelter type. Mar. Res. Indones., 45(2): 67–74 **(8 pages)**.

Ariadji, Z.A.; Suantika, G.; Aditiawati, P., (2024). Trophic state assessment of marine ecosystems used for floating net cage aquaculture: a case study in Pegametan Bay, North Bali, Indonesia. Aquacul. Int., 32(5): 6611–6647 **(37 pages)**.

Asmah, R.; Falconer, L.; Telfer, T.; Karikari, A.; Al Wahaibi, M.; Xia, I.F.; Handisyde, N.; Quansah, K.E.; Amoah, D.; Alshihhi, J.; Ross, L., (2021). Waterbody scale assessment using spatial models to identify suitable locations for cage aquaculture in large lake systems: A case study in Volta Lake, Ghana. Aquacult. Res., 52(8): 3854–3870 **(17 pages)**.

Augie, B.H.; Augie, M.H.; Mansur, R., (2025). Regression and mixed-effects modeling of fish growth, survival, and yield in semi-intensive aquaculture systems in Gusau, Zamfara State, Nigeria. Int. J. Sci. Global Sustainability. 11(4): 87–92 **(6 pages)**.

Balkhair, M.; Al-Mashiki, A.; Chesalin, M.V., (2012). Experimental rearing of spiny lobster, Panulirus homarus (Palinuridae) in land-based tanks at Mirbat station (Sultanate of Oman) in 2009–2010. J. Agric. Mar. Sci., 17: 33–43 **(11 pages).**

Breitburg, D.; Hondorp, D.; Audemard, C.; Carnegie, R.; Burrell, R.B.; Trice, M.; Clark, V., (2015). Landscape-level variation in disease susceptibility related to shallow-water hypoxia. PLoS ONE. 10(2): e0116223 **(27 pages)**.

Brennan, C.E.; Blanchard, H.; Fennel, K., (2016). Putting temperature and oxygen thresholds of marine animals in context of environmental change: A regional perspective for the Scotian Shelf and Gulf of St. Lawrence. PLoS ONE. 11(12): e0167411 **(27 pages)**.

Costa-Pierce, B.A., (2010). Sustainable ecological aquaculture systems: The need for a new social contract for aquaculture development. Mar. Technol. Soc. J., 44(3): 88–112 **(25 pages)**.

Costello, C.; Cao, L.; Gelcich, S.; Cisneros-Mata, M.Á.; Free, C.M.; Froehlich, H.E.; Golden, C.D.; Ishimura, G.; Maier, J.; Macadam-Somer, I.; Mangin, T.; Melnychuk, M.C.; Miyahara, M.; Moor, C.L.d.; Naylor, R.; Nøstbakken, L.; Ojea, E.; O'Reilly, E.; Parma, A.M.; Plantinga, A.J.; Thilsted, S.H.; Lubchenco, J., (2020). The future of food from the sea. Nature. 588(7836): 95–100 **(6 pages)**.

Falconer, L.; Telfer, T.C.; Ross, L.G., (2016). Investigation of a novel approach for aquaculture site selection. J. Environ. Manage., 181: 791–804 **(15 pages)**.

FAO., (2024). The State of World Fisheries and Aquaculture 2024: Blue Transformation in Action. Food and Agriculture Organization of the United Nations, Rome.

Folke, C.; Carpenter, S.R.; Walker, B.; Scheffer, M.; Chapin, T.; Rockström, J., (2010). Resilience thinking: integrating resilience, adaptability and transformability. Ecol. Soc., 15(4): 20.

Green, B.S.; Gardner, C.; Hochmuth, J.D.; Linnane, A., (2014). Environmental effects on fished lobsters and crabs. Rev. Fish Biol. Fish., 24: 613–638 **(26 pages)**.

Giri, N.A.; Irvin, S.; Haryanti; Sudewi, S.; Selamet, B.; Jones, C.M.; Mujiono, (2023). Growth response of lobster Panulirus homarus reared in tanks and in floating net cages fed with compound and fresh feed. J. Nat. Sci., 52(10): 2747–2759 **(13 pages)**.

Hamel, S.; Yoccoz, N.G.; Gaillard, J.M., (2012). Statistical evaluation of parameters estimating autocorrelation and individual heterogeneity in longitudinal studies. Methods Ecol. Evol., 3(4): 731–742 **(12 pages)**.

Hodson, T.O.; Over, T.M.; Smith, T.J.; Marshall, L.M., (2024). How to select an objective function using information theory. Water Resour. Res., 60: e2023WR035803 **(14 pages)**.

Hurvich, C.M.; Tsai, C.L., (1993). A corrected Akaike information criterion for vector autoregressive model selection. J. Time Ser. Anal., 14: 271–279 **(9 pages).**

Ignatz, E.H.; Zanuzzo, F.S.; Sandrelli, R.M.; Clow, K.A.; Rise, M.L.; Gamperl, A.K., (2021). Phenotypic stress response does not influence the upper thermal tolerance of male Atlantic salmon (Salmo salar). J. Therm. Biol., 101: 103102 **(14 pages)**.

Jayanthi, M.; Kumaran, M.; Vijayakumar, S.; Duraisamy, M.; Anand, P.; Samynathan, M.; Thirumurthy, S.; Kabiraj, S.; Vasagam, K.; Panigrahi, A.; Muralidhar, M., (2022). Integration of land and water resources, environmental characteristics, and aquaculture policy regulations into site selection using GIS based spatial decision support system. Mar. Policy. 137: 104946 **(10 pages)**.

Jeong, J.; Awosile, B.; Thakur, K.; Stryhn, H.; Boyce, B.; Vanderstichel, R., (2024). Longitudinal dissolved oxygen patterns in Atlantic salmon aquaculture sites in British Columbia, Canada. Front. Mar. Sci., 10: 1289375 **(15 pages)**.

Jolliffe, I. T., and Cadima, J., (2016). Principal component analysis: A review and recent developments. Philos. Trans. R. Soc. A, 374(2065), 20150202.

Kapetsky, J.M.; Aguilar-Manjarrez, J.; Jenness, J., (2013). A global assessment of offshore mariculture potential from a spatial perspective. FAO Fisheries and Aquaculture Technical Paper No. 549. FAO, Rome.

Kristiana, V.; Mukti, A.T.; Agustono, (2020). Increasing growth performances of Nile tilapia (Oreochromis niloticus) by supplementation of noni Morinda citrifolia fruit extract via diet. Aquacult. Aquarium Conserv. Legislation., 13(1): 159–166 (**8 pages)**.

Kroeker, K.J.; Donham, E.M.; Vylet, K.; Warren, J.K.; Cheresh, J.; Fiechter, J.; Freiwald, J.; Takeshita, Y., (2023). Exposure to extremes in multiple global change drivers: Characterizing pH, dissolved oxygen, and temperature variability in a dynamic, upwelling-dominated ecosystem. Limnol. Oceanogr., 68(7): 1611–1623 **(13 pages)**.

Kulmiye, A.; Mavuti, K., (2005). Growth and moulting of captive Panulirus homarus homarus in Kenya, western Indian Ocean. N. Z. J. Mar. Freshwater Res., 39: 539–549 **(11 pages)**.

Kumar, M.; Chadha, N.K.; Prakash, S.; Pavan-Kumar, A.; Harikrishna, V.; Gireesh-Babu, P.; Krishna, G., (2024). Salinity, stocking density, and their interactive effects on growth performance and physiological parameters of white-leg shrimp, Penaeus vannamei (Boone, 1931), reared in inland ground saline water. Aquacult. Int., 32: 675–690 **(16 pages)**.

Lee, C.W.; Lim, J.H.; Heng, P.L.; Marican, N.F.; Narayanan, K.; Sim, E.U.H.; Bong, C.W., (2020). Influence of elevated river flow on hypoxia occurrence, nutrient concentration and microbial dynamics in a tropical estuary. Environ. Monit. Assess., 192(10): 1–12 **(12 pages)**.

Li, D.; Tang, C.; Xia, C.; Zhang, H., (2017). Acoustic mapping and classification of benthic habitat using unsupervised learning in artificial reef water. Estuarine Coastal Shelf Sci., 185: 11–21 **(11 pages).**

Mabula, M.; Kisanga, D.; Pamba, S.; Limbu, S.M., (2023). Use of GIS-based multicriteria evaluation for improved selection of suitable sites for cage fish farming in Mwanza Gulf, Lake Victoria. Aquacult. Fish Fish., 3(6): 472–286 **(15 pages)**.

Mair, G.; Halwart, M.; Derun, Y.; Costa-Pierce, B., (2023). A decadal outlook for global aquaculture. J. World Aquacult Soc., 54(2): 196–205 **(10 pages)**.

Minjoyo, H.; Rivaei, A.R.R.; Saputra, S.; Puja, Y.; Putro, D.H.; Dhoe, S.B.; Meiyana, M.; Antoro, S.; Slamet, B., (2024). Effect of stocking density on survival and growth of spiny sand lobsters Panulirus homarus in cages at 7-m depth. North Am. J. Aquacult., 86(4): 485–494 **(10 pages)**.

Norman, R.; Crumlish, M.; Stetkiewicz, S., (2019). The importance of fisheries and aquaculture production for nutrition and food security. Sci. Technol. Rev., 38(2): 395–407 **(13 pages)**.

Oldham, T.; Oppedal, F.; Dempster, T., (2018). Cage size affects dissolved oxygen distribution in salmon aquaculture. Aquacult. Environ. Interact., 10: 149–156 **(8 pages)**.

Ostrom, E., (2009). A general framework for analyzing sustainability of social-ecological systems. Science, 325(5939): 419–422 **(4 pages)**.

Radhakrishnan, E.V.; Phillips, B.F.; Achamveetil, G., (2019). Lobsters: Biology, Fisheries and Aquaculture. Springer, Singapore.

Porporato, E.M.D.; Pastres, R.; Brigolin, D., (2020). Site suitability for finfish marine aquaculture in the Central Mediterranean Sea. Front. Mar. Sci., 6: 772 **(12 pages)**.

Prayanti, M.; Lesmana, I.; Kristina, K.; Rusliadi, R., (2026). Growth and production performance of sand lobster (Panulirus homarus) cultured in floating net cages. Asian J. Aquat. Sci., 9(1): 108–117 **(10 pages)**.

Radiarta, I.N.; Saitoh, S.I.; Miyazono, A., (2008). GIS-based multi-criteria evaluation models for identifying suitable sites for Japanese scallop (Mizuhopecten yessoensis) aquaculture in Funka Bay, southwestern Hokkaido, Japan. Aquaculture, 284: 127–135 (9 pages).

Sampantamit, T.; Ho, L.T.; Lachat, C.; Goethals, P.L.M., (2020). Links and trade-offs between fisheries and environmental protection in relation to the Sustainable Development Goals in Thailand. Water. 12(2): 399 **(16 pages)**.

Sarkar, A.; Chowdhury, S.K.; Nahid, S.A.A.; Shimul, S.A.; Rana, S.; Jaber, M.Y.A., (2026). Toward spiny lobster (Panulirus spp.) aquaculture development in Bangladesh: lessons and insights from global research. Aquacult. Res., 2026(1): 7143949 **(22 pages)**.

Shahat, M.A.A.; Sayed, D.S.; Qorqor, M.M.; Abdel Hamed, H.N., (2026). An integrated framework for sustainable natural resources management in freshwater lakes. Global J. Environ. Sci. Manage., 12(4): 2061-2086 **(26 pages).**

Soeyanto, E.; Priyono, B.; Sudaryanto, A.; Fauzi, A.; Hadiyanto, H.; Nugroho, D.; Triwibowo, H.; Sahabuddin, M.; Nurhangga, E.; Handayani, D.P.; Himawati, S.; Morimoto, A., (2026). Seasonal wind forcing and hydrodynamic response as a predictor of ecological change: toward an early warning framework for semi-enclosed tropical bay waters. Reg. Stud. Mar. Sci., 97: 104959 **(17 pages)**.

Sun, X.; Wang, Y., (2024). Growth models in aquaculture for hybrid and natural groupers based on early development stage. Aquaculture. 578: 740026 **(12 pages)**.

Syahrir, S.; Prasetya, A.; Hasidu, L.O.A.F.; Saleh, R.; Riana, A.D.; Umar, N.A.; Yusuf, M., (2024). Suitability of floating net cage system of lobster cultivation site (Panulirus spp.) through Geographic Information System approach in Samaturu Sub-district, Kolaka District, Indonesia. Biodiversity. 25(11): 4105–4116 **(12 pages).**

Takarina, N.D.; Chuan, O.M.; Adiwibowo, A.; Adidharma, M.A., (2025). Modeling the shrimp aquaculture wastewater pollutant removals by clam shell using structural equation model. Global J. Environ. Sci. Manage., 11(1): 1-20 **(20 pages).**

Tho, N.; Ut, V.N.; Merckx, R., (2011). Physico-chemical characteristics of the improved extensive shrimp farming system in the Mekong Delta of Vietnam. Aquacult. Res., 42(11): 1600–1614 **(15 pages)**.

Trenggono, S.W.; Meilano, I.; Latief, H.; Diantara, S.D.; Sakti, W.I.; Ketaren, D.G.K.; Winata, I.N.P.; Yuwono, T.; Syamdidi; Arthatiani, F.Y.; Kasim, K.; Radiarta, I.N., (2025). Innovation in the blue economy and environmental sustainability in marine and fisheries strategy. Global J. Environ. Sci. Manage., 11(2): 497-518 **(22 pages).**

Vidya, K.; Joseph, S., (2012). Effect of salinity on growth and survival of juvenile Indian spiny lobster, Panulirus homarus (Linnaeus). Indian J. Fish., 59(1): 113–118 **(6 pages)**.

Wahjuningrum, D.; Effendi, I.; Hadiroseyani, Y.; Budiardi, T.; Diatin, I.; Setiawati, M.; Hastuti, Y.P.; Sudrajat, A.O.; Yonvitner; Nuryati, S.; Utami, P., (2022). Health status of spiny lobster Panulirus homarus with sub-mersible net cage system in the different depths at Kepulauan Seribu, DKI Jakarta. J. akuakultur Indones., 21(1): 68–80 **(23 pages)**.

Wahyono, H.D.; Santoso, A.D.; Goh, G.G.G.; Setiaji, G.; Yudo, S.; Sudinda, T.; Salim, M.A.; Kustianto, I.; Alhasa, K.M., (2026). An Integrated real-time water quality monitoring system for sustainable management in tropical reservoirs. Global J. Environ. Sci. Manage., 12(2): 873-896 **(24 pages).**

Zheng, C.; Zhao, Q.; Li, E.; Zhao, D.; Sun, S., (2021). Role of hypoxia in the behaviour, physiology, immunity and response mechanisms of crustaceans: A review. Rev. Aquacult., 14(2): 676–687 **(12 pages)**.

Zhou, F.; Mai, Q.; Yu, G.; Li, Y., (2026). Review and outlook for aquaculture of scalloped spiny lobster (Panulirus homarus). Aquat. Life Ecosyst., 2(1): 1 **(12 pages)**.

Zhu, L.; Li, L.; Liang, Z., (2009). Comparison of six statistical approaches in the selection of appropriate fish growth models. Chin. J. Oceanol. Limnol., 27: 457–467 **(11 pages)**.

Zuur, A.F.; Ieno, E.N.; Walker, N.J.; Saveliev, A.A.; Smith, G.M., (2009). Mixed effects models and extensions in ecology with R. Springer, New York.

AUTHOR (S) BIOSKETCHES

Winata, I.N.P., Ph.D. Candidate, Oceanography and Fisheries, Faculty of Earth Science and Technology, Bandung Institute of Technology. Jl. Ganesa No.10, Lb. Siliwangi, Kecamatan Coblong, Kota Bandung, Jawa Barat. Gedung Mina Bahari 2, 17th Floor, Jl. Merdeka Timur, Gambir, Jakarta Pusat, Indonesia.
- Email: *i.winata_itb@yahoo.com*
- ORCID: 0009-0008-9307-0783
- Web of Science ResearcherID: NA
- Scopus Author ID: 59743827100
- Homepage: https://itb.ac.id/fakultas-ilmu-dan-teknologi-kebumian

Radjawane, I.M., Ph.D., Instructor, Physical Oceanography, Bandung Institute of Technology, Jl. Ganesa No.10, Lb. Siliwangi, Kecamatan Coblong, Kota Bandung, Jawa Barat, Indonesia.
- Email: *ivonne.mradjawane@gmail.com*
- ORCID: 0000-0002-8116-3180
- Web of Science ResearcherID: AAD-7783-2021
- Scopus Author ID: 6507931445
- Homepage: https://fitb.itb.ac.id/ivonne-milichristi-radjawane-m-siph-d/

Nurdjaman, S., Ph.D., Instructor, Oceanography, Faculty of Earth Science and Technology, Bandung Institute of Technology. Jl. Ganesa No.10, Lb. Siliwangi, Kecamatan Coblong, Kota Bandung, Jawa Barat. Indonesia.
- Email: *susanna@itb.ac.id*
- ORCID: 0000-0001-7867-1451
- Web of Science ResearcherID: NA
- Scopus Author ID: 6506745840
- Homepage: https://itb.ac.id/fakultas-ilmu-dan-teknologi-kebumian

Radiarta, I.N., Ph.D., Researcher, Remote Sensing, Ministry of Marine Affairs and Fisheries – Gedung Mina Bahari 3, 7th Floor, Jl. Merdeka Timur, Gambir, Jakarta Pusat, Indonesia.
- Email: *radiarta@gmail.com*
- ORCID: 0000-0002-8798-1344
- Web of Science ResearcherID: NA
- Scopus Author ID: 24341932700
- Homepage: https://www.researchgate.net/profile/Nyoman_Radiarta

Sidik, D., M.Aq., Aquaculture Specialist, Ministry of Marine Affairs and Fisheries – Gedung Mina Bahari 2, 17th Floor, Jl. Merdeka Timur, Gambir, Jakarta Pusat, Indonesia.
- Email: *darmawan.sidik@kkp.go.id*
- ORCID: 0009-0006-8160-9134
- Web of Science ResearcherID: NA
- Scopus Author ID: NA
- Homepage: https://lpmukp.kkp.go.id/

Deby, M.Kom., Aquaculture Analyst, Ministry of Marine Affairs and Fisheries – Gedung Mina Bahari 2, 17th Floor, Jl. Merdeka Timur, Gambir, Jakarta Pusat, Indonesia.
- Email: *deby91@kkp.go.id*
- ORCID: 0009-0004-4093-6484
- Web of Science ResearcherID: NA
- Scopus Author ID: NA
- Homepage: https://lpmukp.kkp.go.id/

Pratiwi, S.K., S.Tr.Pi, Aquaculture Analyst, Ministry of Marine Affairs and Fisheries – Gedung Mina Bahari 2, 17th Floor, Jl. Merdeka Timur, Gambir, Jakarta Pusat, Indonesia.
- Email: *salsabilakusumaning@gmail.com*
- ORCID: 0009-0006-3164-8450
- Web of Science ResearcherID: NA
- Scopus Author ID: NA
- Homepage: https://lpmukp.kkp.go.id/

Makmur, S., Dr., Center for Biota System, Research Organization for Life Science and Environment, National Research and Innovation Agency,Kawasan Sains Teknologi Dr. (H.C) Ir. H. Soekarno, Jl. Raya Bogor KM. 46, Cibinong, 16911, West Java, Indonesia
- E-mail: *safranmakmur@gmail.com*
- ORCID: 0000-0002-2459-956X
- Scopus ID: 57212381250
- Web of Science ResearcherID: -
- Homepage: https://www.researchgate.net/profile/Safran-Makmur

Utama., A.A., Ph.D., Research Center for Biota System, Research Organization for Life Science and Environment, National Research and Innovation Agency,Kawasan Sains Teknologi Dr. (H.C) Ir. H. Soekarno, Jl. Raya Bogor KM. 46, Cibinong, 16911, West Java, Indonesia
- E-mail: *andr058@brin.go.id*
- ORCID: 0009-0003-0772-0107
- Scopus ID: 56412055300
- Web of Science ResearcherID: NA
- Homepage: https://www.researchgate.net/scientific-contributions/Andria-Ansri-Utama-2329588454

Suman, A., Dr., Researcher, Research Center for Biota System, Research Organization for Life Science and Environment, National Research and Innovation Agency,Kawasan Sains Teknologi Dr. (H.C) Ir. H. Soekarno, Jl. Raya Bogor KM. 46, Cibinong, 16911, West Java, Indonesia
- E-mail: *alis005@brin.go.id*
- ORCID: 0000-0002-0072-395X
- Scopus ID: 57195403371
- Web of Science ResearcherID: NA
- Homepage: https://scholar.google.com/citations?user=00NSGv8AAAAJ&hl=id

Husnah, Dr., Researcher, Research Center for Biota System, Research Organization for Life Science and Environment, National Research and Innovation Agency,Kawasan Sains Teknologi Dr. (H.C) Ir. H. Soekarno, Jl. Raya Bogor KM. 46, Cibinong, 16911, West Java, Indonesia
- E-mail: *husn008@brin.go.id*
- ORCID: 0000-0001-9260-305X
- Scopus ID: 18935073600
- Web of Science ResearcherID: NA
- Homepage: https://www.researchgate.net/scientific-contributions/Husnah-Samhudi-2168979432

HOW TO CITE THIS ARTICLE:
Winata, I.N.P.; Radjawane, I.M.; Nurdjaman, S.; Radiarta, I.N.; Sidik, D.; Deby; Pratiwi, S.K.; Makmur, S.; Utama, A.A.; Suman, A.; Husnah, (2027). Temporal water-quality variability and its implications for environmental management of sand lobster aquaculture. Global J. Environ. Sci. Manage., 12(3): 369-390.

DOI: 10.22034/gjesm.2027.01.17
URL: https://www.gjesm.net/article_735773.html

Global J. Environ. Sci. Manage. 13(1): 391-412, Winter 2027, Serial #49

Global Journal of Environmental Science and Management
(GJESM)

Homepage: https://www.gjesm.net/

Podcasts

ORIGINAL RESEARCH ARTICLE

Ecological drivers of *Hygrocybe* and *Xylaria* occurrences in a tropical Karst forest

S.H. Larekeng[1,2,*], A.H. Salman[2,3], H.A. Amanah[4], T. Grebenc[5], M.B. Akzad[2,6], M. Restu[2,6], M.D. Usman[7], R. Prayudyaningsih[2,8] Asrianny[1,9]

[1]*Karst Bioprospecting and Society Research Group LPPM Unhas, Hasanuddin University, Jl.Perintis Kemerdekaan, Tamalanrea Indah, Makassar, South Sulawesi, 90245 Indonesia*

[2]*Research Collaboration Center for Karst Microbes, Jl.Perintis Kemerdekaan, Tamalanrea Indah, Makassar, Sulawesi Selatan, 90245 Indonesia*

[3] *Doctoral Program of Forestry, Faculty of Forestry, Hasanuddin University. Jl. Perintis Kemerdekaan, Makassar, South Sulawesi, 90245 Indonesia*

[4]*Graduate School of Hasanuddin University, Jl. Perintis Kemerdekaan, Makassar, South Sulawesi, 90245 Indonesia*

[5]*Slovenian Forestry Institute, Večna pot 2, SI-1000 Ljubljana, Slovenia*

[6]*Faculty of Vocational, Hasanuddin University. Jl. Perintis Kemerdekaan, Makassar, South Sulawesi, 90245 Indonesia*

[7]*Program Study of Forestry Engineering, Faculty of Forestry, Hasanuddin University. Jl. Perintis, Indonesia*

[8]*Research Center for Applied Microbiology, Indonesia National Research and Innovation Agency. Jl. Raya Bogor-Jakarta, Cibinong, Bogor, 16912 Indonesia*

[9]*Department of Forest Conservation, Faculty of Forestry, Hasanuddin University, Jl. Perintis Kemerdekaan, Makassar, South Sulawesi, 90245 Indonesia*

ARTICLE INFO

Article History:
Received 21 June 2026
Revised 24 August 2026
Accepted 29 September 2026

Keywords:
Calcareous soil
Cation exchange capacity
Decomposer fungi
Ecological niche
Karst microhabitat
Lignicolous saprotroph
Soil-associated specialist

ABSTRACT

BACKGROUND AND OBJECTIVES: Tropical karst forests are characterized by heterogeneous microhabitats with nutrient-poor calcareous soils and dynamic microclimatic fluctuations that regulate macrofungal communities. Across such extreme environments, the fungal genera *Xylaria* and *Hygrocybe* exhibit divergent ecological strategies, functioning respectively as lignicolous saprotrophs and edaphic specialists. The study objectives were to evaluate the influence of edaphic and microclimatic variables on the occurrence and niche differentiation of *Hygrocybe* and *Xylaria* assemblages in the Maros–Pangkep karst forest of South Sulawesi, Indonesia.

METHODS: Macrofungal surveys and simultaneous environmental measurements were conducted across representative karst habitat transects. The analyzed edaphic parameters comprised soil potential of hydrogen, organic nitrogen, available phosphorus, exchangeable cations (calcium, magnesium, potassium and sodium), cation exchange capacity, base saturation, soil temperature, and soil moisture. The microclimatic parameters monitored included air temperature, relative humidity, and canopy light intensity. Principal Component Analysis was employed to determine multivariate environmental gradients, and Spearman's rank correlation analysis was applied to assess relationships between fungal abundance and individual environmental parameters.

FINDINGS: Eight macrofungal taxa were identified, comprising five *Xylaria* species (*Xylaria longipes, Xylaria longiana, Xylaria hypoxylon, Xylaria furcata*, and *Xylaria polymorpha*) and three *Hygrocybe* species (*Hygrocybe miniata, Hygrocybe flavescens*, and *Hygrocybe reesiae*). All *Xylaria* specimens, sampled across nine plots, were exclusively associated with decaying coarse woody debris, whereas every *Hygrocybe* specimens, recorded from five plots, was restricted to mineral soils substrates. Principal Component Analysis showed *Xylaria* occurrence aligned mainly with microclimatic gradients, explaining about ninety two percent of total variance, while *Hygrocybe* was more closely linked to soil chemical properties, explaining about eighty four percent of total variance. Spearman's rank correlation analyses revealed no statistically significant relationship between measured environmental parameter and *Xylaria* abundance. This pattern aligns with its established dependence on woody substrates, although specific substrate characteristics were not directly quantified. *Hygrocybe* abundance exhibited a nominally significant negative correlation with cation exchange capacity, aligning with an apparent affinity for nutrient-deficient substrates; however, this relationship warrants cautious interpretation owing to the limited sample size.

CONCLUSION: Microclimatic conditions and soil chemical properties potentially act in synergy to drive macrofungal niche differentiation in tropical karst forests. These findings establish critical baseline ecological indicators essential for biodiversity monitoring, habitat conservation, and the sustainable management of vulnerable karst ecosystems.

DOI:10. 22034.gjesm.2027.01.18

This is an open access article under the CC BY license (http://creativecommons.org/licenses/by/4.0/)

NUMBER OF REFERENCES	NUMBER OF FIGURES	NUMBER OF TABLES
38	6	9

*Corresponding Author:
Email: sittihalimah@unhas.ac.id
Phone: +62851 7150 7458
ORCID: 0000-0002-9749-9500

Note: Discussion period for this manuscript open until March 01, 2027 on GJESM website at the "Show Article".

INTRODUCTION

Macrofungi play a vital ecological role in tropical forest ecosystems as primary decomposers, pathogens, parasites, and symbiotic partners, driving nutrient cycling and maintaining the overall functional stability of the ecosystem (Chen *et al.,* 2018; Petre *et al.,* 2017)**.** Nevertheless, the spatial distribution, abundance, and community structure of macrofungi are notably heterogeneous, being strongly governed by the dynamics of specific micro-environmenta conditions. Canopy composition, available organic substrate, microclimatic fluctuations across the forest floor, and physicochemical soil properties function concurrently as ecological filters, constraining or facilitatingmycelial proliferation and the onset of sporocarp formation (Tuo *et al.,* 2022; Salman *et al.,* 2026). Within the broad functional spectrum of macrofungal communities, the genera *Hygrocybe* and *Xylaria* occupy highly distinct and contrasting ecological and morphological positions. The genus *Hygrocybe* (family Hygrophoraceae) is characterized by brightly pigmented fruiting bodies with a distinctive waxy texture (waxy caps). Ecologically, this genus exhibits pronounced sensitivity to both anthropogenic disturbances and environmental stochasticity; consequently, its biodiversity is frequently coupled with high habitat stability and the integrity of natural ecosystems (Griffith *et al.,* 2002; Lodge *et al.,* 2014). Notably, *Hygrocybe* frequently demonstrates a pronounced spatial preference for nutrient-deficient, marginal soil zones, rendering it a reliable bioindicator for evaluating ecosystem health and the severity of soil degradation. In contrast, the genus *Xylaria* (family Xylariaceae) exhibits a contrasting life strategy, as these fungi typically colonize decaying wood, thick litter, and dead plant tissue undergoing decomposition. As a group of saprotrophic fungi, *Xylaria* plays a crucial role in degrading lignocellulose complexes on the forest floor of tropical forests (Osono *et al.,* 2019). Beyond their established ecological role in the carbon cycle, multiple *Xylaria* species are recognized to exhibit an endophytic phase and synthesize bioactive secondary metabolites of substantial biotechnological and pharmaceutical value (Helaly *et al.,* 2018; Promputtha *et al*., 2010). The distribution patterns, abundance, and temporal occurrence of these two genera in the natural environment are governed by dynamic interactions between microclimatic factors (such as air temperature, humidity, and light intensity) and edaphic factors, such as soil potential of hydrogen (pH), cation exchange capacity (CEC) , and organic matter content) (Hu *et al.,* 2022). Spatial variations in these environmental parameters generate microhabitat heterogeneity, which dictates niche partitioning within fungal communities (Krah *et al.,* 2018). Although the impacts of edaphic and microclimatic variables on soil fungi have received extensive global documentation (Tedersoo *et al.,* 2014; Furtak and Gałązka, 2019), investigations into macrofungal ecology, particularly concerning the adaptive responses of the genera *Hygrocybe* and *Xylaria*, remains notably scarce within the distinctive ecosystems of tropical Indonesia. A prime setting characterized by environmental complexity ideally suited for this ecological study is the Maros-Pangkep Karst region. This high-conservation ecosystem features unique limestone topography, rapid drainage rates, and pronounced substrate heterogeneity (Duli and Mulyadi, 2019). Furthermore, variations in land cover and the structure of secondary vegetation within the Maros–Pangkep Karst region also modify local edaphic conditions, which in turn shape the structure of microbial communities, including macrofungi (Salman *et al.,* 2026; Mujio *et al.,* 2026). Research on macrofungi in Indonesia's karst regions is still dominated by inventory studies that focus on species composition and diversity, while studies on the ecological factors that control the structure of macrofungal communities remain relatively limited (Salman *et al.,* 2026). Globally, the spatial distribution of

macrofungi is governed by complex interactions among diverse environmental determinants, encompassing microclimatic regimes, edaphic properties, vegetation characteristics, and substrate availability (Lodge *et al.,* 2004; Sakti *et al.,* 2026). Specifically, the distribution of the genus *Xylaria* has been reported to be associated with moisture gradients and habitat characteristics (Thomas *et al.,* 2016), whereas *Hygrocybe* exhibits responses to differing soil and microenvironmental conditions across habitats (Halbwachs *et al.,* 2016; Kasim *et al.,* 2026). Nevertheless, to date, empirical evaluations examining the influence of microclimatic and edaphic variables on *Hygrocybe* and *Xylaria* assemblages within the Maros–Pangkep karst landscape remain absent. Consequently, this study addresses this knowledge gap by elucidating the relationships linking governing ecological factors to the community dynamics of these two genera in a tropical karst environment. The specific selection of the genera Hygrocybe and Xylaria as the focus of this study is based on their contrasting lifestyles and ecological adaptation strategies in response to nutrient limitations in karst ecosystems. These two genera are considered ideal models for examining how macrofungal communities partition space and resources through opposing functional pathways. The initial hypothesis of this study posits that Xylaria, functioning as a lignicolous saprotrophic fungus, would demonstrate substantial independence from variations in mineral soil chemistry due to its reliance on dead wood-derived lignocellulose as its primary carbon source. Conversely, *Hygrocybe* is strongly suspected to exhibit a strict ecological preference for nutrient-poor (oligotrophic) marginal soil zones, making it a natural habitat specialist that is highly sensitive to increases in soil chemical fertility. The adopted methodology is anticipated to yield a more comprehensive understanding of the ecological responses exhibited by the two target genera under varying environmental gradients within karst ecosystems (Legendre and Legendre., 2012). Therefore, this study focuses on analyzing the influence of edaphic and microclimatic factors on the distribution patterns of *Hygrocybe* and *Xylaria* communities in the Maros–Pangkep Karst region, with the aim of elucidating the environmental factors associated with the distribution of these two genera and providing scientific information to support a better understanding of the role of macrofungi in decomposition processes, nutrient cycling, and the management and conservation of tropical karst ecosystems. Employing a combination of principal component analysis (PCA) and Spearman's rank correlation, this study aims to identify the main environmental gradients and evaluate the relationships among edaphic properties, microclimatic conditions, and the *Hygrocybe* and *Xylaria* communities. This study has been contacted in the Maros–Pangkep karst region in South Sulawesi Province, Indonesia in 2025- 2026. All authentic specimens are deposited as official scientific reference vouchers at the Laboratory of Biotechnology and Tree Breeding, Faculty of Forestry, Hasanuddin University, Indonesia.

MATERIALS AND METHODS

The study is covering both the rainy and dry seasons. The entire process of collecting macrofungal samples and measuring environmental variables was carried out in an integrated manner in the Maros–Pangkep karst region in South Sulawesi Province, Indonesia (Fig. 1). Geographically, this karst landscape is situated at elevations ranging from 50 to 300 meters above sea level (masl) and is characterized by steep, complex limestone (karst) topography. Climatologically, this region features a humid microclimate characteristic of tropical rainforests, marked by mean annual temperatures of 26 to 30 degrees Celsius (°C), elevated vertical atmospheric moisture, and annual precipitation totals between 2,000 and 3,000 millimeters (mm). Edaphically, the limestone formations dominating this area create a very rapid internal drainage system, high



Fig. 1 : Geographical location of the study area along with the macrofungi sampling locations at Maros–Pangkep karst area, Indonesia

substrate heterogeneity, and variations in the canopy structure of secondary vegetation that directly influence the microhabitats of macrofungi.

Experimental design and sampling of macrofungi

Field sampling utilized an integrated approach combining purposive selection and transect methods to ensure representative assessment of the study area. Transects were established across environmental gradients within the Maros–Pangkep karst area. Along these transects, 20 × 20 meters (m) observation plots were established at locations where *Xylaria* or *Hygrocybe* fruiting bodies were recorded during field surveys. Field surveys were executed over three consecutive days per season (dry season of year 1; rainy season of year 2). Each daily sampling session resumed from the preceding day's terminus, thereby establishing a single continuous transect for each seasonal period. Observation plots (20 × 20 m) were established along this route at locations where fruiting bodies were recorded. A total of 14 observation plots were established, comprising nine plots in which *Xylaria* was recorded and five different plots in which Hygrocybe was recorded. These designated plots served as representative sampling sites for the purposes of this study. Comprehensive macrofungal surveys were conducted within each plot by examining the forest floor, soil surface, and accumulations of decaying wood and leaf litter that served as substrates for macrofungi. To maintain methodological consistency and comparability among sampling locations, macrofungal inventories and the documentation of micro-ecological attributes were performed using standardized sampling protocols. Macrofungal abundance was quantified as the total number of fruiting bodies of each taxon recorded within each

observation plot. Multiple fruiting bodies recorded within a single plot were consequently aggregated to establish plot-level abundance metrics, thereby avoiding pseudoreplication by preventing individual sporocarps from being treated as independent statistical observations. The observation plot was considered the independent sampling unit (n) for statistical analysis.

Taxonomic identification of macrofungi

The macroscopic features of fresh macrofungi fruiting bodies were recorded in detail in the field to serve as a primary identification database, including the shape, color, size, and surface texture of the cap (pileus); the type of gills (lamellae); the structure of the stem (stipe); and the presence of waxy coatings or specific exudates. Taxonomic identification was verified to the genus and species levels through morphological comparison with established monographs and standard field guides, including "guide to mushrooms" (Pacioni, 1982), "How to Identify Mushrooms to Genus I, II, and III: Macroscopic Features" (Largent, 1973), and "Edible and Poisonous Mushrooms of the World" (Hall *et al.*, 2003). Taxonomic nomenclature and validity were authenticated through digital verification against authoritative mycological databases, including MycoWeb, alongside peer-reviewed international scientific publications. The identification of macrofungal specimens was conducted using a morpho-taxonomic evaluation approach based on diagnostic morphological characters, including cap morphology, hymenophore structure, stipe characteristics, spore features, and overall macroscopic traits. Subsequent investigations incorporating molecular phylogenetic analyses are recommended in future studies to validate and confirm the taxonomic affinities of closely related species. The fruiting body collections were then dried using a dehydrator to be processed into dried specimens (herbarium specimens) for long-term taxonomic preservation and reference.

Measurement of edaphic variables (soil physical and chemical properties)

Soil characteristics were observed simultaneously at the same plots where macro fungi were found to detect accurate spatial correlations. In-situ soil physical parameters, specifically soil temperature and moisture, were quantified directly at each sampling plot using a calibrated digital soil tester. For the analysis of soil chemical properties, soil sampling was conducted destructively using the composite method, with samples collected from 5 sub-plot points (4 at the plot corners and 1 at the plot center) at a depth of 0–20 centimeters (cm). Additionally, undisturbed soil samples were collected non-destructively using a sample rings to facilitate standardized physical analysis. Subsequent laboratory preparation involved homogenizing, air-drying, and sieving all soil samples to quantify key chemical attributes, encompassing soil acidity (pH) (H_2O)], organic nitrogen content (N-organic), carbon-to-nitrogen ratio (C/N), available phosphorus (P_2O_5), soluble calcium (Ca), magnesium (Mg), potassium (K), sodium (Na), CEC, base saturation (BS), and calcium carbonate ($CaCO_3$) concentration.

Measurement of microclimate variables

To ascertain the specific microhabitats driving macrofungal proliferation, periodic measurements of microclimatic dynamics were recorded at the center of each sample plot. The microclimate variables measured included:

1. Air temperature (°C): Measured using a digital thermohygrometer placed at a height of approximately 1 meter above the forest floor to avoid direct heat bias from the ground.
2. Air humidity in percent (%): Measured simultaneously using a digital thermohygrometer along with air temperature measurements.
3. Light Intensity (lux): Measured on the forest floor surface above the fungal growth substrate using a calibrated digital lux meter, as an indicator of ambient light availability at the microhabitat level.

Statistical analysis

Raw data of microclimatic and edaphic variables collected from each observation plot were summarized using descriptive statistics (mean ± standard deviation). PCA, derived from a correlation matrix using Minitab (version 22), was utilized to investigate associations between environmental parameters and the sporocarp abundance of *Hygrocybe* and *Xylaria*. The correlation matrix was selected because the environmental variables were measured using different units such as; %, °C, pH, and milligram per kilogram (mg/kg), allowing standardized comparison among variables. PCA was performed separately for each genus and dataset, with n = 9 plots (*Xylaria*) and n = 5 plots (*Hygrocybe*), corresponding to variable-to-observation ratios of 4:9 (microclimate) and 12:9 / 12:5 (edaphic). Owing to these restricted ratios, PCA was implemented as an exploratory ordination method to delineate primary environmental gradients rather than as a confirmatory test. Interpretability was substantiated by the substantial cumulative variance accounted for by the initial two components, structural alignment with Spearman's rank correlations, and underlying ecological plausibility. For the Hygrocybe edaphic ordination, where variables (12) exceeded observations (n = 5), results are presented as a qualitative illustration only. To complement the multivariate analysis, pairwise relationships were assessed using Spearman's rank correlation coefficient (ρ) in IBM SPSS Statistics, with significance set at $P < 0.05$. Spearman's rank correlation was chosen because its non-parametric framework avoids assumptions of normality and exhibits resilience against outliers, rendering it well-suited for the modest sample sizes (n = 5-9) characteristic of this exploratory study. As plots were established only at locations where fruiting bodies were recorded, fungal abundance values were always ≥ 1, requiring no zero-handling transformation. The choice of microclimatic and edaphic parameters was informed by their documented significance in analogous macrofungi–environment studies (Tedersoo *et al.,* 2014; Krah *et al.,* 2018). Standard sampling adequacy tests (KMO, Bartlett's test) were not performed, as sample sizes (n = 5–9) were too small relative to the number of variables for reliable interpretation. The first two principal components were retained for two-dimensional biplot visualization rather than the Kaiser eigenvalue > 1 criterion; notably, the second component of the Xylaria-microclimate PCA had an eigenvalue of 0.9861, below this threshold. This selection was made to facilitate consistent two-dimensional interpretation of the major multivariate patterns across the datasets, while preserving comparability among the separately analysed genus-specific environmental variable combinations. PCAs were performed independently for each genus (*Xylaria*, *Hygrocybe*) across respective variable sets (microclimatic, edaphic). Although the outcomes are tabulated side-by-side for comparative clarity, each ordination represents a distinct, uncoupled statistical computation. PCA results are presented as loading plots (correlation-based ordination diagrams displaying variable vectors only, without individual plot scores), generated in Minitab version 22 using a correlation matrix (equivalent to standardized/scaled variables.

Ethical considerations and field permits

Field surveys, ecological observations, and sampling of soil and macro fungi fruiting bodies in the Maros–Pangkep karst region were conducted after obtaining official permission from local authorities and the relevant area managers. Macrofungal sampling and environmental parameter collection were executed with minimal disturbance to the local microecosystem, strictly adhering to regional biodiversity conservation policies. This study confirms that no protected or endangered species of flora or fauna were exploited or collected during field activities. Because this research involved neither human subjects nor vertebrate animals, formal institutional ethical approval was not required.

RESULTS AND DISCUSSION

Substrate composition and preferences

The survey successfully recorded two predominant macrofungi genera exemplifying distinct phyla and ecological strategies: *Xylaria* (Ascomycota) and *Hygrocybe* (Basidiomycota). From these two genera, eight species were identified based on morphological characters: *Xylaria longipes Nitschke, Xylaria longiana, Xylaria polymorpha, Xylaria hypoxylon, Xylaria furcata, Hygrocybe miniata, Hygrocybe flavescens,* and *Hygrocybe reesiae* (Fig. 2). A total of eight species of macrofungi representing two genera were recorded in the Maros–Pangkep karst forest, consisting of five species of *Xylaria* (Ascomycota: Xylariaceae) and three species of *Hygrocybe* (Basidiomycota: Hygrophoraceae) (Table 1). Specimen distributions exhibited strict substrate specificity: all recorded Xylaria taxa (*X. longipes*, *X. longiana*, *X. hypoxylon*, *X. furcata*, and *X. polymorpha*) were restricted to dead wood substrates, whereas every Hygrocybe representative (*H. miniata*, *H. flavescens*, and *H. reesiae*) occurred solely on edaphic substrates (Table 1). These findings reveal clear differences in substrate utilization between the two genera, indicating distinct ecological strategies for resource acquisition within the Maros–Pangkep karst ecosystem. Among the recorded taxa, the genus *Xylaria* is represented by a greater number of species than the genus *Hygrocybe*, indicating that lignicolous habitats are an important ecological component in the study area. The exclusive presence of Xylaria on dead wood reflects its role as a lignicolous saprotrophic fungus that primarily relies on lignocellulosic substrates as a carbon source. Taxa within this genus synthesize extracellular ligninolytic enzymes, specifically laccases and peroxidases, which efficiently degrade lignin and cellulose, facilitating the colonization of woody debris across diverse stages of decomposition (Osono, 2020). Consequently, the availability of dead wood, decaying branches, and tree stumps provides a substrate that supports the formation of *Xylaria* communities. Similar observations were reported by Purahong *et al.* (2017), who demonstrated that the quantity and decay stage of coarse wood debris significantly influence the composition and structure of lignicolous fungal communities in forest ecosystems. In contrast, all *Hygrocybe* species are found only on mineral soil and have not been observed on woody substrates. This pronounced substrate preference mirrors the ecological profile of *Hygrocybe*, widely recognized as an edaphic genus that predominantly occupies relatively undisturbed habitats characterized by oligotrophic conditions and environmental stability (Griffith *et al.,* 2002; Lodge *et al.,* 2014). Previous research has also shown that *Hygrocybe* species are sensitive to habitat disturbance, soil compaction, eutrophication, and changes in microenvironmental conditions, making them valuable ecological indicators for assessing habitat quality (Griffith *et al.,* 2002). The marked niche segregation in substrate utilization—wherein *Xylaria* colonizes lignocellulosic woody debris and *Hygrocybe* inhabits mineral soil—furnishes robust empirical support for spatial niche partitioning. This segregation mitigates interspecific competition for finite space and resources on the forest floor in harsh karst topography. This functional divergence facilitates the coexistence of both genera within heterogeneous karst environments, reflecting contrasting ecological adaptations and resource-allocation strategies (Boddy *et al.,* 2014; Lodge *et al*., 2014). This serves as an ecological foundation for further analysis evaluating the influence of edaphic and microclimatic variables on the abundance and distribution of these two genera. Direct, species-level comparisons with previous macrofungal inventories from other tropical karst forests remain limited, as prior studies in Indonesian karst regions have primarily been inventory-focused; the relatively modest number of taxa recorded here should therefore be interpreted in light of the limited sampling effort documented in this study rather than necessarily reflecting the true regional species richness of these genera. Because



Fig. 2. Macrofungi of the genera Xylariaceae and Hygrophoraceae found in the Maros-Pangkep Karst Region: A. *Xylaria longipes*, B. *Xylaria longiana*, C. *Xylaria hypoxylon*, D. *Xylaria furcata*, E. *Xylaria polymorpha*, F. *Hygrocybe miniata*, G. *Hygrocybe flavescens*, H. *Hygrocybe reesiae*.

Table 1 : *Xylaria* and *Hygrocybe* found in the Maros–Pangkep karst region

Phyllum	Family	Species	Substrates
Ascomycota	*Xylaria*ceae	*Xylaria longipes* Nitschke	Dead wood
Ascomycota	*Xylaria*ceae	*Xylaria longiana* Rehm	Dead wood
Ascomycota	*Xylaria*ceae	*Xylaria hypoxylon* (L.) Grev.	Dead wood
Ascomycota	*Xylaria*ceae	*Xylaria furcata* Fr.	Dead wood
Ascomycota	*Xylaria*ceae	*Xylaria polymorpha* (Pers.) Grev.	Dead wood
Basidiomycota	Hygrophoraceae	*Hygrocybe miniata (Fr.)* P. Kumm.	Soil
Basidiomycota	Hygrophoraceae	*Hygrocybe flavescens* (Kauffman) Singer	Soil
Basidiomycota	Hygrophoraceae	*Hygrocybe reesiae*	Soil

independent PCAs were executed for each genus using distinct variable sets derived from mutually exclusive, substrate-specific plots, the divergent loading configurations likely stem from intrinsic variations between wood- and soil-associated microhabitats rather than demonstrating an independent axis of niche partitioning beyond the aforementioned substrate segregation.

Microclimatic factors and their effects on macrofungi

Average microclimate conditions during the study period revealed characteristic environmental parameters (Table 2). The convergence of edaphic and physical parameters, particularly in karst ecosystems, revealed pronounced fluctuations in water retention driven by elevated rock porosity, a condition that fosters vegetative mycelial development and promotes sporocarp formation in macrofungi (Krah *et al.,* 2018). However, although the average conditions indicate an ideal environment, fluctuations in these microclimatic factors result in highly varied responses among fungal genera.

Table 2: Average climate in the Maros–Pangkep karst Region

Parameter	Average
Air temperature (°C)	26.6
Air humidity (%)	83.94
Light (lux)	362.71

PCA analysis shows that the distribution of the genus *Xylaria* exhibits different patterns of association with microclimate variables, namely air humidity, air temperature, and light intensity. Based on the loadings plot, the Xylaria vector is located in quadrant IV (PC1 = 0.272; PC2 = −0.887), whereas air humidity (PC1 = 0.598; PC2 = −0.001) and light intensity (PC1 = 0.559; PC2 = 0.015) are oriented toward the positive side of the PC1 axis at angles that are relatively smaller compared to the *Xylaria* vector. These findings reveal an apparent association linking *Xylaria* distribution with both ambient atmospheric humidity and illumination levels. Conversely, air temperature (PC1 = 0.507; PC2 = 0.461) forms a larger angle with the Xylaria vector due to a difference in direction on the second component (PC2), thus indicating a weak association (Fig. 3). This PCA interpretation is supported by the loading values (eigenvectors), where the second component (PC2) contributes more to distinguishing the position of *Xylaria* relative to air temperature than the first component (PC1) (Table 3). These results are consistent with the Spearman correlation analysis (Table 4). The correlation between Xylaria and air humidity showed a moderate positive relationship (ρ = 0.464; p = 0.208), while light intensity also showed a positive relationship, albeit a relatively weak one (ρ = 0.287; p = 0.454). In contrast, air temperature showed a weak negative relationship with *Xylaria* abundance (ρ = −0.268; p = 0.485). Despite directional concordance between the PCA and Spearman's rank correlations, none of the correlation coefficients achieved statistical significance (p > 0.05). Thus, the measured microclimatic factors cannot yet be considered primary predictors of *Xylaria* distribution at the study site, and the observed relationships are more accurately interpreted as ecological associations rather than deterministic influences. *Xylaria* is a group of Ascomycota that employs complex life strategies as both endophytes and saprotrophs. Following an endophytic phase within plant tissues, *Xylaria* can develop into decomposers on wood or litter; thus, the presence of fruiting bodies is not always determined by microclimatic conditions at the time of observation, but also by substrate availability and the stage of its life cycle (Thomas *et al.,* 2016). Owing to superior moisture retention and thermal buffering capacities, decomposing wood establishes a microclimate significantly more stable than the surrounding ambient atmosphere, thereby serving as a primary habitat for lignicolous fungi (Boddy, 2001; Heilmann-Clausen and Christensen, 2004). The positive relationship between *Xylaria* and air humidity indicates that more humid atmospheric conditions have the potential to support fruiting body formation, although this effect was not significant in this study. Although not directly quantified in this study, it is conceivable that atmospheric humidity assists in sustaining substrate moisture content and bolstering fungal physiological metabolism throughout the decomposition process. Conversely, the tendency toward a negative relationship with air temperature suggests that rising temperatures may reduce the microhabitat conditions optimal for fruiting body formation, although this effect is relatively weak. Experimental studies have shown that *Xylaria*'s growth and decomposition activities have specific optimal temperature ranges, whereas higher temperatures can alter enzymatic activity and decomposition efficiency (Osono *et al.,* 2011). *The* positive correlation with light intensity likely does not reflect a direct effect of light on Xylaria growth, but rather is related to the characteristics of the habitat where decomposing substrate is available. As a wood- and litter-decomposing fungus, the spatial distribution of *Xylaria* is more influenced by the presence of organic substrate than by light intensity itself. Consequently, light variations likely function as an indirect proxy for microenvironmental conditions associated with canopy architecture or substrate patchiness (Osono *et al.,* 2011). Overall, the PCA results indicate an exploratory relationship between *Xylaria* abundance and microclimate variables, with ordination patterns suggesting a relationship

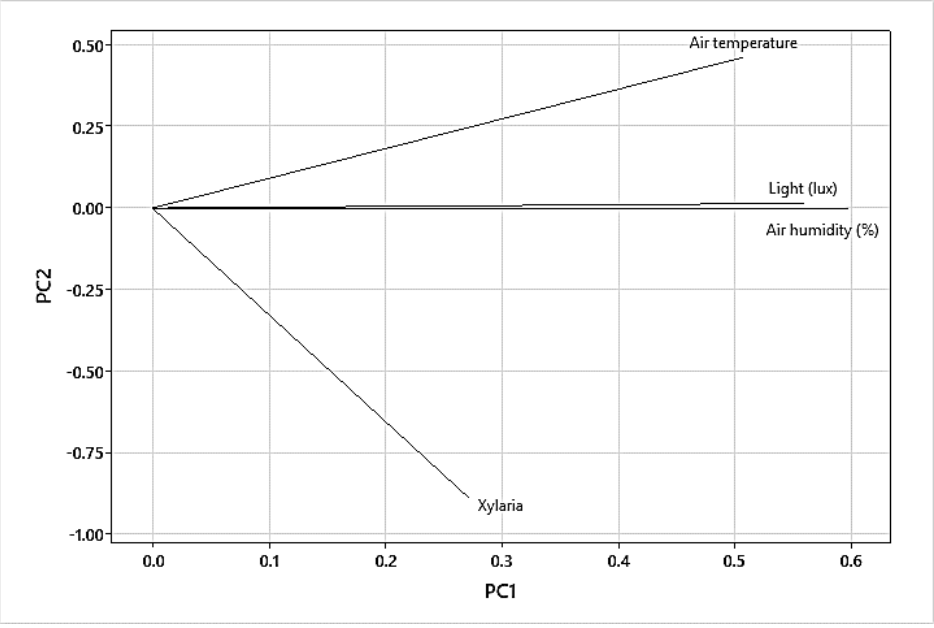

Fig. 3: A PCA loading plot showing the relationships between microclimatic variables and Xylaria in the Maros–Pangkep karst forest (Note: PC1 and PC2 explained 67.1% and 24.7% of the total variance, respectively, with a cumulative explained variance of 91.8%. The corresponding eigenvalues were 2.6856 for PC1 and 0.9861 for PC2)

Table 3: PCA eigenvector values of the microclimate factors associated with the occurrence of *Xylaria* and *Hygrocybe*

Variable	PC1	PC2	Variable	PC1	PC2
Xylaria	0.272	-0.887	*Hygrocybe*	0.380	-0.751
Air humidity	0.598	-0.001	Air humidity	-0.473	-0.633
Air temperature	0.507	0.461	Air temperature	-0.543	0.149
Light (lux)	0.559	0.015	Light (lux)	0.581	0.114

with air humidity and light intensity, as well as a pattern inversely related to air temperature. Nevertheless, subsequent Spearman's rank evaluations revealed no statistically significant associations among these variables. Therefore, these PCA patterns should be interpreted as exploratory ordination patterns, rather than as statistically supported relationships. The results of the study indicate that, within the sample plots, the microclimatic variables do not have a statistically significant relationship with *Xylaria* abundance. Rather than responding directly to immediate microclimatic fluctuations, the spatial distribution of this genus is likely governed by substrate properties, organic debris availability, and its dual ecological strategy as both an endophyte and a saprotroph, traits that confer broad environmental resilience across diverse habitats (Thomas *et al.,* 2016). PCA shows that *Hygrocybe* populations exhibit different responses to microclimate variables, namely air humidity, air temperature, and light intensity (Fig. 4). The loading plot shows that the Hygrocybe vector is located in quadrant IV (PC1 = 0.380; PC2 = –0.751), while light intensity is in quadrant I (PC1 = 0.581; PC2 = 0.114), air temperature in quadrant II (PC1 = –0.543; PC2 = 0.149), and air humidity in quadrant III (PC1 = –0.473; PC2 = –0.633). These positions

Table 4: Spearman's rank correlation between *Xylaria* and microclimatic variables in the Maros–Pangkep karst forest

Variable	Spearman's ρ	p-value
Air humidity	0.464	0.208
Air temperature	-0.268	0.485
Light (lux)	0.287	0.454

Note: ρ = Spearman's correlation coefficient; a relationship is considered significant if $p < 0.05$

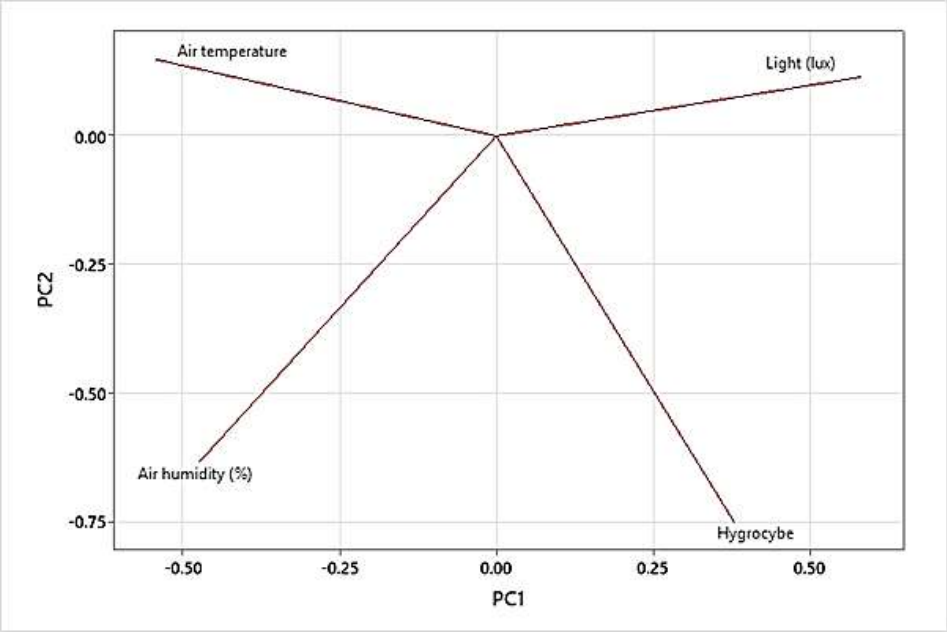

Fig. 4: A PCA loadings plot illustrating the relationship between microclimate variables and *Hygrocybe* in the Maros–Pangkep karst forest (Note: PC1 and PC2 explained 67.8% and 30.9% of the total variance, respectively, with a cumulative explained variance of 98.7%. The corresponding eigenvalues were 2.713 for PC1 and 1.236 for PC2)

indicate exploratory ordination patterns suggesting an association of *Hygrocybe* with light intensity and an opposite ordination pattern with air temperature and air humidity (Fig. 4). This interpretation is supported by the loading values (eigenvectors) on the two principal components (Table 3). *Hygrocybe* has a positive loading on PC1 (0.380) and a strongly negative loading on PC2 (–0.751). Light intensity also has a positive loading on PC1 (0.581) with a relatively small loading on PC2 (0.114), resulting in a relatively similar ordination direction to that of *Hygrocybe*. In contrast, air temperature has a negative loading on PC1 (–0.543) and a positive loading on PC2 (0.149), resulting in a different ordination direction from Hygrocybe. Furthermore, air humidity exhibits a divergent ordination trajectory (PC1 = –0.473; PC2 = –0.633), primarily driven by its inverse loading value along the PC1. These PCA patterns represent exploratory ordination associations rather than statistically supported relationships. The PCA patterns were then compared with Spearman's correlation analysis (Table 5). Light intensity exhibited a moderately strong positive correlation with *Hygrocybe* sporocarp abundance (ρ = 0.783; p = 0.118), whilst air temperature displayed a moderate inverse association (ρ = –0.530; p = 0.358). Air humidity also showed a negative correlation (ρ = –0.447; p = 0.450). Although the directional patterns observed in the PCA were generally consistent with the direction of the Spearman's correlation coefficients, none of these correlations were statistically significant (p > 0.05). In tropical forests, increased light intensity typically occurs in areas with greater canopy openings. Gaps in the forest canopy elevate soil surface temperature, accelerate litter decomposition, and modulate

Table 5: Spearman's rank correlation between Hygrocybe and microclimatic variables in the Maros–Pangkep karst forest

Variable	Spearman's ρ	p-value
Air humidity	-0.447	0.450
Air temperature	-0.530	0.358
Light (lux)	0.783	0.118

Note: ρ = Spearman's correlation coefficient; a relationship is considered significant if p < 0.05

local moisture availability, collectively establishing microenvironmental conditions favorable for sporocarp production in select Hygrocybe species. However, light is not a primary physiological factor for mycelial growth; rather, it serves as an indicator of changes in microhabitat conditions (Halbwachs *et al.,* 2013). This pattern indicates that *Hygrocybe* species in the Maros–Pangkep karst region are more frequently found in microhabitats characterised by a relatively open canopy or forest gaps, thereby allowing greater light penetration. Previous research has reported that waxcaps are generally found in habitats with low vegetation, relatively open canopy cover, and limited competition from vascular plants, including semi-natural grasslands and other open habitats (Griffith *et al.,* 2002; Boertmann, 2010). These habitat characteristics are considered to provide environmental conditions conducive to the emergence of waxcap fruiting bodies, although habitat preferences may vary between species (Halbwachs *et al.,* 2013). The inverse relationship observed between air temperature and the abundance of *Hygrocybe* fruiting bodies suggests that elevated temperatures precipitate a decline in yield. This pattern aligns with the physiological constraints characteristic of the Hygrophoraceae family, which typically proliferate in microhabitats defined by thermal stability and sustained humidity. Rising temperatures can accelerate evaporation and reduce water availability in both the soil surface layer and litter, thereby inhibiting basidiocarp formation (Halbwachs *et al.,* 2018). The combination of PCA (Fig. 4), loading values (Table 3), and Spearman's correlation (Table 5) reveals mutually supportive patterns: *Hygrocybe* tends to show a positive association with light intensity and a negative association with air temperature and humidity. However, However, given the lack of statistically significant correlations ($p > 0.05$), the results of this study indicate that local microclimatic conditions are not strongly associated with the spatial distribution or abundance of *Hygrocybe* species.

The interaction between soil properties and adaptation mechanisms (contrasting lifestyles)

The edaphic characteristics of the Maros–Pangkep karst region reflect typical limestone-derived soils characterized by moderate acidity and moderate CEC, however, they exhibit pronounced macronutrient limitations, as evidenced by low levels of organic nitrogen and base saturation (BS) (Table 6). PCA revealed that the distribution of the genus *Xylaria* exhibits distinct association patterns with the observed edaphic factors (Fig. 5). In the loading plot, the *Xylaria* vector is located in quadrant IV (PC1 = 0.121; PC2 = –0.492), while most soil chemical variables, such as pH, P_2O_5, Ca, Mg, K, Na, and BS are located on the positive side of the PC1 axis with relatively small PC2 values. The ordination pattern shows that *Xylaria* and the variables related to soil fertility occupy different positions along the PCA axes, with pH, P_2O_5, Ca, Mg, K, Na and BS generally oriented towards the positive side of PC1. This pattern illustrates an exploratory association between *Xylaria* and the soil fertility gradient across the sampling plots, rather than robust statistical significance. In contrast, soil moisture lies on the negative side of PC1 (PC1 = –0.124; PC2 = 0.183), resulting in a different ordination direction from that of *Xylaria*. This pattern suggests an exploratory association between *Xylaria* and soil moisture, diverging from the trends observed for soil fertility variables.

Table 6: Average profile of the physical and chemical characteristics of soils in the Maros–Pangkep karst region

Parameter	Average
pH	6.12
N organic (%)	0.15
P_2O_5 (ppm)	11.24
Ca in centimole per kilogram (cmol/kg)	5.35
Mg (cmol/kg)	0.86
K (cmol/kg)	0.24
Na (cmol/kg)	0.24
CEC (cmol/kg)	19.9
Base saturation (%)	33.47
Soil temperature (°C)	26.26
Soil moisture (%)	22

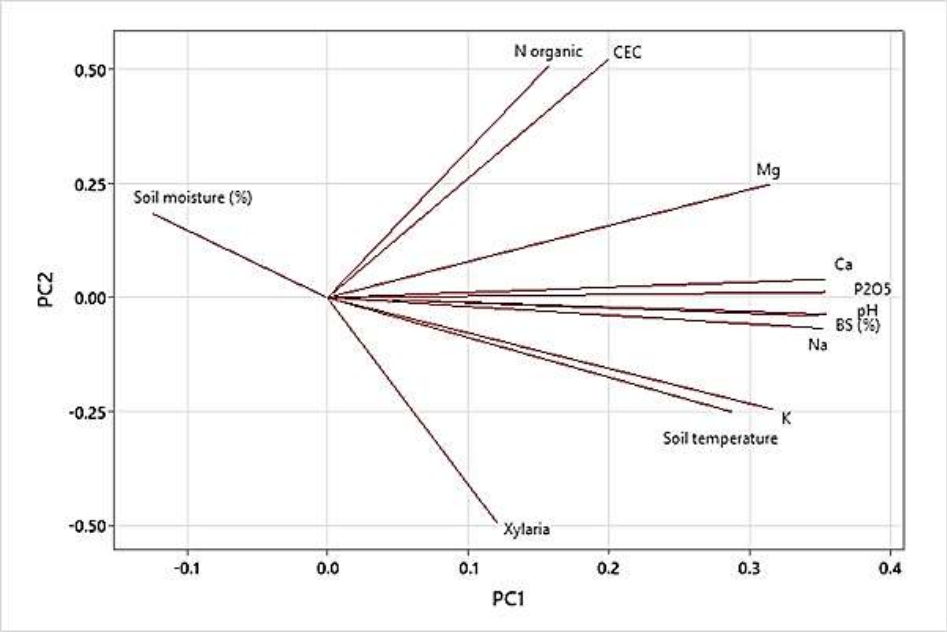

Fig. 5. A PCA loadings plot illustrating the relationship between edaphic factors and Xylaria in the Maros–Pangkep karst forest (Note: PC1 and PC2 explained 65.7% and 14.5% of the total variance, respectively, with a cumulative explained variance of 80.2%. The corresponding eigenvalues were 7.8860 for PC1 and 1.7425 for PC2)

The loading values (eigenvectors) (Table 7) support this interpretation. The variables pH (0.355; –0.036), P_2O_5 (0.354; 0.012), Ca (0.354; 0.041), Mg (0.314; 0.248), K (0.317; –0.245), Na (0.352; –0.067), and BS (%) (0.350; –0.040) are relatively aligned with the *Xylaria* vector on the first principal component (PC1), indicating that the occurrence of *Xylaria* fruiting bodies tends to increase at sites with higher soil fertility. Conversely, soil moisture has a negative loading value on PC1 (–0.124), so its position is opposite to that of *Xylaria*. Meanwhile, CEC and organic nitrogen had fairly high positive PC2 values (0.522 and 0.508, respectively), whereas *Xylaria* had a negative PC2 value (–0.492). The patterns observed in the PCA analysis were compared with the results of the Spearman's correlation analysis (Table 8). The Spearman's correlation analysis revealed a positive correlation between *Xylaria* abundance and pH (ρ = 0.262; p = 0.497), P_2O_5 (ρ = 0.232; p = 0.548), Ca (ρ = 0.186; p = 0.632), Mg (ρ = 0.186; p = 0.632), K (ρ = 0.439; p = 0.237), Na (ρ = 0.211; p = 0.586), and soil temperature (ρ = 0.331; p = 0.385). Conversely, negative correlations were observed between *Xylaria* abundance and soil moisture (ρ = –0.456; p = 0.218), CEC (ρ = –0.211; p = 0.586), BS (ρ = –0.152; p = 0.696), and organic nitrogen (ρ = –0.013; p = 0.974). Although the direction of some Spearman's correlation coefficients was generally consistent with the exploratory patterns observed in the PCA, none were statistically significant (p > 0.05). The PCA pattern revealed exploratory ordination relationships, whereas Spearman rank correlations indicated that no statistically significant associations between *Xylaria* abundance and the evaluated edaphic variables. This apparent discrepancy highlights the distinct analytical functions of the two methods: PCA functions as a descriptive, exploratory ordination technique that summarizes overall covariance without evaluating structure without testing statistical significance, whereas Spearman's rank correlation formally assesses pairwise

Table 7: PCA eigenvector values of the edaphic variables associated with the occurrence of *Xylaria* and *Hygrocybe*

Variable	PC1	PC2	Variable	PC1	PC2
Xylaria	0.121	-0.492	*Hygrocybe*	-0.114	0.511
pH	0.355	-0.036	pH	0.368	0.068
N organic	0.158	0.508	N organic	0.202	-0.486
P_2O_5	0.354	0.012	P_2O_5	0.279	-0.095
Ca	0.354	0.041	Ca	0.373	-0.003
Mg	0.314	0.248	Mg	0.171	-0.025
K	0.317	-0.245	K	0.367	-0.077
Na	0.352	-0.067	Na	0.334	0.055
CEC	0.200	0.522	CEC	-0.091	-0.542
BS (%)	0.350	-0.040	BS (%)	0.372	0.043
Soil temperature	0.287	-0.250	Soil temperature	0.189	0.422
Soil moisture (%)	-0.124	0.183	Soil moisture (%)	0.369	0.075

Table 8: Spearman's rank correlation between *Xylaria* and edaphic factors in the Maros–Pangkep karst forest

Variable	Spearman's ρ	p-value
pH	0.262	0.497
N organic	-0.013	0.974
Phosphorus pentoxide (P_2O_5)	0.232	0.548
Ca	0.186	0.632
Mg	0.186	0.632
K	0.439	0.237
Na	0.211	0.586
CEC	-0.211	0.586
BS (%)	-0.152	0.696
Soil temperature	0.331	0.385
Soil moisture (%)	-0.456	0.218

Note: ρ = Spearman's correlation coefficient; a relationship is considered significant if $p < 0.05$

relationship. Consequently, the PCA loading pattern should be interpreted as a non-significant, exploratory trends rather than definitive associations. As a lignocellulose decomposer, the presence of *Xylaria* is determined more by the availability of wood and litter substrates than by any single edaphic factor. Several *Xylaria* species can efficiently degrade lignin, cellulose, and hemicellulose, enabling them to proliferate across diverse soil conditions provided that sufficient organic substrate is available (Osono, 2020). The tendency toward a positive relationship between *Xylaria* and pH, P_2O_5, Ca, Mg, K, and Na also indicates that the presence of *Xylaria* fruiting bodies is not limited by low nutrient content at the study site. These elements contribute to sustaining microbial metabolic activity and enhancing organic matter decomposition of organic matter. However, given their relatively weak and statistically nonsignificant correlations, these factors likely function merely as supporting conditions, while the primary determinants of *Xylaria* distribution appear linked to the quality and availability of lignocellulosic substrate. Similar findings have been reported in various soil fungal communities, where edaphic variables generally account for only a small portion of the variation in fungal communities compared to habitat and vegetation factors (Detheridge *et al.,* 2018). The inverse trend between *Xylaria* abundance soil moisture indicates that sporocarp density is elevated in drier substrates. This pattern is ecologically plausible because most *Xylaria* species function as lignicolous saprotrophic that colonize coarse woody debris, twigs, stumps, and woody litter at various decomposition stages (Rogers, 2000). As wood-decaying fungi, the growth and decomposition activity of *Xylaria* depend on their ability to utilize lignocellulosic substrates through the production of extracellular enzymes; thus, the characteristics and microhabitat conditions of the substrate are key factors influencing colonization and fruiting body development (Ponting *et al.,* 2003). Consequently, elevated soil moisture does not invariably promote an increase in *Xylaria* fruiting body abundance. It is hypothesized that micro-moisture conditions within the substrate, rather than bulk soil moisture, exert a more pronounced influence on sporocarp formation, although substrate-level moisture was not directly measured in this study. Consequently, the inverse relationship observed

in this study suggests that suitable substrate availability is a more critical driver of *Xylaria* sporocarp emergence than soil moisture variations alone (Rogers, 2000; Pointing *et al.,* 2003). Overall, the PCA results (Fig. 5) and Spearman's correlation coefficients (Table 8) show mutually supportive patterns, namely a tendency toward a positive association between *Xylaria* and most soil fertility parameters (pH, P_2O_5, Ca, Mg, K, Na, and soil temperature), as well as a tendency toward a negative association with soil moisture, CEC, and organic nitrogen. However, given the lack of statistically significant correlations ($p > 0.05$), the results of this study suggest that microclimate variations are not strongly associated with the distribution of *Xylaria*. Instead, the distribution of this genus appears to be governed primarily by an interplay of substrate characteristics, vegetation attributes, and microhabitats, a pattern widely documented in ecological studies of macrofungi in tropical karst ecosystems (Salman *et al.,* 2026). PCA revealed that the fruit body distribution of *Hygrocybe* exhibits distinct patterns of association with edaphic factors (Fig. 6). On the loading plot, the Hygrocybe vector is located in quadrant II (PC1 = –0.114; PC2 = 0.511), while most soil chemical variables, such as pH, Ca, K, Na, BS (%), P_2O_5, soil moisture, and soil temperature, are on the positive side of PC1. Conversely, CEC aligns relatively closely with Hygrocybe due to shared negative PC1 scores, whereas organic N exhibits an opposing vector, particularly along the second principal component (Fig. 6). This interpretation is supported by the loading values (eigenvectors) for the two principal components (Table 7). *Hygrocybe* has loadings of PC1 = –0.114 and PC2 = 0.511, while pH (0.368; 0.068), Ca (0.373; –0.003), K (0.367; –0.077), Na (0.334; 0.055), BS (%) (0.372; 0.043), soil moisture (0.369; 0.075), and soil temperature (0.189; 0.422) are dominated by positive loadings on PC1. These spatial positions indicate that *Hygrocybe* exhibits an inverse relationship with the majority of soil fertility parameters. In contrast, CEC has a negative loading on PC1 (–0.091) and a negative loading on PC2 (–0.542); thus, although it differs on the second component, the same direction on PC1 indicates a relative proximity compared to the other variables. These PCA results are consistent with the Spearman correlation analysis (Table 9). Among all evaluated edaphic parameters, CEC alone exhibited strong, statistically significant inverse relationship with the abundance of *Hygrocybe* fruiting bodies ($\rho = –0.894$; $p = 0.041$). In contrast, soil temperature showed a fairly strong positive trend ($\rho = 0.783$; $p = 0.118$), though it was not yet significant. Soil moisture showed a weak negative correlation ($\rho = –0.224$; $p = 0.718$), while organic nitrogen also exhibited a moderate negative correlation ($\rho = –0.447$; $p = 0.450$). Other soil chemical parameters, such as pH, Ca, K, BS (%), and P_2O_5, showed very weak relationships, all of which were insignificant ($p > 0.05$). Consequently, the PCA and Spearman's correlation analyses provide complementary interpretations, demonstrating that no single edaphic factor robustly accounts for the variance in *Hygrocybe* sporocarp abundance, with the sole exception of a inverse tendency regarding CEC. The negative relationship between Hygrocybe and CEC indicates that the presence of *Hygrocybe* tends to decrease in soils with higher nutrient retention capacity. Elsewhere, *Hygrocybe* species particularly within semi-natural grassland ecosystems, have been documented as sensitive bioindicators of habitat integrity, low soil nutrient availability, and oligotrophic ecosystem stability (Griffith *et al*., 2002; Lodge *et al*., 2014; Halbwachs *et al*., 2018). Although the observation of a negative correlation between *Hygrocybe* abundance and CEC ($\rho = −0.894$, uncorrected $p = 0.041$; as stated in the Study Limitations) aligns with previously reported trends, limitations including a restricted sample size, a single edaphic variable, and tropical karst rather than grassland setting *Hygrocybe* as a preclude designating bioindicator in this system. Confirming this role would require broader evidence, including multiple independent sites, additional habitat variables, and replication across seasons.

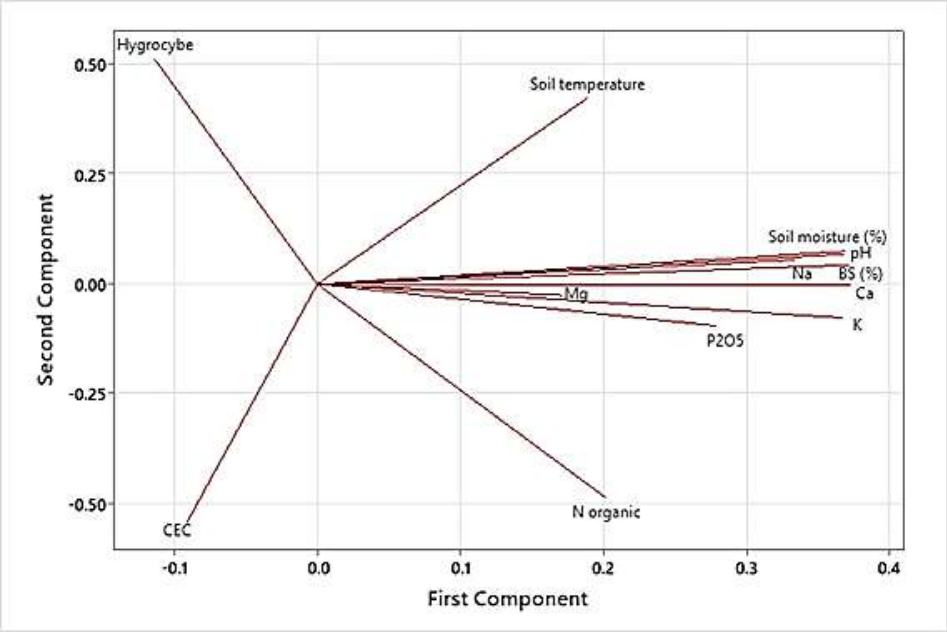

Fig. 6: A PCA loadings plot illustrating the relationship between edaphic factors and Hygrocybe in the Maros–Pangkep karst forest (Note: PC1 and PC2 explained 59.9% and 24.2% of the total variance, respectively, with a cumulative explained variance of 84.1%. The corresponding eigenvalues were 7.190 for PC1 and 2.896 for PC2)

Table 9: Spearman's rank correlation between *Hygrocybe* and edaphic factors in the Maros–Pangkep karst forest

Variable	Spearman's ρ	p-value
pH	-0.224	0.718
P_2O_5	0.112	0.858
Ca	-0.224	0.718
Mg	0.057	0.927
K	-0.224	0.718
Na	0.447	0.450
CEC	-0.894	0.041*
BS (%)	-0.224	0.718
Soil temperature	0.783	0.118
Soil moisture (%)	-0.224	0.718
N organic	-0.447	0.450

(Note: ρ = Spearman's correlation coefficient; a relationship is considered significant if $p < 0.05$)

Therefore, the negative correlation between CEC and *Hygrocybe* observed in this study likely reflects the ecological affinity of these fungi for nutrient-deficient soils, rather than indicating that CEC acts as a direct causal driver.The negative relationship between *Hygrocybe* and organic nitrogen is also consistent with the unique nutritional characteristics of the Hygrophoraceae family. Although the observed correlation was statistically nonsignificant (ρ = –0.447; p = 0.450), stable isotope analyses indicate that waxcaps utilize a nutritional strategy distinct from typical saprotrophic fungi. Evidence from $\delta^{13}C$ and $\delta^{15}N$ isotopes indicates that this group is likely biotrophic or root-endophytic and utilizes different sources of carbon and nitrogen than conventional saprotrophic fungi. Consequently, elevated soil organic nitrogen content is not invariably mirrored by an increase in *Hygrocybe* abundance, given that total nitrogen availability does not necessarily reflect the specific nitrogen sources assimilated by these fungi (Halbwachs *et al*., 2018). Although statistically nonsignificant, soil temperature exhibited a positive correlation trend (ρ = 0.783). These findings indicate that rising soil temperatures do not invariably suppress *Hygrocybe* fruiting body production at the study site. This pattern is likely attributable to local microhabitat conditions wherein thermal elevations remain within the optimal physiological threshold for basidiocarp development. Furthermore, soil temperature may also reflect differences in canopy openness or moisture

dynamics between plots and therefore cannot be interpreted as a direct influence on fungal physiology. Other parameters such as pH, Ca, K, Na, BS (%), and soil moisture showed a relatively weak relationship with the number of *Hygrocybe* fruiting bodies. These results demonstrate that variations in the measured soil chemical parameters do not fully account for the distribution of *Hygrocybe* at the study site. aligns with broader ecological evidence indicating that waxcaps occurrence is governed by multifaceted interactions among habitat conditions, land-management history, vegetative or bryophyte cover, microclimate, and specialized trophic strategies. Consequently, their spatial distribution cannot be explained by any single soil chemical property in isolation (Griffith *et al.,* 2002). Furthermore, the observed negative association with soil moisture suggests that increasing soil moisture may reduce oxygen availability within soil pores, thereby constraining aerobic fungal metabolism and mycelial respiration (Dighton, 2016). Although the correlation between *Hygrocybe* abundance and CEC was nominally significant ($\rho = -0.894$, $p = 0.041$), it was derived from only five plots and should be interpreted cautiously. This limited small sample size diminishes statistical power, rendering the correlation highly sensitive to individual data points. Furthermore, the unfavorable variable-to-observation ratio in the corresponding PCA (12 variables across 5 plots) restricts the robustness of multivariate patterns for this genus. Additionally, because CEC was one of 14 variables tested independently, the possibility of a false-positive result due to multiple testing cannot be excluded. As sampling was restricted to the Maros–Pangkep karst landscape, the generalizability of this finding to alternative ecosystems remains uncertain. The CEC–*Hygrocybe* association, though ecologically plausible given the known oligotrophic affinity of Hygrophoraceae, should therefore be regarded as preliminary and requiring confirmation with larger sample sizes. Furthermore, CEC, BS, and exchangeable cations (Ca, Mg, K, and Na) are chemically interrelated, as they collectively reflect the same underlying soil base-cation status, with soil pH exhibiting a well-documented covariation with this geochemical complex. Because independent Spearman correlations were conducted for each variable without accounting for this relatedness, the CEC–*Hygrocybe* correlation should not be interpreted as evidence of an independent, CEC-specific ecological driver, but rather as one indicator within a broader, intercorrelated soil fertility gradient. Sampling effort was restricted to a single continuous transect per season, surveyed over six field days over two seasons. Combined with the non-random, presence-based plot selection, this captures only a narrow spatial and temporal slice of macrofungal occurrence and should not be assumed to reflect the full spatial or seasonal variability of the Maros–Pangkep karst landscape. Due to the presence-based and purposive design of plot selection, the findings of this study should be interpreted as characteristic of the sampled locations rather than as being statistically representative of the broader Maros–Pangkep karst region. Microclimatic parameters were recorded as instantaneous single-point measurements per visit rather than continuous or diurnally-repeated readings, potentially failing to capture diurnal fluctuations in temperature and light. Combined with the limited number of sampling visits, this constrains the extent to which reported values reflect the full temporal variability relevant to fungal fruiting. Because no formal statistical procedure (e.g., a genus by-environment-interaction test) was performed to ascertain whether the contrasting environmental associations observed between Hygrocybe and Xylaria reflect genuine ecological divergence—as opposed to confounding artifacts of unequal sample size, detectability, or substrate availability, this comparison should be interpreted as descriptive rather than statistically confirmed. Most prior ecological studies of *Hygrocybe* and *Xylaria* originate from temperate or subtropical, non-karst systems; whether the substrate- and

CEC-associated patterns observed here operate similarly under tropical, calcareous karst conditions has not been directly established and represents an important direction for future comparative research across karst and non-karst tropical systems.

CONCLUSION

This study provides one of the first attempts to quantitatively link environmental variation to the occurrence of *Xylaria* and *Hygrocybe* within the Maros–Pangkep karst forest, an ecosystem that, despite its recognized ecological and geomorphological significance, remains substantially understudied with respect to its macrofungal communities. Past investigations of this landscape have focused primarily on taxonomic cataloging and distributional mapping. Building upon this baseline, the current research investigates potential microclimatic and edaphic gradients that may account for the distinct ecological trajectories and distribution patterns observed between the two genera. The selection of *Xylaria* and *Hygrocybe* as a comparative model was grounded in their fundamentally different substrate-use strategies: *Xylaria*, a lignicolous saprotroph reliant on decaying woody debris, and *Hygrocybe*, a genus widely reported as sensitive to soil fertility and associated with oligotrophic conditions in other ecosystems. The complete substrate exclusivity observed in this sample, wherein all recorded *Xylaria* specimens occurred dead wood, and all *Hygrocybe* specimens on mineral or lichen-covered soil, accords with anticipated ecological contrast. This pattern underscores the utility of the comparative framework for investigating substrate-driven niche partitioning in tropical karst environments, although confirmation via expanded sampling remains necessary given the presence-based nature of plot selection in this study. The absence of statistically significant associations between *Xylaria* abundance and any measured microclimatic or edaphic variable constitutes an informative result in its own right. This indicates that the primary environmental drivers governing lignicolous fungi in this ecosystem operate at the substrate level, encompassing wood decay stage, moisture retention , and host wood wood species identity, rather than at the level of ambient soil chemistry or general microclimate. As these substrate-level variables were not directly quantified in the present study, this interpretation remains a hypothesis rather than a demonstrated conclusion, and represents a specific, testable direction for future research. Conversely, the nominally significant negative correlation between *Hygrocybe* abundance and soil CEC provides preliminary, exploratory support for the oligotrophic preferences widely documented for this genus. Nevertheless, given the restricted sample size (n = 5), multiple testing across fourteen independent variables, and the geochemical collinearity of CEC with other base-cation metrics, this observation remains strictly hypothesis-generating rather than confirmatory, underscoring the need for replication via larger, more balanced sampling frameworks. Beyond these genus-specific patterns, this study illustrates several broader methodological considerations relevant to macrofungal ecology research in logistically challenging environments such as karst landscapes. Due to operational constraints—including rugged topography, restricted access, and limited fieldwork duration, a purposive, presence-based sampling strategy was adopted in lieu of a randomized or stratified design. Although this methodology facilitated the collection of ecologically informative data within practical boundaries, it concurrently restricts statistical power, spatial representativeness, and the broader generalizability of the findings across the Maros–Pangkep karst region. Future studies would benefit from expanded, spatially replicated sampling across multiple independent transects and seasons, systematic recording of absence as well as presence data, and the direct quantification of substrate-level and vegetation-

structural variables (including dead-wood volume, decay stage, canopy cover, litter depth, and land-use history) that could not be incorporated here. Where feasible, future investigations employing count-based statistical frameworks such as generalized linear models or generalized linear mixed models, alongside substantially expanded sample sizes, would facilitate a more rigorous and statistically robust identification of environmental drivers than the exploratory correlation, and ordination-based techniques necessitated by this preliminary study. Despite these limitations, this study offers ecologically meaningful, hypothesis-generating baseline information on the potential environmental associations of two contrasting macrofungal genera in an underexplored tropical karst ecosystem. Recognizing the profound susceptibility of karst landscapes to anthropogenic pressures such as habitat degradation, quarrying, and land conversion, baseline ecological surveys of this nature retain significant applied importance. They pinpoint prospective indicator taxa and environmental correlates that can shape the framework of subsequent, long-term monitoring initiatives, while highlighting the critical need to integrate both micro-substrate characteristics and soil chemistry into conservation planning for karst macrofungal communities. It should be emphasized that the patterns documented herein serve as a foundational baseline rather than a definitive characterization of, the ecological drivers governing macrofungal diversity in the Maros–Pangkep karst forest, and future studies are encouraged to expand upon these findings through more extensive, methodologically rigorous investigation.

AUTHOR CONTRIBUTIONS

S.H. Larekeng, the corresponding author, contributed to conceptualization, supervision, funding acquisition, project administration, resources, writing – review and editing. A.H. Salman, contributed to methodology, investigation, data curation, formal analysis, visualization, writing – original draft. H.A. Amanah, contributed to investigation, data curation, validation. T. Grebenc, contributed to methodology, validation, supervision, writing – review and editing. M.B. Akzad, contributed to data collection. M.D. Usman, contributed to resources, validation. M. Restu, contributed to formal analysis, visualization, writing – review and editing. R. Prayudyaningsih, contributed to conceptualization, supervision, validation, writing – review and editing. Asrianny, contributed to formal analysis, data curation. All authors have read and approved the final version of the manuscript.

ACKNOWLEDGEMENT

Authors would like to thank to the Indonesian Endowment Fund for Education (LPDP) on behalf of the Indonesian Ministry of Higher Education, Science and Technology, and managed under the EQUITY Program Contract No. [4307/B3/DT.03.08/2025] and [47103 / UN4.1/PM.01.01/2025]. TG was supported by Research Program P4-0107, Infrastructure Program I0-0012-0404, abd research project J4-70171.

CONFLICT OF INTEREST

The authors declare that there is no conflict of interest regarding the publication of this manuscript. In addition, the authors have fully addressed the ethical issues, including plagiarism, informed consent, misconduct, data fabrication and/or falsification, double publication and/or submission, and redundancy.

OPEN ACCESS

©2027 The author(s). This article is licensed under a Creative Commons Attribution 4.0 International License, which permits use, sharing, adaptation, distribution and reproduction in any medium or format, as long as you give appropriate credit to the original author(s) and the source, provide a link to the Creative Commons license,

and indicate if changes were made. The images or other third-party material in this article are included in the article's Creative Commons license, unless indicated otherwise in a credit line to the material. If material is not included in the article's Creative Commons license and your intended use is not permitted by statutory regulation or exceeds the permitted use, you will need to obtain permission directly from the copyright holder. To view a copy of this license, visit: http://creativecommons.org/licenses/by/4.0/

PUBLISHER'S NOTE

GJESM Publisher remains neutral with regard to jurisdictional claims in published maps and institutional affiliations.

NEGATIVE AI STATEMENT

The author(s) declare that no AI tools or services were used during the preparation of this work.

ABBREVIATIONS

%	Percentage
°C	Degrees Celsius
BS	Base saturation
Ca	Calcium
$CaCO_3$	calcium carbonate
CEC	Cation exchange capacity
cm	Centimeters
cmol/kg	Centimole per kilogram
K	Potassium
m	Meters
masl	Meters above sea level
mg/kg	Milligrams per kilogram
Mg	Magnesium
mm	Millimeters
N	Nitrogen
Na	Sodium
n	Sample size
P	Probability value
P_2O_5	Phosphorus pentoxide
PC	Principal component
PCA	Principal component analysis
pH	Potential of hydrogen
ppm	Part per million
Spearman's ρ	Spearman's rank correlation coefficient

REFERENCES

Boddy, L., (2001). Fungal community ecology and wood decomposition processes in angiosperms: from standing tree to complete decay of coarse woody debris. Ecol. Bull., 49: 43-56 **(14 pages)**.

Boddy, L.; Büntgen, U.; Egli, S.; Gange, A.C.; Heegaard, E.; Kirk, P.M.; Mohammad, A.; Kauserud, H., (2014). Climate variation effects on fungal fruiting. Fungal Ecol., 10: 20-33 **(14 pages).**

Boertmann, D., (2010). The genus *Hygrocybe*, 2nd ed. The Danish Mycological Society **(200 pages).**

Chen, Y.; Svenning, J.C.; Wang, X.; Cao, R.; Yuan, Z.; Ye, Y., (2018). Drivers of macrofungi community structure differ between soil and rotten-wood substrates in a temperate mountain forest in China. Front. Microbiol., 9: 37 (**9 pages).**

Duli, A.; Mulyadi, Y.; Rosmawati., (2019). The mapping out of Maros-Pangkep karst forest as a cultural heritage conservation. IOP Conference Serires: Earth Environ. Sci., 270 (1), 012014 **(19 pages).**

Detheridge, A.P.; Comont, D.; Callaghan, T.M.; Bussel, J.; Brand, G.; Gwyn-jones, D.; Scullion, J.; Griffith, G.W., (2018). Vegetation and edaphic factors influence rapid establishment of distinct fungal communities on former coal-spoil sites. Fungal Ecol., 33: 92-103 **(12 pages).**

Dighton, J., (2016). Fungi in ecosystem processes, 2nd ed. CRC Press, Boca Raton **(434 pages).**

Furtak, K.; Gałązka, A., (2019). Edaphic factors and their influence on the microbiological biodiversity of the soil environment. Adv. Microbiol., 58 (4): 375–384 **(10 pages).**

Griffith, G.W.; Easton, G.L.; Jones, A.W., (2002). Ecology and diversity of waxcap (*Hygrocybe* spp.) fungi. Bot. J. Scotl., 54 (1): 7–22 **(16 Pages)**.

Halbwachs, H.; Simmel, J.; Bässler, C., (2016). Tales and mysteries of fungal fruiting: How morphological and physiological traits affect a pileate lifestyle. Fungal Biol. Rev., 30(1): 36-61 **(26 pages).**

Halbwachs, H.; Dentinger, B.T.M.; Detheridge, A.P.; Karasch, P.; Griffith, G.W., (2013). Hyphae of waxcap fungi colonise plant roots. Fungal Ecol., 6(6): 487-492 **(6 pages)**.

Halbwachs, H.; Easton, G.L.; Bol, R.; Hobbie, E.A.; Garnett, M.H.; Persoh, D.; Dixon,L.; Ostle, N.; Karasch, P.; Griffith, G.W., (2018). Isotopic evidence of biotrophy and unusual nitrogen nutrition in soil-dwelling Hygrophoraceae. Environ. Microbiol., 20(10): 3573-3588 **(16 pages)**.

Hall, I.R.; Stephenson, S.L.; Buchanan, P.K.; Yun, W.; Cole, A.L.J., (2003). Edible and poisonous mushroom of the world. Timber Press, Portland **(369 pages).**

Heilmann-Clausen, J.; Christensen, M., (2004). Does size matter? on the importance of various dead wood fractions for fungal diversity in Danish beech forests. For. Ecol. Manage., (201): 105-117 **(13 pages).**

Helaly, S.E.; Thongbai, B.; Stadler, M., (2018). Diversity of biologically active secondary metabolites from endophytic and saprotrophic fungi of the ascomycete order Xylariales. Nat. Prod. Rep., 35(10): 992-1014 **(23 pages).**

Hu, J.-J.; Zhao, G.-P.; Tuo, Y.-L.; Qi, Z.-X.; Yue, L.; Zhang, B.; Li, Y., (2022). Ecological factors influencing the occurrence of macrofungi from eastern mountainous areas to the central plains of Jilin Province, China. J. Fungi., 8(8): 871 **(50 pages)**.

Kasim, K.; Nurdjaman, S.; Putri, M.R.; Saputra, T.A.; Hermawati, S.; Fikri, I.A.; Nugraha, B.R.D; Triharyuni, S., (2026). Oceanic environmental variability and fishing effort reallocation in data constrain small-scale fishery. Global J. Environ. Sci. Manage., 12(4): 1917-1940 **(24 pages).**

Krah, F.-S., Seibold, S., Brandl, R., Baldrian, P., Müller, J., Bässler, C., (2018). Independent effects of host and environment on the diversity of wood-inhabiting fungi. J. Ecol., (106):1428-1442 **(15 pages)**.

Largent, D.L., (1973). How to Identify Mushrooms to Genus I: Macroscopic Features. Mad River Press, Eureka **(86 pages)**.

Legendre, P.; Legendre, L., (2012). Numerical Ecology, 3rd ed. Elsevier, Amsterdam **(990 pages)**.

Lodge, D.J., Padamsee, M., Matheny, P.B., Aime, M.C., Cantrell, S.A., Boertmann, D., Kovalenko, A., Vizzini, A., Dentinger, B.T.M., Kirk, P.M., Ainsworth, A.M., Moncalvo, J.M., Vilgalys, R., Larsson, E., Lücking, R., Griffith, G.W., Smith, M.E., Norvell, L.L., Desjardin, D.E., Baroni, T.J., (2014). Molecular phylogeny, morphology, pigment chemistry and ecology in Hygrophoraceae (Agaricales). Fungal Divers., (64): 1-99 **(100 pages)**.

Lodge, D. J.; Ammirati, J. F.; O'Dell, T. E.; Mueller, G. M., (2004). Collecting and describing macrofungi. In: Mueler, G.M.; Bills, G.F.; Foster, M.S., (Eds), Biodiversity of Fungi: inventory and mmonitoring methods. Elsevier Academic Press. 128–158 **(31 pages)**.

Mujio.; Natsir, M.; Ermyanyla, M.; Rusdiana, O; Yanuadi, A., (2026). Socio-ecological transformation and biodiversity dynamics under agromaritime development. Global J. Environ. Sci. Manage., 12(4): 2041-2060 **(20 pages).**

Osono, T.; Hagiwara, Y.; Masuya, H., (2011). Effects of temperature and litter type on fungal growth and decomposition of leaf litter. Mycoscience., 52(50): 327-332 **(6 pages)**.

Osono, T.; To-Anun, C.; Hagiwara, Y.; Hirose, D., (2011). Decomposition of wood, petiole and leaf litter by Xylaria species from northern Thailand. Fungal Ecol., 4(3):210-218 **(9 pages)**.

Osono, T., (2019). Functional diversity of ligninolytic fungi associated with leaf litter decomposition. Ecol. Res., 35 (1): 30–43 **(14 pages)**.

Osono, T., (2020). Decomposition of organic chemical components in wood by tropical Xylaria species. J. Fungi., 6 (4): 186 **(8 pages).**

Pacioni, G., (1982). Simon and Schuster's Guide to mushrooms. Mycologia. 75 **(511 pages).**

Petre, C.V.; Dirtu, A.C.; Niculaula, M.; Tanase, C., (2017). Volatile compounds in the aroma of three species of wood rotting basidiomycetes and their antifungal potential. J. Plant Dev., 24: 73-83 **(11 pages).**

Promputtha, I.; Hyde, K.D.; Mckenzie, E.H.C.; Peberdy, J.F.; Lumyong, S., (2010). Can leaf degrading enzymes provide evidence that endophytic fungi becoming saprobes? Fungal Divers., 41: 89-99 **(11 pages).**

Purahong, W.; Pietsch, K.A.; Lentendu, G.; Schöps, R.; Bruelheide, H.; Wirth, C.; Buscot, F.; Wubet, T., (2017). Characterization of unexplored deadwood mycobiome in highly diverse subtropical forests using culture-independent molecular technique. Front. Microbiol., 8:574 **(17 pages).**

Pointing, S.B.; Parungao, M.M.; Hyde, K.D., (2003). Production of wood-decay enzymes, mass loss and lignin solubilization in wood by tropical Xylariaceae. Mycol. Res., 107(2) **(5 pages).**

Rogers, J.D., (2000). Thoughts and musings on tropical Xylariaceae. Mycol. Res., 104: 12 **(9 pages).**

Sakti, W.I.; Radjawane, I.M.; Latief, H.; Meilano, I.; Trenggono, S.W.; Diantara, S.D.; Wahyudin, R.A.; Radiarta, I.N.; Ketaren, D.G.K..; Winata, I.N.P.; Gusmawati, N.F.; Syamdidi; Yuwono, T.; Arthatiani, F.Y.; Maharani, S.; Fahira, N.D.; Kasim, K., (2026). Balancing ecological stability and economic growth under oceanographic variability and coastal interventions in fisheries systems. Global J. Environ. Sci. Manage., 12(3): 1263-1286 **(24 pages).**

Salman, A.H.; Restu, M.; Larekeng, S.H.; Prayudyaningsih, R., (2026). Vegetation structure, microclimate, and edaphic variables as determinants of macrofungi occurrence in the Maros-Pangkep Karst Area, Indonesia. Biodiversitas. 27: 3 **(12 pages).**

Tedersoo, L.; Bahram, M.; Sergei, P.; Kõljalg, U.; Yorou, N.S.; Wijesundera, R.; Ruiz, L.V.; Vasco-Palacios, A.M.; Thu, P.Q.; Suija, A.; Smith, M.E.; Sharp, C.; Saluveer, E.; Saitta, A.; Rosas, M.; Riit, T.; Ratkowsky, D.; Pritsch, K.; Pärtel, K.; Otsing, E.; Nouhra, E.; Njouonkou, A.L.; Nillson, R.H.; Morgado, L.N.; Mayor, J.; May, T.W.; Majuakim, L.; Lodge, D.J.; Lee, S.S.; Larrson, K.H.; Kohout, P.; Hosaka, K.; Hiiesalu, I.; Henkel, T.W.; Harend, H.; Guo, L.D.; Greslebin, A.; Grelet, G.; Geml, J.; Gates, G.; Dunstan, W.; Dunk, C.; Drenkhen, R.; Dearnaley, J.; Kesel, A.D.; Dang, T.; Chen, X.; Buegger, F.; Brearley, F.Q.; Bonito, G.; Anslan, S.; Abell, S.; Abarenkov, K., (2014). Fungal biogeography. global diversity and geography of soil fungi. Science. 28: 346 **(11 pages).**

Thomas, D.C.; Vandergrift, R.; Ludden, A.; Carrol, G.C.; Roy, B.A., (2016). Spatial ecology of the fungal genus *Xylaria* in a tropical cloud forest. Biotropica. 48; 381-393 **(13 pages).**

Tuo, Y; Rong, N.; Hu, J.; Zhao, G.; Wang, Y.; Zhang, Z.; Qi, Z.; Li, Y.; Zhang, B., (2022). Exploring the relationships between macrofungi diversity and major environmental factors in Wunvfeng National Forest Park in Northeast China. J. Fungi. 8: 98 **(39 pages).**

AUTHOR (S) BIOSKETCHES

Larekeng, S.H., Ph.D., Professor, Karst Bioprospecting and Society Research Group LPPM Unhas, Hasanuddin University, Jl.Perintis Kemerdekaan No. km 10, Tamalanrea Indah, Makassar, 90245, South Sulawesi, Indonesia. Research Collaboration Center for Karst Microbes, Jl.Perintis Kemerdekaan No. km 10, Tamalanrea Indah, Makassar, 90245, Sulawesi Selatan, Indonesia.

- Email: *sittihalimah@unhas.ac.id*
- ORCID: 0000-0002-9749-9500
- Web of Science ResearcherID: AAX-2682-2021
- Scopus Author ID: 57200256258
- Homepage: https://bachelor.forestry.unhas.ac.id/dosen/

Salman, A.H., S.Hut, Ph.D. Candidate, Doctoral Program of Forestry, Faculty of Forestry, Hasanuddin University, Jalan Perintis Kemerdekaan Km.10 Makassar, 90245, Indonesia.

- Email: *alihasansalman1213@gmail.com*
- ORCID: 0009-0003-7113-1606
- Web of Science ResearcherID: PMQ-1721-2026
- Scopus Author ID: 59728685900
- Homepage: https://forestry.unhas.ac.id/

Amanah, H.A., Ph.D., Assistant Professor, Graduate School of Hasanuddin University, Jl. Perintis Kemerdekaan Km.10 Makassar, 90245, South Sulawesi, Indonesia.

- Email: *hafizhah.al.amanah@unhas.ac.id*
- ORCID: 0000-0002-4333-185X
- Web of Science ResearcherID: NA
- Scopus Author ID: 59728685900
- Homepage: https://portal.pasca.unhas.ac.id/study-program/

Grebenc, T., Ph.D., Senior Scientist, Slovenian Forestry Institute, Večna pot 2, SI-1000 Ljubljana, Slovenia.

- Email: *tine.grebenc@gozdis.si*
- ORCID: 0000-0003-4035-8587
- Web of Science ResearcherID: NA

- Scopus Author ID: 12041279200
- Homepage: https://www.gozdis.si/en/

Akzad, M.B., M.Hut., Researcher, Karst Bioprospecting and Society Research Group LPPM Unhas, Hasanuddin University, Jl.Perintis Kemerdekaan No. km 10, Tamalanrea Indah, Makassar, 90245, South Sulawesi, Indonesia. Research Collaboration Center for Karst Microbes, Jl.Perintis Kemerdekaan No. km 10, Tamalanrea Indah, Makassar, 90245, Sulawesi Selatan, Indonesia.
- Email: *bimamuhammadakzad@gmail.com*
- ORCID: 0000-0001-7137-3750
- Web of Science ResearcherID: NA
- Scopus Author ID: NA
- Homepage: https://trg.unhas.ac.id/karstbios/

Restu, M., Ph.D., Professor, Research Collaboration Center for Karst Microbes, Jl.Perintis Kemerdekaan No. km 10, Tamalanrea Indah, Makassar, 90245, Sulawesi Selatan. Faculty of Vocational, Hasanuddin University. Jl. Perintis Kemerdekaan Km.10 Makassar, 90245, South Sulawesi, Indonesia.
- Email: *tueid@yahoo.com*
- ORCID: 0000-0002-9434-5194
- Web of Science ResearcherID: NA
- Scopus Author ID: 57200256044
- Homepage: https://trg.unhas.ac.id/karstbios/

Usman, M.D., Researcher, Program Study of Forestry Engineering, Faculty of Forestry, Hasanuddin University. Jl. Perintis Kemerdekaan No. km 10, Tamalanrea Indah, Makassar, 90245, Sulawesi Selatan, Indonesia.
- Email: *didinmks0504@gmail.com*
- ORCID: 0009-0008-2803-8621
- Web of Science ResearcherID: NA
- Scopus Author ID: NA
- Homepage: https://engineering.forestry.unhas.ac.id/

Prayudyaningsih, R., Ph.D., Associate Professor, Principal Researcher, Research Collaboration Center for Karst Microbes, Jl.Perintis Kemerdekaan No. km 10, Tamalanrea Indah, Makassar, 90245, Sulawesi Selatan. Research Center for Applied Microbiology, Indonesia National Research and Innovation Agency. Jl. Raya Bogor-Jakarta km. 47, Cibinong 16912, Bogor, Indonesia.
- Email: *retno.prayudyaningsih@brin.go.id*
- ORCID: 0000-0003-3604-5406
- Web of Science ResearcherID: E-6349-2018
- Scopus Author ID: 57211188858
- Homepage: https://brin.go.id

Asrianny, I., Ph.D., Associate Professor, Karst Bioprospecting and Society Research Group LPPM Unhas, Hasanuddin University, Jl.Perintis Kemerdekaan No. km 10, Tamalanrea Indah, Makassar, 90245, South Sulawesi, Indonesia. Department of Forest Conservation, Faculty of Forestry, Hasanuddin University, Jl. Perintis Kemerdekaan Km.10 Makassar, 90245, South Sulawesi, Indonesia.
- Email: *asrianny@unhas.ac.id*
- ORCID: 57218363864
- Web of Science ResearcherID: GQQ-8540-2022
- Scopus Author ID: 6742781
- Homepage: https://forestry.unhas.ac.id/

HOW TO CITE THIS ARTICLE:
Larekeng, S.H.; Salman, A.H.; Amanah, H.A.; Grebenc, T.; Akzad, M.B.; Restu, M.; Usman, M.D.; Prayudyaningsih, R.; Asrianny, (2027). Ecological drivers of Hygrocybe and Xylaria occurrences in a tropical Karst forest. Global J. Environ. Sci. Manage., 13(1): 391-412.

DOI: 10.22034/gjesm.2027.01.18
URL: https://www.gjesm.net/article_736244.html

Global J. Environ. Sci. Manage. 13(1): 413-432, Winter 2027, Serial #49

Global Journal of Environmental Science and Management
(GJESM)

Homepage: https://www.gjesm.net/

Podcasts

CASE STUDY

Consumer awareness, participation, and accessibility in sustainable electronic waste management

D. Fitria[1], D.R. Nugraheni[1], H. Herdiansyah[2,*], M. Qamruzzaman[3]

[1]Social Environment, Community Engagement, and Environmental Economics Research Cluster, Graduate School of Sustainable Development, Universitas Indonesia, Jalan Salemba Raya, Jakarta Pusat, DKI Jakarta 10430, Indonesia

[2]Department of Environmental Science, Graduate School of Sustainable Development, Universitas Indonesia, Jalan Salemba Raya, Jakarta Pusat, DKI Jakarta 10430, Indonesia

[3]School of Business and Economics, United International University, Dhaka 1212, Bangladesh

ARTICLE INFO

Article History:
Received 29 June 2026
Revised 02 September 2026
Accepted 03 October 2026

Keywords:
Electronic waste
Environmental awareness
Household participation
Recycling facilities
Waste management system

DOI:10. 22034.gjesm.2027.01.19

ABSTRACT

BACKGROUND AND OBJECTIVES: The rapid increase in electronic waste has created increasingly complex environmental and health challenges, especially in developing countries like Indonesia. The study objectives were to examine how household awareness and accessibility of electronic-waste management facilities are associated with consumer participation, controlling for socioeconomic factors, demographics, and the region's spatial characteristics.

METHODS: This study uses a quantitative, cross-sectional survey design to examine household consumers living near electronic waste management facilities in Indonesia. To analyze the data, Spearman's rank correlation was employed to evaluate variable relationships, ordinary least squares regression to estimate the associations of awareness and accessibility with participation levels, Kruskal-Wallis test to examine group differences, and Geographic Information System-based spatial analysis to describe the spatial patterns of facility distance, accessibility, and electronic waste management participation.

FINDINGS: Consumer awareness of the consequences of electronic waste showed a significant positive correlation with the intention to manage electronic waste, with a correlation coefficient of 0.340, but showed no significant correlation with actual behavior, with a correlation coefficient of only 0.067. Accessibility showed a significant positive correlation with both intention and actual behavior, with correlation coefficients of 0.197 and 0.416, respectively. Accessibility had the largest reported regression coefficient for actual behavior (β = 0.449), followed by awareness of consequences (β = 0.182). The Kruskal-Wallis test confirmed significant differences in intention and actual behavior across accessibility levels, with chi-square values of 11.67 and 35.91, respectively. Spatial analysis using the nearest neighbor method produced a nearest neighbor ratio of 0.60 with a z score of -10.01. Spatial analysis revealed that highly aware and active residents are significantly clustered rather than randomly dispersed, with the vast majority residing within a functional catchment area defined by 10 to 30 kilometer distances or 10 to 30 minute travel times from e-waste facilities.

CONCLUSION: The findings underscore the need for electronic waste management policies that prioritise facility accessibility and spatially based approaches to strengthen community participation within a circular economy framework.

This is an open access article under the CC BY license (http://creativecommons.org/licenses/by/4.0/)

NUMBER OF REFERENCES	NUMBER OF FIGURES	NUMBER OF TABLES
64	3	9

*Corresponding Author:
Email: herdis@ui.ac.id
Phone: +622131930251
ORCID: 0000-0003-2684-3551

Note: Discussion period for this manuscript open until March 01, 2027 on GJESM website at the “Show Article”.

INTRODUCTION

The rapid growth in the consumption of electronic devices has made electronic waste (e-waste) one of the fastest-growing waste streams globally (Baldé *et al.,* 2022, 2024; Arumbinang, 2026). Electronic waste (E-waste) contains various hazardous materials, such as heavy metals and toxic chemical compounds, which have the potential to cause severe impacts on the environment and human health if not managed properly (Ankit *et al.,* 2021; Parvez *et al.,* 2021; Ghulam and Abushammala, 2023; Jain *et al.,* 2023; Bhardwaj *et al.,* 2025). Throughout developing economies such as Indonesia, e-waste management remains heavily constrained by institutional and behavioral barriers, frequently leading to significant volumes of discarded electronics to bypass formal channels and terminate in municipal landfills, informal processing nodes, or indefinite domestic storage devoid of treatment (Islam *et al.,* 2021; Andeobu *et al.*, 2023; Jain *et al.,* 2023; Bhardwaj *et al.,* 2025). From an ecological anthropology perspective, behavioral patterns in e-waste management are inseparable from everyday household practices and the social meanings attached to electronic devices (Ebo, 2026). Unused devices are often stored as spare parts because they are considered to have value still and are therefore not immediately treated as waste. Practices like these demonstrate that e-waste management decisions result from negotiations among individual awareness, household norms, and structural conditions within the human waste management system (Harafah *et al.*, 2026; Heeks *et al.,* 2015; Almulhim, 2022; Arya and Kumar, 2020; Wickramasingha *et al.,* 2025). Achieving long-term circular economy objectives depends fundamentally on active consumer engagement—comprising both behavioral intent and practical execution—in sustainable e-waste practices, such as source separation, authorized facility utilization, and community initiatives, all of which form a critical foundation for overarching system efficiency (Duckworth and Gross, 2020; Alhassan *et al.,* 2020; Koshta *et al.,* 2022). However, several studies have found that the level of public participation often does not align with their level of awareness of the negative impacts of e-waste (Attia *et al.*, 2021; Islam *et al.*, 2021; Garg *et al.,* 2023; Muthukumari *et al.*, 2024; Kosarkar and Barthwal, 2025; Zia and Sukri, 2025). In fact, consumer awareness of the environmental and health risks posed by e-waste is a crucial cognitive factor associated with pro-environmental behavioral tendencies (Wibowo *et al.,* 2022; Liang *et al.*, 2024). Furthermore, awareness alone is insufficient to encourage active participation unless supported by adequate external conditions. One of the most frequently cited external factors is access to e-waste management facilities, including distance, travel time, ease of access, availability of information, and convenience of use (Sari *et al.*, 2021; Michael *et al.*, 2025; Wirtu *et al.*, 2025). Evidence from Frigo *et al*. (2025) indicates that residential waste collection is consistently underreported even by households located within a 100-meter radius, illustrating that operational impediments extend beyond mere spatial proximity to encompass economic travel burdens, transit availability, and logistical convenience. This aligns with previous research by Abha *et al.,* (2025) that found that high travel costs and limited transportation options prevent low-income households from recycling electronic waste (Borthakur and Singh, 2021). In Indonesia, accessibility difficulties in the distribution and management of e-waste are known to remain very high. Consumers living near recycling facilities tend to have greater opportunities to participate than those living in areas with limited access (Sari *et al.*, 2021; Michael *et al.*, 2025; Haq, 2026). Building upon these framework conditions, this investigation evaluates consumer awareness and facility accessibility as factors associated with household behavioral intent and active participation in sustainable e-waste management, while controlling for sociodemographic profiles

(Azkiyah, 2026). Geographic information systems (GIS), as an analytical tool for understanding the dynamics of accessibility in e-waste management and the factors that influence it, is used as one approach in this framework (Nuwematsiko *et al.,* 2021). GIS can serve as a powerful tool when integrated with non-spatial criteria (Cheng *et al.,* 2024; Bante *et al.*, 2025), where specific GIS analyses such as weighted overlay analysis and kernel density estimation have proven effective in resolving and balancing conflicting interests (Bante *et al.*, 2025). GIS serves not only to visualize data but also to bridge the gap between designed policies and actual practices by providing actionable solutions. Ultimately, operationalizing this methodological framework seeks to generate robust empirical backing for inclusive, circular-economy-aligned e-waste policies, while concurrently advancing a deeper analytical understanding of electronic waste management efficacy throughout Indonesia. In the value-belief-norm (VBN) theory, environmental values and beliefs are described as being related to consumers' personal norms and intentions to engage in e-waste management practices (Yeh *et al.,* 2024; Yang *et al.,* 2025). In this study, VBN is used as an interpretive perspective for understanding the potential relevance of environmental awareness to behavioral intention rather than as a framework for empirically testing normative mechanisms. However, this study attempts to integrate it with another approach, namely the environmental behavior approach from ecological anthropology, which views consumer participation (intention and actual behavior) as being related to cognitive, structural, and contextual factors (Vijayan *et al.,* 2023). Consumer awareness of e-waste issues is positioned as an internal factor associated with attitudes and behavioral tendencies, while the accessibility of e-waste management facilities is an external factor associated with opportunities for participation (Linder *et al.*, 2021; Michael *et al.*, 2025; Arain *et al.,* 2025). Rather than functioning as a directly tested empirical mechanism in this study, environmental awareness is conceptualized through this methodological amalgamation as an underlying psychological disposition reflecting individual readiness for electronic waste engagement (Maphosa and Maphosa, 2022). Previous studies have also reported associations between participation and the accessibility of facilities, which may be relevant to opportunities for e-waste management participation (Linder *et al.*, 2021; Asibey *et al.*, 2022; Nawaz *et al.*, 2025; Harnita, 2025). Here, sociodemographic factors can serve as control variables in examining the associations among awareness, accessibility, and participation. Furthermore, spatial dimensions are integrated as core analytical parameters, treating both physical distance and transit duration to e-waste infrastructure as vital factors related to regional disparities in public participation capacity (Rusni, 2025). By integrating GIS-based spatial analysis, this theoretical framework provides a spatial description of geographic patterns in relation to awareness, accessibility, intention, and participation in sustainable e-waste management (Arsanti *et al.,* 2024; Yalcinkaya and Kaleli, 2025). Thus, the theoretical framework of this study positions household consumers' participation in e-waste management as a multidimensional phenomenon associated with individual awareness, perceived accessibility, and spatial conditions. Rather than evaluating mediation, moderation, or direct causal pathways, these theoretical frameworks serve to ground the empirical associations identified herein. Accordingly, this study evaluates household e-waste engagement by integrating risk awareness, perceived infrastructural accessibility, behavioral intent, self-reported actions, core sociodemographic attributes, and spatial dispersion patterns. This study aims to: 1) examine the associations between awareness of e-waste consequences, perceived facility accessibility, behavioral intention, and self-reported actual behavior; 2) estimate the associations of awareness and perceived accessibility with the two behavioral outcomes after adjustment for

selected sociodemographic characteristics; 3) compare behavioral intention and actual behavior across accessibility groups; and (4) describe the spatial pattern of the observations included in the GIS analysis. The study was conducted in Surabaya City, East Java Province, Indonesia, in 2025.

MATERIALS AND METHODS

Research design and location

This study employed a quantitative, cross-sectional survey design to examine associations among awareness of e-waste consequences, perceived accessibility of e-waste management facilities, behavioral intention, and self-reported actual behavior. Owing to the cross-sectional nature of the research design—capturing exposure, perceptions, and outcomes simultaneously—the empirical outcomes are interpreted strictly as associative relationships rather than direct causal effects. Cross-sectional studies are useful for estimating relationships and describing patterns but cannot establish temporal precedence or causal direction (Capili, 2021). Surabaya is located in East Java Province and is one of Indonesia's major metropolitan areas (Fig. 1). According to BPS Statistics Surabaya (2025), the city had a population of approximately 3.02 million in 2024. This municipality was chosen as the empirical setting to investigate urban household e-waste management, focusing on how municipal generation rates, infrastructure proximity, and disposal logistics shape public engagement in formal recycling frameworks**.** The study area was limited to Surabaya City; therefore, the sample should not be interpreted as representative of households in other Indonesian cities or of Indonesia as a whole.

Sampling and participants

The analytical sample comprised 250 respondents selected via purposive sampling from households within the Surabaya study area that satisfied specific eligibility criteria and resided in proximity to designated e-waste collection or recycling infrastructure. The unit of analysis was an individual household member who independently managed household waste and was involved in decisions concerning its storage, disposal, or delivery to e-waste collection facilities.

Data collection

Primary data were collected using a structured questionnaire informed by previous research on environmental behavior and e-waste management (Islam *et al.,* 2021; Sari *et al.,* 2021; Garg *et al.,* 2023). The questionnaire included measures of awareness of consequences, perceived accessibility, behavioral intention, self-reported actual behavior, and sociodemographic characteristics. Awareness of consequences was defined as respondents' perceived knowledge of the environmental and health consequences associated with improper e-waste management (Attia *et al.,* 2021; Almulhim, 2022). Behavioral intention operationalized respondents' self-reported willingness or strategic planning to execute future e-waste management practices (Sari *et al.,* 2021; Islam *et al.,* 2021; Nawaz *et al.,* 2025). Self-reported actual behavior referred to reported past actions. Perceived accessibility referred to respondents' assessment of how readily and conveniently e-waste management facilities could be used (Sari *et al.,* 2021; Kosarkar and Barthwal, 2025; Waheed *et al.,* 2023). The operationalization of the awareness construct incorporated two distinct indicators measuring human health and environmental consequences. Furthermore, behavioral intention was evaluated through three items focusing on recycling, donation, and facility utilization, whereas actual behavior was assessed using three indicators capturing prior drop-offs at official collection or recycling nodes, responsible material storage, and involvement in civic programs. Because these actual-behavior items represent related but not identical actions, the resulting score was treated as a composite index of reported e-waste

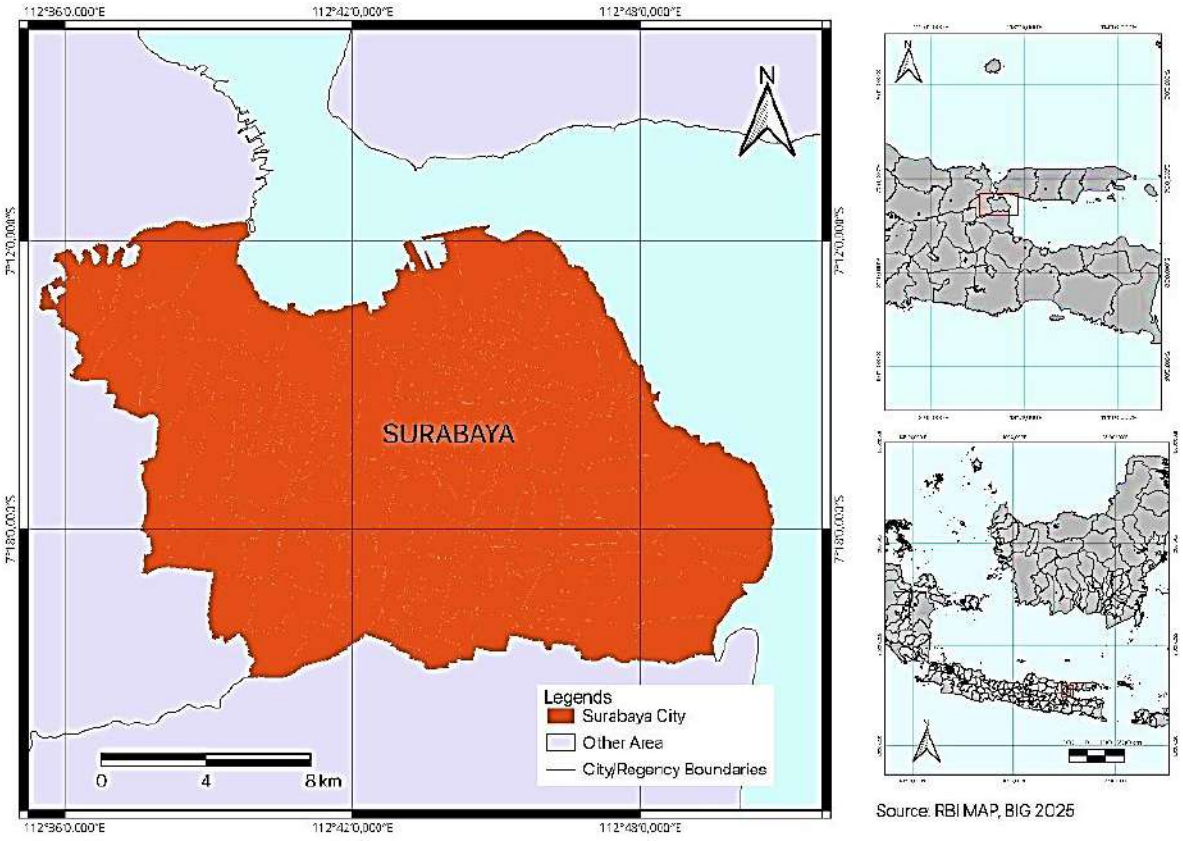

Fig. 1: Geographical location of the study area in Surabaya City, East Java Province, Indonesia

management behavior. The index therefore captures several forms of responsible management rather than formal recycling alone. Perceived accessibility comprised nine items covering facility location, road conditions, directions, number of collection points, operating hours, user-friendliness, perceived distance, willingness to spend time/purchase, and perceived time/energy burden (Alkhazali *et al.,* 2025). Because these indicators capture multiple dimensions of perceived spatial proximity, they were aggregated into a composite index reflecting respondents' overall assessment of facility convenience and operational usability (Sari *et al.,* 2021; Kosarkar and Barthwal, 2025). Perceived accessibility was analyzed separately from objective geographic measures of distance and travel time; the relationship between the two forms of accessibility was not formally tested. All questionnaire items were measured using a five-point Likert response scale from 1 (strongly disagree) to 5 (strongly agree). Composite scores were calculated according to the study's scoring procedure (Huh and Gim, 2025; Koo and Yang, 2025). Spearman correlation was used for bivariate association testing because the item responses were ordinal. Ordinary least squares (OLS) regression was applied to the composite scores as approximately continuous outcomes to estimate adjusted statistical associations. Because the archived manuscript lacks the requisite diagnostic output to explicitly report numerical evaluations for all OLS assumptions, the resulting regression estimates are interpreted with necessary caution and appropriate methodological restraint in this context.

Ethical considerations

Participation was voluntary, respondents were informed about the study before completing the questionnaire, and confidentiality was maintained. No formal institutional ethics approval number or approval date is available for this study; accordingly, the manuscript does not claim that formal institutional ethics approval was obtained.

Data analysis

Data analysis proceeded in four stages. First, descriptive statistics were used to summarise respondent characteristics and the distributions of the study variables. Second, Spearman rank correlation was used to examine bivariate associations among awareness, perceived accessibility, behavioral intention, and actual behavior. Third, OLS regression models estimated the associations of awareness, perceived accessibility, and selected sociodemographic covariates with behavioral intention and actual behavior. The interpretation of OLS coefficients was limited to adjusted statistical associations, not causal effects. The OLS models were used to estimate adjusted associations among the composite study variables and selected covariates. Because the retained manuscript does not include the original diagnostic output, numerical results for residual normality, linearity, homoscedasticity, variance inflation factor (VIF), and influential observations are not reported. Because the archived manuscript lacks the requisite diagnostic output to explicitly report numerical evaluations for all OLS assumptions, the resulting regression estimates are interpreted with necessary caution. Kruskal–Wallis tests were used to compare behavioral intention and actual behavior across the three accessibility groups. Because the available results contain only the omnibus statistics and group mean ranks, pairwise post-hoc comparisons cannot be reconstructed from the retained manuscript data. Effect sizes were estimated from the reported Kruskal–Wallis statistics using epsilon-squared, yielding error $(\varepsilon)^2 = 0.039$ for behavioral intention and $\varepsilon^2 = 0.137$ for actual behavior. Consequently, the statistically significant omnibus findings serve as evidence that at least one accessibility subgroup exhibits a distinct profile, though without identifying the specific pairwise differences. For the spatial analysis, GIS was used to examine the distribution of the observations included in the spatial dataset and their relationship to e-waste facilities. Average nearest neighbor (ANN) analysis was used only to assess whether the analyzed point pattern was more clustered, random, or dispersed than expected under spatial randomness. A nearest-neighbor ratio below 1 indicates clustering, whereas the z-score and associated p-value determine whether the departure from randomness is statistically significant. ANN does not identify the behavioral or social mechanism producing the spatial pattern. The spatial analysis used the household and e-waste facility observations retained in the study's GIS dataset. Although the existing manuscript documents the resulting nearest-neighbor ratio and z-score, it omits critical methodological parameters, including the GIS software and version, geocoding and coordinate source, spatial reference system, facility dataset metadata, and explicit observation-selection criteria used for the spatial analysis and mapping.

Research hypotheses

In light of the theoretical framing, the hypotheses were formulated to examine the associations among awareness, perceived accessibility, behavioral intention, and actual behavior, and to assess differences in behavioral intention and actual behavior across accessibility groups (Fig. 2).

H1: Awareness of the environmental and health consequences of e-waste is positively associated with behavioral intention to manage e-waste.

H2: Awareness of the environmental and health consequences of e-waste is positively associated with self-reported actual e-waste management behavior.

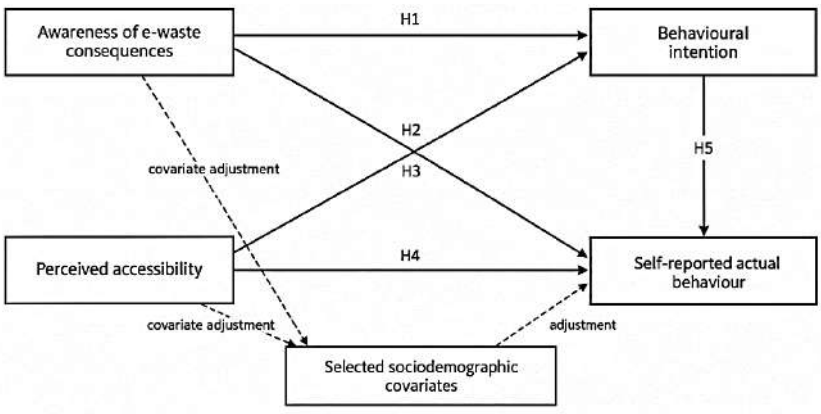

Fig. 2: Research framework showing the tested associations and covariate adjustment

H3: Perceived accessibility of e-waste management facilities is positively associated with behavioral intention to manage e-waste.

H4: Perceived accessibility of e-waste management facilities is positively associated with self-reported actual e-waste management behavior.

H5: Behavioral intention is positively associated with self-reported actual e-waste management behavior.

H6: Behavioral intention differs across levels of perceived facility accessibility.

H7: Self-reported actual e-waste management behavior differs across levels of perceived facility accessibility.

Rather than being evaluated as directional research hypotheses, sociodemographic parameters were treated strictly as analytical covariates, given that the study's primary objective was to control for potential population heterogeneity rather than to establish a priori causal pathways for individual demographic attributes. The framework therefore provides the conceptual basis for the seven hypotheses and for the subsequent correlation, regression, and accessibility-group analyses. Because the study uses a cross-sectional design, these relationships are examined as statistical associations rather than causal effects (Table 1). This approach is known as spatial household behavior analysis using the nearest-neighbor method. Within this spatial analysis framework, the focus of pattern mapping is on households characterised by high awareness, positive behavior, and high participation. The analysis determines the average accessibility to collection facilities for households with positive behavior, allowing the resulting patterns to be categorised as clustered, dispersed, or random (Table 2).

RESULTS AND DISCUSSION

Respondent characteristics

A total of 250 respondents participated in this study, with women comprising 57.6% and men 42.4%. Most respondents were aged 18–35 years (y) (76%), followed by those aged 36–45 y (14.8%). In terms of residential status, 56.8% reported owning a single residence, while the remainder reported other ownership or rental arrangements. The sample's educational attainment leaned heavily toward tertiary or post-secondary credentials. Furthermore, spatial proximity and transit duration relative to e-waste processing facilities were captured across categorical brackets, identifying < 10 kilometers (km) and 10–30 minutes (min.) as the respective modal categories. Beyond the demographic profile, the access-related characteristics presented in Table 3 provide an indication of the physical circumstances surrounding household access to formal e-waste management facilities. Among the

Table 1: Operationalized variables or constructs

Variable	Construct
Awareness of consequences	The accumulation of e-waste will result in long-term negative impacts on human health. E-waste that is not managed properly can lead to environmental pollution.
Behavioral intentions	I intend to recycle my electronic devices in the future. I plan to donate usable electronic devices instead of discarding them. I will actively utilize an e-waste collection facility if one is readily available.
Actual behaviors	I have previously taken my e-waste to an official collection or recycling point. I store my electronic waste so it can be managed responsibly at a later time. I participate in community programs or campaigns focused on e-waste.
Accessibility	The location of the current e-waste drop-off point is easily accessible from where I live/conduct my activities. The road conditions to the e-waste collection location do not pose a problem (example, no traffic jams, good roads). Directions (example, signs or maps) to the e-waste collection location are very clear. The number of e-waste drop-off points available in my area is sufficient. The operating hours of the e-waste collection point are compatible with my free time. The e-waste collection point is user-friendly (example, the drop-off process is quick and uncomplicated). The distance from my house/office to the nearest e-waste collection point is not far. I am willing to take the time to deliver e-waste to the collection point. I feel that the time and energy required to deliver e-waste is not a big burden.

Note: The study applied a 5-point Likert scale to measure all the items in this survey (1 equal to (=) strongly disagree to 5=strongly agree).

Table 2: Pattern categories formed by nearest neighbor analysis

Index	Pattern
Nearest neighbor ratio (T) lower than < 1	Clustered
T= 1	Random
T > 1	Uniform

Table 3: Demographic profile and socioeconomic attributes of household consumers in Surabaya City

Variable/attribute	Component	Frequency	Percentage (%)
Sex	Men	106	42.4
	Women	144	57.6
Age (years)	< 18	11	4.4
	18–35	190	76.0
	36–45	37	14.8
	46–55	12	4.8
Education level	Secondary	7	2.8
	Tertiary	145	58.0
	College	84	33.6
	Master/Doctor	14	5.6
Monthly income	0–2.5 million IDR	157	62.8
	2.5–5 million IDR	49	19.6
	5–7.5 million IDR	36	14.4
	7.5–10 million IDR	8	3.2
Number of household dependents	0	96	38.4
	1–2	88	35.2
	3–4	52	20.8
	5–6	13	5.2
	More than (>) 6	1	0.4
Residential status	Own a single house/residence	142	56.8
	Own more than one house/residence	16	6.4
	Temporary rental/short-term lease	48	19.2
	Long-term rental/lease	44	17.6
Estimated distance from home to electronic waste processing location (km)	< 10	124	49.6
	10–30	84	33.6
	31–50	33	13.2
	51–70	8	3.2
	> 70	1	0.4
Travel time from home to electronic waste processing site (minutes)	< 10	77	30.8
	10–30	116	46.4
	31–45	41	16.4
	46–60	12	4.8
	> 60	4	1.6

250 respondents, 124 (49.6%) reported that the relevant facility was located less than 10 km from their residence, while 84 (33.6%) reported a distance of 10–30 km. The distribution of travel time was somewhat different, with 116 respondents (46.4%) reporting a travel time of 10–30 minutes and 77 (30.8%) reporting less than 10 minutes. This divergence between the two metrics warrants emphasis, given that linear spatial separation fails to capture the true operational burden, encompassing transit time and personal effort, associated with accessing collection facilities. A relatively short distance may still involve longer travel because of road conditions, transport availability, or route characteristics, while a greater distance may be manageable where transport and routes are convenient. When residents must undertake dedicated excursions to discard stored e- waste, cumulative transit duration and logistical demands can severely diminish the perceived utility of formal disposal channels. Conversely, closer facilities may reduce the geographical burden of access, although physical proximity alone does not determine whether households will use them. Previous studies have similarly identified convenience, accessibility, and infrastructure support as important conditions influencing participation in formal e-waste collection and recycling systems (Sari *et al.,* 2021; Nawaz *et al.,* 2025; Kosarkar and Barthwal, 2025). The distance and travel-time distributions in Table 3 therefore provide a useful description of the physical access conditions experienced by the sampled households, while also highlighting why accessibility cannot be represented by distance alone. Accordingly, within this study, these objective parameters were evaluated independently of perceived accessibility, which encapsulates public perceptions regarding the operational convenience, usability, and logistical friction inherent in utilizing e-waste disposal infrastructure (Table 3).

Descriptive statistics and construct reliability

Descriptive statistics show that consequence awareness had the highest mean score (Mean = 4.33; Standard deviation (SD) = 0.706), indicating a relatively high level of respondent awareness of the environmental impacts of e-waste. Behavioral intention also showed a high mean score (Mean = 4.02; SD = 0.682), while accessibility (Mean = 3.55; SD = 0.710) and actual behavior (Mean = 3.66; SD = 0.792) were at a moderate level. Reliability testing showed that the accessibility construct had excellent internal consistency (Cronbach's Alpha = 0.883). The consequence awareness (Cronbach's Alpha = 0.668), behavioral intention (Cronbach's Alpha = 0.647), and actual behavior (Cronbach's Alpha = 0.635) constructs showed more modest internal consistency, but remained within acceptable ranges for exploratory or preliminary confirmatory social research (Table 4). Behavioral intention differed significantly across the low, medium, and high accessibility groups ($\chi^2 = 11.67$, $p = 0.003$), while actual behavior also differed significantly across accessibility groups ($\chi^2 = 35.91$, $p < 0.001$), with the high-accessibility group showing the highest mean ranks for both outcomes.

Spearman correlation analysis

The relationships among the main variables were not uniform across the two behavioral outcomes. Awareness of e-waste consequences had a positive association with behavioral intention ($r = 0.340$, $p < 0.001$), whereas its association with actual behavior was weak and statistically non-significant ($r = 0.067$, $p = 0.293$). Perceived accessibility showed a different pattern, with significant positive associations with both behavioral intention ($r = 0.197$, $p < 0.001$) and

Table 4: Descriptive statistics and reliability test results

Variable/ construct	Mean	SD	Min	Max	Item Total	Cronbach's Alpha
Awareness of consequences	4.33	0.706	1	5	2	0.668
Accessibility	3.55	0.710	1	5	9	0.883
Behavioral intention	4.02	0.682	1	5	3	0.647
Actual behavior	3.66	0.792	1	5	3	0.635

actual behavior ($r = 0.416$, $p < 0.001$). Behavioral intention was also positively associated with actual behavior ($r = 0.407$, $p < 0.001$). The contrast among these coefficients provides an important indication of the relationship between awareness, intention, and reported behavior. While environmental awareness exhibited a stronger correlation with stated behavioral intent than with self-reported past actions, perceived accessibility demonstrated significant associations with both outcomes, displaying a markedly more robust bivariate relationship with actual behavior. This pattern suggests that recognising the health and environmental consequences of e-waste may be relevant to the formation of behavioral intention, but awareness alone does not necessarily correspond to reported engagement in e-waste management practices. Conversely, the pronounced association between perceived accessibility and actual behavior underscores that on-the-ground operational conditions governing facility access exert a profound influence on household participation levels. Previous research has similarly identified gaps between environmental awareness or behavioral intention and actual e-waste participation, particularly where convenience, infrastructure, and other external conditions influence the translation of intention into action (Attia *et al.,* 2021; Kosarkar and Barthwal, 2025; Nawaz *et al.,* 2025). The positive association between behavioral intention and actual behavior ($r = 0.407$, $p < 0.001$) further indicates that intention is related to reported participation, although the relationship does not imply that intention alone is sufficient for behavior to occur. Accordingly, the concurrent correlation of perceived accessibility with both behavioral intent and realized actions highlights how tangible infrastructural access operates as a critical counterpart to individual cognitive awareness and motivation. Awareness and perceived accessibility were themselves weakly and negatively correlated ($r = -0.125$, $p < 0.05$), indicating that these constructs capture relatively distinct dimensions of household e-waste management rather than reflecting the same underlying characteristic (Table 5).

OLS regression analysis

OLS regression results indicate that awareness of consequences (standardized regression coefficient (β) = 0.376; p-value < 0.001) and accessibility (β = 0.253; p-value < 0.001) have a positive and significant association with household intention to manage e-waste. Furthermore, gender was also significantly associated with intention (β = 0.233; p-value = 0.005), indicating differences in intention based on demographic characteristics (Table 6). Regression coefficients are reported as β values as presented in the available manuscript. The original statistical output is not retained, so the coefficients are not further described as standardized or unstandardized beyond this notation. Due to an irreconcilable discrepancy among the coefficient, standard error, and t-statistic reported within the available record for the residential status parameter in Table 6, this specific estimate is excluded from the textual analysis. In the intention model, awareness (β = 0.376, p-value < 0.001), perceived accessibility (β = 0.253, p-value < 0.001), and sex (β = 0.233,

Table 5: Spearman correlation between variables/constructs

Variable/ construct	Awareness of consequences	Accessibility	Behavioral intention	Actual behavior
Awareness of consequences	1.00	-0.125**	0.340***	0.067
Accessibility		1.00	0.197***	0.416***
Behavioral intention			1.00	0.407***
Actual behavior				1.00

Note: *Significant at 10% level; ** Significant at 5% level; ***Significant at 1% level

Table 6: OLS regression results (dependent variable: behavioral intention)

Independent variable	Regression coefficient (β)	Standard error (SE)	t-statistic (t-value)	p-value
Constant	1.293	0.346	3.739	0.000
Awareness of consequences	0.376	0.057	6.574	0.000***
Accessibility	0.253	0.058	4.346	0.000***
Sex	0.233	0.082	2.858	0.005***
Age	-0.104	0.088	-1.188	0.236
Education level	0.091	0.079	1.148	0.252
Monthly income	-0.001	0.067	-0.019	0.985
Number of household	-0.053	0.049	-1.088	0.278
Residential status	-5.09	0.032	-0.002	0.999
Distance to nearest facility (km)	0.019	0.074	0.254	0.800
Travel time to nearest facility (min.)	0.097	0.064	1.511	0.132

Model summary: Coefficient of determination (R^2) = 0.257; Adjusted R^2 = 0.226; F-test statistic (F) = 8.251; p-value < 0.001
Note: *Significant at 10% level; ** Significant at 5% level; ***Significant at 1% level

p-value = 0.005) were statistically associated with behavioral intention after adjustment. Age, education level, monthly income, Number of household dependents, residential status, distance, and travel time were not statistically significant in the reported model. In the actual-behavior model, perceived accessibility (β = 0.449, p-value < 0.001) and awareness (β = 0.182, p-value = 0.008) were statistically associated with the outcome, while sex was not statistically significant at the 5% level (β = 0.177, p-value = 0.068). Within Table 7, the regression coefficients are presented strictly as β values, mirroring the source manuscript. Because the primary statistical output is unavailable, these estimates are deliberately left unclassified as either standardized or unstandardized beyond this specific notation.

Differences in participation (behavioral intention and actual behavior) based on accessibility level

The Kruskal–Wallis test results indicate a significant difference in intention to manage e-waste between the low, medium, and high accessibility groups (Kruskal-Wallis chi-square statistic (χ^2) = 11.67; p-value = 0.003). The high accessibility cohort recorded the highest mean rank, with successively lower values observed across the medium and low accessibility groups. Stronger differences were found in actual behavior/participation. The test results showed a highly significant difference between accessibility groups (χ^2 = 35.91; p-value = 0.000), with a consistent pattern of increasing participation as accessibility levels increased (Table 8). Although the statistically significant omnibus Kruskal–Wallis tests signal overall group-level variations across the accessibility strata, the limitations of the existing manuscript preclude the reconstruction of granular pairwise post-hoc comparisons. Based on the reported H statistics, epsilon-squared was approximately 0.039 for behavioral intention and 0.137 for actual behavior. The findings are therefore reported at the omnibus level only. Effect sizes estimated from the reported Kruskal–

Table 7: OLS regression results (dependent variable: actual behavior)

Independent variable	Regression coefficient (β)	SE	t-value	p-value
Constant	1.153	0.409	2.817	0.005
Awareness of consequences	0.182	0.068	2.686	0.008***
Accessibility	0.449	0.069	6.528	0.000***
Sex	0.177	0.097	1.831	0.068*
Age	-0.165	0.104	-1.589	0.113
Education level	0.025	0.093	0.270	0.787
Monthly income	0.109	0.079	1.379	0.169
Number of household dependents	0.056	0.058	0.962	0.337
Residential status	0.012	0.038	0.311	0.756
Distance to nearest facility (km)	-0.030	0.087	-0.349	0.727
Travel time to nearest facility (minutes)	0.078	0.076	1.029	0.305

Model summary: $R^2 = 0.228$; Adjusted $R^2 = 0.196$; $F = 7.055$; p-value < 0.001
Note: *Significant at 10% level; ** Significant at 5% level; ***Significant at 1% level

Table 8: Kruskal–Wallis test results across accessibility levels

Dependent variable	χ^2	Degrees of freedom (df)	p-value	Mean rank (Low)	Mean rank (Medium)	Mean rank (High)
Behavioral intention	11.67	2	0.003***	112.72	120.28	151.96
Actual behavior	35.91	2	0.000***	95.24	125.07	167.43

Note: *Significant at 10% level; ** Significant at 5% level; ***Significant at 1% level

Wallis statistics were ε^2=0.039 for behavioral intention and ε^2 = 0.137 for actual behavior. While these values quantify the magnitude of overarching group differences; the absence of pairwise post-hoc outputs within the archived manuscript precludes the reporting of specific intergroup contrasts.

Integrated interpretation of the quantitative findings

Collectively, the findings demonstrate that cognitive awareness and perceived accessibility operate as distinct predictors, influencing separate dimensions of household engagement in e-waste management. Awareness was positively associated with behavioral intention but was not significantly associated with self-reported actual behavior in the bivariate analysis. Perceived accessibility was positively associated with both intention and actual behavior, and its adjusted coefficient was larger in the actual-behavior model. These empirical insights align seamlessly with established scholarship, reinforcing the principle that public engagement with e-waste management is fundamentally driven by the interplay between internal psychological motivations and tangible contextual constraints governing disposal (Sari *et al.*, 2021; Mahartin, 2023; Nawaz *et al.*, 2025; Kosarkar and Barthwal, 2025; Haq, 2026). The positive association between awareness and intention is compatible with the Value-Belief-Norm perspective, in which awareness of consequences forms part of the cognitive basis through which environmental concerns can become behaviorally relevant. Prior empirical studies have documented varying associations between environmental awareness and e-waste recycling intention (Elmosaad *et al.*, 2023). However, the effect sizes and underlying mechanisms exhibit considerable heterogeneity across diverse demographic populations and theoretical frameworks (Al Mamun *et al.*, 2022; Duong *et al.*, 2023; Nawaz *et al.*, 2025). The present findings should therefore be interpreted as evidence of an association between consequence awareness and intention rather than

as evidence that awareness causes intention. The absence of a statistically significant bivariate correlation between environmental awareness and actual behavior warrants particular emphasis; rather than representing an analytical contradiction, this finding underscores that cognitive recognition of environmental consequences does not automatically translate into realized action within the specific constraints characterizing this sample. Similar intention–behavior gaps have been documented in pro-environmental behavior research, including e-waste studies, where convenience, perceived control, habits, infrastructure, and institutional arrangements may influence whether an intention is enacted (Trinh and Sakurai, 2025; Nawaz *et al.*, 2025; Kosarkar and Barthwal, 2025). The spatial findings provide a descriptive complement to the survey analysis. They characterize the spatial distribution of the analyzed observations but do not permit these mechanisms to be tested directly. This finding is consistent with Indonesian research indicating that facility accessibility is relevant to e-waste collection intention (Sari *et al.*, 2021) and with recent studies emphasising convenience and formal collection barriers in e-waste management (Alejandro *et al.,* 2025; Nawaz *et al.*, 2025; Kosarkar and Barthwal, 2025). Nevertheless, this outcome must be interpreted strictly as an association with perceived accessibility given that the majority of the accessibility metrics utilized within this study rely on self-reported data. Objective distance and travel time were analyzed separately and should not be treated as interchangeable with perceived accessibility. The regression models further showed that perceived accessibility had the largest reported coefficient in the actual-behavior model (β = 0.449, p-value < 0.001), while awareness was also statistically associated with actual behavior (β = 0.182, p-value = 0.008). Because the retained manuscript lacks the requisite software output to verify whether the estimated coefficients are standardized or unstandardized, their respective magnitudes are intentionally omitted from formal evaluations of predictive strength. The sociodemographic findings were comparatively limited. Gender was statistically associated with behavioral intention in the intention model (β = 0.233, p-value = 0.005), while most other reported covariates were not statistically significant. This observed trend should not be misconstrued as proof that sociodemographic characteristics are universally trivial; rather, within this purposively restricted sample, the majority of evaluated covariates failed to demonstrate statistically significant adjusted associations once all other variables were integrated into the models. The relatively high proportion of respondents with tertiary or college-level education also limits the extent to which these findings can be generalized to more educationally heterogeneous populations.

Spatial analysis

The ANN analysis produced a nearest-neighbor ratio of approximately 0.60 and a z-score of approximately −10.01. Because the ratio is below 1 and the z-score is far from zero, the analyzed point pattern is consistent with statistically significant spatial clustering rather than a random spatial arrangement (p-value < 0.001). However, ANN result outputs do not inherently establish social learning, social contagion, neighborhood effects, collective socialisation, or interpersonal communication. Because none of these underlying mechanisms were directly assessed within the survey framework, ANN serves strictly to characterize the spatial configuration of points rather than elucidate the generative causal processes responsible for that arrangement. Accordingly, statements in the previous version linking the clustering directly to imitation or neighborhood social networks have been

removed. Such mechanisms may be considered as hypotheses for future research rather than conclusions from the present analysis. Table 3 reports distance and travel time as categorical distributions. The modal distance category was < 10 km (49.6%), whereas the modal travel-time category was 10–30 minutes (46.4%). These classifications characterize respondent distributions rather than serving as arithmetic means or definitive accessibility thresholds. Nevertheless, the spatial patterns offer a valuable descriptive complement to the survey evaluation. Specifically, they demonstrate that the analyzed observations exhibit spatial clustering rather than uniform dispersion, highlighting the value of examining the spatial distribution of household participation in relation to collection facility locations. Future studies could extend this approach using network-based travel time, facility capacity, service coverage, population density, and distance-decay models to examine accessibility more directly. Such analyses would be required before proposing a specific facility-planning threshold.

Implications for sustainable e-waste management

The combined findings suggest that awareness-oriented and infrastructure-oriented approaches may address different components of household participation. Awareness campaigns may strengthen recognition of the environmental and health consequences of e-waste, whereas improvements in collection-point availability, operating hours, information, convenience, and service coverage may reduce practical barriers to action. This perspective aligns with contemporary empirical findings indicating that service convenience and structured collection parameters continue to exert a significant influence on e-waste recycling participation (Siringo *et al.,* 2020; Nawaz *et al.*, 2025; Kosarkar and Barthwal, 2025). From a circular-economy perspective, the practical implication is not simply to increase the number of facilities, but to improve the usability and coverage of formal collection pathways and connect them with household routines. Community collection points, retailer take-back schemes, scheduled pick-up services, and clear information on accepted e-waste categories could be considered as complementary measures. Because the current study does not empirically evaluate the efficacy of these interventions, they should be construed strictly as prospective policy options rather than validated causal outcomes. The ecological-anthropological contribution of the study lies in situating household e-waste practices within the material and spatial context in which they occur. Rather than presuming a direct linear trajectory from cognitive awareness to responsible conduct, the findings underscore that contextual disposal conditions play a critical role in turning behavioral intent into actual practice. This contextual interpretation is compatible with research emphasising the role of infrastructure, everyday practices, and institutional arrangements in environmental behavior (Ardoin and Heimlich, 2021; Rippa, 2023; Harafah *et al.*, 2026). H1–H7 correspond to the relationships and group comparisons directly examined in the available analyses. Sociodemographic variables were treated as covariates rather than as separate directional hypotheses. Five hypotheses concerning bivariate associations were supported, whereas H2 was not supported. Awareness of e-waste consequences was positively associated with behavioral intention (H1: $r = 0.340$, $p < 0.001$), but its association with actual behavior was weak and statistically non-significant (H2: $r = 0.067$, $p = 0.293$). This divergence reveals that while individuals possessing a heightened awareness of the ecological and health risks associated with e-waste reported more robust intentions toward proper management, this cognitive recognition failed to manifest correspondingly in their

Table 9: Summary of hypothesis testing

Hypothesis	Testing method	Coefficient/ test statistic	p-value	Decision
H1	Spearman correlation	r = 0.340	< 0.001	Supported
H2	Spearman correlation	r = 0.067	0.293	Not supported
H3	Spearman correlation	r = 0.197	< 0.001	Supported
H4	Spearman correlation	r = 0.416	< 0.001	Supported
H5	Spearman correlation	r = 0.407	< 0.001	Supported
H6	Kruskal–Wallis	χ^2 = 11.67, df = 2	0.003	Supported at omnibus level; post-hoc comparisons required
H7	Kruskal–Wallis	χ^2 = 35.91, df = 2	<0.001	Supported at omnibus level; post-hoc comparisons required

Note: *Significant at 10% level; ** Significant at 5% level; ***Significant at 1% level

self-reported past actions. Comparable disconnects traversing awareness, behavioral intent, and actual disposal practices have been widely documented in previous studies. Attia *et al.* (2021), for example, found that awareness of e-waste issues did not necessarily translate into appropriate disposal practices among households (Table 9).

Spatial analysis results

The Average Nearest Neighbor analysis produced a nearest-neighbor ratio of 0.598616, a z-score of −10.011886, and a p-value of < 0.001 (Fig. 3). The ratio below 1 and the statistically significant z-score indicate that the observed point pattern is significantly clustered rather than consistent with spatial randomness. The ANN result describes the spatial arrangement of the observations included in the analysis and does not demonstrate social learning, social contagion, neighborhood effects, collective socialization, or interpersonal communication. These mechanisms were not directly assessed within the survey framework and therefore cannot be legitimately inferred from ANN spatial metrics alone. The reported distance and travel-time measures are categorical observations. The most frequently reported distance category was < 10 km (49.6%), while the most frequently reported travel-time category was 10–30 minutes (46.4%) (Table 3). These categories describe the observed distribution of respondents and should not be interpreted as arithmetic means or formal accessibility thresholds.

CONCLUSION

This study examined household e-waste participation in Surabaya by considering awareness of e-waste consequences, perceived facility accessibility, behavioral intention, self-reported actual behavior, selected sociodemographic characteristics, and spatial distribution. Awareness was positively associated with behavioral intention (r = 0.340, p-value < 0.001) but not with self-reported actual behavior (r = 0.067, p = 0.293). Perceived accessibility was positively associated with both intention (r = 0.197, p < 0.001) and actual behavior (r = 0.416, p-value < 0.001). In the adjusted OLS models, Perceived accessibility was statistically associated with actual behavior (β = 0.449, p-value < 0.001), while awareness was also statistically associated with actual behavior (β = 0.182, p-value = 0.008). The Kruskal–Wallis tests also indicated differences across accessibility groups for both intention and actual behavior. The ANN evaluation revealed statistically significant spatial clustering across the examined observations, characterized by a nearest-neighbor ratio of approximately 0.60 and a z-score of approximately −10.01. While this outcome delineates an explicit spatial distribution, it must not be construed as indicative of

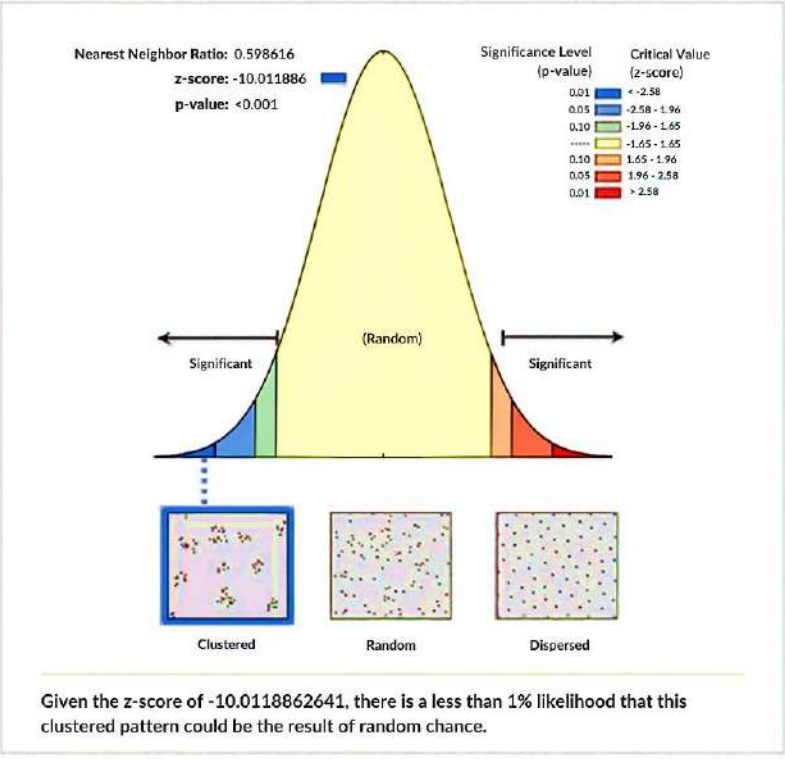

Fig. 3: Spatial distribution of respondents and nearest-neighbor clustering pattern in Surabaya City

neighborhood effects, social learning processes, or alternative underlying causal mechanisms. Similarly, the observed distance and travel-time categories do not establish a specific accessibility threshold. The findings support an integrated interpretation in which household e-waste participation is associated with both cognitive and contextual conditions. Nevertheless, owing to the cross-sectional architecture and purposive sampling strategy employed, these findings preclude definitive causal inferences and broad population-level generalizations. Consequently, the empirical outcomes are most rigorously construed as localized evidence reflecting the sampled households within Surabaya rather than serving as national-level estimates. For practice, the findings suggest that awareness activities can be complemented by improvements in the convenience and usability of formal e-waste collection services. Recommended policy measures encompass expanding geographical service coverage, disseminating transparent information concerning collection points and accepted waste categories, extending operating hours, and integrating e-waste collection mechanisms with existing municipal waste streams or retail take-back programs. These measures should be evaluated through longitudinal, experimental, or quasi-experimental research before their effectiveness is assumed. Several methodological limitations warrant explicit consideration. First, the cross-sectional design inherently precludes the determination of temporal sequencing and directional causality. Second, purposive sampling and the focus on households near e-waste facilities limit generalisability and may introduce facility-proximity selection bias. Third, actual behavior was self-reported and may be affected by recall or social-desirability bias. Fourth, the awareness

construct contained only two items and showed Cronbach's alpha = 0.668, while the actual-behavior construct showed α = 0.635; therefore, the reliability of these measures should be interpreted cautiously. Fifth, perceived accessibility aggregates multiple underlying dimensions that may not constitute a strictly unidimensional construct. Sixth, objective distance and travel time were considered separately from perceived accessibility, but their relationship with perceived accessibility was not formally tested. Finally, the spatial analysis cannot identify behavioral mechanisms underlying clustering. Future research should use probability-based or stratified sampling, stronger multi-item measures, objective behavioral or administrative records, network-based accessibility measures, and longitudinal or quasi-experimental designs. Furthermore, supplementary mediation or moderation modeling could be pursued provided that the underlying constructs of interest have been explicitly and rigorously operationalized. The internal consistency estimates were acceptable for the accessibility construct (Cronbach's alpha = 0.883), whereas the awareness (Cronbach's alpha = 0.668), behavioral intention (Cronbach's alpha = 0.647), and actual-behavior (Cronbach's alpha = 0.635) constructs showed more modest internal consistency. These lower coefficients should be interpreted in light of the limited number of items used to represent these constructs and constitute a measurement limitation of the study.

AUTHOR CONTRIBUTIONS

H. Herdiansyah supervised the study, contributed to the statistical analysis and interpretation, and led manuscript preparation. D. Fitria contributed to interpretation of the statistical findings and manuscript preparation. D.R. Nugraheni prepared the maps and figures and contributed to spatial-data interpretation. M. Qamruzzaman contributed to supervision, data analysis, and interpretation.

ACKNOWLEDGEMENT

This study is funded by the Indonesian Endowment Fund for Education (LPDP) on behalf of the Indonesian Ministry of Higher Education, Science and Technology and managed under the EQUITY Program [Contract No. 4302 / B3 / DT.03.08 / 2025 and 573 / PKS / R / UI / 2025].

CONFLICT OF INTEREST

The authors declare that there is no conflict of interests regarding the publication of this manuscript. In addition, the ethical issues, including plagiarism, informed consent, misconduct, data fabrication and/or falsification, double publication and/or submission, and redundancy have been completely observed by the authors.

OPEN ACCESS

©2027 The author(s). This article is licensed under a Creative Commons Attribution 4.0 International License, which permits use, sharing, adaptation, distribution and reproduction in any medium or format, as long as you give appropriate credit to the original author(s) and the source, provide a link to the Creative Commons license, and indicate if changes were made. The images or other third-party material in this article are included in the article's Creative Commons license, unless indicated otherwise in a credit line to the material. If material is not included in the article's Creative Commons license and your intended use is not permitted by statutory regulation or exceeds the permitted use, you will need to obtain permission directly from the copyright holder. To view a copy of this license, visit: http://creativecommons.org/licenses/by/4.0/

PUBLISHER'S NOTE

GJESM Publisher remains neutral with regard to jurisdictional claims in published maps and institutional affiliations.

NEGATIVE AI STATEMENT

The authors declare that no AI tools or services were used or heavily applied during the preparation of this work.

ABBREVIATIONS

%	Percent
=	Equal to
<	Less than
>	More than
–	Through
β	Regression coefficient
ε	Error
χ^2	Kruskal–Wallis chi-square statistic
ANN	Average Nearest Neighbor
df	Degrees of freedom
e-waste	Electronic waste
F	F-test statistic
GIS	Geographic Information Systems
H	Hypotheses
H1–H7	Hypotheses 1–7
km	Kilometer
Max	Maximum
Min	Minimum
Min.	Minutes
OLS	Ordinary least squares
p-value	Probability value
r	Spearman correlation coefficient
R^2	Coefficient of determination
SD	Standard deviation
SE	Standard error
T	Nearest neighbor ratio
VBN	Value-belief-norm
VIF	Variance inflation factor
t-value	t-statistic
y	Year
Z	Standard score (Z-score)

REFERENCES

Abha, A.T.; Gitifar, A.; Chowdhury, R.; Tasnim, A.; Ng, K.T.W., (2025). Quantification of E-waste collection count at household level. Environ. Sustainable Indic., 28: 100898 **(10 pages).**

Al Mamun, A.; Hayat, N.; Masud, M.M.; Makhbul, Z.K.M.; Jannat, T.; Salleh, M.F.M., (2022). Modelling the Significance of Value-Belief-Norm Theory in Predicting Solid Waste Management Intention and Behavior. Front. Environ. Sci., 10: 906002 **(12 pages).**

Alejandro, J.; Cuellar, A.; Puerto-rojas, E.; Correa-galindo, S.N., (2025). A community-based intervention proposal for municipal solid waste management : analyzing willingness, barriers and spatial strategies. Barriers Spat. Strateg., 17(13): 6206 **(21 pages).**

Alhassan, H.; Kwakwa, P.A.; Owusu-Sekyere, E., (2020). Households' source separation behavior and solid waste disposal options in Ghana's Millennium City. J. Environ. Manage., 259: 110055 **(10 pages).**

Alkhazali, Q.M.; Ooi, K.-B.; Shyu, W.-H.; Wei-Han Tan, G., (2025). Driving toward sustainability: extending the value-belief-norm theory to understand the willingness to purchase full electric vehicles in Jordan. Manage. Sustainable Arab. Rev., 1–21 **(21 pages).**

Almulhim, A.I., (2022). Household's awareness and participation in sustainable electronic waste management practices in Saudi Arabia. Ain Shams Eng. J., 13(4): 101729 **(15 pages).**

Andeobu, L.; Wibowo, S.; Grandhi, S., (2023). Environmental and Health Consequences of E-Waste Dumping and Recycling Carried out by Selected Countries in Asia and Latin America. Sustainility. 15(13): 10405 **(28 pages).**

Ankit, S.; Saha, L.; Kumar, V.;Tiwari, J.; Sweta; Rawat, S.; Singh, J.; Bauddh, K., (2021). Electronic waste and their leachates impact on human health and environment: Global ecological threat and management. Environ. Technol. Innov., 24: 102049 **(28 pages).**

Arain, A.L.; Pummill, R.; Adu-Brimpong, J.; Becker, S.; Green, M.; Ilardi, M.; Dam, E.; Neitzel, R.L., (2020). Analysis of e-waste recycling behavior based on survey at a Midwestern US University. Waste Manage., 105: 119–127 **(9 pages).**

Ardoin, N.M.; Heimlich, J.E., (2021). Environmental learning in everyday life: foundations of meaning and a context for change. Environ. Educ. Res., 27(12): 1681–1699 **(19 pages).**

Arsanti, V.; Kharisma, R.; Ardiansyah, I.; Nugroho, B.; Fajruna, M.; Deswanti, L.; Qori, M., (2024). Spatial Analysis of Waste Management Facility Distribution Using GIS. Adv. Sustainable Sci. Eng. Technol., 6(4): 02404013-01 ~ 02404013-010 **(10 pages).**

Arumbinang, N.A., (2026). Reduce, reuse, regulate: A comparative policy mix analysis of e-waste governance in five emerging economies. Sustain. Urban Dev. Environ. Impact J., 3(2): 87–105 **(19 pages)**.

Arya, S.; Kumar, S., (2020). E-waste in India at a glance: Current trends, regulations, challenges and management strategies. J. Clean. Prod., 271: 122707 **(20 pages).**

Asibey, M.O.; Lykke, A.M.; King, R.S., (2022). Understanding the factors for increased informal electronic waste recycling in Kumasi, Ghana. Int. J. Environ. Health Res., 32(2): 305–320 **(16 pages).**

Attia, Y.; Soori, P.; Ghaith, F., (2021). Analysis of Households' E-Waste Awareness, Disposal Behavior, and Estimation of Potential Waste Mobile Phones towards an Effective E-Waste Management System in Dubai. Toxics. 9(10): 236 **(24 pages).**

Azkiyah, N.H., (2026). Socio-economic factors and community participation in household waste management systems. Waste, Soc. Sustain., 3(1): 108–124 **(17 pages).**

Baldé, C.P.; Angelo, E.D.; Luda, V.; Deubzer, O.; Kuehr, R., (2022). Global Transboundary E-waste Flows Monitor 2022. United Nations Institute for Training and Research (UNITAR), 1–66 **(66 pages).**

Baldé, C.P.; Kuehr, R.; Yamamoto, T.; McDonald, R.; D'Angelo, E.; Althaf, S.; Bel, G.; Deubzer, O.; Fernandez-Cubillo, E.; Forti, V.; Gray, V.; Herat, S.; Honda, S.; Iattoni, G.; Khetriwal, D.S.; Luda di Cortemiglia, V.;

Lobuntsova, Y.; Nnorom, I.; Pralat, N.; Wagner, M., (2024). The global E-waste Monitor 2024 – Electronic Waste Rising Five Times Faster than Documented E-waste Recycling. International Telecommunication Union (ITU) and United Nations Institute for Training and Research (UNITAR), 1–33 **(33 pages).**

Bante, A.B.; Dararo, K.F.; Dejene, I.N., (2025). Solid Waste Dumping Site Suitability Analysis using Geographic Information System: A Case of Tebela Town Administration, South Ethiopia. Clean. Waste Syst., 11: 100310 **(10 pages).**

Bhardwaj, L.K.; Rath, P.; Jain, H.; Choudhury, M., (2025). Exploring the effects of e-waste on soil, water quality and human health. Discov. Civ. Eng., 2: 12 **(16 pages).**

Borthakur, A.; Singh, P., (2021). The journey from products to waste: a pilot study on perception and discarding of electronic waste in contemporary urban India. Environ. Sci. Pollut. Res., 28(19): 24511–24520 **(10 pages).**

BPS Statistics Surabaya, (2025). Surabaya municipality in figures 2025. BPS-Statistics Surabaya Municipality. 1-382 **(382 pages).**

Capili, B., (2021). Cross-Sectional Studies. Am. J. Nurs., 121(10): 59–62 **(4 pages).**

Cheng, X.; Yang, J.; Han, Z.; Shi, G.; Pan, D.; Meng, L.; Shen, Z., (2024). Optimizing rural waste management: Leveraging high-resolution remote sensing and GIS for efficient collection and routing. Int. J. Appl. Earth Obs. Geoinf., 135: 104219 **(13 pages).**

Duckworth, A.L.; Gross, J.J., (2020). Behavior change. Organ. Behav. Hum. Decis. Process., 161: 39–49 **(11 pages).**

Duong, C.D.; Nguyen, B.N.; Doan, X.H.; Nguyen, V.H.; Vu, A.T., (2023). I do believe in karma": understanding consumers' pro-environmental consumption with an integrated framework of theory of planned behavior, norm activation model and self-determination theory. Manag. Environ. Qual. An Int. J., 35(2): 270–298 **(29 pages).**

Ebo, P., (2026). Household waste management, community behavior, and sustainability challenges in urban areas. Waste, Soc. Sustain., 3(1): 1–16 **(16 pages)**.

Elmosaad, Y.M.; Rajeh, A.M.A.; Llaguno, M.B.B.; Alqaimi, S.S.; Alsalman, A.M.; Alkishi, A.Y.; Hussain, H.; Alhoudaib, M.A.; Alnajim, O.S.; Belal, S., (2023). Self-Reported Household Waste Recycling and Segregation Practices among Families in Eastern Region of Saudi Arabia : A Cross-Sectional Study. Int. J. Environ. Res. Public Health. 20(3): 1790 **(16 pages).**

Frigo, G.; Zurbrügg, C.; Giuliani, G.; Hansmann, R.; Binder, C.R., (2025). The geography of waste: Explaining the spatial variation of litter and dumpsites in Indonesia. Environ. Challenges. 21: 101345 **(12 pages).**

Garg, S.; Ahmad, A.; Madsen, D.Ø.; Sohail, S.S., (2023). Sustainable Behavior with Respect to Managing E-Wastes: Factors Influencing E-Waste Management among Young Consumers. Int. J. Environ. Res. Public Health. 20(1): 801 **(15 pages).**

Ghulam, S.T.; Abushammala, H., (2023). Challenges and Opportunities in the Management of Electronic Waste and Its Impact on Human Health and Environment. Sustainability. 15(3): 1837 **(22 pages).**

Haq, M.R.T., (2026). The implementation gap in waste management: A study of discrepancies in awareness, attitude, and practice. J. Char. Environ., 3(2): 95–111 **(17 pages).**

Harnita, N., (2025). Community participation in sustainable solid waste management. Waste, Soc. Sustain., 2(1): 72–91 **(20 pages).**

Harafah, W.O.U.M.P.; Rizky, M.E.A.; Herdiansyah, H.; Istighfarani, S., (2026). Environmental Behavior Driving Household E-Waste Recycling in Emerging Urban Contexts. Environments, 13: 206 (**23 pages).**

Heeks, R.; Subramanian, L.; Jones, C., (2015). Understanding e-Waste Management in Developing Countries: Strategies, Determinants, and Policy Implications in the Indian ICT Sector. Inf. Technol. Dev., 21(4): 653–667 **(15 pages).**

Huh, I.; Gim, J., (2025). Exploration of Likert scale in terms of continuous variable with parametric statistical methods. BMC Med. Res. Methodol., 25: 218 **(10 pages).**

Islam, M.T.; Dias, P.; Huda, N., (2021). Young consumers' e-waste awareness, consumption, disposal, and recycling behavior: A case study of university students in Sydney, Australia. J. Clean. Prod., 282: 124490 **(18 pages).**

Jain, M.; Kumar, D.; Chaudhary, J.; Kumar, S.; Sharma, S.; Singh Verma, A., (2023). Review on E-waste management and its impact on the environment and society. Waste Manage. Bull., 1(3): 34–44 **(11 pages).**

Koo, M.; Yang, S., (2025). Likert-Type Scale. Encyclopedia, 5(1): 18 **(11 pages)**.

Kosarkar, M.; Barthwal, S., (2025). Environmentally conscious but helpless: Consumer challenges for participation in Formal e-waste collection initiatives of India. Clean. Waste Syst., 12: 100363 **(11 pages).**

Koshta, N.; Patra, S.; Singh, S.P., (2022). Sharing economic responsibility: Assessing end user's willingness to support E-waste reverse logistics for circular economy. J. Clean. Prod., 332: 130057 **(11 pages).**

Liang, H.; Wu, Z.; Du, S., (2024). Study on the impact of environmental awareness, health consciousness, and individual basic conditions on the consumption intention of green furniture. Sustainable Futur., 8: 100245 **(11 pages).**

Linder, N.; Rosenthal, S.; Sörqvist, P.; Barthel, S., (2021). Internal and External Factors ' Influence on Recycling. Insights From a Lab. Exp. With Obs. Behav., 12: 699410 **(16 pages).**

Mahartin, T.L., (2023). Waste management plan with reduce, reuse, recycle (3r) method. J. Sustain. Soc. Eco-Welf., 1(1): 49–59 **(11 pages).**

Maphosa, M.; Maphosa, V. (2022). A bibliometric analysis of the effects of electronic waste on the environment. Global J. Environ. Sci.Manage., 8(4): 589-606 **(18 pages).**

Michael, L.K.; Hungund, S.; Sriram, K. V, (2025). Analyzing Factors Influencing E-waste Sustainable Management System. Evergreen. 12(1): 423–438 **(12 pages).**

Muthukumari, W.A.C.S.; Ahn, J.; Kim, M., (2024). Impact of information publicity on Korean residents' E-waste recycling intentions: Applying the norm activation model and theory of planned behavior. Heliyon. 10(14): e34319 **(15 pages).**

Nawaz, N.; Shaik, S.A.; Parayitam, S.; Dutot, V.; Vijayakumar, G., (2025). Electronic waste recycling intention, behavior and environmental benefits: Evidence from Middle East. Clean. Waste Syst., 11: 100320 **(15 pages).**

Nuwematsiko, R.; Oporia, F.; Nabirye, J.; Halage, A.A.; Musoke, D.; Buregyeya, E., (2021). Knowledge, Perceptions, and Practices of Electronic Waste Management among Consumers in Kampala, Uganda. J. Environ. Public Health. 3846428 **(11 pages).**

Parvez, S.M.; Jahan, F.; Brune, M.-N.; Gorman, J.F.; Rahman, M.J.; Carpenter, D.; Islam, Z.; Rahman, M.; Aich, N.; Knibbs, L.D.; Sly, P.D., (2021). Health consequences of exposure to e-waste: an updated systematic review. Lancet. Planet. Heal., 5(12): e905-e920 **(16 pages).**

Rippa, A., (2023). Infrastructure and the environment in anthropology. Soc. Sci. Inf., 63(1): 25–46 **(22 pages).**

Rusni, N.K., (2025). Spatial planning based on urban waste-generating: A streetscape design perspective. J. Placemak. Streetscape Des., 2(2): 155–169 **(15 pages).**

Sari, D.P.; Masruroh, N.A.; Asih, A.M.S., (2021). Consumer intention to participate in e-waste collection programs: A study of smartphone waste in Indonesia. Sustainability. 13(5): 1–28 **(28 pages).**

Siringo, R.; Herdiansyah, H.; Kusumastuti, R.D., (2020). Underlying factors behind the low participation rate in electronic waste recycling. Global J. Environ. Sci. Manage., 6(2): 203-214 **(12 pages).**

Trinh, D.D.; Sakurai, R., (2025). University students' e-waste disposal and recycling behavior: a cross-cultural study using an integrated psychological model. Front. Sustainable. 6: 1607525 **(21 pages).**

Vijayan, R. V; Krishnan, M.M.; Parayitam, S.; Anantharaman Duraisami, S.P.; Saravanaselvan, N.R., (2023). Exploring e-waste recycling behavior intention among the households: Evidence from India. Clean. Mater., 7: 100174 **(12 pages).**

Waheed, K.; Singh, A.; Siddiqua, A.; Gamal, M.; Laeequddin, M., (2023). E-Waste Recycling Behavior in the United Arab Emirates: Investigating the Roles of Environmental Consciousness, Cost, and Infrastructure Support. Sustainability. 15(19): 14365 **(19 pages).**

Wibowo, N.; Nurcahyo, R.; Gabriel, D.S., (2022). Environmental awareness factor of used cell phones. Global J. Environ. Sci. Manage., 8(1): 87-100 **(14 pages).**

Wickramasingha, B.; Nazeer, F.; Nandasena, T.; Nasara, F.; Nayanananda, U.; Nuwantha, S.; Nisansala, L.; Subasinghe, W., (2025). Promoting sustainability in E-waste management: a comparison of household practices and awareness between STEM and non-STEM university students in Sri Lanka. J. Mater. Cycles Waste Manage., 27(5): 3634–3649 **(16 pages).**

Wirtu, Y.D.; Godana, U.A.; Tucho, G.T., (2025). A review of public perception and awareness of e-waste management in developing countries: challenges and opportunities for sustainable solutions. Environ. Rev., 33: 1-12 **(12 pages).**

Yalcinkaya, S.; Kaleli, H.İ., (2025). Optimizing municipal solid waste collection with GIS-Based High-Density routing and zoning. Transp. Res. Part D Transp. Environ., 148: 105012 **(21 pages).**

Yang, M.; Luo, M.; Jin, J., (2025). What Roles Do Attitudes and Recycling Trust Play in the Recycling Behavior of Urban Residents of Used Clothing in China?An Analysis Based on Extended VBN Theory. Sage Open. 15(3): 1-18 **(18 pages).**

Yeh, S.-C.; Tan, A.Y.K.; Lai, R.-L.; Her, R.-S.; Fang, W.-T.; Liu, S.-Y., (2024). Influences of Social-Psychological Constructs in Predicting Taiwanese Pro-Environmental Behaviors. Behav. Sci., 14(4): 261 **(16 pages).**

Zia, G.D.; Sukri, S., (2025). Advancing sustainability: Raising awareness for e-waste management in Penang, 30–39 **(10 pages).**

AUTHOR (S) BIOSKETCHES

Fitria, D., B.Sc., Researcher, Social Environment, Community Engagement, and Environmental Economics Research Cluster, Graduate School of Sustainable Development, Universitas Indonesia Jl. Salemba Raya No 4. Jakarta Pusat, Indonesia.
- Email: *dewifitriadahlan@gmail.com*
- ORCID: 0009-0006-0373-4861
- Web of Science ResearcherID: NA
- Scopus Author ID: NA
- Homepage: https://scholarhub.ui.ac.id/jessd/editorialboard.html

Nugraheni, D.R., B.Sc., Researcher, Social Environment, Community Engagement, and Environmental Economics Research Cluster, Graduate School of Sustainable Development, Universitas Indonesia Jl. Salemba Raya No 4. Jakarta Pusat, Indonesia.
- Email: *dwirahayunugraheni@gmail.com*
- ORCID: 0009-0002-3126-5215
- Web of Science ResearcherID: QUV-0481-2026
- Scopus Author ID: 57216409800
- Homepage: https://sdgswhoswho.org/indonesia/dwi-nugraheni/

Herdiansyah, H., Ph.D., Associate Professor, Graduate School of Sustainable Development, Universitas Indonesia Jl. Salemba Raya No 4. Jakarta Pusat, Indonesia.
- Email: *herdis@ui.ac.id*
- ORCID: 0000-0003-2684-3551
- Web of Science ResearcherID: K-3075-2019
- Scopus Author ID: 57170905600
- Homepage: https://scholar.ui.ac.id/en/persons/herdis-herdiansyah/

Qamruzzaman, M., Ph.D., Professor, School of Business and Economics, United International University, Dhaka, 1212, Bangladesh.
- Email: *qamruzzaman@bus.uiu.ac.bd*
- ORCID: 0000-0002-0854-2600
- Web of Science ResearcherID: G-1194-2017
- Scopus Author ID: 57205082109
- Homepage: https://sobe.uiu.ac.bd/faculty/qamruzzaman/

HOW TO CITE THIS ARTICLE:
Fitria, D.; Nugraheni, D.R; Herdiansyah, H.; Qamruzzaman, M., (2027). Consumer awareness, participation, and accessibility in sustainable electronic waste management. Global J. Environ. Sci. Manage., 13(1): 413-432.

DOI: 10.22034/gjesm.2027.01.19
URL: https://www.gjesm.net/article_736262.html

Global Journal of Environmental Science and Management
(GJESM)

Homepage: https://www.gjesm.net/

Podcasts

CASE STUDY

Integrated system dynamics modeling for sustainable fisheries provisioning services

A.N.K.B.P. Iskandar[1,*], D. Iskandar[1], Sunardi[2], Zahidah[3], R. Adji[4], R. Sunaryanto[5], S.S. Antarlina[5], B.N. Marwoto[6], W. Basuki[7], N. Ismail[7]

[1]Research Center for Industrial Systems and Sustainable Manufacturing, National Research and Innovation Agency, Indonesia

[2]Faculty of Mathematics and Natural Sciences, Padjadjaran University, Indonesia

[3]Faculty of Fisheries and Marine Science, Padjadjaran University, Indonesia

[4]Study Program of Agribusiness, Faculty of Business, President University, Indonesia

[5]Research Center for Food Technology and Processing, National Research and Innovation Agency, Indonesia

[6]Research Center for Pharmaceutical Ingredients and Traditional Medicine, National Research and Innovation Agency, Indonesia

[7]Directorate of Policy Evaluation for Research, Technology, and Innovation, National Research and Innovation Agency, Indonesia

ARTICLE INFO

Article History:
Received 17 May 2026
Revised 20 July 2026
Accepted 24 August 2026

Keywords:
Ecosystem condition
Management model
Reservoir
Sustainable development goals
System dynamics

DOI:10. 22034.gjesm.2027.01.20

ABSTRACT

BACKGROUND AND OBJECTIVES: Fisheries provisioning services deliver food production, livelihoods and ecosystem functions, but are increasingly under pressure from environmental degradation, declining fishery resources and socio-economic stressors. Traditional paradigms in fisheries governance often exhibit a deficiency in accounting for the multidirectional feedback loops linking ecological systems with socio-economic dynamics. The objectives of this study were to develop an integrated system dynamics model to assess interactions between these dimensions and identify management options to improve fisheries provisioning services through long-term scenario simulations.

METHODS: A system dynamics model was integrated, consisting of social, environmental, and economic sub-models using primary and secondary data from 2018-2023. The model includes population, fishermen, floating net cages, alternative employment, willingness to be a fisher, water quality and aquatic conditions, fish restocking, capture fisheries production, fisheries productivity, fish processing innovations, income, costs, and fisher's income. The model was verified and validated using the mean absolute error and average variation error metrics. Subsequently, predictive simulations were projected to 2045 under current, moderate, and optimistic scenarios.

FINDINGS: Actual capture fisheries production declined by 88.9 percent, from 588,100 kilograms in 2018 to 65,035 kilograms in 2023 and was projected to decline to 31,179 kilograms by 2045 under current conditions. Under the moderate and optimistic scenarios, the number of floating net cages was modeled with an annual reduction rate of 30% and 35%, respectively. Production recovery commenced in 2027 under the moderate scenario and in 2026 under the optimistic scenario. Furthermore, target water quality conditions were achieved by 2041 and 2037, respectively, while fisher's net income reached positive values by 2034.

CONCLUSION: The integrated system dynamics model underscores the potential for the sustainability of fishery production services through coordinated actions across social, environmental, and economic dimensions. The faster realization of target outcomes under the optimistic scenario highlights that proactive, coordinated interventions effectively expedite ecological restoration, fisheries output, and socioeconomic progress. This model offers a decision-support framework for assessing long-term fisheries management strategies.

This is an open access article under the CC BY license (http://creativecommons.org/licenses/by/4.0/)

NUMBER OF REFERENCES	NUMBER OF FIGURES	NUMBER OF TABLES
50	6	4

*Corresponding Author:
Email: andi077@brin.go.id
Phone: +62 812 4147 9161
ORCID: 0000-0001-9491-170X

INTRODUCTION

Reservoir fisheries are an important part of the inland food system, providing fish for human consumption, employment, income and ecosystem services, especially for communities with limited alternative livelihoods. Inland fisheries are critical for global food security and livelihoods and are associated with freshwater ecosystem functions and several sustainable development goals (SDGs) (Smith and Bennett, 2019; Lynch *et al*., 2020). In South and Southeast Asia, capture fisheries and aquaculture, encompassing supply and consumption dynamics—are progressively recognized as integral subsystems within the wider food matrix, moving away from traditional treatments as standalone productive domains (Tezzo *et al*., 2021). Thus, the sustainability of reservoir fisheries is not only about fish abundance and fishing practices, but also about the relationships among environmental conditions, community livelihoods, resource use and governance, and economic incentives. Characterized as intricate socio-ecological matrices, reservoirs accommodate competing sectors such as fisheries, aquaculture, hydropower, agriculture, and urban infrastructure, which collectively generate pronounced anthropogenic pressures on aquatic ecosystems. Reservoir fisheries in tropical Asia result from a complex interaction among aquatic ecology, resource users, watershed processes, and institutional decision-making. Therefore, an integrated and transdisciplinary management approach is required (Schiemer *et al*., 2024; Solomon *et al*., 2020). Socio-ecological feedback loops are also important, as changes in fish abundance and catch opportunities may influence human behavior, while fishing decisions and resource use patterns, in turn, influence fish populations and ecosystem conditions (Wilson *et al*., 2020). Consequently, fisheries management frameworks reliant exclusively on biological metrics risk disregarding critical socioeconomic feedback, potentially precipitating unintended adverse consequences. Another significant pressure on reservoir ecosystems is aquaculture. Floating net cage (FNC) operations can increase food production and local income, but high stocking densities, overfeeding, and poor waste management can lead to increased nutrient and organic matter loads. Aquaculture effluents may contain nutrients, suspended solids, organic matter, and other contaminants that can cause eutrophication and environmental degradation (Ahmad *et al*., 2021; Liu *et al*., 2024). Consequently, evaluations of aquaculture carrying capacity must extend beyond physical production limits to explicitly incorporate ecological, social, and economic dimensions (Weitzman and Filgueira, 2020). A holistic assessment should also consider stakeholders, spatial and temporal variability, environmental changes and interactions between ecological and socioeconomic factors (Kluger and Filgueira, 2021; Weitzman *et al*., 2021). These complexities are particularly acute in reservoir ecosystems characterized by spatial competition and resource rivalry between cage aquaculture operations and capture fisheries. The Jatigede Reservoir is an artificial freshwater ecosystem that provides fisheries products and livelihood opportunities to the surrounding communities. The fisheries provisioning services of Jatigede Reservoir were recently classified as moderate due to anthropogenic pressures from residues of FNC, river waste, boat activities, and domestic activities (Iskandar *et al*., 2024). These results suggest that management should consider ecosystem conditions and community resource-use activities simultaneously to sustain fisheries provisioning services. One of the problems in Jatigede Reservoir is the management of FNC activity. FNC aquaculture can generate fish production and economic benefits, but overdevelopment can increase nutrient loads and degrade water quality. A study of the trophic status and carrying capacity of FNC in Jatigede Reservoir revealed significant nutrient enrichment, highlighting the need to

control the growth of FNC within the reservoir's carrying capacity (Marsela *et al*., 2023). findings align with broader evidence demonstrating that intensive aquaculture can generate environmental externalities when production and waste discharge exceed the assimilative capacity of aquatic ecosystems (Ahmad *et al*., 2021; Liu *et al*., 2024). Consequently, evaluating FNC management must extend beyond sectoral aquaculture policies to incorporate comprehensive assessments of water quality, capture fisheries productivity, and local socioeconomic well-being. The capture fisheries in Jatigede Reservoir have a very strong influence on the condition of the aquatic ecosystem. Plankton communities are used as indicators of reservoir environmental conditions, reflecting the importance of aquatic ecological processes in evaluating fish habitats (Dahlan *et al*., 2020; Rosadi, 2020). Recent studies (Iskandar *et al*., 2024) also indicate that the provision of sustainable fisheries services within the Jatigede Reservoir is fundamentally governed by complex interactions between environmental dynamics and anthropogenic stressors. Environmental degradation can affect fish stocks and the production of capture fisheries. Reduced catch and income in the future can affect fishing behavior, livelihood choices, and pressure on resource use; similar feedback loops have been described in freshwater fisheries, where human decisions and fish population dynamics are coupled over time (Wilson *et al*., 2020). The single variable-based management approaches are inadequate for ensuring the long-term viability of fisheries. Because these socio-ecological interactions are inherently complex, they necessitate analytical frameworks capable of capturing feedback loops, time delays, and temporal dynamics. System dynamics provides such a method. It models feedback structures and interrelated variables, and mimics their behavior under different conditions. Its application to environmental and sustainability challenges can assess nonlinear interactions and potential consequences of management actions. Systems modeling is regarded as beneficial for tackling interconnected environmental, social, and economic goals, as well as for evaluating the interactions among the SFGs (Moallemi *et al*., 2021). Integrated socio-economic-ecological models have been used in fisheries management to describe the relationships among fishery resources, communities, economic activities, and environmental conditions (Failler *et al*., 2021). Furthermore, system dynamics modeling has been widely applied in fisheries management to evaluate alternative policy strategies and examine the intricate interactions among biological, social and economic dimensions (Ismail *et al*., 2022). The paper demonstrates the potential of system dynamics as a decision-support tool rather than as a forecasting method. The importance of integrated modeling lies in the fact that fisheries management involves a trade-off between ecological conservation and socio-economic objectives. Application of the European sea bass fishery model demonstrates that management performance is fundamentally governed by the interplay between biological conditions and economic drivers, highlighting the necessity of simultaneously evaluating multiple objectives (Tidbury *et al*., 2021). Similarly, modeling system dynamics in socio-ecological systems can represent feedback loops among human activities, environmental processes, and ecosystem services, and evaluate alternative management pathways (Berrio-Giraldo *et al*., 2021). This enables a shift from separate environmental or economic assessments to a more integrated framework for assessing alternative interventions. However, previous studies on Jatigede Reservoir have focused mainly on specific aspects, including plankton communities, environmental factors, trophic status, fisheries provisioning services, and the carrying capacity of FNC (Dahlan *et al*., 2020; Marsela *et al*., 2023; Iskandar *et al*., 2024). Long-term management strategies frequently overlook the dynamic interactions among environmental variables, fishing practices, social dynamics,

fisheries production, and fisher's income. This is an important gap in literature as interventions targeting one component may have implications for other components. Reducing activities in FNC may relieve environmental pressure. Nonetheless, it will impact livelihoods, while increasing capture fisheries production without restoring environmental conditions may not yield sustainable outcomes in the long run. The innovation of this study lies in the creation of an integrated system dynamics model that connects social, environmental, and economic sub-models to evaluate the long-term sustainability of fisheries provisioning services. The model includes interactions between FNC activities, water conditions, capturing fisheries production, fisheries productivity, innovations in fish processing, fisher income, and social variables. To evaluate the effects of varying management intensities on fisheries provisioning services through 2045, three distinct trajectories were modeled: current, moderate, and optimistic. Quantitative social-ecological modeling can help reveal feedback between human actions and ecological dynamics and offer a basis for assessing alternative fisheries management strategies (Restrepo-Gómez *et al*., 2022). Whereas earlier evaluations typically examined individual indicators in isolation, the present study establishes a scenario-based decision-support framework to trace the systemic management variables through interconnected social, environmental, and economic feedback loops (Schiemer *et al*., 2024). The study examines alternative interventions that affect the activities of FNC, water conditions, fisheries production, and fisher's income. Results of this study are expected to provide a framework to support scientific decision-making for evaluating alternative fisheries management strategies and to support sustainable management of aquatic resources. To improve the long-term sustainability of fisheries provisioning services, this study aims to develop an integrated system dynamics framework designed to parse multidimensional interactions across social, environmental, and economic sectors and identify optimal management pathways. The data used in the study were primary and secondary data obtained in 2018-2023, as well as model projections and scenario simulations until 2045. The study was conducted at the Jatigede Reservoir in West Java, Indonesia. The study was conducted in Jatigede Reservoir, Sumedang Regency, West Java, during 2022 to 2024.

MATERIALS AND METHODS

Data collection method and data analysis

Primary data were collected through field observations, interviews with fishermen and other reservoir stakeholders, and field and laboratory measurements, whereas secondary data were collected from relevant literature and government agencies. Environmental samples were collected at seven stations, and water samples were collected twice during the sampling period; water sampling was conducted only at a depth of 10 meters (m) from the surface. Fishery related data were compiled using field observation and semi-structured interviews. The system dynamics model was parameterized using six years of historical data (2018-2023) and incorporated dedicated sub-models for social, environmental, and economic indicators. The model was constructed and simulated using Powersim software to examine the temporal dynamics of fisheries provisioning services and to evaluate alternative scenarios.

System dynamics model concept

System dynamics analysis was used to understand the model and to simulate a complex system in a simple way, with variables that are reciprocally interconnected (Sterman, 2002). The analytical procedure was conducted in a sequential, stepwise manner. The initial phase focused on objective analysis and problem formulation, identifying core system requirements and defining structural problems to establish pathways toward overarching system goals. The

next step is system identification, which presents the system as a causal loop diagram (CLD) showing the feedback loops between variables in a model. CLDs were constructed by illustrating the feedback loops among variables in the system (Firmansyah *et al*., 2019). This study used three sub-models following aspects of fisheries and sustainability (Charles, 2001):

1) Social sub-model, which accounts for human population dynamics, the scale of FNC cultivation, alternative employment opportunities, total fishermen, and individual willingness occupational preference to enter the fishing sector. 2) The ecological or environmental sub-models, which track water quality status and general aquatic environmental conditions. 3) The economic sub-models, which simulates capture fisheries production, fish restocking rates, overall productivity, the total surface water area of the Jatigede Reservoir, processing volumes, product innovation in fish processing, fisher's income, aggregate revenues and costs, and total revenues generated from fisheries processing.

a. CLD: A CLD l loop diagram was made after system identification. In this study, there will be three sub-models. The variables in each sub-model are described as reciprocal relationships.
b. Data Collection: After making CLD, data collection related to each variable in the system was carried out. The data collected will be included in the stock flow diagram.
c. Stock Flow Diagram: The variables taken come from CLD. Then, classify which variables are included in the level, parameters, and initial conditions.

Model verification and Validation: The subsequent phase involved verifying the logical and mathematical integrity of the conceptual implementation to ensure that the integration of model formulation into the stock-flow diagram variables produced no runtime or computational errors. There are two metrics to validate the model: Absolute mean error (AME) and average variation error (AVE). The acceptable deviation is limited to <10 percent (%). Model validation was conducted using AME and AVE tests for each variable, yielding AME values of 1-7% and AVE values of 2-5%, both within the acceptable threshold of <10%, indicating that the model adequately reproduces the historical patterns within the adopted criteria, for AME and AVE, using Eqs. 1 and 2 (Walukow, 2011):

$$AME = \frac{Si-Ai}{Ai} \quad (1)$$

Where:
Si = Si/N
Ai = Ai/N
A = Actual value
Si = Simulation value
N = Observation time interval

$$AVE = \frac{Ss-Sa}{Sa} \quad (2)$$

$Ss = ((Si-Si)^2N)$
$Sa = ((Ai-Ai)^2N)$
Sa= Deviation of actual value
Ss= Deviation of simulated value

d. Sensitivity analysis: Sensitivity analysis was conducted to evaluate the robustness of the model outcomes to variations in key scenario parameters. The evaluated parameters comprised the reduction of floating net-cage capacity, water-quality intervention, occupational preference for commercial fishing, and technological innovation in fish processing. Each parameter varied by -20%, -10%, baseline, +10%, and +20% relative to the corresponding scenario baseline. The resulting changes in key model outputs, including capture fisheries production, fisher's income, fish catch productivity, processed fish products, water condition, and FNC stocks, were compared across the sensitivity ranges. The sensitivity analysis retained the structural architecture and simulation horizon of the primary scenario

analysis, evaluating model projections evaluated through the year 2045.

e. Projection, Simulation, and Scenario: At this stage, system behavior is studied because of scenario settings. During the simulation phase, model outputs were generated using Powersim initialized with empirical baseline data. The simulation time step was configured to be one year, with model outputs being recorded annually. In the stock flow diagram, several scenarios were run, generating annual variable data from 2025 until 2045. The year 2045 was selected to align with the government program, Indonesia Emas, and the achievement of the SDGs in Indonesia. The scenario parameters were derived, which pertains to the regional management framework, including the Regional Regulation of Sumedang Regency Number 4 of 2018 concerning the Regional Spatial Plan of Sumedang Regency for the period of 2018-2038, as well as the capacity and environmental management context of the Jatigede Reservoir. These parameters were built as policy assumptions, not statistical forecasts. The levels of the FNC s reduction and water-condition intervention were selected to represent varying degrees of management intensity within the local socio-ecological setting. Whereas the moderate scenario represents a lower-intensity intervention pathway, the optimistic scenario is designed as a more stringent policy stress-test. Thus, these values were used to explore system response to different levels of intervention, not to describe empirically predicted future behavior. The scenarios simulated in this study were:

1) Floating net cages: FNC decreased by 30% (moderate scenario) and decreased by 35% (optimistic scenario).

2) Water condition: FNC decreased by 8% (moderate) and decreased by 10% (optimistic). 3) Capture fisheries: The willingness to become a fisherman variable increased by 0.002% (moderate scenario) and the willingness to become a fisher variable by 0.003% (optimistic scenario).

4) Fisher's income: Increases willingness to become a fisher by 0.002% and increases the number of processed fishery product innovations by 6% (Moderate). Increase willingness to become a fisher by 0.003% and increase the number of processed fishery product innovations by 8% (optimistic).

RESULT AND DISCUSSION

Integrated system structure and baseline dynamics

A CLD maps the feedback structures and component interactions underlying capture fisheries sustainability, thereby delineating the causal pathways necessary to achieve management goals. The CLD is then translated into an input-output diagram. A CLD illustrates the correlations among variables in a system with feedback (Firmansyah *et al*., 2019). The causal loop represents the system being modeled; later, it serves as the basis for formulating the stock-flow diagram. The system identification carried out identified 17 interconnected variables that can affect the management system, leading to the creation of a CLD. The CLD depiction is based on quantitative variables identified in the input-output system. The CLD diagram is structured into social, environmental, and economic sub-models. This classification is designed to organize variables according to the core dimensions under investigation, specifically highlighting policy levers governed by public authorities acting as controllers of the fisheries provisioning services management system. The CLD is presented in Fig. 1. Fig. 1 illustrates the feedback structure underlying the interactions among the principal components of the fisheries system and serves as the basis for interpreting the model dynamics. Six major reinforcing feedback systems (R1-R6) are identified to capture the dominant pathways through which changes in fisher participation, FNC activities, environmental conditions, fish

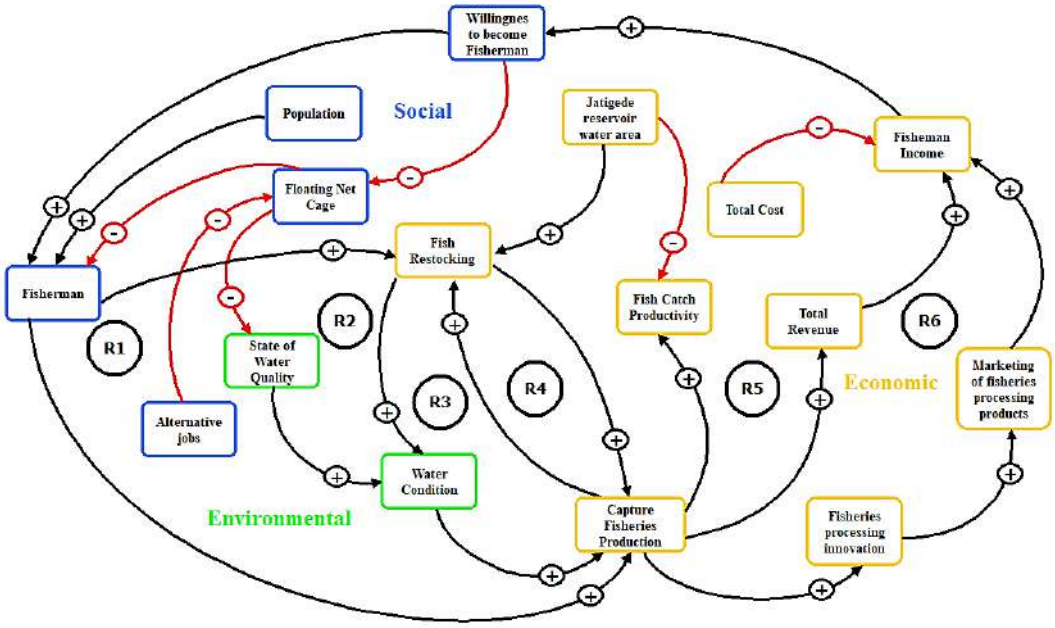

Fig. 1. The CLD for fisheries provisioning services in Jatigede Reservoir

restocking, capture fisheries production and economic performance propagate throughout the system. The polarity symbols (+/−) show the direction of causal influence between variables and the reinforcing loops show feedback processes that amplify changes in the system. Consequently, the CLD establishes a conceptual foundation for exploring the feedback dynamics embedded within the model. These causal pathways are subsequently operationalized and expanded according to the specific objectives of each sub-model.

The *number of FNC decreases*

This objective is the goal of the social sub-model related to anthropogenic pressure or community activities that harm the environment. Given the ongoing annual expansion of floating net-cage aquaculture and its compounding pressures on aquatic environmental quality, this sub-model is designed to simulate and evaluate strategies for mitigating cage density. When viewed from the CLD, the number of FNC is influenced by the variable of alternative jobs and the variable of willingness to become a fisher. System feedback mechanisms link FNC density to socio-economic and ecological variables. Labor market shifts—such as the expansion of alternative employment and fluctuations in occupational preference—exert a negative feedback effect on FNC proliferation. Ecologically, reductions in FNC scale mitigate organic waste accumulation, enhancing water quality scores in the Jatigede Reservoir. Socio-economically, FNC expansion acts as a driver of livelihood diversification, which inversely affects the total number of active fishermen by reducing reliance on capture fisheries (Béné *et al*., 2016; Allison and Ellis, 2001; Stacey *et al*., 2021). Furthermore, the increase in FNC has a negative impact on water quality, as organic waste from fish feed and excrement can increase eutrophication and degrade the ecological condition of the water (FAO, 2009; Cao *et al*., 2007; Liu *et al*., 2024).

Water conditions are in a good category

The environmental sub-model aims to find water conditions that fall into the good category.

Jatigede Reservoir is heavily polluted, requiring a management model that focuses on improving water conditions. Water condition variables are influenced by water quality status (positive relationship). If the water quality status is good, the water condition is also good. In addition, variables that can affect water conditions are fish restocking variables (positive relationship). Aquatic health is determined not only by physicochemical water quality parameters but also by the biological abundance within the ecosystem. Consequently, fish stocking initiatives can enhance aquatic biodiversity and foster equilibrium between biotic communities and water quality conditions. Therefore, the water conditions will also be good if the fish restocking variable increases. Good water conditions can affect fisher's catch (positive relationship). If this variable is in good condition, it supports fish in living, developing, and adapting, which increases the amount of fish life. Successful fish recruitment and reproduction drive population growth, which in turn enhances aggregate harvest rates and tota capture fisheries production. Improved water quality has a positive impact on capturing fisheries production, as habitat quality directly influences the abundance and health of wild fish stocks (Lorenzen, 2008; Welcomme and Bartley, 1998; Smith and Bennett, 2019). On the other hand, fish restocking activities can also improve water conditions by enhancing ecological balance, particularly if the released fish species play an ecological role in controlling certain aquatic organisms or plants (Bell *et al*., 2006; Silva, 2003).

Increased capture fisheries production

The economic sub-model has two objectives, one of which is capturing fisheries production. The restocking variable (positive relationship) influences the capture fisheries production variable. Although the model assumes that increased fish restocking can enhance capture fisheries production, the magnitude and persistence of this contribution remain. This uncertainty stems from the lack of explicit quantification for post-stocking survival, recruitment, ecological interactions, and fishing pressure are not explicitly quantified. This aligns with observed variations in stocking efficacy and reinforces the necessity of treating its contribution as probabilistic rather than assuming a uniform effect on future catch (Stewart and Long, 2016). Another variable that affects the number of fish caught is water conditions (positive relationship). Good water conditions will increase the survival of organisms, increasing the quantity of fish in the waters and the amount of catch. Another variable that affects capture fisheries production is the number of fishermen (positive relationship). The overall catch or capture fisheries production will increase if the number of fishermen increases. The variable influenced by capture fisheries production is the number of restocked fish (positive relationship). Annual fish restocking rates are dynamically linked to total commercial catch volumes. Consequently, an increase in aggregate harvest yields drives a corresponding expansion in subsequent stocking quantities. Another variable influenced by fisher's catch is the innovation of processed fishery products (positive relationship). If the capture fisheries production increases, the processed products of fishermen who do processing business will also increase. The total revenue variable is influenced by fisheries production (positive relationship). The more fishermen catch, the more fish are sold, and the more total revenue increases. The last variable influenced by capturing fisheries production is the fish productivity variable (positive relationship). Elevated catch rates correspond directly with enhanced fisheries productivity. Furthermore, growth in the active fishing population stimulates fish restocking efforts, driven by the critical role of community participation in sustaining stock enhancement programs. This active local involvement simultaneously reinforces the social and institutional capacities necessary for successful restocking interventions (Lorenzen, 2008; Garaway *et al*., 2006; Katre *et al*., 2024). Accordingly, the increase in the number of

fishermen is also positively correlated with capture fisheries production, as increased fishing effort directly boosts total catch up to the optimal capacity limit (Hilborn and Walters, 1992; Charles, 2001). Fish restocking itself has a clear positive relationship with capture fisheries production, as the addition of stock directly increases the fish biomass available for harvest (Lorenzen, 2008; Lorenzen, 2005). This production growth subsequently improves catch productivity, as rising stock abundance facilitates higher catch per unit effort for fishers (Hilborn, 2007; Haddon, 2007; Schiemer *et al*., 2024).

Fisher's income increases

Another purpose of the economic sub-model is to increase fisher's income. The results of interviews with 40 captured fishermen in Jatigede Reservoir show that fisher's income has decreased from previous years. The primary objective of this model is to inform the sustainable management of fisheries and aquatic environments, thereby fostering community well-being through the enhancement of fisher's income. Total revenue (positive relationship) influences the fisher's income variable. The more total revenue fishermen receive from fish sales, the higher their income. The total cost variable is also a variable that affects income (negative relationship). If the total costs incurred by fishermen increase, the net income of fishermen decreases. The variable that affects fisher's income is the marketing variable of processed fishery products (positive relationship). An expansion in the processing of fishery products drives proportional growth in product distribution and commercialization, which consequently enhances household incomes within the fishing community. Increased capture fisheries production also has a direct impact on the total revenue of the fisheries sector, given the linear relationship between production output and fisher's economic income (Lorenzen, 2008; Charles, 2001; Smith *et al*., 2005). This increase in production subsequently spurred innovation in fisheries processing, as the greater availability of raw materials encouraged market actors to develop new processing methods with higher added value (Delgado *et al*., 2003; FAO, 2016). Furthermore, the expansion of the Jatigede Reservoir's surface area has also spurred an increase in restocking activities, as the provision of a larger aquatic space creates ecological opportunities for the development of restocking-based fisheries (FAO, 1998; Lorenzen *et al*., 2001). Economically, expansions in total sectoral revenue directly augment fishers' incomes, reflecting the strong interdependence between individual financial returns and the broader performance of the fisheries sector (Lorenzen, 2008). Within the fisheries value chain, innovations in fish processing drive increased marketing of these innovative products, as a growing variety of value-added products opens new market opportunities (Allison and Ellis, 2001; Smith *et al*., 2005; Stacey *et al*., 2021). Ultimately, this increase in marketing activities for innovative fish products positively influences fishers' earnings, as market expansion and elevated price points for processed products enhance the economic benefits received by fishing households (Béné *et al*., 2016; FAO, 2016).

Baseline projection of fisheries provisioning services

Stock flow diagrams were constructed and expanded based on the variables identified in the CLD. Subsequently, the model was parameterized using empirical primary data and secondary datasets compiled from relevant agencies and previous literature. The resulting stock-flow diagram for the fisheries provisioning services model is presented in Fig. 2. Stock flow diagrams are used to project data trends through 2045 and to create scenarios using the sub-model to inform policy related to the Jatigede reservoir water environment and sustainable fisheries. The actual data used in this study are 2018-2023 data. The data projection on the stock-flow diagram shows the model's projection for variables related to fisheries provisioning services. Projection data in the stock-flow diagram relate to variables for FNC,

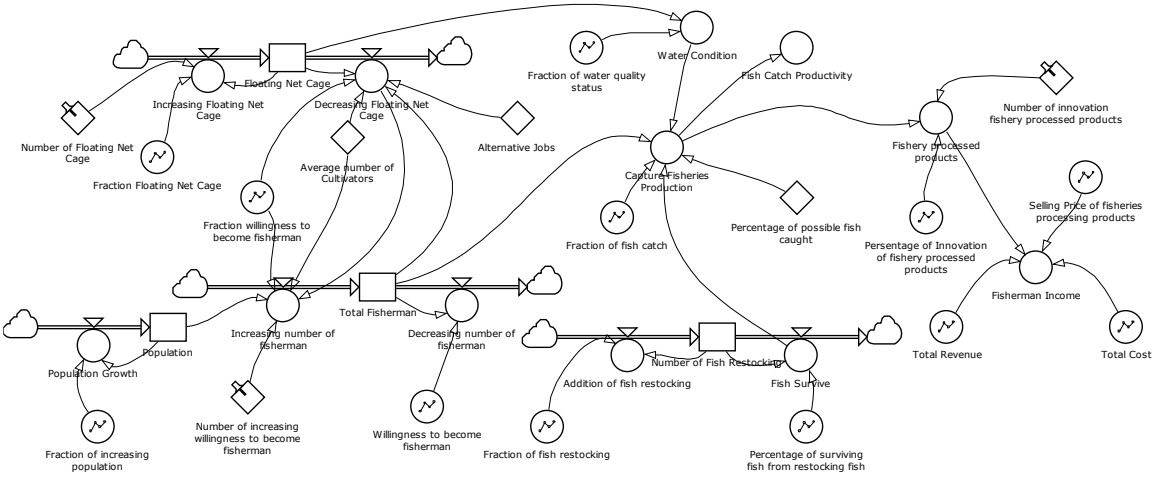

Fig. 2. Stock flow diagram of fisheries provisioning services in Jatigede Reservoir

fishermen, water conditions, capture fisheries production, the number of fish processed into fisheries products, and fisher's income. Projections and data trends for 2018-2045 are shown in Table 1. The trend observed in Table 1 shows the projection increases or decreases in data for each variable until 2045. The FNC data show an increase, indicating that without intervention from economic drivers, public awareness, government intervention, and so on, the number of FNC will continue to rise. As detailed in the preceding data, the total active fishing population exhibits a declining trend that corresponds inversely with the expansion of FNC. According to the results of interviews with 40 fishermen, there are some fishermen who do not want to be fishermen and turn their profession into cultivators in FNC. The condition of Jatigede Reservoir waters shows a trend of increasing pollution, with STORET scores in the hundreds, indicating it has entered the heavily polluted category. This is also in line with the number of FNC, which are a source of pollutants in the waters, and, as described in the causal loop and stock flow diagrams, FNC affect the condition of the waters of Jatigede Reservoir. Aquatic environmental conditions directly influence the viability of aquatic organisms, subsequently constraining aggregate harvest yields in capture fisheries. Furthermore, this dynamic is compounded by the ongoing contraction of the active fishing workforce. Historical and projected simulation data spanning from 2024 to 2045 indicate that capture fisheries production has experienced a declining trend since the initial inundation of the Jatigede Reservoir. The results of interviews with people living in and around the Jatigede Reservoir and fishermen who work in its waters show that only 1 fisher processes his catch into dried fish products, which adds to the fish's selling value. Annual data demonstrates a progressive decline in the volume of fish allocated for value-added processing. Without targeted interventions such as capacity-building programs to increase the number of fishers engaged in product processing, this downward trajectory is projected to persist. Model projections indicate that while capture fisheries yields will rise through 2045, the volume of processed fishery products will experience a continuous decline. Total household income for fishers is calculated as the aggregate revenue generated from both fresh fish harvest sales and processed fishery commodities. Consequently, as processing output contracts over time, annual income exhibits a steady downward trend, reflecting declining production capacity, reduced value addition, and increasing livelihood vulnerability.

Table 1: The number of fish processed into fisheries products, and fisher's income and projections data for 2018-2045

Year	Floating net cage (unit)	Total fishermen (People)	Water condition	Capture fisheries production in kilograms (kg)	Number of fish processed (kg)	Fisher income (USD)
Actual data						
2018	250	123	-7	588,100	1,800	140,849
2019	625	122	-15	489,675	1,800	138,132
2020	750	123	-25	275,125	180	84,400
2021	333	110	-45	238,705	180	55,454
2022	816	111	-52	169,365	90	34,986
2023	885	110	-94	65,035	90	13,270
Projection data						
2024	891	106	-94	62,328	86	13,278
2025	897	101	-95	59,762	82	13,286
2026	904	97	-96	57,331	79	13,294
2027	910	93	-96	55,030	76	13,301
2028	916	90	-97	52,853	73	13,307
2029	922	86	-98	50,796	70	13,314
2030	929	83	-98	48,855	67	13,320
2031	935	80	-99	47,025	65	13,325
2032	942	77	-100	45,301	63	13,331
2033	948	74	-100	43,680	60	13,336
2034	955	72	-101	42,159	58	13,340
2035	961	69	-102	40,734	56	13,345
2036	968	67	-103	39,402	54	13,349
2037	974	65	-103	38,160	53	13,352
2038	981	63	-104	37,006	51	13,356
2039	988	61	-105	35,936	50	13,359
2040	995	59	-105	34,949	48	13,362
2041	1,002	58	-106	34,041	47	13,365
2042	1,008	56	-107	33,213	46	13,368
2043	1,015	55	-108	32,460	45	13,370
2044	1,022	54	-108	31,783	44	13,372
2045	1,029	53	-109	31,179	43	13,374

Initial conditions

The system dynamics model was formulated using the Stock-Flow diagram and the functional relationships among the social, environmental, and economic variables. The initial conditions of the principal stock variables were defined using the 2018 observed values, including 250 FNC, 123 fishermen, a water-condition score of -7, 588,100 kg of capture fisheries production, and 1,800 kg of processed fishery products. Model parameters were derived from official statistics, field observations, interviews, and secondary data sources, as detailed in Table 2.

Verification and validation

Verification and validation were conducted to ensure that the dynamic model adequately represented the 2018-2023 historical system. Model verification involved checking the stock flow diagram and input data, while validation used AME and AVE to compare simulated and actual outputs. The validation results were below 10% for FNC (AME 1%, AVE 5%), water condition (2%, 4%), capture fisheries production (3%, 2%), and fisher's income (7%, 2.6%), indicating that the model was suitable for subsequent scenario analysis (Walukow, 2011).

Scenario simulation and management implications

The scenarios created in this study aim to achieve the objectives of the three sub-models developed in the problem identification section. The sub-models are the social, environmental, and economic sub-models. These three sub-models interact to capture the complex dynamics of the fisheries system and evaluate its broader

Table 2: Variable, unit, and data source of stock flow diagram

Variable	Unit	Stock flow diagram symbol
Population	People	level
Population growth	People/year	Rate
Fraction of increasing population	%	Auxiliary
FNC	FNC	Level
Increasing FNC	FNC	Rate
Fraction of FNC	%	Auxiliary
Decreasing FNC	FNC	Rate
Alternative jobs	%	Constant
Average number of cultivators	People/Floating net cage	Constant
Fraction's willingness to become a fisher	%FNC	Auxiliary
An increasing number of fishermen	People	Rate
Total Fisher	People	level
Decreasing number of fishers	People	Rate
Willingness to become a fisher	%	Auxiliary
Fraction of water quality status	-	Auxiliary
Water Condition	-	Rate
Capture fisheries production	Kg	Rate
Fraction of fish catch	Kg/people	Auxiliary
Percentage of possible fish caught	%	Constant
Fish that survive restocking	Kg	Rate
Number of fish restocking	Kg	level
Addition of fish restocking	Kg	Rate
Fraction of fish restocking	%	Auxiliary
Jatigede Reservoir water area	M^2	Constant
Fish catch productivity	Kg/M^2	Rate
Fishery processed products	Kg	Rate
Percentage of fishery processed products	%	Auxiliary
Selling price of fisheries processing products	Rp	Auxiliary
Total revenue	Rp	Auxiliary
Total cost	Rp	Auxiliary
Fisher income	Rp	Rate

socioeconomic and environmental consequences. Data simulations for each sub-model are conducted across three comparison aspects: actual data trends, trends from moderate simulations, and trends from optimistic simulations. The moderate scenario embodies a lower-intensity policy intervention, whereas the optimistic scenario functions as a more stringent policy stress-test. Optimistic simulation is a data scenario that uses more optimistic variable assumptions, set with the aim of achieving the best results and desired conditions.

Sensitivity analysis

Sensitivity analyses were conducted by perturbing key model parameters across a range of -20%, -10%, +10%, and +20% relative to their baseline values. Model responses were quantified as percent change from baseline and a normalized sensitivity index (SI). The results showed very different sensitivity of the intervention parameters. The sensitivity of FNC reduction was very low, with projected 2045 capture fisheries production changes of less than 0.04 % under the moderate scenario and less than 0.03 % under the optimistic scenario, with absolute SI values less than 0.002. Similarly, water-condition improvement led to less than 0.07% change in projected 2045 production, with absolute SI values below 0.004. The results demonstrate that long-term production exhibit high stability in response to variations in FNC reduction and water-quality improvement across the tested ranges. Conversely, the coupled shift in occupational inclination toward fishing and innovations in fish processing generated substantially greater system sensitivity. The projected 2045 production changed by about ±13% under the moderate

scenario and ±14% under the optimistic scenario for a ±20% change in parameters. The combined SI values ranged from 0.635 to 0.636 and 0.723 to 0.724, respectively. The results show that socioeconomic participation and value-added processing are more powerful leverage points in the modelled system than FNC reduction or water-condition improvement. However, because the inclination toward commercial fishing and fish processing innovation varies simultaneously, their individual contributions cannot be fully isolated, necessitating dedicated one-at-a-time sensitivity analyses.

Sensitivity to milestone year

Sensitivity analysis of the milestone year showed that the robustness of the projected transition timing varied across system outcomes. In the moderate scenario, FNC elimination occurred in 2041-2045, and Water Condition > -30 moved from 2045 to 2038. While production recovery exhibited relative stability between 2027 and 2030, income recovery proved significantly more sensitive. Specifically, non-negative income levels were not achieved under the baseline, -10%, and -20% conditions; however, under the +10% and +20% parameter variations, positive income recovery was attained by 2045 and 2041, respectively. In the optimistic scenario, FNC elimination and the water-condition threshold were reached earlier, varying from 2035 to 2042 and 2035 to 2041, respectively. Production recovery proved exceptionally robust, with 2026 recovery levels remaining consistent across all parameter variations. In contrast, income recovery exhibited the highest temporal sensitivity, spanning a recovery window from 2027 to 2044. Overall, the results show that production recovery is relatively robust to changes in parameters, whereas the timing of environmental and, especially, socio-economic recovery is more sensitive. This milestone year analysis is in addition to the endpoint sensitivity analysis and illustrates the robustness of the timing of the projected transition to uncertainty in the parameters.

Social dimension

The social sub-model includes aspects related to the behavior, activities, and interactions of the community around Jatigede Reservoir, as well as the impact of fisheries on social life. The variables included in the social sub-model in this study are population variables, fishermen, FNC, alternative jobs, and willingness to become a fisher. Within the social sub-model, scenario generation is driven by FNC density, as a primary objective of this module is to simulate the targeted reduction of net-cage infrastructure. In the simulation of the reduction of FNC, scenarios were developed in which the number of FNC in Jatigede Reservoir decreased by 30% annually (moderate scenario) and by 35% annually (optimistic scenario). The simulated reduction in FNC capacity was initiated in 2025. The resulting trajectories of FNC reduction are illustrated in Fig. 3. The simulation results of the FNC after two scenarios, such as the moderate and optimistic scenarios, provide data on the decline in FNC. In both scenarios, it is expected that there will not only be a decrease in the number of FNC but also that there will be no FNC in Jatigede Reservoir following government directives, as FNCs are not allowed in Jatigede Reservoir. As illustrated in Fig. 3, the moderate scenario projects that the complete eradication of FNC in the Jatigede Reservoir will be achieved by 2045. Simulation results under the optimistic scenario indicate that all FNC operations in the Jatigede Reservoir will be fully phased out by 2042. Structurally, the social sub-model interacts dynamically with the economic and environmental sub-models. Specifically, social dynamics such as FNC prevalence influence community occupational choices (i.e., willingness to enter the fishing workforce) and subsequent harvest efficiency. Concurrently, shifts within the environmental and economic subsystems collectively drive overall community welfare.

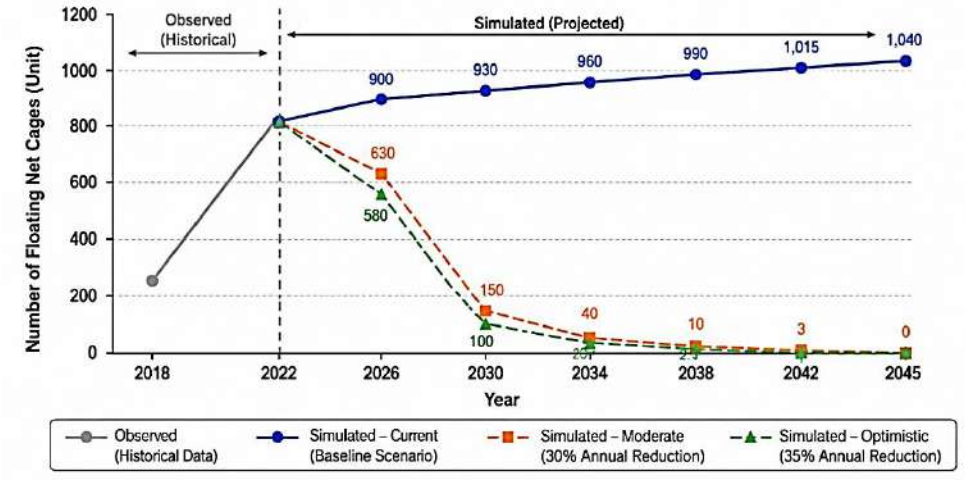

Fig. 3: Graphic simulation of FNCs

Environmental dimension

The Environmental Sub-Model represents ecological aspects related to fisheries provisioning services in Jatigede Reservoir. Variables that become environmental sub-models in this study are water quality and water conditions. The data simulation used in the environmental sub-model is data on the water condition variable, which is influenced by the FNC variable, one of the factors that contributes pollutants to water bodies and affects the condition of Jatigede Reservoir waters. The water-quality scenarios were designed to simulate management interventions aimed at restoring the ecological health of the Jatigede Reservoir to optimal conditions, specifically achieving a STORET index score exceeding -30. The scenario of water conditions is carried out with a controlled input variable of the number of FNC: a decrease of 8% (moderate) and a decrease in FNC by 10% (optimistic). The simulated water-quality trajectories are presented graphically in Fig. 4. Simulation of Jatigede Reservoir water condition data by the moderate scenario, where the number of FNC is reduced by 8% annually; the results of water conditions each year are getting better, and the target to achieve the goal of Jatigede Reservoir water conditions above a score of -30 is achieved in 2041. In the optimistic scenario, where the number of FNC is reduced by 10%, the water conditions improve every year, and the goal of water conditions above -30 is achieved in 2037. The environmental sub-model affects other sub-models (the economic sub-model), which is fish catches to fisher's income.

Economic dimension

In this dynamic system model, the third sub-model is the economic aspect of fisheries and fisheries resource management in Jatigede Reservoir, which includes production, marketing, and income. Variables included in the economic sub-model category in this study are fish restocking, Jatigede Reservoir area, capturing fisheries production, fish catch productivity, fisheries processing innovation, marketing of fisheries processing products, total cost, total revenue, and fishers' income. The economic sub-model simulation focuses on two primary output variables: the volume of capture fisheries production and fishers' incomes. The capture fisheries production variable is simulated under two scenarios: a moderate scenario with controlled inputs, using an increase of 0.002% in the willingness to become a fishers' variable, and an optimistic scenario with an increase of 0.003% over the simulation period. The simulation of the production data of the capture fisheries is illustrated in Fig. 5.

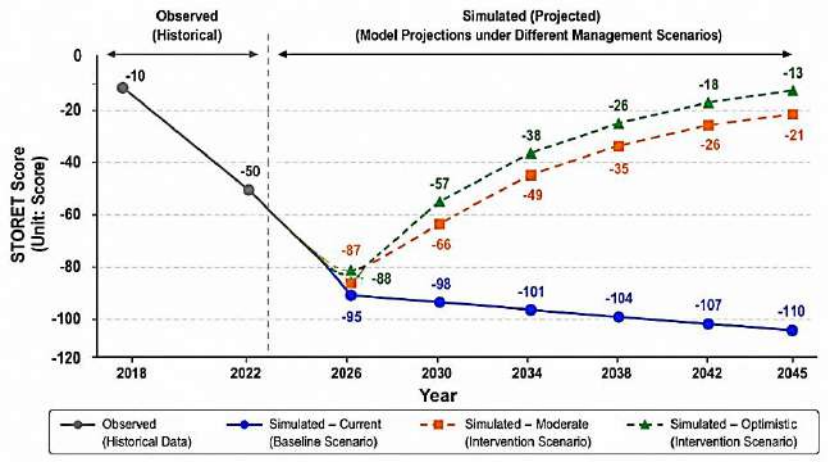

Fig. 4: Graphic simulation of water condition

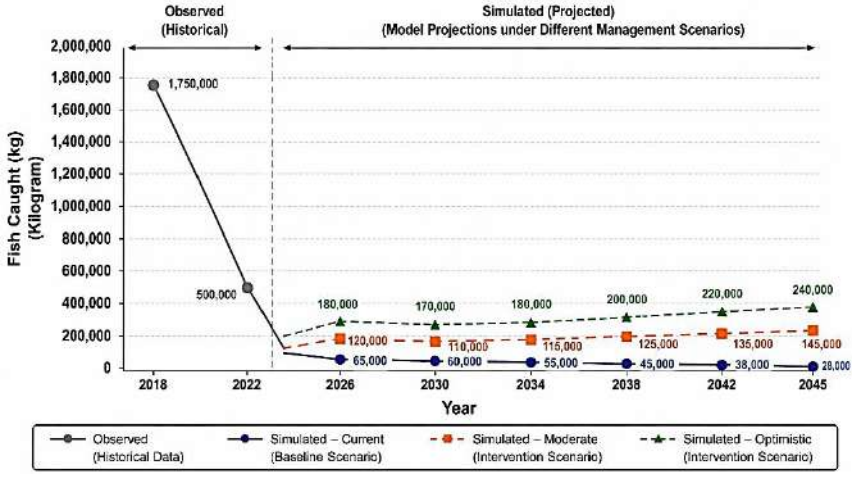

Fig. 5: Graphic simulation of capture fisheries production

The results of the comparison between the trend of actual data and data from the moderate and optimistic scenarios show that when the scenario is applied to increase the willingness to become a fishers variable in 2025, capture fisheries production increases annually. The moderate scenario shows an increase in data starting from 2027, and when the optimistic scenario is applied, fisheries production increases starting in 2026. Fishers' income constitutes a primary target output within the economic sub-model. Total earnings are governed by aggregate revenue, which is directly determined by total revenue, whereas total revenue is influenced by capture fisheries production alongside secondary economic variables, such as innovation in processed fishery products. In the simulation of increased fisher's income, the moderate scenario used is an increase in willingness to become fishermen by 0.002% and an increase in the number of processed fishery product innovations by 6%. The optimistic scenario is an increase in willingness to become a fisher by 0.003% and an increase in the number of innovations in processed fishery products by 8% for improved long-term sustainability. The simulated trajectories of fishers' income are presented in Fig. 6 under scenarios.

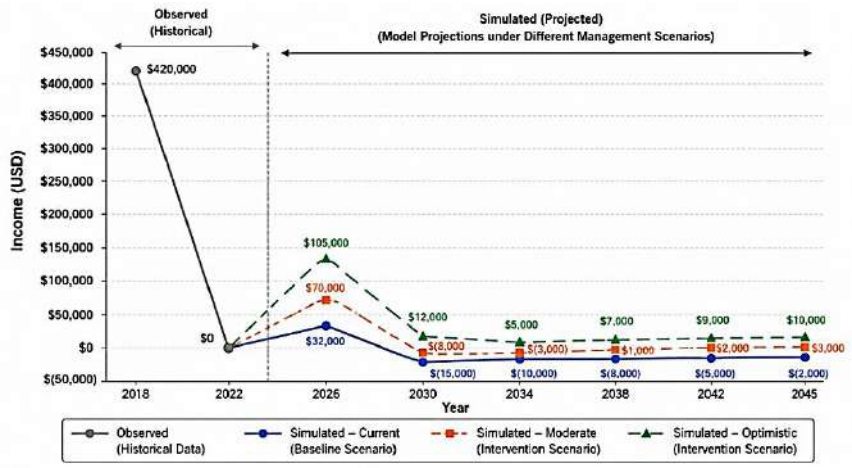

Fig. 6: Graphic simulation of fisher's income

The income of fishermen obtained from 2018 to 2023 is the total income of 40 fishermen for a year. The fisher's income in Jatigede Reservoir indicates community welfare in the economic sector. In 2023, aggregate net income for fishers on the Jatigede Reservoir yielded a negative balance. This deficit was driven by critically low daily catch rates—frequently falling below 3 kg per day or resulting in total zero-catch days—coupled with continuous operational expenditures. These fixed and variable costs encompassed fuel expenses, daily sustenance, and unforeseen losses, such as gear damage caused by submerged structural remnants within the reservoir basin. The results of the dynamic system model for fisher's income, shown in Fig. 6, indicate that under a moderate scenario, fisher's income increases, and in 2042 the total income of fishermen in Jatigede Reservoir is still negative. Under the optimistic scenario, fishers' incomes demonstrated a consistent upward trajectory, with net financial returns shifting from deficit to positive by 2034. The economic sub-model is highly dependent on environmental and social conditions. Environmental degradation can reduce fish stocks, resulting in lower catches and income for fishermen. Conversely, economic changes, such as increases in fisher's income, will affect people's desire to become fishermen and market demand.

Integrated management implications

The simulation results demonstrate strong interconnections among the social, environmental, and economic sub-models, indicating that fisheries provisioning services require an integrated management approach. Three scenarios were evaluated: the current condition, moderate scenario, and optimistic scenario. While the baseline condition maintains the trajectory of current trends absent significant intervention, the moderate and optimistic scenarios reflect realistic and intensive mitigation measures, respectively. A summary of the simulation outcomes is summarized in Table 3. The results show that the current situation is causing the continuous deterioration of environmental quality, fishery resources, and fisher's income. Conversely, while the optimistic scenario attains the primary management objectives ahead of schedule, the moderate scenario achieves them by 2045. Under the optimistic scenario, FNC reaches zero in and the target hydrological condition is attained by 2037, accompanied by an accelerated recovery in capture fisheries production and a transition to positive net income for fishers by 2034. These findings indicate that intensified interventions can significantly accelerate the recovery of fisheries provisioning services.

Table 3: General results of the simulation

Intervention	Scenario	Scenario assumption	Model outcome	Milestone
FNCs reduction	Moderate	30% reduction	FNCs decrease progressively	FNCs reach 0 in 2045
FNCs reduction	optimistic	35% reduction	FNCs decrease more rapidly	FNCs reach 0 in 2042
Water-condition improvement	Moderate	8% FNCs reduction	Water condition improves progressively	Water condition > -30 in 2041
Water-condition improvement	optimistic	10% FNCs reduction	Water condition improves more rapidly	Water condition > -30 in 2037
Integrated socioeconomic intervention	Moderate	0.002% willingness to become fishermen and 6% fish-processing innovation	Capture fisheries production and fisher's income recover gradually	Income becomes still negative in 2045 but getting better
Integrated socioeconomic intervention	optimistic	0.003% willingness to become a fisher and 8% fish processing innovation	Capture fisheries production and fisher's income recover more rapidly	Income becomes non-negative by 2034

This study also reveals that environmental restoration, social engagement, and economic diversification should be developed in parallel. Mitigating FNC alleviates environmental stress, improves hydrological conditions, and enhances aquatic resources alongside capturing fisheries production. Consequently, increased fishery yields, coupled with innovations in fish processing and improved marketing strategies, serve to strengthen fishers' incomes. This means that fisheries management should address feedback interactions among environmental conditions, social behavior, and economic performance, rather than relying on isolated interventions. The model was designed to achieve sustainable fisheries, a healthy aquatic ecosystem, and community welfare by 2045. This long-term vision aligns with the Indonesia Emas 2045 vision and the National Long-Term Development Plan 2025-2045. Thus, the model provides a decision-support framework for evaluating alternative management strategies for the SDGs. Although the optimistic scenario yields the most rapid environmental recovery, it necessitates more stringent policy enforcement and heightened public buy-in, particularly concerning the reduction of FNC. Therefore, successful implementation demands participatory planning, compensation mechanisms, alternative livelihood programs, adequate budget allocation, and cross-agency coordination. Furthermore, the integrated model provides a versatile framework applicable to other reservoirs, provided that model parameterizations are calibrated to reflect local socio-ecological conditions. Overall, the results suggest that coordinated interventions across the social, environmental, and economic dimensions are more likely to accelerate ecological recovery, fisheries production, and community welfare than isolated management actions.

Comparison with previous system dynamics studies

Consistent with prior system dynamics literature, the present model employs feedback-based simulation to evaluate fisheries sustainability and the efficacy of management interventions. Previous studies have mainly considered the environmental capacity of cage-aquaculture, fishing effort, stock management, or biological and economic interactions. For instance, Gunawan *et al.,* (2011) investigated sustainable FNC aquaculture in Cirata Reservoir, integrating cage production, environmental quality, and farm profitability into their analysis (Château *et al.,* 2015). Moreover, Martins *et al.* (2015) and Ismail *et al.,* (2022) showed the usefulness of system dynamics in assessing fisheries management and socioeconomic impacts. A comparison of these studies with the present framework is provided in Table 4. The current study extends these approaches by incorporating environmental

Table 4: Comparison of the present study with previous system dynamics studies on fisheries sustainability and management

Study system / location	Main modelling focus	Dimensions	Management / scenario analysis	Main contribution relative to the present study	Source
FNC aquaculture, Cirata Reservoir, Indonesia	Sustainable management of FNC aquaculture	Ecological: fish productivity, water quality, and eutrophication. Social: limited consideration of social/fisher participation. Economic: fish price and environmental costs.	FNCA regulation, aeration, and stocking-density interventions.	Demonstrated the usefulness of SD for reservoir cage aquaculture management. However, the model primarily focused on aquaculture sustainability and did not integrate capture fisheries, fishermen participation, and livelihood outcomes as explicitly as the present study.	Gunawan *et al.* (2011)
Marine cage culture, Magong Bay, Taiwan	Environmental carrying capacity and farm profitability	Ecological: nutrient enrichment, dissolved oxygen, phytoplankton, and water quality. Social: not explicitly represented. Economic: farm profitability and harvest.	Production-level scenarios and environmental limits.	Integrated environmental and economic consequences of cage production. However, the focus was mainly on cage aquaculture, whereas the present study links FNC reduction with capture fisheries, fishermen participation, processing innovation, income, and environmental recovery.	Château *et al.* (2015)
Artisanal dredge fisheries, southern Portugal	Sustainable fisheries management	Ecological: fish stocks and biological sustainability. Social: fishing activity and fishing effort. Economics: fisheries revenue.	Fishing-effort reduction and temporary closure.	Demonstrated how SD can evaluate regulatory interventions and socioeconomic consequences. However, it did not explicitly integrate reservoir water conditions, FNC management, fish processing innovation, and fishermen participation within one framework.	Martins *et al.* (2015)
Managed fisheries under transferable quota systems	Fisheries management and stock rebuilding	Ecological: fish stocks and stock rebuilding. Social: fishermen incentives and management behavior. Economic: economic incentives associated with quota management.	Individual transferable quotas (ITQ), total allowable catch (TAC), and adaptive management.	Highlighted the importance of feedback between management incentives and fisheries sustainability. However, it focused on quota-based fisheries management rather than reservoir-specific environmental degradation and livelihood transition.	Garrity (2011)
Indian mackerel fishery, Malaysia	Open-access fishery management	Ecological: biological and fishery dynamics. Social: fisher behavior and fishing activity. Economic: economic factors affecting the fishery.	Alternative fisheries-management options.	Provided an integrated biological, social, and economic SD framework for fisheries management. The present study extends this framework by integrating water condition, FNC pressure, fisher participation, processing innovation, restocking, and income within a reservoir fisheries provisioning-service framework.	Ismail *et al.* (2022)
Jatigede Reservoir, West Java, Indonesia	Integrated fisheries provisioning-service sustainability	Ecological: FNC pressure, water condition, capture fisheries production, and restocking. Social: fishermen participation and livelihood transition. Economic: fishermen income and fish-processing innovation.	Moderate and optimistic integrated interventions, including FNC reduction, water-condition improvement, socioeconomic interventions, and milestone assessment.	Develops an integrated social, environmental, economic SD model for reservoir fisheries provisioning services and evaluates intervention intensity, sustainability milestones, parameter sensitivity, and long-term leverage points through 2045.	Present study

degradation and FNC pressure into a comprehensive reservoir fisheries provisioning-service framework that simultaneously accounts for capture fisheries production, fishers' participation, fish processing innovation, restocking, and fishers' income. The comparison suggests that important combinations of ecological, social, and economic dimensions in fisheries management have been addressed in prior system dynamics studies, albeit with different system boundaries and intervention mechanisms than the present study. Whereas scholarship in cage aquaculture has predominantly centered on environmental carrying capacity and economic performance, conventional fisheries management models have largely focused on fish stocks, harvesting dynamics, fishing effort, or economic incentives. The present study extends these approaches by incorporating environmental conditions, FNC pressure, capture fisheries production, fishermen participation, restocking, fish-processing innovation, and income into a single social-environmental-economic framework. Furthermore, the model evaluates alternative intervention intensities, sustainability milestones, and parameter sensitivity through 2045, thereby offering a comprehensive appraisal of long-term fisheries provisioning-service sustainability.

Limitations of the model

Certain limitations should be considered when interpreting the model's outputs. First, the calibration period is restricted to 2018-2023, which is a relatively short period for showing long-term socio-ecological dynamics. Second, because the social and behavioral relationships were informed in part by interviews with 40 fishers, the estimated behavioral parameters may not fully capture the heterogeneity of the broader fishing community. Third, parameters governing behavioral responses such as propensity toward entering the fishery and livelihood transition remain subject to uncertainty, as human behavior adapts dynamically to shifting economic, social, and institutional drivers. Fourth, the water quality component is modelled by a simplified model and may not fully encompass the inherent complexity of hydrological, biogeochemical and ecological processes in the reservoir. the model does not explicitly account for all potential pollution sources; external inputs—such as those from upstream reservoirs, domestic sewage, agricultural runoff, and catchment-wide activities—can substantially influence water quality. Sixth, restocking of fish is seen as a positive contribution to fisheries production. However, the scale and longevity of the effect on future catch is unknown, and might depend on survival, recruitment, ecological interactions and fishing pressure. Seventh, the projection extends to 2045, well beyond the historical calibration period, implying a large potential for uncertainty to grow over the long simulation horizon. Eighth, economic parameters are affected by uncertainty related to inflation, changes in fish prices, operating costs, market conditions, and general economic conditions, which are not fully accounted for in the model. Ninth, the proposed interventions lack explicit evaluation regarding their economic viability through a detailed cost–benefit analysis. Costs of intervention, implementation budgets, enforcement costs, compensation mechanisms, and costs related to markets are not fully included in the model. Consequently, the simulated scenarios should not be construed as cost-optimal investment strategies, or as definitive proof of economic viability. These financial dimensions require rigorous assessment prior to the formulation of practical investment and policy frameworks. Tenth, the aggregation of the relationships between fishers, FNC activities, alternative employment and willingness to become fishermen may oversimplify the livelihood transitions. It thus may not be representative of decision making at the individual level. Alternative employment is presented as a social mechanism for reducing dependence on FNC activities and for indirectly changing the fisher's participation. Nevertheless,

the scenario analysis did not isolate the independent quantitative contribution of this factor to fishing dependence. Finally, the sensitivity analysis is not probabilistic but deterministic, since parameters were varied in established ranges (-20%, -10%, +10% and +20%) rather than probability distributions. Consequently, these projections should be interpreted as output of scenario-based decision support rather than accurate predictions of future fishery trajectories. Longer time-series data could improve future model development on water quality and fish production, spatially resolved environmental measurements, fishing effort and catch-per-unit-effort data, individual-level livelihood and behavioral information, post-stocking survival and recapture data, and more detailed economic data on intervention costs, fish prices, operating costs, and market conditions. Such empirical data would facilitate enhanced model calibration, robust uncertainty quantification, and a more comprehensive appraisal of management feasibility.

CONCLUSION

The integrated system dynamics model developed in this study suggests that interactions among social, environmental, and economic factors highly influence the sustainability of fisheries services in Jatigede Reservoir. Model simulations indicate that fishery sustainability cannot be attained through isolated interventions, as FNC operations, water quality, fishery resources, community participation, and fishers' incomes are intrinsically linked via feedback loops. The baseline scenario indicates that the continued use of FNC is associated with declining water quality, decreasing capture fisheries production, and lower fisher's income. These results suggest the need for an integrated management approach that considers ecological conditions, fishery resources, and community livelihoods. Outputs from the scenario analysis demonstrate that reducing aquaculture pressures from FNC, intensity, improving water quality, enhancing community engagement in capturing fisheries, and fostering innovation in fish processing can collectively reverse the declining trajectory of fisheries provisioning services. In the optimistic scenario, management targets are achieved sooner than in the moderate scenario. In the optimistic scenario, the activities of FNC reach zero by 2042, the targeted water quality is achieved by 2037, and fisher's income, the optimistic scenario reaches non-negative income in 2034. In the moderate scenario, these targets are reached in 2045 and 2041 respectively. Furthermore, the optimistic scenario demonstrates that capture fisheries production undergoes an accelerated recovery, indicating that more intensive and coordinated interventions can significantly expedite both ecological restoration and harvest yields. Collectively, these findings suggest that mitigating the environmental pressure of FNC enhances water quality and establishes optimal conditions for the rehabilitation of captured fisheries. These findings also suggest that socio-economic interventions need to be integrated with ecological restoration. Increased production in capture fisheries does not necessarily improve community well-being if fishermen continue to rely on limited income sources. Important complementary strategies include improving fisher's participation, developing innovations in fish processing, expanding market opportunities, and providing alternative livelihoods. Specifically, the former strategy enhances the economic value of fishery resources, whereas the latter alleviates ecological stress on the reservoir ecosystem. Thus, the interaction between environmental improvement and economic diversification is an important factor in the long-term viability of fisheries. By offering a management-centric architecture for decision support, integrated system dynamics models facilitate the comparative analysis of policy alternatives and the structural trade-offs inherent among environmental, social, and

economic targets. The optimistic scenario would be a faster route to the sustainability horizon of 2045, but it would require greater institutional commitment and broader public acceptability. Any reduction in FNC activities must be accompanied by appropriate incentives, alternative livelihood opportunities, robust financial support, stakeholder engagement, and cross-sectoral coordination to mitigate unintended socio-economic repercussions. Also, there is a need for regular monitoring and occasional evaluation of water quality, fishery production, and welfare of fishermen to change management interventions as the conditions change. Ultimately, this study underscores the capacity of system dynamics modeling to advance the integrated and adaptive governance of fisheries provisioning services, achieving this by embedding ecological restoration, harvest productivity, stakeholder behavioral responses, and economic welfare within a comprehensive analytical framework. The proposed model affords decision-makers and stakeholders an analytical framework to examine alternative management trajectories and prioritize interventions that optimize trade-offs between environmental and socio-economic objectives. This framework may be adapted for use in other reservoir fisheries facing similar sustainability challenges through appropriate parameter adjustments and validation.

AUTHOR CONTRIBUTIONS

A.N.K.B.P. Iskandar, the corresponding author, contributed to conceptualizing and designed the study, acquisition of data, analysis and interpretation of data, drafted the manuscript, statistical analysis and developed the integrated system dynamics model. Sunardi contributed to critical revision of the manuscript for important intellectual content, supervision, and ecological and fisheries aspects. Zahidah contributed to critical revision of the manuscript for important intellectual content, supervision, and ecological and fisheries aspects. D. Iskandar contributed to analysis and interpretation of data, critical revision of the manuscript for important intellectual content, and supervision. R. Adji contributed to acquisition of data, critical revision of the manuscript for important intellectual content, socioeconomic and economic analysis. R. Sunaryanto contributed to acquisition of data, critical revision of the manuscript for important intellectual content, and fisheries processing and value-added analysis. S. S. Antarlina, contributed to acquisition of data, critical revision of the manuscript for important intellectual content, fisheries processing and value-added analysis. B. Marwoto contributed to acquisition of data, critical revision of the manuscript for important intellectual content, fisheries processing and value-added analysis. W. Basuki contributed to administrative, technical, or material support, policy analysis, and management implications. N. Ismail contributed to administrative, technical, or material support, policy analysis, and management implications. All authors reviewed and approved the final manuscript.

ACKNOWLEDGEMENT

The authors would like to express their sincere gratitude to the Jatigede Reservoir Working Unit and the Sukamenak Village community for their valuable support during data collection. The authors also gratefully acknowledge the analysts at the Ecology Laboratory and the Center for Environment and Sustainability Science for their assistance with data collection and analysis. Their contributions were essential to the completion of this study.

CONFLICT OF INTEREST

The authors declare that there is no conflict of interest regarding the publication of this manuscript. In addition, ethical issues, including plagiarism, informed consent, misconduct, data fabrication and/or falsification, double publication and/or submission, and redundancy, have been completely observed by the authors.

OPEN ACCESS

©2027 The author(s). This article is licensed under a Creative Commons Attribution 4.0 International License, which permits use, sharing, adaptation, distribution and reproduction in any medium or format, as long as you give appropriate credit to the original author(s) and the source, provide a link to the Creative Commons license, and indicate if changes were made. The images or other third-party material in this article are included in the article's Creative Commons license, unless indicated otherwise in a credit line to the material. If material is not included in the article's Creative Commons license and your intended use is not permitted by statutory regulation or exceeds the permitted use, you will need to obtain permission directly from the copyright holder. To view a copy of this license, visit: http://creativecommons.org/licenses/by/4.0/

PUBLISHER'S NOTE

GJESM Publisher remains neutral regarding jurisdictional claims in published maps and institutional affiliations.

POSITIVE AI STATEMENT

During the preparation of this work, the author(s) have used Artificial Intelligence (AI), including ChatGPT (OpenAI) for manuscript review, evaluation, and suggestions for improvement; DeepL for English translation; and Grammarly for English grammar and language improvement. After using this tool/service, the authors reviewed and edited the content as needed and take full responsibility for the content of the publication.

ABBREVIATIONS

%	Percent
AME	Absolute mean error
AVE	Average variation error
CLD	Causal loop diagram
FAO	Food and Agriculture Organization
FNC	Floating net cages
kg	Kilogram
SDGs	Sustainable development goals
STORET	STORET is a method
USD	US Dollar (American currency)
y	Year
m	meter

REFERENCES

Ahmad, A.; Abdullah, S.R.S.; Abu Hasan, H.; Othman, A.R.; Ismail, N.I., (2021). Aquaculture industry: Supply and demand, best practices, effluent and its current issues and treatment technology. J. Environ. Manage., 287: 112271 **(14 pages).**

Allison, E.H.; Ellis, F., (2001). The livelihoods approach and management of small-scale fisheries. Mar. Policy., 377–388 **(12 pages).**

Bell, J.D.; Bartley, D.M.; Lorenzen, K.; Loneragan, N.R., (2006). Restocking and stock enhancement of coastal fisheries: Potential, problems and progress. Fish. Res., 80: 1–8 **(8 pages).**

Béné, C.; Arthur, R.; Norbury, H.; Allison, E.H.; Beveridge, M.; Bush, S.; Campling, L.; Leschen, W.; Little, D.; Squires, D.; Thilsted, S.H.; Troell, M.; Williams, M., (2016). Contribution of fisheries and aquaculture to food security and poverty reduction: assessing the current evidence. World Dev., 79: 177–196 **(20 pages).**

Berrio-Giraldo, L.; Villegas-Palacio, C.; Arango-Aramburo, S., (2021). Understanding complex interactions in socio-ecological systems using system dynamics: A case in the tropical Andes. J. Environ. Manage., 291: 112675 **(15 pages).**

Cao, L.; Wang, W.; Yang, Y.; Yang, C.; Yuan, Z.; Xiong, S.; Diana, J., (2007). Environmental impact of aquaculture and countermeasures to aquaculture pollution in China. Environ Sci Pollut Res Int., 14(7): 452–462 **(11 pages).**

Charles, A.T, (2001). Sustainable fishery system. Blackwell Science Ltd **(370 pages).**

Château, P.A.; Huang, Y.C.A.; Chen, C.A.; Chang, Y.C., (2015). Integrated assessment of sustainable marine cage culture through system dynamics modeling. Ecological Modelling., 299: 140–146 **(7 pages)**.

Dahlan, A.; Zahidah.; Andriani, Y.; Herawati, H., (2020). Plankton community structure as a bioindicator in Jatigede Reservoir, West Java, Indonesia. AACL Bioflux., 13(5): 3086–3095 (**10 pages).**

Delgado, C.L.; Wada, N.; Rosegrant, M.W.; Meijer, S.; Ahmed, M., (2003). Fish to 2020. Supply and demand in changing global markets. International Food Policy Research Institute and WorldFish Center **(236 pages).**

Failler, P.; Pan, H.; Akbari, N., (2021). Integrated social-economic-ecological modelling for fisheries: The ECOST model. Front. Mar. Sci., 8: 704371 **(15 pages).**

FAO, (1998). Inland fishery enhancements. FAO Fisheries Technical Paper 374. Food and Agriculture Organization of the United Nations **(463 pages)**.

FAO, (2009). Environmental impact assessment and monitoring in aquaculture. Food And Agriculture Organization of The United Nations **(675 pages).**

FAO, (2016). The state of world fisheries and aquaculture. Food And Agriculture Organization of The United Nations **(204 pages).**

Firmansyah, I.; Widiatmaka; Pramudya, B.; Budiharsono, S., (2019). The dynamic model of paddy field conversion control in Citarum watershed. IOP Conference Series: Earth Environ. Sci., 399(012009): 1-9 **(10 pages)**.

Garaway, C.J.; Arthur, R.I.; Chamsingh, B.; Homekingkeo, P.; Lorenzen, K.; Saengvilaikham, B.; Sidavong, K., (2006). A social science perspective on stock enhancement outcomes: Lessons learned from inland fisheries in southern Lao PDR. Fish. Res., 80: 37–45 **(9 pages).**

Garrity, E.J., (2011). System Dynamics Modeling of Individual Transferable Quota Fisheries and Suggestions for Rebuilding Stocks. Sustainability., 3(1): 184–215 **(32 pages)**.

Gunawan, W.; Hasan, Z.; Tasrif, M., (2011). Sustainable Fish Cage Aquaculture in Cirata Reservoir West Java, Indonesia: A System Dynamics Approach. Prabandhan: Indian J. Manag., 4(6): 3–12 **(10 pages)**.

Haddon, M., (2007). Fisheries and their management. In S. D. C. and B. M. Gillanders (Ed.), Marine Ecology. Oxford University Press., 511–533 **(23 pages).**

Hilborn, R., (2007). Moving to sustainability by learning from successful fisheries. Ambio., 36(4): 296–303 **(8 pages).**

Hilborn, R.; Walters, C.J., (1992). Quantitative fisheries stock assessment choice, dynamics and uncertainty. Springer Nature Media, B.V. **(570 pages).**

Iskandar, A.N.K.B.P.; Zahidah; Iskandar; Sumiarsa, D.; Suwartapradja, O.S.; Kamarudin, M.K.A.; Sunardi., (2024). Measurement of fisheries provisioning services and its pressure to support the sustainability of fisheries in the Jatigede Reservoir, Indonesia. Environ. Sustainability Indic., 100405 **(9 pages).**

Ismail, I.; Failler, P.; March, A.L.A.; Thorpe, A., (2022). A system dynamics approach for improved management of the Indian mackerel fishery in Peninsular Malaysia. Sustainability., 14: 14190 **(21 pages)**.

Katre, N.; Sharma, A.; Ojha, S.N.; Tyagi, L.; Yadav, V., (2024). Reservoir fisheries governance quality index: Development and validation. Eco. Ind., 158: 111562 **(12 pages).**

Kluger, L.C.; Filgueira, R., (2021). Thinking outside the box: Embracing social complexity in aquaculture carrying capacity estimations. ICES J. Mar. Sci., 78(1): 435-442 **(8 pages).**

Liu, X.; Wang, Y.; Liu, H.; Zhang, Y.; Zhou, Q.; Wen, X.; Guo, W.; Zhang, Z., (2024). A systematic review on aquaculture wastewater: Pollutants, impacts, and treatment technology. Environ. Res., 262(Pt 1): 119793 **(21 pages).**

Lorenzen, K., (2005). Population dynamics and potential of fisheries stock enhancement: practical theory for assessment and policy analysis. Phil. Trans. R. Soc. B., 171–189 **(19 pages).**

Lorenzen, K., (2008). Understanding and managing enhancement fisheries systems. Rev. Fish. Sci., 16(2): 10–23 **(14 pages).**

Lorenzen, K.; Amarasinghe, U.S.; Bartley, D.M.; Bell, J.D.; Bilio, M.; Silva, S.S.De.; Garaway, C.J.; Hartmann, W.D.; Kapetsky, J.M.; Laleye, P.; Moreau, J.; Sugunan, V.V.; Swar, D.B., (2001). Strategic review of enhancements and culture-based fisheries strategic review of enhancements and culture-based fisheries. Aquaculture in the third millennium. Technical Proceedings of the Conference on Aquaculture in the Third Millennium., 1–23 **(23 pages).**

Lynch, A.J.; Elliott, V.; Phang, S.C.; Claussen, J.E.; Harrison, I.; Murchie, K.J.; Steel, E.A.; Stokes, G.L., (2020). Inland fish and fisheries integral to achieving the Sustainable Development Goals. Nat. Sustain., 3: 579–587 **(9 pages).**

Marsela, K.; Sumiarsa, D.; Kurniadie, D., (2023). Determination of trophic status and carrying capacity of floating net cages in Jatigede Reservoir. J. Akuakultur Indones., 22(2): 147–155 **(9 pages).**

Martins, J.H.; Camanho, A.S.; Oliveira, M.M.; Gaspar, M.B., (2015). A system dynamics model to support the management of artisanal dredge fisheries in the south coast of Portugal. ITOR., 22: 611–634 **(24 pages)**.

Moallemi, E.A.; Bertone, E.; Eker, S.; Gao, L.; Szetey, K.; Taylor, N.; Bryan, B.A., (2021). A review of systems modelling for local sustainability. Environ. Res. Lett., 16: 113004 **(20 pages)**.

Restrepo-Gómez, D.C.; Zetina-Rejón, M.J.; Zepeda-Domínguez, M.J., (2022). Trends in marine fisheries social-ecological systems studies. Ocean Coast. Manag., 226: 106076 **(14 pages)**.

Rosadi, R.; Musa, M.; Lelono, T.D., (2020). Plankton community structure as bioindicator of trophic status of Jatigede Reservoir. Res. J. of Life Sci., 7(1): 29–40 **(12 pages)**.

Schiemer, F.; Amarasinghe, U.S.; Simon, D.; Vijverberg, J., (2024). Sustainable aquatic resource management and inland fisheries in tropical Asia: Interdisciplinary and transdisciplinary approaches. Ambio., 53(7): 1050–1064 **(15 pages).**

Silva, S.S.De., (2003). Culture-based fisheries: an underutilised opportunity in aquaculture development. Aquaculture., 221: 221–243 **(23 pages).**

Smith, L.E.D.; Khoa, S.N.; Lorenzen, K., (2005). Livelihood functions of inland fisheries: policy implications in developing countries. Water Policy., 359–383 **(25 pages).**

Smith, S. F.; Bennett, A., (2019). A fresh look at inland fisheries and their role in food security and livelihoods. Fish Fish., 1176–1195 **(20 pages).**

Solomon, C.T.; Dassow, C.J.; Iwicki, C.M.; Jensen, O P.; Jones, S.E.; Sass, G.G.; Trudeau, A.; Poorten, B.T.Van.; Whittaker, D., (2020). Frontiers in modelling social-ecological dynamics of recreational fisheries: A review and synthesis. Fish Fish., 21: 973–991 **(19 pages).**

Stacey, N.; Gibson, E.; Loneragan, N.R.; Warren, C.; Wiryawan, B.; Adhuri, D.S.; Steenbergen, D.J.; Fitriana, R., (2021). Developing sustainable small-scale fisheries livelihoods in Indonesia: Trends, enabling and constraining factors, and future opportunities. Mar. Policy., 132, 104654 **(12 pages).**

Sterman, J.D., (2002). System dynamics: systems thinking and modeling for a complex world. In MIT Sloan School of Management, Cambridge **(31 pages).**

Stewart, D.R.; Long, J.M., (2016). Using an experimental manipulation to determine the effectiveness of a stock enhancement program. J. Freshw. Ecol., 31(1): 37–52 **(18 pages)**.

Tezzo, X.; Bush, S.R.; Oosterveer, P.; Belton, B., (2021). Food system perspective on fisheries and aquaculture development in Asia. Agric. Hum. Values., 38: 73–90 **(18 pages).**

Tidbury, H.J.; Muench, A.; Lamb, P.D.; Hyder, K., (2021). Balancing biological and economic goals in commercial and recreational fisheries: Systems modelling of sea bass fisheries. ICES J. Mar. Sci., 78(5): 1793–1803 **(11 pages).**

Walukow, A. F., (2011). The Impact of Population Growth on Pollutant Source Load in Andau Sentani with an Environmentally Sound Dynamical System Model. Purification Journal., 12(2): 63-74 **(12 pages)**.

Weitzman, J.; Filgueira, R., (2020). The evolution and application of carrying capacity in aquaculture: Towards a research agenda. Rev. Aquacult., 12: 1297–1322 **(26 pages).**

Weitzman, J.; Filgueira, R.; Grant, J., (2021). Development of best practices for more holistic assessments of carrying capacity of aquaculture. J. Environ. Manage., 287: 112278 (13 pages).

Welcomme, R.L.; Bartley, D.M., (1998). Current approaches to the enhancement of fisheries. Fish. Manage. Ecol., 5: 351–382 **(32 pages).**

Wilson, K.L.; Foos, A.; Barker, O.E.; Farineau, A.; Gisi, J.De.; Post, J.R., (2020). Social–ecological feedbacks drive spatial exploitation in a northern freshwater fishery: A halo of depletion. J. Appl. Ecol., 57(2): 206-218 **(13 pages).**

AUTHOR (S) BIOSKETCHES

Iskandar, A.N.K.B.P, Ph.D., Post-Doctoral Researcher at Research Center for Industrial Systems and Sustainable Manufacturing, National Research and Innovation Agency, Indonesia.

- Email: *andi077@brin.go.id*
- ORCID: 0000-0001-9491-170X
- Web of Science Researcher ID: QWB-1400-2026
- Scopus Author ID: 58312935100
- Homepage: https://brin.go.id/

Iskandar, D., Ph.D., Senior Researcher at Research Center for Industrial Systems and Sustainable Manufacturing, National Research and Innovation Agency, Indonesia.

- Email: *dudi002@brin.go.id*
- ORCID: 0000-0001-9029-0619

- Web of Science Researcher ID: HRA-9766-2023
- Scopus Author ID: 59746281900
- Homepage: https://brin.go.id/

Sunardi, Ph.D., Professor, Department of Biology, Faculty of Mathematics and Natural Science, Universitas Padjadjaran, Jatinangor, Sumedang, Indonesia.
- Email: *sunardi@unpad.ac.id*
- ORCID: 0000-0002-7972-3580
- Web of Science Researcher ID: HGU-8380-2022
- Scopus Author ID: 7409958211
- Homepage: https://unpad.ac.id/

Zahidah, Ph.D, Professor, Faculty of Fisheries and Marine Science, Universitas Padjadjaran, Jatinangor, Sumedang, Indonesia
- Email: *zahidah@unpad.ac.id*
- ORCID: 0000-0003-0129-2685
- Web of Science Researcher ID: NA
- Scopus Author ID: 57201775006
- Homepage: https://unpad.ac.id/

Adji, R., M.Sc., Senior Researcher at the Study Program of Agribusiness, Faculty of Business, President University, Indonesia.
- Email: *Riyanto.adji@president.ac.id*
- ORCID: 0000-0001-9580-579X
- Web of Science Researcher ID: CAJ-1742-2022
- Scopus Author ID: 58046427500
- Homepage: https://president.ac.id/

Sunaryanto, R., Ph.D., Senior Researcher at Research Center for food technology and processing, National Research and Innovation Agency, Indonesia.
- Email: *rofi001@brin.go.id*
- ORCID: 0000-0002-5035-4195
- Web of Science Researcher ID: NA
- Scopus Author ID: 58763561900
- Homepage: https://brin.go.id/

Antarlina, S.S., Ph.D., Senior Researcher at Research Center for food technology and processing, National Research and Innovation Agency, Indonesia.
- Email: *sris024@brin.go.id*
- ORCID: 0000-0002-7034-4074
- Web of Science Researcher ID: NA
- Scopus Author ID: 57225170925
- Homepage: https://brin.go.id/

Marwoto, B., Ph.D., Senior Researcher at Research Center for pharmaceutical ingredients and traditional medicine, National Research and Innovation Agency, Indonesia.
- Email: *bamb023@brin.go.id*
- ORCID: 0000-0002-5035-4195
- Web of Science Researcher ID: NA
- Scopus Author ID: 58763561900
- Homepage: https://brin.go.id/

Basuki, W., Ph.D., Professor at the Directorate of Policy Evaluation for Research, Technology, and Innovation, National Research and Innovation Agency, Indonesia.
- Email: *witono.basuki@brin.go.id*
- ORCID: 0000- 0003- 1155-495X
- Web of Science Researcher ID: NA
- Scopus Author ID: NA
- Homepage: https://brin.go.id/

Ismail, N., Ph.D., Professor at the Directorate of Policy Evaluation for Research, Technology, and Innovation, National Research and Innovation Agency, Indonesia.
- Email: *nmahmudi86@gmail.com*
- ORCID: 0009-0008-8284-3330
- Web of Science Researcher ID: NA
- Scopus Author ID: 7409955641
- Homepage: https://brin.go.id/

HOW TO CITE THIS ARTICLE:
Iskandar, A.N.K.B.P.; Iskandar, D.; Sunardi; Zahidah; Adji, R.; Sunaryanto, R.; Antarlina, S.S.; Marwoto, B.; Basuki, W.; Ismail, N., (2027). Integrated system dynamics modeling for sustainable fisheries provisioning services. Global J. Environ. Sci. Manage., 13(1): 433-456.

DOI: 10.22034/gjesm.2027.01.20
URL: https://www.gjesm.net/article_735641.html

Global J. Environ. Sci. Manage. 13(1): 457-478, Winter 2027, Serial #49

Global Journal of Environmental Science and Management
(GJESM)

Homepage: https://www.gjesm.net/

Podcasts

CASE STUDY

Environmental health conditions associated with childhood stunting during the first 1000 days of life

A. Muthia[1], D. Utari[2], T.E.B Soesilo[1,*]

[1]Department Environmental Science, Graduated School of Sustainable Development, Universitas Indonesia, Jalan Salemba Raya, Jakarta Pusat, DKI Jakarta 10430 Indonesia

[2]Faculty of Health Science, Universitas Pembangunan Nasional Veteran, Depok, 1651, Indonesia

ARTICLE INFO

Article History:
Received 03 May 2026
Revised 05 July 2026
Accepted 06 August 2026

Keywords:
Environmental health
Environmental perspectives
First 1,000 days of life
Maternal behavior
Stunting

DOI:10. 22034.gjesm.2027.01.21

ABSTRACT

BACKGROUND AND OBJECTIVES: Child stunting is increasingly recognized not only as a nutritional disorder but also as a complex environmental health issue. Household environmental determinants, particularly safe potable water and advanced sanitation infrastructure, exert a fundamental influence on minimizing children's susceptibility to environmental health hazards that compromise linear growth trajectories. Using the transtheoretical model as a behavioral framework, the study objectives were to examine how household environmental conditions, including access to improved drinking water and sanitation, together with maternal environmental health-related behaviors, are associated with child stunting during the first 1,000 days of life in Indonesia.

METHODS: This cross-sectional study used nationally representative data from the fifth wave of the Indonesian Family Life Survey. Maternal behaviors related to nutrition, healthcare utilization, and environmental conditions were operationalized as proxies for advanced stages of behavioral change. Child stunting was defined using height-for-age z-scores based on the World Health Organization Child Growth Standards. A binary logistic regression model was utilized to evaluate the multivariate associations linking maternal behavioral patterns, socio-environmental covariates, and socio-demographic indicators to the latent risk of linear growth retardation in children.

FINDINGS: The prevalence of stunting among children aged 0 to 23 months was 30.32 percent. Low birth weight and higher birth order significantly increased the odds of stunting. Maternal behaviors reflecting progression to the action and maintenance stages were protective, including routine antenatal care attendance, with an odds ratio of 0.642, and delivery assisted by a skilled birth attendant, with an odds ratio of 0.707. Findings indicate that higher maternal educational attainment, improved sanitation facilities, and safe drinking water sources significantly decreased the likelihood of stunting. In contrast, maternal under nutrition elevated the associated risk by 26.5 percent.

CONCLUSION: Household environmental conditions constitute fundamental determinants of child stunting during the first 1,000 days of life. Maternal progression toward advanced stages of stunting prevention behavior, reinforced by adequate health services and enabling environments, plays a critical role in reducing stunting during the first 1,000 days of life. The findings underscore the efficacy of the transtheoretical model as a robust conceptual paradigm for mitigating childhood stunting. By integrating maternal behavioral stages of change with healthcare access and environmental determinants, the research delineates a nuanced, stage-sensitive and contextually grounded architecture for analyzing early childhood growth dynamics.

This is an open access article under the CC BY license (http://creativecommons.org/licenses/by/4.0/)

NUMBER OF REFERENCES	NUMBER OF FIGURES	NUMBER OF TABLES
58	1	3

*Corresponding Author:
Email: tri.edhi@ui.ac.id
Phone: +6221 3193 0251
ORCID: 0000-0002-3188-5812

Note: Discussion period for this manuscript open until March 01, 2027 on GJESM website at the “Show Article”.

INTRODUCTION

Child stunting is increasingly recognized not just as a nutritional disorder, but as a complex environmental health issue. This paradigm shift is reinforced by accumulating evidence indicating that environmental determinants play a critical role in the etiology of stunting, operating alongside conventional nutritional pathways. Contaminated water sources, poor sanitation, and lack of toilets are linked to higher stunting rates due to increased risk of infections and environmental enteropathy, a chronic inflammatory gut disorder that impairs nutrient absorption (Fregonese *et al.*, 2017; Perdananugraha *et al.*, 2026; Ramlan *et al.*, 2025; Vilcins *et al.*, 2018). Consequently, environmental health has emerged as a core pillar of international initiatives designed to mitigate pediatric undernutrition and advance sustainable human development (WHO, 2006; UNICEF, 2019; Astuti, 2026; Firdaus and Maulana, 2025). These environmental covariates exhibit close alignment with sustainable development goal 6 (SDG 6), which underscores universal access to potable water and advanced sanitation infrastructure as foundational prerequisites for optimizing public health outcomes and reducing childhood malnutrition (UNICEF, 2019). Despite global progress in nutrition interventions, reductions in stunting remain uneven, particularly in low- and middle-income countries where environmental inequalities persist (Victora *et al.*, 2021; Astuti, 2026). Improvements in dietary intake alone are insufficient to mitigate the adverse effects of inadequate water, sanitation, and hygiene on child growth (Binamungu and Sanga, 2026; Kusumo *et al.*, 2024; Nisa *et al.*, 2026). This situation underscores the multifactorial nature of stunting, which is shaped by the complex interaction of nutritional, socioeconomic, environmental, and behavioral determinants (Sahiledengle *et al.*, 2023; Saleh *et al.*, 2021; Sukmawati *et al.*, 2025). The first 1,000 days of life constitute a biologically vulnerable window wherein environmental exposures exert lasting effects on physical growth and human development (Aguayo and Menon, 2016; Bloem *et al.*, 2013; Sukmawati *et al.*, 2025). During this period, rapid cellular proliferation and organ development require adequate nutrition supported by healthy environmental conditions. Children who experience repeated exposure to contaminated water, inadequate sanitation, or poor household hygiene are more susceptible to diarrheal diseases and environmental enteric dysfunction (EED). Accumulating empirical data indicates that EED functions as a fundamental physiological mechanism mediating the relationship between degraded environmental conditions and the pathogenesis of linear growth faltering in pediatric populations, notably within low- and middle-income economies (Aguayo and Menon, 2016; Torlesse *et al.*, 2016; UNICEF, 2023; Victora *et al.*, 2021). Compared with later stages of childhood, growth faltering after the age of two is considerably less reversible, making the first 1,000 days the most effective period for interventions to prevent stunting and its lifelong consequences (Victora *et al.*, 2021; WHO, 2006). Accordingly, centering analytical focus on this vulnerable ontogenetic window establishes a rigorous conceptual framework for isolating modifiable environmental covariates prior to the permanent entrenchment of irreversible somatic growth deficits. Globally, approximately 150.2 million children under five were stunted in 2025, with the greatest burden occurring in South Asia and Sub-Saharan Africa (UNICEF, 2025). An increasing number of recent studies demonstrate that access to safely managed drinking water, improved sanitation, and effective environmental hygiene significantly reduces the risk of chronic undernutrition in children. This is achieved by interrupting fecal-oral transmission pathways and lowering the burden of infectious diseases (Arief *et al.*, 2025; Mediani, 2020; Sahiledengle *et al.*, 2023; Saleh *et al.*, 2021). These findings indicate that environmental management must be integrated into national stunting mitigation

frameworks. Despite a notable decrease in prevalence from 37.2% in 2013 to 19.8% in 2024, Indonesia continues to experience one of the most severe stunting burdens in Southeast Asia (Kemenkes, 2025; WHO and UNICEF 2021). These disparities reflect unequal access to environmental infrastructure, including improved sanitation, safe drinking water (Islam and Mostafa, 2024), waste management, and quality maternal healthcare services. The Indonesian government has recognized the multidimensional nature of stunting through presidential regulation Number 72 of 2021, promoting multisectoral collaboration involving nutrition, healthcare, water supply, sanitation, and environmental improvement. Beyond instigating direct biological consequences, ambient household environmental conditions exert a profound regulatory influence on maternal health-related behaviors. Mothers living in supportive environments are more likely to practice appropriate hygiene (Kirana, 2025; Astuti, 2026), access antenatal care (ANC), utilize skilled birth attendance, and adopt preventive childcare practices, whereas environmental constraints may hinder sustained healthy behaviors despite adequate knowledge (Arief *et al.*, 2025; Mediani, 2020; Sahiledengle *et al.*, 2023; Saleh *et al.*, 2021; Zulfitrawati and Mukty, 2025). The transtheoretical model (TTM) provides a useful framework for understanding this process by conceptualizing behavior change as a progression through the stages of precontemplation, contemplation, preparation, action, and maintenance (Prochaska and Velicer, 1997). The TTM offers a stage-oriented framework that more effectively elucidates how preventive health behaviors are initiated, adopted, and sustained over time (Glanz *et al.*, 2015; Spencer *et al.*, 2006). This framework is relevant to maternal behaviors concerning environmental health during the first 1,000 days of life. Preventive measures—such as consistent antenatal care attendance, professionally attended deliveries, hygiene maintenance, and adherence to health guidelines—demand continuous behavioral commitment rather than isolated, discrete choices. Within stunting prevention, these stages can be reflected through the gradual adoption and maintenance of maternal preventive practices during the first 1,000 days of life. Although numerous studies have reported associations between environmental factors and childhood stunting, most have examined environmental conditions and maternal behaviors separately, with maternal practices commonly treated as static or binary outcomes (Arief *et al.*, 2025; Mediani, 2020; Sahiledengle *et al.*, 2023; Saleh *et al.*, 2021). As a result, limited empirical literature addresses how supportive domestic environments facilitate mothers' progression toward sustained preventive health behaviors. Moreover, empirical applications of the Transtheoretical Model to stunting prevention remain scarce, particularly within the critical first 1,000 days of life. Consequently, a paucity of empirical research investigates the precise mechanisms through which supportive domestic environments catalyze maternal progression toward the longitudinal maintenance of preventive behaviors. Despite the theoretical relevance of the TTM, empirical applications of the Stage of Change framework to stunting prevention remain scarce, limiting understanding of the behavioral mechanisms linking household environmental conditions to child growth (Yunitasari *et al.*, 2021). To address these gaps, this study integrates household environmental conditions, particularly access to improved drinking water and sanitation, with maternal environmental health behaviors using the TTM as its behavioral framework. This study conceptualizes maternal preventive behaviors as dynamic mechanisms through which supportive household environments are associated with child growth. Using nationally representative household survey data collected in 13 Indonesian provinces during 2014–2015 by Research and Development (R&D) (Strauss *et al.*, 2016), this study provides a more comprehensive understanding of the environmental determinants of childhood stunting. It generates evidence to

support stage-specific and context-sensitive intervention strategies. Theoretically, this study expands the study of environmental health by transcending the conventional treatment of potable water access and sanitation infrastructure as isolated structural covariates, instead framing them as supportive determinants that catalyze maternal behavioral readiness through the lens of the TTM framework. Practically, these findings support policies that integrate basic infrastructure development (clean water and sanitation) with maternal health promotion based on stages of readiness, rather than separate programs. For other developing countries, these results can serve as a basis for mapping priority areas that consider both stunting prevalence and water, sanitation, and hygiene (WASH) access, allowing for more targeted resource allocation and supporting the simultaneous achievement of SDGs 3 and 6. Because nationally representative household surveys, including the Indonesian Family Life Survey (IFLS) omit direct psychometric assessment of motivational constructs and behavioral readiness, empirical operationalizations of the transtheoretical model in population-based studies routinely leverage observable preventive behaviors as proxy markers for tracking advancement across sequential stages of behavioral modification. Accordingly, in the present study the TTM is used as a theoretical framework for interpreting maternal preventive behaviors rather than as a model whose stages are directly measured or validated. This study seeks to elucidate the associations linking domestic environmental determinants, including advanced sanitation infrastructure and potable water access, to the behavioral stages of change governing maternal stunting mitigation practices across the critical 1,000-day postnatal window, employing the TTM as an overarching conceptual paradigm. This study aims to examine how household environmental conditions, including access to improved drinking water and sanitation, are associated with the stages of change in maternal stunting prevention behaviors during the first 1,000 days of life, using the TTM as a behavioral framework. This study utilizes data from the Indonesia Family Life Survey Wave 5 (IFLS-5), one of the highest-quality nationally representative longitudinal datasets available in Indonesia. Conducted between 2014 and 2015, IFLS-5 covered 13 provinces, including North Sumatra, West Sumatra, South Sumatra, Lampung, Jakarta, West Java, Central Java, Yogyakarta, East Java, Bali, West Nusa Tenggara, South Kalimantan, and South Sulawesi, which together represent the majority of the Indonesian population. IFLS-5 provides comprehensive information on health, nutrition, household environment, demographic characteristics, and socioeconomic conditions, enabling robust analyses of the complex determinants of child health. Its high response rate, rigorous data collection procedures, and extensive use in national and international research make it a reliable data source for examining public health issues and generating evidence to inform policy development in Indonesia.

MATERIALS AND METHODS

This study employed a cross-sectional design using nationally representative data from the fifth wave of the IFLS 5, conducted between 2014 and 2015. IFLS-5 applied a multistage stratified sampling approach covering approximately 83% of the Indonesian population across 13 provinces: North Sumatra, West Sumatra, South Sumatra, Lampung, Jakarta, West Java, Central Java, Yogyakarta, East Java, Bali, West Nusa Tenggara, South Kalimantan, and South Sulawesi. To accurately reflect Indonesia's cultural and socioeconomic heterogeneity and guarantee comprehensive demographic representation, these specific provinces were selected. IFLS-5 was selected because it provides one of the most comprehensive nationally representative household datasets in Indonesia, simultaneously capturing child anthropometry, maternal characteristics, household environmental conditions, healthcare utilization, and

socioeconomic information. Integrating these variables within a single survey framework facilitates the simultaneous investigation of environmental health conditions, maternal behaviors, and their joint associations with childhood stunting (Strauss *et al.*, 2016). A nationally representative sampling frame was used to randomly select 321 enumeration areas (EAs) across the provinces. IFLS-5 was selected because it provides one of the most comprehensive and nationally representative household datasets in Indonesia. IFLS-5 simultaneously encompasses data on child anthropometry, maternal characteristics, household environmental conditions, healthcare service utilization, and economic information. Capturing these variables within a unified framework facilitates the simultaneous examination of their interactive relationships. Households were randomly selected based on lists from the 1993 National Socioeconomic Survey/*Survei Sosial Ekonomi Nasiona*l (SUSENAS) obtained from local offices of the Central Statistics Agency/*Badan Pusat Statistik* (BPS). In total, 20 households were selected from each urban EA and 30 households from each rural EA. The IFLS data are publicly accessible through the RAND Corporation website (Strauss *et al.*, 2016). Restricting the analysis to households with children aged 0-23 months and omitting observations with incomplete data yielded a final analytical sample of 1,260 children. Children aged 0–23 months were selected because they represent the postnatal component of the first 1,000 days of life, the period during which growth faltering is most sensitive to environmental exposures. Observations with missing anthropometric or covariate information were excluded to ensure complete-case analysis. While this methodological refinement enhances data quality, it may compromise sample representativeness if the excluded children differ systematically from those retained in the final cohort. Furthermore, the IFLS-5 survey protocol and data collection procedures were reviewed and approved by the Institutional Review Boards (IRBs) of the RAND Corporation in the United States and Universitas Gadjah Mada (UGM) in Indonesia. Structured to capture extensive household-level data across Indonesia, the IFLS collects critical information concerning demographics, health, education, and income, thereby providing an empirical foundation for public policy formulation and the tracking of national development metrics (Strauss *et al.*, 2016). Given that the IFLS dataset does not explicitly capture motivational or intentional constructs, maternal behavioral indicators (nutrition, WASH, healthcare) were treated as proxies for progressive behavioral stages. This approach follows previous studies that implicitly model behavioral evolution using secondary survey data (Torlesse *et al.*, 2016) and is theoretically consistent with the Transtheoretical Model (Prochaska and Velicer, 1997). Given the absence of direct metrics for motivational constructs and the five stages of behavioral change within the IFLS-5 data architecture, the TTM served as an overarching conceptual framework for behavioral interpretation rather than a directly evaluated variable. Observable preventive behaviors by mothers are operationalized as proxy indicators of progress toward the action and maintenance stages of behavior change. Consequently, the TTM was applied to facilitate interpretation of behavioral patterns within supportive household environmental contexts rather than to empirically classify mothers into specific stages of change. This study integrates the TTM of behavior change with a logistic regression analytical approach to examine the determinants of child stunting. The Transtheoretical Model characterizes health behavior modification as a dynamic, sequential progression encompassing five distinct stages: precontemplation, contemplation, preparation, action, and maintenance (Prochaska and Velicer, 1997). In this study, household environmental conditions constitute the primary analytical context for understanding child stunting during the first 1,000 days of life. Adequate water and

sanitation infrastructure is framed as a foundational household condition that mediates childhood exposure to enteric pathogens, environmental contamination, and chronic infectious illness, all of which drive stunted linear growth trajectories. These environmental conditions also provide enabling environments that facilitate or constrain mothers' adoption and maintenance of preventive health practices. TTM was employed as a behavioral framework to interpret how maternal environmental health-related behaviors evolve within these household environmental contexts. Rather than viewing maternal practices as isolated decisions, the TTM conceptualizes preventive behaviors as a gradual progression through the stages of precontemplation, contemplation, preparation, action, and maintenance (Prochaska and Velicer, 1997). In evaluating environmental health behaviors, consistent antenatal care attendance, skilled birth attendance (SBA) during delivery, sufficient iron intake throughout gestation, and ongoing household environmental maintenance were conceptualized as behavioral metrics indicating progression toward the action and maintenance stages. Although IFLS 5 does not directly measure the construct of motivation or explicit stages of behavioral change, observable maternal practices serve as proxy indicators for more advanced TTM stages. This aligns with previous behavioral health research utilizing secondary survey data. This methodological approach facilitates the interpretation of behavioral patterns within an established theoretical framework while explicitly recognizing the inherent constraints of secondary data. To empirically evaluate these relationships, binary logistic regression analysis was employed in this study. This analysis aims to estimate the probability of childhood stunting as a function of household environmental conditions, maternal behaviors related to environmental health, and relevant child and socio-demographic characteristics. Within this analytical framework, home environmental conditions are treated as a primary environmental determinant. Concurrently, maternal behavior is conceptualized as an underlying behavioral mechanism through which an enabling environment promotes sustainable practices for stunting mitigation, thereby enhancing pediatric growth outcomes. Although TTM emphasizes stage-based behavioral change, regression-based methods are widely used in TTM informed research to identify factors associated with progression toward advanced stages when direct measurement of stages is not available (Grossman *et al.*, 2008; Ma *et al.*, 2015). Consequently, the logistic regression framework employed here does not substitute for the sequential progression of the TTM, but instead operationalizes its constructs by evaluating the association between sustained action- and maintenance-stage preventive behaviors and decreased odds of child stunting. This integrated approach allows statistical findings to be interpreted within a robust behavioral theory, providing a comprehensive understanding of how maternal behavior change contributes to stunting prevention. The primary outcome of this study was children's stunting status among those aged 0- 24 months, a critical period that encompasses the most sensitive window of the first 1,000 days of life, spanning from conception to a child's second birthday. Stunting was categorized dichotomously into stunted (height-for-age more than two standard deviations below the median) and non-stunted or normal (height-for-age equal to or above two standard deviations from the median). A binary coding scheme was applied, where a value of "1" indicated stunted growth and a value of "0" indicated normal growth. Child stunting status was ascertained using height-for-age z-scores derived from age- and sex-standardized growth references. Height and body mass index (BMI) z-scores were computed based on the WHO 2006 Child Growth Standards for children under five years of age. Following the recommendations provided by the World Health Organization (WHO), this study excludes any extreme values in the data, such as height-for-age

Z-scores greater than 6 and less than -6 standard deviations (WHO, 2006). All study variables were constructed following the IFLS guidelines, drawing on data from Book US, Book 1, Book 2, Book 3A, Book 4, and Book 5. Guided by existing literature and a conceptual framework grounded in the TTM, the independent variables were categorized into child-level, maternal, and environmental factors. Child-related variables included sex, age group (Less than (<) 12 months versus (vs.) 12 through (–) 23 months), birth order (firstborn, 2–4, more than or equal to (≥) 5), size at birth (normal vs. low birth weight), and exclusive breastfeeding up to six months (yes/no). Maternal characteristics comprised age (<18, 18–24, 25–34, ≥35 years), education level (primary or below, secondary, higher), nutritional status based on BMI (<18.5, 18.5–24.9, 25–29.9, ≥30 kilograms per square meter (kg/m²), smoking status (yes/no), hypertension status (yes/no), and iron supplementation during pregnancy (received≥60pills/received<60 pills) (Fig. 1). Body mass index (BMI), calculated from objectively measured height and weight, served as the indicator for maternal nutritional status and was classified using established WHO thresholds. BMI was selected because it is the standardized anthropometric indicator consistently available in the IFLS-5 dataset. Household and environmental variables included place of residence (urban/rural), source of drinking water (improved/unimproved), and toilet facility (improved/unimproved). Access to drinking water and toilet facilities was classified as improved or unimproved according to the WHO/UNICEF Joint Monitoring Program (JMP) definitions. Categorized as improved drinking water sources, infrastructure such as piped networks, protected wells, and protected springs are effectively safeguarded against external environmental contamination. Conversely, improved sanitation facilities are defined as infrastructure that hygienically isolates human excreta from direct contact, encompassing flush or pour-flush toilets linked to septic systems or municipal sewerage networks, alongside ventilated or standardized pit latrines. All other water sources and sanitation facilities were classified as unimproved (WHO and UNICEF, 2021). Although other household environmental factors, including housing quality, solid waste management, indoor air pollution, and hygiene practices, may also contribute to childhood stunting, these variables were not included because comparable measures were not consistently available in the IFLS-5 dataset. Consequently, access to improved drinking water and sanitation was designated as the primary proxy for household environmental health. Health service utilization variables consisted of antenatal care attendance (routine/non-routine) and place of delivery assisted by a skilled birth attendant (yes/no). All independent variables were treated as categorical and included simultaneously in the multivariable logistic regression model. Potential confounding variables, determined through a review of existing literature and the underlying conceptual framework, were adjusted for in a multivariable model to isolate the association between household environmental conditions and the incidence of pediatric stunting. Binary logistic regression was selected because the primary outcome variable was dichotomous (Hosmer *et al.,* 2013). The objective of the study was to estimate adjusted associations between household environmental conditions, maternal environmental health-related behaviors, and childhood stunting. To estimate the association between maternal behaviors, socio-demographic characteristics, and child stunting, binary logistic regression was employed. The regression model is specified, using Eq. 1 (Hosmer *et al.,* 2013):

$$logit\ (p_i) = ln\ ln\ \left(\frac{p_i}{1-p_i}\right) = \beta_0 + \beta_1 X_i + \varepsilon_i \quad (1)$$

Where: p_i represents the probability that child i is stunted, X_i denotes maternal stunting prevention behaviors covariates. Odds ratios (ORs) and 95% confidence intervals were reported. An OR less than one for preventive behaviors indicates a

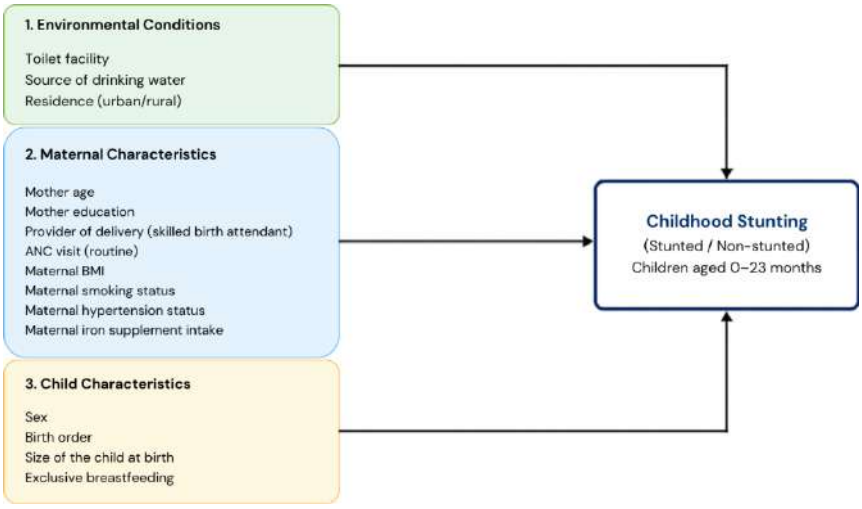

Fig. 1: Conceptual framework of the research

reduced likelihood of stunting, consistent with successful progression to advanced stages of behavior change within the TTM framework. Grounded in the Stage of Change framework, the regression results demonstrate that significant inverse associations between maternal practices and stunting risk signify successful advancement into the action and maintenance stages. Environmental factors were interpreted as enabling or reinforcing mechanisms that support sustained behavioral change and indirectly are associated with child growth outcomes. To guarantee the validity and robustness of the regression specifications, comprehensive diagnostic checks were implemented. Multicollinearity among the independent variables was assessed using the variance inflation factor (VIF), with all VIF values below the commonly accepted threshold, indicating no evidence of problematic multicollinearity. Model calibration was evaluated using the Hosmer–Lemeshow goodness-of-fit test, where a non-significant result (probability value (p-value) >0.05) indicated adequate agreement between the observed and predicted values. Furthermore, the explanatory and discriminative performance of the final logistic regression model was appraised using pseudo-R^2 metrics.

RESULTS AND DISCUSSION

Environmental, maternal, and child characteristics of the study population

The sociodemographic, maternal, and environmental characteristics of the analytical sample, encompassing 1,260 children between 0 and 23 months of age—are summarized in Table 1. The prevalence of stunting in the sample was 30.32%, with 382 children classified as stunted, while 69.68% (n=878) were not stunted. From an environmental health perspective, the majority of households experienced relatively positive environmental conditions. Approximately 87.46% of households had access to improved drinking water sources, while 74.37% used improved sanitation facilities. Furthermore, 58.81% of children resided in urban areas, whereas 41.19% lived in rural settings, reflecting variation in household environmental settings across the study population. Maternal profiles concerning environmental health reflected a substantial engagement with preventive health services. Routine antenatal care (ANC) attendance was reported by 92.22% of mothers, and 72.78% delivered with the assistance of skilled birth attendants. Approximately 67.70% of mothers received at least 60 iron–folic acid tablets during pregnancy. Most mothers were aged 25–34 years

Table 1: The environmental, maternal, and child characteristics of the study sample

Variable	Total	Percentage
Stunting		
Not stunting	878	69.68
Stunting	382	30.32
Sex		
Male	642	50.95
Female	618	49.05
Age (months)		
<12	463	36.75
12 -23	797	63.25
Birth order		
Firstborn	627	49.76
2-4	606	48.10
5 or higher	27	2.14
Size of the child at birth		
Normal	1,182	93.81
Small	78	6.19
Exclusive breastfeeding		
Yes	270	21.43
No	990	78.57
Toilet facility		
Improved	937	74.37
Unimproved	323	25.63
Source of drinking water		
Improved	1,102	87.46
Unimproved	157	12.54
Mother's Age		
<18	13	1.03
18-24	340	26.98
25-34	682	54.13
>=35	225	17.86
Mother's education		
Primary or below	551	43.73
Secondary	495	39.29
Higher	214	16.98
Provided of delivery		
Skilled birth attendant	917	72.78
Non-skilled	343	27.22
ANC visit		
Routine	1,162	92.22
Non-routine	98	7.78
Maternal BMI		
<18.5 (underweight)	109	8.65
18.5-24.9 (normal)	731	58.02
25-29.9 (overweight)	293	23.25
>=30 (obesity)	127	10.08
Residence		
Urban	741	58.81
Rural	519	41.19
Maternal Smoking Status		
Yes	13	1.03
No	1,247	98.97
Maternal Hypertension Status		
Yes	2	0.16
No	1,258	99.84
Maternal Iron Supplement Intake		
Received <60 pills	407	32.30
Received ≥60 pills	853	67.70

(54.13%), while 26.98% were aged 18–24 years, and only 1.03% were adolescents. Regarding educational attainment, 43.73% of individuals had attained primary education or lower, 39.29% had completed secondary education, and 16.98% held higher education credentials. Most mothers had a normal body mass index (58.02%), whereas 8.65% were underweight, 23.25% overweight, and 10.08% obese. Maternal smoking (1.03%) and hypertension (0.16%) were relatively uncommon. Regarding child characteristics, 50.95% were boys and 49.05% were girls. Most children (63.25%) were aged 12–23 months, whereas 36.75% were younger than 12 months. Nearly half (49.76%) were firstborns, 48.10% were of second to fourth birth order, and 2.14% belonged to birth orders of five or higher. Most children (93.81%) had normal birth weight, while 6.19% were born with low birth weight. Despite a high overall breastfeeding rate of 78.89% among surveyed children, the low prevalence of exclusive breastfeeding (21.43%) highlights a persistent gap in achieving optimal infant feeding standards universally.

Bivariate associations between household environmental conditions, maternal characteristics, and child stunting

Table 2 presents the bivariate associations between household environmental conditions, maternal characteristics, and child stunting. Significant disparities in stunting prevalence emerged across varying household environmental conditions, emphasizing the critical role of environmental health in determining early childhood growth trajectories. Children living in rural areas exhibit a significantly higher prevalence of stunting (34.8%) compared to those living in urban areas (27.1%). This indicates that disparities in environmental infrastructure and access to essential services may contribute to inequalities in growth outcomes. Similarly, children from households relying on unimproved drinking water sources experienced a considerably higher prevalence of stunting (37.9%) than those with access to improved water sources (29.3%). This observed pattern corroborates existing evidence that consumption of unsafe drinking water elevates children's susceptibility to enteric pathogens and EED, which consequently compromises nutrient assimilation and impairing linear growth trajectories. A comparable gradient was observed for sanitation, where children living in households with unimproved toilet facilities had a higher prevalence of stunting (35.7%) than those with improved sanitation (28.4%). These results highlight that optimal household environmental conditions are vital for suppressing fecal–oral pathogen transmission and establishing healthier living conditions that support pediatric development. Maternal environmental health-related behaviors also demonstrated clear differences in stunting prevalence. Children whose mothers did not attend routine antenatal care (ANC) experienced substantially higher stunting prevalence (39.7%) than those whose mothers attended ANC regularly (29.5%). Likewise, children delivered by non-skilled birth attendants showed a higher prevalence of stunting (38.4%) than those assisted by skilled birth attendants (27.4%). These findings suggest that sustained maternal health service utilization may enhance environmental health education, nutritional counseling, infection prevention, and other practices supporting healthy growth during the first 1,000 days of life (UNICEF, 2023; Nuraeni *et al.,* 2024). Clean and healthy environmental behavior, adequate sanitation, and appropriate household hygiene practices are particularly important because environmental conditions can influence nutritional status and susceptibility to infectious diseases during early childhood (Nuraeni *et al.,* 2024). In a similar vein, failure to meet the recommended intake of at least 60 iron-folic acid tablets during pregnancy was associated with an elevated stunting prevalence in children (34.2% versus 28.5% for those whose mothers met the threshold). Sustained maternal preventive practices may improve child growth, while maternal characteristics influence vulnerability to stunting.

Table 2: The bivariate associations between household environmental conditions, maternal characteristics, and child stunting

Variable	Stunting status	
	Not stunting	stunting
Sex		
Male	68.9%	31.1%
Female	70.6%	29.4%
Birth order		
Firstborn	71.0%	29.0%
2-4	68.9%	31.1%
5 or higher	57.9%	42.1%
Size of the child at birth		
Normal	70.8%	29.2%
Small	54.0%	46.0%
Exclusive breastfeeding		
No	69.8%	30.2%
Yes	69.3%	30.7%
Toilet facility		
Improved	71.6%	28.4%
Unimproved	64.3%	35.7%
Source of drinking water		
Improved	70.7%	29.3%
Unimproved	62.1%	37.9%
Mother's Age		
<18	69.2%	30.8%
18-24	65.6%	34.4%
25-34	70.9%	29.1%
>=35	71.9%	28.1%
Mother's education		
Primary or below	65.0%	35.0%
Secondary	72.0%	28.0%
Higher	77.0%	23.0%
Provided of delivery		
Skilled birth attendant	72.6%	27.4%
Non-skilled	61.6%	38.4%
ANC visit		
Routine	70.5%	29.5%
Non-routine	60.3%	39.7%
Maternal BMI		
<18.5 (underweight)	70.9%	29.1%
18.5-24.9 (normal)	58.7%	41.3%
25-29.9 (overweight)	69.2%	30.8%
>=30 (obesity)	73.5%	26.5%
Residence		
Urban	72.9%	27.1%
Rural	65.2%	34.8%
Maternal Smoking Status		
No	69.7%	30.3%
Yes	72.2%	27.8%
Maternal Hypertension Status		
No	69.7%	30.3%
Yes	50.0%	50.0%
Maternal Iron Supplement Intake		
Received <60 pills	65.85%	34.15%
Received ≥60 pills	71.51%	28.49%

A clear inverse relationship was observed between maternal educational attainment and stunting prevalence, with rates dropping from 35.0% in the primary education or below category to 23.0 among children whose mothers completed higher education. Higher educational attainment may improve mothers' environmental health literacy, enabling more effective utilization of available household environmental resources, safer childcare practices, and informed health-seeking behaviors (UNICEF, 2023). Maternal nutritional status also showed a pronounced gradient. Children of underweight mothers (BMI <18.5 kg/m²) experienced the highest prevalence of stunting (41.3%), whereas children of mothers with obesity had the lowest prevalence (26.5%), reflecting the intergenerational influence of maternal nutritional status on child growth. Maternal smoking and hypertension were observed at low frequencies within the study cohort. However, children of hypertensive mothers exhibited the highest prevalence of stunting (50.0%), although this finding should be interpreted cautiously because of the limited number of affected mothers. Child characteristics also exhibited variations in stunting prevalence. Male children showed a slightly higher prevalence (31.1%) than females (29.4%). Consistent with existing literature, these results suggest an increased biological vulnerability to early childhood growth faltering and infectious morbidities among male infants. Children born with low birth weight (<2,500 g) had a markedly higher prevalence of stunting (46.0%) than those born with normal birth weight (29.2%), emphasizing the lasting influence of prenatal growth conditions. Likewise, stunting prevalence increased with birth order, reaching 42.1% among children of fifth birth order or higher compared with 29.0% among firstborns. Although conventionally explained by resource dilution mechanisms, expanded household size can intensify environmental pressures pertaining to caregiver capacity, domestic sanitation maintenance, and the availability of water and sanitation infrastructure. Such environmental dimensions are particularly relevant because clean and healthy environmental behavior and adequate sanitation are important components of protecting child health and reducing malnutrition-related vulnerabilities (Nuraeni *et al.,* 2024). In contrast, the prevalence of stunting was similar between exclusively breastfed children (30.7%) and those who were not exclusively breastfed (30.2%). This finding should be interpreted cautiously, as the cross-sectional design cannot account for reverse causality, complementary feeding practices, or dietary quality after six months of age (WHO, 2006). Environmental exposures may also contribute to broader childhood health vulnerability. Evidence linking ambient nitrogen dioxide exposure with increasing asthma incidence among school-aged children demonstrates the potential health consequences of environmental air pollution and highlights the importance of maintaining healthy environmental conditions for vulnerable child populations (Sari *et al.,* 2025). Similarly, climate change can modify environmental and epidemiological conditions that influence vector-borne disease transmission, emphasizing the importance of community-based adaptation, environmental management, and preventive health practices (Akhtar, 2026). These findings reinforce the need to consider child growth and health within a broader environmental-health framework, in which household sanitation, environmental quality, climate-related risks, and preventive health behaviors interact with maternal and child-level determinants.

Result of logistic regression model

Before model estimation, multicollinearity diagnostics showed no evidence of problematic multicollinearity (maximum VIF = 3.86). All VIF values were below 5, indicating that multicollinearity was not a concern in the final regression model (Hair *et al.*, 2019). The Hosmer–Lemeshow goodness-of-fit test indicated that the model adequately fit the data (χ^2 = 4.89, p =

0.768). Furthermore, the final model exhibited satisfactory explanatory and predictive capacity, yielding a pseudo-R^2 of 0.231. Collectively, these results indicate that the final logistic regression model was well calibrated and provided satisfactory discrimination between stunted and non-stunted children. The multivariable logistic regression models evaluating determinants of stunting in children aged 0–23 months are summarized in Table 3. The overall model was statistically significant (Wald chi-square (Wald χ^2) = 54.75; probability value (p-value) <0.001), indicating that the included environmental, maternal, and child-related variables jointly explained variations in child stunting. Domestic environmental conditions materialized as key predictors influencing the onset of pediatric stunting. Children living in households with improved drinking water sources had significantly lower odds of stunting than those relying on unimproved water sources (OR=0.806; p-value=0.047). Similarly, access to improved sanitation facilities was significantly associated with lower odds of stunting (OR=0.943; p-value=0.007). Despite the relatively modest magnitude of the sanitation effect, the attainment of statistical significance demonstrates a persistent protective influence of improved household sanitation on early childhood growth. In contrast, residential location was not significantly associated with stunting after adjustment for other covariates (OR=1.116; p-value=0.417). This implies that disparities between urban and rural settings were primarily accounted for by household environmental and socio-demographic attributes rather than geographical location per se. Maternal environmental health-related behaviors also demonstrated significant protective associations. Children whose mothers attended routine antenatal care (ANC) had 35.8% lower odds of stunting than those whose mothers attended ANC irregularly (OR=0.642; p-value=0.048). Likewise, delivery assisted by a skilled birth attendant was associated with lower odds of stunting by approximately 29% (OR=0.707; p-value=0.014). These results demonstrate that the ongoing utilization of preventive maternal health services, conceptualized within the TTM as advancement toward the action and maintenance stages of behavioral modification, contributes to enhanced child growth outcomes. Although maternal iron supplementation was associated with lower odds of stunting (OR=0.827), the association was not statistically significant (p-value=0.160). Maternal socioeconomic and nutritional characteristics were also associated with child growth. Higher maternal education was significantly associated with lower odds of stunting (OR=0.784; p-value=0.025). Meanwhile children born to underweight mothers (BMI<18.5 kg/m^2) had significantly higher odds of stunting compared with those whose mothers had normal nutritional status (OR=1.265; p-value=0.008). After multivariable adjustment, maternal overweight, obesity, age, smoking, hypertension, and exclusive breastfeeding were not significantly associated with stunting, whereas low birth weight remained one of the strongest child-level predictors of stunting**.** Children born with low birth weight had nearly twice the odds of being stunted compared with those born at normal birth weight (OR=1.898; p-value=0.009). Analysis revealed a positive gradient between birth order and stunting prevalence. Specifically, infants of second-to-fourth birth order experienced a 32% increase in the odds of stunting relative to firstborn children (OR=1.324; p-value=0.041), and fifth-order or higher births showed an elevated risk trend (OR=1.802), although this estimate attained only marginal significance (p-value=0.066). The findings demonstrate that improved water, sanitation, and maternal environmental health practices reduce stunting risk during the first 1,000 days of life, highlighting their complementary roles in supporting optimal child growth and long-term health and development, particularly by reducing exposure to infections, improving hygiene, and strengthening household-level preventive care practices.

Table 3: The result of the logistic regression model

Variable	Coefficient	Odds ratio	Standard error (SE)	p-value	95% CI
Sex					
Male (references (ref))					
Female	-0.078	0.925	0.127	0.536	[-0.327, 0.170]
Birth order					
Firstborn (ref)					
2–4	0.280	1.324	0.137	0.041	[0.012, 0.549]
5 or higher	0.589	1.802	0.426	0.066	[-0.245, 1.423]
Size of the child at birth					
Normal (ref)					
Low birth weight	0.641	1.898	0.244	0.009	[0.162, 1.119]
Exclusive breastfeeding					
No (ref)					
Yes	0.131	1.140	0.154	0.393	[-0.170, 0.433]
Toilet facility					
Unimproved (ref)					
Improved	-0.059	0.943	0.154	0.007	[-0.360, 0.242]
Source of drinking water					
Unimproved (ref)					
Improved	-0.216	0.806	0.186	0.047	[-0.580, 0.149]
Mother's Age					
<18 (ref)					
18–24	0.1836	1.2016	0.6258	0.769	[-0.976, 1.445]
25–34	-0.0468	0.9543	0.6275	0.941	[-1.138, 1.290]
≥35	-0.1456	0.8645	0.6410	0.820	[-1.236, 1.240]
Mother's education					
Primary or below (ref)					
Secondary	-0.059	0.942	0.147	0.086	[-0.347, 0.228]
Higher	-0.243	0.784	0.200	0.025	[-0.635, 0.149]
Provided of delivery					
Non-skilled (ref)					
Skilled birth attendant	-0.346	0.707	0.141	0.014	[-0.623, -0.069]
ANC visit					
Non-routine (ref)					
Routine	-0.443	0.642	0.224	0.048	[-0.883, -0.004]
Maternal BMI					
18.5-24.9 (normal) (ref)					
<18.5 (underweight)	0.235	1.265	0.216	0.008	[-0.976, 1.445]
25-29.9 (overweight)	0.076	1.079	0.157	0.118	[-1.138, 1.290]
≥30 (obesity)	0.002	1.002	0.213	0.357	[-1.236, 1.240]
Residence					
Urban (ref)					
Rural	0.109	1.116	0.135	0.417	[-0.155, 0.374]
Maternal smoking status					
No (ref)					
Yes	0.173	1.189	0.641	0.787	[-1.083, 1.430]
Maternal hypertension status					
No (ref)					
Yes	0.962	2.617	1.408	0.494	[-1.798, 3.723]
Maternal iron supplement intake					
No (ref)					
Yes	-0.189	0.827	0.135	0.160	[-0.453, 0.075]
Constant	-0.235		0.667		[-1.542, 1.073]

Collectively, the regression analysis results suggest that favorable household environments and maternal practices reflecting advancement toward the action and maintenance stages of behavior change correlate inversely with the likelihood of child stunting. These findings highlight that favorable environmental conditions are associated with lower environmental health risks and the adoption and maintenance of preventive maternal behaviors. This supports the relevance of a stage-based behavioral perspective in promoting healthy child growth. The findings can be interpreted through the TTM as a theoretical basis for understanding how maternal preventive behaviors operate within conducive household environmental contexts. Since the IFLS-5 dataset does not directly measure stages of behavioral change, these findings should be interpreted as a reflection of observable preventive behaviors among mothers rather than as a direct empirical measurement of the model itself. Findings from this study imply that early childhood stunting over the first 1,000 days reflects the combined influence of household environmental determinants, maternal preventive behaviors, and biological vulnerability rather than relying exclusively on nutritional status. This interpretation is consistent with previous studies suggesting that behavioral change is influenced not only by individual motivation and self-efficacy but also by contextual and environmental resources that enable sustained behavioral adoption (Haakstad *et al.*, 2013; Jung and Shin, 2021; Prochaska and Velicer, 1997). These findings indicate that home environmental conditions and maternal behaviors pertaining to environmental health function as complementary pathways supporting healthy child development. This underscores the importance of integrating environmental and behavioral approaches into strategies for preventing childhood stunting. These findings aligned with previous research show that inadequate water supply and poor sanitation increase children's exposure to enteric pathogens, recurrent diarrheal infections, and EED. All these factors compromise intestinal integrity, reduce nutrient absorption, and ultimately hinder linear growth (Arief *et al.*, 2025; Sahiledengle *et al.*, 2023; Torlesse *et al.*, 2016). From the perspective of environmental health, the relationship between household environmental conditions and child growth extends beyond simple disease prevention. This biological mechanism has garnered growing recognition as a principal pathway connecting environmental degradation to childhood growth failure, particularly in low- and middle-income countries (LMICs) characterized by deficient environmental infrastructure (Arief *et al.*, 2025; Sahiledengle *et al.*, 2023). The associations of improved drinking water and sanitation observed in this study are consistent with a growing body of evidence from Indonesia and other LMICs. Previous studies conducted in Indonesia, India, East Africa, and the Democratic Republic of the Congo have consistently demonstrated that access to improved water and sanitation is associated with a lower likelihood of childhood stunting by reducing exposure to enteric pathogens, recurrent infections, and EED (Budiastutik *et al.*, 2024; Das *et al.*, 2022; Huo *et al.*, 2022; Rah *et al.*, 2020). The consistency of these findings across diverse LMIC settings suggests that household environmental conditions represent fundamental determinants of child growth regardless of differences in socioeconomic and public health contexts. These results strengthen the mounting consensus that environmental health interventions represent indispensable components of nutrition-sensitive programming. Rather than functioning solely as physical infrastructure, improved household environmental conditions create healthier living environments that reduce environmental health risks and support optimal child development during the first 1,000 days of life. Analyses revealed an independent association between

consistent antenatal care attendance, skilled birth assistance, and decreased likelihood of child stunting. By providing repeated clinical opportunities for nutrition counseling, hygiene education, infection prevention, and early risk screening, routine prenatal evaluations and professional delivery support serve a critical preventive function. All of which contribute to improved maternal and child health (Islam *et al.*, 2020; Kumala Putri *et al.*, 2024; Nyarko *et al.*, 2024). The protective effects of routine antenatal care (ANC) attendance and delivery assisted by skilled birth attendants (SBAs) indicate that maternal environmental health-related behaviors are key pathways through which supportive household environments improve child growth (Kumala Putri *et al.*, 2024; Nurfatimah *et al.*, 2021; Nyarko *et al.*, 2024). Within the TTM, routine antenatal care attendance and skilled birth attendance may be viewed as observable maternal preventive behaviors that are conceptually consistent with progression toward the action and maintenance stages. Thus, these services strengthen mothers' capacity to adopt environmental health practices that protect maternal and child well-being throughout the first 1,000 days of life. The findings further demonstrate that maternal education and nutritional status remain important determinants of child growth. Mothers with advanced educational backgrounds typically exhibit greater proficiency in interpreting health literacy, accessing healthcare services, and adopting preventive measures. In contrast, maternal undernutrition manifests as a accumulation of nutritional and socioeconomic deprivations that exert adverse effects on fetal and pediatric growth (Haque *et al.*, 2022; Porwal *et al.*, 2021). These results indicate that improvements in household environmental conditions alone may not be sufficient unless accompanied by strategies that strengthen maternal capacity to sustain healthy behaviors throughout pregnancy and early childhood. Consistent with previous studies, low birth weight has been identified as one of the strongest predictors of childhood stunting. Such data underscore that impaired developmental growth often has its genesis prior to birth, driven by a confluence of maternal nutritional deficits, repeated pathogenic infections, and unfavorable intrauterine conditions (Nyarko *et al.*, 2024; Taslim *et al.*, 2023). Similarly, the increased likelihood of stunting among children of higher birth order may reflect greater competition for household resources and reduced caregiving capacity, particularly in socioeconomically disadvantaged households. This evidence demonstrates that childhood stunting is shaped by the interplay of biological vulnerability and household environmental conditions, underscoring their roles as interrelated rather than mutually exclusive determinants. These findings support socio-ecological perspectives suggesting that behavior change is shaped not only by individual readiness but also by environmental contexts that enable or constrain long-term behavioral adoption (Haakstad *et al.*, 2013; Jung and Shin, 2021). The absence of a significant association between place of residence and childhood stunting after adjustment suggests that geographic location alone is not the primary determinant of child growth. Instead, household-level socioeconomic and environmental conditions appear to play a more important role than children living in urban or rural areas. This finding aligns with prior research demonstrating that socioeconomic gradients in childhood stunting are primarily mediated by variations in household income, parental educational attainment, and household food security (Poojara *et al.*, 2025), and access to essential environmental health services rather than residential location itself (Amegbor *et al.*, 2020; Kyu *et al.*, 2013). Likewise, inadequate sanitation and limited access to safe drinking water remain important risk factors for childhood stunting in

both urban and rural settings (Ar Rahma *et al.*, 2023; Nor Aisyah Purnamasari *et al.*, 2024; Puteri and Fitria, 2025), indicating that household environmental conditions represent more direct determinants of child growth than geographic residence alone. Synthesized collectively, these empirical insights underscore vital imperatives for the formulation of environmental health policies and the design of efficacious interventions to prevent stunting. Improving access to safe drinking water and sanitation should be implemented alongside maternal health promotion and stage-based behavioral interventions rather than as isolated programs. Such an integrated approach aligns with Indonesia's multisectoral stunting reduction strategy and contributes to achieving SDG-3 on good health and well-being and SDG-6 on clean water and sanitation. Interventions that simultaneously target domestic environmental conditions and maternal preventive practices are more efficacious in engendering long-term improvements in pediatric growth during the critical first 1,000 days. This study has several limitations. First, owing to the cross-sectional nature of the data, the identified relationships linking domestic environmental conditions, maternal practices, and childhood stunting denote statistical associations rather than definitive causal or temporal trajectories. Second, the TTM was applied as an interpretive framework because the IFLS-5 dataset does not directly measure behavioral readiness or the stages of change, and maternal preventive behaviors were therefore represented using proxy indicators. Third, although IFLS-5 utilizes a sophisticated multistage sampling design, sampling weights were not applied in the present analysis; consequently, the estimated associations should be interpreted cautiously when extrapolating the findings to the entire Indonesian population. Fourth, Future studies ought to employ sensitivity analyses across varied analytical specifications and environmental classifications to verify the stability and resilience of the identified relationships. Finally, household environmental indicators were limited primarily to drinking water and sanitation because comparable measures of housing quality, household hygiene, waste management, and indoor air pollution were not consistently available in the dataset. Fifth, maternal behaviors and home environment conditions were based on self-reported information. Moreover, the results are potentially vulnerable to social desirability bias, notably regarding health behaviors perceived as normative or advantageous, including antenatal care utilization and iron supplementation adherence. This may have led to over-reporting of preventive practices and could attenuate or overestimate the true associations between maternal behaviors and childhood stunting. Sixth, although this study included urban/rural residence as a contextual variable, broader regional variations in environmental infrastructure, socioeconomic development, and healthcare accessibility across the 13 provinces were not explicitly modeled. Given the substantial socioeconomic and infrastructural indicators across these administrative regions, residual unmeasured heterogeneity may have exerted a confounding influence on the estimated linkages connecting household environmental conditions, maternal behaviors, and childhood stunting. Future research should employ longitudinal or intervention designs that incorporate broader environmental health indicators. Furthermore, future research ought to analyze the moderation effects linking domestic effects between home environmental conditions and maternal behavioral preparedness, thereby clarifying the mechanisms through which supportive milieus promote long-term preventive behaviors. This will also provide a more comprehensive understanding of effective stunting prevention strategies among vulnerable children during the first 1,000 days of life.

CONCLUSION

This study demonstrates that household environmental conditions are fundamental determinants of childhood stunting during the first 1,000 days of life, with an overall stunting prevalence of 30.32% among children aged 0 to 23 months. Access to improved drinking water (OR=0.806, p-value=0.047) and improved sanitation (OR=0.943, p-value=0.001) was consistently associated with lower odds of stunting, emphasizing that environmental improvements should be regarded as essential components of stunting prevention. Utilizing the TTM framework, these findings provide additional evidence that a conducive home environment accelerates mothers' advancement toward long-term preventive practices. This is reflected in regular prenatal check-ups (which reduced the risk of stunting by 35.8%; OR=0.642, p-value=0.048) and deliveries assisted by skilled health personnel (which reduced the risk by approximately 29%; OR=0.707, p-value=0.014) thereby reinforcing the protective effect of a healthy environment on child growth. These results underscore the significance of combining environmental enhancements with stage-specific behavioral interventions and maternal health services to attain lasting decreases in childhood stunting, thereby contributing to the objectives of SDG 3 and 6. By linking environmental conditions and maternal behavioral readiness through the TTM framework, this study makes a theoretical contribution that has rarely been. However, the cross-sectional design limits causal inference, the IFLS does not directly measure key TTM constructs, and environmental variables were restricted to improved drinking water and sanitation without capturing direct environmental exposures. Such methodological constraints denote that underlying behavioral trajectories were inferred through proxy indicators, raising the possibility that the magnitude of associated environmental risks has been understated. This may stem from the absence of direct exposure measurements, such as water quality testing or assessments of fecal contamination. Nevertheless, these findings indicate that household environmental conditions and maternal behaviors related to environmental health serve as complementary determinants of childhood stunting. Moreover, this findings advances the theoretical utility of the TTM by accentuating the critical function of conducive environmental frameworks in preserving long-term preventive actions. These findings strengthen the evidence that a healthy environment has a protective effect on child growth, while also confirming the close relationship between physical environmental conditions and maternal health behaviors in determining children's nutritional status. This study indicates that initiatives aimed at mitigating childhood stunting must be coupled with enhancements in fundamental household infrastructure—specifically, access to potable water and adequate sanitation—as core components of nutrition-sensitive programming. Furthermore, since environmental impacts on stunting operate through the reinforcement of mothers' preventive behaviors, stage-based behavioral interventions are designed contextually by tailoring health promotion messages and approaches. Health promotion strategies should be tailored to the mothers' perceived stages of readiness, rather than employing a one-size-fits-all approach to all situations. This study also supports the importance of a cross-sectoral approach that supports environmental development while strengthening maternal and child health services, as a dual strategy to simultaneously achieve SDGs 3 and 6, both of which have a direct intersection with the issue of stunting. From a programmatic standpoint, these results underscore the utility of regional priority-mapping frameworks that simultaneously account for stunting prevalence and infrastructural indicators of water and

sanitation, thereby enabling more targeted resource distribution to environmentally vulnerable populationsFuture studies would benefit from employing longitudinal or panel-based designs to establish temporal and causal relationships among environmental improvements, maternal behavioral development, and child growth, while also capturing changes in household conditions, maternal practices, and child nutritional status across different developmental stages over time.Furthermore, the use of validated TTM instruments and direct measurements of environmental exposure would allow for a more precise mapping of the mechanisms underlying the environment–behavior–stunting pathway identified in this study, thereby improving causal interpretation and strengthening evidence for targeted intervention development and implementation.

AUTHOR CONTRIBUTIONS

A. Mutia conceived the research idea and designed the study methodology, prepared the manuscript draft, contributed to reviewing and editing the manuscript, and prepared the visualizations. D. Utari prepared the manuscript draft, contributed to reviewing and editing the manuscript, prepared the visualizations, and supervised the work. T.E.B. Soesilo, the corresponding author, curated the data, carried out the investigation, provided resources, contributed to reviewing and editing the manuscript, administered the project, and secured funding for the research. All authors have read and agreed to the published version of the manuscript.

ACKNOWLEDGEMENT

The authors would like to thank to Directorate of Research and Development, Universitas Indonesia and member of cluster research which facilitates this research to run well. This work was supported by the Hibah Publikasi Terindeks Internasional (PUTI) Q1 2024, Directorate of Research and Development, Universitas Indonesia [Grant numbers NKB-569/UN2.RST/HKP.05.00/2024]

CONFLICT OF INTEREST

The authors declare that there is no conflict of interest regarding the publication of this manuscript. In addition, ethical issues, including plagiarism, informed consent, misconduct, data fabrication and/or falsification, double publication and/or submission, and redundancy have been completely observed by the authors.

OPEN ACCESS

©2027 The author(s). This article is licensed under a Creative Commons Attribution 4.0 International License, which permits use, sharing, adaptation, distribution and reproduction in any medium or format, as long as you give appropriate credit to the original author(s) and the source, provide a link to the Creative Commons license, and indicate if changes were made. The images or other third-party material in this article are included in the article's Creative Commons license, unless indicated otherwise in a credit line to the material. If material is not included in the article's Creative Commons license and your intended use is not permitted by statutory regulation or exceeds the permitted use, you will need to obtain permission directly from the copyright holder. To view a copy of this license, visit: http://creativecommons.org/licenses/by/4.0/

PUBLISHER'S NOTE

GJESM Publisher remains neutral regarding jurisdictional claims in published maps and institutional affiliations.

NEGATIVE AI STATEMENT

The author(s) declared that no AI tools or services were used or not highly applied during the preparation of this work.

ABBREVIATIONS

%	Percent
<	Less than
≥	More than or equal to
–	Through
ANC	Antenatal care
BMI	Body mass index
BPS	Badan Pusat Statistik
EAs	Enumeration areas
EED	Environmental enteric dysfunction
g	gram
HAZ	Height-for-age z-score
IFLS	Indonesian Family Life Survey
IRBs	Institutional Review Boards
JME	Joint child malnutrition estimates
kg	kilograms
kg/m²	kilograms per square metre
LBW	low birth weight
LMICs	low- and middle-income countries
m²	square metre
OR	Odds ratio
p-value	probability value
PNC	Postnatal care
Ref	References
R&D	Research and development
SBA	Skilled birth attendant
SDGs	Sustainable development goals
SE	Standard error
SUSENAS	Survei Sosial Ekonomi Nasional
TTM	Transtheoretical Model
UGM	Universitas Gadjah Mada
UNICEF	United Nations Children's Fund
vs.	Versus
Wald χ^2	Wald chi-square
WASH	Water, sanitation, and hygiene
WHO	World Health Organization

REFERENCES

Aguayo, V.M.; Menon, P., (2016). Stop stunting: improving child feeding, women's nutrition and household sanitation in South Asia. Matern. Child Nutr., 12(S1): 3-11 **(9 pages).**

Akhtar, M.T., (2026). Community-based adaptation strategies to the impact of climate change in vector-borne diseases. Global J. Environ. Sci. Manage., 12(3): 1333-1350 **(18 pages).**

Amegbor, P.M.; Yankey, O.; Sabel, C.E., (2020). Examining the effect of geographic region of residence on childhood malnutrition in Uganda. J. Trop. Pediatr., 66(6): 598-611 **(14 pages).**

Ar Rahma, C.A.; Razak, R.; Septiawati, D., (2023). Analisis spasial kasus stunting berdasarkan fasilitas kesehatan dan korelasi faktor risiko lingkungan pada balita di Kabupaten Ogan Ilir tahun 2023. Media Publ. Promosi Kesehatan Indones. (MPPKI), 6(12): 2588-2598 **(11 pages).**

Arief, Y.S.; Yunita, F.C.; Efendi, F.; Murti, F.A.K.; Pradipta, R.O.; McKenna, L., (2025). Social and environmental determinants of childhood stunting in Indonesia: national cross-sectional study. JMIR Pediatr. Parent. 8: e68918 **(11 pages).**

Astuti, D., (2026). Stunting incidence factors based on environmental health and economic status perspectives: a narrative review. J. Evid. Based Nurs. Public Health, 3(1): 20-36 **(17 pages).**

Binamungu, J.; Sanga, I., (2026). High coverage, limited impact: rethinking the effectiveness of intensive stunting reduction interventions in Njombe Region, Tanzania. Matern. Child Nutr., 22(3) **(6 pages)**.

Bloem, M.; Pee, S.; Hop, L.; Khan, N.; Laillou, A.; Minarto, E.; Moench-Pfanner, R.; Soekarjo, D.; Soekirman, S.; Solon, J.; Theary, C.; Wasantwisut, E., (2013). Key strategies to further reduce stunting in Southeast Asia: lessons from the ASEAN countries workshop. Food Nutr. Bull., 34: S8-16 **(9 pages).**

Budiastutik, I.; Pranaka, R.N.; Amaliyah, N.; Hediyanti, G.; Trisnawati, E., (2024). The relation of infectious diseases, water access, hygiene practice, and sanitation with the stunting: a case-control study in Sambas Regency. Amerta Nutr., 8(1SP): 70-75 **(6 pages).**

Das, M.; Verma, M.; Sahoo, S.S.; Gupta, M., (2022). Regional water availability and WASH indicators as predictors of malnutrition in under-5 children: analysis of the National Family Health Survey, India (2015-16). J. Trop. Pediatr., 68(3) **(11 pages).**

Firdaus, S.E.; Maulana, P.D., (2025). Acceleration of stunting reduction: advancing social and environmental well-being through policy, education, and environmental management. J. Sustain. Soc. Eco-Welf., 2(2): 141-158 **(18 pages).**

Fregonese, F.; Siekmans, K.; Kouanda, S.; Druetz, T.; Ly, A.; Diabaté, S.; Haddad, S., (2017). Impact of contaminated household environment on stunting in children aged 12-59 months in Burkina Faso. J. Epidemiol. Community Health. 71(4): 356-363 **(8 pages).**

Glanz, K.; Rimer, B.K.; Viswanath, K., (Eds.), (2015). Health behavior: theory, research, and practice (5th ed.). Jossey-Bass/Wiley.

Grossman, C.; Hadley, W.; Brown, L.K.; Houck, C.D.; Peters, A.; Tolou-Shams, M., (2008). Adolescent sexual risk: factors predicting condom use across the stages of change. AIDS Behav., 12(6): 913-922 **(10 pages).**

Haakstad, L.A.H.; Voldner, N.; Bo, K., (2013). Stages of change model for participation in physical activity during pregnancy. J. Pregnancy. 2013: 1-7 **(7 pages).**

Hair, J.F.; Risher, J.J.; Sarstedt, M.; Ringle, C.M., (2019). When to use and how to report the results of PLS-SEM. Eur. Bus. Rev., 31(1): 2-24 **(23 pages).**

Haque, R.; Alam, K.; Rahman, S.M.; Mustafa, M.U.R.; Ahammed, B.; Ahmad, K.; Hashmi, R.; Wubishet, B.L.; Keramat, S.A., (2022). Nexus between maternal underweight and child anthropometric status in South and South-East Asian countries. Nutrition. 98: 111628 **(8 pages).**

Huo, S.; Wang, K.; Liu, Z.; Yang, Y.; Hee, J.Y.; He, Q.; Takesue, R.; Tang, K., (2022). Influence of maternal exposure to mass media on growth stunting among children under five: mediation analysis through the water, sanitation, and hygiene program. JMIR Public Health Surveill., 8(4): e33394 **(10 pages).**

Hosmer, D.W.; Lemeshow, S.; Sturdivant, R.X., (2013). Applied Logistic Regression. 3rd Ed. Wiley, Hoboken, NJ. **(510 pages).**

Islam, M.S.; Zafar Ullah, A.N.; Mainali, S.; Imam, M.A.; Hasan, M.I., (2020). Determinants of stunting during the first 1000 days of life in Bangladesh: a review. Food Sci. Nutr., 8(9): 4685-4695 **(11 pages).**

Islam, M.Z.; Mostafa, M.G., (2024). Suitability assessment of groundwater quality for drinking purposes. J. Environ. Sci. Sustain. Dev., 7(1): 512-539 **(28 pages).**

Jung, S.; Shin, S.R., (2021). Factors affecting stages of change in smoking cessation and intention to quit among Asian students in Korea based on the transtheoretical model. Korean J. Adult Nurs., 33(5): 484 **(14 pages).**

Kemenkes, (2025). Survei Kesehatan Indonesia (SKI) Tahun 2023. Survei Kesehatan Indonesia, 1-965 **(965 pages).**

Kirana, T.A., (2025). The relationship between host behavior and environmental sanitation with the incidence of diarrhea in toddlers. Public Health Risk Assess. J., 3(1): 16-34 **(19 pages).**

Kumala Putri, D.S.; Sari, K.; Utami, N.H.; Djaiman, S.P.H., (2024). Influence of maternal and neonatal continuum of care on the risk of intergenerational cycle of stunting: a cross-sectional study. BMJ Open. 14(4): e081774 **(8 pages).**

Kusumo, P.D.; Surbakti, A.; Wiharianti, Y.V., (2024). Correlation between macronutrition and micronutrition intake in stunting children at Babakan Mandang Region. BIO Web Conference. 123: 02007 **(6 pages).**

Kyu, H.H.; Shannon, H.S.; Georgiades, K.; Boyle, M.H., (2013). Association of urban slum residency with infant mortality and child stunting in low and middle income countries. Biomed Res. Int., 2013: 1-12 **(12 pages).**

Ma, J.; Chan, W.; Tsai, C.; Xiong, M.; Tilley, B.C., (2015). Analysis of transtheoretical model of health behavioral changes in a nutrition intervention study, a continuous time Markov chain model with Bayesian approach. Stat. Med., 34(27): 3577-3589 **(13 pages).**

Mediani, H.S., (2020). Predictors of stunting among children under five year of age in Indonesia: a scoping review. Global J. Health Sci., 12(8): 83 **(13 pages).**

Nisa, A.F.; Pratiwi, C.S.; Warsiti., (2026). Association between access to water, sanitation, and hygiene (WASH) practices and stunting among children under five: a systematic review and meta-analysis. J. Evid. Based Nurs. Public Health, 3(1): 80-97 **(18 pages).**

Nuraeni; Hawa, N.I.; Utari, D.; Parahyanti, E., (2024). Clean and healthy environmental behavior in terms of malnutrition and sanitation. Global J. Environ. Sci. Manage., 10(2): 589-604 **(16 pages).**

Nurfatimah, N.; Ramadhan, K.; Entoh, C.; Longgupa, L.W.; Hafid, F., (2021). Continuity of midwifery care implementation to reduce stunting. Open Access Maced. J. Med. Sci., 9(E): 1512-1516 **(5 pages).**

Nyarko, M.J.; van Rooyen, D.; ten Ham-Baloyi, W., (2024). Preventing malnutrition within the first 1000 days of life in under-resourced communities: an integrative literature review. J. Child Health Care. 28(4): 898-913 **(16 pages).**

Perdananugraha, G.M.; Nuryana, M.; Wismayanti, Y.F., (2026). Can air quality data predict stunting prevalence? Aerosol Air Qual. Res., 26(3): 28 **(15 pages).**

Poojara, R.H.; P S, S.; Rose, A.; Somarajan, N., (2025). Composite flours for sustainable food systems: integrating nutritional, environmental, and climate resilience strategies. J. Environ. Sci. Sustain. Dev., 8(2): 490-522 **(33 pages).**

Porwal, A.; Agarwal, P.K.; Ashraf, S.; Acharya, R.; Ramesh, S.; Khan, N.; Johnston, R.; Sarna, A., (2021). Association of maternal height and body mass index with nutrition of children under 5 years of age in India: evidence from Comprehensive National Nutrition Survey 2016-18. Asia Pac. J. Clin. Nutr., 30(4): 675-686 **(12 pages).**

Prochaska, J.O.; Velicer, W.F., (1997). The transtheoretical model of health behavior change. Am. J. Health Promot., 12(1): 38-48 **(11 pages).**

Purnamasari, N.A.; Raharjo, M.; Hanani, Y., (2024). Environmental sanitation and PHBS analysis of stunting incidents in toddler in Paser District. Media Publ. Promosi Kesehatan Indones. (MPPKI), 7(8): 2092-2097 **(6 pages).**

Puteri, N.J.; Fitria, L., (2025). Access to sanitation and its impact on stunting in toddlers in East Nusa Tenggara, Indonesia. Unnes J. Public Health, 14(1): 14-21 **(8 pages).**

Rah, J.H.; Sukotjo, S.; Badgaiyan, N.; Cronin, A.A.; Torlesse, H., (2020). Improved sanitation is associated with reduced child stunting amongst Indonesian children under 3 years of age. Matern. Child Nutr., 16(S2) **(8 pages).**

Ramlan, P.; Sukri, P.; Abdullah, M.T.; Ibrahim, M.A.; Ahmad, J.; Adri, K., (2025). A systematic review of maternal and child health policies in addressing stunting: trends and challenges. J. Public Health Pharm., 5(1): 119-130 **(12 pages).**

Sahiledengle, B.; Agho, K.E.; Petrucka, P.; Kumie, A.; Beressa, G.; Atlaw, D.; Tekalegn, Y.; Zenbaba, D.; Desta, F.; Mwanri, L., (2023). Concurrent wasting and stunting among under-five children in the context of Ethiopia: a generalised mixed-effects modelling. Matern. Child Nutr., 19(2) **(20 pages)**.

Saleh, A.; Syahrul, S.; Hadju, V.; Andriani, I.; Restika, I., (2021). Role of maternal in preventing stunting: a systematic review. Gac. Sanit., 35: S576-S582 **(7 pages).**

Sari, P.N.; Driejana, D.; Yudison, A.P.; Agustian, D.; Kurnia, A.B.; Riqqi, A. (2025). Ambient air nitrogen dioxide concentration and the growing incidence of asthma in school-aged children. Global J. Environ. Sci. Manage., 11(3): 1125-1142 **(18 pages).**

Spencer, L.; Adams, T.B.; Malone, S.; Roy, L.; Yost, E., (2006). Applying the transtheoretical model to exercise: a systematic and comprehensive review of the literature. Health Promot. Pract., 7(4): 428-443 **(16 pages).**

Strauss, J.; Witoelar, F.; Sikoki, B., (2016). The fifth wave of the Indonesia Family Life Survey: overview and field report, volume 1. RAND Corp **(94 pages)**.

Sukmawati, S.; Hermayanti, Y.; Fadlyana, E.; Maulana, I.; Mediani, H.S., (2025). Health cadres' experiences in detecting and preventing childhood stunting in Indonesia: a qualitative study. BMC Public Health. 25(1): 2987 **(10 pages).**

Taslim, N.A.; Farradisya, S.; Gunawan, W.B.; Alfatihah, A.; Barus, R.I.B.; Ratri, L.K.; Arnamalia, A.; Barazani, H.; Samtiya, M.; Mayulu, N.; Kim, B.; Hardinsyah, H.; Surya, E.; Nurkolis, F., (2023). The interlink between chrono-nutrition and stunting: current insights and future perspectives. Front. Nutr., 10 **(10 pages)**.

Torlesse, H.; Cronin, A.A.; Sebayang, S.K.; Nandy, R., (2016). Determinants of stunting in Indonesian children: evidence from a cross-sectional survey indicate a prominent role for the water, sanitation and hygiene sector in stunting reduction. BMC Public Health. 16(1): 669 **(11 pages).**

UNICEF, (2019). The state of the world's children 2019: children, food and nutrition, growing well in a changing world **(258 pages)**.

UNICEF, (2023). The state of the world's children 2023: for every child, vaccination **(24 pages)**.

UNICEF, (2025). Levels and trends in child malnutrition: UNICEF/WHO/World Bank Group joint child malnutrition estimates **(24 pages)**.

Victora, C.G.; Christian, P.; Vidaletti, L.P.; Gatica-Domínguez, G.; Menon, P.; Black, R.E., (2021). Revisiting maternal and child undernutrition in low-income and middle-income countries: variable progress towards an unfinished agenda. Lancet. 397(10282): 1388-1399 **(12 pages).**

Vilcins, D.; Sly, P.D.; Jagals, P., (2018). Environmental risk factors associated with child stunting: a systematic review of literature. Ann. Glob. Health. 84(4): 551 **(12 pages).**

WHO, (2006). WHO child growth standards: length/height-for-age, weight-for-age, weight-for-length, weight-for-height, and body mass index-for-age: methods and development **(336 pages).**

WHO and UNICEF, (2021). Indicators for assessing infant and young child feeding practices: definitions and measurement methods.

Yunitasari, E.; Pradanie, R.; Arifin, H.; Fajrianti, D.; Lee, B.O., (2021). Determinants of stunting prevention among mothers with children aged 6-24 months. Open Access Maced. J. Med. Sci., 9(B): 378-384 **(7 pages).**

Zulfitrawati.; Mukty, M.I., (2025). Maternal knowledge and stunting: a cultural and public health perspective on community health education. Arung: Community Health Insight, 1(1): 27-34 **(8 pages).**

AUTHOR (S) BIOSKETCHES

Muthia, A., M.E.K.K, Junior researcher, Social Environment, Community Engagement, and Environmental Economics, Department Environmental Science, Graduated School of Sustainable Development, Universitas Indonesia, Jalan Salemba Raya, Jakarta Pusat, DKI Jakarta 10430, Indonesia
- Email: *azkamuthia25@gmail.com*
- ORCID: 0000-0002-6189-981X
- Web of Science ResearcherID: QTU-6859-2026
- Scopus Author ID: NA
- Homepage: https://www.researchgate.net/profile/Azka-Muthia-3

Utari, D., Ph.D., Associate Professor, Faculty of Health Science, Universitas Pembangunan Nasional Veteran, Depok, 16514, Indonesia.
- Email: *dyahutari@upnvj.ac.id*
- ORCID: 0000-0002-6808-0209
- Web of Science ResearcherID: HLP-8484-2023
- Scopus Author ID: 57170719700
- Homepage: https://fikes.upnvj.ac.id/id/akademic/staf-pengajar/dosen-tetap-kesehatan-masyarakat-s-1/dr-ns-dyah-utari-s-kep-mkkk.html

Soesilo, T.E.B., Ph.D., Associate Professor, Department Environmental Science, Graduated School of Sustainable Development, Universitas Indonesia, Jalan Salemba Raya, Jakarta Pusat, DKI Jakarta 10430, Indonesia
- Email: *tri.edhi@ui.ac.id*
- ORCID: 0000-0002-3188-5812
- Web of Science ResearcherID: AAD-2398-2021
- Scopus Author ID: 57193915879
- Homepage: https://scholar.ui.ac.id/en/persons/tri-edhi-budhi-soesilo/

HOW TO CITE THIS ARTICLE:
Muthia, A.; Utari, D.; Soesilo, T.E.B., (2027). Environmental health conditions associated with childhood stunting during the first 1000 days of life. Global J. Environ. Sci. Manage., 13(1): 457-478.

DOI: 10.22034/gjesm.2027.01.21
URL: https://www.gjesm.net/article_735561.html

Global J. Environ. Sci. Manage. 13(1): 479-500, Winter 2027, Serial #49

Global Journal of Environmental Science and Management
(GJESM)

Homepage: https://www.gjesm.net/

Podcasts

REVIEW ARTICLE

Artificial intelligence-driven approaches for detection, fate, transport, and remediation of microplastic pollution in aquatic systems

M. Kamaraj[1,2], H.A. Bhavithra[3], B. Rajalakshmi[4], J. Aravind[5,*]

[1]Department of Biotechnology, Faculty of Science and Humanities, SRM Institute of Science and Technology Ramapuram Campus, Chennai, Tamil Nadu, 600089 India

[2]Life Science Division, Faculty of Health and Life Sciences, INTI International University, Nilai, 71800 Malaysia

[3]Department of Mathematics, Faculty of Science and Humanities, SRM Institute of Science and Technology Ramapuram Campus, Chennai, Tamil Nadu, 600089 India

[4]Department of Computer Science and Engineering, Easwari Engineering College, Chennai, Tamil Nadu, 600089 India

[5]Environmental Research Laboratory, Department of General Medicine, Saveetha Medical College and Hospital, Saveetha Institute of Medical and Technical Sciences, Chennai, Tamil Nadu, 602105 India

ARTICLE INFO

Article History:
Received 26 March 2026
Revised 29 June 2026
Accepted 30 July 2026

Keywords:
Artificial intelligence
Artificial intelligence detection
Artificial intelligence remediation
Deep learning
Environmental monitoring
Microplastics

DOI:10. 22034.gjesm.2027.01.22

ABSTRACT

Microplastic pollution in aquatic systems is a global, pervasive and significant aquatic environmental problem with serious ecological and human health consequences. Traditional approaches to monitoring, analyzing, and modeling microplastics are labor-intensive, difficult to scale up and have limited predictive power. However, several large-scale studies have reported the occurrence, distribution and impact of microplastics. In the last few years, artificial intelligence, machine learning and deep learning have shown enormous potential to reshape how we monitor and manage the environment through data and automation. This narrative review critically synthesizes recent advances in artificial intelligence-assisted approaches for detection, characterization, environmental monitoring, fate and transport modeling, ecological risk assessment, and remediation of microplastic pollution in aquatic systems, with an emphasis on their current capabilities, limitations, and future research needs. Artificial intelligence-based image analysis and spectroscopic data processing have demonstrated improved accuracy and efficiency for automated microplastic identification under laboratory and controlled research conditions, although broader field validation remains limited. The use of artificial intelligence in evaluating exposure scenarios and potential impacts on biota and human health has emerged. Artificial intelligence-assisted optimization has shown promise for improving treatment-process performance in experimental studies; however, validation under full-scale operational conditions remains limited. However, several factors have hindered large-scale adoption, including data availability, model generalisability, standardization and interpretability. The study objectives were to synthesize current advances, highlight limitations, and suggest future research directions, such as the development of integrated artificial intelligence frameworks, digital twin technologies, and autonomous monitoring systems. By linking data science and environmental engineering, artificial intelligence-led strategies offer a revolutionary approach to more efficiently and sustainably managing microplastic pollution in aquatic systems. Unlike previous reviews that primarily address individual aspects of microplastic pollution or artificial intelligence applications, this review provides an integrated critical assessment of artificial intelligence -assisted detection, environmental monitoring, fate and transport modeling, ecological risk assessment, and remediation, while identifying key research gaps related to data standardization, model generalizability, field-scale validation, and interdisciplinary integration.

This is an open access article under the CC BY license (http://creativecommons.org/licenses/by/4.0/)

NUMBER OF REFERENCES	NUMBER OF FIGURES	NUMBER OF TABLES
119	5	3

*Corresponding Author:
Email: dr.j.aravind@gmail.com
Phone: +91 9443518878
ORCID: 0000-0001-9699-2312

Note: Discussion period for this manuscript open until March 01, 2027 on GJESM website at the “Show Article”.

INTRODUCTION

Microplastic pollution has become an increasing environmental issue - particularly in water bodies, where it is concentrated as indestructible plastic litter throughout water columns, sediments and aquatic organisms. Their small size and widespread coverage, coupled with their ability to withstand degradation, imply that they can move between numerous environmental compartments and consequently interact with complex physical, chemical and biological processes. These features not only affect their future in the environment but also increase their potential to act as vectors for toxic substances, thereby threatening aquatic ecosystems and human health. Although much research has been reported on the occurrence and impact of microplastics, the dynamic behavior of these particles in water bodies remains a challenge (Yang *et al.,* 2021; Ashrafy *et al.,* 2023; Jeyachandran *et al.,* 2026). Traditional techniques for tracking and analyzing microplastics are more labor-intensive and involve sampling, spectroscopic identification and deterministic modeling. Although such techniques provide valuable insights, in many cases they are constrained in spatial and temporal scales, have low throughput and involve uncertainty in forecasting transport paths and environmental distribution. Moreover, the quantity and diversity of environmental data produced by environmental monitoring programs have increased awareness of the inadequacy of old analytical structures, which are not sufficiently configured to manipulate vast and intricate data sets. Consequently, there is an ever-increasing demand for novel, information-based methodologies that can enhance the accuracy of detection, predictive modeling and decision-making processes (Pal *et al.,* 2025; Jolaosho *et al.,* 2025; Xie *et al.,* 2025). The application of artificial intelligence (AI) and deep learning (DL) has been a revolutionary tool in environmental science over the past few years, enabling us to derive meaningful patterns from large, complex datasets. AI-driven methods have shown great potential to automate the detection and classification of particulate pollutants, combine information from multiple environmental sources, and enhance the predictive capacity of environmental models. Where directional behavioral tendencies of microplastics suggest multifactorial dynamics, as seen in aquatic systems, including hydrodynamics, physicochemical interactions and biological action, AI offers a strong system for capturing nonlinear relationships and spatiotemporal variance. These capabilities render AI particularly well-suited for advancing insight into microplastic dynamics that cannot be achieved with traditional methods (Etin-Osa and Isitua, 2025; Anyanwu *et al.,* 2026). Recent studies have begun to discuss the application of AI-based methods for detecting microplastics, environmental monitoring and optimizing treatment methods. Image-based DL models have been used with much success for automatic particle identification, and machine learning (ML) models coupled with environmental datasets have been used to predict distribution patterns and transport processes. Most importantly, the strategies of AI assistance are explored to improve the efficiency of treatment systems that aim to reduce microplastic contamination. Despite these promising developments, the use of AI in this field is fragmented, with limited attempts to create integrated frameworks that combine detection, environmental behavior and remediation in a unified view (Zhang *et al.,* 2023; Rawat *et al.,* 2025). AI should be regarded as a complementary analytical tool that enhances rather than replaces conventional experimental, analytical, and modeling techniques. AI-assisted algorithms improve the interpretation of data generated from spectroscopy, microscopy, field observations, and hydrodynamic models, thereby facilitating more efficient identification, prediction, and decision-making in microplastic research. In this context, a synthesis of knowledge on AI-driven approaches is needed to fill gaps at

this stage and provide a coherent picture of their role in tackling microplastic pollution in aquatic systems. The study has primarily focused on individual aspects of microplastic pollution, including analytical detection techniques, environmental occurrence, ecological impacts, or specific applications of AI (Agaton, 2025; Amparán *et al.,* 2025; Anyanwu *et al.,* 2026). However, comprehensive critical synthesis integrating AI-assisted detection, environmental monitoring, fate-and-transport modeling, ecological risk assessment, and remediation strategies remains limited. To address this gap, the present narrative review provides a critical synthesis of representative and recent advances in AI-assisted approaches for the detection, environmental monitoring, fate and transport modeling, ecological risk assessment, and remediation of microplastic pollution in aquatic systems. Rather than systematically evaluating all published studies using predefined inclusion criteria, the review critically discusses recent developments, evaluates the current level of technological maturity, identifies key scientific and technological limitations, and highlights future research directions. Emphasis is placed on how AI complements conventional analytical techniques, predictive modeling, and remediation strategies to improve the understanding and management of microplastic pollution in aquatic environments. By combining knowledge from environmental science and data analytics, this study aims to highlight the potential of AI as a key enabler in the effective management of microplastic pollution in aquatic environments. This review study was carried out at Saveetha Institute of Medical and Technical Sciences, Chennai, Tamil Nadu, India, in 2026.

Role of AI in environmental monitoring of microplastics

AI has developed as a game-changing tool in environmental monitoring, offering advanced capabilities in data analysis, pattern recognition and predictive modeling. The complexity of environmental systems and the vast amount and diversity of data have made it clear that traditional analytical approaches based on deterministic models and manual interpretation are inadequate. AI, which uses ML and DL techniques, offers a data-driven framework that can help derive meaningful information from complex datasets to improve the efficiency and accuracy of environmental assessment (Coleman, 2025; Leong, 2025). ML algorithms, such as artificial neural networks (ANNs), random forests (RFs), and support vector machines (SVMs), have proven highly successful at modeling nonlinear relationships among environmental variables. In contrast, DL architectures, especially convolutional neural networks (CNNs), have proven extremely good at analyzing images and, in parallel, performing automated feature extraction. These capabilities have enabled real-time monitoring, improved prediction accuracy, and reduced reliance on labor-intensive analytical procedures (Popescu *et al.,* 2024; Camps-Valls *et al.,* 2025). AI's advantages in environmental monitoring include unique qualities. AI models can work with enormous amounts of multi-source data, including spatial, temporal and spectral data, to analyze complex processes in the environment. AI methods are particularly well-suited to estimate nonlinear interactions and the inherent uncertainties in environmental systems. AI continues to expand its opportunities for continuous monitoring and decision-making through data, along with other emerging technologies such as remote sensing, the Internet of Things (IoT) devices, and geospatial analysis tools (Huang *et al.,* 2025; Blessing and Olateru, 2025). These benefits are especially valuable for addressing water pollution from microplastics. The combination of hydrodynamic processes, physicochemical interactions and biological factors controls the behavior and distribution of microplastics, creating highly dynamic and spatially heterogeneous patterns. Traditional monitoring and modeling practices often fall short of adequately capturing such complexities due to

data constraints, limited analytical and predictive capacity, and insufficient resolution. In this respect, AI can serve as an effective tool for improving the detection, classification, and prediction of microplastics by leveraging large datasets and uncovering invisible patterns that may not have been identified by traditional approaches (Chaukura *et al.,* 2021; Yang *et al.,* 2025). Recent advancements have shown that AI can be automated to detect microplastics by analyzing images, matching them against datasets and environmental data to predict transport paths, and streamlining treatment processes to minimize pollution. Nevertheless, despite these encouraging trends, AI applications in studying microplastics remain at an initial stage, research remains disorganized, and there is a lack of connections between various dimensions of monitoring and management. Proper awareness of AI-based solutions is, consequently, key to exploiting their full potential to address microplastic pollution (Khanam *et al.,* 2025; Olawade *et al.,* 2026). Fig. 1 displays the hypothetical basis for applying AI to environmental monitoring of microplastics in water bodies. Recent studies have highlighted the usefulness of AI for identifying and characterizing microplastics in the water industry. For example, DL techniques have been used in synergy with spectroscopic techniques to improve polymer identification. Kedzierski *et al.* (2019) demonstrated the use of ML algorithms with Fourier transform infrared (FTIR) spectroscopy to achieve automated, high-accuracy classification of microplastics and reduce the error of manual interpretation. Srivastava *et al.* (2025) pointed to the combination of ML with surface-enhanced Raman spectroscopy (SERS) to address high-dimensional spectra, peak overlap and interference from complex environmental matrices. The study highlighted that ML-assisted SERS is a valuable addition to the detection and classification of environmental contaminants, including infectious pathogens and inorganic/organic pollutants, improving analytical sensitivity for more reliable field monitoring. In addition to spectroscopic analysis, the detection of microplastics in images has made huge strides thanks to DL techniques. In one study by Lorenzo-Navarro *et al.* (2021), they developed a CNN-based model for automatic identification of microplastics in microscopy images, achieving high precision and recall. Likewise, recent advancements in computer vision have led to the development of real-time detection systems, with object detection methods such as You Only Look Once (YOLO) adopted for rapid detection and tracking of microplastics in aquatic environments (Sarker *et al.,* 2024). These approaches support continuous monitoring and reduce reliance on labor-intensive manual analysis. Beyond detection, ML techniques have been used to analyze complex datasets related to microplastic pollution. Studies have shown that algorithms such as RF and ANN can model the distribution and transport of microplastics using a combination of hydrodynamic, physicochemical and spatial information (Kannankai *et al.,* 2022).

AI in microplastic detection and monitoring

Identifying and tracking microplastics in water systems is highly significant for understanding their distribution, origin, and potential environmental effects. Visual sorting, FTIR spectroscopy, and Raman spectroscopy are common methods for identifying microplastics. Nevertheless, they are usually lengthy, cumbersome and prone to human error, especially when analyzing large data sets with complex environmental contexts. Moreover, they are not automated, which limits scalability and necessitates sophisticated analytical software. AI, and in particular DL, has become a promising solution to overcome these limitations by enabling automated, accurate, high-throughput analysis of microplastic data. AI-based techniques are useful for handling large volumes of images and spectral data, detecting patterns and performing classifications with minimal human intervention. These capabilities have enabled significant

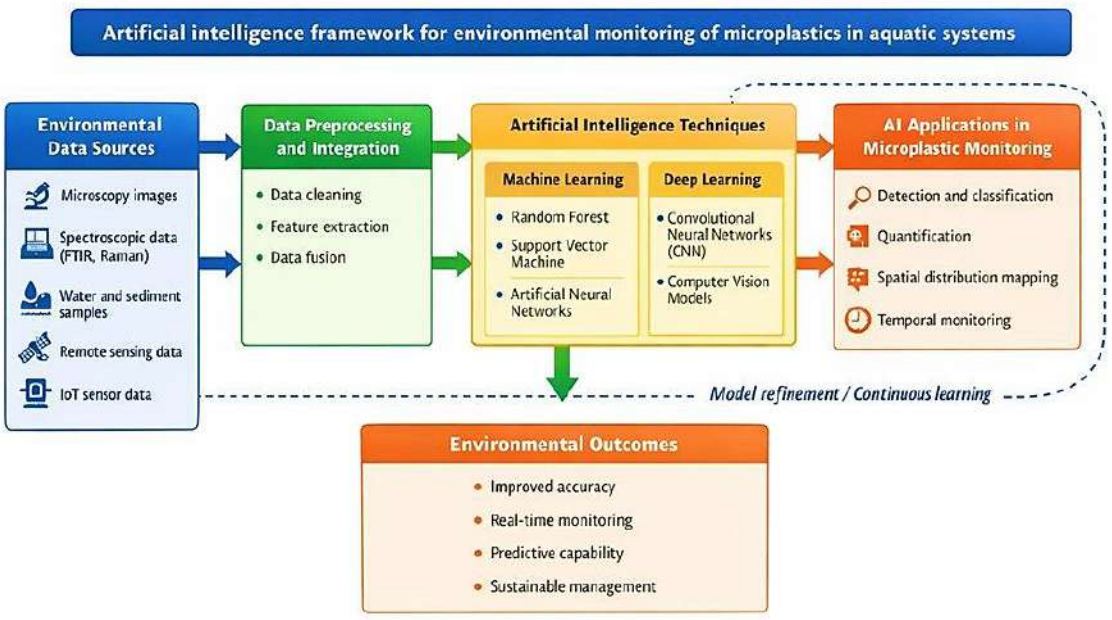

Fig. 1: Conceptual outline demonstrating the application of AI in the environmental monitoring of microplastics

progress in microplastic detection and monitoring through image-based analysis and the interpretation of spectroscopic data (Abimbola *et al.,* 2024; Ardini *et al.,* 2025).

Image analysis using AI for microplastics detection

Given the extensive use of microscopy techniques for environmental monitoring, image-based detection of microplastics has received considerable attention. CNNs and other DL models have achieved remarkable success in particle detection and classification from microplastic images. These models can extract features such as shape, size, and texture, which can be used to differentiate microplastics from natural particulates (Zhu *et al.,* 2021; Elawady *et al.,* 2025). Several studies have reported successful use of CNN architectures for microplastic detection. For instance, CNNs can achieve high precision and recall in recognizing fibrous and fragmented microplastics in microscopy images, thereby significantly reducing manual analysis. Further, transfer learning approaches using pre-trained models such as ResNet and EfficientNet have improved classification performance, especially with limited data. Despite these improvements, difficulties have been encountered in precisely identifying irregularly shaped particles and discriminating microplastics from organic materials with similar visual appearance (Thammasanya *et al.,* 2024; Villegas-Camacho *et al.,* 2025).

Progression of spectroscopic analysis with AI

Spectroscopic techniques (FTIR, Raman) are widely used for chemical characterization of microplastics. But analyzing spectral data can be complicated and labor-intensive, especially with large datasets. Over the years, AI-based approaches such as ML and DL models have been increasingly adopted to streamline the spectral signature classification process and enhance identification accuracy. Various ML algorithms, such as SVM, RF and ANN, have been used for polymer classification using spectral data. DL models are more efficient at detecting signals within spectral patterns, noise and even overlapping signals, particularly CNNs. These

approaches not only reduce analysis time but also minimize operator bias, yielding more consistent and reproducible results. However, the efficacy of AI models relies heavily on access to high-quality datasets for training, which remains a limitation in spectroscopic analysis (Sim *et al.,* 2024; Umurhan *et al.,* 2025; Villegas-Camacho *et al.,* 2025).

Monitoring and integrating data using AI-powered environmental monitoring

AI in relation to detection, is another key component of environmental data integration and analysis to build a full microplastic dataset. Aquatic systems produce massive amounts of heterogeneous information, including spatial, temporal and physicochemical data. These methods can be highly beneficial and efficient for processing such complex data, and AI can detect trends, patterns, and anomalies that might not be evident using traditional methods of analysis (Zhao *et al.,* 2024; Wang *et al.,* 2024). The AI and remote sensing technologies, which include geographical information systems (GIS) and sensors through the IoT, have facilitated tracking of the pollution of microplastics in real-time and at a very large scale. ML models can forecast microplastic concentrations using environmental parameters, and DL models can fully automate the analysis of visual and spectral data. These combined systems provide important insights into the distribution and dynamics of microplastics, supporting effective decision-making (Ibrahim *et al.,* 2025; Khan and Zaidi, 2025; Pan *et al.,* 2025). More recently, studies have demonstrated the effectiveness of AI and ML approaches in detecting and monitoring microplastics in aquatic environments. One major area of development is the application of DL algorithms to datasets of microscopic images for automatic particle identification. Wang *et al.* (2023) proposed the Faster Region-Based Convolutional Neural Network (Faster R-CNN) to detect microplastic particles in microscopy images automatically. The model represents a major advance in identification efficiency, reducing laborious manual sorting of particles and highlighting the potential of computer vision methods for large-scale environmental monitoring of microplastics. Another significant advancement is the integration of AI with spectroscopic methods, such as Raman and FTIR spectroscopy, for automated polymer identification. Ren *et al.* (2023) used micro-Raman spectroscopy with CNNs to categorize various types of microplastic polymers. Their model could produce classification rates exceeding 95 percent (%), indicating the performance of AI-driven spectral analysis methodologies in right-off-the-shelf classification of polymer structures even in environmentally complicated samples. Lim *et al.* (2024) designed a CNN-based method for analyzing Raman spectra to accelerate the detection of microplastics in the 1-10 micrometer (µm) range. The integration of DL and Raman spectral data processing has significantly reduced data collection time without compromising classification performance, resulting in a viable, high-throughput method for detecting microplastics in water. Other more recent studies have attempted to label multiple spectroscopic measurements using DL algorithms to improve identification accuracy further. Li *et al.* (2025) developed a high-order fusion model based on Raman and FTIR spectral data using DL algorithms, achieving over 98% identification accuracy of microplastics in different environmental media. This multi-sensor data fusion reveals the potential of AI to enhance reliability in complex environmental monitoring conditions. Beyond laboratory analysis, AI is also applied to develop real-time monitoring systems for microplastic pollution. Sarker *et al.* (2024) developed an AI-empowered camera sensor apparatus using computer vision to detect and monitor microplastic particles in water streams, including size and velocity parameters. Such practices imply that automated surveillance systems can systematically monitor environmental conditions related to microplastic pollution in water. Furthermore, technological advancements in the creation of low-cost

AI-driven detection platforms are taking shape to support rapid analysis in the domain. Arju *et al.* (2025) recently demonstrated a mobile phone-based microscopy system that incorporates DL algorithms and has the potential to achieve microplastic detection rates of nearly 98%. This method emphasizes the potential of portable, low-cost monitoring technologies to enable mass surveillance of microplastics in resource-scarce settings. Fig. 2 explains a monitoring system for microplastics in water systems via AI. Table 1 summarizes AI-based approaches for detecting, classifying, and monitoring microplastics in aquatic systems.

AI in modeling the fate and transport of microplastics in aquatic systems

The fate and transport of microplastics in aquatic systems involve complex interactions among hydrodynamic processes, physicochemical properties, and environmental conditions. Microplastic particles have a variety of characteristics such as size, density, shape and surface chemistry, which play a major role in their behavior in water bodies. These properties determine such important transport processes as advection, diffusion, sedimentation, resuspension and aggregation. In addition, environmental parameters such as flow velocity, turbulence, temperature, salinity and biological activity oversee the spatial and temporal variability of microplastic distribution. The dynamic nature of these processes poses major challenges for accurately predicting microplastic movement and accumulation using conventional modeling approaches (Du *et al.,* 2021; Jolaosho *et al.,* 2025).

Influencing factors of fate and transport

Microplastic transport depends on both intrinsic particle properties and external environmental conditions. Low-density polymers are likely to be suspended in water columns, and high-density particles are more likely to be in sediments. Particle shape, especially fibers and fragments, influences drag forces and settling velocities, resulting in differences in transport behavior. Surface properties, such as biofilm formation and chemical aging, further alter particle density and associated hydrophobicity, thereby affecting particle interactions with the surrounding media (Kumar *et al.,* 2021; Jiang *et al.,* 2025a). Environmental factors also play an important part in determining microplastic dynamics. Hydrodynamic parameters such as currents, waves and turbulence, as well as physicochemical parameters such as salinity and temperature, affect particle movement and dispersion, whereas physical parameters affect buoyancy and aggregation. Carrier transport pathways and the residence time of microplastics may be affected by biological interactions such as ingestion and biofouling. These interconnected processes result in highly complex, nonlinear systems, and it is not easy to predict microplastic behavior using traditional deterministic approaches (Kye *et al.,* 2023; Guo *et al.,* 2024).

Predictive modeling using AI

AI has emerged as a powerful tool for microplastic fate and transport modeling because it can analyze complex environmental systems in a data-driven manner. ML algorithms such as RF, SVM and ANN possess the potential to detect nonlinear correlations between multiple environmental variables. These models can be trained using historical data to predict microplastic concentrations, distributions and transport routes across different aquatic environments (Astorayme *et al.,* 2024; Cazzetta *et al.,* 2026). AI-based predictive models have been shown to perform better than traditional methods, especially when dealing with large and heterogeneous data. For instance, ML models have been adopted to estimate microplastic concentrations in riverine and coastal water bodies, incorporating hydrological, meteorological and physicochemical parameters. Similarly, temporal variations have been represented, and the transport of microplastics under dynamic environmental conditions has been predicted using DL models

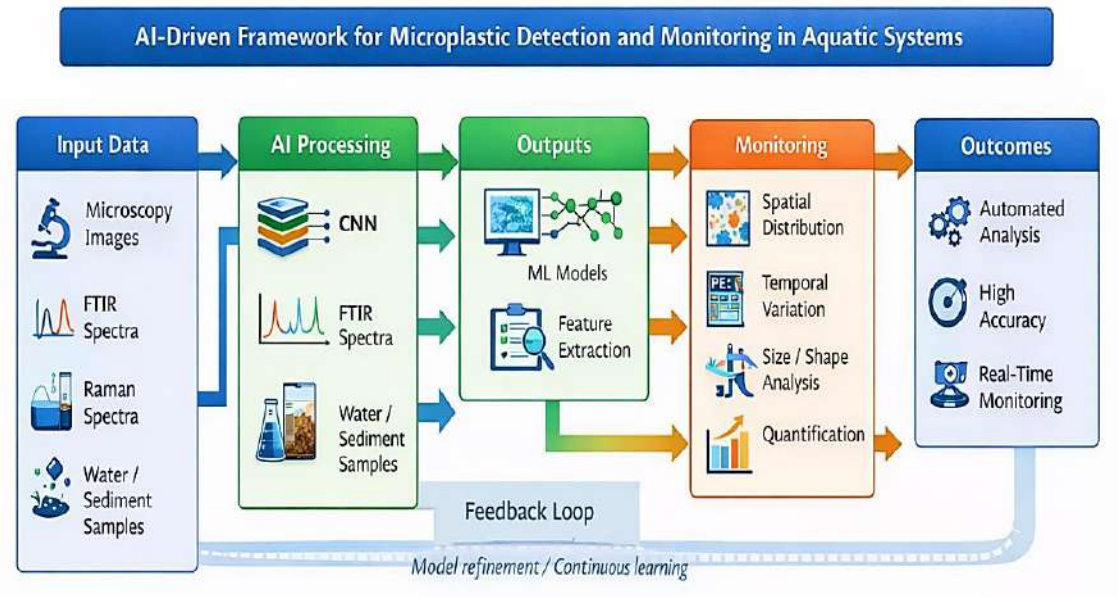

Fig. 2: AI-driven monitoring of microplastics in aquatic systems

Table 1: Summary of AI-based approaches for the detection, classification, and monitoring of microplastics in aquatic systems

AI Model	Data type	Application	Key findings	Sources
CNN	Microscopy images	Detection and classification	Achieved high precision in identifying microplastics, reducing manual analysis	Lorenzo-Navarro *et al.*, 2021
CNN	Raman spectroscopy	Polymer classification	>95% accuracy in microplastic identification	Jeon *et al.*, 2025
ML (SVM)	FTIR spectra	Polymer classification	Automated classification with reduced human bias	Yan *et al.*, 2022
YOLO(v5)	Image data	Real-time detection	Achieved ~96% detection accuracy	Sarker *et al.*, 2024
RF	Spectral data	Polymer identification	Improved classification compared to traditional methods	Valls-Conesa *et al.*, 2023
ANN	Environmental data	Distribution prediction	Accurate prediction of microplastic concentration patterns	Manchu *et al.*, 2024
CNN	FTIR imaging	Automated identification	High-throughput microplastic analysis	Li *et al.*, 2025
ML	FTIR data	Spectral classification	Enhanced spectral library matching	Rosales-Martínez *et al.*, 2025
ML-assisted analysis	Water samples	Monitoring	Improved detection efficiency	Hufnagl *et al.*, 2021
ML	Remote sensing	Marine debris detection	Large-scale monitoring capability	Perera *et al.*, 2025
CNN	Image data	Classification	Improved recognition of complex particle shapes	Wang *et al.*, 2023
CNN	Microscopy images	Microplastic classification	High accuracy with limited datasets	Zeng *et al.*, 2024
ML	FTIR data	Automated identification	Improved speed of analysis	Moses *et al.*, 2023
CNN	Raman spectra	Polymer classification	Accurate classification under noise	Lim *et al.*, 2024
DL	Image + spectral	Multi-modal analysis	Improved classification robustness	Barker *et al.*, 2025
CNN	Image data	Detection	Enhanced detection of irregular particles	Han *et al.*, 2024
RF	Environmental data	Prediction	Identified key influencing factors	Tran *et al.*, 2023
CNN	Image data	Automated detection	Reduced processing time significantly	Zhao *et al.*, 2024
Hybrid ML	Multi-source data	Monitoring	Improved predictive performance	Seggio *et al.*, 2023

such as recurrent neural networks (RNN) and long short-term memory (LSTM) networks. These approaches enable more precise, scalable predictions for improved environmental monitoring and management (Yu and Hu, 2022; Reshadi *et al.,* 2025).

Hybrid modeling approaches

The combination of AI techniques and traditional hydrodynamic models has been adopted to develop hybrid modeling frameworks for simulating microplastic transport. Conventional models, such as particle-tracking and computational fluid dynamics (CFD), are used to obtain physics-based insights into flow dynamics and particle motion. However, these models can be computationally expensive and may fail to account for complex interactions among multiple variables accurately (Ibna Hafiz *et al.,* 2025; Filo *et al.,* 2025). Hybrid models combine physics-based and data-driven techniques to improve prediction accuracy and efficiency. AI algorithms may be applied to calibrate model parameters, reducing uncertainties and better representing nonlinear processes. For instance, ML models can be integrated with hydrodynamic simulations to forecast transport pathways and accumulation areas in rivers, estuaries and coastal areas. These hybrid approaches provide richer frameworks for understanding the dynamics of microplastics in aquatic systems (Velazquez-Araque *et al.,* 2025).

Geospatial analysis and monitoring and research outputs

The addition of geospatial data and remote sensing technologies has significantly strengthened AI-based modeling. Geographic information systems (GIS) and ML algorithms help map the distribution of microplastics in space on a broad geographical scale. These methods provide a simple way to determine microplastic pollution hotspots and to investigate the spatial variability of microplastic concentrations (Manapragada *et al.,* 2025; Hochmair *et al.,* 2025). AI models can also be used to process data from remote sensing platforms, sensor networks, and monitoring programs to enable large-scale, real-time analysis of microplastics. The combination of spatial and temporal information enables us to create predictive models that can quantify the movement and accumulation of microplastics under different environmental conditions. Such capabilities are especially useful for assessing regions and global regions where sampling is often limited with traditional methods (Rawat *et al.,* 2025). Fig. 3 Projects the AI modules for modeling the fate and transport of microplastics in aquatic systems. Recent studies have demonstrated the potential of AI-based approaches for modeling the fate and transport of microplastics in water systems. ML models have been successfully used to predict microplastic concentrations in riverine environments by incorporating hydrological and physicochemical information, offering greater predictive ability than traditional statistical methods. An ANN has been applied to model transport pathways and the key environmental factors that affect the distribution of microplastics (Usman *et al.,* 2026). Hybrid approaches combining hydrodynamic simulations with ML have shown better performance for predicting particle transport and accumulation zones, especially in coastal and estuarine systems. Geospatial models of microplastic pollution using a combination of geographic information systems (GIS) and AI techniques have been applied to map microplastic pollution at larger scales, identify hotspots and track temporal trends (Kida *et al.,* 2024). Various recent studies have demonstrated the potential of ML models to predict microplastic abundance and transport dynamics in riverine and coastal environments. Gong *et al.* (2024) used several ML algorithms to model MP abundance in river waters across several coastal regions in China. Using datasets that included hydrological conditions, land use and anthropogenic factors, it was shown that there are strong relationships between environmental drivers and the distribution patterns of microplastics. The ML models with spatial variations in microplastic

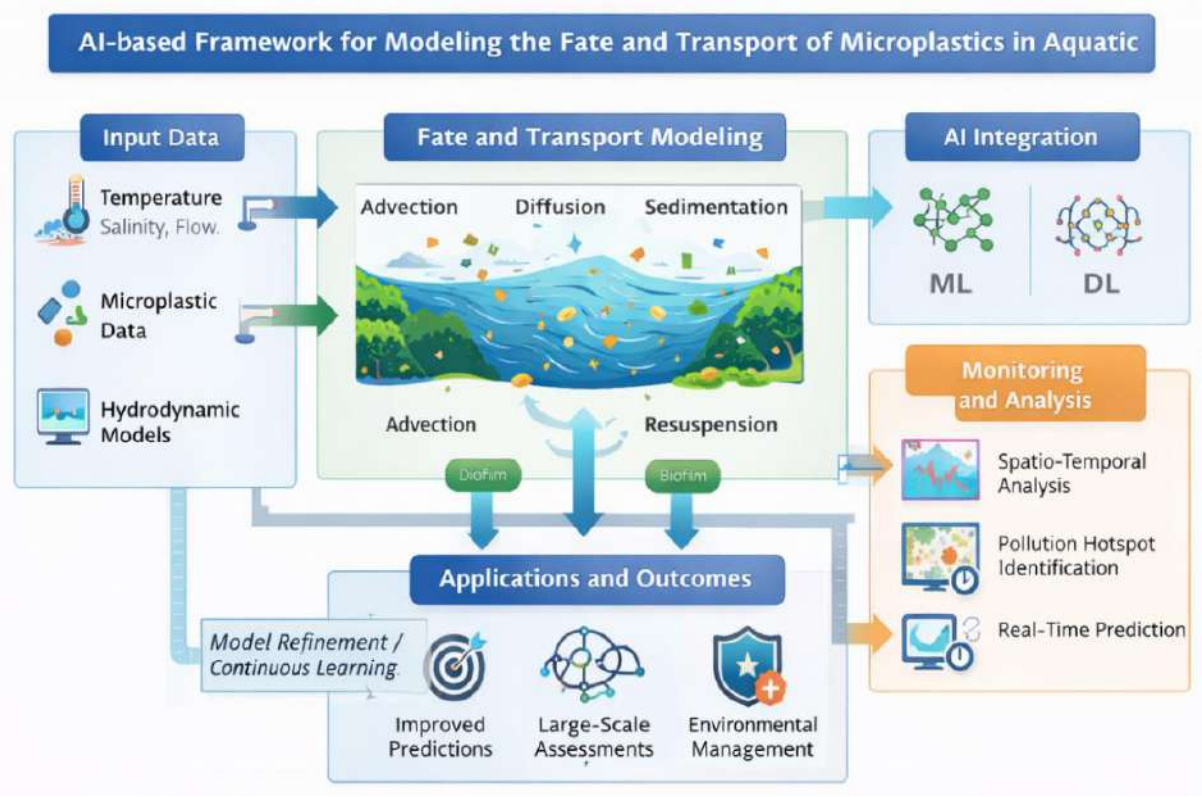

Fig. 3: AI elements for demonstrating the fate and transport of microplastics in aquatic systems

abundance were able to predict these patterns, suggesting the importance of environmental factors, such as population density, runoff dynamics and industrial activity, in regulating microplastic transport. These results demonstrate the potential of AI-based predictive frameworks to reduce the field sampling required and to provide credible estimates of microplastic distribution in complex aquatic systems. Priyanto *et al.* (2025) applied ML algorithms to predict microplastic amounts in river systems in Indonesian provinces using environmental and anthropogenic datasets. The analysis showed that tree-based algorithms were particularly suitable for predicting microplastic concentrations, with a coefficient of determination (R^2) of about 0.84. The model demonstrated the presence of controlling variables of interest. Table 2 lists a few AI-based models of microplastic fate and transport Fig. 4.

AI-based methods for risk assessment and ecotoxicological assessment of microplastics

The widespread occurrence of microplastics in aquatic environments has raised growing concerns regarding their ecological and human health impacts. Microplastics interact with both biotic and abiotic components of aquatic ecosystems, resulting in complex exposure pathways and multiple toxicological responses. They can be ingested by organisms across different trophic levels, causing physical damage, oxidative stress, inflammation, metabolic disruption, and impaired reproduction. In addition, microplastics serve as vectors for heavy metals, persistent organic pollutants, pharmaceuticals, and microbial pathogens, thereby increasing the bioavailability and transport of co-existing contaminants. Several physicochemical characteristics, including particle

Table 2: AI-based modeling of fate and transport of microplastics

AI model	Data type	Aquatic system	Application	Key findings	Sources
ML (Data-driven modeling)	Oceanographic data	Ocean	Transport pathways	Identified global microplastic accumulation zones	Tsiaras *et al.,* 2021
Numerical + ML	Marine data	Ocean	Distribution modeling	Highlighted complexity of microplastic transport	Pilechi *et al.,* 2022
Statistical modelling	Waste data	Coastal	Source estimation	Quantified plastic input into oceans	Wolf *et al.,* 2020
ML + hydrodynamic	Ocean current data	Ocean gyres	Transport prediction	Identified Great Pacific Garbage Patch	Olawade *et al.,* 2026
ANN	Environmental data	River	Concentration prediction	High prediction accuracy for microplastic levels	Fazil *et al.,* 2025
Statistical + modelling	Marine data	Ocean	Distribution analysis	Identified widespread ocean contamination	Aoki K and Furue, 2021
ML/statistical	River discharge data	Rivers	Source apportionment	Rivers as major plastic sources	Sá *et al.,* 2022
ML	Catchment data	River	Transport analysis	Identified key influencing parameters	Windsor *et al.,* 2019
Process-based + AI	Particle properties	Ocean	Vertical transport	Modeled sinking and rising behavior	Sugathapala *et al.*, 2025
Simulation + ML	Sediment data	Freshwater	Fate analysis	Sediment accumulation patterns	Portillo De Arbeloa and Marzadri, 2025
ML	Environmental data	River	Distribution prediction	Improved spatial predictions	Lee *et al.,* 2022
ANN	Water quality data	River	Pollution prediction	High model performance	Olbert *et al.,* 2025
Modeling + ML	Soil-water data	Freshwater	Transport pathways	Identified terrestrial-aquatic link	Rehm *et al.,* 2021
ML	Environmental datasets	Freshwater	Distribution modeling	Identified influencing factors	Hu *et al.,* 2025
Statistical + modeling	Marine surveys	Ocean	Distribution	Global mapping of plastics	Goddijn-Murphy *et al.,* 2025
Numerical + ML	Ocean data	Ocean	Transport simulation	Seasonal variability observed	Pilechi *et al.,* 2022
AI + modeling	Marine data	Ocean	Particle behavior	Modeled microplastic transport processes	Santana *et al.,* 2025
Modeling	Marine data	Ocean	Accumulation zones	Identified Mediterranean pollution	Tsiaras *et al.,* 2021
ML	River data	Global rivers	Source identification	Identified top polluting rivers	Pittroff *et al.,* 2024
Integrated modeling	Global datasets	Ocean	Future scenarios	Predicted plastic emissions	Yan *et al.*, 2024

size, shape, polymer composition, surface chemistry, and aging, influence their toxicity. Smaller particles, particularly nanoplastics, possess greater potential to penetrate biological membranes and accumulate within tissues. In contrast, irregularly shaped particles are more likely to cause mechanical injury and remain in organisms for longer. Furthermore, biofouling and interactions with other environmental contaminants modify particle behavior, transport, and exposure dynamics, making conventional ecological risk assessment increasingly challenging (Karak *et al.,* 2025; Yarahmadi *et al.,* 2024; Mahari *et al.,* 2025; Trivedi *et al.,* 2026).

AI in toxicity prediction

Artificial intelligence has emerged as a powerful tool for predicting microplastic toxicity by

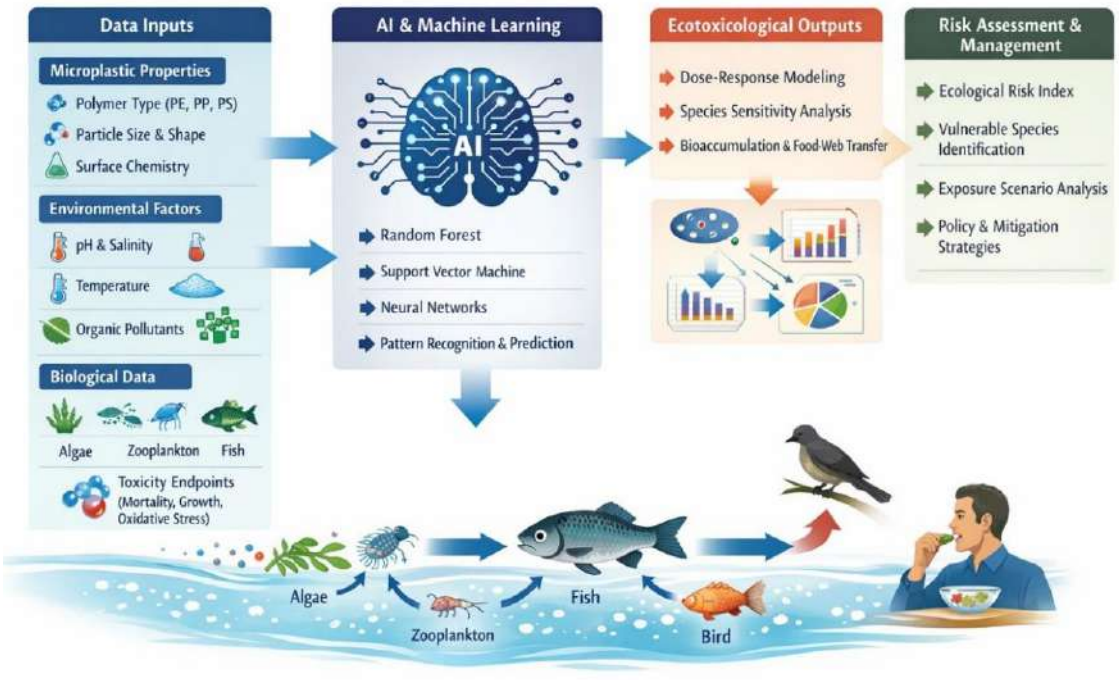

Fig. 4: Conceptual outline indicating the use of AI for microplastic induced ecotoxicological risk assessment

integrating physicochemical properties, environmental conditions, and biological response data. ML algorithms, including Random Forest (RF), Support Vector Machine (SVM), Artificial Neural Networks (ANN), and deep learning (DL), have been widely applied to identify complex nonlinear relationships between particle characteristics and toxicity endpoints such as mortality, growth inhibition, oxidative stress, and biochemical alterations (Astray et al., 2023; Tang, 2025). Deep learning approaches further improve predictive performance by analyzing large and heterogeneous datasets generated from high-throughput toxicity screening and experimental studies. These models facilitate the identification of the most influential variables governing toxicity, including particle size, polymer type, concentration, surface charge, and the presence of sorbed contaminants. Compared with conventional statistical approaches, AI models offer greater flexibility in capturing nonlinear interactions; however, their predictive performance remains highly dependent on the quality, diversity, and representativeness of the available training datasets (Elawady *et al.,* 2025; Jiang *et al.,* 2025b). Recent studies have also combined ML with quantitative structure–activity relationship (QSAR) modeling to predict the toxicity of microplastics and associated additives. Using curated toxicity databases such as ECOTOX, AI-assisted QSAR models provide a rapid screening tool for prioritizing potential hazards and may help reduce reliance on extensive animal testing by supporting early-stage toxicity assessment. However, AI-based predictions should be regarded as complementary to experimental ecotoxicological studies until broader external validation and regulatory acceptance are achieved. These approaches provide rapid screening for potential hazards and improve the efficiency of environmental risk assessment by identifying the key physicochemical properties

that control biological responses (Liu *et al.,* 2023). The interpretation of AI-based toxicity predictions should consider the biological and experimental context of the underlying datasets. Toxicity responses vary substantially with species, developmental stage, exposure duration, particle size, polymer composition, concentration metrics, particle aging or weathering, chemical additives, and the presence of co-contaminants. Consequently, the predictive performance and applicability of AI models depend not only on the modeling algorithm but also on the quality, representativeness, and standardization of the input data. Future studies should prioritize harmonized toxicity datasets and standardized reporting to improve the robustness and transferability of AI-assisted ecotoxicological assessments.

AI in ecological risk assessment

AI complements conventional ecological risk assessment by integrating environmental monitoring data, biological observations, and physicochemical information to improve exposure prediction and toxicity assessment of microplastics. Unlike conventional ecological indices and statistical analyses, AI models identify complex nonlinear relationships and support predictive modeling for ecological risk evaluation. ML models have been employed to predict exposure levels, estimate bioaccumulation potential, identify vulnerable species, and assess ecological risks across different aquatic ecosystems (Hu *et al.,* 2024; Hoang *et al.,* 2025). In addition, probabilistic AI models can incorporate uncertainty within environmental datasets, enabling scenario analysis under varying pollution conditions and improving decision-making for environmental management (Wardani *et al.,* 2024; El-Sokkary *et al.,* 2026). Beyond toxicity prediction, AI has increasingly been applied to model trophic transfer and bioaccumulation in aquatic food webs. Data-driven ecological models integrating field observations, species traits, and environmental variables have been used to estimate exposure probabilities and accumulation potential across multiple trophic levels, from plankton and benthic invertebrates to fish species. ML techniques, including gradient boosting and neural networks, have demonstrated that particle characteristics, feeding behavior, habitat conditions, and environmental variables strongly influence trophic transfer. Integrating heterogeneous ecological datasets through AI provides a more comprehensive understanding of long-term ecosystem impacts and supports the development of next-generation ecological risk assessment frameworks for emerging contaminants such as microplastics (Jiang *et al.,* 2025c; Zhang *et al.,* 2025; Jachimowicz *et al.,* 2025; Yang *et al.,* 2026). Overall, AI-based approaches have demonstrated considerable potential to improve the prediction of microplastic toxicity and ecological risk by integrating diverse environmental, physicochemical, and biological datasets and by identifying complex nonlinear relationships among exposure variables. These approaches can complement conventional ecotoxicological assessments by supporting toxicity prediction, exposure modeling, and scenario analysis. However, the predictive performance and reliability of AI models remain strongly dependent on the quality, diversity, and representativeness of the underlying datasets. Most published models have been developed using a limited range of polymer types, test organisms, toxicity endpoints, and controlled laboratory exposure conditions, which may not adequately capture the complexity and spatial-temporal variability of natural aquatic ecosystems. Consequently, AI model predictions should be interpreted within the training data's applicability domain, and caution should be exercised. Fig. 4 conceptualizes the potential application and integration of AI for microplastic ecotoxicological risk assessment.

AI in microplastic remediation and treatment technologies

The growing presence of microplastics in aquatic habitats has highlighted the need for effective remediation and treatment methods. Conventional methods of microplastic removal include physical, chemical and biological processes, such as filtration, coagulation-flocculation, sedimentation, adsorption and membrane separation. While these techniques have shown different levels of efficiency, they tend to be limited by factors such as incomplete removal, high operation costs, energy use, and difficulties in dealing with different forms of microplastics. The variation in particle size, shape, and composition further complicates the design and optimization of treatment systems (Amparán *et al.,* 2025; Dayal *et al.,* 2024; Bodzek *et al.,* 2024). AI-assisted remediation technologies target different treatment objectives, including the physical removal, capture, retention, transfer, or degradation of microplastics. These outcomes should not be regarded as environmentally equivalent. Physical separation processes such as membrane filtration, coagulation–flocculation, sedimentation, and adsorption primarily remove or transfer microplastics from the aqueous phase to concentrated residual streams (e.g., sludge or spent adsorbents), requiring appropriate downstream management. In contrast, advanced oxidation and photocatalytic processes aim to chemically degrade polymer structures, although complete mineralization is rarely achieved under practical conditions. Consequently, AI-based optimization strategies should be interpreted in light of the specific treatment objective and the environmental fate of the resulting products, rather than solely on apparent removal efficiency.

AI in process optimization

AI has been utilized as a potent solution to streamline microplastic remediation procedures, leveraging a data-driven decision-making approach and real-time control. ML models can predict treatment efficiency based on pH, coagulant dosage, temperature, and flow rate. Algorithms, including ANN, RF, and support vector machines, have been utilized to predict operating conditions to achieve higher removal efficiencies and reduce energy usage and operational costs. The key parameters affecting treatment performance can also be calculated using AI-based optimization models, enabling system design optimization. In fact, ML strategies have been implemented to optimize adsorption processes by predicting interactions between microplastics and adsorbent materials. In these models, the number of experimental steps can be greatly reduced, enabling the design of better treatment variations (Lowe *et al.,* 2022; Cairone *et al.,* 2024; Valle-Bravo *et al.,* 2026). Although many AI-assisted optimization strategies have been developed for conventional wastewater treatment processes, direct applications specifically targeting microplastic removal remain comparatively limited. Nevertheless, these approaches provide a useful framework for improving operational conditions that may enhance microplastic capture and separation efficiency.

AI-powered treatment solutions

The combination of AI and the latest treatment technologies has led to the development of intelligent systems for removing microplastics. AI-assisted membrane systems can track fouling behavior and make on-the-fly changes to operational parameters to ensure optimal performance. Similarly, AI models can be used in conjunction with adsorption and filtration systems to predict removal efficiency and optimize system design. Emerging approaches combining AI, nanomaterials and advanced oxidation processes have also shown potential to improve the degradation and removal of microplastics. Using

AI models, it is possible to design and optimize nanomaterial-based adsorbents that can be even more selective and efficient. In addition, AI-enabled analysis of treatment processes can help identify the right conditions for microplastic degradation (Xu and Liu, 2025; Agaton, 2025).

Smart and autonomous remediation systems

AI and IoT technologies, combined, have enabled the development of intelligent, autonomous remediation systems. To verify the concepts of the AI models, sensor arrays will be used to continuously monitor water quality parameters and the level of microplastics and report in real time. These systems can automatically adjust treatment conditions in response to changing environmental conditions to achieve optimal performance. Autonomous environmental monitoring and remediation can also be conducted at large scale using systems that run AI algorithms. For instance, AI can be used to detect polluted areas via platforms and prioritize them for cleaning. These systems can provide the prospect of dramatically improving the effectiveness of microplastics management (Essamlali *et al.,* 2024; Govindarajan *et al.,* 2025). Table 3 lists AI-based approaches for microplastic remediation. Fig. 5 Shows conceptual microplastic removal with AI assistance (Valdiviezo-Gonzales *et al.,* 2026). Current AI-assisted remediation technologies can be broadly categorized into i) conceptual frameworks proposed for future implementation, ii) laboratory-scale proof-of-concept systems, iii) pilot-scale demonstrations, and iv) emerging applications integrated into conventional wastewater treatment processes. However, reports of fully autonomous, full-scale microplastic remediation systems remain scarce. Overall, AI has emerged as a valuable tool for enhancing the efficiency, automation, and optimization of microplastic remediation technologies. By integrating predictive modeling, intelligent process control, and real-time monitoring, AI can support the development of adaptive and energy-efficient treatment systems. Although many applications remain at the laboratory or pilot scale, continued advances in ML, sensor technologies, and process automation are expected to facilitate the practical implementation of AI-assisted remediation strategies for sustainable microplastic management. Evidence from AI-assisted processes in wastewater treatment suggests potential applicability to microplastic removal; however, direct studies focusing specifically on microplastic adsorption remain scarce. An important consideration in AI-assisted microplastic remediation is the subsequent fate of particles retained during treatment. Many physical separation technologies, including membrane filtration, coagulation–flocculation, adsorption, and granular filtration, do not destroy microplastics but instead transfer them to residual streams such as sludge, spent adsorbents, filter media, membrane concentrates, or backwash water. Consequently, the environmental effectiveness of these technologies depends not only on their removal efficiency but also on the safe handling, treatment, disposal, or potential recovery of these residual materials to prevent secondary environmental release. Future AI-based optimization frameworks should therefore incorporate residual management strategies alongside treatment performance to support more sustainable microplastic remediation.

CONCLUSION

Microplastic pollution continues to pose a significant threat to freshwater and marine ecosystems, creating an urgent need for efficient approaches to its detection, monitoring, prediction, and mitigation. This review demonstrates that AI, ML, and DL are increasingly contributing to microplastic research by

Table 3: AI-based approaches for microplastic remediation

Remediation technology	Role of AI	Optimised parameters	Current limitations
Coagulation–flocculation	Process optimisation	Coagulant dose, pH	Limited real-world validation
Membrane filtration	Fouling prediction and process control	Flux, TMP, cleaning cycles	Small datasets
Adsorption	Prediction of adsorption efficiency	Adsorbent dosage, contact time	Material-specific models
Photocatalysis	Catalyst/process optimization	Catalyst loading, irradiation time	Mostly laboratory studies
Advanced oxidation	Process optimisation	Oxidant dosage, reaction time	Limited AI applications
Smart treatment systems	Real-time monitoring and control	Sensor integration, operational parameters	Pilot-scale implementation

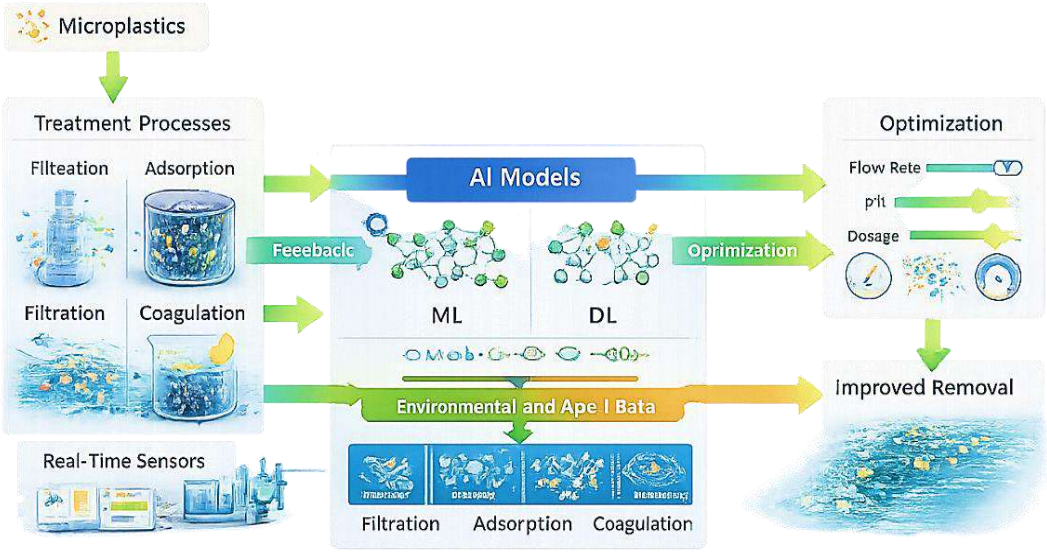

Fig. 5: AI-assisted microplastics remediation

enhancing data analysis, improving predictive capabilities, and supporting more efficient environmental monitoring and decision-making. Among the current applications, AI-assisted image analysis, automated microscopy, and spectroscopic classification represent the most mature and widely validated technologies, providing substantial improvements in the speed and accuracy of microplastic identification. AI has also shown considerable promise in modeling the environmental fate and transport of microplastics and supporting ecotoxicological risk assessment. However, the reliability of these applications remains dependent on the quality and representativeness of the available datasets. By comparison, several emerging applications, including AI-assisted remediation, digital twins, autonomous treatment systems, and large-scale toxicity prediction, are still at an early stage of development. Much of the current evidence for these applications is derived from laboratory investigations, pilot-scale studies, or AI-assisted optimization of conventional wastewater treatment processes rather than direct modeling of microplastic removal under real-world operating conditions. Consequently, these technologies should be regarded as promising research directions rather than fully established

environmental management tools. Similarly, while AI-assisted optimization may improve treatment efficiency under specific conditions, quantitative evidence demonstrating consistent reductions in operational costs and energy consumption for microplastic-specific treatment systems remains limited. Despite the rapid progress achieved in recent years, several important challenges continue to limit the broader implementation of AI in microplastic research. Many published models have been developed using relatively small, geographically restricted, and heterogeneous datasets, limiting their generalizability across different aquatic environments. Furthermore, inconsistent sampling protocols, analytical methodologies, reporting metrics, and benchmark datasets hinder model comparison and independent validation. Additional challenges include limited model interpretability, insufficient external validation, restricted transferability across environmental conditions, and the scarcity of field-scale deployment studies. Addressing these issues will require greater standardization of analytical workflows, development of high-quality open-access datasets, rigorous external validation, and closer collaboration among environmental scientists, engineers, data scientists, and regulatory agencies.

AUTHOR CONTRIBUTIONS

M. Kamaraj wrote the original draft and conceptualized the paper. H.A. Bhavithra helped with visualization, validation, writing, review and editing. B. Rajalakshmi collected literature, created the figures and helped in writing and editing. J. Aravind, as the corresponding author, supervised the work and wrote the original draft and conceptualized the paper.

ACKNOWLEDGEMENT

Authors are thankful for the support and facilities provided by SRM Group of Educational Institutions, Ramapuram, Chennai, Tamil Nadu, India, and Saveetha Institute of Medical and Technical Sciences, Chennai, Tamil Nadu, India.

CONFLICT OF INTEREST

The authors declare no potential conflict of interest regarding the publication of this work. In addition, the ethical issues, including plagiarism, informed consent, misconduct, data fabrication and/or falsification, double publication and/or submission, and redundancy, have been completely witnessed by the authors.

OPEN ACCESS

©2027 The author(s). This article is licensed under a Creative Commons Attribution 4.0 International License, which permits use, sharing, adaptation, distribution and reproduction in any medium or format, as long as you give appropriate credit to the original author(s) and the source, provide a link to the Creative Commons license, and indicate if changes were made. The images or other third-party material in this article are included in the article's Creative Commons license, unless indicated otherwise in a credit line to the material. If material is not included in the article's Creative Commons license and your intended use is not permitted by statutory regulation or exceeds the permitted use, you will need to obtain permission directly from the copyright holder. To view a copy of this license, visit: http://creativecommons.org/licenses/by/4.0/

PUBLISHER'S NOTE

GJESM Publisher remains neutral regarding jurisdictional claims in published maps and institutional affiliations.

NEGATIVE AI STATEMENT

The author(s) declared that no AI tools or services were used or highly applied during the preparation of this work.

ABBREVIATIONS

%	Percent
µm	Micrometers
AI	Artificial intelligence
ANN	Artificial neural network
CFD	Computational fluid dynamics
CNN	Convolutional neural network
DL	Deep learning
Faster R-CNN	Faster region-based convolutional neural network
FTIR	Fourier transform infrared
GIS	Geographic information system
IoT	Internet of things
LSTM	Long short-term memory
ML	Machine learning
R^2	Coefficient of determination
RF	Random forest
RNN	Recurrent neural network
SDGs	Sustainable development goals
SERS	Surface-enhanced raman spectroscopy
SVM	Support vector machine
YOLO	You only look once

REFERENCES

Abimbola, I.; McAfee, M.; Creedon, L.; Gharbia, S., (2024). In-situ detection of microplastics in the aquatic environment: A systematic literature review. Sci. Total Environ. 934: 173111 **(18 pages)**.

Agaton, C.B., (2025). Nature-Based Solutions for Removal of Microplastics from Wastewater: Technologies, Challenges, and Prospects. Microplastics. 4(4): 107 **(23 pages)**.

Amparán, M.A.A.; Palacios, A.; Flores, G.M.; Olivera, P.M.C., (2025). Review and future outlook for the removal of microplastics by physical, biological and chemical methods in water bodies and wastewaters. Environ. Monitor. Assess., 197(4):429 **(35 pages)**.

Anyanwu, C.; Agunwamba, J.C.; Tiza, M., (2026). Artificial intelligence in removal of emerging contaminants: A sustainable approach for environmental cleanup and circular economy. In Applications of artificial intelligence in removal of emerging contaminants. Elsevier. 77–108 **(32 pages)**.

Aoki, K.; Furue, R., (2021). A model for the size distribution of marine microplastics: A statistical mechanics approach. PLOS One. 16(11): e0259781 **(19 pages)**.

Ardini, B.; Pittura, L.; Frontini, A.; Benedetti, M.; Gorbi, S.; Regoli, F.; Cerullo, G.; Valentini, G.; Manzoni, C., (2025). Fast detection and classification of microplastics by a wide-field fourier transform Raman microscope. Environ. Sci. Technol., 59(18): 9255–9264 **(10 pages)**.

Arju, B.Z.M.Z.; Hridi, N.A.; Dewan, L.; Suhaila; Amin, M.N.; Rashid, T.; Azad, A.K.; Rahman, S.; Hossain, M.; Habib, A., (2025). Deep-learning enabled rapid and low-cost detection of microplastics in consumer products following on-site extraction and image processing. RSC Adv., 15(14): 10473–10483 **(11 pages)**.

Ashrafy, A.; Liza, A.A.; Islam, M.N.; Billah, M.M.; Arafat, S.T.; Rahman, M.M.; Rahman, S.M., (2023). Microplastics pollution: A brief review of its source and abundance in different aquatic ecosystems. J. Hazard. Mater. Adv., 9: 100215 **(12 pages)**.

Astorayme, M.A.; Vázquez-Rowe, I.; Kahhat, R., (2024). The use of artificial intelligence algorithms to detect macroplastics in aquatic environments: A critical review. Sci. Total Environ., 945: 173843 **(19 pages)**.

Astray, G.; Soria-Lopez, A.; Barreiro, E.; Mejuto, J.C.; Cid-Samamed, A., (2023). Machine learning to predict the adsorption capacity of microplastics. Nanomaterials. 13(6): 1061 **(17 pages)**.

Barker, M.; Singha, T.; Willans, M.; Hackett, M.; Pham, D.-S., (2025). A domain-adaptive deep learning approach for microplastic classification. Microplastics. 4(4):69 **(22 pages)**.

Blessing, A.-A.; Olateru, K., (2025). AI-driven optimization of bioremediation strategies for river pollution: A comprehensive review and future directions. Front. Microbiol., 16: 1504254 **(8 pages)**.

Bodzek, M.; Pohl, A.; Rosik-Dulewska, C., (2024). Microplastics in wastewater treatment plants: Characteristics, occurrence and removal technologies. Water. 16(24): 3574 **(21 pages)**.

Cairone, S.; Hasan, S.W.; Choo, K.-H.; Li, C.-W.; Zorpas, A.A.; Ksib, M.; Zarra, T.; Belgiorno, V.; Naddeo, V., (2024). Enhancing membrane fouling control in wastewater treatment processes through artificial intelligence modeling: Research progress and future perspectives. Euro-Mediterr. J. Environ. Integr., 9(4): 1887–1905 **(9 pages)**.

Camps-Valls, G.; Fernández-Torres, M.-Á.; Cohrs, K.-H.; Höhl, A.; Castelletti, A.; Pacal, A.; Robin, C.; Martinuzzi, F.; Papoutsis, I.; Prapas, I.; Pérez-Aracil, J.; Weigel, K.; Gonzalez-Calabuig, M.; Reichstein, M.; Rabel, M.; Giuliani, M.; Mahecha, M. D.; Popescu, O.-I.; Pellicer-Valero, O. J.; Ouala, S.; Salcedo-Sanz, S.; Sippel, S.; Kondylatos, S,; Happé, T.; Williams, T., (2025). Artificial intelligence for modeling and understanding extreme weather and climate events. Nat. Commun., 16(1): 1919 **(14 pages)**.

Cazzetta, A.; Zangaro, F.; Marcucci, F.; Julius, O.T.; Rainò, M.; Shauer, M.; Massaro, R.; Semeraro, T.; Basset, A.; Pinna, M., (2026). Applying Artificial Intelligence (AI) Innovative Tools for Ecological Research and Monitoring of Transitional Water Ecosystems: A Systematic Review. Environments. 13(4): 193 **(71 pages)**.

Chaukura, N.; Kefeni, K.K.; Chikurunhe, I.; Nyambiya, I.; Gwenzi, W.; Moyo, W.; Nkambule, T.T.I.; Mamba, B.B.; Abulude, F.O., (2021). Microplastics in the aquatic environment—The occurrence, sources, ecological impacts, fate, and remediation challenges. Pollutants. 1(2): 95–118 **(24 pages)**.

Coleman, B.R., (2025). An introduction to machine learning tools for the analysis of microplastics in complex matrices. Environ. Sci. Process. Impacts. 27(1): 10–23 **(14 pages)**.

Dayal, L.; Yadav, K.; Dey, U.; Das, K.; Kumari, P.; Raj, D.; Mandal, R.R., (2024). Recent advancement in microplastic removal process from wastewater-a critical review. J. Hazard. Mater. Adv., 16: 100460 **(15 pages)**.

Du, S.; Zhu, R.; Cai, Y.; Xu, N.; Yap, P.-S.; Zhang, Y.; He, Y.; Zhang, Y., (2021). Environmental fate and impacts of microplastics in aquatic ecosystems: A review. RSC Adv., 11(26): 15762–15784 **(23 pages)**.

Elawady, A.; Mohammed, J. A.; bin Abid, M., (2025). Advancements in microplastics detection techniques and their multidimensional impacts on aquatic ecosystems and human health. Journal of Hazardous Materials: Plastics. 2: 100025 **(23 pages)**.

El-Sokkary, N.; Arafa, A.A.; Zahran, E. G.; Hefny, H. A.; Ramdan, N., (2026). Recent trends of machine learning techniques for risk assessment in hazardous environments. Artif. Intell. Rev., 59(3): 108 **(60 pages)**.

Essamlali, I.; Nhaila, H.; El Khaili, M. (2024). Advances in machine learning and IoT for water quality monitoring: A comprehensive review. Heliyon. 10(6): e27920 **(28 pages)**.

Etin-Osa, D.; Isitua, C.C., (2025). Artificial intelligence/machine learning techniques in the management of environmental issues. In: Integrated biotechnological solutions for the treatment of industrial wastewater: 487–525. Elsevier **(39 pages)**.

Fazil, A.Z.; Dhawala Wijeratna, D.D.S.; Gomes, P.I.A., (2025). Predicting microplastic transport in open channels with different bed types and river regulation with machine learning techniques. Environ. Pollut., 384: 126912 **(11 pages)**.

Filo, G.; Lempa, P.; Wisowski, K., (2025). Review of deterministic and AI-based methods for fluid motion modelling and sloshing analysis. Energies. 18(5): 1263 **(21 pages)**.

Goddijn-Murphy, L.; Woolf, D.; James, N.A., (2025). Patterns and trends in marine microplastics density distributions using a long-term, global, field database. Mar. Pollut Bull., 212: 117528 **(11 pages)**.

Gong, X.; Hu, J.; Situ, Z.; Zhou, Q.; Zhao, Z., (2024). Exploring action-law of microplastic abundance variation in river waters at coastal regions of China based on machine learning prediction. Sci. Total Environ., 955: 176965 **(14 pages)**.

Govindarajan, P., Shahapuram, V. K., Ganesh, P. S., Basavalingappa, V. M., Balarama, K. Y., Sarangi, K. P., Cheong, J.Y.; Padil, V.V.T., (2025). Tracking microplastic pathways: Real-time IoT monitoring for water quality and public health. MethodsX. 15: 103674 **(15 pages)**.

Guo, M.; Noori, R.; Abolfathi, S., (2024). Microplastics in freshwater systems: Dynamic behaviour and transport processes. Resour. Conserv. Recycl., 205: 107578 **(21 pages)**.

Han, K.; Huang, M.; Wang, Z.; Shi, C.; Wang, Z.; Guo, J.; Liu, W.; Lei, L.; Guo, Q., (2024). Innovative methods for microplastic characterization and detection: Deep learning supported by photoacoustic imaging and automated pre-processing data. J. Environ. Manag., 359: 120954 **(11 pages)**.

Hoang, H.G.; Nguyen, N.S.H.; Zhang, T.; Tran, H.-T.; Mukherjee, S.; Naidu, R., (2025). A review of microplastic pollution and human health risk assessment: Current knowledge and future outlook. Front. Environ. Sci., 13: 1606332 **(17 pages)**.

Hochmair, H. H.; Juhász, L.; Li, H., (2025). Advancing AI-driven geospatial analysis and data generation: Methods, applications and future directions. ISPRS Int. J. Geo-Inf., 14(2): 56 **(8 pages)**.

Hu, B.; Dai, Y.; Zhou, H.; Sun, Y.; Yu, H.; Dai, Y.; Wang, M.; Ergu, D.; Zhou, P. (2024). Using artificial intelligence to rapidly identify microplastics pollution and predict microplastics environmental behaviors. J, Haz. Mat., 474: 134865 **(17 pages)**.

Hu, J.; Li, C.; Deng, L.; Yan, Z.; Gong, X., (2025). Spatial distribution, key influencing factors, and ecological risk of microplastics in Pearl River estuary water and sediments. Water. 17(17): 2572 **(18 pages)**.

Huang, L.; Duan, Q.; Liu, Y.; Wu, Y.; Li, Z.; Guo, Z.; Liu, M.; Lu, X.; Wang, P.; Liu, F.; Ren, F.; Li, C.; Wang, J.; Huang, Y.; Yan, B.; Kioumourtzoglou, M.-A.; Kinney, P.L., (2025). Artificial intelligence: A key fulcrum for addressing complex environmental health issues. Environ. Int., 198: 109389 **(19 pages)**.

Hufnagl, B.; Stibi, M.; Martirosyan, H.; Wilczek, U.; Möller, J.N.; Löder, M.G.J.; Laforsch, C.; Lohninger, H., (2021). Computer-assisted analysis of microplastics in environmental samples based on FTIR imaging in combination with machine learning. Environ. Sci. Technol. Let., 9(1): 90–95 **(6 pages)**.

Ibna Hafiz, A.M.; Ahmadisharaf, E.; Salehi, M.; Farner, J.; White, J. C.; Zeng, E. Y.; Nazari, B., (2025). A review of processes and models for the export of microplastics from terrestrial to aquatic systems. WIREs Water. 12(1): 70004 (**35 pages**).

Ibrahim, N.; Rahman, A.M.N.A.A.; Shafiq, M. D.; Lockman, Z.; Jaafar, M.; Kameda, Y., (2025). Microplastic pollution: Sources, degradation mechanisms, analytical advances, and mitigation strategies for environmental sustainability. Rev. Environ. Contam. Toxicol., 263(1): 27 **(42 pages)**.

Jachimowicz, P.; Babkiewicz, E.; Gavlova, A.; Lang, J.; Mądzielewska, W.I.; Maszczyk, P.; Mierzyńska K.; Zieliński, P., (2025). Global microplastic contamination in freshwater lakes: Spatial patterns, environmental drivers, and methodological challenges. Environ. Res., 291: 123585 **(19 pages)**.

Jeon, J.W.; Choi, J.W.; Shin, Y.; Kang, T.; Chung, B.G., (2025). Machine learning-integrated droplet microfluidic system for accurate quantification and classification of microplastics. Water Res., 274: 123161 **(11 pages)**.

Jeyachandran, S.; Vibhute, P.; Dahms, H.-U.; Mudigonda, S.; Manavalan, A.; Heese, K., (2026). Microplastic pollution in aquaculture: Challenges and mitigation. Water Environ. J., 40(1): 3–20 **(18 pages)**.

Jiang, Y.; Zhang, F.; Xia, S.; Chen, J.; Yue, L.; Xu, X.; Dong, W.; Pan, Y.; Fan, W.; Qu, M.; Chen, Y., (2025a). Evaluating microplastics and antibiotics induced genotoxicity in marine mussels through deep learning-based processing images of comet assay. Ecotoxicol. Environ. Saf., 305: 119295 (10 pages).

Jiang, H.; Li, Z.; Zhu, L.; Zhou, J.; Huang, Y.; Sun, D., (2025b). Comprehensive review of the co-transport of microplastics and suspended sediments in aquatic environments: Macroscopic transport and microscopic mechanisms. Environ. Sci. Eur., 37(1): 210 **(19 pages)**.

Jiang, H.-H.; Che, T.-H.; Su, Q.; Jin, B.; Lu, Y.; Zhou, H.-X.; Fu, M.-J.; Zhou, J.-Y., (2025c). Machine learning-enhanced meta-analysis unravels the global patterns of microplastic-heavy metal co-toxicity in terrestrial ecosystems. Environ. Pollut., 386: 127273 **(13 pages)**.

Jolaosho, T.L.; Rasaq, M.F.; Omotoye, E.V.; Araomo, O.V.; Adekoya, O.S.; Abolaji, O.Y.; Hungbo, J.J., (2025). Microplastics in freshwater and marine ecosystems: Occurrence, characterization, sources, distribution dynamics, fate, transport processes, potential mitigation strategies, and policy interventions. Ecotoxicol. Environ. Saf., 294: 118036 **(36 pages)**.

Kannankai, M.P.; Babu, A.J.; Radhakrishnan, A.; Alex, R.K.; Borah, A.; Devipriya, S.P., (2022). Machine learning aided meta-analysis of microplastic polymer composition in global marine environment. J. Haz. Mat., 440: 129801 **(8 pages)**.

Karak, P.; Parveen, A.; Modak, A.; Adhikari, A.; Chakrabortty, S., (2025). Microplastic pollution: A global environmental crisis impacting marine life, human health, and potential innovative sustainable solutions. Int. J. Environ. Res. Public Health. 22(6): 889 **(22 pages)**.

Kedzierski, M.; Falcou-Préfol, M.; Kerros, M.E.; Henry, M.; Pedrotti, M.L.; Bruzaud, S., (2019). A machine learning algorithm for high throughput identification of FTIR spectra: Application on microplastics collected in the Mediterranean Sea. Chemosphere. 234: 242–251 **(10 pages)**.

Khan, A.L; Zaidi, A.A., (2025). Separation and detection of microplastics in human exposure pathways: Challenges, analytical techniques, and emerging solutions. J. Xenobiot., 15(5): 154 **(30 pages)**.

Khanam, M.M.; Uddin, M.K.; Kazi, J.U., (2025). Advances in machine learning for the detection and characterization of microplastics in the environment. Front. Environ. Sci., 13: 1573579 **(15 pages)**.

Kida, M.; Pochwat, K.; Ziembowicz, S., (2024). Assessment of machine learning-based methods predictive suitability for migration pollutants from microplastics degradation. J. Haz. Mat., 461: 132565 **(12 pages)**.

Kumar, R.; Sharma, P.; Verma, A.; Jha, P.K.; Singh, P.; Gupta, P.K.; Chandra, R.; Prasad, P.V.V., (2021). Effect of physical characteristics and hydrodynamic conditions on transport and deposition of microplastics in riverine ecosystem. Water. 13(19): 2710 **(20 pages)**.

Kye, H.; Kim, J.; Ju, S.; Lee, J.; Lim, C.; Yoon, Y., (2023). Microplastics in water systems: A review of their impacts on the environment and their potential hazards. Heliyon. 9(3): e14359 **(31 pages)**.

Lee, H.W., Kim, M.; Son, H.W.; Min, B.; Choi, J.H., (2022). Machine-learning-based water quality management of river with serial impoundments in the Republic of Korea. Journal of Hydrology: Reg. Stud., 41: 101069 **(23 pages)**.

Leong, W.Y., (2025). Artificial Intelligence-Driven Analytics for Monitoring and Mitigating Climate Change Impacts. Engineering Proceedings. 108(1), 7 **(8 pages)**.

Li, F.; Tian, J.; Guo, X.; Xu, L., (2025). Hybrid deep learning framework for environmental microplastic classification: Integrating CNN-based spectral feature extraction and transformer models. Environmen. Pollut., 384: 126989 **(8 pages)**.

Lim, J.; Shin, G.; Shin, D., (2024). Fast detection and classification of microplastics below 10 µm using CNN with Raman spectroscopy. Anal. Chem., 96(17): 6819–6825 **(7 pages)**.

Liu, C.; Zong, C.; Chen, S.; Chu, J.; Yang, Y.; Pan, Y.; Yuan, B.; Zhang, H., (2024). Machine learning-driven QSAR models for predicting the cytotoxicity of five common microplastics. Toxicology. 508: 153918 **(9 pages)**.

Lorenzo-Navarro, J.; Castrillón-Santana, M.; Sánchez-Nielsen, E.; Zarco, B.; Herrera, A.; Martínez, I.; Gómez, M., (2021). Deep learning approach for automatic microplastics counting and classification. Sci. Total Environ., 765: 142728 **(7 pages)**.

Lowe, M.; Qin, R.; Mao, X., (2022). A review on machine learning, artificial intelligence, and smart technology in water treatment and monitoring. Water. 14(9): 1384 **(28 pages)**.

Mahari, W.A.W.; Anuar, S.T.; Lam, S.S.; Ibrahim, Y.S.; Bhubalan, K.; Vijayan, A.S.; Joseph, A.; Vandana, S.; Juraij, K.; Priya, K.; Santos, J.H.; Govinda.; Katiyar, J. K.; Ayyamperumal, R.; Gaur, A.P.S.; Chinglenthoiba, C., (2026). Perspective into bio-fouled microplastic behaviour, transportation and characterization in water bodies. J. Haz. Mat. Plast., 2: 100017 **(18 pages)**.

Manapragada, N.V.S.K.; Mandelmilch, M.; Roitberg, E.; Kizel, F.; Natanian, J., (2025). Remote sensing for environmentally responsive urban built environment: A review of tools, methods and gaps. Remote Sensing Applications: Soc. Environ., 38: 101529 (22 pages).

Manchu, M.; Felsy, C.; Joselin Kavitha, M., (2024). Microplastic predictive modelling with the integration of Artificial Neural Networks and Hidden Markov Models (ANN-HMM). J. Environ. Health Sci. Eng., 22(2): 579 **(14 pages)**.

Moses, S.R.; Roscher, L.; Primpke, S.; Hufnagl, B.; Löder, M.G.J.; Gerdts, G.; Laforsch, C., (2023). Comparison of two rapid automated analysis tools for large FTIR microplastic datasets. Anal. Bioanal. Chem., 415(15): 2975–2987 **(13 pages)**.

Olawade, D.B.; Ijiwade, J.O.; Ige, A.O.; Wada, O.Z., (2026). Artificial intelligence for modeling and reducing microplastic in marine environments: A review of current evidence. Mar. Pollut. Bull., 226: 119379 **(18 pages)**.

Olbert, A.I.; Diganta, M.T.M.; Bamal, A.; Burke, W.; Sajib, A.M.; Abioui, M.; Ashekuzzaman, S.M.; Rahman, A.; Uddin, M.G., (2025). Developing river water quality prediction model incorporating reliable indexing approach. J. Environ. Sci., 164: 581–598 **(18 pages)**.

Pal, D.; Prabhakar, R.; Barua, V.B.; Zekker, I.; Burlakovs, J.; Krauklis, A.; Hogland, W.; Vincevica-Gaile, Z., (2025). Microplastics in aquatic systems: A comprehensive review of its distribution, environmental interactions, and health risks. Environ. Sci. Pollut. Res., 32(1): 56–88 **(33 pages)**.

Pan, D.; Deng, Y.; Yang, S.X.; Gharabaghi, B. (2025). Recent advances in remote sensing and artificial intelligence for river water quality forecasting: A review. Environments. 12(5): 158 **(34 pages)**.

Perera, I.J.J.U.N., Sandaruwan, R.D.C.; Bellanthudawa, B.K.A., (2025). Coastal and marine plastic pollution monitoring and control using remote sensing (RS) and artificial intelligence (AI) technologies. In: Vithanage, M.; Samarasekara, S.M.; James, B.D.; Reddy, C.M. (Eds.), Coastal and marine pollution: Source to sink, mitigation and management: 329–345. John Wiley & Sons **(17 pages)**.

Pilechi, A.; Mohammadian, A.; Murphy, E., (2022). A numerical framework for modeling fate and transport of microplastics in inland and coastal waters. Mar. Pollut. Bull., 184: 114119 **(15 pages)**.

Pittroff, M.; Loui, C.; Oswald, S.E.; Bochow, M.; Kamp, J.; Dierkes, G.; Lensing, H.-J.; Munz, M., (2024). Riverbed depth-specific microplastics distribution and potential use as process marker. Environ. Sci. Pollut. Res., 31(32): 45326–45340 **(15 pages)**.

Popescu, S.M.; Mansoor, S.; Wani, O.A.; Kumar, S.S.; Sharma, V.; Sharma, A.; Arya, V.M.; Kirkham, M.B.; Hou, D.; Bolan, N.; Chung, Y.S., (2024). Artificial intelligence and IoT driven technologies for environmental pollution monitoring and management. Front. Environ. Sci., 12: 1336088 **(19 pages)**.

Portillo De Arbeloa, N.; Marzadri, A., (2025). Modeling microplastic dynamics in riverine systems: Fate and transport analysis. Environ. Sci. Pollut. Res., 32(34): 20659–20677 **(19 pages)**.

Priyanto, A.; Hapidin, D.A.; Edikresnha, D.; Aji, MP; Khairurrijal, K., (2025). Predicting microplastic quantities in Indonesian provincial rivers using machine learning models. Sci. Total Environ., 961: 178411 (12 pages).

Rawat, H.; Gaur, A.; Singh, N.; Selvaraj, M.; Karnwal, A.; Pant, G.; Malik, T., (2025). Artificial intelligence-driven detection of microplastics in food: A comprehensive review of sources, health risks, detection techniques, and emerging artificial intelligence solutions. Food Chem. X. 29: 102687 **(12 pages)**.

Rehm, R.; Zeyer, T.; Schmidt, A.; Fiener, P., (2021). Soil erosion as transport pathway of microplastic from agriculture soils to aquatic ecosystems. Sci. Total Environ., 795: 148774 **(12 pages)**.

Ren, L.; Liu, S.; Huang, S.; Wang, Q.; Lu, Y.; Song, J.; Guo, J., (2023). Identification of microplastics using a convolutional neural network based on micro-Raman spectroscopy. Talanta. 260: 124611 **(7 pages)**.

Reshadi, M.A.M.; Rezanezhad, F.; Shahvaran, A.R.; Ghajari, A.; Kaykhosravi, S.; Slowinski, S.; Van Cappellen, P., (2025). Assessment of environmental and socioeconomic drivers of urban stormwater microplastics using machine learning. Sci. Rep., 15(1): 6299 **(15 pages)**.

Rosales-Martínez, O.; Granda-Gutiérrez, E.E.; García-Hernández, R.A.; Alejo-Eleuterio, R.; Flores-Fuentes, A.A., (2025). Spectral derivatives improve FTIR-based machine learning classification of plastic polymers. Modelling. 6(4): 115 **(22 pages)**.

Sá, B.; Pais, J.; Antunes, J.; Pequeno, J.; Pires, A.; Sobral, P., (2022). Seasonal abundance and distribution patterns of microplastics in the Lis River, Portugal. Sustainability. 14(4): 2255 **(18 pages)**.

Santana, M.F.M.; Tonin, H.; Vamvounis, G.; van Herwerden, L.; Motti, C.A.; Kroon, F.J., (2025). Predicting microplastic dynamics in coral reefs: Presence, distribution, and bioavailability through field data and numerical simulation analysis. Environ. Sci. Pollut. Res., 32(15): 9655–9675 **(21 pages)**.

Sarker, M.A.B.; Imtiaz, M.H.; Holsen, T.M.; Baki, A.B.M., (2024). Real-time detection of microplastics using an AI camera. Sensors. 24(13): 4394 **(15 pages)**.

Seggio, M.; Arcadio, F.; Radicchi, E.; Cennamo, N.; Zeni, L.; Bossi, A.M., (2024). Toward nano- and microplastic sensors: Identification of nano- and microplastic particles via artificial intelligence combined with a plasmonic probe functionalized with an estrogen receptor. ACS Omega. 9(17): 18984–18994 **(11 pages)**.

Sim, W.; Song, S.W.; Park, S.; Jang, J.I.; Kim, J.H.; Cho, Y.-M.; Kim, H.M., (2024). Unveiling microplastics with hyperspectral Raman imaging: From macroscale observations to real-world applications. J. Haz. Mat., 463: 132861 **(10 pages)**.

Srivastava, S.; Wang, W.; Zhou, W.; Jin, M.; Vikesland, P.J., (2024). Machine learning-assisted surface-enhanced Raman spectroscopy detection for environmental applications: A review. Environ. Sci. Technol., 58(47): 20830–20848 **(19 pages)**.

Sugathapala, T.M.; Capuano, T.; Brandt, L.; Iudicone, D.; Sardina, G., (2025). Vertical transport of buoyant microplastic particles in the ocean: The role of turbulence and biofouling. Environ. Pollut., 36: 125819 **(9 pages)**.

Tang, K.H.D., (2025). The role of artificial intelligence in microplastic pollution studies and management. Recent Prog. Sci. Eng., 1(4): 1–11 **(10 pages)**.

Thammasanya, T.; Patiam, S.; Rodcharoen, E.; Chotikarn, P., (2024). A new approach to classifying polymer type of microplastics based on

Faster-RCNN-FPN and spectroscopic imagery under ultraviolet light. Sci. Rep., 14(1): 3529 **(11 pages)**.

Tran, H.-T.; Hadi, M.; Nguyen, T.T.H.; Hoang, H.G.; Nguyen, M.-K.; Nguyen, K.N.; Vo, D.N., (2023). Machine learning approaches for predicting microplastic pollution in peatland areas. Mar. Pollut. Bull., 194(A); 115417 **(10 pages)**.

Trivedi, A.; Bakhasha, J.; Saxena, V.; Arya, N.; Kumar, P.; Srivastava, A.; Mishra, S.; Yadav, K. K.; Trivedi, S.P.; Banaee, M.; Faggio, C., (2026). Microplastic-metal interactions and their toxicological effects in fish: A comprehensive review. J. Haz. Mat. Adv., 21: 101005 **(18 pages)**.

Tsiaras, K.; Hatzonikolakis, Y.; Kalaroni, S.; Pollani, A.; Triantafyllou, G., (2021). Modeling the pathways and accumulation patterns of micro- and macro-plastics in the Mediterranean. Front. Mar. Sci., 8: 743117 **(23 pages)**.

Umurhan, Y.; Songsart-Power, M.; Limbu, T.B.; Phan, T., (2025). Applications of Raman spectroscopy for microplastic detection and characterization: A comprehensive spectral reference. Environ. Sci. Pollut. Res., 32(50): 28630–28677 **(48 pages)**.

Usman, A.G.; Almongy, H.M.; Samsudin, M.S.; Mati, S.; Ashraf, M.W.; Abba, S.I.; Almetwally, E.M.; Tajer, K.W.N., (2026). Integration of bio-inspired algorithms with machine learning for modeling microplastic contamination transport processes in natural aquatic habitats using morphological features. J. Radiat. Res. Appl. Sci., 19(1): 102216 **(13 pages)**.

Valdiviezo-Gonzales, L.; Huaman, M.; Huachopoma, J., (2026). Microplastic removal by coagulation/flocculation: A review and bibliometric analysis. J. Haz. Mat. Adv., 101098 **(12 pages)**.

Valle-Bravo, A.V.; González, C.L.; González-Soto, R.A.; Serrano, L.A.G.; García, J.A.C.; Flores-Huicochea, E., (2026). Integrating artificial intelligence into circular strategies for plastic recycling and upcycling. Polymers. 18(2): 306 (42 pages).

Valls-Conesa, J.; Winterauer, D.J.; Kröger-Lui, N.; Roth, S.; Liu, F.; Lüttjohann, S.; Harig, R.; Vollertsen, J., (2023). Random forest microplastic classification using spectral subsamples of FT-IR hyperspectral images. Anal. Met. Adv. Met. Appl., 15(18): 2226–2233 **(8 pages)**.

Velazquez-Araque, L.; Flor, J.; Méndez, A.; Cárdenas-Calle, M., (2025). Modeling microplastic dispersion in the Salado estuary using computational fluid dynamics. Fluids. 10(5): 118 **(29 pages)**.

Villegas-Camacho, O.; Francisco-Valencia, I.; Alejo-Eleuterio, R.; Granda-Gutiérrez, E.E.; Martínez-Gallegos, S.; Villanueva-Vásquez, D., (2025). FTIR-based microplastic classification: A comprehensive study on normalization and ML techniques. Recycling. 10(2): 46 **(20 pages)**.

Wang, J.; Dong, J.; Tang, M.; Yao, J.; Li, X.; Kong, D.; Zhao, K., (2023). Identification and detection of microplastic particles in marine environment by using improved faster R–CNN model. J. Environ. Manag., 345: 118802 **(11 pages)**.

Wang, Z.; Pal, D.; Pilechi, A.; Ariya, P.A., (2024). Nanoplastics in water: Artificial intelligence-assisted 4D physicochemical characterization and rapid in situ detection. Environ. Sci. Technol., 58(20): 8919–8931 **(13 pages)**.

Wardani, I.; Hazimah Mohamed Nor, N.H.M.; Wright, S.L.; Kooter, I.M.; Koelmans, A.A., (2024). Nano- and microplastic PBK modeling in the context of human exposure and risk assessment. Environ. Int., 186: 108504 **(14 pages)**.

Windsor, F.M.; Durance, I.; Horton, A.A.; Thompson, R.C.; Tyler, C.R.; Ormerod, S.J., (2019). A catchment-scale perspective of plastic pollution. Glob. Change Biol., 25(4): 1207–1221 **(15 pages)**.

Wolf, M.; Van Den Berg, K.; Garaba, S.P.; Gnann, N.; Sattler, K.; Stahl, F.; Zielinski, O., (2020). Machine learning for aquatic plastic litter detection, classification and quantification (APLASTIC-Q). Environ. Res. Let., 15(11): 114042 **(12 pages)**.

Xie, L.; Ma, M.; Ge, Q.; Liu, Y.; Zhang, L., (2025). Machine learning advancements and strategies in microplastic and nanoplastic detection. Environ. Sci. Technol., 59(18): 8885–8899 **(14 pages)**.

Xu, M.; Liu, D., (2025). AI-enabled membrane bioreactors: A review of control architectures and operating-parameter optimization for nitrogen and phosphorus removal. Water. 17(19): 2899 **(29 pages)**.

Yan, H.; Cordier, M.; Uehara, T., (2024). Future projections of global plastic pollution: Scenario analyses and policy implications. Sustainability. 16(2): 643 **(18 pages)**.

Yan, X.; Cao, Z.; Murphy, A.; Qiao, Y., (2022). An ensemble machine learning method for microplastics identification with FTIR spectrum. J. Environ. Chem. Eng., 10(4): 108130 **(8 pages)**.

Yang, H.; Chen, G.; Wang, J., (2021). Microplastics in the marine environment: Sources, fates, impacts and microbial degradation. Toxics. 9(2): 41 **(19 pages)**.

Yang, J.; Li, H.; Ling, W.; Li, Y.; Zhang, K.; Zhang, P., (2025). Sources, status, and potential risks of microplastics in marine organisms of the Bohai Sea: A systematic review. Toxics. 13(5): 400 **(23 pages)**.

Yang, Y.; Kong, F.; You, X.; Wu, R.; Shen, J. (2026). Assessing microplastic impacts on insect behaviour through artificial intelligence tools. TrAC Trends Anal. Chem., 198: 118784 **(8 pages)**.

Yarahmadi, A.; Heidari, S.: Sepahvand, P.: Afkhami, H.: Kheradjoo, H., (2024). Microplastics and environmental effects: Investigating the effects of microplastics on aquatic habitats and their impact on human health. Front. in Public Health. 12: 1411389 **(22 pages)**.

Yu, F.; Hu, X., (2022). Machine learning may accelerate the recognition and control of microplastic pollution: Future prospects. J. Haz. Mat., 432: 128730 **(8 pages)**.

Zeng, G.; Ma, Y.; Du, M.; Chen, T.: Lin, L.; Dai, M.; Luo, H.; Hu, L.; Zhou, Q.; Pan, X., (2024). Deep convolutional neural networks for aged microplastics identification by Fourier transform infrared spectra classification. Sci. Total Environ., 913: 169623 **(13 pages)**.

Zhang, Y.; Li, J.; Zhou, Y.; Zhang, X.; Liu, X., (2024). Artificial intelligence-based microfluidic platform for detecting contaminants in water: A review. Sensors. 24(13): 4350 **(19 pages)**.

Zhang, Y.; Zhang, D.; Zhang, Z., (2023). A critical review on artificial intelligence—Based microplastics imaging technology: Recent advances, hotspots and challenges. Int. J. Environ. Res. Public Health. 20(2): 1150 (30 pages).

Zhang, J.; Li, X.; Chen, H.; Liu, G.; Yan, X.; Yan, B., (2025). Unraveling the ecotoxicity of micro (nano) plastics loaded with environmental pollutants using ensemble machine learning. J. Haz. Mat. 495: 138911 **(11 pages)**.

Zhao, B.; Richardson, R.E.; You, F., (2024). Advancing microplastic analysis in the era of artificial intelligence: From current applications to the promise of generative AI. Nexus. 1(4): 100043 **(19 pages)**.

Zhu, Y.; Hang Yeung, C.; Lam, E.Y., (2021). Microplastic pollution monitoring with holographic classification and deep learning. Journal of Physics: Photonics. 3(2): 024013 **(12 pages)**.

AUTHOR (S) BIOSKETCHES

Kamaraj, M., Ph.D., Associate Professor, Department of Biotechnology, Faculty of Science and Humanities, SRM Institute of Science and Technology Ramapuram Campus, Chennai 600089, Tamil Nadu, India.
- Email: *drkamarajm@gmail.com*
- ORCID: 0000-0002-0111-8524
- Web of Science ResearcherID: AAP-1422-2020
- Scopus Author ID: 55645159500
- Homepage: https://fsh.srmrmp.edu.in/department-of-biotechnology/faculty/dr-kamaraj-m/

Bhavithra, H.A., Ph.D., Assistant Professor, Department of Mathematics, Faculty of Science and Humanities, SRM Institute of Science and Technology Ramapuram Campus, Chennai 600089, Tamil Nadu, India.
- Email: *bhavimani09@gmail.com*
- ORCID: 0009-0007-8318-2805
- Web of Science ResearcherID: GWU-4897-2022
- Scopus Author ID: 58899580500
- Homepage: https://in.linkedin.com/in/h-a-bhavithra-b65b10343

Rajalakshmi, B., M.E, Assistant Professor, Department of Computer Science and Engineering, Easwari Engineering College, Chennai-600089, Tamil Nadu, India.
- Email: *bsr.raji@gmail.com*
- ORCID: 0009-0008-9481-4430
- Web of Science ResearcherID:
- Scopus Author ID: 58988933200
- Homepage: https://www.linkedin.com/in/rajalakshmi-b-a8706a344/

Aravind, J., Professor, Environmental Biotechnology Lab, Department of General Medicine, Saveetha Institute of Medical and Technical Sciences, Chennai 602105, Tamil Nadu, India
- Email: *dr.j.aravind@gmail.com*
- ORCID: 0000-0003-0623-0037
- Web of Science ResearcherID: O-9296-2015
- Scopus Author ID: 23569355700
- Homepage: https://www.scopus.com/authid/detail.uri?authorId=23569355700

HOW TO CITE THIS ARTICLE:
Kamaraj, M.; Bhavithra, H.A.; Rajalakshmi, B.; Aravind, J., (2027). Artificial intelligence-driven approaches for detection, fate, transport, and remediation of microplastic pollution in aquatic systems. Global J. Environ. Sci. Manage., 13(1): 479-500.

DOI: 10.22034/gjesm.2007.01.22
URL: https://www.gjesm.net/article_735544.html

Global J. Environ. Sci. Manage. 13(1): 501-522, Winter 2027, Serial #49

Global Journal of Environmental Science and Management
(GJESM)

Homepage: https://www.gjesm.net/

Podcasts

REVIEW ARTICLE

Environmental risks of pest management practices in smallholder coconut plantations

M.L.A. Hosang[1], Susilawati[1], J.C. Alouw[1,2,*], M. Puspitasari[1], R.E. Senewe[1], Sujak[1], R. Rohimatun[1], R.T. Hutasoit[1], Subiyakto[1], Nurindah[1], D.A. Sunarto[1], R.G.U.I. Meththananda[3], B.A.N. Pinaria[4]

[1]*Research Centre for Estate Crops, National Research and Innovation Agency, Cibinong Science Center, Jl. Raya Jakarta - Bogor, Cibinong, Bogor, 16911 Indonesia*

[2]*International Coconut Community, Jakarta 10430, Indonesia*

[3]*Department of Computational Mathematics, Faculty of Computing, General Sir John Kotelawala Defence University, Rathmalana, Sri Lanka*

[4]*Department of Plant Protection, Faculty of Agriculture, Sam Ratulangi University, Manado City, North Sulawesi, Indonesia*

ARTICLE INFO

Article History:
Received 01 June 2026
Revised 05 August 2026
Accepted 08 September 2026

Keywords:
Coconut rhinoceros beetle
Environmental risk assessment
Integrated pest management
Oryctes rhinoceros
Smallholder agriculture

ABSTRACT

Oryctes rhinoceros, the coconut rhinoceros beetle, remains one of the most damaging pests of coconut (*Cocos nucifera*) across South and Southeast Asia, the Pacific, and increasingly, new invasion fronts in the Americas. Although climatic alterations may redistribute the geographic footprint of the hazard, predictive assessments underscore non-linear and variable outcomes. Regional expansions in vulnerable or suitable extents are largely contingent upon the analytical scenario and structural parameters of the model utilized. This reinforces the case for treating its management as an environmental, not solely agronomic, concern. The study objectives were to characterize how smallholder-level management choices translate into differentiated environmental and health risk. Smallholder coconut plantations, which supply most world coconut production, are disproportionately exposed because of fragmented land holdings, limited capital, and constrained extension access. This review evaluates the translation of management interventions into distinct environmental and health hazards by systematically reviewing evidence on coconut rhinoceros beetle biology, intervention efficacy, smallholder socioeconomic dynamics, and insecticide risk literature through a standardized four-tier risk framework. Smallholders commonly rely on chemical control options such as organophosphates and pyrethroids. These options carry documented risks: non-target toxicity, soil and water contamination, and occupational exposure. In the absence of beetle-specific metrics, elevated occupational exposure risks are inferred from prevailing normative practices in smallholder agriculture concerning the omission of protective equipment. Biological and cultural alternatives include *O. rhinoceros nudivirus*, *Metarhizium anisopliae*, *Bacillus thuringiensis*, botanical larvicides, and pheromone-based trapping. These present a substantially lower environmental risk profile: laboratory bioassays report 90 to 100 percent larval mortality for *Metarhizium* isolates from East Java, comparable to the up to 98 percent larval and 90 percent adult mortality reported for a granular carbamate alternative, indicating technical efficacy is not the limiting factor, with field-deployed monitoring documented in Jepara and Bengkulu. Uptake of these lower-risk options is nonetheless constrained less by technical efficacy than by production economics, extension access, and the fragmented governance of smallholder replanting and pest-management programs. The evidence suggests that attenuating this risk burden is predominantly constrained by the disparity between existing lower-risk technological interventions and their operational uptake, among other compounding determinants. Risk-management strategies must therefore be designed around smallholder economic and institutional realities rather than efficacy data alone.

DOI:10. 22034.gjesm.2027.01.23

This is an open access article under the CC BY license (http://creativecommons.org/licenses/by/4.0/)

NUMBER OF REFERENCES	NUMBER OF FIGURES	NUMBER OF TABLES
120	5	4

*Corresponding Author:
Email: jelf001@brin.go.id
Phone: +62821 9424 7398
ORCID: 0000-0002-4831-125X

Note: Discussion period for this manuscript open until March 01, 2027 on GJESM website at the "Show Article".

INTRODUCTION

Coconut (*Cocos nucifera* L.) underpins the livelihoods of tens of millions of smallholder farmers across the tropics, and in most producing countries the crop is grown predominantly on smallholdings rather than large corporate estates. Comparative economic assessments within Indonesia indicate that diversified coconut intercropping practices consistently outperform monocropping by securing enhanced returns for smallholders under both national and private economic accounting criteria. Development programs have nonetheless historically still encouraged monocropping (Rani *et al.,* 2018). More broadly, technical efficiency, profitability, and sustainability of coconut smallholdings remain sensitive to several production constraints. These range from ageing palm stands to limited access to credit and extension (Omar and Fasleen, 2020, 2021; Rusli and Isa, 2021; Agus, 2025; Bahri *et al.*, 2026). Among the biotic constraints on smallholder coconut production, the coconut rhinoceros beetle (CRB), *Oryctes rhinoceros* (Linnaeus) (Coleoptera: Scarabaeidae), is one of the most persistent and economically damaging. Adult beetles bore into the crown of the palm to feed, damaging developing fronds and, under repeated attack, killing young or already-stressed palms (Bedford, 1976; Zelazny and Alfiler, 1987; Manley *et al.*, 2018). Larvae develop in decaying organic matter that is often abundant around smallholder plantings, including felled trunks, compost, and other breeding substrates (Fauzana and Ustadi, 2020; Shen *et al.*, 2025). The species' life-history characteristics exacerbate control challenges in smallholder agricultural matrices, wherein fragmented and decentralized breeding substrates limit the efficacy of the centralized sanitation protocols typically enforceable on managed estates. The geographic range of CRB has continued to expand. Beyond its long-established distribution across South and Southeast Asia and the Pacific, recent reports document continuing damage around Port Moresby, Papua New Guinea (Jackson *et al.*, 2025a). Confirmed presence in Timor-Leste carries attendant biosecurity implications (Paudel *et al.*, 2025). Further documentation confirms a sustained outbreak on Efate, Vanuatu (Paudel *et al.*, 2023), marking both this regional expansion and the initial geographic establishment of the species within the Americas (Jackson *et al.*, 2025b). Compounding the invasion risk, a genetically distinct haplotype, historically referred to as Guam biotype (CRB-G)-has been shown to escape control by the region's primary biological control agent, *O. rhinoceros* nudivirus (OrNV) (Marshall *et al.*, 2017; Tanaka *et al.*, 2021). This haplotype has driven renewed outbreaks across several Pacific islands (Anggraini, 2023; Weston *et al.*, 2023), although recent genomic analyses confirm this invasive lineage did not disperse from Guam (Tay *et al.*, 2024). Within Indonesia, field damage and infestation have been documented from East Java (Prastowo *et al.*, 2022), and Rote-Ndao, East Nusa Tenggara (Nenotek *et al.*, 2024). Further cases are reported from Jepara, Central Java (Indriyanti, 2017; Indriyanti *et al.*, 2018), and Yogyakarta (Adi *et al.*, 2023, 2025). This underscores that the problem recurs across the archipelago's smallholder coconut belt, rather than being geographically confined. The management framework for the CRB bridges a continuum from broad-spectrum chemical treatments to precise biological and cultural measures, wherein each intervention tier carries a distinct spectrum of environmental and occupational health hazards. A substantial general literature has established that insecticide use carries environmental risks extending well beyond the target pest. These include risks to pollinators and other non-target organisms (Goulson, 2013; Sponsler *et al.*, 2019; Wan *et al.*, 2025) and contamination of surface water and sediment (Sousa *et al.*, 2016; Top *et al.*, 2023). Occupational and residential exposure of applicators and nearby communities is also documented (Dereumeaux *et al.*, 2020; Oltramare *et al.*, 2023). General studies

on smallholder agriculture practices highlights substantial vulnerabilities during pesticide administration, including negligible use of personal protective equipment, imprecise application dosing, and minimal formal risk-appraisal capacity. In the absence of CRB-specific empirical datasets, these systemic trends are considered broadly applicable to CRB management frameworks. As a result, the environmental risk profile of any CRB control program depends as much on who applies it and under what conditions as on the intrinsic toxicity of the product used. This study synthesizes evidence on CRB management options in smallholder coconut systems through an explicit environmental risk-assessment lens. Existing comprehensive literature has predominantly examined CRB biology and intervention efficacy as standalone objectives (Hassaan *et al.*, 2025; Hosang *et al.*, 2025). The aim of this study is to characterize the comparative hazard, exposure, and risk profile of the control strategies actually available to and adopted by smallholders. This study also examines, through Indonesian and comparable Southeast Asian and Pacific case evidence, why lower-risk options remain under-adopted despite their documented field performance. This study was carried out at the Research Centre for Estate Crops, National Research and Innovation Agency (BRIN), Bogor, Indonesia, in 2026.

METHODOLOGY

Methodologically, this review adopts a narrative synthesis rather than a systematic or quantitative protocol, aligning its scope with the evaluation of operational management cases across smallholder coconut systems rather than providing an exhaustive bibliographic catalog of CRB literature. The evidence base draws on 121 peer-reviewed references across four domains: (i) CRB biology, invasion ecology, and genomics; (ii) chemical, biological, and cultural control efficacy; (iii) smallholder production economics and sociology; and (iv) general insecticide risk-assessment literature, used as a comparative frame where CRB-specific ecotoxicological data are lacking. Findings are presented as direct evidence when derived from studies on *Oryctes rhinoceros* or its management; otherwise, broader insecticide or smallholder literature is used for context and identified accordingly. Following a standardized environmental risk assessment paradigm (hazard identification, exposure assessment, risk characterization, and risk management), the initial phase focuses on the biological and invasive attributes of the CRB that perpetuate its persistent impact. Exposure assessment examines chemical and biological control practices reported in smallholder contexts, with emphasis on Indonesian cases. Risk characterization compares environmental and health profiles of these practices, while risk management considers institutional, economic, and technological factors shaping adoption of lower-risk options. Within this framework, “hazard” denotes intrinsic toxicological or biological properties; “exposure” refers to pathways, dose, frequency, route, and receptor; and “risk” reflects their combination. Socioeconomic vulnerability is explicitly integrated as the structural determinant governing intervention accessibility, which subsequently configures realized hazard-exposure trajectories. Geographic emphasis is on Indonesia, with comparative evidence from Malaysia, India, the Philippines, and Pacific Island systems where smallholder structures are similar. The review process followed the general framework proposed by Fink (2014). Literature was retrieved from Scopus, Web of Science, Google Scholar, and CAB Abstracts using combinations of the search terms "Oryctes rhinoceros", "coconut rhinoceros beetle", "coconut", "Cocos nucifera", "integrated pest management", "biological invasion", "climate change", "nudivirus", "biosecurity", "pesticide pollution", "insecticide", "ecotoxicology", and "biopesticide", covering publications from 1976 to

2026. Records were screened for relevance to CRB biology, invasion ecology, control efficacy, or smallholder coconut socioeconomics; general insecticide environmental risk-assessment literature was included where CRB-specific ecotoxicological data were unavailable. Conformant with the stated narrative-review architecture, formal systematic screening protocols, including PRISMA guidelines, were not implemented in the article selection process. Of the 960 records identified, 363 remained after title screening, and 121 were retained following full-text assessment for relevance, availability, and language, as summarised in Fig. 1. The geographic scope of this review is illustrated in Fig. 2, which maps the five Indonesian smallholder case locations discussed in the "Case review synthesis" section: East Java (Prastowo *et al.*, 2022), Jepara in Central Java (Indriyanti *et al.*, 2018), Yogyakarta (Adi *et al.*, 2023, 2025), Bengkulu (Ginting *et al.*, 2025), and Rote-Ndao in East Nusa Tenggara (Nenotek *et al.*, 2024). Encompassing a broad spectrum of agroecological and socioeconomic gradients across four major islands—from the high-density smallholder configurations of Java to the dispersed, moisture-stressed coconut systems of eastern Indonesia, these cases illustrate that the environmental risk profiles analyzed in this review are structurally pervasive throughout the archipelago's smallholder agricultural landscape. The analytical framework used to structure this synthesis, mapping each guiding theme to its corresponding focus and extraction criteria, is presented in Table 1. Socioeconomic vulnerability is conceptualized within this structure not as a parallel risk dimension, but as the operational filter that dictates intervention accessibility for smallholders, thereby fundamentally conditioning the realized hazard-exposure trajectory. Where lower-risk biological or cultural options are technically available but inaccessible due to capital, extension, or institutional constraints, the higher-risk chemical alternative becomes the default realized exposure pathway, linking Table 2 (technical risk) and Table 3 (socioeconomic constraint) as a single integrated risk-management framework.

Hazard identification: CRB *as a persistent threat to smallholder coconut*

Adult *O. rhinoceros* bore into the unopened crown of the coconut palm to feed on sap, and the resulting V-shaped cuts in emerging fronds are the pest's most visible field sign. Persistent herbivory on immature or replanted palms frequently causes terminal destruction of the meristematic growing point, a damage dynamic well-documented throughout multiple invasion zones (Mansfield *et al.*, 2024). Larval development depends on decaying organic matter. Felled coconut trunks, sawdust, compost heaps, and other cellulose-rich debris common around smallholder plots and replanting sites function as breeding sites that are difficult to eliminate at the scale of an individual smallholding (Bedford, 1976; Zelazny and Alfiler, 1987; Manley *et al.*, 2018). Environmental conditions, including moisture and substrate composition, materially influence larval survival and breeding success. Hazard intensity is therefore partly determined by land-management practices within the smallholder's control, such as trunk disposal after felling or land clearing (Fauzana and Ustadi, 2020; Shen *et al.*, 2025). The severity of this hazard is structurally compounded by concurrent geographic dispersal and the proliferation of a genetically distinct haplotype impervious to standard biocontrol interventions. The CRB-G haplotype has spread across several Pacific islands where it was not historically established, evading suppression by OrNV isolates that had previously kept older haplotype populations in check (Marshall *et al.*, 2017; Tanaka *et al.*, 2021; Anggraini, 2023; Weston *et al.*, 2023). Its continued detection includes confirmation that it did not disperse to the Solomon Islands or Palau from Guam as initially suspected (Tay *et al.*, 2024). This illustrates how invasion pathways for this pest remain only partly understood. Independent confirmations of new or continuing incursions come from Papua New Guinea

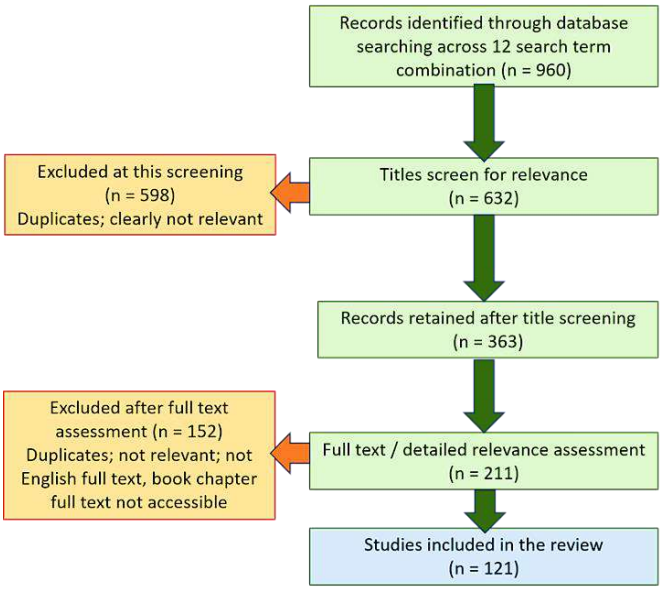

Fig. 1. Flow diagram of the literature search and selection process, showing the number of records identified, screened, and included at each stage, with reasons for exclusion



Fig. 2: Geographical location of the study area of the smallholder CRB infestation cases reviewed

Table 1: Analytical framework guiding the synthesis of literature

No	Analytical theme	Focus	Extraction criteria
1	Hazard and exposure identification	How CRB biology, invasion status, and smallholder management practices jointly determine exposure to different control options	Biological and damage records, documented chemical and biological control practices, application methods
2	Environmental and health risk characterization	Comparative environmental and health risk profile of chemical versus biological/cultural control components	Reported toxicity and ecotoxicological data, contamination indicators, mode of action, occupational exposure pathways
3	Risk management and adoption evidence	What socioeconomic and institutional evidence from Indonesian smallholder systems implies for adoption of lower-risk management	Field-scale case outcomes, adoption constraints, extension and financing evidence, institutional capacity indicators

Table 2: Comparative environmental and health risk profile of *O. rhinoceros* control options reported in smallholder and community plantation settings

Control agent	Active ingredients/ organism	Application route	Target stage	Evidence level	Principal environmental receptor	Occupational exposure pathway	Documented adverse effects	Confidence/ uncertainty	Source
Cypermethrin, dimethoate	Cypermethrin (pyrethroid); dimethoate (organophosphate)	Foliar/crown broadcast spray	Larvae/ adults	Laboratory	Non-target neurosecretory systems; soil/water (class-level)	Dermal/ inhalation during mixing/ application	Dimethoate: measurable neurosecretory changes at 0.125–0.5% concentration, 8–24h exposure	CRB-specific data limited to lab bioassay; broader risk drawn from comparative literature	Larval/adult treatment (Venkatarajappa, 2001; Padmasheela and Delvi, 2004)
Acephate (trunk injection)	Acephate (organophosphate)	Trunk injection/ implant	Adults (systemic)	Semi-field	Palm vascular tissue; feeding organisms	Reduced vs. broadcast spraying	Not specified beyond efficacy	Single study; long-term fate not evaluated	Tall palms via petiole bioassay (Rafie and Amit, 2024)
Marshal 5G / systemic (UAV/manual)	Carbosulfan 5% (carbamate)	Granular soil/leaf-axil; UAV aerial	Larvae/ adults	Laboratory + field	Soil/water (runoff, leaching)	Dermal/ inhalation during mixing/ application; reduced during UAV step	95–98% larval mortality (5–9g); 90% adult mortality (day 7), declining to 70–75% (10–15 days)	Efficacy well-documented; drift/deposition exposure not evaluated	Community oil palm, Riau (Tito *et al.*, 2026); O'ahu, Hawai'i (Russo *et al.*, 2026); UAV application (Roudhiyah *et al.*, 2024; Lan *et al.*, 2024)
Metarhizium anisopliae	Entomopathogenic fungus	Breeding-site inoculation	Larvae (3rd instar)	Laboratory bioassay (field-sourced isolates)	Non-target soil arthropods (broader host range)	Minimal; no chemical toxicant	None identified in literature; 90–100% mortality (day 13–15)	Field-scale/non-target/logistics less established	East Java (Prastowo *et al.*, 2022); compost-based "metankos" (Fauzana *et al.*, 2023)
Bacillus thuringiensis	Bacterium (Cry-toxin dependent)	Pot-based soil application	Larvae	Laboratory / pot trial	Non-target insects (strain-dependent)	Host-specific; non-target effects documented	None identified in literature	Strain-specific host range not fully characterized	Pot-based soil application trial (Pujiastuti *et al.*, 2020, 2021, 2023)
OrNV	Virus (host-specific)	Field release/ regional	Larvae/adults	Field/operational	None beyond target host	Minimal; no chemical toxicant	None identified	Long release history; limited by CRB-G resistance	Long-standing regional releases (Huger, 2005; Ramle *et al.*, 2005)
Pheromone trapping	Ethyl 4-methyloctanoate	Trap deployment	Adults	Field/ village-level	None (non-toxicant)	None	None	Suppression not demonstrated; non-target attraction and trap/lure disposal footprint untested	North Sulawesi (Hosang *et al.*, 2022); Jepara (Indriyanti *et al.*, 2018); Bengkulu (Ginting *et al.*, 2025)
Botanical larvicides	Plant-derived compounds	Lab/small-scale application	Larvae	Laboratory /small field trial	Non-target insects (compound-dependent)	Minimal; not established	Not established at scale	Limited evidence; non-target toxicity and application-frequency trade-offs untested	Laboratory/small field trials (Mohan and Padmanaban, 2013; Kumar *et al.*, 2018, 2019; Wandri *et al.*, 2024)

Table 3: Socioeconomic and institutional contexts of smallholder coconut production relevant to technology adoption

Constraint	Description	Supporting evidence
Capital/production economics	General coconut-sector studies document limited surplus capital among smallholders, which plausibly favors low-upfront-cost chemical sprays over the production/ monitoring infrastructure biological control requires	Godoy and Bennett, 1991; Omar and Fasleen, 2020, 2021;
Extension access	General studies document uneven extension access among Indonesian coconut smallholders, plausibly limiting farmer knowledge of and confidence in biological/cultural alternatives	Rusli and Isa, 2021
Replanting and financing schemes	General studies document historically low implementation of coordinated financing for smallholder long-term investment; sustained biocontrol production would plausibly face similar barriers	Sondakh and Hardaker, 1983; Wulandari and Alouw, 2021
Institutional/development strategy	General coconut-sector studies indicate sector-wide sustainability depends on coordinated strategy rather than farmer-level intervention alone, a principle plausibly relevant to CRB biocontrol adoption	Goltiano and Feliciano, 2022; Agus, 2025; Khopade *et al.*, 2025; Bahri *et al.*, 2026

(Jackson *et al.*, 2025a), Timor-Leste (Paudel *et al.*, 2025), Vanuatu (Paudel *et al.*, 2023), and the Americas (Jackson *et al.*, 2025b). Climatic scenario modeling for CRB indicates non-uniform distributional shifts, wherein regional assessments across China estimate an upward projection of highly suitable acreage by 5.48 percent (%) to 39.43% under different Representative Concentration Pathway scenarios by the 2050s and 2090s (Xu *et al.*, 2022), while global-scale modeling suggests responses vary by region and may include habitat contractions depending on localized environmental parameters (Hao *et al.*, 2022). These habitat suitability projections represent potential distribution rather than definitive predictions of actual presence or population abundance, with uncertainty arising from species occurrence data, predictor variables, climate scenarios, and modeling approach. Together with formal biosecurity interception records (Hoffmann *et al.*, 2024), these indicators reveal a pervasive hazard characterized by ongoing geographic expansion and insufficient containment under prevailing quarantine measures. In Indonesia specifically, field studies document CRB pressure across a wide range of smallholder coconut and oil palm growing areas: East Java (Prastowo *et al.*, 2022), Jepara in Central Java (Indriyanti, 2017; Indriyanti *et al.*, 2018), Rote-Ndao in East Nusa Tenggara (Nenotek *et al.*, 2024), and Yogyakarta (Adi *et al.*, 2023, 2025). The Yogyakarta studies also document co-occurrence with the Asiatic palm weevil (*Rhynchophorus vulneratus*). This spatial spread across islands with very different agroecological and socioeconomic contexts reinforces that CRB hazard identification in Indonesia cannot be reduced to a single regional problem. It must instead be understood as a recurring, archipelago-wide constraint on smallholder coconut production. As demonstrated in Fig. 3, the co-localization of diverse developmental cohorts within individual substrate matrices underscores the systemic difficulties of executing sanitation protocols at a localized smallholding scale. Concurrently, the characteristic foliar mutilation and bore-hole artifacts presented in Fig. 4 delineate the primary phenotypic symptoms upon which prevalent field-level surveillance continues to depend.

Exposure assessment: smallholder management practices and their exposure pathways

Chemical control practices

Chemical insecticides remain a common first response to CRB infestation in smallholder and community-managed plantations because they are locally available and provide a rapid, visible knockdown effect (Table 2). Documented applications within smallholder frameworks encompass the deployment of cypermethrin against CRB larvae, which yields significant and quantifiable residual toxicity profiles in the treated cohorts (Venkatarajappa, 2001). Dimethoate, an organophosphate, has been shown to produce neurosecretory damage in the brain of third-instar grubs, evidence that is itself indicative of the

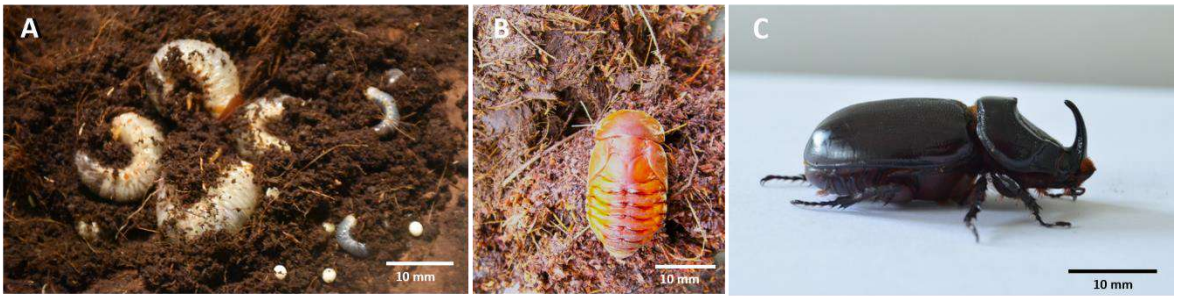

Fig. 3: Co-occurrence of multiple CRB life stages within a single decaying coconut trunk breeding site, illustrating why sanitation-based control is difficult to sustain at the scale of an individual smallholding: (A) eggs and larvae of different instars found together in the same breeding substrate, (B) pupa, (C) adult male poised for dispersal to the coconut palm crown. Scale bars = 10 millimeters (mm)



Fig. 4: Symptoms of CRB infestation on coconut palms: (A) characteristic triangular frond-cutting damage on a young palm, (B) adult *O. rhinoceros* feeding at the base of a young coconut frond, showing a bore hole that can extend toward the growing point, (C) infestation symptoms on a tall coconut palm (*Cocos nucifera* var. Tall) approximately 50 years (y) old

compound's neurotoxic mode of action in non-target contexts (Padmasheela and Delvi, 2004; Sadhu *et al.*, 2024). Other applications include acephate delivered via trunk injection or trunk-implanted controlled-release formulations, intended specifically to reduce broadcast exposure on tall palms (Rafie and Amit, 2024). The granular formulation Marshal 5G has also been tested against CRB larvae and adults in a community oil palm plantation in Riau, Indonesia (Tito *et al.*, 2026). To circumvent conventional canopy application routes, systemic insecticides have been assessed as an alternative control modality against CRB populations in Hawai'i (Russo *et al.*, 2026). UAV application has been trialed to reduce applicator exposure in immature oil palm (Roudhiyah *et al.*, 2024). Recent delivery methods—trunk injection, controlled-release implants, and UAV spraying—are framed as lower-exposure alternatives to conventional broadcast spraying, which remains the baseline practice for broad-spectrum products like cypermethrin and dimethoate. Operational constraints in smallholder frameworks—characterized by manual application protocols and deficient personal protective equipment availability—establish direct occupational exposure pathways to organophosphate and pyrethroid active ingredients during mixing and dispersion phases. These patterns reflect broader systemic trends wherein smallholder chemical management is governed by intrinsic risk appraisal and constrained health literacy, echoing documented exposure modalities across

organophosphate- and organochlorine-intensive agricultural landscapes. (Sulaiman *et al*., 2020). Repeated chemical pesticide use in smallholder coconut plantations can disrupt soil microbial communities and nutrient-cycling organisms, potentially reducing soil productivity and ecological resilience, with persistent residues compounding this pressure (Jeyaseelan *et al.,* 2024; Köninger *et al.,* 2026). Since CRB can also be controlled biologically via *Metarhizium* spp. and OrNV, routine chemical reliance risks undermining these ecological benefits unnecessarily (Paudel *et al.,* 2021; Villamizar *et al.,* 2024). Organophosphates, pyrethroids, and neonicotinoids used against CRB differ mechanistically-acetylcholinesterase inhibition, sodium-channel modulation, and nicotinic receptor modulation, respectively (IRAC, 2026)-with corresponding differences in environmental behavior. Organophosphates pose variable persistence and acute non-target toxicity depending on the active ingredient (Mali *et al.,* 2023; Rajan *et al.,* 2024); pyrethroids adsorb strongly to soil but remain toxic to aquatic organisms via rainfall runoff (Liu *et al.,* 2024); and neonicotinoids are more water-soluble and systemic, favoring leaching and prolonged non-target exposure (Fouad and Abdel-Raheem, 2024; Mandal *et al.,* 2025). Consequently, optimization of insecticide selection protocols for CRB mandates the comprehensive evaluation of chemical persistence, mobility, and ecotoxicological impacts alongside operational efficacy. Such strategies should favor judicious, threshold-driven interventions embedded within an integrated pest management (IPM) paradigm that prioritizes sanitation, pheromone trapping, and biological regulation (Paudel *et al.,* 2021; Villamizar *et al.,* 2024).

Biological and cultural control practices

A substantial body of field evidence documents biological and cultural alternatives already deployed against CRB in smallholder or near-smallholder settings. Entomopathogenic fungi, principally *Metarhizium anisopliae*, have long been used to control CRB larvae (Gopal *et al.*, 2006; Yapo *et al*., 2017). Recent Indonesian studies confirm continued local relevance: isolates recovered from infected larvae around coconut plantations in East Java (Prastowo *et al.*, 2022) (Fig. 5), a compost-based biopesticide formulation ("metankos") incorporating local *M. anisopliae* flour (Fauzana *et al.*, 2023), and virulence testing of *M. anisopliae* in liquid media against CRB larvae (Rozziansha *et al.*, 2025). Field-scale bio-formulation trials combining indigenous *Bacillus thuringiensis* and *Metarhizium* strains have also demonstrated management potential (Manjunatha *et al.*, 2023). Bt-based formulations isolated from Indonesian soils and evaluated in liquid and crude-extract forms have shown insecticidal activity against CRB larvae specifically in oil palm plantation contexts (Pujiastuti *et al.*, 2020, 2021, 2023; Anggraini *et al.*, 2021). OrNV persists as the historically dominant classical biological control agent against CRB, with a long record of field release and establishment across the Pacific and South Asia. This sustained efficacy stems from the agent's capacity for long-term persistence and self-dissemination once released-an ecological attribute that, while diminishing the need for repeated intervention, also means the agent cannot subsequently be withdrawn from the environment (Gorick, 1980; Bedford, 1986; Huger, 2005; Marshall *et al*., 2017; Tanaka *et al*., 2021; Anggraini *et al*., 2023). Documented use also spans Malaysian oil palm plantations (Ramle *et al.*, 2005) and the Andaman Islands (Prasad, 2008a; Prasad *et al.*, 2008b). Pheromone-based aggregation trapping protocols are broadly cited within Indonesian agricultural frameworks, including comparative assessments of pheromone variants conducted in North Sulawesi (Hosang *et al.*, 2022), alongside observational trap deployments in Jepara (Indriyanti *et al.*, 2018). Further studies cover attack-intensity and trapping-effectiveness studies in Bengkulu (Ginting *et al.*, 2025), and packaging-design work aimed at improving pheromone product usability

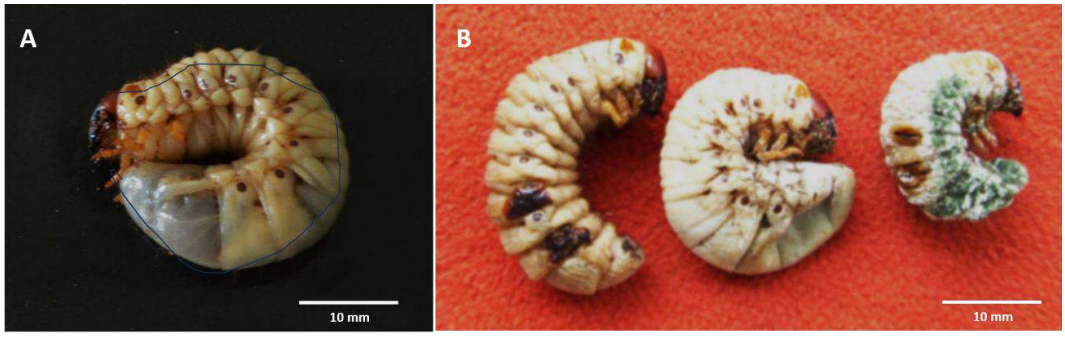

Fig. 5: *Oryctes rhinoceros* larvae: (A) healthy larva showing normal cuticle coloration and morphology, (B) larvae infected with the entomopathogenic fungus *Metarhizium anisopliae*, showing progressive mycosis symptoms including cuticle darkening and dense greenish conidial sporulation covering the body surface in advanced infection. Scale bars = 10 mm

for field application (Pradana *et al.*, 2023). Botanical control options with reported larvicidal or growth-disrupting activity include compounds isolated from *Adiantum latifolium* (Kumar *et al.*, 2018, 2019), various botanical formulations and neem-based products (Mohan and Padmanaban, 2013). *Senna multijuga* has recently been identified as a dual-action plant exhibiting both an attractant and bioinsecticide (Wandri *et al.*, 2024). Entomopathogenic nematodes have also demonstrated biocontrol potential under laboratory conditions (Zelazny, 1985; Sujithra *et al.*, 2022). Evidence shows that lower-risk biological and cultural alternatives to chemical control are viable for Indonesian smallholders. *Metarhizium*-based biopesticides and pheromone trapping have documented field trials in community plantations from East Java to Bengkulu. These regional OrNV programs build on earlier introduction trials in the Andaman Islands and biological suppression efforts against CRB in Andhra Pradesh, India. (Rao *et al.*, 2018). Empirical documentation from Malaysian oil palm plantations encompasses the quantification of pheromone-trapping dynamics, infestation gradients, and mortality outcomes (Kamarudin *et al.*, 2007), thereby corroborating concurrent molecular investigations into the genetic diversity of underlying genetic diversity of local CRB populations and regional derived via RAM marker profiling (Manjeri *et al.*, 2011).

Risk characterization: comparative environmental and health risk of control options

Chemical control risk

The active ingredients reported against CRB in smallholder and community plantation settings include, cypermethrin (a pyrethroid), dimethoate and acephate (organophosphates), and carbamate/ organochlorine adjacent formulations. These belong to chemical classes with well-characterized environmental and health risk profiles in the broader ecotoxicological literature, even where CRB-specific risk data are sparse. Pesticide movement pathways in coconut plantations are functionally dependent upon the operational application modality and the structural height of the target palms. For young/short palms, canopy application is used; synthetic pyrethroids (e.g., deltamethrin, cypermethrin, lambda-cyhalothrin) retain residual activity against CRB for at least 12 weeks, unlike organic pyrethrins, with residues potentially washed by rain into soil (Wei *et al.*, 2025). In tall palm management, trunk- and root-zone methods are operationally preferable despite distinct environmental pathways: soil drenching drives subsurface leaching toward groundwater, surface residues disperse into aquatic systems via runoff, and trunk injection minimizes direct soil loading, notwithstanding eventual environmental reentry through vegetative decay or root uptake. Flow magnitude depends on active-ingredient

properties, soil characteristics, rainfall, and application frequency (Araya *et al*., 2024; Sarker *et al*., 2024). Rainfall intensity, soil texture, and organic matter jointly determine pesticide mobility: heavy post-application rainfall and sandy soils increase leaching, fine soils increase runoff but permit rapid leaching through macropores, and organic matter enhances retention while potentially prolonging persistence (Sarker *et al*., 2024; Wendell *et al*., 2024). Organophosphates and other cholinesterase-inhibiting insecticides carry documented environmental risk through their shared mode of neurotoxic action, which is not restricted to target pests (Thetkathuek *et al*., 2017; Kori *et al.*, 2019). Empirical evidence directly couples occupational exposure to organochlorine and derivative insecticides with amplified health vulnerability profiles among agricultural workforces operating within smallholder frameworks (Carvalho, 1991). Pyrethroids, while generally less persistent than organochlorines, have been shown to pose environmental risk to aquatic systems following surface runoff, with transport modelling studies used specifically to characterize this pathway (Liu *et al.*, 2023). Chlorpyrifos, an organophosphate structurally related to compounds used against CRB, has documented ecotoxicological risk to aquatic indicator species (Marques *et al.*, 2021). Furthermore, neonicotinoid and associated systemic insecticides, frequently implemented to mitigate drift hazards inherent to broadcast dispersion, generate specialized environmental risk profile. This includes risk to pollinators and non-target invertebrates (Goulson, 2013; Hladik *et al.*, 2018; Longing *et al.* 2020), and human exposure through the food chain (Zhao *et al.*, 2020). Two features of smallholder application practice plausibly elevate this baseline risk profile. First, application techniques and dosage configurations characteristic of smallholder operations are infrequently calibrated against standardized risk-assessment frameworks. Frameworks such as the Pesticide Risk Tool and the Environmental Impact Quotient exist precisely to quantify comparative insecticide risk for decision-making (Meys *et al.*, 2024), but no evidence in the reviewed literature indicates that such tools are in routine use at the smallholder level for CRB management. Second, the manual and proximate nature of application routines renders established occupational exposure routes—such as dermal and inhalation contact during mixing and dispersion phases—directly relevant to smallholders conducting crown treatments or trunk injections absent consistent personal protective equipment. While direct ecotoxicological and occupational risk data specific to CRB-targeted chemical use remain limited, the broader insecticide environmental risk-assessment literature offers relevant contextual evidence for the same chemical classes. These studies were conducted in unrelated pest-management and public-health systems and are cited here for comparative context rather than as direct measurements of CRB-management risk: soil-insecticide risk in maize IPM (Furlan *et al.*, 2017), neonicotinoid substitution effects in U.S. maize (Perry and Moschini, 2020) and insecticide risk in tsetse and trypanosomiasis control. Further examples include neonicotinoid contamination of engineered waterways in China (Zhang *et al.*, 2024), metamidophos risk to non-target aquatic organisms (Iannacone, 2007), and fipronil and imidacloprid risk to river shrimp (Cáceres-Del Carpio and Iannacone, 2021). Extended case paradigms involve the analytical review of insecticide-treated bed-net safety in malaria mitigation initiatives, the systemic risks posed by sublethal mosquito control compounds, and comprehensive risk evaluation frameworks for acetamiprid. Other studies report insect movement responses used as environmental-risk indicators, an environmental risk index for insecticides used in Mato Grosso, Brazil, and a quantitative pollinator hazard model for sulfoxaflor. Further evidence covers insecticide contamination of tropical river systems in China regulatory risk considerations for herbicide-

tolerant crops, and honeybee toxicity of broflanilide. Moreover, empirical investigations utilizing rodent models indicate prospective neurobehavioral and psychiatric hazards linked to developmental insecticide exposure, running parallel to structured exposure-window management models intended for pollinator protection. This body of comparative literature indicates that the chemical classes used against CRB are not risk-free in principle; however, direct, CRB-specific exposure and ecotoxicological data would be needed to confirm the magnitude of risk under actual smallholder application conditions. These three classes differ mechanistically: organophosphates and carbamates share a cholinesterase-inhibiting mode of action, while pyrethroids act on nerve sodium channels. While carbamates such as carbosulfan demonstrate accelerated soil dissipation kinetics relative to organophosphates, corresponding comparative metrics regarding mobility and bioaccumulation under coconut plantation environments remain uncharacterized.

Biological and cultural control: a lower-risk but unevenly adopted alternative

CRB differ substantially in their host-range and mode of action. OrNV is highly host-specific to *Oryctes* species. *Metarhizium anisopliae*, an entomopathogenic fungus, has a comparatively broader host range among insect taxa, although its practical deployment at CRB breeding sites limits exposure of most non-target organisms. The host-range specificity of *Bacillus thuringiensis* is governed by the Cry-toxin profile of the respective strain used; the coleopteran-active strains detailed herein exhibit a more restricted host spectrum than Bt variants targeting other insect orders. Entomopathogenic nematodes have host ranges that vary by species and are generally broader than that of OrNV. Botanical products, unlike the biological agents above, act as natural chemical toxicants rather than host-specific organisms, and their non-target toxicity depends on the specific bioactive compounds involved rather than on host specificity by design. Their mode of biological control was itself modelled explicitly to assess population-level suppression rather than broad-spectrum toxicity (Hochberg and Waage, 1991). Although the reviewed biological control literature lacks the occupational exposure documentation characteristic of chemical-control studies, the broader Bacillus thuringiensis literature indicates that Bt applications can elicit direct or indirect effects on soil microorganisms, non-target invertebrates, and higher trophic (Belousova *et al*., 2021). Furthermore, assessments of the related subspecies *Bti* in mosquito control similarly documents non-target ecological impacts, though the long-term ecosystem-level consequences warrant further investigation (Brühl *et al*., 2020). This evidence is drawn from a different insect order (Diptera) than the coleopteran-active Bt strains discussed here and is therefore comparative rather than CRB-specific. The principal documented limitation of these agents is instead field performance, adoption logistics, and the practical burden of production and distribution at scale, echoed for CRB specifically in the integrated pest management synthesis of Alouw *et al.* (2020) and the applied IPM guidance of Hosang *et al.* (2025). Given its mechanism of action—which avoids broadcast toxicant application—pheromone trapping is not anticipated to entail substantial environmental or health risks; however, dedicated non-target or occupational exposure studies specific to this method were not uncovered in the surveyed literature. The Indonesian studies reviewed here measure trap-catch performance and attack intensity, factors addressed directly in packaging-design research (Pradana *et al*., 2023) and comparative trap-catch trials (Hosang *et al*., 2022; Ginting *et al*., 2025). Consequently, these deployments function primarily in surveillance and early detection rather than serving as mass-trapping control strategies or demonstrating population suppression, as neither of the latter two endpoints was assessed in the referenced

sources. Botanical larvicides similarly avoid the persistence and bioaccumulation concerns associated with synthetic insecticides. Their reported efficacy in the literature, however, is generally from laboratory or small field trials (Mohan and Padmanaban, 2013; Kumar *et al.*, 2018, 2019; Wandri *et al.*, 2024) rather than at the commercial scale reported for chemical alternatives. The overall risk contrast is therefore asymmetric. Chemical options carry a well-documented, non-trivial environmental and occupational risk burden but are readily available and provide fast, visible results; whereas biological and cultural options are not associated with the same documented risk pathways in the literature reviewed, though the extent to which these options have themselves been subject to comparable non-target or occupational risk testing remains limited. Nevertheless, the deployment of such methodologies necessitates advanced technical proficiencies regarding production, storage, and field management—capabilities that typically lie beyond the independent reach of individual smallholders. Broader Indonesian evidence on the gut microbiome of CRB, including its bacterial diversity and protease/lipase-producing potential (Aini *et al.*, 2023), points to further biologically-based management avenues under active investigation. This includes the biocontrol potential of CRB-associated gut bacteria against the oil-palm pathogen *Ganoderma boninense* (Surbakti and Marheni, 2025), alongside broader reviews of advances in rhinoceros beetle control in oil palm (Bedford, 2014).

Case review synthesis: Indonesian smallholder coconut systems

Field evidence from across Indonesia—encompassing East Java, Central Java, East Nusa Tenggara, Yogyakarta, and Bengkulu, demonstrates the previously discussed risk trade-offs within concrete, geographically dispersed settings rather than through abstract comparison. In East Java, *Metarhizium* isolates recovered directly from CRB-infested coconut plantations demonstrated laboratory-confirmed virulence against larvae (Prastowo *et al.*, 2022), providing a locally sourced biological alternative that does not depend on imported formulations. In Rote-Ndao, East Nusa Tenggara, damage intensity and geographic distribution mapping of CRB infestation (Nenotek *et al.*, 2024) illustrates the kind of spatial monitoring needed to target biological control deployment efficiently in a resource-constrained provincial setting. Furthermore, the execution of broad-spectrum chemical interventions across decentralized smallholder plots introduces substantial financial burdens and supervisory complexities within this operational framework. In Jepara, Central Java, pheromone trap monitoring has been implemented directly at village level (Indriyanti *et al.*, 2018), demonstrating that community-scale, low-toxicity monitoring infrastructure is technically feasible in a smallholder setting. Comparative pheromone trials conducted in Bengkulu systematically quantified both attack intensity and trap efficacy under conditions adjacent to oil palm and coconut cultivations (Ginting *et al.*, 2025). Packaging-design research has also addressed a genuinely practical barrier-product usability and shelf stability to pheromone adoption in the field (Pradana *et al.*, 2023). A summary of these Indonesian smallholder CRB case studies, including their locations, intervention types, principal findings, management relevance, and scale of evidence, is provided in Table 4. These cases share a common pattern: the lower-risk biological or cultural intervention was not merely tested under laboratory conditions but taken into the field in the same smallholder landscapes where CRB damage was documented. This indicates that the technical feasibility barrier to implementing safer management practices in Indonesia is less pronounced than commonly presumed. What the case evidence does not show, however, is systematic scale-up: each of these studies documents a localized trial or monitoring program

Table 4: Summary of Indonesian smallholder coconut rhinoceros beetle case evidence reviewed

Location	Study Type	Approach documented	Key finding	Source
Jember East Java	Control efficacy trial (laboratory)	*Metarhizium* anisopliae isolation from field cadavers	Locally-sourced isolates show laboratory-demonstrated virulence against larvae	Prastowo *et al.*, 2022
Jepara Central Java	Operational implementation study	Pheromone aggregation trapping	Village-level monitoring infrastructure technically feasible at community scale	Indriyanti *et al.*, 2018
Rote-Ndao East Nusa Tenggara	Hazard/damage surveillance	Damage/distribution mapping	Mild average damage intensity [8.89%) spread across 10 sub-districts	Nenotek *et al.*, 2024
Yogyakarta D.I. Yogyakarta	Diagnostic/distribution study	GIS-based distribution mapping	Co-occurrence with Asiatic palm weevil documented	Adi *et al.*, 2023, 2025
Bengkulu Bengkulu	Hazard surveillance + control efficacy trial	Pheromone trapping efficacy trial	Attack intensity and trap effectiveness quantified under oil palm/coconut-adjacent conditions	Ginting *et al.*, 2025

rather than province- or nation-wide deployment. This is consistent with the broader observation that historical coconut replanting and support initiatives in Indonesia have necessitated dedicated, scheme-level coordination to effectively reach smallholders at scale (Heriyanto *et al*., 2019; Wulandari and Alouw, 2021). These capital and institutional constraints sit within a much longer history of smallholder-dominated coconut and oil-palm production. Smallholder involvement in tree-crop cultivation in Malaya, including coconut and oil palm in Johor, has been documented back to the 1860s (Pakiam, 2020). Historically, smallholder coconut plantation management practices, such as canopy-level pasture composition in Malaita, Solomon Islands, have been dictated by the identical land- and labor-constrained mechanics that currently restrict the uptake of biological control (Manaros and Gurbuz, 2020).

RECOMMENDATION

Drawing upon the risk asymmetry and adoption gaps established across review, subsequent recommendations are categorized into practical management implications for smallholders and extension personnel, policy-level directives for institutional and financial stakeholders, and prioritized research agendas aimed at resolving remaining critical empirical and operational knowledge and implementation gaps.

Management implications

Routine pheromone-trap surveillance should form the baseline activity for smallholder CRB management, escalating to sanitation once a locally defined action threshold is exceeded, then to intensified pheromone trapping combined with biological control (OrNV, *Metarhizium*, or *B. thuringiensis*) where infestation persists. Targeted chemical intervention ought to be designated as a final recourse, preferably administered via trunk injection or controlled-release implants rather than broadcast spraying, with implementation proving more viable at a cooperative or program level than at the individual farmer scale.

Policy implications

Closing the adoption gap for lower-risk controls depends on the same institutional and financing mechanisms that support Indonesian coconut smallholders more broadly: extension access (Rusli and Isa, 2021), coordinated replanting and financing schemes (Sondakh and Hardaker, 1983; Wulandari and Alouw, 2021), and sector-wide development strategy (Agus, 2025; Khopade *et al*., 2025; Bahri *et al*., 2026). The continued spread of the OrNV-tolerant CRB-G haplotype (Jackson *et al*., 2025a, 2025b) requires actively maintained regionally coordinated capacity. Incorporating CRB risk mitigation strategies within overarching coconut-sector sustainability and climate-resilience paradigms would harmonize capital

allocation with pre-existing financial architectures designed to address alternative smallholder limitations.

Research priorities

Structured risk-quantification tools such as the pesticide risktool (Meys *et al*., 2024), alongside life-cycle assessment or comparative environmental footprint approaches, have not yet been applied to CRB management and warrant evaluation. Capital allocations directed toward locally manufactured, economically viable biological agents—exemplified by liquid-media *Metarhizium* cultivation systems (Rozziansha *et al*., 2025), would effectively attenuate the cost disparities relative to conventional chemical alternatives. Farm-scale intervention studies directly measuring pesticide-use reduction, environmental contamination, and non-target exposure following integrated CRB management deployment would address a gap not filled by the individual-component evidence reviewed here. More broadly, the evidence base and policy frameworks presented here would be significantly enhanced by future research that applies standardized risk-assessment methodologies and CRB-specific exposure data, tracks environmental and occupational outcomes longitudinally, and identifies which combinations of financing, extension services, and institutional arrangement most effectively bridge the adoption gap.

LIMITATIONS

This review has several limitations. First, as a narrative rather than a systematic review, no formal PRISMA-style screening protocol with tracked exclusion reasons at each stage was applied; a simplified literature-flow diagram (Fig. 1) is provided based on global rather than per-database search records. Second, because the individual studies synthesized here utilize non-standardized toxicological and exposure endpoints, constructing a harmonized quantitative risk index across all control strategies proved unfeasible; consequently, the risk comparisons presented in Table 2 remain qualitative in nature. Third, the apparent absence of non-target or occupational risk findings for biological and cultural control options should not be interpreted as confirmed evidence of environmental safety; it more likely reflects limited investigation of these agents relative to chemical insecticides. Fourth, evidentiary strength varies substantially, ranging from controlled laboratory bioassays to replicated field trials and village-level monitoring, with these distinctions noted explicitly where they materially influence interpretation. Fifth, a substantial proportion of the chemical, biopesticide, and pheromone-trapping evidence derives from oil-palm rather than coconut systems (Ramle *et al*., 2005; Kamarudin *et al*., 2007; Tito *et al*., 2026; Roudhiyah *et al*., 2024); differences in canopy structure, planting density, and exposure pathways mean such findings are comparative rather than directly equivalent for coconut. Sixth, no systematic dataset comparing farmer adoption, cost, extension access, and institutional support was identified, limiting the institutional-capacity interpretation offered in the Conclusion. Several gaps remain unaddressed within the reviewed literature: the cumulative ecological consequences of recurring *Metarhizium* application over multiple seasons; systematic cross-regional comparison of environmental risk profiles; localized non-target impacts on beneficial insects, pollinators, and soil or aquatic microorganisms within coconut agroecosystems; the pesticide handling life-cycle (including storage, transportation, container disposal and equipment washing) and associated household and livestock spillover risks in smallholder environments; and the adequacy of pesticide regulatory frameworks and monitoring mechanisms in Indonesia. Finally, the evidence base is geographically concentrated in a small number of Indonesian provinces and source countries, and publication bias toward positive efficacy findings cannot be excluded, as is common in the pest-management literature more broadly generally.

CONCLUSION

Oryctes rhinoceros remains a persistent and geographically expanding hazard to smallholder coconut plantations. Ultimately, the environmental and health hazards associated with its management are dictated less by the intrinsic biology of the pest than by the specific control option that smallholder can practically access and afford. Chemical control, while effective and widely available, carries a documented risk burden spanning ecotoxicological, occupational, and environmental-contamination pathways, a burden that is plausibly amplified under typical smallholder application conditions. Biological and cultural alternatives, by contrast, carry a substantially lower risk profile, with laboratory bioassays using field-sourced *Metarhizium* isolates in East Java and field-deployed pheromone monitoring in Jepara and Bengkulu illustrating that the technical feasibility barrier to safer management in Indonesia is smaller than is sometimes assumed. The evidence assembled here suggests that limited adoption, despite documented technical efficacy of several lower-risk options, is more consistent with institutional and economic capacity constraints than with a simple lack of viable technology. Although the narrative design of this synthesis precludes causal inferences, future *CRB* risk-management interventions must nevertheless be conceptualized and appraised through a dual lens—balancing biological efficacy against their practical compatibility with smallholder economic structures and pre-existing extension and replanting frameworks. Closing this gap is, in the authors' assessment, as much an institutional priority as a technical one; the specific surveillance, financing, and technology priorities this implies are set out in the Recommendation above. Subsequent investigations employing standardized risk-assessment methodologies and CRB-specific exposure metrics, coupled with longitudinal monitoring of farm-level environmental and occupational consequences, would substantially reinforce the evidentiary foundation supporting these priorities. This review also did not identify CRB-specific evidence on insecticide resistance or its potential role in driving escalating application frequency and dose; given the established role of such feedback loops in other insect pest systems, this represents a further gap warranting dedicated monitoring in Indonesian smallholder contexts.

AUTHOR CONTRIBUTIONS

M.L.A. Hosang developed the review concept, prepared the visualizations, and reviewed and edited the manuscript. S. Susilawati wrote the original draft, conducted the literature search, and reviewed and edited the manuscript. N. Nurindah performed the analysis and synthesis and reviewed and edited the manuscript. J.C. Alouw wrote the original draft and reviewed and edited the manuscript. M. Puspitasari reviewed and edited the manuscript. R. Semewe reviewed and edited the manuscript. R. Rohimatun reviewed and edited the manuscript. R.T. Hutasoit reviewed and edited the manuscript. S. Subiyakto reviewed and edited the manuscript. S. Sujak reviewed and edited the manuscript. D.A. Sunarto reviewed and edited the manuscript. R.G.U.I. Meththananda reviewed and edited the manuscript. B.A.N. Pinaria reviewed and edited the manuscript. All authors reviewed and approved the final version of the manuscript carefully and jointly before formal submission.

ACKNOWLEDGEMENT

The authors thank colleagues at the Research Centre for Plantation Crops, BRIN and International Coconut Community (ICC), for discussion and access to institutional data on CRB management in Indonesia. Furthermore, the authors affirm full adherence to relevant ethical standards. These standards encompass plagiarism, informed consent, and research misconduct. In addition, these standards address data fabrication and/or falsification, duplicate publication and/or submission, and redundant publication.

CONFLICT OF INTEREST

The authors declare no conflicting interests in relation to the publication of this manuscript. Furthermore, all ethical standards of scholarly publishing that include encompassing plagiarism, informed consent, research misconduct, data fabrication and/or falsification, duplicate publication and/or submission, and redundant publication, have been fully adhered to by the authors throughout the research and publication process.

OPEN ACCESS

©2027 The author(s). This article is licensed under a Creative Commons Attribution 4.0 International License, which permits use, sharing, adaptation, distribution and reproduction in any medium or format, as long as you give appropriate credit to the original author(s) and the source, provide a link to the Creative Commons license, and indicate if changes were made. The images or other third-party material in this article are included in the article's Creative Commons license, unless indicated otherwise in a credit line to the material. If material is not included in the article's Creative Commons license and your intended use is not permitted by statutory regulation or exceeds the permitted use, you will need to obtain permission directly from the copyright holder. To view a copy of this license, visit: http://creativecommons.org/licenses/by/4.0/

PUBLISHER'S NOTE

GJESM Publisher remains neutral with regard to jurisdictional claims in published maps and institutional affiliations.

POSITIVE AI STATEMENT

During the preparation of this work the author(s) have used Artificial Intelligence (AI) ChatGPT Plus in order to correct English sentences. After using this tool/service, the authors reviewed and edited the content as needed and took full responsibility for the content of the publication.

ABBREVIATIONS

%	Per cent
CRB	Coconut rhinoceros beetle
CRB-G	Coconut rhinoceros beetle-Guam biotype
E4-MO	Ethyl 4-methyloctanoate
GIS	Geographic information system
IPM	Integrated pest management
mm	Millimeter
OrNV	*Oryctes rhinoceros* nudivirus
PCR	Polymerase chain reaction
RPA	Recombinase polymerase amplification
SNP	Single nucleotide polymorphism
UAV	Unmanned aerial vehicle
y	Year

REFERENCES

Adi, H.; Soesilohadi, R.H.; Nugroho, A.P.; Hadisusanto, S.; Aldawood, A.S.; Sukirno, S., (2023). Distribution analysis of asiatic palm weevil Rhynchophorus vulneratus Panzer (Coleoptera: Dryphthoridae) using GIS Technique and the Interaction with Coconut Beetle Oryctes rhinoceros L. (Coleoptera: Scarabaeidae). Hayati J. Biosci., 30(5): 918-926 (**9 pages**).

Adi, H.; Lestari, P.; Sofiana, D.; Adella, P.; Ilma, H.; Sukirno, S., (2025). Abundance of Rhynchophorus vulneratus (Coleoptera: Dryophthoridae) and Oryctes rhinoceros (Coleoptera: Scarabaeidae) in Gadjah Mada University, Yogyakarta, Indonesia. IOP Conference Series: Earth nd Environmental Science, 1470(1): 012008 **(11 pages).**

Agus, H.N., (2025). Development strategy for smallholder oil palm and coconut plantation in Pesisir Selatan Regency. J. Saudi Soc. Agric. Sci., 24(35) (**14 pages**).

Aini, L.Q.; Sulistyowati, L.; Muhibuddin, A.; Sukmawati, D., (2023). Diversity of bacterial gut microbiome of Oryctes rhinoceros larvae and their potency as source of protease and lipase enzymes. Agrivita, 45(3): 580-588 (**9 pages**).

Alouw, J.C.; Hosang, M.L.; Nguyen, Q., (2020). Biotechnology contributing to integrated pest management: the example of two major coconut pests, Oryctes rhinoceros and Brontispa longissima. In: Coconut Biotechnology Towards the Sustainability of the Tree of Life. Springer, Cham., 151-168 (**18 pages**).

Anggraini, E., (2023). Complete genome sequences of Oryctes rhinoceros nudivirus strains detected in haplotype-G Oryctes rhinoceros from Johor, Malaysia. Microbiol. Resour. Announc., 12(3) e00019-23 **(18 pages).**

Anggraini, E.I.; Vadamalai, G.; Kong, L.L.; Mat, M.; Lau, W.H., (2023). Variants in the mitochondrial genome sequence of Oryctes rhinoceros (Coleoptera: Scarabaeidae) infected with Oryctes rhinoceros nudivirus in oil palm and coconut plantations. Sci. Rep., 13: 16850 (**13 pages**).

Anggraini, F.I.; Sugiharti, M.; Suwanto, A.; Rachmania, N.; Lay, B.W., (2021). Bacillus thuringiensis isolated from soil in oil palm plantation with high toxicity against Oryctes rhinoceros larvae. Malays. J. Microbiol., 17(4): 345-351 (**7 pages**).

Araya, G.; Perfetti-Bolaño, A.; Sandoval, M.; Araneda, A.; Barra, R.O., (2024). Groundwater leaching potential of pesticides: A historic review and critical analysis. Environ. Toxicol. Chem., 43(12): 2478–2491 (**14 pages**).

Bahri, S.; Vaulina, S.; Mulyani, S.; Dewi, I.; Hadi, K., (2026). Sustainability performance and its determinants in smallholder coconut farming in an island region: evidence from Kepulauan Meranti Regency, Riau Province, Indonesia. Open Agric., 11(1) (**15 pages**).

Bedford, G., (1976). Observations on the biology and ecology of Oryctes rhinoceros and Scapanes australis (Coleoptera: Scarabaeidae: Dynastinae): pests of coconut palms in Melanesia. Aust. J. Entomol., 15(3): 241-251 (**11 pages**).

Bedford, G., (1986). Biological control of the rhinoceros beetle (Oryctes rhinoceros) in the South Pacific by baculovirus. Agric. Ecosyst. Environ., 15(2): 141-147 (**7 pages**).

Bedford, G.O., (2014). Advances in the control of rhinoceros beetle, Oryctes rhinoceros in oil palm. J. Oil Palm Res., 26(3): 183-194 **(12 pages).**

Belousova, M.E.; Malovichko, Y.V.; Shikov, A.E.; Nizhnikov, A.A.; Antonets, K.S., (2021). Dissecting the environmental consequences of Bacillus thuringiensis application for natural ecosystems. Toxins, 13(5): 355 (**25 pages**).

Brühl, C.A.; Després, L.; Frör, O.; Patil, C.D.; Poulin, B.; Tetreau, G.; Allgeier, S., (2020). Environmental and socioeconomic effects of mosquito control in Europe using the biocide Bacillus thuringiensis subsp. israelensis (Bti). Sci. Total Environ., 724: 137800 (**11 pages**).

Cáceres-Del Carpio, F.A.; Iannacone, J., (2021). Environmental risk assessment by fipronil and imidacloprid insecticides in river shrimp (Cryphiops caementarius). Granja, 33(1): 103-113 (**11 pages**).

Carvalho, W., (1991). Risk factors related to occupational and environmental exposure to organochlorine insecticides in the state of Bahia, Brazil, 1985. Bol. Ofic. Sanit. Panam., 111(6): 512-524 (**13 pages**).

Dereumeaux, C.; Fillol, C.; Quénel, P.; Denys, S., (2020). Pesticide exposures for residents living close to agricultural lands: A review. Environ. Int., 134, 105210 (**14 pages**).

Fauzana, H.; Ustadi, U., (2020). The development of rhinoceros beetle larvae (Oryctes rhinoceros L.) in various growing media of the Arecaceae. J. Entomol. Indon., 17(2): 89-96 (**8 pages**).

Fauzana, H.; Nelvia, Rustam, R.; Puspita, F.; Feronica, R., (2023). The dosage of biopesticide formulation of local Metarhizium anisopliae flour in compost (metankos) against Oryctes rhinoceros L. IOP Conference Series: Earth Environ. Sci., 1160(1): 012046 (**10 pages**).

Fink, A., (2014). Conducting research literature reviews: from the internet to paper (4th ed.). Sage Publications, Thousand Oaks, CA.

Fouad, M.R.; Abdel-Raheem, S.A.A., (2024). An overview on the fate and behavior of imidacloprid in agricultural environments. Environ. Sci. Pollut. Res., 31(52): 61345–61355 (**11 pages**).

Furlan, L.; Contiero, B.; Chiarini, F.; Colauzzi, M.; Sartori, E.; Benvegnù, I.; Fracasso F.; Giandon, P., (2017). Risk assessment of maize damage by wireworms (Coleoptera: Elateridae) as the first step in implementing IPM and in reducing the environmental impact of soil insecticides. Environ. Sci. Pollut. Res., 24(1): 236-251 (**16 pages**).

Ginting, S.; Ddjamilah; Pryatiningsih; Gusnitha, F.W.; Sariasih, Y.S.I., (2025). Attack intensity and effectiveness pheromone on Oryctes rhinoceros L. in oil palm, Seluma district, Bengkulu. Int. J. Agric. Technol., 21(1): 29-42 (**14 pages**).

Godoy, R.; Bennett, C.P.A., (1991). The economics of monocropping and intercropping by smallholders: the case of coconuts in Indonesia. Hum. Ecol., 19(1): 83-98 (**16 pages**).

Goltiano, H.Y.; Feliciano, G.S., (2022). Social impacts of a coconet enterprise on smallholder coconut farming families: the case of Panaon Island Farmers Federation Inc in the Philippines. Ann. Trop. Res., 44(2): 119-149 (**31 pages**).

Gopal, M.; Gupta, A.; Thomas, G.V., (2006). Prospects of using Metarhizium anisopliae to check the breeding of insect pest, Oryctes rhinoceros L. in coconut leaf vermicomposting sites. Bioresour. Technol., 97(15): 1801-1806 (**6 pages**).

Gorick, B., (1980). Release and establishment of the baculovirus disease of Oryctes rhinoceros (L.) (Coleoptera: Scarabaeidae) in Papua New Guinea. Bull. Entomol. Res., 70(3): 445-453 (**9 pages**).

Goulson, D., (2013). An overview of the environmental risks posed by neonicotinoid insecticides. J. Appl. Ecol., 50(4): 977-987 (**11 pages**).

Hao, M.; Aidoo, O.F.; Qian, Y.; Wang, D.; Ding, F.; Ma, T.; Tettey, E.; Ninsin, K.D.; Osabutey, A.F.; Borgemeister, C., (2022). Global potential distribution of Oryctes rhinoceros, as predicted by Boosted Regression Tree model. Glob. Ecol. Conserv., 37: e02175 (**13 pages**).

Hassaan, M.A.; Sajjad, Z.U.; Rehman, C.U.; Krishnan, K.T.; Jhammat, M.I., (2025). Oryctes rhinoceros (Coleoptera: Scarabaeidae) as a key pest of oil palm: a systematic review of its biology, establishment, and integrated management strategies in Malaysia. Plant Prot., 9(4): 1081-1093 (**13 pages**).

Heriyanto, A.; Karya, D., (2019). Prototype the Economic of Coconut Farmer Household in Indragiri Hilir Municipality, Riau Province. Proc. 2nd Int. Conf. Soc., Econ., Educ. Humanit, (ICoSEEH 2019) – Sustainable Development in Developing Country for Facing Industrial Revolution 4.0, 69–78 (**10 pages**).

Hladik, M.L.; Main, A.R.; Goulson, D., (2018). Environmental risks and challenges associated with neonicotinoid insecticides. Environ. Sci. Technol., 52(6): 3329-3335 (**7 pages**).

Hochberg, M.E.; Waage, J.K., (1991). A model for the biological control of Oryctes rhinoceros (Coleoptera: Scarabaeidae) by means of pathogens. J. Appl. Ecol., 28(2): 514-531 (**18 pages**).

Hoffmann, B.D.; Tay, W.T.; Blas, A.L., (2024). Biosecurity interceptions of coconut rhinoceros beetle Oryctes rhinoceros. Manage. Biol. Invasions, 15(3): 437-443 (**7 pages**).

Hosang, M.L.A.; Rahma; Maskromo, I.; Alouw, J.C., (2022). Comparative effectiveness of three types of pheromones against Rhynchophorus vulneratus (Panzer) and Oryctes rhinoceros (L.) in Indonesia. IOP Conference Series: Earth Environ. Sci.,, 974(1) (**9 pages**).

Hosang, M.L.A.; Indriati, G.; Alouw, J.C.; Maris, P.; Santosa, B., (2025). Pests of coconut and its innovative management strategies: integrated pest management of coconut rhinoceros beetle, Oryctes rhinoceros (Coleoptera: Scarabaeidae). Science Based Pest Management for a Sustainable and Resilient Coconut Sector: 305-316 (**12 pages**).

Huger, A.M., (2005). The Oryctes virus: its detection, identification, and implementation in biological control of the coconut palm rhinoceros beetle, Oryctes rhinoceros (Coleoptera: Scarabaeidae). J. Invertebr. Pathol., 89(1): 78-84 (**7 pages**).

Iannacone, J., (2007). Environmental risk assessment of the insecticide metamidophos in bioassays with four non-target aquatic organisms. Agric. Tec., 67(2): 126-138 (**13 pages**).

Indriyanti, D.R.; Lutfiana, J.E.; Widiyaningrum, P.; Susilowati, E.; Slamet, M., (2018). Aggregation pheromones for monitoring the coconut rhinoceros beetle (Oryctes rhinoceros) in Jerukwangi Village, Jepara, Indonesia. J. Phys. Conference Series: 983(1): 012177 (**5 pages**).

Indriyanti, D.R., (2017). Density and composition of Oryctes rhinoceros (Coleoptera: Scarabaeidae) stadia in field. ARPN J. Eng. Appl. Sci., 12(22): 6364-6371 (**8 pages**).

IRAC, (2026). IRAC Mode of Action Classification Scheme. Insecticide Resistance Action Committee.

Jackson, T.; Kemoi, M.; Asigau, B.; Oki, L.; Tenakanai, D.; Sar, S.; Paudel, S., (2025a). Coconut rhinoceros beetle, Oryctes rhinoceros (Coleoptera: Scarabaeidae), continues to devastate coconut palms around Port Moresby, Papua New Guinea. EPPO Bull., 55(1): 151-157 (**7 pages**).

Jackson, T.A.; Nájera-Rincón, M.; Paudel, S.; Weston, M.K.; Beattie, A.; Marshall, S.D.G., (2025b). Coconut rhinoceros beetle Oryctes rhinoceros (Coleoptera: Scarabaeidae) confirmed in the Americas. EPPO Bull., 55(3): 511-517 (**7 pages**).

Jeyaseelan, A.; Murugesan, K.; Thayanithi, S.; Palanisamy, S.B., (2024). A review of the impact of herbicides and insecticides on the microbial communities. Environ. Res., 245: 118020 (**12 pages**).

Kamarudin, N.H.; Wahid, M.B.; Moslim, R.; Ali, S.R.A., (2007). The effects of mortality and influence of pheromone trapping on the infestation of Oryctes rhinoceros in an oil palm plantation. J. Asia Pac. Entomol., 10(3): 239-250 (**12 pages**).

Khopade, R.; Sawargaonkar, G.; Kale, S.; Davala, M.; Rakesh, S.; Das, S.S.; Verma, R.V.; Raje, K.; Singh, R.; Jat, M.L., (2025). Sustainable intensification in coconut for building system resilience and nutritional security of smallholders in Eastern India. NPJ Sustain. Agric., 3(1): 1-10 (**10 pages**).

Köninger, J.; Labouyrie, M.; Ballabio, C.; Dulya, O.; Mikryukov, V.; Romero, F.; Franco, A.; Bahram, M.; Panagos, P.; Jones, A.; Tedersoo, L.; Orgiazzi, A.; Briones, M.J.I.; van der Heijden, M.G.A., (2026). Pesticide residues alter taxonomic and functional biodiversity in soils. Nature, 650(8101): 367–373 (**7 pages**).

Kori, R.K.; Hasan, W.; Jain, A.K.; Yadav, R.S., (2019). Cholinesterase inhibition and its association with hematological, biochemical and oxidative stress markers in chronic pesticide exposed agriculture workers. J. Biochem. Mol. Toxicol., 33(9): 1–10 (**10 pages**).

Kumar, R.P.; John, A.; Kumar, P.; Babu, K.V.D.; Evans, D.A., (2018). Larvicidal efficacy of adiantobischrysene from Adiantum latifolium against Oryctes rhinoceros through disrupting metamorphosis and impeding microbial mediated digestion. Pest Manage. Sci., 74(8): 1821-1828 (**8 pages**).

Kumar, R.P.; Babu, K.D.; Evans, D.A., (2019). Isolation, characterization and mode of action of a larvicidal compound, 22-hydroxyhopane from Adiantum latifolium Lam. against Oryctes rhinoceros Linn. Pestic. Biochem. Physiol., 153: 161-170 (**10 pages**).

Lan, X.; Wang, J.; Chen, P.; Liang, Q.; Zhang, L.; Ma, C. (2024). Risk Assessment of Environmental and Bystander Exposure from Agricultural Unmanned Aerial Vehicle Sprayers in Golden Coconut Plantations: Effects of Droplet Size and Spray Volume. Ecotox. Environ. Safety 282: 116675 (**13 pages**).

Liu, S.; Li, X.; Ding, R.; Pan, Y.; Ge, X.; Ma, W., (2023). Transport model simulation prediction and environmental risk assessment of pyrethroid insecticides in urban artificial lakes caused by rainfall: a case study of Cloud Mountain Park in subhumid climate zone. J. Environ. Manage. 343 (**13 pages**).

Liu, S.; Yan, J.; Xu, B.; Huang, X.; Qin, H.; Zhao, J.; Xia, C.; Yan, S.; Liu, G., (2024). Fates and models for exposure pathways of pyrethroid pesticide residues: A review. Ecotoxicol. Environ. Saf., 277: 116342 (**10 pages**).

Longing, R.R.; Hladik, M.L.; Anderson, T.A., (2020). Reduced species richness of native bees in field margins associated with neonicotinoid concentrations in non-target soils. Agric. Ecosyst. Environ., 287: 106693 (**8 pages**).

Mali, H.; Shah, C.; Raghunandan, B.H.; Prajapati, A.S.; Patel, D.H.; Trivedi, U.; Subramanian, R.B., (2023). Organophosphate pesticides an emerging environmental contaminant: Pollution, toxicity, bioremediation progress, and remaining challenges. J. Environ. Sci., 127: 234–250 (**17 pages**).

Mandal, A.H.; Sadhu, A.; Ghosh, S.; Saha, N.C.; Mossotto, C.; Pastorino, P.; Saha, S.; Faggio, C., (2025). Evaluating the impact of neonicotinoids on aquatic non-target species: A comprehensive review. Environ. Toxicol. Pharmacol., 113: 104606 (**10 pages**).

Manaros, M.; Gurbuz, I.B., (2020). Assessment of labor issues faced by the coconut producer in Lanao del Norte Province. Erwerbs-Obstbau, 62(2): 195–200 (**6 pages**).

Manjeri, G.; Muhamad, R.; Faridah, Q.Z.; Tan, S.G., (2011). Genetic variation studies in Oryctes rhinoceros (L.) (Coleoptera: Scarabaeidae) from oil palm plantations using random amplified microsatellite (RAMs) markers. Afr. J. Biotechnol., 10(14): 2611-2617 (**7 pages**).

Manjunatha, C.; Velavan, V.; Rangeshwaran, R.; Mohan, M.; Kandan, A.; Sivakumar, G.; Shylesha, A.N.; Kumar, M.P.; Pramesh, D.; Sujithra, M.; Ranganath, H.K., (2023). Assessment of bio-formulations of indigenous strains of Bacillus thuringiensis, Metarhizium robertsii and Metarhizium majus for management of the rhinoceros beetle, Oryctes rhinoceros L., in field. Egypt. J. Biol. Pest Cont., 33(1): 45 (**6 pages**).

Manley, M.; Melzer, M.J.; Spafford, H., (2018). Oviposition preferences and behavior of wild-caught and laboratory-reared coconut rhinoceros beetle, Oryctes rhinoceros (Coleoptera: Scarabaeidae), in relation to substrate particle size. Insects, 9(4) 141 (**7 pages**).

Mansfield, S.; Asigau, B.; van Koten, C.; Paudel, S.; Bowie, M.; Jackson, T.; Marshall, S., (2024). Assessment of coconut palm damage caused by coconut rhinoceros beetle, Oryctes rhinoceros (Coleoptera: Scarabaeidae). N.Z. J. Crop Hortic. Sci., 52(4): 336-357 (**22 pages**).

Marques, M.B.L.; Brunetti, I.A.; Faleiros, C.A.; da Cruz, C.; Iqbal, H.M.N.; Bilal, M.; Américo-Pinheiro, J.H.P., (2021). Ecotoxicological assessment and environmental risk of the insecticide chlorpyrifos for aquatic neotropical indicators. Water Air Soil Pollut. 232(10) 428 (**14 pages**).

Marshall, S.D.G.; Moore, A.; Vaqalo, M.; Noble, A.; Jackson, T.A., (2017). A new haplotype of the coconut rhinoceros beetle, Oryctes rhinoceros, has escaped biological control by Oryctes rhinoceros nudivirus and is invading Pacific Islands. J. Invertebr. Pathol., 149: 127-134 (**8 pages**).

Meys, E.L.; Mineau, P.; Werts, P.; Nelson, S.G.A.; Larson, A.; Hutchison, W.D, (2024). Assessment of insecticide risk quantification methods: Introducing the pesticide risktool and its improvements over the environmental impact Quotient. J. Integr. Pest Manag., 15(1) (**14 pages**).

Mohan, K.; Padmanaban, A.M., (2013). Biotoxicity assay of neem (Azadirachta indica) products and distillery effluent on the third instar larvae of coconut rhinoceros beetle Oryctes rhinoceros. International J. Pharma Bio Sci., 4(4): 102-110 (**9 pages**).

Nenotek, P.S.; Simamora, A.V.; Hahuly, M.V.; Nahas, A.E.; Ludji, R.; Henuk, J.B.D.; Mudita, I.W.; Pratama, F.; Kune, M.R.B., (2024). Damage intensity and geographic distribution of Oryctes rhinoceros on coconut in Rote-Ndao, East Nusa Tenggara Province, Indonesia. IOP Conference Series: Earth Environ. Sci.,, 1346(1): 012015 (**10 pages**).

Oltramare, C.; Mediouni, Z.; Shoman, Y.; Hopf, N.B.; Graczyk, H.; Berthet, A., (2023). Determinants of pesticide exposure in occupational studies: A meta-analysis. Toxics, 11(7), 623 (**20 pages**).

Omar, Z.; Fasleen, A.P., (2020). Unravelling the factors affecting agriculture profitability enterprise: Evidence from coconut smallholder production. Accounting, 6(4): 493-500 012013 (**8 pages**).

Omar, Z.; Fasleen, A.P., (2021). Determinants of technical efficiency among coconut smallholder production in Johor, Malaysia: a cobb douglas stochastic frontier production approach. IOP Conference Series: Earth Environ. Sci.,, 757(1) (**11 pages**).

Padmasheela, N.C.; Delvi, M.R., (2004). Effect of dimethoate (Rogor 30% EC) on the brain neurosecretory cells of third instar grubs of Oryctes rhinoceros L. (Coleoptera: Scarabaeidae). J. Environ. Biol., 25(4): 451-455 (**5 pages**).

Pakiam, G.K., (2020). Smallholder involvement in tree crops in malaya, with special reference to oil and coconut palms in Johor, 1862–1963. Aust. Econ. Hist. Rev., 60(2): 268-275 (**8 pages**).

Paudel, S.; Mansfield, S.; Villamizar, L.F.; Jackson, T.A.; Marshall, S.D.G., (2021). Can biological control overcome the threat from newly invasive coconut rhinoceros beetle populations (Coleoptera: Scarabaeidae)? A review. Ann. Entomol. Soc. Am., 114(2): 247–256 (**10 pages**).

Paudel, S.; Jackson, T.A.; Boulekouran, S.; Tasale, J.; Garae, B.; Allanson, P.; Ero, M.; Marshall, S.D.G., (2023). The coconut rhinoceros beetle (Oryctes rhinoceros) outbreak is well established on Efate, Vanuatu. EPPO Bull., 53(2): 404-410 (**7 pages**).

Paudel, S.; Soares, G.; Ximenes, A.; Richards, N.K.; Jackson, T.A.; Marshall, S.D.G., (2025). Confirmation of presence of coconut rhinoceros beetle Oryctes rhinoceros (Coleoptera: Scarabaeidae) from Timor-Leste and biosecurity implications. EPPO Bull., 55(2): 250-254 (**5 pages**).

Perry, E.D.; Moschini, G.C., (2020). Neonicotinoids in U.S. maize: Insecticide substitution effects and environmental risk. J. Environ. Econ. Manag., 102: 102320 (**19 pages**).

Pradana, M.G.; Siallagan, I.A.; Guntoro, G.; Susanto, A., (2023). Evaluation of packaging design for pheromone product to control Oryctes rhinoceros in oil palm plantation. IOP Conference Series: Earth Environ. Sci.,, 1133(1) (**6 pages**).

Prasad, G.S., (2008a). Bio-suppression of coconut rhinoceros beetle, Oryctes rhinoceros L. (Coleoptera: Scarabaeidae) by Oryctes baculovirus (Kerala isolate) in South Andaman, India. Crop Prot. 27(6): 959-964 (**6 pages**).

Prasad, G.M.; Jayakumar, V.; Ranganath, H.R.; Bhagwat, V.R., (2008b). Management of coconut rhinoceros beetle (Oryctes rhinoceros) by augmentation of Oryctes baculovirus (Kerala isolate) in Little Andaman Islands. India. J. Agric. Sci., 78(11): 962-965 (**4 pages**).

Prastowo, S.; Rondonuwu, S.B.; Wahid, A., (2022). Virulence of Metarhizium isolated from infected Oryctes rhinoceros L. (Coleoptera: Scarabaeidae) larvae around coconut plantations in East Java, Indonesia. Egypt. J. Biol. Pest Cont., 32(1): 146 (**11 pages**).

Pujiastuti, Y.; Sandi, S.; Arsi, A.; Sulistyani, D.P., (2020). Toxicity of Bacillus thuringiensis Berl. KJ3P1 and DLM isolates towards pest of oil palm Oryctes rhinoceros (Coleoptera: Scarabaeidae). IOP Conference Series: Earth Environ. Sci.,, 497(1): 012029 (**7 pages**).

Pujiastuti, Y.; Sandi, S.; Arsi, A.; Sulistyani, D.P., (2021). Insecticidal activity of supernatant and crude extract of Bacillus thuringiensis-based bio-insecticide towards oil palm pests Oryctes rhinoceros (Coleoptera: Scarabaeidae). IOP Conference Series: Earth Environ. Sci., 709(1): 012070 (**6 pages**).

Pujiastuti, Y.; Suparman, S.H.K.; Umayah, A., (2023). Potency of Bacillus thuringiensis in liquid formulation as a biological agent in controlling larvae of Oryctes rhinoceros (Coleoptera: Scarabaeidae). E3S Web Conference, 373: 07010 (**7 pages**).

Rafie, M.B.S.A.; Amit, S., (2024). Susceptibility of Oryctes rhinoceros beetle to trunk-injected acephate and trunk-implanted acephate controlled-release insecticide on tall palms via petiole bioassay. Serangga, 29(2): 200-209 (**10 pages**).

Rajan, D.K.; Mohan, K.; Rajarajeswaran, J.; Divya, D.; Thanigaivel, S.; Zhang, S., (2024). Toxic effects of organophosphate pesticide monocrotophos in aquatic organisms: A review of challenges, regulations and future perspectives. Environ. Res., 244: 117947 (**12 pages**).

Ramle, M.; Wahid, M.B.; Norman, K.; Glare, T.R.; Jackson, T.A., (2005). The incidence and use of Oryctes virus for control of rhinoceros beetle in oil palm plantations in Malaysia. J. Invertebr. Pathol., 89(1): 85-90 (**6 pages**).

Rani, S.; Rajakumar, D.; Shoba, N.; Maheswarappa, H.P., (2018). Productivity and economic advantages of flower crops in coconut based intercropping system. Indian J. Hortic., 75(2), 279–282 (**4 pages**).

Rao, N.B.V.C.; Snehalatharani, A.; Nischala, A.; Ramanandam, G.; Maheswarappa, H.P., (2018). Management of rhinoceros beetle (Oryctes rhinoceros L.) by biological suppression with oryctes baculovirus in Andhra Pradesh. J. Plant. Crops. 46(2): 124-127 (**4 pages**).

Roudhiyah, H.N.; Saepuloh, A.; Wibowo, A.S.; Irwansyah, (2024). The use of unmanned aerial vehicle for controlling Oryctes rhinoceros beetle on immature oil palm. IOP Conference Series: Earth Environ. Sci., 1308(1): 012042 (**11 pages**).

Rozziansha, T.A.P.; Simarmata, N.; Wijayanti, E.; Tantawi, A.R., (2025). Development and virulence of Metarhizium anisopliae in several liquid media against Oryctes rhinoceros larvae (Coleoptera: Scarabaeidae). IOP Conference Series: Earth Environ. Sci., 1494: 012028 (**9 pages**).

Rusli, A.L.; Isa, N., (2021). Smallholders perception on the roles of extension agent - coconut industry sustainability in Tanjong Karang, Selangor, Malaysia. Food Res., 5: 83-91 (**9 pages**).

Russo, M.; Waisen, P.; Choi, K.; Cheng, Z., (2026). Efficacies of systemic insecticides against the coconut rhinoceros beetle, Oryctes rhinoceros (Coleoptera, Scarabaeidae), on O'ahu, Hawai'i. Int. J. Trop. Insect Sci., 46(2): 1633-1642 (**10 pages**).

Sadhu, A.; Mandal, A.H.; Ghosh, S.; Lakdawala, P.; Saha, S., (2024). Dimethoate-induced toxicity: A comprehensive review of its aquatic environmental hazards. Toxicol. Environ. Health Sci., 16(3): 243–258 (**16 pages**).

Sarker, A.; Kim, D.; Jeong, W.-T., (2024). Environmental fate and sustainable management of pesticides in soils: A critical review focusing on sustainable agriculture. Sustainability, 16(23): 10741 (**25 pages**).

Shen, M.W.; Chen, H-C.; Chen, S-T., (2025). Environmental factors in Oryctes rhinoceros (Coleoptera: Scarabaeidae) Breeding. J. Appl. Entomol., 149(2): 178-186 (**9 pages**).

Sondakh, L.; Hardaker, J.B., (1983). Growth and equity aspects of alternative credit allocation policies for the smallholder coconut development programme in Indonesia. Rural Development Growth and Inequity Papers from 18th IAAE Conference: 194-201 (**8 pages**).

Sousa, A.S.; Duaví, W.C.; Cavalcante, R.M.; Milhome, M.A.L.; do Nascimento, R.F., (2016). Estimated levels of environmental contamination and health risk assessment for Herbicides and Insecticides in Surface Water of Ceará, Brazil. Bull. Environ. Contam. Toxicol., 96(1): 90-95 (**6 pages**).

Sponsler, D.B.; Grozinger, C.M.; Hitaj, C.; Rundlöf, M.; Botías, C.; Code, A.; Lonsdorf, E.V.; Melathopoulos, A.P.; Smith, D.J. Suryanarayanan, S.; Thogmartin, W.E.; Williams, N.M.; Zhang, M.; Douglas, M.R. (2019). Pesticides and pollinators: A socioecological synthesis. Sci. Total Environ., 662, 1012–1027 (**16 pages**).

Sujithra, M.; Rajkumar, M.; Mhatre, P.H.; Guru-Pirasanna-Pandi, G., (2022). Biocontrol potential of native entomopathogenic nematodes against coconut rhinoceros beetle, Oryctes rhinoceros (L.) (Coleoptera: Scarabaeidae) under laboratory conditions. Egypt. J. Biol. Pest Control. 32(1): 1-9 (**9 pages**).

Sulaiman, S.K.B.; Ibrahim, Y.; Jeffree, M.S., (2020). Evaluating the perception of farmers towards pesticides and the health effect of pesticides: A cross-sectional study in the oil palm plantations of Papar, Malaysia. Interdiscip. Toxicol., 12(1): 15–25 (**11 pages**).

Surbakti, R.L.B.; Marheni; Bakti, D., (2025). Evaluating the potential of gut bacteria in Oryctes rhinoceros larvae as biocontrol agents against Ganoderma boninense pathogen in oil palm plantations. Biodiversitas, 26(3): 1414-1423 (**10 pages**).

Tanaka, S.; Harrison, R.L.; Arai, H.; Katayama, Y.; Mizutani, T.; Inoue, M.N.; Miles, J.; Marshall, S.D.G.; Kitalong, C.; Nakai, M., (2021). Confirmation of Oryctes rhinoceros nudivirus infections in G-haplotype coconut rhinoceros beetles (Oryctes rhinoceros) from Palauan PCR-positive populations. Sci. Rep., 11(1): 18820 (**12 pages**).

Tay, W.T.; Marshall, S.D.G.; Popa-Baez, A.D.; Dulla, G.F.J.; Blas, A.L.; Sambiran, J.W.; Hosang, M.; Millado, J.B.H.; Melzer, M.; Rane, R.V.; Hogarty, T.; Cho D.Yi-C.; Alouw, J.C.; Faheem, M.; Hoffmann, B.D., (2024). Alternative DNA markers to detect Guam-specific CRB-G (clade I) Oryctes rhinoceros (Coleoptera: Scarabaeidae) indicate that the beetle did not disperse from Guam to the Solomon Islands or Palau. Diversity, 16(10): 634 (**12 pages**).

Thetkathuek, A.; Yenjai, P.; Jaidee, W.; Jaidee, P.; Sriprapat, P., (2017). Pesticide exposure and cholinesterase levels in migrant farm workers in Thailand. J. Agromed., 22(2): 118–130 (**13 pages).**

Tito, S.I.; Zayadi, H.; Laili, S.; Djuhari, (2026). Effectiveness test of Marshal 5G on larvae and imago Oryctes rhinoceros in a community oil palm plantation Pelalawan Regency, Riau, Indonesia. BIO Web Conference, 209: 01011 (**9 pages**).

Top, Z.N.; Tiriyaki, O.; Polat, B., (2023). Monitoring and environmental risk assessment of agricultural fungicide and insecticides in water, sediment from Kumkale Plain, Çanakkale-Turkey. J. Environ. Sci. Health Part B., Pesticides Food Contaminants and Agricultural Wastes. 58(4): 304-315 (**12 pages**).

Venkatarajappa, P., (2001). Residual toxicity of Cypermethrin in the larvae of coconut pest Oryctes rhinoceros (Coleoptera: Scarabaeidae). J. Environ. Biol., 22(1): 19-21 (**3 pages**).

Villamizar, L.F.; Barrera, G.P.; Luange, A.; Sagata, K.; Gende, P.; Chris, S.; Tsatsia, H.; Mudu, F.; Weston, M.; van Koten, C.; Mansfield, S.; Jackson, T.A.; Marshall, S.D.G., (2024). Characterization and screening of new Metarhizium isolates to control the coconut rhinoceros beetle in the Pacific islands. Fungal Biol., 128(7): 2127–2138 (**12 pages**).

Wan, N-F.; Fu, L.; Dainese, M.; Kiær, L.P.; Hu, Y-Q.; Xin, F.; Goulson, D.; Woodcock, B.A.; Vanbergen, A.J.; Spurgeon, D.J.; Shen, S.; Scherber, C., (2025). Pesticides have negative effects on non-target organisms. Nat. Comm., 16(1), 1360 (**16 pages**).

Wandri, R.; Alam, S.; Ayundra, S.D.; Apriansa, A.; Asmono, D.; Subeki, S.; Fitriana, Y.; Hasibuan, R.; Suharjo, R., (2024). First report: Senna multijuga subsp. multijuga (Fabales: Fabaceae) as an attractant and bioinsecticide for Oryctes rhinoceros (Coleoptera: Scarabaeidae). Agriculture, 14(9): 1477 (**16 pages**).

Wei, X.; Vowell, T.; Nikaido, S.; Ho, J.; Kong, A.; Weiser, K.; Jenkins, D.; Melzer, M., (2025). Evaluating the persistence of pyrethrin and pyrethroid insecticides in coconut palm (Cocos nucifera) canopies for coconut rhinoceros beetle (Oryctes rhinoceros) management. Proc. Hawaii. Entomol. Soc., 57: 25–34 (**10 pages**).

Wendell, A.-K.; Guse, B.; Bieger, K.; Wagner, P.D.; Kiesel, J.; Ulrich, U.; Fohrer, N., (2024). A spatio-temporal analysis of environmental fate and transport processes of pesticides and their transformation products in agricultural landscapes dominated by subsurface drainage with SWAT+. Sci. Total Environ., 945: 173629 (**12 pages**).

Weston, M.K.; Hefer, C.A.; Jacobs, J.M.E.; Marshall, S.D.G., (2023). Complete genome sequences of six isolates of the Oryctes rhinoceros nudivirus. Microbiol. Resour. Announc., 12(8) (**2 pages**).

Wulandari, S.; Alouw, J.C., (2021). Scheme to support coconut replanting program on smallholder plantation. IOP Conference Series: Earth Environ. Sci.,, 892(1) 012088 (**10 pages**).

Xu, D.; Zhuo, Z.; Li, X.; Wang, R., (2022). Distribution and invasion risk assessment of Oryctes rhinoceros (L.) in China under changing climate. J. Appl. Entomol., 146: 385–395 (**11 pages**).

Yapo, K.M.A.A.; Cissé, M.C.; Nigué, L.; Sess, D., (2017). Variations in cholinesterase activity in oil palm plantation workers exposed to pesticides. Greener J. Biol. Sci., 7(1): 008–014 (**6 pages**).

Zelazny, B., (1985). Susceptibility of two coconut Pests, Oryctes rhinoceros [Col.: Scarabaeidae] and Tirathaba rufivena [Lep.: Pyralidae], to the entomoparasitic nematode Steinernema feltiae [= Neoaplectana carpocapsae]. Entomophaga, 30(2): 121-124 (**4 pages**).

Zelazny, B.; Alfiler, A.L., (1987). Ecological methods for adult populations of Oryctes rhinoceros (Coleoptera, Scarabaeidae). Ecol. Entomol., 12(2): 227-238 (**12 pages**).

Zhang, X.; Cao, Y.; Zhang, Z.; Li, Q.; Yan, Y.,(2024). Residues of neonicotinoid insecticides in artificial waterways of the Eastern Route of the South-to North water diversion project, China: implications for environmental risks and human health. Environ. Pollut., 363: 123132 (**10 pages**).

Zhao, Y.; Yang, J.; Ren, J.; Hou, Y.; Han, Z.; Xiao, J.; Li, Y., (2020). Exposure level of neonicotinoid insecticides in the food chain and the evaluation of their human health impact and environmental risk: an overview. Sustainability, 12(18): 7523 (**26 pages**).

AUTHOR (S) BIOSKETCHES

Hosang, M.L.A., Dr., Professor, Research Center for Estate Crops, National Research and Innovation Agency, Jl. Raya Jakarta-Bogor, Cibinong, Bogor 16911, Indonesia.
- Email: *meld001@brin.co.id*
- ORCID: 0009-0003-7173-1388
- Web of Science Researcher ID: KDO-7152-2024
- Scopus Author ID: 6603962646
- Homepage: https://brin.go.id/orpp

Susilawati, M.Sc., Researcher, Research Center for Estate Crops, National Research and Innovation Agency, Jl. Raya Jakarta-Bogor, Cibinong, Bogor 16911, Indonesia.
- Email: *susi018@brin.go.id*
- ORCID: 0009-0001-6684-7576
- Web of Science Researcher ID: NOF-2032-2025
- Scopus Author ID: 60024156100
- Homepage: https://brin.go.id/orpp

Alouw, J.C., Ph.D., Researcher, Research Centre for Estate Crops, National Research and Innovation Agency, Jl. Raya Jakarta-Bogor, Cibinong, Bogor 16911, Indonesia.
- Email: *jelf001@brin.go.id*
- ORCID: 0000-0002-4831-125X
- Web of Science Researcher ID: PPI-1326-2026
- Scopus Author ID: 37013146700
- Homepage: https://brin.go.id/orpp

Puspitasari, M., M.Sc., Researcher, Research Centre for Estate Crops, National Research and Innovation Agency, Jl. Raya Jakarta-Bogor, Cibinong, Bogor 16911, Indonesia.
- Email: *maha011@brin.go.id*
- ORCID: 0009-0001-5492-8985
- Web of Science Researcher ID: DRV-9885-2022
- Scopus Author ID: 57223910872
- Homepage: https://fp.ub.ac.id

Senewe, R.E., Dr. Ir., M.Sc., Researcher, Research Centre for Estate Crops, National Research and Innovation Agency, Jl. Raya Jakarta-Bogor, Cibinong, Bogor 16911, Indonesia.
- Email: *rein001@brin.go.id*
- ORCID: 0000-0001-5137-1248
- Web of Science Researcher ID: NA
- Scopus Author ID: 57222319762
- Homepage: https://brin.go.id/orpp

Sujak, M.Sc., Researcher, Research Centre for Estate Crops, National Research and Innovation Agency, Jl. Raya Jakarta-Bogor, Cibinong, Bogor 16911, Indonesia.
- Email: *suja007@brin.go.id*
- ORCID: 0000-0003-3815-5908
- Web of Science Researcher ID: GDR-8435-2022
- Scopus Author ID: 58074704800
- Homepage: https://brin.go.id/orpp

Rohimatun, R., Dr., Researcher, Research Center for Estate Crops, National Research and Innovation Agency, Jl. Raya Jakarta-Bogor KM 46, Cibinong 16911, Indonesia.
- Email: *rohimatun@brin.go.id*
- ORCID: 0000-0003-4403-7553
- Web of Science Researcher ID: JFK-5318-2023
- Scopus Author ID: 57200729272
- Homepage: https://brin.go.id/orpp

Hutasoit, R.T., M.Sc., Researcher, Research Centre for Estate Crops, National Research and Innovation Agency, Jl. Raya Jakarta-Bogor, Cibinong, Bogor 16911, Indonesia.
- Email: *rudi026@brin.go.id*
- ORCID: 0000-0002-7954-5016
- Web of Science Researcher ID: QTT-3603-2026
- Scopus Author ID: 57218268990
- Homepage: https://brin.go.id/orpp

Subiyakto, Dr., Senior Researcher, Research Centre for Estate Crops, National Research and Innovation Agency, Jl. Raya Jakarta-Bogor, Cibinong, Bogor 16911, Indonesia.
- Email: *subi007@brin.go.id*
- ORCID: 0000-0002-0047-7373
- Web of Science Researcher ID: GDS-2144-2022
- Scopus Author ID: 58314357300
- Homepage: https://brin.go.id/orpp

Nurindah, Ph.D., Professor, Research Centre for Estate Crops, National Research and Innovation Agency, Jl. Raya Jakarta-Bogor, Cibinong, Bogor 16911, Indonesia.
- Email: *nurindah@brin.go.id*
- ORCID: 0000-0003-4389-0261
- Web of Science Researcher ID: E-3444-2014
- Scopus Author ID: 58315849300
- Homepage: https://brin.go.id/orpp

Sunarto, D.A., Dr., Senior researcher, Research Center for Estate Crops, National Research and Innovation Agency, Jl. Raya Jakarta-Bogor, Cibinong, Bogor 16915, Indonesia.
- Email: *dwia021@brin.co.id*
- ORCID: 0000-0002-5579-8369
- Web of Science Researcher ID: GCB-0905-2022
- Scopus Author ID: 57203264481
- Homepage: https://brin.go.id/orpp

Meththananda, R.G.U.I., MPhil., Researcher, Department of Computational Mathematics, Faculty of Computing, General Sir John Kotelawala Defence University, Rathmalana, Sri Lanka
- Email: *umameththananda@kdu.ac.lk*
- ORCID: 0000-0003-1251-364X
- Web of Science Researcher ID: NA
- Scopus Author ID: 57216924210
- Homepage: https://foc.kdu.ac.lk

Pinaria, B.A.N., Dr., Lecturer, Department of Plant Protection, Faculty of Agriculture, Sam Ratulangi University, Manado, Indonesia.
- Email: *betsypinaria@unsrat.ac.id*
- ORCID: 0009-0005-5338-5105
- Web of Science Researcher ID: GQB-2083-2022
- Scopus Author ID: 57226505427
- Homepage: https://foc.kdu.ac.lk

HOW TO CITE THIS ARTICLE:
Hosang, M.L.A.; Susilawati; Alouw, J.C.; Puspitasari, M.; Senewe, R.E.; Sujak; Rohimatun, R.; Hutasoit, R.T., Subiyakto; Nurindah; Sunarto, D.A., Meththananda, R.G.U.I.; Pinaria, B.A.N., (2027). Environmental risks of pest management practices in smallholder coconut plantations. Global J. Environ. Sci. Manage., 13(1): 501-522.

DOI: 10.22034/gjesm.2027.01.23
URL: https://www.gjesm.net/article_735736.html

Global J. Environ. Sci. Manage. 13(1): 523-552, Winter 2027, Serial #49

Global Journal of Environmental Science and Management
(GJESM)

Homepage: https://www.gjesm.net/

Podcasts

REVIEW ARTICLE

A bibliometric and systematic analysis of artificial intelligence and the transition towards smart geotourism

T. Aguirre-Suárez[1,*], M. Pérez-Chiquito[1], H. Cochea-Tomalá[2], P. Escandón-Panchana[3,4]

[1]*Facultad de Ciencias Administrativas, Universidad Estatal Península de Santa Elena, La Libertad, 240204 Ecuador*

[2]*Facultad de Ciencias Sociales y de la Salud, Universidad Estatal Península de Santa Elena, La Libertad, 240204 Ecuador*

[3]*Escuela de Ciencias Ambientales, Universidad Espíritu Santo, Samborondón, Ecuador*

[4]*Departamento de Ingeniería Cartográfica y Topografía, Universidad Politécnica de Madrid, Crta. Valencia km 7, 28031-Madrid, Spain*

ARTICLE INFO

Article History:
Received 28 May 2026
Revised 05 July 2026
Accepted 12 August 2026

Keywords:
Artificial intelligence
Geoheritage
Smart geotourism
Smart tourism
Territorial planning
Sustainability

DOI:10. 22034.gjesm.2027.01.24

ABSTRACT

The rapid digital transformation of tourism has positioned artificial intelligence as a key enabler of destination intelligence, data-driven decision-making, and sustainable tourism management. Although artificial intelligence has become increasingly important in smart tourism research, its application to geotourism remains fragmented, particularly regarding geoheritage conservation, geodiversity management, and territorial planning. Employing a retrospective approach, this study delineates the developmental trajectory of artificial intelligence applications in sustainable tourism while interrogating their integration into the paradigm of smart geotourism. An integrated bibliometric analysis and systematic literature review were conducted to evaluate scientific developments and empirical applications of artificial intelligence within geotourism contexts. Such findings delineate a burgeoning field of inquiry structured through the convergence of three intersecting axes: technological advancement, analytical intelligence, and visitor-focused experiential paradigms. The review study identified four principal domains through which artificial intelligence contributes to geotourism: predictive analytics, smart destination management, geoheritage interpretation, and environmental monitoring and geoconservation. The findings further highlight significant regional differences in technological adoption and reveal a limited integration between artificial intelligence, geoheritage conservation, and sustainable territorial governance. Based on these findings, the study proposes a smart geotourism framework that connects artificial intelligence, smart tourism, geoheritage conservation, and territorial planning within a unified conceptual structure. By delivering an integrated appraisal of artificial intelligence within geotourism, this study contributes to extant scholarship by conceptualizing artificial intelligence beyond its technical dimensions—positioning it as a fundamental enabler of empirical territorial planning, destination analytics, and the sustainable preservation of geological resources. The study objectives were to propose an integrated conceptual framework that connects artificial intelligence, smart tourism, geoheritage conservation, and territorial planning to support the development of smart geotourism.

This is an open access article under the CC BY license (http://creativecommons.org/licenses/by/4.0/)

NUMBER OF REFERENCES	NUMBER OF FIGURES	NUMBER OF TABLES
131	9	3

*Corresponding Author:
Email: taguirre@upse.edu.ec
Phone: +593 98 512 8886
ORCID: 0000-0001-8077-8522

Note: Discussion period for this manuscript open until March 01, 2027 on GJESM website at the “Show Article”.

INTRODUCTION

The digital transformation of tourism is reshaping how destinations are planned, governed, and experienced. Advances in digital infrastructures, geospatial technologies, and data-driven decision-making have accelerated the transition from conventional tourism management towards smart tourism (Mehraliyev *et al.,* 2020; Zhang *et al.,* 2022). Rather than representing only the adoption of digital technologies, smart tourism constitutes a new governance paradigm based on interconnected ecosystems, intelligent networks, collaborative destination management, and data-driven decision-making (Gretzel *et al.,* 2015). Thus, smart tourism effectively couples technological innovation with sustainable destination stewardship and elevated experiential outcomes for visitors (Madzík *et al.,* 2023; Wu *et al.,* 2024). In the context of this transformation, artificial intelligence (AI) has emerged as one of the principal enabling technologies of smart destinations (Knani *et al.,* 2022; Saydam *et al.,* 2022). Recent advances in machine learning (ML), deep learning (DL), natural language processing (NLP), and predictive analytics have significantly expanded the analytical capacity of tourism organisations by facilitating demand forecasting, visitor behavior analysis, mobility modelling, and personalised service provision (Alhaddar and Kummitha, 2025; Hu *et al.,* 2022; Laesser *et al.,* 2025; Núñez *et al.,* 2024). Moreover, AI applications augment operational efficacy by leveraging recommender frameworks, conversational interfaces, and automated decision-support architectures, thereby facilitating more responsive destination management in the face of fluctuating tourism demands (Alves *et al.,* 2023; Ku and Chen, 2024). Consequently, AI is recognized not only as a technological innovation but also as a strategic instrument for destination intelligence and adaptive tourism governance within increasingly complex tourism systems (Baggio and Del Chiappa, 2014). AI is becoming increasingly relevant for addressing the sustainability challenges facing tourism destinations. The growing pressure on natural resources, biodiversity, and local communities requires planning approaches that balance tourism development with environmental conservation and social well-being (Hall, 2019; Santos *et al.,* 2021; Silva *et al.,* 2024). AI contributes to this objective through predictive modelling, environmental monitoring, optimisation of resource consumption, intelligent transport management, and spatial analysis, supporting more sustainable destination planning (García-Madurga and Grilló-Méndez, 2023; Majid *et al.,* 2023). By integrating geospatial technologies, remote sensing, and big data analytics, AI underpins territorial intelligence, harmonizing heterogeneous environmental and tourism streams into comprehensive decision-support systems (Flórez *et al.,* 2024; Parra-Sanchez and Viviescas-Jaimes, 2024). This convergence aligns with the sustainable development goals (SDGs), particularly those promoting sustainable cities, responsible consumption, climate action, and ecosystem conservation (Naciones Unidas, 2025). These advances are particularly relevant for geotourism, a specialized form of sustainable tourism centered on the conservation, interpretation, and appreciation of geoheritage and geodiversity (Gupta *et al.,* 2024; Kubalíková *et al.,* 2021). Diverging from conventional nature-based tourism paradigms, geotourism explicitly synthesizes geoconservation efforts with academic education, scientific knowledge transfer, and local economic stimulation via the valorization of geosites, geoparks, and distinctive geomorphological landscapes (Drinia *et al.,* 2023; Quesada-Valverde and Quesada-Román, 2023; Spyrou *et al.,* 2024). This territorial perspective is consistent with place-based approaches to tourism development that emphasise resilience, destination stewardship, and landscape management (Lew, 2014). In this context, geoparks function as territorial governance systems where conservation, community

participation, education, and sustainable development are integrated within a place-based management framework (Rosado-González *et al.,* 2023; Salgado-Jauregui *et al.,* 2025). This perspective on governance is intrinsically linked to sustainability transitions that frame tourism destinations as complex socio-ecological systems demanding adaptive territorial stewardship (Saarinen, 2013). Consequently, the long-term success of geotourism increasingly depends on destinations' capacity to combine geoheritage conservation with intelligent territorial planning, adaptive governance, and data-driven management. While investigation into AI applications in tourism has grown exponentially and geotourism is recognized as a cornerstone of sustainable tourism literature, the two areas continue to progress largely decoupled from each other. This separation also reflects the broader evolution of tourism research towards experience-oriented and creative destination development, where technological innovation has often progressed independently of place-based heritage management (Richards, 2021). Within the proposed framework, smart geotourism is distinguished from related concepts by its simultaneous integration of geoheritage conservation, geodiversity management, destination intelligence, and evidence-based territorial governance. Smart tourism primarily emphasises digital innovation and intelligent destination services (Koo *et al.,* 2025a); geotourism focuses on the appreciation and conservation of geological heritage (Ferdowsi and Németh, 2026); sustainable tourism seeks balanced environmental, social, and economic development (Khater *et al.,* 2025); and geological heritage tourism concentrates on visitation associated with geosites and geological assets (Salvadeo *et al.,* 2025). Smart geotourism advances these frameworks through the incorporation of intelligent spatial analytics and adaptive governance mechanisms, thereby ensuring the enduring viability and conservation of geoheritage. Existing studies primarily investigate AI applications for tourism demand forecasting, recommendation systems, destination management, and visitor behavior analysis (Ma, 2025; Wang *et al.,* 2025), whereas geotourism research mainly focuses on geoheritage conservation, environmental education, geosite assessment, and territorial development (Carrillo-Hernández *et al.,* 2024; Gupta *et al.,* 2024; Quesada-Román *et al.,* 2021). Consequently, a significant gap remains in understanding how AI mechanisms can be leveraged to advance the governance, strategic planning, preservation, and sustainable administration of geoheritage within contemporary smart tourism destinations. From the perspective of the mobilities paradigm, tourism destinations are increasingly understood as dynamic networks of people, technologies, information, and places rather than static geographical locations (Sheller and Urry, 2006). Consequently, understanding how AI interacts with geoheritage requires integrating technological innovation with territorial mobility, governance, and destination intelligence. This fragmentation also characterises the review literature. The proposed framework is underpinned by the theoretical nexus of smart tourism theory, territorial governance theory, socio-ecological systems theory, and destination intelligence paradigms. Smart tourism theory explains how digital infrastructures and AI support intelligent destination management (Koo *et al.,* 2025b); territorial governance theory emphasises coordination among public, private, and community actors (Torre, 2025); socio-ecological systems theory conceptualises geoheritage destinations as coupled human–environment systems (Esengulova *et al.,* 2026); and destination intelligence provides the analytical link through which AI-generated knowledge informs geoconservation, geodiversity management, and adaptive territorial decision-making (Ferdowsi *et al.,* 2025). Current bibliometric investigations characterize the application of artificial intelligence in tourism through technical or

managerial paradigms, whereas scholarly reviews on geotourism tend to isolate conservation, educational dimensions, and geosite assessment. To the best of our knowledge, there is a significant paucity of research that combines bibliometric analysis with a systematic literature review to investigate how AI specifically contributes to smart geotourism through geoheritage conservation, territorial planning, and destination intelligence. To explicitly position the current research gap and the distinct value proposition of this study, Table 1 offers a comparative synthesis of existing reviews addressing artificial intelligence within tourism, smart destination frameworks, and geoheritage contexts. This comparison demonstrates that previous studies have mainly focused on technological adoption, operational efficiency, destination management, or sustainability dimensions. At the same time, limited attention has been given to integrating AI with geoheritage conservation, territorial planning, and geotourism governance. Therefore, despite the growing body of research on AI in tourism, an integrated understanding of how AI can support smart geotourism remains insufficiently developed. Consequently, this study addresses this void by synthesizing bibliometric techniques and systematic review protocols, thereby elucidating the developmental trajectory, empirical scope, and conceptual architecture of AI applications in geotourism development. This knowledge gap significantly limits both the conceptual understanding of smart geotourism and the development of robust, context-specific, and practically relevant evidence-based strategies that integrate technological innovation with territorial sustainability.Accordingly, this study addresses the following research questions (RQ): (i) RQ1: How has scientific knowledge on AI in sustainable tourism evolved, and what intellectual structures, collaboration patterns, and emerging research themes support the transition towards smart geotourism? (ii) RQ2: How is AI contributing to territorial planning, destination governance, geoheritage conservation, and sustainable management within geotourism? In order to examine these questions, the present study analyzes scientific publications on AI in sustainable tourism through a dual methodological design: an integrated bibliometric analysis utilizing Scopus and Web of Science (WoS), paired with a systematic literature review dedicated to geotourism applications. Specifically, the bibliometric component maps the intellectual landscape, thematic evolution, and international collaboration networks of the overarching discipline, complemented by a systematic review that consolidates empirical findings on AI technologies, application domains, sustainability dimensions, geoconservation outcomes, and smart tourism paradigms within geotourism. This study makes three principal contributions: i) it provides an integrated synthesis linking AI, smart tourism, geoheritage conservation, and geotourism through a combined bibliometric and systematic review approach. ii) proposes a conceptual framework that explains how AI functions as an enabler of smart geotourism by connecting destination intelligence, territorial planning, geoconservation, and sustainable tourism governance. iii) identifies four strategic domains through which AI is transforming geotourism: predictive analytics, smart destination management, geoheritage interpretation, and environmental monitoring and geoconservation, while highlighting current research gaps and future directions. These findings furnish both conceptual advancements regarding the emerging domain of smart geotourism and strategic implications for destination administrators, regulatory authorities, and regional planners striving to integrate digital innovation into the long-term management of geological heritage. The study aims is to propose an integrated conceptual framework that connects AI, smart tourism, geoheritage conservation, and territorial planning to support the development of smart geotourism. The study was carried out at UPSE University, Santa Elena, Ecuador, in 2026.

Table 1: Comparative overview of previous review studies on AI in tourism/geotourism and the distinctive contribution of the present study

S.N.	Author and year	Review type	Geoheritage / geotourism	Territorial planning / geoconservation	Bibliometric and systematic integration	Research scope and main contribution
1	(Knani *et al.,* 2022)	Bibliometric	No	No	No	Maps the evolution, intellectual structure, and future research agenda of AI applications in tourism and hospitality through large-scale bibliometric analysis.
2	(Doborjeh *et al.,* 2022)	Systematic literature review	No	No	No	Reviews AI methods, algorithms, data sources, and applications in hospitality and tourism, highlighting their role in forecasting, destination management, visitor behavior analysis, and personalised services.
3	(Samara *et al.,* 2020)	Systematic literature review	No	No	No	Examines the role of AI and big data in tourism, focusing on value creation, operational efficiency, personalised experiences, and the challenges of strategic adoption.
4	(Florido-Benítez and del Alcázar Martínez, 2024)	Literature review	No	Partial	No	Analyses how AI supports smart tourist destinations through marketing, personalised services, predictive analytics, enhanced visitor experiences, and digital destination management.
5	(Nannelli *et al.,* 2023)	Bibliometric and literature review	No	Partial	Partial	Examines the evolution of AI applications in hospitality and tourism, identifying emerging research directions and future opportunities for the sector.
6	(Aliyah *et al.,* 2023)	Conceptual review / literature-based study	No	Partial	No	Explores the integration of AI and Internet of Things (IoT) in smart tourism destinations, emphasising data-driven management, connectivity, and improved tourist experiences.
7	(Kirtil and Aşkun, 2021)	Bibliometric	No	No	No	Identifies influential authors, institutions, thematic structures, and emerging trends in AI research applied to tourism.
8	(El Archi *et al.,* 2023)	Systematic literature review	No	Partial	No	Synthesises research on smart tourism destinations and sustainable development, addressing economic, social, and environmental dimensions of destination management.
9	(Jabeen *et al.,* 2022)	Conceptual and empirical framework	No	No	No	Analyses organisational factors influencing the adoption of AI and automation in hospitality and tourism, including technological, human, and institutional dimensions.
10	(Solakis *et al.,* 2024)	Literature review	No	No	No	Examines AI-enabled value co-creation in tourism by identifying technological, behavioral, organisational, and relational factors shaping AI-mediated tourist experiences.
11	(Omosanya *et al.,* 2026)	Conceptual	Yes	Yes	No	Explores digital technologies for geoheritage conservation and sustainable geotourism, proposing a framework for digital transformation based on conservation, interpretation, and management needs.
12	(Sánchez-Sánchez *et al.,* 2026)	Bibliometric analysis and content analysis	No	Partial	Partial	Analyses the evolution of AI research in sustainable rural tourism, identifying trends related to governance, sustainability, employment, ethics, and community development.
13	(Henriques *et al.,* 2025)	Conceptual	Yes	Yes	No	Discusses digital geovisualization and AI-supported geointerpretation for geoheritage management, including inventory, education, visitor engagement, and conservation applications.

METHODOLOGY

This study employed an integrated approach, combining bibliometric analysis and a systematic review to investigate the relationships among AI, sustainable tourism, and geotourism. The analytical architecture of this study implements a multi-scale framework structured across two mutually reinforcing levels: i) a macro-level bibliometric analysis examining the evolution of AI in sustainable tourism, and ii) a micro-level systematic review focused on AI applications in geoheritage and geodiversity contexts. Integrating these two levels provides the basis for conceptualising the emerging field of smart geotourism. This dual-method strategy amalgamates quantitative and qualitative frameworks to comprehensively capture the trajectory of scientific growth, thematic transformation, and empirical applications characterizing the field. Fig. 1 presents the methodological framework adopted in the study. The methodological design followed a sequential analytical logic in which a macro-level bibliometric analysis characterized the evolution, intellectual structure, thematic dynamics, and international collaboration patterns of AI research in sustainable tourism, and a micro-level preferred reporting items for systematic reviews and meta-analyses (PRISMA)-based systematic review synthesized empirical evidence on AI applications in geoheritage, geodiversity, and geotourism. Ultimately, the insights yielded across both analytical scales were brought together to furnish the theoretical underpinning that defines smart geotourism as the convergence of destination intelligence, territorial planning, geoheritage conservation, and sustainable tourism governance. The first phase of the study consisted of identifying and collecting information through structured search strategies conducted on 15 March 2026 in the Scopus and WoS databases (Escandón-Panchana *et al.*, 2024; Mongeon and Paul-Hus, 2016). All data retrieval procedures were completed on a single day to control for temporal fluctuations in database indexing, thereby preserving the consistency and comparability of the dataset. Scopus and WoS were selected because they are the two most widely used multidisciplinary databases in bibliometric research, offering high-quality indexing standards, extensive international coverage, citation metadata, and export compatibility with bibliometric software such as Bibliometrix and VOSviewer (Martín-Martín *et al.*, 2018; Belu and Marinoiu, 2025). The synergistic use of these sources curtails database-driven bias, optimizes literature representation across tourism, sustainability, geoscience, and information technology domains, and elevates the analytical rigor of cross-disciplinary analyses (Mondal, 2026). The search strategy was designed to capture publications addressing AI within tourism and sustainability contexts. Searches were conducted in the title, abstract, and keywords fields in both databases without restricting subject categories.

Scopus query: TITLE-ABS-KEY [("artificial intelligence" OR AI OR "machine learning" OR "deep learning") AND ("tourism" OR "sustainable tourism" OR "ecotourism" OR "nature-based tourism" OR "smart tourism"]

WoS query: TS=[("artificial intelligence" OR AI OR "machine learning" OR "deep learning") AND ("tourism" OR "sustainable tourism" OR "ecotourism" OR "nature-based tourism" OR "smart tourism")]

No restrictions were applied regarding publication year, country, or subject area. The scope of the analyzed publication period spans 1993 through 2026—commencing with the earliest appearance of records satisfying the search protocol in Scopus and WoS, and concluding with the latest fully compiled annual data available during the retrieval phase. The analysis therefore covers the full historical range of retrievable publications on AI in tourism and

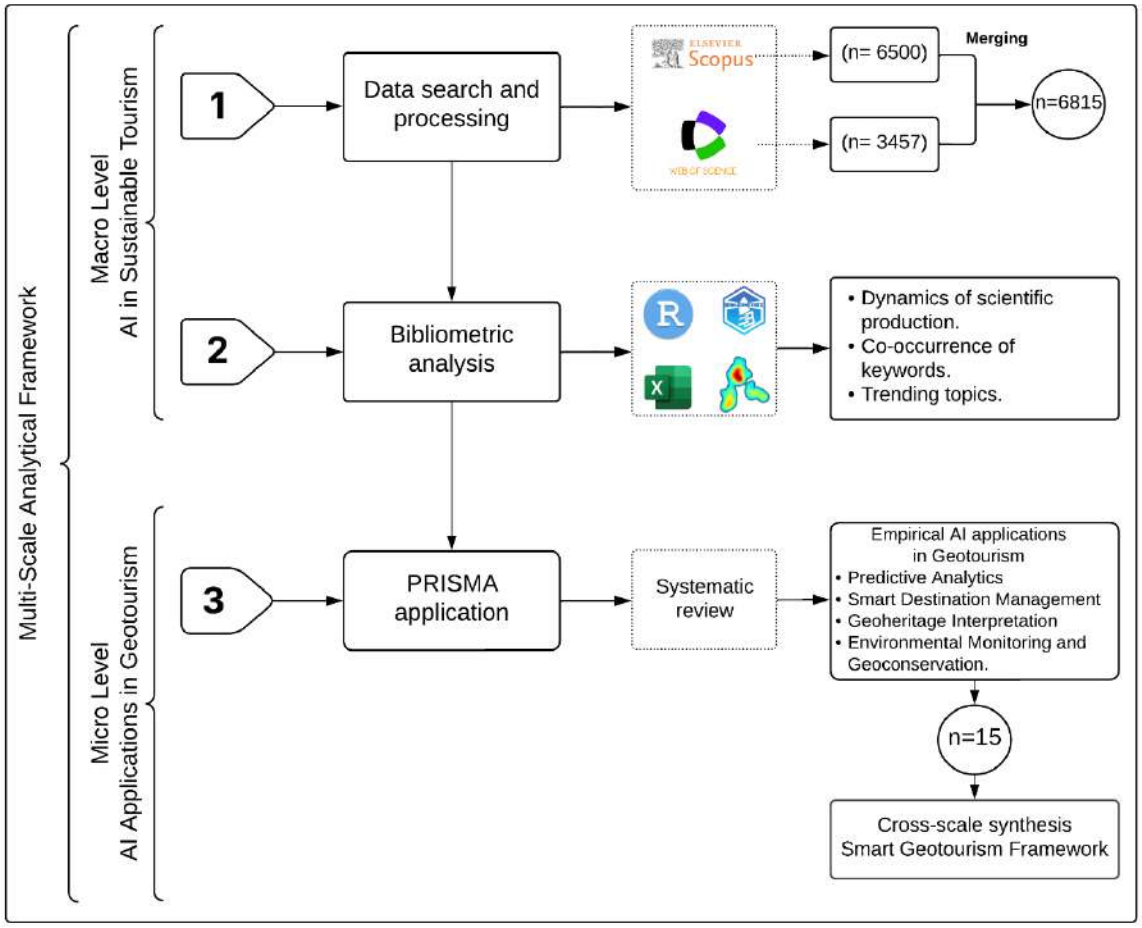

Fig. 1: Multi-scale methodological and conceptual framework integrating macro-level bibliometric analysis with a micro-level PRISMA-based systematic review to establish the foundations of the smart geotourism framework

sustainability rather than an arbitrarily selected period. It enables a longitudinal interpretation of technological evolution, capturing the transition from early exploratory AI applications in tourism during the 1990s, through the expansion of big data and digital tourism platforms after 2008, to the rapid development of ML, DL, conversational AI, and generative AI since 2017. Consequently, this observation window permits a comprehensive assessment of how artificial intelligence evolved from a minor technological interest into a central component governing destination intelligence, smart tourism frameworks, and the developing field of smart geotourism research. The retrieved records were exported in BibTeX (Scopus) and Plain Text (WoS) formats for subsequent integration and cleaning (Mitha and Omarsaib, 2025). To facilitate reproducibility, the bibliometric procedure followed four sequential steps: (i) execution of the Scopus and WoS queries on 15 March 2026; (ii) export of records in BibTeX and Plain Text formats; (iii) integration and duplicate removal using the Bibliometrix package in RStudio; and (iv) manual verification and cleaning prior to bibliometric analysis in Biblioshiny and VOSviewer. The same search strings, export formats, software versions, and cleaning criteria were applied throughout the process. No language filter was applied during the bibliometric retrieval stage in Scopus and WoS.

Consequently, to ensure comprehensive coverage, records indexed across all languages were systematically retrieved and compiled into the bibliometric database whenever they aligned with the search criteria. The language restriction was applied only during the PRISMA-based systematic review, where English-language publications were retained to ensure consistent screening, interpretation, and comparison of empirical evidence. Peer-reviewed journal articles and conference papers indexed in Scopus or WoS were selected for inclusion in the bibliometric dataset given their status as primary scholarly outputs capable of capturing cutting-edge artificial intelligence implementations prior to journal-bound release. In contrast, review articles, conference reviews, book chapters, editorials, notes, and other secondary publications were excluded from the systematic review to avoid double counting and to ensure that the synthesis was based on original empirical evidence. Owing to inconsistent indexing in Scopus and WoS and the frequent absence of rigorous peer review and complete bibliographic metadata, grey literature comprising theses, technical reports, policy briefs, and institutional outputs, was not subjected to systematic retrieval. Given the fragmented nature of the literature on AI applications in geotourism, the search strategy was developed iteratively through preliminary pilot searches. These pilot tests combined AI-related terms with geoheritage- and geotourism-specific descriptors, including geotourism, geoheritage, geodiversity, geopark, geosite, and geological tourism. The retrieved records were manually inspected to evaluate thematic relevance and indexing consistency across Scopus and WoS. This assessment showed that many potentially relevant publications were indexed under broader tourism, heritage, environmental, or geoscience categories and did not consistently use geotourism-specific keywords, resulting in fragmented retrieval and unstable search performance. Consequently, to minimize potential omissions of relevant research, a more expansive search strategy centered on AI and sustainable tourism terms was implemented to enhance retrieval sensitivity and assemble a representative corpus of scientific production. The resulting dataset was then refined through a PRISMA-based systematic review using geoheritage- and geodiversity-specific screening criteria to increase thematic specificity. This two-stage strategy combined broad bibliometric coverage with targeted geoheritage screening and was designed to maximize the identification of AI studies relevant to geotourism, geoheritage conservation, and territorial planning. As a result, 9957 publications were retrieved, including 6500 records from Scopus and 3457 from WoS. The datasets were subsequently merged and cleaned using the Bibliometrix package in RStudio version 4.1.1 (Pratama *et al.,* 2024)—duplicate removal combined automated and manual verification procedures. To resolve duplicate entries stemming from database redundancy, records were prioritized and matched using digital object identifiers (DOIs), while entries devoid of DOIs underwent subsequent cross-verification based on composite criteria including title, authors, publication year, and source title. Candidate duplicates generated by Bibliometrix were manually inspected to confirm true duplicates and avoid the erroneous deletion of records with similar titles or revised metadata. Database duplication was systematically controlled by evaluating unique identifiers across pre- and post-deduplication stages, effectively streamlining the dataset from 9957 retrieved records down to 7211 unique records. A final manual quality-control review identified residual duplicates, incomplete metadata, records without authors (298 publications), and unavailable documents (98), resulting in a final dataset of 6815 publications. The combined database was exported to Microsoft Excel 365 for data organisation and subsequently analyzed using Biblioshiny version 4.1.2 and VOSviewer version 1.6.16 for bibliometric analysis, network visualization, and identification of emerging research patterns (Gupta and Chakravarty, 2021; Arruda *et al.,* 2022;

Espinel *et al.,* 2024). Phase two of the methodology incorporated scientific mapping, utilizing a bibliometric approach designed to map the intellectual structure and thematic progression of the scholarly landscape (Chandler *et al.,* 2018). This analysis evaluated the dynamics of scientific production based on the number of publications and citations per year, as well as contributions and collaboration between countries (Moral-Muñoz *et al.,* 2020). Co-occurrence analysis was performed using author keywords, thereby identifying thematic relationships and field development patterns (Ali and Gölgeci, 2019). The terms were organised into networks, where nodes represent keywords and links reflect their degree of association. These nodes are systematically aggregated into clusters reflecting their interconnectivity levels, employing algorithms standard to bibliometric analytical tools (Velastegui-Montoya *et al.,* 2023). Additionally, emerging trends were analyzed using normalization techniques, parameter grouping, and overlay visualization (Lozano *et al.,* 2019), which enabled the identification of the temporal evolution of research topics. By examining the relationship between keywords and publication timestamps, the thematic trend analysis uncovered the emergence of more recent research trajectories (Correia and Kozak, 2022). Co-occurrence networks were generated from author keywords using full counting, association-strength normalization, and the VOSviewer clustering algorithm with default resolution settings. To evaluate thematic progression, longitudinal analyses were executed in Biblioshiny on the basis of author keywords, applying annual time-slicing parameters. Network visualization employed default attraction–repulsion parameters in VOSviewer, with node size proportional to keyword occurrence and link thickness proportional to co-occurrence strength. The third phase consisted of a systematic review using the PRISMA method, which ensures transparency, methodological rigour, and reproducibility in the selection of studies (Page *et al.,* 2022). The screening process involved reviewing titles, abstracts, and keywords and considering the specific inclusion and exclusion criteria defined in Table 2. Irrelevant documents, publications in other languages, reviews, book chapters, documents with limited access, and studies without explicit AI application were excluded, including theoretical models, geospatial analyses without AI, and conceptual approaches without applied evidence. The primary screening process was performed manually by the investigators and subsequently corroborated through an automated RStudio routine containing essential geotourism keywords, such as geoheritage, geopark, geosite, geodiversity, and natural heritage. To improve reliability and reduce subjective selection bias, two researchers independently screened articles, assessed eligibility, and extracted data. Discrepancies were discussed and resolved by consensus through joint review of the publications and predefined eligibility criteria (Sunarti *et al.,* 2024). The final dataset and extracted variables were subsequently cross-checked before synthesis. This procedure ensured consistency and accuracy in identifying relevant studies. Fig. 2 presents a schematic summary of the entire selection process, mapping the methodological flow from the preliminary identification stage through to the final incorporation of studies. Fig. 2 reports the number of records excluded at each screening stage and the specific reason for exclusion, including language, full-text availability, document type, and thematic relevance to AI applications in geoheritage, geodiversity, geoparks, geosites, and geotourism. Consequently, a total of fifteen case studies centering on AI implementations within sustainable tourism associated with geodiversity and geoheritage were selected. The reviewed corpus consisted predominantly of empirical analyses driven by observed spatial, environmental, tourism, or behavioral metrics, supplemented by one conceptual evaluation on smart tourism and volunteering (Kumar, 2025), resulting in a definitive sample comprised fifteen

Table 2: Inclusion and exclusion criteria

Inclusion	Exclusion
Publications in English	Publications written in languages other than English
Articles focusing on AI applications in geotourism	Irrelevant documents (other approaches)
Document types: Articles and conference papers	Document types: review, book chapter, and conference review
Publications with accessible full text	Publications with limited or inaccessible full text

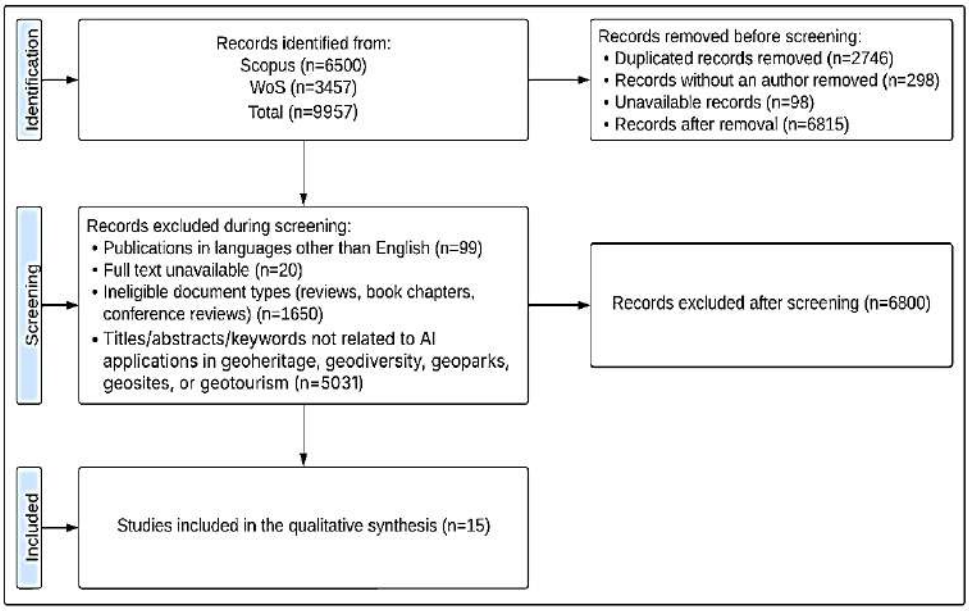

Fig. 2: PRISMA flow diagram showing the identification, screening, eligibility assessment, and inclusion process

empirical studies. Although this number may appear limited relative to the broader bibliometric corpus, it reflects the current state of the literature on AI applications explicitly linked to geoheritage, geodiversity, geoparks, geosites, and geotourism. The review aimed to synthesise the available empirical evidence within this emerging research field, and the selected studies were considered sufficiently representative because they cover multiple geographical regions, territorial contexts, and AI techniques. From these studies, the following variables were extracted: country, type of AI technology, application in tourism, type of resources, type of data, relationship with the dimensions of sustainability, target user, impact on geoconservation, and integration with the smart tourism. Formal methodological quality appraisal was not conducted because the present study adopts an exploratory and conceptual framework, prioritizing the identification of artificial intelligence application domains in geotourism over the estimation of effect sizes. Nevertheless, a structured quality screening was conducted during the eligibility stage. Studies were retained only when they explicitly applied AI techniques, clearly described the tourism or geoheritage context, identified the data sources, and reported the analytical procedure with sufficient methodological detail. Any publications lacking these minimum criteria were systematically excluded during the full-text evaluation process. The final synthesis therefore emphasises recurring functional patterns across studies, and the conclusions should be interpreted as an evidence-informed conceptual synthesis rather than a quality-weighted quantitative assessment. Finally, the selected cases were classified into four

thematic domains: i) AI for Predictive Analytics, ii) AI for Smart Destination Management, iii) AI for Geoheritage Interpretation, and iv) AI for Environmental Monitoring and Geoconservation. These four domains represent the principal empirical manifestations of AI in geotourism identified through the systematic review. Together with the macro-level bibliometric findings, they provide the analytical basis for interpreting the emergence of smart geotourism as an integrated research field.

Time and productivity trends

Fig. 3 depicts the chronological trajectory of publications investigating AI applications within sustainable tourism over the period spanning 1993 to 2026. During this period, the dataset comprised 6815 publications from 2861 scientific sources, indicating the consolidation of a broad, interdisciplinary body of knowledge. The annual growth rate of 20.36 percent (%) demonstrates the rapid expansion of this research field, while the average of 11.93 citations per document reflects its increasing scientific relevance and international visibility. Collectively, these metrics indicate that AI has evolved from a niche topic into a core research area driving innovation, sustainability, and data-informed destination management. The temporal evolution of scientific production reveals three developmental stages (Fig. 4). The initial stage (1993–2008) was characterized by limited scientific output, reflecting the early development of AI technologies and their restricted application within tourism research. During the intermediate stage (2009–2016), publication activity increased steadily alongside the widespread adoption of big data, cloud computing, and digital tourism platforms, which substantially expanded the availability of tourism-related data for analysis (Li *et al.,* 2018; Xiang *et al.,* 2015). Finally, since 2017, there has been a pronounced acceleration in both publications and citations, coinciding with major advances in ML, DL, and intelligent decision-support systems, as well as the consolidation of the smart tourism paradigm (Yu and Chen, 2022; Zhang *et al.,* 2021). Furthermore, the Coronavirus-2019 (COVID-19) pandemic expedited tourism's digital transition by stimulating the adoption of AI tools for visitor management, service customization, operational resilience, and sustainability (Gretzel *et al.,* 2020; Sigala, 2020). From a macro-level perspective, this evolution demonstrates that AI research has progressively shifted from technology-oriented applications towards integrated approaches centered on destination intelligence, sustainable governance, and evidence-based territorial management. This broader scientific context provides the foundation upon which more specialized fields, such as AI applications in geotourism, have recently begun to emerge. Future research priorities in smart geotourism were delineated through the analysis of emerging keywords, thematic progression, and citation-intensity patterns. The increasing prominence of generative AI, conversational AI, digital transformation, sustainability, and advanced geospatial analytics indicates a transition towards intelligent territorial governance, real-time destination management, and personalised geoheritage interpretation. These trends informed the future research agenda proposed in this study, including digital twins, explainable artificial intelligence (XAI), ethical AI governance, and integrated geospatial intelligence for geoheritage management.

An analysis of the geographical distribution of scientific publications demonstrates the worldwide dissemination of AI research in sustainable tourism while revealing distinct regional disparities in academic leadership (Fig. 5). Asia dominates the field, accounting for approximately half of the top 10 most productive countries, with China (27.37%) and India (9.15%) leading. This leadership is likely associated with investments in AI research, rapid digital transformation, and the growing strategic importance of smart tourism initiatives across the region. Europe contributes nearly 40% of the

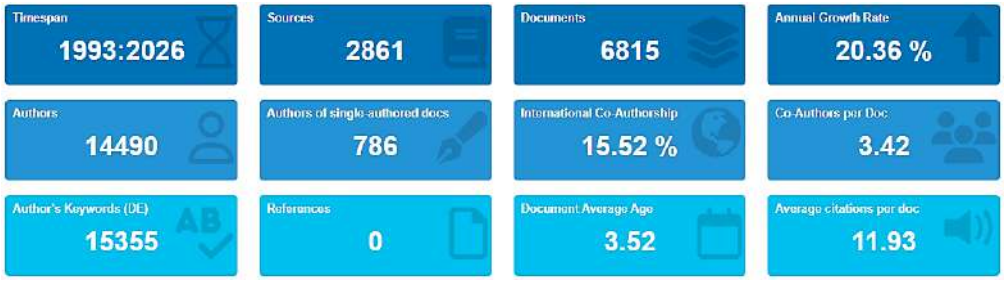

Fig. 3: Main bibliometric indicators of the dataset

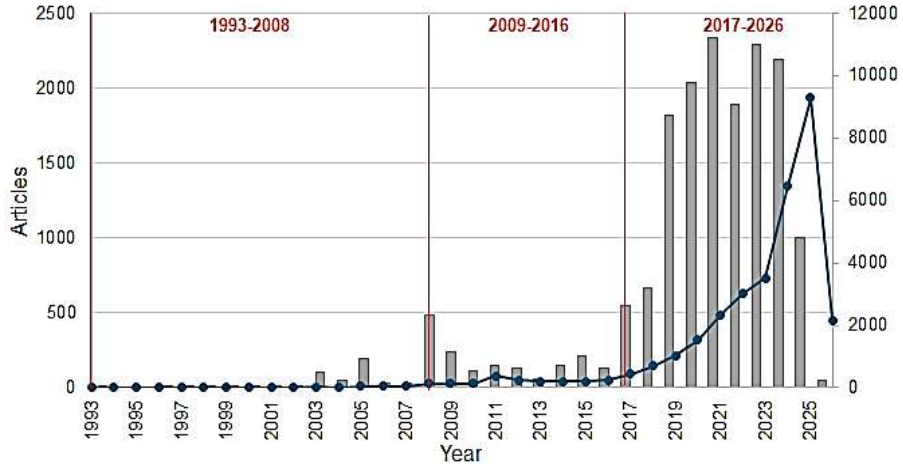

Fig. 4: Annual publication trends on AI applications in sustainable tourism

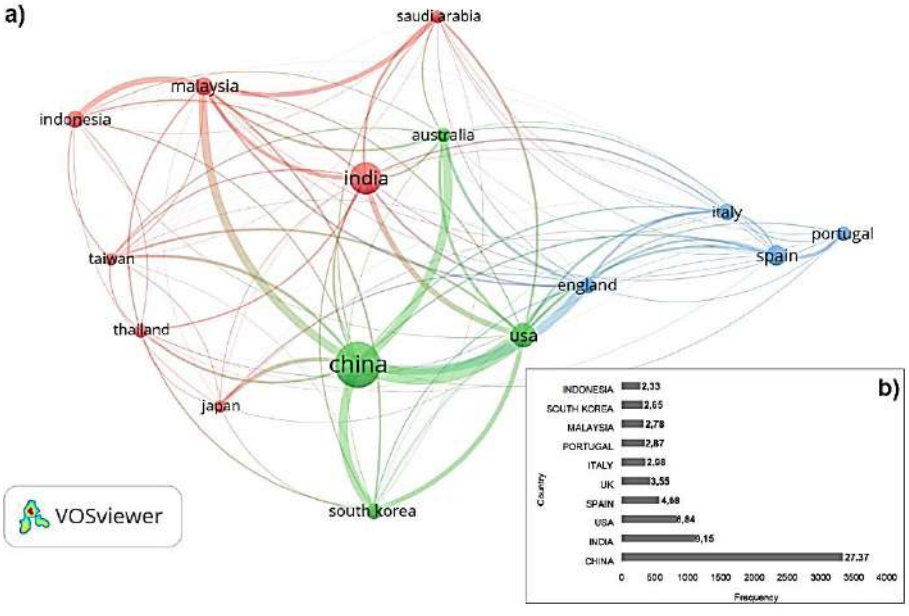

Fig. 5: International collaboration in AI research on sustainable tourism: (a) country co-authorship network generated with VOSviewer and (b) scientific output of the ten most productive countries

leading countries, with Spain (4.68%) and the United Kingdom (3.55%) drive this leadership through research intersecting technological innovation, sustainability and destination governance. The United States (6.84%) represents the principal contributor from North America, remaining among the three most productive countries worldwide. The co-authorship network further reveals a highly interconnected international research community in which China and the United States function as central knowledge hubs, establishing strong collaborative links with European countries (such as the United Kingdom, Spain, and Italy) and Asian countries (including India, South Korea, and Malaysia) (Fig. 5a). These collaboration patterns indicate that advances in AI for sustainable tourism are driven by transnational research networks that integrate technological expertise, multidisciplinary knowledge, and diverse territorial contexts. At the-analytical level, this international scientific matrix provides the epistemological foundation that drives the incremental evolution of specialized applications, encompassing geoheritage conservation, rationalized spatial planning, and smart geotourism. The collaboration networks also facilitate the diffusion of AI innovations into geotourism by enabling knowledge transfer, methodological exchange, shared datasets, and joint technological development among tourism, geoscience, and information-technology researchers. Countries occupying central positions in the collaboration network act as innovation hubs that accelerate the dissemination of analytical tools, geospatial methods, and smart destination practices into geopark management, geoheritage interpretation, and territorial planning. These temporal and geographical patterns demonstrate the rapid consolidation of AI research in sustainable tourism; however, they do not explain how the field is intellectually organised. To address this objective, the following section investigates the conceptual framework and thematic trajectory of the extant literature utilizing bibliometric science mapping methodologies.

Thematic structure and evolutionary dynamics of the study

The macro-level bibliometric analysis reveals that AI research in sustainable tourism has evolved through the progressive integration of three complementary knowledge domains that constitute the scientific foundations of smart tourism. Instead of operating as isolated domains, these thematic areas highlight the synchronized development of technological advancements, analytical capabilities, and visitor-oriented applications, creating the necessary epistemological conditions for the adoption of AI within specialized niches such as geotourism (Fig. 6). The thematic clusters were identified using the VOSviewer modularity-based clustering algorithm and subsequently validated through qualitative consistency assessment. Validation considered the semantic coherence of keywords within each cluster, the strength of co-occurrence links, and the stability of the three-cluster structure under the selected normalization and counting settings. The pronounced demarcation separating technological infrastructure, analytical intelligence, and visitor-centered applications, reinforced by the dense network of internal keyword connections, validates the premise that these clusters reliably capture the primary intellectual domains of AI research in tourism sector. Cluster 1 (red) represents the strategic and technological infrastructure supporting the digital transformation of tourism. This cluster connects concepts such as digital transformation, sustainable tourism, smart tourism, big data, blockchain, IoT, and immersive technologies such as virtual reality (VR) and augmented reality (AR), indicating that research has progressively shifted from isolated technological innovations towards integrated destination ecosystems. Moreover, this thematic grouping highlights the ways in which advanced technological infrastructures increasingly reinforce territorial governance, long-

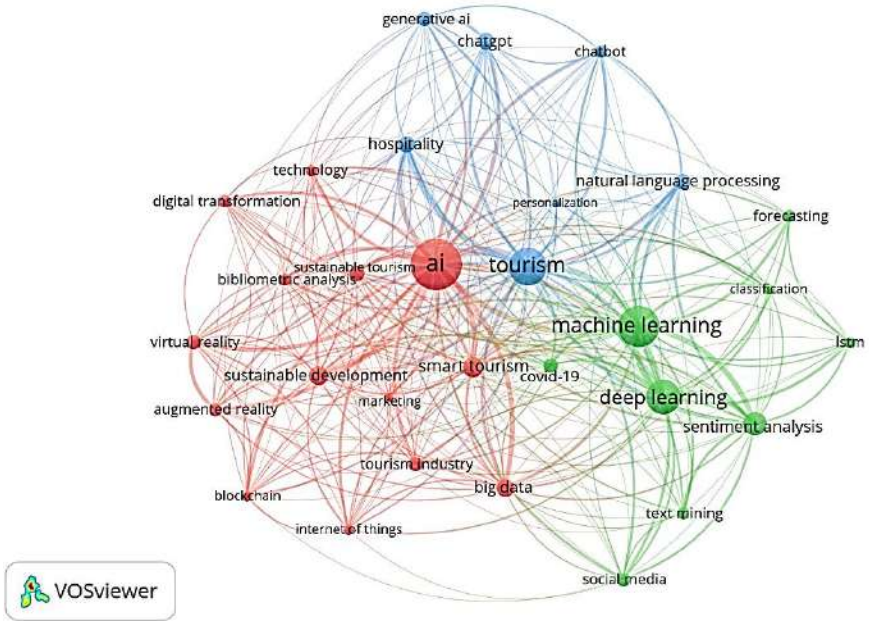

Fig. 6: Keyword co-occurrence network generated with VOSviewer showing the three main thematic clusters of AI research in sustainable tourism

term sustainability, and overall destination competitiveness. These developments provide the technological foundation upon which geoheritage destinations may later implement intelligent planning and management strategies. Cluster 2 (green) represents the analytical intelligence underpinning smart tourism. ML, DL, sentiment analysis, text mining, forecasting, and classification occupy central positions within the network, reflecting the growing importance of predictive analytics for understanding tourism dynamics. The presence of COVID-19 in this cluster illustrates how external disruptions accelerated the adoption of AI-based analytical approaches that support adaptive destination management and resilience. Thus, this grouping marks the critical progression from data proliferation to knowledge creation and empirical, evidence-based policy formulation. Cluster 3 (blue) reflects the evolution of AI towards human-centered tourism experiences. NLP, conversational agents, ChatGPT, generative AI, personalization, and hospitality demonstrate how recent research focuses on improving tourist interaction rather than merely automating operational processes. This evolution suggests that AI is serving as an interface between visitors and destinations, facilitating interpretation, communication, and personalised experiences that are particularly relevant to heritage-based tourism. The three clusters illustrate a broader scientific transition from technological development towards intelligent destination governance. The interaction between digital infrastructures, analytical capabilities, and visitor-oriented provisions reveals that smart tourism transcends its origins as a technological artifact, emerging instead as a holistic paradigm for territorial management. This macro-level evidence provides the conceptual rationale for examining how these AI capabilities are currently being adopted within the more specialized context of geotourism.

From a temporal perspective, the field's evolution shows a clear transition towards greater complexity and specialisation (Fig. 7). To minimize synonym variation and optimize conceptual consistency, keyword standardization procedures

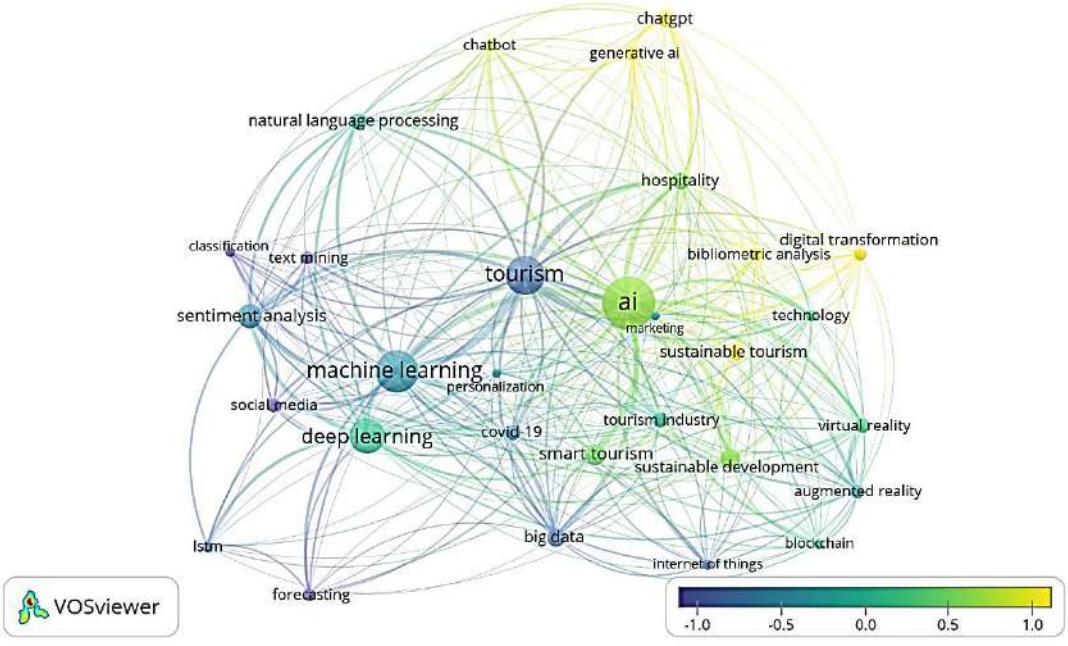

Fig. 7: Overlay visualization of author keywords showing the temporal evolution of AI research in sustainable tourism between 2022 and 2024

were executed prior to the construction of the network. Equivalent terms and spelling variants were merged using a thesaurus file in VOSviewer, including artificial intelligence/AI, machine learning/ML, deep learning/DL, and smart tourism/smart tourism destination. Singular–plural variants, hyphenation differences, and capitalisation inconsistencies were also standardized. The normalization procedure preserved the conceptual distinction between AI, ML, DL, and smart tourism while reducing redundant nodes and improving the interpretability of thematic relationships and temporal trends. The earliest phase (from -1.0 to -0.5) is characterized by data-oriented AI applications, in which research focused on exploiting digital information generated by tourism activities through techniques such as text mining, classification, forecasting, and social media analytics. The intermediate phase (0.0) reflects methodological consolidation, with ML and DL becoming central analytical approaches that generate predictive knowledge rather than descriptive information. The latest developmental phase (normalized from 0.5 to 1.0) highlights a pronounced evolution towards intelligent destination ecosystems, with digital transformation, sustainable tourism, generative AI, ChatGPT, and advanced conversational systems establishing themselves as primary research focal points. Rather than introducing isolated technologies, these topics indicate the convergence of AI, sustainability, and governance within smart tourism. This temporal evolution suggests that smart tourism is no longer defined solely by technological innovation but increasingly by the capacity to integrate AI into destination governance, sustainability, and visitor experience. Consequently, specialized tourism niches necessitating territorial intelligence, exemplified by geotourism—manifest as natural extensions of this overarching scientific progression, establishing the epistemological foundation for the micro-analytical investigation pursued hereafter. The temporal persistence analysis (Fig. 8) complements the previous findings by

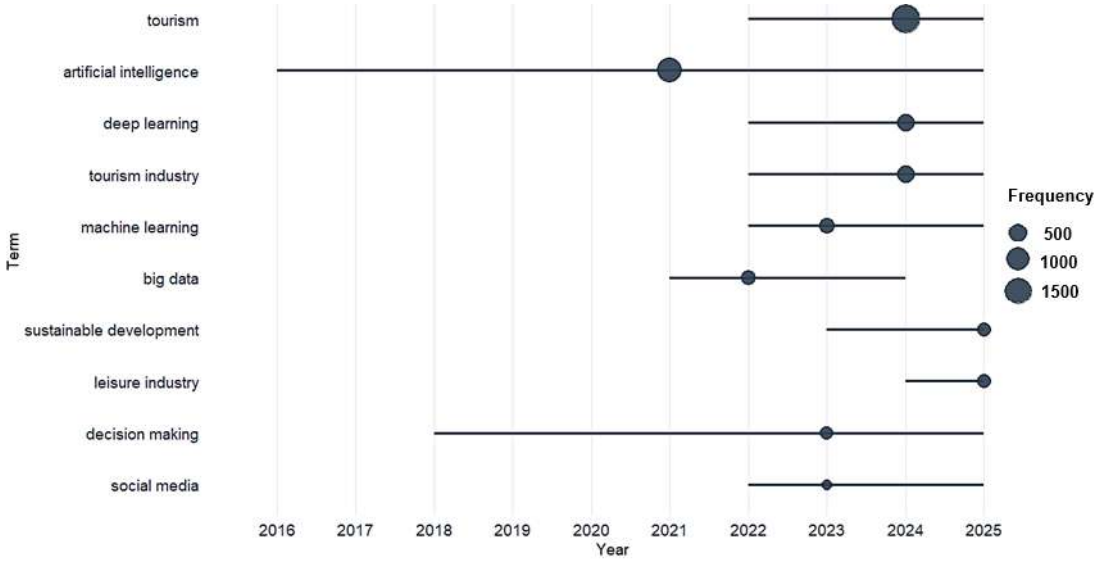

Fig. 8: Temporal evolution and persistence of the principal research topics in AI applied to sustainable tourism

distinguishing between foundational concepts and emerging specialisations. Tourism and AI remain the structural pillars of the field. In contrast, ML, DL, sustainable development, and the tourism industry represent rapidly expanding research domains that have achieved notable structural consolidation in recent years. This pattern indicates that the scientific evolution of AI in tourism is characterized not only by the emergence of new technologies but also by their progressive integration into sustainability-oriented destination management. Furthermore, this trajectory highlights a progression from foundational terms to nuanced, localized concepts, thereby supporting the premise that the maturation of smart tourism and geotourism relies on the systematic convergence of advanced technological tools with strategic and sustainable methodologies. These macro-level trends demonstrate that the scientific community has progressively developed the technological and conceptual foundations required to transfer AI applications to specialized sustainability contexts. The following systematic review explores how these broader scientometric developments translate into geotourism practices through empirical implementations in geotourism through empirical applications in geoheritage interpretation, destination management, predictive modeling, and environmental surveillance.

Empirical AI applications in geotourism: functional typologies from the systematic review

Operating in tandem with the macro-level bibliometric analysis, this systematic review furnishes empirical validation of the deployment of AI in geotourism. Whereas the bibliometric evaluation highlights sustainable tourism as a broader scientometric framework, the chosen case analyses reveal how underlying technological proficiencies convert into applied mechanisms reinforcing geoheritage conservation, destination planning, visitor dynamics, and environmental management (Table 3). The reviewed studies illustrate the emerging transition from smart tourism towards smart geotourism through the integration of AI with destination governance,

Table 3: Empirical evidence on AI applications in geotourism synthesized into four functional domains supporting smart geotourism: (i) predictive analytics, (ii) smart destination management, (iii) geoheritage interpretation, and (iv) environmental monitoring and geoconservation.

S.N.	Author	Country	AI Technology	Application in tourism	Resource type	Application purpose	Data types	Target user
Predictive analytics								
1	(Das *et al.*, 2025)	India	ML / Topic Modelling (BERTopic, NLP, BERT embeddings)	Strategic planning	Natural heritage / Geoheritage	Identification and mapping of key sustainable tourism themes	Textual	Policymakers / Academics
2	(Distefano *et al.*, 2025)	Italy	ML/Space Clustering	Tourism planning / Territorial analysis / Destination management	Cultural heritage	Identification of the likelihood of tourist attraction in museums	Spatial and attraction variables	Tourism planners and cultural managers
Smart destination management								
3	(Li *et al.*, 2022)	China	ML/Big Data/Intelligent systems	Destination Management	Cultural heritage	AI model promoting sustainable and smart heritage tourism	Tourism, behavioral and management data	Destination Managers / Tourism Planners
4	(Kumar, 2025)	India	Smart technologies	Tourism Management / Social Tourism	Community / Cultural	Smart tourism in the transformation of tourism volunteering	Theoretical and descriptive information	Local Communities / Volunteer Tourists / Managers
Geoheritage interpretation								
5	(Bozkurt and Şeker, 2023)	China	ML / DL / ANN	Tourism Planning / Sustainability Assessment	World Heritage Sites	ANN's role in sustainable tourism assessment	Socioeconomic, environmental, and tourism-related factors	Conservation organizations / Tourism planners
6	(Luo *et al.*, 2021)	China	ML / NLP / Text mining	Tourist Behavior Analysis	Geopark / Geoheritage	Analysis of tourist perceptions in geoparks	Tourist reviews and digital platforms	Geopark managers/Tourism marketers
7	(Karadayı *et al.*, 2026)	Türkiye	Metaverse / VR / AR	Heritage Interpretation / Digital Accessibility	Geosite / Geoheritage / Geodiversity	Use of metaverse technologies for the valuation of isolated geosites	Multimedia, virtual environments, and 3D models	Tourists, educators, and managers
8	(Zhao *et al.*, 2025)	China	ML / Data mining	Tourist Experience Analysis / Perceptual Assessment	Natural heritage / Geoheritage	Quantification of the aesthetic value of karst landscapes	Multimedia, reviews, and digital platforms	Destination managers / Tourism planners
9	(Cheng *et al.*, 2025)	-	LLMs / NLP / Text Mining	Tourist Perception Analysis / Sustainability Assessment	Natural heritage / World Heritage	Analysis of sustainability characteristics in natural heritage destinations	Tourist reviews and big data	Destination managers / Policymakers
10	(Benantar *et al.*, 2025)	Spain	HBIM	Digital Conservation / Heritage Interpretation / Cultural Dissemination	Cultural heritage	Sustainable conservation of built heritage	Point clouds, geospatial data, and 3D models	Heritage managers / Researchers / Planners

Environmental monitoring and geoconservation								
11	(Bravo-Jaico *et al.*, 2026)	Brazil	ML / DL / MLP / ANN	Tourism governance / Environmental management	Geodiversity / Natural heritage	Analysis and prediction of the relationship between biodiversity and tourism in sustainable governance contexts	Ecological, tourism, and territorial indicators	Policymakers / Environmental Managers
12	(Pham *et al.*, 2024)	China	DL / CNN / Computer Vision	Environmental monitoring / Destination management	Geopark / Geoheritage / Geodiversity	Monitoring landscape changes in a geopark for its sustainable management	Satellite imagery, geospatial data, and time series	Geopark Managers / Environmental Authorities
13	(Nugraha *et al.*, 2025)	Indonesia	ML / DL / ANN	Tourism planning / Development assessment / Territorial management	Geopark / Geoheritage / Geodiversity	Quantification of the geopark's contribution to the development of local communities	Socioeconomic, territorial, and VDI indicators	Policymakers / Geopark Managers
14	(Shahabi *et al.*, 2026)	China	ML	Tourism planning / Destination management / Territorial management	Geoheritage / Geopark / Geotourism	Analysis of geotourism resilience considering spatio-temporal dynamics	Geographic, time series, and tourism indicators	Policymakers / Destination Managers
15	(Naimi *et al.*, 2024)	Morocco	ML	Geotourism planning / Territorial assessment / Resource management	Geosite / Geoheritage / Geodiversity	Identification and classification of geosites with potential for geotourism development	Geomorphological, Geographic information system (GIS), and environmental criteria	Land Planners / Tourism Managers

Note: Fourteen of the fifteen studies synthesized in Table 3 are empirical studies based on observed or measured data, whereas one study is conceptual (Kumar, 2025). BERT: Bidirectional Encoder Representations from Transformers, ANN: Artificial Neural Network, LLMs: Large Language Models, HBIM: Heritage Building Information Modelling, MLP: Multilayer Perceptron, CNN: Convolutional Neural Network, VDI: Village Development Index and GIS.

geoconservation, and place-based sustainability. Rather than representing isolated technological developments, the reviewed studies reveal a coherent functional evolution of AI applications. Across diverse geographic contexts, AI supports decision-making throughout the geotourism management cycle, from predictive analytics and territorial planning to heritage interpretation and environmental monitoring. This diverse functionality highlights that AI has increasingly shifted beyond its role as a decision-support utility, emerging instead as a foundational catalyst for intelligent territorial governance. The empirical evidence also highlights the increasing integration of heterogeneous data sources, including textual information, social media content, geospatial databases, satellite imagery, environmental indicators, three-dimensional models, and multimedia resources. Through the integration of these complementary datasets enables AI systems are capable of generating multi-dimensional territorial intelligence that collectively reinforces tourism planning, resource management, visitor interaction, and geoheritage conservation. Another consistent finding concerns the diversity of stakeholders involved in AI implementation. Destination managers, policymakers, geopark authorities, environmental agencies, researchers, educators, local communities, and tourists all appear as active users of AI-based systems. This multidimensional participation suggests that smart geotourism

should be understood as the adoption of digital technologies and a governance model in which multiple actors interact through data-driven decision-making processes. Grounded in these insights, the synthesized corpus was structured into four key functional domains, delineating the core pathways by which AI drives smart geotourism.

These four functional domains illustrate the progressive operationaliZation of AI within geotourism. Predictive analytics supports anticipatory planning and decision-making; smart destination management strengthens governance and territorial coordination; geoheritage interpretation enhances visitor engagement through intelligent digital experiences; and environmental monitoring reinforces geoconservation through continuous assessment of landscape dynamics. These distinct domains illustrate that the emergence of smart geotourism is predicated on embedding complementary AI functionalities into sustainable destination management paradigms. The reviewed studies also reveal clear technological patterns. Predictive analytics is mainly supported by ML algorithms such as random forests, support vector machines, and neural networks. In contrast, image recognition and automated geosite detection are more closely associated with DL and computer vision, particularly CNNs. Geospatial modelling is significantly enhanced by coupling ML with GIS and spatial statistics, whereas environmental monitoring commonly leverages DL techniques applied to temporal sequences of remote sensing time series. NLP, LLMs, recommender systems, and immersive AI platforms increasingly support geoheritage interpretation and visitor interaction. ML and geospatial AI improve geoheritage assessment by integrating geomorphological, geological, topographic, environmental, and tourism variables within predictive spatial models (Sousa *et al.,* 2024). Through these approaches, automated geosite identification is achieved alongside the hierarchical categorization of geoheritage resources relative to their scientific and touristic utility, as well as multi-faceted vulnerability evaluations accounting for erosion, anthropogenic land-use modification, climate vulnerability, accessibility constraints, and visitor intensity. The evidence further highlights opportunities for integrating remote sensing, unmanned aerial vehicles (UAVs), light detection and ranging (LiDAR), GIS, and AI into smart geotourism management systems. Satellite imagery provides continuous regional monitoring (Bhattacharjee *et al.,* 2026), UAVs enable high-resolution local observation (Williams *et al.,* 2025), LiDAR supports detailed terrain modelling (Sahahiri *et al.,* 2026), GIS integrates spatial information (Sahahiri, 2025), and AI supports automated classification, change detection, risk assessment, and scenario simulation (Tang, 2025). Thus, the deployment of integrated geospatial intelligence platforms serves to bolster environmental surveillance, visitor management, carrying-capacity evaluation, early hazard detection, and adaptive conservation planning. Moreover, AI contributes to real-time environmental tracking in vulnerable tourist destinations by integrating diverse observational inputs—such as sensor arrays, mobile tracking data, UAV observations, remote sensing temporal series, and comprehensive environmental monitoring systems. ML models can identify crowding hotspots, detect early signs of erosion or vegetation degradation, and support dynamic carrying-capacity assessment (Xiong *et al.,* 2026). In hazard-prone areas, AI-based change detection and forecasting can assist in monitoring landslides, rockfalls, flooding, and geomorphological instability (Bera *et al.,* 2025). Effective, large-scale implementation requires the establishment of interoperable geospatial infrastructures combining GIS, remote sensing repositories, environmental sensor networks, tourism databases, and cultural heritage inventories. Open geospatial standards, interoperable metadata protocols, common spatial reference systems, and standardized geoheritage taxonomies constitute

fundamental prerequisites for effective data sharing across institutional and destination boundaries (da Silva Mano *et al.,* 2024). Cloud-based spatial infrastructures can facilitate multi-source integration and collaborative territorial management (Zhidebayeva *et al.,* 2025). Emerging opportunities also include integration with Digital Twins, AR, VR, and immersive geospatial visualization platforms. Digital Twins can simulate visitor flows and conservation scenarios in real time (Durden, 2025), while AR and VR can enhance geoheritage interpretation, accessibility, and virtual access to fragile geosites (Vandelli *et al.,* 2024). When synthesized with AI-enabled personalization and advanced geospatial visualization, these systems serve to augment visitor education and risk mitigation awareness, thereby bolstering both destination management and conservation planning initiatives. Their adoption, however, remains uneven across regions due to differences in technological maturity, governance capacity, environmental priorities, and territorial conditions.

Regional comparative assessment of sustainability and tourism intelligence in geotourism

Fig. 9 provides a comparative assessment of the fifteen empirical case studies according to three complementary dimensions that underpin the smart geotourism framework proposed in this study: geoconservation, smart tourism integration, and sustainability. As depicted in Fig. 6, different geographical settings combine these structural dimensions to advance AI-driven geotourism, exposing a multiplicity of pathways towards smart geotourism. Asia represents the largest body of empirical evidence and exhibits the greatest variability across the three dimensions. Several studies demonstrate high levels of smart tourism integration, supported by advanced AI techniques such as ML, DL, computer vision, and large-scale spatial analytics. At the same time, the empirical cases highlight considerable divergence concerning the degree to which geoconservation priorities and broader sustainability outcomes parallel technological advancements. This diversity suggests that Asian research is characterized by rapid technological experimentation while simultaneously exploring different governance models for integrating AI into geoheritage management. European studies present a comparatively more balanced profile. Despite the limited corpus of empirical cases identified, these instances consistently align advanced technologies with the core objectives of heritage conservation and sustainability objectives. European research tends to position AI as a decision-support tool within integrated territorial governance, reinforcing the relationship between destination intelligence, heritage interpretation, and sustainable planning. North American evidence is characterized by strong smart tourism integration combined with moderate levels of geoconservation and sustainability. Empirical findings reveal that the investigated instances predominantly utilize AI to advance destination intelligence and administrative efficiency, thereby suggesting a management-driven approach where technological adoption outpaces broader environmental integration. In contrast, Latin American and African case studies demonstrate a more balanced interaction among the three analytical dimensions. Although the technological sophistication of AI applications is generally lower than in Asia, these studies consistently link AI to local territorial planning, environmental conservation, and community-oriented sustainability. Consequently, these observations implies that smart geotourism is forged not solely through technological evolution, but fundamentally through the deepened integration of territorial governance and conservation mandates. Overall, the regional comparison demonstrates that smart geotourism does not follow a single developmental trajectory. Instead, destinations combine AI, sustainability, and geoconservation across different territorial contexts, with varying governance capacities and levels of technological maturity. Consequently,

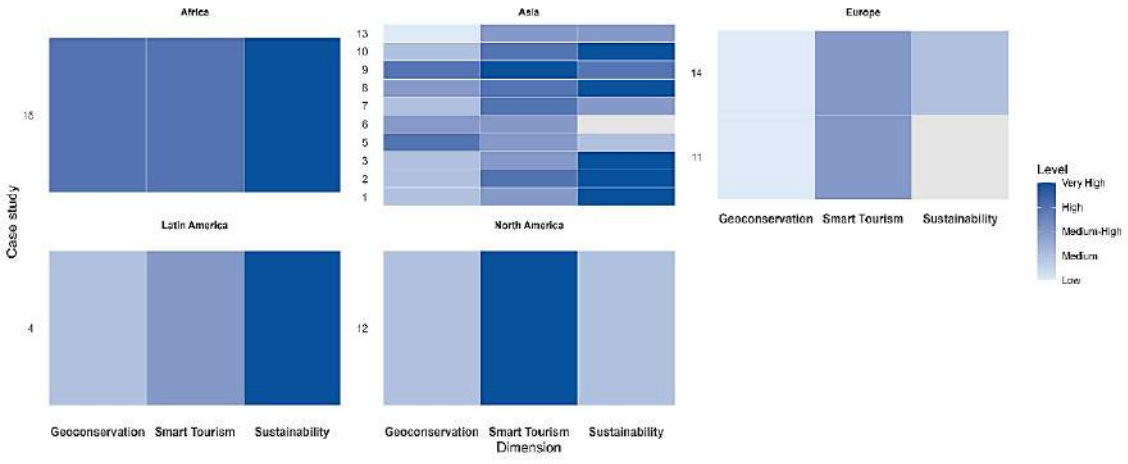

Fig. 9: Regional implementation patterns of the smart geotourism framework based on geoconservation, smart tourism integration, and sustainability

these findings validate that the evolution of smart geotourism is governed less by the standalone adoption of advanced AI capabilities than by their functional efficacy in underpinning integrated destination intelligence, evidence-based territorial planning, and long-term geoheritage conservation. The integration of bibliometric analysis and systematic review provides a multi-scale interpretation of the evolution of AI in tourism. The results indicate a transition from isolated digital applications towards a scientific system in which analytical intelligence, territorial governance, and sustainability increasingly converge. This evolution provides the conceptual basis for understanding smart geotourism as a specialized extension of the smart tourism paradigm. In this perspective, smart geotourism emerges within this framework as a complex socio-technical system driven by the ongoing, reciprocal feedback loops connecting technological innovation, environmental stewardship, tourist behavior, and regional progression (Zheng *et al.,* 2025). AI-based monitoring and analytics inform management decisions, while visitor responses generate new behavioral and spatial information that supports adaptive territorial management (Gacu *et al.,* 2025). Bibliometric evidence shows that the rapid growth of scientific production reflects a structural transformation of the field rather than merely an increase in publications. The temporal evolution of publications (Fig. 4), the consolidation of international collaboration networks (Fig. 5), and the progressive thematic maturation demonstrate that AI has become a central component of destination intelligence. This trajectory corresponds with the transition from digitization to data-driven smart tourism ecosystems highlighted by recent studies (Gajdošík and Marciš, 2025; Mondol *et al.,* 2026). Furthermore, the findings of this analysis reveal that these developments constitute the empirical and theoretical bedrock for novel geoheritage-oriented applications. Co-occurrence analysis reveals three complementary domains (Fig. 6), digital infrastructures, analytical intelligence, and visitor-centered services, which together illustrate the progressive integration of AI within smart tourism systems. This pattern supports previous research on AI-based destination planning (Ku and Chen, 2024; Wang *et al.,* 2025) and suggests that smart tourism is increasingly incorporating territorial conservation and geoheritage management objectives (Ferdowsi, 2025). The substantial contributions spanning tourism studies, computer science, geosciences,

geography, environmental sciences, remote sensing, GIS, and sustainability studies clearly validate the inherently multidisciplinary paradigm of the field. The temporal evolution of keywords indicates a transition from data-processing-oriented research towards themes such as digital transformation (Fig. 7), generative AI, and sustainability, suggesting that AI is being embedded within broader territorial governance frameworks. Thus, smart tourism is evolving beyond a technology-centric efficiency paradigm, reorienting instead toward destination intelligence, adaptive planning, and sustainability, a trajectory consistent with contemporary frameworks of resilient tourism and smart governance (Gómez Rodríguez, 2025; Song and Chen, 2025). Comparison with previous reviews highlights an important gap between AI-oriented tourism research and geotourism research. AI reviews mainly focus on visitor analytics, recommendation systems, and smart destination management (Bingöl and Yang, 2025; Panigrahy and Verma, 2025), whereas geotourism reviews emphasise geoheritage assessment, conservation, education, and territorial development (Reynard and Brilha, 2025). The reviewed empirical studies indicate that these research traditions remain only partially connected. Moreover, while increasingly sophisticated AI applications tend to concentrate on destination intelligence and visitor management, concrete evidence demonstrating their direct impact on measurable geoheritage conservation outcomes remains limited (Bingöl and Yang, 2025; Tuo *et al.,* 2025). In contrast, several Latin American and African studies demonstrate stronger integration between territorial planning and conservation despite using less advanced AI techniques (Córdoba Azcárate, 2025), suggesting that governance capacity may be as important as technological maturity. This study fundamentally contributes by coupling macro-level bibliometric evidence with micro-level data within the domains of geoheritage and geotourism. This combined approach facilitates the extraction of four recurring functional categories: predictive analytics, smart destination management, geoheritage interpretation, and environmental monitoring, which collectively underpin the proposed smart geotourism framework (Table 3). Although the empirical sample is limited to fifteen studies, the diversity of territorial contexts, governance arrangements, heritage types, and AI techniques strengthens the robustness of these recurring patterns. Synthesizing the reviewed findings, AI underpins evidence-based territorial planning by interconnecting four core processes: data acquisition, spatial intelligence, decision support, and adaptive management (Hao *et al.,* 2024). By integrating geospatial, environmental, tourism, and behavioral data, AI can generate predictive models, suitability assessments, risk maps, carrying-capacity indicators, and alternative planning scenarios that support conservation prioritization, visitor management, and monitoring of landscape change (Kim *et al.,* 2026). Reported conservation outcomes involve more efficient tracking of landscape alterations, the precise identification of at-risk geosites, the systematic prioritization of remedial measures, and the reinforcement of adaptive management frameworks within geoparks and protected geological regions. Predictive models can also identify emerging threats associated with erosion, climate change, uncontrolled tourism, and land-use transformation (Goyal *et al.,* 2025), while AI-based decision-support systems can help balance tourism development with conservation objectives (Vujko *et al.,* 2025). Sustainability considerations across the reviewed studies encompass environmental, social, economic, cultural, and governance dimensions, including landscape conservation, community participation, tourism development, heritage interpretation, and institutional coordination. The available data imply that the successful implementation of smart geotourism relies on complex, multi-level governance structures comprising UNESCO Global Geoparks, environmental authorities, tourism bureaus, planning agencies, research bodies, and

host communities (Xanthakis *et al.,* 2024). AI-enabled decision-support systems can facilitate collaboration among these stakeholders through shared geospatial planning platforms. At the same time, responsible AI adoption requires data governance, interoperability standards, ethical guidelines, and community participation mechanisms. Regional disparities in AI adoption are associated with differences in institutional capacity, investment, digital infrastructure, geospatial data availability, technical expertise, and education (Fig. 9). Consistent with antecedent literature highlighting the mediating influence of institutional frameworks on smart technology adoption and territorial innovation, these patterns reinforce the significance of local governance contexts (Frenzel *et al.,* 2022; Reverte and Luque, 2021). Asian cases generally reflect stronger technological ecosystems, whereas several Latin American and African studies demonstrate that effective smart geotourism can emerge through stronger integration between conservation objectives, governance arrangements, and community participation. Thus, successful execution seems governed less by standalone technologies than by the strategic synthesis of AI applications with clear institutional governance and conservation-driven planning (Güngör *et al.,* 2026). Persistent barriers include data ownership restrictions, limited interoperability, fragmented institutional responsibilities, insufficient financing, and weak technological governance frameworks. Recent technological developments indicate that smart geotourism is entering a new phase. Generative AI and LLMs are increasingly used for multilingual geoheritage interpretation, conversational visitor assistance, educational content generation, and personalised storytelling (Mah, 2025), while Digital Twins offer opportunities for real-time simulation of visitor flows and conservation scenarios (Florido-Benítez, 2024). Simultaneously, these technological strides present profound governance complexities associated with transparency, interpretability, data privacy, algorithmic equity, accountability, and civic engagement (Ma *et al.,* 2026). The limited attention to responsible AI governance in the reviewed studies highlights a significant research gap. Overall, the findings support the interpretation of AI not merely as a tourism technology but as a strategic enabler of territorial intelligence. Consequently, smart geotourism emerges as an integrative paradigm uniting AI, territorial governance, geoconservation, and sustainability under the umbrella of a unified destination management system. Future studies should prioritize operational indicators, longitudinal validation, comparative destination studies, ethical governance frameworks, and interdisciplinary integration among AI, geoscience, tourism management, spatial planning, environmental governance, and sustainability science.

Limitations of the study

This study presents some limitations that should be considered for the correct interpretation of the results: i) the bibliometric search was conducted in Scopus and WoS without language restrictions; however, the systematic review was restricted to English-language publications. Thus, relevant literature published across diverse linguistic contexts, regional outlets, or grey literature repositories could be inadvertently overlooked, potentially imparting geographical and intellectual skewness to the aggregation of empirical data. ii) the systematic review identified fifteen empirical case studies explicitly applying AI within geoheritage and geotourism contexts. This limited number reflects the emerging nature of smart geotourism and the current scarcity of empirically documented applications. Nevertheless, the selected studies were intentionally retained because they represent diverse geographical regions, territorial settings, and AI application domains. Additionally, given that a formal methodological quality appraisal tool was omitted from the study selection process, the present synthesis captures the existing empirical literature without quantitative adjustment for individual

study rigor. (iii) the regional comparative assessment relied on qualitative interpretation of the relationships among geoconservation, sustainability, and smart tourism integration. Although the comparative framework enabled systematic interpretation across heterogeneous studies, differences in methodologies, AI techniques, geographical contexts, and evaluation criteria limited the possibility of quantitative meta-analysis. The proposed smart geotourism framework remains conceptual and has not yet been empirically validated through expert assessment, pilot implementation, or comparative case-study testing. Thus, rather than functioning as a verified operational model, its pragmatic value lies in serving as a structured planning and governance reference drawn from the synthesis of current empirical findings. Future research should validate and operationalise the framework through Delphi studies, longitudinal assessments, comparative case studies, and the development of standardized performance indicators.

Political implications

The findings have important implications for tourism governance and territorial planning. Public policies should integrate AI into broader strategies linking destination intelligence, geoheritage conservation, and sustainable territorial development. As evidenced by the regional comparison, standalone technological advancements fall short of achieving smart geotourism; rather, effective implementation is contingent upon institutional readiness, interdisciplinary synergy, equitable geospatial data stewardship, and comprehensive planning systems capable of unifying tourism, environmental tracking, and cultural heritage management. To improve the operational value of the smart geotourism framework, the following stakeholder-specific recommendations are proposed:

- For policymakers, priorities include establishing national and regional smart geotourism strategies, promoting open geospatial data infrastructures, strengthening local AI capabilities, and adopting ethical and transparent governance frameworks.
- Geopark managers and conservation authorities should prioritize AI-supported visitor monitoring, carrying-capacity assessment, digital interpretation, environmental monitoring, and interoperable geospatial databases that support adaptive geoheritage management.
- Tourism planners should incorporate predictive analytics, mobility modelling, and geospatial decision-support tools into destination planning and conservation-sensitive zoning.

Policy priorities should be adapted to regional conditions. Developing regions require investment in digital infrastructure, access to geospatial data, technical training, and institutional strengthening for AI-enabled territorial governance. Consequently, in advanced technological contexts, policy frameworks should increasingly incorporate geoconservation objectives into smart tourism strategies, ensuring that digital and technical innovations serve directly to safeguard geological heritage over the long term. Overall, the proposed smart geotourism framework provides a practical governance reference for coordinating AI, destination management, sustainability, and territorial planning, supporting a transition from technology-driven tourism towards evidence-based territorial management aligned with the SDGs.

CONCLUSION

This study demonstrates that research on AI in sustainable tourism has evolved from isolated technological applications towards a broader scientific paradigm centered on destination intelligence, sustainability, and evidence-based governance. The bibliometric analysis confirms the field's progressive maturation. Simultaneously, the findings of the systematic review reveal that AI applications in geotourism

cluster primarily into four distinct functional domains: predictive analytics, smart destination management, geoheritage interpretation, and environmental monitoring and geoconservation. In addition, the synthesis reveals that AI integration across geotourism sectors is unevenly distributed geographically. Such adoption is fundamentally contingent upon a triad of factors: technological maturity, institutional capacity, and the embeddedness of sustainability and geoconservation into tourism planning. By integrating macro-level bibliometric evidence and micro-level empirical studies, the present study advances a smart geotourism framework designed to unify destination intelligence, spatial planning, geoheritage conservation, and sustainable tourism stewardship. This framework should be interpreted as a conceptual synthesis derived from the reviewed literature rather than as an empirically validated operational model. Accordingly, the study contributes to the emerging smart geotourism literature by offering an integrated analytical perspective that connects AI, territorial governance, and geoheritage management. Looking ahead, future inquiries must move beyond the current empirical boundaries to address operational implementation, ethical and trustworthy AI governance, and the interdisciplinary appraisal of smart geotourism frameworks. Further research should prioritize empirical validation of the framework through comparative case studies, longitudinal assessments, and the development of standardized indicators for destination intelligence, geoheritage conservation, governance capacity, and sustainability outcomes. Cutting-edge technological paradigms, encompassing as generative AI, digital twins, sophisticated geospatial analytics, XAI, and Earth observation systems, establish valuable avenues for operational validation in practical geotourism contexts. These directions should be interpreted as priorities for future research rather than as conclusions demonstrated by the present review.

AUTHOR CONTRIBUTIONS

T. Aguirre-Suárez contributed to the conceptualisation, formal analysis, data curation, investigation, methodology, writing - original draft, writing - review and editing, project administration, software and validation. M. Pérez-Chiquito contributed to the conceptualisation, formal analysis, data curation, methodology, writing - original draft and writing - review and editing. H. Cochea-Tomalá contributed to the formal analysis, investigation, methodology, writing - original draft, writing - review and editing and project administration. P. Escandón-Panchana contributed to the conceptualisation, data curation, investigation, methodology, writing - original draft, writing - review and editing, project administration and software.

CONFLICT OF INTEREST

The authors declare that there is no conflict of interests regarding the publication of this manuscript. In addition, the ethical issues, including plagiarism, informed consent, misconduct, data fabrication and/or falsification, double publication and/or submission, and redundancy have been completely observed by the authors.

OPEN ACCESS

©2027 The author(s). This article is licensed under a Creative Commons Attribution 4.0 International License, which permits use, sharing, adaptation, distribution and reproduction in any medium or format, as long as you give appropriate credit to the original author(s) and the source, provide a link to the Creative Commons license, and indicate if changes were made. The images or other third-party material in this article are included in the article's Creative Commons license, unless indicated otherwise in a credit line to the material. If material is not included in the article's Creative Commons license and your

intended use is not permitted by statutory regulation or exceeds the permitted use, you will need to obtain permission directly from the copyright holder. To view a copy of this license, visit: http://creativecommons.org/licenses/by/4.0/

PUBLISHER'S NOTE

GJESM Publisher remains neutral with regard to jurisdictional claims in published maps and institutional affiliations.

NEGATIVE AI STATEMENT

The author(s) declare that no AI tools or services were not used or not highly applied during the preparation of this work.

ABBREVIATIONS

%	Percent
AI	Artificial intelligence
ANN	Artificial neural network
AR	Augmented reality
BERT	Bidirectional encoder representations from transformers
CNN	Convolutional neural network
COVID-19	*Corronavirus-2019*
DL	Deep learning
DOIs	Digital object identifiers
e.g.	Exempli gratia (for example)
GIS	Geographic information system
HBIM	Heritage building information modelling
IoT	Internet of Things
LiDAR	Light detection and ranging
LLMs	Large language models
ML	Machine learning
MLP	Multilayer perceptron
NLP	Natural language processing
PRISMA	Preferred reporting items for systematic reviews and meta-analyses
RQ	Research questions
SDGs	Sustainable development goals
UAVs	Unmanned aerial vehicles
VDI	Village development index
VR	Virtual reality
WoS	Web of Science
XAI	Explainable artificial intelligence

REFERENCES

Alhaddar, M.; Kummitha, H., (2025). Digitalization and sustainable branding in tourism destinations from a systematic review perspective. Discover Sustainability. 6(1): 1167 **(18 pages).**

Ali, I.; Gölgeci, I., (2019). Where is supply chain resilience research heading? A systematic and co-occurrence analysis. Int. J. Phys. Distrib. Logist. Manage., 49(8): 793–815 **(23 pages).**

Aliyah, C.; Lukita, C.; Pangilinan, G.; Chakim, M.; Saputra, D., (2023). Examining the Impact of Artificial Intelligence and Internet of Things on Smart Tourism Destinations: A Comprehensive Study. Aptisi Trans. Technopreneurship (ATT), 5(2sp): 135–145 **(11 pages).**

Alves, P.; Martins, H.; Saraiva, P.; Carneiro, J.; Novais, P.; Marreiros, G., (2023). Group recommender systems for tourism: how does personality predict preferences for attractions, travel motivations, preferences and concerns? User Model User-Adap Inter., 33(5): 1141–1210 **(70 pages).**

Arruda, H.; Silva, E.; Lessa, M.; Proença J.; Bartholo, R., (2022). VOSviewer and Bibliometrix. J. Med. Lib. Assoc., 110(3): 392–395 **(4 pages).**

Baggio, R.; Del Chiappa, G., (2014). Real and virtual relationships in tourism digital ecosystems. Inf. Technol. Tourism. 14(1): 3–19 **(17 pages).**

Belu, M.; Marinoiu, A., (2025). AI-Enabled Supply Chain Management: A Bibliometric Analysis Using VOSviewer and RStudio Bibliometrix Software Tools. Sustainability, 17(5): 2092 **(28 pages).**

Benantar, H.; de Larriva, J.; Triviño-Tarradas, P., (2025). Scan to HBIM: A Pathway to Sustainable Divulgation of the Built Heritage. Adv. Mechanics, Design Eng. Manufactur., V. 917–930 **(14 pages).**

Bera, S.; Talukdar, S.; Nguyen, K.; Liou, Y.; Guru, B.; Chatterjee, R.; Ramana, G., (2025). Enhancing evacuation shelter suitability in compound hazard-prone regions with a Bayesian optimized convolutional neural network approach. Int. J. Disaster Risk Reduct., 119: 105306 **(22 pages).**

Bhattacharjee, T.; Sarkar, S.; De, D., (2026). FedGeoTour: Federated learning-based geostatistical approach to privacy-preserving mobile crowdsensing for sustainable tourism. Inf. Technol. Tourism, 28(1): 24 **(34 pages).**

Bingöl, S.; Yang, Y., (2025). Integrating smart technologies and artificial intelligence to build smart tourism destination ecosystems: A model for smart destination management. Tourism Manage. Perspect., 58: 101380 **(12 pages).**

Bozkurt, A.; Şeker, F., (2023). Harmonizing Heritage and Artificial Neural Networks: The Role of Sustainable Tourism in UNESCO World Heritage Sites. Sustainability. 15(17): 13031 **(17 pages).**

Bravo-Jaico, J.; Serquén, O.; Alarcón, R.; Suarez-Rivadeneira, J.; Ruiz-Camacho, W.; Manayay, F., (2026). Artificial intelligence for biodiversity and tourism governance: predictive insights from multilayer perceptron models in Amazonia. Front. Artif. Intell., 9:1-13 **(13 pages).**

Carrillo-Hernández, Y.; Ríos-Reyes, C.; Villarreal-Jaimes, C., (2024). Geotourism and Geoeducation: A Holistic Approach for Socioeconomic Development in Rural Areas of Los Santos Municipality, Santander, Colombia. Geoheritage. 16(4):94 **(26 pages).**

Chandler, B.; Lovell, H.; Boston, C.; Lukas, S.; Barr, I.; Benediktsson, Í.; Benn, D.; Clark, C.; Darvill, C.; Evans, D.; Ewertowski, M.; Loibl, D.; Margold, M.; Otto, J.; Roberts, D.; Stokes, C.; Storrar, R.; Stroeven, A., (2018). Glacial geomorphological mapping: A review of approaches and

frameworks for best practice. Earth Sci. Rev., 185: 806–846 **(41 pages).**

Cheng, X.; Chen, Y.; Kim, S., (2025). A tourist review mining framework for the sustainability features of world natural heritage based on AI large models. Curr. Issues in Tourism. 28(11): 1701–1709 **(8 pages).**

Córdoba Azcárate, M., (2025). Tourism, space, and place: bridging past, present and future research. Tourism Geographies, 27(3–4): 735–755 **(21 pages).**

Correia, A.; Kozak, M., (2022). Past, present and future: trends in tourism research. Curr. Issues in Tourism. 25(6): 995–1010 **(15 pages).**

da Silva Mano, A.; Silva, B.; Mocho, P.; Ortega, F., (2024). Location-Based Management of Paleontological Collections using Open Source GIS Software. Geoheritage, 16(2): 38 **(16 pages).**

Das, P.; Mandal, S.; Nedungadi, P.; Raman, R., (2025). Unveiling sustainable tourism themes with machine learning based topic modeling. Discover Sustainability. 6(1): 280 **(28 pages).**

Distefano, V.; De Iaco, S.; Maggio, S., (2025). Improving spatial clustering through a weight system on multilevel permanent museum attraction probability. Qual. Quant., 59(2): 1059–1088 **(30 pages).**

Doborjeh, Z.; Hemmington, N.; Doborjeh, M.; Kasabov, N., (2022). Artificial intelligence: a systematic review of methods and applications in hospitality and tourism. Int. J. Contemp. Hospitality Manage., 34(3): 1154–1176 **(23 pages).**

Drinia, H.; Voudouris, P.; Antonarakou, A., (2023). Geoheritage and Geotourism Resources: Education, Recreation, Sustainability II. Geosci., 13(11): 350 **(7 pages).**

Durden, J., (2025). Environmental management using a digital twin. Environ. Sci. Policy , 164: 104018 **(9 pages).**

El Archi, Y.; Benbba, B.; Nizamatdinova, Z.; Issakov, Y.; Vargáné, G.; Dávid, L., (2023). Systematic Literature Review Analysing Smart Tourism Destinations in Context of Sustainable Development: Current Applications and Future Directions. Sustainability, 15(6); 5086 **(14 pages).**

Escandón-Panchana, P.; Herrera-Franco, G.; Jaya-Montalvo, M.; Martínez-Cuevas, S., (2024). Geomatic tools used in the management of agricultural activities: a systematic review. Environ. Dev. Sustainability. 27(7): 15275–15309 **(35 pages).**

Esengulova, N.; Lopolito, A.; Pazienza, P.; Lucia, C., (2026). The UNESCO Global Geopark model for sustainable development in marginalised areas: Investigating perceptions and social acceptance in a local context. Land Use Policy, 168: 108090 **(14 pages).**

Espinel, R.; Herrera-Franco, G.; Rivadeneira García, J.; Escandón-Panchana, P., (2024). Artificial Intelligence in Agricultural Mapping: A Review. Agric., 14(7): 1071 **(36 pages).**

Ferdowsi, S., (2025). Management of geoheritage conservation and vulnerability in tourism destinations. Tourism Rev., 80(2): 601–623 **(23 pages).**

Ferdowsi, S.; Németh, K., (2026). Geoparks Management in Tourism Destinations: Integrating Development and Conservation. Sustainable Dev., 34(S2): 1034–1056 **(23 pages).**

Ferdowsi, S.; Tavana, M.; Heydari, R.; Štrba, Ľ., (2025). Geoeducation: the key to geoheritage conservation in tourism destinations. Int. Geol. Rev., 67(13): 1674–1696 **(23 pages).**

Flórez, M.; Becerra, O.; Carrillo, E.; Villa, M.; Álvarez, Y.; Suárez, J.; Mendes, F., (2024). Deep Learning Application for Biodiversity Conservation and Educational Tourism in Natural Reserves. ISPRS Int. J. Geo-Inf., 13(10): 358 **(20 pages).**

Florido-Benítez, L., (2024). The Use of Digital Twins to Address Smart Tourist Destinations' Future Challenges. Platforms, 2(4): 234–254 **(21 pages).**

Florido-Benítez, L.; del Alcázar Martínez, B., (2024). How Artificial Intelligence (AI) Is Powering New Tourism Marketing and the Future Agenda for Smart Tourist Destinations. Electron., 13(21): 4151 **(20 pages).**

Frenzel, F.; Giddy, J.; Frisch, T., (2022). Digital technology, tourism and geographies of inequality. Tourism Geographies. 24(6–7): 923–933 **(11 pages).**

Gacu, J.; Monjardin, C.; Mangulabnan, R.; Pugat, G.; Solmerin, J., (2025). Artificial Intelligence (AI) in Surface Water Management: A Comprehensive Review of Methods, Applications, and Challenges. Water, 17(11): 1707 **(27 pages).**

Gajdošík, T.; Marciš, M., (2025). Data-Driven Practices in European Smart Tourism Destinations: Towards a Tourism Data Space. Information and Communication Technologies in Tourism 2025. ENTER 2025. Springer. 39–49 **(11 pages).**

García-Madurga, M.; Grilló-Méndez, A., (2023). Artificial Intelligence in the Tourism Industry: An Overview of Reviews. Admin. Sci., 13(8): 172 **(22 pages).**

Gómez Rodríguez, D., (2025). The convergence between artificial intelligence and tourism: perspectives for sustainable development and operational efficiency. Investigación, Tecnología e Innovación. 17(23): 125–136 **(13 pages).**

Goyal, N.; Dandotiya, M.; Qurashi, J.; Kumari, M.; Sharma, S., (2025). AI-Driven Predictive Analytics for Disease Management. IGI Global Sci. Publishing, 231–276 **(46 pages).**

Gretzel, U.; Fuchs, M.; Baggio, R.; Hoepken, W.; Law, R.; Neidhardt, J.; Pesonen, J.; Zanker, M.; Xiang, Z., (2020). e-Tourism beyond COVID-19: a call for transformative research. Inf. Technol. Tourism, 22(2): 187–203 **(17 pages).**

Gretzel, U.; Sigala, M.; Xiang, Z.; Koo, C., (2015). Smart tourism: foundations and developments. Electron. Mark., 25(3): 179–188 **(10 pages).**

Güngör, Y.; Zülfikar, R.; Zülfikar, Z.; Bakırcıoğlu, N.; Güngör, A.; Azaz, D.; Işık, O.; Turan, A., (2026). Proposal for Transitioning From Traditional Tourism to Geotourism: İnceğiz Caves (Çatalca/Istanbul/Turkey). Geoheritage, 18(3): 151 **(23 pages).**

Gupta, N.; Chakravarty, R., (2021). Research visualization of Indian LIS research using VOSviewer and Bibliometrix. Lib. Hi Tech News, 38(8): 6–8 **(3 pages)**.

Gupta, V.; Anand, S.; Wei, D.; Wang, G.; Tripathi, S., (2024). Exploring applied sustainable strategies through geoheritage and geotourism: A systematic literature review. Int. J. Geoheritage Parks, 12(4): 660–677 **(18 pages).**

Hall, C., (2019). Constructing sustainable tourism development: The 2030 agenda and the managerial ecology of sustainable tourism. J. Sustainable Tourism. 27(7): 1044–1060 **(17 pages).**

Hao, H.; Wang, Y.; Chen, J., (2024). Empowering Scenario Planning with Artificial Intelligence: A Perspective on Building Smart and Resilient Cities. Eng., 43: 272–283 **(12 pages).**

Henriques, R.; Cayla, N.; Santos, I.; Martin, S.; Mariano, G., (2025). Digital technologies for geovisualization and AI-powered geointerpretation applied to geoheritage management. In Geoheritage, Elsevier, 457–478 **(22 pages).**

Hu, M.; Li, H.; Song, H.; Li, X.; Law, R., (2022). Tourism demand forecasting using tourist-generated online review data. Tourism Manage., 90: 104490 **(19 pages).**

Jabeen, F.; Al Zaidi, S.; Al Dhaheri, M., (2022). Automation and artificial intelligence in hospitality and tourism. Tourism Rev., 77(4): 1043–1061 **(19 pages).**

Karadayı, Z.; Yaşar, C.; Çalık, A.; Ulugergerli, E., (2026). Metaverse Technologies for Accessing Isolated Geosites: A Digital Bridge for Immersive Geotourism. Geoheritage. 18(1): 36 **(11 pages).**

Khater, M.; Ibrahim, O.; Sayed, M.; Faik, M., (2025). Legal frameworks for sustainable tourism: balancing environmental conservation and economic development. Curr. Issues Tourism, 28(22): 3693–3714 **(22 pages).**

Kim, J.; Jang, S.; Gretzel, U.; Koo, C., (2026). Special issue on "Smart tourism 2.0: Perspectives with geospatial data and AI." Electron. Mark., 36(1): 3 **(5 pages).**

Kirtil, I.; Aşkun, V., (2021). Artificial Intelligence in Tourism: A Review and Bibliometrics Research. Adv. Hospitality Tourism Res., 9(1): 205–233 **(29 pages).**

Knani, M.; Echchakoui, S.; Ladhari, R., (2022). Artificial intelligence in tourism and hospitality: Bibliometric analysis and research agenda. Int. J. Hospitality Manage., 107: 103317 **(15 pages).**

Koo, C.; Shin, S.; Gretzel, U.; Xiang, Z., (2025a). AI-powered smart tourism 2.0: A 10-year retrospective and updated model. Electron. Mark., 35(1): 108 **(17 pages).**

Koo, I.; Zaman, U.; Ha, H.; Nawaz, S., (2025b). Assessing the interplay of trust dynamics, personalization, ethical AI practices, and tourist behavior in the adoption of AI-driven smart tourism technologies. J. Open Innovation: Technol., Mark., Complexity, 11(1): 100455 **(10 pages).**

Ku, E.; Chen, C., (2024). Artificial intelligence innovation of tourism businesses: From satisfied tourists to continued service usage intention. Int. J. Inf. Manage., 76: 102757 **(15 pages).**

Kubalíková, L.; Drápela, E.; Kirchner, K.; Bajer, A.; Balková, M.; Kuda, F., (2021). Urban geotourism development and geoconservation: Is it possible to find a balance? Environ. Sci. Policy, 121: 1–10 **(10 pages).**

Kumar, N. (2025). Smart Tourism and the Future of Volunteerism: Transforming India's Travel Landscape. In R. Coutinho, J. Fraiz, and B. Sousa (Eds.), Impacts of AI on International Volunteering, 209-230 **(22 pages).**

Laesser, C.; Reinhold, S.; Beritelli, P., (2025). The 2024 consensus on advances in destination management. J. Destination Mark. and Manage., 38: 101038 **(13 pages).**

Lew, A., (2014). Scale, change and resilience in community tourism planning. Tourism Geographies. 16(1): 14–22 **(9 pages).**

Li, D.; Du, P.; He, H., (2022). Artificial Intelligence-Based Sustainable Development of Smart Heritage Tourism. Wireless Commun. Mobile Comput., 2022(1): 5441170 **(13 pages).**

Li, J.; Xu, L.; Tang, L.; Wang, S.; Li, L., (2018). Big data in tourism research: A literature review. Tourism Manage., 68: 301–323 **(23 pages).**

Lozano, S.; Calzada-Infante, L.; Adenso-Díaz, B.; García, S., (2019). Complex network analysis of keywords co-occurrence in the recent efficiency analysis literature. Scientometrics. 120(2): 609–629 **(21 pages).**

Luo, Y.; He, J.; Mou, Y.; Wang, J.; Liu, T., (2021). Exploring China's 5A global geoparks through online tourism reviews: A mining model based on machine learning approach. Tourism Manage. Perspect., 37: 100769 **(15 pages).**

Ma, J., (2025). Demand forecasting of smart tourism integrating spatial metrology and deep learning. Sci. Rep., 15(1): 42646 **(14 pages).**

Ma, D.; Peng, S.; Lin, Z.; Zhu, J.; Pan, X.; Jiao, Y.; Zhu, Z.; Shi, S.; Cui, B.; Jin, R., (2026). Explainable artificial intelligence reveals heterogeneous erosion responses to extreme rainfall: A new framework for conservation prioritization. Int. J. Appl. Earth Obs. Geoinf., 147: 105181 **(15 pages).**

Madzík, P.; Falát, L.; Copuš, L.; Valeri, M., (2023). Digital transformation in tourism: bibliometric literature review based on machine learning approach. Eur. J. Innovation Manage., 26(7): 177–205 **(29 pages).**

Mah, P. M., (2025). Unlocking Cameroon's geomaterials heritage via 3D AI-driven intelligence and NLP-based resource analysis. npj Heritage Sci., 13(1): 532 **(22 pages).**

Majid, G.; Tussyadiah, I.; Kim, Y.; Pal, A., (2023). Intelligent automation for sustainable tourism: a systematic review. J. Sustainable Tourism. 31(11): 2421–2440 **(20 pages).**

Martín-Martín, A.; Orduna-Malea, E.; Thelwall, M.; Delgado López-Cózar, E., (2018). Google Scholar, Web of Science, and Scopus: A systematic comparison of citations in 252 subject categories. J. Informetrics. 12(4): 1160–1177 **(18 pages).**

Mehraliyev, F.; Chan, I.; Choi, Y.; Koseoglu, M.; Law, R., (2020). A state-of-the-art review of smart tourism research. J. Travel Tourism Mark., 37(1): 78–91 **(13 pages).**

Mitha, S.; Omarsaib, M., (2025). Emerging technologies and higher education libraries: a bibliometric analysis of the global literature. Lib. Hi Tech, 43(2–3): 1248–1270 **(23 pages).**

Mondal, H., (2026). A Technical Note on Bibliometric Analysis by Biblioshiny and VOSviewer. Indian J. Radiol. Imaging, 36(02): 167–174 **(8 pages).**

Mondol, N.; Takee, M.; Ahad, A.; Joardar, S.; Hossain, S., (2026). Smart Tourism Technologies in the Industry 4.0 Era: A PRISMA-Based Systematic Review of Adoption, Implications, Outcome and Future Direction. J. Comput. Sci. Inf. Technol., 3(1): 43–69 **(26 pages).**

Mongeon, P.; Paul-Hus, A., (2016). The journal coverage of Web of Science and Scopus: a comparative analysis. Scientometrics. 106(1): 213–228 **(15 pages).**

Moral-Muñoz, J.; Herrera-Viedma, E.; Santisteban-Espejo, A.; Cobo, M., (2020). Software tools for conducting bibliometric analysis in science: An up-to-date review. El Profesional de La Información, 29(1): e290103 **(20 pages).**

Naciones Unidas, (2025). Objetivos y metas de desarrollo sostenible.

Naimi, L.; Manaouch, M.; Jakimi, A., (2024). Leveraging machine learning algorithms to identify potential geosites for geotourism promotion in ziz upper watershed in Southeastern Morocco. Geoj. Tourism Geosites. 57(4 supplement): 2041–2051 **(11 pages).**

Nannelli, M.; Capone, F.; Lazzeretti, L., (2023). Artificial intelligence in hospitality and tourism. State of the art and future research avenues. Eur. Plann. Stud., 31(7): 1325–1344 **(20 pages).**

Nugraha, R.; Fauzi, A.; Rustiadi, E.; Basuni, S., (2025). Quantifying the Geopark Contribution to the Village Development Index Using Machine Learning—A Deep Learning Approach: A Case Study in Gunung Sewu UNESCO Global Geopark, Indonesia. Sustainability. 17(15): 6707 **(31 pages).**

Núñez, J.; Gómez-Pulido, J.; Ramírez, R., (2024). Machine learning applied to tourism: A systematic review. WIREs Data Min. Knowl. Discovery. 14(5): e1549 **(35 pages).**

Omosanya, K.; Oludipe, V.; Lawal, R.; Lawal, T.; Mosuro, G.; Saka, H., (2026). Smart Geoheritage: Using Digital Technologies for Geoheritage Conservation and Sustainable Geotourism in Nigeria. Geoheritage, 18(2): 72 **(21 pages).**

Page, M.; Moher, D.; McKenzie, J., (2022). Introduction to PRISMA 2020 and implications for research synthesis methodologists. Res. Synth. Methods. 13(2): 156–163 **(8 pages).**

Panigrahy, A.; Verma, A., (2025). Tourist experiences: a systematic literature review of computer vision technologies in smart destination visits. J. Tourism Futures, 11(2): 187–202 **(16 pages).**

Parra-Sanchez, D.; Viviescas-Jaimes, P., (2024). Application of digital technologies in nature-based tourism: A scientometric analysis. J. Digital Econ., 3: 249–259 **(11 pages).**

Pham, T.; Dang, K.; Giang, T.; Hoang, T.; Le, V.; Ha, H., (2024). Deep learning models for monitoring landscape changes in a UNESCO Global Geopark. J. Environ. Manage., 354: 120497 **(15 pages).**

Pratama, J.; Rahmawati, Z.; Widyanto, A.; Gunawan, T.; Wan Abdullah, W.; Azua Jamari, N.; Hamzah, A.; Fansuri, H., (2024). Advancements in green diesel production for energy sustainability: a comprehensive bibliometric analysis. RSC Adv., 14(48): 36040–36062 **(23 pages).**

Quesada-Román, A.; Torres-Bernhard, L.; Ruiz-Álvarez, M.; Rodríguez-Maradiaga, M.; Velázquez-Espinoza, G.; Espinosa-Vega, C.; Toral, J.; Rodríguez-Bolaños, H., (2021). Geodiversity, Geoconservation, and Geotourism in Central America. Land. 11(1): 48 **(16 pages).**

Quesada-Valverde, M.; Quesada-Román, A., (2023). Worldwide Trends in Methods and Resources Promoting Geoconservation, Geotourism, and Geoheritage. Geosci., 13(2): 39 **(12 pages).**

Reynard, E.; Brilha, J., (2025). Geoheritage: a multidisciplinary and applied research topic. In Geoheritage, Elsevier. 3–12 **(10 pages).**

Reverte, F.; Luque, P., (2021). Digital Divide in E-Tourism. In: Xiang, Z., Fuchs, M., Gretzel, U., Höpken, W. (eds) Handbook of e-Tourism. Springer, Cham., 1-21 **(22 pages).**

Richards, G. (2021). Rethinking Cultural Tourism (Edward Elgar Publishing, Ed.), 1-161 **(162 pages).**

Rosado-González, E.; Lourenço, J.; Palacio-Prieto, J.; Sá, A., (2023). Collaborative mapping on sustainable development goals in Latin America UNESCO Global Geopark: A methodological discussion. Int. J. Geoheritage Parks, 11(2): 203–220 **(18 pages).**

Saarinen, J., (2013). Critical Sustainability: Setting the Limits to Growth and Responsibility in Tourism. Sustainability, 6(1): 1–17 **(18 pages).**

Sahahiri, R., (2025). Integrating smart technologies in ecotourism opportunities development. The Int. Arch. Photogramm., Remote Sens. Spatial Inf. Sci., XLVIII-G-2025, 1299–1307 **(9 pages).**

Sahahiri, R.; Alattas, A.; Fallatah, A.; Mandourah, A., (2026). Sustainable Tourist Walking Trails Development Using GIS and RS. Urban Sci., 10(4): 218 **(22 pages).**

Salgado-Jauregui, E.; Ellins, K.; Henry, D.; Gordon-Smith, D.; Martindale, R., (2025). A Participatory Decision-making Strategy for Geoconservation Implemented in Portland, Jamaica. Geoheritage. 17(4): 122 **(20 pages).**

Salvadeo, V.; Medina, W.; Cisterna, G., (2025). Geosites as Tourism Resources in the Laguna Brava Andean High Lagoon, a Ramsar Site from La Rioja, Argentina. Geoheritage, 17(2): 41 **(17 pages).**

Samara, D.; Magnisalis, I.; Peristeras, V., (2020). Artificial intelligence and big data in tourism: a systematic literature review. J. Hospitality Tourism Technol., 11(2): 343–367 **(25 pages).**

Sánchez-Sánchez, A.; Ruiz-Muñoz, D.; Sánchez-Sánchez, F., (2026). Trends and Challenges of Sustainable Rural Tourism in the Face of Artificial Intelligence: A Bibliometric Analysis. Sustainable Dev., 34(1): 676–695 **(20 pages).**

Santos, V.; Sousa, M.; Costa, C.; Au-Yong-Oliveira, M., (2021). Tourism towards Sustainability and Innovation: A Systematic Literature Review. Sustainability. 13(20): 11440 **(20 pages).**

Saydam, M.; Arici, H.; Koseoglu, M., (2022). How does the tourism and hospitality industry use artificial intelligence? A review of empirical studies and future research agenda. J. Hospitality Mark. Manage., 31(8): 908–936 **(27 pages).**

Shahabi, H.; Jamini, D.; Shirzadi, A.; Sadeghi, H.; Komasi, H.; Elkhrachy, I.; Salvati, A.; Clague, J.; Ghaderi, Z., (2026). Spatiotemporal dynamics of geotourism resilience: Machine learning methodologies and key insights. Int. J. Geoheritage Parks., 14(1): 91–107 **(17 pages).**

Sheller, M.; Urry, J., (2006). The New Mobilities Paradigm. Environ. Plann. A: Econ. Space, 38(2): 207–226 **(20 pages).**

Sigala, M., (2020). Tourism and COVID-19: Impacts and implications for advancing and resetting industry and research. J. Bus. Res., 117: 312–321 **(10 pages).**

Silva, I.; Costa, V.; Malheiro, A., (2024). Sustainable Tourism: A Systematic Literature Review and Bibliometric Analysis. Eur. J. Tourism, Hospitality Recreat., 14(1): 127–139 **(13 pages).**

Solakis, K.; Katsoni, V.; Mahmoud, A.; Grigoriou, N., (2024). Factors affecting value co-creation through artificial intelligence in tourism: a general literature review. J. Tourism Futures, 10(1): 116–130 **(15 pages).**

Song, D.; Chen, H., (2025). Artificial Intelligence as a Catalyst for Sustainable Tourism: A Case Study from China. Syst., 13(5): 333 **(20 pages).**

Sousa, J.; Lin, J.; Wang, Q.; Liu, G.; Fan, J.; Bai, S.; Zhao, H.; Pan, H.; Wei, W.; Rittlinger, V.; Mayrhofer, P.; Sonnenschein, R.; Steger, S.; Reis, L., (2024). Using machine learning and satellite data from multiple sources to analyze mining, water management, and preservation of cultural heritage. Geo-spatial Inf. Sci., 27(3): 552–571 **(20 pages).**

Spyrou, E.; Maroukian, H.; Saitis, G.; Evelpidou, N.; Karkani, A., (2024). Promoting geo-education and geotourism through geosite assessment: A case study from Acheron-Parga, Epirus, Greece. Int. J. Geoheritage Parks. 12(2): 256–277 **(22 pages).**

Sunarti S.; Nuryana, M.; Wiryanto, W.; Aswin, A.; Permatasari, C.; Tjakraatmadja, J., (2024). Intervention strategy for sustainable waste management systems in developing countries using community of practice. Global J. Environ. Sci. Manage., 10: 323–348 **(26 pages).**

Tang, S., (2025). Monitoring geomorphological evolution and assessing conservation priorities of geoheritage sites using multi-temporal DEMs and deep learning. Geocarto Int., 40(1): 2602979 **(19 pages).**

Torre, A., (2025). Contribution to the theory of territorial development: a territorial innovations approach. Reg. Stud., 59(1): 2193218 **(16 pages).**

Tuo, Y.; Wu, J.; Zhao, J.; Si, X., (2025). Artificial intelligence in tourism: insights and future research agenda. Tourism Rev., 80(4): 793–812 **(20 pages).**

Vandelli, V.; Migoń, P.; Palmgren, Y.; Spyrou, E.; Saitis, G.; Andrikopoulou, M.; Coratza, P.; Medjkane, M.; Prieto, C.; Kalovrektis, K.; Lissak, C.; Papadopoulos, A.; Papastamatiou, N.; Evelpidou, N.; Maquaire, O.; Psycharis, S.; Stroeven, A.; Soldati, M., (2024). Towards Enhanced Understanding and Experience of Landforms, Geohazards, and Geoheritage through Virtual Reality Technologies in Education: Lessons from the GeoVT Project. Geosci., 14(5): 127 **(21 pages).**

Velastegui-Montoya, A.; Escandón-Panchana, P.; Peña-Villacreses, G.; Herrera-Franco, G., (2023). Land use/land cover of petroleum activities in the framework of sustainable development. Cleaner Eng. Technol., 15: 100659 **(12 pages).**

Vujko, A.; Karabašević, D.; Panić, A.; Arsić, M.; Mirčetić, V., (2025). AI Transparency and Sustainable Travel Under Climate Risk: A Geographical Perspective on Trust, Spatial Decision-Making, and Rural Destination Resilience. Sustainability, 17(24): 11200 **(32 pages).**

Wang, S.; Wang, Q.; Cui, Q.; Lan, T., (2025). Artificial Intelligence in Tourism: A Systematic Literature Review and Future Research Agenda. Sustainability. 17(20): 9080 **(25 pages).**

Williams, M.; Tronti, G.; Peruzzo, R.; García-Rodríguez, M.; Fazio, E.; Zucali, M.; Bollati, I., (2025). Geoscience popularisation in Geoparks: A common workflow for digital outcrop modelling. Comput. Geosci., 201: 105945 **(15 pages).**

Wu, W.; Xu, C.; Zhao, M.; Li, X.; Law, R., (2024). Digital Tourism and Smart Development: State-of-the-Art Review. Sustainability. 16(23): 10382 **(19 pages).**

Xanthakis, M.; Simatou, A.; Antonopoulos, N.; Kanavos, A.; Mylonas, N., (2024). Alternative Forms of Tourism: A Comparative Study of Website Effectiveness in Promoting UNESCO Global Geoparks and International Dark Sky Parks. Sustainability, 16(2): 864 **(20 pages).**

Xiang, Z.; Schwartz, Z.; Gerdes, J.; Uysal, M., (2015). What can big data and text analytics tell us about hotel guest experience and satisfaction? Int. J. Hospitality Manage., 44: 120–130 **(11 pages).**

Xiong, W.; Senathirajah, A.; Bin S.; Li, Y.; Yan, X.; Shui, Z.; Zhou, Y., (2026). GIS-based tourist flow prediction for smart scenic areas using multi-source data fusion and deep learning. Geoj., 91(4): 117 **(22 pages).**

Yu, N.; Chen, J., (2022). Design of Machine Learning Algorithm for Tourism Demand Prediction. Comput. Math. Methods Med., 2022: 1–9 **(9 pages).**

Zhang, H.; Huang, R.; Zhang, Y.; Buhalis, D., (2022). Cultural ecosystem services evaluation using geolocated social media data: a review. Tourism Geographies. 24(4–5): 646–668 **(23 pages).**

Zhang, Y.; Li, G.; Muskat, B.; Law, R., (2021). Tourism Demand Forecasting: A Decomposed Deep Learning Approach. J. Travel Res., 60(5): 981–997 **(17 pages).**

Zhao, X.; Xiong, K.; Zhang, M., (2025). Quantitative research on aesthetic value of the world heritage karst based on UGC data: A case study of Huangguoshu Scenic Area. PLoS One. 20(2): e0317304 **(22 pages)**.

Zheng, X.; Lin, Y.; Cheng, X.; Ahn, Y.; Chi, X., (2025). An Investigation into the Formation of Tourists' Pro-Environmental Behavior in Geotourism: Balancing Tourism and Ecosystem Preservation. Sustainability, 17(4): 1422 **(23 pages).**

Zhidebayeva, A.; Syrlybekkyzy, S.; Taizhanova, L.; Koibakova, S.; Altybaeva, Z.; Koishina, A.; Seidaliyeva, L.; Mkilima, T., (2025). Emerging frontiers in ecosystem and biodiversity monitoring using remote sensing and geographic information systems. Global J. Environ. Sci. Manage., 11(4): 1791–1818 **(28 pages).**

AUTHOR (S) BIOSKETCHES

Aguirre-Suárez, T., Ph.D., Researcher, University Professor, and Doctoral Candidate, Facultad de Ciencias Administrativas, Universidad Estatal Península de Santa Elena, La Libertad, 240204 Ecuador.
- Email: *taguirre@upse.edu.ec*
- ORCID: 0000-0001-8077-8522
- Web of Science ResearcherID: NA
- Scopus Author ID: 60074587100
- Homepage: https://scholar.google.com/citations?user=5kvsyUQAAAAJ&hl=es

Pérez-Chiquito, M., Ph.D., Researcher, and University Professor, Facultad de Ciencias Administrativas, Universidad Estatal Península de Santa Elena, La Libertad, 240204 Ecuador.
- Email: *mperez@upse.edu.ec*
- ORCID: 0000-0003-0912-1928
- Web of Science ResearcherID: NA
- Scopus Author ID: 57214998124
- Homepage: https://scholar.google.com/citations?user=M7QoA7gAAAAJ&hl=es&oi=ao

Cochea-Tomalá, H., M.Sc., Researcher, Facultad de Ciencias Sociales y de la Salud, Universidad Estatal Península de Santa Elena, La Libertad, 240204 Ecuador.
- Email: *hcochea@upse.edu.ec*
- ORCID: 0000-0002-1507-1245
- Web of Science ResearcherID: NA
- Scopus Author ID: NA
- Homepage: https://scholar.google.com/citations?user=mrgQ20kAAAAJ&hl=es&oi=ao

Escandón-Panchana, P., Ph.D. Candidate, Escuela de Ciencias Ambientales, Universidad Espíritu Santo, Samborondón, Ecuador; Departamento de Ingeniería Cartográfica y Topografía, Universidad Politécnica de Madrid, Crta. Valencia km 7, 28031-Madrid, Spain.
- Email: *pc.escandon@alumnos.upm.es*
- ORCID: 0000-0002-7788-3118
- Web of Science ResearcherID: EVU-4344-2022
- Scopus Author ID: 57200918370
- Homepage: https://sciprofiles.com/profile/2309195

HOW TO CITE THIS ARTICLE:
Aguirre-Suárez, T.; Pérez-Chiquito, M.; Cochea-Tomalá, H.; Escandón-Panchana, P., (2027). A bibliometric and systematic analysis of artificial intelligence and the transition towards smart geotourism. Global J. Environ. Sci. Manage., 13(1): 523-552.

DOI: 10.22034/gjesm.2027.01.24
URL: https://www.gjesm.net/article_735589.html

Global J. Environ. Sci. Manage. 13(1): 553-574, Winter 2027, Serial #49

Global Journal of Environmental Science and Management
(GJESM)

Homepage: https://www.gjesm.net/

Podcasts

REVIEW ARTICLE

Bridging single-species models to ecosystem-based maximum sustainable yield for environmental sustainability in marine fisheries

S. Triharyuni[1], A.K. Supriatna [1,*], N. Anggriani [1], R. Puspasari[2]

[1]Department of Mathematics, Faculty of Mathematics and Natural Sciences, Universitas Padjadjaran, Sumedang, West Java, 45363 Indonesia

[2]Research Center for Biota System, Research Organization for Life Science and Environment, National Research and Innovation Agency, West Java, 16911 Indonesia

ARTICLE INFO

Article History:
Received 06 June 2026
Revised 10 August 2026
Accepted 13 September 2026

Keywords:
Ecosystem-based fisheries management
Maximum sustainable yield
Marine environmental sustainability
Multispecies models
Precautionary reference points
Trophic interactions

DOI:10. 22034.gjesm.2027.01.25

ABSTRACT

Maximum sustainable yield remains a central biological reference concept in fisheries management. Its reliability is shaped by model assumptions, uncertainty, ecological interactions, and environmental change. The study objectives were to reconstruct the mathematical progression of maximum sustainable yield, from single-species deterministic models to ecosystem-based, multispecies formulations. The critical narrative review synthesizes the paradigm shift in ecological modeling, tracing its trajectory from equilibrium-based single-species frameworks to holistic, ecosystem-aware formulations. Classical production models are compared with age-structured, stock-recruitment, bioeconomic, precautionary, and multispecies approaches. The assumptions, data needs, uncertainty, and management implications are evaluated. Eight fisheries cases are used to illustrate contrasts in data availability, assessment methods, harvest rules, ecosystem awareness, and shared-stock governance. These cases are treated as illustrative examples rather than a representative validation sample. Evidence shows that trophic interactions can alter species-specific and system-level reference points. The direction of change depends on food-web structure, selectivity, interaction strength, environmental productivity, and management objectives. Environmental variation can also affect growth, recruitment, natural mortality, habitat capacity, and species interactions. Accordingly, biological reference points require adaptive updating when stock productivity exhibits nonstationarity, precluding their interpretation as rigid constants amidst shifting environmental conditions. Economic objectives, social needs, and conservation goals must also be distinguished from biological yield objectives. A five-dimension readiness framework is proposed as a preliminary hypothesis-generating heuristic. Alternative weighting schemes indicate that some borderline classifications are sensitive to assumptions. Independent validation and inter-rater testing are therefore required before operational use. While substantial data constraints persist across multiple Indonesian fisheries, these limitations must not be regarded as the sole impediment to comprehensive management. Governance, enforcement, fleet structure, socioeconomic incentives, habitat condition, and climate variability can independently affect performance. Greater use of adaptive monitoring, precautionary harvest rules, uncertainty analysis, and ecosystem indicators is therefore recommended. Multispecies assessment should be prioritized where trophic or technical interactions materially influence stock dynamics. Maximum sustainable yield is best retained as an analytical reference point rather than a literal catch target. Environmentally sustainable application requires precautionary, adaptive, and ecosystem-based governance frameworks dynamically aligned with local empirical data quality, ecological conditions, and institutional capabilities.

This is an open access article under the CC BY license (http://creativecommons.org/licenses/by/4.0/)

NUMBER OF REFERENCES	NUMBER OF FIGURES	NUMBER OF TABLES
101	1	5

*Corresponding Author:
Email: a.k.supriatna@unpad.ac.id
Phone: +6281 6420 3861
ORCID: 0000-0003-0129-6344

Note: Discussion period for this manuscript open until March 01, 2027 on GJESM website at the “Show Article”.

INTRODUCTION

Fisheries management is essential to sustain fish resources as overexploitation, climate change, and habitat loss intensify. The Food and Agriculture Organization (FAO) estimates that 37.7 percent (%) of global marine fish stocks are overexploited and 50.5% are fished at maximum sustainable levels (FAO, 2024). Global fisheries production potential has contracted by roughly 4% since 1930 as a consequence of ocean warming (Free *et al*., 2019), compounded by illegal, unreported, and unregulated (IUU) fishing, which extracts an estimated 11-26 million tons annually outside formal management accounting (Agnew *et al*., 2009). Industrial fishing effort is concentrated among a small number of distant-water fleets (Kroodsma *et al*., 2018; McCauley *et al*., 2018), supported by about United States Dollar (US$)22 billion a year in capacity-enhancing subsidies (Sumaila *et al*., 2019). In Indonesia, enforcement against foreign IUU fishing after 2014 reduced fishing effort without reducing domestic catch (Cabral *et al*., 2018). Sustainable development goal (SDG) 14.4, calls for ending overfishing and restoring stocks to maximum sustainable yield (MSY) levels. National fisheries policy in Indonesia dictates that the annual total allowable catch (TAC) is established at 80% of the aggregate maximum sustainable yield (MSY) (Bappenas, 2020). Accordingly, Ministerial Decree No. 19 of 2022 sets a TAC of 8.6 million tons against an estimated national fish resource potential of 12.01 million tons annually (MMAF, 2022). However, independent assessment has found many Indonesian stocks overfished (Muawanah *et al*., 2018). The Ministry of Marine Affairs and Fisheries has also paired the quota system with a broader blue-economy program, although inter-agency coordination and funding remain challenges (Trenggono *et al*., 2025). The 80% provision is therefore treated as a policy buffer, not as evidence of ecological sustainability, because Its effectiveness depends on assessment quality, reporting, compliance, enforcement, ecosystem condition, and adaptive harvest control. While the theoretical origins of MSY precede Schaefer, Schaefer (1954) formulated its most influential mathematical framework, defining the upper bound of long-term sustainable yield under specific model constraints—a metric that subsequently became a cornerstone policy reference in the 1982 United Nations Convention on the Law of the Sea (UNCLOS), the 1995 United Nations Fish Stocks Agreement, the FAO Code of Conduct for Responsible Fisheries (FAO, 1995), and European fisheries policy (European Union, 2013). Mace (2001) described the shift from MSY as target toward a ceiling not to be exceeded. Nevertheless, Larkin (1977) challenged single-species MSY models, arguing that they inherently neglect ecological variability, multitrophic interactions, operational fishing costs, and socio-political distortion. Subsequent work developed age-structured, stock-recruitment, bioeconomic, precautionary, and ecosystem-aware, and management strategy evaluation (MSE) approaches (Punt *et al*., 2014). Global evidence indicates that actively managed fisheries can rebuild toward biomass levels compatible with sustainable harvest (Worm *et al*., 2009, Costello *et al*., 2016, Hilborn *et al*., 2020), suggesting that poor outcomes reflect misuse, overcapacity, uncertainty, and ecosystem effects rather than one mathematical concept alone (Beddington *et al*., 2007; Pauly and Froese, 2021). Recent studies continue to extend MSY-related modelling (Gillis *et al*., 2024; Chamera *et al*., 2025). This review therefore links model assumptions with environmental non stationarity, trophic interactions, uncertainty, management objectives, and implementation conditions. The current study pursues four primary objectives. First, the mathematical progression of MSY is critically reconstructed from deterministic single-species models to ecosystem-aware formulations. Second, conditions that weaken equilibrium reference points are identified. These conditions include environmental nonstationarity, trophic

coupling, and data uncertainty. Third, contrasting fisheries cases are compared without presuming the statistical equivalence of management units. Fourth, a preliminary readiness heuristic is proposed for organizing implementation evidence. Published literature and secondary sources available in 2026 were used. The study was conducted in the Department of Mathematics, Faculty of Mathematics and Natural Sciences, Universitas Padjadjaran, Sumedang, Indonesia in 2026.

METHODOLOGY

Review design and methodological identity. The manuscript is a critical structured narrative review combining conceptual and mathematical synthesis with illustrative comparative case analysis. It is not a systematic review, meta-analysis, primary stock assessment, or validation study. Classical mathematical derivations are re-evaluated to compare foundational assumptions and contrast the outcomes yielded by alternative reference points. No new mathematical model is claimed. The readiness framework is an author-developed heuristic whose construction is separated from evidence describing individual fisheries. Search strategy and eligibility. Literature was searched in Scopus, ScienceDirect, Google Scholar, and direct institutional sources. Searches combined “maximum sustainable yield” or “MSY” with “surplus production”, “Schaefer”, “Pella-Tomlinson”, “Fox”, “Beverton-Holt”, “Ricker”, “bioeconomic”, “management strategy evaluation”, “multispecies”, “ecosystem-based”, “trophic”, “climate”, and “Indonesia”. Foundational studies published before 2015 were retained when they defined a model, reference point, or management concept. To maintain currency in empirical applications and current policy contexts, precedence was given to recent scholarly literature. Eligible sources addressed model assumptions, reference points, uncertainty, ecological interactions, or implementation. Sources were excluded when MSY served merely as an incidental parameter, the targeted management unit remained ambiguous, or foundational key claims lacked traceable scientific or official support. No prospective protocol complete deduplication log, or screening flow count was available. Evidence appraisal and synthesis. Peer-reviewed stock assessments, MSE studies, and ecosystem models were used for scientific inference. Official regulations and advice documents characterized operational rules. These reviews established the necessary historical and conceptual framework. Robust policy assertions were maintained exclusively when corroborated by multiple evidentiary forms, whereas model-dependent insights were articulated conditionally. Regarding case-study selection and comparability, eight distinct cases were chosen via maximum-variation purposive sampling, spanning data-rich versus data-limited, temperate versus tropical, single-stock versus multispecies, and domestic versus multilateral contexts. Each case was documented across data infrastructure, assessment methodology, harvest-rule enforceability, ecosystem awareness, and shared-stock governance. The heterogeneous cases illustrate contrasts rather than prevalence or causal effects. Framework construction and uncertainty. The five dimensions were scored on a three-level ordinal scale. Equal weighting was adopted as a transparent baseline configuration, with data-intensive, governance-intensive, and ecosystem-intensive alternatives evaluated via sensitivity testing. Weighted mean scores below 1.5 were classified as emerging, 1.5 to below 2.5 as transitional, and 2.5 or higher as advanced. Owing to the absence of an independent validation dataset and inter-rater testing, this framework should be interpreted as exploratory rather than a validated instrument (Table1).

Deterministic single-species models for MSY

All deterministic MSY derivations rest on a common mass balance identity. The rate of change of exploitable biomass equals biological

Table 1: Comparative synthesis of major MSY approaches

Approach	Core assumption/ objective	Ecological realism	Uncertainty treatment	Typical data need	Appropriate management use
Schaefer	Logistic surplus production; equilibrium MSY	Low; single stock, fixed productivity	Usually parameter/ process uncertainty only if extended	Catch-effort/CPUE time series	Transparent baseline when stock and environment are relatively stable
Pella-Tomlinson / Fox	Flexible production-curve shape	Low-moderate; still aggregate single stock	Sensitive to shape and parameter estimation	Catch-effort/CPUE with enough contrast to estimate shape	Alternative production forms; structural-uncertainty comparison
Beverton-Holt / Ricker + Y/R	Age/size processes and stock-recruitment feedback	Moderate; recruitment mechanism explicit but usually single stock	Can propagate recruitment and life-history uncertainty in modern assessments	Age/length composition, growth, mortality, maturity, recruitment	Stock-specific reference points when demographic data are available
Gordon-Schaefer/ MEY	Economic rent, prices, costs, fleet behavior	Biological realism similar to production model; economic dimension explicit	Economic and biological uncertainty can be simulated	Biological data plus prices, costs, effort behavior	Economic target setting; not a substitute for ecological limits
Precautionary HCR + MSE	Management procedure tested under observation, assessment, and implementation error	Potentially high if operating model includes ecosystem/climate processes	Explicit simulation of multiple uncertainty sources	Assessment data plus plausible operating-model scenarios	Testing robustness and trade-offs before implementation
Multispecies / ecosystem models	Species interactions and/or system-level objectives	High relative to single-species models, but model dependent	Parameter and structural uncertainty can be substantial and should be ensemble-tested	Diet/trophic, abundance, fleet/selectivity, environmental data depending on model	When trophic/technical interactions materially alter single-stock advice; results are context dependent

production minus removal by fisheries, $dB/dt = G(B) - C(B,E)$, where $B(t)$ is exploitable biomass at time t, $G(B)$ is a density dependent production function, and $C(B,E)$ is catch expressed as a function of biomass and fishing effort E. MSY is defined as the global maximum of the equilibrium yield curve $Y^*(E)$, obtained by setting $dB/dt = 0$ and solving for catch as a function of effort; MSY is then defined as the maximum of the resulting equilibrium yield curve.

The Schaefer logistic surplus production model

The simplest and most widely taught surplus production model treats production as a quadratic function of biomass, using Eq. 1 (Schaefer, 1954):

$$\frac{dB}{dt} = rB\left(1 - \frac{B}{K}\right) - qEB \quad (1)$$

Differentiating and setting the result to zero gives the classical Schaefer reference points, using Eq. 3 (Hilborn and Walters, 1992; Schaefer, 1954). Here, r is the intrinsic rate of population growth (per year), K is the carrying capacity (in biomass), q is catchability coefficient under fishing conditions, and E is fishing effort. Catch is defined as $C = q\,E\,B$ and instantaneous fishing mortality is $F = q\,E$. At equilibrium, given constant F, biomass is calculated as $B^* = K\,(1 - F/r)$, so equilibrium yield as a function of F, using Eq. 2 (Schaefer, 1954):

$$Y^*(F) = FK\left(1 - \frac{F}{r}\right) \quad (2)$$

Differentiating and setting the results to zero gives the classical Schaefer reference points, using Eq. 3 (Hilborn and Walters, 1992; Schaefer, 1954):

$$B_{MSY} = \frac{K}{2}, \quad F_{MSY} = \frac{r}{2q}, \quad MSY = \frac{rK}{4} \tag{3}$$

The Schaefer solution places maximum production at half of carrying capacity under the logistic assumption. While the Schaefer model dictates that fishing mortality at MSY equals half the intrinsic growth rate, this relationship constitutes an artifact of model architecture rather than a universal biological law. Furthermore, because real-world fish stocks frequently exhibit delayed responses to exploitation and asymmetric surplus production curves, the Schaefer formulation should function as a transparent analytical baseline rather than an unconditional default.

The pella-tomlinson generalized production model

Empirical yield curves for many stocks are skewed rather than symmetric, with maximum production occurring away from *K/2.* Pella and Tomlinson (1969) generalized the Schaefer model with a shape parameter *p*., using Eq. 4 (Pella and Tomlinson, 1969):

$$\frac{dB}{dt} = \left(\frac{r}{p}\right) B \left[1 - \left(\frac{B}{K}\right)^{p}\right] - qEB \tag{4}$$

The Pella-Tomlinson model generalizes the logistic production function by adding a shape parameter *p*. This parameter changes the biomass location of maximum production. Under the parameterization used here, *p = 1* recovers the Schaefer logistic model. Values below one give BMSY below *K/2*. Values above one give B_{MSY} above *K/2*. The terms "left-skewed" and "right-skewed" are avoided because their interpretation depends on the plotted variable. Reference points should instead be interpreted directly from B_{MSY}/K and F_{MSY}. The reference points are Eqs. 5 to 7 (Pella and Tomlinson, 1969):

$$\frac{B_{MSY}}{K} = \left(\frac{1}{p+1}\right)^{1/p} \Rightarrow B_{MSY} = K\left(\frac{1}{p+1}\right)^{1/p} \tag{5}$$

$$F_{MSY} = \frac{r}{P+1} \tag{6}$$

$$MSY = rK\left(\frac{1}{P+1}\right)^{\frac{p+1}{p}} \tag{7}$$

At *p = 1* this recovers the Schaefer result *MSY=rK/4* (Hilborn and Walters, 1992; Schaefer, 1954). As *p* approaches zero ($p \rightarrow 0$), both F_{MSY} approaches r and MSY approaches *rK/e* recovering the Fox (1970) exponential model as a special case. The implied F_{MSY} and B_{MSY} therefore depend on *p*. A shape-invariant Schaefer benchmark can bias reference points when the true production curve is asymmetric. The direction and magnitude of potential estimation bias should be rigorously assessed directly from the characteristics of fitted parameterization. A universal mapping between p and ecological guild is not assumed (Haddon, 2011; Polacheck *et al*., 1993). Other variations can also be found in Supriatna for different interpretations (Supriatna, 2012).

The fox and Gompert exponential model

A third model which replaces the logistic with a Gompertz growth function is expressed as Eq. 8 (Fox, 1970):

$$\frac{dB}{dt} = rB\ ln\left(\frac{K}{B}\right) - qEB \tag{8}$$

This produces a left-skewed yield curve with explicit reference points, using Eq. 9 (Fox, 1970):

$$F_{MSY} = r, \quad B_{MSY} = \frac{K}{e}, \quad MSY = \frac{rK}{e} \tag{9}$$

The Fox model's asymmetric curve yields higher MSY and F_{MSY} estimates than the Schaefer, making Schaefer the more conservative benchmark (Haddon, 2011), though Fox model has been widely applied to tropical tuna and small pelagic stocks (Fox, 1970). See also Supriatna and Husniah (2015) for further modification of this model.

Age-structured yield: Beverton-Holt yield-per-recruit

For long-lived demersal stocks, age at first capture matters as much as total effort. Under von Bertalanffy growth, exponential natural mortality, knife-edge selectivity, and a closed cohort, yield-per-recruit *(Y/R),* using Eq. 10 (Beverton and Holt, 1957):

$$\frac{Y}{R} = F\, e^{\{-M(t_c - t_r)\}}\, W_\infty \sum_{n=0..3} u_n\, e^{\{-\mathrm{n\,K}(t_c - t_0)\}} /(F + M + nK) \quad (10)$$

where $U_n = (-1)^n 3!/[n!\,(3-n)!]$. In Eq. 10, *M* denotes natural mortality and t_c denotes age at first capture. Age of recruitment is denoted by t_r. The von Bertalanffy parameters are t_0 and K. Asymptotic weight is denoted by W_∞. The remaining terms are standard summation coefficients. Maximizing yield per recruit over *F* provides Fmax. The more precautionary $F_{0.1}$ is defined where the yield-per-recruit slope falls to 10% of its value at the origin. $F_{0.1}$ is often used when stock-recruitment information is weak (Gulland and Boerema, 1973; Hilborn and Walters, 1992).

Stock-recruitment functions

Y/R analysis assumes constant recruitment per spawner, rarely defensible empirically. The Beverton-Holt function is asymptotic, using Eq. 11 (Beverton and Holt, 1957):

$$R = \alpha S/(1 + \beta S) \quad (11)$$

where *R* is recruitment, S is spawning biomass, α is the maximum per-capita recruitment, and β is a density-dependent saturation coefficient, giving a finite ceiling $R_\infty = \alpha/\beta$. The function is instead dome-shaped, using Eq. 12 (Ricker, 1954):

$$R = \alpha S e^{\{-\beta S\}} \quad (12)$$

Peaking at $S^* = 1/\beta$ before declining, consistent with density-dependent cannibalism or nursery habitat degradation. Both can be reparametrized in terms of the steepness $h = R(0.2S_0)/R_0$, the parameter of choice in modern integrated assessments such as Stock Synthesis (Methot and Wetzel, 2013). Combining yield-per-recruit with a stock-recruitment relationship, while maintaining self-consistency between the predicted recruitment and the spawning stock biomass, it generates yield F_{MSY}, using Eq. 13 (Beverton and Holt, 1957; Methot and Wetzel, 2013):

$$F_{MSY} = \arg\max_F \left[\frac{\alpha\emptyset(F) - 1}{\beta\emptyset(F)} . \frac{Y}{R}(F)\right] \quad (13)$$

where $\phi(F)$ is spawning biomass per recruit at fishing mortality *F.* The spawning potential ratio (SPR) function is expressed, using Eq. 14 (Clark, 1991):

$$SPR(F) = \frac{\emptyset(F)}{\emptyset_0} \quad (14)$$

Clark (1991) found $F_{35\%}$SPR approximates F_{MSY} across diverse groundfish, later revised to the more conservative $F_{40\%}$SPR (Mace, 1994) when the stock-recruitment relationship is unresolved. These diagnostics can also support data-limited assessment. Recent stock evaluations in Jakarta Bay reveal severe exploitation pressures alongside critically low spawning-potential ratios for key target species (Yuliana *et al.*, 2026). Fishing to natural mortality ratios also exceeded one under two length-based methods. This outcome illustrates the utility of demographic proxies in detecting stock overexploitation in data-limited environments where complete stock-recruitment relationships are absent.

Equilibria and local stability

The Schaefer model has three dynamical regimes depending on *F* relative to *r*. For *F < r,* equilibrium *B* = K (1 − F/r) > 0* is biologically meaningful and locally stable. At *F = r* the non-zero equilibrium collides with the origin in a trans

critical bifurcation, for $F > r$ only $B = 0$ is stable, and the stock declines to extinction. Even an analytically perfect Schaefer fishery is fragility around $F_{MSY} = r/2$, a doubling of effort, from fleet expansion or technical creep halving catchability, is enough to cross this bifurcation (Hilborn and Walters, 1992), underlying Mace's (2001) case for treating F_{MSY} as a limit rather than a target.

Yield curves and the asymmetry of production

The Schaefer equilibrium yield curve manifests as a symmetric inverted parabola, reflecting the mathematical constraints of the logistic production function rather than a universal biological property. Pella-Tomlinson and Fox formulations allow asymmetric production curves. Empirical life-history studies also show that B_{MSY}/K varies among stocks (Thorson *et al*., 2012; Zhou *et al*., 2012). Model choice can therefore alter FMSY and BMSY. Fig. 1. compares the mathematical forms without assigning a universal curve shape to any ecological guild.

Non stationarity and climate-sensitive reference points

Equilibrium MSY assumes sufficiently stable productivity and stock-environment relationships over the management horizon. This core assumption is compromised under conditions of temporal variability in recruitment, growth, natural mortality, habitat carrying capacity, or trophic structure. Given that thermal regimes and community dynamics systematically alter stock productivity and associated reference points (Free *et al*., 2019; Fulton *et al*., 2022), biomass and fishing mortality benchmarks must be operationalized as conditional parameters rather than immutable values. Periodic re-estimation, state-dependent reference points, or climate-conditioned operating models may therefore be appropriate under strong non stationarity. MSE is subsequently applied to test the resilience of candidate management procedures against a suite of plausible future conditions.

Identifiability problem of MSY parameters

Schaefer reference points depend on r and K. These parameters can be difficult to estimate from CPUE series. Their likelihood surface may contain a strong correlation ridge. MSY can sometimes be better determined than r or K separately (Hilborn and Walters, 1992; Punt, 2003). Responses include life-history based priors on r (Froese *et al*., 2016) and catch only and length-based methods such as catch-MSY (Martell and Froese, 2012) and length-based spawning potential ratio (Hordyk *et al*., 2015), though their assumptions require stock-by-stock basis (Free *et al*., 2020). Furthermore, structural uncertainty persists because alternative surplus production frameworks, including the Schaefer, Pella-Tomlinson, and Fox models can generate contrasting reference points when applied to the same stock.

Bioeconomic extensions: from MSY to MEY

The Gordon-Schaefer open-access model

Schaefer's biological model says nothing about the behavior. Gordon (1954) supplied the economic complement, with total revenue $TR(E) = p\,Y^*(E) = p\,q\,E\,K\,(1 - qE/r)$, where p is the unit price of catch, and total cost is $TC(E) = c\,E$, where c is the cost per unit of effort. Sustained economic rent, using Eq. 15 (Gordon, 1954):

$$\pi(E) = p\,q\,E\,K\left(1 - \frac{qE}{r}\right) - c\,E \qquad (15)$$

Setting $d\pi/dE = 0$ gives the effort maximizing sustainable rent, using Eq. 16 (Gordon, 1954):

$$E_{MEY} = \left(\frac{r}{2q}\right)\left(1 - \frac{c}{(pqK)}\right) \qquad (16)$$

In an open-access fishery, equilibrium effort is dictated by the complete dissipation of economic rent. When harvesting remains financially viable under conditions of low biomass, open-access effort frequently exceed levels corresponding to biological MSY, thereby driving fleet overcapacity

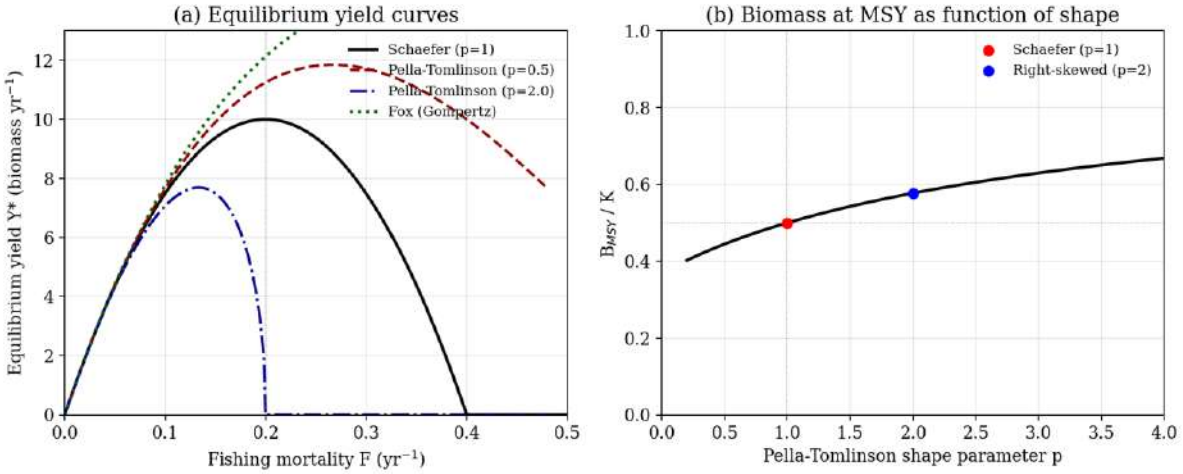

Fig 1: (a) Equilibrium yield curves for the Schaefer logistic (p = 1), two Pella-Tomlinson variations (p = 0.5 and p = 2), and the Fox-Gompertz model, calculated with r = 0.4 per year and K = 100. (b) Biomass at MSY as a fraction of carrying capacity as a function of the Pella-Tomlinson shape parameter p

and stock depletion. MSY, MEY, optimum yield (OY), and MSE each address distinct dimensions of fisheries governance: MEY serves as a biological production reference point; MEY integrates economic variables such as prices, operational costs, and fleet dynamics to establish an economic objective; OY accommodates broader social and ecological considerations; and MSE provides a simulation framework to test the robustness of alternative management procedures under uncertainty. Trade-offs among yield, profit, employment, food security, biodiversity, and catch stability require explicit performance criteria (Punt *et al*., 2014).

MEY as a management target

Several jurisdictions have formally adopted MEY. The Australian Commonwealth Fisheries Harvest Strategy Policy of 2007 (revised 2018) manage toward B_{MEY} as the target reference point, with half of B_{MSY} as the limit (Dichmont *et al*., 2010). Analyzing four distinct fisheries, Grafton *et al*. (2007) established that dynamic maximum economic yield corresponds to greater stock biomass and superior discounted economic returns relative to MSY. Global evidence also suggests that catch shares can reduce collapse risk (Costello *et al*., 2008). These benefits remain conditional on economic assumptions. Clark's (1973) showed that sufficiently high discount rates, the liquidation of a natural resource can constitute an economically rational strategy, even when secure property rights are established.

Optimal sustainable yield and multi-objective trade-offs

Both MSY and MEY remain single objective constructs, while real fisheries serve multiple legitimate objectives, employment, food security, biodiversity, and recreational. The United States 1976 Fishery Conservation and Management Act introduced the concept of OY as the catch providing the greatest overall national benefit, explicitly modifying MSY by economic, social, and ecological factors (National Research Council, 1998). In a parallel policy shift, the 2013 Common Fisheries Policy of the European Union integrates ecosystem and social considerations into its application of MSY (European Union, 2013). MSE fulfills a fundamentally different operational role, utilizing simulation testing to assess the performance of candidate management procedures across multiple performance metrics under uncertainty (Punt *et al*., 2014).

Precautionary and limit reference points

Mace (2001) reformulated F_{MSY} as a limit that fishing mortality should rarely or never exceed,

with a target set below it to buffer for assessment and implementation error. The International Council for the Exploration of the Sea (ICES) operationalizes this through paired target and limit reference points *(B_{pa}, F_{pa}) and (B_{lim}, F_{lim})* (ICES, 2021). Biological reference points define critical boundaries below which recruitment success is compromised, whereas target reference points are positioned with a sufficient margin of safety to maintain the probability of falling below B_{lim} stays around 5%. F_{MSY} in the ICES framework is now a precautionary target defined only in this buffered context (ICES, 2021; Mace, 2001), an architecture several reviews consider essential to any defensible operationalization of MSY (Punt *et al*., 2014).

Management strategy evaluation

MSE is a simulation framework for testing candidate management procedures under uncertainty (Punt *et al*., 2014; Smith, 1994). It links an operating model of "stock and ecosystem dynamics", an observation model, and a harvest control rule (HCR), then evaluated metrics such as mean yield, probability of being below B_{lim}, and catch variability across many simulated trajectories. MSE is now the standard procedure at the Commission for the Conservation of Southern Bluefin Tuna (CCSBT), the International Pacific Halibut Commission, the International Commission for the Conservation of Atlantic Tunas (ICCAT), and ICES. Its value lies in testing whether management procedures maintain resilience under real-world uncertainty, rather than presuming that a deterministic optimum will be operationally dependable (Punt, 2015; Punt *et al*., 2014).

Toward ecosystem-based MSY

Critique of single-species MSY

Larkin (1977) identified five shortcomings of single-species MSY, neglect of natural variability, spatial heterogeneity, species interactions, fishing costs, and political pressure. Later work developed responses to these limitations (Sissenwine, 1978; Mace, 2001; Walters *et al*., 2005). Among the evaluated dimensions, species interaction proved the most analytically tractable, owing to the availability of established discrete predator-prey formulations (Supriatna and Possingham, 1998, 1999). The following section focuses on continuous models. Institutional design can also address ecosystem concerns, the Commission for the Conservation of Antarctic Marine Living Resources (CCAMLR) established precautionary, ecosystem-based mandate from the outset, setting catch limits that account for the needs of dependent predator populations rather than single-species yield alone (Constable *et al*., 2000).

Predator-prey foundations of multispecies MSY

The classical Lotka-Volterra system represents prey density N and predator density *P* using coupled formulas, using Eq. 17 (Lotka, 1925):

$$\frac{dN}{dt} = rN - aNP, \qquad \frac{dP}{dt} = eaNP - mP \tag{17}$$

where *r* is intrinsic prey growth rate, *a* is the predator attack rate, *e* is the trophic transfer efficiency, and *m* is the predator natural mortality (Lotka, 1925). The non-trivial equilibrium *(N*, P*) = (m / (e a), r / a)* show equilibrium prey density set entirely by predator life-history parameters and equilibrium predator density set entirely by prey productivity and attack rate. The simultaneous integration of top-down predation pressure and bottom-up trophic limitation is formally expressed through coupled differential equations that underpin contemporary ecosystem-based fisheries theory (Andersen and Beyer, 2013; Walters *et al*., 2005). Introducing fishing mortality F_N and F_P on prey and predator, defined in Eq. 18 (May *et al*., 1979):

$$\frac{dN}{dt} = rN - aNP - F_N N, \qquad \frac{dP}{dt} = eaNP - mP - F_P P \tag{18}$$

Solving at equilibrium yields, using Eq. 19 (May *et al*., 1979):

$$N^*(F_N, F_P) = \frac{m + F_P}{e\ a}, \quad P^*(F_N, F_P) = \frac{r - F_N}{a} \tag{19}$$

At the unexploited equilibrium, net growth rates for both species drop to zero, leaving single species MSY undefined (May *et al.*, 1979). Operationally, management must ensure that every population maintains a positive effective growth rate amidst the regulated exploitation of its trophic counterpart. For the prey, holding predator at $\bar{P} < P^*$ through predator fishing gives an effective prey growth rate $r_{eff,N} = r - a\,\bar{P} > 0$. The surplus production model is operationalized under these reduced prey dynamics by implementing Eq. 20 (May *et al.*, 1979):

$$F_{MSY,N} = \frac{r - a\,\bar{P}}{2}, B_{MSY,N} = \frac{K_{eff,N}}{2}, MSY_N = \frac{(r - a\,\bar{P})K_{eff,N}}{4} \tag{20}$$

where $K_{eff,N}$ is the effective prey carrying capacity under background predation pressure $\bar{P}$. By parallel reasoning, maintaining prey at sub-equilibrium density $\bar{N} < N^*$ through prey fishing reduces the predator's net growth rate to $rr_{eff,P} = ea\,\bar{N} - m > 0$. Here, the effective prey carrying capacity is conditional on background predation pressure. Exploitation of the prey pool can depress abundance below unfished equilibrium levels, thereby constraining predator growth rates. Within this conceptual framework, the corresponding predator reference points are subsequently calculated using Eq. 21 (May *et al.*, 1979):

$$F_{MSY,P} = \frac{ea\,\bar{N} - m}{2}, B_{MSY,P} = \frac{K_{eff,P}}{2}, MSY_P = \frac{(ea\,\bar{N})K_{eff,P}}{4} \tag{21}$$

The predator reference points in Eq. 21 depend on background prey availability. Eqs. 20 to 21 therefore show that F_{MSY}, B_{MSY}, and MSY are conditional on trophic state rather than fixed biological constants. Augmenting predator exploitation can mitigate predation mortality and stimulate prey productivity, whereas increasing the extraction of prey populations restricts resource availability, leading to a corresponding decline in predator productivity. Consequently, optimizing one species can alter the reference points of another, and independently calculated single-species yields may not reproduce the system-level optimum (Mueter and Megrey, 2006; Walters *et al.*, 2005). The Lotka-Volterra formulation is too idealized for direct quantitative advice, but it demonstrates why ecologically significant predator-prey coupling can mis-specify single-species reference points (Andersen and Beyer, 2013). This result does not imply that every ecosystem-consistent fishing mortality must be lower than a single-species estimate or that summed single-species benchmarks, nor does it imply that cumulative single-species yield invariably surpass community-level optima. The direction and magnitude of adjustment depend on interaction strength, food-web structure, selectivity, environmental productivity, and management objectives (Walters *et al.*, 2005; Fulton *et al.*, 2022; Del Santo O'Neill *et al.*, 2024).

Example and Implication of MSY Implementation in towards Sustainable Fisheries

Empirical applications of MSY span a wide spectrum, from the data-rich, institutionally advanced fisheries of the North Atlantic and data-rich and data-limited fisheries. Rather than serving as statistically equivalent management units, the chosen case studies illustrate underlying ecological and institutional diversity. Given that these cases diverge across spatial scale, taxonomy, assessment method, and governance frameworks, cross-case comparisons are strictly bounded by five shared descriptive dimensions. These are data infrastructure, assessment methodology, harvest-control-rule enforceability, ecosystem awareness, and shared-stock governance. Case outcomes are not used to estimate prevalence or causal effects (Tabel 2). Additionally, the CMSY approach utilized in multiple data-limited instances has undergone continuous methodological refinement,

culminating in the CMSY++ implementation, which enhances the specification and empirical validation of catch-only priors against benchmark stock histories (Froese *et al*., 2023). Across the illustrative cases, data infrastructure, harvest rules bindingness, and multispecies/ecosystem awareness recur as important implementation dimensions. While fishery-independent surveys bolster analytical inference, standardized fishery-dependent observations and explicit uncertainty accounting can likewise underpin reliable scientific advice. Legally specified HCRs may reduce discretion, although outcomes still depend on compliance, enforcement, political economy, and ecosystem conditions. Where biological or technical interactions are intense, multispecies considerations assume critical importance. These findings represent descriptive signals extracted from a heterogeneous purposive sample, rather than direct measures of causal effect. The cases in Table 2 collectively reveal three recurring structural determinants of MSY implementation effectiveness, which are compared across geographic contexts in Table 3. Environmental pressures can alter MSY through biological and observational mechanisms. Warming can change growth, recruitment, natural mortality, distribution, and prey availability (Free *et al.,* 2019). Deoxygenation and acidification can reduce habitat quality and physiological performance (Breitburg *et al.,* 2018; Schmidtko *et al.,* 2017; Tai *et al*., 2021). Loss of reefs, mangroves, and seagrass can reduce carrying capacity or recruitment (Eddy *et al*., 2021; Lefcheck *et al.,* 2019). Trophic depletion can change effective productivity (Daskalov *et al.,* 2007; Walters *et al*., 2005), while discards, ghost fishing, and unreported catch add or conceal (Gilman *et al*., 2020; Richardson *et al*., 2019; Pauly and Zeller, 2016). These processes can alter *r, K*, recruitment, natural mortality, selectivity, interaction coefficients, or observation error. Consequently, operationalizing environmentally sustainable MSY mandates continuous parameter re-estimation, ecosystem indicators, strict habitat protections, and precautionary HCRs. The analyzed cases indicate that implementation outcomes are collectively shaped by underlying data infrastructure, institutional bindingness, and the incorporation of multispecies awareness. Fishery t-independent surveys can strengthen reference points relative to unstandardized commercial CPUE data, but the review does not establish data as the dominant causal constraint. Although binding rules effectively minimize management discretion, negotiated catches frequently surpass scientific recommendations, leaving conservation outcomes dependent on robust enforcement. Additionally, where predator-prey interactions are pronounced, explicit trophic adjustment become necessary (Walters *et al*., 2005; Del Santo O'Neill *et al*., 2024). An older evaluation of RFMOs found substantial governance gaps and depleted stocks (Cullis-Suzuki and Pauly, 2010), it is used only as a historical baseline, while the more recent fishery-specific evidence in Table 3 characterizes current institutional conditions.

Environmental implications for resource sustainability

MSY has direct environmental implications because fishing one trophic group can alter productivity in another. Predator depletion has caused cascading reorganization in the Black Sea (Daskalov *et al*., 2007), illustrating risks that may also arise in mixed fisheries when interacting stocks are managed independently (Walters *et al*., 2005; Del Santo O'Neill *et al*., 2024). Modifications of this nature can impair ecological resilience and erode the productive capacity underpinning food security and coastal livelihoods (Pauly *et al*., 2005; Pikitch *et al*., 2004). Climate and habitat pressures can compound these trophic effects. Empirical evidence indicates that ocean warming restricts fisheries productivity (Free *et al*., 2019), while accompanying deoxygenation and acidification processes drive structural shifts in habitat suitability and trophic networks (Schmidtko *et al*., 2017; Breitburg *et al*., 2018; Diaz and Rosenberg, 2008; Tai *et al*., 2021). Deoxygenation is particularly relevant to Southeast Asian waters (Kim *et al*., 2023). Furthermore, habitat degradation constrains carrying capacity and recruitment dynamics; global provisioning of coral reef ecosystem services has experienced widespread decline (Eddy *et al*., 2021), whereas

Table 2: Comparative synthesis of MSY application case studies from outside Indonesia and within Indonesia

No.	Species/ location	Assessment approach	MSY mechanism	Key findings	Identified weaknesses	Precautionary implications	Source
A. Applications outside Indonesia							
1	Atlantic cod (*Gadus morhua*) North Sea, Europe	VPA and SAM fitted to multi-decadal age-structured catch and acoustic survey data	EU CFP Reg. 1380/2013: mandatory F_{MSY} compliance by 2020; annual TAC set by European Union (EU) Council against ICES advice	Overfished stock share fell from about 74% (mid-2000s) to 26% (2020s); about 75% of Greater North Sea stocks are now below F_{MSY}, but North Sea cod itself remains overfished.	Single-species F_{MSY} on interacting mixed fisheries overestimates ecosystem-consistent yield (ΣMSYi); EU Council TACs have sometimes exceeded advice, though less often over time	F_{MSY} must function as a limit, not a target; multispecies trade-off models and multi-annual plans are needed to insulate advice from politics	Gras *et al.* (2024); ICES (2024); Del Santo O'Neill *et al.* (2024)
2	Northeast Arctic cod (*Gadus morhua*) Barents Sea Norway–Russia	SAM calibrated against >40 yr bilateral acoustic survey; F_{MSY} range 0.40–0.60	JNRFC bilateral HCR: ±20% TAC-change cap while SSB > Bpa; benchmark reassessment cycle	Record catches in the early 2010s; TAC cut 20% in 2024 (453,427 t) and 31% in 2025 (311,587 t); SSB fell below Bpa for the first time since 2002	±20% stability rule is suspended once SSB < Bpa, enabling larger 2025 cut; even so, the negotiated TAC stayed above advice; F_{MSY} stationarity breaks down under shifting productivity	More frequent benchmark assessments are needed under climate change; F_{MSY} should be time-varying; negotiated TACs should be more tightly bound to scientific advice, not just to the stability rule ceiling.	JRN-AFWG (2023) ;JRN-AFWG (2024)
3	Skipjack tuna (*Katsuwonus pelamis*) — Western and Central Pacific Ocean data period 1972–2024	8-region integrated stock assessment model; data 1972–2024; MSE framework for MP evaluation	CMM 2022-01 Management Procedure with explicit HCR and TRP; Management Procedure run set 2024–2026 effort limits (±10% cap)	Stock at about 98% of TRP (2024); catch record 2.1 Mt; $F/F_{MSY} \approx 0.35$; 0% overfishing risk; record catch about 2.1 Mt	Around 88% catch in Pacific Island EEZs, making revenue sharing as contested as biology; free-school sets suppress bigeye tuna; ENSO drives productivity variability beyond static MSY	±10% HCR guardrails limit abrupt effort change; needs better growth/age, tagging, and East Asia data	Teears *et al.* (2025)
4	Multispecies demersal pelagic complex (13 species groups) Gulf of Thailand, DoF 1971–2017	Non-equilibrium Schaefer and Fox surplus production models; aggregate system-level production model; supported by Ecopath-Ecosim model	Aggregate Multispecies MSY (MMSY) vs. sum of single-species MSYs (ΣMSYi); Thailand's TAC policy set at ~95% of aggregate MSY	MMSY only 65–80% of ΣMSYi; MMSY estimates highly sensitive to the baseline period chosen (degradation), recent states yield higher apparent MMSY, Fox model often fails for pelagics/long series, Schaefer more robust	ΣMSYi substantially exceeds MMSY; ecosystem degradation invisible in MSY-aggregate metrics; consistent catch-effort series	MMSY should complement, not replace, single-species checks (since ΣMSYi > MMSY); enforceable effort caps are essential; degraded systems need limit reference points below MSY; multispecies assessment should be prioritized where trophic and technical interactions are demonstrably strong	Fulton *et al.* (2022)

5	Kawakawa (*Euthynnus affinis*) Bay of Bengal Tamil Nadu, India 2001–2020	Multi-model: CMSY + BSM + SPiCT applied in parallel to 20-yr catch and CPUE data	No formal management procedure; assessment provides a reference point recommendation (effort reduction to achieve sustainable fishery)	All three models confirm overfishing and trend toward overfished state; models diverge quantitatively in h_{MSY} and F_{MSY} estimates	Model divergence quantifies the uncertainty envelope rarely reported to policymakers; no independent survey for validation; heterogeneous fleet complicates CPUE standardization	Where feasible, multi-model comparison can be used to characterize structural uncertainty in data-limited fisheries; uncertainty envelopes must be explicitly reported	Abinaya and Sajeevan (2025)
B. Applications in Indonesia							
6	Small pelagic aggregate Java Sea (FMA 712)	Schaefer and Fox surplus production models; CPUE from purse seine fleet; non-equilibrium biomass dynamics with risk analysis	TAC = 80% MSY; commodity FMA-specific reference points; FAO EAFM indicator integration	Sustained CPUE decline; production exceeds estimated MSY in successive years	Three biologically distinct species aggregated into one production unit; CPUE not standardized across heterogeneous fleet; systematic underreporting at informal landing sites	Species-level disaggregation is required as the minimum standard; GLM-based CPUE standardization essential; risk-analysis alongside MSY point estimates should become national practice	Suman *et al*. (2016, 2018); Sadhotomo and Admaja (2012); Zamroni *et al*. (2020); MMAF (2022)
7	Penaeid shrimp and demersal fish Arafura Sea (FMA 718)	Surplus production models; CMSY and BSM for post-moratorium reassessment	TAC = 80% MSY; moratorium on ex-foreign vessels (2014)	$B/B_{MSY} < 1.0$ and $F/F_{MSY} > 1.0$ for demersal groups, overfished, and actively overfishing; partial stock recovery observed post-moratorium	Industrial shrimp trawl bycatch largely unrecorded; small-scale fleet effort invisible in official statistics; surplus production models poorly suited to penaeid biology (ovigerous female selectivity)	Multispecies modeling of shrimp and demersal fish interactions is the minimum appropriate standard; fleet-wide data collection covering all segments is a prerequisite, not an optional improvement	Nurhakim (2004); MMAF (2022)
8	Multi-commodity national framework (11 FMA) Indonesia	CMSY and BSM alongside Schaefer/Fox; commodity- and FMA-specific assessments; FAO EAFM indicator frameworks	Kepmen KP 19/2022: 80% MSY TAC for 9 commodity groups in 11 FMA; procedural basis for licensing; integration into national SDG 14.4 monitoring	35/99 units overexploited; 53/99 fully exploited; national MSY estimate 12.01 Mt/yr; TAC 8.6 Mt/yr	Systematic underreporting of small-scale fleet effort; species aggregation masks within-group status heterogeneity; absence of formal uncertainty quantification in published reference points	80% MSY buffer is meaningful only with enforceable licensing caps; formal HCR linking assessment outputs to licence decisions is needed; multi-model uncertainty reporting should replace single-point MSY estimates in policy documents	MMAF (2022); Suman *et al*. (2016, 2018)

Note: VPA = Virtual Population Analysis; SAM = State-space Assessment Model; CMSY = Catch-based MSY; BSM = Bayesian State-space Schaefer Model; SPiCT = Stochastic Production in Continuous Time; HCR = Harvest Control Rule; TRP = Target Reference Point; TAC = Total Allowable Catch; F_{MSY} = Fishing Mortality at MSY; MMSY = Multispecies MSY; SSB = Spawning Stock Biomass; Bpa = Biomass at Precautionary Approach; JNRFC = Joint Norwegian–Russian Fisheries Commission; WCPFC = Western and Central Pacific Fisheries Commission; DoF = Department of Fisheries (Thailand); FMA = Fisheries Management Area; CPUE = Catch per unit effort; EAFM = Ecosystem Approach to Fisheries Management.

Table 3: Cross-contextual comparison of MSY implementation determinants between fisheries outside Indonesia and Indonesian FMA cases, with corresponding management implications

Dimension	Outside Indonesia	Indonesia	Management implication
Data infrastructure	Fishery-independent data dominate long-term acoustic/age-structured surveys, tagging programs, and observer systems	Fishery-dependent catch-CPUE only; no standardized survey; underreporting at small-scale/informal sites	Build fishery-independent surveys; mandate disaggregated, fleet-wide reporting
Assessment methodology	Spans age-structured models (SAM/VPA) to multi-model ensembles (CMSY+BSM+SPiCT) with explicit uncertainty reporting	Mostly aggregate surplus-production models (Schaefer/Fox/CMSY); uncertainty rarely reported	Use multi-model comparison where data and capacity permit; report uncertainty, not single-point MSY
HCRs	Legally binding HCRs	TAC = 80% MSY established (Decree of MMAF 19/2022 uniform across all stocks, no biomass-triggered adjustment)	Replace flat buffer with stock-specific, biomass-conditional HCRs linked to licensing
Multispecies and ecosystem awareness	Mixed-fisheries advice and ecosystem models in use (like Ecopath with Ecosim, MMSY vs. ΣMSYi)	Species/commodity aggregation masks individual stock status; no ecosystem model exists	Disaggregate species; pilot multispecies/ecosystem models for key mixed fisheries
Shared stock governance	Advanced bilateral/multilateral bodies (JNRFC, WCPFC) set shared-stock TACs	Domestic-only governance; access control, no shared harvest mechanism; limited Regional Fisheries Management Organization (RFMO) and WCPFC coordination.	Develop formal bilateral/regional cooperation for stocks linked to shared/migratory resources

mangroves and seagrass habitats remain essential for sustaining juvenile density and growth (Lefcheck *et al*., 2019). Fishing mortality can also be underestimated when discards, lost gear, small-scale catches, or unreported landings are omitted (Gilman *et al*., 2020; Richardson *et al*., 2019; Pauly and Zeller, 2016). Evidence from Indonesia similarly indicates a decoupling between habitat condition and fisheries productivity (Arthatiani *et al*., 2026), while deoxyribonucleic acid barcoding provides the resolution needed to detect biodiversity patterns obscured by aggregate biomass measures (Limmon *et al*., 2020). At ecosystem scale, catch-to-production ratios indicate widespread risk of ecosystem overfishing (Link and Watson, 2019), and climate-driven biomass losses can be amplified at higher trophic levels (Lotze *et al*., 2019). These findings support ecosystem-aware reference points and precautionary buffers (Säterberg *et al*., 2019; FAO, 1996). Mechanistically, thermal stress and deoxygenation lower intrinsic growth or carrying capacity parameters in production models; habitat loss shifts stock-recruitment parameters in stock-recruitment dynamics; and unmonitored extraction bias effective fishing mortality estimates upward. Rather than representing a fully coupled environmental model, these linkages remain conceptual, and comprehensive quantitative application to Indonesian fisheries management areas extends beyond the boundaries of this synthesis.

Toward a framework for assessing MSY implementation readiness

Tables 2 and 3 show that MSY implementation outcomes depend on structural determinants. ubsequently, this comparison is operationalized as a diagnostic tool that maps fisheries along a developmental gradient, moving from data-limited advisory MSY to institutionally sophisticated, ecosystem-consistent, adaptive and precautionary management, thereby highlighting the priority investments required to advance performance. The instrument converts the five features in Table 3 into an ordinal scale, applies it to the eight cases in Table 2, following the logic of tiered assessment frameworks already in use, notably the Australian Commonwealth Harvest Strategy Policy (Dowling *et al*., 2016) and the ICES stock data category scheme (ICES, 2021). This

progression corresponds with wider empirical evidence indicating that co-management frameworks involving both government authorities and resource users outperform strictly top-down regimes (Cinner *et al*., 2012). Additionally, composite indicates from small-scale Indonesian fisheries, such as an assessment of a coastal fishery in Biak Numfor, Papua, which exhibited strong economic performance alongside moderate habitat condition, imply that livelihood-oriented reforms frequently outpace ecological monitoring capabilities (Sakti *et al*., 2026).

Framework dimensions and scoring

Each dimension is scored at three ordinal levels, emerging, transitional, and advanced, with each score traceable to evidence in Table 2. In terms of data infrastructure, emerging management frameworks depend predominantly on unstandardized catch or CPUE metrics subject to underreporting, transitional systems incorporate multi-decadal catch-effort series or periodic survey; whereas advance regimes maintain sustained fishery-independent monitoring programs. Comparable tuna assessments illustrate the institutional and data investment required for advanced systems (Magnusson *et al*., 2023). In terms of assessment methodology, emerging systems rely on a single production model devoid of uncertainty quantification, transitional frameworks evaluate multiple models with partial uncertainty reporting; whereas advanced regimes employ age or size structured state-space models or management-strategy-evaluation-tested ensembles. For HCR enforceability, emerging regimes apply catch ceiling without biomass trigger, transitional regimes use stock-specific negotiated limits, and advanced regimes employ legally binding rules with explicit biomass triggers. For multispecies and ecosystem awareness, emerging regimes aggregate species without ecosystem modelling, transitional regimes estimate multispecies MSY alongside single-species MSYs, and advanced regimes use trophic model to adjust advice for interacting stocks (Del Santo O'Neill *et al.,* 2024; Walters *et al.*, 2005). Mechanisms for shared-stock governance vary along a continuum: spanning purely domestic management, regional coordination lacking binding authority and fully empowered bilateral or multilateral commission capable of fixing joint catch limits. Under equal weighting, the illustrative cases produce mean scores from 1.2 to 2.8. Although specific categorical assignments remain robust under alternative weighting parameters, numerous borderline cases undergo reclassification. Atlantic cod changes under the ecosystem-heavy scheme. Gulf of Thailand changes under the governance-heavy scheme. Kawakawa also shifts between emerging and transitional categories. This instability shows that the tier boundaries are not empirically validated. Accordingly, the empirical covariance between data quality and assessment performance is treated as a working hypothesis, leaving open whether data infrastructure constitutes the dominant limiting factor. Enforcement, governance, political economy, fleet structure, socioeconomic incentives, habitat degradation, and climate variability can independently limit performance.

Illustrative scoring and sensitivity

Under the equal-weight descriptive baseline, the eight illustrative cases yield composite scores reported in Table 4. These metrics merely summarize the compiled evidence without estimating actual management effectiveness, and the corresponding tier boundaries remain unvalidated thresholds. Equal-weight scores provide a descriptive ordering of the selected cases. Data-rich cases generally score infrastructure and assessment, while several Indonesian cases score lower on those dimensions. Because this covariance partially mirrors the criteria embedded in the scoring definitions, it cannot be taken as proof that data infrastructure serves as the overriding causal bottleneck. Enforcement, governance, political economy, fleet structure, socioeconomic

Table 4: Illustrative scoring of MSY implementation readiness across the case studies in Table 2

Case	Infrastructure	Assessment	HCR Enforceability	Ecosystem awareness	Shared Governance	Composite	Regime
Atlantic cod, North Sea (EU CFP)	3	3	2	2	3	13	Advanced, data-rich
Northeast Arctic cod (JNRFC)	3	3	3	2	3	14	Advanced, data-rich
WCPO skipjack tuna (WCPFC)	3	3	3	2	3	14	Advanced, data-rich
Gulf of Thailand multispecies	2	2	1	2	1	8	Transitional
Kawakawa, Bay of Bengal	2	2	1	1	1	7	Emerging, borderline
Java Sea small pelagic (FMA 712)	1	1	2	1	1	6	Emerging, data-limited
Arafura penaeid shrimp (FMA 718)	1	1	2	1	1	6	Emerging, data-limited
Indonesia national framework	1	1	2	1	1	6	Emerging, data-limited

incentives, habitat degradation, and climate variability can independently limit performance. Accordingly, prioritization should proceed via case-by-case evaluation, deploying expanded monitoring frameworks where operational conditions allow, and falling back on data-limited models where fishery-independent surveys are unfeasible.

Sensitivity of the classification to alternative scoring weights

Equal weighting is a baseline convention without independent empirical justification. Alternative weighting left the broad ordering of the highest- and lowest-scoring cases relatively stable but shifted several borderline classifications. Accordingly, the established category boundaries are inherently provisional. While sensitivity analysis mitigates concerns regarding weighting uncertainty, they do not supplant the necessity for systematic inter-rater testing or forma external validation.

Corroboration with findings reported elsewhere in literature

Table 5 summarizes literature that corroborates or qualifies themes identified in this review. Given that these studies share common elements with the underlying evidence base of the synthesis, the resulting comparison functions solely as functions solely as corroboration and does not provide an independent validation of the readiness framework. Corroborating evidence spans single-fishery cases (Chamera *et al*., 2025; Sakti *et al*., 2026) to global compilations (Zhou *et al*., 2012; Hilborn *et al*., 2020) and governance audits (Cullis-Suzuki and Pauly, 2010). While their alignment reinforces the credibility of several underlying themes, it does not constitute formal validation of the readiness heuristic. Although MSY remains a valuable heuristic when assumptions and uncertainties are transparently stated, multispecies dynamics and environmental variability can drive reference points in opposing direction. Consequently, the empirical case studies fail to identify one universally dominant management bottleneck.

Scope and limitations

The review and readiness framework has several limitations. No prospective systematic-review protocol, complete screening log, or deduplication record was available. The eight purposively selected cases differ in geography, management unit, data structure, model type, and period. It cannot support prevalence estimates or causal rankings. Given that the underlying heuristic was formulated from thematic elements also present within the selected cases, a certain level of circularity is inherent to the analysis. The five

Table 5: Corroboration of this review's key findings with evidence reported elsewhere in the literature

The present review finding	Independent evidence	Source
Trophic interactions can require different fishing mortality than single-species F_{MSY}; the direction is context dependent	Life-history synthesis links F_{MSY} to resilience traits, multispecies simulations report the same downward adjustment	Zhou *et al*., 2012; Walters *et al*., 2005
Data infrastructure and assessment sophistication cover in the illustrative cases, but causal dominance is not established	A data-limited Malawi assessment relied on catch-only proxies; CMSY++ development responds to the same global data gap	Chamera *et al*., 2025; Froese *et al*., 2023
Indonesia's 80% MSY-based TAC coexists with stocks independently found overfished	A small-scale Indonesian fishery index likewise found economic indicators outpacing ecological ones	Muawanah *et al*., 2018; Sakti *et al*., 2026
Binding HCRs improve outcomes but are insufficient without enforcement	About 50% of best-practice governance criteria, most managed stocks remain depleted	Cullis-Suzuki and Pauly, 2010
Active, science-based MSY management is linked to stock rebuilding, not collapse	Global stock-status compilations find actively managed fisheries rebuilding toward MSY-consistent biomass	Worm *et al*., 2009; Costello *et al*., 2016; Hilborn *et al*., 2020

dimensions are ordinal, equal weighting is only a baseline convention, and formal confidence ratings, inter-rater reliability, independent external validation are unavailable. Socioeconomic conditions, stakeholder legitimacy, market incentives, habitat state, and climate exposure are incompletely represented. The equilibrium and Lotka-Volterra derivations simplify stochastic, spatial, age-structured, technical, or climate-dependent dynamics. Accordingly, this framework functions strictly as a hypothesis generating instrument pending empirical testing on independent fisheries through formal inter-rater scoring, pre-determined weights, and calibrated confidence thresholds.

CONCLUSION

The reviewed evidence supports MSY as an analytical reference point rather than a fixed catch target. Equilibrium single-species models remain useful baselines, but their reliability declines when productivity, recruitment, habitat capacity, or species interactions change through time. While Schaefer, Pella-Tomlinson, and Fox formulations exhibit distinct production-curve shapes and reference points, age-structured and stock-recruitment dynamics introduce vital demographic detail. Furthermore, bioeconomic extensions account for market prices, operating costs, and fleet behavior, while precautionary reference points establish explicit safety buffers against assessment and implementation error, all of which are tested under uncertainty via. Multispecies and ecosystem approaches address interactions that single-species models cannot resolve. Predation, competition, prey availability, and technical interactions can shift sustainable exploitation levels upward or downward, so a universal adjustment to single-species fishing mortality is not supported. Environmental non stationarity further limits static reference points because warming, deoxygenation, acidification, and habitat degradation can alter growth, recruitment, natural mortality, distribution, or carrying capacity. Accordingly, routine stock reassessment, accompanied by state-dependent reference points where warranted, is mandatory to maintain management efficacy. The case synthesis also indicates that implementation depends on data quality enforcement, governance, fleet structure, market incentives, habitat condition and climate exposure. No single dominant constraint can be inferred from eight purposively selected cases. For Indonesian, standardized reporting, broader monitoring, fishery-independent information where feasible, and transparent data-limited methods can strengthen assessment. Harvest rules should also be linked to enforceable actions and periodically updated stock information. Operating as a tentative heuristic rather than a verified regulatory score, the readiness framework exhibits weighting sensitivity that underscores the requirement for independent validation and inter-rater reliability testing. Future research should

test climate-sensitive reference points, multispecies and single-species advice under realistic uncertainty, integrate socioeconomic and governance variables, and expand management strategy evaluation in data-limited tropical systems. In practice, MSY should be embedded within precautionary, adaptive, and ecosystem-aware management. Where ecological interactions play a critical role, ecosystem and habitat indicators ought to supplement stock-based reference points; concurrently, economic and livelihood targets should remain explicitly distinct from biological yield objectives. Management decisions should also be periodically revised as new ecological, climatic, and socioeconomic evidence becomes available through continuous monitoring and stakeholder engagement**.** This integrated approach provides a more defensible basis for productive fisheries, ecosystem resilience, and long-term environmental sustainability.

AUTHOR CONTRIBUTIONS

S. Triharyuni was responsible for conceptualizing the draft, searching the bibliography, selecting the relevant references, writing the initial manuscript draft, synthesizing the manuscript, and revising the final manuscript version. A. K. Supriatna was responsible for conceptualizing the draft, analyzing the references' coding, reviewing the whole manuscript, revising the final manuscript version and supervision. N. Anggriani was responsible for conceptualizing the draft, defining the bibliographic search, reviewing the whole manuscript, revising the final manuscript version and supervision. R. Puspasari was responsible for the work plan preparation, selecting the relevant references, reviewing the analysis in the manuscript, revising the final manuscript version and supervision.

ACKNOWLEDGEMENT

This study is funded by Universitas Padjadjaran through the Indonesian Endowment Fund for Education (LPDP) on behalf of the Indonesian Ministry of Higher Education, Science and Technology and managed under the EQUITY Program [Contract No. 4303/83/ DT.03.08/ 2025 and 3927/ UN6. RKT/HK.07.00/2025], also under the Universitas Padjadjaran Research Grant under RMMP with project contract number [5597/UN6.3.1/PT.00/2025]. The authors would like to thank the Department of Mathematics, Faculty of Mathematics and Natural Sciences, Universitas Padjadjaran, for the facilities and resources provided throughout this research. The authors also gratefully acknowledge the National Research and Innovation Agency (BRIN) for financial support through the doctoral scholarship program [Decree Number 1261/II.2.3/KP/2026].

CONFLICT OF INTEREST

The authors declare no potential conflict of interest regarding the publication of this work. In addition, the ethical issues including plagiarism, informed consent, misconduct, data fabrication and, or falsification, double publication and, or submission, and redundancy have been completely witnessed by the authors.

OPEN ACCESS

©2027 The author(s). This article is licensed under a Creative Commons Attribution 4.0 International License, which permits use, sharing, adaptation, distribution and reproduction in any medium or format, as long as you give appropriate credit to the original author(s) and the source, provide a link to the Creative Commons license, and indicate if changes were made. The images or other third-party material in this article are included in the article's Creative Commons license, unless indicated otherwise in a credit line to the material. If material is not included in the article's Creative Commons license and your intended use is not permitted by statutory regulation or exceeds the permitted use, you will need to obtain permission directly from the copyright holder. To view a copy of this license, visit: http://creativecommons.org/licenses/by/4.0/

PUBLISHER'S NOTE

GJESM Publisher remains neutral regarding jurisdictional claims in published maps and institutional affiliations.

POSITIVE AI STATEMENT

During the preparation of this work, the authors used Claude Sonnet 4.6 Pro for assistance in drafting and refining the manuscript, which significantly improved the clarity and quality of the text. After using this tool, the authors reviewed and edited the content as needed and took full responsibility for the content of the published article.

ABBREVIATIONS

%	Per cent
AFWG	Arctic Fisheries Working Group
B_{msy}	Biomass at maximum sustainable yield
Bpa	Biomass at Precautionary Approach
BSM	Bayesian State-space Schaefer Model
CCAMLR	Commission for the Conservation of Antarctic Marine Living Resources
CCSBT	Commission for the Conservation of Southern Bluefin Tuna
CFP	Common fisheries policy
CMM	Conservation and management measure
CMSY	Catch-based maximum sustainable yield
CPUE	Catch per unit effort
DNA	DeoxyriboNucleic Acid
DoF	Department of Fisheries (Thailand)
EAFM	Ecosystem Approach to Fisheries Management
EBFM	Ecosystem-Based Fisheries Management
EU	European Union
FAO	Food and Agriculture Organization of the United Nations
Fig.	Figure
FMA	Fisheries management area
F_{msy}	Fishing mortality at maximum sustainable yield
HCR	Harvest Control Rule
ICCAT	International Commission for the Conservation of Atlantic Tunas
ICES	International Council for the Exploration of the Sea
IUU	Illegal, Unreported, and Unregulated
JNRFC	Joint Norwegian Russian Fisheries Commission
MEY	Maximum economic yield
MMAF	Ministry of Marine Affairs and Fisheries (Indonesia)
MMSY	Multispecies maximum sustainable yield
MSE	Management Strategy Evaluation
MSY	Maximum sustainable yield
OA	Open Access (bioeconomic equilibrium)
OY	Optimum sustainable yield
RFMO	Regional Fisheries Management Organization
SAM	State-space assessment model
SDG	Sustainable Development Goal
SPiCT	Stochastic production in continuous time
SPR	Spawning potential ratio
SSB	Spawning stock biomass
STECF	Scientific, technical and economic committee for fisheries
TAC	Total allowable catch
TRP	Target reference point
UNCLOS	United Nations Convention on the Law of the Sea
VPA	Virtual population analysis
WCPFC	Western and Central Pacific Fisheries Commission
WCPO	Western and Central Pacific Ocean
Y/R	Yield per recruit

REFERENCES

Abinaya, R.; Sajeevan, M.K., (2025). Stock status of kawakawa Euthynnus affinis (Cantor, 1849) fishery using surplus production model: An assessment from coastal waters of Tamil Nadu, Bay of Bengal, Southeast coast of India. Aquacult. Fish., 10(1): 132–140 (9 pages).

Agnew, D.J.; Pearce, J.; Pramod, G.; Peatman, T.; Watson, R.; Beddington, J.R.; Pitcher, T.J., (2009). Estimating the worldwide extent of illegal fishing. PLoS ONE. 4(2): 1-8 (8 pages).

Andersen, K.H.; Beyer, J.E., (2013). Size structure, not metabolic scaling rules, determines fisheries reference points. Fish Fish., 1–22 (22 pages).

Arthatiani, F.; Putri, M.R.; Bernawis, L.; Gusmawati, N.; Trenggono, S.; Kasim, K.; Yuwono, T.; Hidayat, F., (2026). Ocean health index status and the conservation priorities associated with marine protected park. Global J. Environ. Sci. Manage., 12(2): 603–624 (22 pages).

Bappenas, (2020). Metadata for Sustainable Development Goals (SDGs) Indonesia Indicators: Environmental Development Pillar (2nd ed.). The Ministry of National Development Planning.

Beddington, J.R.; Agnew, D.J.; Clark, C.W., (2007). Current problems in the management of marine fisheries. Science. 316(5832): 1713–1716 (4 pages).

Beverton, R.J.H.; Holt, S.J., (1957). On the Dynamics of Exploited Fish Populations (1st ed.). Springer Science+Business Media Dordrecht, United Kingdom (543 pages).

Breitburg, D.; Levin, L.A.; Oschlies, A.; Grégoire, M.; Chavez, F.P.; Conley, D.J.; Garçon, V.; Gilbert, D.; Gutiérrez, D.; Isensee, K.; Jacinto, G.S.; Limburg, K.E.; Montes, I.; Naqvi, S.W.A.; Pitcher, G.C.; Rabalais, N.N.; Roman, M.R.; Rose, K.A.; Seibel, B.A.; Telszewski, M.; Yasuhara, M.; Zhang, J., (2018). Declining oxygen in the global ocean and coastal waters. Science. 359(6371): 1-13 (13 pages).

Cabral, R.B.; Mayorga, J.; Clemence, M.; Lynham, J.; Koeshendrajana, S.; Muawanah, U.; Nugroho, D.; Anna, Z.; Mira; Ghofar, A.; Zulbainarni, N.; Gaines, S.D.; Costello, C., (2018). Rapid and lasting gains from solving illegal fishing. Nat. Ecol. Evol., 2(4): 650–658 (9 pages).

Chamera, F.; Kamndaya, M.; Kadaleka, S.; Phepa, P.; Mwamtobe, P.M.; Soko, A., (2025). Fish Stock Assessment Models for Developing Nations with Emphasis on the Use of the Classic Gordon–Schaefer Model: A Review. Fishes. 10(442): 1–19 (19 pages).

Cinner, J.E.; McClanahan, T.R.; MacNeil, M.A.; Graham, N.A.J.; Daw, T.M.; Mukminin, A.; Feary, D.A.; Rabearisoa, A.L.; Wamukota, A.; Jiddawi, N.; Campbell, S.J.; Baird, A.H.; Januchowski-Hartley, F.A.; Hamed, S.; Lahari, R.; Morove, T.; Kuange, J., (2012). Comanagement of coral reef social-ecological systems. PINAS. 109(14): 5219–5222 (4 pages).

Clark, W.G., (1991). Groundfish Exploitation Rates Based on Life History Parameters. Can. J. Fish. Aquat. Sci., 48: 734–750 (17 pages).

Clark, C.W., (1973). Profit maximization and the extinction of animal species. J. Polit. Econ., 81(4): 950–961 (12 pages).

Constable, A.J.; de la Mare, W.K.; Agnew, D.J.; Everson, I.; Miller, D., (2000). Managing fisheries to conserve the Antarctic marine ecosystem: practical implementation of the Convention on the Conservation of Antarctic Marine Living Resources (CCAMLR). ICES J. Mar. Sci., 57(3): 778–791 (14 pages).

Costello, C.; Ovando, D.; Clavelle, T.; Strauss, C.K.; Hilborn, R.; Melnychuk, M.C.; Branch, T.A.; Gaines, S.D.; Szuwalski, C.S.; Cabral, R.B.; Rader, D.N.; Leland, A., (2016). Global fishery prospects under contrasting management regimes. PINAS. 113(18): 5125–5129 (5 pages).

Costello, C.; Gaines, S.D.; Lynham, J., (2008). Can catch shares prevent fisheries collapse?. Science, 321(5896): 1678–1681 (4 pages).

Cullis-Suzuki, S.; Pauly, D., (2010). Failing the high seas: a global evaluation of regional fisheries management organizations. Mar. Policy. 34(5): 1036–1042 (7 pages).

Daskalov, G.M.; Grishin, A.N.; Rodionov, S.; Mihneva, V., (2007). Trophic cascades triggered by overfishing reveal possible mechanisms of ecosystem regime shifts. Proc. Natl. Acad. Sci. U.S.A., 104(25): 10518–10523 (6 pages).

Del Santo O'Neill, T.J.; Rossberg, A.G.; Thorpe, R.B., (2024). An efficient tool to find multispecies MSY for interacting fish stocks. Fish Fish., 25(3): 441–454 (14 pages).

Diaz, R.J.; Rosenberg, R., (2008). Spreading dead zones and consequences for marine ecosystems. Science, 321(5891): 926–929 (4 pages).

Dichmont, C.M.; Pascoe, S.; Kompas, T.; Punt, A.E.; Deng, R., (2010). On implementing maximum economic yield in commercial fisheries. Econ. Sci., 107(1): 16–21 (6 pages).

Dowling, N.A.; Punt, A.E.; Little, L.R.; Dichmont, C.M.; Smith, D.C.; Haddon, M.; Sporcic, M.; Fulton, E.A.; Gorton, R.J., (2016). Assessing a multilevel tier system: The role and implications of data quality and availability. Fish. Res., 183: 1–6 (6 pages).

Eddy, T.D.; Lam, V.W.Y.; Reygondeau, G.; Cisneros-Montemayor, A.M.; Greer, K.; Palomares, M.L.D.; Bruno, J.F.; Ota, Y.; Cheung, W.W.L., (2021). Global decline in capacity of coral reefs to provide ecosystem services. One Earth, 4(9): 1278–1285 (8 pages).

European Union, (2013). Regulation (EU) No 1380/2013 of the European Parliament and of the Council of 11 December 2013 on the Common Fisheries Policy, amending Council Regulations (EC) No 1954/2003 and (EC) No 1224/2009 and repealing Council Regulations (EC) No 2371/2002 and (EC. (pp. 1–63). European Parliament and Council of the European Union (63 pages).

FAO, (1995). Code of Conduct for Responsible Fisheries. FAO, Rome (49 pages).

FAO, (2024). The State of World Fisheries and Aquaculture 2024 – Blue Transformation in Action. FAO, Rome (264 pages).

FAO, (1996). Precautionary approach to capture fisheries and species introductions. FAO Technical Guidelines for Responsible Fisheries No. 2. FAO, Rome (54 pages).

Fox, W.W., (1970). An Exponential Surplus-Yield Model for Optimizing Exploited Fish Populations. Transactions of the American Fisheries Society, 99(1): 80–88 (9 pages).

Free, C.M.; Jensen, O.P.; Anderson, S.C.; Gutierrez, N.L.; Kleisner, K.M.; Longo, C.; Minto, C.; Osio, G.C.; Walsh, J.C., (2020). Blood from a stone: Performance of catch-only methods in estimating stock biomass status. Fish. Res., 223: 105452 (10 pages).

Free, C.M.; Thorson, J.T.; Pinsky, M.L.; Oken, K.L.; Wiedenmann, J.; Jensen, O.P., (2019). Impacts of historical warming on marine fisheries production. Science, 363(6430): 979–983 (5 pages).

Froese, R.; Demirel, N.; Coro, G.; Kleisner, K.M.; Winker, H., (2016). Estimating fisheries reference points from catch and resilience. Fish Fish., 18(3): 506-526 (21 pages).

Froese, R.; Winker, H.; Coro, G.; Palomares, M.L.D.; Tsikliras, A.C.; Dimarchopoulou, D.; Touloumis, K.; Demirel, N.; Vianna, G.M.S.; Scarcella, G.; Schijns, R.; Liang, C.; Pauly, D., (2023). New developments in the analysis of catch time series as the basis for fish stock assessments: the CMSY++ method. Acta Ichthyol. Piscat., 53: 173–189 (17 pages).

Fulton, E.A.; Sainsbury, K.; Noranarttragoon, P.; Leadbitter, D.; Staples, D.J.; Porobic, J.; Ye, Y.; Phoonsawat, R.; Kulanujaree, N., (2022). Shifting baselines and deciding on the desirable form of multispecies maximum sustainable yield. ICES J. Mar. Sci., 79(7): 2138–2154 (17 pages).

Gillis, D.M.; Koscielny, J.; Blanz, B., (2024). Maximum sustainable yield as a reference point in the presence of fishing effort that follows an ideal free distribution. Nat. Resour. Model., 37(1): 1–19 (19 pages).

Gilman, E.; Perez Roda, A.; Huntington, T.; Kennelly, S.J.; Suuronen, P.; Chaloupka, M.; Medley, P.A.H., (2020). Benchmarking global fisheries discards. Sci. Rep., 10: 14017 (8 pages).

Gordon, H.S., (1954). The economic theory of a common-property resource: the fishery. Journal of Political Economy, 62(2): 124–142 (19 pages).

Grafton, R.Q.; Kompas, T.; Hilborn, R.W., (2007). Economics of overexploitation revisited. Science, 318 (5856): 1601 (1 page).

Gras, M.; Pierucci, A.; Mantopoulou Palouka, D.; Kupschus, S.; Konrad, C., (2024). European Commission, Joint Research Centre, Scientific Technical and Economic Committee for Fisheries (STECF) Monitoring the Performance of the Common Fisheries Policy (STECF-Adhoc-24-01). Publications Office of the European Union (127 pages).

Gulland, J.A.; Boerema, L.K., (1973). Scientific Advice on Catch Levels. Fishery Bulletin, 71(2): 325–335 (11 pages).

Haddon, M., (2011). Modelling and Quantitative Methods in Fisheries (2nd ed.). Chapman and Hall/CRC, New York (465 pages).

Hilborn, R.; Walters, C.J., (1992). Quantitative Fisheries Stock Assessment: Choice, Dynamics and Uncertainty. Chapman and Hall, London (585 pages).

Hilborn, R.; Amoroso, R.O.; Anderson, C.M.; Baum, J.K.; Branch, T.A.; Costello, C.; de Moor, C.L.; Faraj, A.; Hively, D.; Jensen, O.P.; Kurota, H.; Little, L.R.; Mace, P.; McClanahan, T.; Melnychuk, M.C.; Minto, C.; Osio, G.C.; Parma, A.M.; Pons, M.; Segurado, S.; Szuwalski, C.S.; Wilson, J.; Ye, Y., (2020). Effective fisheries management instrumental in improving fish stock status. Proc. Natl. Acad. Sci. U.S.A., 117(4): 2218–2224 (7 pages).

Hordyk, A.; Ono, K.; Sainsbury, K.; Loneragan, N.; Prince, J., (2015). Some explorations of the life history ratios to describe length composition, spawning-per-recruit, and the spawning potential ratio. ICES J. Mar. Sci., 72(1): 204–216 (13 pages).

ICES, (2021). ICES fisheries management reference points for category 1 and 2 stocks. Technical Guidelines. In Report of the ICES Advisory Committee, 2021. ICES Advice 2021, Section 16.4.3.1. (19 pages).

ICES, (2024). Greater North Sea Ecoregion - Fisheries Overview. In Report of the ICES Advisory Committee, 2024. ICES Advice 2024, section 9.2. (58 pages).

JRN-AFWG, (2023). Advice on fishing opportunities for Northeast Arctic cod in 2024 in ICES subareas 1 and 2 (Report series IMR-PINRO 2023-5) (14 pages).

JRN-AFWG, (2024). Advice on fishing opportunities for Northeast Arctic cod in 2025 in ICES subareas 1 and 2 (Report series IMR-PINRO 2024-6) (17 pages).

Kim, H.; Franco, A.C.; Sumaila, U.R., (2023). A selected review of impacts of ocean deoxygenation on fish and fisheries. Fishes, 8(6): 1-18 (18 pages).

Kroodsma, D.A.; Mayorga, J.; Hochberg, T.; Miller, N.A.; Boerder, K.; Ferretti, F.; Wilson, A.; Bergman, B.; White, T.D.; Block, B.A.; Woods, P.; Sullivan, B.; Costello, C.; Worm, B., (2018). Tracking the global footprint of fisheries. Science, 359(6378): 904–908 (5 pages).

Larkin, P.A., (1977). An epitaph for the concept of maximum sustained yield. Trans. Am. Fish. Soc., 106(1): 1–11 (11 pages).

Lefcheck, J.S.; Hughes, B.B.; Johnson, A.J.; Pfirrmann, B.W.; Rasher, D.B.; Smyth, A.R.; Williams, B.L.; Beck, M.W.; Orth, R.J., (2019). Are coastal habitats important nurseries? A meta-analysis. Conserv. Lett., 12(4): 1-12 (12 pages).

Limmon, G.; Delrieu-Trottin, E.; Patikawa, J.; Rijoly, F.; Dahruddin, H.; Busson, F.; Steinke, D.; Hubert, N., (2020). Assessing species diversity of Coral Triangle artisanal fisheries: a DNA barcode reference library for the shore fishes retailed at Ambon harbor (Indonesia). Ecol. Evol., 10(7): 3356–3366 (11 pages).

Link, J.S.; Watson, R.A., (2019). Global ecosystem overfishing: clear delineation within real limits to production. Sci. Adv., 5(6): 1-11 (11 pages).

Lotka, A.J., (1925). ELements of physical biology. Baltimore: Williams and Wilkins, London (494 pages).

Lotze, H.K.; Tittensor, D.P.; Bryndum-Buchholz, A.; Eddy, T.D.; Cheung, W.W.L.; Galbraith, E.D.; et al., (2019). Global ensemble projections reveal trophic amplification of ocean biomass declines with climate change. Proc. Natl. Acad. Sci. U.S.A., 116(26): 12907–12912 (6 pages).

Mace, P.M., (1994). Relationships between Common Biological Reference Points Used as Thresholds and Targets of Fisheries Management Strategies. Can. J. Fish. Aquat.Sci., 51 (1): 110–122 (13 pages).

Mace, P.M., (2001). A new role for MSY in single-species and ecosystem approaches to fisheries stock assessment and management. Fish Fish., 2: 2–32 (31 pages).

Magnusson, A.; Hampton, J.; Day, J.; Davies, N.; Teears, T.; Peatman, T.; Castillón-Jordán, C.; Pilling, G.; Scott, R.; Hamer, P., (2023). Stock assessment of yellowfin tuna in the Western and Central Pacific Ocean: 2023. WCPFC Technical Report WCPFC-SC19-2023/SC19-SA-WP-04 (160 pages).

Martell, S.; Froese, R., (2012). A simple method for estimating MSY from catch and resilience. Fish Fish., 14: 504-514 (11 pages).

May, R.M.; Beddington, J.R.; Holt, S.J.; Clark, C.W.; Laws, R.M., (1979). Management of Multispecies Fisheries. Science, 205(4403): 267–277 (11 pages).

McCauley, D.J.; Jablonicky, C.; Allison, E.H.; Golden, C.D.; Joyce, F.H.; Mayorga, J.; Kroodsma, D., (2018). Wealthy countries dominate industrial fishing. Sci. Adv., 4(8): 1-9 (9 pages).

Methot, R.D.; Wetzel, C.R., (2013). Stock synthesis: A biological and statistical framework for fish stock assessment and fishery management. Fish. Res., 142: 86–99 (14 pages).

MMAF, (2022). Decree of the Minister of Marine Affairs and Fisheries of the Republic of Indonesia Number 19 of 2022 concerning Estimated Potential of Fish Resources, Allowable Catch, and Utilization Rate of Fish Resources in the Fisheries Management Areas of the Republ. Ministry of Marine Affairs and Fisheries (MMAF) of the Republic of Indonesia. 1-7 (7 pages).

Muawanah, U.; Yusuf, G.; Adrianto, L.; Kalther, J.; Pomeroy, R.; Abdullah, H.; Ruchimat, T., (2018). Review of national laws and regulation in Indonesia in relation to an ecosystem approach to fisheries management. Mar. Policy. 91: 150–160 (11 pages).

Mueter, F.J.; Megrey, B.A., (2006). Using multi-species surplus production models to estimate ecosystem-level maximum sustainable yields. Fish. Res., 81(2006): 189–201 (13 pages).

National Research Council, (1998). Improving fish stock assessments. National Academy Press, Washington, D.C (327 pages).

Nurhakim, S., (2004). Estimation of Maximum Sustainable Yield of Shrimp Resources in The Arafura Sea using A Surplus Production Model [In Bahasa Indonesia]. J. Lit. Perikan. Ind., 10(6): 85–93 (9 pages).

Pauly, D.; Froese, R., (2021). MSY needs no epitaph—but it was abused. ICES J. Mar. Sci., 78(6): 2204–2210 (7 pages).

Pauly, D.; Watson, R.; Alder, J., (2005). Global trends in world fisheries: impacts on marine ecosystems and food security. Phil. Trans. R. Soc. B., 360(1453): 5–12 (8 pages).

Pauly, D.; Zeller, D., (2016). Catch reconstructions reveal that global marine fisheries catches are higher than reported and declining. Nat. Commun., 7: 10244: 1-9 (9 pages).

Pella, J.J.; Tomlinson, P.K., (1969). A Generalized Stock Production Model. Bulletin of the Inter-American Tropical Tuna Commission, 13(3): 419–496 (78 pages).

Pikitch, E.K.; Santora, C.; Babcock, E.A.; Bakun, A.; Bonfil, R.; Conover, D.O.; Dayton, P.; Doukakis, P.; Fluharty, D.; Heneman, B.; Houde, E.D.; Link, J.; Livingston, P.A.; Mangel, M.; McAllister, M.K.; Pope, J.; Sainsbury, K.J., (2004). Ecosystem-based fishery management. Science. 305: 346–347 (2 pages).

Polacheck, T.; Hilborn, R.; Punt, A.E., (1993). Fitting Surplus Production Models: Comparing Methods and Measuring Uncertainty. Can. J. Fish. Aquat.Sci., 50 (12): 2597–2607 (11 pages).

Punt, A.E., (2003). Extending production models to include process error in the population dynamics. Can. J. Fish. Aquat. Sci., 60(10): 1217–1228 (12 pages).

Punt, A.E., (2015). Strategic management decision-making in a complex world: Quantifying, understanding, and using trade-offs. ICES J. Mar. Sci., 74(2): 499-519 (12 pages).

Punt, A.E.; Butterworth, D.S.; de Moor, C.L.; De Oliveira, J.A.A.; Haddon, M., (2014). Management strategy evaluation: Best practices. Fish Fish., 17(2): 303-334 (32 pages).

Richardson, K.; Hardesty, B.D.; Wilcox, C., (2019). Estimates of fishing gear loss rates at a global scale: a literature review and meta-analysis. Fish Fish., 20(6): 1218–1231 (14 pages).

Ricker, W.E., (1954). Stock and Recruitment. J. Fish. Res. Board Can., 11(5): 559–623 (65 pages).

Sadhotomo, B.; Admaja, S.B., (2012). A synthesis on small pelagic fisheries assessment in The Java Sea [In Indonesia]. J. Lit. Perikan. Ind., 18(4): 221–232 (12 pages).

Sakti, W.I.; Radjawane, I.M.; Latief, H.; Meilano, I.; Trenggono, S.W.; Diantara, S.D.; Wahyudin, R.A.; Radiarta, I.N.; Ketaren, D.G.K.; Winata, I.N.P.; Gusmawati, N.F.; Syamdidi; Yuwono, T.; Arthatiani, F.Y.; Fahira, N.D.; Maharani, S.; Kasim, K., (2026). Balancing ecological stability and economic growth under oceanographic variability and coastal interventions in fisheries systems. Global J. Environ. Sci. Manage., 12(3): 1263–1286 (24 pages).

Schaefer, M.B., (1954). Some Aspects of the Dynamics of Populations Important to the Management of the Commercial Marine Fisheries. Bulletin of the Inter-American Tropical Tuna Commission, 1(2): 26–56 (30 pages).

Schmidtko, S.; Stramma, L.; Visbeck, M., (2017). Decline in global oceanic oxygen content during the past five decades. Nature, 542: 335–339 (5 pages).

Sissenwine, M.P., (1978). Is MSY an Adequate Foundation for Optimum Yield?. Fisheries, 3(6): 22–42 (21 pages).

Smith, T.D., (1994). Scaling Fisheries: The Science of Measuring the Effects of Fishing, 1855-1955. Cambridge University Press, Cambridge, UK (392 pages).

Sumaila, U.R.; Ebrahim, N.; Schuhbauer, A.; Skerritt, D.; Li, Y.; Kim, H.S.; Mallory, T.G.; Lam, V.W.L.; Pauly, D., (2019). Updated estimates and analysis of global fisheries subsidies. Mar. Policy, 109: 103695 (11 pages).

Suman, A.; Eko Irianto, H.; Satria, F.; Amri, D.K., (2016). Potency and Exploitation Level of Fish Resources 2015 in Fisheries Management Area of Indonesian Republic (FMAs) and Its Management Option [In Indonesia]. J.Kebijak.Perikan.Ind., 8(2): 97–110 (14 pages).

Suman, A.; Satria, F.; Nugraha, B.; Priatna, A.; Amri, K.; Mahiswara, (2018). The Stock Status of Fish Resources in 2016 at Fisheries Management Area of Indonesian Republic (FMAs) and Its Management Alternative [In Indonesia]. J. Kebijak. Perikan. Ind., 10(2): 107–128 (22 pages).

Supriatna, A.K., (2012). Maximum sustainable yield for marine metapopulation governed by coupled generalized logistic equations. J. Sustainable Sci. Manage., 7(2): 201–206 (6 pages).

Supriatna, A.K.; Husniah, H., (2015). Sustainable harvesting strategy for natural resources having a coupled Gompertz production function. Interdisciplinary Behavior and Social Sciences– Lumban Gaol., (Ed.), 91–95 (5 pages).

Supriatna, A.K.; Possingham, H.P., (1998). Optimal Harvesting for a Predator – Prey Metapopulation. Bull. Math. Biol., 60(1): 49–65 (17 pages).

Supriatna, A.K.; Possingham, H.P., (1999). Harvesting a two-patch predator-prey metapopulation. Nat. Resour. Model., 12(4): 481–498 (18 pages).

Säterberg, T.; Casini, M.; Gårdmark, A., (2019). Ecologically sustainable exploitation rates: a multispecies approach for fisheries management. Fish Fish., 20(5): 952–961 (10 pages).

Tai, T.C.; Sumaila, U.R.; Cheung, W.W.L., (2021). Ocean acidification amplifies multi-stressor impacts on global marine invertebrate fisheries. Front. Mar. Sci., 8: 596644 (12 pages).

Teears, T.; Davies, N.; Hamer, P.; Magnusson, A.; Peatman, T.; Phillips, J.S.; Pilling, G.; Scott, R.; Vidal, T.; Hampton, J., (2025). Stock assessment of skipjack tuna in the western and central Pacific Ocean: 2025. Report. WCPFC-SC21-2025/SA-WP-02 (REV3), Nuku'alofa, Tonga (174 pages).

Thorson, J.T.; Cope, J.M.; Branch, T.A.; Jensen, O.P., (2012). Spawning biomass reference points for exploited marine fishes, incorporating taxonomic and body size information. Can. J. Fish. Aquat.Sci., 69(9): 1556–1568 (13 pages).

Trenggono, S.; Meilano, I.; Latief, H.; Diantara, S.; Sakti, W.; Ketaren, D.; Winata, I.; Yuwono, T.; Arthatiani, F.; Kasim, K.; Radiarta, I., (2025). Innovation in the blue economy and environmental sustainability in marine and fisheries strategy. Global J. Environ. Sci. Manage., 11(2): 497–518 (22 pages).

Walters, C.J.; Christensen, V.; Martell, S.J.; Kitchell, J.F., (2005). Possible ecosystem impacts of applying MSY policies from single-species assessment. ICES J. Mar. Sci., 62(3): 558–568 (11 pages).

Worm, B.; Hilborn, R.; Baum, J.K.; Branch, T.A.; Collie, J.S.; Costello, C.; Fogarty, M.J.; Fulton, E.A.; Hutchings, J.A.; Jennings, S.; Jensen, O.P.; Lotze, H.K.; Mace, P.M.; McClanahan, T.R.; Minto, C.; Palumbi, S.R.; Parma, A.M.; Ricard, D.; Rosenberg, A.A.; Watson, R.; Zeller, D., (2009). Rebuilding global fisheries. Science, 325(5940): 578–585 (8 pages).

Yuliana, E.; Nurilmala, M.; Rahadiati, A.; Farida, I.; Kurniawati, H.; Agustina, S.; Difah, D.; Pertiwi, P.; Wicaksana, B.; Ramillo, R.; Djatmiko, W., (2026). Provisioning ecosystem services through the sustainable management of fish resources extracted by small-scale fishers. Global J. Environ. Sci. Manage., 12(3): 1311-1332 (22 pages).

Zamroni, A.; Widiyastuti, H.; Suwarso, S., (2020). Stock Status and Exploitation Risk of Small Pelagic Fisheries in Based Sarang Landing Site, Rembang, Central Java [In Indonesia]. J. Lit. Perikan. Ind., 26(4): 189–199 (11 pages).

Zhou, S.; Yin, S.; Thorson, J.T.; Smith, A.D.M.; Fuller, M., (2012). Linking fishing mortality reference points to life history traits: An empirical study. Can. J. Fish. Aquat.Sci., 69(8): 1292–1301 (10 pages).

AUTHOR (S) BIOSKETCHES

Triharyuni, S., Doctoral Student of Department of Mathematics, Faculty of Mathematics and Natural Sciences, Universitas Padjadjaran, Sumedang 45363, West Java, Indonesia.
- Email: *setiya25001@mail.unpad.ac.id*
- ORCID: 0000-0002-6413-0600
- Web of Science ResearcherID: OEO-8109-2025
- Scopus Author ID: 57195199813
- Homepage: https://www.researchgate.net/profile/Setiya-Triharyuni-2

Supriatna, A.K., Ph.D., Professor of Applied Mathematics, Department of Mathematics, Faculty of Mathematics and Natural Sciences, Universitas Padjadjaran, Sumedang 45363, West Java, Indonesia.
- Email: *a.k.supriatna@unpad.ac.id*
- ORCID: 0000-0003-0129-6344
- Web of Science ResearcherID: AAI-4496-2020
- Scopus Author ID: 8318439700
- Homepage: Homepage: https://www.researchgate.net/profile/Asep-Supriatna-2

Anggriani, N., Ph.D., Professor of Applied Mathematics, Department of Mathematics, Faculty of Mathematics and Natural Sciences, Universitas Padjadjaran, Sumedang 45363, West Java, Indonesia.
- Email: *nursanti.anggriani@unpad.ac.id*
- ORCID: 0000-0003-3609-6203
- Web of Science ResearcherID: AAD-7549-2021
- Scopus Author ID: 55669296500
- Homepage: https://www.researchgate.net/scientific-contributions/Nursanti-Anggriani-2228370649

Puspasari, R., Ph.D., Senior Researcher of Marine Ecologist, Research Center for Biota System, Research Organization for Life Science and Environment, National Research and Innovation Agency, Kawasan Sains Teknologi Dr. (H.C) Ir. H. Soekarno, Jl. Raya Bogor KM. 46, Cibinong, 16911, West Java, Indonesia.
- Email: *reny005@brin.go.id*
- ORCID: 0000-0001-5989-8837
- Web of Science ResearcherID: FSX-9448-2022
- Scopus Author ID: 57203353265
- Homepage: https://www.researchgate.net/profile/Reny-Puspasari

HOW TO CITE THIS ARTICLE:
Triharyuni, S.; Supriatna, A.K.; Anggriani, N.; Puspasari, R., (2027). Bridging single-species models to ecosystem-based maximum sustainable yield for environmental sustainability in marine fisheries. Global J. Environ. Sci. Manage., 13(1): 553-574.

DOI: 10.22034/gjesm.2027.01.25
URL: https://www.gjesm.net/article_735745.html

PUBLICATION ETHICS

The ethical policy of GJESM is based on the Committee on Publication Ethics (COPE) guidelines and complies with International Committee of GJESM Editorial Board codes of conduct. Readers, authors, reviewers and editors should follow these ethical policies once working with GJESM. The ethical policy of GJESM is liable to determine which of the typical research papers or articles submitted to the journal should be published in the concerned issue. For information on this matter in publishing and ethical guidelines please visit http://publicationethics.org

Duties and Responsibilities of Publishers

1. GJESM is committing to ensure that editorial decisions on manuscript submissions are the final.
2. GJESM is promising to ensure that the decision on manuscript submissions is only made based on professional judgment and will not be affected by any commercial interests.
3. GJESM is committing to maintain the integrity of academic and research records.
4. GJESM is monitoring the ethics by Editor-in-Chief, Associate Editors, Editorial Board Members, Reviewers, Authors, and Readers.
5. GJESM is always checking the plagiarism and fraudulent data issues involving in the submitted manuscript.
6. GJESM is always willing to publish corrections, clarifications and retractions involving its publications as and when needed.

Duties and Responsibilities of Editors

1. The Editors of the journal should have the full authority to reject/accept a manuscript.
2. The Editors of the journal should maintain the confidentiality of submitted manuscripts under review or until they are published.
3. The Editor-in-Chief should take a decision on submitted manuscripts, whether to be published or not with other editors and reviewers
4. The Editors of the journal should preserve the anonymity of reviewers.
5. The Editors of the journal should disclose and try to avoid any conflict of interest.
6. The Editors of the journal should maintain academic integrity and strive to meet the needs of readers and authors.
7. The Editors of the journal should be willing to investigate plagiarism and fraudulent data issues and willing to publish corrections, clarifications, retractions, and apologies when needed.
8. The Editors of the journal should have the limit themselves only to the intellectual content.
9. The Editors of the journal must not disclose any information about submitted manuscripts to anyone other than the corresponding author, reviewers, potential reviewers, other editorial advisers, and the publisher, as appropriate.
10. Unpublished materials disclosed in a submitted paper will not be used by the editor or the members of the editorial board for their own research purposes without the author's explicit written consent.

Duties and Responsibilities of Reviewers

1. The Reviewers of the journal should assist the Editors in taking the decision for publishing the submitted manuscripts.
2. The Reviewers should maintain the confidentiality of manuscripts, which they are invited to review.
3. The Reviewers should provide comments in time that will help editors to make decision on the submitted manuscript to be published or not.
4. The Reviewers are bound to treat the manuscript received for peer reviewing as confidential, and must not use the information obtained through peer review for personal advantage.
5. The Reviewers comments against each invited manuscript should be technical, professional and objective.
6. The Reviewers should not review the manuscripts in which they have found conflicts of interest with any of the authors, companies, or institutions.
7. The Reviewers should disclose and try to avoid any conflict of interest.

Duties and Responsibilities of Authors

1. Manuscripts must be submitted only in English and should be written according to sound grammar and proper terminology.
2. Manuscripts must be submitted with the understanding that they have not been published elsewhere (except in the form of an abstract or as part of a published lecture, review, or thesis) and are not currently under consideration by another journal published by or any other publisher.
3. The submitting (corresponding) author is responsible for ensuring that the manuscript article's publication has been approved by all the other coauthors.
4. In order to sustain the peer review system, authors have an obligation to participate in peer review process to evaluate manuscripts from others.
5. It is also the authors' responsibility to ensure that the manuscripts emanating from a particular institution are submitted with the approval of the necessary institution.
6. It is a condition for submission of a manuscript that the authors permit editing of the paper for readability.
7. Authors are requested to clearly identify who provided financial support for the conduct of research and/or preparation of the manuscript and briefly describe the role of the funder/sponsor in any part of the work.
8. A copy right release and conflict of interest disclosure form must be signed by the corresponding author in case of multiple authorships, prior to the acceptation of the

manuscript, by all authors, for publication to be legally responsible towards the Journal ethics and privacy policy.

9. Under open access license, authors retain ownership of the copyright for their content, but allow anyone to download, reuse, reprint, modify, distribute, and/ or copy the content as long as the original authors and source are cited properly.
10. All authors have agreed to allow the corresponding author to serve as the primary correspondent with the editorial office, to review the edited manuscript and proof.
11. When author(s) discovers a significant error or inaccuracy in his/her own published work, it is the author's obligation to promptly notify the journal editor or publisher to retract or correct the manuscript.
12. All authors must know that that the submitted manuscripts under review or published with GJESM are subject to screening using Plagiarism Prevention Software. Plagiarism is a serious violation of publication ethics.

Violation of Publication Ethics

1. **Plagiarism:** Plagiarism is intentionally using someone else's ideas or other original material as if they are one's own. Copying even one sentence from someone else's manuscript, or even one of your own that has previously been published, without proper citation is considered by GJESM Journals as plagiarism. All manuscripts under review or published with GJESM are subject to screening using plagiarism prevention software. Thus, plagiarism is a serious violation of publication ethics. The development of CrossCheck is a service that helps editors to verify the originality of papers. CrossCheck is powered by the Ithenticate software from iParadigms, known in the academic community as providers of Turnitin. For a searchable list of all journals in the CrossCheck database, please visit: www.ithenticate.com/search
2. **Data Fabrication and Falsification:** Data fabrication and falsification means the researcher did not really carry out the study, but made up data or results and had recorded or reported the fabricated information. Data falsification means the researcher did the experiment, but manipulated, changed, or omitted data or results from the research findings.
3. **Simultaneous Submission:** Simultaneous submission occurs when a manuscript (or substantial sections from a manuscript) is submitted to a journal when it is already under consideration by another journal.
4. **Duplicate Publication:** Duplicate publication occurs when two or more papers, without full cross referencing, share essentially the same hypotheses, data, discussion points, and conclusions.
5. **Redundant Publications:** Redundant publications involve the inappropriate division of study outcomes into several articles, most often consequent to the desire to plump academic vitae.
6. **Improper Author Contribution or Attribution:** All listed authors must have made a significant scientific contribution to the research in the manuscript and approved all its claims. Don't forget to list everyone who made a significant scientific contribution, including students and laboratory technicians.
7. **Citation Manipulation:** Citation Manipulation is including excessive citations, in the submitted manuscript, that do not contribute to the scholarly content of the article and have been included solely for the purpose of increasing citations to a given author's work, or to articles published in a particular journal. This leads to misrepresenting the importance of the specific work and journal in which it appears and is thus a form of scientific misconduct.

Handling Cases of Misconduct

Once GJESM confirms a violation against GJESM's publication ethics, GJESM addresses ethical concerns diligently following an issue-specific standard practice as summarized below.

1. The first action of the journal Editor is to inform the Editorial Office of GJESM by supplying copies of the relevant material and a draft letter to the corresponding author asking for an explanation in a nonjudgmental manner.
2. If the author's explanation is unacceptable and it seems that serious unethical conduct has taken place, the matter is referred to the Publication Committee via Editorial Office. After deliberation, the Committee will decide whether the case is sufficiently serious to warrant a ban on future submissions.
3. If the infraction is less severe, the Editor, upon the advice of the Publication Committee, sends the author a letter of reprimand and reminds the author of GJESM publication policies; if the manuscript has been published, the Editor may request the author to publish an apology in the journal to correct the record.
4. Notification will be sent to corresponding author and any work by the author responsible for the violation or any work these persons coauthored that is under review by GJESM journal will be rejected immediately.
5. The authors are prohibited from serving on GJESM editorial board and serving as a reviewer for GJESM Journal. GJESM reserves the right to take more actions.
6. In extreme cases, notifications will be sent to the affiliations of the authors and the authors are prohibited from submitting their work to GJESM for 5 years.
7. In serious cases of fraud that result in retraction of the article, a retraction notice will be published in the journal and will be linked to the article in the online version. The online version will also be marked "retracted" with the retraction date.

GUIDE FOR AUTHORS

"Global Journal of Environmental Science and Management" (GJESM) is a double blind peer reviewed electronic and print quarterly publication concerned with all aspects of environmental science and management. GJESM publishes original research papers, review papers, case reports and short communications, letters to editor and authors' response about letters to editor across the broad field of environment. These include but are not limited to environmental science, environmental management, environmental engineering, environmental planning and design, urban and regional landscape design and industrial ecology. Environmentalist disciplines are invited to contribute their knowledge and experience. The publication appears at regular intervals time quarterly. The Journal database is fully open access and full text of published articles are available for everyone who can get access to the Journal website free of cost. The authors never pay any charges for submission, article processing and publication.

Guide for Authors: More details on guide for authors refer: http://gjesm.net/journal/authors.note

GENERAL

1. Authors should submit their contributions electronically through the GJESM website submission system to the Editorial Office.

2. Manuscripts must be submitted only in English and should be written according to sound grammar and proper terminology. Manuscripts should be typed in Times New Roman of 11 pt. font and in MS-Word format in one column with 2.5 cm margin at each side. Manuscript submission must be applied once in order to obtain only one submission ID number. More than one submission for a single manuscript can lose the chance of the manuscript consideration. Manuscript must be accompanied by a covering letter including title and author(s) name.

3. There are no strict formatting requirements but all manuscripts must contain the essential elements needed to convey your manuscript, for example Abstract, Keywords, Introduction, Materials and Methods, Results, Conclusions, Artwork and Tables with Captions. Please ensure the figures and the tables included in the single file are placed next to the relevant text in the manuscript, rather than at the bottom or the top of the file. There are no strict requirements on reference formatting at submission. References can be in any style or format as long as the style is consistent.

BEFORE YOU BEGIN

1. Peer-Review Process: In order to sustain the peer review system, authors have an obligation to participate in peer review process to evaluate manuscripts from others. When appropriate, authors are obliged to provide retractions and/or corrections of errors to the editors and the Publisher. All papers submitted to GJESM journal will be peer reviewed for at least one round. GJESM journal adopts a double-blinded review policy: authors are blind to reviewers, but reviewers are not blind to authors. After receiving reviewers' comments, the editorial team member makes a decision. Because reviewers sometimes do not agree with each other, the final decision sent to the author may not exactly reflect recommendations by any of the reviewers. The decision after each round of peer review may include (a) Accept without any further changes, (b) Accept with minor revision, (c) Major changes are necessary for resubmission and (d) Decline without encouraging resubmission.

2. Post-Publication Evaluation: In addition to rapid Peer Review Process, the GJESM Journal has Post-Publication Evaluation by the scientific community. Post-Publication Evaluation is concentrated to ensure that the quality of published research, review and case report meets certain standards and the conclusions that are presented are justified. The post-publication evaluation includes online comments and citations on published papers. Authors may respond to the comments of the scientific community and may revise their manuscript. The Post-Publication Evaluation is described in such a way; it is allowing authors to publish quickly about Environmental science, management, engineering and technology concepts.

3. Publication Ethics: The ethical policy of GJESM is based on the Committee on Publication Ethics (COPE) guidelines and complies with International Committee of GJESM Editorial Board codes of conduct. Readers, authors, reviewers and editors should follow these ethical policies once working with GJESM. The ethical policy of GJESM is liable to determine which of the typical research papers or articles submitted to the journal should be published in the concerned issue. The ethical policy insisted the Editor-in-Chief, may confer with other editors or reviewers in making the decision. Visit at: http://publicationethics.org

4. Conflict of Interest: Authors are requested to evident whether impending conflicts do or do not exist. A copyright transfer agreement is signed by the corresponding author, upon the acceptance of the manuscript, on behalf of all authors, for publication to be legally responsible towards the journal ethics and privacy policy. Authors will be notified as soon as possible of decisions concerning the suitability of their manuscripts for publication in the journal. The submitted materials may be considered for inclusion but cannot be returned and Editors of the journal reserve the right to accept or reject any article in any stage, if necessary. Conflict of Interest Disclosure form can be found at: www.gjesm.org/conflict_of_interest_discloure_form.docx

5. Submission Declaration and Verification: While submitting a manuscript to GJESM, all contributing author(s) must verify that the manuscript represents authentic and valid work and that neither this manuscript nor one with significantly similar content under their authorship has been published or is being considered for publication elsewhere including electronically in the same form, in English or in other language, without the written consent the copy right holder.

6. Authorship: All contributing authors should qualify for authorship and corresponding author should sign the authorship form while submitting the manuscript. It can be found at:
(http://www.gjesm.net/data/gjesm/news/authorship_form.docx).

7. Changes to Authorship: After the manuscript is submitted or accepted for publication, the corresponding author is required to send a request to add or remove an author or to rearrange the author names of the submitted/accepted manuscript by sending the change of authorship form to editorial office. No authorship change is allowed after publication of manuscript. More details may be found at:
(http://www.gjesm.net/data/gjesm/news/change_of_authorship_form.docx)

8. Retained Author Rights: As an author, author or authors' employer or institution retains certain rights. For more information on author rights, found at:
www.gjesm.org/retained_authors_right.docx.

9. Copy Right: Journals should make clear the type of copyright under which authors' work will be published. For open access articles the publisher uses an exclusive licensing agreement in which authors retain copyright in their manuscript. More details may be found at: (www.gjesm.org/copyright_form.docx)

10. User license Agreement: GJESM provides access to archived material through GJESM archives. Manuscripts are the parts of an open archive are made freely available from GJESM website after certain period, which begins from the final publication date of the manuscript. All articles published open access will be immediately and permanently free for everyone to read and download. Permitted reuse is defined by Creative Commons user license called ***Creative Commons Attribution***. Visit at: **(**Creative Commons Attribution 4.0 International (CC BY 4.0)**)**

11. Plagiarism Prevention and Violation of Publication Ethics: All manuscripts under review or published with GJESM are subject to screening using Plagiarism Prevention Software. Plagiarism is a serious violation of publication ethics. Other violations include duplicate publication, data fabrication and falsification, and improper credit of author contribution. Thus, the Plagiarism or Fraudulent or knowingly inaccurate statements constitute unethical behavior are unacceptable and submitting the same manuscript to more than one journal concurrently constitutes unethical publishing behavior and is unacceptable. The development of CrossCheck is a service that helps editors to verify the originality of papers. CrossCheck is powered by the Ithenticate software from iParadigms, known in the academic community as providers of Turnitin. For more details visit at: www.ithenticate.com/search

12. Handling Cases of Misconduct: Once GJESM confirms a violation against GJESM's publication ethics, the following actions will be taken.

a. The work is rejected / retracted immediately. Notification will be sent to corresponding authors. In extreme cases, notifications will be sent to the affiliations of the authors.
b. The authors are prohibited from submitting their work to GJESM for 5 years.
c. Any work by the authors responsible for the violation or any work these persons coauthored that is under review by any GJESM journal will be rejected immediately.
d. The authors are prohibited from serving on GJESM editorial board. GJESM reserves the right to take more actions.

MANUSCRIPT PREPARATION

1. Title Page: The title page should include: the name(s) of the author(s), a concise and informative title, the affiliation(s) and address (es) of the author(s), and e-mail address, telephone and fax numbers of the corresponding author.

2. Manuscript Title: Title of up to 17 words should not contain the name of locations, countries or cities of the research as well as abbreviations. The title should be oriented to Environmental issues while not being obscure or meaningless.

3. Abstract: An abstract of 150 to 250 words that sketches the purpose of the study; basic procedures; main findings its novelty; discussions and the principal conclusions, should not contain any undefined abbreviations or references.

4. Keywords: Provide 5 to 7 keywords which can be used for indexing purposes. Keywords should not repeat the words of the manuscript title or contain abbreviations and shall be written in alphabetical order as separated by semicolon.

5. Introduction: The Introduction should state the purpose of the investigation and identify clearly the gap of knowledge that will be filled in the Literature review study. Date and location of the research carried out throughout the study must be mentioned at the end of this section.

6. Materials and methods: The Materials and Methods section should provide enough information to permit repetition of the experimental work. It should include clear descriptions and explanations of sampling procedures, experimental design, and essential sample characteristics and descriptive statistics, hypothesis tested, exact references to literature describing the tests used in the manuscript, number of data involved in statistical tests, etc.

7. Results and Discussion: The Results section should describe the outcome of the study. Data should be presented as concisely as possible - if appropriate in the form of tables or figures, although very large tables should be avoided. The Discussion should be an interpretation of the results and their significance with reference to work by other authors. Please note that the policy of the Journal with respect to units and symbols is that of SI symbols.

8. Tables: Do not submit tables and graphs as photograph. Place explanatory matters in footnotes, not in the heading. Do not use internal horizontal and vertical rules. Tables should be called out in the text and should have a clear and rational structure and consecutive numerical order. All tables should be numbered 1, 2, 3, etc. Give enough information in subtitles so that each table is understandable without reference to the text. Footnotes to tables should be indicated by superscript lower-case letters (or asterisks for significance values and other statistical data) and included beneath the table body.

9. Figures: Figures/ illustrations should be in high quality art work, within 200-300 dpi and separately provided in Excel format. Ensure that figures are clear, labeled, and of a size that can be reproduced legibly in the journal. Each figure should have a concise caption describing accurately what the figure depicts. Figure captions begin with the term Fig. Figures should be with the captions placed below in limited numbers. No punctuation is to be placed at the end of the caption.

10. Conclusion: This section should highlight the major, firm discoveries, and state what the added value of the main finding is, without literature references.

11. Acknowledgements: Acknowledgments of people, grants, funds, etc. should be placed in a separate section before the reference list. The names of funding organizations should be written in full. Financial support affiliation of the study, if exists, must be mentioned in this section. Thereby, the Grant number of financial support must be included.

12. References: All the references should be cited throughout the manuscript text as well as in the Reference section organized in accordance with Harvard system. Groups of references should be listed first alphabetically, then chronologically. The number of references extracted from each journal should not exceed 3 to 5 citations, which is the average acceptable amount. The number of references should not be less than 30 for original paper, less than 100 for review paper. It is substantially recommended to the authors to refer to more recent references rather than old and out of date ones. Volume, issue and pages of the whole references must be specified according to the GJESM format.

Citing and listing of Web references: As a minimum, the full URL should be given. Any further information, if known (Author names, dates, reference to a source publication, etc.), should also be given.

Text: All citations in the text should refer to: 1. Single author: the author's name (without initials, unless there is ambiguity) and the year of publication; 2. Two authors: both authors' names and the year of publication; and 3. Three or more authors: first author's name followed by "et al." and the year of publication. Citations may be made directly (or parenthetically). Groups of references should be listed first alphabetically, then chronologically. Examples: "as demonstrated (Allan, 1996a, 1996b, 1999; Allan and Jones, 1995). Kramer *et al.,* (2000) have recently shown …".

List: References should be arranged first alphabetically and then further sorted chronologically if necessary. More than one reference from the same Author(s) in the same year must be identified by the letters "a", "b", "c", etc., placed after the year of publication.

Journal article: Nouri J.; Lorestani B.; Yousefi N.; Khorasani N.; Hassani A. H.; Seif, F.; Cheraghi M., (2011). Phytoremediation potential of native plants grown in the vicinity of Ahangaran lead-zinc mine. Environ. Earth Sci., 62(3): 639-644.

Book: Davis, M. L., (2005). Introduction to Environmental Engineering, 3rd. Ed. McGraw Hill Inc.

Book chapter: Mettam, G. R.; Adams, L. B., (1999). How to prepare an electronic version of your article, in: Jones, B. S., Smith, R. Z. (Eds.), Introduction to the electronic age. E-Publishing Inc., New York.

Conference paper: Brown, J., (2005). Evaluating surveys of transparent governance. In UNDESA, 6th. Global forum on reinventing government: towards participatory and transparent governance. Seoul, Republic of Korea 24-27 May. United Nations: New York.

Dissertation: Trent, J. W., (1975). Experimental acute renal failure. Ph.D. Dissertation, University of California. USA.

Online document: Cartwright, J., (2007). Big stars have weather too. IOP Publishing Physics Web.
http://physicsworld.com/cws/article/news/2007/jun/26/big-stars-have-weather-too

AFTER ACCEPTANCE

1. Online Proof Correction: Corresponding authors will receive an e-mail with a link to our online proofing system, allowing annotation and correction of proofs online. Use this proof only for checking the typesetting, editing, completeness and correctness of the text, tables and figures. Significant changes to the article as accepted for publication will only be considered at this stage with permission from the Editor-in-Chief. It is important to ensure that all corrections are sent back to us in one communication. Please check carefully before replying, as inclusion of any subsequent corrections cannot be guaranteed. Proofreading is solely the corresponding author responsibility.

2. Offprints: The offprints can be downloading from the GJESM website once the final corrected manuscripts are disseminated.

AUTHORS INQUIRIES

Authors can track their submitted article through GJESM website on author's login section at: http://gjesm.net/contacts?_action=login

Global Journal of Environmental Science and Management (GJESM)

Copyright Transfer Agreement

1. Parties of the agreement

Author (s):

Manuscript Title:

Manuscript ID:

(Herewith referred to as the "materials"),

Journal Title: Global Journal of Environmental Science and Management (GJESM)

2. Subject of the agreement

A) Copyright
1- The Author and each co-authors shall transfer and sell to the Publisher for the length of the copyright starting from the moment the present agreement comes into force the exclusive rights to the materials, including the rights to translate, reproduce, transfer, distribute or otherwise use the materials or parts (fragments) contained therein, for publication in scientific, academic, technical or professional journals or other periodicals and in derivative works thereof, worldwide, in English, in print or in electronic editions of such journals, periodicals and derivative works in all media or formats now existing or that may exist in future, as well as the right to license (or give permission to) third parties to use the materials for publication in such journals, periodicals and derivative works worldwide. The transfer under this agreement includes the right to adapt the presentation of the materials for use in conjunction with computer systems and programs, reproduction or publication in machine-readable format and incorporation into retrieval systems.
2- Reproduction, placement, transfer or any other distribution or use of the materials, or any parts of the materials contained therein, in any way permitted under this Agreement, shall be accompanied by reference to the Journal and mentioning of the Publisher, namely: the title of the article, the name of the Author (Co-authors), the name of the Journal, volume/number, copyright of the publisher.

B) Reserved Rights
The Author (Co-authors) or the employer of the Author (Co-authors) of the materials shall retain all proprietary rights (with the exception of the rights transferred to the Publisher under the present Agreement).

C) Author Guarantee
The Author (Co-authors) guarantees that the materials are an original work, submitted only to GJESM, and have not been published previously.
In case the materials were written jointly with co-authors, the Author guarantees that he/she has informed them of the terms of this Agreement and obtained their signatures or written permission to singe on their behalf.
The Author guarantees as well that:
The materials do not contain libelous statements.
The materials do not infringe on other persons' rights (including without limitation copyrights, patent rights and the trademark right).
The materials do not contain facts or instructions that can cause damage or injury to third parties and their publication does not cause the disclosure of any secret or confidential information

---

Author (Corresponding Author):

Correspondence Address:

Phone:

Fax:

Email:

Corresponding Author Name: Signature Date

On Behalf of the Publisher:

Iran Solid Waste Association,
Faculty of Environment, University of Tehran,
Postal Code: 1417854511, Tehran,
Iran

Telefax: (+9821) 2610 5110

Email: *editor@gjesm.net*
Gjesm.publication@gmail.com

Website: www.gjesm.net

Accepted for publication ☑ Signature Date

PLEASE NOTE: The accepted manuscript cannot be processed for publication until the publisher has received this signed form. The form MUST be signed by the Corresponding Author and then scanned and sent through the system or email. If the manuscript is not published in the Journal, this release will not take effect.

The sole responsibility for the whole content (s) of the article remains only with the corresponding author. However, Editor would reserve the right to adjust the style to certain standards of uniformity before publication.

CONFLICT OF INTEREST DISCLOSURE FORM

Conflict of Interest is defined as a set of conditions in which professional judgment concerning a primary interest, such as the validity of research, may be influenced by a secondary interest, such as financial gain. A Conflict of Interest Disclosure is an agreement or notification from the authors that they have not been paid for the work, or if they have, stating the source of their payment. The purpose of Conflict of Interest Disclosure form is to provide readers of authors' manuscript with information about authors' interests that could influence how the authors receive the work. The corresponding author (on behalf of all co-authors) should submit a conflict of interest disclosure form and is responsible for the accuracy and completeness of the submitted manuscript. Conflict of Interest Disclosure form can be signed by the corresponding author on behalf of all co-authors and stating that the submitted manuscript is the authors' original work, has not received prior publication and is not under consideration for publication elsewhere, permission has been received to use any material in the manuscript much as tables, figures etc. or no permissions have necessary to publish the authors' work.

1. Name of the corresponding author

2. Affiliation including e-mail and phone number

3. Manuscript Title

4. Do the authors or authors' institution at any time receive payment or services from a third party (government, commercial, private foundation, etc.) for any aspect of the submitted manuscript (including but not limited to grants, data monitoring board, study design, manuscript preparation, statistical analysis, etc.)?

   Are there any relevant conflicts of interest? Yes / No

5. Do the authors have any patents, whether planned, pending or issued, broadly relevant to the work?

   Are there any relevant conflicts of interest? Yes / No

6. Are there other relationships or activities that readers could perceive to have influenced, or that give the appearance of potentially influencing, what the authors' information in the submitted manuscript?

   Are there any relevant conflicts of interest? Yes / No

7. Are there any aspect of the work covered in this manuscript that has involved either experimental animals or human patients has been conducted with the ethical approval of all relevant bodies or not.

   Are there any relevant conflicts of interest? Yes / No

Corresponding Author Signature | Print Name | Date

AUTHORSHIP FORM

By completing and signing the following statements, the corresponding author acknowledges and accepts the responsibility on behalf of all contributing authors, if any, concerning Authorship Responsibility.

Manuscript title:

Corresponding author:

Affiliation:

Email:

Phone No:

By signing and filling this form, the corresponding author certifies that each author has met all criteria below (A, B, C, and D) and indicates each author general and specific contributions by listing his or her name next to the relevant section.

A. I certify that

- The manuscript is authentic and valid and that neither this manuscript nor one with considerably similar content under my authorship has been published or is being considered for publication elsewhere, except as described in an attachment, nor copies of closely related manuscripts are provided.
- I will provide the data or will contribute fully in providing and obtaining the data on which the manuscript is based for examination by the editors or their assignees, if requested.
- Every author has agreed to allow the corresponding author to serve as the primary correspondent with the editorial office, to review the edited manuscript and proof.

B. Each author has given final approval of the submitted manuscript.

C. Each author has participated sufficiently in the work to take public responsibility for the whole content.

D. Each author qualifies for authorship by listing his or her name on the appropriate line of the categories of contributions listed below. List appropriate author next to each section – each author must be listed in at least 1 field. More than 1 author can be listed in each field.

- conception and design
- acquisition of data
- analysis and interpretation of data
- drafting of the manuscript
- critical revision of the manuscript for important intellectual content
- statistical analysis
- obtaining funding
- administrative, technical, or material support
- supervision
- no additional contributions
- other (specify)

Corresponding Author Signature **Print Name** **Date**

CHANGE OF AUTHORSHIP FORM

Manuscript Title:

Corresponding Author:

Please check all that apply.

☐ New author(s) have been added.

☐ There is a change in the order of authorship.

☐ An author wishes to remove his/her name. An author's name may only be removed at his/her own request in writing.

ORIGINAL AUTHORSHIP

List ALL AUTHORS in the same order as the original (first) submission.

Print Name	Print Name
Name (1)	Name (6)
Name (2)	Name (7)
Name (3)	Name (8)
Name (4)	Name (9)
Name (5)	Name (10)

NEW AUTHORSHIP

List the ALL AUTHORS in same order as the new version.

Print Name	Print Name
Name (1)	Name (6)
Name (2)	Name (7)
Name (3)	Name (8)
Name (4)	Name (9)
Name (5)	Name (10)

I attest that:

1. The manuscript is not currently under consideration, in press, or published elsewhere, and the research reported will not be submitted for publication elsewhere until a final decision has been made as to its acceptability by the journal (posting of submitted material on a web site may be considered prior publication-note this in your cover letter).
2. The manuscript is truthfully original work without fabrication, fraud, or plagiarism.
3. I have made an important scientific contribution to the study and am thoroughly familiar with the primary data.
4. I have read the complete manuscript and take responsibility for the content and completeness of the manuscript and understand that I share responsibility if the paper, or part of the paper, is found to be faulty or fraudulent.

Corresponding Author Signature Name Date

Global
Journal of Environmental Science and Management

Volume 13, Issue 1, Winter 2027

1. Integration of the online river water quality monitoring management framework based on inclusive governance
2. Environmental deoxyribonucleic acid metabarcoding reveals fish diversity in subtropical island mangrove rivers
3. The effect of agricultural taxes and local agricultural policies onenhancing food security and environmental sustainability
4. Polymer-specific mechanical recycling of pre-sorted post-consumer municipal plastics for enhanced environmental sustainability
5. Sustainability assessment for multi-activity coastal areas using an integrated hierarchical decision-making framework
6. Satellite-based assessment of high Andean wetlands and carbon sequestration under the influence of climate change
7. Environmental status of silky sharks in Eastern Indian Ocean from length-based catch data
8. The impact of environmental, economic, and social sustainability under intensive agriculture
9. Inflow modeling strategies designed to enhance the ecological sustainability of hydroelectric reservoir operation planning
10. Driving sustainable development goal alignment through green consumption marketing and public mind
11. Ecological diversity in soil properties and bacterial communities in tropical coastal areas with contrasting electrical conductivity
12. Multivariate and index-based evaluation of long-term reclaimed wastewater quality and reuse suitability
13. Environmental modeling of yellowfin tuna fishing grounds integrating oceanographic and biological parameters using generalized additive model
14. Life cycle assessment and identification of embodied carbon hotspots in a reinforced concrete factory
15. Valorization and physicochemical characterization of municipal solid waste gasification tar derived aliphatic hydrocarbon-rich oils
16. Analytic hierarchy process-based criterion weighting for water resources management projects
17. Temporal water-quality variability and its implications for environmental management of sand lobster aquaculture
18. Ecological drivers of Hygrocybe and Xylaria occurrences in a tropical Karst forest
19. Consumer awareness, participation, and accessibility in sustainable electronic waste management
20. Integrated system dynamics modeling for sustainable fisheries provisioning services
21. Environmental health conditions associated with childhood stunting during the first 1000 days of life
22. Artificial intelligence-driven approaches for detection, fate, transport, and remediation of microplastic pollution in aquatic systems
23. Environmental risks of pest management practices in smallholder coconut plantations
24. A bibliometric and systematic analysis of artificial intelligence and the transition towards smart geotourism
25. Bridging single-species models to ecosystem-based maximum sustainable yield for environmental sustainability in marine fisheries